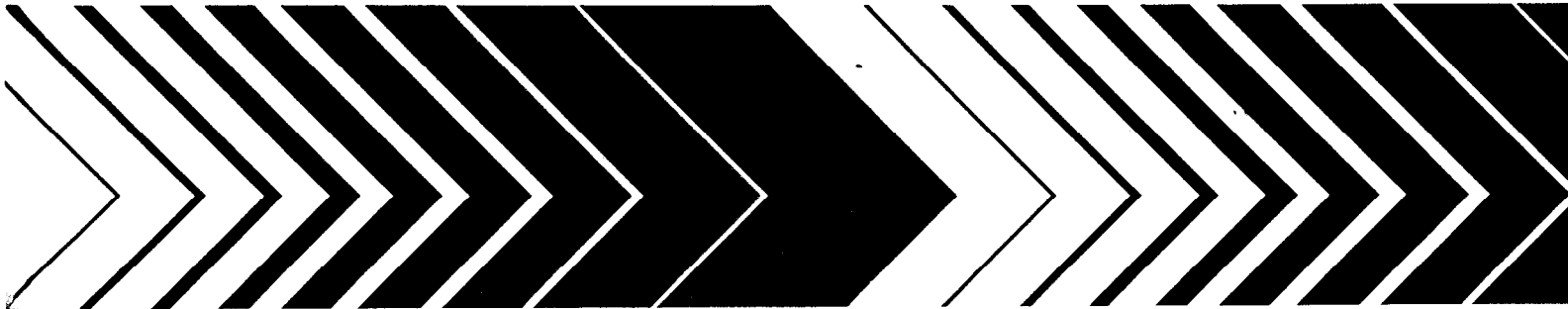




# Air Quality Criteria for Particulate Matter

## Volume II of III



## DISCLAIMER

This document has been reviewed in accordance with U.S. Environmental Protection Agency policy and approved for publication. Mention of trade names or commercial products does not constitute endorsement or recommendation for use.

## PREFACE

On April 30, 1971 (Federal Register, 1971), in accordance with the Clean Air Act (CAA) Amendments of 1970, the U.S. Environmental Protection Agency (EPA) promulgated the original primary and secondary National Ambient Air Quality Standard (NAAQS) for particulate matter (PM). The reference method for measuring attainment of these standards was the "high-volume" sampler (Code of Federal Regulations, 1977), which collected PM up to a nominal size of 25 to 45  $\mu\text{m}$  (so-called "total suspended particulate," or "TSP"). Thus, TSP was the original indicator for the PM standards. The primary standards for PM, measured as TSP, were 260  $\mu\text{g}/\text{m}^3$ , 24-h average not to be exceeded more than once per year, and 75  $\mu\text{g}/\text{m}^3$ , annual geometric mean. The secondary standard was 150  $\mu\text{g}/\text{m}^3$ , 24-h average not to be exceeded more than once per year.

In accordance with the CAA Amendments of 1977, the U.S. EPA conducted a re-evaluation of the scientific data for PM, resulting in publication of a revised air quality criteria document (AQCD) for PM in December 1982 and a later Addendum to that document in 1986. On July 1, 1987, the U.S. EPA published final revisions to the NAAQS for PM. The principle revisions to the 1971 NAAQS included (1) replacing TSP as the indicator for the ambient standards with a new indicator that includes particles with an aerodynamic diameter less than or equal to a nominal 10  $\mu\text{m}$  ("PM<sub>10</sub>"), (2) replacing the 24-h primary TSP standard with a 24-h PM<sub>10</sub> standard of 150  $\mu\text{g}/\text{m}^3$ , (3) replacing the annual primary TSP standard with an annual PM<sub>10</sub> standard of 50  $\mu\text{g}/\text{m}^3$ , and (4) replacing the secondary TSP standard with 24-h and annual PM<sub>10</sub> standards identical in all respects to the primary standards.

The present PM AQCD has been prepared in accordance with the CAA, requiring the EPA Administrator periodically to review and revise, as appropriate, the criteria and NAAQS for listed criteria pollutants. Emphasis has been placed on the presentation and evaluation of the latest available dosimetric and health effects data; however, other scientific data are also presented to provide information on the nature, sources, size distribution, measurement, and concentrations of PM in the environment and contributions of ambient PM to total human exposure. This document is comprised of three volumes, with the present one (Volume II) containing Chapters 8 through 11.

## PREFACE (cont'd)

This document was prepared by U.S. EPA's National Center for Environmental Assessment-RTP, with assistance by scientists from other EPA Office of Research and Development laboratories (NERL; NHEERL) and non-EPA expert consultants. Several earlier drafts of the document were reviewed by experts from academia, various U.S. Federal and State government units, non-governmental health and environmental organizations, and private industry. Several versions of this AQCD have also been reviewed in public meetings by the Agency's Clean Air Scientific Advisory Committee (CASAC). The National Center for Environmental Assessment (formerly the Environmental Criteria and Assessment Office) of the U.S. EPA's Office of Research and Development acknowledges with appreciation the valuable contributions made by the many authors, contributors, and reviewers, as well as the diligence of its staff and contractors in the preparation of this document.

# Air Quality Criteria for Particulate Matter

## TABLE OF CONTENTS

### Volume I

1. EXECUTIVE SUMMARY .....	1-1
2. INTRODUCTION .....	2-1
3. PHYSICS AND CHEMISTRY OF PARTICULATE MATTER .....	3-1
4. SAMPLING AND ANALYSIS METHODS FOR PARTICULATE MATTER AND ACID DEPOSITION .....	4-1
5. SOURCES AND EMISSIONS OF ATMOSPHERIC PARTICLES .....	5-1
6. ENVIRONMENTAL CONCENTRATIONS .....	6-1
Appendix 6A: Tables of Chemical Composition of Particulate Matter .....	6A-1
7. HUMAN EXPOSURE TO PARTICULATE MATTER: RELATIONS TO AMBIENT AND INDOOR CONCENTRATIONS .....	7-1

### Volume II

8. EFFECTS ON VISIBILITY AND CLIMATE .....	8-1
9. EFFECTS ON MATERIALS .....	9-1
10. DOSIMETRY OF INHALED PARTICLES IN THE RESPIRATORY TRACT .....	10-1
Appendix 10A: Prediction of Regional Deposition in the Human Respiratory Tract Using the International Commission on Radiological Protection Publication 66 Model .....	10A-1
Appendix 10B: Selected Model Parameters .....	10B-1
Appendix 10C: Selected Ambient Aerosol Particle Distributions .....	10C-1
11. TOXICOLOGICAL STUDIES OF PARTICULATE MATTER .....	11-1

# Air Quality Criteria for Particulate Matter

## TABLE OF CONTENTS (cont'd)

### Volume III

12. EPIDEMIOLOGY STUDIES OF HEALTH EFFECTS ASSOCIATED WITH EXPOSURE TO AIRBORNE PARTICLES/ACID AEROSOLS .....	12-1
13. INTEGRATIVE SYNTHESIS OF KEY POINTS: PARTICULATE MATTER EXPOSURE, DOSIMETRY, AND HEALTH RISKS .....	13-1
Appendix 13A: References Used To Derive Cell Ratings in the Text Tables 13-6 and 13-7 for Assessing Qualitative Strength of Evidence for Particulate Matter-Related Health Effects .....	13A-1

## TABLE OF CONTENTS

	<u>Page</u>
LIST OF TABLES .....	II-xiv
LIST OF FIGURES .....	II-xx
AUTHORS, CONTRIBUTORS, AND REVIEWERS .....	II-xxix
U.S. ENVIRONMENTAL PROTECTION AGENCY SCIENCE ADVISORY BOARD, CLEAN AIR SCIENTIFIC ADVISORY COMMITTEE .....	II-xxxv
U.S. ENVIRONMENTAL PROTECTION AGENCY PROJECT TEAM FOR DEVELOPMENT OF AIR QUALITY CRITERIA FOR PARTICULATE MATTER .....	II-xxxix
8. EFFECTS ON VISIBILITY AND CLIMATE .....	8-1
8.1 INTRODUCTION .....	8-1
8.1.1 Background .....	8-1
8.1.2 Definition of Visibility .....	8-3
8.1.3 Human Vision .....	8-4
8.2 FUNDAMENTALS OF ATMOSPHERIC VISIBILITY .....	8-8
8.2.1 Geometry of the Atmosphere .....	8-8
8.2.2 Illumination of the Atmosphere .....	8-9
8.2.3 Optical Properties of the Atmosphere .....	8-11
8.2.4 Multiple Scattering .....	8-15
8.2.5 Transmitted Radiance Versus Path Radiance .....	8-23
8.2.6 Contrast and Contrast Transmittance as Quantitative Measures of Visibility .....	8-26
8.2.7 Contrast Reduction by the Atmosphere .....	8-27
8.2.8 Relation Between Contrast Transmittance and Light Extinction .....	8-33
8.3 OPTICAL PROPERTIES OF PARTICLES .....	8-34
8.3.1 Optical Properties of Spheres .....	8-36
8.3.2 Optical Properties of Fine and Coarse Particles .....	8-42
8.3.3 Effect of Relative Humidity on Particle Size .....	8-44
8.3.4 Extinction Efficiencies and Budgets .....	8-47
8.4 INDICATORS OF VISIBILITY AND AIR QUALITY .....	8-51
8.4.1 Introduction .....	8-51
8.4.2 Visual Range from Human Observation .....	8-53
8.4.3 Light-Extinction Coefficient .....	8-54
8.4.4 Parameters Calculated from the Light Extinction Coefficient .....	8-56
8.4.4.1 Visual Range .....	8-56
8.4.4.2 Deciview Haze Index .....	8-57
8.4.5 Light-Scattering Coefficient Due to Particles .....	8-57
8.4.6 Contrast of Terrain Features .....	8-60
8.4.7 Particulate Matter Concentrations .....	8-61
8.4.8 Measures of Discoloration .....	8-63

TABLE OF CONTENTS (cont'd)

	<u>Page</u>
8.5	VISIBILITY IMPAIRMENT . . . . . 8-64
8.5.1	National Patterns and Trends . . . . . 8-64
8.5.2	Visibility Monitoring . . . . . 8-64
8.5.2.1	Point Versus Sight-Path Measurements . . . . . 8-64
8.5.2.2	Instrumental Monitoring Networks . . . . . 8-65
8.5.3	Recent Observations . . . . . 8-66
8.6	VISIBILITY MODELING . . . . . 8-73
8.6.1	Plume Visibility Models . . . . . 8-74
8.6.2	Regional Haze Models . . . . . 8-75
8.6.3	Photographic Representations of Haze . . . . . 8-79
8.7	ECONOMIC VALUATION OF EFFECTS OF PARTICULATE MATTER ON VISIBILITY . . . . . 8-80
8.7.1	Basic Concepts of Economic Valuation . . . . . 8-80
8.7.2	Economic Valuation Methods for Visibility . . . . . 8-81
8.7.3	Studies of Economic Valuation of Visibility . . . . . 8-82
8.7.3.1	Economic Valuation Studies for Air Pollution Plumes . . . . . 8-82
8.7.3.2	Economic Valuation Studies for Urban Haze . . . . . 8-84
8.8	CLIMATIC EFFECTS . . . . . 8-89
8.8.1	Introduction . . . . . 8-89
8.8.2	Radiative Forcing . . . . . 8-90
8.8.3	Solar Radiative Forcing by Aerosols . . . . . 8-93
8.8.3.1	Modeling Aerosol Direct Solar Radiative Forcing . . . . . 8-97
8.8.3.2	Global Annual Mean Radiative Forcing . . . . . 8-100
8.8.4	Climate Response . . . . . 8-102
8.8.4.1	Early Studies . . . . . 8-102
8.8.4.2	Recent Regional Studies . . . . . 8-104
8.8.4.3	Integrated Global Studies . . . . . 8-106
8.8.5	Aerosol Effects on Clouds and Precipitation . . . . . 8-112
8.8.5.1	Indirect Solar Radiative Forcing . . . . . 8-112
8.8.5.2	Observational Evidence . . . . . 8-116
8.8.5.3	Modeling Indirect Aerosol Forcing . . . . . 8-118
8.9	SUMMARY . . . . . 8-120
8.9.1	Visibility Effects . . . . . 8-120
8.9.2	Climate Change . . . . . 8-126
	REFERENCES . . . . . 8-128
9.	EFFECTS ON MATERIALS . . . . . 9-1
9.1	CORROSION AND EROSION . . . . . 9-1
9.1.1	Factors Affecting Metal Corrosion . . . . . 9-1
9.1.1.1	Moisture . . . . . 9-2
9.1.1.2	Temperature . . . . . 9-5
9.1.1.3	Formation of a Protective Film . . . . . 9-6
9.1.2	Development of a Generic Dose-Response Function . . . . . 9-7

TABLE OF CONTENTS (cont'd)

	<u>Page</u>
9.1.3	Studies on Metals . . . . . 9-8
9.1.3.1	Acid-Forming Aerosols . . . . . 9-8
9.1.3.2	Particles . . . . . 9-15
9.1.4	Paints . . . . . 9-17
9.1.4.1	Acid-Forming Aerosols . . . . . 9-17
9.1.4.2	Particles . . . . . 9-22
9.1.5	Stone and Concrete . . . . . 9-22
9.1.6	Corrosive Effects of Acid-Forming Aerosols and Particles on Other Materials . . . . . 9-30
9.2	SOILING AND DISCOLORATION . . . . . 9-31
9.2.1	Building Materials . . . . . 9-32
9.2.1.1	Fabrics . . . . . 9-34
9.2.1.2	Household and Industrial Paints . . . . . 9-34
9.2.1.3	Soiling of Works of Art . . . . . 9-37
9.3	ECONOMIC ESTIMATES . . . . . 9-37
9.3.1	Methods for Determining Economic Loss from Pollutant Exposure . . . . . 9-38
9.3.2	Economic Loss Associated with Materials Damage and Soiling . . . . 9-40
9.4	SUMMARY . . . . . 9-44
	REFERENCES . . . . . 9-46
10.	DOSIMETRY OF INHALED PARTICLES IN THE RESPIRATORY TRACT . . . . . 10-1
10.1	INTRODUCTION . . . . . 10-1
10.2	CHARACTERISTICS OF INHALED PARTICLES . . . . . 10-6
10.3	ANATOMY AND PHYSIOLOGY OF THE RESPIRATORY TRACT . . . . 10-13
10.4	FACTORS CONTROLLING COMPARATIVE INHALED DOSE . . . . . 10-27
10.4.1	Deposition Mechanisms . . . . . 10-34
10.4.1.1	Gravitational Settling or Sedimentation . . . . . 10-35
10.4.1.2	Inertial Impaction . . . . . 10-36
10.4.1.3	Brownian Diffusion . . . . . 10-38
10.4.1.4	Interception . . . . . 10-39
10.4.1.5	Electrostatic Precipitation . . . . . 10-41
10.4.1.6	Additional Factors Modifying Deposition . . . . . 10-43
10.4.1.7	Comparative Aspects of Deposition . . . . . 10-46
10.4.2	Clearance and Translocation Mechanisms . . . . . 10-52
10.4.2.1	Extrathoracic Region . . . . . 10-53
10.4.2.2	Tracheobronchial Region . . . . . 10-55
10.4.2.3	Alveolar Region . . . . . 10-56
10.4.2.4	Clearance Kinetics . . . . . 10-59
10.4.2.5	Factors Modifying Clearance . . . . . 10-66
10.4.2.6	Comparative Aspects of Clearance . . . . . 10-70
10.4.2.7	Lung Overload . . . . . 10-71
10.4.3	Acidic Aerosols . . . . . 10-73

TABLE OF CONTENTS (cont'd)

	<u>Page</u>
10.4.3.1	Hygroscopicity of Acidic Aerosols . . . . . 10-73
10.4.3.2	Neutralization and Buffering of Acidic Particles . . . . . 10-81
10.5	DEPOSITION DATA AND MODELS . . . . . 10-85
10.5.1	Humans . . . . . 10-85
10.5.1.1	Total Deposition . . . . . 10-86
10.5.1.2	Extrathoracic Deposition . . . . . 10-89
10.5.1.3	Tracheobronchial Deposition . . . . . 10-94
10.5.1.4	Alveolar Deposition . . . . . 10-97
10.5.1.5	Nonuniform Distribution of Deposition and Local Deposition Hot Spots . . . . . 10-99
10.5.1.6	Approaches to Deposition Modeling . . . . . 10-101
10.5.2	Laboratory Animals . . . . . 10-106
10.6	CLEARANCE DATA AND MODELS . . . . . 10-119
10.6.1	Humans . . . . . 10-121
10.6.2	Laboratory Animals . . . . . 10-131
10.6.3	Species Similarities and Differences . . . . . 10-133
10.6.4	Models To Estimate Retained Dose . . . . . 10-140
10.6.4.1	Extrathoracic and Conducting Airways . . . . . 10-142
10.6.4.2	Alveolar Region . . . . . 10-145
10.7	APPLICATION OF DOSIMETRY MODELS TO DOSE-RESPONSE ASSESSMENT . . . . . 10-146
10.7.1	General Considerations for Extrapolation Modeling . . . . . 10-147
10.7.1.1	Model Structure and Parameterization . . . . . 10-148
10.7.1.2	Interspecies Variability . . . . . 10-148
10.7.1.3	Extrapolation of Laboratory Animal Data to Humans . . . . . 10-149
10.7.2	Dosimetry Model Selection . . . . . 10-151
10.7.2.1	Human Model . . . . . 10-151
10.7.2.2	Laboratory Animal Model . . . . . 10-154
10.7.3	Choice of Dose Metrics . . . . . 10-155
10.7.3.1	Interspecies Extrapolation . . . . . 10-156
10.7.4	Choice of Exposure Metrics . . . . . 10-162
10.7.4.1	Human Exposure Data . . . . . 10-162
10.7.4.2	Laboratory Animal Data . . . . . 10-163
10.7.5	Deposited Dose Estimations . . . . . 10-163
10.7.5.1	Human Estimates . . . . . 10-163
10.7.5.2	Laboratory Animal Estimates . . . . . 10-194
10.7.6	Retained Dose Estimates . . . . . 10-199
10.7.6.1	Human Estimates . . . . . 10-199
10.7.6.2	Laboratory Animal Estimates . . . . . 10-204
10.7.7	Summary . . . . . 10-212
REFERENCES	. . . . . 10-218

TABLE OF CONTENTS (cont'd)

	<u>Page</u>
APPENDIX 10A: Prediction of Regional Deposition in the Human Respiratory Tract Using the International Commission on Radiological Protection Publication 66 Model .....	10A-1
APPENDIX 10B: Selected Model Parameters .....	10B-1
APPENDIX 10C: Selected Ambient Aerosol Particle Distributions .....	10C-1
11. TOXICOLOGICAL STUDIES OF PARTICULATE MATTER .....	11-1
11.1 INTRODUCTION .....	11-1
11.2 ACID AEROSOLS .....	11-5
11.2.1 Controlled Human Exposure Studies .....	11-6
11.2.1.1 Introduction .....	11-6
11.2.1.2 Pulmonary Function Effects of Sulfuric Acid in Healthy Subjects .....	11-9
11.2.1.3 Pulmonary Function Effects of Sulfuric Acid in Asthmatic Subjects .....	11-17
11.2.1.4 Effects of Acid Aerosols on Airway Responsiveness .....	11-32
11.2.1.5 Effects of Acid Aerosols on Lung Clearance Mechanisms .....	11-34
11.2.1.6 Effects of Acid Aerosols Studied by Bronchoscopy and Airway Lavage .....	11-36
11.2.1.7 Human Exposure Studies of Acid Aerosol Mixtures .....	11-37
11.2.1.8 Summary and Conclusions .....	11-39
11.2.2 Laboratory Animal Studies .....	11-42
11.2.2.1 Introduction .....	11-42
11.2.2.2 Mortality .....	11-42
11.2.2.3 Pulmonary Mechanical Function .....	11-43
11.2.2.4 Pulmonary Morphology and Biochemistry .....	11-49
11.2.2.5 Pulmonary Defenses .....	11-55
11.2.3 Mixtures Containing Acidic Sulfate Particles .....	11-69
11.3 METALS .....	11-76
11.3.1 Introduction .....	11-76
11.3.2 Arsenic .....	11-77
11.3.3 Cadmium .....	11-82
11.3.3.1 Health Effects .....	11-83
11.3.4 Copper .....	11-85
11.3.5 Iron .....	11-87
11.3.6 Vanadium .....	11-89
11.3.7 Zinc .....	11-92
11.3.8 Transition Metals .....	11-92
11.3.9 Summary .....	11-95

TABLE OF CONTENTS (cont'd)

	<u>Page</u>
11.4	ULTRAFINE PARTICLES . . . . . 11-96
11.5	DIESEL EXHAUST EMISSIONS . . . . . 11-102
	11.5.1 Effects of Diesel Exhaust on Humans . . . . . 11-103
	11.5.2 Effects of Diesel Exhaust on Laboratory Animals . . . . . 11-109
	11.5.3 Species Differences . . . . . 11-120
	11.5.4 Effects of Mixtures Containing Diesel Exhaust . . . . . 11-122
	11.5.5 Particle Effect in Diesel Exhaust Studies . . . . . 11-122
	11.5.6 Gasoline Engine Emissions . . . . . 11-124
	11.5.7 Summary . . . . . 11-125
11.6	SILICA . . . . . 11-126
	11.6.1 Physical and Chemical Properties of Silica . . . . . 11-126
	11.6.2 Health Effects of Silica . . . . . 11-127
	11.6.3 Differences Between Chemical Forms of Silica . . . . . 11-128
	11.6.4 Species Differences . . . . . 11-130
11.7	BIOAEROSOLS . . . . . 11-131
	11.7.1 Types of Health Effects Associated with Bioaerosols . . . . . 11-131
	11.7.1.1 Infections . . . . . 11-131
	11.7.1.2 Hypersensitivity Diseases . . . . . 11-132
	11.7.1.3 Toxicoses . . . . . 11-133
	11.7.2 Ambient Bioaerosols . . . . . 11-134
11.8	TOXICOLOGY OF OTHER PARTICULATE MATTER . . . . . 11-136
	11.8.1 Introduction . . . . . 11-136
	11.8.2 Mortality . . . . . 11-137
	11.8.3 Pulmonary Mechanical Function . . . . . 11-137
	11.8.4 Pulmonary Morphology and Biochemistry . . . . . 11-141
	11.8.5 Pulmonary Defenses . . . . . 11-151
	11.8.5.1 Clearance Function . . . . . 11-151
	11.8.5.2 Resistance to Infectious Disease . . . . . 11-154
	11.8.5.3 Immunologic Defense . . . . . 11-158
	11.8.6 Systemic Effects . . . . . 11-158
	11.8.7 Toxicological Interactions of Other Particulate Matter
	Mixtures . . . . . 11-160
	11.8.7.1 Laboratory Animal Toxicology Studies of
	Particulate Matter Mixtures . . . . . 11-160
	11.8.7.2 Human Studies of Particulate Matter Mixtures
	Other Than Acid Aerosols . . . . . 11-166
11.9	PHYSICOCHEMICAL AND HOST FACTORS INFLUENCING PARTICULATE
	MATTER TOXICITY . . . . . 11-169
	11.9.1 Physicochemical Factors Affecting Particulate Matter
	Toxicity . . . . . 11-169
	11.9.2 Host Factors Affecting Particulate Matter Toxicity . . . . . 11-174

TABLE OF CONTENTS (cont'd)

	<u>Page</u>
11.10 POTENTIAL PATHOPHYSIOLOGICAL MECHANISMS FOR THE EFFECTS OF LOW CONCENTRATIONS OF PARTICULATE POLLUTION .....	11-179
11.10.1 Physiological Mechanisms .....	11-179
11.10.2 Physiological-Particle Interaction .....	11-180
11.10.3 Pathophysiologic Mechanisms .....	11-181
11.11 SUMMARY AND CONCLUSIONS .....	11-185
11.11.1 Acid Aerosols .....	11-185
11.11.2 Metals .....	11-188
11.11.3 Ultrafine Particles .....	11-191
11.11.4 Diesel Emissions .....	11-192
11.11.5 Silica .....	11-193
11.11.6 Bioaerosols .....	11-194
11.11.7 "Other Particulate Matter" .....	11-194
REFERENCES .....	11-196

LIST OF TABLES

<u>Number</u>		<u>Page</u>
8-1	Approximate Distances for Selected Increases in Height of an Initially Horizontal Sight Path . . . . .	8-9
8-2	Relative Importance of Light from Ground, Sky, and Sun in Contributing to the Source Function and the Path Radiance When the Absorption is Negligible and the Normalized Phase Function Has a Value of 0.4 . . . . .	8-22
8-3	Long-Term Visibility and Aerosol Databases . . . . .	8-67
8-4	Short-Term Intensive Visibility and Aerosol Studies . . . . .	8-70
8-5	Economic Valuation Studies for Air Pollution Plumes . . . . .	8-83
8-6	Economic Valuation Studies on Urban Haze . . . . .	8-85
8-7	Radiative Forcing and Climate Statistics . . . . .	8-111
9-1	Annual Average and Maximum Values of the Hourly Averages for Sulfur Dioxide, Nitrogen Oxide, and Ozone and Annual Averages of the Monthly Averages of Rain pH at the Five Material Exposure Sites, Based on Data Acquired During 1986 . . . . .	9-10
9-2	Average Corrosion Rates for 3003-H14 Aluminum Obtained During the National Acid Precipitation Assessment Program Between 1982 and 1987 . . . . .	9-10
9-3	Average Corrosion Rates for Rolled Zinc and Galvanized Steel Obtained During the National Acid Precipitation Assessment Program Field Experiments . . . . .	9-14
9-4	Summary of Measured Parameters in Jacksonville, Florida . . . . .	9-23
10-1	Respiratory Tract Regions . . . . .	10-15
10-2	Architecture of the Human Lung According to Weibel's (1963) Model A, with Regularized Dichotomy . . . . .	10-25
10-3	Morphology, Cytology, Histology, Function, and Structure of the Respiratory Tract and Regions Used in the International Commission on Radiological Protection Publication 66 (1994) Human Dosimetry Model . . . . .	10-28
10-4	Deposition Data for Men and Women . . . . .	10-44
10-5	Interspecies Comparison of Nasal Cavity Characteristics . . . . .	10-49

LIST OF TABLES (cont'd)

<u>Number</u>		<u>Page</u>
10-6	Comparative Lower Airway Anatomy as Revealed on Casts .....	10-50
10-7	Acinar Morphometry .....	10-51
10-8	Overview of Respiratory Tract Particle Clearance and Translocation Mechanisms .....	10-53
10-9	Long-Term Retention of Poorly Soluble Particles in the Alveolar Region of Nonsmoking Humans .....	10-63
10-10	Fraction of Ventilatory Airflow Passing Through the Nose in Human "Normal Augmenter" and "Mouth Breather" .....	10-100
10-11	Regional Fractional Deposition .....	10-111
10-12	Deposition Efficiency Equation Estimated Parameters and 95% Asymptotic Confidence Intervals .....	10-114
10-13	Comparative Alveolar Retention Parameters for Poorly Soluble Particles Inhaled by Laboratory Animals and Humans .....	10-135
10-14	Average Alveolar Retention Parameters for Poorly Soluble Particles Inhaled by Selected Laboratory Animal Species and Humans .....	10-138
10-15	Physical Clearance Rates .....	10-139
10-16	Physical Clearance Rates for Modeling Alveolar Clearance of Particles Inhaled by Selected Mammalian Species .....	10-146
10-17	Hierarchy of Model Structures for Dosimetry and Extrapolation .....	10-149
10-18	Species Comparisons by Miller et al. (1995) of Various Dose Metrics as a Function of Particle Size for 24-Hour Exposures to 150 $\mu\text{g}/\text{m}^3$ .....	10-157
10-19	Daily Mass Deposition of Particles from Aerosol Defined in Figure 10C-1 in the Respiratory Tract of "Normal Augmenter" Adult Male Humans Exposed to a Particle Mass Concentration of 50 $\mu\text{g}/\text{m}^3$ .....	10-164
10-20	Daily Mass Deposition of Particles from Aerosol Defined in Figure 10C-1 in the Respiratory Tract of "Mouth Breather" Adult Male Humans Exposed to a Particle Mass Concentration of 50 $\mu\text{g}/\text{m}^3$ .....	10-165

LIST OF TABLES (cont'd)

<u>Number</u>		<u>Page</u>
10-21	Daily Mass Deposition of Particles from Philadelphia Aerosol Defined in Figure 10C-2a in the Respiratory Tract of "Normal Augmenter" Adult Male Humans Exposed to a Particle Mass Concentration of 50 $\mu\text{g}/\text{m}^3$ . . . . .	10-166
10-22	Daily Mass Deposition of Particles from Philadelphia Aerosol Defined in Figure 10C-2a in the Respiratory Tract of "Mouth Breather" Adult Male Humans Exposed to a Particle Mass Concentration of 50 $\mu\text{g}/\text{m}^3$ . . . . .	10-167
10-23	Daily Mass Deposition of Particles from Phoenix Aerosol Defined in Figure 10C-2b in the Respiratory Tract of "Normal Augmenter" Adult Male Humans Exposed to a Particle Mass Concentration of 50 $\mu\text{g}/\text{m}^3$ . . . . .	10-168
10-24	Daily Mass Deposition of Particles from Phoenix Aerosol Defined in Figure 10C-2b in the Respiratory Tract of "Mouth Breather" Adult Male Humans Exposed to a Particle Mass Concentration of 50 $\mu\text{g}/\text{m}^3$ . . . . .	10-169
10-25	Daily Mass Deposition of Aerosol Particles in the Respiratory Tracts of "Normal Augmenter" and "Mouth Breather" Adult Male Humans Exposed to 50 $\mu\text{g}$ Particles per Cubic Meter . . . . .	10-174
10-26	Extrathoracic Deposition Fractions of Inhaled Monodisperse Aerosols in Rats and Human "Normal Augmenter" and "Mouth Breather" . . . . .	10-195
10-27	Extrathoracic Deposition Fractions of Inhaled Polydisperse Aerosols in Rats and Human "Normal Augmenter" and "Mouth Breather" . . . . .	10-195
10-28	Tracheobronchial Deposition Fractions of Inhaled Monodisperse Aerosols in Rats and Human "Normal Augmenter" and "Mouth Breather" . . . . .	10-195
10-29	Tracheobronchial Deposition Fractions of Inhaled Polydisperse Aerosols in Rats and Human "Normal Augmenter" and "Mouth Breather" . . . . .	10-196
10-30	Alveolar Deposition Fractions of Inhaled Monodisperse Aerosols in Rats and Human "Normal Augmenter" and "Mouth Breather" . . . . .	10-196
10-31	Alveolar Deposition Fractions of Inhaled Polydisperse Aerosols in Rats and Human "Normal Augmenter" and "Mouth Breather" . . . . .	10-196
10-32	Predicted Relative Particle Mass in Lungs of Adult Male "Normal Augmenter" Exposed Chronically to Phoenix Trimodel Aerosol Versus Philadelphia Trimodal Aerosol . . . . .	10-202

LIST OF TABLES (cont'd)

<u>Number</u>		<u>Page</u>
10-33	Fraction of Inhaled Particles Deposited in the Alveolar Region of the Respiratory Tract for Rats and Adult Male Humans . . . . .	10-204
10-34	Fraction of Inhaled Particles Deposited in the Alveolar Region of the Respiratory Tract for Different Demographic Groups . . . . .	10-205
10-35	Particle Deposition Rates in the Alveolar Region . . . . .	10-205
10-36	Summary of Common and Specific Inhalation Exposure Parameters Used for Predicting Alveolar Burdens of Particles Inhaled by Rats and Humans . . . . .	10-206
10-37	Alveolar Particle Burdens of Exposure to 50 $\mu\text{g}/\text{m}^3$ of 1.0- $\mu\text{m}$ Mass Median Aerodynamic Diameter Aerosol, Assuming Particle Dissolution-Absorption Half-Time of 10, 100, or 1,000 Days . . . . .	10-207
10-38	Alveolar Particle Burdens of Exposure to 50 $\mu\text{g}/\text{m}^3$ of 2.55- $\mu\text{m}$ Mass Median Aerodynamic Diameter Aerosol, Assuming Particle Dissolution-Absorption Half-Time of 10, 100, or 1,000 Days . . . . .	10-208
10B-1a	Body Weight and Respiratory Tract Region Surface Areas . . . . .	10B-2
10B-1b	Human Activity Patterns and Associated Respiratory Minute Ventilation . . . . .	10B-2
10B-2	Body Weights, Lung Weights, Respiratory Minute Ventilation, and Respiratory Tract Region Surface Area for Selected Laboratory Animal Species . . . . .	10B-3
10C-1	Distribution of Particle Count, Surface Area, or Mass in the Trimodal Polydisperse Aerosol Defined in Figure 10C-1 . . . . .	10C-3
10C-2a	Distribution of Particle Number in the Trimodal Polydisperse Aerosol Defined in Figure 10C-1 . . . . .	10C-4
10C-2b	Distribution of Particle Surface Area in the Trimodal Polydisperse Aerosol Defined in Figure 10C-1 . . . . .	10C-6
10C-2c	Distribution of Particle Mass in the Trimodal Polydisperse Aerosol Defined in Figure 10C-1 . . . . .	10C-8
10C-3	Distribution of Particle Count, Surface Area, or Mass in the Trimodal Polydisperse Aerosol for Philadelphia Defined in Figure 10-C-2a . . . . .	10C-11

LIST OF TABLES (cont'd)

<u>Number</u>		<u>Page</u>
10C-4a	Distribution of Particle Number in the Trimodal Polydisperse Philadelphia Aerosol Defined in Figure 10C-2a .....	10C-12
10C-4b	Distribution of Particle Surface Area in the Trimodal Polydisperse Philadelphia Aerosol Defined in Figure 10C-2a .....	10C-14
10C-4c	Distribution of Particle Mass in the Trimodal Polydisperse Philadelphia Aerosol Defined in Figure 10C-2a .....	10C-16
10C-5	Distribution of Particle Count, Surface Area, or Mass in the Trimodal Polydisperse Aerosol for Phoenix Defined in Figure 10C-2b .....	10C-18
10C-6a	Distribution of Particle Number in the Trimodal Polydisperse Phoenix Aerosol Defined in Figure 10C-2b .....	10C-19
10C-6b	Distribution of Particle Surface Area in the Trimodal Polydisperse Phoenix Aerosol Defined in Figure 10C-2b .....	10C-21
10C-6c	Distribution of Particle Mass in the Trimodal Polydisperse Phoenix Aerosol Defined in Figure 10C-2b .....	10C-23
11-1	Numbers and Surface Areas of Monodisperse Particles of Unit Density of Different Sizes at a Mass Concentration of $10 \mu\text{g}/\text{m}^3$ .....	11-4
11-2	Controlled Human Exposures to Acid Aerosols and Other Particles .....	11-10
11-3	Asthma Severity in Studies of Acid Aerosols and Other Particles .....	11-18
11-4	Pulmonary Function Responses After Aerosol and Ozone Exposures in Subjects with Asthma .....	11-40
11-5	Effects of Acidic Sulfate Particles on Pulmonary Mechanical Function .....	11-45
11-6	Effects of Acidic Sulfate Particles on Respiratory Tract Morphology .....	11-50
11-7	Effects of Acidic Sulfate Particles on Respiratory Tract Clearance .....	11-57
11-8	Effects of Acid Sulfates on Bacterial Infectivity in Vivo .....	11-68
11-9	Toxicologic Effects of Mixtures Containing Acidic Aerosols .....	11-71
11-10	Respiratory System Effects of Inhaled Metals on Humans and Laboratory Animals .....	11-78

LIST OF TABLES (cont'd)

<u>Number</u>		<u>Page</u>
11-11	Human Studies of Diesel Exhaust Exposure . . . . .	11-105
11-12	Short-Term Effects of Diesel Exhaust on Laboratory Animals . . . . .	11-110
11-13	Effects of Chronic Exposures to Diesel Exhaust on Survival and Growth of Laboratory Animals . . . . .	11-112
11-14	Effects of Diesel Exhaust on Pulmonary Function of Laboratory Animals . . . . .	11-113
11-15	Histopathological Effects of Diesel Exhaust in the Lungs of Laboratory Animals . . . . .	11-114
11-16	Effects of Exposure to Diesel Exhaust on the Pulmonary Defense Mechanisms of Laboratory Animals . . . . .	11-117
11-17	Comparative Inhalation Toxicity Studies with Different Silica Polymorphs . . . . .	11-129
11-18	Effects of Particulate Matter on Mortality . . . . .	11-138
11-19	Effects of Inhaled Particulate Matter on Pulmonary Mechanical Function . . . . .	11-139
11-20	Effects of Particulate Matter on Respiratory Tract Morphology . . . . .	11-144
11-21	Effects of Particulate Matter on Markers in Lavage Fluid . . . . .	11-148
11-22	Effects of Particulate Matter on Lung Biochemistry . . . . .	11-150
11-23	Effects of Particulate Matter on Alveolar Macrophage Function . . . . .	11-152
11-24	Effects of Particulate Matter on Microbial Infectivity . . . . .	11-155
11-25	Effects of Particulate Matter on Respiratory Tract Immune Function . . . . .	11-159
11-26	Toxicologic Interactions to Mixtures Containing Non-Acid Aerosol Particles . . . . .	11-163
11-27	Controlled Human Exposure Studies of Particulate Matter Mixtures Other Than Acid Aerosols . . . . .	11-167

## LIST OF FIGURES

<u>Number</u>		<u>Page</u>
8-1	Diagrams showing the definitions of contrast and modulation . . . . .	8-6
8-2	Spectrum of direct solar rays at the top of the atmosphere and at the surface of the earth for various values of the air mass . . . . .	8-10
8-3	The approach of radiances in the atmosphere to the equilibrium radiance or source function . . . . .	8-17
8-4	Data for the ratio of the total flux of skylight $F_{\text{incident}}$ of the earth's to the solar flux $F_0 \cos\theta$ on a horizontal surface at the top of the atmosphere . . . . .	8-20
8-5	Illustration of the transmitted radiance and the path radiance for a sight path toward a hillside . . . . .	8-24
8-6	Nomograms for the estimation of the contrast transmittance in a uniform region of the atmosphere and in a nonuniform atmosphere . . . . .	8-31
8-7	Hour-average values of the modulation transfer and transmittance measured in a 2.20-km sight path during the 1987 summer intensive of the Southern California Air Quality Study . . . . .	8-35
8-8a	Light-scattering efficiency factor for a homogeneous sphere with an index of refraction of 1.50 as a function of the size parameter $\alpha = \pi D/\lambda$ . . . . .	8-37
8-8b	Maximum and minimum values for light-scattering efficiency factors for homogeneous spheres with indices between 1.33 and 1.50 as a function of the normalized size parameter . . . . .	8-38
8-9	Volume-specific light-scattering efficiency as a function of particle diameter $D_p$ . . . . .	8-39
8-10	Volume-specific light-scattering efficiency as a function of geometric mean particle diameter $D_{gv}$ for log-normal size distributions . . . . .	8-41
8-11	Humidogram showing the dependence of the light-scattering coefficient of ambient aerosol on the relative humidity . . . . .	8-45
8-12	Relative size growth is shown as a function of relative humidity for an ammonium sulfate particle at 25° C . . . . .	8-46

LIST OF FIGURES (cont'd)

<u>Number</u>		<u>Page</u>
8-13	Summary of all relative humidity-dependent particle growth factors for 0.2- $\mu\text{m}$ diameter particles measured in Claremont, California, during the Southern California Air Quality Study and at Hopi Point in the Grand Canyon National Park during the Navajo Generating Station Visibility Study . . . . .	8-48
8-14	Hypothetical curves showing the effect of nonlinearities on the mass-specific light-scattering efficiency . . . . .	8-52
8-15	Changes in radiative forcing due to increases in greenhouse gas concentrations between 1765 and 1990 . . . . .	8-91
8-16	A schematic diagram showing the relationship between the radiative forcing of sulfate aerosols and climate response . . . . .	8-93
8-17	Extinction of direct solar radiation by aerosols showing the diffusely transmitted and reflected components, as well as the absorbed components . . . . .	8-94
8-18	Global, direct, and diffuse spectral solar irradiance on a horizontal surface for a solar zenith angle of $60^\circ$ and ground reflectance of 0.2 . . . . .	8-96
8-19	Surface measurements of direct, diffuse, and global solar radiation expressed as illuminance, at Albany, New York, on August 23, 1992, and August 26, 1993 . . . . .	8-98
8-20	Single scattering albedo of monodispersed spherical aerosols of varying radius and three different refractive indices at a wavelength of $0.63 \mu\text{m}$ . . . . .	8-99
8-21a	Annual mean direct radiative forcing resulting from anthropogenic sulfate aerosols . . . . .	8-108
8-21b	Annual mean direct radiative forcing resulting from anthropogenic and natural sulfate aerosols . . . . .	8-108
8-22a	Annual averaged greenhouse gas radiative forcing from increases in carbon dioxide, methane, nitrous oxide, and chlorfluorocarbons 11 and 12, from preindustrial time to the present . . . . .	8-110
8-22b	Annual averaged greenhouse gas forcing plus anthropogenic sulfate aerosol forcing . . . . .	8-110

LIST OF FIGURES (cont'd)

<u>Number</u>		<u>Page</u>
8-23	Schematic illustration of the difference between response times of climate forcing due to carbon dioxide (heating) and sulfate (cooling) during different patterns of global fossil fuel consumption . . . . .	8-113
9-1	Empirical relationship between average relative humidity and fraction of time when a zinc sheet specimen is wet . . . . .	9-4
9-2	Geographic distribution of paint soiling costs . . . . .	9-42
10-1	Schematic characterization of comprehensive exposure-dose-response continuum and the evolution of protective to predictive dose-response estimates . . . . .	10-2
10-2	Biological marker components in sequential progression between exposure and disease . . . . .	10-4
10-3	Lognormal particle size distribution for a hypothetical polydisperse aerosol . . . . .	10-9
10-4	These normalized plots of number, surface, and volume (mass) distributions from Whitby (1975) show a bimodal mass distribution in a smog aerosol . . . . .	10-11
10-5	Diagrammatic representation of respiratory tract regions in humans . . . . .	10-16
10-6	Schematic representation of five major mechanisms causing particle deposition . . . . .	10-17
10-7	Lung volumes and capacities . . . . .	10-23
10-8	Estimated tracheobronchial deposition in the rat lung, via the trachea, with no interceptional deposition . . . . .	10-40
10-9	Deposition increment data versus particle electronic charge for three particle diameters at 0.3, 0.6, and 1.0 $\mu\text{m}$ . . . . .	10-42
10-10	Total deposition data in children with or during spontaneous breathing as a function of particle diameter . . . . .	10-45
10-11	Calculated mass deposition from polydisperse aerosols of unit density with various geometric standard deviations as a function of mass median diameter for quiet breathing . . . . .	10-47

LIST OF FIGURES (cont'd)

<u>Number</u>		<u>Page</u>
10-12	Major physical clearance pathways from the extrathoracic region and tracheobronchial tree . . . . .	10-54
10-13	Diagram of known and suspected clearance pathways for poorly soluble particles depositing in the alveolar region . . . . .	10-54
10-14	Regional deposition data in rats versus particle size for sulfuric acid mists and dry particles . . . . .	10-75
10-15	Theoretical growth curves for sodium chloride, sulfuric acid, ammonium bisulfate, and ammonium sulfate aerosols in terms of the initial and final size of the particle . . . . .	10-76
10-16	Regional deposition of hygroscopic sulfuric acid and control iron oxide particles at quiet breathing in the human lung as a function of subject age . . . . .	10-77
10-17	Distinctions in growth of aqueous ammonium sulfate droplets of 0.1 and 1.0 $\mu\text{m}$ initial size are depicted as a function of their initial solute concentrations . . . . .	10-78
10-18	The initial diameter of dry sodium chloride particles and equilibrium diameter achieved are shown for three relative humidity assumptions . . . . .	10-79
10-19	The initial dry diameter of three different salts is assumed to be 1.0 $\mu\text{m}$ . . . . .	10-80
10-20	Total deposition data (percentage deposition of amount inhaled) in humans as a function of particle size . . . . .	10-87
10-21	Total deposition as a function of the diameter of unit density spheres in humans for variable tidal volume and breathing frequency . . . . .	10-88
10-22	Inspiratory deposition of the human nose as a function of particle aerodynamic diameter and flow rate . . . . .	10-91
10-23	Inspiratory extrathoracic deposition data in humans during mouth breathing as a function of particle aerodynamic diameter, flow rate, and tidal volume . . . . .	10-92
10-24	Inspiratory deposition efficiency data and fitted curve for human nasal casts plotted versus $Q^{-1/8}D^{1/2} (\text{Lmin}^{-1})^{-1/8}(\text{cm}^2\text{s}^{-1})^{1/2}$ . . . . .	10-93

LIST OF FIGURES (cont'd)

<u>Number</u>		<u>Page</u>
10-25	Inspiratory deposition efficiency data in human oral casts plotted versus flow rate and particle diffusion coefficient . . . . .	10-95
10-26	Tracheobronchial deposition data in humans at mouth breathing as a function of particle aerodynamic diameter . . . . .	10-97
10-27	Alveolar deposition data in humans as a function of particle aerodynamic diameter . . . . .	10-98
10-28	Percentage of total ventilatory airflow passing through the nasal route in human "normal augmenter" and in habitual "mouth breather" . . . . .	10-100
10-29	Local deposition pattern in a bifurcating tube for inhalation and exhalation . . . . .	10-102
10-30	Regional deposition fraction in laboratory animals as a function of particle size . . . . .	10-107
10-31	Regional deposition efficiency in the rat extrathroacic region versus an impaction parameter as predicted by the model of Ménache et al. (1996) . . . . .	10-113
10-32	Comparison of regional deposition efficiencies and fractions for the rat . . . . .	10-116
10-33	Experimental deposition fraction data and predicted estimates using model of Ménache et al. (1996) . . . . .	10-120
10-34	Schematic of the International Commission on Radiological Protection Publication 66 (1994) model . . . . .	10-125
10-35	Comparison of regional deposition fractions predicted by the proposed National Council on Radiation Protection model with those of the International Commission on Radiological Protection Publication 66 (1994) model . . . . .	10-128
10-36	Comparison of regional deposition fractions predicted by the proposed National Council on Radiation Protection model with those of the International Commission on Radiological Protection Publication 66 (1994) model . . . . .	10-129

LIST OF FIGURES (cont'd)

<u>Number</u>		<u>Page</u>
10-37	Comparison of regional deposition fractions predicted by the proposed National Council on Radiation Protection model with those of the International Commission on Radiological Protection Publication 66 (1994) model . . . . .	10-130
10-38	Compartments of the simulation model used to predict alveolar burdens of particles acutely inhaled by mice, hamsters, rats, guinea pigs, monkeys, and dogs . . . . .	10-132
10-39	Schematic showing integration of inhalability with deposition efficiency functions . . . . .	10-171
10-40	Daily mass deposition in tracheobronchial and alveolar regions for normal augmenter versus mouth breather adult males using International Commission on Radiological Protection Publication 66 (1994) minute volume activity patterns . . . . .	10-172
10-41	Daily mass deposition in tracheobronchial and alveolar regions for normal augmenter versus mouth breather adult males using International Commission on Radiological Protection Publication 66 (1994) minute volume activity patterns . . . . .	10-173
10-42	Deposition fraction in each respiratory tract region as predicted by the International Commission on Radiological Protection Publication 66 (1994) model . . . . .	10-177
10-43	Daily mass particle deposition rates for 24-hour exposure at 50 $\mu\text{g}/\text{m}^3$ in each respiratory tract region as predicted by the International Commission on Radiological Protection Publication 66 (1994) model . . . . .	10-178
10-44	Respiratory tract deposition fractions and $\text{PM}_{10}$ sampler collection versus mass median aerodynamic diameter with two different geometric standard deviations . . . . .	10-181
10-45	Respiratory tract deposition fractions and $\text{PM}_{10}$ or $\text{PM}_{2.5}$ sampler collection versus mass median aerodynamic diameter with two different geometric standard deviations . . . . .	10-182
10-46	Respiratory tract deposition fractions and $\text{PM}_{10}$ or $\text{PM}_{2.5}$ sampler collection fractions versus mass median aerodynamic diameter with two different geometric standard deviations . . . . .	10-183

LIST OF FIGURES (cont'd)

<u>Number</u>		<u>Page</u>
10-47	Schematic illustration of how ambient aerosol distribution data were integrated with respiratory tract deposition efficiency or sampler efficiency to calculate deposition in respiratory tract regions or mass collected by sampler . . . . .	10-185
10-48	Mass deposition fraction in normal augmenter versus mouth breather adult male with a general population minute volume activity pattern predicted by the International Commission on Radiological Protection Publication 66 (1994) model and the mass collected by PM <sub>10</sub> or PM <sub>2.5</sub> samplers for Philadelphia aerosol . . . . .	10-186
10-49	Mass deposition fraction in normal augmenter versus mouth breather adult male with a general population minute volume activity pattern predicted by the International Commission on Radiological Protection Publication 66 (1994) model and the mass collected by PM <sub>10</sub> or PM <sub>2.5</sub> samplers for Phoenix aerosol . . . . .	10-187
10-50	Fractional number deposition in each respiratory tract region for normal augmenter versus mouth breather adult male with a general population activity pattern as predicted by the International Commission on Radiological Protection Publication 66 (1994) model for an exposure to the Philadelphia aerosol . . . . .	10-188
10-51	Number of particles deposited per day in each respiratory tract region for normal augmenter versus mouth breather adult male with a general population activity pattern predicted by the International Commission on Radiological Protection Publication 66 (1994) model for an exposure to the Philadelphia aerosol at a concentration of 50 $\mu\text{g}/\text{m}^3$ . . . . .	10-189
10-52	Fractional number deposition in normal augmenter versus mouth breather adult male with a general population activity pattern predicted by the International Commission on Radiological Protection Publication 66 (1994) model for an exposure to the Phoenix aerosol . . . . .	10-191
10-53	Number of particles deposited per day in each respiratory tract region for normal augmenter versus mouth breather adult male with a general population activity pattern predicted by the International Commission on Radiological Protection Publication 66 (1994) model for an exposure to the Phoenix aerosol at a concentration of 50 $\mu\text{g}/\text{m}^3$ . . . . .	10-192
10-54	Predicted extrathoracic deposition fractions versus mass median aerodynamic diameter of inhaled monodisperse aerosols or polydisperse aerosols for humans and rats for the extrathoracic region, the tracheobronchial region, and the alveolar region . . . . .	10-197

LIST OF FIGURES (cont'd)

<u>Number</u>		<u>Page</u>
10-55	Particle mass retained in the lung versus time predicted by the International Commission on Radiological Protection Publication 66 (1994) model, assuming dissolution-absorption half-times of 10, 100, and 1,000 days for the accumulation, intermodal, and coarse modes, respectively, of continuous exposures to Philadelphia and Phoenix aerosols at $50 \mu\text{g}/\text{m}^3$ . . . . .	10-201
10-56	Specific lung burden versus time predicted by the International Commission on Radiological Protection Publication 66 (1994) model, assuming dissolution-absorption half-times of 10, 100, and 1,000 days for the accumulation, intermodal, and coarse modes, respectively, of continuous exposures to Philadelphia and Phoenix aerosols at $50 \mu\text{g}/\text{m}^3$ . . . . .	10-203
10-57	Predicted retained alveolar dose in normal augmenter human or in a rat for exposure at $50 \mu\text{g}/\text{m}^3$ to $1.0\text{-}\mu\text{m}$ mass median aerodynamic diameter monodisperse aerosol, assuming a dissolution-absorption half-time of 10, 100, or 1,000 days . . . . .	10-210
10-58	Predicted retained alveolar dose in a normal augmenter human or in a rat for exposure at $50 \mu\text{g}/\text{m}^3$ to $2.55\text{-}\mu\text{m}$ mass median aerodynamic diameter polydisperse aerosol, assuming a dissolution-absorption half-time of 10, 100, or 1,000 days . . . . .	10-211
10-59	Predicted alveolar region retained dose ratios in rats versus humans for chronically inhaled exposure at $50 \mu\text{g}/\text{m}^3$ to $1.0\text{-}\mu\text{m}$ mass median aerodynamic diameter (MMAD) monodisperse and $2.55\text{-}\mu\text{m}$ MMAD polydisperse aerosols, assuming a dissolution-absorption half-time of 10, 100, or 1,000 days . . . . .	10-213
10A-1	Nasal deposition efficiency measured in adult Caucasian males during normal breathing and data on extrathoracic deposition when particles are inhaled and exhaled through a mouthpiece . . . . .	10A-5
10A-2	Comparisons of the "fast cleared" fraction of lung deposition measured at the GSF Frankfurt Laboratory with the tracheobronchiolar deposition predicted by the theoretical model of Egan et al. (1989) . . . . .	10A-8
10A-3	Comparisons of the "slow cleared" fraction of lung deposition measured at the GSF Frankfurt Laboratory with the alveolar deposition predicted by the theoretical model of Egan et al. (1989) . . . . .	10A-9

LIST OF FIGURES (cont'd)

<u>Number</u>		<u>Page</u>
10A-4	Comparison of fractional deposition measured by Foord et al. (1978) and Emmett and Aitken (1982) in different subjects with values given by the International Commission on Radiological Protection Publication 66 (1994) lung model . . . . .	10A-12
10A-5	Comparison of total respiratory tract deposition of submicron-sized alumino-silicate particles measured by Tu and Knutson (1984) in two subjects, with the values calculated as a function of particle diameter by Egan et al. (1989) . . . . .	10A-14
10A-6	Comparison of the distributions of total respiratory tract deposition measured in 20 different subjects breathing spontaneously at rest or breathing at a controlled rate at rest . . . . .	10A-15
10A-7	Experimental data on deposition efficiency of the tracheobronchial region and fractional deposition in the alveolar region for the large group of subjects studied at New York University . . . . .	10A-17
10B-1	Daily minute volume pattern for male demographic groups . . . . .	10B-4
10B-2	Daily minute volume pattern for female demographic groups . . . . .	10B-5
10B-3	Daily minute volume pattern for demographic groups for children . . . . .	10B-6
10C-1	An example of histogram display and fitting to log-normal functions for particle-counting size distribution data . . . . .	10C-2
10C-2	Impactor size distribution measurement generated by Lundgen et al. with the Wide Range Aerosol Classifier: Philadelphia and Phoenix . . . . .	10C-10
11-1	Mean plus or minus standard error of the mean specific airway resistance before and after a 16-minute exposure for nine subjects who inhaled low relative-humidity (RH) sodium chloride (NaCl), low-RH sulfuric acid (H <sub>2</sub> SO <sub>4</sub> ), and high-RH H <sub>2</sub> SO <sub>4</sub> aerosols at rest, and six subjects who inhaled low-RH NaCl and low-RH H <sub>2</sub> SO <sub>4</sub> aerosols during exercise . . . . .	11-29
11-2	Decrements in forced expiratory volume in one second following 6.5-hour exposures on two successive days . . . . .	11-38
11-3	Asthmatic subjects . . . . .	11-41

## AUTHORS, CONTRIBUTORS, AND REVIEWERS

### CHAPTER 8. EFFECTS ON VISIBILITY AND CLIMATE

#### *Principal Authors*

Dr. Harshvardhan—Purdue University, Department of Earth and Atmospheric Sciences,  
W. Lafayette, IN 47907-1397

Dr. Willard Richards—Sonoma Technology, Inc., 5510 Skyline Blvd., Santa Rosa, CA 95403

#### *Contributors and Reviewers*

Dr. Michael A. Berry—National Center for Environmental Assessment (MD-52),  
U.S. Environmental Protection Agency, Research Triangle Park, NC 27711

Ms. Beverly Comfort—National Center for Environmental Assessment (MD-52),  
U.S. Environmental Protection Agency, Research Triangle Park, NC 27711

Dr. Adarsh Deepak—Science and Technology, 101 Research Drive, Hampton, VA 23666

Dr. Derrick Montaque—University of Wyoming, Department of Atmospheric Sciences,  
P.O. Box 3038, University Station, Laramie, WY 82071

Dr. Joseph P. Pinto—National Center for Environmental Assessment (MD-52),  
U.S. Environmental Protection Agency, Research Triangle Park, NC 27711

Dr. Joseph Sickles—National Exposure Research Laboratory (MD-80A), U.S. Environmental  
Protection Agency, Research Triangle Park, NC 27711

Dr. William E. Wilson—National Center for Environmental Assessment (MD-52),  
U.S. Environmental Protection Agency, Research Triangle Park, NC 27711

### CHAPTER 9. EFFECTS ON MATERIALS

#### *Principal Authors*

Ms. Beverly Comfort—National Center for Environmental Assessment (MD-52),  
U.S. Environmental Protection Agency, Research Triangle Park, NC 27711

Mr. Fred Haynie—300 Oak Ridge Road, Cary, NC 27511

## AUTHORS, CONTRIBUTORS, AND REVIEWERS (cont'd)

### *Contributors and Reviewers*

Dr. Michael A. Berry—National Center for Environmental Assessment (MD-52),  
U.S. Environmental Protection Agency, Research Triangle Park, NC 27711

Dr. Edward Edney—National Exposure Research Laboratory (MD-84), U.S. Environmental  
Protection Agency, Research Triangle Park, NC 27711

Dr. Douglas Murray—TRC Environmental Corporation, 5 Waterside Crossing, Windsor,  
CT 06095

Dr. John Spence—National Exposure Research Laboratory (MD-75), U.S. Environmental  
Protection Agency, Research Triangle Park, NC 27711

Dr. John Yocom—Environmental Consultant, 12 Fox Den Road, West Simsbury, CT 06092

## CHAPTER 10. DOSIMETRY OF INHALED PARTICLES IN THE RESPIRATORY TRACT

### *Principal Authors*

Dr. Anthony C. James—ACJ and Associates, 129 Patton Street, Richland, WA 99352-1618

Ms. Annie M. Jarabek—National Center for Environmental Assessment (MD-52),  
U.S. Environmental Protection Agency, Research Triangle Park, NC 27711

Dr. Paul E. Morrow—University of Rochester Medical Center, School of Medicine and  
Dentistry, Rochester, NY 14614

Dr. Richard B. Schlesinger—New York University, Department of Environmental Medicine,  
550 First Avenue, New York, NY 10016

Dr. Morris Burton Snipes—Inhalation Toxicology Research Institute, Lovelace Biomedical and  
Environmental Research Institute, Albuquerque, NM 87185-5890

Dr. C.P. Yu—State University of New York, Department of Mechanical and Aerospace  
Engineering, Buffalo, NY 14260-4400

AUTHORS, CONTRIBUTORS, AND REVIEWERS (cont'd)

*Contributors and Reviewers*

Dr. William J. Bair—Battelle, Pacific Northwest Laboratories, K1-50, P.O. Box 999, Richland, WA 99352

Dr. Lawrence J. Folinsbee—National Center for Environmental Assessment (MD-52), U.S. Environmental Protection Agency, Research Triangle Park, NC 27711

Dr. Timothy R. Gerrity—Veterans Administration, Acting Deputy Director, Medical Research, 810 Vermont Avenue, NW, Washington, DC 20420

Dr. Judith A. Graham—National Exposure Research Laboratory (MD-75), U.S. Environmental Protection Agency, Research Triangle Park, NC 27711

Dr. Raymond A. Guilmette—Inhalation Toxicology Research Institute, Lovelace Biomedical and Environmental Research Institute, Inc., P.O. Box 5890, Albuquerque, NM 87185

Dr. F. Charles Hiller—University of Arkansas for Medical Science, 4301 W. Markham, Little Rock, AR 72212

Dr. Wolfgang G. Kreyling—GSF, Institute for Inhalation Biology, Ganghoferstr, 40 Unterschleissheit, Germany D-85716

Dr. Ted Martonen—National Health and Environmental Effects Research Laboratory (MD-74), U.S. Environmental Protection Agency, Research Triangle Park, NC 27711

Ms. Margaret G. Menache—Duke University Medical Center, Center for Extrapolation Modeling, P.O. Box 3210, First Union Plaza/Suite B-200, Durham, NC 27710

Dr. Gunter Oberdörster—University of Rochester, Department of Environmental Medicine, 575 Elmwood Avenue, Rochester, NY 14642

Dr. Robert F. Phalen—University of California—Irvine, Department of Community and Environmental Medicine, Air Pollution Health Effects Laboratory, Irvine, CA 92717-1825

Dr. Otto G. Raabe—University of California—Davis, Institute of Toxicology and Environmental Health, Old Davis Road, Davis, CA 95616

Dr. Sid Söderholm—National Institute for Occupational Safety and Health, 1095 Willowdale Road, Morgantown, WV 26505

Dr. Magnus Svartengren—Karolinska Institute of Huddinge University Hospital, Department of Occupational Medicine, S-141 86 Hugginge, Sweden

AUTHORS, CONTRIBUTORS, AND REVIEWERS (cont'd)

CHAPTER 11. TOXICOLOGICAL STUDIES OF PARTICULATE MATTER

*Principal Authors*

Dr. Lawrence J. Folinsbee—National Center for Environmental Assessment (MD-52),  
U.S. Environmental Protection Agency, Research Triangle Park, NC 27711

Dr. Mark Frampton—University of Rochester Medical Center, Pulmonary Disease Unit,  
601 Elmwood Avenue, Rochester, NY 14642-8692

Dr. Rogene Henderson—Lovelace Biomedical and Environmental Research Institute,  
Inhalation Toxicology Research Institute, Albuquerque, NM 87105

Ms. Annie M. Jarabek—National Center for Environmental Assessment (MD-52),  
U.S. Environmental Protection Agency, Research Triangle Park, NC 27711

Dr. James McGrath—National Center for Environmental Assessment (MD-52),  
U.S. Environmental Protection Agency, Research Triangle Park, NC 27711

Dr. Gunter Oberdörster—University of Rochester, Department of Environmental Medicine, 575  
Elmwood Avenue, Rochester, NY 14642

Dr. Richard B. Schlesinger—New York University, Department of Environmental Medicine,  
550 First Avenue, New York, NY 10016

Dr. David B. Warheit—Haskell Laboratory, E.I. Du Pont de Nemours, P.O. Box 50, Elkton  
Road, Newark, DE 19714

*Contributors and Reviewers*

Dr. Daniel L. Costa—National Health and Environmental Effects Research Laboratory  
(MD-82), U.S. Environmental Protection Agency, Research Triangle Park, NC 27711

Dr. Kevin E. Driscoll—The Miami Valley Laboratories, Procter & Gamble Company, P.O. Box  
538707, Cincinnati, OH 45253-8707

Dr. Don Dungworth—6260 Cape George Road, Port Townsend, WA 98368

Dr. Gary Foureman—National Center for Environmental Assessment (MD-52),  
U.S. Environmental Protection Agency, Research Triangle Park, NC 27711

Dr. Donald Gardner—P.O. Box 97605, Raleigh, NC 27624-7605

AUTHORS, CONTRIBUTORS, AND REVIEWERS (cont'd)

*Contributors and Reviewers (cont'd)*

Dr. Andy Ghio—Duke University Medical Center, Division of Pulmonary Medicine and Critical Care Medicine, P.O. Box 3177, Durham, NC 27710

Dr. Jeff Gift—National Center for Environmental Assessment (MD-52), U.S. Environmental Protection Agency, Research Triangle Park, NC 27711

Dr. Judith A. Graham—National Exposure Research Laboratory (MD-75), U.S. Environmental Protection Agency, Research Triangle Park, NC 27711

Dr. Lester D. Grant—National Center for Environmental Assessment (MD-52), U.S. Environmental Protection Agency, Research Triangle Park, NC 27711

Dr. Daniel Guth—National Center for Environmental Assessment (MD-52), U.S. Environmental Protection Agency, Research Triangle Park, NC 27711

Dr. Jack Harkema—Michigan State University, Department of Pathology, College of Veterinary Medicine, Veterinary Medical Center, East Lansing, MI 48824

Dr. Gary Hatch—National Health and Environmental Effects Research Laboratory (MD-82), U.S. Environmental Protection Agency, Research Triangle Park, NC 27711

Dr. Michael T. Kleinman—University of California—Irvine, Department of Community and Environmental Medicine, Irvine, CA 92717-1825

Dr. Dennis Kotchmar—National Center for Environmental Assessment (MD-52), U.S. Environmental Protection Agency, Research Triangle Park, NC 27711

Dr. Gunter Oberdörster—University of Rochester, Department of Environmental Medicine 575 Elmwood Avenue, Rochester, NY 14642

Dr. MaryJane Selgrade—National Health and Environmental Effects Research Laboratory (MD-92), U.S. Environmental Protection Agency, Research Triangle Park, NC 27711

Dr. Jeff Tepper—Genetech, Inc., Pulmonary Research, 460 Point San Bruno Boulevard, South San Francisco, CA 94080-4990

Dr. Hanspeter Witschi—University of California—Davis, Laboratory for Energy-Related Health Research, Davis, CA 95616



U.S. ENVIRONMENTAL PROTECTION AGENCY  
SCIENCE ADVISORY BOARD  
CLEAN AIR SCIENTIFIC ADVISORY COMMITTEE

PARTICULATE MATTER CRITERIA DOCUMENT REVIEW

*Chairman*

Dr. George T. Wolff—General Motors Corporation, Environmental and Energy Staff,  
General Motors Bldg., 12th Floor, 3044 West Grand Blvd., Detroit, MI 48202

*Members*

Dr. Stephen Ayres—Office of International Health Programs, Virginia Commonwealth  
University, Medical College of Virginia, Box 980565, Richmond, VA 23298

Dr. Jay Jacobson—Boyce Thompson Institute, Tower Road, Cornell University, Ithaca,  
NY 14853

Dr. Philip Hopke—Clarkson University, Box 5810, Potsdam, NY 13699-5810

Dr. Joseph Mauderly—Inhalation Toxicology Research Institute, Lovelace Biomedical and  
Environmental Research Institute, P.O. Box 5890, Albuquerque, NM 87185

Dr. Paulette Middleton—Science and Policy Associates, 3445 Penrose Place, Suite 140,  
Boulder, CO 80301

Dr. James H. Price, Jr.—Research and Technology Section, Texas Natural Resources  
Conservation Commission, P.O. Box 13087, Austin, TX 78711-3087

*Invited Scientific Advisory Board Members*

Dr. Morton Lippmann—Institute of Environmental Medicine, New York University Medical  
Center, Long Meadow Road, Tuxedo, NY 10987

Dr. Roger O. McClellan—Chemical Industry Institute of Toxicology, P.O. Box 12137, Research  
Triangle Park, NC 27711

*Consultants*

Dr. Petros Koutrakis—Harvard School of Public Health, 665 Huntington Avenue, Boston,  
MA 02115

U.S. ENVIRONMENTAL PROTECTION AGENCY  
SCIENCE ADVISORY BOARD  
CLEAN AIR SCIENTIFIC ADVISORY COMMITTEE  
(cont'd)

*Consultants* (cont'd)

Dr. Kinley Larntz—Department of Applied Statistics, University of Minnesota, 352 COB,  
1994 Buford Avenue, St. Paul, MN 55108-6042

Dr. Allan Legge—Biosphere Solutions, 1601 11th Avenue, N.W., Calgary, Alberta T2N 1H1,  
Canada

Dr. Daniel Menzel—Department of Community and Environmental Medicine, University of  
California—Irvine, 19172 Jamboree Boulevard, Irvine, CA 92717-1825

Dr. William R. Pierson—Energy and Environmental Engineering Center, Desert Research  
Institute, P.O. Box 60220, Reno, NV 89506-0220

Dr. Jonathan Samet—Johns Hopkins University, School of Hygiene and Public Health,  
Department of Epidemiology, 615 N. Wolfe Street, Baltimore, MD 21205

Dr. Christian Seigneur—Atmospheric and Environmental Research, Inc., 6909 Snake Road,  
Oakland, CA 94611

Dr. Carl M. Shy—Department of Epidemiology, School of Public Health, University of North  
Carolina, CB #7400 McGavran-Greenberg Hall, Chapel Hill, NC 27599-7400

Dr. Frank Speizer—Harvard Medical School, Channing Laboratory, 180 Longwood Avenue,  
Boston, MA 02115

Dr. Jan Stolwijk—Epidemiology and Public Health, Yale University, 60 College Street,  
New Haven, CT 06510

Dr. Mark J. Utell—Pulmonary Disease Unit, Box 692, University of Rochester Medical Center,  
601 Elmwood Avenue, Rochester, NY 14642

Dr. Warren White—Washington University, Campus Box 1134, One Brookings Drive,  
St. Louis, MO 63130-4899

U.S. ENVIRONMENTAL PROTECTION AGENCY  
SCIENCE ADVISORY BOARD  
CLEAN AIR SCIENTIFIC ADVISORY COMMITTEE  
(cont'd)

*Designated Federal Official*

Mr. Randall C. Bond—Science Advisory Board (1400), U.S. Environmental Protection Agency, 401 M Street, S.W., Washington, DC 20460

Mr. A. Robert Flaak—Science Advisory Board (1400), U.S. Environmental Protection Agency, 401 M Street, S.W., Washington, DC 20460

*Staff Assistant*

Ms. Janice M. Cuevas—Science Advisory Board (1400), U.S. Environmental Protection Agency, 401 M Street, S.W., Washington, DC 20460

*Secretary*

Ms. Lori Anne Gross—Science Advisory Board (1400), U.S. Environmental Protection Agency, 401 M Street, S.W., Washington, DC 20460

Ms. Connie Valentine—Science Advisory Board (1400), U.S. Environmental Protection Agency, 401 M Street, S.W., Washington, DC 20460



U.S. ENVIRONMENTAL PROTECTION AGENCY  
PROJECT TEAM FOR DEVELOPMENT OF AIR QUALITY CRITERIA  
FOR PARTICULATE MATTER

*Scientific Staff*

Dr. Lester D. Grant—Director, National Center for Environmental Assessment (MD-52), U.S. Environmental Protection Agency, Research Triangle Park, NC 27711

Dr. Michael A. Berry—Deputy Director, National Center for Environmental Assessment, (MD-52), U.S. Environmental Protection Agency, Research Triangle Park, NC 27711

Dr. Dennis Kotchmar—Project Manager, Medical Officer, National Center for Environmental Assessment (MD-52), U.S. Environmental Protection Agency, Research Triangle Park, NC 27711

Ms. Beverly Comfort—Deputy Project Manager/Technical Project Officer, Health Scientist, National Center for Environmental Assessment (MD-52), U.S. Environmental Protection Agency, Research Triangle Park, NC 27711

Dr. Lawrence J. Folinsbee—Chief, Environmental Media Assessment Group, National Center for Environmental Assessment (MD-52), U.S. Environmental Protection Agency, Research Triangle Park, NC 27711

Dr. A. Paul Altshuller—Technical Consultant, National Center for Environmental Assessment (MD-52), U.S. Environmental Protection Agency, Research Triangle Park, NC 27711 (Retired)

Dr. Robert Chapman—Technical Consultant, Medical Officer, National Center for Environmental Assessment (MD-52), U.S. Environmental Protection Agency, Research Triangle Park, NC 27711

Mr. William Ewald—Technical Project Officer, Health Scientist, National Center for Environmental Assessment (MD-52), U.S. Environmental Protection Agency, Research Triangle Park, NC 27711

Mr. Norman Childs—Chief, Environmental Media Assessment Branch, National Center for Environmental Assessment (MD-52), U.S. Environmental Protection Agency, Research Triangle Park, NC 27711 (Retired)

Dr. Judith A. Graham—Associate Director for Health, National Exposure Research Laboratory (MD-77), U.S. Environmental Protection Agency, Research Triangle Park, NC 27711

U.S. ENVIRONMENTAL PROTECTION AGENCY  
PROJECT TEAM FOR DEVELOPMENT OF AIR QUALITY CRITERIA  
FOR PARTICULATE MATTER  
(cont'd)

*Scientific Staff* (cont'd)

Ms. Annie M. Jarabek—Technical Project Officer, Toxicologist, National Center for Environmental Assessment (MD-52), U.S. Environmental Protection Agency, Research Triangle Park, NC 27711

Dr. Allan Marcus—Technical Project Officer, Statistician, National Center for Environmental Assessment (MD-52), U.S. Environmental Protection Agency, Research Triangle Park, NC 27711

Dr. James McGrath—Technical Project Officer, Visiting Senior Health Scientist, National Center for Environmental Assessment (MD-52), U.S. Environmental Protection Agency, Research Triangle Park, NC 27711

Dr. Joseph P. Pinto—Technical Project Officer, Physical Scientist, National Center for Environmental Assessment, U.S. Environmental Protection Agency, Research Triangle Park, NC 27711

Ms. Beverly Tilton—Technical Project Officer, Physical Scientist, National Center for Environmental Assessment (MD-52), U.S. Environmental Protection Agency, Research Triangle Park, NC 27711 (Retired)

Dr. William E. Wilson—Technical Consultant, Physical Scientist, National Center for Environmental Assessment (MD-52), U.S. Environmental Protection Agency, Research Triangle Park, NC 27711

*Technical Support Staff*

Mr. Douglas B. Fennell—Technical Information Specialist, National Center for Environmental Assessment (MD-52), U.S. Environmental Protection Agency, Research Triangle Park, NC 27711

Ms. Emily R. Lee—Management Analyst, National Center for Environmental Assessment (MD-52), U.S. Environmental Protection Agency, Research Triangle Park, NC 27711

Ms. Diane H. Ray—Program Analyst, National Center for Environmental Assessment (MD-52), U.S. Environmental Protection Agency, Research Triangle Park, NC 27711

U.S. ENVIRONMENTAL PROTECTION AGENCY  
PROJECT TEAM FOR DEVELOPMENT OF AIR QUALITY CRITERIA  
FOR PARTICULATE MATTER  
(cont'd)

*Technical Support Staff (cont'd)*

Ms. Eleanor Speh—Office Manager, Environmental Media Assessment Branch, National Center for Environmental Assessment (MD-52), U.S. Environmental Protection Agency, Research Triangle Park, NC 27711

Ms. Donna Wicker—Administrative Officer, National Center for Environmental Assessment (MD-52), U.S. Environmental Protection Agency, Research Triangle Park, NC 27711

Mr. Richard Wilson—Clerk, National Center for Environmental Assessment (MD-52), U.S. Environmental Protection Agency, Research Triangle Park, NC 27711

*Document Production Staff*

Ms. Marianne Barrier—Graphic Artist, ManTech Environmental Technology, Inc., P.O. Box 12313, Research Triangle Park, NC 27709

Mr. John R. Barton—Document Production Coordinator, ManTech Environmental Technology, Inc., P.O. Box 12313, Research Triangle Park, NC 27709

Mr. Donald L. Duke—Project Director, ManTech Environmental Technology, Inc., P.O. Box 12313, Research Triangle Park, NC 27709

Ms. Shelia H. Elliott—Word Processor, ManTech Environmental Technology, Inc., P.O. Box 12313, Research Triangle Park, NC 27709

Ms. Sandra K. Eltz—Word Processor, ManTech Environmental Technology, Inc., P.O. Box 12313, Research Triangle Park, NC 27709

Ms. Sheila R. Lassiter—Word Processor, ManTech Environmental Technology, Inc., P.O. Box 12313, Research Triangle Park, NC 27709

Ms. Wendy B. Lloyd—Word Processor, ManTech Environmental Technology, Inc., P.O. Box 12313, Research Triangle Park, NC 27709

Ms. Carolyn T. Perry—Word Processor, ManTech Environmental Technology, Inc., P.O. Box 12313, Research Triangle Park, NC 27709

Ms. Terri D. Ragan—Personal Computer Technician, ManTech Environmental Technology, Inc., P.O. Box 12313, Research Triangle Park, NC 27709

U.S. ENVIRONMENTAL PROTECTION AGENCY  
PROJECT TEAM FOR DEVELOPMENT OF AIR QUALITY CRITERIA  
FOR PARTICULATE MATTER  
(cont'd)

*Document Production Staff (cont'd)*

Mr. Derrick Stout—Local Area Network System Administrator, ManTech Environmental Technology, Inc., P.O. Box 12313, Research Triangle Park, NC 27709

Ms. Cheryl B. Thomas—Word Processor, ManTech Environmental Technology, Inc., P.O. Box 12313, Research Triangle Park, NC 27709

*Technical Reference Staff*

Ms. Ginny M. Belcher—Bibliographic Editor, ManTech Environmental Technology, Inc., P.O. Box 12313, Research Triangle Park, NC 27709

Mr. Robert D. Belton—Bibliographic Editor, Information Organizers, Inc., P.O. Box 14391, Research Triangle Park, NC 27709

Mr. John A. Bennett—Bibliographic Editor, ManTech Environmental Technology, Inc., P.O. Box 12313, Research Triangle Park, NC 27709

Ms. S. Blythe Hatcher—Bibliographic Editor, Information Organizers, Inc., P.O. Box 14391, Research Triangle Park, NC 27709

Ms. Susan L. McDonald—Bibliographic Editor, Information Organizers, Inc., P.O. Box 14391, Research Triangle Park, NC 27709

Ms. Deborah L. Staves—Bibliographic Editor, Information Organizers, Inc., P.O. Box 14391, Research Triangle Park, NC 27709

Ms. Patricia R. Tierney—Bibliographic Editor, ManTech Environmental Technology, Inc., P.O. Box 12313, Research Triangle Park, NC 27709

## **8. EFFECTS ON VISIBILITY AND CLIMATE**

### **8.1 INTRODUCTION**

Visibility is the yardstick by which the layman measures air quality every day. Air pollutants can change the way he sees the world. The air pollutant that makes the largest contribution to visibility impairment is usually fine particulate matter, more specifically the accumulation mode, ~0.3 to 1.0  $\mu\text{m}$  diameter (see Chapter 3).

The primary objective of the visibility discussion in this chapter is to present the technical basis for understanding the linkage between air pollution, especially particulate matter, and visibility. This linkage can be used to (1) evaluate the visibility effects of different levels for the primary standards for particulate matter concentrations designed to protect public health and (2) evaluate the need for a secondary standard designed to reduce visibility impairment.

The visibility sections of this chapter are complementary to recent reviews of visibility published by the National Research Council (National Research Council, 1993), the National Acid Precipitation Assessment Program (Trijonis et al., 1991), and the U.S. EPA (U.S. Environmental Protection Agency, 1995e). Little of the information in those reviews has been presented again here, with the result that this review does not attempt to present a fully comprehensive overview of the effect of particulate matter on visibility. Instead, the visibility sections of this chapter focus on presenting additional information relevant to the consideration of visibility protection that does not appear in the prior reviews.

#### **8.1.1 Background**

In August 1977, Congress amended the Clean Air Act (CAA) to establish as a national goal "the prevention of any future and remedying of any existing impairment of visibility in mandatory Class I Federal areas, which impairment results from manmade air pollution" (Title I Part C Section 169A; 42 U.S.C. 7491). Class I areas include many national parks and wilderness areas, especially in the western portion of the United States. These areas were generally large national parks and federal wilderness areas and included all national parks in existence on August 7, 1977. The visibility protection provisions of section 169A

required the U.S. Environmental Protection Agency (EPA) to establish a regulatory program to assure reasonable progress toward this national goal. In 1980, the EPA established regulatory requirements under section 169A to address Class I protection from visibility impairment that could be reasonably attributed to major stationary air pollution sources. At that time, regulatory action on regional haze (pollution transported long distances from a multitude of sources) was deferred until better scientific tools were developed. The 1977 Amendments also included provisions requiring applicants for new major source permits to assess the potential for their projects to cause adverse impacts on the air quality-related values, including visibility, in nearby Class I areas.

The mandate to protect visibility in national parks and wilderness areas led to the development of the Interagency Monitoring of Protected Visual Environments (IMPROVE), a cooperative visibility monitoring network managed and operated by federal land management agencies, the U.S. EPA, and State air quality organizations (Malm et al., 1994; Sisler et al., 1993). The 1977 CAA amendments also (a) led to major visibility research studies, such as (1) the Visibility Impairment due to Sulfur Transformation and Transport in the Atmosphere (VISTTA) study (Blumenthal et al., 1981); (2) the Subregional Cooperative Electric Utility, and the Department of Defense, National Park Service, and Environmental Protection Agency Study (SCENES) (Mueller et al., 1986); and (b) included the requirement to control sulfur dioxide (SO<sub>2</sub>) emissions from the Navajo Generating Station, which is near the Grand Canyon National Park (56 FR 38399, 1991).

The CAA was amended in 1990 by adding section 169B, which authorized the EPA (a) to conduct research on regional visibility impairment and (b) to establish the Grand Canyon Visibility Transport Commission (GCVTC) for the assessment of appropriate actions under section 169A for protecting the Grand Canyon from regional visibility impairment caused by man-made sources. This charge was expanded by the U.S. EPA to include the 15 other Class I parks and wilderness areas on the Colorado Plateau. Work is now being performed to assess the scientific and technical data, studies, and other available information pertaining to adverse impacts on visibility from projected growth in emissions from sources located in the region. The U.S. EPA has also initiated a tracer study to evaluate the effects of emissions from the Mohave Power Project on visibility in the Grand Canyon National Park and other Class I areas in the Colorado Plateau. Because of these events, a major portion of

the funding for visibility research during the last two decades has been directed toward protecting pristine and scenic areas.

Interest in protecting visibility in urban areas has a much longer history and is strong at the present time. Smoke in European cities, especially London, has been a concern for centuries. Many of the modern advances in the understanding of atmospheric fine particles were made during the 1969 Pasadena Smog Experiment (see, for example, Whitby et al., 1972), which was followed by the Aerosol Characterization Experiment (ACHEX) sponsored by the California Air Resources Board (Hidy et al., 1980). The continuing interest in urban visibility is indicated in the list of short-term intensive visibility and aerosol studies summarized by the National Acid Precipitation Assessment Program (NAPAP) report on visibility (Trijonis et al., 1991) and discussed later in this chapter. Many of the studies focused on urban visibility.

Visibility impairment carries significant social and economic costs, which are discussed below.

Particulate matter also affects climate by increasing the absorption of solar radiation within the atmosphere and by increasing the fraction of solar radiation reflected into space (Charlson et al., 1992). The first effect causes heating within the atmosphere, especially where the concentrations of light-absorbing particles are elevated, and the second effect causes a cooling of the Earth. This cooling counteracts the heating caused by the greenhouse effect of gases that absorb infrared radiation.

### **8.1.2 Definition of Visibility**

The National Research Council's Committee on Haze in National Parks and Wilderness Areas said, "Visibility is the degree to which the atmosphere is transparent to visible light." (National Research Council, 1993). Section 169A of the 1977 CAA Amendments (42 U.S.C. 7491) and the 1979 Report to Congress (U.S. Environmental Protection Agency, 1979) define visibility impairment as a reduction in visual range and atmospheric discoloration. Equating visibility to the visual range is consistent with historical visibility measurements at airports, where human observers recorded the greatest distance at which one of a number of pre-selected targets could be perceived.

Visibility may also be defined as the clarity (transparency) and color fidelity of the atmosphere. Transparency can be quantified by the contrast transmittance of the atmosphere. This definition of visibility is consistent with both (1) the historical records based on human observation of the perceptibility of targets, which include both the longest duration and most widespread records now available, and (2) the definition of visibility recommended by the National Research Council (National Research Council, 1993).

Air pollution can also alter the colors of the atmosphere and the perceived colors of objects viewed through the atmosphere. A complete quantification of visibility should include a measure of the color changes caused by the atmosphere. Such measures have been included in plume visibility models (e.g., Latimer et al., 1978), but there is no consensus on the best parameter to quantify color changes caused by air pollution from many sources.

Visibility is an effect of air quality and, unlike the particulate matter concentration, it is not a property of an element of volume in the atmosphere. Visibility can be defined only for a sight path and depends on the illumination of the atmosphere and the direction of view. The factors that control this dependence are described in the succeeding sections of this chapter.

### **8.1.3 Human Vision**

Vision results from the human response to the electromagnetic radiation that enters the eye. Therefore, this presentation of the theory of visibility begins with a brief outline of the relevant properties of human vision.

The eye is most sensitive to green wavelengths, near 550 nm, and can perceive radiation between approximately 400 and 700 nm. The sensitivity of the eye is greatly diminished near the longest and shortest visible wavelengths. When measurements or calculations at only one wavelength are used to characterize visibility, it is customary to select a wavelength between 500 and 550 nm because these wavelengths are in the middle of the visible spectrum and the eye is most sensitive in this range.

The retina of the eye contains two types of receptor cells, rods and cones. The rods, used for nighttime vision, are not capable of perceiving color and are most concentrated in the parts of the retina used for peripheral vision. Rods are most sensitive at a wavelength of 510 nm and are insensitive to wavelengths longer than about 630 nm. The foveal pit, which

subtends an angle of about 1 degree, contains only cones, which are used for daytime color vision. There are no rods in approximately the central 2 degrees of the field of view. As a result, a faint light is best detected at night by looking in a slightly different direction. On the other hand, visual acuity is greatly diminished in peripheral vision. For example, at normal levels of illumination, text which is quite readable becomes unreadable when the direction of view is displaced by a few degrees so that the image of the text no longer falls on the fovea.

Human vision has a dynamic range of about  $10^{12}$  cd/m<sup>2</sup> (candelas per square meter). Radiation becomes perceptible to the completely dark adapted eye at levels of about  $10^{-6}$  cd/m<sup>2</sup>. Cones begin to be activated at levels of about  $10^{-3}$  cd/m<sup>2</sup>, the rods cease to function at about 125 cd/m<sup>2</sup>, and light levels above  $10^6$  cd/m<sup>2</sup> cause the observer to be uncomfortable and to feel blinded. The visibility regulations are usually interpreted as addressing daytime visibility, which is provided by the cones and is called photopic vision.

Contrast is widely used as a measure of the perceptibility of faint objects because of the following property of human vision. Weber's law, sometimes called Fechner's law or the Weber-Fechner law, states that for a wide range of luminance levels, to be just noticeably brighter, one patch of light must exceed the luminance of another by a constant fraction. Figure 8-1 and Equation 8-1 illustrate the definition of the contrast, C, of an object (target) of radiance, I, viewed against a background of radiance, I<sub>b</sub>

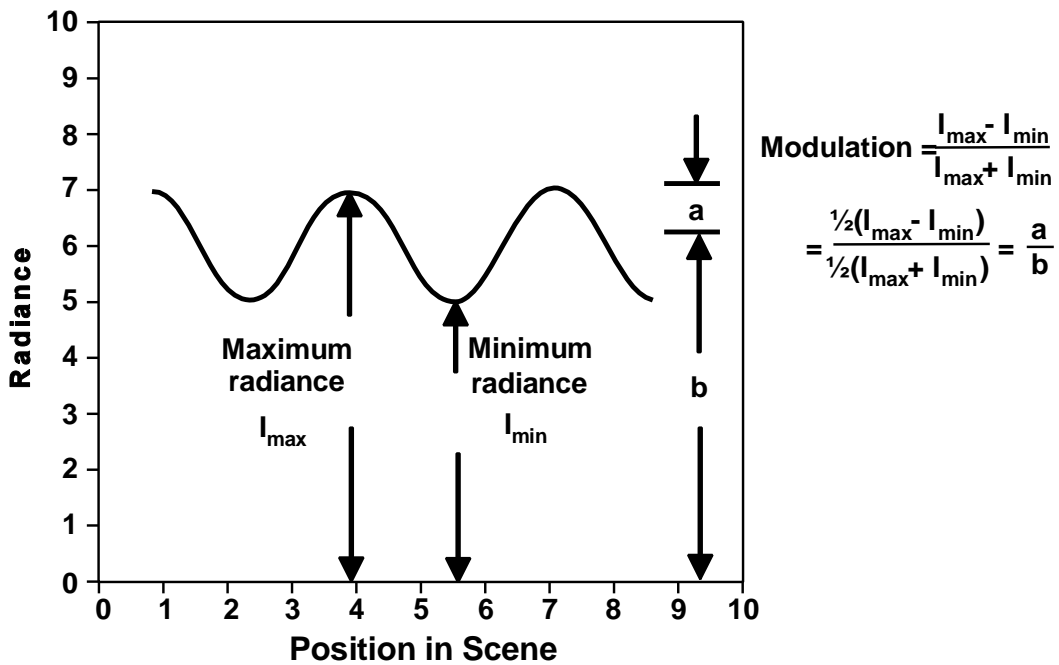
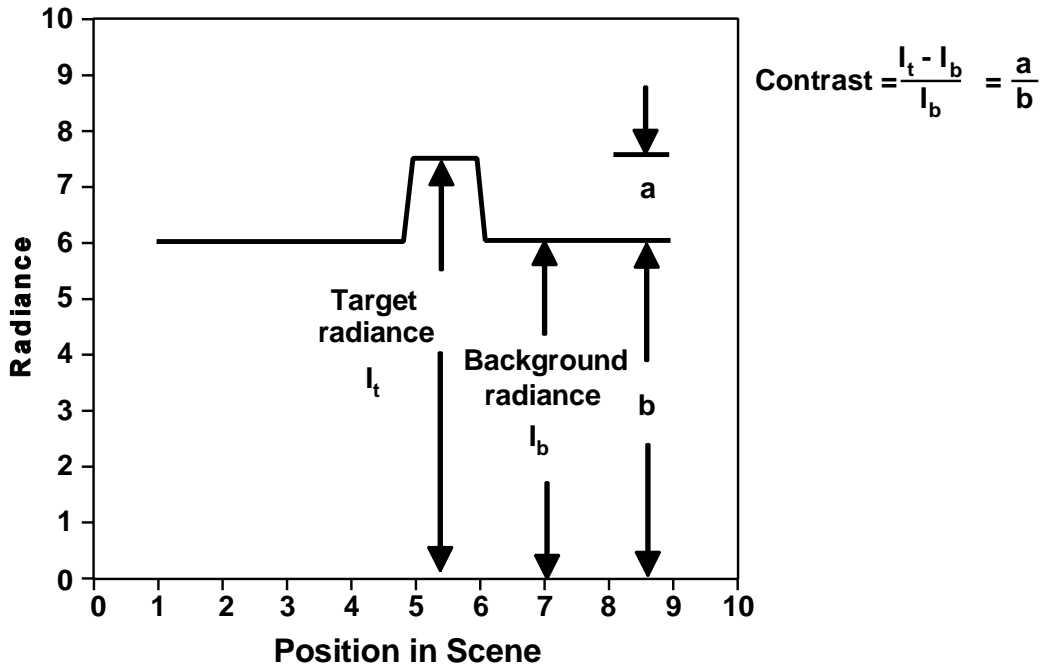
$$C = (I - I_b) / I_b . \quad (8-1)$$

Figure 8-1 also illustrates the definition of modulation, M, of a sine wave with maximum and minimum radiances, I<sub>max</sub> and I<sub>min</sub>, respectively

$$M = (I_{max} - I_{min}) / (I_{max} + I_{min}) . \quad (8-2)$$

If the average radiance of the sine wave is indicated by I<sub>b</sub>, then Equation 8-2 can be written

$$M = (I_{max} - I_b) / I_b \quad (8-3)$$



**Figure 8-1. Diagrams showing the definitions of contrast and modulation. If the background radiance in the definition of contrast is equated to the average radiance in the definition of modulation, the definitions have the same mathematical form.**

Source: Richards (1990).

which is identical in form to Equation 8-1. This transformation allows contrast and modulation to be used interchangeably in visibility calculations. It is shown below that the average radiance or background radiance in Equations 8-1 and 8-3 plays a key role in visibility calculations.

The accommodation of the eye, and its ability to perceive contrasts, changes in response to the general light level. The above definitions of contrast and modulation assume that the eye is accommodated to the background radiance. The effects of the accommodation of the eye can be experienced by first viewing objects in a relatively dark room, then going outside into bright daylight and viewing the same objects through an open window. Radiance differences that were perceptible when the eye was accommodated to those radiances become imperceptible when the eye becomes accommodated to a much greater radiance.

The perception of discoloration in the atmosphere depends on the properties of human color vision. Studies with color matches have shown that color vision is three dimensional. For example, images on color television or computer monitors are made up of red, green, and blue dots. All colors that the screen is capable of displaying can be specified by three numbers that quantify the intensity of the light from each of the three phosphors. For purposes of determining color matches, it is possible to characterize colors by these three numbers, X, Y, and Z, which are called tristimulus values. Colors that have the same tristimulus values will appear to match. In 1931, the Commission Internationale de l'Eclairage (CIE, or International Commission for Illumination) adopted a standard method of calculating these numbers from the spectrum of the light reflected from an object.

The perception of color depends on illumination and setting. For example, when there is a brilliant sunset, a white picket fence will appear to be white, but will be distinctly yellow in a color photograph. A nitrogen dioxide (NO<sub>2</sub>) containing plume appears to be yellow against a blue sky even when a photograph or spectral measurement shows that the plume is blue, but less blue than the surrounding sky. The eye correctly perceives that a yellow gas is present in the plume. Spectral measurements have shown that the "Denver brown cloud" is a neutral gray (Waggoner et al., 1983).

These properties of human vision been described and explained by MacAdam (1981). The eye tends to perceive the lightest and brightest object in a scene as white, and to determine the color of other objects by comparison. For example, water clouds are typically

present in the sky above Denver. Spectral measurements show that they are blue compared to the color of sunlight, but the eye perceives them as white. The urban haze is not as blue as the water clouds in the sky, and by comparison, appears yellow or brown.

Because of this property of human vision, plume visibility models calculate the spectral radiance and tristimulus values of a "reference white." This reference is then used in the color calculations in the models.

## **8.2 FUNDAMENTALS OF ATMOSPHERIC VISIBILITY**

This section presents a simple, complete, and reasonably accurate theory of daytime visibility for approximately horizontal sight paths. This theory provides the linkage between the nature and concentration of particulate matter in the atmosphere and visibility.

### **8.2.1 Geometry of the Atmosphere**

The atmosphere is an extremely thin layer on the surface of the Earth, and all of its physical properties have strong vertical gradients. Half the mass of the atmosphere is at altitudes below 5.7 km (18,700 ft) mean sea level. The average of the equatorial and polar radii of the Earth is 6,370 km (3958 mi). Thus, most of the mass of the atmosphere is within a shell having a thickness 0.09% of the radius of the Earth.

The atmosphere is thin enough compared to the radius of the Earth that its curvature can be neglected in most optical calculations. This is not the case for sight paths that are horizontal or nearly so (Malm, 1979). Because of the curvature of the Earth, a sight path that is initially horizontal will have an altitude that increases with distance. Table 8-1 gives the approximate distances for selected increases in height above ground level. Sight paths longer than approximately 100 km (60 mi) are always subject to substantial changes in the properties of the atmosphere over the length of the sight path because of the changes in altitude. The atmosphere rarely has uniform optical properties over distances greater than a few tens of kilometers, even at a constant height above ground. Tabulations of air quality or visibility data that report visual ranges much greater than 100 km are based on assumptions that cannot be valid in the Earth's atmosphere.

**TABLE 8-1. APPROXIMATE DISTANCES FOR SELECTED INCREASES IN HEIGHT OF AN INITIALLY HORIZONTAL SIGHT PATH**

Height		Distance	
(m)	(ft)	(km)	(mi)
300	1,000	62	39
1,000	3,280	113	70
2,000	6,560	160	99
3,000	9,840	196	122
4,000	13,120	226	140

Optical calculations for the Earth's atmosphere are simplified if it is assumed that the Earth is flat and the atmosphere is horizontally uniform. Except for horizontal, or nearly horizontal, sight paths, it is an excellent approximation to neglect the Earth's curvature. An initially horizontal sight path above a curved Earth can be simulated in the calculations for a flat Earth by a sight path approximately 1.5 degrees above the horizontal sight path (Bergstrom et al., 1981). This angle depends on the vertical profile of the atmospheric haze, and can be calculated from an analytic expression in Latimer et al. (1978).

The variation in the optical properties of the atmosphere in the vertical dimension has received little attention in visibility monitoring and data reporting. Interest in the effects of particulate matter on climate forcing is causing a rapid expansion of the available information on haze aloft (see Section 8.8).

### **8.2.2 Illumination of the Atmosphere**

Illumination of the atmosphere and factors affecting illumination of the sight path will affect visibility and visibility observations. Figure 8-2 shows the spectrum of the direct solar rays at the top of the atmosphere. Much of solar energy is in the visible wavelength range. Figure 8-2 also shows the spectra at the surface of the Earth for increasing amounts of atmospheric attenuation as the sun moves lower in the sky.

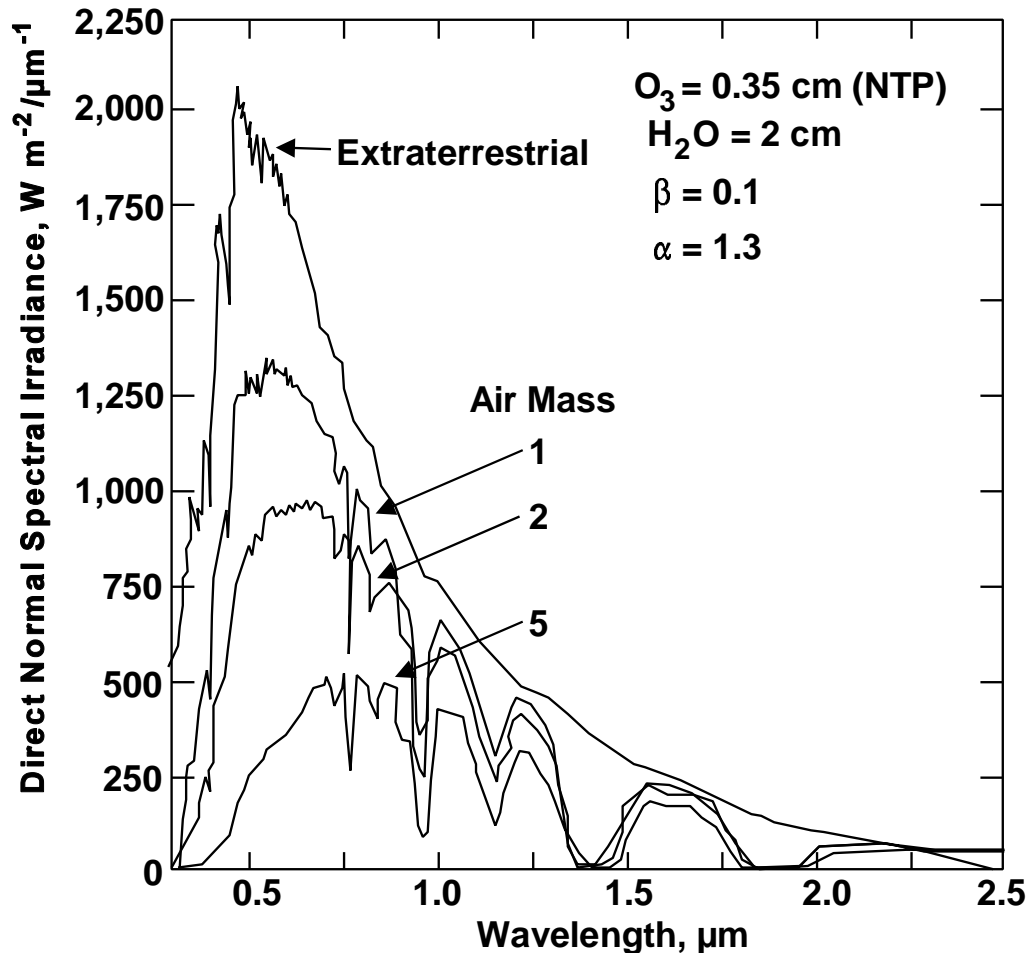


**Figure 8-2.** Spectrum of direct solar rays at the top of the atmosphere and at the surface of the Earth for various values of the air mass ( $m$ ). The air mass equals 1 for an overhead sun and increases in proportion to the mass of atmosphere between the observer and the sun as the sun moves lower in the sky. The aerosol optical depth is  $m \beta \lambda^{-\alpha}$ , where  $\lambda$  is the wavelength in  $\mu m$ .

Source: Duffie and Beckman (1991).

The data in Figure 8-2 show that the atmospheric attenuation is greater at the shorter visible wavelengths than the longer visible wavelengths. This is because light scattering by air molecules depends inversely on the fourth power of the wavelength (as expressed in Equation 8-5). The greater atmospheric light scattering at the shorter wavelengths causes the blue sky in daytime and the familiar red and yellow colors at dawn and sunset. These color changes occur naturally, and are very great. They are much greater than would be caused by typical amounts of  $NO_2$  in haze layers.

On a clear day, 80 to 90% of the visible solar radiation reaches the surface of the Earth without being scattered or absorbed when the sun is high in the sky. At the surface, a variable fraction is reflected upwards, so the atmosphere is illuminated both from above and below. The fraction of the radiation incident on the surface of the Earth that is reflected is known as the surface reflectance or the albedo. Both visibility and visibility observations are affected by clouds in the viewing background or overhead. The effects of clouds are readily apparent and are very great. The illumination of a terrain feature or the atmosphere in a sight path can change by a factor of 10 or more in a few minutes as clouds pass overhead. Very dark terrain can reflect only one tenth as much radiation as snow-covered terrain.

The derivations in the following subsections show that visibility is determined both by the illumination of the sight path and by the air quality in the sight path. The effects of the illumination are great enough and variable enough that it is not appropriate to omit them from quantitative discussions of visibility.

### **8.2.3 Optical Properties of the Atmosphere**

The fate of the solar radiation that enters the Earth's atmosphere is determined by the geometry and optical properties of the atmosphere and the Earth's surface. This section presents definitions of the atmospheric optical properties that affect visibility and also presents data for the optical properties of gases. Data for the optical properties of particles are presented in Section 8.3. All of these optical properties are functions of the wavelength of light.

The atmosphere is a turbid medium, which both scatters and absorbs light. A ray of light passing through the atmosphere is weakened by both of these processes. The distance-rate of energy loss is proportional to the radiance of the ray, and the proportionality constant is the light-extinction coefficient,  $\sigma_{\text{ext}}$ , which has units of  $\text{length}^{-1}$ . The light-extinction coefficient is the sum of the light-scattering coefficient,  $\sigma_{\text{scat}}$ , and the light-absorption coefficient,  $\sigma_{\text{abs}}$ , which are the proportionality constants for energy loss from the ray caused by scattering and absorption, respectively.

The light-extinction coefficient can be further divided into coefficients for the following components:

$\sigma_{ag}$ , light absorption by gases,  
 $\sigma_{sg}$ , light scattering by gases,  
 $\sigma_{ap}$ , light absorption by particles, and  
 $\sigma_{sp}$ , light scattering by particles.

Because of their different origins and composition, atmospheric particles are frequently divided into coarse and fine particles (see Chapters 3 and 6). The corresponding division of  $\sigma_{sp}$  is

$\sigma_{sfp}$ , light scattering by fine particles and  
 $\sigma_{scp}$ , light scattering by coarse particles.

These components of the light-extinction coefficient are related as follows:

$$\begin{aligned}
 \sigma_{ext} &= \sigma_{abs} + \sigma_{scat} \\
 \sigma_{ab} &= \sigma_{ag} + \sigma_{ap} \\
 \sigma_{scat} &= \sigma_{sg} + \sigma_{sp} \\
 \sigma_{sp} &= \sigma_{sfp} + \sigma_{scp}
 \end{aligned}
 \tag{8-4}$$

Light scattering by gases is also known as Rayleigh scattering, and the coefficient can be calculated from the equation

$$\sigma_{sg} = 16.51 (p/1013.25 \text{ mb}) (273.15 \text{ K}/t) \lambda^{-4.07} \text{ Mm}
 \tag{8-5}$$

where  $p$  and  $t$  are the ambient pressure and temperature and the wavelength,  $\lambda$ , is in micrometers (Edlen, 1953; Penndorf, 1957). Equation 8-5 was obtained by fitting values reported by Bodhaine (1979). At modest elevations and daytime temperatures, the coefficient for light scattering by gases has a value near  $10 \text{ Mm}^{-1}$  (or  $0.01 \text{ km}^{-1}$ ) at a wavelength of 550 nm. This corresponds to an attenuation of a ray of green light in particle-free air of 1% per kilometer.

Light absorption by gases is predominantly caused by  $\text{NO}_2$ , and typically accounts for a few percent of the total light extinction in urban atmospheres. It is typically negligible in

remote areas. Nitrogen dioxide absorbs blue light more strongly than other visible wavelengths, and thus contributes to the yellow or brown appearance of urban hazes.

Ozone (O<sub>3</sub>) absorbs ultraviolet light strongly and, in the visible range, has a weak absorption at green wavelengths. The absorption in the green wavelength could cause perceptible effects only if the O<sub>3</sub> concentration were much greater than 0.2 ppmv in a long sight path through a very clean atmosphere. These conditions are quite improbable.

The optical properties of particles are complicated enough that all of Section 8.3 is devoted to a summary of current knowledge. The remaining discussions in this section make use of that information as if it were presented here.

The appearance of the atmosphere, especially near the horizon, is affected by the relative importance of light scattering and absorption, which is measured by the single scattering albedo,  $\omega_0$ ,

$$\omega_0 = \sigma_{\text{scat}} / \sigma_{\text{ext}} = \sigma_{\text{scat}} / (\sigma_{\text{scat}} + \sigma_{\text{abs}}) . \quad (8-6)$$

When there is no light absorption,  $\omega_0 = 1$ . As light absorption increases, the single scattering albedo becomes smaller, and hazes and the horizon sky become darker. Typical values for  $\omega_0$  range between 0.8 and 1.0, even in smoke from fires.

When the direction of travel of radiation is changed by light scattering, the redirected radiation is not evenly distributed into all possible angles. The angular distribution of the scattered light is described by the phase function. This function was named by astronomers, and an example of its use is provided by the phases of the moon. The moon scatters light back toward the sun more strongly than in other directions, so the moonlight is strongest when the moon is full. Measuring the light from the moon during the progression from a new moon to a full moon would provide data for the phase function of the moon. The scattering angle is the angle through which radiation is deflected by the scattering process. This angle is near 0 degrees for a new moon and is 180 degrees for a full moon. (The infinitesimal deflection of radiation that passes near the moon is neglected in this discussion.)

The phase function for the scattering of unpolarized light by clear air (Rayleigh scattering) is

$$P(\theta) = (3/4)(1 + \cos^2\theta) \quad (8-7)$$

where  $\theta$  is the scattering angle. This function is normalized so that the integral from 0 to  $\pi$  radians equals 2.

$$\int_0^{\pi} P(\theta) \sin\theta d\theta = 2 \quad (8-8)$$

This normalization is customarily used for all phase functions, and causes the integral over all scattering angles to equal  $4\pi$ .

The optical depth,  $\tau$ , associated with a distance in a turbid medium is equal to the definite integral of the light-extinction coefficient over that distance

$$\tau = \int \sigma_{\text{ext}} dx = \bar{\sigma}_{\text{ext}} x \quad (8-9)$$

where  $dx$  is the element of distance and  $\bar{\sigma}_{\text{ext}}$  is the average of the light-extinction coefficient over the distance  $x$ . The transmittance,  $T$ , for a ray of light that passes through a medium of optical depth is

$$T = e^{-\tau}. \quad (8-10)$$

When distances in the atmosphere are specified in terms of the optical depth, the phase function and the single scattering albedo provide all the information about the optical properties of the atmosphere required for visibility calculations. As mentioned above, these quantities must be known as a function of wavelength.

Polarization has not been included. If polarization were included, radiances would be described by the Stokes vector and the phase function would be replaced by a phase matrix. In general, polarization effects are small enough that they can be neglected when considering the effects of air quality on visibility. However, polarization effects are readily apparent, and can be used to infer information about air quality (White, 1975).

Visibility is affected by atmospheric refraction (Minnaert, 1954). Those effects are often important, but are not discussed in any depth here because they are not closely linked to air quality. Atmospheric refraction causes mirages and looming, i.e., causes sight paths to be bent so the apparent positions of objects are displaced from their actual position. The refraction associated with thermal turbulence causes the stars to twinkle at night and distant objects to shimmer in the daytime. In general, an effort is made to eliminate the effects of atmospheric refraction from measurements and analyses to determine the effects of air quality on visibility.

This subsection has listed all the optical properties of the atmosphere that must be known to understand and calculate atmospheric visibility. With the inclusion of the absorption spectrum of NO<sub>2</sub> (Davidson et al., 1988), this section also presents all the required optical data for gases. The necessary optical data for particles are discussed in Section 8.3.

#### **8.2.4 Multiple Scattering**

The term, multiple scattering, is used when light is scattered more than once in a turbid medium. Light passing through a turbid medium transmits energy, and this process is known as radiative transfer. (Convective and conductive transfer of energy are also possible.) The equation that governs the light intensities, and hence the radiative transmission of energy in a turbid medium, is known as the equation of radiative transfer. Obtaining solutions of this equation for the Earth's atmosphere requires a knowledge of the optical properties of the atmosphere listed in Section 8.2.3 as a function of position and also a knowledge of the boundary conditions. The boundary conditions at the top of the atmosphere are (1) the atmosphere is illuminated by the solar radiation, and (2) radiation that leaves the top of the atmosphere does not return. The boundary condition at the bottom of the atmosphere is specified by the bidirectional reflectance of the Earth's surface. The reflectance albedo

indicates the fraction of the radiation incident on the Earth's surface that is reflected, and the bidirectional reflectance specifies both this fraction and the angular distribution of the reflected light as a function of the angle of incidence.

The equation of radiative transfer can be written

$$dI/dx = -\sigma_{ext} ( I - I_e ) \quad (8-11)$$

where  $dI/dx$  is the rate of change with distance  $x$  of a ray of radiance  $I$  and  $I_e$  is the source function. All of these quantities (except the distance  $x$ ) are functions of the wavelength.

Middleton used the name equilibrium radiance for the source function. This name conveys the idea that the radiance of a ray always tends toward the "equilibrium" value as the ray progresses through the atmosphere. Also, if the radiance of a ray is equal to the source function, its value will not change with distance in the atmosphere. These properties are represented in Figure 8-3, which Middleton adapted from Hugon (1930). The rate of approach to the "equilibrium" is determined by the light-extinction coefficient. When the light-extinction coefficient has high values, e.g., in a fog, radiances approach the source function (equilibrium radiance) in short distances.

When the optical depth defined in Equation 8-9 is used in place of distance  $x$  in Equation 8-11, the equation of radiative transfer becomes

$$dI/d\tau = I_e - I . \quad (8-12)$$

This equation focuses attention on the source function. An intuitive understanding of the properties of radiation in the Earth's atmosphere must be based on an understanding of the source function and the factors that determine its value.

For horizontal sight paths, the horizon sky radiance typically provides a reasonable estimate of the source function. If the surface of the Earth were perfectly flat and the atmosphere and its illumination were perfectly uniform, the sight path into the horizon sky

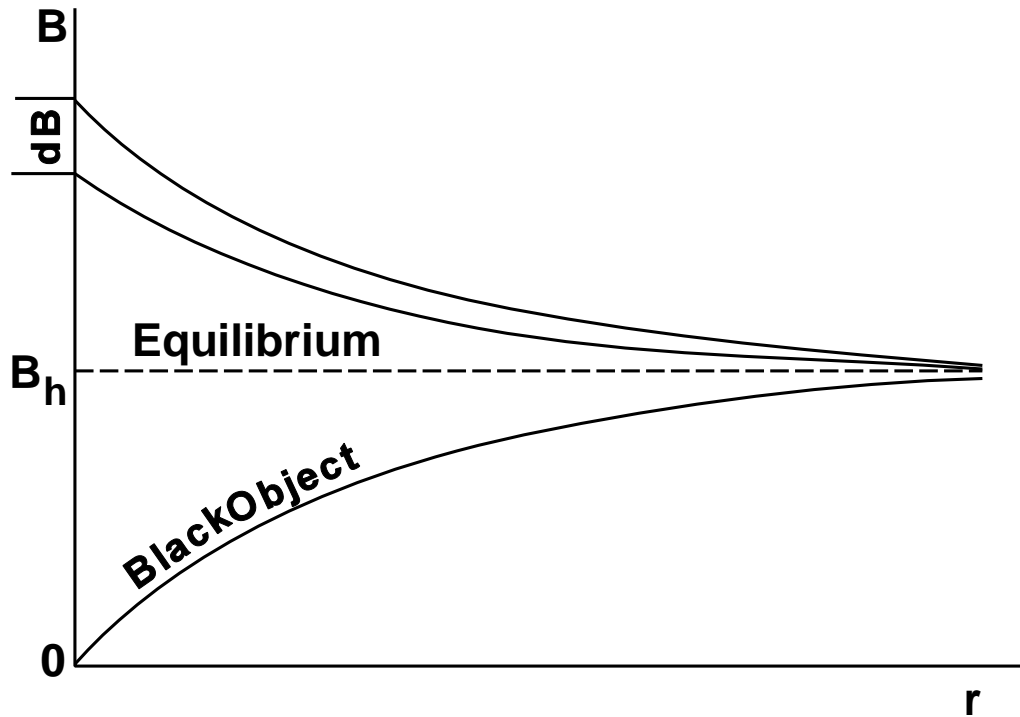


**Figure 8-3. The approach of radiances in the atmosphere to the equilibrium radiance or source function.**

Source: Middleton (1952).

would be limited in length by the atmospheric extinction. The curves in Figure 8-3 indicate that in this case, the horizon sky radiance would be equal to the source function. In the real world, the horizon sky radiance provides a good estimate of the source function if the light-extinction coefficient is great enough that the curvature of the Earth and nonuniformities of the atmosphere can be neglected for distances with an optical depth approaching a value of 3. This condition can be satisfied in fogs or moderate hazes. In practice, the greatest errors in equating the source function to the horizon sky radiance are due to variations in the optical properties of the atmosphere and its illumination along the sight path toward the horizon and beyond.

Further insight into the properties of the source function can be obtained from the equation of radiative transfer. When the radiance of a ray is equal to the source function, the radiance does not change as the ray is propagated. In this case, the removal of energy

from the ray by light extinction is balanced by scattering of light into the direction of the ray. This balance is expressed by the equation

$$\sigma_{\text{ext}} I_e = (\sigma_{\text{scat}}/4\pi) \int_{4\pi} I(\Omega') P(\Omega, \Omega') d\Omega' \quad (8-13)$$

The left side indicates the removal of energy by extinction per unit distance. The right side indicates the addition of energy by scattering per unit distance. The quantity,  $I(\Omega')$ , specifies the strength of the illumination of the path of the ray by radiation from the angle  $\Omega'$ . The quantity  $(\sigma_{\text{scat}}/4\pi)P(\Omega, \Omega')$  describes the amount of this illumination scattered into the direction of the ray. The phase function for scattering of radiation from the direction  $\Omega'$  of the illumination into the direction  $\Omega$  of the ray is  $P(\Omega, \Omega')$ . Because this function is normalized (see discussion of Equation 8-8), it is necessary to multiply by the light-scattering coefficient, which specifies the strength of the light scattering. The factor of  $4\pi$  results from the conventions used in the normalization of the phase function. The integration extends over all angles.

Dividing both sides of Equation 8-13 by the light-extinction coefficient and using Equation 8-6 gives

$$I_e = (\omega_o/4\pi) \int_{4\pi} I(\Omega') P(\Omega, \Omega') d\Omega' \quad (8-14)$$

which is the customary form of the equation for the source function. All the complications of radiative transfer calculations are contained in this equation. The value of the source function at each point in the atmosphere depends on the illumination at that point, which is affected by all the nearby surroundings.

Equation 8-14 can be simplified by making some reasonable, but not strictly valid, assumptions. The purpose of this simplification is to derive a formula that shows the dominant factors that affect the source function for an approximately horizontal sight path. This formula can then be used to develop an intuition for the factors that control visibility in the atmosphere and also to perform simple, approximate visibility calculations.

The first assumption is that the skylight is perfectly diffuse, i.e., that the radiance of the sky is the same in all directions. The second assumption is that the light reflected from the surface of the Earth is also perfectly diffuse. Richards et al. (1983) and Richards (1988) showed that these assumptions permit the integration in Equation 8-14 to be divided into integrations over each of two hemispheres to obtain

$$I_e = (\omega_o / 4\pi) [2F_+ + 2F_- + F_s P(\Omega, \Omega_s)] \quad (8-15)$$

where  $\omega_o$  is the single scattering albedo defined in Equation 8-6,  $F_+$  is the flux of diffuse light reflected upward from the Earth's surface,  $F_-$  is the flux of diffuse skylight incident on the Earth's surface,  $F_s$  is the direct solar flux on the sight path measured normal to the solar rays, and  $P(\Omega, \Omega_s)$  is the phase function for the scattering of radiation from the direction  $\Omega_s$  of the solar rays into the direction  $\Omega$  of the line of sight. Near the surface of the Earth, Equation 8-15 can be simplified by the relationship

$$F_+ = \alpha(F_- + F_s \cos\theta) \quad (8-16)$$

where  $\alpha$  is the diffuse reflectance albedo of the Earth's surface and  $\theta$  is the angle between the sun's rays and the normal to the Earth's surface. It is known that the assumptions used to derive Equations 8-15 and 8-16 are not strictly valid; the radiance reflected from the Earth's surface is not perfectly diffuse (Gordon, 1964), the skylight is also not perfectly diffuse, and these assumptions are worst when the sun is near the horizon.

The use of Equations 8-15 and 8-16 requires data for the flux of diffuse skylight. Figure 8-4 provides the necessary information for a broad range of cases in which the sky is cloud free. The curves in Figure 8-4 were calculated using the data and calculation methods in Richards et al. (1986). The atmosphere is represented by four layers of different composition. The composition and optical properties of the top three layers are kept constant. The curves in Figure 8-4 show the effects of increasing amounts of haze in the

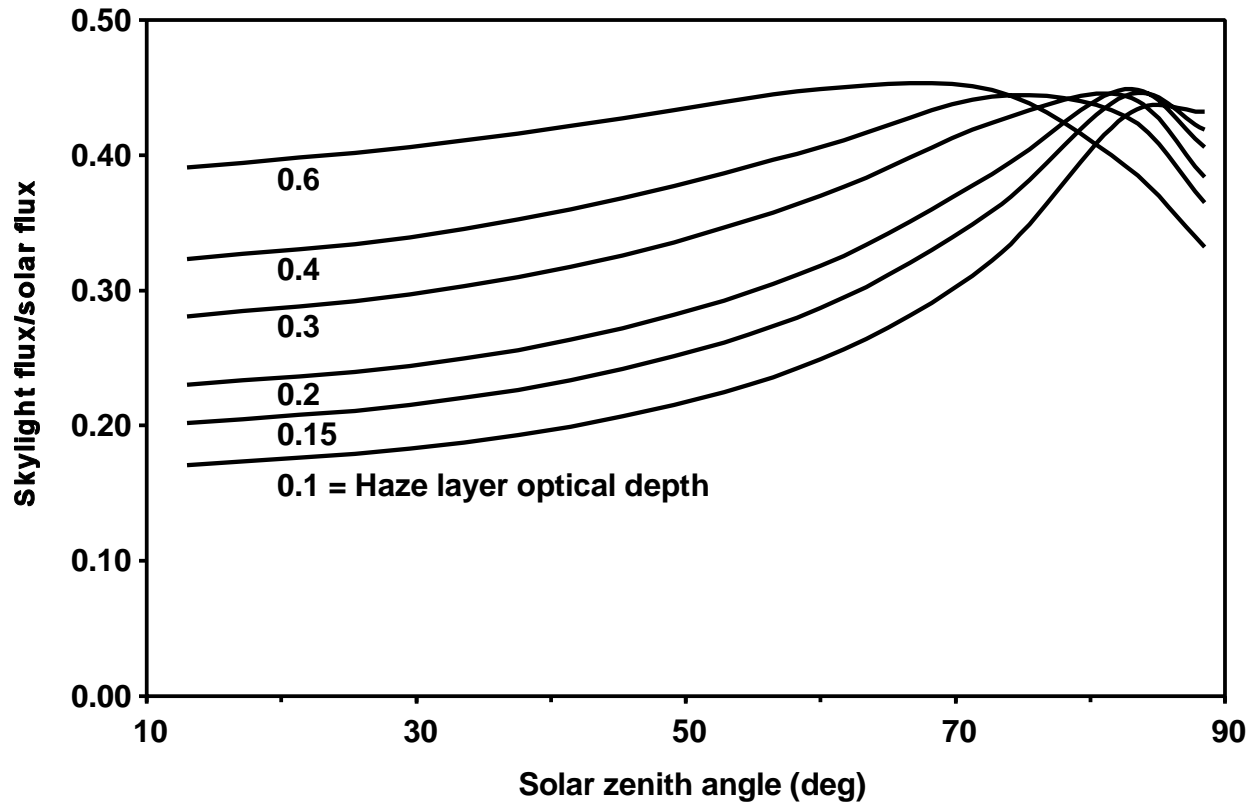


**Figure 8-4.** Data for the ratio of the total flux of skylight  $F_{\text{skylight}}$  incident of the earth's surface to the solar flux  $F_0 \cos \theta$  on a horizontal surface at the top of the atmosphere. These data are a function of the solar zenith angle and the optical depth of the haze layer, which is the bottom of four layers used to represent the atmosphere.

Source: Richards et al. (1986).

bottom layer of the atmosphere. The amount of haze is measured by the optical depth, defined in Equation 8-9.

The aerosol in the bottom layer is composed of fine, coarse, and carbon particles with the same physical and optical properties as the bottom haze layer described by Richards et al. (1986). The relative volume concentrations of fine, coarse, and carbon aerosol are 46, 51, and 3%, respectively. The relative contributions to the light-extinction coefficients are 75, 12.5, and 12.5%, respectively. These proportions were kept constant as the total aerosol concentration was changed to vary the optical depth of the haze,  $\tau_h$ .

The ordinate in Figure 8-4 is the total flux of skylight incident on the Earth's surface divided by the total flux of sunlight incident on a horizontal surface at the top of the

atmosphere,  $F_0 \cos \theta$ . Equation 8-10 can be used to relate the solar flux at the Earth's surface,  $F_s$ , to the solar flux at the top of the atmosphere

$$F_s = F_0 e^{-(\tau_3 + \tau_h / \cos \theta)} \quad (8-17)$$

where  $\tau_3$  is the optical depth of the top three layers of the atmosphere used in the calculations (Richards et al., 1986). The optical depth is equal to 0.50, 0.134, and 0.079 at wavelengths of 370, 550, and 650 nm, respectively. These fluxes are for surfaces normal to the solar rays.

Equations 8-15 and 8-16 can be used to evaluate the relative roles of the factors that determine the source function, and hence the horizon sky radiance and path radiance (defined below). The role of the single scattering albedo defined in Equation 8-6 is immediately apparent; light absorption darkens the horizon sky by an amount proportional to the decrease in the single scattering albedo. The relative importance of (1) the direct solar radiation, (2) skylight, and (3) light reflected from the ground can also be evaluated. Table 8-2 presents data showing that light reflected from the ground always makes a significant contribution to the source function, and that sometimes this contribution is dominant. Past reviews of the optics of visibility have not adequately recognized the role of light reflected from the surface of the Earth. Mariners have long known that land over the horizon can be detected by the change in color of the horizon sky (U.S. Naval Oceanographic Office, 1966).

These calculations are simplified in the case of a uniformly overcast sky. In this case, the direct solar flux on the sight path measured normal to the solar rays,  $F_s$ , in Equations 8-15 and 8-16 is equal to zero, and these equations can be combined to obtain

$$I_e = (\omega_0 / 2\pi) (1 + \alpha) F_- \quad (8-18)$$

where  $F_-$  is the downward flux of diffuse light from the cloud layer. The ratio of the source function to the downward flux depends on the single scattering albedo and the diffuse reflectance albedo.

**TABLE 8-2. RELATIVE IMPORTANCE OF LIGHT FROM GROUND, SKY, AND SUN IN CONTRIBUTING TO THE SOURCE FUNCTION AND THE PATH RADIANCE WHEN THE ABSORPTION IS NEGLIGIBLE AND THE NORMALIZED PHASE FUNCTION HAS A VALUE OF 0.4.**

Conditions		Ratio of Source Function to Sunlight Flux (%) $100 I_0/F_s$	Percentage of Source Function or Path Radiance Due to Light from the		
Ground Reflectance $\alpha$	Ratio of Sky Light to Sunlight $F/F_s$		Ground	Sky	Sun
0.10	0.10	6.53	26.83	24.39	48.78
0.15	0.10	7.40	35.48	21.51	43.01
0.20	0.10	8.28	42.31	19.23	38.46
0.40	0.10	11.78	59.46	13.51	27.03
0.80	0.10	18.78	74.58	8.47	16.95
0.10	0.20	8.28	23.08	38.46	38.46
0.15	0.20	9.23	31.03	34.48	34.48
0.20	0.20	10.19	37.50	31.25	31.25
0.40	0.20	14.01	54.55	22.73	22.73
0.80	0.20	21.65	70.59	14.71	14.71

$F_d$  = the flux of diffuse light incident on the Earth's surface.  
 $\alpha$  = diffuse reflectance albedo.  
 $I_0$  = source function for a ray of radiance.  
 $F_s$  = the direct solar flux on the sight path measured normal to the solar rays.

Source: Richards (1988).

The equations in this section provide the basis for the radiative transfer calculations required to understand visibility as defined by the clarity (transparency) and color fidelity of the atmosphere (see Section 8.1.2).

The equations apply to a single wavelength; radiative transfer calculations must be performed for a representative series of wavelengths for a complete description of visibility. However, it would be compatible with current practice to perform these calculations only for one wavelength of green light, such as 500 nm or 550 nm, to determine the visibility. When addressing practical problems, it is essential to adequately address the strong temporal and spatial variations in the illumination and the optical properties of the atmosphere.

### 8.2.5 Transmitted Radiance Versus Path Radiance

The appearance of a distant object is determined by light from two sources. One source is the light reflected from the object itself. This reflected light is attenuated by scattering and absorption as it travels through the atmosphere toward the observer. The portion that reaches the observer is the transmitted radiance,  $I_t$ . These processes are illustrated in the top panel in Figure 8-5, where an observer looks at a distant hillside illuminated by direct sunlight, diffuse skylight, and light reflected from the surrounding terrain. The horizontal black bar indicates the light reflected from the hillside into the sight path. The small arrows pointing away from this bar indicate that some light is scattered into other directions. The decrease in the transmitted radiance with distance along the sight path caused by scattering and absorption is indicated by the horizontal bar becoming narrower as the distance increases.

The other source of light seen by the observer is the intervening atmosphere. During the daytime, the sight path is illuminated by the direct rays of the sun, diffuse skylight, light that has been reflected from the surface of the Earth, etc. This is indicated in the bottom panel of Figure 8-5 by the small arrows pointing toward the sight path. Some of this illumination is scattered by the air and particulate matter in the sight path toward the observer. The horizontal bar in the lower panel indicates the path radiance,  $I_p$ , which is an accumulation of this light scattered into the sight path. The width of the horizontal bar indicates that the path radiance has a value of zero at the start of the sight path at the hillside and increases with increasing distance along the sight path. Not all of the light scattered into the sight path reaches the observer. Some is absorbed and some is scattered into other directions as indicated by the small arrows pointing away from the sight path. Because the path radiance arises in the atmosphere, it is sometimes referred to as air light. The radiance seen by the observer looking at the hillside is the sum of the transmitted radiance and the path radiance.

The transmitted radiance carries the information about the object; this is the radiance which tells us what the object looks like. The path radiance only carries information about the intervening atmosphere and is often quite featureless. In a dense fog, the transmitted radiance from nearby objects can be seen, but the transmitted radiance from more distant

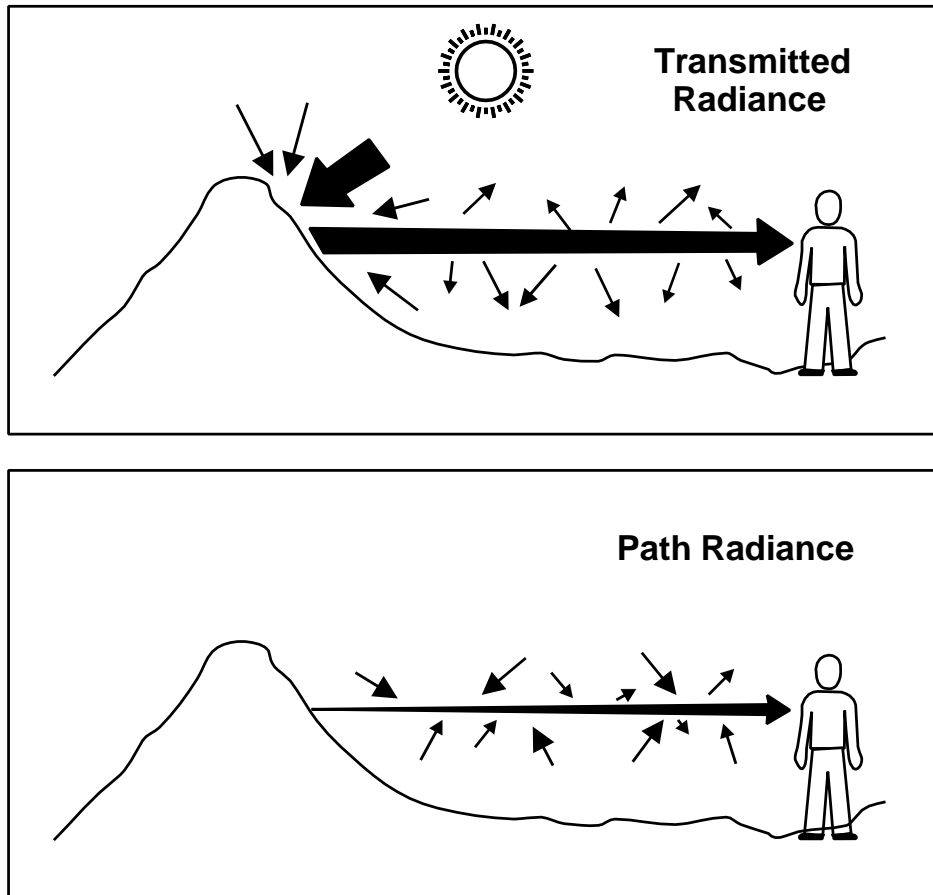


**Figure 8-5. (A) Illustration of the transmitted radiance and (B) the path radiance for a sight path toward a hillside.**

objects is completely overwhelmed by the path radiance, i.e., the light scattered by the fog. Distant objects are lost in the white (or gray) of the fog.

Visibility is determined by the competition between the transmitted radiance and the path radiance. The effects of this competition can be observed anytime the sun is low in the sky. Distant hillsides viewed toward the sun appear to be silhouettes; all details on their surface are lost in the haze. The reason is that the hillsides are in a shadow and, therefore, are dark. Only a small amount of light is reflected from them, so the transmitted radiance is small and is easily overwhelmed by the path radiance. Hillsides at a similar distance viewed looking away from the sun clearly show the details of trees, gullies, grass patches, etc. A large amount of light is reflected from these hillsides because they are sunlit, so the transmitted radiance is large. These effects can also be observed when portions of a scene

are shadowed by clouds and adjacent portions are sunlit. Cloud shadows on the atmosphere decrease the path radiance and improve the ability to see distant objects, but shadows on the objects themselves decrease the transmitted radiance and make it more difficult to see details in those objects. With practice, a discerning observer can visually evaluate the separate effects of the transmitted radiance and the path radiance on the appearance of a scene.

The remainder of this subsection presents a mathematical description of these effects. The radiance transmitted from an object at a distance  $x$  is equal to the initial radiance,  $I_o$ , of that object (measured at the object) multiplied by the transmittance,  $T$ , of the atmosphere in the sight path (see Equation 8-10).

$$I_t = I_o T = I_o e^{-\tau} \quad (8-19)$$

In general, the value of the light-extinction coefficient will not be uniform over the sight path, and this should be accounted for in the calculation of the optical depth (see Equation 8-9).

The completely general calculation of the path radiance requires solving the equation of radiative transfer for the atmosphere. However, if the illumination and optical properties of the atmosphere were uniform over the sight path, the path radiance could be calculated from the equation

$$I_p = I_e (1 - T) . \quad (8-20)$$

Equations 8-19 and 8-20 are typically used to calculate photographic images that show the effects of haze (see, for example, Equations 1 and 2 in Molenaar et al., 1994). With rare exceptions, the calculations used to generate photographic images assume that the atmosphere is uniform.

The apparent radiance,  $I$ , is the radiance that enters the eye of an observer or the aperture of a measurement instrument, and is the sum of the transmitted and path radiance.

$$I = I_t + I_p \quad (8-21)$$

The radiances from these two sources must be considered in all visibility calculations. As stated above, it is the competition between the transmitted radiance and the path radiance that determines the visibility.

Because of the role of the path radiance in determining visibility, and because the path radiance is strongly influenced by the illumination of the sight path, daytime visibility is inextricably linked to the illumination of the atmosphere. A knowledge of the atmospheric optical properties alone (e.g., the value of the light-extinction coefficient) is not adequate to predict the visibility. These ideas are quantified in the next section, where contrast and contrast transmittance are used as measures of visibility.

### **8.2.6 Contrast and Contrast Transmittance as Quantitative Measures of Visibility**

It is standard practice in science to define numerical scales that can be used to quantify observations. Because of the properties of human vision described in Section 8.1.3, contrast provides a numerical scale that can be used to quantify visibility. When investigating the ability to perceive faint objects, the use of contrast to quantify visibility is based directly on Weber's law and experiments with perception thresholds (see, for example, Blackwell, 1946). Contrast is defined in Equation 8-1 in Section 8.1.3.

The contrast of a distant object is determined by its initial contrast,  $C_o$ , and the contrast transmittance of the atmosphere,  $C/C_o$ . The definition of contrast transmittance is analogous to the definition of the transmittance. If  $C$  is the apparent contrast, i.e., the observed or measured contrast at the end of the sight path, and  $C_o$  is the initial contrast, i.e., the contrast at the start of the sight path, then

$$\text{Contrast transmittance} = C/C_o. \quad (8-22)$$

Modulation is defined in Equation 8-2 in Section 8.1.3. If  $M$  is the apparent modulation and  $M_0$  the initial modulation, then

$$\text{Modulation transfer} = M/M_0. \quad (8-23)$$

As indicated by Equation 8-3, modulation and contrast can be used interchangeably. Similarly, contrast transmittance and modulation transfer can be used interchangeably. The more familiar contrast and contrast transmittance are used in this chapter.

The contrast transmittance of the atmosphere in the sight path to a distant object largely determines whether or not that object can be perceived. Thus, the quantitative calculation of contrast transmittance plays a key role in the investigation of the perceptibility of distant objects. At these distances, the contrast transmittance of the atmosphere and the apparent contrast of the object can be used to quantify visibility. If these parameters are used for objects at all distances, then the same numerical scales can be used to quantify the visibility of objects at all distances.

The National Park Service used contrast measurements to quantify visibility for approximately a decade beginning in the late 1970s. This monitoring method is continued in the use of photographs and video images to characterize visibility. Computer-generated photographs are often used to demonstrate the visual effects of haze, and they are generated by calculating the contrast transmittance of the atmosphere and the contrast of objects in the scene.

### **8.2.7 Contrast Reduction by the Atmosphere**

Because of the quantitative relationship between visibility and contrast reduction by the atmosphere, the investigation of the effect of the atmosphere on apparent contrasts has a long history, which has been reviewed by Middleton (1952). An early result was obtained by Haecker (1905), who showed that radiance differences are attenuated by the atmosphere to the same degree as the radiance of a single ray. For example, if two objects at the same distance with initial radiances  $I_{10}$  and  $I_{20}$  are viewed through the same sight path, Equations 8-19 and 8-21 give the result that the difference in the apparent radiances is

$$- I_2 = (I_{10}e^{-\tau} + I_{1p}) - (I_{20}e^{-\tau} + I_{2p}) = (I_{10} - I_{20})e^{-\tau} \quad (8-24)$$

For the same sight path, the two path radiances have the same value, and therefore have no effect on the radiance difference. Also, the optical depth is the same for both sight paths. This result is valid regardless of the uniformity of the atmosphere and the illumination. If human perception were controlled by radiance differences instead of radiance ratios (as in the formula for contrasts), optical calculations for visibility analyses would have been greatly simplified.

Equation 8-24 applies to any two adjacent objects viewed through sight paths close enough together to have the same optical depths and path radiances. In the following derivation, this equation is applied to a case in which an object with initial radiance,  $I_o$ , is viewed against a background with initial radiance,  $I_{bo}$ . The definition of contrast in Equation 8-1 and contrast transmittance in Equation 8-22 can be combined to obtain

$$C/C_o = [(I - I_b)/I_b]/[(I_o - I_{bo})/I_{bo}] \quad (8-25)$$

Replacing  $I - I_b$  by the right-hand side of Equation 8-24 and using Equation 8-19 gives the result

$$C/C_o = I_{bo}e^{-\tau}/I_b = I_{bt}/I_b \quad (8-26)$$

In other words, the contrast transmittance of the atmosphere is the transmitted radiance of the background,  $I_{bt}$ , divided by the apparent radiance of the background,  $I_b$ . The role of the path radiance is made more apparent by writing Equation 8-26 as

$$C/C_o = I_{bt}/(I_{bt} + I_p) \quad (8-27)$$

where the apparent radiance of the background is equal to the sum of the background transmitted radiance and the path radiance. Equations 8-26 and 8-27 are completely general and contain no assumptions about the uniformity of the atmosphere or its illumination. They are included in the paper of Duntley et al. (1957), which contains an excellent overview of contrast reduction by the atmosphere.

Exactly the same derivation can be performed using the modulation defined in Equation 8-3 and modulation transfer defined in Equation 8-23 instead of contrast and transmittance. The result is

$$M/M_0 = I_b / (I_{bt} + I_p) \quad (8-28)$$

where  $I_b$  is now the average radiance of the sine wave instead of the background radiance used in the definition of contrast. Equations 8-27 and 8-28 are identical in form and in interpretation.

Equations 8-19 and 8-21 can be used to show the dependence of contrast transmittance and modulation transfer on the variables  $T$ ,  $I_{b_0}$ , and  $I_e$  in cases where the atmosphere and the illumination are uniform over the length of the sight path

$$\begin{aligned} C/C_0 &= I_{b_0} T / [I_{b_0} T + I_e (1 - T)] \\ M/M_0 &= I_{b_0} T / [I_{b_0} T + I_e (1 - T)] \end{aligned} \quad (8-29)$$

The dependence of the  $T$  on the average light-extinction coefficient for the sight path is given by Equations 8-9 and 8-10.

Koschmieder (1924) derived a simple equation for the contrast of distant objects viewed against the horizon sky. He assumed that the radiance of the background horizon sky at the target initial background radiance is the same as at the apparent background radiance, with the result that Equation 8-26 becomes

$$C/C_0 = e^{-\tau} \quad (8-30)$$

This assumption would be valid if the atmosphere and its illumination were uniform, which accounts for the long list of assumptions often associated with discussions of Equation 8-30 (Malm, 1979; U.S. Environmental Protection Agency, 1979). Only the one assumption above is necessary, and that assumption could be valid in a nonuniform atmosphere. If it is further assumed that the target is black, so that  $C_0 = -1$ , Equation 8-30 becomes

$$C = -e^{-\tau} \quad (8-31)$$

but this assumption is not necessary if the value of  $C_0$  is measured or can be estimated with sufficient accuracy (see, for example, Malm et al., 1982). The average value of the light-extinction coefficient for the sight path is equal to the optical depth divided by the length of the sight path (see Equation 8-9). Equation 8-31 can be used to estimate the average value of the light-extinction coefficient from only a measurement of the apparent contrast of a dark object against the sky and the distance to the object. However, the assumptions used in the derivation of Equation 8-31 are generally not satisfied, with the result that the values of the light-extinction coefficient obtained from it may not be appropriate when illumination along the sight path is not uniform (White and Macias, 1987).

The nomogram in Figure 8-6A provides an instructive visualization of the factors that determine the visibility. In this figure, the abscissa is a linear measure of the light transmittance or light extinction. This is a change from Figure 8-3, where the abscissa is linear in distance. This change causes the curves for radiances in a uniform atmosphere to be straight lines instead of exponential curves.

The lines at the left side of Figure 8-6A show the radiances measured at the target. The initial radiance of the background (used in the calculation of contrast) measured at the target is  $I_{b0}$ . The path radiance is equal to zero. As the distance from the target increases, the initial radiance of the background and the transmittance decreases linearly towards zero. By definition, this line is always straight. With increasing distance, the path radiance (air light) typically increases. If the atmosphere were uniform, Equation 8-20 could be used to

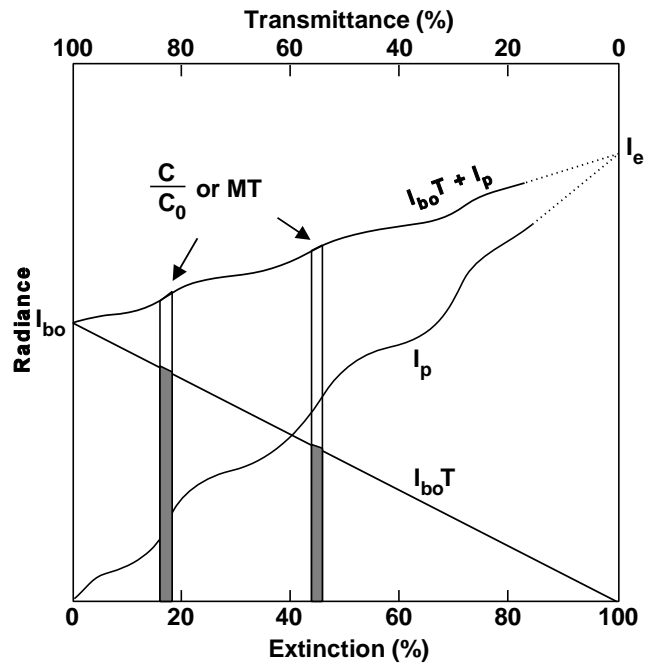
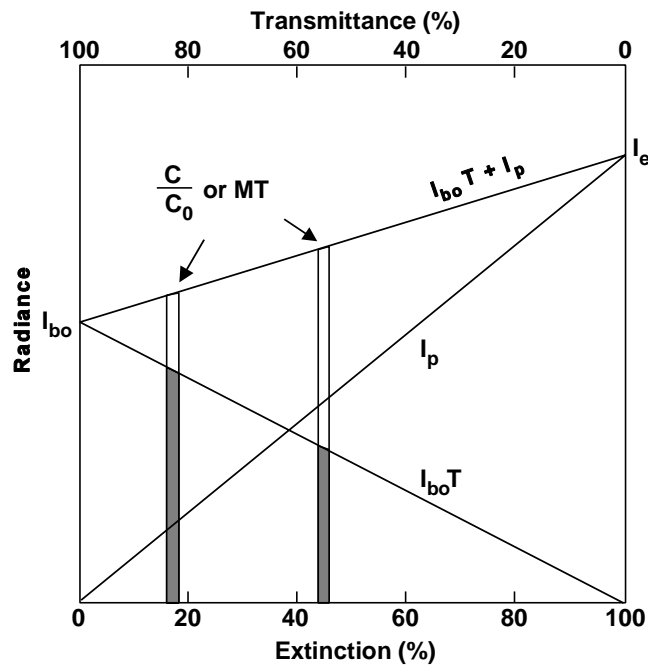


**Figure 8-6. (A) Nomogram for the estimation of the contrast transmittance in a uniform region of the atmosphere; (B) Nomogram for the estimation of contrast transmittance in a nonuniform atmosphere. In a nonuniform atmosphere, the curve representing the path radiance will typically not be a straight line.**

Source: Richards (1990).

calculate the path radiance, and the values would form a straight line as in Figure 8-6A. When the distance from the target becomes sufficiently great (which is possible in the Earth's atmosphere only for relatively large values of the light-extinction coefficient, the transmitted radiance becomes zero and the path radiance becomes equal to the source function, as at the right edge of the figure. This condition is easily observed in dense fogs.

The apparent radiance is equal to the sum of the transmitted and path radiances, and is shown by the upper line in the figure. The contrast transmittance can be calculated at any place in the figure by drawing a vertical line between the x-axis and the apparent radiance. The contrast transmittance is the fraction of the line due to the transmitted radiance. These fractions are illustrated by the shaded portions of the vertical lines in Figure 8-6A.

This nomogram shows how the relative values of the initial background radiance used to calculate contrast and the source function interact with the transmittance of the sight path to determine the contrast transmittance of a sight path, i.e., the visibility. When the initial background radiance is small compared to source function, the transmitted radiance rather quickly becomes a small part of the apparent radiance, and the visibility in that sight path is rapidly degraded by increasing light extinction. However, if the initial background radiance is much larger than source function, as is the case for snowcapped mountains, the transmitted radiance is not so quickly dominated by the apparent radiance as the light extinction in the sight path increases. Sometimes, snowcapped peaks at a distance appear to float in the sky because the transmitted radiance from the dark mountainsides below the snow line is completely dominated by the path radiance, making the dark mountainsides invisible.

The initial and apparent background radiances may be assigned to different parts of the scene in different calculations. If the contrast of an object against the horizon sky is to be calculated, the background is the horizon sky. When the horizon sky radiance is approximately equal to the source function, initial background radiance is approximately equal to the source function. However, if the contrast of a feature on a hillside, such as a tree or a rock, is to be calculated, then the background is the hillside. In this case, it is necessary to determine the ratio of the initial radiance of the hillside to the source function. In cases where the horizon sky radiance is approximately equal to the source function, this ratio is equal to the initial contrast used in contrast teleradiometry. Data for these initial contrasts have been tabulated for a range of types of ground cover and illumination (Malm et al.,

1982). These data provide an acceptable basis for estimating values of the background initial radiance/source function when measurements are not available.

The nomogram for a nonuniform atmosphere is shown in Figure 8-6B. Because the source function varies along the sight path, the path radiance does not vary linearly with the light extinction. This is indicated by the curve in Figure 8-6B. Regardless of the form of the curve for the path radiance, the apparent radiance is the sum of the transmitted and path radiances and the contrast transmittance is the transmitted radiance divided by the apparent radiance. Therefore, the calculations represented in the nomogram remain exactly valid for any curve representing the dependence of the path radiance on the fraction of the initial radiance removed by light extinction along the sight path. If the curve for the path radiance is properly calculated, the relations shown by the nomogram in Figure 8-6B are exact and contain no approximations.

### **8.2.8 Relation Between Contrast Transmittance and Light Extinction**

The light-extinction coefficient determines the transmittance of a sight path (see Equations 8-9 and 8-10). The nomogram in Figure 8-6A shows that the transmittance provides a reasonable estimate of the contrast transmittance only when the initial radiance of the background is approximately equal to the source function (or equilibrium radiance). The only situation where this approximation is reliable enough to be useful is for a target viewed against the horizon sky when it is hazy enough that the horizon sky radiance is approximately equal to the source function. The southern and eastern United States have many days that are hazy enough to satisfy this criterion, so the use of the light-extinction coefficient as a measure of visibility frequently gives a satisfactory indication of the perceptibility of targets against the sky in those locations. However, the light-extinction coefficient may not provide a satisfactory indication of the perceptibility of features viewed against other backgrounds (e.g., trees on a hillside), because the radiances of other backgrounds will not, in general, be approximately equal to the source function.

Data for both the transmittance and modulation transfer of a sight path were measured during the Southern California Air Quality Study (SCAQS) (Richards, 1989) and are shown in Figure 8-7. Modulation and modulation transfer were used to present these data because the white and black pattern of the target were more like the sine wave pattern in Figure 8-1

than the pattern in that figure used to define contrast. It is shown in Equation 8-28 that the modulation transfer is mathematically equivalent to the contrast transmittance. It is apparent that the data for modulation transfer in Figure 8-7 are poorly correlated with the sight path transmittance. In particular, when the sight path transmittance was 50%, the modulation transfer varied from 5 to 70%. When the modulation transfer was 5%, the target was barely perceptible. A modulation transfer of 70% corresponds to the visibility for a 30-km (19-mi) sight path through particle-free air under conditions where the Koschmieder equation is valid. Thus, at the same value of the light-extinction coefficient, the visibility ranged from excellent to nearly obscured. However, the inability of the light-extinction coefficient to represent the perceived visibility of any specific scene does not affect its ability to characterize the visual effects on a sensitive scene caused by the combination of air pollutants and relative humidity. The data points in Figure 8-7 are scattered in the vertical direction, and do not tend to cluster along a simple relationship between modulation transfer and transmittance.

The lack of correlation between modulation transfer and light extinction in Figure 8-7 shows that the light-extinction coefficient does not, in the general case, provide a reliable quantitative measure of the visibility and specifically not under conditions of varying illumination. When using airport visibility data to estimate values for the light-extinction coefficient, it is common practice to select only midday data. This practice minimizes variations in the illumination of the atmosphere, and would reduce the variability of the data in plots such as Figure 8-7.

On the other hand, the light-extinction coefficient is an optical property of each point in the atmosphere and is closely linked to air quality. It also plays a key role in radiative transfer calculations. However, although the light-extinction coefficient is a key input to visibility calculations, it does not, by itself, provide a reliable quantitative measure of the degree to which the atmosphere is transparent to visible light under varying illuminations.

### **8.3 OPTICAL PROPERTIES OF PARTICLES**

The 1978 report on the technical basis for visibility protection in Class I areas that was prepared for the Council on Economic Quality stated, "From a scientific and technical point of view, the optical effects of particles are also the best understood and most easily measured

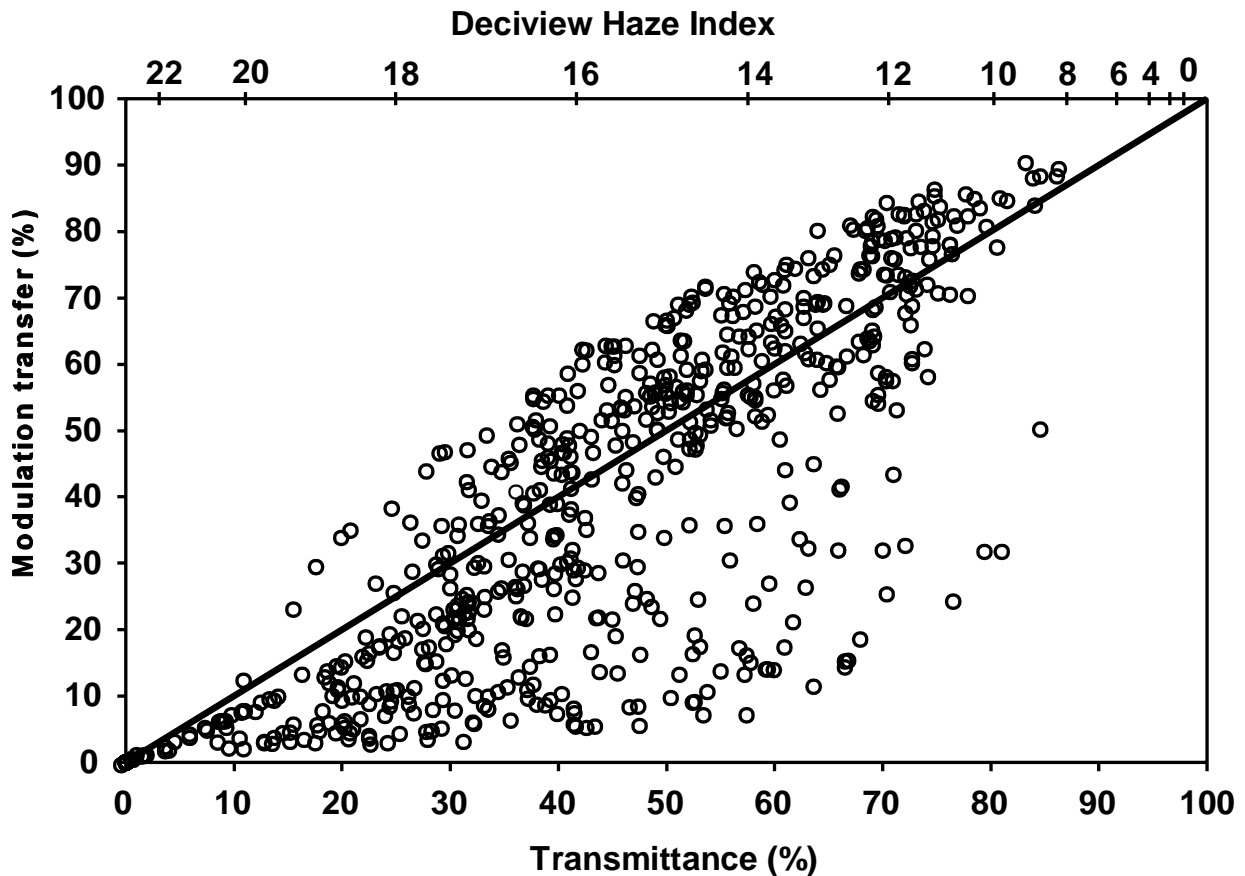


**Figure 8-7. Hour-average values of the modulation transfer and transmittance measured in a 2.20-km sight path during the 1987 summer intensive of the Southern California Air Quality Study. These data show that the modulation transfer (and contrast transmittance) are poorly correlated with the light-extinction coefficient. At 50% transmittance ( $\sigma_{\text{ext}} = 315 \text{ Mm}^{-1}$ ), the visibility ranged from excellent to nearly obscured. The scale at the top shows the value of the deciview haze index, an index of haze that is scaled to correspond to properties of human vision.**

Source: Richards (1989).

effects of air pollution." (Charlson et al., 1978). There was much truth in that statement, but since then, significant advances have been made in the understanding of the physical, chemical, and optical properties of fine particulate matter. At the present time, this is an active area of research and an area where significant future advances can be expected.

### 8.3.1 Optical Properties of Spheres

Fine particles, which are typically the dominant cause of visibility impairment, are small enough in comparison with the wavelength of visible light that their optical properties are nearly the same as those of homogeneous spheres of the same volume and average index of refraction. This approximation is good enough that by far the greatest uncertainty in using light-scattering equations for homogeneous spheres to calculate the optical properties of fine particles is due to uncertainties in their size distribution. Uncertainties in the index of refraction, due to lack of knowledge of the detailed particle composition, is the next greatest source of uncertainty in these calculations.

These assertions are supported by an example from the pigment industry. Titanium dioxide ( $\text{TiO}_2$ ), the universally used white pigment, has a size distribution similar to atmospheric fine particles. Titanium dioxide particles are crystalline, and therefore have angular shapes. Titanium dioxide is birefringent, i.e., has different indices of refraction for different directions in the crystal. The size distribution of  $\text{TiO}_2$  samples can be estimated by measuring the size of 1000 particles in an electron micrograph. Alternatively, it can be estimated by measuring the light-extinction coefficient as a function of wavelength for a dilute suspension and comparing the result with theoretical curves calculated assuming the particles were homogeneous spheres. It was found that one light-extinction spectrum gave a better estimate of the size distribution determined from repeated counts of 1000 particles than did one count of 1000 particles (Richards, 1973). A knowledge of the size distribution is key to calculating the optical properties of fine particles.

The equations for calculating the optical properties of homogeneous spheres in the size range of atmospheric particles are known as the Mie equations (Mie, 1908), but Lorenz, Debye, and others made substantial contributions to this theory (Kerker, 1969). The only inputs to these calculations are the particle-size parameter  $\alpha = \pi D/\lambda$ , where  $D$  is the particle diameter and  $\lambda$  is the wavelength of light, and the ratio of the index of refraction of the particle to the index of refraction of the medium surrounding the particle. For collections of particles, it is assumed that there is no phase coherence in the scattering by neighboring particles, so that the intensity of the light scattered by an ensemble of particles is the sum of the intensities scattered by the individual particles. Therefore, the optical properties of atmospheric particles are calculated by representing the aerosol particle-size distribution by a

histogram, performing Mie calculations for each particle-size bin in the histogram, weighting the results by the amount of aerosol in each bin, and calculating the sum.

The output of the Mie calculations includes efficiency factors for extinction, scattering, and absorption,  $Q_{\text{ext}}$ ,  $Q_{\text{scat}}$ , and  $Q_{\text{abs}}$ , respectively. These factors give the fraction of the incident radiation falling on a circle with the same diameter as the particle that is either scattered or absorbed, only scattered, or only absorbed, respectively. Figure 8-8A shows the scattering efficiency factor for a sphere with an index of refraction of 1.5 as a function of the size parameter,  $\alpha$ . Many fine aerosol particles have an index of refraction near this value. Because of diffraction, all particles with an index of refraction of 1.5 and a size parameter larger than about 1.6 scatter more radiation than falls on the geometrical cross section of the particle. The scattering efficiency factor tends toward a value of 2.0 for large particles.

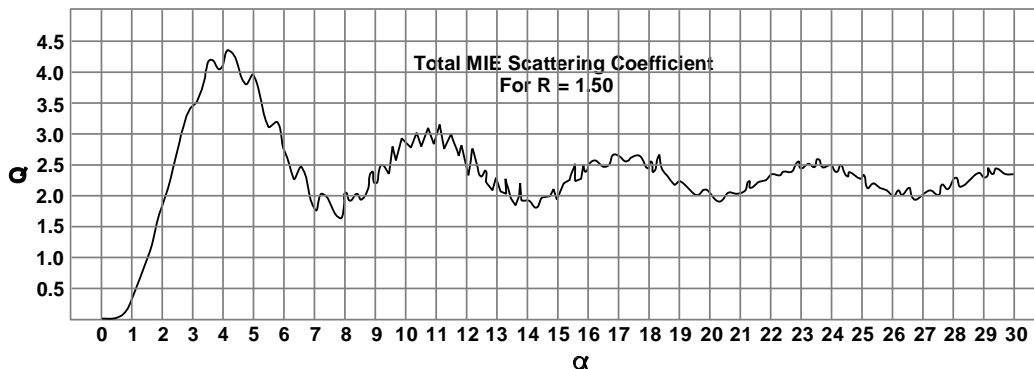


**Figure 8-8a. Light-scattering efficiency factor for a homogeneous sphere with an index of refraction of 1.50 as a function of the size parameter  $\alpha = \pi D/\lambda$ .**

Source: Penndorf (1958).

The major oscillations and ripples in the curve in Figure 8-8A are typical. The data in Figure 8-8B show that when the size parameter is scaled by the index of refraction minus 1, scattering efficiency factors for a range of indices of refraction fall in a narrow range of efficiency factors. The index of refraction range extends from water ( $n = 1.33$ ) to a reasonable value for dry fine particulate matter ( $n = 1.5$ ). For example, Hering and McMurry (1991) found that calibration of an optical particle counter with oleic acid, with an

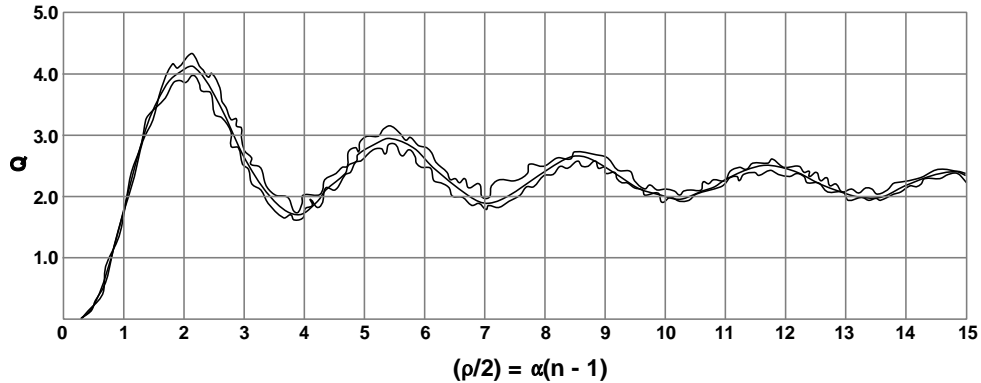


**Figure 8-8b. Maximum and minimum values for light-scattering efficiency factors for homogeneous spheres with indices of refraction between 1.33 and 1.50 as a function of the normalized size parameter.**

Source: Penndorf (1958).

index of refraction of 1.46, gave better results than did calibration with polystyrene latex spheres, with an index refraction of 1.59, for monodisperse samples of Los Angeles aerosol obtained from a differential mobility analyzer. Thus, within the range of indices of refraction that most commonly occur in atmospheric fine particles, the results of Mie calculations can be scaled to account for the effect of the index of refraction.

Figure 8-9 shows the same data as in Figure 8-8b, except that the scattering efficiency factor  $Q$  was multiplied by the cross section of the sphere to obtain the scattering cross section and divided by the volume of the sphere to obtain the volume-specific light-scattering efficiency factor,  $E_v$ , in units of  $\mu\text{m}^{-1}$ . A wavelength of 550 nm was assumed in these calculations. Multiplying the values of the light-scattering efficiency factor by the aerosol volume concentration (in units of  $\mu\text{m}^3/\text{cm}^3$ ) gives the value of light-scattering coefficient,  $\sigma_{sp}$ , (in units of  $\text{Mm}^{-1}$ ) for these particles. Thus, the curves in Figure 8-9 gives the light-scattering coefficient for a unit concentration of aerosol if all particles have the same diameter and index of refraction.

Dividing the curves in Figure 8-9 by the density of the particulate material (in units of  $\text{g}/\text{cm}^3$ ) gives the mass-specific light-scattering efficiency,  $E_m$  (in units of  $\text{m}^2/\text{g}$ ). Multiplying the values of the mass-specific light-scattering efficiency by the aerosol mass concentration (in units of  $\mu\text{g}/\text{m}^3$ ) gives the value of the light-scattering coefficient (in units of  $\text{Mm}^{-1}$ ) for these particles. Thus, the mass-specific light-scattering efficiency for water, which has an

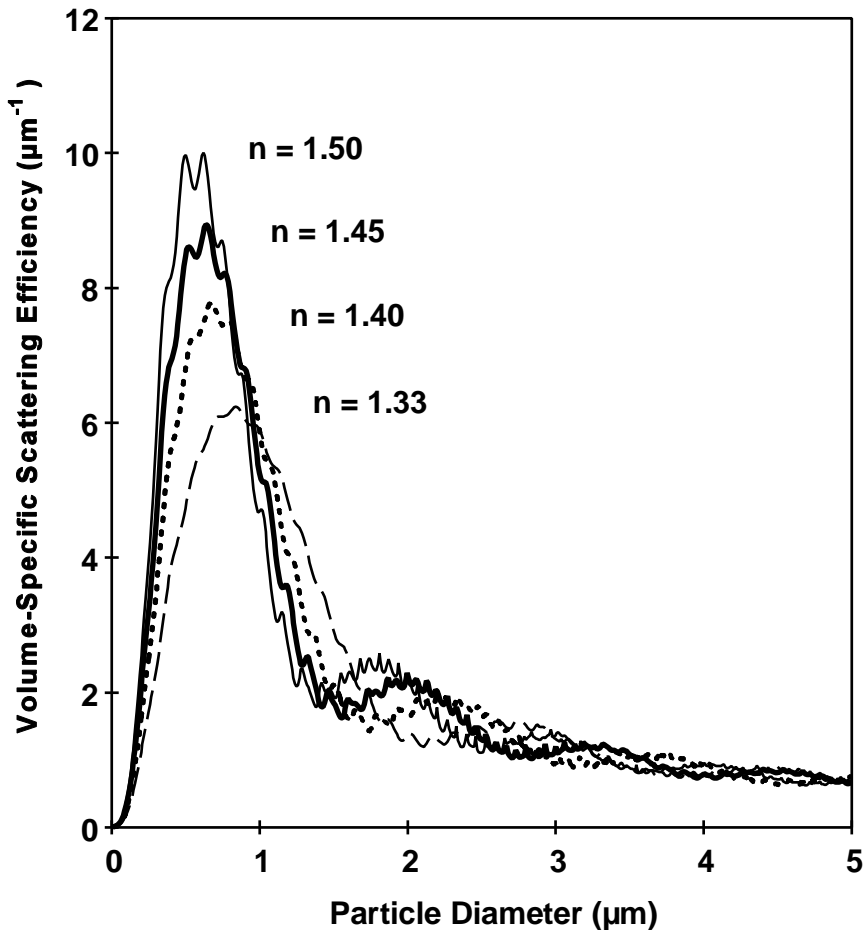


**Figure 8-9.** Volume-specific light-scattering efficiency as a function of particle diameter  $D_p$ . The calculations were performed for the indicated indices of refraction and a wavelength of 550 nm. For large particle diameters the scattering efficiencies tend toward a value of  $3/D_p$ . Mass-specific light-scattering efficiencies (in units of  $m^2/g$ ) can be obtained by dividing the values of the curves by the particle density (in units of  $g/cm^3$ ).

index of refraction of 1.33 and a density of 1.0, is shown by the curve for  $n = 1.33$  in Figure 8-9. Ammonia salts have a density near  $1.75 g/cm^3$  and an index of refraction near 1.5, so the mass-specific light-scattering efficiency for these compounds can be obtained by dividing the curve for  $n = 1.5$  in Figure 8-9 by  $1.75 g/cm^3$ . The maximum value for mass-specific light-scattering efficiency for both water and ammonia salts is close to  $6 m^2/g$ .

The particle diameter at the maximum light-scattering efficiency for green light with a wavelength of 550 nm is approximately given by the relationship

$$D = 0.28 / (n - 1) \mu\text{m} \quad (8-32)$$

although the exact value depends on the ripples in the curve. This formula gives a diameter of  $0.85 \mu\text{m}$  for an index of refraction of 1.33 and a diameter of  $0.56 \mu\text{m}$  for an index of refraction of 1.5. Most fine aerosol particles are smaller, so it is generally true that processes which tend to increase the size of fine particles tend to increase their scattering efficiency. The absorption of water at high humidity is an example of such a process.

The Mie equations can also be used to calculate the efficiency factors for light absorption by particles. The results of these calculations contain significant uncertainties because (1) the imaginary component of the refractive index of the particles is usually not accurately known, and (2) light-absorbing particles are frequently chained agglomerates that do not have a spherical shape. In some aerosol particles, light absorption is caused by elemental carbon particles coated with chemical species that absorb light much less strongly (see, for example, Husar et al., 1976). For these reasons, the theoretical calculation of the strength of light absorption by atmospheric particles is significantly less reliable than the calculation of light scattering.

Computer codes are available for calculating the light scattering and light absorption by particles composed of a spherical core and a concentric shell (Toon and Ackerman, 1981; Appendix B of Bohren and Huffman, 1983; Kerker and Aden, 1991). These codes are used to determine the optical properties of particles with a solid core and a liquid shell, which can be formed by the absorption of water at high humidities by particles that contain insoluble species. A core-and-shell particle can also be formed by condensation and coagulation of materials of one refractive index on pre-existing particles that have a different refractive index.

The data for the volume-specific light-scattering efficiency for particles of one size in Figure 8-9 can be made more useful by averaging the values for log-normal size distributions. Results from such calculations are presented in Figure 8-10. As before, the calculations are performed for a wavelength of 550 nm. A value of 2.0 was used for the sigma of the log-normal size distributions, and the scattering efficiency was calculated as a function of the geometric mean diameter,  $D_{gv}$ . For water, the index of refraction is 1.33 and

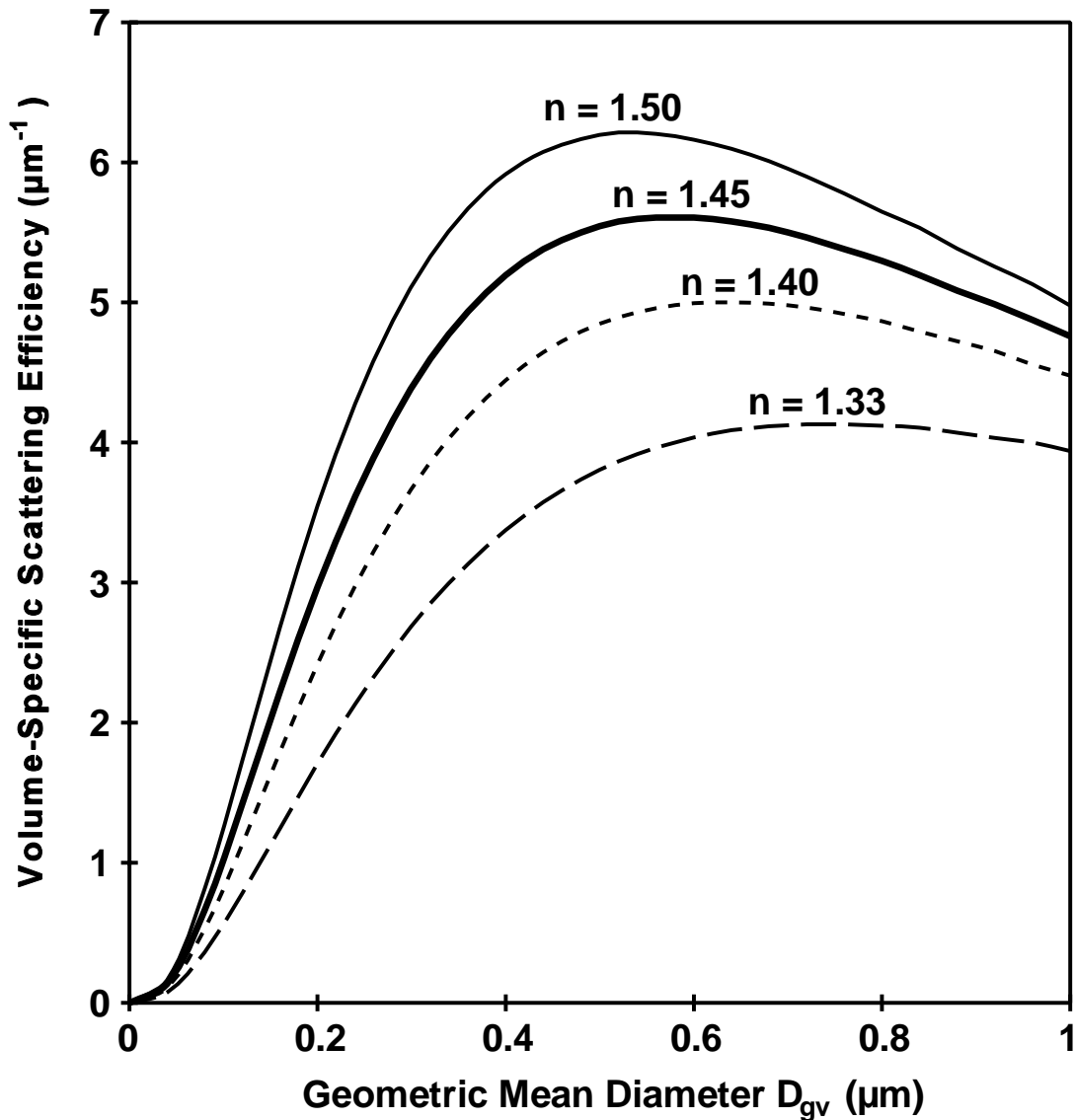


**Figure 8-10.** Volume-specific light-scattering efficiency as a function of geometric mean particle diameter  $D_{gv}$  for log-normal size distributions. The calculations were performed for the indicated indices of refraction, a wavelength of 550 nm, and size distributions with a sigma of 2.0. Mass-specific light-scattering efficiencies (in units of  $\text{m}^2/\text{g}$ ) can be obtained by dividing the values of the curves by the particle density (in units of  $\text{g}/\text{cm}^3$ ).

the maximum volume-specific scattering efficiency of  $4.1 \mu\text{m}^{-1}$  occurs at a geometric mean diameter of  $0.74 \mu\text{m}$ . For the index of refraction of 1.5, the maximum volume-specific scattering efficiency of  $6.2 \mu\text{m}^{-1}$  occurs at a geometric mean diameter of  $0.53 \mu\text{m}$ . If these particles had a density of  $1.75$ , then the maximum mass-specific scattering efficiency would be  $3.5 \text{ m}^2/\text{g}$ . The curves in Figure 8-10 show that the scattering efficiency increases rapidly

with increasing particle size in the 0.2- to 0.4- $\mu\text{m}$ -diameter range. The accumulation-mode aerosol is typically in this size range. Therefore, the uptake of water by aerosol particles can cause significant increases in the light-scattering coefficient.

Computer codes to calculate the optical properties of log-normal size distributions of homogeneous spheres can be obtained from the U.S. Environmental Protection Agency Support Center for Regulatory Air Models (SCRAM) by calling 919-541-5742 and downloading the files for the PLUVUE II plume visibility model. The FORTRAN source code is in the file RNPLUVU2.ZIP, code compiled for Intel 386- or 486-compatible computers is in the file RUNPLUVU.ZIP, and the manual is in PLVU2MAN.ZIP. These codes are available at no charge, and the program MIETBL.EXE calculates the normalized phase function and the efficiencies for light scattering, absorption, and extinction. These codes will run on any personal computer with enough speed, memory, and hard drive space to run Microsoft Windows®. If the parameters of the log-normal size distribution and the index of refraction can be satisfactorily estimated, these codes will generate all the information on the optical properties of particles required for the calculations described in Section 8.2.

Coarse particles in the atmosphere are large enough that the effects caused by their non-spherical shape can be detected (see, for example, Holland and Gagne, 1970; Wiscombe and Mugnai, 1988). However, in most actual cases, the dominant uncertainty in using the Mie equations to calculate the optical properties of coarse particles in the atmosphere is due to uncertainties in their size distribution. Therefore, obtaining data for particle-size distributions is more important than determining the shape of coarse particles in the atmosphere.

### **8.3.2 Optical Properties of Fine and Coarse Particles**

Field measurements of the optical properties of fine and coarse particles have produced results compatible with the theoretical results described above. The mass-specific light-scattering efficiency is usually used to report these results. The mass-specific light-scattering efficiency (in units of  $\text{m}^2/\text{g}$ ) multiplied by the particle concentration,  $c$ , (in units of  $\mu\text{g}/\text{m}^3$ ) is equal to the light-scattering coefficient for particles (in units of  $\text{Mm}^{-1}$ ). For these units, no

conversion factor is required. As discussed above, the value of the mass-specific light-scattering efficiency is different for different particle-size fractions.

White et al. (1994) determined the value of  $E_{fp}$ , the scattering efficiency for particles smaller than 2.5- $\mu\text{m}$  diameter, at two sites in the desert southwest and obtained values of 2.4 and 2.5  $\text{m}^2/\text{g}$ . These experiments were unique in that both the light scattering and particulate-mass concentration measurements were made with a 2.5- $\mu\text{m}$ -diameter cutpoint. The relative humidity was generally low, so these values are appropriate for dry particles.

In the same experiments, White et al. (1994) also determined the value of  $E_{cp}$ , the scattering efficiency for coarse particles, and obtained values that ranged from 0.34 to 0.45  $\text{m}^2/\text{g}$ . Earlier, White and Macias (1990) obtained an estimate of 0.4  $\text{m}^2/\text{g}$ . Watson et al. (1991) also obtained a value of 0.4  $\text{m}^2/\text{g}$ . One of the first determinations of the scattering efficiency for coarse particles was by Trijonis and Pitchford (1987), who obtained the value of 0.6  $\text{m}^2/\text{g}$ . In all cases, these authors estimated that the integrating nephelometer responds to approximately half the light scattered by coarse particles (White et al., 1994), so the scattering efficiency for coarse particles observed by the nephelometer would be approximately 0.2  $\text{m}^2/\text{g}$ . This is mentioned here to provide assurance that the values of the scattering efficiency for coarse particles near 0.4  $\text{m}^2/\text{g}$  are not biased by the failure of nephelometers to detect light scattered at angles near 0 and 180 degrees.

A review article by Waggoner et al. (1981) indicates that at moderate or low humidities, the mass-specific light-scattering efficiency, measured by a nephelometer without a size-selective inlet, was equal to  $3.1 \pm 0.2 \text{ m}^2/\text{g}$  using the fine-particle mass concentration. A good correlation was obtained even though the nephelometer measurements included both coarse and fine particles because of the small scattering efficiency of coarse particles. The nephelometer response to all particles reported by White et al. (1994) was 2.8 and 3.1  $\text{m}^2/\text{g}$  times the fine-particle mass concentration at their two sites.

As a general rule, the above values of mass-specific light-scattering efficiencies can be used at moderate to low humidities. The effect of water uptake by particles at high humidities is discussed in Section 8.3.3.

Widely varying mass-specific scattering efficiencies can be observed near sources, in plumes, and in cases where particle formation occurred in clouds and fog. Particles formed in power station plumes in clean areas can be quite small. For example, during the Navajo

Generating Station Visibility Study (NGSVS), a pulse of SO<sub>2</sub> and sulfate from the station was observed at Hopi Point, 100 km from the source. Mie calculations based on the measured size distribution of the sulfate formed in the plume indicated a light-scattering efficiency for ammonium sulfate of 1.2 m<sup>2</sup>/g, and this result agreed with the value determined from the integrating nephelometer readings and the sulfate concentrations determined by filter sampling (Richards et al., 1991). Closer to the source, the sulfate formed in the plume was in still smaller particles with an even smaller light-scattering efficiency (Richards et al., 1981).

Larger light-scattering efficiencies for fine particles have been observed when significant numbers of the particles are in the 0.5- to 1.0- $\mu$ m size range. The measurements of John et al. (1990) provide an example of data for particles in this size range. Secondary particles in this size range are the result of heterogeneous gas-to-particle conversion in fogs or clouds (Meng and Seinfeld, 1994). However, heterogeneous particle formation in fogs or clouds does not always produce large particles. Events in which large amounts of sulfate were rapidly formed in clouds were observed in the NSGVS, and these typically produced sulfate with a smaller mean diameter than the background aerosol (Richards et al., 1991).

Because of the strong dependence of both the light-scattering efficiency and settling velocity of coarse particles on particle size, it would be expected that the light-scattering efficiency of coarse particles in an air parcel would vary with time. In cases where coarse particles are not being added to the air parcel, the light-scattering efficiency of the coarse particles would increase with time.

The great majority of light absorption by particles is caused by elemental carbon (Rosen et al., 1978, Japar et al., 1986). Determinations of the mass-specific light-absorption efficiency of elemental carbon gives values in the range of 9 to 10 m<sup>2</sup>/g (Japar et al., 1984; Adams et al., 1989). A value of 9 m<sup>2</sup>/g has been used in recent studies of urban haze with satisfactory results (Watson et al., 1988, 1991).

### **8.3.3 Effect of Relative Humidity on Particle Size**

Water in the atmosphere exists in both the particle and vapor phases. Great reductions in visibility occur when water condenses to form fog or clouds. Water is also present in all

ambient particles, even on relatively clear days. The increase in the amount of water in the particle phase that occurs at high relative humidity (RH) has a significant effect on visibility.

The effect of water has been understood for many decades, and was one of the key areas of investigation in the Aerosol Characterization Experiment (ACHEX) in California in the 1970s (Hidy et al., 1980). Figure 8-11 shows a summary of Humidogram data measured in several parts of the United States. These data were obtained by comparing the integrating nephelometer signal from an ambient aerosol sample conditioned to 30-% RH with the signal from the same aerosol conditioned to a higher RH (Covert et al., 1980). The increase in light scattering with increasing RH is due to two factors: (1) the absorption of water by the aerosol particles increases the volume of the particle phase, and (2) the absorption of water increases the size of the aerosol particles, which increases the light-scattering efficiency of most particles.

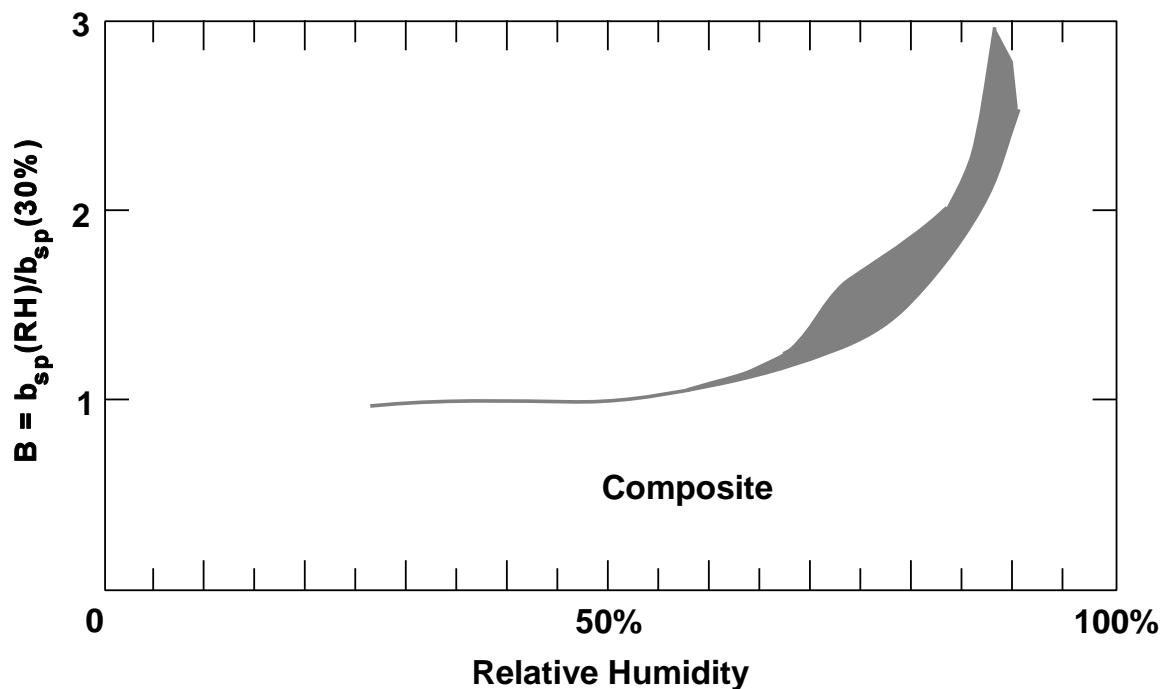


**Figure 8-11. Humidogram showing the dependence of the light-scattering coefficient of ambient aerosol on the relative humidity. The shaded area shows the range of values obtained in various areas of the United States. The vertically hatched area shows data for strongly deliquescent sulfate aerosol observed at Tyson, MO and marine aerosol at Point Reyes, CA.**

Source: Covert et al. (1980).

Ammonium salts are an aerosol component that contribute to the absorption of water at high RH. Figure 8-12 shows the relative diameter of a pure ammonium sulfate particle as a function of RH. At humidities above the deliquescence point of 80%, the particle is a liquid solution, the higher the RH, the more dilute the solution and the larger the particle. When the RH is below 80%, the particle is a dry ammonium sulfate crystal at equilibrium. If the RH of the air surrounding liquid ammonium sulfate decreases through the deliquescence RH, it is necessary for a crystal to nucleate for the conversion from liquid to solid to occur. For pure solutions, this can require either tens of minutes to hours or the reduction of the RH far below the deliquescence point. Thus in ambient air deliquescence particles frequently exist in a non-equilibrium state, containing water even though the RH is below the deliquescence point.

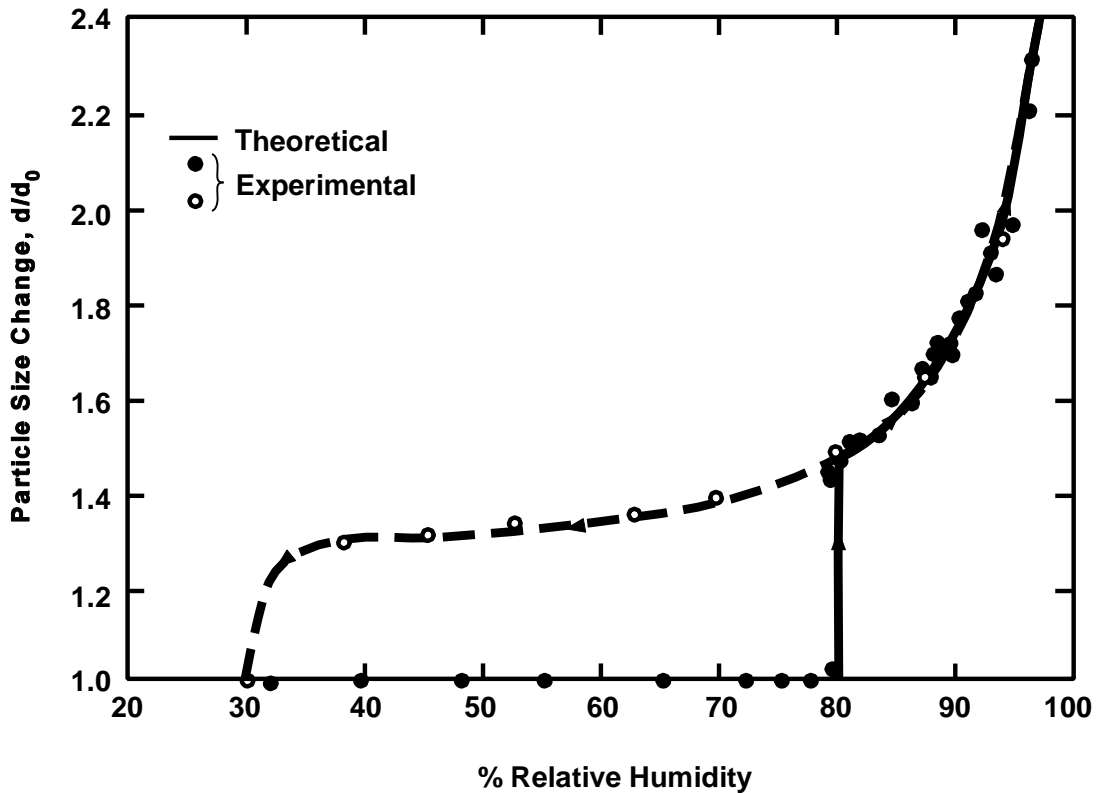


**Figure 8-12.** Relative size growth is shown as a function of relative humidity for an ammonium sulfate particle at 25° C. The dotted line indicates the size of the liquid particles when the RH decreases below the deliquescence point without nucleation of the solid phase.

Source: Tang et al. (1981).

Ambient particles are always a mixture of chemical compounds. Different salts have different deliquescence points, and some aerosol components, such as sulfuric acid and perhaps some organic compounds, have water absorption properties represented by a smooth curve. Therefore, a typical sample of ambient aerosol shows a smooth dependence of light scattering on RH, as shown in Figure 8-11. Figure 8-13 shows data from experiments that can detect the change in size of individual particles in response to a change in RH. These data show that the ambient particles in the Los Angeles Basin tended to fall either in a more hygroscopic class, presumably containing inorganic salts and acids, and a less hygroscopic class, which may be predominantly composed of primary organic species (McMurry and Stolzenburg, 1989). The particles in the desert Southwest tended to grow more with increasing RH, suggesting that ammonium salts are present in most fine particles (Zhang et al., 1993, 1994) and that the organic compounds in the particles are more oxidized (Saxena et al., 1995).

The RH of the atmosphere is nonuniform in both space and time, so the ambient aerosol is continually subjected to cycles of RH. Radiational cooling increases the RH at night near the surface of the Earth, and this tends to increase the haze in the early morning. Also, atmospheric convection frequently cycles the aerosol particles through clouds during the day. Rood et al. (1989) have shown that hysteresis like that shown in Figure 8-12 exists in the atmosphere, so it is reasonable to believe that the ambient particles are commonly on the upper curve, which represents the properties of the particles that have recently been exposed to high values of RH.

Data for the dependence of the particle size of the ambient aerosol on RH have also been obtained by cascade impactor measurements in urban and rural environments, and are in reasonable agreement with the Humidogram in Figure 8-11. Good examples of this type of measurement appear in a report by Watson et al. (1991) and papers by Zhang et al. (1993, 1994). A more detailed discussion of the effects of RH on the size distribution of ambient particles is given in Chapter 3.

#### **8.3.4 Extinction Efficiencies and Budgets**

The attribution of visibility impairment to emission sources can proceed through a series of steps in which the following are determined in sequence: (1) emissions,

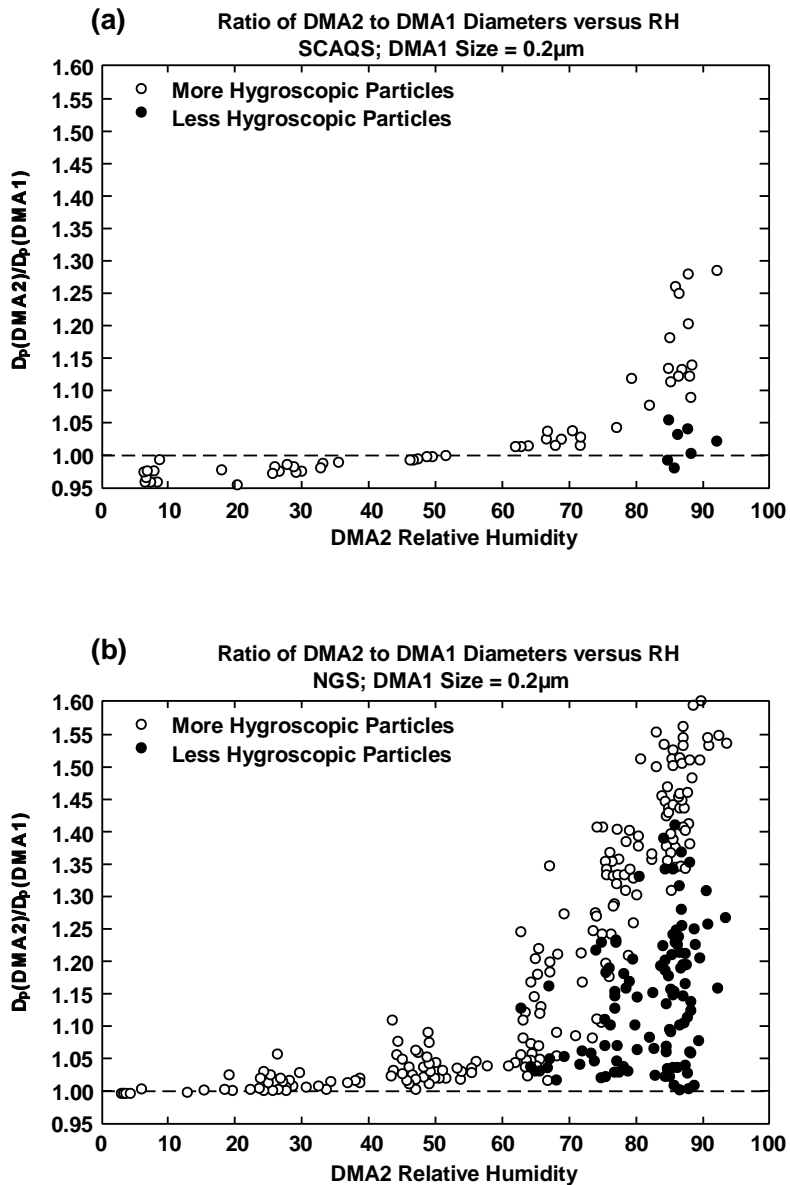


**Figure 8-13. Summary of all relative humidity-dependent particle growth factors for 0.2  $\mu$ m diameter particles measured (a) in Claremont, CA during the SCAQS and (b) at Hopi Point in the Grand Canyon National Park during the Navajo Generating Station Visibility Study.**

Source: McMurry and Stolzenburg (1989); Zhang et al. (1993).

(2) composition of the atmosphere, (3) optical properties of the atmosphere, (4) optical properties of sight paths, and (5) visibility. In principle, the effects of selected emissions can be determined by performing the above analysis steps with and without those emissions.

This section addresses the calculation of the optical properties of the atmosphere from a knowledge of its composition. This is an essential step in the source attribution of visibility impairment. This calculation is also useful in understanding current visibility conditions. Portions of this calculation proceed through simple addition. Section 8.2.3 showed how the optical properties of the atmosphere can be represented as the sum of the components of light extinction. It also indicated that the light-scattering coefficient for particles can be represented as the sum of the scattering by coarse and fine particles. Operationally, the separate contributions of coarse and fine particles to the light-scattering coefficient can be determined by using instruments with size-selective inlets.

It would be convenient if the light-scattering coefficient for fine and coarse particles,  $\sigma_{sfp}$  and  $\sigma_{scp}$ , could each be represented as the sum of the light scattering by the chemical constituents of those particles. Then the components of light extinction could be calculated from

$$\sigma_{sfp} = \sum E_j C_j \quad (8-33)$$

where  $E_j$  is the light-scattering efficiency of fine-particle species  $j$  whose concentration is  $c_j$  and the sum includes all species. Unfortunately, there is no theoretical basis for such a representation, because the light-scattering efficiency depends strongly on the particle size, and changing the atmospheric concentration of one chemical species can change the size distribution of the other particulate species (White, 1986; Sloane, 1986; Sloane and White, 1986).

Simple additive calculations can be justified theoretically only in the hypothetical case of an externally mixed aerosol, in which each particle contains only one chemical species. In this case, the contribution of each chemical species to light extinction can be determined by summing the contributions of the particles of each species. The calculation in Equation 8-33 can be performed on either a particle volume or particle mass basis. The mass basis is customarily used because aerosol mass concentrations are more easily monitored, so most ambient data are for particulate mass concentrations.

In practice, useful approximations exist that allow the estimation of light extinction by ambient particles from the aerosol composition. White (1986) showed that it made little

difference in the calculated optical properties of an aerosol mixture to assume either that the chemical species are externally mixed, as described above, or internally mixed. In an internally mixed aerosol, all particles in a stated particle-size cut have the same composition, i.e., they each have the same proportions of all chemical species. This finding has been confirmed by other authors, including Lowenthal et al. (1995). Lowenthal et al. (1995) showed that for an internally mixed aerosol, it made little difference whether each particle was assumed to be homogeneous, or assumed to be composed of a core of insoluble species and a shell of species that form a solution at high humidities. Thus, useful estimates of the aerosol optical properties can be constructed by assigning extinction efficiencies to chemical species, multiplying the ambient concentrations by the efficiencies, and summing the results.

Two key inputs to this estimation are (1) estimates of the size of the (dry) particles and (2) estimates of the water uptake associated with each chemical species with increasing RH. If it is known that the chemical species were mostly formed in homogeneous (i.e., dry) photochemical reactions, then it can be assumed that most particles are in a size mode with a diameter in the 0.2- to 0.3- $\mu\text{m}$  size range (see, for example, Meng and Seinfeld, 1994; John et al., 1990). However, in locations where particle formation is active, the particle-size distribution can be shifted toward smaller particle sizes. If it is known that most particles were formed heterogeneously (i.e., in liquid particles), then the particle size is less certain. John et al. (1990) observed that the droplet mode particles formed in the Los Angeles Basin typically had a mean size near 0.7  $\mu\text{m}$ . Sulfur particle-size distributions measured in the NGSVS show that droplet mode particles formed in a relatively clean environment could have a mean size near 0.2- $\mu\text{m}$  diameter (Richards et al., 1991). Small particles are formed when only a small amount of particulate matter is formed in each cloud drop. The effects of water uptake on light extinction are discussed in Section 8.3.3.

When designing control strategies to improve visibility, it is necessary to estimate the change in light extinction that would result from a change in the atmospheric composition. It would be convenient if Equation 8-34 could be used for this calculation.

$$\Delta\sigma_{\text{sf}} = \sum E_j \Delta C_j \quad (8-34)$$

However, as illustrated by the hypothetical curves in Figure 8-14, the light-scattering efficiency of fine particle species  $j$  is typically not a linear function of the species concentration. Therefore, the value of the light-scattering efficiency for fine particles to be used in Equation 8-33 to calculate the contribution of species  $j$  to light scattering when its concentration has the value indicated by point a, (shown by the slope of the dashed line through the origin), is typically different from the value of the light-scattering efficiency of fine particle species  $j$  to be used in Equation 8-34 to calculate the change in the contribution to light scattering when the concentration is reduced from point a to point b (shown by the slope of the dotted line that passes through points a and b).

The literature contains data for extinction efficiencies defined both ways, so the reader should maintain an awareness of this distinction. Lowenthal et al. (1995) have published an analysis of the sensitivity of light-extinction efficiencies to the methods and assumptions used in their calculation and have presented values calculated using different assumptions.

Light-extinction budgets have the objective of estimating the fraction of the total light extinction contributed by each chemical species. Because the chemical species in particles do not scatter light independently, light-extinction budgets are somewhat arbitrary. Budgets can be calculated from estimated extinction efficiencies and measured species concentrations using Equation 8-33, but the values obtained depend on the assumptions used. Many tabulations of light-extinction efficiencies and budgets have been published. Some of the more recent data and reviews are in the National Acid Precipitation Assessment Program report (Trijonis et al., 1991), a separate publication of some of those data (White, 1990), a summary of IMPROVE data (Malm et al., 1994), and a review of light-extinction calculation methods and the results from their application to data from recent field studies (Lowenthal et al., 1995).

## **8.4 INDICATORS OF VISIBILITY AND AIR QUALITY**

### **8.4.1 Introduction**

Air quality standards to protect human health designate an indicator, which is the atmospheric constituent (such as  $O_3$ ) whose concentration is regulated. The standards also specify a concentration level and a form. The form specifies such variables as the averaging

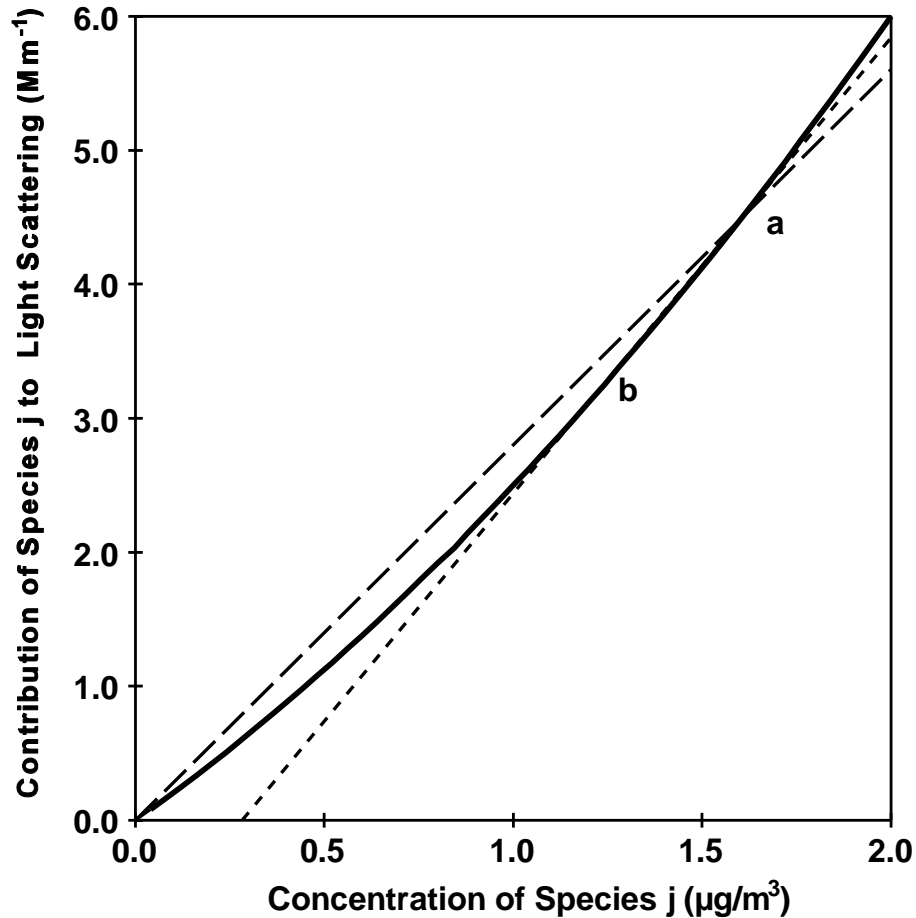


**Figure 8-14. Hypothetical curves showing the effect of nonlinearities on the mass-specific light-scattering efficiency. The bold curve shows the contribution of species  $j$  to the light-scattering coefficient as a function of the concentration of species  $j$ . The slope of the dashed curve gives the mass-specific light-scattering efficiency to be used in Equation 8-33 for the species concentration at point  $a$ . The slope of the dotted curve gives the efficiency to be used in Equation 8-34 when the species concentration changes from point  $a$  to point  $b$ .**

time and the number of times the average concentration may exceed the concentration level of the standard in a specified length of time. Indicators are selected on the basis of their linkage to the human health of populations, and the levels are set based on data for the health of classes of sensitive individuals.

A similar approach is also useful when considering visibility standards; some property of the atmosphere related to visibility must be selected as an indicator. Factors which may be considered in making this selection include (1) the linkage between the indicator and

visibility, (2) the cost and feasibility of monitoring the indicator to determine compliance with the standard as well as progress toward achieving the standard, (3) the nature and severity of the interferences inherent in the available monitoring methods, (4) the relationship between the visibility indicator and indicators for other air quality standards, and (5) the usefulness of monitoring data in analyses which have the purpose of determining the optimum control measures to achieve the standard.

Even though contrast and contrast transmittance provide numerical scales that can be used to quantify visibility, they are not suitable indicators of visibility for regulation of visibility protection based on air quality. Visibility is strongly affected by the illumination of the sight path, which is largely determined by natural processes that are not subject to regulation. Visibility is also affected by meteorological conditions, such as very high humidity, precipitation, and fog, which are also not subject to regulation. Furthermore, the derivations presented above show that complex calculations are required to relate contrast and contrast transmittance to air quality.

A secondary standard to protect visibility has the objective of setting an air quality standard that ensures visibility protection. Therefore, it is appropriate to select an indicator more closely linked to air quality than to visibility. In this case, the indicator would not be closely linked to the visibility along a specific sight path at a specific time. Instead, the indicator would be linked to the distribution of visibilities observed as a function of the value of the indicator. The level of the standard could be set to protect sensitive views under specified illumination conditions. This relationship between the indicator and visibility is similar to that for standards set to protect human health.

The following sections discuss parameters that could be used as indicators for regulation of visibility protection based on air quality.

#### **8.4.2 Visual Range from Human Observation**

The use of visual range from human observation as an indicator of visibility is listed here for historical reasons. The National Weather Service is discontinuing the observations at airports, so the number of locations at which observations are being made is now declining rapidly. In 1989, the California Air Resources Board changed the standard for visibility

reducing particles, replacing the observation of visual range with an instrumental measurement (VanCuren, 1989a,b).

There is a long history of recording the most distant target that can be perceived, or alternatively, whether or not a distant target can be perceived. For example, Husar et al. (1981) cited data from visibility observations at the Blue Hill Observatory in Massachusetts that extended from the 1880s to the 1950s. During recent decades, visibility at all major airports throughout the United States has been recorded hourly during the daytime by human observation. These data have been used to determine visibility trends in the United States as well as the spatial distribution of current visibility conditions (see, for example, Trijonis et al., 1991; Husar and Wilson, 1993). No other visibility measurement provides an historical record for the United States of comparable usefulness.

The advantages of human observations of visibility are: (1) they provide a direct measure of the visibility as defined in Section 8.1.2, (2) no special equipment is required, and (3) manpower requirements are minimal if an observer is already present for other reasons. The disadvantages are: (1) the results depend on the observer and the available visibility targets, and (2) in general, the data are poorly related to air quality. However, the linkage to air quality can be improved by using only midday observations not influenced by meteorological effects such as fog, precipitation, or very high humidities.

Middleton (1952) reports data from experiments in which photometric measurements were made in parallel with routine visibility observations. There was a wide range in the measured contrasts of the targets selected by the observers to indicate the visual range. These data document only one source of uncertainty in human observations.

### **8.4.3 Light-Extinction Coefficient**

The light-extinction coefficient is the parameter most frequently used by the air quality community to characterize visibility because it is closely linked to air quality. The advantages of using the light-extinction coefficient are that it is: (1) an intensive property of the atmosphere (i.e., a property of an element of volume of the atmosphere), (2) closely linked to air quality, (3) can be directly measured by a commercially available instrument, and (4) is a key input for the radiative transfer calculations needed to calculate the visibility.

The light-extinction coefficient can be directly measured by a transmissometer (Molenar et al., 1990, 1992) or it can be estimated by measuring the components of light extinction listed in Equation 8-4 (dry scattering and absorption, or ambient scattering and absorption) and calculating the sum (see, for example, Malm et al., 1994; Richards, 1995). There are several key disadvantages of using the transmissometer to monitor the light extinction coefficient. These disadvantages include: (1) transmissometer measurements respond to meteorological effects such as fog and precipitation, and (2) the commercially available transmissometer is difficult to calibrate and maintain. For example, the optical windows need to be cleaned frequently. It is a further disadvantage of transmissometer measurements that the measurement error is large compared to the effects of air pollution when the atmosphere is very clear.

The effects of meteorological conditions on light extinction can be very great; they frequently completely obscure the sight path. In applications such as airport runway control, where visibility is the prime concern, it is appropriate to include these effects in the monitoring data. However, when the effect of air quality on visibility is the prime concern, it is important to remove meteorological effects from the monitoring data. This is recognized by the IMPROVE protocols for processing transmissometer data. Measurements made at relative humidities above 90% are flagged because they may be affected by meteorological effects such as fog, clouds, or precipitation (Blandford, 1994). It is standard practice to exclude these data from statistical summaries (Mercer, 1994). However, it is nearly impossible to remove these effects to a satisfactory degree because it is nearly impossible to distinguish between snow flurries or rain showers on the one hand or puffs of haze on the other. Subjective judgement enters into the flagging of transmissometer data. Furthermore, particle formation is often enhanced at high humidity, so failing to collect visibility-related air quality data at high humidities is a significant omission (Richards, 1994).

The value of the light-extinction coefficient calculated from the sum of its components listed in Equation 8-4 could be used in place of transmissometer measurements as an indicator of visibility. In this case, it is an option to exclude the contribution of gases to the light-extinction coefficient and to include only the contribution of particles. Light scattering by gases can be omitted because it is nearly constant and cannot be regulated. Light absorption by gases can be omitted because it is primarily due to  $\text{NO}_2$ , whose concentrations

are (1) already subject to regulation, and (2) typically too small outside urban areas to have a significant effect on visibility. If such calculations use the ambient scattering, the light-extinction coefficient, as is the case with transmissometer measurements, will be strongly dependent upon the relative humidity and so will not be a good indicator of air quality. If the air sample is dried the light-extinction coefficient will be a better indicator of air quality but a poorer indicator of visibility.

In 1989, the California Air Resources Board adopted a standard for visibility reducing particles that is calculated from the sum of the light-scattering coefficient for particles and the light-absorption coefficient for particles. Light scattering by particles is measured by a heated, enclosed integrating nephelometer (see Section 8.4.5) and light absorption by particles is measured with a tape sampler (VanCuren, 1989a,b).

## **8.4.4 Parameters Calculated From the Light-Extinction Coefficient**

### **8.4.4.1 Visual Range**

The visual range can be calculated from a measurement of the light-extinction coefficient at a point by assuming (1) that the atmosphere and the illumination over the sight path is uniform and (2) the threshold contrast is 2%. Then, for a black target, the left side of Equation 8-31 has the value -0.02 and Equation 8-9 can be used to obtain

$$\text{Visual Range} = 3.91 / \sigma_{\text{ext}} \quad (8-35)$$

which is known as the Koschmieder equation. This equation is useful when the value of the light-extinction coefficient is large enough that the visual range is small enough for the assumptions to be valid. The assumptions are quite questionable for visual ranges larger than 10 to 20 km, and invalid for visual ranges greater than about 100 km (see Section 8.2.1).

In addition, the use of visual range calculated from a point measurement of the light-extinction coefficient is useful as an indicator of visibility related to air quality. It does, however, have the same disadvantages as associated with the use of transmissometer measurements of light-extinction coefficients listed in Section 8.4.3.

#### 8.4.4.2 Deciview Haze Index

The deciview haze index,  $dv$ , was proposed by Pitchford and Malm (1994) to provide an indicator of haze that is scaled to correspond to the properties of human vision. It is calculated from the light-extinction coefficient for green light by the equation

$$dv = 10 \log_{10} (\sigma_{\text{ext}} / 10 \text{ Mm}^{-1}) \quad (8-36)$$

This index has a value of zero, approximately  $10 \text{ Mm}^{-1}$  at sea level, where the light-extinction coefficient has the value for particle-free air (see Equation 8-5) and increases by one unit for each 10% increase in the value of the light-extinction coefficient. The logarithmic scaling is similar to that of the decibel scale, which is also related to human perception.

As described in Section 8.2.8 and the above sections, the light-extinction coefficient is closely linked to air quality. Therefore, the deciview haze index is similarly a measure of haze, and is closely related to air quality. The scale at the top of Figure 8-7 indicates that for a given sight path, the deciview haze index is linked to the visibility only in the range of light-extinction values that correspond to sight path transmittances between roughly 20 and 80%. Outside this range, changes in the deciview haze index have a greatly decreased effect on visibility. For example, increases in the deciview haze index will not change the appearance of features that are already completely obscured by haze.

The deciview haze index is well suited for presenting data for spatial and temporal trends of haze. It is not influenced by the many factors unrelated to air quality that affect visibility, and it is scaled to approximately linearize the relationship between human perception and the haze index. However, its use as an indicator of visibility has the disadvantages associated with the use of transmissometer measurements of light-extinction coefficients listed in Section 8.4.3.

#### 8.4.5 Light-Scattering Coefficient Due to Particles

There are several advantages to using the light-scattering coefficient for particles as an indicator of visibility effects. They include: (1) it is the component of the light-extinction

coefficient primarily responsible for visibility impairment; (2) it is closely linked to fine particle concentrations; (3) a number of monitoring methods and commercial instruments are available; (4) the cost of implementing the monitoring methods and maintaining measurement instruments is competitive with those for other indicators; (5) accurate instrument calibration methods are available; (6) interferences can be reduced to an acceptable level and are as well understood as for any other indicator; (7) it is typically measured continuously; and (8) commercial instruments are available that are either designed to include or designed to exclude meteorological effects.

There is a linkage between the light-scattering coefficient for particles and visibility because the dominant cause of visibility impairment is light scattering by particles. The components of the light-extinction coefficient other than the coefficient for light scattering by particles are the coefficient for light scattering by gases, which is nearly constant, and the coefficient for light absorption by gases and particles. Light absorption does not contribute to the path radiance, and under some circumstances, decreases it significantly. Therefore, under some lighting conditions, light absorption does not degrade visibility as effectively as does light scattering. In extreme cases, the addition of absorption to the sight path has no effect on visibility (e.g., sun glasses), or can even increase the apparent contrast of bright objects viewed against the horizon sky by darkening the background sky and thereby increasing the initial contrast (Dessens, 1944; Middleton, 1952). On the other hand, increasing the light-scattering coefficient for particles always decreases the transmitted radiance and increases the path radiance, so it always impairs visibility, which depends on the competition between the transmitted radiance and path radiance. However, although the light-absorption coefficient is not significant to visibility impairment for every scene as is the light-scattering coefficient, the light-absorption component of the light-extinction coefficient is important in overall visibility impairment.

The available monitoring instruments include: (1) the enclosed integrating nephelometer (Ahlquist and Charlson, 1967), (2) the open integrating nephelometer (Molenaar et al., 1992), and (3) forward scatter visibility monitors (see, for example, National Oceanic and Atmospheric Administration, 1992). The enclosed nephelometer can be fitted with a size-selective inlet, which excludes the large particles that cause meteorological interferences and provides control over the particle-size fraction that is sampled (White et al., 1994; Richards,

1994). Enclosed nephelometers that use an incandescent lamp heat the sample a few degrees, but this heating can be less than 1 °C in nephelometers that use a flashlamp. Sample heating reduces the RH of the sample air, which causes absorbed water to evaporate from particles in the sample chamber.

The California Air Resources Board Method V for monitoring ambient concentrations of visibility-reducing particles uses an enclosed nephelometer that is deliberately heated to minimize the effects of high humidities on the monitoring data (VanCuren, 1989a, 1989b). This drying of the aerosol particles is similar to the drying which occurs when filter samples are conditioned to a standard humidity before being weighed in the laboratory.

Open nephelometers were designed to reduce the heating of the sample to a fraction of a degree, and to admit a broad range of particle sizes (Molenaar et al., 1992). Therefore, open nephelometers respond to meteorological effects such as fog and snow. The standard IMPROVE protocol flags open nephelometer data influenced by meteorological effects and excludes them from some the statistical presentations of the data (Cismoski, 1994). The difficulties associated with this data flagging are the same as those for flagging light-extinction coefficient data listed in Section 8.4.3.

Forward scatter meters have been selected by the National Weather Service to replace human observers for visibility measurements at airports (National Oceanic and Atmospheric Administration, 1992). The sample volume is in the open air, so the instrument responds to meteorological effects as well as air quality effects. This instrument is significant because it is in use at approximately 600 locations as of the end of 1995, and additional installations are planned. Data from this instrument have the potential to provide a database for the evaluation of spatial and temporal trends in the light-scattering coefficient for particles that is more useful than the historical records of visual range at airports. However, this will require a change in the way data are archived by the National Weather Service because current practice is to report all visibilities greater than 10 mi in one bin.

The cost of most instruments to measure the light-scattering coefficient for particles is in the range of typical monitoring instruments. They operate for long periods of time unattended, but do require routine lamp replacement and occasional cleaning.

Integrating nephelometers can be accurately calibrated with gases of varying scattering coefficients (see, for example, Bodhaine, 1979; Ruby and Waggoner, 1981). These

calibrations are applicable to the measurement of light scattering by fine particles. Because integrating nephelometers are blind to light scattered near 0 and 180 degrees, their response to particles in the 2.5- to 15- $\mu\text{m}$ -diameter range is roughly half the correct value (White et al., 1994). This property of nephelometers, known as the truncation error, has been quantified (Ensor and Waggoner, 1970; Heintzenberg and Quenzel, 1973; Heintzenberg, 1978; Hasan and Lewis, 1983; White et al., 1994).

The measurement of the light-scattering coefficient has the potential to be an indicator for health effects as well as visibility effects. Enclosed nephelometer readings are highly correlated with the mass of fine particles collected on a filter (see, for example, Waggoner et al., 1981). The correlation between nephelometer readings and the mass concentration of fine particles is improved by using the same size selective inlet on both the nephelometer and filter sampler (White et al., 1994). Filter samples are typically equilibrated to a standard RH before being weighed. The correlation between nephelometer readings and mass concentrations measured by filter can be improved minimizing the occurrence of high RH in the nephelometer scattering chamber. This can be accomplished by heating the sample air a few degrees, as in the California Air Resources Board Method V (VanCuren, 1989a,b) or by passing the air sample through a dryer that removes water. Heating the air sample has the potential to volatilize particulate species other than water.

#### **8.4.6 Contrast of Terrain Features**

Data for the contrast of terrain features provides a direct measure of the visibility. In current practice, the contrasts of features in a scene are most commonly monitored photographically and determined by film densitometry (Johnson et al., 1985).

Because of the close relationship to visibility, contrast measurements were used by the National Park Service when instrumental visibility monitoring in Class I areas began in the late 1970s (Malm, 1979). A teloradiometer was used to measure the contrast of a distant terrain feature against the horizon sky.

When contrasts and background radiances are measured at both ends of the sight path, Equations 8-26 and 8-9 can be used to accurately determine the average light-extinction coefficient of the atmosphere in the sight path. These measurements are rarely made. It is more common to assume that the background radiances are equal at each end of the sight

path (Malm, 1979) to estimate the initial contrast (Malm et al., 1982) and to calculate the average light-extinction coefficient from Equations 8-30 and 8-9. Values of the light-extinction coefficient calculated by this method have been found to be unreliable (White and Macias, 1987). For this reason, the National Park Service has discontinued making instrumental contrast measurements in favor of the direct measurement of the light-extinction coefficient or the light-extinction coefficient due to particles.

The contrast monitoring data provide a direct measure of the visibility, which is affected by many factors other than the air quality (see Section 8.2.9). Sections 8.2.5 through 8.2.8 provide the methods for calculating contrasts and contrast transmittances from air quality data. It is expected that improvements in these calculation methods will lead to, increasing emphasis on the contrasts of terrain features and contrast transmittances for specific sight paths as measures of visibility. The calculation methods presented in this chapter can be used to calculate contrasts of terrain features when the air quality and land-use data are available and the skies are either reasonably free of clouds or are uniformly overcast.

#### **8.4.7 Particulate Matter Concentrations**

The fine-particle concentration could be used as an indicator of visibility because (1) the data cited below show that the coefficient for light-scattering by particles is closely linked to the mass concentration of fine particles, and (2) the coefficient for light-scattering by particles is the component of light extinction primarily responsible for visibility impairment. This alternative would be attractive if fine particle concentrations were monitored to determine compliance with a primary air quality standard because no additional monitoring would be required to determine compliance with a visibility standard. The calculation methods presented in Sections 8.2 and 8.3 could be used to relate the visibility (as measured by contrast and contrast transmittance) to the fine-particle concentration for purposes of evaluating various options for the level and form of a fine-particle standard designed to protect visibility.

A number of studies report data for the relationship between the coefficient for light-scattering by particles (as measured by an integrating nephelometer) and the fine-particle concentration. Most of these studies report correlation coefficients of 0.9 or greater. Early

results were reported by Waggoner and Weiss (1980), who measured correlation coefficients greater than 0.95 at Mesa Verde, CO, and at industrial, residential, and rural sites in the Pacific Northwest. The nephelometer measurements were made using an enclosed nephelometer without a size selective inlet and with some sample heating caused by the lamp. Dichotomous samplers with a 3  $\mu\text{m}$  cutpoint were used to collect fine particles on teflon or Nuclepore substrates. No special precautions were taken in the filter sampling to prevent the evaporation or collection of semi-volatile species. The mass-specific light-scattering efficiencies determined from regression analysis of the data from each of the five sites ranged from 2.9 to 3.2  $\text{m}^2/\text{g}$ . These data were also reported by Waggoner et al. (1981).

The results of Koenig et al. (1993) are of interest because pulmonary function changes in children were associated with integrating nephelometer readings in Seattle, WA. The studies were conducted during two winter heating seasons in areas affected by wood smoke. The year following these studies,  $\text{PM}_{2.5}$  samples collected at pre-set time intervals over 1-week periods from January 17 to December 12, 1991, were compared with integrating nephelometer measurements averaged over the sample collection times. Regression analysis gave a mass-specific light-scattering efficiency of 4.9  $\text{m}^2/\text{g}$ , which is larger than typically observed, and a regression coefficient of 0.97.

The results of White et al. (1994) are of interest because size-selective inlets with cutpoints of 2.5 and 15  $\mu\text{m}$  were used on both the integrating nephelometer and the filter sampler. As in the previous studies, the nephelometer sample chamber was heated by the lamp. The samples were collected in a desert climate in northern Arizona. As described in Section 8.3.2, the mass-specific light-scattering efficiency of particles that pass the 2.5  $\mu\text{m}$  cutpoint at two sites was 2.8 and 3.1  $\text{m}^2/\text{g}$  and the correlation coefficients were 0.86 and 0.84.

Integrating nephelometer readings are not as well correlated with total suspended particulate concentrations (Waggoner et al., 1981) or with particle concentrations measured with a 15  $\mu\text{m}$  cutpoint (White et al., 1994). The reasons are (1) fine particles have mass-specific light-scattering efficiencies 5 to 10 times greater than the efficiencies of coarse particles, (2) the integrating nephelometer responds to roughly half the light scattered by coarse particles (White et al., 1994), and (3) the relative amounts of coarse and fine particles in the atmosphere are typically quite variable. Therefore, the coefficient for light-scattering

by particles is much less closely linked to the  $PM_{10}$  concentration than to the fine-particle concentration, making  $PM_{10}$  less satisfactory as an indicator of visibility than the fine-particle concentration.

#### **8.4.8 Measures of Discoloration**

The 1977 Clean Air Act Amendments define visibility impairment as a reduction in the visual range or atmospheric discoloration. Color calculations have been included in plume visibility models (see, for example, Latimer et al., 1978), and quantitative color measurements have been made for urban hazes (e.g., Waggoner et al., 1983). Less emphasis has been placed on the color of regional hazes. A brief review of methods for specifying the colors of hazes appears in the National Acid Precipitation Assessment Program report on visibility (Trijonis et al., 1991).

For plume visibility analyses, the most commonly used parameter is the color difference  $\Delta E(L^*a^*b^*)$  between the apparent spectral radiances for a sight path with and without the plume. The equations for calculating this parameter are presented in an EPA workbook (U.S. Environmental Protection Agency, 1988). It is the intent of these equations to linearize the human perception of color differences, so color differences with equal values of  $\Delta E(L^*a^*b^*)$  are equally perceptible. It was also an intent of these equations to assign a  $\Delta E(L^*a^*b^*)$  value of unity to color differences that were just perceptible when presented as two, side-by-side, uniform areas of color that each subtended angles of a few degrees or more. For plume visibility analyses, the threshold for the perception of color differences is greater than for color patches separated by a sharp edge because of the diffuse edges of the plume. It also depends on the apparent angle subtended by the plume, i.e., the apparent width of the plume (U.S. Environmental Protection Agency, 1988).

The apparent color of an urban or regional haze depends on the element of the scene used by the human visual system as a reference white (MacAdam, 1981). Water clouds in the sky typically have spectra that are strong in the blue. If such water clouds are used as the reference white for color perception, hazes that have a more neutral spectrum (Waggoner et al., 1983) can appear yellowish or brown by comparison. Thus, an analysis of haze colors requires an analysis of both the spectral radiance of the haze and the spectral radiance of the elements of the scene used by the observer as the reference white (MacAdam, 1981).

## **8.5 VISIBILITY IMPAIRMENT**

### **8.5.1 National Patterns and Trends**

National patterns and historical visibility trends are summarized in the National Acid Precipitation Assessment Program report by Trijonis et al. (1991). They were also reviewed in the National Research Council report prepared by the Committee on Haze in National Parks and Wilderness Areas (National Research Council, 1993). Data for spatial and temporal patterns of haze measured by the IMPROVE (Interagency Monitoring of Protected Visual Environments) protocol in Class I areas, mostly in the western United States, have been summarized by Sisler et al. (1993) and Malm et al. (1994).

Patterns and trends in visibility are closely linked to patterns and trends in particulate matter concentrations, which are reviewed in Chapter 6 of this document. Because of the close linkage to data appearing elsewhere in this document and the availability of good, current reviews in publications of the federal government, the data for visibility patterns and trends are not summarized again here.

### **8.5.2 Visibility Monitoring**

Visibility observations have long been made as part of weather observations. Since the advent of aviation, visibility observations have routinely been made at airports. The 1977 Amendments to the Clean Air Act generated a need for visibility and air quality monitoring to determine the visibility conditions in Class I areas and a need to monitor progress toward the national goal of eliminating man-made air pollution in Class I areas.

A recent report summarizes current visibility monitoring activities (U.S Environmental Protection Agency, 1995e). The following sections give additional information which supplements the information in the U.S Environmental Protection Agency report.

#### **8.5.2.1 Point Versus Sight Path Measurements**

The monitoring methods used in visibility studies can be divided into point measurements, which measure properties of the atmosphere at the sampler inlets, and path measurements, which determine the optical properties of a sight path through the atmosphere. This distinction is blurred only in mobile or airborne sampling, where the sampler inlets can be moved through a sight path.

Visibility, by definition, is linked to sight paths and can be quantified only after a sight path is specified. Sight path measurements, such as human observations of the visual range, the instrumental measurement of the contrast of distant terrain features, or contrasts measured from photographs provide a direct measure of the visibility.

Most air quality measurements measure the air quality at the sampler inlets. This is typically true of trace gas monitors, aerosol filter samplers, and optical monitors such as the integrating nephelometer. Some remote sensing instruments measure air quality parameters, such as trace gas concentrations or light extinction, for a sight path. However, the sight paths for these instruments are typically short enough that the measurements are more appropriately classified as point measurements rather than sight path measurements.

The Optec Transmissometer is an example of a remote sensing instrument that typically produces data that can be classified as a point measurement. To conserve electric power in remote locations, the IMPROVE protocol for the transmissometer calls for collecting data for 10 min each hour. For typical wind velocities, the spatial and temporal averaging resulting from a 10-min measurement each hour for a sight path a few kilometers in length is comparable to the hour-average data continuously measured at a sampler inlet. An exception to this classification occurs when the transmissometer sight path is strongly slanted, with the result that different layers in a stable atmosphere may be sampled. An example is the transmissometer with one end of the sight path at Hopi Point on the rim of the Grand Canyon and the other end of the sight path at Indian Gardens within the Canyon.

When air quality measurements made at a point satisfactorily represent the conditions in the surrounding region, the methods in Section 8.2 can be used to calculate the visibility from the air quality data. Uncertainties in the representativeness of the air quality data should be evaluated when estimating the uncertainties in the visibility calculations.

### **8.5.2.2 Instrumental Monitoring Networks**

According to present plans, the largest instrumental visibility monitoring network in the United States will be operated by the National Oceanic and Atmospheric Administration and cooperating agencies to measure airport visibility. The primary purpose of this network is to provide real-time data for runway visibility to aid in controlling airport operations. The visibility measurements are one component of the Automated Surface Observing System

(ASOS) and are made by the Belfort Visibility Sensor (National Oceanic and Atmospheric Administration, 1992). This instrument uses a flash lamp to illuminate a volume of open air and a sensor to measure the scattering of visible light at angles near 40 degrees. The signals from the visibility sensor have been calibrated by comparison with transmissometer measurements during episodes of haze, fog, rain, snow, etc., and a calibration curve is used to convert the sensor readings to units of light extinction and visual range. Between 400 and 600 installations are now operating.

The IMPROVE is the largest network that includes both visibility and air quality measurements. Most sites are operated by the National Park Service, but sites are also operated by the U.S. Forest Service and other agencies. Data are being collected using the IMPROVE protocols at more than 40 sites, most of which are in or near federal Class I areas (Malm et al., 1994; Sisler et al., 1993; U.S. Environmental Protection Agency, 1995e).

The Clean Air Status and Trends Network (CASTNET), which is no longer in operation, included the CASTNET Visibility Network, which had nine sites, primarily in the eastern United States (U.S. Environmental Protection Agency, 1995e). The California Air Resources Board operates integrating nephelometers (to measure light scattering by visibility-reducing particles) at approximately 16 sites and tape samplers (to measure light absorption by particles) at nearly 40 sites (VanCuren, 1989a,b). Data from many of these sites are used when forecasting agricultural burn days. Other monitoring activities are listed in a recent U.S. Environmental Protection Agency report (U.S. Environmental Protection Agency, 1995e) and in Tables 8-3 and 8-4 adapted from the National Acid Precipitation Assessment Program report (Trijonis et al., 1991).

### **8.5.3 Recent Observations**

This section briefly summarizes results presented in selected papers published since the U.S. Environmental Protection Agency review was prepared (U.S. Environmental Protection Agency, 1995e).

Vasconcelos et al. (1994) examined data from Subregional Cooperative Electric Utility, Department of Defense, National Park Service, and EPA Study (SCENES) conducted from 1984 to 1989 in the area surrounding the Grand Canyon. Aerosol concentrations showed

**TABLE 8-3. LONG-TERM VISIBILITY AND AEROSOL DATA BASES**

Study/Data Base	Air Sheds	Period	Type of Data <sup>a</sup>	Purpose of Study	Comments	References
<b>National and Regional Networks</b>						
Analyses of National Weather Service (NWS) Airport Visibility Data	Rural and urban airports all over the nation.	1918 to present	Human estimates of prevailing visibility mainly in support of aircraft operations	To assess visibility trends; Assessment of the role of meteorology on visibility impairment.	Quality varies from site to site; natural causes of visibility impairment (rain, snow, fog) included in data.	Trijonis (1979, 1982a,b); Sloane (1982 a,b, 1983); Patterson et al. (1980); Husar and Patterson (1984)
Interagency Monitoring of Protected Visual Environments (IMPROVE)	Twenty remote locations nationwide, though primarily in the West.	1987 to present	Aerosol and visibility; PM <sub>10</sub> and fine particle mass. Fine particle elements, ions, organic and light absorbing carbon. $\sigma_{ext}$ , $\sigma_{ap}$ , and $\sigma_{sp}$ and photography.	To establish baseline values and identify existing impairment in visibility protected federal Class I areas.	Employs "state-of-art" methods for long term routine monitoring. Operated jointly by U.S. EPA four federal land managers.	Joseph et al. (1987) Sisler et al. (1993) Malm et al. (1994)
Eastern Fine Particle Visibility Network	Five eastern rural locations.	1988-89 five sites; after 1989 two sites	Aerosol and visibility; fine particle elements organic and soot carbon. $\sigma_{ext}$ , $\sigma_{ap}$ , and $\sigma_{ag}$ , and photography.	A research monitoring program to provide information needed to quality support development of a secondary fine particle standard.	An U.S. EPA operated network. Sites are collocated with other air monitoring programs.	Handler (1989)
National Park Service Network (NPS)	About 37 remote locations nationwide, though primarily in the west.	1987 to present Seventeen sites started in 1987.	Aerosol & visibility; 17 sites operated with IMPROVE measurements. Other have some subset of the IMPROVE measurements.	To document visibility and aerosol levels and to identify sources of visibility impairment measurements in NPS.	Represents the longest period of record for visibility and aerosol monitoring at remote locations.	Joseph et al. (1987)
SCENES	Eleven rural and remote southwestern locations.	1984-1989	Aerosol and visibility; PM <sub>15</sub> and fine particle mass, elements, organic and light carbon at most sites. $\sigma_{ext}$ or $\sigma_{sp}$ and $\sigma_{sg}$ , and photography at most sites.	To document levels and causes of visibility impairment in northern Arizona and southern Utah.	This cooperative research program included several intensive and special studies. An ambitious quality assurance protocol identified many monitoring method difficulties which new techniques ultimately solved.	McDade and Tombach (1987)
Western Regional Air Quality Study (WRAQS)	Eleven nonurban locations in the western U.S.	1981-1982	Aerosol and visibility; PM <sub>15</sub> and fine particle mass, elements, ion.	To document background levels of visibility and related aerosols, organic and elemental carbon. $\sigma_{sg}$ and $\sigma_{sp}$ , observed visual range and photography.	Represents the highest times resolution for routinely collected filter samples (two four-hour samples each day).	Macias et al. (1987)

**TABLE 8-3 (cont'd). LONG-TERM VISIBILITY AND AEROSOL DATA BASES**

Study/Data Base	Air Sheds	Period	Type of Data <sup>a</sup>	Purpose of Study	Comments	References
National Air Surveillance Network (NASH)	Urban & rural areas of U.S.	1975 to present	Aerosol only; TSP ions, and some elements.	Air quality monitoring.	No size-fractionated data; collected only once every six days; artifact on filter possible.	Shah et al. (1986) Mueller and Hidy (1983)
Inhalable Particle Network (IP Network)	Urban and rural areas of U.S. Evans (84) Rodes and Evans (85)	June 1979 to present	Aerosol only; fine and coarse aerosol mass, PM <sub>15</sub> mass, elements, and ions (every fourth sample).	Characterize inhalable particles.	Discrepancy exists between PM <sub>15</sub> and IP mass (sum of fine and coarse). Screening of the data required to remove invalid data points (~25%).	Pace et al. (1981) Watson et al. (1981)
Sulfate Regional Experiment (SURE)	Nonurban areas of eastern U.S. (9 Class I sites and 45 Class II sites)	1977-1978	Aerosol only; TSP, fine and coarse aerosol mass, ions and elements.	Sulfate characterization pollutant source characterization	Class I sites operated for 18 months continuously; Class II sites operated for one month every season for a total of six.	Mueller and Hidy (1983)
Eastern Regional Air Quality Studies (ERAQS)	Nine nonurban areas in northeastern U.S. SURE Class I sites.	1978-1979	Aerosol and visibility; TSP, fine and coarse aerosol mass, ions, elements, $\sigma_{sg}$ and $\sigma_{sp}$ , $\sigma_{ext}$ , and photography.	To characterize visibility (at two sites only) and air quality in the northeastern U.S. region.	The only long-term instrumental visibility data set generated in the eastern U.S. Visibility monitored only at 2 sites; intercomparison of visibility measurement methods made.	Mueller and Watson (1982) Tombach and Allard (1983)
Ohio River Valley Study	Three rural sites in Ohio River Valley.	May 1980-August 1981	Aerosol only; fine and coarse aerosol mass and elements.	Characterization of fine and coarse aerosols in the region.	Portion of aerosol composition was not accounted for due to limitations in XRF analysis used. A long-term daily monitoring of aerosol in rural areas of the Ohio River Valley.	Shaw and Paur (1983)
Harvard School of Public Health's Six Cities Study	Portage, WI; Topeka, KS; Kingston, TN; Watertown, MA; St. Louis, MO; Steubenville, OH	Spring 1979	Aerosol and visibility; fine and coarse aerosol mass, elements, SO <sub>4</sub> <sup>2-</sup> , $\sigma_{sg}$ and $\sigma_{sp}$ .	Mass and elemental characterization of aerosol and their temporal variations to assess health effects of air pollution.	Portion of aerosol composition was not accounted for due to limitations in XRF analysis used.	Spengler and Thurston (1983)

**TABLE 8-3 (cont'd). LONG-TERM VISIBILITY AND AEROSOL DATA BASES**

Study/Data Base	Air Sheds	Period	Type of Data <sup>a</sup>	Purpose of Study	Comments	References
RESOLVE	Seven remote sites in the California Mojave Desert	1983-1985	Aerosol and visibility; PM <sub>10</sub> and fine particle mass, elements, organic and elemental carbon, $\sigma_{\text{ext}}$ , $\sigma_{\text{sp}}$ and $\sigma_{\text{sg}}$ , $\sigma_{\text{ap}}$ and $\sigma_{\text{sg}}$ , and photography.	To document levels and identify causes of visibility impairment in the R-2508 military air space.	DOD sponsored study to provide information needed to limit future additional degradation of military testing by visibility impairment.	Blumenthal et al. (1987)
<b>Single Air Shed Studies</b>						
Great Smoky Mountain National Park Visibility and Air Quality Study (TVA)	Great Smoky Mountain National Park	1980-1983	Aerosol and visibility; fine and coarse aerosol mass and elements; $\sigma_{\text{sp}}$ and $\sigma_{\text{sg}}$ and $\sigma_{\text{ext}}$ ; photography.	Characterize visibility and aerosol.	Because of instrument problems, teleradiometer data were lost. Total particulate matter mass only estimated in some cases. PIXE analysis could not provide some major elemental data.	Valente and Reisinger (1983) Reisinger and Valente (1984, 1985)
Regional Air Pollution Study (RAPS)	100 km region around St. Louis, MO	1974-1977	Aerosol only; fine and coarse mass, SO <sub>4</sub> <sup>2-</sup> , elements.	Develop and evaluate regional air quality models.	Comparison of Hi-Vol and dichotomous samplers.	Jaklevic et al. (1981) Altshuller (1982, 1985)
Portland Aerosol Characterization Study (PACS)	Two rural and four urban areas in Portland, OR	July 1977-April 1978	Visibility and aerosol; fine and coarse mass, TSP, ions, elements, $\sigma_{\text{sp}}$ and $\sigma_{\text{sg}}$ .	Aerosol characterization source apportionment.	Significant role of carbonaceous aerosols recorded.	Copper and Watson (1979) Shah et al. (1984)

<sup>a</sup>Visibility data include light scattering and light extinction measurements using integrating nephelometer, teleradiometers, cameras, and human observers.

Adapted from: Trijonis et al. (1991).

**TABLE 8-4. SHORT-TERM INTENSIVE VISIBILITY AND AEROSOL STUDIES**

Study/Data Base	Air Sheds	Period	Type of Data <sup>a</sup>	Purpose of Study	Comments	References
<b>Rural Studies</b>						
Allegheny Mountain Studies	Rural Allegheny Mountain site	24 July-11 Aug 1977 and Aug 1993	Visibility and aerosol; TSP, fine and coarse aerosol mass, ions, elements, $\sigma_{sp}$ and $\sigma_{sg}$ .	Characterization of visibility and $SO_4^{2-}$ in the region.	Filter artifact investigated; no size fractionated data in 1977.	Pierson et al. (1980a,b)
Shenandoah Valley Studies	Rural Shenandoah Valley	15 July - 15 Aug 1980	Visibility and aerosol; fine and coarse aerosol mass, ions, elements, $\sigma_{ext}$ , human estimates of visibility.	To characterize visibility and aerosol in the rural eastern U.S.	Since three different groups performed the study, intercomparability of data possible.	Stevens et al. (1984) Weiss et al. (1982) Ferman et al. (1981) Wolff et al. (1983)
Great Smoky Mountain Study (EPA)	Great Smoky Mountain National Park	20-26 Sept 1978	Aerosol and gaseous pollutants; fine and coarse aerosol mass and elements.	Characterize aerosol in a rural area.	Comparison of day and night aerosol data made.	Stevens et al. (1980)
Research Triangle Park Visibility Study	Rural Research Triangle Park, NC	8 June - 3 Aug 1979	Visibility and aerosol; fine and coarse aerosol mass, elements, $\sigma_{ext}$ , and $\sigma_{sp}$ and $\sigma_{sg}$ .	Characterize visibility and aerosol in the region.	Comparison of different visibility measurement methods studies.	Dzubay and Clubb (1981)
Louisiana Gulf Coast Study	Gulf Coast	8 Aug - 7 Sept 1979	Visibility and aerosol; fine and coarse aerosol mass, ions, elements, $\sigma_{sp}$ and $\sigma_{sg}$ .	Investigation of sources of $O_3$ and haze.	Calibration errors of MRI 1550 integrating nephelometer applied to data.	Wolff et al. (1982)
Atlantic Coastal Study	Lewes, DE	1-31 Aug 82, 25 Jan - 28 Feb 1983	Visibility and aerosol; fine and coarse aerosol mass and chemistry, $\sigma_{sp}$ and $\sigma_{sg}$ .	Air quality and sources of haze.		Wolff et al. (1985a)
Pacific Northwest Regional Aerosol Mass Apportionment (PANORAMAS)	Twenty-six rural and remote locations in Washington, Oregon, and Idaho	May - Nov 1984	Visibility and aerosol; fine particle mass, elements, and ions. $\sigma_{ext}$ , $\sigma_{ap}$ , $\sigma_{sg}$ , and photography.	To document the levels and sources of summer visibility impairment in the Northwest.	This cooperative monitoring program identified smoke as a major contributor to visibility impairment.	Core et al. (1987)

**TABLE 8-4 (cont'd). SHORT-TERM INTENSIVE VISIBILITY AND AEROSOL STUDIES**

Study/Data Base	Air Sheds	Period	Type of Data <sup>a</sup>	Purpose of Study	Comments	References
<b>Rural Studies</b>						
California Aerosol Characterization Study (ACHEX)	Fourteen southern California cities	July- Nov 72, July - Oct 73	Aerosol and visibility TSP, fine and coarse aerosol mass, ions, elements, $\sigma_{sg}$ and $\sigma_{sp}$ .	Characterization of urban aerosols in California.	The most complete classic aerosol experiment. New methods sampling and analysis tested.	Hidy et al. (1975) Hidy et al. (1980) Charlson et al. (1972)
Denver Winter Haze Study I	Denver, CO	Nov - Dec 78	Visibility and aerosol; fine and coarse aerosol mass, ions, elements, $\sigma_{sg}$ and $\sigma_{sp}$ , and $\sigma_{ext}$ .	Investigation of sources of Denver haze.	Role of local sources and the significant role of carbon in the air documented.	Countess et al. (1980, 1981) Wolff et al. (1981) Groblicki et al. (1981) Heisler et al. (1980a,b)
Denver Winter Haze Study II	Denver, CO	Jan 1982	Visibility and aerosol; fine and coarse aerosol mass, ions, elements, $\sigma_{sp}$ and $\sigma_{sg}$ .	Investigation of sources of Denver haze.	Role of local sources and the significant role of carbon in the air documented.	Lewis and Stevens (1983) Hasan and Dzubay (1987)
Metro Denver Brown Cloud Study	Denver, CO	Nov 1987 - Jan 1988	Visibility and aerosol; fine particle elements ions, organic and light absorbing carbon, $\sigma_{ext}$ , $\sigma_{sp}$ and $\sigma_{sg}$ , $\sigma_{ap}$ and $\sigma_{ag}$ , and photography.	Investigate the sources of Denver haze.	Comprehensive spatial and temporal measurements included fuel switching to see effects of source modulation.	Watson et al. (1988)
Detroit Visibility Study	Urban Detroit, MI	15-21 July 1981	Aerosol and visibility; fine and coarse aerosol, ions, elements, $\sigma_{sp}$ and $\sigma_{sg}$ .	Identification of chemical components of TSP.	Data from a major industrial and urban areas.	Wolff et al. (1982, 1985b) Sloane and Wolff (1984, 1985)
Houston Visibility Study	Houston, TX	11-19 Sept 1980	Visibility and aerosol; fine and coarse aerosol, ions, elements, $\sigma_{sp}$ and $\sigma_{sg}$ , and $\sigma_{ext}$ .	Characterization of visibility and aerosol.	Comparison of day and night aerosols and different visibility measurement devices made.	Dzubay et al. (1982)
CARB Los Angeles Basin Study	Los Angeles Basin	Aug 1992	Visibility and aerosol; fine and coarse aerosol mass, ions, and $\sigma_{sp}$ and $\sigma_{sp}$ .	Characterize visibility and aerosol in the basin.	Significant roles of $NO_3^-$ and organics shown; the importance of filter artifacts reported.	Appel et al. (1983)

**TABLE 8-4 (cont'd). SHORT-TERM INTENSIVE VISIBILITY AND AEROSOL STUDIES**

Study/Data Base	Air Sheds	Period	Type of Data <sup>a</sup>	Purpose of Study	Comments	References
Northern New Jersey Air Pollution Study	Newark, NJ Elizabeth, NJ Camden, NJ Ringwood, NJ	Winter 1982-1983	Aerosol only.	Inhalation toxicology studies.	Urban contributions of carbonaceous particles to air pollution episodes.	Lioy et al. (1983, 1985)
Willamette Valley Field and Slash Burning Study	Willamette Valley, OR	Summer 1978	Aerosol; fine and coarse mass, TSP, elements (carbon), ions	Assessment of field and slash burning on air quality.	Significant role of carbonaceous particles in fine aerosol demonstrated.	Lyons and Tombach (1979)
San Joaquin Valley Aerosol Study	San Joaquin Valley, CA	Nov-Dec 78, Jul and Sept. 79	Aerosol only; fine and coarse mass, ions.	Characterize ambient aerosols termittent data sets.		Heisler and Baskett (1981)
Southern California Air Quality Study (SCAQS)	Los Angeles Basin	June-Sepemter and December 1987	Meteorological air quality data to address O <sub>3</sub> and aerosol formation.	Characterization of air quality, including aerosol and visibility in the basin.	Comprehensive data base for O <sub>3</sub> and aerosol analyses.	Lawson (1990) Air and Waste Management (1993)

<sup>a</sup>Visibility data include light scattering and light extinction measurements using integrating nephelometer, teleradiometers, cameras, and human observers.

Adapted from: Trijonis et al. (1991).

substantial seasonal variation but little systematic diurnal variation. Aerosol composition, but not total concentration, depended strongly on ambient relative humidity, with crustal materials augmented at low humidities and sulfates augmented at high humidities. Total fine-particle concentrations showed the expected strong correlation with light scattering, but the aerosol composition was essentially the same on clear days and hazy days.

Saxena et al. (1995) analyzed data for particle growth as a function of RH and particle composition to evaluate the effect of organic compounds on water uptake. They analyzed the data from which the examples in Figure 8-13 were taken. They compared the observed water content with the water content expected to be associated with the inorganic fraction, and found that the aggregate hygroscopic properties of inorganic particles were altered substantially when organic compounds are also present. The alterations can be positive or negative. For the nonurban location near the Grand Canyon, organics enhance water absorption by inorganics. In the RH range of 80 to 88%, organics account for 25 to 40% of the total water uptake, on average. For the urban location in the Los Angeles Basin, the net effect of organics is to diminish water absorption of the inorganics by 25 to 35% in the RH range of 83 to 95%.

## **8.6 VISIBILITY MODELING**

Three types of models are discussed in this section: plume models; regional haze models; and models for photographic representation of haze. Plume visibility models and regional haze models are source models which simulate the transport, dispersion, and transformation of chemical species in the atmosphere. Plume models use the resulting air quality data to calculate the values of parameters related to human perception, such as contrast and color difference. Regional haze models currently calculate aerosol species concentrations and the light-extinction coefficient. Models for the photographic representation of haze use air quality data as an input, and perform the optical calculations required to create images that represent the visual effects of the air quality.

### **8.6.1 Plume Visibility Models**

As part of the 1977 amendments of the Clean Air Act (Section 169A to Part C) of Title I), the U.S. Environmental Protection Agency sponsored the development of the plume visibility model (PLUVUE) to be used during the preparation of a permit application to determine whether or not a proposed new facility would cause visibility impairment in a class I area (Latimer et al., 1978; Johnson et al., 1980; White et al., 1985). Plume visibility models estimate the value of optical parameters related to human perception, such as contrast and color differences. The calculated values for these parameters are then compared with perception thresholds to determine whether or not the plume would be perceptible in each simulated case (U.S. Environmental Protection Agency, 1988; Latimer, 1988).

Other plume visibility models have been developed by the Los Alamos National Laboratory (Williams et al., 1980, 1981), Environmental Research and Technology, Inc. (Drivas et al., 1981), and the University of Washington (Eltgroth and Hobbs, 1979). Additional citations for these models and a comparison of results from PLUVUE and the other models with experimental data have been reported by White et al. (1985). The PLUVUE model (PLUVUE I) has been refined, now known as PLUVUE II (Seigneur et al., 1983; Seigneur et al., 1984) and has been evaluated (White et al., 1986).

To minimize the cost of visibility analyses in cases where a full plume visibility analysis is not necessary, the U.S. Environmental Protection Agency sponsored the development of a visibility screening model, VISCREEN (U.S. Environmental Protection Agency, 1988). When used for Level-1 analyses, default values are used for most input data to evaluate the visibility effects of a worst case scenario. If necessary, a Level-2 analysis is performed with more realistic values for the input data. If these screening analyses indicate a potential for visible effects, a full Level-3 analysis must be performed with a plume visibility model.

It is anticipated that an improved version of the PLUVUE II plume visibility model will be available on the U.S. Environmental Protection Agency's Support Center for Regulatory Air Models bulletin board in 1995.

## 8.6.2 Regional Haze Models

The primary sources of anthropogenically induced, regional visibility degradation (also referred to as regional haze) measured as light extinction, are fine particles in the atmosphere. In the eastern United States, these anthropogenic particles are composed primarily of sulfate compounds, organic compounds, and to a much lesser extent nitrate compounds. These are important constituents in other areas of the United States as well; their relative importance, however, changes. For example, in some areas of the Pacific Northwest, organic aerosols are as, or more, important than sulfate aerosols. In some parts of Southern California, nitrate aerosols are the dominant species.

Sulfate aerosols are mostly formed from SO<sub>2</sub> emissions, which are predominantly due to fuel combustion. The sources of organic aerosols can be both natural and anthropogenic. Organic aerosols may be primary, emitted directly from a source, or secondary products of chemical reactions which occur in the atmosphere during transport and dispersion downwind from the source. The processes which lead to their formation are not altogether well understood.

For the purposes of calculating regional visibility degradation due to specific sources of air pollution, the primary focus has been on the contribution to light extinction of fine particles of sulfate and nitrate compounds. Once these particles are formed, their size can change, and thus their light scattering efficiency, due to changes in the RH of the atmosphere. In order to account for the contribution for light extinction of either sulfate or nitrate compounds, the mass of these constituents and the RH of the atmosphere in which these particles reside must be known. The calculations of the extinction due to primary fine particles are assumed to be non-hygroscopic.

Depending on the modeling situation, regional haze assessment can involve one to several sources, or it can involve a multitude of sources spanning several states. The first situation (involving isolated source impacts) most often arises within the context of assessing air quality impacts on Class I wilderness areas, which often involve transport of 50 km or more. The second situation (involving nationwide or regional impact assessments) most often arises within the context of assessing the impacts of new or existing air quality regulations. The modeling requirements for regional-scale multiple-source haze models are nearly identical to the modeling requirements for simulations of regional-scale multiple-source fine

particle impacts. Hence, the Eulerian-based grid models currently under development to support fine particle impact assessments will be relied upon to provide a means for assessing large-scale multiple-source haze impacts. Middleton (1996) described the findings of such a modeling effort; the Denver Air Quality Modeling Study (DAQMS). The Denver Air Quality Model was designed to apportion sources of visibility degradation and to evaluate the benefits of future emission controls in the Denver Metropolitan area. The results of the study demonstrated an association between visibility and air quality issues in the Colorado Front Range area. As this latter modeling is still under development, the following discussion summarizes recent efforts to improve the Lagrangian-based modeling products available for characterizing isolated source impacts involving long-range transport and dispersion.

A requirement of the CAA concerns air pollution impacts of proposed new sources on federal Class I areas and prevention of significant deterioration. The Class I areas (e.g., national parks, national wilderness areas, and other areas of special national value) are the responsibility of Federal Land Managers. The responsibility for prevention of significant deterioration is shared with U.S. Environmental Protection Agency and the States. However, the air quality assessment for proposed new sources often involves the simulation of air transport and dispersion over large distances (greater than 50 km). This creates a problem since Lagrangian-based simulation methods capable of reliably handling the complex transport and dispersive process unique to such long-range transport assessments have not been developed as yet to a point where guidance can be offered on how to apply these methods routinely (see section 7.6.2 of the Guideline on Air Quality Modeling, 40 CFR Appendix W to Part 51).

To address the joint responsibilities of various governmental agencies involved, a memorandum of understanding was established in November 1991 which formed a working group, known as the Interagency Workgroup for Air Quality Modeling. The purpose of the working group was to foster cooperation among the U.S. Environmental Protection Agency, the U.S. Forest Service, the Fish and Wildlife Service, the National Park Service, and selected State representatives. The goal was to foster development of applied mathematical modeling techniques needed by Federal Land Managers, and others, to make informed

decisions regarding the protection of federal Class I areas, especially within the context of assessing individual source impacts.

A two phased approach was devised (U.S. Environmental Protection Agency, 1992), given (1) the immediate need for guidance on modeling techniques for impact assessments involving regional scale (greater than 50 km) transport, (2) the complexity of applicable modeling systems and data bases, and (3) the spatial scales and potential numbers of sources for consideration. The first phase involved a review of available modeling techniques and construction of an interim recommendation for use by concerned technical and regulatory communities until such time that more permanent guidance could be offered. The second phase involved development, testing and application of state-of-the-art meteorological processors and dispersion modeling systems, to establish a basis for enhancement and perhaps replacement of the Phase I interim recommendations..

Following a series of model comparison and sensitivity analyses, a technical review was completed of meteorological data processing and dispersion modeling systems (U.S. Environmental Protection Agency, 1993b). This served as the basis for the Phase I interim recommendations. These findings facilitated use of the MESOPUFF II system (U.S. Environmental Protection Agency, 1994) within established national guidance provided in the Guideline on Air Quality Modeling. For the purposes of assessing regional haze impacts, the light extinction is estimated using 3- to 24-h concentration averages for the sulfate and nitrate compounds. The use of longer-period concentration averages to compute a light extinction coefficient (inverse of visual range) provides a pragmatic surrogate for assessing visibility degradation and avoids the overwhelming complications introduced when one attempts to invoke a line of sight visibility assessment for an actual vista.

The interim recommendations were applied in simulating pollutant impacts on the Shenandoah National Park to provide further technical information on the strengths and weaknesses of the available modeling systems (U.S. Environmental Protection Agency, 1995a). These results demonstrated that sources beyond 100 km might be expected to contribute and should not be arbitrarily excluded from assessments. They also demonstrated that such assessments are currently best accomplished on a case-by-case basis using expert judgement.

The technical work associated with phase II involves: (1) testing and assessment of possible benefits to be achieved through the use of state-of-the-art mesoscale meteorological (MM) processors employing four dimensional data assimilation (FDDA); (2) development of a state-of-the-art Lagrangian puff modeling system; and (3) testing of the developed modeling methods. Following completion of these technical efforts, an update to the Guideline on Air Quality Modeling can be proposed describing the modeling methods to be routinely accepted for characterization of long-range transport and dispersion from isolated sources.

The first step was addressed by initiating an analysis, in which MM-FDDA meteorological model was used to develop an hourly characterization of meteorological conditions (on a 80-km resolution) for an entire one-year period for the contiguous United States, northern Mexico and southern Canada. It was shown that MM-FDDA meteorological models could be applied operationally. Use of sophisticated meteorological processors provides a means for realistic characterization of long-range transport trajectories.

The second step involved enhancement of an advanced modeling system, entitled CALPUFF, capable of processing mesoscale meteorological data and capable of addressing dispersive processes of a regional nature. The modeling system was evaluated demonstrating the benefits of MM-FDDA meteorological data in characterizing long-range pollutant trajectories. Simulated trajectories were successfully compared to results from a field study involving transport to 1000 km downwind (U.S. Environmental Protection Agency, 1995b). The CALPUFF system was incorporated into a user-friendly windows-based environment with an on-line electronic user's guide (U.S. Environmental Protection Agency 1995c,d).

Previous evaluation results of puff dispersion models for transport distances of 30 to 100 km (Carhart et al., 1989), have illustrated the difficulty in characterizing the transport trajectory, but have seen a bias on the order of 30% on average towards overestimating the magnitude of the maximum surface concentration values. One of the findings of the trajectory comparisons (U.S. Environmental Protection Agency, 1995b), was that Lagrangian puff dispersion modeling involving transport of 200 km or more will underestimate the horizontal extent of the dispersion, thereby overestimate surface concentration values if delayed shear enhancement of dispersion (Moran and Pielke, 1994) is not addressed. In anticipation that CALPUFF will likely find widespread use in a variety of situations, a puff splitting algorithm was added to CALPUFF.

However, there remains a need to determine how best to invoke this algorithm for improved characterization of surface concentration values.

The third step towards providing enhanced guidance on methods for characterizing long-range dispersion for individual sources has been initiated by placing the CALMET/CALPUFF modeling system on the Support Center for Regulatory Models electronic bulletin board system for testing. Currently, this stage of the process must primarily rely on volunteer efforts from the public at large. It is hoped these efforts will prove successful in resolving the remaining technical issues, and that an update to the modeling guidance can be drafted for comment and review late in 1997.

### **8.6.3 Photographic Representations of Haze**

Photographs are frequently used to illustrate visibility conditions. However, it is difficult to take a series of photographs of an actual scene under known, uniform conditions to illustrate the effects of various intensities of haze. Therefore, computer-generated photographs have been used for this purpose. Examples of this use of photographs appear at the back of the National Acidic Precipitation Assessment Program report on visibility (Trijonis et al., 1991). The current status of photographic representations of haze has been described by Molenaar et al. (1994) and Eldering et al. (1993).

A photograph is taken on a very clean, cloud-free day and scanned to generate an initial image. The most laborious step is the creation of a distance map, which assigns a distance to each element in the scene. The estimated value of the light-extinction coefficient when the photograph was taken is used to calculate the initial radiances for each element in the scene. The horizon sky radiance can be used to estimate the source function in the calculations for the clean day.

The equations to generate images showing the effects of haze must calculate the value of the source function appropriate for the haze represented. Larson et al. (1988) have shown that the common practice of using the horizon sky radiance in the clean photograph as an estimate of the source function produces distorted results. Radiative transfer calculations can be used to derive the source function from the haze composition (Molenaar et al., 1994; Eldering et al., 1993). Equations 8-19 and 8-20 are used to calculate the radiances presented in the photographic images.

The use of photographic models for representation of haze requires many approximations. The softening of shadows caused by the diffuse lighting when it is hazy is neglected, and it is usually assumed that the haze is uniformly distributed throughout the scene. Photographs also have the limitation that they are expensive to produce, so are typically used to illustrate only a few conditions. Often, the selected conditions are idealized, so the full range of conditions that occur in a scene are not represented.

## **8.7 ECONOMIC VALUATION OF EFFECTS OF PARTICULATE MATTER ON VISIBILITY**

The effects of particulate matter on visibility were described in previous sections of this chapter and are hazes and reductions in visual range in all of the United States. This section discusses the available economic evidence concerning the value of preventing or reducing these types of effects on visibility. The following brief summary of economic estimation methods and available results is derived from the document, Air Quality Criteria for Oxides of Nitrogen (U.S. Environmental Protection Agency, 1993a). A comprehensive study on the economic impact of visibility impairment on national parks and wilderness areas and the cost of controls is currently being conducted by the Grand Canyon Visibility Transport Commission.

### **8.7.1 Basic Concepts of Economic Valuation**

Studies on the economic impact of visibility degradation have mainly focused on consumer activities, specifically on the individuals response to the aesthetic aspects. Studies on the effects of visibility degradation on commercial activities are limited. However, airport operations may be affected by visibility degradation, but available evidence suggests that the economic magnitude of the effects of haze on commercial operations probably is very small. Based on a 1985 report by the U.S. Environmental Protection Agency the percentage of the visibility impairment incidents sufficient to affect air traffic activity might be attributable, at least in part, to manmade air pollutants (possibly 2% to 12% in summer in the eastern United States).

That people notice changes in visibility conditions and that visibility conditions affect the well-being of individuals has been verified in scenic and visual air quality rating studies (Middleton et al., 1983; Latimer et al., 1981; Daniel and Hill, 1987), through the observation that individuals spend less time at scenic vistas on days with lower visibility (MacFarland et al., 1983), and through use of attitudinal surveys (Ross et al., 1987).

### **8.7.2 Economic Valuation Methods for Visibility**

Two main economic valuation methods have been used to estimate dollar values for changes in visibility conditions in various settings: (1) the contingent valuation method (CVM), and (2) the hedonic property value method. Both methods have important limitations, and uncertainties surround the accuracy of available results for visibility. Ongoing research continues to address important methodological issues, but at this time some fundamental questions remain unresolved (Chestnut and Rowe, 1990a; Mitchell and Carson, 1989; Fischhoff and Furby, 1988; Cummings et al., 1986). See Fischhoff and Fauby (1988), Kahneman and Knetsch (1992), Rowe and Chestnut (1982), Mitchell and Carson (1989), and Cummings et al. (1986) for details on these methods and its usefulness in economic valuations.

The CVM involves the use of surveys to elicit values that respondents place on changes in visibility conditions. The most common variation of the CVM relies on questions that directly ask respondents to estimate their maximum willingness to pay (WTP) to obtain or prevent various changes in visibility conditions based on photographs and verbal descriptions, and some hypothetical payment mechanism, such as a general price increase or a utility bill increase.

Among the fundamental issues concerning the adequacy of CVM for estimating visibility values are (1) the ability of researchers to present visibility conditions in a manner relevant to respondents and to design instruments that can elicit unbiased values; and (2) the ability of respondents to formulate and report values with acceptable accuracy. Another important issue in CVM visibility research concerns the ability of respondents to isolate values related to visibility aesthetics from other potential benefits of air pollution control such as protection of human health.

The hedonic property value method uses relationships between property values and air quality conditions to infer values for differences in air quality. The approach is used to determine the implicit, or "hedonic," price for air quality in a residential housing market, based on the theoretical expectation that differences in property values that are associated with differences in air quality will reveal how much households are willing to pay for different levels of air quality in the areas where they live. This approach uses real market data that reflect what people actually pay to obtain improvements in air quality in association with the purchase of their homes. Hedonic property value studies provide estimates of total value for all perceived impacts resulting from air pollution at the residence, including health, visibility, soiling, and damage to materials and vegetation. The most important limitation is the difficulty in isolating values for visibility from other effects of air pollution at the residence.

### **8.7.3 Studies of Economic Valuation of Visibility**

Economic studies have estimated values for two types of visibility effects potentially related to particulate matter and  $\text{NO}_x$ : (1) use and non-use values for preventing the types of plumes caused by power plant emissions, visible from recreation areas in the southwestern United States; and (2) use values of local residents for reducing or preventing increases in urban hazes in several different locations.

#### **8.7.3.1 Economic Valuation Studies for Air Pollution Plumes**

Three CVM studies have estimated on-site use values for preventing an air pollution plume visible from recreation areas in the southwestern United States (Table 8-5). One of these studies (Schulze et al., 1983) also estimated total preservation (use and non-use) values held by visitors and non-visitors for preventing a plume at the Grand Canyon. The plumes in all three studies were illustrated with actual or simulated photographs showing a dark, thin plume across the sky above scenic landscape features, but specific measures such as contrast and thickness of the plume were not reported. The estimated on-site use values for the prevention or elimination of the plume ranged from about \$3 to \$6 (1989 dollars) per day per visitor-party at the park. A potential problem common to all of these studies is the use of daily entrance fees as a payment vehicle.

**TABLE 8-5. ECONOMIC VALUATION STUDIES FOR AIR POLLUTION PLUMES**

Study	Location of Plume	Study Subjects	Year of Interviews	Type of Value	Valuation Method <sup>a</sup>	Payment Vehicle	Mean Results (\$ 1989)
Schulze et al. (1983)	Grand Canyon National Park	Urban residents who have visited or plan to visit Grand Canyon	1980	Daily use value at park per household	Contingent valuation, direct WTP question	Daily park entrance fee	\$6.17 per day at park per household
		Urban residents in Denver, Los Angeles, Chicago, Albuquerque; visitors and non-visitors	1980	Monthly preservation value per household	Contingent valuation, direct WTP question	Monthly utility bill increase	\$5.31 per month per household
MacFarland et al. (1983)	Grand Canyon National Park	Park visitors	1980	Daily use value at park per visitor-party (household)	Contingent valuation, direct WTP question	Daily park entrance fee	\$2.84 per day at park per visitor-party (household)
Brookshire et al. (1976)	Glen Canyon National Recreation Area (Lake Powell)	Nearby residents and lake visitors	1974	Daily use value at recreation area per visitor-party (household)	Contingent valuation, direct WTP question	Daily entrance fee	Visitors: \$3.32 per day additional to prevent visible plume Residents: \$2.21 per day additional to prevent visible plume

<sup>a</sup>WTP = Willingness to pay.

The Schulze et al. (1983) study suggest that on-site preservation values for preventing a plume at the Grand Canyon every day, based on 1.3 million visitor-parties of about three people per party, would be about \$8 million. Based on their results, the implied preservation value for preventing a visible plume most days (the exact frequency was not specified) at the Grand Canyon would be about \$5.7 billion each year when applied to the total U.S. population. However, Chestnut and Rowe (1990b) reported that the Schulze et al. (1983) preservation value estimates for haze at national parks in the Southwest are probably overstated by a factor of two or three and the same probably applies to the preservation value estimates for plumes.

### **8.7.3.2 Economic Valuation Studies for Urban Haze**

Six economic studies concerning urban haze caused by air pollution are summarized in Table 8-6. The implicit values obtained for a 10% change in visual range are reported in Table 8-6 to allow a comparison of results across the studies. Values for a 10% change are shown to illustrate the range of results across the different studies. These estimates are based on a model developed for comparison purposes that assumes economic values are proportional to the percentage change in visual range. Values for a 20% change, for example, would be about twice as large as those shown for a 10% change, given the underlying comparison model. Each of these studies relied on a reasonably representative sample of residents in the study area, such that a range of socioeconomic characteristics and of neighborhood pollution levels was included in each sample.

The first five studies in Table 8-6 all focused on changes in urban hazes with fairly uniform features that can be described as changes in visual range. The sixth study (Irwin et al., 1990) focused on visual air quality in Denver, where a distinct edge to the haze is often noticeable, making visual range a less useful descriptive measure because it would vary depending on the viewpoint of the individual and whether the target was in or above the haze layer. The studies conducted in Denver and in the California cities are likely to have a higher  $\text{NO}_x$  component than in the eastern cities.

Both of the CVM studies in California asked respondents to consider health and visual effects but used different techniques to have respondents partition the total values. They found that, on average, respondents attributed about one-third to one-half of their total values

**TABLE 8-6. ECONOMIC VALUATION STUDIES ON URBAN HAZE**

Study	Location	Year	Valuation Method <sup>a</sup>	Payment Vehicle	Presentation/Definition of Change in Visibility	Implied Mean Annual WTP <sup>a</sup> for a 10% Change in Visual Range (\$ 1989)
<b>PART I. UNIFORM URBAN HAZE</b>						
<u>Western Cities</u>						
Loehman et al. (1981)	San Francisco	1980	Contingent valuation, direct WTP question	Monthly utility bill increases	Change in frequency distribution illustrated with local photos for 3 levels of air quality	\$106 per household
Brookshire et al. (1982)	Los Angeles	1978	Contingent valuation, direct WTP question	Monthly utility bill increases	Change in average visibility illustrated with local photos for 3 levels of air quality	\$10 per household
Trijonis et al. (1984)	San Francisco	1978-79	Hedonic property value		Light extinction based on airport visibility data	\$208-231 per household
	Los Angeles	1978-79	Hedonic property value		Light extinction based on airport visibility data	\$112-226 per household
<u>Eastern Cities</u>						
Tolley et al. (1986)	Chicago; Atlanta; Boston; Mobile; Washington, D.C.; Miami; Cincinnati	1982	Contingent valuation, direct WTP question	Monthly payment for visibility improvement program	Change in average visibility illustrated with Chicago photos for levels of air quality	\$8-51 per household

**TABLE 8-6 (cont'd). ECONOMIC VALUATION STUDIES ON URBAN HAZE**

Study	Location	Year	Valuation Method <sup>a</sup>	Payment Vehicle	Presentation/Definition of Change in Visibility	Implied Mean Annual WTP <sup>a</sup> for a 10% Change in Visual Range (\$ 1989)
<b>PART I (cont'd). UNIFORM URBAN HAZE</b>						
Rae (1984)	Cincinnati	1982	Contingent valuation, direct WTP question	Monthly payment for visibility improvement program	Change in average visibility illustrated with Chicago photos for 3 levels of air quality	\$48 per household
<b>PART II. URBAN HAZE WITH BORDER</b>						
Irwin et al. (1990)	Denver	1989	Contingent valuation, direct WTP question	General higher prices each year	1-step change in 7-point air quality scale, illustrated with photos	<u>Preliminary</u> results indicate mean annual WTP of about \$100 per household for a 1-step change in the 7-point scale, with about one-third of the value attributed to visibility alone

<sup>a</sup>WTP = Willingness to pay.

to aesthetic visual effects. In spite of many similarities in the approaches used, the CVM results for San Francisco are notably higher than for Los Angeles when adjusted to a comparable percentage change in visual range. One potentially important difference in the presentations was that Loehman et al. (1981) defined the change in visibility as a change in a frequency distribution rather than simply a change in average conditions. This type of presentation is more realistic but more complex; and it is unclear how it may affect responses relative to presentation of a change in the average. It is possible that the distribution presentation might elicit higher WTP responses because it may focus respondents' attention on the reduction in the number of relatively bad days (and on the increase in the number of relatively good days), whereas the associated change in the average may not appear as significant. The implied change in average conditions in the Loehman et al. (1981) San Francisco study was considerably smaller than that presented in the Brookshire et al. (1982) Los Angeles study, which may have also resulted in a higher value when adjusted to a comparable size change in average visual range because of diminishing marginal utility (i.e., the first incremental improvement is expected to be worth more than the second).

The California studies in Los Angeles and San Francisco provide some interesting comparisons because two different estimation techniques were applied for the same locations. Property value results for changes in air quality for both cities were found to be higher than comparable values (for changes in total air quality) obtained in the CVM studies. This is as expected given the theoretical underpinnings of each estimation method, although Graves et al. (1988) have reported that subsequent analysis of the property value data revealed that the estimates are more variable than the original results suggest. These property value results are not reported here because they are for changes in air pollution indices that are not tied to visual air quality.

The property value study results reported in Table 8-6 from Trijonis et al. (1984) were estimated using light extinction as the measure of air quality. However, as discussed in the previous section on the hedonic property value method, these estimates are still likely to include perceived benefits to human health for reductions in air pollution as well as values for visual aesthetics. Consistent with this expectation, the results for a 10% change in light extinction are higher than the CVM results for visual range changes for the same cities. Respondents in several CVM studies have reported that, on average, they would attribute to

visibility aesthetics about one-fourth to one-half of their total WTP for improvements in air quality. This would imply that the Trijonis et al. (1984) results may reflect \$25 to \$100 for a change in visibility alone.

The results for the uniform urban haze studies in cities in the eastern United States fall between the respective CVM results for the California cities. The changes in visual range presented in these studies were similar to those presented in the Los Angeles study. In all of the eastern studies respondents were simply asked to consider only the visual effects when answering the WTP questions. This approach is now considered to be inadequate (Irwin et al., 1990; Carson et al., 1990).

McClelland et al. (1991) conducted a mail survey in 1990 in Chicago and Atlanta. Residents were asked what they would be willing to pay to have an improvement in air quality, which amounted to about a 14% improvement in annual average visual range. Respondents were then asked to say what percentage of their response was attributable to concern about health effects, soiling, visibility, or other air quality effects. Respondents, on average, attributed about 20% of their total WTP to visibility. The authors conducted two analyses and adjustments on the responses. One was to estimate and eliminate the potential selection bias resulting from non-response to the WTP questions (including what has been called protest responses). The other was to account for the potential skewed distribution of errors caused by the skewed distribution of responses (the long tail at the high end). Both of these adjustments caused the mean value to decrease. The annual average household WTP for the designated visibility improvement was \$39 before the adjustments and \$18 after the adjustments. This adjusted mean value implies about \$13 per household for a 10% improvement in visual range. This is at the low end of the range of estimates shown in Table 8-6. If peer-review of this research effort confirms the appropriateness of the study design and analysis, the results suggest that greater confidence should be placed in the lower end of the range of results shown in Table 8-6 because this study represents an improvement in approach over the other eastern-cities studies.

Irwin et al. (1990) have reported preliminary results for the Denver study (Part II, Table 8-6). Comparison of these preliminary results with results from other studies is difficult because the photographs used to illustrate different levels of air quality were not tied to visual range levels. Instead, they were rated on a seven-point air quality scale by the

respondents, who were then asked their maximum WTP for a one-step improvement in the scale. This study reports some important methodological findings. One of these is confirmation that simply asking respondents to think only about visibility results in higher WTP responses for visibility changes than when respondents are asked to give WTP for the change in air quality and then to say what portion of that total they would attribute to visibility only. The latter approach produced a mean WTP estimate for a one-step change in visibility that was about one-half the size of the mean WTP estimate given when respondents were simply asked to think only about visibility. This may result from the effect of budget constraints on marginal values (the respondent has less to spend on visibility when he also is buying health); however, the authors express the concern that some, but not all, of the value for health may be included in the response when respondents are told to think only about visibility. They recommend that respondents be asked to give total values for changes in urban air quality and then be asked to say what portion is for visibility.

## **8.8 CLIMATIC EFFECTS**

### **8.8.1 Introduction**

Aerosols of submicron size in the atmosphere can affect the Earth's climate directly through the absorption of radiation and indirectly by modifying the optical properties and lifetime of clouds (perturbation of the radiative field). Perturbation of the radiation field generally is expressed as a *radiative forcing*, which is the change in average net radiation at the top of the troposphere because of a change in solar (shortwave) or terrestrial (longwave) radiation (Houghton et al., 1990). Note that it is the net effect at the top of the troposphere (i.e., the tropopause) that forces climate, and not the change at the surface, because the surface and troposphere are intimately coupled through atmospheric energy exchange processes such as dry and moist convection (Ramanathan et al., 1987). The radiative forcing due to aerosols is negative (i.e., aerosols have a cooling effect through the enhanced reflection of solar energy). This is in contrast to radiatively active trace ("greenhouse") gases associated with industrial and agricultural activities, which produce a positive longwave radiative forcing (i.e., "greenhouse" gases cause a warming of the earth-troposphere system). A large fraction of atmospheric particulate matter is of anthropogenic origin, the chief

sources being the emission of sulfur-containing aerosols by industry and the large-scale burning of biomass.

### 8.8.2 Radiative Forcing

There is now little doubt that long-lived, optically thick, aerosol layers may have modified the Earth's climate in the past. Geologic evidence suggests that there have been episodic injections of massive amounts of material into the Earth's atmosphere as a result of the impact of large asteroids or comets. The diminution of solar radiation reaching the surface has been suggested as the most likely cause of mass extinctions of species at the Cretaceous-Tertiary boundary (Alvarez et al., 1980) and also in the Late Devonian (Claeys et al., 1992). The possibility of a similar climatic catastrophe following a nuclear war has also been raised (Turco et al., 1983, 1990). However, these are examples of massive injections of particulate matter that result in extremely large radiative forcings. Current interest is focused on much more modest injections of materials that form thin aerosol layers in the troposphere. Although the radiative effects are smaller and have been generally ignored in climate model simulations (Hansen and Lacis, 1990), recent studies have estimated that they are not negligible and that their radiative forcing may be comparable (but opposite in sign) to the radiative effects of increased greenhouse gas emissions (Wigley, 1991; Charlson et al., 1992; Penner et al., 1992). Because there is so much concern regarding greenhouse gas-induced climate change, the study of this potential opposite effect of industrial emissions is expected to be quite intense in the near future (Penner et al., 1994).

To appreciate what is at issue here, it is necessary to understand the concept of radiative forcing. Averaged globally and annually, about 240 watts per meter squared ( $\text{W m}^{-2}$ ) of solar energy is absorbed by the earth-atmosphere system (Hartmann, 1994). This must be balanced by an equal emission of thermal energy back to space for equilibrium. A *change* in average net radiation at the tropopause, because of a change in either solar or terrestrial radiation, perturbs the system and this perturbation is defined as the *radiative forcing*. In response to this perturbation, the climate system will try and reach a new equilibrium state. For example, the increase in longwave opacity of the atmosphere resulting from enhanced concentrations of greenhouse gases such as carbon dioxide ( $\text{CO}_2$ ) and methane ( $\text{CH}_4$ ) is a positive radiative forcing because it leads to a reduction in outgoing thermal

radiation. For equilibrium, given that there is no change in solar input, the temperature of the surface-troposphere system must increase. The individual contributions to this positive forcing, since pre-industrial times, is shown in Figure 8-15 (Houghton et al., 1990). Carbon dioxide is the single most important contributor with a radiative forcing of  $1.50 \text{ W m}^{-2}$  for the period 1765 to 1990. The total for all greenhouse gases attributable to anthropogenic sources is  $2.45 \text{ W m}^{-2}$ .

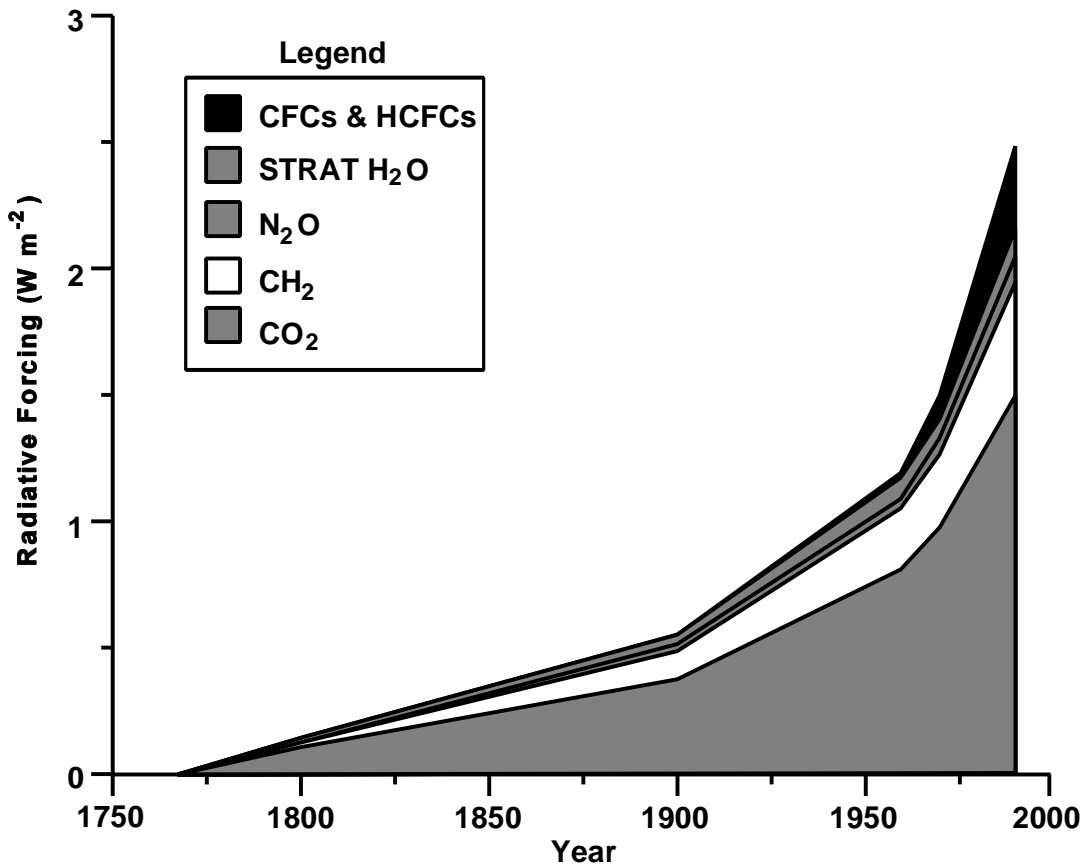


**Figure 8-15. Changes in radiative forcing ( $\text{W m}^{-2}$ ) due to increases in greenhouse gas concentrations between 1765 and 1990. Values are changes in forcing from 1765 concentrations.**

Source: Houghton et al. (1990).

Human activity has also led to an increase in the abundance of tropospheric aerosols, primarily as a result of enhanced  $\text{SO}_2$  emission, but also from biomass burning. This aerosol

layer produces a radiative forcing by perturbing the amount of solar energy that is absorbed by the earth-atmosphere system. By increasing the amount of solar energy reflected by the planet, aerosols produce a direct radiative forcing. They can also force the climate system indirectly by modifying the microphysical properties of clouds, primarily by reducing the effective drop size of water clouds. Both the direct and indirect radiative forcing of aerosols are negative (i.e., in response to this perturbation, the planet will cool).

Aerosols in the stratosphere have been implicated in the loss of O<sub>3</sub> through heterogeneous chemistry involving chlorine compounds (Hoffman and Solomon, 1989; Schoeberl et al., 1993; Hoffman et al., 1994). Although the chlorine is primarily of anthropogenic origin, the enhanced concentrations of aerosols are a result of volcanic eruptions. Anthropogenic SO<sub>2</sub> does not change the stratospheric aerosol burden appreciably. Therefore, this effect of aerosols is not relevant to this discussion.

The succeeding sections of this chapter are devoted to the estimation of aerosol radiative forcing. Translating this forcing into a climate response requires the incorporation of the forcing into a climate model. The model simulations, of course, are only as reliable as the models, which typically incorporate numerous feedbacks in the climate system that are only represented to some degree of approximation. There are certainly many feedbacks missing from current climate models, and it is quite possible that some feedbacks have been modeled quite incorrectly. Moreover, the radiative forcing due to anthropogenic aerosols needs to be estimated separately from that due to naturally occurring aerosols in order to evaluate the impact of human activity. The relationship between these aspects of the problem is shown in Figure 8-16.

As has been mentioned, the radiative forcing due to aerosols is opposite in sign to that due to greenhouse gases, but the degree of offset in forcing may not translate into offsetting climatic consequences. We can only judge these by studying model simulations. Also, it must be kept in mind that climate variations occur in the absence of radiative forcing as a result of interactions between the atmosphere, oceans, and the various elements of the land surface such as snow cover and vegetation.

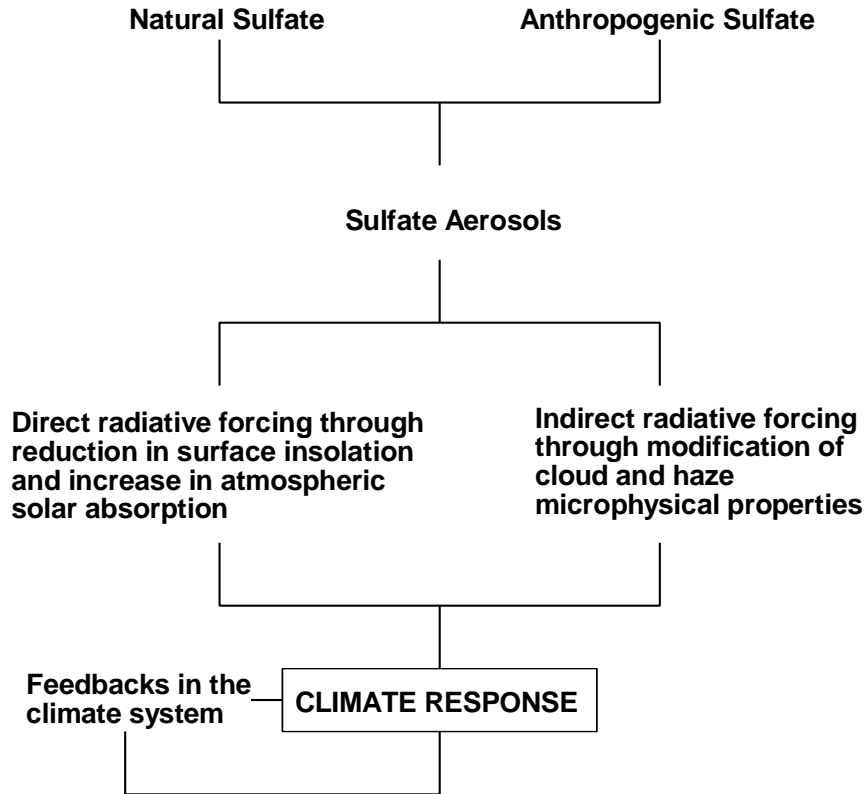


**Figure 8-16.** A schematic diagram showing the relationship between the radiative forcing of sulfate aerosols and climate response.

Source: Harshvardhan (1993).

### 8.8.3 Solar Radiative Forcing by Aerosols

Aerosol radiative forcing results from enhanced reflection of solar energy which enters the top of the Earth's atmosphere as a collimated beam of infinite width, but is subsequently scattered and absorbed to some degree even on the clearest day. Figure 8-17 shows this process schematically. Throughout the troposphere molecules, constituting the atmosphere, scatter sunlight by Rayleigh scattering (see the discussion of visibility for the definition of Rayleigh scattering), which is highly wavelength dependent. In the lower troposphere, sunlight is scattered by aerosols or haze and absorbed by aerosols and water vapor. Because the aerosol loading is quite variable, this component of aerosol scattered solar radiation is also variable.

The degree to which a layer of particles scatters solar radiation is primarily determined by the nondimensional parameter referred to as the scattering optical depth of the layer,  $\tau_s$ ,

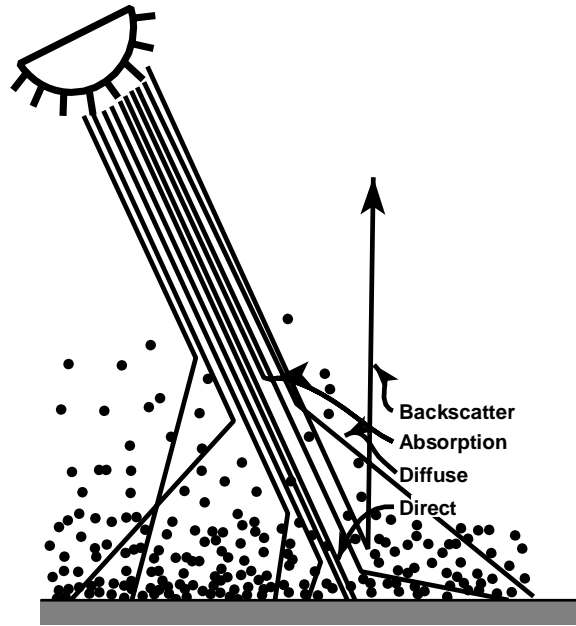


**Figure 8-17. Extinction of direct solar radiation by aerosols showing the diffusely transmitted and reflected components, as well as the absorbed components.**

which in turn is the column integrated volume scattering coefficient for particles,  $\sigma_{sp}$  (units are  $\text{km}^{-1}$ , see sections on visibility for details). Because the scattering coefficient for particles depends on wavelength, the attenuation of the direct beam of sunlight is also wavelength dependent. This spectral behavior is usually expressed by the proportionality

$$\sigma_{sp} \propto \lambda^{-\alpha} \quad (8-37)$$

where  $\lambda$  is the wavelength in micrometers ( $\mu\text{m}$ ). The exponent,  $\alpha$ , is the turbidity parameter introduced by Ångström (1964) and varies between 0.5 and 1.5 for aerosols (Twomey, 1977). For particles that are very small compared to the wavelength (Rayleigh scattering),  $\alpha = 4$ , and for relatively larger particles, such as cloud drops,  $\alpha = 0$ . The downwelling portion of the radiation scattered by molecules and aerosols forms diffuse skylight whereas the unattenuated beam of solar radiation is said to be the directly transmitted or beam radiation. The upwelling portion of scattered radiation, together with energy reflected by the surface, is the diffuse reflection of the earth-atmosphere system. It is the perturbation in this

component of radiant energy by enhanced aerosol loadings that constitutes the radiative forcing to the system by aerosols. The sum of directly and diffusely transmitted solar energy is the global solar radiation incident on a surface.

Figure 8-18, from Iqbal (1983), shows computations of the spectral distribution of a solar energy incident on a horizontal surface for a solar zenith angle of  $60^\circ$  (air mass = 2) and standard clear conditions. The atmosphere contains 350 Dobson units of ozone ( $O_3$ ), 2 ppt/cm of water vapor, and a nonabsorbing aerosol layer corresponding to a surface visibility of 28 km. The ground reflectance is 0.2. Some features of Figure 8-18 are worth noting. Virtually all solar radiation at wavelengths less than  $0.29 \mu\text{m}$  is removed by  $O_3$  absorption. Rayleigh scattering by molecules is the predominant source of the diffuse radiation at shorter wavelengths, but the contribution falls off very dramatically with increasing wavelength because of the inverse fourth power dependence. Aerosol scattering contributes to the diffuse component at visible and near-infrared wavelengths. Absorption by the strong water vapor bands is quite evident in the near-infrared.

An increase in the optical depth of aerosols results in a decrease in the direct beam radiation, which could be substantial, but the downwelling portion of the enhanced scattered radiation compensates for this to a large extent. This is illustrated in Figure 8-19, which shows surface measurements of direct, diffuse, and global solar radiation, made using a multifilter rotating shadowband radiometer (Harrison and Michalsky, 1994; Harrison et al., 1994) at Albany, NY, on two clear days in August of 1992 and 1993. The total atmospheric optical depth in 1992 was influenced by the eruption of Mt. Pinatubo in June 1991. Although the volcanic aerosols were in the stratosphere, their effect on direct and diffuse transmitted radiation is similar to that due to tropospheric aerosols. The quantity plotted is the spectral irradiance convolved with the average human eye response that peaks at 550 nm and falls to zero at 400 and 700 nm. The main feature of the plot is the substantial difference in direct and diffuse radiation, but quite similar global irradiances. Close inspection shows that on the hazier day (in 1992), the global transmitted radiation was somewhat less (i.e., the volcanic aerosol caused a negative radiative forcing to the earth-atmosphere system by increasing the planetary albedo). Locally, tropospheric aerosol optical

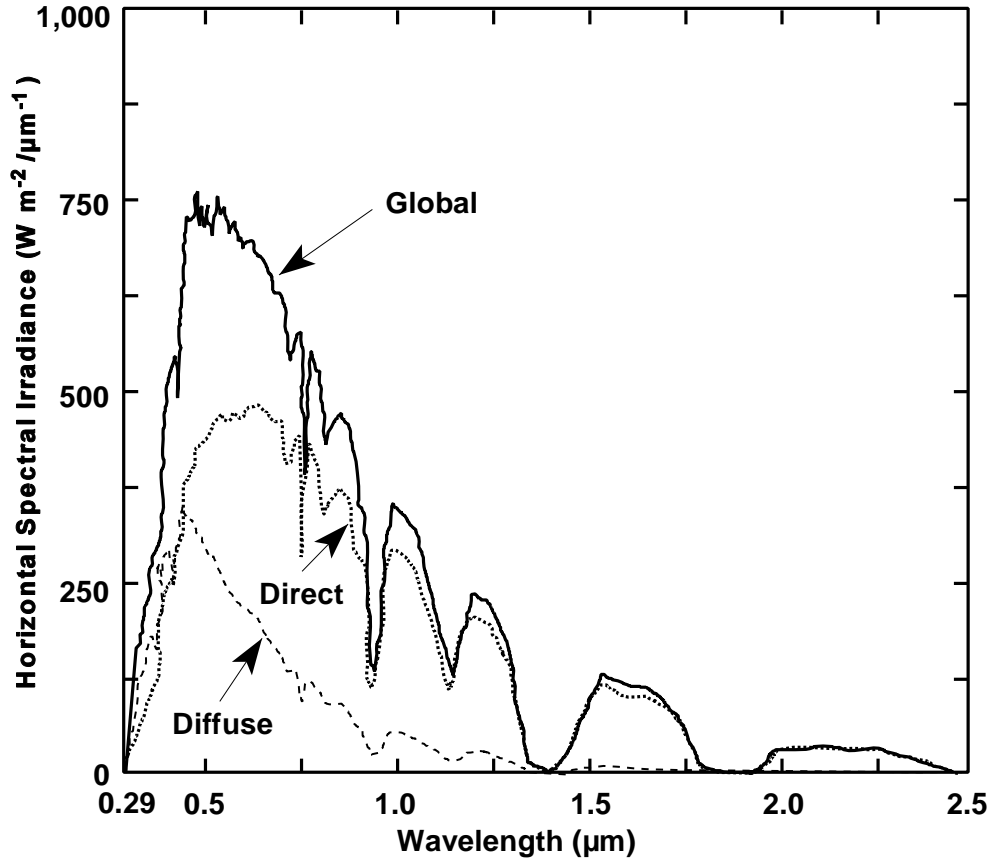


**Figure 8-18.** Global, direct, and diffuse spectral solar irradiance on a horizontal surface for a solar zenith angle of  $60^\circ$  and ground reflectance of 0.2. Atmospheric conditions are visibility, 28 km; water vapor, 2 ppt/cm.; ozone, 350 Dobson units.

Source: Iqbal (1983).

depths are much larger than the stratospheric optical depth and one would expect a more obvious diminution of global transmitted radiation than is shown here.

Figure 8-19 is for the spectrally integrated irradiance. Within the solar spectrum, wavelengths are affected to different degrees by the presence of aerosols. In particular there have been some studies on the effect of aerosols on transmitted UV to the surface. This an important consideration, especially for UV-B ( $280 \text{ nm} < \lambda < 320 \text{ nm}$ ). Many theoretical studies have been made of the effect of stratospheric aerosols on transmitted UV (Michelangeli et al., 1989, 1992; Davies, 1993; Box, 1995). They have shown that global transmitted UV can increase with the addition of a thin aerosol layer when the sun is low in

the sky and the layer is above the absorption region. The process responsible for this is single scattering which changes the direction of the incident radiation such that there is a shorter path through the absorbing layer and more is transmitted to the ground. However, when the sun is high in the sky or the scattering layer is below the absorbers this effect does not occur.

For tropospheric aerosols, the net effect is a reduction in global irradiance at all wavelengths similar to the total energy shown in Figure 8-19. Frederick et al. (1989) have calculated the expected change in Robertson-Berger meter readings from 1969 to 1986 for 34.5°N based on changes in column ozone as reported by Watson et al. (1988). They compared ratios with and without an aerosol layer of optical depth 0.1 independent of wavelength in the lowest 2 km for 1986 only. For clear atmospheres, the ratio changed from 1.02 without the aerosol to 0.92 with the aerosol indicating that the effect on UV-B transmission of the depletion in column ozone from 1969 to 1986 could be compensated by a concomitant increase in particulate matter. Measurements made at Barcelona, Spain, by Lorente et al. (1994) show that the UV-B at the surface is reduced by 37% during the most polluted days and UV-A is reduced by 30% compared to the clearest days. By reflecting some UV back to space, tropospheric aerosols actually decrease the irradiance of this flux to the surface.

### **8.8.3.1 Modeling Aerosol Direct Solar Radiative Forcing**

Some basic aspects of scattering and absorption by small particles typically present in aerosol layers govern the sign and magnitude of the direct radiative forcing by aerosols. These properties are discussed in Section 8.2 of this chapter. The reflectance of an aerosol layer is chiefly determined by the optical depth, single scattering albedo,  $\omega_{00}$ , and some measure of the scattering phase function. The single scattering albedo, the ratio of the light-scattering coefficient and the light-extinction coefficient, is a measure of the absorptance of the aerosol layer. Related quantities are the specific extinction and specific scattering coefficients,  $\psi_{ext}$  and  $\psi_{scat}$ , which are defined as the coefficients per unit mass in units of  $m^2g^{-1}$ . The phase function determines the probability that incident radiation will scatter into a particular direction given by the scattering angle measured from the forward direction of the incident radiation.

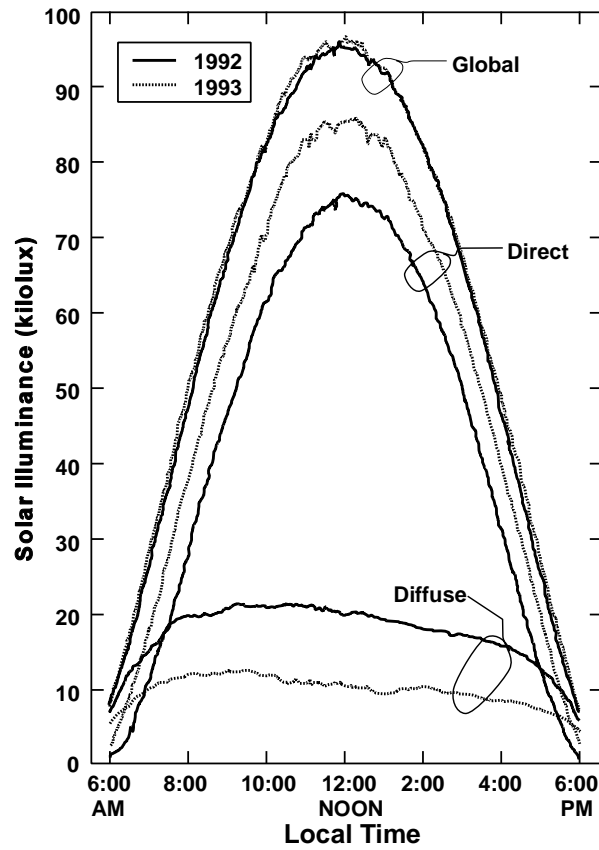


**Figure 8-19. Surface measurements of direct, diffuse, and global solar radiation expressed as illuminance, at Albany, NY, on August 23, 1992, and August 26, 1993.**

Source: Harrison and Michalsky (1994).

At visible wavelengths, the optical depth of tropospheric aerosols ranges from less than 0.05 in remote, pristine environments to about 1.0 near the source of copious emissions (Weller and Leiterer, 1988). The optical depth decreases quite rapidly with increasing wavelength if the layer is composed of fine particles as can be seen from Equation 8-37. Aerosol layers, therefore, tend to be fairly transparent at thermal wavelengths and their radiative forcing is confined to solar wavelengths. Because there are strong water vapor absorption bands in the solar near-infrared (see Figure 8-20), the dominant effect of tropospheric aerosols is in the visible wavelengths. Harshvardhan (1993) has shown that, to the first order, the change in the albedo with the addition of a thin aerosol layer over a surface of reflectance,  $R_s$ , is

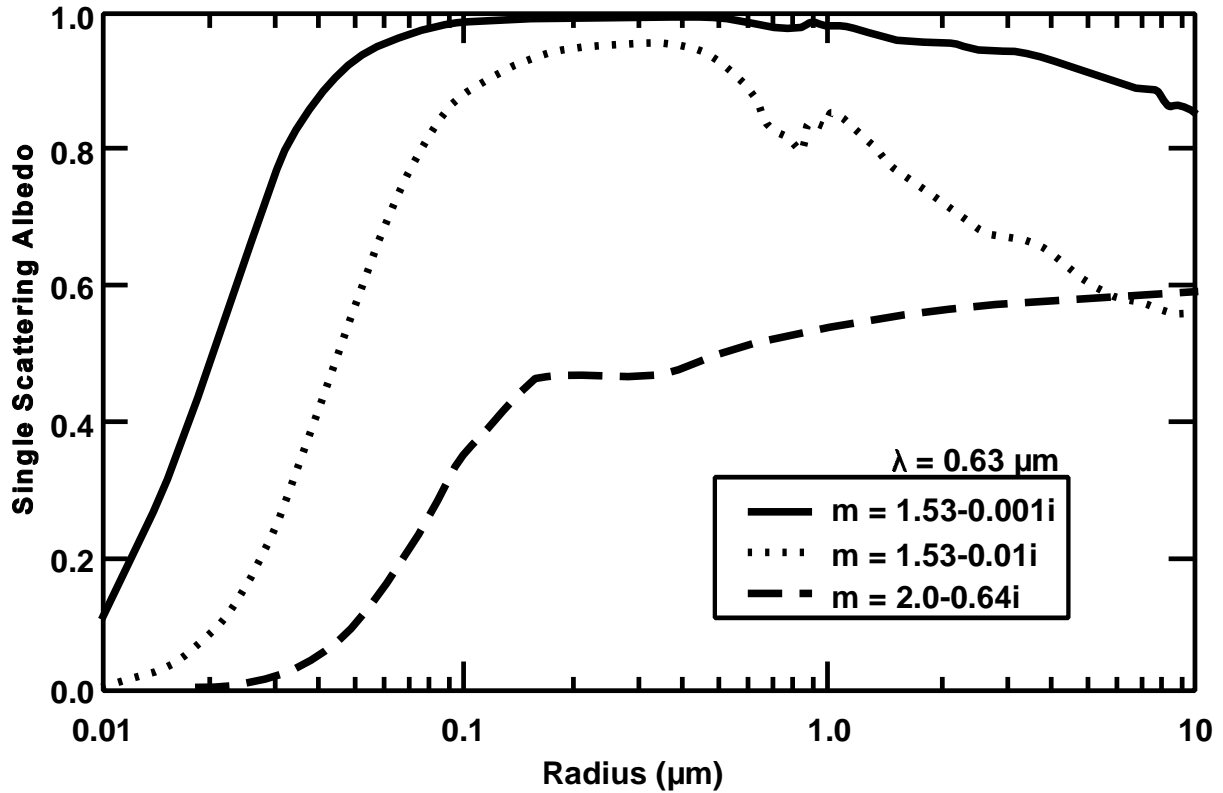


**Figure 8-20. Single scattering albedo of monodispersed spherical aerosols of varying radius and three different refractive indices at a wavelength of  $0.63 \mu\text{m}$ .**

Source: Harshvardhan (1993).

$$\Delta R \approx R_a(1 - R_s)^2 - 2A_aR_s \quad (8-38)$$

where  $R_a$  and  $A_a$  are the reflectance and absorptance, respectively, of the aerosol layer. The perturbation,  $\Delta R$ , will be positive when

$$(1 - \omega_0)/\omega_0\beta < (1 - R_s)^2/2R_s \quad (8-39)$$

where  $\beta$  is the average backscatter fraction and can be computed from the scattering phase function. A positive value for the change in albedo implies a negative solar radiative forcing because the planetary albedo increases and less solar energy is absorbed by the earth-atmosphere system.

From Equation 8-39, it is obvious that the sign of the forcing will be determined to a large extent by the single scattering albedo. At visible wavelengths, most constituents of tropospheric aerosols, with the exception of elemental carbon, are nonabsorbing and  $\omega_{00} = 1.0$  (Bohren and Huffman, 1983) so that the change in albedo will be positive. Aerosols with absorbing components can be modeled as equivalent scatterers of refractive index,  $m = n - ik$ , with the imaginary index being a measure of particle absorption. Figure 8-20, shows the computed values of single scattering albedo at a wavelength of  $0.63 \mu\text{m}$  for single particles of varying radius. The three separate curves are for aerosols composed of carbon ( $m = 2.0 - 0.64i$ ) and two models of sulfate aerosols containing absorptive components. Given the properties of an aerosol layer, the change in albedo can be computed from Equation 8-38. To calculate the radiative forcing, one must also include the effects of other atmospheric constituents such as molecular scattering, stratospheric  $\text{O}_3$ , water vapor absorption, and, most importantly, cloud cover.

### 8.8.3.2 Global Annual Mean Radiative Forcing

Charlson et al. (1991) calculated the global mean radiative forcing due to anthropogenic aerosols by making the following assumptions. They assumed that the perturbation would be exceedingly small over cloudy areas because cloud optical depths are one to two orders of magnitude greater than aerosol optical depths (Rossow and Schiffer, 1991). For nonabsorbing aerosols, they found that the change in planetary albedo could be expressed as

$$\Delta R_p \approx T^2 (1 - N_c) (1 - R_s^2) (2\beta\tau) \quad (8-40)$$

where  $T$  is the transmittance of the atmosphere above the aerosol layer and  $N_c$  is the global mean cloud fraction. The planetary mean radiative forcing is then

$$\Delta F_R = \Delta R_p S_0 / 4 \quad (8-41)$$

where  $S_0/4$  is the annual global mean insolation of the earth-atmosphere system (Hartmann, 1994) with  $S_0$  being the solar constant, which equals to  $1,370 \text{ W m}^{-2}$ . For the generally accepted values of  $T = 0.71$ ,  $N_c = 0.6$ ,  $R_s = 0.15$  and  $\beta = 0.3$ , Charlson et al. (1991)

$$\Delta F_R = 30.0 \tau \quad (8-42)$$

obtained such that for  $\tau$ , the optical depth at visible wavelengths ranging from 0.05 to 0.10, the direct solar radiative forcing is  $1.5$  to  $3.0 \text{ W m}^{-2}$ , a value comparable to the long-wave radiative forcing of all the anthropogenic greenhouse gases (Section 8.8.2).

The above estimate was refined by Charlson et al. (1992) in which the anthropogenic sulfate aerosol burden was actually related to the source strength of anthropogenic  $\text{SO}_2$ , the fractional yield of emitted  $\text{SO}_2$  that reacts to produce sulfate aerosol and the sulfate lifetime in the atmosphere. The scattering properties of the sulfate aerosol were also modeled in terms of a relative humidity factor that accounts for the increase in particle size associated with deliquescent or hygroscopic accretion of water with increasing RH. The relationship between optical depth and the areal mean column burden of anthropogenic sulfate aerosol,  $B_{\text{sulfate}}$ , is

$$\tau = \chi_{\text{sulfate}} f(\text{RH}) B_{\text{sulfate}} \quad (8-43)$$

where  $\chi_{\text{sulfate}}$  is the molar scattering cross section of sulfate at a reference low RH (30%) and  $f(\text{RH})$  is the relative humidity factor. The sulfate burden, is related to  $\text{SO}_2$  emissions and sulfate lifetime. For an emission rate of  $90 \times 10^{12} \text{ g}$  of sulfur per year, a yield fraction of 0.4, a sulfate lifetime of 0.02 years (7 days) and the molar scattering cross section of sulfate of  $500 \text{ m}^2 \text{ mol}^{-1}$  (corresponding to specific extinction coefficient of  $5 \text{ m}^2 \text{ g}^{-1}$ ), Charlson et al. (1992) estimated that  $\Delta F_R = 1.0 \text{ W m}^{-2}$ , with an uncertainty factor of 2, which perhaps should be more considering that the uncertainty in the specific extinction coefficient alone is higher (Hegg et al., 1993, 1994; Anderson et al., 1994).

The above is an estimate for the forcing due to industrial emissions. Another anthropogenic source of aerosols is biomass burning. Penner et al. (1992) have estimated

that the radiative forcing due to this activity could be as much as  $0.9 \text{ W m}^{-2}$ , which is comparable to the sulfate forcing. One difference is that the smoke produced is somewhat absorbing and the atmosphere would experience a positive forcing of  $0.5 \text{ W m}^{-2}$ . Estimates of the global forcing due to biomass burning are even more uncertain than those for sulfate because of the sparsity of data on the relevant radiative properties of biomass aerosols.

## 8.8.4 Climate Response

### 8.8.4.1 Early Studies

#### *Global Background Aerosols*

The role of aerosols in modifying the Earth's climate through solar radiative forcing has been a topic of discussion for many decades. Modeling studies assumed a climatological background distribution of aerosols such as that of Toon and Pollack (1976). Two simple types of climate models were used to calculate the effects of aerosols on climate: (1) the radiative-convective model, which resolves radiative perturbations in an atmospheric column, and (2) the energy balance model, which allows for latitudinal dependence, but parameterizes all processes in terms of the surface temperature. A typical study was that of Charlock and Sellers (1980) who used an enhanced one-dimensional radiative-convective model that included the effects of meridional heat transport and heat storage. The model was run with and without a prescribed aerosol layer of visible optical depth equal to 0.125 for conditions representative of  $40^\circ$  and  $50^\circ$  N latitude. The annual mean surface temperature with aerosols was  $1.6^\circ\text{C}$  lower than that for the aerosol-free run.

Coakley et al. (1983) were the first to use an energy balance model to compute the latitudinally dependent radiative forcing for the Toon and Pollack (1976) aerosol distribution, including the effects of absorbing components. Even for moderately absorbing aerosols ( $m = 1.5 - 0.01i$ ), the solar radiative forcing was negative, except in the  $80^\circ$  to  $90^\circ$  N latitude belt, which has a very high surface albedo. Here the criterion given by Equation 8-31 is not satisfied and the change in albedo is negative (i.e., the solar radiative forcing is positive). The model results showed global mean surface temperature decreases ranging from  $3.3^\circ\text{C}$  for nonabsorbing aerosols to  $2.0^\circ\text{C}$  for the absorbing aerosols. The maximum temperature drop was at polar latitudes even for the absorbing layer because advective processes responded to the aerosol-

induced cooling at low- and middle-latitudes. Other two-dimensional model studies have confirmed this basic picture (Jung and Bach, 1987).

### ***Regional and Seasonal Effects***

Apart from global studies, there have been several programs devoted to ascertaining the effects of aerosols on regional and seasonal scales. An example is the radiative effect of aerosols in the Arctic (Rosen et al., 1981). A field experiment, the Arctic Gas and Aerosol Sampling Program, was conducted in 1983 (Schnell, 1984). It was determined that aerosols had a substantial absorbing component. The study by MacCracken et al. (1986) used both one- and two-dimensional climate models to evaluate the climatic effects. They found that the initial forcing of the surface-atmosphere system is positive for surface albedos greater than 0.17, and the equilibrium response of the one-dimensional radiative-convective model showed surface temperature increases of 8 °C. Infrared emission from the warmer atmosphere was found to be an important forcing agent of the surface. The two-dimensional model was run through the seasonal cycle and had an interactive cryosphere. Peak warming occurred in May, a month later than the peak radiative forcing, as a result of earlier snow melt.

### ***Massive Aerosol Loads***

In the 1980s, there were several studies related to what became known as the "nuclear winter" phenomenon (Turco et al., 1983) (i.e., the climatic consequences of widespread nuclear war). Modeling efforts ranged from radiative-convective models (Cess et al., 1985) to three-dimensional general circulation models (GCM) (Thompson et al., 1987; Ghan et al., 1988), and mesoscale models (Giorgi and Visconti, 1989) with interactive smoke generation and removal processes and fairly detailed smoke optics. A review of modeling efforts has been made by Schneider and Thompson (1988) and Turco et al. (1990). The latter study summarized the best estimates of possible reduction in surface temperature from the smoke lofted into the atmosphere during the initial acute phase.

General Circulation Model studies (Thompson et al., 1987; Ghan et al., 1988) indicate that for a July smoke injection, the average land temperatures over the latitude zone from 30° to 70° N, over a 5-day period, would decrease by 5 °C for smoke of optical depth equal to 0.3, but could decrease by 22 °C for large loadings of optical depth equal to

3.0. However, the temperature in the interior of land masses could drop by as much as 30 °C. The temperature perturbations for smoke injections in other seasons are smaller. At lower latitudes, the cooling is moderated by the delay in smoke transport (assuming initial injection in high northern latitudes), and the more humid climate. Model studies also indicate a dramatic decrease in rainfall over land and a failure of the Asian monsoon (Ghan et al., 1988).

#### **8.8.4.2 Recent Regional Studies**

There have been more recent studies of possible climatic effects resulting from severe aerosol loading on regional scales. The Arctic haze problem has been investigated extensively. Blanchet (1989, 1991), using a GCM, studied the effects of increasing aerosol loads north of 60° N. Although the solar heating rate in the troposphere increased quite dramatically, the temperature did not rise substantially. The positive forcing of 0.1 to 0.3 Kday<sup>-1</sup> resulted in a decrease in the meridional heat flux. Quite importantly, the simulated cloud cover in the experiment was altered sufficiently to produce changes in net radiative fluxes at the top were locally an order of magnitude greater than the initial forcing. This implies that it may be very difficult to identify climate change effects due to aerosols alone. Another effect of aerosols at high latitudes that has the potential for affecting climate is the change in surface albedo due to deposition of soot. This was studied by Vogelmann et al. (1988) with respect to the nuclear winter problem. They found that the cooling due to smoke aerosol could be moderated somewhat by the "dirty" snow at very high latitudes.

Several studies have examined the effect of smoke from forest fires on climate. Since these are natural phenomena, it is important to understand their effects in order to place anthropogenic effects in context. Evidence of substantial climatic effects is present only when the smoke loading is substantial. For example, Robock (1988) examined the situation in northern California where a subsidence inversion trapped smoke in mountain valleys for several days in September 1987. One station recorded an anomaly in the maximum temperature of -20 °C. Veltischev et al. (1988) analyzed data covering the period of major historical fires in Siberia, Europe, and Canada. They estimated that the optical depth of

smoke following fires in Siberia in 1915 was about 3.0 and surface temperature dropped by 5 °C.

Other studies have also shown a relationship between smoke and surface temperature. Robock (1991) studied the smoke from Canadian fires in July 1982. He compared forecasted temperatures with observations and found that regions of negative anomaly were well correlated with the smoke layer. Westphal and Toon (1991) used a mesoscale model with interactive smoke physics and optics to simulate the smoke plume and its meteorological effects. They calculated the albedo of the smoke-covered area to be 35%, and the resulting surface cooling was 5 °C.

Perhaps the most extensive recent investigation of the possible climatic effects of heavy aerosol burdens was the study of the Kuwait oil fires in 1991. Several modeling studies were undertaken. Browning et al. (1991) simulated the smoke plume with a long-range dispersion model and concluded that the smoke would remain in the troposphere and not be lofted into the stratosphere where the residence time would be much longer. They estimated a maximum temperature drop of 10 °C beneath the plume, within about 200 km (i.e., only a regional, not global climatic effect). Bakan et al. (1991) used a GCM with an interactive tracer model to simulate the plume dispersion and climatic effects. The maximum temperature drop was estimated to be about 4 °C near the source. The local and regional nature of the effect was confirmed during a field experiment undertaken in May/June, 1991. The smoke from the oil fires had insignificant global effects because (1) particle emissions were less than expected, (2) the smoke was not as black as expected, (3) the smoke was not carried high in the atmosphere, and (4) the smoke had a short atmospheric residence time (Hobbs and Radke, 1992).

The study of severe events such as those described above is useful for investigating model response since such strong forcings usually provide unambiguous climate response signals. The simulated climate response to the more modest radiative forcing due to the distribution of natural and usual anthropogenic sulfate or smoke aerosols is well within the internal model variability. However, an estimate of the magnitude of possible effects can be obtained by model simulations that integrate the chemistry, optics, and meteorology of anthropogenic aerosols.

### 8.8.4.3 Integrated Global Studies

Ideally, one should study the problem in an integrated manner, in which the emissions of sulfate precursors are tracked globally and the radiative forcing of the resulting aerosols computed locally in space and time. A further step would be to let the radiative response impact climate interactively. This latter step could be carried out by a GCM coupled to an oceanic model. Recent studies have accomplished various elements in this scenario.

Global three-dimensional models of the tropospheric sulfur cycle consider emission, transport, chemistry, and removal processes for both natural and anthropogenic sources. The primary natural source is dimethylsulfide (DMS), which is released by oceanic phytoplankton (Nguyen et al., 1983; Shaw, 1983; Charlson et al., 1987). The DMS reacts in air to form sulfate aerosols. Anthropogenic emissions are over land, especially in the heavily industrialized areas of the Northern Hemisphere. Examples of such sulfur cycle models are the Lagrangian model of Walton et al. (1988) and Erickson et al. (1991), known as the GRANTOUR model, and the Eulerian transport model of Langner and Rodhe (1991) and Langner et al. (1992), known as the MOGUNTIA model. Both models use prescribed mean winds, typically obtained from GCM simulations, to provide monthly mean concentrations of sulfate aerosols.

With such detailed input, it is possible to construct global maps of the radiative forcing due to sulfate and compare the magnitude with that due to greenhouse gases. Kiehl and Briegleb (1993) carried out such a study using the monthly mean sulfate abundances from the MOGUNTIA model. For meteorological parameters, they used 1989 monthly mean temperature and moisture fields data from the European Center for Medium Range Weather Forecasting. Vertical distributions of clouds were taken from a GCM simulation using the National Center for Atmospheric Research Community Climate Model (CCM2) since such detailed observations are lacking. However, attempts were made to adjust the total cloud cover to correspond to observations.

The radiative forcing was calculated by Kiehl and Briegleb using an 18-band  $\delta$ -Eddington model in the shortwave and a  $100\text{ cm}^{-1}$  resolution band model in the longwave, which includes the contributions due to trace gases such as  $\text{CH}_4$ ,  $\text{NO}_2$ , and chlorofluorocarbons. The optical properties of sulfate aerosol were calculated spectrally using the refractive indices for 75% sulfuric acid ( $\text{H}_2\text{SO}_4$ ) and 25% water ( $\text{H}_2\text{O}$ ) and an

assumed log-normal size distribution that has a geometric mean diameter by volume of  $0.42 \mu\text{m}$ . The specific extinction coefficient of the dry particles was found to be a very strong function of wavelength, decreasing from  $10 \text{ m}^2\text{g}^{-1}$  at  $0.3 \mu\text{m}$  to less than  $2.0 \text{ m}^2\text{g}^{-1}$  at  $1.0 \mu\text{m}$ . This is significant in interpreting the computed forcing when comparisons are made with earlier studies that used a constant value for the specific extinction coefficient.

The value of the specific extinction coefficient depends on the size distribution of the aerosols but that also affects the phase function such that changes in the coarse particle or fine particle mode do not greatly affect the total radiative forcing (Kiehl and Briegleb, 1993). This is because the extinction cross section has a sharp maximum for particles that are of the same dimension as the wavelength and falls off rapidly for smaller and larger particles (Covert et al., 1980).

The direct radiative forcing is calculated by adding the sulfate burden to the model and computing the change in absorbed solar radiation. Figures 8-21a and 8-21b, from Kiehl and Briegleb (1993) show the annual mean direct solar radiative forcing resulting from anthropogenic sulfate aerosols (global mean =  $-0.28 \text{ W m}^{-2}$ ) and anthropogenic plus natural sulfate (global mean =  $-0.54 \text{ W m}^{-2}$ ). The patterns are similar to those obtained earlier by Charlson et al. (1991), but the magnitude is roughly half. Most of the difference is due to the assumption of a constant value of  $5.0 \text{ m}^2\text{g}^{-1}$  for the specific extinction coefficient in the earlier study, but there was also a difference in the phase function used. Therefore, assumptions regarding radiative properties were able to account for all the differences. Points to note in the figure are the local concentrations of anthropogenic forcing and particularly the hemispheric asymmetry in the forcing, even when natural sulfate is included. Although the southern hemisphere is largely ocean, the direct forcing due to natural sulfate is substantial only in the clear oceanic areas since, in the presence of clouds, the additional sulfate effect is minimal.

To place the role of anthropogenic sulfate in perspective, Kiehl and Briegleb (1993) compared the direct radiative forcing with that of increasing greenhouse gases from preindustrial times to the present. The greenhouse gas forcing is calculated by computing the spatial distribution of the change in the net longwave flux at the tropopause for the trace gas increases from the preindustrial period to the present. The annual averaged results for

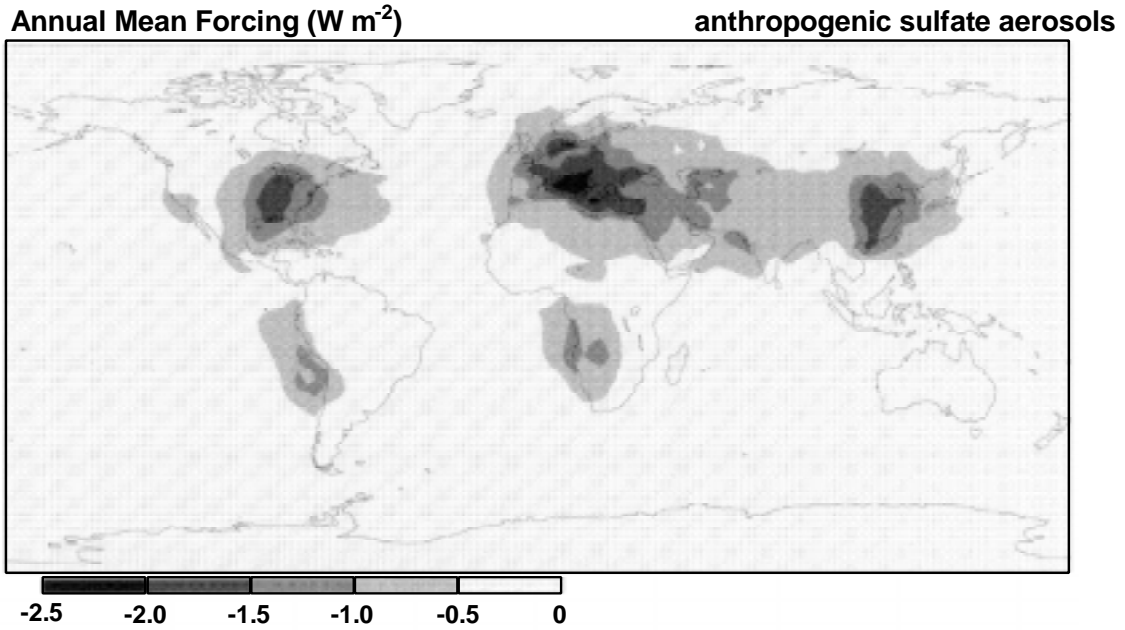


**Figure 8-21a.** Annual mean direct radiative forcing ( $W m^{-2}$ ) resulting from anthropogenic sulfate aerosols.

Source: Kiehl and Briegleb (1993).

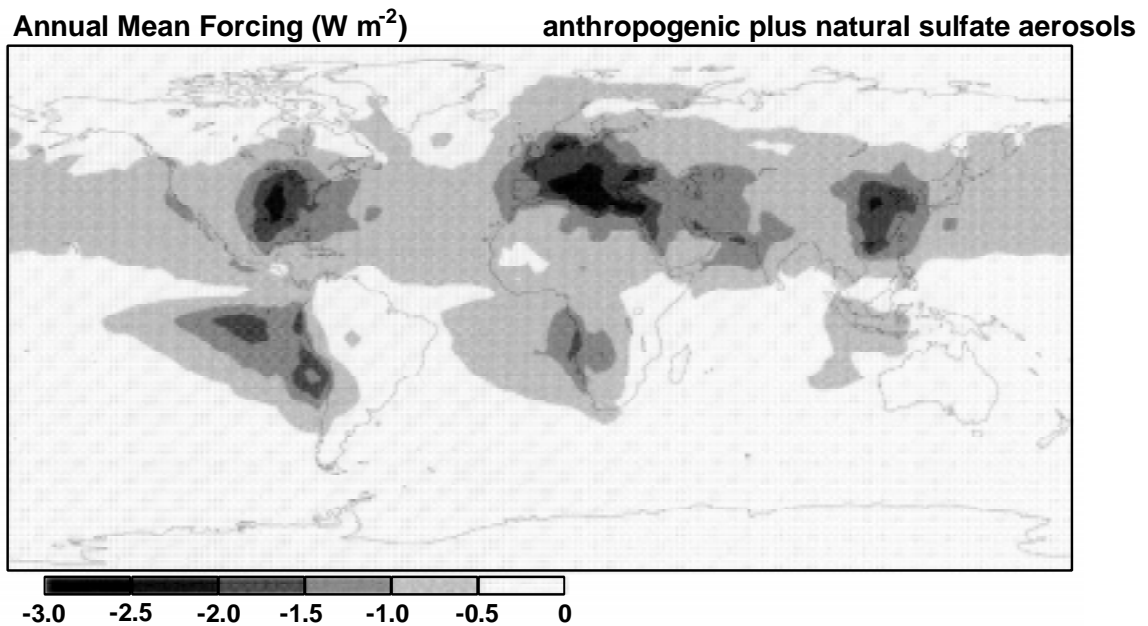


**Figure 8-21b.** Annual mean direct radiative forcing ( $W m^{-2}$ ) resulting from anthropogenic and natural sulfate aerosols.

Source: Kiehl and Briegleb (1993).

greenhouse gases alone and in combination with anthropogenic sulfate are shown in Figure 8-22a and 8-22b, respectively. The greenhouse gas forcing is, of course, positive and is the greatest in the clear regions over the land and oceanic deserts. The global annual mean is  $2.1 \text{ W m}^{-2}$ . When the negative forcing of aerosols is added, the global annual mean direct radiative forcing due to anthropogenic activities is  $1.8 \text{ W m}^{-2}$ . However, locally, there are regions where the anthropogenic sulfate forcing cancels the greenhouse forcing.

The forcing is simply an initial perturbation. Because the sulfate forcing is in the shortwave and felt primarily at the surface (for nonabsorbing aerosols), a coupled atmospheric-oceanic climate model is required to determine the effect on climate. Taylor and Penner (1994) have used the GRANTOUR model to provide the sulfate input to a GCM (CCM1), which was coupled to a 50 m mixed-layer ocean model with sea ice and a specified meridional oceanic heat flux.

To assess the anticipated patterns of climate response to anthropogenic emissions of both  $\text{SO}_2$  and  $\text{CO}_2$ , Taylor and Penner performed four 20-simulated-year integrations in which the atmospheric  $\text{CO}_2$  concentration was fixed at either the preindustrial level (275 ppm) or the present day concentration (345 ppm). Anthropogenic sulfur emissions, corresponding to 1980, were either included or excluded. Table 8-7 summarizes their annual average results. The global average anthropogenic sulfate forcing was found to be  $-0.95 \text{ W m}^{-2}$ ; more than three times larger than calculated by Kiehl and Briegleb (1993). The differences in the annual anthropogenic sulfate forcing value in the two studies is due partially to the sulfate chemistry in the model used by Taylor and Penner, (1994). For example, there is a stronger seasonal cycle with enhanced northern hemisphere concentrations in summer. The remainder may be contributed to the use of a constant specific scattering coefficient ( $8.5 \text{ m}^2\text{g}^{-1}$  at  $0.55 \mu\text{m}$ ) instead of the RH-dependent model used by Kiehl and Briegleb (1993). As noted earlier, the value of the specific scattering coefficient chosen could be a gross overestimate and, therefore the values of the sulfate forcing shown in Table 8-7 are probably much too high.

Some noteworthy features of Table 8-7 are that the combined  $\text{CO}_2$  and sulfate forcing is not linearly additive and there is a pronounced asymmetry in the climate response in the two hemispheres. What is clear is that the anthropogenic sulfate is expected to reduce somewhat the anticipated warming resulting from the increased emission of greenhouse gases, especially

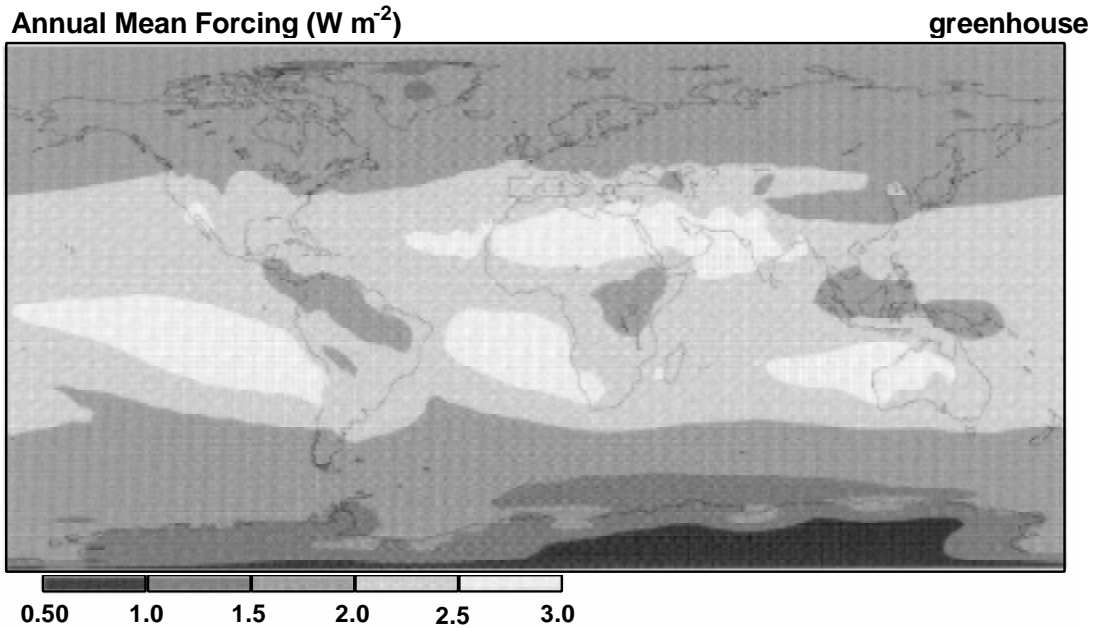


**Figure 8-22a.** Annual averaged greenhouse gas radiative forcing ( $\text{W m}^{-2}$ ) from increases in  $\text{CO}_2$ ,  $\text{CH}_4$ ,  $\text{N}_2\text{O}$ , CFC-11, and CFC-12 from preindustrial time to the present.

Source: Kiehl and Briegleb (1993).

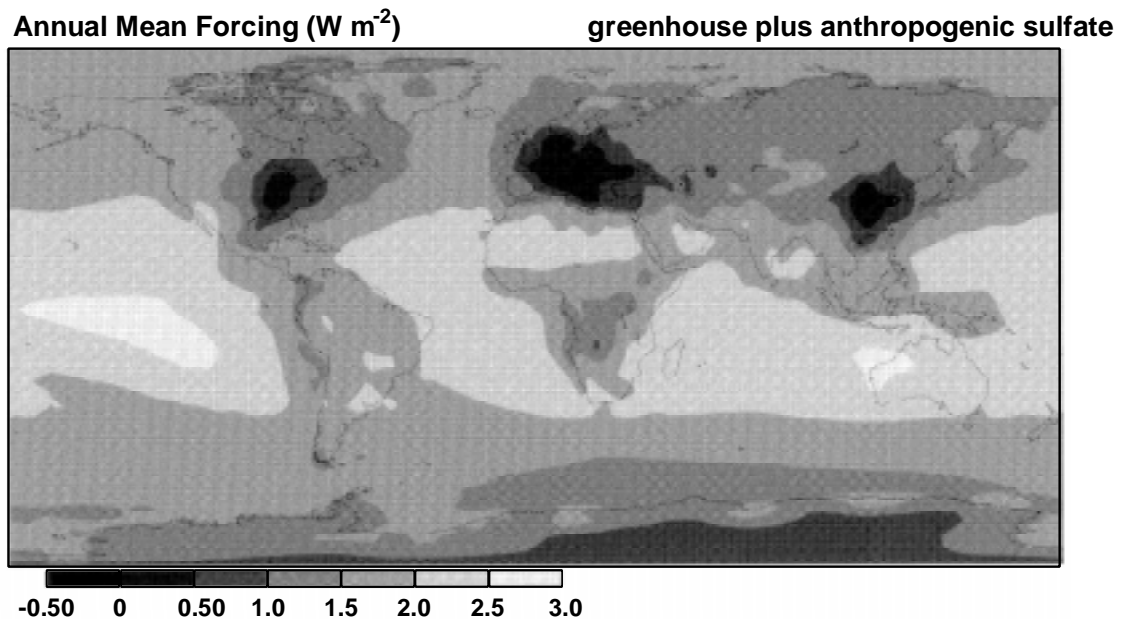


**Figure 8-22b.** Annual averaged greenhouse gas forcing plus anthropogenic sulfate aerosol forcing ( $\text{W m}^{-2}$ ).

Source: Kiehl and Briegleb (1993).

**TABLE 8-7. RADIATIVE FORCING AND CLIMATE STATISTICS**

Case	$\Delta F$ (W m <sup>-2</sup> )	T <sub>s</sub> (°C)	$\Delta T_s$ (°C)	P (mm d <sup>-1</sup> )	$\Delta P$ (mm d <sup>-1</sup> )	C (%)	$\Delta C$ (%)	SI (%)	$\Delta SI$ (%)
Northern Hemisphere									
Preindustrial		12.5		3.40		56.6		4.87	
Present-day CO <sub>2</sub>	1.26	14.5	1.9	3.48	0.09	55.0	-1.7	4.13	-0.74
Present-day sulfate	-1.60	11.3	-1.2	3.36	-0.04	56.9	0.3	5.54	0.67
Combined CO <sub>2</sub> and sulfate	-0.34	13.0	0.5	3.43	0.03	55.8	-0.9	4.85	-0.02
Observed climate statistics		14.9		2.6		58.9		4.4	
Southern Hemisphere									
Preindustrial		12.5		3.54		62.4		6.64	
Present-day CO <sub>2</sub>	1.25	14.8	2.3	3.61	0.08	61.1	-1.3	4.39	-2.26
Present-day sulfate	-0.30	11.7	-0.8	3.48	-0.06	63.1	0.7	7.24	0.59
Combined CO <sub>2</sub> and sulfate	0.95	13.6	1.1	3.56	0.02	62.1	-0.3	5.40	-1.24
Observed climate statistics		13.5		2.7		65.6		4.5	
Global average									
Preindustrial		12.5		3.47		59.5		5.76	
Present-day CO <sub>2</sub>	1.26	14.6	2.1	3.55	0.08	58.0	-1.5	4.26	-1.50
Present-day sulfate	-0.95	11.5	-1.0	3.42	-0.05	60.0	0.5	6.39	0.63
Combined CO <sub>2</sub> and sulfate	0.31	13.3	0.8	3.49	0.02	58.9	-0.6	5.13	-0.63
Observed climate statistics		14.2		2.7		62.2		4.5	

$\Delta F$  = radiative forcing; T<sub>s</sub> = surface temperature; P = precipitation; C = cloud cover; SI = sea ice coverage.

Source: Taylor and Penner (1994).

in the Northern Hemisphere. On a regional scale, Taylor and Penner (1994) found that the strongest response was in the polar regions associated with an increase in sea ice. Note that the change in sea ice coverage, ( $\Delta SI$ ), in the northern hemisphere is essentially zero as the sulfate completely cancels the  $CO_2$  effect. Also, the greatest cooling is found over broad regions of the Northern Hemisphere continents where all the sulfur emission is occurring. However, the maximum cooling is not over Europe where the maximum radiative forcing occurs, but further north, and associated with changes in sea ice.

### ***Comparative Lifetimes of the Forcing***

One extremely important aspect in comparing the effects of  $CO_2$  and sulfur emissions is the disparate lifetimes of the forcing mechanisms. The residence times of trace gases that result in a positive longwave forcing of the climate system is from decades to a century or more (Houghton et al., 1990). On the other hand, the cycling time for sulfate in the troposphere is only about a week (Langner and Rodhe, 1991), which is dependent on the frequency of precipitation removal (Charlson et al., 1992). Therefore, any changes in industrial emission patterns will be reflected immediately in the sulfate forcing, but the concentration of  $CO_2$  and the accompanying forcing will continue to rise for more than a century even if emissions were kept constant at present levels. See Figure 8-23.

One could infer from the above discussion that sulfate emissions are providing some amelioration of greenhouse warming, and that a curtailment of such emissions might result in enhanced global warming. However, given the uncertainties in present estimates of the effects of aerosols, especially the fact that many feedbacks are not fully included, it would be premature to base any decisions on these current discussions of the possible effects of aerosols on climate.

## **8.8.5 Aerosol Effects on Clouds and Precipitation**

### **8.8.5.1 Indirect Solar Radiative Forcing**

#### ***Cloud Microphysical Properties***

A substantial portion of the solar energy reflected back to space by the earth system is due to clouds. The albedo (i.e., reflectivity) of clouds, in turn, depends to a large extent on the optical thickness, which is the column integrated light-extinction coefficient (see

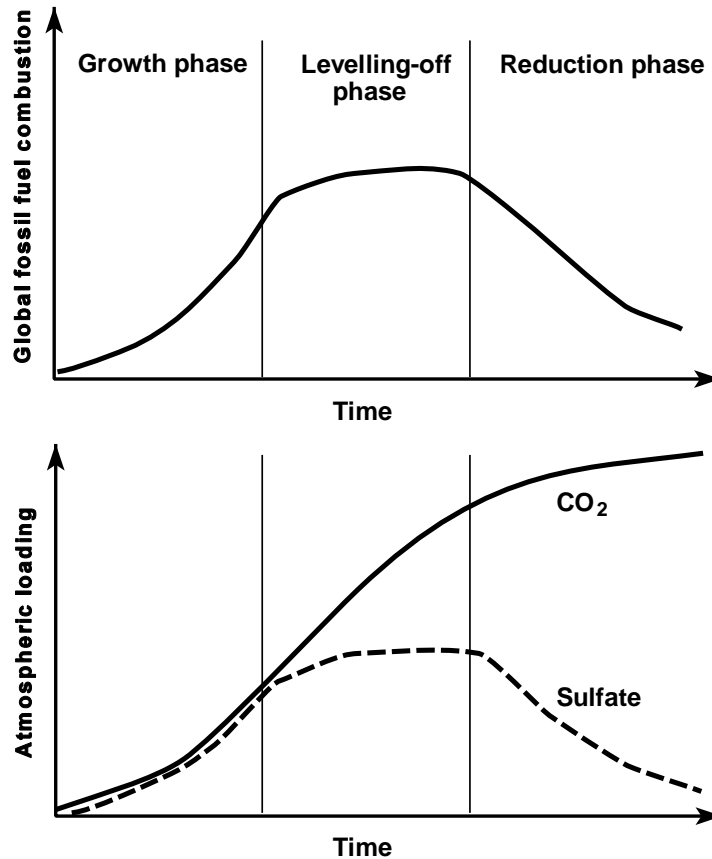


**Figure 8-23.** Schematic illustration of the difference between response times of climate forcing due to CO<sub>2</sub> (heating) and sulfate (cooling) during different patterns of global fossil fuel consumption.

Source: Charlson et al. (1991)

Section 8.8.3). The light-extinction coefficient is related to the size distribution and number concentration of cloud droplets. Because these cloud droplets nucleate on aerosols, it is to be expected that changes in aerosol loading could affect cloud albedo, particularly that marine stratiform clouds. Because of their effect on the Earth's radiative energy budget, marine stratus and stratocumulus cloud systems are likely to influence climate and climate change. Their high albedo compared with ocean background provide a large negative shortwave forcing which is not compensated in thermal wavelengths because of their low altitude (Randall et al., 1984). Recent studies by Ramanathan et al. (1995) and Cess et al. (1995) indicate that more solar radiation is being absorbed by clouds in cloudy atmospheres than originally believed. This finding has, however, not been confirmed.

Stephens (1994) gave the volume light-extinction coefficient of a cloud of spherical polydispersed drops ranging in size as:

$$\sigma_{\text{ext}} = \pi \int_{r_{\text{min}}}^{r_{\text{max}}} n(r) Q_{\text{ext}}(r) r^2 dr \quad (8-44)$$

where  $n(r)$  represents the size distribution and is the number concentration per unit volume per unit radius increment and  $Q_{\text{ext}}$  is the extinction efficiency factor (see Section 8.3.1) which approaches the value of 2.0 for drops that are large relative to the wavelength. At visible wavelengths, this limit for the extinction efficiency factor is satisfied by cloud drops that are typically  $10 \mu\text{m}$  in radius. Therefore,

$$\sigma_{\text{ext}} \propto \int_{r_{\text{min}}}^{r_{\text{max}}} n(r) r^2 dr. \quad (8-45)$$

The mass concentration of water in clouds, called the liquid water content,  $M$  (in  $\text{kg}^{-3}$ ), is proportional to the total volume of liquid water in a unit volume of air. This may be written as

$$M \propto \int_{r_{\text{min}}}^{r_{\text{max}}} n(r) r^3 dr \quad (8-46)$$

because the volume of each cloud drop is  $(4/3) \pi r^3$ . Comparing Equations 8-45 and 8-46, one can see that

$$\sigma_{\text{ext}} \propto M/r_e \quad (8-47)$$

where  $r_e$  is the effective radius, defined as the ratio

$$r_e = \frac{\int_{r_{\min}}^{r_{\max}} n(r) r^3 dr}{\int_{r_{\min}}^{r_{\max}} n(r) r^2 dr} . \quad (8-48)$$

For identical meteorological conditions, the liquid water content will be the same in two cloud layers that are composed of droplets of different effective radius. If other parameters remain the same, the light-extinction coefficient will increase as the effective radius decreases (Equation 8-47). Therefore, if the geometric depth of two cloud layers is the same and the column amount of liquid water is the same, the cloud with more numerous, but smaller drops, will have a larger optical depth and a higher albedo. This sets the stage for a potentially important indirect effect of anthropogenic aerosols on the Earth's radiation balance. As suggested by Twomey (1974), the addition of cloud nuclei by pollution can lead to an increase in the solar radiation reflected by clouds, a negative radiative forcing that is in addition to the direct radiative forcing discussed in Section 8.8.3.

Another radiative consequence of pollution is the emission of elemental carbon, which can be incorporated into clouds and increase the absorptance at visible wavelengths at which pure water is nonabsorbing. This mechanism decreases the single scattering albedo of the cloud material (see Figure 8-20), causing a decrease in the reflectance of the layer. There are, therefore, two competing mechanisms, but Twomey et al. (1984) assessed the relative magnitudes of the two effects based on observations of clean and polluted air in Arizona, and concluded that increases in albedo from increases in cloud droplet concentration would dominate over the absorption effect.

### ***Cloud Lifetimes***

Another possible indirect effect of aerosols on clouds and precipitation is that of increased cloud condensation nuclei (CCN), the inhibition of precipitation (Albrecht, 1989; Twomey, 1991). Cloud condensation nuclei can be either hygroscopic or deliquescent, having large light scattering efficiency due to hygroscopic growth. With more droplets, coagulative growth, which is the mechanism of water removal in liquid water clouds, will be hindered. This will result in

longer residence times for clouds and a higher mean albedo time, which, again, is indirect negative solar radiative forcing.

There is some observational evidence that cloud amounts have increased during the recent decades. Henderson-Sellers (1986, 1989) has analyzed surface based meteorological observations from several stations in the United States and Canada. There is coherent increase in cloud amount in all seasons between 1900 and 1982 with most of the increase occurring between 1930 and 1950. Attribution of this increase to anthropogenic causes is very difficult. The possibility of jet contrails playing a role has been mentioned by Changnon (1981) but this would not explain the increase in the 1930-1950 time frame. Warren et al. (1988) have also noted a positive trend in the total cloud amount and also for all classes of clouds globally over the oceans. An increase in aerosol concentration is compatible with an increase in cloud lifetimes for low level clouds so there is a plausible link between these observations and anthropogenic activities but nothing definitive can be said at the moment.

### ***Cloud Chemistry***

Novakov and Penner (1993) pointed out that anthropogenic activity could modify the nucleating properties of anthropogenic sulfate. It has already been mentioned that carbon black influences the direct radiative forcing. The presence of carbon black and other organics can also alter the hygroscopic properties of sulfate aerosols. For instance, the condensation of hydrophobic organics onto preexisting sulfate particles may render these inactive as CCN. On the other hand, the condensation of sulfuric acid vapor on a hydrophobic organic aerosol may convert it to a hydrophilic particle. Because the indirect radiative forcing depends on the ability of sulfate to nucleate, organics may enhance or diminish the potential indirect radiative forcing.

#### **8.8.5.2 Observational Evidence**

The relationship between the availability of CCN and cloud droplet size distribution has been a subject of research in cloud physics for decades. It has been known, for instance, that continental clouds are composed of far more numerous, but smaller drops than maritime clouds (Wallace and Hobbs, 1977). The more difficult question is whether the additional

contribution to CCN by anthropogenic activities has increased the reflectance of clouds over large areas of the Earth. If so, this would be an additional indirect radiative forcing attributable to sulfate emissions.

The most dramatic evidence of such an indirect effect (albeit on a small scale) is the observation of "ship tracks" in marine stratocumulus (Conover, 1966; Coakley et al., 1987). These are visible in satellite images as white lines against a gray background and follow the path of ships that have been emitting effluents. King et al. (1993) reported the first radiation and microphysics measurements on ship tracks obtained from a research aircraft as it flew within marine stratocumulus clouds off California. Comparing the flight track with satellite images, they were able to locate two distinct ship tracks in which they measured enhanced droplet concentration, and liquid water contents, greater than in the surrounding clouds. They also derived the effective radius of the cloud drops and found that there was a significant decrease within the ship tracks. The radiation measurements were consistent with increased optical depths in the ship tracks. The increased liquid water content is compatible with the suppression of drizzle as a result of slower coagulative growth (Albrecht, 1989), an indirect aerosol effect.

Twomey (1991) estimated that the visible reflectance of clouds,  $R$ , is affected by cloud droplet concentration,  $N$ , according to the following relationship for a fixed liquid water content,  $M$ .

$$\left( \frac{dR}{dN} \right)_M = \frac{R(1-R)}{3N} \quad (8-42)$$

The parameter,  $dR/dN$ , the susceptibility, is a measure of the sensitivity of cloud reflectance to changes in microphysics (Platnick and Twomey, 1994). It has a maximum value at  $R = 0.5$  and is inversely proportional to the cloud droplet concentration such that when the cloud droplet concentration is low as in marine clouds, the susceptibility is high. It is, therefore, not surprising that emissions from ships can influence cloud albedo.

To determine whether the indirect effect of aerosols on clouds is detectable on a global scale, Schwartz (1988) compared cloud albedos in the two hemispheres and also historic changes in surface temperature from preindustrial times. The sulfate signal is expected in

both: cloud albedos in the Northern Hemisphere should be higher, and the rate of greenhouse warming should be slower. The results of his study were inconclusive in that no inter-hemispheric differences were found. However, more recent studies suggest some influence of sulfate emissions.

Falkowski et al. (1992) showed that cloud albedos in the central North Atlantic Ocean, far from continental emission sources, were well correlated with chlorophyll in surface waters. These correspond to higher ocean productivity and DMS emissions, indicating that natural sources of sulfate emission can influence cloud albedo. More substantial evidence of the effect of sulfate aerosol has been presented by Han et al. (1994) who made a near-global survey of the effective droplet radii in liquid water clouds by inverting satellite visible radiances obtained from advanced very-high-resolution radiometer (AVHRR) measurements. Han et al. (1994) found systematic differences between the effective radius of continental clouds (global mean effective radius =  $8.5 \mu\text{m}$ ) and maritime clouds (global mean effective radius =  $11.8 \mu\text{m}$ ), which is the expected result based on differences in CCN concentrations. In addition, they found inter-hemispheric differences in the effective radius over both land and ocean. Northern Hemisphere clouds had smaller effective radii, the difference being  $0.4 \mu\text{m}$  for ocean and  $0.8 \mu\text{m}$  for land. However, Southern Hemisphere clouds tended to be optically thicker, which explains why Schwartz (1988) was unable to detect inter-hemispheric albedo differences.

### **8.8.5.3 Modeling Indirect Aerosol Forcing**

If the appropriate radiative properties of aerosols are known, it is fairly straightforward to model the direct solar radiative forcing of aerosols (Section 8.8.3) and estimate possible climatic responses (Section 8.8.4). Calculations of the indirect forcing of aerosols, on the other hand, is much more difficult since several steps are involved and the uncertainty at each level is high. Charlson et al. (1992) proposed that enhancements in albedo would occur only for marine stratocumulus clouds and for a uniform global increase of droplet concentration of 15% in only these clouds, the global mean solar radiative forcing would be  $-1.0 \text{ W m}^{-2}$ , which is comparable to the direct forcing (Section 8.8.4) and of the same sign. The greatest uncertainty in this estimate is the degree that cloud droplet number concentration is enhanced by increasing emissions. The uncertainty has been estimated by Kaufman et al.

(1991) to be at least a factor of 2. Leaitch and Isaac (1994) have addressed this issue based on their observations of the relationship between cloud droplet concentrations and cloud water sulfate concentrations. They find that the assumptions in Kaufman et al. (1991) are within reasonable bounds. The Scientific Steering Committee for the International Global Aerosol Program concluded that the uncertainties involved in determining the indirect effects of aerosols on the Earth's radiation balance are so great that no formal value can be given at this time (Hobbs, 1994).

The indirect forcing has been included in climate model simulations by Kaufman and Chou (1993) who used a zonally averaged multilayer energy balance model and by Jones et al. (1994) who used a GCM. Kaufman and Chou (1993) modeled the competing effects of enhanced anthropogenic emissions of CO<sub>2</sub> and SO<sub>2</sub> since preindustrial times. They concluded that SO<sub>2</sub> has the potential of offsetting CO<sub>2</sub>-induced warming by 60% for present conditions and 25% by the year 2060 given the Intergovernmental Panel on Climate Change BAU (business as usual) scenario of industrial growth (Intergovernmental Panel on Climate Change, 1994). They also found a small inter-hemispheric difference in climate response, with the Northern Hemisphere cooler than Southern Hemisphere by about -0.2 °C.

Jones et al. (1994) used a GCM with a prognostic cloud scheme and a parameterization of the effective radius of cloud water droplets that links effective radius to cloud type, aerosol concentration and liquid water content. The parameterization is based on extensive aircraft measurements. The distribution of column sulfate mass loading was obtained from the model of Langner and Rodhe (1991) separately for natural and anthropogenic sources. Simulated effective radius distributions of low-level clouds showed land-ocean contrasts and also inter-hemispheric differences as observed by Han et al. (1994). The indirect forcing due to anthropogenic sulfate was estimated by performing a series of single-timestep calculations with the GCM. For present conditions, the mean northern hemisphere forcing was calculated to be -1.54 W m<sup>-2</sup> and the southern hemisphere forcing was -0.97 W m<sup>-2</sup>. This is comparable to the estimates of Charlson et al. (1992) and Kaufman and Chou (1993) and substantially larger than the direct forcing estimates of Kiehl and Briegleb (1993). The combined direct and indirect forcing is more than half the total positive forcing of greenhouse gas emissions. It should be noted that the indirect effect is greatest when the atmosphere is very clean and so, in principle, could saturate with time. The direct effect is

linear with emissions and may dominate in the future. In any case, the negative forcing of sulfate aerosols must be considered in any overall estimate of the total anthropogenic effect on climate.

## **8.9 SUMMARY**

### **8.9.1 Visibility Effects**

This chapter presents (1) an overview of the effects of particulate matter on visibility, and combines information from this chapter and other recent reviews by the National Research Council (NRC), the National Acid Precipitation Assessment Program (NAPAP), and Environmental Protection Agency (U.S. EPA) and (2) a discussion on the effects of particulate matter on climate.

Several definitions of visibility have been noted in this chapter, and they are generally consistent with each other. Section 169A of the 1977 Clean Air Act Amendments (42 U.S.C. 7491) and the U.S. EPA 1979 Report to Congress defined visibility impairment as a reduction in visual range and atmospheric discoloration. The National Research Council's Committee on Haze in National and Wilderness Areas said, "Visibility is the degree to which the atmosphere is transparent to visible light." These definitions indicate that visibility is determined by the clarity (or transparency) and color fidelity of the atmosphere. Visibility can be numerically quantified by equating it with the contrast transmittance of the atmosphere. This quantification is consistent with both (1) the use of visual range to quantify visibility, and (2) the definition recommended by the NRC.

All evaluations of visibility have focused on daytime visibility as perceived by a human observer looking through one or more sight paths in the Earth's atmosphere. Weber's Law indicates that if an object is just perceptible, the brightness of the object differs from the brightness of its surroundings by a constant fraction, i.e., a constant percentage of the surrounding brightness. A perception threshold of 2% brightness change is most commonly used, but 5% is sometimes used in visibility analyses. Either contrast or modulation can be used to quantify changes in brightness. Weber's law is not exact, so perception thresholds depend on the viewing conditions. The eye is the most sensitive to objects that subtend an angle of

approximately 1/3 degree, is somewhat less sensitive to objects that subtend larger angles, and becomes rapidly less sensitive as the size of the object is decreased below a subtended angle of 0.1 degree. Many factors, such as the brightness level and the pattern of brightness surrounding the object being viewed can affect the perception threshold. The contrast threshold of 2% generally applies to objects that subtend an angle between 0.1 and 1.0 degree and are viewed against uniform backgrounds.

The atmosphere is a very thin layer on the Earth and has strong vertical gradients. Because of these gradients and the curvature of the Earth, the properties of the atmosphere exhibit substantial variations in sight paths longer than roughly 100 km. The visual range is the greatest distance at which a dark target can be perceived against the horizontal sky. Because of the non-uniformities in the atmosphere, the visual range provides a meaningful characterization of the Earth's atmosphere only for haze levels that cause the visual range to be much less than 100 km.

A sight path through the atmosphere is illuminated by direct sunlight, diffused skylight, and light reflected by the Earth's surface. An observer looking through the atmosphere sees light from two sources: (1) the light reflected from the object or terrain feature being viewed that is transmitted through the sight path to the observer, and (2) the light scattered by the atmosphere into the line of sight and then transmitted to the observer. These are known as the transmitted radiance and the path radiance (air light), respectively.

Visibility is determined by the competition between the transmitted radiance and the path radiance. The transmitted radiance carries all of the information about the nature of the object being viewed. When this radiance is dominant, the features of the object can be easily perceived and the visibility is good. The path radiance contains information only about the uniformity of the intervening atmosphere, and no information about the object being viewed. When the path radiance is dominant, it tends to obscure the object. These effects are easily seen by viewing objects at various distances in a dense fog, but can also be seen on a clear day if sight paths of sufficient length are available.

The transmitted radiance is attenuated by light extinction. The strength of that attenuation is quantified by the light-extinction coefficient, which describes the rate of energy loss with distance from a beam of light. The light-extinction coefficient for green light in particle-free air (Rayleigh scattering) is 1% per km, or  $0.01 \text{ km}^{-1}$ . Extinction coefficients are

most often measured in units of inverse megameters ( $\text{Mn}^{-1}$ ), and in these units the extinction coefficient for clean air is  $10 \text{ Mn}^{-1}$ .

Light extinction is caused by light scattering and light absorption by particles and gases. In visibility analyses it is useful to consider each of these separate contributions to the light-extinction coefficient; the coefficients for light absorption by gases ( $\sigma_{\text{ag}}$ ), light scattering by gases ( $\sigma_{\text{sg}}$ ), light absorption by particles ( $\sigma_{\text{ap}}$ ), and light scattering by particles ( $\sigma_{\text{sp}}$ ). Because of their different origins and composition, atmospheric particles are frequently divided into coarse and fine particles. The corresponding division of coefficients for light scattering and absorption then becomes, the coefficient for light-scattering and light-absorption by fine particles ( $\sigma_{\text{sfp}}$  and  $\sigma_{\text{afp}}$ ) and the coefficient for light scattering and light-absorption by coarse particles ( $\sigma_{\text{scp}}$  and  $\sigma_{\text{acp}}$ ). The components of the light-extinction coefficient are related as follows:

$$\sigma_{\text{ext}} = \sigma_{\text{abs}} + \sigma_{\text{scat}}$$

$$\sigma_{\text{ab}} = \sigma_{\text{ag}} + \sigma_{\text{ap}}$$

$$\sigma_{\text{scat}} = \sigma_{\text{sg}} + \sigma_{\text{sp}}$$

$$\sigma_{\text{sp}} = \sigma_{\text{sfp}} + \sigma_{\text{scp}}$$

$$\sigma_{\text{ap}} = \sigma_{\text{afp}} + \sigma_{\text{acp}}$$

Light scattering by gases (Raleigh Scattering) is nearly constant, but decreases with increasing altitude. Light absorption by gases is almost entirely due to  $\text{NO}_2$ , and is typically significant only near  $\text{NO}_2$  sources, e.g., in or downwind of urban areas or in plumes. Light absorption by particles is principally caused by elemental carbon. Light scattering by particles is typically the most important component of light extinction in causing visibility degradation. Further discussion of this component of light extinction appears below.

If the average light-extinction coefficient and path length are known, the light transmittance of a sight path can be calculated. Thus, the effect of light extinction on the transmitted radiance is easily quantified.

The calculation of the path radiance is much more difficult. It requires a knowledge of (1) the illumination of the sight path at each point along its length, (2) the light scattering properties of the atmosphere at each point, and (3) the transmittance of the atmosphere

between each point and the observer. The illumination is affected by the clouds in the sky, the haze that contributes to diffuse skylight, and the variations of the reflectance of the Earth's surface under the sight path. Light scattering and light absorption contribute differently, because light absorption does not contribute to the scattering of light into the sight path. Thus, a given amount of light extinction due to light absorption causes less visibility impairment than the same amount of light extinction due to light scattering. Because of the differing effects of scattering and absorption and the highly variable effects of the illumination, the path radiance is not closely linked to light extinction. As a result, the visibility for a specific sight path under specific illumination conditions is not closely linked to the light-extinction coefficient.

All of these effects can be mathematically simulated, and a simple theory for these simulations is present in the text. The theoretical development includes the equations used to generate photographs showing the visual effects with various amounts of haze. For simple situations, e.g., a cloud-free sky and uniform haze, photographic simulation are quite realistic. Examples appear in the National Acid Precipitation Assessment Program study. These photographs, and other comparisons, indicated that the relationship between air pollution and visibility is well understood.

As previously stated, the most important component of light extinction in causing visibility degradation is typically light scattering by particles. Except in dust storms or during fog, snow, or rain, most light scattering by particles is caused by fine particles, i.e. the accumulation mode, ~0.3 to 1.0  $\mu\text{m}$  diameter. Coarse particles typically have a light-scattering efficiency 5 to 10 times less than the efficiency of fine particles. Coarse particles can have important visibility effects in dusty or desert areas, but fine particles dominate the visibility effects in most of the eastern United States.

The light-scattering efficiency of particles is a maximum for particles with a diameter approximately equal to the wavelength of visible light. For a single particle, the maximum in light-scattering efficiency occurs at a diameter approximately equal to

$$D = 0.28/(n-1) \mu\text{m}$$

where  $n$  is the index of refraction of the particulate matter. This formula gives a diameter of  $0.85 \mu\text{m}$  for an index of refraction of 1.33 (e.g. water) and a diameter of  $0.56 \mu\text{m}$  for an index of refraction of 1.5, which is larger than typical for ambient aerosol mixtures. Most fine particles have smaller diameters. Therefore, processes that increase the particle size of fine particles tend to increase the light-scattering efficiency of the particles.

Coagulation of nuclei particles, which can be smaller than  $0.1 \mu\text{m}$  in diameter, in the atmosphere will increase their light-scattering efficiency. Particles in the  $0.2$  to  $0.3 \mu\text{m}$  in diameter range are small enough that their light-scattering efficiency is roughly half that of particles with the optimum size. Particles in this range coagulate very slowly, so they tend to maintain their size in the atmosphere as long as they are not processed by clouds or fog. Heterogeneous processes in clouds and fogs can form particles in any size range, but these processes are the dominant source of particles with a diameter near  $0.7 \mu\text{m}$ , which is near the optimum size for light scattering. Particles in this size range are frequently observed in air samples processed by clouds or fog.

The dominant chemical components of fine particulate matter are sulfates, organic species, nitrates, crustal species, and elemental carbon. Sulfates and organic species dominate visibility impairment in the eastern United States, and nitrates and organic species are dominant in many western urban areas as well as the California Central Valley during winter months. Crustal species are important contributors in dry areas, especially when these areas are farmed. Elemental carbon is most important in urban areas, and in Phoenix, AZ can contribute about one-third of the light extinction during some episodes.

Water uptake, which occurs when hygroscopic aerosol is exposed to elevated humidities, increase light scattering by two mechanisms: (1) the mass concentration of particulate matter is increased, and (2) the increase particle size causes the light scattering efficiency to increase. Thus, the materials present before the water uptake makes a larger contribution to light scattering because they are now a component of larger particles. The overall effect on increasing humidity on light scattering by particles was quantified nearly 20 years ago, but current research is greatly increasing the detailed understanding of the response of aerosol particles to changing humidities and the relationship of this response to the chemical composition of the particles. Humidity effects generally become important at relative humidities between 60 and 70%, and increase the light scattering by a factor of 2 at

approximately 85% relative humidity. The light scattering increase rapidly with relative humidity when the humidity exceeds 90%.

Potential indicators for a visibility and air quality include: (a) fine particle mass and composition, or only fine particle mass; (b) light scattering by dried ambient particles; (c) light scattering by particles under ambient conditions; (d) light extinction calculated from separate measurements of dry scattering and absorption or ambient scattering and absorption; (e) light extinction measured directly; and (f) contrast transmittance of a sight path.

The selection of an indicator should consider such factors as (1) the linkage between the indicator and visibility, (2) the cost and feasibility of monitoring the indicator to determine both compliance with the standard and progress toward achieving the standard, (3) the nature and severity of the interferences inherent in the available monitoring methods, (4) the relationship between the visibility indicator and indicators for other air quality standards, and (5) the usefulness of monitoring data in analyses which have the purpose of determining the optimum control measures to achieve the standard.

In general there is an inverse relationship between an indicator's ability to characterize air quality and its ability to characterize visibility.

There is general agreement in the technical community that contrast transmittance would not be a suitable indicator for regulatory purposes. It is affected by too many factors other than air quality, such as cloud shadows, precipitation, fog, etc. Therefore, only the other indicators merit consideration.

Visibility has value to individual economic agents primarily through its impact upon the activities of consumers. Most economic studies of the effects of air pollution on visibility have focused on the aesthetic effects to the individual, which are, at this time, believed to be the most significant economic impacts of visibility degradation caused by air pollution in the United States. It is well established that people notice those changes in visibility conditions that are significant enough to be perceptible to the human observer, and that visibility conditions affect the well-being of individuals.

One way of defining the impact of visibility degradation on the consumer is to determine the maximum amount the individual would be willing to pay to obtain improvements in visibility or prevent visibility degradation. Two economic valuation techniques have been used to estimate willingness to pay for changes in visibility: (1) the

contingent valuation method, and (2) the hedonic property value method. Both methods have important limitations, and uncertainties exist in the available results. Recognizing these uncertainties is important, but the body of evidence as a whole suggests that economic values for changes in visibility conditions are probably substantial in some cases, and that a sense of the likely magnitude of these values can be derived from available results in some instances. Economic studies have estimated values for two types of visibility effects potentially related to particulate air pollution: (1) use and non-use values for preventing the types of plumes caused by power plant emissions, visible from recreation areas in the southwestern United States; and (2) use values of local residents for reducing or preventing increases in urban hazes in several different locations.

### **8.9.2 Climate Change**

Aerosols of submicron size in the Earth's atmosphere perturb the radiation field. There is no doubt that anthropogenic aerosol emissions, primarily sulfur oxides, have the potential to affect climate; the question is by how much. There are two chief avenues through which aerosols impact the radiation budget of the Earth. The direct effect is that of enhanced solar reflection by the cloud-free atmosphere. Since aerosols, even those containing some absorptive component, are primarily reflective, their impact is felt as a negative radiative forcing (i.e., a cooling) on the climate system. Although there is some uncertainty in the global distribution of such aerosols and in the chemical and radiative properties of the aerosols, the radiative effects can still be modeled within certain bounds. Estimates of this forcing range from  $-0.3 \text{ W m}^{-2}$  to about twice that value for current conditions over pre-industrial times.

The indirect forcing results from the way in which aerosols affect cloud microphysical properties. The most important is the effective radius of cloud droplets, which decrease in the presence of higher concentrations of Cloud Condensation Nuclei (CCN) since more nucleating sites are available for droplets to form. This effect is most pronounced when the concentration,  $N$ , is very low, and clouds are moderately reflective. Other effects are the enhancement of cloud lifetimes and also changes in the nucleating ability of CCN through chemical changes. Although estimates of the indirect effect are uncertain by at least a factor of 2, but perhaps much more, it appears to be potentially more important than the direct

effect. Taken together, on a global mean basis, anthropogenic emissions of aerosols could have offset substantially the positive radiative forcing due to greenhouse gas emissions. High priority should be given to acquiring the measurements needed to quantifying these effects with greater accuracy.

The one crucial difference between aerosol forcing and greenhouse (gas) forcing is the atmospheric lifetime of aerosols and gases and hence, forcing. The aerosol forcing is fairly localized, whereas the greenhouse forcing is global. One should, therefore, expect inter-hemispheric differences in the forcing and perhaps climate response. However, climate models are not currently at the level of sophistication needed to determine climate response unambiguously. With few exceptions, global observations of surface temperature can not separate natural and anthropogenic causal mechanisms.

## REFERENCES

- Adams, K. M.; Kavis, L. I., Jr.; Japar, S. M.; Pierson, W. R. (1989) Real-time, *in situ* measurements of atmospheric optical absorption in the visible via photoacoustic spectroscopy - II. validation for atmospheric elemental carbon aerosol. *Atmos. Environ.* 23: 693-700.
- Ahlquist, N. C.; Charlson, R. J. (1967) A new instrument for evaluating the visual quality of air. *J. Air Pollut. Control Assoc.* 17: 467-469.
- Air & Waste Management Association. (1993) Southern California air quality study data analysis: proceedings of an international specialty conference; July 1992; Los Angeles, CA. Pittsburgh, PA: Air & Waste Management Association.
- Albrecht, B. A. (1989) Aerosols, cloud microphysics, and fractional cloudiness. *Science (Washington, DC)* 245: 1227-1230.
- Altshuller, A. P. (1982) Relationships involving particle mass and sulfur content at sites in and around St. Louis, Missouri. *Atmos. Environ.* 16: 837-843.
- Altshuller, A. P. (1985) Relationships involving fine particle mass, fine particle sulfur and ozone during episodic periods at sites in and around St. Louis, MO. *Atmos. Environ.* 19: 265-276.
- Alvarez, L. W.; Alvarez, W.; Asaro, F.; Michel, H. V. (1980) Extraterrestrial cause for the Cretaceous-Tertiary extinction. *Science (Washington, DC)* 208: 1095-1108.
- Anderson, T. L.; Charlson, R. J.; White, W. H.; McMurry, P. H. (1994) Comment on "Light scattering and cloud condensation nucleus activity of sulfate aerosol measured over the northeast Atlantic Ocean" by D. A. Hegg et al. *J. Geophys. Res. [Atmos.]* 99: 25,947-25,949.
- Ångström, A. (1964) The parameters of atmospheric turbidity. *Tellus* 16: 64-75.
- Appel, B. R.; Tokiwa, Y.; Hsu, J.; Kothny, E. L.; Hahn, E.; Wesolowski, J. J. (1983) Visibility reduction as related to aerosol constituents. Sacramento, CA: State of California, Air Resources Board; report no. CA/DOH/AIHL/SP-29. Available from: NTIS, Springfield, VA; PB84-243617.
- Appel, B. R.; Tokiwa, Y.; Hsu, J.; Kothny, E. L.; Hahn, E. (1985) Visibility as related to atmospheric aerosol constituents. *Atmos. Environ.* 19: 1525-1534.
- Bakan, S.; Chlond, A.; Cubasch, U.; Feichter, J.; Graf, H.; Grassl, H.; Hasselmann, K.; Kirchner, I.; Latif, M.; Roeckner, E.; Sausen, R.; Schlese, U.; Schriever, D.; Schult, I.; Schumann, U.; Sielmann, F.; Welke, W. (1991) Climate response to smoke from the burning oil wells in Kuwait. *Nature (London)* 351: 367-371.
- Bergstrom, R. W.; Seigneur, C.; Babson, B. L.; Holman, H.-Y.; Wojcik, M. A. (1981) Comparison of the observed and predicted visual effects caused by power plant plumes. *Atmos. Environ.* 15: 2135-2150.
- Blackwell, H. R. (1946) Contrast thresholds of the human eye. *J. Opt. Soc. Am.* 36: 624-643.
- Blanchet, J.-P. (1989) Toward estimation of climatic effects due to Arctic aerosols. *Atmos. Environ.* 23: 2609-2625.
- Blanchet, J.-P. (1991) Potential climate change from Arctic aerosol pollution. In: Sturges, W. T., ed. *Pollution of the Arctic atmosphere*. New York, NY: Elsevier Science Publishers; pp. 289-322. (Cairns, J.; Harrison, R. M., eds. *Environmental management series*).
- Blandford, J. C. (1994) Transmissometer data reduction and validation (IMPROVE protocol). Fort Collins, CO: Air Resource Specialists, Inc.; technical instruction no. 4400-5000.

- Blumenthal, D. L.; Richards, L. W.; Macias, E. S.; Bergstrom, R. W.; Wilson, W. E.; Bhardwaja, P. S. (1981) Effects of a coal-fired power plant and other sources on southwestern visibility (interim summary of EPA's project VISTTA). In: White, W. H.; Moore, D. J.; Lodge, J. P., Jr., eds. *Plumes and visibility: measurements and model components, proceedings of the symposium; November 1980; Grand Canyon National Park, AZ.* Atmos. Environ. 15: 1955-1969.
- Blumenthal, D.; Trijonis, J.; Kelso, R.; Pitchford, M.; McGown, M.; Dodson, T.; Flocchini, R.; Pitchford, A.; Waggoner, A.; Ouimette, J. (1987) Design and initial findings of the RESOLVE (research on operations-limiting visual extinction) desert visibility study. In: Bhardwaja, P. S., ed. *Visibility protection: research and policy aspects, an APCA international specialty conference; September 1986; Grand Teton National Park, WY.* Pittsburgh, PA: Air Pollution Control Association; pp. 87-98. (APCA transactions series no. TR-10).
- Bodhaine, B. A. (1979) Measurement of the Rayleigh scattering properties of some gases with a nephelometer. *Appl. Opt.* 18: 121-125.
- Bohren, C. F.; Huffman, D. R. (1983) *Absorption and scattering of light by small particles.* New York, NY: John Wiley & Sons.
- Box, M. A. (1995) Changes in surface radiation caused by a scattering layer as calculated using radiative perturbation theory. *J. Geophys. Res. [Atmos.]* 100: 11,581-11,584.
- Brookshire, D. S.; Ives, B. C.; Schulze, W. D. (1976) The valuation of aesthetic preferences. *J. Environ. Econ. Manage.* 3: 325-346.
- Brookshire, D. S.; Thayer, M. A.; Schulze, W. D.; d'Arge, R. C. (1982) Valuing public goods: a comparison of survey and hedonic approaches. *Am. Econ. Rev.* 72: 165-177.
- Browning, K. A.; Allam, R. J.; Ballard, S. P.; Barnes, R. T. H.; Bennetts, D. A.; Maryon, R. H.; Mason, P. J.; McKenna, D.; Mitchell, J. F. B.; Senior, C. A.; Slingo, A.; Smith, F. B. (1991) Environmental effects from burning oil wells in Kuwait. *Nature (London)* 351: 363-371.
- Carhart, R. A.; Policastro, A. J.; Wastag, M.; Coke, L. (1989) Evaluation of eight short-term long-range transport models using field data. *Atmos. Environ.* 23: 85-105.
- Carson, R. T.; Mitchell, R. C.; Ruud, P. A. (1990) Valuing air quality improvements: simulating a hedonic equation in the context of a contingent valuation scenario. In: Mathai, C. V., ed. *Visibility and fine particles: an A&WMA/EPA international specialty conference; October 1989; Estes Park, CO.* Pittsburgh, PA: Air & Waste Management Association; pp. 639-646. (A&WMA transactions series no. TR-17).
- Cess, R. D.; Potter, G. L.; Ghan, S. J.; Gates, W. L. (1985) The climatic effects of large injections of atmospheric smoke and dust: a study of climate feedback mechanisms with one- and three-dimensional climate models. *J. Geophys. Res. [Atmos.]* 90: 12,937-12,950.
- Cess, R. D.; Zhang, M. H.; Minnis, P.; Corsetti, L.; Dutton, E. G.; Forgan, B. W.; Garber, D. P.; Gates, W. L.; Hack, J. J.; Harrison, E. F.; Jing, X.; Kiehl, J. T.; Long, C. N.; Morcrette, J.-J.; Potter, G. L.; Ramanathan, V.; Subasilar, B.; Whitlock, C. H.; Young, D. F.; Zhou, Y. (1995) Absorption of solar radiation by clouds: observations versus models. *Science (Washington, DC)* 267: 496-499.
- Changnon, S. A. (1981) Midwestern cloud, sunshine and temperature trends since 1901: possible evidence of jet contrail effects. *J. Appl. Meteorol.* 20: 496-508.
- Charlock, T. P.; Sellers, W. D. (1980) Aerosol effects on climate: calculations with time-dependent and steady-state radiative-convective models. *J. Atmos. Sci.* 37: 1327-1341.

- Charlson, R. J.; Covert, D. S.; Tokiwa, Y.; Mueller, P. K. (1972) Multiwavelength nephelometer measurements in Los Angeles smog aerosol: III. comparison to light extinction by  $\text{NO}_2$ . In: Hidy, G. M., ed. *Aerosols and atmospheric chemistry: the Kendall award symposium at the proceedings of the American Chemical Society*; March-April 1971; Los Angeles, CA. New York, NY: Academic Press, Inc.; pp. 333-338.
- Charlson, R. J.; Covert, D. S.; Larson, T. V.; Waggoner, A. P. (1978) Chemical properties of tropospheric sulfur aerosols. In: Husar, R. B.; Lodge, J. P., Jr.; Moore, D. J., eds. *Sulfur in the atmosphere: proceedings of the international symposium*; September 1977; Dubrovnik, Yugoslavia. *Atmos. Environ.* 12: 39-53.
- Charlson, R. J.; Lovelock, J. E.; Andreae, M. O.; Warren, S. G. (1987) Oceanic phytoplankton, atmospheric sulphur, cloud albedo and climate. *Nature (London)* 326: 655-661.
- Charlson, R. J.; Langner, J.; Rodhe, H.; Leovy, C. B.; Warren, S. G. (1991) Perturbation of the northern hemisphere radiative balance by backscattering from anthropogenic sulfate aerosols. *Tellus* 43AB: 152-163.
- Charlson, R. J.; Schwartz, S. E.; Hales, J. M.; Cess, R. D.; Coakley, J. A., Jr.; Hansen, J. E.; Hofmann, D. J. (1992) Climate forcing by anthropogenic aerosols. *Science (Washington, DC)* 255: 423-430.
- Chestnut, L. G.; Rowe, R. D. (1990a) Methods for valuing acidic deposition and air pollution effects. Section B5. Economic valuation of changes in visibility: a state of the science assessment for NAPAP. In: Irving, P. M., ed. *Acidic deposition: state of science and technology, volume IV, control technologies, future emissions, and effects valuation*. Washington, DC: The U.S. National Acid Precipitation Assessment Program; pp. 27-153 - 27-175. (State of science and technology report no. 27).
- Chestnut, L. G.; Rowe, R. D. (1990b) Preservation values for visibility in the national parks. Washington, DC: U.S. Environmental Protection Agency.
- Cismoski, D. S. (1994) nephelometer data reduction and validation (IMPROVE protocol). Fort Collins, CO: Air Resource Specialists, Inc.; August.
- Claeys, P.; Casier, J.-G.; Margolis, S. V. (1992) Microtektites and mass extinctions: evidence for a Late Devonian asteroid impact. *Science (Washington, DC)* 257: 1102-1104.
- Coakley, J. A., Jr.; Cess, R. D.; Yurevich, F. B. (1983) The effect of tropospheric aerosols on the earth's radiation budget: a parameterization for climate models. *J. Atmos. Sci.* 40: 116-138.
- Coakley, J. A., Jr.; Bernstein, R. L.; Durkee, P. A. (1987) Effect of ship-stack effluents on cloud reflectivity. *Science (Washington, DC)* 237: 1020-1022.
- Conover, J. H. (1966) Anomalous cloud lines. *J. Atmos. Sci.* 23: 778-785.
- Cooper, J. A.; Watson, J. G. (1979) Portland aerosol characterization study (PACS). Final report for Portland Air Quality Maintenance Area Advisory Committee and Oregon Department of Environmental Quality.

- Core, J. E.; Maykut, N.; Weaver, D.; Boylan, J.; Hooper, M. (1987) PANORAMAS: a summary of major findings from the Pacific northwest regional aerosol mass apportionment study. In: Bhardwaja, P. S., ed. Visibility protection: research and policy aspects, an APCA international specialty conference; September 1986; Grand Teton National Park, WY. Pittsburgh, PA: Air Pollution Control Association; pp. 99-112. (APCA transactions series no. TR-10).
- Cornsweet, T. N. (1970) Factors other than wavelength that influence hue. In: Visual perception. New York, NY: Academic Press, Inc.; pp. 236-240.
- Countess, R. J.; Wolff, G. T.; Cadle, S. H. (1980) The Denver winter aerosol: a comprehensive chemical characterization. *J. Air Pollut. Control Assoc.* 30: 1194-1200.
- Countess, R. J.; Cadle, S. H.; Groblicki, P. J.; Wolff, G. T. (1981) Chemical analysis of size-segregated samples of Denver's ambient particulate. *J. Air Pollut. Control Assoc.* 31: 247-252.
- Covert, D. S.; Waggoner, A. P.; Weiss, R. E.; Ahlquist, N. C.; Charlson, R. J. (1980) Atmospheric aerosols, humidity, and visibility. In: Hidy, G. M.; Mueller, P. K.; Grosjean, D.; Appel, B. R.; Wesolowski, J. J., eds. The character and origins of smog aerosols: a digest of results from the California Aerosol Characterization Experiment (ACHEX). New York, NY: John Wiley & Sons, Inc.; pp. 559-581. (Advances in environmental science and technology: v. 9).
- Cummings, R. G.; Brookshire, D. S.; Schulze, W. D., eds. (1986) Valuing environmental goods: an assessment of the contingent valuation method. Totowa, NJ: Rowman and Allanheld.
- Daniel, T. C.; Hill, A. C. (1987) Measuring visibility values: comparison of perceptual assessment methods. In: Bhardwaja, P. S., ed. Visibility protection: research and policy aspects, an APCA international specialty conference; September 1986; Grand Teton National Park, WY. Pittsburgh, PA: Air Pollution Control Association; pp. 287-303. (APCA transactions series no. TR-10).
- Davidson, J. A.; Cantrell, C. A.; McDaniel, A. H.; Shetter, R. E.; Madronich, S.; Calvert, J. G. (1988) Visible-ultraviolet absorption cross sections for NO<sub>2</sub> as a function of temperature. *J. Geophys. Res. [Atmos.]* 93: 7105-7112.
- Davies, R. (1993) Increased transmission of ultraviolet radiation to the surface due to stratospheric scattering. *J. Geophys. Res. [Atmos.]* 98: 7251-7253.
- Dessens, H. (1944) Relation entre l'absorption par l'atmosphère et la visibilité [Relationship between atmospheric absorption and visibility]. *Comptes Rendus* 218: 685-687.
- Drivas, P. J.; Bass, A.; Heinold, D. W. (1981) A plume blight visibility model for regulatory use. In: White, W. H.; Moore, D. J.; Lodge, J. P., Jr. Plumes and visibility: measurements and model components: proceedings of the symposium; November 1980; Grand Canyon National Park, AZ. *Atmos. Environ.* 15: 2179-2184.
- Duffie, J. A.; Beckman, W. A. (1991) Solar engineering of thermal processes. 2nd ed. New York, NY: John Wiley & Sons, Inc.
- Duntley, S. Q.; Boileau, A. R.; Preisendorfer, R. W. (1957) Image transmission by the troposphere I. *J. Opt. Soc. Am.* 47: 499-506.
- Dzubay, T. G.; Clubb, K. W. (1981) Comparison of telephotometer measurements of extinction coefficients with scattering and absorption coefficients. In: White, W. H.; Moore, D. J.; Lodge, J. P., Jr., eds. Plumes and visibility: measurements and model components, proceedings of the symposium; November 1980; Grand Canyon National Park, AZ. *Atmos. Environ.* 15: 2617-2624.
- Dzubay, T. G.; Stevens, R. K.; Lewis, C. W.; Hern, D. H.; Courtney, W. J.; Tesch, J. W.; Mason, M. A. (1982) Visibility and aerosol composition in Houston, Texas. *Environ. Sci. Technol.* 16: 514-525.

- Edlén, B. (1953) The dispersion of standard air. *J. Opt. Soc. Am.* 43: 339-344.
- Eldering, A.; Larson, S. M.; Hall, J. R.; Hussey, K. J.; Cass, G. R. (1993) Development of an improved image processing based visibility model. *Environ. Sci. Technol.* 27: 626-635.
- Eldred, R. A.; Cahill, T. A. (1994) Trends in elemental concentrations of fine particles at remote sites in the United States of America. *Atmos. Environ.* 28: 1009-1019.
- Eltgroth, M. W.; Hobbs, P. V. (1979) Evolution of particles in the plumes of coal-fired power plants— II. A numerical model and comparisons with field measurements. *Atmos. Environ.* 13: 953-975.
- Ensor, D. S.; Waggoner, A. P. (1970) Angular truncation error in the integrating nephelometer. *Atmos. Environ.* 4: 481-487.
- Erickson, D. J., III; Walton, J. J.; Ghan, S. J.; Penner, J. E. (1991) Three-dimensional modeling of the global atmospheric sulfur cycle: a first step. *Atmos. Environ. Part A* 25: 2513-2520.
- Falkowski, P. G.; Kim, Y.; Kolber, Z.; Wilson, C.; Wirrick, C.; Cess, R. D. (1992) Natural versus anthropogenic factors affecting low-level cloud albedo over the north Atlantic. *Science (Washington, DC)* 256: 1311-1313.
- Ferman, M. A.; Wolff, G. T.; Kelly, N. A. (1981) The nature and sources of haze in the Shenandoah Valley/Blue Ridge Mountains area. *J. Air Pollut. Control Assoc.* 31: 1074-1082.
- Fischhoff, B.; Furby, L. (1988) Measuring values: a conceptual framework for interpreting transactions with special reference to contingent valuation of visibility. *J. Risk Uncertainty* 1: 147-184.
- Frederick, J. E.; Snell, H. E.; Haywood, E. K. (1989) Solar ultraviolet radiation at the earth's surface. *Photochem. Photobiol.* 50: 443-450.
- Ghan, S. J.; MacCracken, M. C.; Walton, J. J. (1988) Climate response to large atmospheric smoke injections: sensitivity studies with a tropospheric general circulation model. *J. Geophys. Res. [Atmos.]* 93: 8315-8337.
- Giorgi, F.; Visconti, G. (1989) Two-dimensional simulations of possible mesoscale effects of nuclear war fires: 2. model results. *J. Geophys. Res. [Atmos.]* 94: 1145-1163.
- Gordon, J. I. (1964) Visibility III: optical properties of objects and backgrounds. *Appl. Opt.* 3: 556-562.
- Graves, P.; Murdoch, J. C.; Thayer, M. A.; Waldman, D. (1988) The robustness of hedonic price estimation: urban air quality. *Land Econ.* 64: 220-233.
- Groblicki, P. J.; Wolff, G. T.; Countess, R. J. (1981) Visibility-reducing species in the Denver "brown cloud" - I. relationships between extinction and chemical composition. In: White, W. H.; Moore, D. J.; Lodge, J. P., Jr., eds. *Plumes and visibility: measurements and model components, proceedings of the symposium, November 1980; Grand Canyon National Park, AZ.* *Atmos. Environ.* 15: 2473-2484.
- Haecker, G. (1905) Untersuchungen über Nebeltransparenz [Fog transparency investigations]. *Meteorol. Zeit.* 22: 343-353.
- Han, Q.; Rossow, W. B.; Lacis, A. A. (1994) Near-global survey of effective droplet radii in liquid water clouds using ISCCP data. *J. Clim.* 7: 465-497.
- Handler, A. (1989) Annual report on the establishment and operation of the eastern pine particle visibility network. search Triangle Park, NC: U.S. Environmental Protection Agency; EPA report no. 600/3-89/026. Available from: NTIS, Springfield, VA; PB89-165948.

- Hansen, J. E.; Lacis, A. A. (1990) Sun and dust versus greenhouse gases: an assessment of their relative roles in global climate change. *Nature (London)* 346: 713-719.
- Harrison, L.; Michalsky, J. (1994) Objective algorithms for the retrieval of optical depths from ground-based measurements. *Appl. Opt.* 33: 5126-5132.
- Harrison, L.; Michalsky, J.; Berndt, J. (1994) Automated multifilter rotating shadow-band radiometer: an instrument for optical depth and radiation measurements. *Appl. Opt.* 33: 5118-5125.
- Harshvardhan. (1993) Aerosol—climate interactions. In: Hobbs, P. V., ed. *Aerosol-cloud-climate interactions*. New York, NY: Academic Press; pp. 75-95.
- Hartmann, D. L. (1994) Emission temperature of a planet. In: *Global physical climatology*. New York, NY: Academic Press; p. 25.
- Hasan, H.; Dzubay, T. G. (1987) Size distributions of species in fine particles in Denver using a microorifice impactor. *Aerosol Sci. Technol.* 6: 29-39.
- Hasan, H.; Lewis, C. W. (1983) Integrating nephelometer response corrections for bimodal size distributions. *Aerosol Sci. Technol.* 2: 443-453.
- Hegg, D. A.; Ferek, R. J.; Hobbs, P. V. (1993) Light scattering and cloud condensation nucleus activity of sulfate aerosol measured over the northeast Atlantic Ocean. *J. Geophys. Res. [Atmos.]* 98: 14,887-14,894.
- Hegg, D. A.; Ferek, R. J.; Hobbs, P. V. (1994) Reply. *J. Geophys. Res. [Atmos.]* 99: 25,951-25,954.
- Heintzenberg, J. (1978) The angular calibration of the total scatter/backscatter nephelometer: consequences and applications. *Staub Reinhalt. Luft* 38: 62-63.
- Heintzenberg, J.; Quenzel, H. (1973) On the effect of the loss of large particles on the determination of scattering coefficients with integrating nephelometers. *Atmos. Environ.* 7: 503-507.
- Heisler, S. L.; Baskett, R. (1981) Particle sampling and analysis in the California San Joaquin Valley. Westlake Village, CA: Environmental Research & Technology, Inc.; ERT document no. P-5381-701.
- Heisler, S. L.; Henry, R. C.; Watson, J. G.; Hidy, G. M. (1980a) The 1978 Denver winter haze study. Westlake Village, CA: Environmental Research & Technology, Inc.; document no. P-5417-1.
- Heisler, S. L.; Henry, R. C.; Watson, J. G. (1980b) The sources of the Denver haze in November and December of 1978. Presented at: 73rd annual meeting of the Air Pollution Control Association; June; Montreal, PQ, Canada. Pittsburgh, PA: Air Pollution Control Association; paper no. 80-58.6.
- Henderson-Sellers, A. (1986) Increasing cloud in a warming world. *Clim. Change* 9: 267-309.
- Henderson-Sellers, A. (1989) North American total cloud amount variations this century. *Paleogeog. Paleoclim. Paleoecol.* 75: 175-194.
- Hering, S. V.; McMurry, P. H. (1991) Optical counter response to monodisperse atmospheric aerosols. *Atmos. Environ. Part A* 25: 463-468.
- Hidy, G. M.; Appel, B. R.; Charlson, R. J.; Clark, W. E.; Friedlander, S. K.; Hutchison, D. H.; Smith, T. B.; Suder, J.; Wesolowski, J. J.; Whitby, K. T. (1975) Summary of the California Aerosol Characterization Experiment. *J. Air Pollut. Control Assoc.* 25: 1106-1114.

- Hidy, G. M.; Mueller, P. K.; Grosjean, D.; Appel, B. R.; Wesolowski, J. J., eds. (1980) The character and origins of smog aerosols: a digest of results from the California Aerosol Characterization Experiment (ACHEX). New York, NY: John Wiley & Sons.
- Hildemann, L. M.; Mazurek, M. A.; Cass, G. R.; Simoneit, B. R. T. (1994) Seasonal trends in Los Angeles ambient organic aerosol observed by high-resolution gas chromatography. *Aerosol Sci. Technol.* 20: 303-317.
- Hobbs, P. V., ed. (1994) A plan for an international global aerosol program (IGAP). Seattle, WA: University of Washington; p. 3.
- Hobbs, P. V.; Radke, L. F. (1992) Airborne studies of the smoke from the Kuwait oil fires. *Science* (Washington, DC) 256: 987-991.
- Hoffman, D. J.; Solomon, S. (1989) Ozone destruction through heterogeneous chemistry following the eruption of El Chichón. *J. Geophys. Res. [Atmos.]* 94: 5029-5041.
- Hoffman, D. J.; Oltmans, S. J.; Komhyr, W. D.; Harris, J. M.; Lathrop, J. A.; Langford, A. O.; Deshler, T.; Johnson, B. J.; Torres, A.; Matthews, W. A. (1994) Ozone loss in the lower atmosphere over the United States in 1992-1993: evidence for heterogeneous chemistry on the Pinatubo aerosol. *Geophys. Res. Letters* 21: 65-68.
- Hofmann, D. J. (1993) Twenty years of balloon-borne tropospheric aerosol measurements at Laramie, Wyoming. *J. Geophys. Res. [Atmos.]* 98: 12,753-12,766.
- Holland, A. C.; Gagne, G. (1970) The scattering of polarized light by polydisperse systems of irregular particles. *Appl. Opt.* 9: 1113-1121.
- Houghton, J. T.; Jenkins, G. J.; Ephraums, J. J., eds. (1990) Climate change: the IPCC scientific assessment. Cambridge, MA: Cambridge University Press; p. 55.
- Hugon, M. (1930) Variation de la brillance des lointains avec la distance. *Sci. Ind. Phot.* 1: 161-168, 201-212.
- Husar, R. B.; Patterson, D. E. (1984) Haze climate of United States. Research Triangle Park, NC: U.S. Environmental Protection Agency, Atmospheric Sciences Research Laboratory; EPA report no. EPA-600/3-86/07. Available from: NTIS, Springfield, VA; PB87-141057.
- Husar, R. B.; Poirot, R. (1992) Exploration of the AIRS database: weekly cycle of ozone and PM 10 aerosols. Presented at: 85th annual meeting of the Air & Waste Management Association; June; Kansas City, MO. Pittsburgh, PA: Air & Waste Management Association; paper no. 92-77.06.
- Husar, R. B.; Wilson, W. E. (1993) Haze and sulfur emission trends in the eastern United States. *Environ. Sci. Technol.* 27: 12-16.
- Husar, R. B.; White, W. H.; Blumenthal, D. L. (1976) Direct evidence of heterogeneous aerosol formation in Los Angeles smog. *Environ. Sci. Technol.* 10: 490-491.
- Husar, R. B.; Holloway, J. M.; Patterson, D. E.; Wilson, W. E. (1981) Spatial and temporal pattern of eastern U.S. haziness: a summary. *Atmos. Environ.* 15: 1919-1928.
- Intergovernmental Panel on Climate Change. (1994) Climate change 1994: radiative forcing of climate and an evaluation of the IPCC 1S92 emission scenarios. Cambridge, United Kingdom: Cambridge University Press.
- Iqbal, M. (1983) An introduction to solar radiation. New York, NY: Academic Press; p. 162.
- Irwin, J.; Schenk, D.; McClelland, G. H.; Schulze, W. D.; Stewart, T.; Thayer, M. (1990) Urban visibility: some experiments on the contingent valuation method. In: Mathai, C. V., ed. *Visibility and fine particles: an*

- A&WMA/EPA international specialty conference; October 1989; Estes Park, CO. Pittsburgh, PA: Air & Waste Management Association; pp. 647-658. (A&WMA transactions series no. TR-17).
- Jaklevic, J. M.; Gattis, R. C.; Goulding, F. S.; Loo, B. W.; Thompson, A. C.. (1981) Aerosol analysis for the regional air pollution study. Research Triangle Park, NC: U.S. Environmental Protection Agency; EPA report no. 600/4-81-006. Available from: NTIS, Springfield, VA; PB81-157141.
- Japar, S. M.; Szkarlat, A. C.; Pierson, W. R. (1984) The determination of the optical properties of airborne particle emissions from diesel vehicles. *Sci. Total Environ.* 36: 121-130.
- Japar, S. M.; Brachaczek, W. W.; Gorse, R. A., Jr.; Norbeck, J. M.; Pierson, W. R. (1986) The contribution of elemental carbon to the optical properties of rural atmospheric aerosols. *Atmos. Environ.* 20: 1281-1289.
- John, W.; Wall, S. M.; Ondo, J. L.; Winklmayr, W. (1990) Modes in the size distributions of atmospheric inorganic aerosol. *Atmos. Environ. Part A* 24: 2349-2359.
- Johnson, C. D.; Latimer, D. A.; Bergstrom, R. W.; Hogo, H. (1980) User's manual for the plume visibility model (PLUVUE). Research Triangle Park, NC: U.S. Environmental Protection Agency; EPA report no. EPA-450/4-80-032. Available from: NTIS, Springfield, VA; PB81-163297.
- Johnson, C. E.; Malm, W. C.; Persha, G.; Molenaar, J. V.; Hein, J. R. (1985) Statistical comparisons between teleradiometer-derived and slide-derived visibility parameters. *J. Air Pollut. Control Assoc.* 35: 1261-1265.
- Jones, A.; Roberts, D. L.; Slingo, A. (1994) A climate model study of indirect radiative forcing by anthropogenic sulfate aerosols. *Nature (London)* 370: 450-453.
- Joseph, D. B.; Metsa, J.; Malm, W. C.; Pitchford, M. (1987) Plans for IMPROVE: a federal program to monitor visibility in class I areas. In: Bhardwaja, P. S., ed. *Visibility protection: research and policy aspects*, an APCA international specialty conference; September 1986; Grand Teton National Park, WY. Pittsburgh, PA: Air Pollution Control Association; pp. 113-125. (APCA transactions series no. TR-10).
- Judd, D. B.; Wyszecski, G (1975) *Color in business, science and industry*. 3rd ed. New York, NY: John Wiley & Sons.
- Jung, H. J.; Bach, W. (1987) The effects of aerosols on the response of a two-dimensional zonally-averaged climate model. *Theor. Appl. Climatol.* 38: 222-233.
- Kahneman, D.; Knetsch, J. L. (1992) Valuing public goods: the purchase of moral satisfaction. *J. Environ. Econ. Manage.* 22: 57-70.
- Kaufman, Y. J.; Chou, M.-D. (1993) Model simulations of the competing climatic effects of SO<sub>2</sub> and CO<sub>2</sub>. *J. Clim.* 6: 1241-1252.
- Kaufman, Y. J.; Fraser, R. S.; Mahoney, R. L. (1991) Fossil fuel and biomass burning effect on climate—heating or cooling? *J. Clim.* 4: 578-588.
- Kerker, M. (1969) *The scattering of light and other electromagnetic radiation*. New York, NY: Academic Press, Inc. (Loebl, E. M., ed. *Physical chemistry: a series of monographs*, no. 16).
- Kerker, M.; Aden, A. L (1991) Scattering of electromagnetic waves from two concentric spheres. *J. Appl. Physiol.* 22: 1242-1246.
- Kiehl, J. T.; Briegleb, B. P. (1993) The relative roles of sulfate aerosols and greenhouse gases in climate forcing. *Science (Washington, DC)* 260: 311-314.

- King, M. D.; Radke, L. F.; Hobbs, P. V. (1993) Optical properties of marine stratocumulus clouds modified by ships. *J. Geophys. Res. [Atmos.]* 98: 2729-2739.
- Koenig, J. Q.; Larson, T. V.; Hanley, Q. S.; Rebolledo, V.; Dumler, K.; Checkoway, H.; Wang, S.-Z.; Lin, D.; Pierson, W. E. (1993) Pulmonary function changes in children associated with fine particulate matter. *Environ. Res.* 63: 26-38.
- Koschmieder, H. (1924) Theorie der horizontalen Sichtweite II: Kontrast und Sichtweite [Theory of horizontal visibility]. *Beitr. Phys. Atmos.* 12: 171-181.
- Langner, J.; Rodhe, H. (1991) A global three-dimensional model of the tropospheric sulfur cycle. *J. Atmos. Chem.* 13: 225-263.
- Langner, J.; Rodhe, H.; Crutzen, P. J.; Zimmermann, P. (1992) Anthropogenic influence on the distribution of tropospheric sulphate aerosol. *Nature (London)* 359: 712-716.
- Larson, S. M.; Cass, G. R.; Hussey, K. J.; Luce, F. (1988) Verification of image processing based visibility models. *Environ. Sci. Technol.* 22: 629-637.
- Latimer, D. A. (1988) Plume perceptibility thresholds. Presented at: 81st annual meeting of the Air Pollution Control Association; June; Dallas, TX. Pittsburgh, PA: Air Pollution Control Association; paper no. 88-56.6.
- Latimer, D. A.; Bergstrom, R. W.; Hayes, S. R.; Liu, M.-K.; Seinfeld, J. H.; Whitten, G. Z.; Wojcik, M. A.; Hillyer, M. J. (1978) The development of mathematical models for the prediction of anthropogenic visibility impairment: volumes I-III. Research Triangle Park, NC: U.S. Environmental Protection Agency, Office of Air Quality Planning and Standards; EPA report no. EPA-450/3-78-110a-c. Available from: NTIS, Springfield, VA; PB-293118-SET.
- Latimer, D. A.; Hogo, H.; Daniel, T. C. (1981) The effects of atmospheric optical conditions on perceived scenic beauty. *Atmos. Environ.* 15: 1865-1874.
- Lawson, D. R. (1990) The Southern California Air Quality Study. *J. Air Waste Manage. Assoc.* 40: 156-165.
- Leaich, W. R.; Isaac, G. A. (1994) On the relationship between sulfate and cloud droplet number concentrations. *J. Clim.* 7: 206-212.

- Lewis, C. W.; Stevens, R. K. (1983) Comparison of factors influencing visual air quality during the winter in Denver, derived from measurements made by General Motors and Motor Vehicle Manufacturers Association in 1978 and Environmental Protection Agency in 1982. Research Triangle Park, NC: U.S. Environmental Protection Agency; EPA preliminary report.
- Lioy, P. J.; Daisey, J. M.; Reiss, N. M.; Harkov, R. (1983) Characterization of inhalable particulate matter, volatile organic compounds and other chemical species measured in urban areas in New Jersey— I. summertime episodes. *Atmos. Environ.* 17: 2321-2330.
- Lioy, P. J.; Daisey, J. M.; Greenberg, A.; Harkov, R. (1985) A major wintertime (1983) pollution episode in northern New Jersey: analyses of the accumulation and spatial distribution of inhalable particulate matter, extractable organic matter and other species. *Atmos. Environ.* 19: 429-436.
- Loehman, E.; Boldt, D.; Chaikin, K. (1981) Measuring the benefits of air quality improvements in the San Francisco Bay area. Washington, DC: U.S. Environmental Protection Agency.
- Lorente, J.; Redaño, A.; de Cabo, X. (1994) Influence of urban aerosol on spectral solar irradiance. *J. Appl. Meteorol.* 33: 406-415.
- Lowenthal, D. H.; Rogers, C. F.; Saxena, P.; Watson, J. G.; Chow, J. C. (1995) Sensitivity of estimated light extinction coefficients to model assumptions and measurement errors. *Atmos. Environ.* 29: 751-766.
- Lyons, C.; Tombach, I. (1979) Willamette Valley field and slash burning impact air surveillance network data evaluation, v. 2. Pasadena, CA: Aerovironment Inc.
- MacAdam, D. L. (1981) Perceptual significance of colorimetric data for colors of plumes and haze. *Atmos. Environ.* 15: 1797-1803.
- MacCracken, M. C.; Cess, R. D.; Potter, G. L. (1986) Climatic effects of anthropogenic Arctic aerosols: an illustration of climate feedback mechanisms with one- and two-dimensional climate models. *J. Geophys. Res. [Atmos.]* 91: 14,445-14,450.
- MacFarland, K. K.; Malm, W.; Molenaar, J. (1983) An examination of methodologies for assessing the value of visibility. In: Rowe, R. D.; Chestnut, L. G., eds. *Managing air quality and scenic resources at national parks and wilderness areas*. Boulder, CO: Westview Press; pp. 151-172.
- Macias, E. S.; Vossler, T. L.; White, W. H. (1987) Carbon and sulfate particles in the western U.S. In: Bhardwaja, P. S., ed. *Visibility protection: research and policy aspects, an APCA international specialty conference; September 1986; Grand Teton National Park, WY*. Pittsburgh, PA: Air Pollution Control Association; pp. 361-372. (APCA transactions series no. TR-10).
- Malm, W. (1979) Considerations in the measurement of visibility. *J. Air Pollut. Control Assoc.* 29: 1042-1052.
- Malm, W.; Pitchford, M.; Pitchford, A. (1982) Site specific factors influencing the visual range calculated from teleradiometer measurements. *Atmos. Environ.* 16: 2323-2333.
- Malm, W. C.; Sisler, J. F.; Huffman, D.; Eldred, R. A.; Cahill, T. A. (1994) Spatial and seasonal trends in particle concentration and optical extinction in the United States. *J. Geophys. Res. [Atmos.]* 99: 1347-1370.
- Marians, M.; Trijonis, J. (1979) *Empirical studies of the relationship between emissions and visibility in the Southwest*. Research Triangle Park, NC: U.S. Environmental Protection Agency, Office of Air Quality Planning and Standards; EPA report no. EPA-450/5-79-009. Available from: NTIS, Springfield, VA; PB80-156136.

- McClelland, G.; Schulze, W.; Waldman, D.; Irwin, J.; Schenk, D.; Stewart, T.; Deck, L.; Thayer, M. (1991) Valuing eastern visibility: a field test of the contingent valuation method. Washington, DC: draft report to the U.S. Environmental Protection Agency; cooperative agreement no. CR-815183-01-3.
- McDade, C. E.; Tombach, I. H. (1987) Goals and initial findings from SCENES. In: Bhardwaja, P. S., ed. Visibility protection: research and policy aspects, an APCA international specialty conference; September 1986; Grand Teton National Park, WY. Pittsburgh, PA: Air Pollution Control Association; pp. 76-86. (APCA transactions series no. TR-10).
- McMurry, P. H.; Stolzenburg, M. R. (1989) On the sensitivity of particle size to relative humidity for Los Angeles aerosols. *Atmos. Environ.* 23: 497-507.
- Meng, Z.; Seinfeld, J. H. (1994) On the source of the submicrometer droplet mode of urban and regional aerosols. *Aerosol Sci. Technol.* 20: 253-265.
- Mercer, G. S. (1994) Transmissometer data reporting (IMPROVE protocol). Fort Collins, CO: Air Resource Specialists, Inc.; technical instruction no. 4500-5100.
- Michelangeli, D. V.; Allen, M.; Yung, Y. L. (1989) The effect of El Chichon volcanic aerosols: impact of radiative, thermal, and chemical perturbations. *J. Geophys. Res. [Atmos.]* 94: 18,429-18,443.
- Michelangeli, D. V.; Allen, M.; Yung, Y. L.; Shia, R.-L.; Crisp, D.; Eluszkiewicz, J. (1992) Enhancement of atmospheric radiation by an aerosol layer. *J. Geophys. Res. [Atmos.]* 97: 865-874.
- Middleton, W. E. K. (1952) *Vision through the atmosphere*. Toronto, ON, Canada: University of Toronto Press.
- Middleton, P. (1996) DAQM-simulated spatial and temporal differences among visibility, PM and other air quality concerns under realistic emission change scenarios. *J. Air Waste Manage. Assoc.*: accepted.
- Middleton, P.; Stewart, T. R.; Dennis, R. L. (1983) Modeling human judgments of urban visual air quality. *Atmos. Environ.* 17: 1015-1021.
- Mie, G. (1908) Beiträge zur Optik trüber Medien, speziell kolloidaler Metallosungen [Optics of cloudy media, especially colloidal metal solutions]. *Ann. Phys. (Leipzig)* 25: 377-445.
- Minnaert, M. (1954) *The nature of light and colour in the open air*. New York, NY: Dover Publications, Inc.
- Mitchell, R. C.; Carson, R. T. (1989) *Using surveys to value public goods: the contingent valuation method*. Washington, DC: Resources for the Future.
- Molenaar, J. V.; Persha, G.; Malm, W. C. (1990) Long path transmissometer for measuring ambient atmospheric extinction. In: Mathai, C. V., ed. *Visibility and fine particles: transactions of an Air & Waste Management Association/U.S. Environmental Protection Agency international specialty conference; October 1989; Estes Park, CO*. Pittsburgh PA: Air & Waste Management Association; pp. 293-304. (Transactions TR-17).
- Molenaar, J. V.; Cismoski, D. S.; Tree, R. M. (1992) Intercomparison of ambient optical monitoring techniques. Presented at: 85th annual meeting of the Air & Waste Management Association; June; Kansas City, MO.
- Molenaar, J. V.; Malm, W. C.; Johnson, C. E. (1994) Visual air quality simulation techniques. *Atmos. Environ.* 28: 1055-1063.
- Moran, M. D.; Pielke, R. A. (1994) Delayed shear enhancement in mesoscale atmospheric dispersion. Presented at: 8th joint conference on applications of air pollution meteorology with A&WMA; January; Nashville, TN. Boston, MA: Meteorological Society; pp. 96-103.

- Mueller, P. K.; Watson, J. G. (1982) Eastern regional air quality measurements, v. I. Palo Alto, CA: Electric Power Research Institute; report no. EA-1914.
- Mueller, P. K.; Hidy, G. M. (1983) The sulfate regional experiment (SURE): report of findings. Palo Alto, CA: Electric Power Research Institute; EPRI report no. EA-1901. 3v.
- Mueller, P. K.; Hansen, D. A.; Watson, J. G., Jr. (1986) The subregional cooperative electric utility, Department of Defense, National Park Service, and EPA study (SCENES) on visibility: an overview. Palo Alto, CA: Electric Power Research Institute; report no. EA-4664-SR.
- National Oceanic and Atmospheric Administration. (1992) ASOS (automated surface observing system) user's guide. Washington, DC: National Oceanic and Atmospheric Administration.
- National Research Council. (1993) Protecting visibility in national parks and wilderness areas. Washington, DC: National Academy Press. 3v.
- Nguyen, B. C.; Bonsang, B.; Gaudry, A. (1983) The role of the ocean in the global atmospheric sulfur cycle. *J. Geophys. Res. C: Oceans Atmos.* 88: 10,903-10,914.
- Novakov, T.; Penner, J. E. (1993) Large contribution of organic aerosols to cloud-condensation-nuclei concentrations. *Nature (London)* 365: 823-826.
- Orr, C., Jr.; Hurd, F. K.; Corbett, W. J. (1958) Aerosol size and relative humidity. *J. Colloid Sci.* 13: 472-482.
- Pace, Y. G.; Watson, J. G.; Rodes, C. E. (1981) Preliminary interpretation of Inhalable Particulate Network data. Presented at: 74th annual meeting of the Air Pollution Control Association; June; Philadelphia, PA. Pittsburgh, PA: Air Pollution Control Association; paper no. 81-5.2.
- Patterson, E. M. (1977) Atmospheric extinction between 0.55  $\mu\text{m}$  and 10.6  $\mu\text{m}$  due to soil-derived aerosols. *Appl. Opt.* 16: 2414-2418.
- Patterson, D. E.; Holloway, J. M.; Husar, R. B. (1980) Historical visibility over the eastern U.S.: daily and quarterly extinction coefficient contour maps. Research Triangle Park, NC: U.S. Environmental Protection Agency, Environmental Sciences Research Laboratory; EPA report no. EPA-600/3-80-043a. Available from: NTIS, Springfield, VA; PB81-196974.
- Penndorf, R. B. (1958) An approximation method to the Mie theory for colloidal spheres. *J. Phys. Chem.* 62: 1537-1542.
- Penndorf, R. (1957) Tables of the refractive index for standard air and the Rayleigh scattering coefficient for the spectral region between 0.2 and 20.0  $\mu$  and their application to atmospheric optics. *J. Opt. Soc. Am.* 47: 176-182.
- Penner, J. E.; Dickinson, R. E.; O'Neill, C. A. (1992) Effects of aerosol from biomass burning on the global radiation budget. *Science (Washington, DC)* 256: 1432-1433.
- Penner, J. E.; Charlson, R. J.; Hales, J. M.; Laulainen, N. S.; Leifer, R.; Novakov, T.; Ogren, J.; Radke, L. F.; Schwartz, S. E.; Travis, L. (1994) Quantifying and minimizing uncertainty of climate forcing by anthropogenic aerosols. *Bull. Am. Meteorol. Soc.* 75: 375-400.
- Pierson, W. R.; Brachaczek, W. W.; Korniski, T. J.; Truex, T. J.; Butler, J. W. (1980a) Artifact formation of sulfate, nitrate, and hydrogen ion on backup filters: Allegheny Mountain experiment. *J. Air Pollut. Control Assoc.* 30: 30-34.

- Pierson, W. R.; Brachaczek, W. W.; Truex, T. J.; Butler, J. W.; Korniski, T. J. (1980b) Ambient sulfate measurements on Allegheny Mountain and the question of atmospheric sulfate in the northeastern United States. *Ann. N. Y. Acad. Sci.* 338: 145-173.
- Pinnick, R. G.; Fernandez, G.; Martinez-Andazola, E.; Hinds, B. D.; Hansen, A. D. A.; Fuller, K. (1993) Aerosol in the arid southwestern United States: measurements of mass loading, volatility, size distribution, absorption characteristics, black carbon content, and vertical structure to 7 km above sea level. *J. Geophys. Res. [Atmos.]* 98: 2651-2666.
- Pitchford, M. L.; Malm, W. C. (1994) Development and applications of a standard visual index. *Atmos. Environ.* 28: 1049-1054.
- Platnick, S.; Twomey, S. (1994) Determining the susceptibility of cloud albedo to changes in droplet concentration with the advanced very high resolution radiometer. *J. Appl. Meteorol.* 33: 334-347.
- Rae, D. A. (1984) Benefits of visual air quality in Cincinnati - results of a contingent ranking survey, final report. Palo Alto, CA: Electric Power Research Institute; report no. RP-1742.
- Ramanathan, V.; Callis, L.; Cess, R.; Hansen, J.; Isaksen, I.; Kuhn, W.; Lacis, A.; Luther, F.; Mahlman, J.; Reck, R.; Schlesinger, M. (1987) Climate-chemical interactions and effects of changing atmospheric trace gases. *Rev. Geophys.* 25: 1441-1482.
- Ramanathan, V.; Subasilar, B.; Zhang, G. J.; Conant, W.; Cess, R. D.; Kiehl, J. T.; Grassl, H.; Shi, L. (1995) Warm pool heat budget and shortwave cloud forcing: a missing physics? *Science (Washington, DC)* 267: 499-503.
- Randall, D. A.; Coakley, J. A., Jr.; Fairall, C. W.; Kropfli, R. A.; Lenschow, D. H. (1984) Outlook for research on subtropical marine stratiform clouds. *Bull. Am. Meteorol. Soc.* 65: 1290-1301.
- Reisinger, L. M.; Valenti, R. J. (1984) Visibility and air quality impairment in the southeastern United States - 1983. Presented at: 77th annual meeting of the Air Pollution Control Association; paper no. 84-59.3.
- Reisinger, L. M.; Valente, R. J. (1985) Visibility and other air quality measurements made at the Great Smoky Mountains National Park. Muscle Shoals, AL: Tennessee Valley Authority; TVA/ON RED AWR -86/6.
- Richards, L. W. (1973) Size distribution of pigment particles: measurement and characterization by light-scattering techniques. In: Patton, T. C., ed. *Pigment handbook: volume III, characterization and physical relationships*. New York NY: John Wiley & Sons; pp. 89-100.
- Richards, L. W. (1988) Sight path measurements for visibility monitoring and research. *JAPCA* 38: 784-791.
- Richards, L. W. (1989) Atmospheric light transmittance and path radiance measurements during the southern California air quality study. Presented at: Air & Waste Management Association 82nd annual meeting; June; Anaheim, CA. Pittsburgh, PA: Air & Waste Management Association; paper no. 89-154.6.
- Richards, L. W. (1990) Effect of the atmosphere on visibility. In: Mathai, C. V., ed. *Visibility and fine particles: an A&WMA/EPA international specialty conference; October 1989; Estes Park, CO*. Pittsburgh, PA: Air & Waste Management Association; pp. 261-270. (A&WMA transactions series no. TR-17).
- Richards, L. W. (1994) Recommendations for monitoring the effects of air quality on visibility. In: *Proceedings of the international specialty conference, aerosols and atmospheric optics: radiative balance and visual air quality, v. A; September; Showbird, UT*. Pittsburgh, PA: Air & Waste Management Association; pp. 6-15.
- Richards, L. W.; Anderson, J. A.; Blumenthal, D. L.; Brandt, A. A.; McDonald, J. A.; Waters, N.; Macias, E. S.; Bhardwaja, P. S. (1981) The chemistry, aerosol physics, and optical properties of a western coal-fired power plant plume. *Atmos. Environ.* 15: 2111-2134.

- Richards, L. W.; Anderson, J. A.; Blumenthal, D. L.; McDonald, J. A.; Kok, G. L.; Lazrus, A. L. (1983) Hydrogen peroxide and sulfur (IV) in Los Angeles cloud water. *Atmos. Environ.* 17: 911-914.
- Richards, L. W.; Bergstrom, R. W., Jr.; Ackerman, T. P. (1986) The optical effects of fine-particle carbon on urban atmospheres. *Atmos. Environ.* 20: 387-396.
- Richards, L. W.; Blanchard, C. L.; Blumenthal, D. L. (1991) Navajo generating station visibility study, draft #2. Santa Rosa, CA: Sonoma Technology, Inc.; final report STI-90200-1124-FRD2.
- Richards, L. W.; Prouty, J. D.; Stoelting, M.; Korc, M. E.; Jones, C. M. (1995) Visual impact analysis of the plume from the Owens Lake Soda Ash Company soda ash mining and processing project on nearby Class I areas. San Mateo, CA: MHA Environmental Consulting, Inc.; final report no. STI-94490-1445-FR.
- Robock, A. (1988) Enhancement of surface cooling due to forest fire smoke. *Science (Washington, DC)* 242: 911-913.
- Robock, A. (1991) Surface cooling due to forest fire smoke. *J. Geophys. Res. [Atmos.]* 96: 20,869-20,878.
- Rood, M. J.; Shaw, M. A.; Larson, T. V.; Covert, D. S. (1989) Ubiquitous nature of ambient metastable aerosol. *Nature (London)* 337: 537-539.
- Rosen, H.; Hansen, A. D. A.; Gundel, L.; Novakov, T. (1978) Identification of the optically absorbing component in urban aerosols. *Appl. Opt.* 17: 3859-3861.
- Rosen, H.; Novakov, T.; Bodhaine, B. A. (1981) Soot in the Arctic. Presented at: the second symposium on Arctic air chemistry; May 1980; Kingston, RI. *Atmos. Environ.* 15: 1371-1374.
- Ross, D. M.; Malm, W. C.; Loomis, R. J. (1987) An examination of the relative importance of park attributes at several national parks. In: Bhardwaja, P. S., ed. *Visibility protection: research and policy aspects, an APCA international specialty conference; September 1986; Grand Teton National Park, WY.* Pittsburgh, PA: Air Pollution Control Association; pp. 304-319. (APCA transactions series no. TR-10).
- Rossow, W. B.; Schiffer, R. A. (1991) ISCCP cloud data products. *Bull. Am. Meteorol. Soc.* 72: 2-20.
- Rowe, R. D.; Chestnut, L. G. (1982) *The value of visibility: economic theory and applications for air pollution control.* Cambridge, MA: Abt Books.
- Ruby, M. G.; Waggoner, A. P. (1981) Intercomparison of integrating nephelometer measurements. *Environ. Sci. Technol.* 15: 109-113.
- Saxena, P.; Hildemann, L. M.; McMurry, P. H.; Seinfeld, J. H. (1995) Organics alter hygroscopic behavior of atmospheric particles. *J. Geophys. Res. [Atmos.]*: in press.
- Schneider, S. H.; Thompson, S. L. (1988) Simulating the climatic effects of nuclear war. *Nature (London)* 333: 221-227.
- Schnell, R. C. (1984) Arctic haze: editorial. *Geophys. Res. Lett.* 11: 359.
- Schoeberl, M. R.; Bhartia, P. K.; Hilsenrath, E. (1993) Tropical ozone loss following the eruption of Mt. Pinatubo. *Geophys. Res. Letters* 20: 29-32.
- Schulze, W. D.; Brookshire, D. S.; Walther, E. G.; MacFarland, K. K.; Thayer, M. A.; Whitworth, R. L.; Ben-David, S.; Malm, W.; Molenar, J. (1983) The economic benefits of preserving visibility in the national parklands of the southwest. *Nat. Resour. J.* 23: 149-173.

- Schwartz, S. E. (1988) Are global cloud albedo and climate controlled by marine phytoplankton? *Nature (London)* 336: 441-445.
- Seigneur, C.; Johnson, C. D.; Latimer, D. A.; Bergstrom, R. W.; Hogo, H. (1983) User's manual for the plume visibility model (PLUVUE II). San Rafael, CA: Systems Applications, Inc.; report no. SYSAPP-83/221.
- Seigneur, C.; Johnson, C. D.; Latimer, D. A.; Bergstrom, R. W.; Hogo, H. (1984) User's manual for the plume visibility model (PLUVUE II). Research Triangle Park, NC: U.S. Environmental Protection Agency, Environmental Sciences Research Laboratory; EPA report no. EPA-600/8-84-005. Available from: NTIS, Springfield, VA; PB84-158302.
- Shah, J. J.; Watson, J. G., Jr.; Cooper, J. A.; Huntzicker, J. J. (1984) Aerosol chemical composition and light scattering in Portland, Oregon: the role of carbon. *Atmos. Environ.* 18: 235-240.
- Shah, J. J.; Johnson, R. L.; Heyerdahl, E. K.; Huntzicker, J. J. (1986) Carbonaceous aerosol at urban and rural sites in the United States. *J. Air Pollut. Control Assoc.* 36: 254-257.
- Shaw, G. E. (1983) Bio-controlled thermostasis involving the sulfur cycle. *Clim. Change* 5: 297-303.
- Shaw, R. W., Jr.; Paur, R. J. (1983) Measurements of sulfur in gases and particles during sixteen months in the Ohio River Valley. *Atmos. Environ.* 17: 1431-1438.
- Sisler, J. F.; Huffman, D.; Lattimer, D. A.; Malm, W. C.; Pitchford, M. L. (1993) Spatial and temporal patterns and the chemical composition of the haze in the United States: an analysis of data from the IMPROVE network, 1988-1991. Fort Collins, CO: Colorado State University, Cooperative Institute for Research in the Atmosphere (CIRA).
- Sloane, C. S. (1982a) Visibility trends—I. methods of analysis. *Atmos. Environ.* 16: 41-51.
- Sloane, C. S. (1982b) Visibility trends—II. mideastern United States 1948-1978. *Atmos. Environ.* 16: 2309-2321.
- Sloane, C. S. (1983) Summertime visibility declines: meteorological influences. *Atmos. Environ.* 17: 763-774.
- Sloane, C. S. (1986) Effect of composition on aerosol light scattering efficiencies. *Atmos. Environ.* 20: 1025-1037.
- Sloane, C. S.; White, W. H. (1986) Visibility: an evolving issue. *Environ. Sci. Technol.* 20: 760-766.
- Sloane, C. S.; Wolff, G. T. (1984) Relating ambient visibilities to aerosol composition. Presented at: 77th annual meeting of the Air Pollution Control Association; June; San Francisco, CA; Pittsburgh, PA: Air Pollution Control Association; paper no. 84-115.1.
- Sloane, C. S.; Wolff, G. T. (1985) Prediction of ambient light scattering using a physical model responsive to relative humidity: validation with measurements from Detroit. *Atmos. Environ.* 19: 669-680.
- Spengler, J. D.; Thurston, G. D. (1983) Mass and elemental composition of fine and coarse particles in six U.S. cities. *J. Air Pollut. Control Assoc.* 33: 1162-1171.
- Stephens, G. L. (1994) Remote sensing of the lower atmosphere: an introduction. New York, NY: Oxford University Press; p. 214.
- Stevens, R. K.; Dzubay, T. G.; Russwurm, G.; Rickel, D. (1978) Sampling and analysis of atmospheric sulfates and related species. *Atmos. Environ.* 12: 55-68.
- Stevens, R. K.; Dzubay, T. G.; Shaw, R. W., Jr.; McClenny, W. A.; Lewis, C. W.; Wilson, W. E. (1980) Characterization of the aerosol in the Great Smoky Mountains. *Environ. Sci. Technol.* 14: 1491-1498.

- Stevens, R. K.; Dzubay, T. G.; Lewis, C. W.; Shaw, R. W., Jr. (1984) Source apportionment methods applied to the determination of the origin of ambient aerosols that affect visibility in forested areas. *Atmos. Environ.* 18: 261-272.
- Tang, I. N. (1980) Deliquescence properties and particle size change of hygroscopic aerosols. In: Willeke, K., ed. *Generation of aerosols and facilities for exposure experiments*. Ann Arbor, MI: Ann Arbor Science; pp. 153-167.
- Tang, I. N.; Wong, W. T.; Munkelwitz, H. R. (1981) The relative importance of atmospheric sulfates and nitrates in visibility reduction. *Atmos. Environ.* 15: 2463-2471.
- Taylor, K. E.; Penner, J. E. (1994) Response of the climate system to atmospheric aerosols and greenhouse gases. *Nature (London)* 369: 734-737.
- Thompson, S. L.; Ramaswamy, V.; Covey, C. (1987) Atmospheric effects of nuclear war aerosols in general circulation model simulations: influence of smoke optical properties. *J. Geophys. Res. [Atmos.]* 92: 10,942-10,960.
- Tolley, G. A.; Randall, A.; Blomquist, G.; Fabian, R.; Fishelson, G.; Frankel, A.; Hoehn, J.; Krumm, R.; Mensah, E.; Smith, T. (1986) *Establishing and valuing the effects of improved visibility in eastern United States*. Washington, DC: U.S. Environmental Protection Agency.
- Tombach, I.; Allard, D. (1983) *Comparison of visibility measurement techniques: eastern United States*. Palo Alto, CA: Electric Power Research Institute; EPRI report no. EA-4903.
- Toon, O. B.; Ackerman, T. P. (1981) Algorithms for the calculation of scattering by stratified spheres. *Appl. Opt.* 20: 3657-3660.
- Toon, O. B.; Pollack, J. B. (1976) A global average model of atmospheric aerosols for radiative transfer calculations. *J. Appl. Meteorol.* 15: 225-246.
- Trijonis, J. (1979) Visibility in the southwest—an exploration of the historical data base. *Atmos. Environ.* 13: 833-843.
- Trijonis, J. (1982a) Existing and natural background levels of visibility and fine particles in the rural East. *Atmos. Environ.* 16: 2431-2445.
- Trijonis, J. (1982b) Visibility in California. *J. Air Pollut. Control Assoc.* 32: 165-169.
- Trijonis, J.; Yuan, K. (1978) *Visibility in the southwest: an exploration of the historical data base*. Research Triangle Park, NC: U.S. Environmental Protection Agency, Environmental Sciences Research Laboratory; EPA report no. EPA-600/3-78-039. Available from: NTIS, Springfield, VA; PB-282942.
- Trijonis, J.; Thayer, M.; Murdoch, J.; Hagemen, R. (1984) *Air quality benefits analysis for Los Angeles and San Francisco based on housing values and visibility*. Sacramento, CA: California Air Resources Board.
- Trijonis, J.; Thayer, M.; Murdoch, J.; Hageman, R. (1985) *Air quality benefit analysis for Los Angeles and San Francisco based on housing values and visibility*. Final report. Sacramento, CA: California Air Resources Board; report no. ARB/R-85/237. Available from: NTIS, Springfield, VA; PB85-166049.
- Trijonis, J. C.; Pitchford, M.; McGown, M. (1987) Preliminary extinction budget results from the RESOLVE program. In: Bhardwaja, P. S., ed. *Visibility protection: research and policy aspects, an APCA international specialty conference*; September 1986; Grand Teton National Park, WY. Pittsburgh, PA: Air Pollution Control Association; pp. 872-883. (APCA transactions series no. TR-10).
- Trijonis, J. C.; Malm, W. C.; Pitchford, M.; White, W. H. (1991) Visibility: existing and historical conditions—causes and effects. In: Irving, P. M., ed. *Acidic deposition: state of science and technology, volume III: terrestrial*,

- materials, health and visibility effects. Washington, DC: The U.S. National Acid Precipitation Assessment Program. (State of science and technology report no. 24).
- Turco, R. P.; Toon, O. B.; Ackerman, T. P.; Pollack, J. B.; Sagan, C. (1983) Nuclear winter: global consequences of multiple nuclear explosions. *Science* (Washington, DC) 222: 1283-1292.
- Turco, R. P.; Toon, O. B.; Ackerman, T. P.; Pollack, J. B.; Sagan, C. (1990) Climate and smoke: an appraisal of nuclear winter. *Science* (Washington, DC) 247: 166-176.
- Twomey, S. (1974) Pollution and the planetary albedo. *Atmos. Environ.* 8: 1251-1256.
- Twomey, S. (1977) Atmospheric aerosols. Amsterdam, The Netherlands: Elsevier Scientific Publishing Company; p. 237.
- Twomey, S. (1991) Aerosols, clouds and radiation. *Atmos. Environ. Part A* 25: 2435-2442.
- Twomey, S. A.; Piepgrass, M.; Wolfe, T. L. (1984) An assessment of the impact of pollution on global cloud albedo. *Tellus Ser. B* 36B: 356-366.
- U.S. Environmental Protection Agency. (1979) Protecting visibility: an EPA report to Congress. Research Triangle Park, NC: Office of Air Quality Planning and Standards; EPA report no. EPA-450/5-79-008. Available from: NTIS, Springfield, VA; PB80-220320.
- U.S. Environmental Protection Agency. (1982) Air quality criteria for particulate matter and sulfur oxides. Research Triangle Park, NC: Office of Health and Environmental Assessment, Environmental Criteria and Assessment Office; EPA report no. EPA-600/8-82-029aF-cF. 3v. Available from: NTIS, Springfield, VA; PB84-156777.
- U.S. Environmental Protection Agency. (1985) Developing long-term strategies for regional haze: findings and recommendations of the visibility task force. Research Triangle Park, NC.
- U.S. Environmental Protection Agency. (1988) Workbook for plume visual impact screening and analysis. Research Triangle Park, NC: U.S. Environmental Protection Agency; EPA report no. EPA-450/4-88-015. Available from: NTIS, Springfield, VA; PB89-131286.
- U.S. Environmental Protection Agency. (1992) Interagency workgroup on air quality modeling (IWAQM): work plan rationale. Research Triangle Park, NC: Office of Air Quality Planning and Standards; EPA report no. EPA-454/R-92-001.
- U.S. Environmental Protection Agency. (1993a) Air quality criteria for oxides of nitrogen. Research Triangle Park, NC: Office of Health and Environmental Assessment, Environmental Criteria and Assessment Office; EPA report no. EPA/600/8-91/049aF-cF. 3v. Available from: NTIS, Springfield, VA; PB95-124533, PB95-124525, PB95-124517.
- U.S. Environmental Protection Agency. (1993b) Interagency workgroup on air quality modeling (IWAQM): interim recommendation for modeling long range transport and impacts on regional visibility. Research Triangle Park, NC: Office of Air Quality Planning and Standards; EPA report no. EPA-454/R-93-015.
- U.S. Environmental Protection Agency. (1994) A revised user's guide to MESOPUFF II (V5.1). Research Triangle Park, NC: Office of Air Quality Planning and Standards; EPA report no. EPA-454/B-94-025.
- U.S. Environmental Protection Agency. (1995a) Interagency workgroup on air quality modeling (IWAQM): assessment of phase I recommendations regarding the use of MESOPUFF II. Research Triangle Park, NC: Office of Air Quality Planning and Standards; EPA report no. EPA-454/R-95-006.

- U.S. Environmental Protection Agency. (1995b) Testing of meteorological and dispersion models for use in regional air quality modeling. Research Triangle Park, NC: Office of Air Quality Planning and Standards; EPA report no. EPA-454/B-95-005.
- U.S. Environmental Protection Agency. (1995c) A user's guide for the CALMET meteorological model. Research Triangle Park, NC: Office of Air Quality Planning and Standards; EPA report no. EPA-454/B-95-002.
- U.S. Environmental Protection Agency. (1995d) A user's guide for the CALPUFF dispersion model. Research Triangle Park, NC: Office of Air Quality Planning and Standards; EPA report no. EPA-454/B-95-006.
- U.S. Environmental Protection Agency. (1995e) Interim findings on the status of visibility research. Research Triangle Park, NC: Office of Air and Radiation; EPA report no. EPA-600/R-95/021.
- U.S. Naval Oceanographic Office. (1966) Signs of land. Section 2623; p. 660; H. O. publication no. 9.
- Valente, R. J.; Reisinger, L. M. (1983) Data summary: visibility and ambient air quality in the Great Smoky Mountain Park research project. TVA/ONR/AQB-83/4.
- VanCuren, T. (1989a) Instrumental measurement of visibility reducing particles: staff report. Sacramento, Ca: California Air Resources Board, Research Division; January.
- VanCuren, T. (1989b) Instrumental measurement of visibility reducing particles: technical support document. Sacramento, CA: California Air Resources Board, Research Division.
- Vasconcelos, L. A. de P.; Macias, E. S.; White, W. H. (1994) Aerosol composition as a function of haze and humidity levels in the southwestern U.S. *Atmos. Environ.* 28: 3679-3691.
- Vel'tishchev, N. N.; Ginzburg, A. S.; Golitsyn, G. S. (1988) Climatic effects of massive fires. *Izv. Acad. Sci. USSR Atmos. Oceanic Phys. Engl. Transl.* 24: 217-223.
- Veress, S. A. (1972) Extinction coefficient. *Photogramm. Eng.* 38: 183-191.
- Vogelmann, A. M.; Robock, A.; Ellingson, R. G. (1988) Effects of dirty snow in nuclear winter simulations. *J. Geophys. Res. [Atmos.]* 93: 5319-5332.
- Wagener, R.; Schwartz, S. E. (1994) Comparison of seasonal and zonal patterns of the direct and indirect radiative forcing of climate by aerosols. Presented at: International Aerosol Research Assembly and American Association for Aerosol Research fourth international aerosol conference; August-September; Los Angeles, CA.
- Waggoner, A. P.; Weiss, R. E. (1980) Comparison of fine particle mass concentration and light scattering extinction in ambient aerosol. *Atmos. Environ.* 14: 623-626.
- Waggoner, A. P.; Weiss, R. E.; Ahlquist, N. C.; Covert, D. S.; Will, S.; Charlson, R. J. (1981) Optical characteristics of atmospheric aerosols. In: White, W. H.; Moore, D. J.; Lodge, J. P., Jr., eds. *Plumes and visibility: measurements and model components: proceedings of the symposium; November 1980; Grand Canyon National Park, AZ.* *Atmos. Environ.* 15: 1891-1909.
- Waggoner, A. P.; Weiss, R. E.; Ahlquist, N. C. (1983) The color of Denver haze. *Atmos. Environ.* 17: 2081-2086.
- Wall, S. M.; John, W.; Ondo, J. L. (1988) Measurement of aerosol size distributions for nitrate and major ionic species. *Atmos. Environ.* 22: 1649-1656.
- Wallace, J. M.; Hobbs, P. V. (1977) *Atmospheric science: an introductory survey.* New York, NY: Academic Press, Inc.

- Walton, J. J.; MacCracken, M. C.; Ghan, S. J. (1988) A global-scale Lagrangian trace species model of transport, transformation, and removal processes. *J. Geophys. Res. [Atmos.]* 93: 8339-8354.
- Warren, S. G.; Hahn, C. J.; London, J.; Chervin, R. M.; Jenne, R. L. (1988) Global distribution of total cloud cover and cloud type over the ocean. Boulder, CO: DOE report no. DOE/ER-0406; NCAR/TN-317+STR.
- Watson, J. G.; Chow, J. C.; Shah, J. J. (1981) Analysis of inhalable and fine particulate matter measurements. Research Triangle Park, NC: U.S. Environmental Protection Agency, Office of Air Quality Planning and Standards; EPA report no. EPA-450/4-81-035. Available from: NTIS, Springfield, VA; PB83-111336.
- Watson, J. G.; Chow, J. C.; Richards, L. W.; Neff, W. D.; Andersen, S. R.; Dietrich, D. L.; Houck, J. E.; Olney, I. (1988) The 1987-88 metro Denver brown cloud study: v. I, II, III. Reno, NV: Desert Research Institute; final report no. 8810.1F(1-3).
- Watson, J. G.; Chow, J. C.; Richards, L. W.; Haase, D. L.; McDade, C.; Dietrich, D. L.; Moon, D.; Sloane, C. (1991) The 1989-90 Phoenix urban haze study, volume II: the apportionment of light extinction to sources [final report]. Reno, NV: University and Community College System of Nevada, Desert Research Institute; DRI document no. 8931.5F1.
- Weiss, R. E.; Larson, T. V.; Waggoner, A. P. (1982) In situ rapid-response measurement of  $\text{H}_2\text{SO}_4/(\text{NH}_4)_2\text{SO}_4$  aerosols in rural Virginia. *Environ. Sci. Technol.* 16: 525-532.
- Weller, M.; Leiterer, U. (1988) Experimental data on spectral aerosol optical thickness and its global distribution. *Contrib. Atmos. Phys.* 61: 1-9.
- Westphal, D. L.; Toon, O. B. (1991) Simulations of microphysical, radiative, and dynamical processes in a continental-scale forest fire smoke plume. *J. Geophys. Res. [Atmos.]* 96: 22,379-22,400.
- Whitby, K. T.; Husar, R. B.; Liu, B. Y. H. (1972) The aerosol size distribution of Los Angeles smog. *J. Colloid Interface Sci.* 39: 177-204.
- White, W. H. (1975) Estimating the size range of smog aerosol particles with a pair of sunglasses. *Atmos. Environ.* 9: 1036-1037.
- White, W. H. (1986) On the theoretical and empirical basis for apportioning extinction by aerosols: a critical review. *Atmos. Environ.* 20: 1659-1672.
- White, W. H. (1990) The components of atmospheric light extinction: a survey of ground-level budgets. *Atmos. Environ. Part A* 24: 2673-2679.
- White, W. H.; Macias, E. S. (1987) On measurements error and the empirical relationship of atmospheric extinction to aerosol composition in the non-urban west. In: Bhardwaja, P. S., ed. *Visibility protection: research and policy aspects*, an APCA international specialty conference; September 1986; Grand Teton National Park, WY. Pittsburgh, PA: Air Pollution Control Association; pp. 783-794. (APCA transactions series no. TR-10).
- White, W. H.; Macias, E. S. (1990) Light scattering by haze and dust at Spirit Mountain, Nevada. In: Mathai, C. V., ed. *Visibility and fine particles: an A&WMA/EPA international specialty conference*; October 1989; Estes Park, CO. Pittsburgh, PA: Air & Waste Management Association; pp. 914-922. (A&WMA transactions series no. TR-17).
- White, W. H.; Seigneur, C.; Heinold, D. W.; Eltgroth, M. W.; Richards, L. W.; Roberts, P. T.; Bhardwaja, P. S.; Conner, W. D.; Wilson, W. E., Jr. (1985) Predicting the visibility of chimney plumes: an intercomparison of four models with observations at a well-controlled power plant. *Atmos. Environ.* 19: 515-528.

- White, W. H.; Seigneur, C.; Heinold, D. W.; Richards, L. W.; Wilson, W. E.; Roberts, P. T. (1986) Radiative transfer budgets for scattering and absorbing plumes: measurements and model predictions. *Atmos. Environ.* 20: 2243-2257.
- White, W. H.; Macias, E. S.; Nininger, R. C.; Schorran, D. (1994) Size-resolved measurements of light scattering by ambient particles in the southwestern U.S.A. *Atmos. Environ.* 28: 909-921.
- Wigley, T. M. L. (1991) Could reducing fossil-fuel emissions cause global warming? *Nature (London)* 349: 503-506.
- Williams, M. D.; Treiman, E.; Wecksung, M. (1980) Plume blight visibility modeling with a simulated photograph technique. *J. Air Pollut. Control Assoc.* 30: 131-134.
- Williams, M.; Chan, L. Y.; Lewis, R. (1981) Validation and sensitivity of a simulated-photograph technique for visibility modeling. *Atmos. Environ.* 15: 2151-2170.
- Wiscombe, W. J.; Mugnai, A. (1988) Scattering from nonspherical Chebyshev particles. 2: means of angular scattering patterns. *Appl. Opt.* 27: 2405-2421.
- Wolff, G. T.; Countess, R. J.; Groblicki, P. J.; Ferman, M. A.; Cadle, S. H.; Muhlbaier, J. L. (1981) Visibility-reducing species in the Denver "brown cloud"—II. sources and temporal patterns. *Atmos. Environ.* 15: 2485-2502.
- Wolff, G. T.; Kelly, N. A.; Ferman, M. A. (1982) Source regions of summertime ozone and haze episodes in the eastern United States. *Water Air Soil Pollut.* 18: 65-81.
- Wolff, G. T.; Kelly, N. A.; Ferman, M. A.; Morrissey, M. L. (1983) Rural measurements of the chemical composition of airborne particles in the eastern United States. *J. Geophys. Res. C: Oceans Atmos.* 88: 10,769-10,775.
- Wolff, G. T.; Korsog, P. E.; Kelly, N. A.; Ferman, M. A. (1985a) Relationships between fine particulate species, gaseous pollutants and meteorological parameters in Detroit. *Atmos. Environ.* 19: 1341-1349.
- Wolff, G. T.; Korsog, P. E.; Stroup, D. P.; Ruthkosky, M. S.; Morrissey, M. L. (1985b) The influence of local and regional sources on the concentration of inhalable particulate matter in southeastern Michigan. *Atmos. Environ.* 19: 305-313.
- Wysecki, G.; Stiles, W. S. (1967) *Color science: concepts and methods, quantitative data and formulas.* New York, NY: John Wiley & Sons.
- Zhang, X. Q.; McMurry, P. H.; Hering, S. V.; Casuccio, G. S. (1993) Mixing characteristics and water content of submicron aerosols measured in Los Angeles and at the Grand Canyon. *Atmos. Environ. Part A* 27: 1593-1607.
- Zhang, X.; Turpin, B. J.; McMurry, P. J.; Herring, S. V.; Stolzenburg, M. R. (1994) Mie theory evaluation of species contributions to the 1990 wintertime visibility reduction in the Grand Canyon. *J. Air Waste Manage. Assoc.* 44: 153-162.

## **9. EFFECTS ON MATERIALS**

The deposition of airborne particles on the surface of building materials and culturally important articles (e.g., statuary) can cause damage and soiling, thus reducing the life usefulness and aesthetic appeal of such structures (National Research Council, 1979; Baedecker et al., 1991). Furthermore, the presence of particles on surfaces may also exacerbate the physical and chemical degradation of materials that normally occur when these materials are exposed to environmental factors such as wind, sun, temperature fluctuations, and moisture. Beyond these effects, particles, whether suspended in the atmosphere, or already deposited on a surface, also adsorb or absorb acidic gases from other pollutants like sulfur dioxide (SO<sub>2</sub>) and nitrogen dioxide (NO<sub>2</sub>), thus serving as nucleation sites for these gases. The deposition of "acidified" particles on a susceptible material surface is capable of accelerating chemical degradation of the material. Therefore, concerns about effects of particles on materials are relate both to impacts on aesthetic appeal and physical damage to material surfaces, both of which may have serious economic consequences. Insufficient data are available regarding perception thresholds with respect to pollutant concentration, particle size, and chemical composition to determine the relative roles these factors play in contributing to materials damage.

This chapter briefly discusses the effects of particle exposure on the aesthetic appeal and physical damage to different types of building materials. This chapter also discusses the effects of dry deposition of acid forming gases on economically important materials. For more detailed discussion of the effects of acid gases on materials, see the 1991 National Acid Precipitation Assessment Program report (Baedecker et al., 1991).

### **9.1 CORROSION AND EROSION**

#### **9.1.1 Factors Affecting Metal Corrosion**

The mechanisms controlling atmospheric corrosion of metals have been thoroughly discussed in the National Acid Precipitation Assessment Program (Baedecker et al., 1991). In summary, metals undergo corrosion in the absence of pollutant exposure through a series of physical, chemical, and biological interactions involving moisture, temperature, oxygen, and

various types of biological agents. In addition to these environmental factors, atmospheric pollutant exposure may accelerate the corrosion process. Pollutant-induced corrosion arises from complex interactions of the pollutant with the metal surface and the metal corrosion film. In the absence of moisture, there would be limited pollutant-induced or nonpollutant-induced corrosion.

The atmospheric corrosion of most metals is a diffusion-controlled electrochemical process. For an electrochemical reaction to take place, there must exist an electromotive force between points on the metal surface; a mechanism for charge transfer between the electronic conductors; and a conduction path between the cathode and anode reaction centers (Haynie, 1980). The rate of corrosion is still, however, dependent upon the deposition rate and nature of the pollutant (discussed in Chapter 3 of this document); the variability in the electrochemical reactions; the influence of the metal protective corrosion film; the effects of the pollutant coupled with the amount of moisture present (time-of-wetness; relative humidity) (Zhang et al., 1993; Pitchford and McMurry, 1994; Li et al., 1993); the presence and concentration of other surface electrolytes; and the orientation of the metal surface.

The principal form of atmospheric metal corrosion is the uniform corrosion of the metal surface. Other forms of corrosion include pitting, grain-boundary corrosion, and stress-corrosion cracking.

#### **9.1.1.1 Moisture**

The formation of a moisture layer (condensation) on the metal surface is dependent upon precipitation in the form of rain, fog, mist, thawing snow and sleet, and dew. The moisture layer provides a medium for conductive paths for electrochemical reactions and a medium for water soluble air pollutants.

A moisture layer may also form as the result of the reaction of adsorbed water with the metal surface or protective corrosion film, deposited particles and salts from the reaction of the metal surface, and deposited particles with reactive gases. Of particular importance is the production of hydrated corrosion products that increase the absorption rate of moisture. The presence of these hygroscopic salts can drastically decrease the critical relative humidity, resulting in large amounts of moisture on the metal surface.

When the temperature of a metal is below the ambient dew point, water condenses on the metal surface. Whether or not the metal reaches the temperature at which condensation occurs varies with heat transfer between ground and metal and between air and metal. Condensation occurs when the relative humidity adjacent to the surface exceeds a value in equilibrium with the vapor pressure of a saturated solution of whatever salts are on the surface. The solution may contain corrosion products, other hygroscopic contaminants, or both. Temperature, wind, sunshine, and night sky cover then become factors in establishing corrosion rates, since they determine whether there will be sufficient dew condensation.

The first evidence of ambient relative humidity-dependent atmospheric corrosion was demonstrated by Vernon (1931, 1935). Vernon showed a dramatic increase in weight gain in magnesium and iron samples when the relative humidity exceeded certain values (critical relative humidities) in the presence of SO<sub>2</sub>. More recently, researchers have shown particle size related effects based on relative humidity (Pitchford and McMurry, 1994). A more detailed discussion on the water content of atmospheric aerosols and its dependence on relative humidity appears in Chapter 3 of this document.

According to Schwartz (1972), the corrosion rate of a metal could increase by 20% for each increase of 1% in the relative humidity above the critical relative humidity value. It is evident that relative humidity has a considerable influence on the corrosion rate, as established in laboratory trials by Haynie and Upham (1974) and Sydberger and Ericsson (1977). Although these experimental results do not support the exact rate predicted by Schwartz (1972), they do indicate that the corrosion rate of steel increases with increasing relative humidity.

Since average relative humidity is calculated from the relative humidity distribution, an empirical relationship exists between average relative humidity and the fraction of time some "critical humidity value" (minimum concentration of water vapor required for corrosion to proceed) is exceeded, assuming a relatively constant standard deviation of relative humidity (Mansfeld and Kenkel, 1976; Sereda, 1974). The fraction of time that the surface is wet must be zero when the average relative humidity is zero and unity when the average relative humidity is 100%. According to Haynie (1980), the following equation is the simplest single-constant first-order curve that can be fitted to observed data:

$$f = (1 - k)/(100 - k)RH \quad (9-1)$$

where

$f$  = fraction of time relative humidity exceeds the critical value,

$RH$  = average relative humidity, and

$k$  = an empirical constant less than unity.

Haynie (1980) analyzed and fitted, by the least-squares method, ten quarter-year periods of relative humidity data from St. Louis International Airport to this equation. The fraction of time the relative humidity exceeded 90% gave a value of 0.86 for  $k$ . This fraction and the data points are plotted in Figure 9-1.

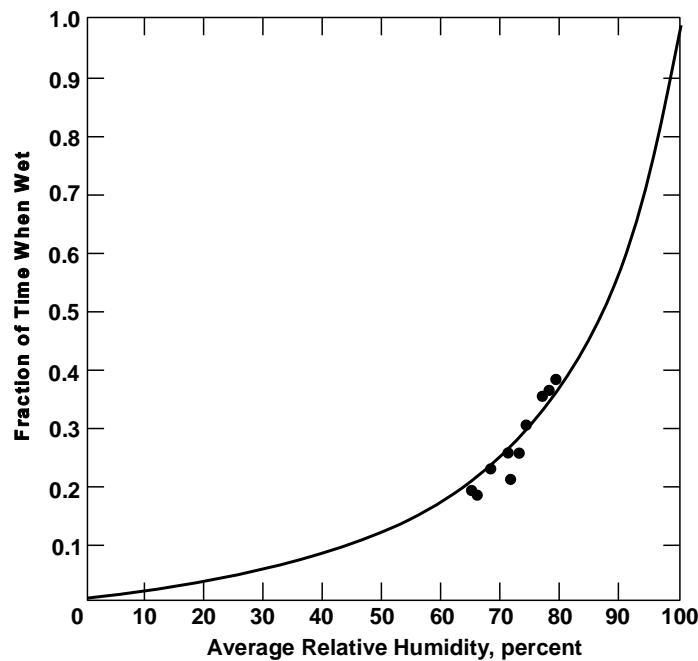


**Figure 9-1. Empirical relationship between average relative humidity and fraction of time when a zinc sheet specimen is wet.**

Source: Haynie (1980).

### *Time-of-Wetness Sensors*

Time-of-wetness sensors, sensors that detect moisture using an electrochemical cell, have been developed to better determine critical relative humidities. The first of these

sensors, developed by Sereda (1958) and Tomashov (1966), measured voltage and current changes across galvanic cells. More recently, Mansfeld and Vijaykumar (1988) reported a technique that uses single metal electrodes for detection of moisture and measurement of the corrosion rate.

Haynie and Stiles (1992) evaluated the Mansfeld type Atmospheric Corrosion Rate Monitor (ACRM) with 19 mo of exposure in an hourly monitored field environment. Duplicate sensors were exposed each at 30° and 90° C. The distribution of measured currents were bimodal for all sensors with definite minimums at around a cell resistance of  $10^{6.5}$  ohms between wet and dry modes. Thus, the sensors can be used to measure time-of-wetness with good reproducibility between sensors exposed at the same time in the same manner. An analysis of variance of the results revealed statistically significant differences between exposure months and angles but not between sensors. Also, there was a significant interaction between month and exposure angle. From these results it was concluded that the sensors are sensitive enough to detect changes with time that are not associated with the primary effects of surface temperature or air moisture content. The magnitude of the dew point/surface temperature difference when a surface becomes wet changes with time, possibly as corrosion products and pollutant concentrations change on the surface. Exposure angle affects time-of-wetness by changing the surface temperature. The surface temperature is related to the relative sun angle and the angle with respect to the night sky. The angle affects radiant heat transfer. This effect was observed as an interaction between seasonal change and exposure angle. Further analysis of the magnitude of the sensor responses when they were wet and comparing the results with weight loss data and model predictions indicated that they were measuring cell resistance rather than polarization resistance (Haynie and Stiles, 1992).

### **9.1.1.2 Temperature**

Few recent studies were found on the effects of temperature on the corrosion process, and earlier studies (Guttman and Sereda, 1968; Barton, 1976; Haynie et al., 1976; Guttman, 1968; Haynie and Upham, 1974; Harker et al., 1980) disagree on the role temperature plays in the rate of corrosion. How temperature affects the corrosion rate of metal was probably best explained by Haynie (1980). He reported that the rate of metal corrosion is diffusion-

controlled, and that under normal temperature conditions, effects on the rate of corrosion would likely not be observed. A decrease in temperature would raise the relative humidity but decrease diffusivity. When the temperature reaches freezing, a decrease in the overall corrosion rate occurs because diffusion has to take place through a solid (Haynie, 1980; Biefer, 1981; Sereda, 1974). Available recent studies on the effects of temperature on metal corrosion are discussed below in various subsections on pollutant-induced corrosion of various specific metals.

### **9.1.1.3 Formation of a Protective Film**

The rust layer on steel is somewhat protective against further corrosion, though far less so than the corrosion layer on zinc and copper. The content of soluble compounds in rust limits its protection of steel. Rust samples analyzed by Chandler and Kilcullen (1968) and Stanners (1970) contained 2 to 2.5% soluble  $\text{SO}_4^{2-}$  and 3 to 6% total  $\text{SO}_4^{2-}$ . The outer rust layer contained a small amount (0.04 to 0.2%) of soluble  $\text{SO}_4^{2-}$ , compared with 2% in the inner rust layer. The concentration of insoluble  $\text{SO}_4^{2-}$  was fairly uniform throughout the rust layers.

The composition of the rust layer has led to studies of the corrosion protective properties of rust as a function of exposure pattern (Nriagu, 1978; Sydberger, 1976). Steel samples initially exposed to low concentrations of sulfur oxides ( $\text{SO}_x$ ) and then moved to sites of higher  $\text{SO}_x$  concentrations corroded at a slower rate than did samples continuously exposed to the higher concentrations. Exposure tests started in summer showed slower corrosion rates during the first years of exposure than those started in winter.

The long-term corrosion rate of steel appears to depend on changes in the composition and structure of the rust layer. During the initiation period, which varies with the  $\text{SO}_2$  concentration and other accelerating factors, the rate of corrosion increases with time (Barton, 1976). Because it is porous and non-adherent, the rust initially formed offers no protection and may accelerate corrosion by retaining hygroscopic sulfates and chlorides, producing a micro-environment with a high moisture content. This is consistent with the concept of sulfate nests discussed by Kucera and Mattsson (1987). After the initiation stage, the corrosion rate decreases as the protective properties of the rust layer improve. Satake and Moroishi (1974) relate this slowing down to a decrease in the porosity of the rust layer.

During a third and final stage, corrosion attains a constant rate and the amount of  $\text{SO}_4^{2-}$  in rust is proportional to atmospheric  $\text{SO}_2$  concentrations. The quantitative determination and subsequent interpretation of corrosion rates becomes difficult if it is not known how long the metal has had a surface layer of electrolyte. Variations in the "wet states" occur with relative humidity, temperature, rain, dew, fog, evaporation, wind, and surface orientation. Capillary condensation in rust can be related to the minimum atmospheric moisture content that allows corrosion to occur (i.e., critical relative humidity). Centers of capillary condensation of moisture on metals can occur in cracks, on dust particles on the metal surface, and in the pores of the rust (Tomashov, 1966).

### 9.1.2 Development of a Generic Dose-Response Function

There are several factors that are important in the corrosion process. First, the rate of corrosion is decreased in the absence of moisture (moisture layer). Secondly, the deposition rate of a pollutant is more important in determining the rate of corrosion than the pollutant concentration. Lastly, the protective corrosion layer may be affected by either dry or wet deposition. A generic semi-theoretical model has been developed that takes into account these factors (Edney et al., 1986; Haynie, 1988; Haynie et al., 1990; and Spence et al., 1992). The model is based on the relative rates of the competing processes of buildup and dissolution of protective corrosion product films. It is a mathematical function that expresses the relationship between corrosion and environmental factors. The general form of the equation is:

$$C = bt_w + a/(Dc/dt_w) \quad (9-2)$$

or a transcendental form:

$$C = bt_w + a(1 - \exp[-Bc/a])/b \quad (9-3)$$

where  $C$  is the amount of corrosion,  $t_w$  is time-of-wetness,  $a$  is a film diffusivity term, and  $b$  is a film dissolution rate. The last two terms are associated with the conditions of the environment and the corrosion product film. For long-term exposures, the exponential term approaches zero and the film reaches a steady state thickness. The equation simplifies to the linear form:

$$C = bt_w + a/b. \quad (9-4)$$

It is in determining the magnitude of the term  $b$  that the effects of pollution on corrosion can be analyzed. More detailed discussion of a generic dose-response function comparing metal corrosion in the absence of pollution and acidic dry deposition of acidic aerosols appears in Baedecker et al. (1991).

### 9.1.3 Studies on Metals

#### 9.1.3.1 Acid-Forming Aerosols

##### *Ferrous Metals*

Ferrous metals include iron, steel, and steel alloys. Stainless steels, incorporating chromium, molybdenum, and nickel, are highly corrosion resistant because of the protective properties of the oxide corrosion film; however, in more polluted areas, the oxide corrosion film becomes less protective. Based on early studies, reported in the National Acid Precipitation Assessment Program report (Baedecker et al., 1991), most steels are susceptible to corrosion from pollutant exposure unless covered by an organic or metallic covering. The rate of corrosion was related to the amount of  $SO_2$  in the atmosphere, showing increasing rates of corrosion with increasing concentrations of  $SO_2$ . The rate of corrosion was also found to depend on the deposition rate of  $SO_2$ .

A recent report by Butlin et al. (1992a) also demonstrated that the corrosion of mild steel and galvanized steel was  $SO_2$ -dependent. These researchers monitored the corrosion of steel samples by  $SO_2$  and ozone ( $O_3$ ) under artificially fumigated environmental conditions, and  $NO_2$  under natural conditions. The natural meteorological conditions of the areas were unaltered. Annual average  $SO_2$  concentrations ranged from  $2.1 \mu\text{g}/\text{m}^3$  in a rural area to  $60 \mu\text{g}/\text{m}^3$  in one of the  $SO_2$ -fumigated locations. Annual average  $NO_2$  concentrations ranged from  $1.5 \mu\text{g}/\text{m}^3$  in the most rural area to  $61.8 \mu\text{g}/\text{m}^3$  in the most polluted area. They found that corrosion of the steel samples was more dependent on the long-term  $SO_2$  concentration and was only minimally affected by nitrogen oxides ( $NO_x$ ).

### ***Aluminum and Aluminum Alloys***

Aluminum is generally considered corrosion resistant, but when exposed to very high SO<sub>2</sub> concentrations and relative humidities above 50%, aluminum will corrode rapidly, forming a hydrated aluminum sulfate. When aluminum is exposed to low concentrations of acid sulfate particles, a protective aluminum oxide film is formed.

Early evaluations of the effects of SO<sub>2</sub> exposure on aluminum indicated that corrosion of aluminum by SO<sub>2</sub> was exposure-dependent and insignificant, based on loss of metal thickness (Haynie, 1976; Fink et al., 1971). However, Haynie (1976) reported SO<sub>2</sub> exposure-related loss in bending strength in the aluminum samples.

In a more recent study, Butlin et al. (1992a) reported that aluminum corrosion was insignificant in SO<sub>2</sub>-spiked environments. The aluminum samples were exposed under natural environmental conditions (29 sites) for up to 2 years. The corrosion was greater and often more patchy on the underside of some of the metal samples. The authors attributed the increased corrosion on the underside of some samples to the lack of pollutant washoff by rain and an increased concentration of particulate matter (dust) in those test areas.

Aluminum alloy 3003-H14 was exposed to various acid forming aerosols and particles as part of the National Acid Precipitation Assessment Program (Baedecker et al., 1991). Aluminum samples were exposed at 5 sites (Newcomb, NY, Chester, NJ, Washington, DC, Steubenville, OH, and Research Triangle Park, NC). Corrosion after 60 mo of exposure, as measured by weight loss, was more than three times greater at the industrial site (NJ) than at rural sites. Particulate matter concentrations ranged from 14 μg/m<sup>3</sup> in NY to 60 μg/m<sup>3</sup> in OH and DC. The concentration ranges for other pollutants at the 5 sites appears in Table 9-1. Even at the industrial site the corrosion rate was very low at a factor of about 10 less than for Galvalume (aluminum-zinc). The exposure time and the average corrosion rate by site is listed in Table 9-2.

### ***Copper and Copper Alloys***

Graedel et al. (1987) studied the chemical composition of patinas exposed in the greater New York area for from 1 to 100 years and compared the results with estimated dry and wet deposition of pollutants between 1886 and 1983. They concluded that the long-term corrosion of copper was not controlled by deposition of pollutants, but rather, it was more

**TABLE 9-1. ANNUAL AVERAGE AND MAXIMUM VALUES OF THE HOURLY AVERAGES FOR SULFUR DIOXIDE (SO<sub>2</sub>), NITROGEN OXIDE (NO<sub>x</sub>), AND OZONE (O<sub>3</sub>) AND ANNUAL AVERAGES OF THE MONTHLY AVERAGES OF RAIN pH AT THE FIVE MATERIAL EXPOSURE SITES, BASED ON DATA ACQUIRED DURING 1986<sup>a</sup>**

Site	SO <sub>2</sub> (ppb)		NO <sub>2</sub> (ppb)		O <sub>3</sub> (ppb)		Particulate Matter (μg/m <sup>3</sup> )	
	Avg.	Max.	Avg.	Max.	Avg.	Max.	Avg.	Avg.
NC	2±4	45	14±9	65	25±21	99	35	4.33
DC	12±9	91	28±12	91	17±16	99	60	4.10
NJ	6±7	87	14±10	98	30±20	114	30	4.16
NY	2±3	29	2±2	21	30±14	99	14	4.28
OH	15±17	450	19±11	98	19±17	94	60	3.90

<sup>a</sup>The ± errors are estimates of one standard deviation on a single hourly average based on the dispersion of the data.

Source: Baedecker et al. (1991).

**TABLE 9-2. AVERAGE CORROSION RATES FOR 3003-H14 ALUMINUM OBTAINED DURING THE NATIONAL ACID PRECIPITATION ASSESSMENT PROGRAM BETWEEN 1982 AND 1987**

Site	Exposure Time (y)	Average Corrosion Rate (μm/y)
NC	5	0.036
DC	5	0.069
NJ	5	0.106
NY	5	0.036
OH	1	0.056

Source: Baedecker et al. (1991).

likely controlled by the availability of copper to react with deposited pollutants. The patina, that is mostly basic sulfate, is not readily dissolved by acids and thus provides significant protection for the substrate metal. However, according to Simpson and Horrobin (1970), the formation of these basic copper salts can take as long as 5 or more years and will vary with the concentration of SO<sub>2</sub> or chloride particles, the humidity, and the temperature.

Butlin et al. (1992a) reported an average rate for copper corrosion of  $1 \pm 0.2 \mu\text{m}/\text{y}$  in 19 of 29 sites evaluated. In areas where there was above average  $\text{SO}_2$ , mass loss ranged from 1.5 to  $1.75 \mu\text{m}/\text{y}$ . The lowest recorded mass loss was  $0.66 \mu\text{m}/\text{y}$  in an area with low precipitation and low  $\text{SO}_2$ . The maximum pit depth over a 2-year period was  $63 \mu\text{m}$ .

Meakin et al. (1992) reported on the atmospheric degradation of monumental bronzes. They measured ion concentrations in rain run off from brigade markers at the Gettysburg National Military Park as well as rain samples. There was a very strong correlation between copper and sulfate ions with a regression coefficient not significantly different from the stoichiometric value for cupric sulfate. There appeared to be little correlation between the acidity of the run off and the acidity of the rain fall on the markers. Dry deposition between rain events was concluded to dominate the soluble corrosion of the bronze.

Because of the complexity of the patina formation, few damage functions have been reported and most of those that have been reported were based on short-term data when the patina had not developed. Corrosion rates of  $0.5$  to  $1 \mu\text{m}/\text{y}$  have been predicted by these equations. However, the values greatly over estimate long-term damage and would be misleading in an economic assessment.

Although limited to 5 years of exposure, the National Acid Precipitation Assessment Program study (Baedecker et al., 1991; Cramer et al., 1989) may be useful in evaluating the affects of  $\text{SO}_2$  on copper because it analyzed 110 Cu soluble corrosion data with components of the previously discussed generic damage function. The average total corrosion rate between 3 and 5 years was about  $1 \mu\text{m}/\text{y}$  but the soluble portion was less than a third of that which could be statistically attributed to  $\text{SO}_2$ . The resulting coefficient for the product of  $\text{SO}_2$  times the time-of-wetness was  $0.18 \text{ cm}/\text{s}$  which has the units of a deposition velocity. This term may be multiplied by a stoichiometric conversion factor to get a corrosion rate. With  $\text{SO}_2$  expressed in  $\text{mg}/\text{m}^3$  and time-of-wetness in years, the conversion factor for  $\mu\text{m}/\text{y}$  of Cu to cupric sulfate is  $0.035$ . The coefficient is  $0.0063$  and for an average concentration of  $20 \text{ mg}/\text{m}^3$  of  $\text{SO}_2$  the resulting corrosion rate is  $0.126 \mu\text{m}/\text{y}$  of wetness. If the surface is wet only a quarter of the time, the corrosion rate attributable to  $\text{SO}_2$  is around  $0.03 \mu\text{m}/\text{y}$ . If the patina color has aesthetic value, and  $\text{SO}_2$  accelerates the formation, then, in the case of Cu, the presence of  $\text{SO}_2$  may be beneficial.

### ***Zinc and Galvanized Steel***

In the presence of moisture and oxygen, zinc will form an initial corrosion product of zinc hydroxide. Carbon dioxide (CO<sub>2</sub>) in the atmosphere further reacts with this film to form basic zinc carbonates. This corrosion product is insoluble in neutral environments but dissolves in both strong acids and strong bases. Zinc is electrochemically more active than iron. Coating steel with zinc provides a protection to the steel substrate against atmospheric corrosion.

Many studies conducted on the corrosive properties of zinc and zinc products are extensively evaluated in the National Acid Precipitation Assessment Program report (Baedecker et al., 1991). Two of the studies, conducted over a 20-year period, showed zinc corrosion rates of 0.22 to 7.85  $\mu\text{m}/\text{y}$  from 1931 to 1951 and 0.6 to 3.6  $\mu\text{m}/\text{y}$  from 1957 to 1977 (Anderson, 1956; Showak and Dunbar, 1982). State College, PA was the only site common to both studies. The corrosion rates were 1.13 and 1.2  $\mu\text{m}/\text{y}$ .

Harker et al. (1980) examined the variables controlling the corrosion of zinc by SO<sub>2</sub> and sulfuric acid (H<sub>2</sub>SO<sub>4</sub>). Experimental conditions were selected from the following ranges:

Temperature	12 to 20 °C
Relative humidity	65 to 100%
Mean flow velocity	0.5 to 8 m/s
Sulfur dioxide concentration	46 to 216 ppb
Sulfate aerosol mass concentration	1.2 mg/m <sup>3</sup>
Aerosol size distribution	0.1 to 1.0 $\mu\text{m}$

The factors controlling the rate of corrosion were found to be relative humidity, pollutant flux, and the chemical form of the pollutant. Corrosion occurred only when the relative humidity was greater than 60%. The deposition velocities were 0.07 cm/s for 0.1 to 1.0 ppm H<sub>2</sub>SO<sub>4</sub> aerosols and 0.93 cm/s for SO<sub>2</sub> at a friction velocity of 35 cm/s. The results indicate that SO<sub>2</sub>-induced corrosion of zinc proceeds at a rate approximately a factor of two greater than that for the equivalent amount of deposited H<sub>2</sub>SO<sub>4</sub> aerosol. Temperature did not appear to be a controlling factor within the range 12 to 20 °C.

Edney et al. (1986) conducted controlled environmental chamber experiments on unexposed galvanized steel panels to determine the rate at which SO<sub>2</sub> deposits to fresh test panels and the fate of the deposited compound. During exposure, dew was periodically produced on some of the panels. After exposure, samples were washed with sprays of different pH levels to simulate acidic wet deposition. The runoff samples were analyzed for corrosion product ions.

In the absence of dew, deposited SO<sub>2</sub> was absorbed. With dew present, the absorption rate increased substantially. At a chamber flow rate of 3 m/s, the flux of SO<sub>2</sub> to the panel surfaces was directly proportional to the air concentration and the regression slope represents a deposition velocity of 0.9 cm/s. A linear regression slope between zinc and sulfate in the runoff was 1.06, which is consistent with a stoichiometric reaction.

The National Acid Precipitation Assessment Program (Baedecker et al., 1991; Cramer et al., 1989) included zinc and galvanized steel panels in its field exposure experiments in Newcomb, NY, Newark, NJ, Washington, DC, Research Triangle Park, NC, and Steubenville, OH. The NC and OH sites were the only two of the 5 sites that had covers and spray devices set up to separate the effects of wet and dry deposition of pollutants. Air quality, meteorological parameters, and rain chemistry were determined at all sites. Runoff samples were collected and analyzed for both ambient rain and the deionized water spray.

In general, the rolled zinc corrosion rates were larger than those found for the galvanized steel panels, most likely because of a protective chromate treatment that had been factory applied to the galvanized steel. The deposition of SO<sub>2</sub> was one of several corrosion contributing factors. The concentrations of SO<sub>2</sub> at the different sites varied by as much as a factor of 10, but the corrosion rates were within a factor of 2 (see Table 9-3). Pollutant concentrations at the 5 exposure sites appear in Table 9-1.

At the NC and OH sites, exposed samples of both zinc and galvanized steel corroded more than similar samples exposed to the clean simulated rain. Although SO<sub>2</sub> levels were higher at the OH site, the deionized water spray samples corroded about the same at both sites. This result, together with high levels of particles at the industrial OH site, may indicate that much of the deposited SO<sub>2</sub> was neutralized by dry deposited alkaline particles.

Cramer et al. (1989) did a preliminary analysis of the soluble fraction of the total zinc corrosion with respect to the model of the generic damage function. The multiple regression

**TABLE 9-3. AVERAGE CORROSION RATES FOR ROLLED ZINC AND GALVANIZED STEEL OBTAINED DURING THE NATIONAL ACID PRECIPITATION ASSESSMENT PROGRAM FIELD EXPERIMENTS**

Site	Exposure Time (y)	Average Corrosion Rate ( $\mu\text{m}/\text{y}$ )	
		Rolled Zinc	Galvanized Steel
NC	5	0.81	0.73
DC	5	1.27	0.71
NJ	5	1.32	0.99
NY	5	0.63	0.63
OH	1	1.33	0.99

Source: Baedecker et al. (1991)

analysis gave significant coefficients for  $\text{SO}_2$ , hydrogen ions ( $\text{H}^+$ ), and  $\text{CO}_2$  in precipitation. The coefficient for  $\text{SO}_2$  was not significantly different from stoichiometric for both the rolled zinc and the chromated galvanized steel. Most of the zinc corrosion product was soluble. Haynie et al. (1990) have calculated the solubility of basic zinc carbonate in equilibrium with water containing  $\text{CO}_2$ . Zinc solubility is very temperature dependent due to the strong inverse dependence of  $\text{CO}_2$  solubility in water, leading to increased dissolution of the corrosion products as the ambient temperature decreases.

In the study reported by Butlin et al. (1992a), galvanized steel was found to corrode at a rate of  $1.45 \mu\text{m}/\text{y}$  (high precipitation, low  $\text{SO}_2$ ) to  $4.25 \mu\text{m}/\text{y}$  (high  $\text{SO}_2$ ). Galvanized steel samples from the area of low rainfall and low  $\text{SO}_2$  had a corrosion rate of  $1.53 \mu\text{m}/\text{y}$ . Metallographical evaluation of the galvanized steel samples showed only superficial corrosion with no penetration of the zinc coating.

The various factors that contribute to the corrosion of zinc and galvanized steel are discussed in more detail in terms of the model of the generic damage function in Spence and Haynie (1990), Haynie et al. (1990), and Spence et al. (1992). The combined terms of the long-term form of the model are:

$$\mathbf{C} = \mathbf{F} + \mathbf{C}_d + \mathbf{C}_{RA} + \mathbf{C}_{RC} \quad (9-5)$$

where  $C$  is total corrosion in  $\mu\text{m}$ ,  $F$  is the equivalent thickness of zinc remaining in the insoluble corrosion product film and, at steady state, is equal to  $a/b$ ,  $C_d$  is the corrosion

associated with deposition of SO<sub>2</sub> both in wet and dry periods, and C<sub>RC</sub> is the corrosion due to rain acidity (H<sup>+</sup> and dissolved CO<sub>2</sub>). The SO<sub>2</sub> contribution, C<sub>d</sub>, is expressed as follows:

$$C_d = 0.045 V_d(SO_2)t_w + 1.29 \times 10^{-4} A_r N \quad (9-6)$$

where,

C<sub>d</sub> = zinc corrosion, μm

V<sub>d</sub> = deposition velocity (wind speed, shape, and size dependent), cm/s

SO<sub>2</sub> = ambient SO<sub>2</sub> concentration, mg/m<sup>3</sup>.

A<sub>r</sub> = ratio of actual to apparent surface area

N = number of times surface is dry during the exposure period.

The first additive term represents corrosion from the dry deposition of SO<sub>2</sub> during periods of wetness caused by condensation (dew), and the second term is the corrosion associated with the adsorption of a monolayer of SO<sub>2</sub> during periods of dryness.

In the absence of sufficient data to accurately determine each of the terms, Haynie et al. (1990), and Spence et al. (1992) have applied assumed values for flat galvanized specimens (different sizes), large sheets, and wire with reasonable success. More recently, Cramer and Baker (1993) have applied the generic damage function to predict the expected life of the restored tin plated roof of Monticello. Thus, the model can be used to assess the economic effects of atmospheric corrosion on several metals, especially zinc.

### 9.1.3.2 Particles

Only limited information is available on the effects of particles alone on metals. Goodwin et al. (1969) reported damage to steel, protected with a nylon screen, exposed to quartz particles. The damage did not, however, become substantial until the particle size exceeded 5 μm. Barton (1958) found that dust contributed to the early stages of metal corrosion. The effect of dust was lessened as the rust layer formed. Other early studies also indicated that suspended particles can play a significant role in metal corrosion. Sanyal and Singhania (1956) wrote that particles, along with other cofactors and SO<sub>2</sub>, promoted the corrosion of metals in India. Yocom and Grappone (1976) and Johnson et al. (1977) reported that moist air containing both particles and SO<sub>2</sub> resulted in a more rapid corrosion rate than air polluted with SO<sub>2</sub> alone. Russell (1976) stated that particles serve as points for

the concentration of active ionic species on electrical contact surfaces, thereby increasing the corrosion rate of  $\text{SO}_x$ . However, other studies have not established a conclusive statistical correlation between total suspended particulates (TSP) and corrosion, possibly due to data limitations (Mansfeld, 1980; Haynie and Upham, 1974; and Upham, 1967; Yocom and Upham, 1977).

Edney et al. (1989) reported on the effects of particles,  $\text{SO}_2$ ,  $\text{NO}_x$ , and  $\text{O}_3$  on galvanized steel panels exposed under actual field conditions in Research Triangle Park, NC, and Steubenville, OH, between April 25 and December 28, 1987. The panels were exposed under the following conditions: (1) dry deposition only; (2) dry plus ambient wet deposition; and (3) dry deposition plus deionized water. The average concentrations for  $\text{SO}_2$  (in ppb) and particulate matter (in  $\mu\text{g}/\text{m}^3$ ) was 22 ppb and  $70 \mu\text{g}/\text{m}^3$  and  $<1$  ppb and  $32 \mu\text{g}/\text{m}^3$  for Steubenville and Research Triangle Park, respectively. By analyzing the runoff from the steel panel the authors concluded that the dissolution of the steel corrosion products for both sites was likely the result of deposited gas phase  $\text{SO}_2$  on the metal surface and not particulate sulfate.

Dean and Anthony (1988) investigated the atmospheric corrosion of unstressed wrought aluminum alloys at three sites representing industrial, marine, and coastal-industrial environments. After 10 years of exposure, degradation was measured by several means. They reached the following conclusions: (1) a sooty industrial environment is far more damaging than a warm, salt-laden seacoast atmosphere, (2) by far the most noticeable effect of prolonged atmospheric exposure is loss of ductility in susceptible alloys, and (3) sacrificial cladding completely eliminates ductility loss.

Walton et al. (1982) performed a laboratory study of the direct and synergistic effects of different types of particles and  $\text{SO}_x$  on the corrosion of aluminum, iron, and zinc. The four most aggressive species were salt and salt/sand from marine or deiced locations, ash from iron smelters, ash from municipal incinerators, and coal mine dusts. Fly ashes of various types were less aggressive. Coal ash with  $\text{SO}_x$  did promote corrosion but oil fly ash was relatively noncorrosive. This suggests that catalytic species in the ash promote the oxidation of  $\text{SO}_x$  and the presence of  $\text{SO}_x$  alone is not sufficient to accelerate corrosion. Other laboratory studies of metal corrosion provide considerable evidence that the catalytic effect is not significant and that atmospheric corrosion rates are dependent on the

conductance of the thin-film surface electrolyte and that the first-order effect of contaminant particles is to increase solution conductance, and, hence corrosion rates (Skerry et al., 1988a,b; Askey et al., 1993).

#### **9.1.4 Paints**

Paints, opaque film coatings, are by far the dominant class of manmade materials exposed to air pollutants in both indoor and outdoor environments. Paints are used as decorative coverings and protective coatings against environmental elements on a variety of finishes including woods, metals, cement, asphalt, etc.

Paints primarily consists of two components: the film forming component and the pigments. Paints undergo natural weathering processes from exposure to environmental factors such as sunlight (ultraviolet light), moisture, fungi, and varying temperatures. In addition to the natural weathering from exposure to environmental factors, evidence exists that demonstrates pollutants affect the durability of paint (National Research Council, 1979).

Paint failure may be manifested by two general degradation modes. The first involves the paint surface and includes paint discoloration, chalking, loss of gloss, and erosion. Paint erosion can be measured by loss of thickness of the paint layer. The second is degradation at the paint/substrate interface, which can be manifested as loss of adhesion leading to blistering and peeling.

In paint formulas, the ratio of pigments to film formers is important to the overall properties of gloss, hardness, and permeability to water. If the amount of film former is too low, soiling is increased and the paint may lose the film flexibility needed for durability and become brittle.

##### **9.1.4.1 Acid-Forming Aerosols**

Paint films permeable to water are also susceptible to penetration by  $\text{SO}_2$  and  $\text{SO}_4^{2-}$  aerosols. Baedecker et al. (1991) reviewed about twenty papers (1958 to 1985) dealing with solubility and permeability of  $\text{SO}_2$  in paints and polymer films. Permeation and adsorption rates varied by as much as several orders of magnitude depending on formulation. They concluded that unpigmented polymer films have a large range of permeabilities but that the polymers used in paint formulations generally do not form barriers to  $\text{SO}_2$  either in the

gaseous state or in solution as sulfurous acid. Although 20% of the absorbed SO<sub>2</sub> was retained in alkyd/melamine and epoxide films and probably reacted with the polymer, there appears to be little degradation to the polymer itself from SO<sub>2</sub> at low concentrations. Absorption is inhibited by pigments; those pigments that can catalyze the oxidation of SO<sub>2</sub> and scavenge the resulting sulfate ions can limit the penetration even more than can typical pigments.

Concentrations of SO<sub>2</sub> found in fog or near industrial sites can increase the drying and hardening times of certain kinds of paints. Holbrow (1962) found that the drying time of linseed, tung, and certain castor oil paint films increased by 50 to 100% on exposure to 2,620 to 5,240 μg/m<sup>3</sup> (1 to 2 ppm) SO<sub>2</sub>. The touch-dry and hard-dry times of alkyl and oleoresinous paints with titanium dioxide pigments were also reported to increase substantially; however, the exposure time of the wet films was not reported. Analysis of the dried films indicated that SO<sub>2</sub> chemically reacted with the drying oils, altering the oxidation-polymerization process. No studies have been reported on the effects of SO<sub>2</sub> on the drying of latex paints.

Spence et al. (1975) conducted a controlled exposure study to determine the effects of gaseous pollutants on four classes of exterior paints: oil-base house paint, vinyl-acrylic latex house paint, and vinyl and acrylic coil coatings for metals. The house paints were sprayed on aluminum panels. The coil coating panels were cut from commercially painted stock. Recorded paint thickness was oil-base paint film, 58 μm; acrylic latex, 45 μm; vinyl coil coating, 27 μm; and acrylic coil coating, 20 μm. Temperature, humidity, and SO<sub>2</sub>, (78.6 and 1,310 μg/m<sup>3</sup>), NO<sub>2</sub> (94 and 940 μg/m<sup>3</sup>), and O<sub>3</sub> (156.8 and 980 μg/m<sup>3</sup>) exposures were controlled. Each exposure chamber had a xenon arc lamp to provide ultraviolet radiation. A dew/light cycle was included; light exposure time was followed by a dark period during which coolant circulated through racks holding the specimens, thereby forming dew on the panels. Each dew/light cycle lasted 40 min and consisted of 20 min of darkness with formation of dew, followed by 20 min under the xenon arc. The total exposure time was 1,000 h. Damage was measured after 200 h, 500 h, and 1,000 h by loss of both weight and film thickness. In evaluating the data, loss of weight was converted to equivalent loss of film thickness.

Visual examination of the panels coated with oil-base house paint revealed that all exposure conditions caused considerable damage. The erosion rate varied from 28.3 to 79.14  $\mu\text{m}/\text{y}$ , with an average of 60  $\mu\text{m}/\text{y}$ . The investigators concluded that  $\text{SO}_2$  and relative humidity markedly affected the rate of erosion of oil-base house paint. The presence of  $\text{NO}_2$  increased the weight of the paint film. A multiple linear regression on  $\text{SO}_2$  concentration and relative humidity yielded the following relation:

$$E = 14.3 + 0.0151 \text{SO}_2 + 0.388 \text{RH} \quad (9-7)$$

where

E = erosion rate in  $\mu\text{m}/\text{y}$ ,

$\text{SO}_2$  = concentration of  $\text{SO}_2$  in  $\mu\text{g}/\text{m}^3$ , and

RH = relative humidity in percent.

The authors reported the 95% tolerance limits on 99% of the calculated rates to be  $\pm 44 \mu\text{m}/\text{y}$ .

Blisters formed on the acrylic latex house paint at the high  $\text{SO}_2$  levels. The blisters resulted from severe pitting and buildup of aluminum corrosion products on the substrate. The paint acted as a membrane retaining moisture under the surface and excluding oxygen that would passivate the aluminum. The vinyl coating and the acrylic coating are resistant to  $\text{SO}_2$ . The visual appearance of the vinyl coil coating showed no damage. The average erosion rate was low, 3.29  $\mu\text{m}/\text{y}$ . The average erosion rate for a clean air exposure was 1.29  $\mu\text{m}/\text{y}$ . The acrylic coil coating showed an average erosion rate of 0.57  $\mu\text{m}/\text{y}$  (Spence et al., 1975).

A study of the effects of air pollutants on paint, under laboratory controlled conditions, was conducted by Campbell et al. (1974). The paints studied included oil and acrylic latex house paints, a coil coating, automotive refinish, and an alkyd industrial maintenance coating. These coatings were exposed to clean air,  $\text{SO}_2$  at 262 and 2,620  $\mu\text{g}/\text{m}^3$ , and  $\text{O}_3$  at 196 and 1,960  $\mu\text{g}/\text{m}^3$ . Light, temperature, and relative humidity were controlled. In addition, one-half of the coatings were shaded during the laboratory exposures. Similar panels (half facing north) were exposed at field sites in Leeds, ND; Valparaiso, IN; Research Center, Chicago, IL; and Los Angeles, CA.

The laboratory exposure chamber operated on a 2-h light-dew cycle (i.e., 1 h of xenon light at 70% relative humidity and a temperature of 66 °C followed by 1 h of darkness at 100% relative humidity and a temperature of 49 °C). Coating erosion rates were calculated after exposure periods of 400, 700, and 1,000 h. Erosion rates for samples exposed to the lowest exposure concentrations were not significantly different from values for clean air exposures due to the high variability of the data. The erosion rates on the shaded specimens were significantly less than the unshaded panel results; panels facing north were also less eroded. At the highest exposure concentrations, erosion rates were significantly greater than controls for both pollutants, with oil-base house paint experiencing the largest erosion rate increases, latex and coil coatings moderate increases, and the industrial maintenance coating and automotive refinish the smallest increases (Yocom and Grappone, 1976; Yocom and Upham, 1977; and Campbell et al., 1974). Coatings that contained extender pigments, particularly calcium carbonate ( $\text{CaCO}_3$ ), showed the greatest erosion rates from the  $\text{SO}_2$  exposures. Results of field exposures also support these conclusions (Campbell et al., 1974).

Haynie and Spence (1984) evaluated data on two house paints that were exposed for up to 30 mo at 9 environmental monitoring sites in the St. Louis, MO area. The paints were formulated with and without  $\text{CaCO}_3$  and applied to stainless steel panels. Multiple regression analysis of mass loss versus the environmental variables revealed no statistical differences associated with  $\text{SO}_2$ .

Hendricks and Balik (1990) evaluated the effects of  $\text{SO}_2$  on free films of paint and the latex polymer for one of the paints and established diffusion coefficients for  $\text{SO}_2$  in the various formulations. Pigments, as well as fillers such as  $\text{CaCO}_3$ , were found to decrease the diffusion coefficient. A latex polymer desorbed all  $\text{SO}_2$  when placed in a vacuum but an alkyd retained approximately 15 to 20%  $\text{SO}_2$  even after several days. Xu and Balik (1989, 1990) concluded that the gas had reacted with the polymer in the paint. They also determined quantitatively the rate of  $\text{CaCO}_3$  removal from paints exposed to different pH levels of sulfurous acid or distilled water (weak carbonic acid). The rates of dissolution were dependent on acid strength but removal was complete for all acids. The mass loss was 27%. A similar paint without  $\text{CaCO}_3$  lost only 7%.

Patil et al. (1990) reported that certain combinations of  $\text{SO}_2/\text{H}_2\text{O}/\text{UV}$  light (high  $\text{SO}_2$  levels) had detrimental effects when they were evaluating various techniques for measuring

film degradation. Mechanical properties were dominated by cross-linking. While SO<sub>2</sub> had little effect when dry, there was considerable chain scissioning when exposed wet. Sanker et al. (1990) found that after exposing the polymer to SO<sub>2</sub>/UV light that there was a decrease in carbonyl signal associated with the acrylate group, whereas no decrease in carbonyl signal was associated with samples exposed to UV light alone. They reported a synergistic effect on polymer degradation between UV light and SO<sub>2</sub> under both wet and dry conditions.

Edney (1989) and Edney et al. (1988, 1989) measured the chemical composition of runoff from painted red cedar and zinc panels exposed at field sites in Raleigh, NC, and Steubenville, OH, and in controlled chambers. Acidic gases such as SO<sub>2</sub> and nitric acid dissolved alkaline (CaCO<sub>3</sub> or ZnO) components in the paint.

Williams et al. (1987) demonstrated that weathering of wood prior to painting decreases the adhesion of paint. Significant decreases in paint adhesion were noted in panels weathered for 4 weeks and those weathered for 16 weeks had about a 50% decrease in adhesive strength. In similar studies, it was shown that acid treatment of specimens during weathering increased the rate of surface deterioration; the rate of wood weathering increased by as much as 50% when it was exposed to sulfurous, sulfuric, or nitric acids (Williams, 1987, 1988).

As part of the National Acid Precipitation Assessment Program, Davis et al. (1990) studied the effects of SO<sub>2</sub> on oil/alkyd systems on steel using a custom designed exposure chamber in which a dew cycle could be simulated. Energy dispersive X-ray microscopy scans were made across primer/paint cross-sections. Samples were exposed to 1 ppm SO<sub>2</sub> at 90 to 95% relative humidity, and thermally cycled (12-h dew cycle followed by 12-h drying period) or the chamber was maintained at a constant temperature. Controls were exposed under similar conditions but without SO<sub>2</sub>. All samples gained weight after 7 days of exposure. The greatest weight gain was noted in the cyclic samples (30 to 40% more than those samples maintained under constant temperatures). After 28 days to cyclic (dew/drying) conditions samples exposed to SO<sub>2</sub> had rusted scribe marks while the controls showed only light rust.

As the specimens were exposed in the chamber, the tensile strength decreased significantly and the locus of failure shifted from within the coating system to the primer-metal interface. The relationship of tensile strength to metal/primer failure was

approximately linear, suggesting that the decrease in tensile strength was dominated by a loss or weakening of adhesion between the substrate and the primer (Davis et al., 1990).

#### **9.1.4.2 Particles**

Several studies suggest that particles serve as carriers of other more corrosive pollutants, allowing the pollutants to reach the underlying surface or serve as concentration sites for other pollutants (Cowling and Roberts, 1954).

Reports have indicated that particles can damage automobile finishes. In an early study, staining and pitting of automobile finishes was reported in industrial areas. The damage was traced to iron particles emitted for nearby plants (Fochtman and Langer, 1957). General Motors conducted a field test to determine the effect of various meteorological events, the chemical composition of rain and dew, and the ambient air composition during the event, on automotive paint finishes. The study was conducted in Jacksonville, FL. Painted (basecoat/clearcoat technology) steel panels were exposed for varying time periods, under protected and unprotected conditions. Damage to paint finishes appeared as circular, elliptical, or irregular spots, that remained after washing. Using scanning electron microscopy (high magnification) the spots appeared as crater-like deformities in the paint finish. Chemical analyses of the deposit determined calcium sulfate to be the predominant species. It was concluded that calcium sulfate was formed on the paints surface by the reaction of calcium from dust and sulfuric acid contained in rain or dew. The damage to the paint finish increased with increasing days of exposure (Wolff et al., 1990). Table 9-4 contains the atmospheric pollutants and their concentrations during the study.

The formulation of the paint will affect the paint's durability under exposure to varying environmental factors and pollution; however, failure of the paint system results in the need for more frequent repainting and additional cost.

#### **9.1.5 Stone and Concrete**

Air pollutants are known to damage various building stones. Some of the more susceptible stones are the calcareous stones, such as limestone, marble and carbonated cemented stone. The deterioration of inorganic building materials occurs initially through surface weathering. Moisture and salts are considered the most important factors in building

**TABLE 9-4. SUMMARY OF MEASURED PARAMETERS IN  
JACKSONVILLE, FLORIDA  
(Statistics based on 8-h samples)**

Variable	Overall <sup>a</sup>		
	Mean <sup>b</sup>	Standard Deviation	Maximum <sup>c</sup>
Fine particulates <sup>d</sup> ( $\mu\text{g}/\text{m}^3$ )	22.2	11.0	58.2
Particulate matter <sup>e</sup> ( $\mu\text{g}/\text{m}^3$ )	38.7	15.9	89.8
Total suspended particulates ( $\mu\text{g}/\text{m}^3$ )	55.8	22.2	129.2
Fine sulfates <sup>f</sup> ( $\mu\text{g}/\text{m}^3$ )	6.9	4.6	18.1
Sulfates <sup>e</sup> ( $\mu\text{g}/\text{m}^3$ )	7.7	4.9	18.9
Sulfur dioxide ( $\mu\text{g}/\text{m}^3$ )	6.7	9.8	56.6
Fine ammonium ( $\mu\text{g}/\text{m}^3$ )	2.5	1.5	7.8
Fine organic carbon ( $\mu\text{g}/\text{m}^3$ )	2.0	1.3	6.4
Organic carbon <sup>e</sup> ( $\mu\text{g}/\text{m}^3$ )	4.4	2.8	12.9
Fine elemental carbon ( $\mu\text{g}/\text{m}^3$ )	1.3	1.1	5.4
Elemental carbon <sup>e</sup> ( $\mu\text{g}/\text{m}^3$ )	1.8	1.8	8.5
Fine calcium ( $\text{ng}/\text{m}^3$ )	284.0	224.0	1,145.0
Calcium ( $\text{ng}/\text{m}^3$ )	3,572.0	3,850.0	21,073.0
Fine silica ( $\text{ng}/\text{m}^3$ )	132.0	214.0	1,797.0
Silica <sup>e</sup> ( $\text{ng}/\text{m}^3$ )	995.0	909.0	6,572.0
Potassium <sup>e</sup> ( $\text{ng}/\text{m}^3$ )	348.0	140.0	920.0
Titanium <sup>e</sup> ( $\text{ng}/\text{m}^3$ )	42.0	38.0	237.0
Iron <sup>e</sup> ( $\text{ng}/\text{m}^3$ )	421.0	388.0	3,090.0
Total nitrates ( $\mu\text{g}/\text{m}^3$ )	1.3	1.3	8.4
Nitric acid ( $\mu\text{g}/\text{m}^3$ )	0.7	1.2	7.8
Fine nitrates ( $\mu\text{g}/\text{m}^3$ )	0.6	0.3	1.5
Nitrogen oxide (ppb)	3.1	4.0	19.2
Nitrogen dioxide (ppb)	8.8	5.9	32.3
Oxone (maximum) (ppb)	48.0	20.2	93.0

<sup>a</sup>Overall = combination of three daily 8-h samples.

<sup>b</sup>Mean daily ozone maximum.

<sup>c</sup>Maximum ozone concentration over the study period.

<sup>d</sup><2.5  $\mu\text{m}$ .

<sup>e</sup>PM<sub>10</sub> variables.

<sup>f</sup> $\leq$ 2.5  $\mu\text{m}$ .

Source: Wolff et al. (1990).

material damage. Many researchers believe that the mechanism of damage from air pollution involves the formation of salts from reactions in the stone; subsequently, these surface salts dissolve in moist air and are washed away by rainfall. Luckat (1977) reported good correlation with stone damage and SO<sub>2</sub> uptake. Riederer (1974) and Niesel (1979) reported that stone damage is predominantly associated with relative humidity >65% and freeze/thaw weathering. Still other researchers suggest that microorganisms must also be considered in order to quantify damage to building materials due to ambient pollutant exposure (Winkler, 1966; Riederer, 1974; Krumbein and Lange, 1978; Eckhardt, 1978; Hansen, 1980). Sulfur chemoautotrophs are well known for the damage they can cause to inorganic materials. These microorganisms (e.g., Thiobacillus) convert reduced forms of sulfur to H<sub>2</sub>SO<sub>4</sub> (Anderson, 1978) and the presence of sulfur oxidizing bacteria on exposed monuments has been confirmed (Vero and Sila, 1976). The relative importance of biological, chemical, and physical mechanisms, however, have not been systematically investigated. Thus, damage functions definitely quantifying the relationship of pollutant concentrations to stone and concrete deterioration are not available in the literature.

Baedecker et al. (1991) reviewed the published literature on calcareous stones and concluded that the most significant damage to these stones resulted from the exposure to natural constituents of nonpolluted rain water; carbonic acid from the reaction of CO<sub>2</sub> with rain reacts with the calcium in the stone. Based on the work conducted by the National Acid Precipitation Assessment Program, 10% of chemical weathering of marble and limestone was caused by wet deposition of hydrogen ions from all acid species. Dry deposition of SO<sub>2</sub> between rain events caused 5 to 20% of the chemical erosion of stone and the dry deposition of nitric acid was responsible for 2 to 6% of the erosion (Baedecker et al., 1991).

Niesel (1979) completed a literature review on the weathering of building stone in atmospheres containing SO<sub>x</sub>, which includes references from 1700 to 1979. In summary, he reported that weathering of porous building stone containing lime is generally characterized by accumulation of calcium sulfate dihydrate in the near-surface region. The effect of atmospheric pollutants on the rate of weathering is believed to be predominantly controlled by the stone's permeability and moisture content. Migrating moisture serves primarily as a transport medium. Sulfur dioxide is sorbed and thus can be translocated internally while being oxidized to sulfates. Reacting components of the building stone are

thus leached, the more soluble compounds inward and the less soluble toward the surface, often forming a surface crust.

Sengupta and de Gast (1972) reported that  $\text{SO}_2$  sorption causes physical changes in stone involving changes in porosity and water retention. Removal of  $\text{CaCO}_3$  changes the physical nature of the stone surface. The hard, nonporous layer that forms as a result of alternate freezing and thawing may blister, exfoliate, and separate from the surface. If the stone contains some substances that are unaffected by  $\text{SO}_2$ , the surface can deteriorate unevenly. The conversion of  $\text{CaCO}_3$  to calcium sulfate results in a type of efflorescence called "crystallization spalling."

Baedecker et al. (1992) reported the results of a study on carbonate stone conducted as a part of National Acid Precipitation Assessment Program. Physical measurements of the recession of test stones exposed to ambient conditions at an angle of  $30^\circ$  to horizontal at 5 sites ranged from 15 to 30  $\mu\text{m}/\text{y}$  for marble and from 25 to 45  $\mu\text{m}/\text{y}$  for limestone and were approximately double the recession estimates based on the observed calcium content of run-off solutions from test slabs. The difference between the physical and chemical recession measurements was attributed to the loss of mineral grains from the stone surfaces that were not measured in the run-off experiments. The erosion due to grain loss did not appear to be influenced by rainfall acidity, however, preliminary evidence suggested that grain loss may be influenced by dry deposition of  $\text{SO}_2$  between rain events. Chemical analysis of the run-off solutions and associated rainfall blanks suggested 30% of erosion by dissolution could be attributed to the wet deposition of hydrogen ion and the dry deposition of  $\text{SO}_2$  and nitric acid between rain events. The remaining 70% of erosion by dissolution is accounted for by the solubility of carbonate stone in rain that is in equilibrium with atmospheric  $\text{CO}_2$  (clean rain). These results are for slabs exposed at  $30^\circ$  angles. The relative contribution of  $\text{SO}_2$  to chemical erosion was significantly enhanced for slab having an inclination of  $60^\circ$  to  $85^\circ$ . The dry deposition of alkaline particles at the two urban sites competed with the stone surface for reaction with acidic species.

Sweevers and Van Grieken (1992) studied the deterioration of sandstone, marble and granite under ambient atmospheric conditions. Specially constructed sampling devices, called "micro catchment units", were installed to sample the run-off water (i.e. the rain that flows over the stones). Several analysis techniques were invoked for the analysis of the bulk

runoff water, as well as electron probe X-ray microanalysis for individual particles in the runoff. There was a strong calcium to sulfate correlation on sandstone but not on granite after extended exposures.

Webb et al. (1992) studied the effects of air pollution on limestone degradation in Great Britain. There was a significant trend to increased weight loss with increased average  $\text{SO}_2$  concentration, but a negative trend with total  $\text{NO}_x$  and with  $\text{NO}_2$ . Rainfall did not significantly affect limestone degradation. Based on a mass and ion balance model, the natural solubility of limestone in water was the dominant term in describing the stone loss. The average overall recession rate was  $24 \mu\text{m}/\text{y}$ . The increase in stone loss due to  $\text{SO}_2$  was less than  $1 \mu\text{m}/\text{year}/\text{ppb}$ .

Butlin et al. (1992b) correlated damage to stone samples exposed at 29 monitoring sites in Great Britain. Portland limestone, White Mansfield dolomitic sandstone, and Monks Park limestone tablets ( $50 \times 50 \times 8 \mu\text{m}$ ) were exposed both under sheltered and unsheltered conditions. Weight change and ionic composition of surface powders were determined after one and two years of exposure.

The results showed the expected increases in acidic species and soluble calcium in the sheltered tablets. The stone deterioration data were statistically analyzed with respect to the environmental variables at the sites. Significant correlations existed between the mean annual  $\text{SO}_2$  concentration, rainfall volume, and hydrogen ion loading and the weight changes. These three correlations contain the three components that appear to be responsible for the degradation of calcareous stone, (1) dry deposition of acid gases and aerosols, (2) dissolution by acid species in rain water, and (3) the dissolution of stone by unpolluted rain water.

By analyzing storm runoff from a Vermont marble sample and comparing the results with the pollution exposure history, Schuster et al. (1994) have determined the relative contributions of wet and dry deposition to accelerated damage. Data were compared with runoff from glass for the same seven selected summer storms. Even though the exposure site had low concentrations of  $\text{SO}_2$ , it was estimated that between 10 and 50% of calcium washed from the marble surface during a storm was from the dissolution of gypsum formed by the reaction of  $\text{SO}_2$  during dry periods.

Yerrapragada et al. (1994) exposed samples of Carrara and Georgia marble for 6, 12, or 20 mo under normal atmospheric conditions. The samples were exposed outside, but

protected from the rain, at sites in Jefferson County, KY. These authors also analyzed samples of Georgia marble of varying ages from cemeteries in the Los Angeles basin. The researchers reported that SO<sub>2</sub> is more reactive with the calcium in marble under higher NO<sub>2</sub> conditions. The effects were noted even under relatively low SO<sub>2</sub> and NO<sub>2</sub> concentrations (10 to 20 and 22 to 32 ppb, respectively). Carrara marble was found to be more reactive with SO<sub>2</sub> than Georgia marble, possibly due to the more compactness of the Georgia marble.

The effect of dry deposition of SO<sub>2</sub>, NO<sub>2</sub>, and NO both with and without O<sub>3</sub> on limestones and dolomitic sandstone was reported by Haneef et al. (1993). Samples of Portland limestone, Massamgis Jaune Roche limestone, and White Mansfield dolomitic sandstone were exposed to 10 ppm of each of the pollutants at a controlled relative humidity of 84% and a temperature of 292 °K. The stone samples were exposed to the controlled environment for 30 days. There was a small increase in sample weights after the 30 day exposure for all samples. Those samples exposed to O<sub>3</sub> in addition to one of the other pollutants (SO<sub>2</sub>, NO<sub>2</sub>, or NO) showed a significant increase in weight gain. All stone samples also showed retained sulfates or nitrates, particularly in the presence of O<sub>3</sub>. When viewed by electron/optical techniques, a crust was noted on the surface and lining the pores of the stones exposed to SO<sub>2</sub> but not those exposed to NO<sub>2</sub> or NO.

Wittenburg and Dannecker (1992) measured dry deposition and deposition velocities of airborne acidic species on different sandstones. During different air-monitoring campaigns carried out in urban sites in East and West Germany, the dry deposition of particles and gaseous sulfur and nitrogen containing species on three different sandstones and on an inert substrate were measured. The measured depositions were related to the ambient air concentrations of the most important gaseous and particulate species. Dry deposition velocities were calculated and the proportions of particle and gas input depositions on the sandstones were estimated.

Salt accumulation in building stones was mainly caused by the gaseous components, especially SO<sub>2</sub>. The deposition velocities were strongly dependent upon stone type. The contribution of sulfate particle deposition on sandstones was around 5 to 10% for vertical surfaces depending on the atmospheric conditions (Wittenburg and Dannecker, 1992).

Cobourn et al. (1993) used a continuing monitoring technique to measure the deposition velocity of SO<sub>2</sub> on marble and dolomite stone surfaces in a humid atmosphere over a

2,000 ppm-h exposure period at approximately 10 ppm SO<sub>2</sub> and 100% relative humidity. The measured average deposition velocities of SO<sub>2</sub> over the two stones were comparable in magnitude. For dolomite, the measured deposition velocity varied between 0.02 and 0.10 cm/s, whereas for the marble, the deposition velocity varied between 0.03 and 0.23 cm/s. The measured deposition velocity for both types of stone changed as a function of time. The deposition velocity over dolomite increased gradually with time. The increase was attributed to a gradual increase of liquid water on the surface, brought about by the formation of the deliquescent mineral epsomite. The wide variation appeared to be associated with the absence or presence of condensed moisture on the marble sample surfaces. For most of the marble runs, the deposition velocity generally decreased slightly with time, after an initial period. The decrease could have been due to the build-up of reactions products on the stone surface.

Under high wind conditions, particles have been reported to result in slow erosion of marble surfaces, similar to sandblasting (Yocom and Upham, 1977). Mansfeld (1980), after performing statistical analysis of damage to marble samples exposed for 30 mo at 9 air quality monitoring sites in St. Louis, MO, concluded that exposure to TSP and nitrates were correlated with stone degradation. However, there is some concern over the statistical techniques used.

Generally, black and white areas can be observed on the exposed surfaces of any building. The black areas, found in zones protected from direct rainfall and from surface runs, are covered by an irregular, dendrite-like, hard crust composed of crystals of gypsum mixed with dust, aerosols, and particles of atmospheric origin. Among these the most abundant are black carbonaceous particles originating from oil and coal combustion. On the other hand, surfaces directly exposed to rainfall show a white color, since the deterioration products formed on the stone surface are continuously washed out.

The accumulation of gypsum on carbonate stone has been investigated by McGee and Mossotti (1992) through exposure of fresh samples of limestone and marble at monitored sites, examination of alteration crusts from old buildings, and laboratory experiments. McGee and Mossotti (1992) concluded that several factors contribute to gypsum accumulation on carbonate stone. Marble or limestone that is sheltered from direct washing by rain in an urban environment with elevated pollution levels is likely to accumulate a gypsum crust.

Crust development may be enhanced if the stone is porous or has an irregular surface area. Gypsum crusts are a superficial alteration feature; gypsum crystals form at the pore opening/air interface, where evaporation is greatest. Particles of dirt and pollutants are readily trapped by the bladed network of gypsum crystals that cover the stone surface, but the particles do not appear to cause the formation of gypsum crusts. Sabbioni and Zappia (1992) analyzed samples of damaged layers on marble and limestone monuments and historical buildings from 8 urban sites in Northern and Central Italy. Samples of black crust were taken from various locations at each site to be representative of the entire site. The predominant species in the black crust matrix was calcium sulphate dihydrate (gypsum). The evaluation of enrichment factors with respect to the stone and to the soil dust showed the main components of the atmospheric deposition to be from the combustion of fuels and incineration. Saiz-Jimenez (1993) also found, after analyzing the organic compounds extracted for black crusts removed for building surfaces in polluted areas, that the main components were composed of molecular markers characteristic of petroleum derivatives. The composition of each crust, however, is governed by the composition of the particular airborne pollutants in the area.

Sabbioni et al. (1992) conducted a laboratory study on the interaction between carbonaceous particles and carbonate building stones. Three types of building stones with the common characteristic of a carbonate matrix were used: (1) Carrar marble, (2) Travertine, and (3) Trani stone. Samples of the emissions from two oil-combustion sources, representative of a centralized domestic heating system and an electric generating plant, were characterized by means of chemical and physical analysis and spread manually on the stone samples. Any excess was removed using compressed air. The distribution of the particles on the surface of the samples was controlled by optical microscopy. The stone samples were weighed before and after the particle deposition. Stones without particles were also exposed as reference samples. The samples with particles containing the highest carbon content had the lowest reactivity in the sulfation process. Particles with high sulphur content enhanced the reactivity of the stone samples with SO<sub>2</sub> (Sabbioni et al., 1992).

Del Monte et al. (1981) reported evidence of a major role for carbonaceous particles in marble deterioration, using scanning electron microscopy. The majority of the carbonaceous

particles were identified as products of oil fired boiler/combustion. Particle median diameter was  $\approx 10 \mu\text{m}$ .

Delopoulou and Sikiotis (1992) compared the corrosive action of nitrates and sulfates on pentelic marble with that of  $\text{NO}_x$  and  $\text{SO}_2$ . This was achieved by passing the polluted ambient air through a filter pack before it entered the reactor chamber holding the marble grains. As a consequence, the air reaching the marble was free of nitrates and sulfates while it contained all the  $\text{NO}_x$  and  $\text{SO}_2$ . The effects on the marble grains were quantified and compared with those from a reactor through which unfiltered ambient air was passed simultaneously and under the same conditions. They reported that the action of the acids was much greater than that of the oxides, despite the fact that the concentrations of the latter were much greater.

### **9.1.6 Corrosive Effects of Acid-Forming Aerosols and Particles on Other Materials**

Exposure to ionic dust particles can contribute significantly to the corrosion rate of electronic devices, ultimately leading to failure of such device. Anthropogenically and naturally derived particles ranging in size from tens of angstroms to  $1 \mu\text{m}$  cause corrosion of electronics because many are sufficiently hygroscopic and corrosive at normal relative humidities to react directly with non-noble metals and passive oxides, or to form sufficiently conductive moisture films on insulating surfaces to cause electrical leakage. The effects of particles on electronic components were first reported by telephone companies, when particles high in nitrates caused stress corrosion cracking and ultimate failure of the wire spring relays (Hermance, 1966; McKinney and Hermance, 1967). More recently, attention has been directed to the effects of particles on electronic components, primarily in the indoor environment.

Sinclair (1992) discussed the relevance of particle contamination to corrosion of electronics. Data collected during the 1980s show that the indoor mass concentrations of anthropogenically derived airborne particles and their arrival rates at surfaces are comparable to the concentrations and arrival rates of corrosive gases for many urban environments.

Frankenthal et al. (1993) examined the effects of ionic dust particles, ranging from 0.01 to  $1 \mu\text{m}$  in size, on copper coupons under laboratory conditions. The copper coupons,

after being polished with diamond paste, were inoculated with ammonium sulfate  $[(\text{NH}_4)_2\text{SO}_4]$  particles and exposed to air at 100 °C and relative humidities ranging from 65 to 100% for up to 600 h. The particles were deposited on the metal surface by thermophoretic deposition and cascade impaction.

Exposure of the copper coupons to  $(\text{NH}_4)_2\text{SO}_4$  at 65% relative humidity had little effect on the corrosion rate. However, when the relative humidity was increased to 75%, the critical relative humidity for  $(\text{NH}_4)_2\text{SO}_4$  at 100 °C, localized areas of corrosion were noted on the metal surface. The corrosion product, determined to be brochantite, was only found in areas where the  $(\text{NH}_4)_2\text{SO}_4$  was deposited on the metal surface. When relative humidity was increased to 100%, the corrosion became widespread (Frankenthal et al., 1993).

## 9.2 SOILING AND DISCOLORATION

A significant detrimental effect of particle pollution is the soiling of manmade surfaces. Soiling may be defined as a degradation mechanism that can be remedied by cleaning or washing, and depending on the soiled material, repainting. Faith (1976) described soiling as the deposition of particles of less than 10  $\mu\text{m}$  on surfaces by impingement. Carey (1959) observed when particles descended continuously onto paper in a room with dusty air, the paper appeared to remain clean for a period of time and then suddenly appeared dirty. Increased frequency of cleaning, washing, or repainting over soiled surfaces becomes an economic burden and can reduce the life usefulness of the material soiled. In addition to the aesthetic effect, soiling produces a change in reflectance from opaque materials and reduces light transmission through transparent materials (Beloin and Haynie, 1975; National Research Council, 1979). For dark surfaces, light colored particles can increase reflectance (Beloin and Haynie, 1975).

Determining at what accumulated level particle pollution leads to increased cleaning is difficult. For instance, in the study by Carey (1959), it was found that the appearance of soiling only occurred when the surface of the paper was covered with dust specks spaced 10 to 20 diameters apart. When the contrast was strong, e.g., black on white, it was possible to distinguish a clean surface from a surrounding dirty surface when only 0.2% of the areas was covered with specks, while 0.4% of the surface had to be covered with specks

with a weaker color contrast. Still, the effect is subjective and not easy to judge between coverages.

Support for the Carey (1959) work was reported by Hancock et al. (1976). These authors also found that with maximum contrast, a 0.2% surface coverage (effective area coverage; EAC) by dust can be perceived against a clean background. A dust deposition level of 0.7% EAC was needed before the object was considered unfit for use. The minimum perceivable difference between varying gradations of shading was a change of about 0.45% EAC. Using the information on visually perceived dust accumulation and a telephone survey, Hancock et al. (1976) concluded that a dustfall rate of less than 0.17% EAC/day would be tolerable to the general public.

Some materials that are soiled are indoors. In general, particle pollution levels indoors may be affected by outdoor ambient levels; however, other factors generally have greater effects on concentration and composition (Yocom, 1982). For that reason, discussion of indoor soiling will be limited primarily to works of art.

### **9.2.1 Building Materials**

Dose-response relationships for particle soiling were developed by Beloin and Haynie (1975) using a comparison of the rates of soiling and TSP concentrations on different building materials (painted cedar siding, concrete block, brick, limestone, asphalt singles, and window glass) at 5 different study sites over a 2-y period. Particle concentrations ranged from 60 to 250 mg/m<sup>3</sup> for a rural residential location and an industrial residential location, respectively. The results were expressed as regression functions of reflectance loss (soiling) directly proportional to the square root of the dose. With TSP expressed in mg/m<sup>3</sup> and time in months, the regression coefficients ranged from -0.11 for yellow brick to +0.08 for a coated limestone depending on the substrate color and original reflectance. For dark surfaces, light colored particles can increase reflectance. Not all of the coefficients were significantly different from zero.

A theoretical model of soiling of surfaces by airborne particles has been developed and reported by Haynie (1986). This model provides an explanation of how ambient concentrations of particulate matter are related to the accumulation of particles on surfaces and ultimately the effect of soiling by changing reflectance. Soiling is assumed to be the

contrast in reflectance of the particles on the substrate to the reflectance of the bare substrate. Thus, the average reflectance from the substrate ( $R$ ) equals the reflectance from the substrate not covered by particles [ $R_o(1-X)$ ] plus the reflectance from the particles ( $R_pX$ ) where  $X$  is the fraction of surface covered by particles.

Under constant conditions, the rate of change in fraction of surface covered is directly proportional to the fraction of surface yet to be covered. Therefore, after integration:  $X = 1 - \exp(-kt)$  where  $k$  is a function of particle size distribution and dynamics and  $t$  is time. Lanting (1986) evaluated similar models with respect to soiling by particulate elemental carbon (PEC) in the Netherlands. He determined that the models were good predictors of soiling of building materials by fine mode black smoke. Based on the existing levels of PEC, he concluded that the cleaning frequency would be doubled.

An important particle dynamic is deposition velocity which is defined as flux divided by concentration and is a function of particle diameter, surface orientation, and surface roughness, as well as other factors such as wind speed, atmospheric stability, and particle density. Thus, soiling is expected to vary with the size distribution of particles within an ambient concentration, whether a surface is facing skyward (horizontal versus vertical), and whether a surface is rough or smooth.

Van Aalst (1986) reviewed particle deposition models existing at that time and pointed out both their benefits and their faults. The lack of significant experimental verification was a major fault. Since then, Hamilton and Mansfield (1991, 1993) have applied the model reported by Haynie (1986) and Haynie and Lemmons (1990) to soiling experiments with relatively good predictive success.

Terrat and Joumard (1990) found that the simple plate method (a measurement of the number of particles deposited on a flat inert plate of material), as well as the measurement of reflectance and transmission of the light really showed the amount of soiling deposit in a town. The simple plates are more suitable for high particle polluted areas and the optical methods are more suitable for low pollution areas. This study also provided evidence that motor vehicles are mainly responsible for soiling the facades along roads.

### **9.2.1.1 Fabrics**

No recent information on the effects of particles on fabrics was located in the published literature. Earlier studies indicate particles are only damaging to fabrics when they are abrasive. Yocom and Upham (1977) reported that curtains hanging in an open window often split in parallel lines along the fold after being weakened by particle exposure. The appearance and life usefulness also may be lessened from increased frequencies of washing as a result of particle "soiling". Rees (1958) described the mechanisms (mechanical, thermal, and electrostatic) by which cloth is soiled. Tightly woven cloth exposed to moving air containing fine carbon particles was found to be the most resistant to soiling. Soiling by thermal precipitation was related to the surface temperature of the cloth versus that of the air. When the surface temperature of the cloth was greater than that of the air, the cloth resisted soiling. When cloth samples were exposed to air at both positive and negative pressure, the samples exposed to positive pressure showed greater soiling than those exposed to equivalent negative pressure.

### **9.2.1.2 Household and Industrial Paints**

Research suggest that particles can serve as carriers of more corrosive pollutants, allowing the pollutants to reach the underlying surface or serve as concentration sites for other pollutants on painted surfaces (Cowling and Roberts, 1954). Paints may also be soiled by liquids and solid particles composed of elemental carbon, tarry acids, and various other constituents.

Haynie and Lemmons (1990) conducted a soiling study at an air monitoring site in a relatively rural environment in Research Triangle Park, NC. The study was designed to determine how various environmental factors contribute to the rate of soiling of white painted surfaces. White painted surfaces are highly sensitive to soiling by dark particles and represent a large fraction of all manmade surfaces exposed to the environment. Hourly rainfall and wind speed, and weekly data for dichotomous sampler measurements and TSP concentrations were monitored. Gloss and flat white paints were applied to hardboard house siding surfaces and exposed vertically and horizontally for 16 weeks, either shielded from or exposed to rainfall. Particle mass concentration, percentage of surfaces covered by fine and coarse mode fractions, average wind speed and rainfall amounts, and paint reflectance

changes were measured at 2, 4, 8, and 16 weeks. The scanning electron microscopy stubs, that had been flush-mounted on the hardboard house siding prior to painting, were also removed and replaced with unpainted stubs at these intervals.

The unsheltered panels were initially more soiled by ambient pollutants than the sheltered panels; however, washing by rain reduced the effect. The vertically exposed panels soiled at a slower rate than the horizontally exposed panels. This was attributed to additional contribution to particle flux from gravity. The reflectivity was found to decrease faster on glossy paint than on the flat paint (Haynie and Lemmons, 1990).

Least squares fits through zero of the amounts on the surfaces with respect to exposure doses provided the deposition velocities. There was no statistical difference between the horizontal and vertical surfaces for the fine mode and the combined data given a deposition velocity of  $0.00074 + 0.000048 \text{ cm/s}$  (which is lower than some reported values). The coarse mode deposition velocity to the horizontal surfaces at  $1.55 \text{ cm/s}$  is around five times greater than to vertical surfaces at  $0.355 \text{ cm/s}$ . By applying assumptions these deposition velocities can be used to calculate rates of soiling for sheltered surfaces. The empirical prediction equation for gloss paint to a vertical surface based on a theoretical model (Haynie, 1986) is:

$$\mathbf{R = R_0 \exp (-0.0003[0.0363C_f + 0.29C_c]t)} \quad (9-8)$$

where  $R$  and  $R_0$  are reflectance and original reflectance, respectively,  $C_f$  and  $C_c$  are coarse and fine mode particle concentrations in  $\mu\text{g}/\text{m}^3$ , respectively, and  $t$  is time in weeks of exposure.

The fine mode ( $<2.5 \mu\text{m}$ ) did not appear to be washed away by rain, but most of the coarse mode ( $>2.5 \mu\text{m}$  to  $10 \mu\text{m}$ ) was either dissolved to form a stain or was washed away. Therefore, for the surfaces exposed to rain, the 0.0363 coefficient for the fine mode should remain the same as it is for sheltered surfaces but there should be a time-dependent difference in the coefficient for the coarse mode.

Based on the results of this study, the authors concluded that: (1) coarse mode particles initially contribute more to soiling of both horizontal and vertical surfaces than fine mode

particles; (2) coarse mode particles, however, are more easily removed by rain than are fine mode particles; (3) for sheltered surfaces reflectance changes is proportional to surface coverage by particles, and particle accumulation is consistent with the deposition theory; (4) rain interacts with particles to contribute to soiling by dissolving or desegregating particles and leaving stains; and (5) very long-term remedial actions are probably taken because of the accumulation of fine rather than coarse particles (Haynie and Lemmons, 1990).

Similar results were also reported by Creighton et al. (1990). They found that horizontal surfaces, under the test conditions, soiled faster than did the vertical surfaces, and that large particles were primarily responsible for the soiling of horizontal surfaces not exposed to rainfall. Soiling was related to the accumulated mass of particles from both the fine and coarse fractions. Exposed horizontal panels stain because of dissolved chemical constituents in the deposited particles. The size distribution of deposited particles was bimodal, and the area of coverage by deposited particles was also bimodal with a minimum at approximately  $5 \mu\text{m}$ . The deposition velocities for each of the size ranges onto the horizontal, sheltered panel was in general agreement with both the theoretical settling velocity of density  $2.54 \text{ g/cm}^3$  spheres and the reported results of laboratory tests. An exponential model (Haynie, 1986) was applied to the data set and gave a good fit.

Spence and Haynie (1972) reported on the published data on the effects of particles on the painted exterior surfaces of homes in Steubenville and Uniontown, OH, Suitland and Rockville, MD, and Fairfax, VA. There was a direct correlation between the ambient concentration of particulate matter in the city and the number of years between repainting. The average repainting time for homes in Steubenville, where particulate matter concentrations averaged  $235 \mu\text{g/m}^3$ , was approximately one year. In the less polluted city, Fairfax, where the particulate matter concentrations only reached  $60 \mu\text{g/m}^3$  (arithmetic means), the time between repainting was 4 years. Parker (1955) reported the occurrence of black specks on the freshly paint surface of a building in an industrial area. The black specks were not only aesthetically unappealing, but also physically damaged the painted surface. Depending on the particle concentration, the building required repainting every 2 to 3 years.

### **9.2.1.3 Soiling of Works of Art**

Ligocki et al. (1993) studied potential soiling of works of art. The concentrations and chemical composition of suspended particles were measured in both the fine and coarse size modes inside and outside five Southern California museums during summer and winter months. The seasonally averaged indoor/outdoor ratios for particle mass concentrations ranged from 0.16 to 0.96 for fine particles and from 0.06 to 0.53 for coarse particles, with lower values observed for buildings with sophisticated ventilation systems that include filters for particle removal. Museums with deliberate particle filtration systems showed indoor fine particle concentrations generally averaging less than  $10 \mu\text{g}/\text{m}^3$ . One museum with no environmental control system showed indoor fine particles concentrations averaging nearly  $60 \mu\text{g}/\text{m}^3$ . Analysis of indoor versus outdoor concentrations of major chemical species indicated that indoor sources of organics may exist at all sites, but that none of the other measured species appear to have major indoor sources at the museums studied. The authors concluded that a significant fractions of the dark-colored fine elemental carbon and soil dust particles present in the outdoor environment had penetrated to the indoor atmosphere of the museums studied and may constitute a soiling hazard to displayed works of art.

Methods for reducing the soiling rate in museums that included reducing the building ventilation rate, increasing the effectiveness of particle filtration, reducing the particle deposition velocity onto surfaces of concern, placing objects within display cases or glass frames, managing a site to achieve lower outdoor aerosol concentrations, and eliminating indoor particle sources were proposed by Nazaroff and Cass (1991). According to model results, the soiling rate can be reduced by at least two orders of magnitude through practical application of these control measures. Combining improved filtration with either a reduced ventilation rate for the entire building or low-air-exchange display cases would likely reduce the soiling hazard in museums.

## **9.3 ECONOMIC ESTIMATES**

Only limited new information was located in the published literature on the economic cost of soiling and corrosion by particles. Many of these studies are flawed or represent monetary cost for materials damage and soiling that are not representative of monetary losses

today. A detailed discussion of earlier studies on economic loss from exposure to acid forming aerosols and other particles can be found in the previous criteria document for particulate matter (U.S. Environmental Protection Agency, 1982). The following sections describe methods for determining economic losses from materials damage and soiling from air pollution and includes the limited body of new information available since publication of the 1982 particulate matter criteria document.

### **9.3.1 Methods for Determining Economic Loss from Pollutant Exposure**

Several types of economic losses result from materials damage and soiling. Financial or out-of-pocket losses include the reduction in service life of a material, decreased utility, substitution of a more expensive material, losses due to an inferior substitute, protection of susceptible materials, and additional required maintenance, including cleaning. The major losses of amenity, as defined by Mäler and Wyzga (1976), are associated with enduring and suffering soiled, damaged, or inferior products and materials because of particle pollution and any corrosive pollutant that may be absorbed on or adsorbed to particles. In addition, amenity losses are suffered when pollution damage repair or maintenance procedures result in inconvenience or other delays in normal operations. Some of these losses, such as effects on monuments and works of art, are especially difficult to specify (Mäler and Wyzga, 1976).

The compilation and assessment of materials damage and soiling research reveals a variety of techniques employed by different disciplines to estimate economic losses associated with soiling and materials damage. Attempts have been made to address the following questions.

- At what concentration or deposition rate is materials damage and soiling perceived?
- What is the relationship between the color of the particle and perceived materials damage and soiling?
- What is the physical or economic life of various materials, coatings, structures, etc.?
- What is the inventory of pollution sensitive materials, coatings, structures, etc.?
- What behaviors are undertaken to avert, mitigate, or repair pollution-related damages?

- What is the economic cost of materials damage and soiling due to exposure to acid forming aerosols and other particles?

The answers to these questions are certainly relevant to the structure of a modeling framework, the collection of data, and the estimation of effects of materials damage and soiling on economic values. The analytical approach selected depends on whether financial losses or losses of amenity are emphasized, the type of damage being considered, and the availability of cost information. Economic losses from pollutant exposure can be estimated using the damage function approach or using direct economic methods.

In the damage function approach, physical damage (any undesirable change in the function of specific materials, including appearance, leading to failure of specific components) is determined before economic cost is estimated. Physical damage is estimated from ambient pollutant concentrations over a specified period of time. Depending on the material damaged, both short-term and long-term exposure data may be necessary to determine a more accurate estimate of damage related to pollution exposure. The damage function is expressed in terms appropriate to the interaction of the pollutant and material. For example, the corrosion of metal may be expressed in units of thickness lost, while the deterioration of paint from soiling may be expressed in units of reflectance lost. A willingness-to-pay value, mitigation, or replacement cost is then applied to estimate a monetary value of damages caused by changes in pollutant concentrations. It is, however, difficult to estimate fully the financial losses because reliable information is not available on the physical damage of all economically important materials, and on the spatial and temporal distribution of these materials. Further, current techniques do not reflect the use of more resistant and reduced-maintenance materials, and loss estimates may assume that substitute materials cost more than the original materials, and that the cost differential is attributable solely to pollution.

Another major problem in developing reliable damage functions is the inability to separate pollutant effects from natural weathering processes due to various meteorological parameters (temperature, relative humidity, wind speed, and surface wetness). Since weathering is a natural phenomenon, proceeding at a finite rate irrespective of anthropogenic pollution, materials damage estimates must represent only that damage directly produced by

anthropogenic pollutant exposure. Also, this approach cannot account for irreplaceable items such as works of art or national monuments.

In the studies that do not use the physical damage approach to derive monetized economic damages reflecting the estimates of damages associated with pollution, the loss of amenity or direct financial losses are estimated econometrically. These approaches have been used to relate changes in air pollution directly with the economic value of avoidance or mitigation of damages. A major source of error using these approaches is the requirement that all factors that affect cost other than air quality have to be accounted for. In general all approaches to estimating costs of air pollution effects on materials are limited by the difficulty in quantifying the human response to damage based upon the ability and the incentive to pay additional costs (Yocom and Grappone, 1976).

### **9.3.2 Economic Loss Associated with Materials Damage and Soiling**

Information on the geographic distribution of various types of exposed materials may provide an indication of the extent of potential economic costs of damage to materials from air pollution. Lipfert and Daum (1992) analyzed the efforts made to determine the geographic distribution of various types of materials. They focused on the identification, evaluation and interpretation of data describing the distribution of exterior construction materials, primarily in the United States. Materials distribution surveys for 16 cities in the United States and Canada and five related data bases from government agencies and trade organizations were examined. Data on residential buildings were more available than non-residential buildings; little geographically resolved information on distributions on materials in infrastructure was found.

Lipfert and Daum (1992) observed several important factors relating pollution to distribution of materials. In the United States, buildings constitute the largest category of surface areas potentially at risk to pollution damage. Within this category, residential buildings are the most important. On average, commercial and industrial buildings tend to be larger than residential buildings and to use more durable materials. However, because they are more numerous (and use less durable materials) more surface area for residential buildings is exposed to potentially damaging pollutants. For residential buildings in general, painted surfaces are preferred over masonry in the Northeastern United States (with the

exception of large inner cities), brick is popular in the South and Midwest) and stucco in the West. The use of brick appears to be declining, painted wood increasing, and the use of vinyl siding is gaining over aluminum. One of the factors underlying the present regional distribution of materials is their durability under the environmental conditions which exist when they were installed. Thus, changing pollution levels have possibly affected materials selection, and is expected to do so.

Haynie (1990) examined the potential effects of  $PM_{10}$  nonattainment on the costs of repainting exterior residential walls due to soiling in 123 counties. The analysis was based on a damage function methodology developed for a risk assessment of soiling of painted exterior residential walls (Haynie, 1989). The data base was updated with 1988 and 1989 AIRS data. An extreme value statistical model was used to adjust every sixth day monitoring to 365 days for counting violation days (one violation in 60 does not translate to 6 violations in 360). The resulting paint cost due to soiling was subjected to a sensitivity analysis using various assumed values. When the model is restricted to only a national average of 10% of households repainting because of soiling, the effects of other assumptions become inversely related and tend to cancel out each other (possibly associated with individual cost minimization choices).

The top twenty counties were ranked by estimated soiling costs. Fourteen of the counties with actual violation days in 1989 were in this group. All but three were west of the Mississippi. A total of 29 counties with measured violations are in the set of 123 counties for which  $PM_{10}$  nonattainment soiling costs were calculated. When the given set of behavior assumptions was used, there were no costs calculated for 19 counties that actually measured violations in 1989. The distribution of a national estimated \$1 billion in painted exterior residential wall soiling costs is shown in Figure 9-2.

An experimentally determined soiling function for unsheltered, vertically exposed house paint was used to determine painting frequency (Haynie and Lemmons, 1990). An equation was set up to express paint life in integer years because the painting of exterior surfaces is usually controlled by season (weather). Different values for normal paint life without soiling and levels of unacceptable soiling could be used in the equation. If four was taken as the most likely average paint life for other than soiling reasons, then painting because of soiling would likely be done at 1, 2, or 3 year intervals.

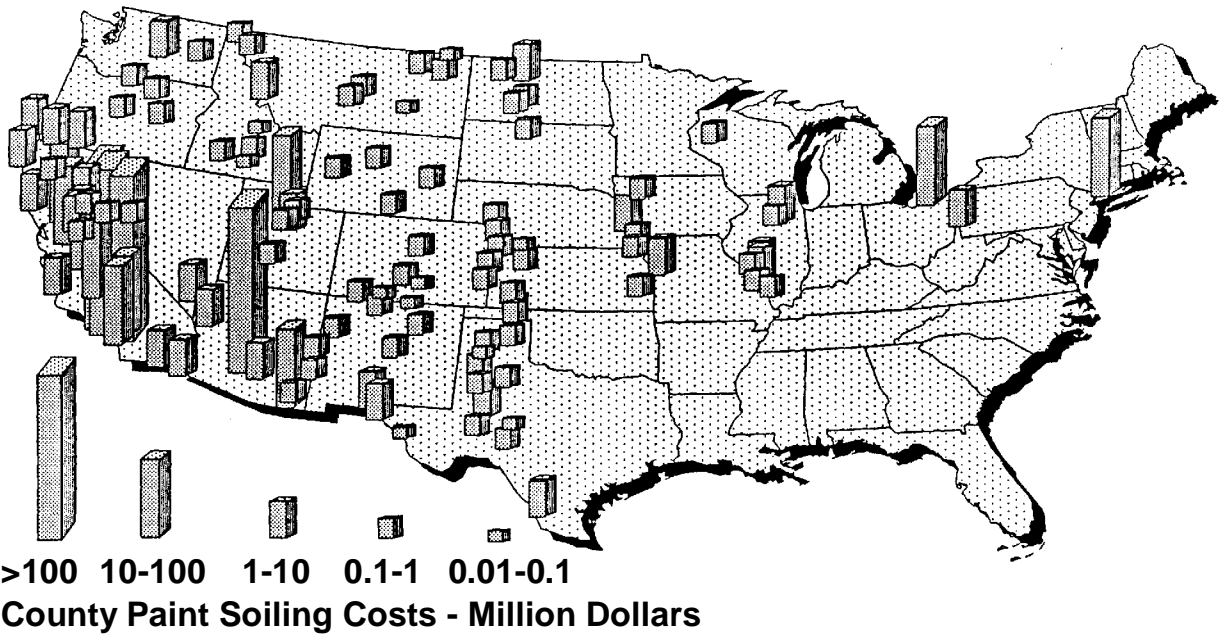


**Figure 9-2. Geographic distribution of paint soiling costs.**

Source: Haynie (1990).

Soiling costs by county were calculated and ranked by decreasing amounts and the logarithm of costs plotted by rank. The plot consisted of three distinct straight lines with intersections at ranks 4 and 45. The calculated cost values provide a reasonable ranking of the soiling problem by county, but do not necessarily reflect actual painting cost associated with extreme concentrations of particles. Households exposed to extremes are not expected to respond with average behavior. The authors concluded that repainting costs could be lowered if: (1) individuals can learn to live with higher particle pollution, accepting greater reductions in reflectance before painting; (2) painted surfaces were washed rather than repainted; and (3) if materials or paint colors that do not tend to show dirt were used.

Extrapolating the middle distribution of costs to the top four ranked counties reduces their estimated costs considerably. For example Maricopa County, AR, was calculated to rank first at \$70.2 million if all households painted each year as predicted, but was calculated to be only \$29.7 million based on the distribution extrapolation.

Based on these calculations and error analysis, the national soiling costs associated with repainting the exterior walls of houses probably were within the range of \$400 to \$800 million a year in 1990. This sector represents about 70% of the exterior paint market, so that extrapolating to all exterior paint surfaces gives a range of from \$570 to \$1,140 million (Haynie and Lemmons, 1990).

A number of other studies have attempted to model the economic losses of soiling due to particulate air pollution. Based on the hypothesis that air pollution affects the budget allocation decisions of individuals, MathTech (1983) used a household sector model to establish a statistical relationship between TSP and the demand for laundry and cleaning products and services using 1972-1973 Bureau of Labor Statistics Consumer Expenditure data. Given knowledge of the pattern of demand for these goods, standard methods of welfare economics were used to estimate the benefits (or compensating variation) of changes in TSP concentrations. The results of this study indicated that the annual benefits of attaining the primary  $PM_{10}$  standard were approximately \$88.3 million to \$1.2 billion in 1980 dollars for the period 1989 to 1995. The applicability of the underlying relationship to current air quality and economic conditions is uncertain given that potential changes in consumer tastes and the opportunity set of goods influencing budget allocation decisions could have changed over the intervening 20 years.

MathTech (1990) also assessed the effects of acidic deposition on painted wood surfaces using individual maintenance behavior data. The effects were a function of the repainting frequency of the houses as well as pollution levels.

Gilbert (1985) used a household production function framework to design and estimate the short-run costs of soiling. The results were comparable to those reported by MathTech (1983). Smith and Gilbert (1985) also used a hedonic property value model to analyze the effects of particles in the long term, examining the possibility of households moving in response to air pollution.

McClelland et al. (1991) conducted a field study valuing eastern visibility using the contingent valuation method. Given the problem of embedding between closely associated attributes, the survey instrument provided for separation of the visibility, soiling, and health components of the willingness-to-pay estimates. Households were found to be willing to pay \$2.70 per  $\mu\text{g}/\text{m}^3$  change in particle pollution to avoid soiling effects.

The findings of the aforementioned studies are consistent with the hypotheses that there are economic costs associated with elevated pollution levels across multiple sectors and that households are willing to pay positive amounts to reduce particle concentrations to reduce the risk of materials damage and soiling. However, these studies have done little to advance our knowledge of perception thresholds in relationship to concentration, particle size, and chemical composition. Without such information it is very difficult and highly uncertain to quantify the relationship between ambient particle concentrations and soiling and associated economic cost.

#### **9.4 SUMMARY**

Available information supports the fact that exposure to acid forming aerosols promotes the corrosion of metals beyond the corrosion rates expected from exposure to natural environmental elements (wind, rain, sun, temperature fluctuations, etc.). Many metals form a protective film that protects against corrosion; however, high concentrations of anthropogenic pollutants, lessen the effectiveness of the protective film. Acid forming aerosols have also been found to limit the life expectancy of paints by causing discoloration, loss of gloss, and loss of thickness of the paint film layer.

Various building stones and cement products are damaged from exposure to acid-forming aerosols. However, the extent of the damage to building stones and cement products produced by the pollutant species, beyond that expected as part of the natural weathering process is uncertain. Several investigators have suggested that the damage attributed to acid forming pollutants is overestimated and that stone damage is predominantly associated with relative humidity, temperature, and, to a lesser degree, air pollution.

A significant detrimental effect of particle pollution is the soiling of painted surfaces and other building materials. Soiling is defined as a degradation mechanism that can be remedied by cleaning or washing, and depending on the soiled surface, repainting. Available data on pollution exposure indicates that particles can result in increased cleaning frequency of the exposed surface, and may reduce the life usefulness of the material soiled. Data on the effects of particulate matter on other surfaces are not as well understood. Some evidence does, however, suggest that exposure to particles may damage fabrics, electronics, and works

of art composed of one or more materials, but this evidence is largely qualitative and sketchy.

The damaging and soiling of materials by acid forming aerosols and other particles have an economic impact, but this impact is difficult to measure. One problem is the lack of sufficient data to separate costs between various pollutants and to separate cost of pollutant exposure from that of normal maintenance. Attempts have been made to quantify the pollutants exposure levels at which materials damage and soiling have been perceived. However, to date, insufficient data are available to advance our knowledge regarding perception thresholds with respect to pollutant concentration, particle size, and chemical composition.

## REFERENCES

- Anderson, E. A. (1956) The atmospheric corrosion of rolled zinc. In: Symposium on atmospheric corrosion of non-ferrous metals; June 1955; Atlantic City, NJ. Philadelphia, PA: American Society for Testing and Materials; pp. 126-134. (ASTM special technical publication no. 175).
- Anderson, J. W. (1978) Transformations of inorganic sulphur by organisms. In: Sulphur in biology. Baltimore, MD: University Park Press; pp. 11-22 (The Institute of Biology's studies in biology no. 101).
- Askey, A.; Lyon, S. B.; Thompson, G. E.; Johnson, J. B.; Wood, G. C.; Sage, P. W.; Cooke, M. J. (1993) The effect of fly-ash particulates on the atmospheric corrosion of zinc and mild steel. *Corros. Sci.* 34: 1055-1081.
- Baedecker, P. A.; Edney, E. O.; Moran, P. J.; Simpson, T. C.; Williams, R. S. (1991) Effects of acidic deposition on materials. In: Irving, P. M., ed. Acidic deposition: state of science and technology, volume III: terrestrial, materials, health and visibility effects. Washington, DC: The U.S. National Acid Precipitation Assessment Program. (State of science and technology report no. 19).
- Baedecker, P. A.; Reddy, M. M.; Reimann, K. J.; Sciammarella, C. A. (1992) Effects of acidic deposition on the erosion of carbonate stone—experimental results from the U.S. National Acid Precipitation Assessment Program (NAPAP). *Atmos. Environ. Part B* 26: 147-158.
- Barton, K. (1958) The influence of dust on atmospheric corrosion of metals. *Werkst. Korros.* 8/9: 547-549.
- Barton, K. (1976) Protection against atmospheric corrosion: theories and methods. Duncan, J. R., trans. London, United Kingdom: John Wiley and Sons, Ltd.
- Beloin, N. J.; Haynie, F. H. (1975) Soiling of building materials. *J. Air Pollut. Control Assoc.* 25: 399-403.
- Biefer, G. J. (1981) Atmospheric corrosion of steel in the Canadian Arctic. *Mater. Perform.* 20: 16-19.
- Butlin, R. N.; Coote, A. T.; Devenish, M.; Hughes, I. S. C.; Hutchens, C. M.; Irwin, J. G.; Lloyd, G. O.; Massey, S. W.; Webb, A. H.; Yates, T. J. S. (1992a) Preliminary results from the analysis of metal samples from the National Materials Exposure Programme (NMEP). *Atmos. Environ. Part B* 26: 199-206.
- Butlin, R. N.; Coote, A. T.; Devenish, M.; Hughes, I. S. C.; Hutchens, C. M.; Irwin, J. G.; Lloyd, G. O.; Massey, S. W.; Webb, A. H.; Yates, T. J. S. (1992b) Preliminary results from the analysis of stone tablets from the National Materials Exposure Programme (NMEP). *Atmos. Environ. Part B* 26: 189-198.
- Campbell, G. G.; Schurr, G. G.; Slawikowski, D. E.; Spence, J. W. (1974) Assessing air pollution damage to coatings. *J. Paint Technol.* 46: 59-71.
- Carey, W. F. (1959) Atmospheric deposits in Britain: a study of dinginess. *Int. J. Air Pollut.* 2: 1-26.
- Chandler, K. A.; Kilcullen, M. B. (1968) Survey of corrosion and atmospheric pollution in and around Sheffield. *Br. Corros. J.* 3: 80-84.
- Cobourn, W. G.; Gauri, K. L.; Tambe, S.; Li, S.; Saltik, E. (1993) Laboratory measurements of sulfur dioxide deposition velocity on marble and dolomite stone surfaces. *Atmos. Environ. Part B* 27: 193-201.
- Cowling, J. E.; Roberts, M. E. (1954) Paints, varnishes, enamels, and lacquers. In: Greathouse, G. A.; Wessel, C. J., eds. Deterioration of materials: causes and preventive techniques. New York, NY: Reinhold Publishing Corporation; pp. 596-645.
- Cramer, S. D.; Baker, M. J. (1993) Monticello roof restoration. *Mater. Perform.* 32: 61-64.

- Cramer, S. D.; McDonald, L. G.; Bhagia, G.; Flinn, D. R.; Linstrom, P. J.; Carter, J. P. (1989) Effects of acid deposition on the atmospheric corrosion of structural metals. Research Triangle Park, NC: U.S. Environmental Protection Agency; internal report.
- Creighton, P. J.; Lioy, P. J.; Haynie, F. H.; Lemmons, T. J.; Miller, J. L.; Gerhart, J. (1990) Soiling by atmospheric aerosols in an urban industrial area. *J. Air Waste Manage. Assoc.* 40: 1285-1289.
- Davis, G. D.; Shaw, B. A.; Arah, C. O.; Fritz, T. L.; Moshier, W. C.; Simpson, T. C.; Moran, P. J.; Zankel, K. L. (1990) Effects of SO<sub>2</sub> deposition on painted steel surfaces. *Surf. Interface Anal.* 15: 107-112.
- Dean, S. W.; Anthony, W. H. (1988) Atmospheric corrosion of wrought aluminum alloys during a ten-year period. In: Dean, S. W.; Lee, T. S., eds. *Degradation of metals in the atmosphere: a symposium sponsored by ASTM committee G-1 on corrosion of metals; May 1986; Philadelphia, PA.* Philadelphia, PA: American Society for Testing and Materials; pp. 191-205. (ASTM special technical publication 965).
- Del Monte, M.; Sabbioni, C.; Vittori, O. (1981) Airborne carbon particles and marble deterioration. *Atmos. Environ.* 15: 645-652.
- Delopoulou, P.; Sikiotis, D. (1992) A comparison of the corrosive action on pentelic marble of nitrates and sulphates with the action of nitrogen oxides and sulphur dioxide. *Atmos. Environ. Part B* 26: 183-188.
- Eckhardt, F. E. W. (1978) Microorganisms and weathering of a sandstone monument. In: Krumbein, W. E., ed. *Environmental biogeochemistry and geomicrobiology, volume 2: the terrestrial environment: proceedings of the third international symposium on environmental biogeochemistry; 1977; Wolfenbüttel, Germany.* Ann Arbor, MI: Ann Arbor Science Publishers, Inc.; pp. 675-686.
- Edney, E. O. (1989) Paint coatings: controlled field and chamber experiments. Research Triangle Park, NC: U.S. Environmental Protection Agency; EPA report no. EPA/600/S3-89/032.
- Edney, E. O.; Stiles, D. C.; Spence, J. W.; Haynie, F. H.; Wilson, W. E. (1986) A laboratory study to evaluate the impact of NO<sub>x</sub>, SO<sub>x</sub>, and oxidants on atmospheric corrosion of galvanized steel. In: Baboian, R., ed. *Materials degradation caused by acid rain: developed from the 20th state-of-the-art symposium of the American Chemical Society; June 1985; Arlington, VA.* Washington, DC: American Chemical Society; pp. 172-193. (ACS symposium series 318).
- Edney, E. O.; Cheek, S. F.; Stiles, D. C.; Corse, E. W.; Wheeler, M. L.; Spence, J. W.; Haynie, F. H.; Wilson, W. E., Jr. (1988) Effects of acid deposition on paints and metals: results of a controlled field study. *Atmos. Environ.* 22: 2263-2274.
- Edney, E. O.; Cheek, S. F.; Corse, E. W.; Spence, J. W.; Haynie, F. H. (1989) Atmospheric weathering caused by dry deposition of acidic compounds. *J. Environ. Sci. Health Part A* 24: 439-457.
- Faith, W. L. (1976) Effects of atmospheric pollutants. In: Pfafflin, J. R.; Ziegler, E. N., eds. *Encyclopedia of environmental science and engineering: volume one, A-M.* New York, NY: Gordon and Breach Science Publishers; pp. 219-233.
- Fink, F. W.; Buttner, F. H.; Boyd, W. K. (1971) Final report on technical-economic evaluation of air-pollution corrosion costs on metals in the U.S. Columbus, OH: Battelle Memorial Institute, Columbus Laboratories; EPA contract no. CPA 70-86; EPA report no. APTD-0654. Available from: NTIS, Springfield, VA; PB-198-453.
- Fochtman, E. G.; Langer, G. (1957) Automobile paint damaged by airborne iron particles. *J. Air Pollut. Control Assoc.* 6: 243-247.
- Frankenthal, R. P.; Lobnig, R.; Siconolfi, D. J.; Sinclair, J. D. (1993) Role of particle contamination in the corrosion of electronic materials and devices. *J. Vac. Sci. Technol. A* 11: 2274-2279.

- Gilbert, C. C. S. (1985) Household adjustment and the measurement of benefits from environmental quality improvements [Ph.D. dissertation]. Chapel Hill, NC: University of North Carolina at Chapel Hill.
- Goodwin, J. E.; Sage, W.; Tilly, G. P. (1969) Study of erosion by solid particles. *Proc. Inst. Mech. Eng.* 184: 279-292.
- Graedel, T. E.; Nassau, K.; Franey, J. P. (1987) Copper patinas formed in the atmosphere—I. introduction. *Corros. Sci.* 27: 639-657.
- Guttman, H. (1968) Effects of atmospheric factors on the corrosion of rolled zinc. In: *Metal corrosion in the atmosphere; a symposium presented at the seventieth annual meeting of the American Society for Testing and Materials; June 1967; Boston, MA. Philadelphia, PA: American Society for Testing and Materials; pp. 223-239.*
- Guttman, H.; Sereda, P. J. (1968) Measurement of atmospheric factors affecting the corrosion of metals. In: *Metal corrosion in the atmosphere: a symposium presented at the 70th annual meeting of the American Society for Testing and Materials; June 1967; Boston, MA. Philadelphia, PA: American Society for Testing and Materials; pp. 326-359. (ASTM special technical publication 435).*
- Hamilton, R. S.; Mansfield, T. A. (1991) Airborne particulate elemental carbon: its sources, transport and contribution to dark smoke and soiling. *Atmos. Environ. Part A* 25: 715-723.
- Hamilton, R. S.; Mansfield, T. A. (1993) The soiling of materials in the ambient atmosphere. *Atmos. Environ. Part A* 27: 1369-1374.
- Hancock, R. P.; Esmen, N. A.; Furber, C. P. (1976) Visual response to dustiness. *J. Air Pollut. Control Assoc.* 26: 54-57.
- Haneef, S. J.; Johnson, J. B.; Thompson, G. E.; Wood, G. C. (1993) Simulation of the degradation of limestones and dolomitic sandstone under dry deposition conditions. In: *Proceedings of the 12th international corrosion congress: corrosion control and low-cost reliability, v. 2. Houston, TX: National Association of Corrosion Engineers (NACE); pp. 700-710.*
- Hansen, J. (1980) Ailing treasures. *Science (Washington, DC)* 1: 58-61.
- Harker, A. B.; Mansfeld, F. B.; Strauss, D. R.; Landis, D. D. (1980) Mechanism of SO<sub>2</sub> and H<sub>2</sub>SO<sub>4</sub> aerosol zinc corrosion. Research Triangle Park, NC: U.S. Environmental Protection Agency, Environmental Sciences Research Laboratory; EPA report no. EPA-600/3-80-018. Available from: NTIS, Springfield, VA; PB80-167018.
- Haynie, F. H. (1976) Air pollution effects on stress induced intergranular corrosion of 7005-t53 aluminum alloy. In: *Stress corrosion: new approaches. Philadelphia, PA: American Society for Testing and Materials; pp. 32-43. (ASTM special technical publication 610).*
- Haynie, F. H. (1980) Theoretical air pollution and climate effects on materials confirmed by zinc corrosion data. In: Sereda, P. J.; Litvan, G. G., eds. *Durability of building materials and components: proceedings of the 1st international conference; August 1978; Ottawa, ON, Canada. Philadelphia, PA: American Society for Testing and Materials; pp. 157-175. (ASTM special technical publication 691).*
- Haynie, F. H. (1986) Environmental factors affecting corrosion of weathering steel. In: Baboian, R., ed. *Materials degradation caused by acid rain: developed from the 20th state-of-the-art symposium of the American Chemical Society; June 1985; Arlington, VA. Washington, DC: American Chemical Society; pp. 163-171. (ACS symposium series 318).*
- Haynie, F. H. (1988) Environmental factors affecting the corrosion of galvanized steel. In: Dean, S. W.; Lee, T. S., eds. *Degradation of metals in the atmosphere: a symposium sponsored by ASTM committee G-1 on corrosion of*

- metals; May 1986; Philadelphia, PA . Philadelphia, PA: American Society for Testing and Materials; pp. 282-289. (ASTM special technical publication 965).
- Haynie, F. H. (1989) Risk assessment of particulate matter soiling of exterior house paints. Research Triangle Park, NC: U.S. Environmental Protection Agency, Atmospheric Research and Exposure Assessment Laboratory; EPA report no. EPA/600/X-89/304.
- Haynie, F. H. (1990) Effects of PM10 nonattainment on soiling of painted surfaces. Research Triangle Park, NC: U.S. Environmental Protection Agency, Atmospheric Research and Exposure Assessment Laboratory.
- Haynie, F. H.; Lemmons, T. J. (1990) Particulate matter soiling of exterior paints at a rural site. *Aerosol Sci. Technol.* 13: 356-367.
- Haynie, F. H.; Spence, J. W. (1984) Air pollution damage to exterior household paints. *J. Air Pollut. Control Assoc.* 34: 941-944.
- Haynie, F. H.; Stiles, D. C. (1992) Evaluation of an atmospheric corrosion rate monitor as a time-of-wetness meter. *Mater. Perform.* 31: 48-52.
- Haynie, F. H.; Upham, J. B. (1974) Correlation between corrosion behavior of steel and atmospheric pollution data. In: Coburn, S. K., ed. *Corrosion in natural environments: presented at the 76th annual meeting American Society for Testing and Materials; June 1973; Philadelphia, PA.* Philadelphia, PA: American Society for Testing and Materials; pp. 33-51. (ASTM special technical publication 558).
- Haynie, F. H.; Spence, J. W.; Upham, J. B. (1976) Effects of gaseous pollutants on materials - a chamber study. Research Triangle Park, NC: U.S. Environmental Protection Agency, Environmental Sciences Research Laboratory; EPA report no. EPA-600/3-76/015. Available from: NTIS, Springfield, VA; PB-251580.
- Haynie, F. H.; Spence, J. W.; Lipfert, F. W.; Cramer, S. D.; McDonald, L. G. (1990) Evaluation of an atmospheric damage function for galvanized steel. In: Baboian, R.; Dean, S. W., eds. *Corrosion testing and evaluation: silver anniversary volume.* Philadelphia, PA: American Society for Testing and Materials; pp. 225-240. (ASTM special technical publication 1000).
- Hendricks, B. J.; Balik, C. M. (1990) Solubility and diffusivity of sulfur dioxide in latex paint films. *J. Appl. Polym. Sci.* 40: 953-961.
- Hermance, H. W. (1966) Combatting the effects of smog on wire-spring relays. *Bell Lab. Rec.* (February): 48-52.
- Holbrow, G. L. (1962) Atmospheric pollution: its measurement and some effects on paint. *J. Oil Colour Chem. Assoc.* 45: 701-718.
- Johnson, J. B.; Elliott, P.; Winterbottom, M. A.; Wood, G. C. (1977) Short-term atmospheric corrosion of mild steel at two weather and pollution monitored sites. *Corros. Sci.* 17: 691-700.
- Krumbein, W. E.; Lange, C. (1978) Decay of plaster, paintings and wall material of the interior of buildings via microbial activity. In: Krumbein, W. E., ed. *Environmental biogeochemistry and geomicrobiology, volume 2: the terrestrial environment: proceedings of the third international symposium on environmental biogeochemistry; 1977; Wolfenbüttel, Germany.* Ann Arbor, MI: Ann Arbor Science Publishers Inc.; pp. 687-697.
- Kucera, V.; Mattsson, E. (1987) Atmospheric corrosion. In: Mansfeld, F., ed. *Corrosion mechanisms.* New York, NY: Marcel Dekker, Inc.; pp. 211-284.

- Lanting, R. W. (1986) Black smoke and soiling. In: Lee, S. D.; Schneider, T.; Grant, L. D.; Verkerk, P. J., eds. *Aerosols: research, risk assessment and control strategies: proceedings of the second U.S.-Dutch international symposium*; May 1985; Williamsburg, VA. Chelsea, MI: Lewis Publishers, Inc.; pp. 923-932.
- Li, S.-M.; Anlauf, K. G.; Wiebe, H. A. (1993) Heterogeneous nighttime production and deposition of particle nitrate at a rural site in North America during summer 1988. *J. Geophys. Res. [Atmos.]* 98: 5139-5157.
- Ligocki, M. P.; Salmon, L. G.; Fall, T.; Jones, M. C.; Nazaroff, W. W.; Cass, G. R. (1993) Characteristics of airborne particles inside southern California museums. *Atmos. Environ. Part A* 27: 697-711.
- Lipfert, F. W.; Daum, M. L. (1992) The distribution of common construction materials at risk to acid deposition in the United States. *Atmos. Environ. Part B* 26: 217-226.
- Luckat, S. (1977) Stone deterioration at the Cologne Cathedral and other monuments due to action of air pollutants. In: *Proceedings of the fourth international clean air congress*; May; Tokyo, Japan. Tokyo, Japan: Japanese Union of Air Pollution Prevention Associations; pp. 128-130.
- Mäler, K. G.; Wyzga, R. E. (1976) *Economic measurement of environmental damage: a technical handbook*. Paris, France: Organisation for Economic Co-operation and Development.
- Mansfeld, F. (1980) *Regional air pollution study: effects of airborne sulfur pollutants on materials*. Research Triangle Park, NC: U.S. Environmental Protection Agency, Environmental Sciences Research Laboratory; EPA report no. EPA-600/4-80-007. Available from: NTIS, Springfield, VA; PB81-126351.
- Mansfeld, F.; Kenkel, J. V. (1976) Electrochemical monitoring of atmospheric corrosion phenomena. *Corros. Sci.* 16: 111-122.
- Mansfeld, F.; Vijaykumar, R. (1988) Atmospheric corrosion behavior in Southern California. *Corros. Sci.* 28: 939-946.
- MathTech, Inc. (1983) *Benefit and net benefit analysis of alternative national ambient air quality standards for particulate matter*. Research Triangle Park, NC: U.S. Environmental Protection Agency, Strategies and Air Standards Division; contract no. 68-02-3579.
- MathTech, Inc. (1990) *Economic assessment of materials damage in the South Coast Air Basin: a case study of acid deposition effects on painted wood surfaces using individual maintenance behavior data*. Sacramento CA: California Air Resources Board; May.
- McClelland, G.; Schulze, W.; Waldman, D.; Irwin, J.; Schenk, D.; Stewart, T.; Deck, L.; Thayer, M. (1991) *Valuing eastern visibility: a field test of the contingent valuation method*. Washington, DC: draft report to the U.S. Environmental Protection Agency; cooperative agreement no. CR-815183-01-3.
- McGee, E. S.; Mossotti, V. G. (1992) Gypsum accumulation on carbonate stone. *Atmos. Environ. Part B* 26: 249-253.
- McKinney, N.; Hermance, H. W. (1967) Stress corrosion cracking rates of a nickel-brass alloy under applied potential. In: *Stress corrosion testing: a symposium presented at the sixty-ninth annual meeting of the American Society for Testing and Materials*; June-July 1966; Atlantic City, NJ. Philadelphia, PA: American Society for Testing and Materials; pp. 274-291. (ASTM special technical publication 425).
- Meakin, J. D.; Ames, D. L.; Dolske, D. A. (1992) Degradation of monumental bronzes. *Atmos. Environ. Part B* 26: 207-215.
- National Research Council. (1979) *Airborne particles*. Baltimore, MD: University Park Press.
- Nazaroff, W. W.; Cass, G. R. (1991) Protecting museum collections from soiling due to the deposition of airborne particles. *Atmos. Environ. Part A* 25: 841-852.

- Niesel, K. (1979) The weathering of building materials in atmospheres containing sulfur oxides - a literature discussion. *Fortschr. Mineral.* 57: 68-124.
- Nriagu, J. O. (1978) Deteriorative effects of sulfur pollution on materials. In: Nriagu, J. O., ed. *Sulfur in the environment, part II: ecological impacts*. New York, NY: John Wiley & Sons; pp. 1-59.
- Parker, A. (1955) The destructive effects of air pollution on materials. In: *Proceedings of the 22nd annual conference of the National Smoke Abatement Society; September; Bournemouth, United Kingdom*. London, United Kingdom: National Smoke Abatement Society; pp. 3-15.
- Patil, D.; Gilbert, R. D.; Fornes, R. E. (1990) Environmental effects on latex paint coatings. I. Base polymer degradation. *J. Appl. Polym. Sci.* 41: 1641-1650.
- Pitchford, M. L.; McMurry, P. H. (1994) Relationship between measured water vapor growth and chemistry of atmospheric aerosol for Grand Canyon, Arizona, in winter 1990. *Atmos. Environ.* 28: 827-839.
- Rees, W. H. (1958) Atmospheric pollution and the soiling of textile materials. *Br. J. Appl. Phys.* 9: 301-305.
- Riederer, J. (1974) Pollution damage to works of art. *Experientia Suppl.* 20: 73-85.
- Russell, C. A. (1976) How environmental pollutants diminish contact reliability. *Insul. Circuits* 22: 43-46.
- Sabbioni, C.; Zappia, G. (1992) Atmospheric-derived element tracers on damaged stone. *Sci. Total Environ.* 126: 35-48.
- Sabbioni, C.; Zappia, G.; Gobbi, G. (1992) Carbonaceous particles on carbonate building stones in a simulated system. In: *Proceedings of the 1992 European aerosol conference; September; Oxford, United Kingdom*. *J. Aerosol Sci.* 23(suppl. 1): S921-S924.
- Saiz-Jimenez, C. (1993) Deposition of airborne organic pollutants on historic buildings. *Atmos. Environ. Part B* 27: 77-85.
- Sankar, S. S.; Patil, D.; Schadt, R.; Fornes, R. E.; Gilbert, R. D. (1990) Environmental effects on latex paint coatings. II. CP/MAS <sup>13</sup>C-NMR and XPS investigations of structural changes in the base polymer. *J. Appl. Polym. Sci.* 41: 1251-1260.
- Sanyal, B.; Singhanian, G. K. (1956) Atmospheric corrosion of metals: part I. *J. Sci. Ind. Res. Sect. B* 15: 448-455.
- Satake, J.; Moroishi, T. (1974) Various factors affecting atmospheric corrosion of steels. In: *Proceedings of the fifth international congress on metallic corrosion; May 1972; Tokyo, Japan*. Houston, TX: National Association of Corrosion Engineers; pp. 744-749.
- Schuster, P. F.; Reddy, M. M.; Sherwood, S. I. (1994) Effects of acid rain and sulfur dioxide on marble dissolution. *Mater. Perform.* 33: 76-80.
- Schwarz, H. (1972) On the effect of magnetite on atmospheric rust and on rust under a coat of paint. *Werkst. Korros.* 23: 648-663.
- Sengupta, M.; de Gast, A. A. (1972) Environmental deterioration and evaluation for dimension stone. *CIM Bull.* 65: 54-58.
- Sereda, P. J. (1958) Measurement of surface moisture. *ASTM Bull.* (228): 53-55.
- Sereda, P. J. (1974) Weather factors affecting corrosion of metals. In: *Corrosion in natural environments: three symposia presented at the 76th annual meeting of the American Society for Testing and Materials; June 1973*;

- Philadelphia, PA. Philadelphia, PA: American Society for Testing and Materials; pp. 7-22. (ASTM special technical publication 558).
- Showak, W.; Dunbar, S. R. (1982) Effect of 1 percent copper addition on atmospheric corrosion of rolled zinc after 20 years' exposure. In: Dean, S. W.; Rhea, E. C., eds. Atmospheric corrosion of metals: a symposium; May 1980; Denver, CO. Philadelphia, PA: American Society for Testing and Materials; pp. 135-162. (ASTM special technical publication 767).
- Simpson, J. W.; Horrobin, P. J., eds. (1970) The weathering and performance of building materials. New York, NY: Wiley-Interscience.
- Sinclair, J. D. (1992) The relevance of particle contamination to corrosion of electronics in processing and field environments. *Proc. Electrochem. Soc.* 93-1: 325-335.
- Skerry, B. S.; Johnson, J. B.; Wood, G. C. (1988a) Corrosion in smoke, hydrocarbon and SO<sub>2</sub> polluted atmospheres—I. general behaviour of iron. *Corros. Sci.* 28: 657-695.
- Skerry, B. S.; Wood, J. C.; Johnson, J. B.; Wood, G. C. (1988b) Corrosion in smoke, hydrocarbon and SO<sub>2</sub> polluted atmospheres—II. mechanistic implications for iron from surface analytical and allied techniques. *Corros. Sci.* 28: 697-719.
- Smith, V. K.; Gilbert, C. C. S. (1985) The valuation of environmental risks using hedonic wage models. In: Martin, D.; Smeeding, T., eds. Horizontal equity, uncertainty, and economic well-being. Chicago, IL: University of Chicago Press; pp. 359-391.
- Spence, J. W.; Haynie, F. H. (1972) Paint technology and air pollution: a survey and economic assessment. Research Triangle Park, NC: U.S. Environmental Protection Agency, Office of Air Programs; publication no. AP-103. Available from: NTIS, Springfield, VA; PB-210736.
- Spence, J. W.; Haynie, F. H. (1990) Derivation of a damage function for galvanized steel structures: corrosion kinetics and thermodynamic considerations. In: Baboian, R.; Dean, S. W., eds. Corrosion testing and evaluation: silver anniversary volume. Philadelphia, PA: American Society for Testing and Materials; pp. 208-224. (ASTM special technical publication 1000).
- Spence, J. W.; Haynie, F.; Upham, J. B. (1975) Effects of gaseous pollutants on paints: a chamber study. *J. Paint Technol.* 47: 57-63.
- Spence, J. W.; Haynie, F. H.; Lipfert, F. W.; Cramer, S. D.; McDonald, L. G. (1992) Atmospheric corrosion model for galvanized steel structures. *Corrosion* 48: 1009-1019.
- Stanners, J. F. (1970) Use of environmental data in atmospheric corrosion studies. *Br. Corros. J.* 5: 117-121.
- Sweevers, H.; Van Grieken, R. (1992) Analytical study of the deterioration of sandstone, marble and granite. *Atmos. Environ. Part B* 26: 159-163.
- Sydberger, T. (1976) Influence of sulfur pollution on the atmospheric corrosion of steel. Goteborg, Sweden: Chalmers University of Technology and University of Gothenburg, Department of Inorganic Chemistry.
- Sydberger, T.; Ericsson, R. (1977) Laboratory testing of the atmospheric corrosion of steel. *Werkst. Korros.* 28: 154-158.
- Terrat, M.-N.; Joumard, R.. (1990) The measurement of soiling. *Sci. Total Environ.* 93: 131-138.
- Tomashov, N. D. (1966) Theory of corrosion and protection of metals: the science of corrosion. New York, NY: The Macmillan Company.

- U.S. Environmental Protection Agency. (1982) Air quality criteria for particulate matter and sulfur oxides. Research Triangle Park, NC: Office of Health and Environmental Assessment, Environmental Criteria and Assessment Office; EPA report no. EPA-600/8-82-029aF-cF. 3v. Available from: NTIS, Springfield, VA; PB84-156777.
- Upham, J. B. (1967) Atmospheric corrosion studies in two metropolitan areas. *J. Air Pollut. Control Assoc.* 17: 398-402.
- van Aalst, R. M. (1986) Dry deposition of aerosol particles. In: Lee, S. D.; Schneider, T.; Grant, L. D.; Verkerk, P. J., eds. *Aerosols: research, risk assessment and control strategies, proceedings of the second U.S.-Dutch international symposium*; May 1985; Williamsburg, VA. Chelsea, MI: Lewis Publishers, Inc.; pp. 933-949.
- Vernon, W. H. J. (1931) A laboratory study of the atmospheric corrosion of metals. Part I.—The corrosion of copper in certain synthetic atmospheres, with particular reference to the influence of sulphur dioxide in air of various relative humidities. *Trans. Faraday Soc.* 27: 255-277.
- Vernon, W. H. J. (1935) A laboratory study of the atmospheric corrosion of metals. *Trans. Faraday Soc.* 31: 1668-1700.
- Vero, L. B.; Sila, M. M. (1976) Isolation of various sulphur-oxidizing bacteria from stone monuments. In: *The conservation of stone: proceedings of the international symposium*; June; Bologna, Italy.
- Walton, J. R.; Johnson, J. B.; Wood, G. C. (1982) Atmospheric corrosion initiation by sulphur dioxide and particulate matter: I. test-cell apparatus for simulated atmospheric corrosion studies. *Br. Corros. J.* 17: 59-64.
- Webb, A. H.; Bawden, R. J.; Busby, A. K.; Hopkins, J. N. (1992) Studies on the effects of air pollution on limestone degradation in Great Britain. *Atmos. Environ. Part B* 26: 165-181.
- Williams, R. S. (1987) Acid effects on accelerated wood weathering. *For. Prod. J.* 37: 37-38.
- Williams, R. S. (1988) Effect of dilute acid on the accelerated weathering of wood. *JAPCA* 38: 148-151.
- Williams, R. S.; Winandy, J. E.; Feist, W. C. (1987) Paint adhesion to weathered wood. *J. Coat. Technol.* 59: 43-49.
- Winkler, E. M. (1966) Important agents of weathering for building and monumental stone. *Eng. Geol. (Amsterdam)* 1: 381-400.
- Wittenburg, C.; Dannecker, W. (1992) Dry deposition and deposition velocity of airborne acidic species upon different sandstones. In: *Proceedings of the 1992 European aerosol conference*; September; Oxford, United Kingdom. *J. Aerosol Sci.* 23(suppl. 1): S869-S872.
- Wolff, G. T.; Collins, D. C.; Rodgers, W. R.; Verma, M. H.; Wong, C. A. (1990) Spotting of automotive finishes from the interactions between dry deposition of crustal material and wet deposition of sulfate. *J. Air Waste Manage. Assoc.* 40: 1638-1648.
- Xu, J. R.; Balik, C. M. (1989) Infrared attenuated total reflectance study of latex paint films exposed to aqueous sulfur dioxide. *J. Appl. Polym. Sci.* 38: 173-183.
- Xu, J. R.; Balik, C. M. (1990) Studies of latex paint films exposed to aqueous SO<sub>2</sub>: pH effects. *J. Appl. Polym. Sci.* 39: 1957-1966.
- Yerrapragada, S. S.; Jaynes, J. H.; Chirra, S. R.; Gauri, K. L. (1994) Rate of weathering of marble due to dry deposition of ambient sulfur and nitrogen dioxides. *Anal. Chem.* 66: 655-659.
- Yocom, J. E. (1982) Indoor-outdoor air quality relationships: a critical review. *J. Air Pollut. Control Assoc.* 32: 500-520.

Yocom, J. E.; Grappone, N. (1976) Effects of power plant emissions on materials. Palo Alto, CA: Electric Power Research Institute; report no. EPRI/EC-139. Available from: NTIS, Springfield, VA; PB-257 539.

Yocom, J. E.; Upham, J. B. (1977) Effects of economic materials and structures. In: Air pollution: v. 11, the effects of air pollution. 3rd ed. New York, NY: Academic Press, Inc.; pp. 93-94.

Zhang, X. Q.; McMurry, P. H.; Hering, S. V.; Casuccio, G. S. (1993) Mixing characteristics and water content of submicron aerosols measured in Los Angeles and at the Grand Canyon. Atmos. Environ. Part A 27: 1593-1607.

# 10. DOSIMETRY OF INHALED PARTICLES IN THE RESPIRATORY TRACT

## 10.1 INTRODUCTION

Development of an efficient air-breathing respiratory tract was a critical requirement for mammalian evolution. The combination of airways and airspaces in an internalized and arborized arrangement that expands with incoming tidal air and contracts with its ebb led to the vertebrate lung. This very design that led to the close proximity of the alveolar air spaces to the outside environment for efficient air exchange also makes the lung vulnerable to insult by inorganic and organic dusts, and by microorganisms. The intense perfusion of these spaces by essentially the entire cardiac output also makes the lung vulnerable to many blood-borne, chemical, microbial, and immunologic agents.

It is a basic tenet of toxicology that the dose delivered to the target site, not the external exposure, is the proximal cause of a response. Therefore, there is increased emphasis on understanding the exposure-dose-response relationship. In the case of PM, exposure is what gets measured (or estimated) in the typical study and what gets regulated; inhaled dose is the causative factor. Even if inhaled dose could be easily defined, it fits within a complex continuum. For example, as illustrated in Figure 10-1, it is ultimately desirable to have a comprehensive biologically-based dose-response model that incorporates the mechanistic determinants of chemical disposition, toxicant-target interactions, and tissue response integrated into an overall model of pathogenesis. Mathematical dosimetry models that incorporate mechanistic determinants of disposition (deposition, absorption, distribution, metabolism, and elimination) of chemicals have been useful in describing relationships along this continuum (e.g., between exposure concentration and target tissue dose), particularly as applied to describing these relationships for the exposure-dose-response component of risk assessment. With each progressive level, incorporation and integration of mechanistic determinants allow further elucidation of the exposure-dose-response continuum and, depending on the knowledge of model parameters and fidelity to the biological system, a more accurate characterization of the pathogenetic process. Thus, once the site and

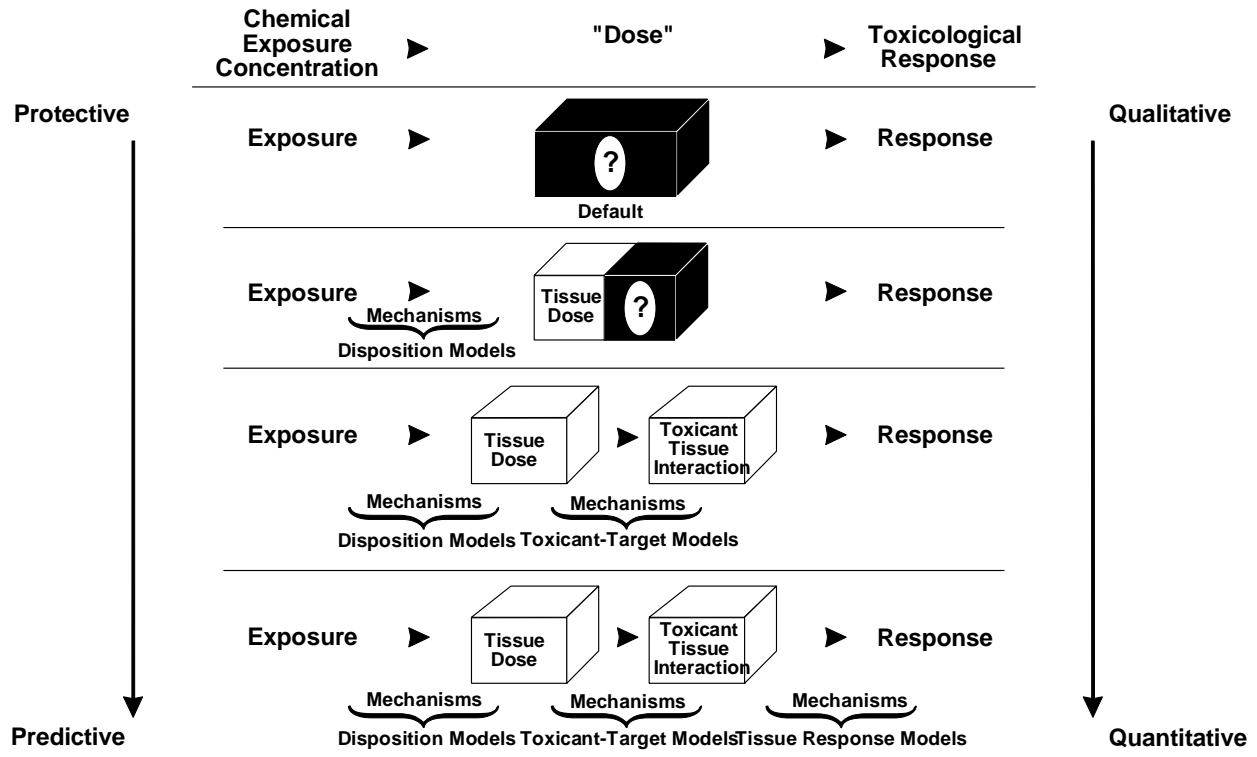


**Figure 10-1. Schematic characterization of comprehensive exposure-dose-response continuum and the evolution of protective to predictive dose-response estimates.**

Source: Adapted from Conolly (1990) and Andersen et al. (1992).

mechanisms are known, dosimetry may prove useful in linking exposure to internal dose and effects, and to the extrapolation of variability both within and across species. For example, a healthy individual and a person with emphysema will not get identical doses to specific lung regions even if their external exposure is identical. Knowledge of how and to what extent disease factors affect dose can assist in characterizing susceptible subpopulations. If a rat and a human are identically exposed, they will receive different doses to regions of the respiratory tract. Insofar as this is quantitatively understood, laboratory animal data can be made more useful in assessing human health risks.

Characterization of the exposure-dose-response continuum for PM requires the elucidation and understanding of the mechanistic determinants of inhaled particle dose, toxicant-target interactions, and tissue responses. Only the first level of characterization, i.e., description of the factors that influence inhaled dose has been accomplished to any degree for PM. Inhaled particles are deposited in the respiratory tract by mechanisms of interception, impaction, sedimentation, diffusion, and electrostatic precipitation. The relative contribution of each deposition mechanism to the fraction of inhaled particles deposited varies for each region of the respiratory tract (extrathoracic, ET; tracheobronchial, TB; and alveolar, A). Subsequent clearance of deposited particles depends on the initial deposition site, physicochemical properties of the particles (e.g., solubility), translocation mechanisms such as mucociliary transport and endocytosis by macrophages or epithelial cells, and on the time since initial deposition. Retained particle burdens and ultimate particle disposition are determined by the dynamic relationship between deposition and clearance mechanisms.

The biologically effective dose resulting from inhalation of airborne particles can be defined as the time integral of total inhaled particle mass, particle number, or particle surface area per unit of surface area (e.g., surface area of a given region such as the TB) or per unit mass of the respiratory tract. Choice of the metric to characterize the biologically effective inhaled dose should be motivated by insight on the mechanisms of action of the compound (or particles) in question. Conceptually, as illustrated in Figure 10-2, the exposure-dose-response continuum can be represented as events in the progression from exposure to disease. The components depicted in Figure 10-2 are not necessarily discrete, nor the only events in the continuum, and represent a conceptual temporal sequence. The left-most component of the continuum generally precedes any component to the right, but some impacts may be detectable in parallel. As our understanding of the continuum is supplemented by identification of the important intervening relationships and the components are characterized more precisely or with greater detail, the health events of concern can be viewed as a series of changes from homeostatic adaptation, through dysfunction, to disease and death. The critical effect could become that biologic marker deemed most pathognomonic or of prognostic significance, based on validated hypotheses of the role of the marker in the development of disease. The appropriate dose metric would then be defined by a measure

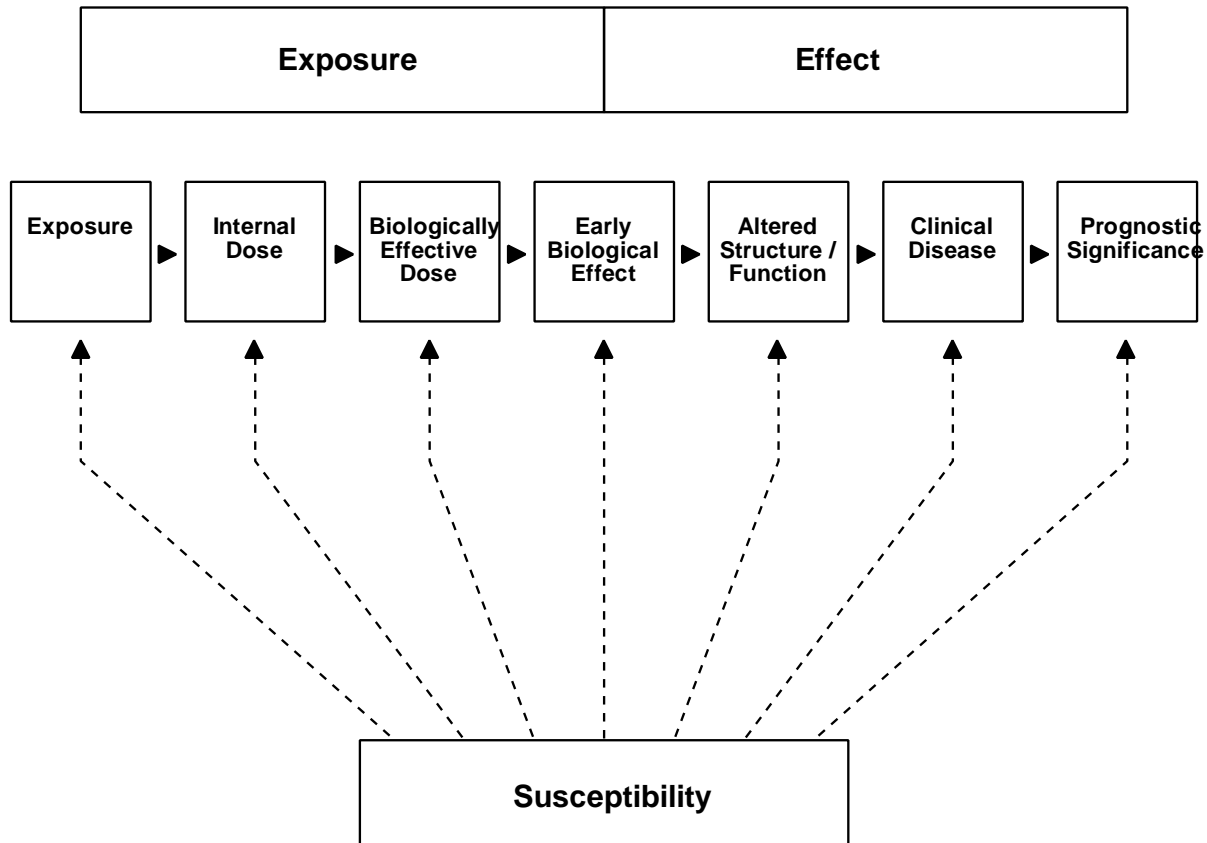


**Figure 10-2. Biological marker components in sequential progression between exposure and disease.**

Source: Schulte (1989).

that characterizes the biologically effective dose for the mechanism of action causing that critical effect.

Elucidation of the toxic moiety as well as the mechanism of action for PM have remained elusive, however. The link to the epidemiological findings discussed in Chapter 12 lies in understanding the sites of injury and the types of injury. The appropriate dose metric for PM might accurately be described by particle deposition alone of the particles exert their primary action on the surface contacted (Dahl et al., 1991). For longer-term effects, the deposited dose may not be a decisive metric, since particles clear at varying rates from the different respiratory tract regions. At this point, when considering the epidemiologic data, dose metrics can only be separated into two major categories: (1) the pattern and quantity of deposited particle burdens,

and (2) the pattern and quantity of retained particle burdens. The deposited dose or initial acute deposition (e.g., particle mass burden per 24-hours) may be relevant to "acute" effects observed in the epidemiologic studies such as "acute" mortality, hospital admissions, work loss days, etc. On the other hand, retained dose may be more appropriate for chronic responses such as induction of chronic disease, shortening of life-span ("premature mortality"), morbidity, or diminished quality of life.

Another aspect of the definition of the dose metric that would benefit from mechanism of action information include whether mass is the appropriate measure of particle burden and how to normalize the inhaled particle burdens. To date, most of the epidemiologic studies have relied upon the particle mass concentration ( $\mu\text{g}/\text{m}^3$ ) to characterize particle exposures. Alternative expressions that may be more relevant to certain mechanisms of injury include numbers of particles or aggregate particle surface area. For example, the fine fraction contains by far the largest number of particles and those particles have a large aggregate surface area. Oberdörster et al. (1992) have shown ultrafine particles are less effectively phagocytosed by macrophages than larger particles. Anderson et al. (1990) have shown that the deposition of ultrafine particles in patients with COPD is greater than in healthy subjects. The need to consider particle number is accentuated when the high deposition efficiency of small particle numbers in the lower respiratory tract, the putative target for both the mortality and morbidity effects of PM exposures, is taken into account.

Insight on how PM causes injury would also inform what normalizing factor to use to define the dose metric. Particle mass or number burdens could be normalized to respiratory tract surface area, to lung mass, or to other anatomical or functional units critical to determining the toxicity such as ventilatory units, alveoli, or macrophages. Clearly, inhaled dose is important, but the most appropriate dose metric or metrics to quantitatively link with the observed acute or chronic health outcomes await elucidation of the pertinent mechanisms of injury and tissue response.

For the present document, average daily deposited particle mass burden in each region of the respiratory tract has been selected as the dose metric to characterize "acute" effects. Average retained particle mass burden in each region for humans and in the lower respiratory tract for laboratory animals has been selected as the dose metric for "chronic" effects. As discussed in Section 10.7.3., these choices were dictated by the selection of the dosimetry models and the

availability of anatomical and morphometric information. Both deposited particle mass and number burdens in each respiratory tract region are estimated for human exposures. Retained particle burdens are normalized per gram of lung tissue.

The chapter first describes important particle characteristics and the basic mechanisms of particle deposition and clearance in the respiratory tract. The available mathematical dosimetry models for humans and laboratory animals are reviewed as a background to the application presented in Section 10.7. Dosimetry models are selected for human exposure simulations and to perform interspecies extrapolation of laboratory animal toxicity studies. The rationale for selection of the extrapolation models is provided. An attempt is made to ascertain whether dosimetry modeling can provide insight into the apparent discrepancies between the epidemiologic and laboratory animal data, to identify plausible dose metrics of relevance to the available health endpoints, and to identify modifying factors that may enhance susceptibility to inhaled particles. Simulations of variability due to key modifying factors (age, gender, disease status) are also attempted. This information should be useful to the interpretation of health effects data in Chapters 11 and 12.

The chapter deals exclusively and generically with aerosols (i.e., both airborne droplets and solid particles, including the hygroscopic, acidic variety). It briefly reviews selected studies that have been reported in the literature on particle deposition and retention since the publication of the 1982 Air Quality Criteria Documents on Particulate Matter and Sulfur Oxides and the 1989 Acid Aerosols Issue Paper (U.S. Environmental Protection Agency; 1982, 1989), but the focus is on newer information.

## **10.2 CHARACTERISTICS OF INHALED PARTICLES**

Information about particle size distribution aids in the evaluation of the effective inhaled dose. Because the characteristics of inhaled particles interact with the other major factors controlling comparative inhaled dose, this section discusses aerosol attributes requiring characterization and provides general definitions.

An aerosol is a suspension of finely dispersed solids or liquids in air. It is intrinsically unstable, and hence, tends to deposit both continuously and inelastically onto exposed surfaces. From the perspective of health-related actions of aerosols, interest is limited to particles that can

at least penetrate into the nose or mouth and that deposit on respiratory tract surfaces. For humans, this constraint ordinarily eliminates very coarse particles, viz., greater than about 100  $\mu\text{m}$  diameter. Particles between 1  $\mu\text{m}$  and 20  $\mu\text{m}$  diameter are commonly encountered in the work place and the ambient air. Still smaller, i.e., submicron diameter particles (less than 1  $\mu\text{m}$  in diameter) are generally the most numerous in the environmental air, with the number concentration of particles tending to increase markedly for smaller particles. Even particles down to the nanometer (nm) size domain are found in the atmosphere and are of interest, although until recently, these "ultrafine" particles were of greater interest to atmospheric scientists than to biomedical scientists. Typically, "ultrafine" aerosols are produced by highly energetic reactions (e.g., high temperature sublimation and combustion, or by gas phase reactions involving atmospheric pollutants). Note that 10 nm = 100 Ångstroms = 0.01  $\mu\text{m}$  or  $1 \times 10^{-6}$  cm diameter.

Because aerosols can consist of almost any material, descriptions of aerosols in simple geometric terms can be misleading unless important factors relating to size, shape, and density are considered. Aerosol constituents are usually described in terms of their chemical composition and geometric or aerodynamic sizes. Additionally, aerosol particles may be defined in terms of particle surface area. It is important to note that aerosols present in natural and work environments all have polydisperse size distributions. This means that the particles comprising the aerosols have a range of geometric size, aerodynamic size, and surface area and are more appropriately described in terms of size distribution parameters. Aerosol sampling devices can be used to collect bulk or size fractions of aerosols to allow defining the size distribution parameters. In this procedure, the amount of particles in defined size parameter groups (number, mass, or surface area) is divided by the total number, mass, or surface of all particles collected and divided also by the size interval for each group. Data from the sampling device are then expressed in terms of the fraction of particles per unit size interval. The next step is to use this information to define an appropriate particle size distribution.

The lognormal distribution has been widely used for describing size distributions of radioactive aerosols (Hatch and Choate, 1929; Raabe, 1971) and is also generally used as a function to describe other kinds of aerosols. For many aerosols, their size distribution may be described by a lognormal distribution, meaning that the distribution will resemble the bell-shaped Gaussian error curve, if the frequency distribution is based on the logarithms of the

particle size. The lognormal distribution is a skewed distribution characterized by the fact that the logarithms of particle diameter are normally distributed. In linear form, the logarithmic mean is the median of the distribution. The standard deviation,  $\sigma$ , of this logarithmic normal distribution is a logarithm, so that addition and subtraction of this logarithm to and from the logarithmic mean is equivalent to multiplying and dividing the median by the factor  $\sigma_g$ , with  $\ln \sigma_g = \sigma$ . The factor  $\sigma_g$  is defined as the geometric standard deviation. When any aerosol distribution is "normalized", it acquires parameters and properties equivalent to those of the Gaussian distribution. Accordingly, the only two parameters needed to describe the log normal distribution are the median diameter and the geometric standard deviation,  $\sigma_g$ , (ratio of the log 84%/log 50% size cut or log 50%/log 16% size cut, where the 50% size cut is the median). For a distribution formed by counting particles, the median is called the count median diameter (CMD). While there may be occasions when the number of the particles is of the greatest interest, the distribution of mass in an aerosol according to particle size is of interest if particle mass determines the dose of interest. Derivation of the particle mass distribution is essentially a matter of converting a diameter distribution to a diameter-cubed distribution since the volume of a sphere with diameter  $d$  is  $\pi d^3/6$  and mass is simply the product of particle volume and physical density.

The cumulative distribution of a lognormally distributed size distribution is conveniently evaluated using log-probability graph paper on which the cumulative distribution forms a straight line (Figure 10-3). This distribution can be used for all three lognormally distributed particle size parameters discussed above, which are related as indicated in Figure 10-3. The characteristic parameters of this distribution are the size and  $\sigma_g$ . The CMD is characterized by the fact that half of the particles in the size distribution are larger than the CMD and half of the particles are smaller. Multiplying and dividing the CMD by  $\sigma_g$  yields the particle size interval for the distribution that contains about 68% of the particles by number.

When particles are not spherical, equivalent diameters can be used in place of the physical diameters of particles. A calculated parameter, the projected area diameter (diameter of a circle having a cross sectional area equivalent to the particles in the distribution of interest) is often used as the equivalent diameter.

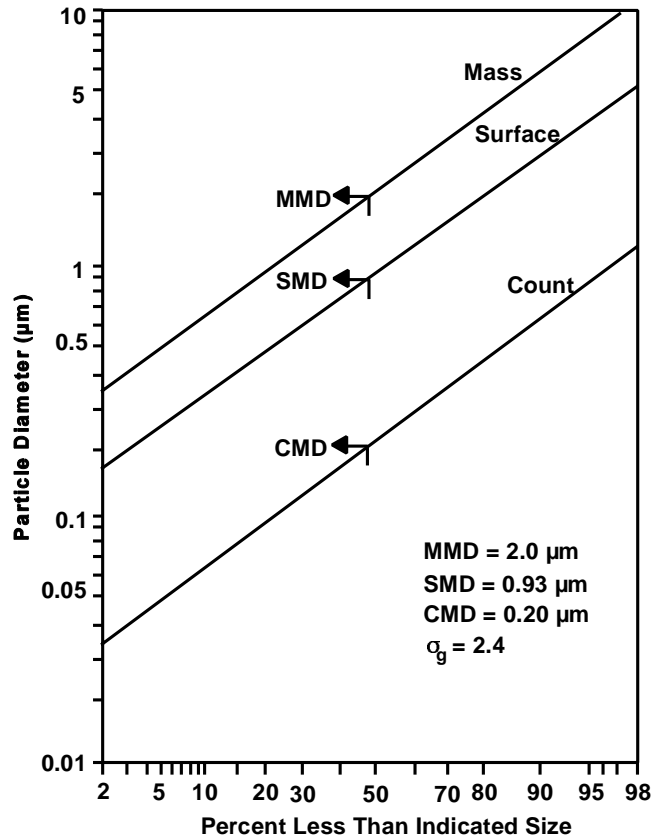


**Figure 10-3. Lognormal particle size distribution for a hypothetical polydisperse aerosol.**

The mass median diameter (MMD) and surface median diameter (SMD), also shown in Figure 10-3, are additional ways to describe size distributions of lognormally distributed aerosols. In these distributions, half of the mass or surface area of particles is associated with particles smaller than the MMD or SMD; the other half of the particles is associated with particles larger than the MMD or SMD, respectively.

The relationship of the various lognormal distribution parameters based on geometric diameter of particles is unique, since the CMD, SMD, and MMD are all lognormal with the same  $\sigma_g$ , but with different means that can be calculated. The CMD and  $\sigma_g$  can be determined and extrapolated to MMD, and SMD using the following relationships

$$\ln(\text{MMD}) = \ln(\text{CMD}) + 3(\ln\sigma_g)^2, \quad (10-1)$$

and

$$\ln(\text{SMD}) = \ln(\text{CMD}) + 2(\ln\sigma_g)^2. \quad (10-2)$$

For most aerosols, it is useful to define a particle's size in terms of its aerodynamic size whereby particles of differing geometric size, shape and density are compared aerodynamically with the instability behavior of particles that are unit density ( $1 \text{ gm/cm}^3$ ) spheres. The aerodynamic behavior of unit density spherical particles can be determined, both experimentally and theoretically, consequently, the aerodynamic diameter constitutes a useful standard by which all particles can be compared in matters of inertial impaction and gravitational settling. Thus, if the terminal settling velocity of a unit density sphere of  $10 \text{ }\mu\text{m}$  diameter is measured in still air, the velocity induced by gravity would be  $\sim 3 \times 10^{-1} \text{ cm/s}$ . If the gravitational settling of an irregularly shaped particle of unknown density was measured and the same terminal velocity was obtained, the particle would have a  $10 \text{ }\mu\text{m}$  aerodynamic diameter ( $d_{ae}$ ). Its tendency to deposit by inertial processes on environmental surfaces or onto the surfaces of the human respiratory tract will be the same as for the  $10 \text{ }\mu\text{m}$  unit density sphere.

A term that is frequently encountered is mass median aerodynamic diameter (MMAD), which refers to the mass median of the distribution of mass with respect to aerodynamic diameter. With commonly-encountered aerosols having low to moderate polydispersity,  $\sigma_g \leq 2.5$ , the Task Group on Lung Dynamics (TGLD) (1966) showed that mass deposition in the human respiratory tract could be approximated by the deposition behavior of the particle of median aerodynamic size in the mass distribution, the so-called MMAD. This is successful because the particles which dominate the mass distribution are those which deposit mainly by settling and inertial impaction.

In many urban environments, the aerosol frequency and mass distributions have been found to be bimodal or trimodal (Figure 10-4), usually indicating a composite of several log normal distributions where each aerosol mode was presumably derived from different formation mechanisms or emission sources (John et al., 1986). Conversely, in the laboratory, experimentalists often create aerosol distributions which are lognormal or normal, and very frequently, they generate monodisperse aerosols consisting of particles of nearly one size. The use of monodisperse aerosols of nearly uniform, unit density, spherical particles

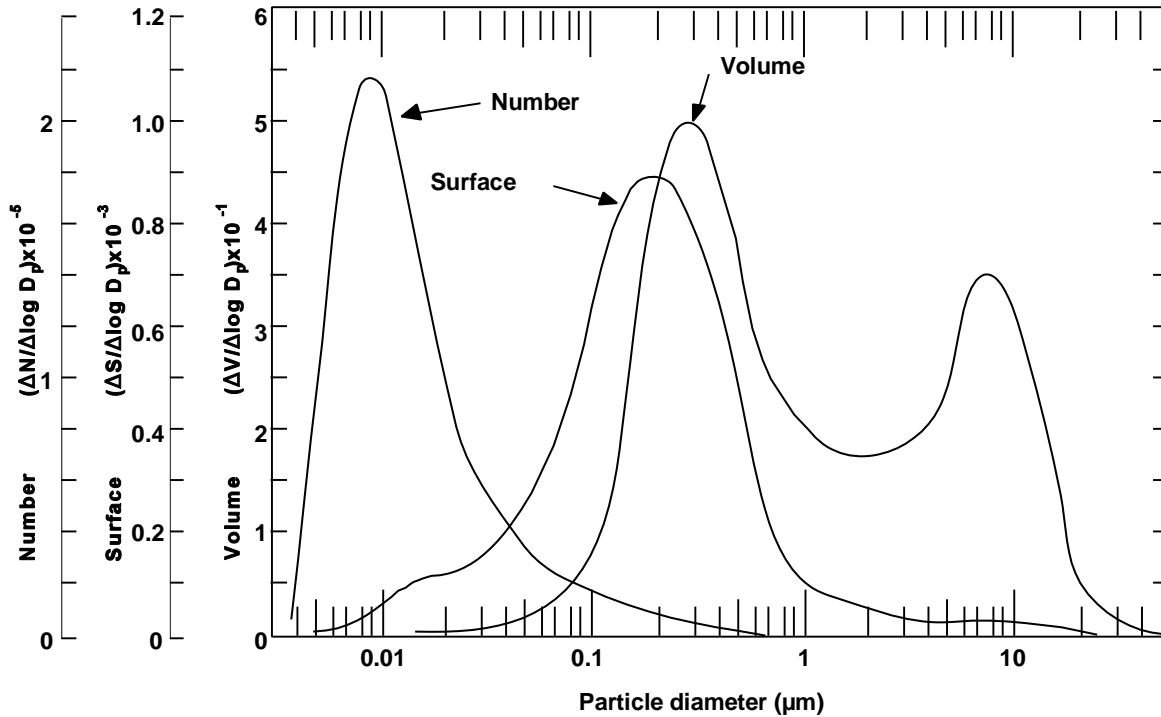


**Figure 10-4.** These normalized plots of number, surface, and volume (mass) distributions from Whitby (1975) show a bimodal mass distribution in a smog aerosol. Historically, such particle size plots were described as consisting of a coarse mode (2.5 to 15  $\mu\text{m}$ ), a fine mode (0.1 to 2.5  $\mu\text{m}$ ), and a nuclei mode ( $< 0.05\mu\text{m}$ ). The nuclei mode would currently fall within the ultrafine particle range (0.005 to 0.1  $\mu\text{m}$ ).

greatly simplifies experimental deposition and retention measurements and also instrument calibrations. With nearly uniform particles, the mass, surface area and frequency distributions are nearly identical, another important simplification.

The terms count median aerodynamic diameter (CMAD) and surface median aerodynamic diameter (SMAD) might be encountered. These distributions are useful in that they include consideration of aerodynamic properties of the particles. If the particle aerodynamic or diffusive diameter is determined when sizing is done, then the median of the particle size distribution is the CMAD, or count median diffusive (or thermodynamic) diameter (CMDD or CMTD), respectively. If the mass of particles is of concern, then the median that is derived is the MMAD or mass median diffusive (or thermodynamic) diameter (MMDD or MMTD). Generally, MMTDs or MMADs are generally used to evaluate particle deposition patterns in the respiratory tract because deposition of inhaled aerosol particles, as discussed in detail later in this chapter, is

determined primarily by particle diffusive and aerodynamic properties of the particles rather than simply particle physical size, surface area, volume, or mass. Activity median aerodynamic diameter (AMAD) is the median of the distribution of radioactivity or toxicological or biological activity with respect to size. Both MMAD and AMAD are determined using aerosol sampling devices such as multistage impactors. When particles become smaller than about 0.1  $\mu\text{m}$  diameter, their instability as an aerosol depends mainly on their interaction with air molecules. Like particles in Brownian motion, they are caused to "diffuse". For these small particles and especially for ultrafine particles, this interaction is independent of the particle density and varies only with geometric particle diameter. Very small particles are not expressed in aerodynamic equivalency, but instead to a thermodynamic-equivalent size. The thermodynamic particle diameter ( $d_{\text{TH}}$ ) is the diameter of a spherical particle that has the same diffusion coefficient in air as the particle of interest. The activity median thermodynamic diameter (AMTD) is the diameter associated with 50 percent of the activity for particles classified thermodynamically.

The selection of the particle size distribution to associate with health effects depends on decisions about the importance of number of particles, mass of particles, or surface area of particles in producing the effects. In some situations, numbers of particles or mass of particles phagocytized by alveolar macrophages may be important; in other cases, especially for particles that contain toxic constituents, surface area may be the most important parameter that associates exposures with biological responses or pathology. These particle distributions should all be considered during the course of evaluating relationships between inhalation exposures to particles and effects resulting from the exposures.

Most of the discussion in the remainder of this chapter will focus on MMAD because it is the most commonly used measure of aerosol distributions. If MMAD is not measured directly, an alternative is to estimate MMAD from one of the particle size distributions that is based on physical size of the particles (CMD, MMD, and SMD), which can all be readily converted to MMAD. The approximate conversion of MMD to MMAD is made using the following relationship (neglecting correction for slip)

$$\text{MMAD} = \text{MMD} \cdot (\text{particle density})^{0.5}. \quad (10-3)$$

By definition, MMDD = CMTD, because behavior of particles in this size category does not usually depend on aerodynamic properties.

Because small particles have a large aggregate surface area, aerosols comprised of such particles have increased potential for reactivity. For example, tantalum is a very stable, unreactive metal, whereas aerosols of tantalum particles can be caused to explode by a spark. The rates of oxidation and solubility are proportional to surface area as are the processes of gas adsorption and desorption, and vapor condensation and evaporation. Accordingly, special concerns arise from gas-particle mixtures and from "coated" particles. For a general review of atmospheric aerosols, their characteristics and behavior, the publication *Airborne Particles* prepared under the aegis of the National Research Council (1979) is recommended.

### **10.3 ANATOMY AND PHYSIOLOGY OF THE RESPIRATORY TRACT**

The respiratory systems of humans and various laboratory animals differ in anatomy and physiology in many quantitative and qualitative ways. These differences affect air flow patterns in the respiratory tract, and in turn, the deposition of an inhaled aerosol. Particle deposition connotes the removal of particles from their airborne state due to their inherent instabilities in air as well as to additional instabilities in air induced when additional external forces are applied. For example, in tranquil air, a 10  $\mu\text{m}$  diameter unit-density particle only undergoes sedimentation due to the force of gravity. If a 10  $\mu\text{m}$  particle is transported in a fast moving air stream, it acquires an inertial force that can cause it to deposit on a surface projecting into the air stream without significant regard to gravitational settling. For health-related issues, interest in particle deposition is limited to that which occurs in the respiratory tract of humans and laboratory animals during the respiration of dust-laden air.

Once particles have deposited onto the surfaces of the respiratory tract, some will undergo transformation, others will not, but subsequently, all will be subjected either to absorptive or non-absorptive particulate removal processes, e.g., mucociliary transport, or a combination thereof. This will result in their removal from the respiratory tract surfaces. Following this, they will undergo further transport which will remove them, to a greater or less degree, from the respiratory tract. Such particulate matter is said to have undergone clearance. To the extent

particulate matter is not cleared, it is retained. The temporal persistence of uncleared (retained) particles within the structure of the respiratory tract is termed retention.

Thus, either the deposited or retained dose of inhaled particles in each region is governed by the exposure concentration, by the individual species anatomy (e.g., airway size and branching pattern, cell types) and physiology (e.g., breathing rate, and clearance mechanisms), and by the physicochemical properties (e.g., particle size, distribution, hygroscopicity, solubility) of the aerosol. The anatomic and physiologic factors are discussed in this section. The physicochemical properties of particles were discussed in Section 10.2. Deposition and clearance mechanisms will be discussed in Section 10.4.

The respiratory tract in both humans and various experimental mammals can be divided into three regions on the basis of structure, size, and function: the extrathoracic (ET) region or upper respiratory tract (URT) that extends from just posterior to the external nares to the larynx, i.e., just anterior to the trachea; the tracheobronchial region (TB) defined as the trachea to the terminal bronchioles where proximal mucociliary transport begins; and the alveolar (A) or pulmonary region including the respiratory bronchioles and alveolar sacs. The thoracic (TH) region is defined as the TB and A regions combined. The anatomic structures included in each of these respiratory tract regions are listed in Table 10-1, and Figure 10-5 provides a diagrammatic representation of these regions as described in the International Commission on Radiological Protection (ICRP) Human Respiratory Tract Model (ICRP66, 1994).

Figure 10-6 depicts how the architecture of the respiratory tract influences the airflow in each region and thereby the dominant deposition mechanisms. The 5 major mechanisms (gravitational settling, inertial impaction, Brownian diffusion, interception and electrostatic attraction) responsible for particle deposition are schematically portrayed in Figure 10-6 and will be discussed in detail in Section 10.4.1.

In humans, the nasal hairs, anterior nares, turbinates of the nose, and glottic aperture in the larynx are areas of especially high air velocities, abrupt directional changes, and turbulence, hence, the predominant deposition mechanism in the ET region for large particles is inertial impaction. In this process, changes in the inhaled airstream direction or magnitude of air velocity streamlines or eddy components are not followed by airborne particles because of their inertia. Large particles ( $>5 \mu\text{m}$  in humans) are more efficiently removed from the

**TABLE 10-1. RESPIRATORY TRACT REGIONS**

Region	Anatomic Structure	Other Terminology
Extrathoracic (ET)	Nose	Head airways region
	Mouth	Nasopharynx (NP)
	Nasopharynx	Upper respiratory tract (URT)
	Oropharynx	Naso-Oro-Pharyngo-Laryngeal (NOPL)
	Laryngopharynx	
	Larynx	
Tracheobronchial (TB)	Trachea	Lower conducting airways
	Bronchi	
	Bronchioles (including terminal bronchioles)	
Alveolar (A)	Respiratory bronchioles	Gas exchange region
	Alveolar ducts	Pulmonary region
	Alveolar sacs	
	Alveoli	

Adapted from: Phalen et al. (1988).

airstream in this region. The respiratory surfaces of the nasal turbinates are in very close proximity to and designed to warm and humidify the incoming air, consequently they can also function effectively as a diffusion deposition site for very small particles and an effective absorption site for water-soluble gases. The turbinates and nasal sinuses are lined with cilia which propel the overlying mucous layer posteriorly via the nasopharynx to the laryngeal region. Thus, the airways of the human head are major deposition sites for the largest inhalable particles ( $>10\ \mu\text{m}$  aerodynamic diameter) as well as the smallest particles ( $<0.1$  micrometers diameter). For the most part, the ET structures are lined with a squamous, non-ciliated mucous membrane. Collectively, the movement of upper airway mucus, whether transported by cilia or gravity, is mainly into the gastrointestinal (GI) tract.

As air is conducted into the airways of the head and neck during inspiration, it first passes through either the nasal passages or mouth. Whereas nasal breathing is normal with most people most of the time, the breathing mode usually depends upon the work load. Work loads which tend to treble or quadruple minute ventilation i.e., go from 10 L/m to

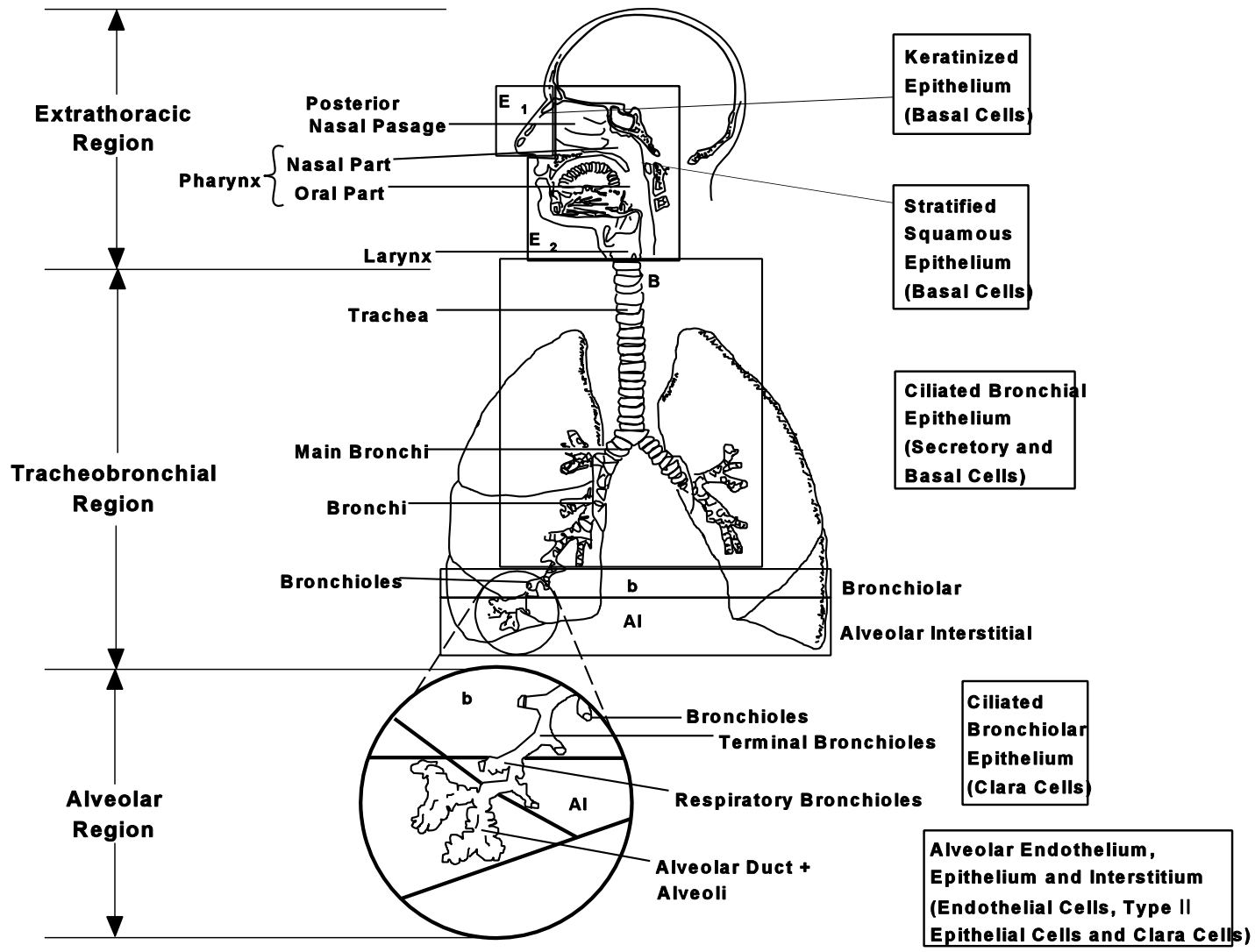
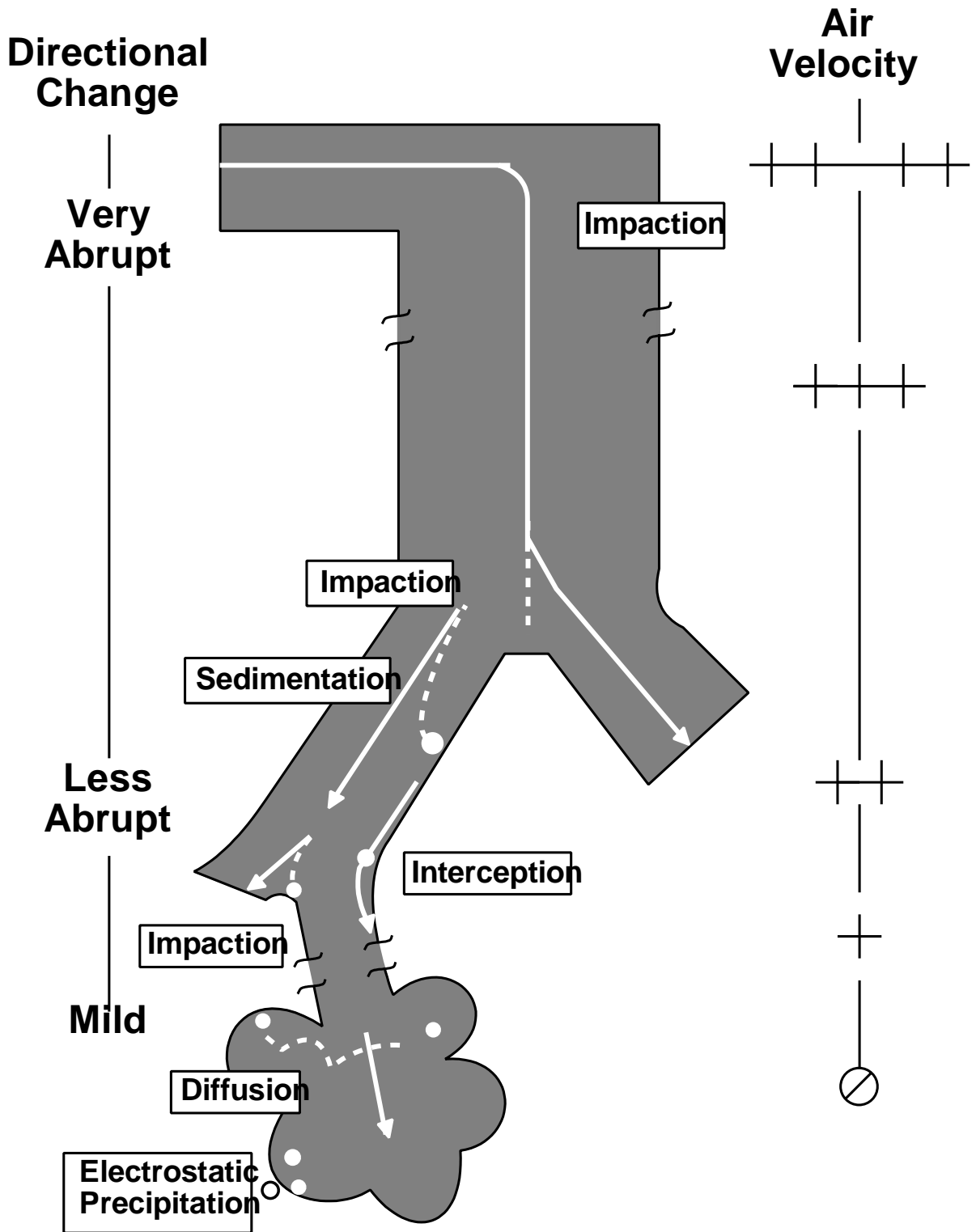


Figure 10-5. Diagrammatic representation of respiratory tract regions in humans.



**Figure 10-6. Schematic representation of five major mechanisms causing particle deposition where airflow is signified by the arrows and particle trajectories by the dashed line.**

Source: Adapted from Casarett (1975); Raabe (1979); Lippmann and Schlesinger (1984).

30 to 40 L/m, cause most subjects to change from nasal to oronasal breathing. In either case, the inspired air then passes through the pharyngeal region into the larynx.

From the larynx, inspired air passes into the trachea, a cylindrical muscular- cartilaginous tube. The trachea measures approximately 1.8 cm diameter  $\times$  12 cm long in humans. The trachea, like other conducting airways of the lungs, is ciliated and richly endowed with secretory glands and mucus-producing goblet cells. The major or main stem bronchi are the first of approximately 16 generations of branching that occur in the human bronchial "tree". For modeling purposes, Weibel (1963;1980) described bronchial branching as regular and dichotomous, i.e., where the branching parent tube gives rise, symmetrically, to two smaller (by approximately  $\sqrt[3]{2}$ ) tubes of the same diameter. While this pattern provides a simplification for modeling, the human bronchial tree actually has irregular dichotomous branching, wherein the parent bronchi gives rise to two smaller tubes of differing diameter and length. The number of generations of branching occurring before the inspired air reaches the first alveolated structures varies from about 8 to 18 (Raabe et al., 1976; Weibel, 1980). The junction of conducting and respiratory airways appears to be a key anatomic focus. Many inhaled particles of critical size are deposited in the respiratory bronchioles that lie just distal to this junction, and many of the changes characteristic of chronic respiratory disease involve respiratory bronchioles and alveolar ducts.

Impaction remains a significant deposition mechanism for particles larger than  $2.5 \mu\text{m}$  aerodynamic equivalent diameter ( $d_{\text{ae}}$ ) in the larger airways of the TB region in humans and competes with sedimentation, with each mechanism being influenced by mean flow rate and residence time, respectively. As the airways successively bifurcate, the total cross-sectional area increases. This increases airway volume in the region, and the air velocity is decreased. With decreases in velocity and more gradual changes in air flow direction as the branching continues, there is more time for gravitational forces (sedimentation) to deposit the particle. Sedimentation occurs because of the influence of the earth's gravity on airborne particles. Deposition by this mechanism can occur in all airways except those very few that are vertical. For particles  $\approx 4 \mu\text{m}$   $d_{\text{ae}}$ , a transition zone between the two mechanisms, from impaction to predominantly sedimentation, has been observed (U.S. Environmental Protection Agency, 1982). This transition zone shifts toward smaller particles for nose breathing.

The surface area of the adult human TB region is estimated to be about 200 cm<sup>2</sup> and its volume is about 150 to 180 mL. At the level of the terminal bronchiole, the most peripheral of the distal conducting airways, the mean airway diameter is about 0.3 to 0.4 mm and their number is estimated at about  $6 \times 10^4$ . As to the variability of bronchial airways of a given size, Weibel's model (1963) considered 0.2 cm diameter airways and noted that such airways occur from the 4th to 14th generations of branching, peaking in frequency around the 8th generation. An insight into the variabilities in various lung models was provided by Forrest (1993) who indicated that the number of terminal bronchioles incorporated in Weibel's model was about 66,000, whereas, Findeisen (1935) used 54,000 and Horsfield and Cumming (1968) estimated only 28,000. The transitional airways of the human lung, the respiratory bronchioles and alveolar ducts, undergo an average of another 6 generations of branching according to Weibel (1980) before they become alveolar sacs. On this basis, the dichotomous lung model indicates there should be about  $8.4 \times 10^6$  branches ( $2^{23}$ ), serving  $3 \times 10^8$  alveoli. The "typical path" model of Yeh and Schum (1980), adopted by the National Council on Radiation Protection (NCRP) (Cuddihy et al., 1988), cites approximately 33,000 terminal bronchioles. The International Commission on Radiological Protection (ICRP) utilized the dimensions from three sources in its human respiratory tract model (ICRP66, 1994).

The parenchymal tissue of the lungs surrounds all of the distal conducting airways except the trachea and portions of the mainstem bronchi. This major branch point area is termed the mediastinum; it is where the lungs are suspended in the thorax by a band of pleura called the pulmonary ligament, the major blood vessels enter and leave the hilus of each lung, and the site of the mediastinal pleura which envelopes the heart and essentially subdivides the thoracic cavity.

Humans lungs are demarcated into 3 right lobes and 2 left lobes by the pleural lining. The suspension of the lungs in an upright human gives rise to a gradient of compliance increasing from apex to base and thereby controls the sequential filling and emptying of the lungs. Subdivisions of the lobes (segments) are not symmetrical due to a fusion of 2 (middle left lung) of the 10 lobar segments of the lung and occasionally an underdeveloped segment in the lower left lobe. Lobar segments can be related to specific segmental bronchi and are useful anatomical delineators for bronchoalveolar lavage.

The lung parenchyma is composed primarily of alveolated structures of the A region and the associated blood vessels and lymphatics. The parenchyma is organized into functional units called acini which consist of the dependent structures of the first order respiratory bronchioles. The alveoli are polyhedral, thin-walled structures numbering approximately  $3 \times 10^8$  in the adult human lung. Schreider and Raabe (1981) provided a range of values, viz,  $2 \times 10^8$  to  $5.7 \times 10^8$ . The parenchymal lung tissue can be likened to a thin sheet of pneumocytes (0.5 to 1.0  $\mu\text{m}$  thickness) that envelops the pulmonary capillary bed and is supported by a lattice of connective tissue fibers: these fibers enclose the alveolar ducts (entrance rings), support the alveolar septa, and anchor the parenchymal structures axially (e.g. from pulmonary veins) and peripherally (from the pleural surface).

The alveolar walls or septa are constructed of a network of meandering capillaries consisting mainly of endothelial cells, an overlying epithelium made of Type I cells or membranous pneumocytes (95% of the surface) with Type II cells or metabolically-active cuboidal pneumocytes (5% of the surface), and an interstitium or interseptal connective tissue space that contains interstitial histiocytes and fibroblasts (Stone et al., 1992). For about one-half of the alveolar surface, the Type I pneumocytes and the capillary endothelia share a fused basement membrane. Otherwise, there is an interstitial space within the septa which communicates along the capillaries to the connective tissue cuffs around the airways and blood vessels. The connective tissue spaces or basal lamina of these structures are served by pulmonary lymphatic vessels whose lymph drainage, mainly perivascular and peribronchial, is toward the hilar region where it is processed en route by islets of lymphoid tissue and filtered principally by the TB lymph nodes before being returned to the circulation via the subclavian veins. From the subpleural connective tissue, lymphatic vessels also arise whose drainage is along the lobar surfaces to the hilar region (Morrow, 1972).

The epithelial surface of the A region is covered with a complex lipo-proteinaceous liquid called pulmonary surfactant. This complex liquid contains a number of surface-active materials, primarily phospholipids, with a predominance of dipalmitoyl lecithin. The surfactant materials exist on the respiratory epithelium non-uniformly as a thin film ( $<0.01 \mu\text{m}$  thick) on a hypophase approximately 10 times thicker. This lining layer stabilizes alveoli of differing dimensions from collapsing spontaneously and helps to prevent the normal capillary effusate from diffusing from the interstitium into the alveolar spaces. The role of the lining layer as an environmental

interface is barely understood, especially in terms of how the layer may modify the physicochemical state of deposited particles and vice versa.

The epithelial surface of the A region, which can exceed 100 m<sup>2</sup> in humans, maintains a population of mobile phagocytic cells, the alveolar macrophage (AM), that have many important functions, e.g. removing cellular debris, eliminating bacteria and elaborating many cytologic factors. The AM is also considered to play a major role in non-viable particle clearance. The resident AM population varies, *inter alia*, according to conditions of particle intake, as does their state of activation. An estimate of the normal AM population in the lungs of non-smokers is about  $7 \times 10^9$  (Crapo et al. 1982) while in the Fischer 344 rat, estimates are about  $2.2 \times 10^7$  to  $2.91 \times 10^7$  AM (Lehnert et al., 1985; Stone et al., 1992). According to prevailing views, the importance of AM-mediated particle clearance via the bronchial airways in the rat and human lungs may be different (refer to Section 10.4.2.).

The respiratory tract is a dynamic structure. During respiration, the caliber and length of the airways changes as do the angles of branching at each bifurcation. The structural changes that occur during inspiration and expiration differ. Since respiration, itself, is a constantly changing volumetric flow, the combined effect produces a complex pattern of airflows during the respiratory cycle within the conducting airways and volumetric variations within the A region. Even if the conducting airways were rigid structures and a constant airflow was passed through the diverging bronchial tree, the behavior of air flow within these structures would differ from that produced by the identical constant flow passed in the reverse or converging direction. Consequently, important distinctions exist between inspiratory and expiratory airflows through the airways, especially those associated with the glottic aperture and nasal turbinates. Distinctions occurring in particle deposition during inspiration and expiration are not as marked as those in airflow. This is because the particles with the greatest tendency to deposit, will deposit during inspiration and will mostly be absent from the expired air.

At rest, the amount of air that is inspired, the tidal volume ( $V_T$ ), is normally about 500 mL. If a maximum inspiration is attempted, about 3300 mL of air can be added; this constitutes the inspiratory reserve volume (IRV). During breathing at rest, the average expired  $V_T$  is essentially unchanged from the average inspired  $V_T$ . At the end of a normal expiration, there still remains in the lungs about 2200 mL, the functional residual capacity (FRC). When a maximum expiration is made at the end of a normal tidal volume, approximately 1000 mL of additional air

will move out of the lung: this constitutes the expiratory reserve volume (ERV). Remaining in the lungs after a maximal expiration is the residual volume (RV) of approximately 1200 mL. These volumes and capacities are illustrated in Figure 10-7. From the perspective of air volumes within the respiratory tract, estimates are based on both anatomic and physiologic measurements. The ET airways have a volume in the average adult of about 80 mL, whereas the composite volume of the transitional airways is about 440 mL. At rest, the total volume in the lungs at end exhalation is usually around 2200 mL and is called the functional residual capacity (FRC). Both the RV and FRC tend to increase with age and in some forms of lung disease (e.g., COPD). The gas exchange volume of the lungs contacts with between 60 and 100 m<sup>2</sup> of alveolar epithelium depending on the state of lung inflation, viz,  $Alv_{sa} = 22 (V_L)^{2/3}$  where the surface area ( $Alv_{sa}$ ) is in m<sup>2</sup> and the lung volume ( $V_L$ ) in liters (or cubic decimeters). The alveolar volume is juxtaposed with a pulmonary capillary blood volume (70 to 230 mL) which varies with cardiac output and contacts an endothelial surface area of comparable size to that of the alveoli.

The average respiratory frequency of an adult human at rest is about 12 to 18 cycles per min. This indicates a cycle length of 4 to 5 s: about 40% for inspiration and 60% for expiration. With a 500 mL  $V_T$ , this results in a minute ventilation ( $V_E$ ) of about 6 to 7.5 L/min: about 60 to 70% of the  $V_E$  is considered alveolar ventilation due to the dead space volume constituting about 30 to 40% of the  $V_T$ . With the foregoing assumptions, the mean inspiratory and expiratory air flows will be about 250 mL/s and 166 mL/s, respectively. During moderate to heavy exercise, the  $V_E$  will increase by up to 10-fold or more (35 to 70 L/min or more). This is accomplished initially and primarily by an increase in  $V_T$  ( $V_T$  reaches approximately 2.0 L and frequency approximately 30 to 35 per min at a ventilation of 60 to 70 L per min). There is considerable variation in response. One impact of such an assumed change in  $V_E$  is that the duration of the respiratory phases become shorter and more similar, consequently, the mean inspired and expired air flows will both likely increase to about  $\geq 2,000$  mL/s. With nose breathing, an inspiratory airflow of

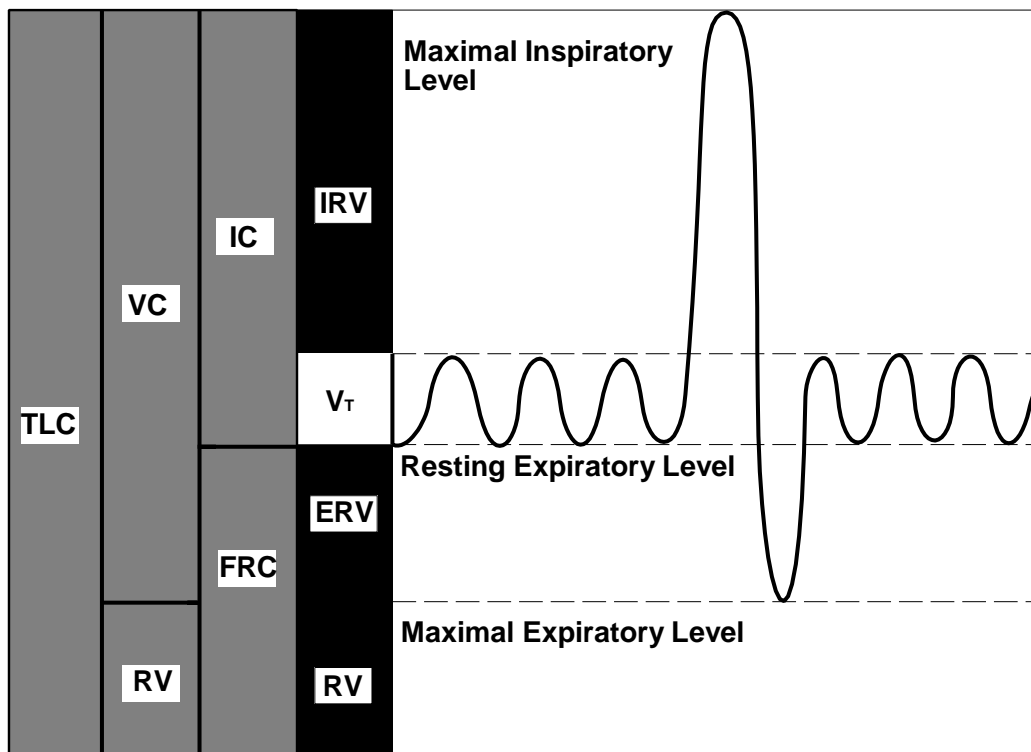


**Figure 10-7. Lung volumes and capacities. Diagrammatic representation of various lung compartments, based on a typical spirogram. TLC, total lung capacity; VC, vital capacity; RV, residual volume; FRC, functional residual capacity; IC, inspiratory capacity; V<sub>T</sub>, tidal volume; IRV, inspiratory reserve volume; ERV, expiratory reserve volume. Shaded areas indicate relationships between the subdivisions and relative sizes as compared to the TLC. The resting expiratory level should be noted, since it remains more stable than other identifiable points during repeated spiograms, hence is used as a starting point for FRC determinations, etc.**

Source: Ruppel (1979).

800 mL/s would be expected to produce linear velocities in the anterior nares greater than 10 m/s.

Because of the irregular anatomic architecture of the nasal passages, the incoming air induces many eddies and turbulence in the ET airways. This is also true in the upper portions of the TB region largely due to the turbulence created by the glottic aperture. As the collective volume and cross sectional area of the bronchial airways increases, the mean airflow rates fall, but "parabolic airflow", a characteristic of laminar airflow does not develop because of the

renewed development of secondary flows due to the repetitive airway branching. Conditions of true laminar flow probably do not occur until the inspired air reaches the transitional airways. Whether air flow in a straight circular tube is laminar or turbulent is determined by a dimensionless parameter known as the Reynolds number (Re) which is defined by the ratio  $\rho_a D_a U / \mu$  where  $\rho_a$  is the air density,  $D_a$  is the tube diameter,  $U$  is the air velocity, and  $\mu$  is the viscosity of air. As a general rule, when Re is below 2000, the flow is expected to be laminar (Owen, 1969). See Table 10-2.

Pattle (1961) was the first investigator to demonstrate that the nasal deposition of particles was proportional to the product of the aerodynamic diameter ( $d_{ac}$ ) squared and the mean inspiratory flow rate (Q); where the aerodynamic diameter is the diameter of a unit density sphere having the same terminal settling velocity (see Section 10.2) as the particle of concern. Albert et al. (1967) and Lippmann and Albert (1969) were among the earliest to report experimentally that the same general relationship governed inertial deposition of different uniformly-sized particles in the conducting airways of the TB region. Recent papers by Martonen et al. (1994a,b,c) have considered the influence of both the cartilaginous rings and the carinal ridges of the upper TB airways on the dynamics of airflow. As in the case of the glottic aperture, these structures appear to contribute to the non-uniformity of particulate deposition sites within these airways. Concomitantly, Martonen et al. have pointed to the limitations incurred by assuming smooth tubes in modeling the aerodynamics of the upper TB airways (see also Section 10.5.1.5).

Smaller particles, i.e. those with an aerodynamic size of between 0.1 and 0.5  $\mu\text{m}$ , are the particles with the greatest airborne stability. They are too small to gravitate appreciably and are too large to diffuse; hence they tend to persist in the inspired air as a gas would, but in teams of alveolar mixing, they behave as "non-diffusible" gas. The study of these particles has provided very useful information on the distribution of tidal air under different physiologic conditions (Heyder et al., 1985). A recent analysis of airflow dynamics in human airways, conducted by Chang and Menon (1993), concluded that the measurement of flow dynamics aids in the understanding of particle transport and the development of enhanced areas of particle deposition.

Sedimentation becomes insignificant relative to diffusion as the particles become smaller. Deposition by diffusion results from the random (Brownian) motion of very small

**TABLE 10-2. ARCHITECTURE OF THE HUMAN LUNG ACCORDING TO WEIBEL'S (1963)  
MODEL A, WITH REGULARIZED DICHOTOMY**

Region	Generation	Number	Diameter (mm)	Length (mm)	Cum. <sup>b</sup> Length (mm)	Area <sup>a</sup> (cm <sup>2</sup> )	Volume (mL)	Cum. <sup>b</sup> Volume (mL)	At flow of 1 L/sec	
									Speed (cm/s)	Reynolds Number
Trachea <sup>c</sup>	0	1	18	120.0	120	2.6	31	31	393	4,350
Main bronchus	1	2	12.2	47.6	167	2.3	11	42	427	3,210
Lobar bronchus	2	4	8.3	19.0	186	2.2	4	46	462	2,390
Segmental bronchus	3	8	5.6	7.6	194	2.0	2	47	507	1,720
	4	16	4.5	12.7	206	2.6	3	51	392	1,110
Bronchi with cartilage in wall	5	32	3.5	10.7	217	3.1	3	54	325	690
	6	64	2.8	9.0	226	4.0	4	57	254	434
	7	128	2.3	7.6	234	5.1	4	61	188	277
	8	256	1.86	6.4	240	7.0	4	66	144	164
Terminal bronchus	9	512	1.54	5.4	246	9.6	5	71	105	99
	10	1,020	1.30	4.6	250	13	6	77	73.6	60
	11	2,050	1.09	3.9	254	19	7	85	52.3	34
Bronchioles with muscle in wall	12	4,100	0.95	3.3	257	29	10	95	34.4	20
	13	8,190	0.82	2.7	260	44	12	106	23.1	11
	14	16,400	0.74	2.3	262	70	16	123	14.1	6.5
	15	32,800	0.66	2.0	264	113	22	145	8.92	3.6
Terminal bronchiole	16	65,500	0.60	1.65	266	180	30	175	5.40	2.0
Resp. bronchiole	17	131 × 10 <sup>3</sup>	0.54	1.41	267	300	42	217	3.33	1.1
Resp. bronchiole	18	262 × 10 <sup>3</sup>	0.50	1.17	269	534	61	278	1.94	0.57
Resp. bronchiole	19	524 × 10 <sup>3</sup>	0.47	0.99	270	944	93	370	1.10	0.31
Alveolar duct	20	1.05 × 10 <sup>6</sup>	0.45	0.83	271	1,600	139	510	0.60	0.17
Alveolar duct	21	2.10 × 10 <sup>6</sup>	0.43	0.70	271	3,200	224	734	0.32	0.08
Alveolar duct	22	4.19 × 10 <sup>6</sup>	0.41	0.59	272	5,900	350	1,085	0.18	0.04
Alveolar sac	23	8.39 × 10 <sup>6</sup>	0.41	0.50	273	12,000	591	1,675	0.09	—
Alveoli, 21 per duct		300 × 10 <sup>6</sup>	0.28	0.23	273		3,200	4,800		

<sup>a</sup>Area = total cross sectional area.

<sup>b</sup>Cum. = cumulative.

<sup>c</sup>Dead space, approx. 175 mL + 40 mL for mouth.

Source: Y.C. Fung (1990).

particles caused by the collision of gas molecules in air. The terminal settling velocity of a particle approaches 0.001 cm/s for a unit density sphere with a physical diameter of 0.5  $\mu\text{m}$ , so that gravitational forces become negligible at smaller diameters. The main deposition mechanism is diffusion for a particle having physical (geometric) size  $<0.5 \mu\text{m}$ . Impaction and sedimentation are the main deposition mechanisms for a particle whose size is greater than 0.5  $\mu\text{m}$ . Hence,  $d_{\text{ac}} = 0.5 \mu\text{m}$  is convenient for use as the boundary between the diffusion and aerodynamic regimes. Although this convention may lead to confusion in the case of very dense particles, most environmental aerosols have densities below 3 g/cm<sup>3</sup> (U.S. Environmental Protection Agency, 1982). Diffusional deposition is important in the small airways and in the A region where distances between the particles and airway epithelium are small. Diffusion has also been shown to be an important deposition mechanism in the ET region for small particles (Cheng et al., 1988, 1990).

With mouth-only breathing, the regional deposition pattern changes dramatically when compared to nasal breathing, with ET deposition being reduced and both TB and A deposition enhanced. Oronasal breathing (partly via the mouth and partly nasally), however, typically occurs in healthy adults while undergoing exercise. Therefore, the appropriate activity pattern of subjects for risk assessment estimation remains an important issue. Miller et al. (1988) examined ET and thoracic deposition as a function of particle size for ventilation rates ranging from normal respiration to heavy exercise. A family of estimated deposition curves was generated as a function of breathing pattern (See Section 10.5.1.4.). Anatomical and functional differences between adults and children are likely to interact with the major mechanisms affecting respiratory tract deposition in a complex way which will have important implications for risk assessment.

Humidification and warming of the inspired air begins in the nasal passages and continues into the deep lung. This conditioning of the ambient air does not significantly affect particle deposition unless the particulate material is intrinsically hygroscopic, in which case, it is very important. For both liquid and solid aerosol particles that are hygroscopic, there are physical laws that control both particle growth and deposition, and these have been modeled extensively. In a review of this general subject (Morrow, 1986), many experimental measurements of the humidity (RH) and temperature of the air within the respiratory tract have been reported, but because of the technical problems involved, uncertainties remain. Two major problems prevail:

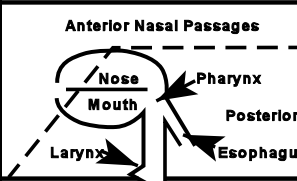
(1) the accurate measurement of temperature requires a sensor with a very rapid response time; and (2) hygrometric measurements of conditions of near saturation (>99% RH) are the most difficult to make. The latter technicality is of special significance, because the growth of hygroscopic aerosols are greatest near saturation. For example, the effect of a difference in humidity between 99.0% and 99.9% is more important than the difference between 20 and 80% RH. A more complete discussion of models and experimental determinations of the deposition of hygroscopic aerosols is given in Section 10.4.

The differences in respiratory tract anatomy summarized briefly in this section are the structural basis for the species differences in particle deposition. In addition to the structure of the respiratory tract, the regional thickness and composition of the airway epithelium (a function of cell types and distributions) are important factors in clearance (Section 10.4). Characteristic values and ranges for many respiratory parameters have been published for "Reference Man" by the International Commission on Radiological Protection (ICRP) (1975) and they are also available from many reference sources (Altose, 1980; Collett et al., 1988; Cotes, 1979). A typical description of respiratory tract morphology, cytology, histology, structure, and function is given in Table 10-3. This description of the respiratory tract is used in the human dosimetry model applied in Section 10.7 (ICRP66, 1994). For additional information on human respiratory tract structure, the papers of Weibel (1963; 1980), Hatch and Gross (1964), Proctor (1977), Forrest (1993), and Gehr (1994) are recommended.

## **10.4 FACTORS CONTROLLING COMPARATIVE INHALED DOSE**

As discussed in Section 10.1, comprehensive characterization of the exposure-dose-response continuum is the fundamental objective of any dose-response assessment. Within human and interspecies differences in anatomical and physiological characteristics, the physicochemical properties of the inhaled aerosol, the diversity of cell types that may be affected, and a myriad of mechanistic and metabolic differences all combine to make the characterization particularly complex for the respiratory tract as the portal of entry. This section attempts to discuss these factors within the exposure-dose-response context in order to present unifying concepts. These concepts are used to construct a framework by which to

**TABLE 10-3. MORPHOLOGY, CYTOLOGY, HISTOLOGY, FUNCTION, AND STRUCTURE OF THE RESPIRATORY TRACT AND REGIONS USED IN THE ICRP66 (1994) HUMAN DOSIMETRY MODEL**

Functions	Cytology (Epithelium)	Histology (Walls)	Generation Number	Anatomy	Regions used in Model		Zones (Air)	Location	Airway Surface <sup>(a)</sup>	Number of Airways		
					New	Old <sup>(d)</sup>						
Air Conditioning Temperature and Humidity, and Cleaning; Fast Particle Clearance; Air Conduction	Respiratory Epithelium with Goblet Cells Cell Types: • Ciliated Cells • Nonciliated Cells: Goblet Cells Mucous (Secretory) Cells Serous Cells Brush Cells Endocrine Cells Basal Cells Intermediate Cells	Mucous Membrane, Respiratory Epithelium (Pseudostratified, Ciliated, Mucous), Glands			ET <sub>1</sub>		0.175 x 10 <sup>3</sup> m <sup>3</sup> (Anatomical Dead Space)	Extrathoracic	Extrapulmonary	2 x 10 <sup>-3</sup> m <sup>2</sup>	—	
		Mucous Membrane, Respiratory or Stratified Epithelium, Glands			ET <sub>2</sub>	LN <sub>ET</sub>				(N-P)	4.5 x 10 <sup>-2</sup> m <sup>2</sup>	—
		Mucous Membrane, Respiratory Epithelium Cartilage Rings, Glands	0	Trachea	BB	(T-B)		Conduction	Thoracic	Pulmonary	2.9 x 10 <sup>-2</sup> m <sup>2</sup> (a)	511 (a)
		Mucous Membrane, Respiratory Epithelium, Cartilage plates, Smooth Muscle Layer, Glands	1	Main Bronchi							2.4 x 10 <sup>-1</sup> m <sup>2</sup> (a)	6.5 x 10 <sup>4</sup> (a)
	Mucous Membrane, Respiratory Epithelium, No Cartilage, No Glands, Smooth Muscle Layer	2-8	Bronchi	bb							LN <sub>TH</sub> <sup>(c)</sup>	7.5 m <sup>2</sup>
	Respiratory Epithelium with Clara Cells (No Goblet Cells) Cell Types: • Ciliated Cells • Nonciliated Cells: Clara (Secretory) Cells	Mucous Membrane, Respiratory Epithelium, No Cartilage, No Glands, Smooth Muscle Layer	9-14	Bronchioles								
Mucous Membrane, Single-Layer Respiratory Epithelium, Less Ciliated, Smooth Muscle Layer	15	Terminal Bronchioles										
Air Conduction; Gas Exchange; Slow Particle Clearance	Respiratory Epithelium Consisting Mainly of Clara Cells (Secretory) and Few Ciliated Cells	Mucous Membrane, Single-Layer Respiratory Epithelium of Cuboidal Cells, Smooth Muscle Layer	16-18	Respiratory Bronchioles								
Gas Exchange; Very Slow Particle Clearance	Squamous Alveolar Epithelial Cells (Type I), Covering 93% of Alveolar Surface Areas	Wall Consists of Alveolar Entrance Rings, Squamous Epithelial Layer, Surfactant	(c)	Alveolar Ducts	AI							
	Cuboidal Alveolar Epithelial Cells (Type II, Surfactant-Producing), Covering 7% of Alveolar Surface Areas Alveolar Macrophages	Interalveolar Septa Covered by Squamous Epithelium, Containing Capillaries, Surfactant	(c)	Alveolar Sacs								
				Lymphatics		L						

10-28

<sup>a</sup> Dimensions from three sources (James, 1988; adapted from Weibel, 1963; Yeh and Schum, 1980; and Phalen et al., 1985) were averaged after all were adjusted to a functional residual capacity (FRC) of 3.3 x 10<sup>3</sup> m<sup>3</sup> (Yu and Dui, 1982a; James, 1988).

<sup>b</sup> Calculated from Hansen and Ampaya (1975) and scaled to a functional residual capacity (FRC) of 3.3 x 10<sup>3</sup> m<sup>3</sup>.

<sup>c</sup> Unnumbered because of imprecise information.

<sup>d</sup> Previous ICRP Model.

• As described in the text, lymph nodes are located only in BB region but drain the broncholar and alveolar interstitial regions as well as the bronchial region.

evaluate the different available dosimetry models; to appreciate why they are constructed differently, and to determine which are the most appropriate for extrapolation of the available toxicity data. The section discusses the major factors controlling the disposition of inhaled particles. Note that disposition is defined as encompassing the processes of deposition, absorption, distribution, metabolism, and elimination.

It must be emphasized that dissection of the factors that control inhaled dose into discrete topic discussions is deceptive and masks the dynamic and interdependent nature of the intact respiratory system. For example, although deposition in a particular respiratory region will be discussed separately from the clearance mechanisms for that region, retention (the actual amount of inhaled agent found in the respiratory tract at any time) is determined by the relative rates of deposition and clearance. Retention and the toxicologic properties of the inhaled agent are related to the magnitude of the pharmacologic, physiologic, or pathologic response. Therefore, although the deposition mechanisms, clearance mechanisms, and physicochemical characteristics of particles are described in distinct sections, assessment of the overall dosimetry and toxic response requires integration of the various factors.

Inasmuch as particles which are too massive to be inhaled occur in the environmental air, the description "inhalability" has been used to denote the overall spectrum of particle sizes which are potentially capable of entering the respiratory tract of humans and depositing therein. Except under conditions of microgravity (spaceflight) and possibly some other rare circumstances, unit density particles  $>100\ \mu\text{m}$  diameter have a low probability of entering the mouth or nose in still air. Nevertheless, there is no sharp cutoff to zero probability because air velocities into the nose or mouth during heavy breathing, or in the presence of a high wind, may be comparable to the settling velocity of  $>100\text{-}\mu\text{m}$  particles. Even though the settling velocity of particles of this size is  $>25\ \text{cm/s}$ , wind velocities of several  $\text{m/s}$  can result in them being blown into the nose or mouth. Inhalability can be defined as the ratio of the number concentration of particles of a certain aerodynamic diameter,  $d_{\text{ae}}$ , that are inspired through the nose or mouth to the number concentration of the same  $d_{\text{ae}}$  present in the inspired volume of ambient air (ICRP66, 1994). The concept of aerodynamic diameter is discussed in Section 10.2. In studies with head and torso models, inhalability has been considered generally under conditions of different wind velocities and horizontal head orientations.

The American Conference of Governmental Industrial Hygienists (ACGIH) (1985) expressed inhalability in terms of an intake efficiency of a hypothetical sampler. This expression was replaced in 1989 by international definitions for inspirable (also called inhalable), thoracic, and respirable fractions of airborne particle (Soderholm, 1989). Agreement on these definitions has been achieved between the International Standards Organization (ISO) and the ACGIH (Vincent, 1995). Health-related sampling should be based on one or more of the three, progressively very-finer, particle size-selective fractions; inhalable, thoracic, and respirable.

Each definition is expressed as a sampling efficiency (S) which is a function of particle aerodynamic diameter ( $d_{ae}$ ) and specifies the fraction of the ambient concentration of airborne particles collected by an ideal sampler. For the inspirable fraction,

$$\mathbf{SI}(d_{ae}) = \mathbf{0.5(1 + e^{-0.06d_{ae}})}. \quad (10-4)$$

For the thoracic fraction,

$$\mathbf{ST}(d_{ae}) = \mathbf{SI}(d_{ae}) [1 - \mathbf{F(x)}], \quad (10-5)$$

where

$$\mathbf{F(x)} = \frac{\mathbf{\ln(d_{ae}/\Gamma)}}{\mathbf{\ln(\Sigma)}}, \quad \mathbf{\Gamma = 11.64 \mu m, \Sigma = 1.5}. \quad (10-6)$$

F(x) is the cumulative probability function of a standardized normal random variable. For the respirable fraction,

$$\mathbf{SR}(d_{ae}) = \mathbf{SI}(d_{ae}) [1 - \mathbf{F(x)}], \quad (10-7)$$

where

$$\mathbf{\Gamma = 4.25 \mu m, \Sigma = 1.5}. \quad (10-8)$$

It should be emphasized that these conventions do not purport to reflect deposition per se, but are rather intended to be representative of the penetration of particles to a region and hence their availability for deposition. The thoracic fraction corresponds to penetration to the TB plus A regions, and the respirable fraction to the A region. Inhalability for laboratory animals is discussed in Section 10.5.2.

Swift (1976) estimated the deposition of particles by impaction in the nose, based on a nasal entrance velocity of 2.3 m/s and a nasal entrance width of 0.5 cm, and deduced that particles  $>61 \mu\text{m } d_{ae}$  have a negligible probability of entering the nasal passages due to the high impaction efficiency of the external nares. Experiments by Breysse and Swift (1990) in tranquil air estimated a practical upper limit for inhalability to be  $\sim 40 \mu\text{m } d_{ae}$  for individuals breathing at 15 breaths per min at rest. No information on tidal volumes was provided. Studies reported by Vincent (1990) of inhalability made use of a mannequin with mouth and nasal orifices that could be placed in a wind tunnel and rotated 360 degrees horizontally. At low wind speeds, the intake efficiency approached 0.5 for particle sizes between  $20 \mu\text{m}$  and  $100 \mu\text{m } d_{ae}$ . Vincent derived the following empirical relationship from these studies

$$\eta_1 (\text{sampler}) = 0.5 [1 + \exp(-0.06 d_{ae})] = 1 \times 10^{-5} U^{2.75} \exp(0.055 d_{ae}), \quad (10-9)$$

where  $\eta_1$  is the intake efficiency of the sampler,  $d_{ae}$  is the aerodynamic diameter, and  $U$  is the wind speed. For particles with  $d_{ae}$  less than about  $40 \mu\text{m}$ , intake efficiency generally tends to decrease with increasing  $d_{ae}$ . However, for large particles, the intake efficiency tends to increase with windspeed. For particles with  $d_{ae} < 10 \mu\text{m}$ , the ICRP modified Vincent's expression to increase the accuracy in representing the data. Thus, in the 1994 ICRP66 model (ICRP66, 1994) the intake efficiency of the head,  $\eta_1$ , i.e., the particle inhalability, is represented by

$$\eta_1 = 1 - 0.5 (1 - [7.6 \times 10^{-4} (d_{ae})^{2.8} + 1]^{-1}) + 1 \times 10^{-5} U^{2.75} \exp(0.055 d_{ae}), \quad (10-10)$$

where  $d_{ae}$  is in  $\mu\text{m}$  and  $U$  is the windspeed in  $(\text{m s}^{-1})$  (for  $0 \leq U \leq 10 \text{ ms}^{-1}$ ).

While there is some contention about the practical upper size limit of inhalable particles in humans, there is no lower limit to inhalability as long as the particle exceeds a critical

(Kelvin) size where the aggregation of atomic or molecular units is stable enough to endow it with "particulate" properties, in distinction to those of free ions or gas molecules. *Inter alia*, particles are considered to experience inelastic collisions with surfaces and with each other. The lower limit for the existence of aerosol particles is assumed to be around 1 nanometers for some materials (refer to Section 10.2.). If the particulate material has an appreciable vapor pressure, particles of a certain size may "evaporate" as fast as they are formed. For example, pure water droplets as large as 1  $\mu\text{m}$  diameter will evaporate in less than 1 second even when they are in water-saturated air at 20° Celsius (Greene and Lane, 1957).

Description of a "respirable dust fraction" was first suggested by the British Medical Research Council and implemented by C.N. Davies (1952) using the experimentally-estimated alveolar deposition curve of Brown et al. (1950). This curve described the respirable dust fraction as that which would be available to deposit in the alveolated lung structures including the respiratory bronchioles, thereby making "respirable dusts" applicable to pneumoconiosis-producing dusts. The horizontal elutriator was chosen as a particle size selector, and respirable dust was defined as that dust passing an ideal horizontal elutriator. The elutriator cutoff was chosen to result in the best agreement with experimental lung deposition data. The Johannesburg International Conference on Pneumoconiosis in 1959 adopted the same standard (Orenstein, 1960). Later, an Atomic Energy Commission working group defined "respirable dust" by a deposition curve which indicated 0% deposition at 10  $\mu\text{m}$   $d_{ae}$  and 100% deposition for particles  $\leq 2.0$   $\mu\text{m}$   $d_{ae}$ . "Respirable dust" was defined as that portion of the inhaled dust which penetrates to the nonciliated portions of the lung (Hatch and Gross, 1964). The AEC respirable size deposition curve was pragmatically adjusted to 100% deposition for  $\leq 2$   $\mu\text{m}$   $d_{ae}$  particles so that the "respirable" curve could be approximated by a two-stage selective sampler and because comparatively little dust mass was represented by these small particles (Mercer 1973a). This definition was not intended to be applicable to dusts that are readily soluble in body fluids or are primarily chemical intoxicants, but rather only for poorly soluble particles that exhibit prolonged retention in the lung.

Other groups, such as the American Conference of Governmental Industrial Hygienists (ACGIH), incorporated respirable dust sampling concepts in setting acceptable exposure levels for other toxic dusts. Such applications are more complicated, since laboratory animal

and human exposure data, rather than predictive calculations, form the data base for standards. The size-selector characteristic specified in the ACGIH standard for respirable dust (Threshold Limits Committee, 1968) was almost identical to that of the AEC, differing only at  $2 \mu\text{m } d_{ac}$ , where it allowed for 90% passing the first-stage collector instead of 100 percent. The difference between them appeared to be a recognition of the properties of real particle separators, so that, for practical purposes, the two standards could be considered equivalent (Lippmann, 1978).

The cutoff characteristics of the precollectors preceding respirable dust samplers are defined by these criteria. The two sampler acceptance curves have similar, but not identical, characteristics, due mainly to the use of different types of collectors. The BMRC curve was chosen to give the best fit between the calculated characteristics of an ideal horizontal elutriator and available lung deposition data; on the other hand, the design for the AEC curve was based primarily on the upper respiratory tract deposition data of Brown et al. (1950). The separation characteristics of cyclone type collectors simulate the AEC curve. Whenever the particle size distribution has a  $\sigma_g > 2$ , samples collected with instruments meeting either criterion will be comparable (Lippmann, 1978). Various comparisons of samples collected on the basis of the two criteria are available (Knight and Lichti, 1970; Breuer, 1971; Maquire and Barker, 1969; Lynch, 1970; Coenen, 1971; Moss and Ettinger, 1970).

The various definitions of respirable dust were somewhat arbitrary, with the BMRC and AEC definitions being based on the poorly soluble particles that reach the A region. Since part of the aerosol that penetrates to the alveoli remains suspended in the exhaled air, respirable dust samples are not intended to be a measure of A deposition but only a measure of aerosol concentration for those particles that are the primary candidates for A deposition. Given that the "respirable" dust standards were intended for "insoluble dusts", most of the samplers developed to satisfy their criteria have been relatively simple two-stage instruments. In addition to an overall size-mass distribution curve, multistage aerosol sampler data can provide estimates of the "respirable" fraction and deposition in other functional regions. Field application of these samplers has been limited because of the increased number and cost of sample analyses and the lack of suitable instrumentation. Many of the various samplers, along with their limitations and deficiencies, were reviewed by Lippmann (1978).

PM<sub>10</sub> dust is based on the PM10 sampler efficiency curve promulgated by the U.S. Environmental Protection Agency. This sample is equivalent to the thoracic dust sample defined by the American Conference of Governmental Industrial Hygienists (Raabe, 1984).

The medical field also refers to a "respirable fraction". Aerosols are widely used for both therapy and diagnosis (Swift, 1993). Aerosols are used to deliver bioactive substances to the respiratory tract to affect a physiological change (e.g., nasal or bronchial medication), provocation tests in the diagnosis of bronchial asthma, and the administration of contrast substances for radiological studies. In pharmaceutical applications, the "respirable fraction" refers to particles with an aerodynamic diameter between 0.5 and 5  $\mu\text{m}$  for most therapeutic products, although larger size particles (up to 10  $\mu\text{m}$ ) are recognized as important in certain situations (Hallworth, 1993; Lourenco and Cotromanes, 1982). Aerosols produced by metered-dose-inhaler (MDI) systems are about 2.5 to 2.8  $\mu\text{m}$  in size upon entering the lung (Kim et al., 1985) and 40 to 50% of these aerosols are expected to deposit during normal tidal breathing. The lung deposition, however, is usually higher in the abnormal lung, and can be further increased by changing the mode of breathing.

#### 10.4.1 Deposition Mechanisms

This section will review briefly the aerosol physics that both explains how and why particle deposition occurs and provides the theoretician a capability to develop predictive deposition models. Some of these models will be described in Section 10.5, together with recent experimental results on particle deposition. The ability of the experimentalist to measure deposition quantitatively has continued to advance, but theoretical models remain the only practical way for predicting the impact of aerosol exposures and for delineating the patterns of intra-regional deposition.

The motion of an airborne particle between 1 and 100  $\mu\text{m}$   $d_{ae}$  is primarily related to its mass, and the resulting resistive force of air which is proportional to

$$\mu v d, \quad (10-11)$$

where  $\mu$  is the viscosity of air,  $v$  is the velocity of the particle relative to the air, and  $d$  is the particle diameter. This is a statement of Stokes law for viscous resistance which is

appropriate to a sphere moving in air at low particle Reynolds numbers, i.e., less than 1. The particle Reynolds number ( $Re_p$ ) is defined as

$$\rho_a dv/\mu, \quad (10-12)$$

where  $\rho_a$  is the density of air. When the particle velocity relative to air is sufficiently slow that the airflow pattern around the sphere is symmetrical and only viscous stresses resist the sphere's motion, Stokes law applies. As the value of  $Re_p$  increases, asymmetrical flow about the moving sphere and a pressure drop across the sphere, both progressively develop. These changes in flow signify that the condition of inertial resistance prevails and Stokes law does not pertain (Mercer, 1973b).

For the range of particle sizes just discussed (1 to 100  $\mu\text{m}$ ), the motion of airborne particles is characterized by a rapid attainment of a constant velocity whereby the viscous resistance of air matches the force(s) on the sphere responsible for its motion. This constant velocity is termed the terminal velocity of the particle. For the size region below 1  $\mu\text{m}$  diameter, particle motion is also based on the viscous resistance of air and described by its terminal velocity. In this particle size region, the viscous resistance of air on the particle, using Stokes law, begins to be overestimated and the particle's terminal velocity, underestimated. This general phenomenon is termed "slip"; consequently, Slip Correction Factors have been developed. These slip corrections become more important as the particle diameter nears, or is less than, the mean free path of air molecules ( $\approx 0.068 \mu\text{m}$  at 25 °C and 760 mm Hg air pressure).

#### **10.4.1.1 Gravitational Settling or Sedimentation**

All aerosol particles are continuously influenced by gravity, but for practical purposes, particles with an  $d_{ac} > 0.5 \mu\text{m}$  are mainly involved. Within the respiratory tract, an  $d_{ac}$  of 100  $\mu\text{m}$  will be considered as an upper cut-off. A spherical, compact particle within these arbitrary limits will acquire a terminal settling velocity when a balance is achieved between the acceleration of gravity,  $g$ , acting on the particle of density,  $\rho$ , ( $\text{g}/\text{cm}^3$ ) and the viscous resistance of the air according to Stokes law

$$(\pi/6)\rho d^3 g = 3\pi\mu d v_t \quad (10-13)$$

The left hand side of Equation 10-13 is the force of gravity on the particle, neglecting the effect of the density of air. Solving for the terminal velocity,  $v_t$ , gives

$$v_t = d_{ae}^2 \rho g K_s / 18\mu \quad (10-14)$$

In Equation 10-14 a slip correction factor,  $K_s$ , is added to account for the slip effect on particles with diameters about or below 1  $\mu\text{m}$ . For particles as small as 0.02  $\mu\text{m}$ , the  $K_s$  used by Knudsen and Weber increases  $v_t$  six fold (cited by Mercer, 1973c).

The relationship for the terminal settling velocity, just described, is not restricted to measurements in tranquil air. For example, moving air in a horizontal airway will tend to carry the particle at right angles to gravity at an average velocity,  $U$ . The action of gravity on the particle will nonetheless result in a terminal settling velocity,  $v_t$ ; consequently the particle will follow, vectorially, the two velocities; and, provided the airway is sufficiently long or the settling velocity is relatively high, the particle will sediment in the airway. For every orientation of the airways with respect to gravity, it is possible to calculate the particle's settling behavior using Stokes law.

#### 10.4.1.2 Inertial Impaction

Sudden changes in airstream direction and velocity, cause particles to fail to follow the streamlines of airflow as depicted in Figure 10-5. As a consequence, the relatively massive particles impact on the walls or branch points of the conducting airways. The ET and upper TB airways have been described as the dominant sites of high air velocities and sharp directional changes; hence, they dominate as sites of inertial impaction. Because the air (and particle) velocities are affected by the breathing pattern, it is easy to imagine that even small particles also experience some inertial impaction. Moreover, as nasal breathing shifts to oral breathing during work or exercise, the particle that would normally be expected to impact in the ET region will pass into the TB region, greatly increasing TB deposition. That all

impaction sites occur lower down in the TB region when such a shift takes place is also expected.

The probability that a particle with a diameter,  $d$ , moving in an air stream with an average velocity,  $U$ , will impact at a bifurcation is related to a parameter called the Stokes number,  $Stk$ ; defined as

$$\rho d^2 U / 9\mu D_a , \quad (10-15)$$

or

$$\rho d_{ae}^2 U / 9\mu D_a . \quad (10-16)$$

As far as particulate properties are concerned, the aerodynamic diameter ( $d_{ae}$ ) is again the significant parameter (see Section 10.2). In Landahl's lung deposition model (1950a) of impaction in the TB region, impaction efficiency was proportional to

$$\rho d^2 U_i \sin \theta_i / D_{ai} S_{i-1} , \quad (10-17)$$

where  $U_i$  is the air velocity in the airway generation  $i$ ,  $\theta_i$  is the branching angle between generations  $i$  and  $i-1$ ,  $D_{ai}$  is diameter of the airway of generation  $i$ , and  $S_{i-1}$  is the total cross sectional area of airway generation  $i-1$ .

Prevailing TB models have simplistically represented the airways as smooth, bifurcating tubes. Martonen et al. (1993; 1994a,b,c) have predicted that the cartilaginous rings and carinal ridges perturb the dynamics of airflow and help to explain the non-uniformity of particle deposition.

It should be evident that both gravitational settling and inertial impaction cause the deposition of many particles within the same size range. These deposition forces are always acting together in the ET and TB regions, with inertial impaction dominating in the upper airways and gravitational settling becoming increasingly dominant in the lower conducting

airways, and especially for the largest of the particles which can penetrate into the transitional airways and alveolar spaces.

For sedimenting particles with diameters between 0.1  $\mu\text{m}$  to 1.0  $\mu\text{m}$ , their Slip Correction Factor will be greater than 1.0, although the magnitude of their respective  $v_t$  will only range from about 1  $\mu\text{m/s}$  to 35  $\mu\text{m/s}$ . Concurrently, 0.1  $\mu\text{m}$  diameter particles are affected by diffusion such that the root mean displacement they experience in one second is about 0.3  $\mu\text{m}$ . The size region, 1.0  $\mu\text{m}$  down to about 0.1  $\mu\text{m}$ , is frequently described as consisting of particles which are too small to settle and too large to diffuse. Indeed, it is this circumstance that makes them the most persistent and stable particles in aerosols and those which undergo the least deposition in the respiratory tract. As any aerosol ages and continuously undergoes deposition without particle replenishment, the ultimate aerosol will exist largely within this same size range, i.e., have a median size of about 0.5  $\mu\text{m}$  diameter.

#### **10.4.1.3 Brownian Diffusion**

Particles  $<1 \mu\text{m}$  diameter are increasingly subjected to diffusive deposition as their size decreases. Even particles in the nanometer diameter range are large compared to individual air molecules, hence, the collisions resulting between air molecules, undergoing random thermal motion, and the surface of a particle produce numerous very small changes in the particle's spatial position. These frequent, minute excursions are each made at a constant or terminal velocity due to the viscous resistance of air. The root mean square (r.m.s.) displacement that the particle experiences in a unit of time along a given cartesian coordinate, x, y or z is a measure of its diffusivity. For instance, a 0.1  $\mu\text{m}$  diameter particle has a r.m.s. displacement of about 37  $\mu\text{m}$  during one s. This 1  $\mu\text{m}$  displacement in one s does not describe a velocity of particle motion because the displacement resulted from numerous relatively high velocity excursions.

The diffusion of particles by Brownian motion is described by the Einstein-Stokes' equation

$$\Delta_x = \sqrt{2Dt}, \quad (10-18)$$

where  $\Delta_x$  is the root-mean-square displacement in one second along coordinate x,  $D$  is the diffusion coefficient for the particle expressed in  $\text{cm}^2/\text{s}$ ,  $t$  is time in seconds. The diffusion coefficient of a particle of diameter,  $d$ , is

$$D = \kappa T K_s / 3\pi \mu d, \quad (10-19)$$

where  $\kappa$  is the Boltzmann constant, and  $T$  the absolute temperature, collectively describing the average kinetic energy of the gas molecules.

It is apparent that the density of the particle is ordinarily unimportant in determining particle diffusivity which increases as  $K_s$  increases and  $d$  decreases. Instead of having an aerodynamic equivalent size, diffusive particles of different shapes can be related to the diffusivity of a thermodynamic equivalent size based on spherical particles (Heyder and Scheuch, 1983). In terms of the architecture of the respiratory tract, diffusive deposition of particles is favored by proximate surfaces and by relatively long residence times for particles, both conditions occurring in the alveolated structures of the lungs, the A region. Experimental studies with diffusive particles ( $<0.5 \mu\text{m}$ ) in replicate casts of the human nose and theoretical predictions both indicate a rising deposition efficiency for the nasal airways as  $d$  becomes very small (Cheng et al., 1988).

#### 10.4.1.4 Interception

The interception potential of any particle depends on its physical size. As a practical matter, particles that approach sizes  $> 150 \mu\text{m}$  or more in one dimension will be too massive to be inhaled. Airborne fibers (length/diameter  $\geq 3$ ), however, frequently exceed  $150 \mu\text{m}$  in length and appear to be relatively stable in air. This is because their aerodynamic size is determined predominantly by their diameter, not their length. Fibers, therefore, are the chief concern in the interception process, especially as their length approaches the diameters of peripheral airways ( $>150 \mu\text{m}$ ).

The theoretical model of Asgharian and Yu (1988, 1989) for the deposition of fibrous particles in the respiratory tract is complex. While the model includes interception as an important process for long fibers, it also depends on a combination of inertial, gravitational

and diffusional forces to explain fiber deposition. The deposition efficiencies of the three deposition mechanisms cited have been developed for spherical particles, but these can be extended to fibrous particles by considering orientation effects which are strongly related to the direction of airflow. The orientation of fibers depends upon the velocity shear of the airflow and Brownian motion.

For their analysis of orientational effects throughout the respiratory tract, Asgharian and Yu (1988, 1989) defined the equivalent mass diameter,  $d_{em}$ , of fibers as

$$d_{em} = d_f \beta^{1/3}, \quad (10-20)$$

where  $d_f$  is the fiber diameter and  $\beta$  is its aspect ratio (length/diameter). For example, a fiber 100  $\mu\text{m}$  long and 3  $\mu\text{m}$  diameter has a  $d_{em}$  of 10  $\mu\text{m}$  diameter. In Figure 10-8, two sets of TB deposition predictions for the rat are reproduced from Asgharian and Yu (1989) that clearly show an example of the relative importance of particle interception.

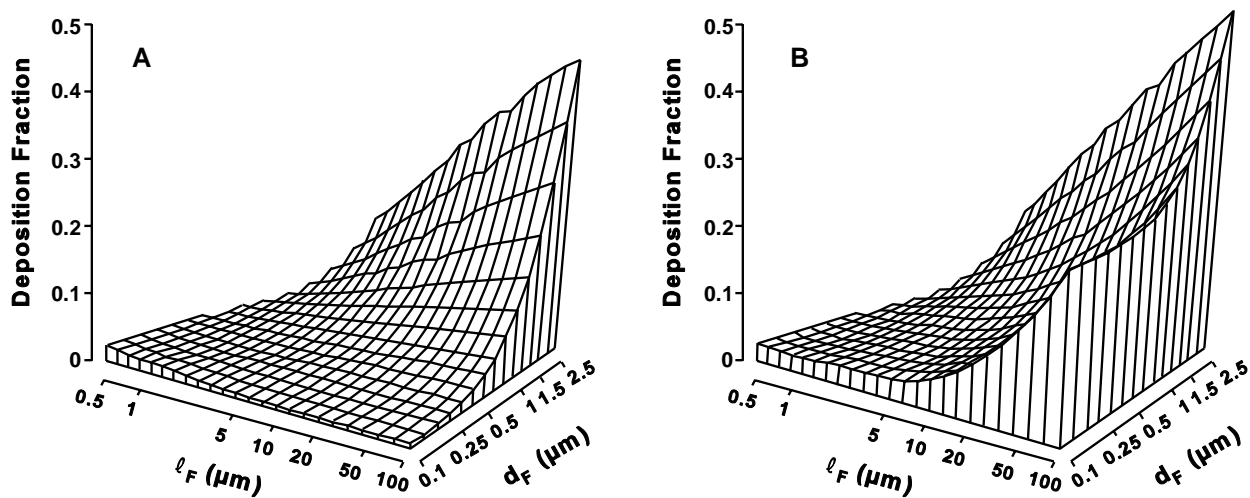


**Figure 10-8. Estimated tracheobronchial (TB) deposition in the rat lung, via the trachea, with no interceptional deposition. Graph A is shown in relation to total TB deposition, via the trachea; Graph B for the same fibrous aerosol under identical respiratory conditions including interception.**

Source: Asgharian and Yu (1989).

Several general reviews of particle deposition mechanisms in the human respiratory tract have been published, e.g, Stuart (1973), Lippmann (1977), and Brain and Blanchard (1993), and are recommended to the reader, as is the excellent review of particle deposition mechanisms prepared by Phalen (1984).

#### **10.4.1.5 Electrostatic Precipitation**

The minimum charge an aerosol particle can have is zero, when it is electrically neutral. This condition is rarely achieved because of the random charging of aerosol particles by the omnipresent air ions. Every cubic centimeter of air contains about  $10^3$  ions in approximately equal numbers of positive and negative ions. Aerosol particles that are initially neutral will acquire charges from these ions by collisions with them due to their random thermal motion. Aerosols that are initially charged will lose their charge slowly as the charged particles attract oppositely charged ions. An equilibrium state of these competing processes is eventually achieved. The Boltzmann equilibrium represents the charge distribution of an aerosol in charge equilibrium with bipolar ions. The minimum amount of charge is very small, with a statistical probability that some particles will have no charge and others will have one or more charges.

The electrical charge on some particles may result in an enhanced deposition over what would be expected from size alone. This is due to image charges induced on the surface of the airway by these particles or to space-charge effects whereby repulsion of particles containing like charges results in increased migration toward the airway wall. The effect of charge is inversely proportional to particle size and airflow rate. This deposition is probably small compared to the effects of turbulence and other deposition mechanisms and is generally a minor contributor to overall particle deposition, but it may be important in some laboratory studies. This deposition is also negligible for particles below  $0.01 \mu\text{m}$  because so few of these particles carry any charge at Boltzmann equilibrium.

Many of freshly generated particles are electrostatically charged. Experimental studies in a lung cast (Chan et al., 1978) and measurements in rats and humans (Melandri et al., 1977, 1983; Tarroni et al., 1980; Jones et al., 1988; Scheuch et al., 1990) all showed that particle charge increased deposition. For low particle number concentration ( $<10^5 \text{ cm}^{-3}$ ), the deposition increase is due to the presence of electrostatic image force acting on the

particle by particle-wall interaction (Yu, 1985). Figure 10-8 shows the experimental data on human deposition of Melandri et al. (1983) and Tarroni et al. (1980) for three particle sizes and the modeling results by Yu (1985). The vertical axis in Figure 10-9 is the deposition increment, defined as

$$\Delta T = (DE - DE_0)/(1 - DE_0), \quad (10-21)$$

where DE is total deposition at particle charge level, q, and  $DE_0$  is the total deposition of particles at Boltzmann charge equilibrium. As seen for each particle size, deposition increments increase linearly with q. Figure 10-9 also shows that there exists a threshold charge level above which the increase in deposition becomes significant. For 1  $\mu\text{m}$  particles, the threshold charge was estimated to be about 54 elementary charges (Yu, 1985).

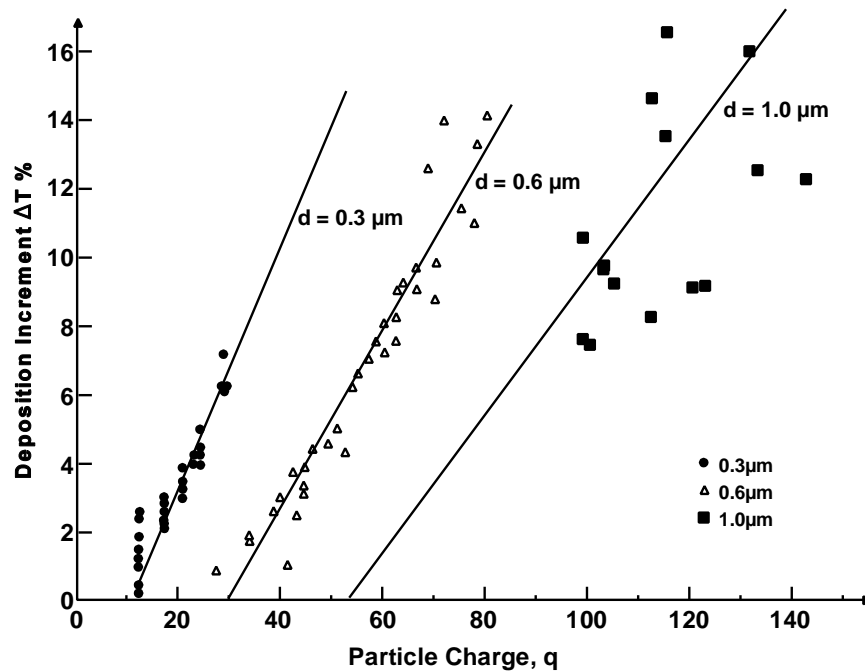


**Figure 10-9.** Deposition increment data versus particle electronic charge (q) for three particle diameters at 0.3, 0.6, and 1.0  $\mu\text{m}$  (unit density). The solid lines represent the theoretical predictions.

Source: Yu (1985).

#### **10.4.1.6 Additional Factors Modifying Deposition**

The available experimental deposition data in humans are commonly for healthy adult Caucasian males using stable, monodisperse particles in charge equilibrium. When these conditions do not hold, changes in deposition are expected to occur. In the following, the effects of different factors on deposition are summarized based upon the information reported from various studies.

##### ***Gender***

The average size of the adult human female thorax is smaller than the average thorax size in adult human males. The diameter of the female trachea is approximately 75% that of the male (Warwick and Williams, 1973), and the size of the bronchi is proportional to the size of the trachea (Weibel, 1963). In addition, the minute ventilation and inspiratory flow rate are smaller for females. It is therefore expected that deposition will be different in females than males. Using radioactive-labeled polystyrene particles in the 2.5 to 7.5  $\mu\text{m}$  size range, Pritchard et al. (1986) measured total and regional deposition in 13 healthy nonsmoking female adults at mouth breathing through a tube. Because deposition of particles in this particle size range in the ET region is controlled by impaction, they reported the data as a function of  $d_{ae}^2 Q$  to accommodate the difference in flow rate between male and female. The data of Pritchard et al. (1986) for females are shown together with data obtained for a group of male nonsmokers using the same technique in Table 10-4. At a comparative value of  $d_{ae}^2 Q$ , females were found to have higher ET and TB deposition and smaller A deposition. The ratio of A deposition to total thoracic deposition in females was also found to be smaller. The differences in depositions were attributed by Pritchard et al. (1986) to the differences in the airway size between males and females.

##### ***Age***

As a human grows from birth to adulthood, both airway structure and respiratory conditions vary with age. These variations are likely to alter the deposition pattern of inhaled particles. Total deposition data for particles of 1 to 3.1  $\mu\text{m}$  size range were reported by Becquemin et al. (1987, 1991) for a group of 41 children at 5 to 15 years of age and by Schiller-Scotland et al. (1992) for 29 children at two age groups (6.7 and 10.9 years).

**TABLE 10-4. DEPOSITION DATA FOR MEN AND WOMEN**

Sex	$d_{ae}^2 Q$ ( $\mu\text{m}^2 \text{Lmin}^{-1}$ )	Deposition as a Fraction of Inhaled Material (%) $\pm$ Standard Error			
		Total	ET	TB	A
Female	405 $\pm$ 47	75.9 $\pm$ 1.7	21.2 $\pm$ 2.4	16.9 $\pm$ 1.5	37.5 $\pm$ 2.5
Male	430 $\pm$ 41	81.5 $\pm$ 1.8	19.9 $\pm$ 2.5	14.7 $\pm$ 1.7	46.9 $\pm$ 2.7

Although Becquemin et al. (1987, 1991) did not find a clear dependence of total deposition on age, slightly higher deposition was found by Schiller-Scotland et al. (1992), for each diameter when children breathed at their normal rates (see Figure 10-10), than was found in adults.

Mathematical models for children have been developed by many workers (Hofmann, 1982; Crawford, 1982; Xu and Yu, 1986; Yu and Xu, 1987; Phalen et al., 1988; Hofmann et al., 1989; Yu et al., 1992; Martonon and Zhang, 1993). Phalen et al. (1988) reported morphometric data of twenty TB airway casts of children and young adults from 21 days to 21 years. With the use of these data, they calculated a higher TB deposition in children during inhalation for particle diameters between 0.01 and 10  $\mu\text{m}$ . If the entire respiratory tract and a complete breathing cycle at normal rate are considered in the model, the results show that ET deposition in children is higher than adults, but that TB and A deposition in children may be either higher or lower than the adult depending upon the particle size (Xu and Yu, 1986).

### ***Respiratory Tract Disease***

Effect of airway diseases on deposition have been studied extensively. In 8 healthy nonsmokers, Svartengren et al. (1986, 1989) found A deposition at different flow rates to be lower (26% versus 48% of thoracic deposition) in subjects after induced bronchoconstriction. The degree of bronchoconstriction was quantified by measurements of airway resistance using a whole-body plethysmograph. An inverse relationship between airway resistance and A deposition was found. Data from the same laboratory (Svartengren et al., 1990, 1991) using 2.6  $\mu\text{m}$   $d_{ae}$  particles with maximally deep slow inhalations at 0.5 L/min showed no

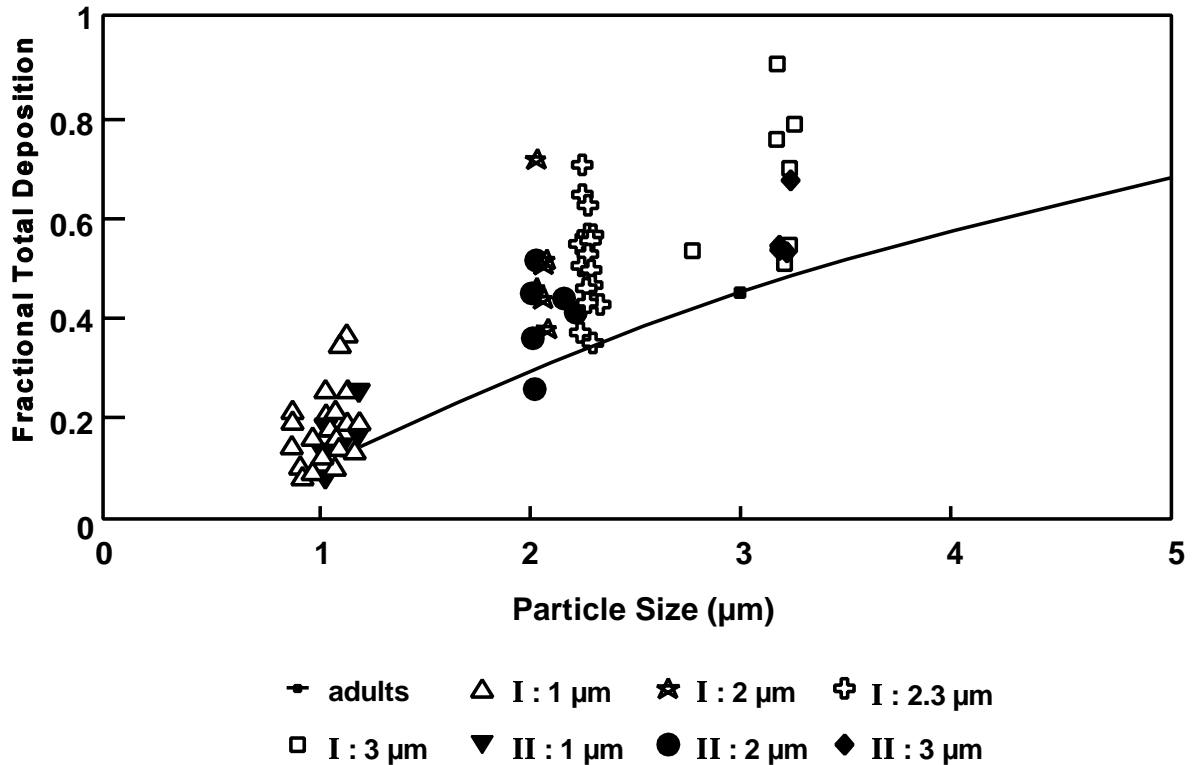


**Figure 10-10.** Total deposition data in children with or during spontaneous breathing as a function of particle diameter (unit density). Group I ( $10.6 \pm 2.0$  yrs); Group II ( $5.3 \pm 1.5$  yrs). The adult curve represents the mean value of deposition from the data of Stahlhofen et al. (1989).

Source: Schiller-Scotland et al. (1992).

significant differences in mouth and throat deposition in asthmatics versus healthy subjects, but thoracic deposition was higher in asthmatics than in healthy subjects (83% versus 73% of total deposition). TB deposition was also found to be higher in asthmatics. The results are similar to those found in subjects with obstructive lung disease (e.g., Dolovich et al., 1976; Itoh et al., 1981; Anderson et al., 1990).

Another extensive study of the relationship between deposition and lung abnormality was made by Kim et al. (1988). One-hundred human subjects with various lung conditions (normal, asymptomatic smoker, smoker with small airway disease, chronic simple bronchitis and chronic obstructive bronchitis) breathed  $1 \mu\text{m}$  test particles from a bag at a rate of 30 breaths/min. The number of rebreathing breaths needed to produce a 90% loss of aerosol

from the bag was determined. From these data, they estimated total deposition and found that total deposition increased with increasing level of airway obstruction.

### ***Particle Polydispersity***

Aerosol particles are often generated polydisperse and can be approximated by a lognormal distribution (Section 10.2). The mass deposition of spherical particles in the respiratory tract depends upon mass median diameter (MMD), geometric standard deviation,  $\sigma_g$ , and physical density (Diu and Yu, 1983; Rudolf et al., 1988). For large particles ( $d_{ae} > 1 \mu\text{m}$ ), deposition is governed by impaction and sedimentation. The dependence on MMD and mass density can be combined with the use of mass medium aerodynamic diameter (MMAD), as suggested by TGLD (1966). However, this method is not valid for particles in the size range where diffusion deposition becomes important. Figure 10-11 shows the calculated total and regional mass deposition results by Yeh et al. (1993) for polydisperse aerosols of unit density with various  $\sigma_g$  as function of MMD at quiet mouth breathing. The variation of deposition with  $\sigma_g$  depends strongly on the MMD of the aerosol. At certain MMD's, variability with  $\sigma_g$  is zero; however, variations at other MMD's can be very large. One of the main effects of polydisperse deposition is the flattening of the deposition curves as a function of particle size, as shown in Figure 10-11.

### ***Particle Hygroscopicity***

Another important particle factor that affects deposition is the hygroscopicity of the particle. Many atmospheric particles such as acid particles are water soluble. As these particles travel along the humid respiratory tract, they grow in size and, as a result, the deposition pattern is altered. A discussion on deposition of hygroscopic particles follows in Section 10.4.3.

#### **10.4.1.7 Comparative Aspects of Deposition**

The various species used in inhalation toxicology studies that serve as the basis for dose-response assessment do not receive identical doses in a comparable respiratory tract region (ET, TB, or A) when exposed to the same aerosol or gas (Brain and Mensah, 1983). Such interspecies differences are important because the adverse toxic effect is likely more

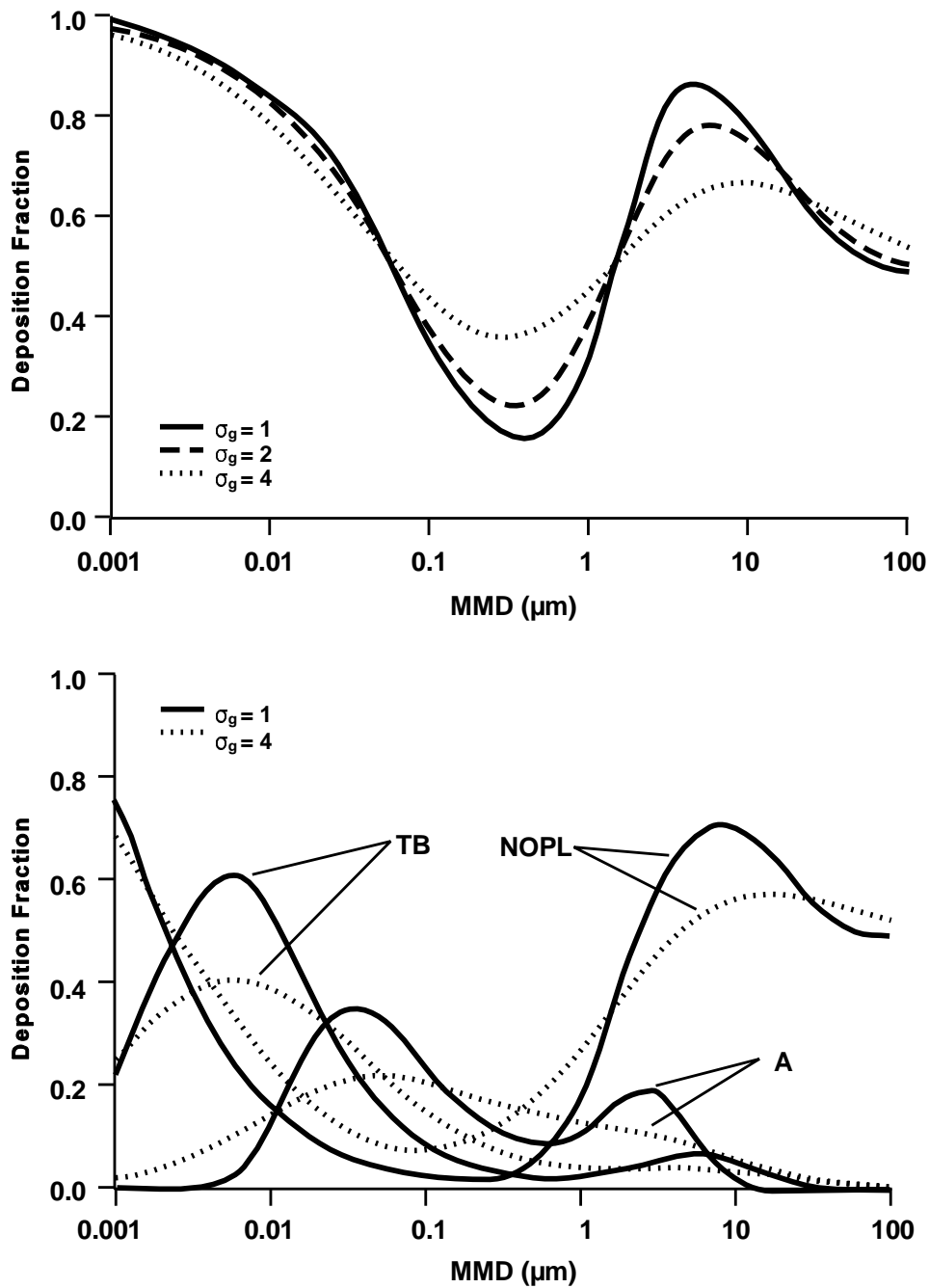


**Figure 10-11.** Calculated mass deposition from polydisperse aerosols of unit density with various geometric standard deviations ( $\sigma_g$ ) as a function of mass median diameter (MMD) for quiet breathing (tidal volume = 750 mL, breathing frequency = 15  $\text{min}^{-1}$ ). The upper panel is total deposition and the lower panel is regional deposition (NOPL = Naso-oro-pharyngo-laryngeal, TB = Tracheobronchial, A = Alveolar). The range of  $\sigma_g$  values demonstrates the extremes of monodisperse to extremely polydisperse.

Source: Yeh et al. (1993).

related to the quantitative pattern of deposition within the respiratory tract than to the exposure concentration; this pattern determines not only the initial respiratory tract tissue dose but also the specific pathways by which the inhaled material is cleared and redistributed (Schlesinger, 1985b). Differences in ventilation rates and in the URT structure and size and branching pattern of the lower respiratory tract between species result in significantly different patterns of airflow and particle deposition. Disposition varies across species and with the respiratory tract region. For example, interspecies variations in cell morphology, numbers, types, distributions, and functional capabilities contribute to variations in clearance of initially deposited dose. Tables 10-5, 10-6, and 10-7 summarize some of these differences for the ET, TB, and A regions, respectively. This section only briefly summarizes these considerations. Comprehensive and detailed reviews of species differences have been published (Phalen and Oldham, 1983; Patra, 1986; Mercer and Crapo, 1987; Gross and Morgan, 1992; Mercer and Crapo, 1992; Parent, 1992).

The geometry of the upper respiratory tract exhibits major interspecies differences (Gross and Morgan, 1992). In general, laboratory animals have much more convoluted nasal turbinate systems than do humans, and the length of the nasopharynx in relation to the entire length of the nasal passage also differs between species. This greater complexity of the nasal passages, coupled with the obligate nasal breathing of rodents, is generally thought to result in greater deposition in the upper respiratory tract (or ET region) of rodents than in humans breathing orally or even nasally (Dahl et al., 1991), although limited comparative data are available. Species differences in gross anatomy, nasal airway epithelia (e.g., cell types and location) and the distribution and composition of mucous secretory products have been noted (Harkema, 1991; Guilmette et al., 1989). The extent of upper respiratory tract removal affects the amount of particles or gas available to the distal respiratory tract.

Airway size (length and diameter) and branching pattern affect the aerodynamics of the respiratory system in the following ways:

- The airway diameter affects the aerodynamics of the air flow and the distance from the particle to the airway surface.
- The cross-sectional area of the airway determines the airflow velocity for a given volumetric flow.
- Airway length, airway diameter, and branching pattern variations affect the mixing between tidal and residual air.

**TABLE 10-5. INTERSPECIES COMPARISON OF NASAL CAVITY CHARACTERISTICS**

	Sprague-Dawley Rat	Guinea Pig	Beagle Dog	Rhesus Monkey	Human <sup>a</sup>
Body weight	250 g	600 g	10 kg	7 kg	≈70 kg
Naris cross-section	0.7 mm	2.5 mm <sup>2</sup>	16.7 mm <sup>2</sup>	22.9 mm <sup>2</sup>	140 mm <sup>2</sup>
Bend in naris	40°	40°	30°	30°	
Length	23 cm	3.4 cm	10 cm	5.3 cm	7-8 cm
Greatest vertical diameter	9.6 mm	12.8 mm	23 mm	27 mm	40-45 mm
Surface area (both sides of nasal cavity)	10.4 cm <sup>2</sup>	27.4 cm <sup>2</sup>	220.7 cm <sup>2</sup>	61.6 cm <sup>2</sup>	181 cm <sup>2</sup>
Volume (both sides)	0.4 cm <sup>3</sup>	0.9 cm <sup>3</sup>	20 cm <sup>3</sup>	8 cm <sup>3</sup>	16-19 cm <sup>3</sup> (does not include sinuses)
Bend in nasopharynx	15°	30°	30°	80°	≈90°
Turbinate complexity	Complex scroll	Complex scroll	Very complex membranous	Simple scroll	Simple scroll

<sup>a</sup>Adult male.

Source: Schreider (1983); Gross and Morgan (1992).

**TABLE 10-6. COMPARATIVE LOWER AIRWAY ANATOMY AS REVEALED ON CASTS**

	Gross Structure					Typical Structure (Generation 6)				
	Mammal/ Body Mass	Left Lung Lobes	Right Lung Lobes	Airway Branching	Trachea Length/Diameter (cm)	Major Airway Bifurcations	Average Airway L/D (ratio)	Branch Angles (Major Daughter/ Minor Daughter) (degrees)	Typical Number of Branches to Terminal Bronchiole	Respiratory Bronchioles
10-50	Human/70 kg	Upper and lower	Upper, middle, and lower	Relatively symmetric	12/2	Sharp for about the first 10 generations, relatively blunt thereafter	2.2	11/33	14-17	About 3-5 orders
	Rhesus monkey/2 kg	Superior, middle, and inferior	Superior, middle, and inferior, azygous	Monopodial	3/0.3	Mixed blunt and sharp	2.6	20/62	10-18	About 4 orders
	Beagle dog/10 kg	Apical, intermediate, and basal	Apical, intermediate, and basal	Strongly monopodial	17/1.6	Blunt tracheal bifurcation, others sharp	1.3	8/62	15-22	About 3-5 orders
	Ferret/0.61 kg	NR <sup>a</sup>	NR	strongly monopodial	10/0.5	Sharp	2.0	16/57	12-20	About 3-4 orders
	Guinea pig/1 kg	Superior and inferior	Superior, middle, and inferior	Monopodial	5.7/0.4	Very sharp and high	1.7	7/76	12-20	About 1 order
	Rabbit/4.5 kg	Superior and inferior	Cranial, middle, caudal, and postcaval	Strongly monopodial	6/0.5	Sharp	1.9	15/75	12-20	About 1-2 orders
	Rat/0.3 kg	One lobe	Cranial, middle, caudal, and postcaval	Strongly monopodial	2.3/0.26	Very sharp and very high throughout lung	1.5	13/60	12-20	Rudimentary
	Golden hamster/0.14 kg	Superior and inferior	Cranial, middle, caudal, and postcaval	Strongly monopodial	2.4/0.26	Very sharp	1.2	15/63	10-18	About 1 order

<sup>a</sup>NR = Not reported.

Source: Phalen and Oldham (1983); Patra (1986); Mercer and Crapo (1987).

**TABLE 10-7. ACINAR MORPHOMETRY**

Species	Fixation	Number of Acini/Lung	V (mm <sup>3</sup> )	D or L (mm) <sup>2</sup>	Number Alveoli/Acinus	Alveolar Duct Generations	References
Human		27,992	1.33-30.9		15,000 10,714	6	Pump (1964) Horsfield and Cumming (1968); Parker et al. (1971)
	75% TLC	23,000	160.8	7.04 (L)	14,000-20,000	9	Hansen and Ampaya (1975); Hansen et al. (1975)
		80,000	15.6	5.1 (L)	7,100	2-5 8-12	Boyden (1972) Schreider and Raabe (1981)
	TLC	26,000-32,000	187.0	8.8 (L)	10,344	9	Haefeli-Bleuer and Weibel (1988)
	FRC	43,000	51.0	6.0 (D)	8,000	9	Mercer, and Crapo (1992)
Rabbit		17,900	2.54				Kliment (1973)
	55% TLC	18,000	3.46	1.95 (L)		6	Rodriguez et al. (1971)
Guinea pig		5,100	1.25				Kliment (1973)
	FRC	4,097	1.09	1.56 (D)	6,890	9-12	Mercer and Crapo (1992)
Rat		2,500	1.0				Kliment (1973)
		2,487	5.06				Yeh et al. (1979)
	FRC	2,020	1.9	1.5 (D)	5,243	10-12	Mercer et al., 1987
	70% TLC	5,993	1.46	1.5 (L)		6	Rodriguez et al. (1987)

<sup>1</sup>Volume of lung at fixation (TLC, total lung capacity; FRC, functional residual capacity).

<sup>2</sup>Acinar size (D, diameter; L, length).

Source: Mercer and Crapo (1992).

The airways show a considerable degree of variability within species (e.g., size and branching pattern) and this is most likely the primary factor responsible for the deposition variability seen within single species (Schlesinger, 1985a).

Larger airway diameter results in greater turbulence for the same relative flow velocity (e.g., between a particle and air). Therefore, flow may be turbulent in the large airways of humans, whereas for an identical flow velocity, it would be laminar in the smaller laboratory animal. Relative to humans, laboratory animals also tend to have tracheas that are much longer in relation to their diameter. This could result in increased relative deposition in humans because of the increased likelihood of laryngeal jet flow extending into the bronchi. Human airways are characterized by a more symmetrical dichotomous branching than that found in most laboratory mammals, which have highly asymmetrical airway branching (monopodial). The more symmetrical dichotomous pattern in humans is susceptible to deposition at the carina because of its exposure to high air flow velocities toward the center of the air flow profile.

Alveolar size also differs between species, which may affect deposition efficiency due to variations on the distance between the airborne particle and alveolar walls (Dahl et al., 1991).

Addressing species differences in ventilation, which affects the tidal volume and ventilation to perfusion ratios, is also critical to estimating initial absorbed dose. Due to the expected variations in airflows within the respiratory tract, the variability among lungs in the human or laboratory animal population, and the variations in respiratory performance that members of the population experience during their normal activities, e.g. sleep and exercise, must be considered in order to gain some insight into the variability that might be expected in particle deposition, total and regional, of particles in the urban atmosphere. The experimentalist must try to keep respiratory parameters relatively constant to obtain reasonably consistent deposition data.

#### **10.4.2 Clearance and Translocation Mechanisms**

Particles that deposit upon airway surfaces may be cleared from the respiratory tract completely, or may be translocated to other sites within this system, by various regionally distinct processes. These clearance mechanisms, which are outlined in Table 10-8, can be

**TABLE 10-8. OVERVIEW OF RESPIRATORY TRACT PARTICLE CLEARANCE AND TRANSLOCATION MECHANISMS**

---



---

Extrathoracic region
Mucociliary transport
Sneezing
Nose wiping and blowing
Dissolution (for "soluble" particles) and absorption into blood
Tracheobronchial region
Mucociliary transport
Endocytosis by macrophages/epithelial cells
Coughing
Dissolution (for "soluble" particles) and absorption into blood
Alveolar region
Macrophages, epithelial cells
Interstitial
Dissolution for "soluble" and "insoluble" particles (intra-and extracellular)

---



---

Source: Schlesinger (1995).

categorized as either absorptive (i.e., dissolution) or nonabsorptive (i.e., transport of intact particles) and may occur simultaneously or with temporal variations. It should be mentioned that particle solubility in terms of clearance refers to solubility within the respiratory tract fluids and cells. Thus, an "insoluble" particle is considered to be one whose rate of clearance by dissolution is insignificant compared to its rate of clearance as an intact particle. For the most part, all deposited particles are subject to clearance by the same mechanisms, with their ultimate fate a function of deposition site, physicochemical properties (including any toxicity), and sometimes deposited mass or number concentration. Clearance routes from the various regions of the respiratory tract are schematically outlined in Figures 10-12 and 10-13. Furthermore, clearance is a continuous process and all mechanisms operate simultaneously for deposited particles.

#### **10.4.2.1 Extrathoracic Region**

The clearance of insoluble particles deposited in the nonolfactory portion of nasal passages occurs via mucociliary transport, and the general flow of mucus is backwards, i.e., towards the nasopharynx (Figure 10-12). However, the epithelium of the most anterior portion of the nasal passages is not ciliated, and mucus flow just distal to this is forward,

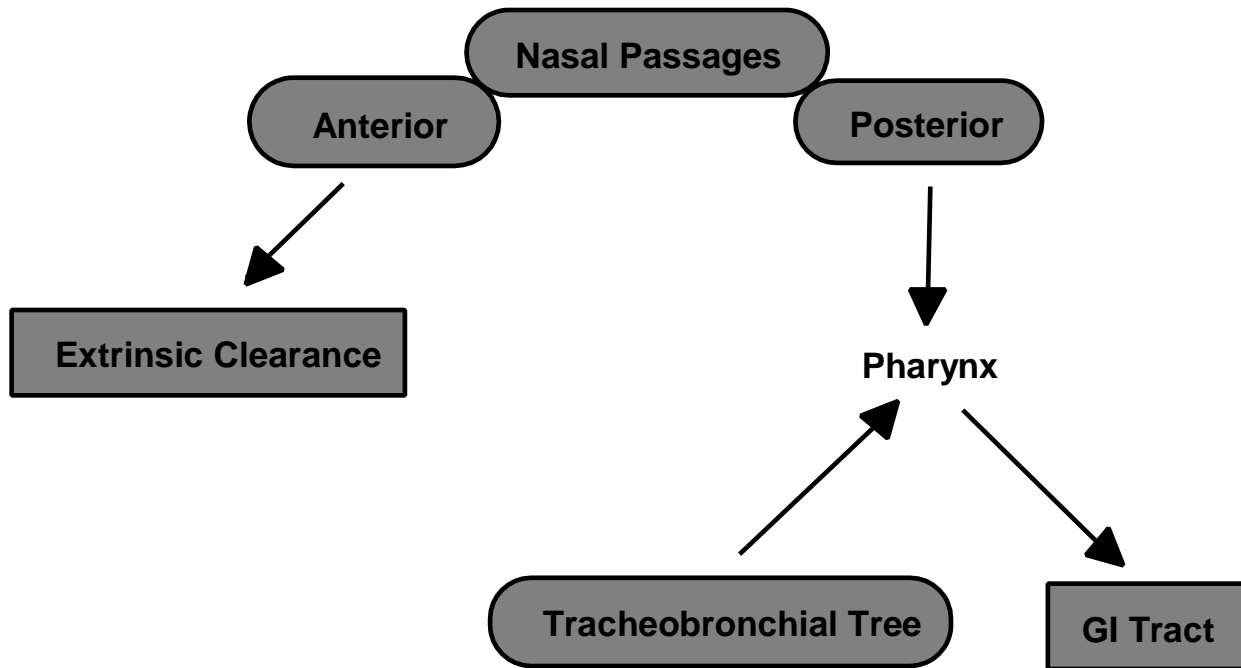


Figure 10-12. Major physical clearance pathways from the extrathoracic region and tracheobronchial tree.

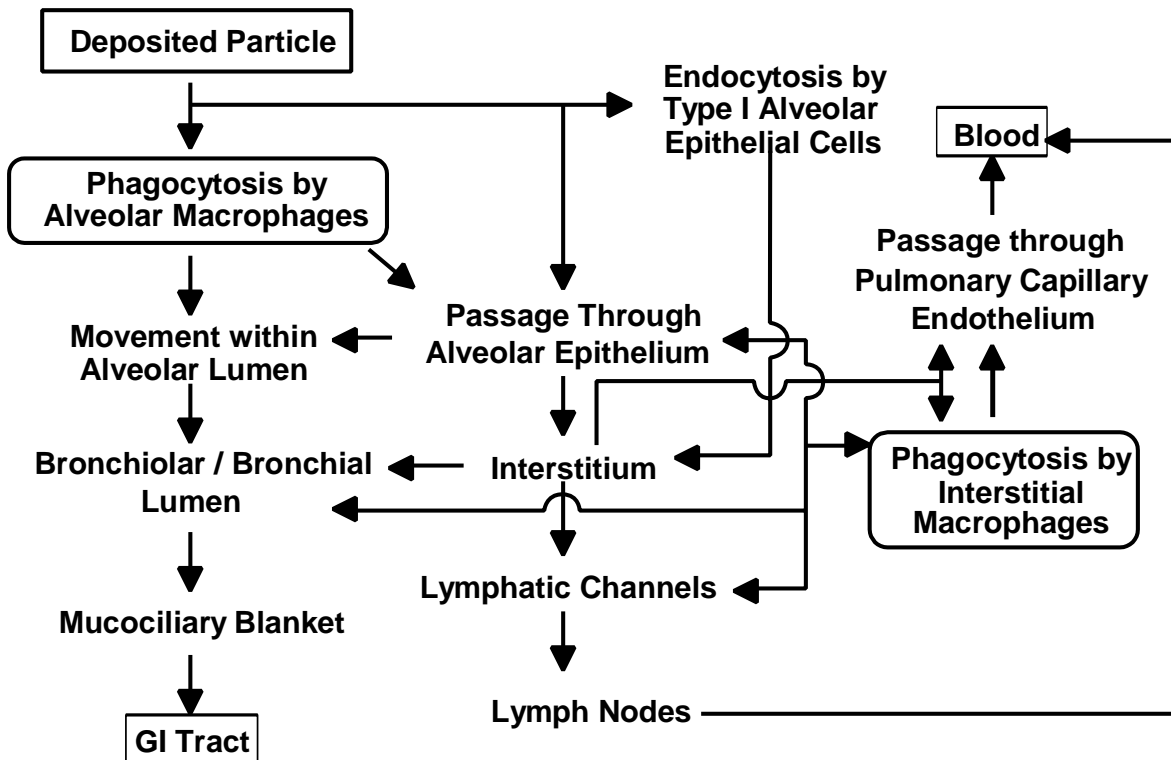


Figure 10-13. Diagram of known and suspected clearance pathways for poorly soluble particles depositing in the alveolar region.

Source: Modified from Schlessinger (1995).

clearing deposited particles to a site (vestibular region) where removal is by sneezing (a reflex response), wiping, or blowing (mechanisms known as extrinsic clearance).

Soluble material deposited on the nasal epithelium will be accessible to underlying cells if it can diffuse to them through the mucus prior to removal via mucociliary transport. Dissolved substances may be subsequently translocated into the bloodstream following movement within intercellular pathways between epithelial cell tight junctions or by active or passive transcellular transport mechanisms. The nasal passages have a rich vasculature, and uptake into the blood from this region may occur rapidly.

Clearance of poorly soluble particles deposited in the oral passages is by coughing and expectoration or by swallowing into the gastrointestinal tract. Soluble particles are likely to be rapidly absorbed after deposition (Swift and Proctor, 1988).

#### **10.4.2.2 Tracheobronchial Region**

Poorly soluble particles deposited within the tracheobronchial tree are cleared primarily by mucociliary transport, with the net movement of fluid towards the oropharynx, followed by swallowing. Some poorly soluble particles may traverse the epithelium by endocytotic processes, entering the peribronchial region (Masse et al., 1974; Sorokin and Brain, 1975). Clearance may also occur following phagocytosis by airway macrophages, located on or beneath the mucous lining throughout the bronchial tree. They then move cephalad on the mucociliary blanket, or via macrophages which enter the airway lumen from the bronchial or bronchiolar mucosa (Robertson, 1980).

As in the nasal passages, soluble particles may be absorbed through the mucous layer of the tracheobronchial airways and into the blood, via intercellular pathways between epithelial cell tight junctions or by active or passive transcellular transport mechanisms.

The bronchial surfaces are not homogeneous; there are openings of daughter bronchi and islands of non-ciliated cells at bifurcation regions. In the latter, the usual progress of mucous movement is interrupted, and bifurcations may be sites of relatively retarded clearance. The efficiency with which such non-ciliated regions are traversed is dependent upon the traction of the mucous layer.

Another method of clearance from the tracheobronchial region, under some circumstances, is cough, which can be triggered by receptors located in the area from the

trachea through the first few bronchial branching levels. While cough is generally a reaction to some inhaled stimulus, in some cases, especially respiratory disease, it can also serve to clear the upper bronchial airways of deposited substances by dislodging mucus from the airway surface.

### **10.4.2.3 Alveolar Region**

Clearance from the alveolar (A) region occurs via a number of mechanisms and pathways, but the relative importance of each is not always certain and may vary between species.

Particle removal by macrophages comprises the main nonabsorptive clearance process in the A region. Alveolar macrophages reside on the epithelium, where they phagocytize and transport deposited material. They come into contact with phagocytized material by random motion, or more likely via directed migration under the influence of local chemotactic factors (Warheit et al, 1988). Contact may be facilitated as some deposited particles are translocated, due to pressure gradients or via capillary action within the alveolar surfactant lining, to sites where macrophages congregate (Schurch et al., 1990; Parra et al., 1986).

Alveolar macrophages normally comprise  $\approx 3 - 5\%$  of the total alveolar cells in healthy (non-smoking) humans and other mammals, and represent the largest subpopulation of nonvascular macrophages in the respiratory tract (Gehr, 1984; Lehnert, 1992). However, the actual cell count may be altered by particle loading. While a slight increase of deposited particles may not result in an increase in cell number, macrophage numbers will increase proportionally to particle number until some peak accumulation is reached (Adamson and Bowden, 1981; Brain, 1971). Since the magnitude of this increase is related more to the number of deposited particles than to total deposition by weight, equivalent masses of an identically deposited substance would not produce the same response if particle sizes differed; thus, deposition of smaller particles would tend to result in a greater elevation in macrophage number than would larger particle deposition.

Particle-laden macrophages may be cleared from the A region along a number of pathways (Figure 10-13). One route is cephalad transport via the mucociliary system after the cells reach the distal terminus of the mucus blanket. However, the manner by which macrophages actually reach the ciliated airways is not certain. The possibilities are chance

encounter; passive movement along the alveolar surface due to surface tension gradients between the alveoli and conducting airways; directed locomotion along a gradient produced by chemotactic factors released by macrophages ingesting deposited material; or passage through the alveolar epithelium and the interstitium, perhaps through aggregates of lymphoid tissue known as bronchus associated lymphoid tissue (BALT) located at bronchoalveolar junctions (Sorokin and Brain, 1975; Kilburn, 1968; Brundel, 1965; Green, 1973; Corry et al., 1984; Harmsen et al., 1985).

Some of the cells which follow interstitial clearance pathways are likely resident interstitial macrophages that have ingested particles which were transported through the alveolar epithelium, probably via endocytosis by Type I pneumocytes (Brody et al., 1981; Bowden and Adamson, 1984). Particle-laden interstitial macrophages can also migrate across the alveolar epithelium, becoming part of the alveolar macrophage cell population (Adamson and Bowden, 1978).

Macrophages that are not cleared via the bronchial tree may actively migrate within the interstitium to a nearby lymphatic channel or, along with uningested particles, be carried in the flow of interstitial fluid towards and into the lymphatic system (Harmsen et al., 1985). Passive entry into lymphatic vessels is fairly easy, since the vessels have loosely connected endothelial cells with wide intercellular junctions (Lauweryns and Baert, 1974). Lymphatic endothelium may also actively engulf particles from the surrounding interstitium (Leak, 1980). Particles within the lymphatic system may be translocated to tracheobronchial lymph nodes, which often become reservoirs of retained material. Particles penetrating the nodes and subsequently reaching the post-nodal lymphatic circulation may enter the blood.

Uningested particles or macrophages in the interstitium may traverse the alveolar-capillary endothelium, directly entering the blood (Raabe, 1982; Holt, 1981); endocytosis by endothelial cells followed by exocytosis into the vessel lumen seems, however, to be restricted to particles  $<0.1 \mu\text{m}$  diameter, and may increase with increasing lung burden (Lee et al., 1989; Oberdörster, 1988). Once in the systemic circulation, transmigrated macrophages, as well as uningested particles, can travel to extrapulmonary organs. Some mammalian species have alveolar intravascular macrophages, which can remove particles from circulating blood and which may play some role in the clearance of material deposited in the alveoli (Warner and Brain, 1990).

Uningested particles and macrophages within the interstitium may travel to perivenous, peribronchiolar or subpleural sites, where they become trapped, increasing particle burden. The migration and grouping of particles and macrophages within the lungs can lead to the redistribution of initially diffuse deposits into focal aggregates (Heppleston, 1953). Some particles can be found in the pleural space, often within macrophages which have migrated across the visceral pleura (Sebastien et al., 1977; Hagerstrand and Siefert, 1973). Resident pleural macrophages do occur, but their role in clearance, if any, is not certain.

During clearance, particles can be redistributed within the alveolar macrophage population (Lehnert, 1992). This can occur following death of a macrophage, and release of free particles to the epithelium, followed by uptake by other macrophages. Some of these newly freed particles may, however, translocate to other clearance routes.

Clearance by the absorptive mechanism involves dissolution in the alveolar surface fluid, followed by transport through the epithelium and into the interstitium, and diffusion into the lymph or blood. Some soluble particles translocated to and trapped in interstitial sites may be absorbed there. Although the factors affecting the dissolution of deposited particles are poorly understood, solubility is influenced by the particle's surface to volume ratio and other surface properties (Morrow, 1973; Mercer, 1967). Thus, materials generally considered to be relatively insoluble may still have high dissolution rates and short dissolution half-times if the particle size is small.

Some deposited particles may undergo dissolution in the acidic milieu of the phagolysosomes after ingestion by macrophages, and such intracellular dissolution may be the initial step in translocation from the lungs for these particles (Kreyling, 1992; Lundborg et al., 1985). Following dissolution, the material can be absorbed into the blood. Dissolved materials may then leave the lungs at rates which are more rapid than would be expected based upon their normal dissolution rate in lung fluid. For example, while insoluble (in lung fluid)  $\text{MnO}_2$  dissolves in the macrophage following ingestion, soluble manganese chloride ( $\text{MnCl}_2$ ) likely dissolves extracellularly and is not ingested, resulting in manganese clearing at different initial rates depending upon the form in which it was initially inhaled (Camner et al, 1985). Differences in rates of clearance may also occur for particles whose rate of dissolution is pH dependent (Marafante et al., 1987).

Finally, some particles can bind to epithelial cell membranes or macromolecules, or other cell components, delaying clearance from the lungs.

#### **10.4.2.4 Clearance Kinetics**

Deposited particles may be cleared completely from the respiratory tract. However, the actual time frame over which clearance occurs affects the cumulative dose delivered to the respiratory tract, as well as to extrapulmonary organs. Particle-tissue contact and retained dose in the extrathoracic region and tracheobronchial tree are often limited by rapid clearance from these regions. On the other hand, the retained dose from material deposited in the A region is more dependent upon the physicochemical characteristics of the particles.

Various experimental techniques have been used to assess clearance rates in both humans and laboratory animals (Schlesinger, 1985b). Because of technical differences and the fact that measured rates are strongly influenced by the specific methodology, comparisons between studies are often difficult to perform. However, regional clearance rates, i.e., the fraction of the deposit which is cleared per unit time, are well defined functional characteristics of an individual human or laboratory animal when repeated tests are performed under the same conditions; but, as with deposition, there is a substantial degree of inter-individual variability.

#### ***Extrathoracic Region***

Mucus flow rates in the posterior nasal passages are highly nonuniform. Regional velocities in the healthy adult human may range from  $< 2$  to  $> 20$  mm/min (Proctor, 1980), with the fastest flow occurring in the midportion of the nasal passages. The median rate in a healthy adult human is about 5 mm/min, the net result being a mean anterior to posterior transport time of about 10-20 min for poorly soluble particles deposited within the nasal passages (Stanley et al., 1985; Rutland and Cole, 1981). However, particles deposited in the anterior portion of the nasal passages are cleared more slowly, at a rate of 1-2 mm/h (Hilding, 1963). Since clearance at this rate may take upwards of 12 h, such deposits are usually more effectively removed by sneezing, wiping, or nose blowing, in which case clearance may occur in 0.5 h (Morrow, 1977; Fry and Black, 1973).

### ***Tracheobronchial Region***

Mucus transport in the tracheobronchial tree occurs at different rates in different local regions; the velocity of movement is fastest in the trachea, and it becomes progressively slower in more distal airways. In healthy non-smoking humans, and using non-invasive procedures and no anesthesia, average tracheal mucus transport rates have been measured at 4.3 to 5.7 mm/min (Leikauf et al., 1981, 1984; Yeates et al., 1975, 1981b; Foster et al., 1980), while that in the main bronchi has been measured at  $\approx 2.4$  mm/min (Foster et al., 1980). While rates of movement in smaller airways have not been directly determined, estimates for human medium bronchi range between 0.2-1.3 mm/min, while those in the most distal ciliated airways range down to 0.001 mm/min (Yeates and Aspin, 1978; Morrow et al., 1967b; Cuddihy and Yeh, 1988).

It is not certain whether the transport rate for deposited poorly soluble particles is independent of their nature, i.e., shape, size, composition. While particles of different materials and sizes have been shown to clear at the same rate in the trachea in some studies (Man et al., 1980; Patrick, 1983; Connolly et al., 1978), other studies (using instillation) have indicated that the rate of mucociliary clearance may be greater for smaller particles ( $\leq 2\mu\text{m}$ ) than for larger ones (Takahashi et al, 1992). Reasons for such particle-size related differences are not known. There may, however, be more than one phase of clearance within individual tracheobronchial airways. For example, the rat trachea shows a biphasic clearance pattern, consisting of a rapid phase within the first 2-4 h after deposition, clearing up to 90% of deposited particles with a half time of  $< 0.5$  h, followed by a second, slower phase, clearing most of the remaining particles with a half-time of 8-19 h (Takahashi et al, 1992).

The total duration of bronchial clearance, or some other time parameter, is often used as an index of mucociliary kinetics, yet the temporal clearance pattern is not certain. In healthy adult non-smoking humans, 90% of poorly soluble particles depositing within the tracheobronchial tree were found to be cleared from 2.5 to 20 h after deposition, depending upon the individual subject and the size of the particles (Albert et al., 1973). While particle size does not affect surface transport, it does affect the depth of particle penetration and deposition and the subsequent pathway length for clearance. Due to differences in regional transport rates, clearance times from different regions of the bronchial tree will differ.

While removal of a TB deposit is generally 99% completed by 48 h after exposure (Bailey et al., 1985a), there is the possibility of longer-term retention under certain circumstances.

Studies with rodents, rabbits, and humans have indicated that a small fraction ( $\approx 1\%$ ) of insoluble material may be retained for a prolonged period of time within the upper respiratory tract (nasal passages) or tracheobronchial tree (Patrick and Stirling, 1977; Gore and Patrick, 1982; Watson and Brain, 1979; Radford and Martell, 1977; Svartengren et al., 1981). The mechanism(s) underlying this long-term retention is unknown, but may involve endocytosis by epithelial cells with subsequent translocation into deeper (submucosal) tissue, or merely passive movement into this tissue. In addition, uptake by the epithelium may depend upon the nature, or size, of the deposited particle (Watson and Brain, 1980). The retained particles may eventually be cleared to regional lymph nodes, but with a long half time that may be  $> 80$  days (Patrick, 1989; Oghiso and Matsuoka, 1979).

There is some suggestion of a greater extent of long term retention in the bronchial tree. Stahlhofen et al. (1986), using a specialized inhalation procedure, noted that a significant fraction, up to 40%, of particles which were likely deposited in the conducting airways were not cleared up to six days post-deposition. They also noted that the size of the particles influenced this retention, with smaller ones being retained to a greater extent than were larger ones (Stahlhofen et al., 1987, 1990). Although the reason for this is not certain, the suggested presence of a surfactant film on the mucous lining of the airways (Gehr et al., 1990) may result in a reduced surface tension which, in turn, influences the displacement of particles into the gel layer and, subsequently, into the sol layer towards the epithelial cells. Particles that reach these cells may then be phagocytized, increasing retention time in the lungs. However, the issue of retention of large fractions of tracheobronchial deposit is not resolved.

Long-term TB retention patterns are not uniform. There is an enhancement at bifurcation regions (Cohen et al., 1988; Radford and Martell, 1977; Henshaw and Fews, 1984), the likely result of both greater deposition and less effective mucus clearance within these areas. Thus, doses calculated based upon uniform surface retention density may be misleading, especially if the material is, toxicologically, slow acting. Solubilized material may also undergo long-term retention in ciliated airways due to binding to cells or macromolecules.

### ***Alveolar Region***

Clearance kinetics in the A region are not definitively understood, although particles deposited there generally remain longer than do those deposited in airways cleared by mucociliary transport. There are limited data on rates in humans, while within any species rates vary widely due to different properties of the particles used in the various studies. Furthermore, some of these studies employed high concentrations of poorly soluble particles, which may have interfered with normal clearance mechanisms, producing rates different from those which would typically occur at lower exposure levels. Prolonged exposure to high particle concentrations is associated with what is termed particle "overload." This is discussed in greater detail in Section 10.4.2.7.

There are numerous pathways of A region clearance, and these may depend upon the nature of the particles being cleared. Thus, generalizations about clearance kinetics are difficult to make, especially since the manner in which particle characteristics affect clearance kinetics is not resolved. Nevertheless, A region clearance can be described as a multiphasic process, each phased considered to represent removal by a different mechanism or pathway, and often characterized by increased retention half-times with time post-exposure.

Clearance of inert, poorly soluble particles in healthy, nonsmoking humans has been generally observed to consist of two phases, with the first having a half-time measured in days, and the second in hundreds of days. Table 10-9 presents some observed times for the longer, second phase of clearance as reported in a number of studies. Differences in technique, chemistry, and solubility of the particles in Table 10-9 are largely responsible for the variations. Although wide variations in retention reflect a dependence upon the nature of the deposited material (e.g., particle size) once dissolution is accounted for, mechanical removal to the gastrointestinal tract and/or lymphatic system appears to be independent of size, especially for particles  $< 5 \mu\text{m}$  (Snipes et al., 1983). Although not evident from Table 10-9, there is considerable intersubject variability in the clearance rates of identical particles, which appears to increase with time post-exposure (Philipson et al., 1985; Bailey et al., 1985a). The large differences in clearance kinetics among different individuals suggest that equivalent chronic exposures to poorly soluble particles may result in large variations in respiratory tract burdens.

**TABLE 10-9. LONG-TERM RETENTION OF POORLY SOLUBLE PARTICLES IN THE ALVEOLAR REGION OF NON-SMOKING HUMANS**

Particle		Retention Half-Time <sup>a</sup> (days)	Reference
Material	Size ( $\mu\text{m}$ )		
Polystyrene latex	5	150 to 300	Booker et al. (1967)
Polystyrene latex	5	144 to 340	Newton et al. (1978)
Polystyrene latex	0.5	33 to 602	Jammett et al. (1978)
Polystyrene latex	3.6	296	Bohning et al. (1982)
Teflon	4	100 to 2,500	Philipson et al. (1985)
Aluminosilicate	1.2	330	Bailey et al. (1982)
Aluminosilicate	3.9	420	Bailey et al. (1982)
Iron oxide ( $\text{Fe}_2\text{O}_3$ )	0.8	62	Morrow et al. (1967a,b)
Iron oxide ( $\text{Fe}_2\text{O}_3$ )	0.1	270	Waite and Ramsden (1971)
Iron oxide ( $\text{Fe}_3\text{O}_4$ )	2.8	70	Cohen et al. (1979)

<sup>a</sup>Represent the half-time for the slowest clearance phase observed.

While the kinetics of overall clearance from the A region have been assessed to some extent, much less is known concerning relative rates along specific pathways, and any available information is generally from studies with laboratory animals. The usual initial step in clearance, i.e., uptake of deposited particles by alveolar macrophages, is very rapid. Ingestion by macrophages generally occurs within 24 h of a single inhalation (Naumann and Schlesinger, 1986; Lehnert and Morrow, 1985). But the actual rate of subsequent macrophage clearance is not certain; perhaps 5% or less of their total number is translocated from the lungs each day in rodents (Lehnert and Morrow, 1985; Masse et al., 1974).

The rate and amount of particle uptake by macrophages is likely governed by particle size and surface properties (Tabata and Ikada, 1988), although these experiments were performed with peritoneal macrophages and not with alveolar macrophages. For example, the effect of particle size was examined by incubating mouse peritoneal macrophages with polymer microspheres (0.5 to 5  $\mu\text{m}$ ). Both the number of particles ingested per cell and the volume of these particles per cell reached a maximum for particle diameters of 1-2  $\mu\text{m}$ , declining on either side of this range. In terms of particle surface, those with hydrophobic surfaces were ingested to a greater extent than were those with hydrophilic surfaces. Phagocytosis also increased as the

surface charge density of a particle increased, but for the same charge density there was no difference in uptake between positively or negatively charged particles.

The time for clearance of particle-laden alveolar macrophages via the mucociliary system depends upon the site of uptake relative to the distal terminus of the mucus blanket at the bronchiolar level. Furthermore, clearance pathways, and subsequent kinetics, may depend to some extent upon particle size. For example, some smaller ultrafine particles (perhaps  $< 0.02 \mu\text{m}$ ) may be less effectively phagocytosed than are larger ones (Oberdörster, 1993). But once ingestion occurs, alveolar macrophage-mediated kinetics are independent of the particle involved, as long as solubility and cytotoxicity are low.

In terms of other clearance pathways, uningested particles may penetrate into the interstitium, largely by Type I cell endocytosis, within a few hours following deposition (Ferin and Feldstein, 1978; Sorokin and Brain, 1975; Brody et al., 1981). This transepithelial passage seems to increase as particle loading increases, especially to a level above the saturation point for increasing macrophage number (Adamson and Bowden, 1981; Ferin, 1977). It may also be particle size dependent, since insoluble ultrafine particles ( $< 0.1 \mu\text{m}$  diameter) of low intrinsic toxicity show increased access to and greater lymphatic uptake than do larger ones of the same material (Oberdörster et al., 1992). However, ultrafine particles of different materials may not enter the interstitium to the same extent. Similarly, any depression of phagocytic activity or the deposition of large numbers of smaller ultrafine particles may increase the number of free particles in the alveoli, enhancing removal by other routes. In any case, free particles and alveolar macrophages may reach the lymph nodes, perhaps within a few days after deposition (Lehnert et al., 1988; Harmsen et al., 1985), although this route is not certain and may be species dependent.

The extent of lymphatic uptake of particles may depend upon the effectiveness of other clearance pathways. For example, lymphatic translocation probably increases when phagocytic activity of alveolar macrophages is decreased (Greenspan, et al., 1988). This may be a factor in lung overload, as discussed in Section 10.4.2.7. However, it seems that the deposited mass or number of particles must reach some threshold below which increases in loading do not affect translocation rate to the lymph nodes (Ferin and Feldstein, 1978; LaBelle and Brieger, 1961).

The rate of translocation to the lymphatic system may be somewhat particle size dependent. Although no human data are available, translocation of latex particles to the lymph nodes of rats was greater for 0.5 to 2  $\mu\text{m}$  particles than for 5 and 9  $\mu\text{m}$  particles (Takahashi et al., 1992), and smaller particles within the 3 to 15  $\mu\text{m}$  size range were found to be translocated at faster rates than were larger sizes (Snipes and Clem, 1981). On the other hand, translocation to the lymph nodes was similar for both 0.4  $\mu\text{m}$  barium sulfate or 0.02  $\mu\text{m}$  gold colloid particles (Takahashi et al., 1987). It seems that particles  $\leq 2 \mu\text{m}$  clear to the lymphatic system at a rate independent of size, and it is particles of this size, rather than those  $\geq 5 \mu\text{m}$ , that would have significant deposition within the A region following inhalation.

In any case, and regardless of any particle size dependence, the normal rate of translocation to the lymphatic system is quite slow, on the order of 0.02-0.003%/day (Snipes, 1989), and elimination from the lymph nodes is even slower, with half-times estimated in tens of years (Roy, 1989).

Soluble particles depositing in the A region may be rapidly cleared via absorption through the epithelial surface into the blood, but there are few data on dissolution and transfer rates to blood in humans. Actual rates depend upon the size of the particle (i.e., solute size), with smaller ones clearing faster than larger ones. Chemistry also plays a role, since water soluble compounds generally clear at a slower rate than do lipid soluble materials.

Absorption may be considered as a two stage process, with the first stage dissociation of the deposited particles into material that can be absorbed into the circulation (dissolution) and the second stage the uptake of this material. Each of these stages may be time dependent. The rate of dissolution depends upon a number of factors, including particle surface area and chemical structure. Uptake into the circulation is generally considered as instantaneous, although a portion of the dissolved material may be absorbed more slowly due to binding to respiratory tract components. Accordingly, there is a very wide range for absorption rates depending upon the physicochemical properties of the material deposited. For example, a highly soluble particle may be absorbed at a rate faster than the particle transport rate and significant uptake may occur in the conducting airways. On the other

hand, a particle that is less soluble and remains in the lungs for years would have a much lower rate, perhaps <0.0001%/day.

#### **10.4.2.5 Factors Modifying Clearance**

A number of host and environmental factors may modify normal clearance patterns, affecting the dose delivered by exposure to inhaled particles. These include aging, gender, workload, disease and irritant inhalation. However, in many cases, the exact role of these factors is not resolved.

##### ***Age***

The evidence for aging-related effects on mucociliary function in healthy individuals is equivocal, with studies showing either no changes or some slowing in mucous clearance function with age after maturity (Goodman et al., 1978; Yeates et al., 1981a; Puchelle et al., 1979). However, it is often difficult to determine whether any observed functional decrement was due to aging alone, or to long-term, low level ambient pollutant exposure (Wanner, 1977). In any case, the change in mucous velocity between approximately age 20 and 70 in humans is about a factor of two (Wolff, 1992) and would likely not significantly affect overall kinetics.

There are few data to allow assessment of aging-related changes in clearance from the A region. Although functional differences have been found between alveolar macrophages of mature and senescent mice (Esposito and Pennington, 1983), no age-related decline in macrophage function has been seen in humans (Gardner et al., 1981).

There are also insufficient data to assess changes in clearance in the growing lung. Nasal mucociliary clearance time in a group of children (average age = 7 yrs) was found to be  $\approx 10$  min (Passali and Bianchini Ciampoli, 1985); this is within the range for adults. There is one report of bronchial clearance in children (12 yrs old), but this was performed in patients hospitalized for renal disease (Huhnerbein et al., 1984).

##### ***Gender***

No gender related differences were found in nasal mucociliary clearance rates in children (Passali and Bianchini Ciampoli, 1985) nor in tracheal transport rates in adults

(Yeates et al., 1975). Slower bronchial clearance has been noted in male compared to female adults, but this was attributed to differences in lung size (and resultant clearance pathway length) rather than to inherent gender related differences in transport velocities (Gerrard et al., 1986).

### ***Physical Activity***

The effect of increased physical activity upon mucociliary clearance is unresolved, with the available data indicating either no effect or an increased clearance rate with exercise (Wolff et al., 1977; Pavia, 1984). There are no data concerning changes in A region clearance with increased activity levels, but CO<sub>2</sub>-stimulated hyperpnea (rapid, deep breathing) was found to have no effect on early alveolar clearance and redistribution of particles (Valberg et al., 1985). Breathing with an increased tidal volume was noted to increase the rate of particle clearance from the A region, and this was suggested to be due to distension related evacuation of surfactant into proximal airways, resulting in a facilitated movement of particle-laden macrophages or uningested particles due to the accelerated motion of the alveolar fluid film (John et al., 1994).

### ***Respiratory Tract Disease***

Various respiratory tract diseases are associated with clearance alterations. The examination of clearance in individuals with lung disease requires careful interpretation of results, since differences in deposition of tracer particles used to assess clearance function may occur between normal individuals and those with respiratory disease, and this would directly impact upon the measured clearance rates, especially in the tracheobronchial tree. In any case, nasal mucociliary clearance is prolonged in humans with chronic sinusitis, bronchiectasis, or rhinitis (Majima et al., 1983; Stanley et al., 1985), and in cystic fibrosis (Rutland and Cole, 1981). Bronchial mucus transport may be impaired in people with bronchial carcinoma (Matthys et al., 1983), chronic bronchitis (Vastag et al., 1986), asthma (Pavia et al., 1985), and in association with various acute infections (Lourenco et al., 1971; Camner et al., 1979; Puchelle et al., 1980). In certain of these cases, coughing may enhance mucus clearance, but it generally is effective only if excess secretions are present.

Normal mucociliary function is essential to respiratory tract health. Studies of individuals with a syndrome characterized by impaired clearance, i.e., primary ciliary dyskinesia (PCD),

may be used to assess the importance of mucociliary transport and the effect of its dysfunction upon respiratory disease, and to provide information on the role of clearance in maintaining the integrity of the lungs. The lack of mucociliary function in PCD is directly responsible for the early development of recurrent respiratory tract infections and, eventually, chronic bronchitis and bronchiectasis (Rossman et al., 1984; Wanner, 1980). It is, however, not certain whether partial impairment of the mucociliary system will increase the risk of lung disease.

Rates of A region particle clearance appear to be reduced in humans with chronic obstructive lung disease (Bohning et al., 1982) and in laboratory animals with viral infections (Creasia et al., 1973). The viability and functional activity of macrophages was found to be impaired in human asthmatics (Godard et al., 1982).

Studies with laboratory animals have also found disease related clearance changes. Hamsters with interstitial fibrosis showed an increased degree of alveolar clearance (Tryka et al., 1985). Rats with emphysema showed no clearance difference from control (Damon et al., 1983), although the co-presence of inflammation resulted in prolonged retention (Hahn and Hobbs, 1979). On the other hand, inflammation may enhance particle and macrophage penetration through the alveolar epithelium into the interstitium, by increasing the permeability of the epithelium and the lymphatic endothelium (Corry et al., 1984). Neutrophils, which are phagocytic cells present in alveoli during inflammation, may contribute to the clearance of particles via the mucociliary system (Bice et al., 1990).

Macrophages have specific functional properties, namely phagocytic activity and mobility, which allow them to adequately perform their role in clearance. Alveolar macrophages from calves with an induced interstitial inflammation (pneumonitis) were found to have enhanced phagocytic activity compared to normal animals (Slauson et al., 1989). On the other hand, depressed phagocytosis was found with virus-induced acute bronchiolitis and alveolitis (Slauson et al., 1987). How such alterations affect clearance from the A region is not certain, since the relationship between macrophage functional characteristics and overall clearance is not always straightforward. While changes in macrophage function do impact upon clearance, the manner by which they do so may not always be easily

predictable. In any case, the modification of functional properties of macrophages appear to be injury specific, in that they reflect the nature and anatomic pattern of disease.

### ***Inhaled Irritants***

Inhaled irritants have been shown to have an effect upon mucociliary clearance function in both humans and laboratory animals (Schlesinger, 1990; Wolff, 1986). Single exposures to a particular material may increase or decrease the overall rate of tracheobronchial clearance, often depending upon the exposure concentration (Schlesinger, 1986). Alterations in clearance rate following single exposures to moderate concentrations of irritants are generally transient, lasting < 24 h. However, repeated exposures may result in an increase in intra-individual variability of clearance rate and persistently retarded clearance. The effects of irritant exposure may be enhanced by exercise, or by coexposure to other materials.

Acute and chronic exposures to inhaled irritants may also alter A region clearance (Cohen et al., 1979; Ferin and Leach, 1977; Schlesinger et al., 1986; Phalen et al., 1994), which may be accelerated or depressed, depending upon the specific material and/or length of exposure. While the clearance of poorly soluble particles from conducting airways is due largely to only one mechanism, i.e., mucociliary transport, clearance from the respiratory region involves a complex of multiple pathways and processes. Because transit times along these different pathways vary widely, a toxicant-induced change in clearance rate could be due to a change in the time for removal along a particular pathway and/or to a change in the actual route taken. Thus, it is often quite difficult to delineate specific mechanisms of action for toxicants which alter overall clearance from respiratory airways. Alterations in alveolar macrophages likely underlay some of the observed changes, since numerous irritants have been shown to impair the numbers and functional properties of these cells (Gardner, 1984).

Since a great number of people are exposed to cigarette smoke, it is of interest to summarize effects of this irritant upon clearance processes. Smoke exposed animals and humans show increased number of macrophages recoverable by bronchopulmonary lavage (Brody and Davis, 1982; Warr and Martin, 1978; Matulionis, 1984; Zwicker et al., 1978). However, the rate of particle clearance from the A region of the lungs appears to be reduced in cigarette smokers (Bohning et al., 1982; Cohen et al., 1979).

While cigarette smoking has been shown to affect tracheobronchial mucociliary clearance function, the effects range from acceleration to slowing. Some of the apparent discrepancies in different studies is related to differences in the effects of short-term versus long-term effects of cigarette smoke. Long term smokers appear to have mucociliary clearance which is slower than that in nonsmokers (Lourenco et al., 1971; Albert et al., 1971) and which also show certain anomalies, such as periods of intermittent clearance stasis. On the other hand, the short term effects of cigarette smoke range from acceleration to retardation depending upon the number of cigarettes smoked (Albert et al., 1971; Lippmann et al., 1977; Albert et al., 1974).

#### **10.4.2.6 Comparative Aspects of Clearance**

As with deposition analyses, the inability to study the retention of certain materials in humans for direct risk assessment requires use of laboratory animals. Since dosimetry depends upon clearance rates and routes, adequate toxicologic assessment necessitates that clearance kinetics in these animals be related to those in humans. The basic mechanisms and overall patterns of clearance from the respiratory tract appear to be similar in humans and most other mammals. However, regional clearance rates can show substantial variation between species, even for similar particles deposited under comparable exposure conditions (Snipes, 1989).

Dissolution rates and rates of transfer of dissolved substances into the blood may or may not be species independent, depending upon certain chemical properties of the deposited material (Griffith et al., 1983; Bailey et al., 1985b; Roy, 1989). For example, lipophilic compounds of comparable molecular weight are cleared from the lungs of various species at the same rate (dependent solely upon solute molecular weight and the lipid/water partition coefficient), but hydrophilic compounds do show species differences.

On the other hand, there are distinct interspecies differences in rates of mechanical transport in the conducting and A airways. While mucous transport rates in the nasal passages seem to be similar in humans and the limited other species examined (Morgan et al., 1986; Whaley, 1987), tracheal mucous velocities vary among species as a function of body weight (Felicetti et al., 1981; Wolff, 1992).

In the A region, macrophage-mediated clearance of poorly soluble particles is species dependent, with small mammalian species generally exhibiting faster clearance than larger species, with the exception of the guinea pig which clears slower than laboratory rodents. This may result from interspecies differences in macrophage-mediated clearance of poorly soluble particles (Valberg and Blanchard, 1992; Bailey et al., 1985b), transport of particles from the A region to alveolar lymph nodes (Snipes et al., 1983; Mueller et al., 1990), phagocytic rates and chemotactic responses of alveolar macrophages (Warheit and Hartsky, 1994), or the prevalence of BALT (Murray and Driscoll, 1992). These likely result in species-dependent rate constants for these clearance pathways, and differences in regional (and perhaps total) clearance rates between some species are a reflection of these differences in mechanical processes. For example, the relative proportion of particles cleared from the A region in the short and longer term phases of clearance differs between laboratory rodents and larger mammals, with a greater percentage cleared in the faster first phase in laboratory rodents. The end result of interspecies differences in deposition and clearance is that the retention of deposited particles can differ between species, and this may result in differences in response to similar particulate exposure atmospheres.

#### **10.4.2.7 Lung Overload**

Some experimental studies using laboratory rodents employed high exposure concentrations of relatively nontoxic, poorly soluble particles, which interfered with normal clearance mechanisms, producing clearance rates different from those which would occur at lower exposure levels. Prolonged exposure to high particle concentrations is associated with what is termed particle "overload." This is defined as the overwhelming of macrophage-mediated clearance by the deposition of particles at a rate which exceeds the capacity of that clearance pathway. It is a nonspecific effect noted in experimental studies, generally in rats, using many different kinds of poorly soluble particles (including TiO<sub>2</sub>, volcanic ash, diesel exhaust particles, carbon black, and fly ash) and results in A region clearance slowing or stasis, with an associated inflammation and aggregation of macrophages in the lungs and increased translocation of particles into the interstitium (Muhle et al., 1990; Lehnert, 1990; Morrow, 1994). While some overload induced effects are reversible, the extent of such reversibility decreases as the degree of overloading increases (Muhle et al., 1990). Once

some critical particle burden is reached, particles of all sizes (those studies ranged from ultrafine to 4  $\mu\text{m}$ ) show increased translocation into the interstitium (Oberdörster et al., 1992). This phenomenon has been suggested to be due to the inhibition of alveolar macrophage mobility.

While the exact amount of deposition needed to induce overload is uncertain, it has been hypothesized that it will begin, in the rat, when deposition approaches 1 mg particles/g lung tissue (Morrow, 1988). When the concentration reaches 10 mg particles/g lung tissue, macrophage-mediated clearance of particles would effectively cease. Overload may be related more to the volume of particles ingested than to the total mass (Morrow, 1988; Oberdörster et al., 1992b). Following overloading, the subsequent retardation of lung clearance, accumulation of particles, inflammation, and the interaction of inflammatory mediators with cell proliferative processes and DNA may lead to the development of tumors and fibrosis in rats (Mauderly, 1994).

Alternative hypotheses exist for the events that define the onset of lung overload. One hypothesis is that if repeated exposures to poorly soluble particles occurs, some critical lung burden may be reached. Until the critical lung burden is reached, clearance is normal; above the critical lung burden, clearance becomes progressively retarded and associated other changes occur. The other hypothesis is that overload is a function of the amount of poorly soluble particles which deposit daily, i.e., deposition rate (Muhle, 1988; Creutzenberg et al., 1989; Bellmann et al., 1990). Clearance retardation was suggested to occur at exposure levels of 3  $\text{mg}/\text{m}^3$  or higher. Thus, some critical deposition rate over a sufficient exposure duration would result in retardation of clearance (Yu et al., 1989).

The relevance of lung overload to humans, and even to species other than laboratory rats and mice, is not clear. While it likely to be of little relevance for most "real world" ambient exposures of humans, it is of concern in interpreting some long-term experimental exposure data. It may, however, be of some concern to humans occupationally exposed to some particle types (Mauderly, 1994), since overload may involve all insoluble materials and affect all species if the particles are deposited at a sufficient rate (Pritchard, 1989), (i.e., if the deposition rate exceeds the clearance rate). In addition, the relevance to humans is also clouded by the suggestion that macrophage-mediated clearance is normally slower and

perhaps less important in humans than in rats (Morrow, 1994), and that there will be significant differences in macrophage loading between the two species.

### **10.4.3 Acidic Aerosols**

An Issue Paper on Acid Aerosols was published by the Environmental Protection Agency in 1989. Section 3 of that document was devoted to the deposition and fate of acid aerosols. Moreover, that Section provided an update of particle deposition data from both human and laboratory animal studies, described hygroscopic aerosol studies reported between 1977 and 1987, and presented a thorough discussion of the neutralization of acid aerosols by airway secretions and absorbed ammonia.

This section consists of two subsections: the first concerns the phenomenon of hygroscopicity; and the second presents current information on acidic aerosol neutralization.

#### **10.4.3.1 Hygroscopicity of Acidic Aerosols**

Hygroscopicity can be defined as the propensity of a material for taking up and retaining moisture under certain conditions of humidity and temperature. It is well known that action of ocean waves continuously disperses tons of hygroscopic saline particles into the atmosphere and these contribute to worldwide meteorologic phenomena. As industrialization has expanded, the evolution of gaseous pollutants, especially the oxides of sulfur and nitrogen, has caused a greatly increased atmospheric burden of aerosols mainly derived from gas-phase reactions. These aerosols are predominantly both acidic and hygroscopic, consisting of mixtures of partially neutralized nitric, sulfuric and hydrochloric acids: i.e., inorganic salts, such as nitrites, bisulfates, sulfates and chlorides. In addition, small amounts of organic acid salts, e.g., formate and acetate, are present as are a variety of trace elements, e.g., cadmium, carbon, vanadium, chromium and phosphorus, whose oxides and other chemical forms tend also to be acid forming (Aerosols, 1986).

Experimental studies on deposition of acid aerosols are limited. There have been two studies in laboratory animals using  $\text{H}_2\text{SO}_4$  aerosols. Dahl and Griffith (1983) measured regional deposition of these aerosols in the size range from 0.4 to 1.2  $\mu\text{m}$  MMAD generated at 20% and 80% relative humidities. Their data showed greater total and regional deposition of  $\text{H}_2\text{SO}_4$  aerosols in rats compared to nonhygroscopic aerosols having the same MMAD's

(Figure 10-14). Deposition of  $\text{H}_2\text{SO}_4$  aerosols generated at 20% RH was also higher than those generated at 80% RH, indicating that the increase in deposition was caused by the growth of the particles in the highly humid environment of the respiratory tract.

However, a similar study by Dahl et al. (1983) found that deposition of  $\text{H}_2\text{SO}_4$  aerosols in beagle dogs at these two relative humidities was similar to that of nonhygroscopic aerosols having the same size although deposition at 20% RH was again higher than that at 80% RH. The inconsistent results were explained by Dahl et al. (1985) to be caused by the large intersubject variability of deposition in dogs.

Two reviews (Morrow, 1986; Hiller, 1991) have been published on hygroscopic aerosols which consider the implications of hygroscopic particle growth on deposition in the human respiratory tract. Much of the treatment of hygroscopic particle growth is based on theoretical models (e.g., Xu and Yu, 1985; Ferron et al., 1988; Martonen and Zhang, 1993). Suffice it to say, particulate sodium chloride has been commonly utilized in these models and to a lesser extent, sulfuric acid droplets, and ammonium sulfate and ammonium bisulfate particles. There are no major distinctions in the growth of these hygroscopic materials except that sulfuric acid does not manifest a deliquescent point (when the particle becomes an aqueous droplet). It can be seen in Figure 10-15 that the growth rate of hygroscopic particles is controlled by the relative humidity (RH): the closer to saturation (100% RH), the faster the growth rate.

In humans, deposition of acid aerosols in the respiratory tract has only been estimated by model studies. Martonen and Zhang (1993) estimated deposition of  $\text{H}_2\text{SO}_4$  aerosols in the human lung for various ages and three different activity levels. The  $\text{H}_2\text{SO}_4$  aerosol was considered to be in equilibrium with atmospheric conditions outside the lung prior to being inhaled. The results of their calculation for rest breathing without considering extrathoracic deposition are shown in Figure 10-16. Comparing to nonhygroscopic aerosols such as  $\text{Fe}_2\text{SO}_3$ , deposition of  $\text{H}_2\text{SO}_4$  aerosols in different regions of the lung may be higher or lower depending upon the initial particle size. There is a critical initial size of  $\text{H}_2\text{SO}_4$  in the 0.2 to 0.4  $\mu\text{m}$  range. For larger particles the influence of hygroscopicity of  $\text{H}_2\text{SO}_4$  aerosols is to increase total lung deposition, whereas for smaller particles the opposite occurs.

Hygroscopic particles or droplets of different initial size will experience different growth rates: the smallest particles being the fastest to reach an equilibrium size. For

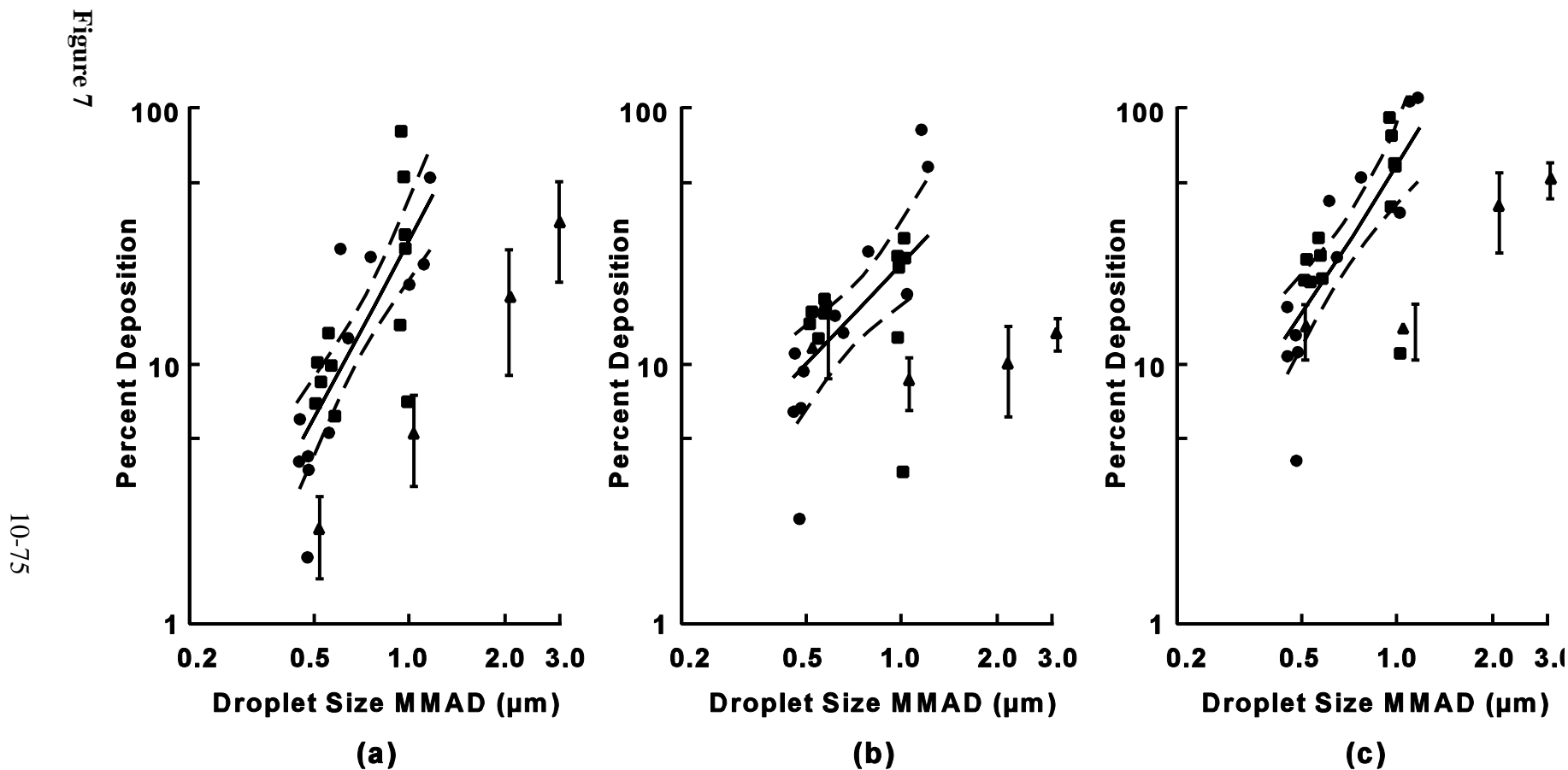


**Figure 10-14.** Regional deposition data in rats versus particle size for sulfuric acid mists and dry particles. Panel (a) = upper airway deposition; (b) = lower airway deposition; and (c) = total deposition. Circles are 20% relative humidity; squares are 80% relative humidity; triangles are dry nonhygroscopic particles. Solid curves represent the mean of the data for sulfuric acid mists. Error bars and broken curves represent 95% confidence limits.

Source: Dahl and Griffith (1983).

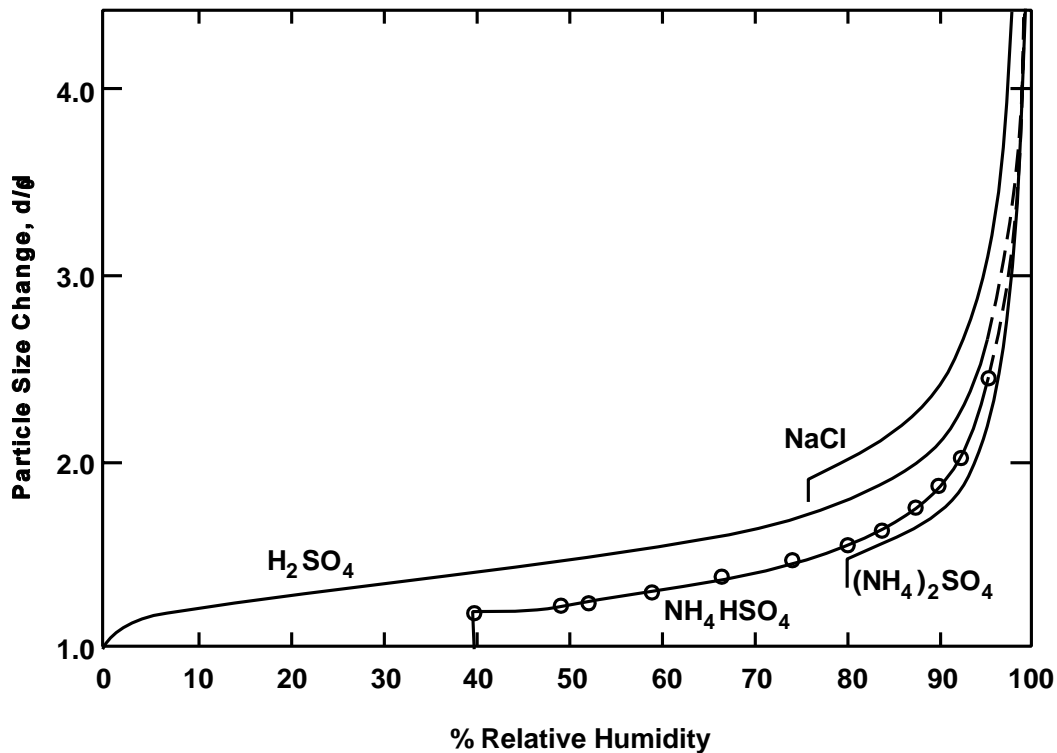


**Figure 10-15. Theoretical growth curves for sodium chloride, sulfuric acid, ammonium bisulfate, and ammonium sulfate aerosols in terms of the initial ( $d_0$ ) and final ( $d$ ) size of the particle. Note that the  $H_2SO_4$  curve, unlike those for the three salts, has no deliquescence point.**

Source: Tang and Munkelwitz (1977).

example, a  $0.5 \mu\text{m}$  diameter particle will require approximately 1 s, whereas a  $2.0 \mu\text{m}$  particle will require close to 10 s. It is immediately evident that many inhaled hygroscopic particles will not reach their equilibrium size (maximum growth) during the duration of a single respiratory cycle (ca 4 s). Conversely, the growth of ultrafine particles does not resemble that for particles  $>0.1 \mu\text{m}$  and thereby represents a special case. Moreover, the hygroscopic growth characteristics of aqueous droplets, containing one or more solutes, depend not only on their initial size, but their initial composition. The study of Cocks and Fernando (1982), using the condensation model of Fukuta and Walter (1970), with ammonium sulfate droplets illustrate both of these last points (Figure 10-17).

The direct measurement of the RH of alveolar air and the temperature of air at the alveolar surface have been attempted, but because of technical limitations, the direct

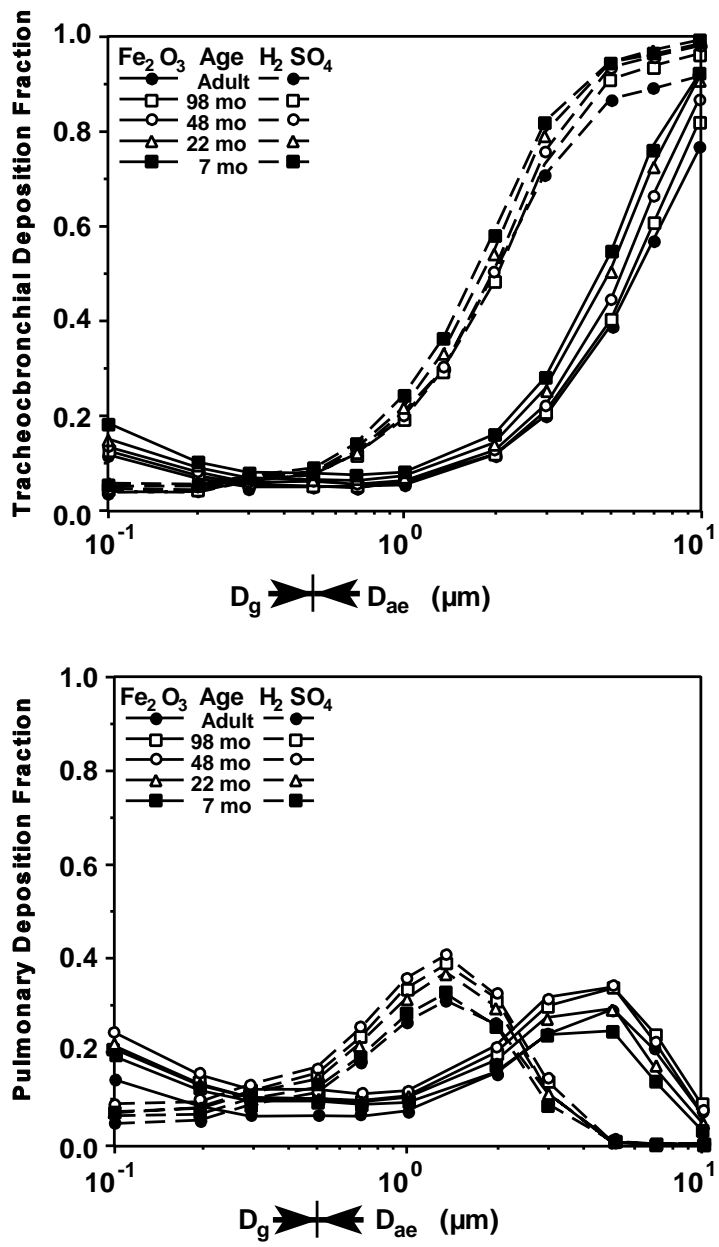


**Figure 10-16. Regional deposition of hygroscopic sulfuric acid ( $\text{H}_2\text{SO}_4$ ) and control iron oxide ( $\text{Fe}_2\text{O}_3$ ) particles at quiet breathing in the human lung as a function of subject age.**

Source: Martonen and Zhang (1993).

experimental determinations of these and other values at different levels of the respiratory tract have only been considered reliable for conditions in the conducting airways (Morrow, 1986). Fortunately, indirect methods for these determinations have been

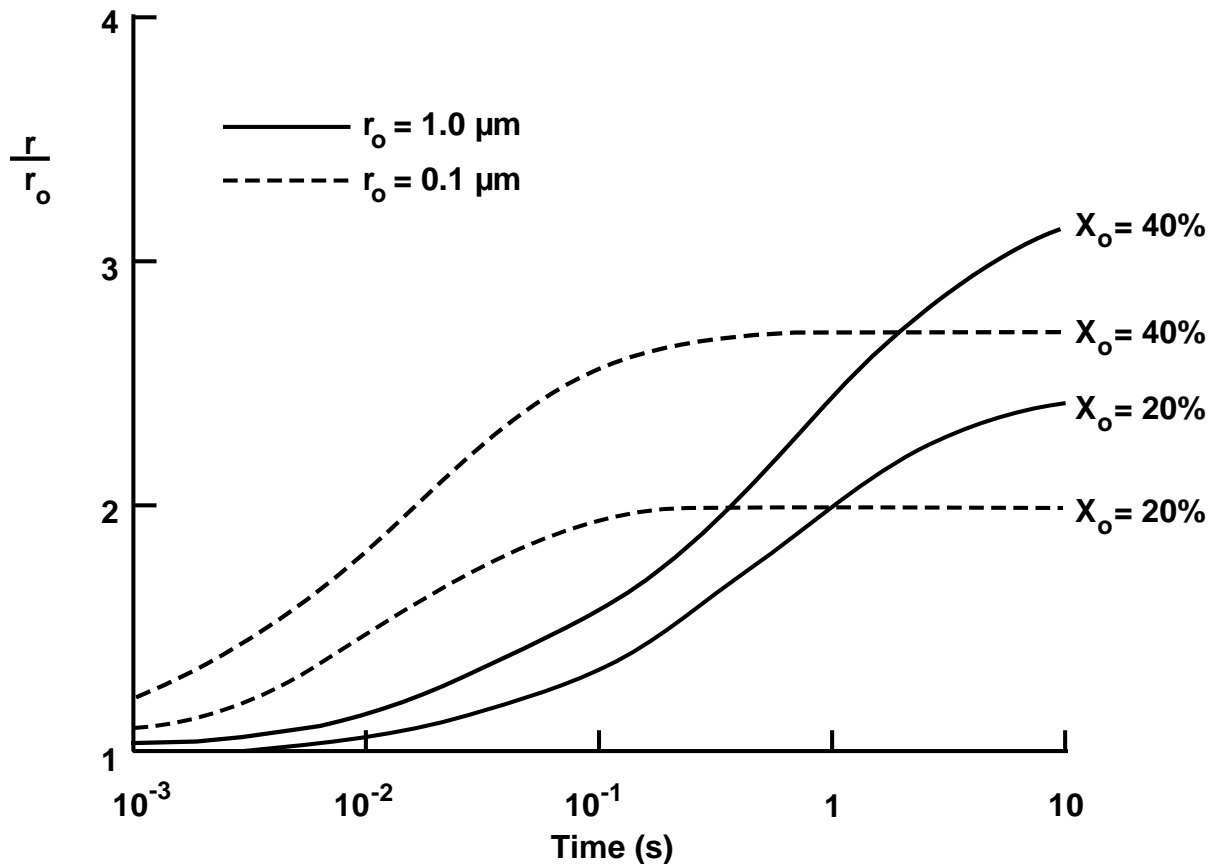


**Figure 10-17.** Distinctions in growth ( $r/r_0$ ) of aqueous ammonium sulfate  $[(\text{NH}_4)_2\text{SO}_4]$  droplets of 0.1 and 1.0  $\mu\text{m}$  initial size are depicted as a function of their initial solute concentrations ( $X_0$ ).

Source: Cocks and Fernando (1982).

successful. For deep-lung temperature, Edwards et al. (1963) used solubility of a helium-argon mixture in arterial blood. By this approach they found the mean pulmonary capillary temperature in five normal subjects to be 37.52 °C. Because of individual variability, they also provided an equation for estimating the deep lung temperature in an individual from a measurement of rectal temperature.

Ferron and co-workers (1983, 1985) made the logical assumption that the RH of the alveolar air was determined by an equilibrium with the vapor pressure of blood serum at the capillary level. The osmolarity of serum at 37 °C ( $287 \pm 4$  mmol/kg) provided these investigators a sound basis for selecting 99.5% RH as the value to use in all of the modeling estimations. In Figure 10-18 (from Xu and Yu, 1985) the calculated equilibrium diameters

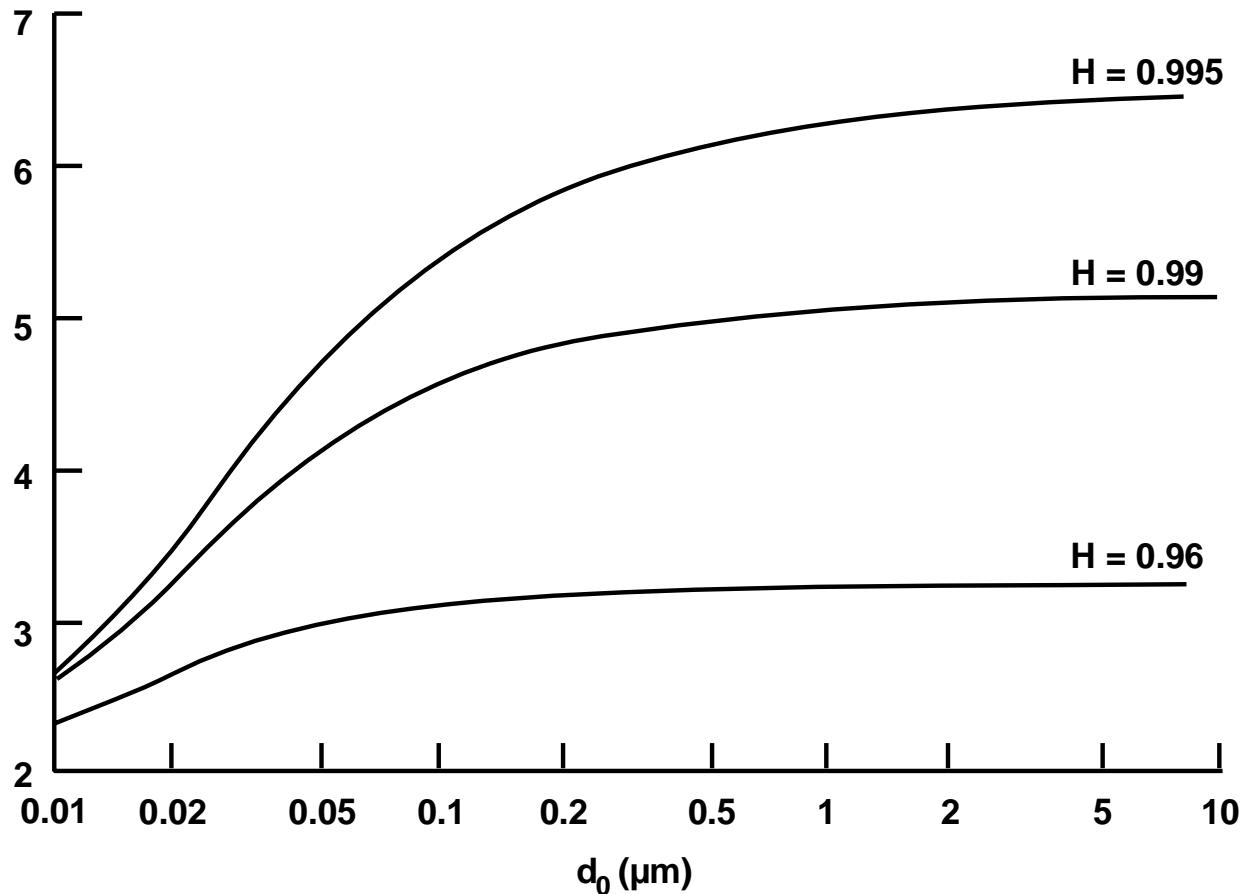


**Figure 10-18. The initial diameter of dry sodium chloride particles ( $d_0$ ) and equilibrium diameter achieved ( $d$ ) are shown for three relative humidity assumptions.**

Source: Xu and Yu (1985).

for sodium chloride particles on the basis of their initial size ( $d_0$ ) is depicted. The equilibrium diameters ( $d_{oo}$ ) that can be achieved theoretically for each particle size is shown as a function of three different RH values. For an RH of 99.5%, the growth of salt particles with an initial size greater than  $0.5 \mu\text{m}$ , yields about a 6-fold increase in diameter.

Ferron et al. (1988) calculated the RH in the human airways by employing a transport theory for heat and water vapor using cylindrical coordinates. Several parameters of the theory were chosen to best fit the available experimental data. These authors also used the transport theory to model the growth and deposition of three salts, viz., NaCl,  $\text{CoCl}_2 \cdot 6\text{H}_2\text{O}$ ,

and  $\text{ZnSO}_4 \cdot 7\text{H}_2\text{O}$ , which were selected because these differentially hydrated particles have large, moderate and small hygroscopic growth potentials, respectively. Figure 10-19 depicts the growth of these three salts when their initial dry particle size is  $1.0 \mu\text{m}$  diameter, the average inspired airflow is  $250 \text{ cc/s}$ , and the inhalation is by mouth. In this depiction, the particle growth is expressed as the ratio of the achieved aerodynamic diameter to the initial aerodynamic size.

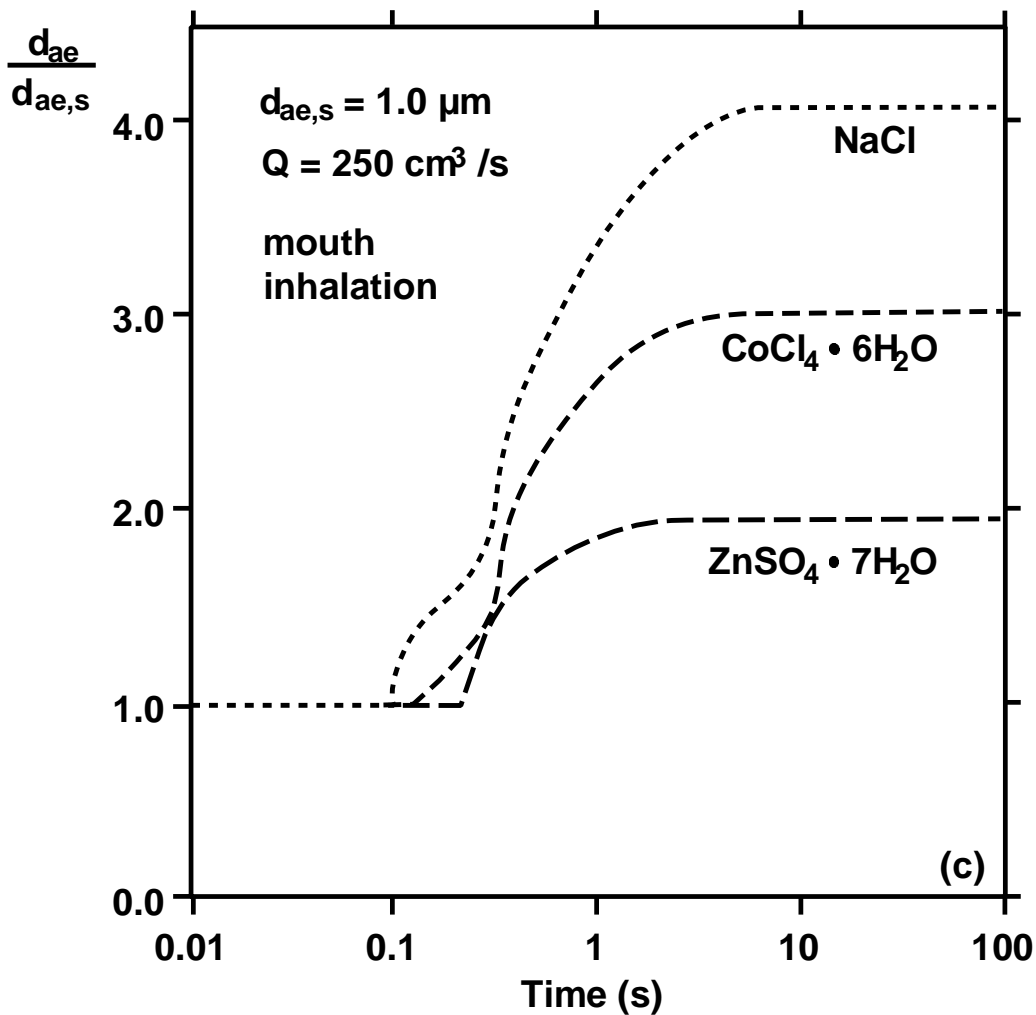


**Figure 10-19.** The initial dry diameter ( $d_{ae,s}$ ) of three different salts is assumed to be  $1.0 \mu\text{m}$ . Their subsequent growth to an equilibrium diameter at 99.5%RH is shown by the ratio ( $d_{ae}/d_{ae,s}$ ). The highly hydrated salts of cobalt chloride and zinc sulfate exhibit a reduced growth potential compared to sodium chloride.

Source: Ferron et al. (1988).

A recent experimental study by Anselm et al. (1990) used an indirect method, similar to that employed earlier by Tu and Knudsen (1984), to validate the 99.5% RH assumption for alveolar air. In this instance, monodisperse NaCl particles between 0.2 and 0.5  $\mu\text{m}$  were made by vibrating orifice generator and administered, by mouth, as boli during a constant inspiratory airflow. During expiration, the particles suspended in the same volume element were size classified. To determine equilibrium particle sizes, 600 mL of aerosol was inspired followed by 400 mL of clean air. Expiration was initiated after different periods of breath holding and the behavior of NaCl particles (loss and settling velocities) was compared to that of a stable (nonhygroscopic) aerosol. Through this approach, the investigators found that the diameters of the NaCl particles initially 0.2  $\mu\text{m}$  and 0.25  $\mu\text{m}$ , increased 5.55 and 5.79-fold, respectively. These values were found to be consistent with a 99.5% RH.

To make the transport theory model estimations more pragmatic, Ferron and coworkers (1992, 1993) made estimations for heterodisperse aerosols of salts with the range of growth potentials used in their 1988 study. Also, deposition estimates for  $\text{H}_2\text{SO}_4$  aerosols, incorporating variabilities in age-related airway morphometry and in physical activity levels, have been reported by Martonen and Zhang (1993) using some innovative modeling assumptions.

In his excellent review of hygroscopic particle growth and deposition and their implications to human health, Hiller (1991) concluded that despite the importance of models, there remains insufficient experimental data on total and regional deposition of hygroscopic aerosols in humans to confirm these models adequately.

#### **10.4.3.2 Neutralization and Buffering of Acidic Particles**

The toxicity of acidic particles may be modulated following their inhalation. This may occur within the inhaled air, by neutralization reaction with endogenous respiratory tract ammonia, or following deposition, due to buffering within the fluid lining of the airways.

##### ***Reaction of Acidic Particles with Respiratory Tract Ammonia***

Ammonia ( $\text{NH}_3$ ) is present in the air within the respiratory tract. Measurements taken in exhaled air have found that the  $\text{NH}_3$  concentration varies, depending upon the site of measurement, with levels obtained via oral breathing greater than those measured in the nose

or trachea (Larson et al., 1977; Vollmuth and Schlesinger, 1984). Because of these concentration differences between the oral and nasal passages, the route of acidic particle inhalation likely plays a significant role in determining the hydrogen ion ( $H^+$ ) available for deposition in the lower respiratory tract. Thus, for the same mass concentration of acidic particles, inhalation via the mouth will result in more neutralization compared to inhalation via the nose, and less  $H^+$  available for deposition in the lungs (Larson et al., 1982). The toxicity of acidic particles is likely due to the  $H^+$ , as discussed in Chapter 11.

The possibility that endogenous ammonia could chemically neutralize inhaled acidic particles to their ammonium salts prior to deposition on airway surfaces, thereby reducing toxicity, was originally proposed by Larson et al. (1977) in relation to acidic sulfate aerosols. Since, stoichiometrically, 1  $\mu g$  of  $NH_3$  can convert 5.8  $\mu g$  of  $H_2SO_4$  to ammonium bisulfate ( $NH_4HSO_4$ ), or 2.9  $\mu g$  of  $H_2SO_4$  to ammonium sulfate [ $(NH_4)_2SO_4$ ], they determined, based upon the range of  $NH_3$  levels measured in the exhaled air of humans, that up to 1,500  $\mu g/m^3$  of inhaled  $H_2SO_4$  could be converted to  $(NH_4)_2SO_4$ . For a given sulfate content in an exposure atmosphere, both ammonium bisulfate and ammonium sulfate are less potent irritants than is sulfuric acid.

Complete neutralization of inhaled sulfuric acid or ammonium bisulfate would produce ammonium sulfate. However, partial neutralization of sulfuric acid would reduce to varying extents the amount of  $H^+$  available for deposition, thereby modulating toxicity. The extent of neutralization has been shown to play a role in measured toxicity from inhaled sulfuric acid. Utell et al. (1989) exposed asthmatic subjects to sulfuric acid under conditions of high or low levels of expired ammonia. The response to inhaled acid exposure was greater when exposure was conducted under conditions of low oral ammonia levels.

The extent of reaction of ammonia with acid sulfates depends upon a number of factors. These include residence time within the airway, which is a function of ventilation rate, and inhaled particle size. In terms of the latter, for a given amount of ammonia, the extent of neutralization is inversely proportional to particle size, at least within the diameter range of 0.1-10  $\mu m$  (Larson et al., 1993). In addition, for any given ammonia concentration, the extent of neutralization of sulfuric acid increases as mass concentration of the acid aerosol decreases (Schlesinger and Chen, 1994).

Cocks and McElroy (1984) presented a model analysis for neutralization of sulfuric acid particles in human airways. Particle acidity was a function of both dilution by particle growth and neutralization by ammonia. As an example of their results, neutralization would be complete in 3 sec for  $\text{H}_2\text{SO}_4$  (3M) having a particle size of  $0.5 \mu\text{m}$  and a mass concentration of  $100 \mu\text{g}/\text{m}^3$ , with the ammonia level at  $500 \mu\text{g}/\text{m}^3$ . If the  $\text{NH}_3$  level is reduced to  $50 \mu\text{g}/\text{m}^3$ , neutralization would take longer.

Larson (1989) presented another model for neutralization of inhaled acidic sulfate aerosols in humans. It was concluded that significant deposition of acid in the lower respiratory tract would occur in the presence of typical respiratory tract  $\text{NH}_3$  levels, for both oral or nasal inhalation of  $\text{H}_2\text{SO}_4$  particles at  $0.3 \mu\text{m}$ . However, particles at  $0.03 \mu\text{m}$  should be completely neutralized in the upper respiratory tract. While this latter seems to contradict findings of significant biological responses in guinea pigs following exposure to ultrafine acid particles (Chapter 11), this could reflect differences in residence times and ammonia levels between different species. Furthermore, it is likely that under most circumstances, only partial neutralization of inhaled sulfuric acid occurs prior to deposition (Larson et al., 1977). In any case, these conclusions support toxicological findings of biological effects following inhalation of sulfuric acid concentrations that should, based solely upon stoichiometric considerations, be completely neutralized, and highlights the complexity of neutralization processes in the respiratory tract.

Larson et al. (1993) examined the role of ammonia and ventilation rate on response to inhaled (oral) sulfuric acid by estimating, using the model of Larson (1989), the acid concentrations to which the lungs would be exposed during oral inhalation. They concluded that combinations of high ammonia and low ventilation rate or low ammonia and high ventilation rate produce smaller or larger amounts of acid deposition, respectively, even if the acid concentration at the point of inhalation remained constant. The former condition resulted in greater neutralization than did the latter.

### ***Buffering by Airway Surface Fluid (Mucus)***

Mucus lining the conducting airways has the ability to buffer acid particles which deposit within it. The pH of mammalian tracheobronchial mucus has been reported to be within a range of about 6.5 to 8.2 (Boat et al., 1994; Gatto, 1981; Holma et al., 1977).

This variability may be due to differences in the methods used and species examined, as well as the likelihood that the acid-base equilibrium differs at different levels of the tracheobronchial tree, but may also reflect variations in secretion rate and the occurrence of inflammation. The influence on pH of various other endogenous factors, such as secretion of hydrogen or bicarbonate ions, and the role of specific mucus constituents, such as secreted acidic glycoproteins and basic macromolecules, have not been extensively examined.

The buffering capacity of human sputum, a mixture of saliva and mucus, was examined by Holma (1985), by titrating sputum equilibrated with 5% carbon dioxide at 37 °C and 100% relative humidity (RH) with sulfuric acid. While the buffering capacity was variable, depending upon the sputum sample examined, depression of pH from 7.25 to 6.5 required the addition of approximately 6  $\mu\text{mol}$  of hydrogen ion ( $\text{H}^+$ ) per milliliter of sputum. Assuming a tracheobronchial mucus volume of 2.1 mL, between 8 and 16  $\mu\text{mol}$  of  $\text{H}^+$ , if evenly distributed through the airways, would be required to depress mucus pH from 7.4 to 6.5. Since 1  $\mu\text{g}$   $\text{H}^+$  is obtained from 49  $\mu\text{g}$  of sulfuric acid, between 390 and 780  $\mu\text{g}$  of sulfuric acid would be required to cause this change in pH. With an inhalation exposure duration of 0.5 h, ventilation at 20 L/min and 50% deposition (in the total respiratory tract) of 100  $\mu\text{g}/\text{m}^3$  sulfuric acid (at 1M), 0.6  $\mu\text{mol}$  of  $\text{H}^+$  would be deposited in the lungs. However, the distribution of submicrometer acid particles in the respiratory tract is not uniform and, therefore, greater changes in pH may be anticipated on a regional basis in those areas having higher than average deposition. If, for example, 30  $\mu\text{g}$  of acid deposited in 0.2 mL of mucus, a greater change in pH would likely occur.

The above example may apply to healthy individuals. However, the buffering capacity of mucus may be altered in individuals with compromised lungs. For example, sputum from asthmatics had a lower pH than that from healthy subjects, and a reduced buffering capacity (Holma, 1985). This group may, therefore, represent a portion of the population which is especially sensitive to inhaled acidic particles. The potential sensitivity of asthmatics to acid particles is discussed in greater detail in Chapter 11.

While biological responses following the inhalation of acidic aerosols are likely due to the  $\text{H}^+$  component of these particles, it has been suggested that pH may not be the sole determinant of response to acid particles, but that response may actually depend upon total available hydrogen ion, or titratable acidity, depositing upon airway surfaces. Fine et al.

(1987) hypothesized that buffered acid aerosols (with a greater  $H^+$  pool) would cause a greater biological response than would unbuffered acid aerosols having the same pH. Since airway surface fluids have a considerable capacity to buffer acid, it was suggested that the buffered acid would cause a more persistent decrease in airway surface fluid pH. Thus, it appears that the specific metric of acidity used, i.e., pH or titratable acid, would, therefore, be reflected in the relationship between amount of deposited acidity and resultant biological response.

## **10.5 DEPOSITION DATA AND MODELS**

The background information in Sections 10.4 demonstrates that a knowledge of where particles of different sizes deposit in the respiratory tract and the amount of their deposition is necessary for understanding and interpreting the health effects associated with exposure to particles. As was seen, the respiratory tract can be divided into the ET, TB and A regions on the basis of structure, size and function. Particles deposited in the various regions have large differences in clearance pathways and, consequently, retention times. This section discusses the available data on particle deposition in humans and laboratory animals. Different approaches for modeling these data are also discussed. Theoretical models must assume average values and simplifying conditions of respiratory performance in order to make reasonable estimates. This latter approach was initiated by the meteorologist Findeisen (1935) over fifty years ago, when he developed a simplified anatomic model of the respiratory tract and assumed steady inspiratory and expiratory air flows in order to estimate the interactions between the anatomy of the respiratory tract and particle deposition based on physical laws. Despite much progress in respiratory modeling, there are not major distinctions in total particle deposition predictions among models and experimental verifications have been generally satisfactory.

### **10.5.1 Humans**

The deposition of particles within the human respiratory tract have been assessed using a number of techniques (Valberg, 1985). Unfortunately, the use of different experimental methods and assumptions results in considerable variations in reported values. This section

discusses the available particle deposition data in humans for either the total respiratory tract or in terms of regional deposition.

### 10.5.1.1 Total Deposition

If the quantity of aerosol particles deposited in the entire respiratory tract is divided by that inhaled, the result is called total deposition fraction or total deposition. Thus, total deposition can be measured by comparing particle concentrations of the inhaled and exhaled, but the regional involvement cannot be distinguished. By the use of test aerosol particles with radiolabels, investigators have been able to separate deposition by region, beginning from the ET region with either nasal and nasopharyngeal deposition for nose breathing or oral and pharyngeal deposition for mouth breathing. The measurement of clearance of the radiolabeled particles from the thorax can be used to separate fast clearance, usually assumed to be an indicator of TB deposition, from the more slowly cleared A deposition (see below for more discussion).

Total human deposition data, as a function of particle size with nose and mouth breathing compiled by Schlesinger (1988) are depicted in Figure 10-20. These data were obtained by various investigators using different sizes of test spherical particles in healthy male adults under different ventilation conditions. Deposition with nose breathing is generally higher than that with mouth breathing because mouth breathing bypasses the filtration capabilities of the nasal passages. For large particles with aerodynamic diameters  $d_{ae}$  greater than  $1 \mu\text{m}$ , deposition is governed by impaction and sedimentation and it increases with increasing  $d_{ae}$ . When  $d_{ae} > 10 \mu\text{m}$ , almost all inhaled particles are deposited. As the particle size decreases from  $0.1 \mu\text{m}$ , diffusional deposition becomes dominant and total deposition depends more upon the physical diameter  $d$  of the particle. Decreasing particle diameter leads to an increase in total deposition in this particle size range. Total deposition shows a minimum for particle diameters in the range of  $0.1 \mu\text{m}$  to  $0.5 \mu\text{m}$  where neither sedimentation nor diffusion deposition are effective. The particle diameter at which the minimum deposition occurs is different for nose breathing and mouth breathing and it depends upon flow rate and airway dimensions. For all particle sizes, mixing of the tidal air and functional residual air can enhance particle deposition by providing a mechanism for keeping the inhaled particles in the lung for a longer time and

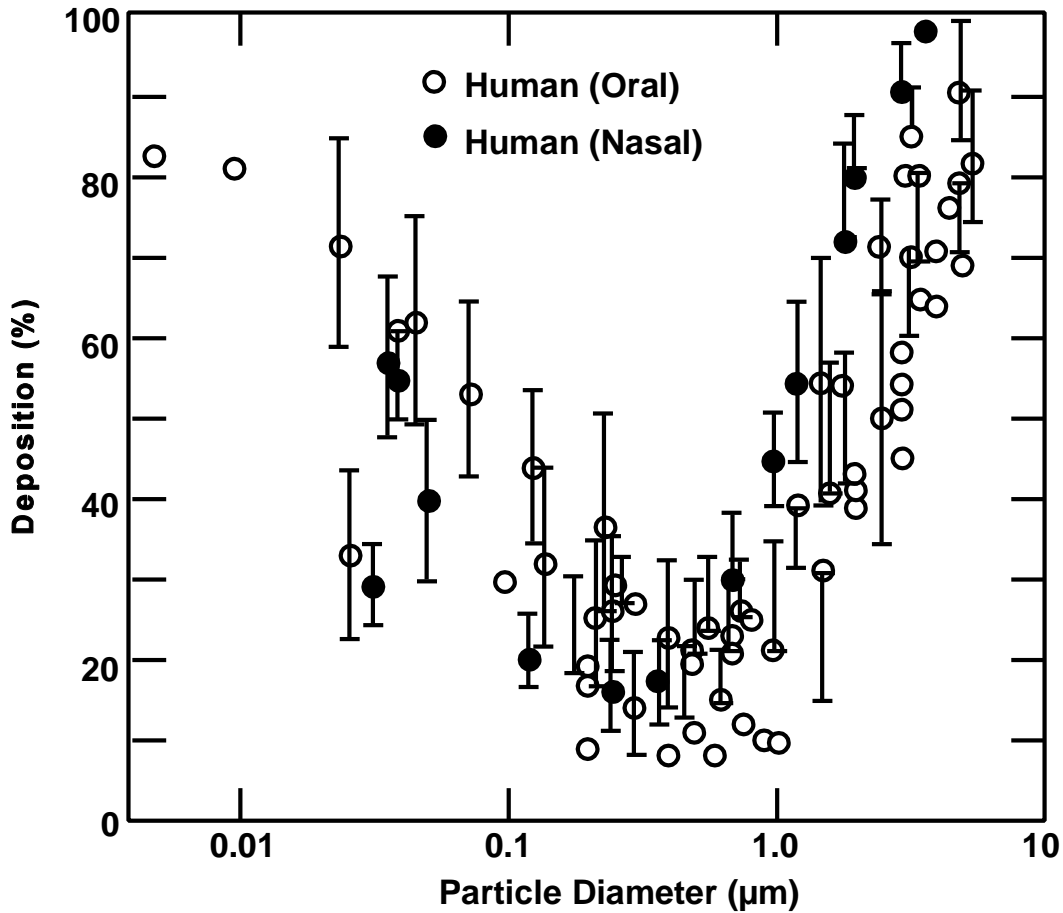


**Figure 10-20. Total deposition data (percentage deposition of amount inhaled) in humans as a function of particle size. All values are means with standard deviations when available. Particle diameters are aerodynamic (MMAD) for those  $\geq 0.5 \mu\text{m}$ .**

Source: Schlessinger (1988).

thereby increasing the probability of the particles to deposit. This factor is more significant for particle sizes for which deposition is low. Good deposition experiments therefore should account for mixing into the residual volume by requiring subjects to fully exhale.

Although various studies in Figure 10-20 all appear to show the same trend, there is a significant amount of scatter in the data. Much of this scatter can be explained by the use of different test particles and methods in the experimental studies, as well as different breathing modes and ventilation conditions employed by the subjects. However, a good portion of the scatter is caused by the differences in airway morphology and breathing pattern among

subjects (Heyder et al., 1982, 1988; Yu et al., 1979; Yu and Diu, 1982a,b; Bennett and Smaldone, 1987; Bennett, 1988). In addressing the health-related issues of inhaled particles, this intersubject variability is an important factor which must be taken into consideration.

Indeed, for well controlled experiments and controlled breathing patterns (constant inspiratory flow in half a cycle and constant expiratory flow in another half cycle and no pause), total deposition data do not have the amount of scatter shown in Figure 10-20. Figure 10-21 shows the data by Heyder et al. (1986) and Schiller et al. (1986, 1988) reported by Stahlhofen et al. (1989) at controlled mouth breathing for particle size ranging from 0.005  $\mu\text{m}$  to 15  $\mu\text{m}$  and three different ventilation conditions. Total deposition was found higher for larger tidal volume while the minimum deposition occurred at about 0.4  $\mu\text{m}$  for all three ventilation conditions.

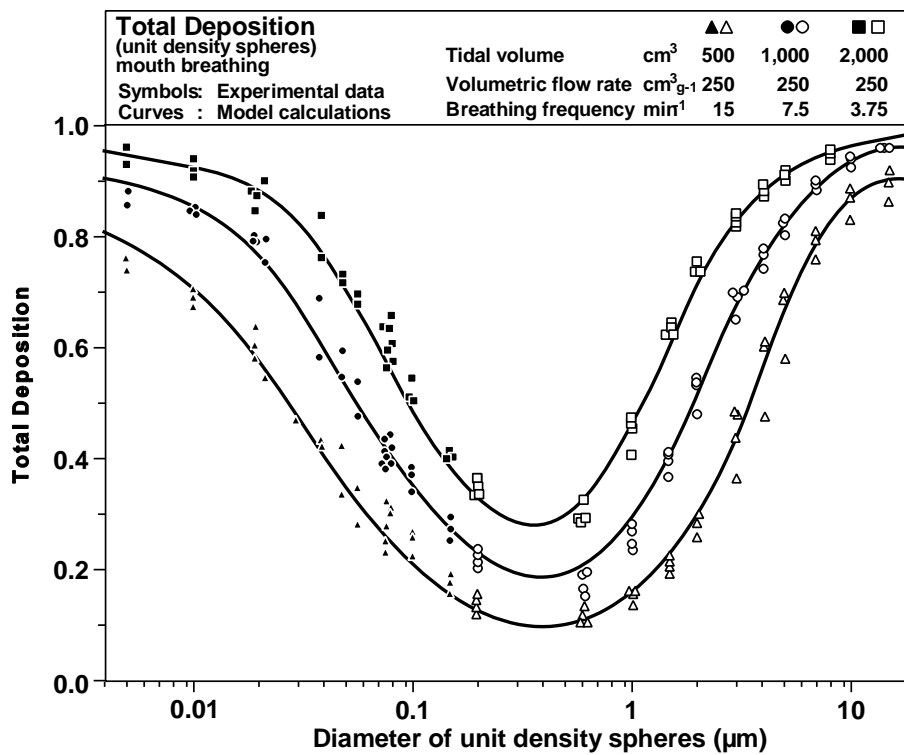


**Figure 10-21. Total deposition as a function of the diameter of unit density spheres in humans for variable tidal volume and breathing frequency. Experimental data are by Heyder et al. (1986) and Schiller et al. (1988). The curves represent empirical fitting.**

Source: Stahlhofen et al. (1988).

### 10.5.1.2 Extrathoracic Deposition

The fraction of inhaled particles depositing in the ET region can be quite variable, depending on particle size, flow rate, breathing frequency and whether the breathing is through the nose or through the mouth. During exertion, the flow resistance of the nasal passages cause a shift to mouth breathing in almost all individuals, thereby bypassing much of the filtration capabilities of the head and leading to increased deposition in the lung (TB and A regions). For nose breathing, the usual technique for measuring inspiratory deposition is to draw the aerosol through the nose and out of the mouth while the subject holds his mouth open (Pattle, 1961; Lippmann, 1970; Hounam et al., 1969, 1971). The aerosol concentration is measured before it enters the nose and after it leaves the mouth. Neglecting mouth deposition during expiration, inspiratory nasal deposition can be calculated from the concentration difference. Another method to measure the nasal deposition is to use the lung as a part of the experimental system (Giacomelli-Maltoni et al., 1972; Martens and Jacobi, 1973; Rudolf, 1975). The deposition of particles in the nose is calculated from total deposition of particles in the entire respiratory tract for mouth, nose, mouth-nose and nose-mouth breathing. Because mouth deposition is not significant under the experimental conditions, this method allows the determination of nasal deposition for both inspiration and expiration.

Deposition in the mouth for expiration is normally assumed to be negligible. For inspiration, the deposition in mouth has been measured using radioactive aerosol particles (Rudolf, 1975; Lippmann, 1977; Foord et al., 1978; Stahlhofen et al., 1980; Chan and Lippmann, 1980; Stahlhofen et al., 1981, 1983). The amount of deposition is obtained from the difference of activity measurements, one immediately after exposure and the other after the deposited particles are removed with mouthwash or other means. Because the subjects in these experiments breathe through a large bore tube, the deposition via the mouth occurs predominantly in the larynx. Rudolf et al. (1984, 1986) have suggested to name this laryngeal deposition. Mouth deposition by natural mouth breathing without using a mouthpiece was measured in an earlier study by Dennis (1961) and recently by Bowes and Swift (1989) during natural oronasal breathing at moderate and heavy exercise conditions. The data showed a much greater deposition than breathing through a mouth-piece.

For  $d_{ac} > 0.2 \mu\text{m}$ , ET deposition is usually expressed as a function of  $d_{ac}^2 Q$ , where  $Q$  is the flow rate. This is the appropriate parameter for normalizing impaction-dominated deposition when the actual flow rates in the experimental studies are not identical. Even with this normalization, deposition data in the extrathoracic region by various workers exhibit a very large amount of scatter as shown in Figures 10-22 and 10-23, respectively, for inspiratory nasal and mouth deposition. Besides uncertainty in measurement techniques, one major source of this scatter, similar to the case of total deposition, comes from intersubject and intrasubject variabilities. The intersubject variability may arise from the difference in anatomical structure and dimensions, number of nasal hairs, breathing pattern, etc., while the intrasubject variability may be caused by the degree of mouth opening and by the nasal resistance cycle in which airflow may be redistributed from one side to the other side, by as much as 20 to 80%.

Mathematical model studies on the deposition in the nose and mouth are very limited. There have been only two attempts to determine nasal deposition during inspiration (Landahl, 1950b; Scott et al., 1978). At present, formulas useful for predicting ET deposition are derived empirically from experimental data (Pattle, 1961; Yu et al., 1981; Rudolf et al., 1983, 1984, 1986; Miller et al., 1988; Zhang and Yu, 1993). The formulas by Rudolf et al. (1983, 1984, 1986) given below, with some modification, have been adopted by the International Commission on Radiological Protection (ICRP, 1994) in their dosimetry model. Deposition efficiency via the nose ( $\eta_N$ ) or mouth ( $\eta_M$ ) is expressed in terms of an impaction parameter ( $d_{ac}^2 Q$ ), as

$$\eta_N = 1 - [3.0 \times 10^{-4} (d_{ac}^2 Q) + 1]^{-1}, \quad (10-22)$$

or

$$\eta_M = 1 - [1.1 \times 10^{-4} (d_{ac} Q^{0.6} V_T^{-0.2})^{1.4} + 1]^{-1}. \quad (10-23)$$

where  $d_{ac}$  is in the unit of  $\mu\text{m}$ ,  $Q$  in  $\text{cm}^3/\text{s}$ , and  $V_T$  is the tidal volume in  $\text{cm}^3$ . Equation 10-22 applies to both inspiration and expiration since the data by Heyder and Rudolf (1977) do not show a systematic difference between the two efficiencies. The

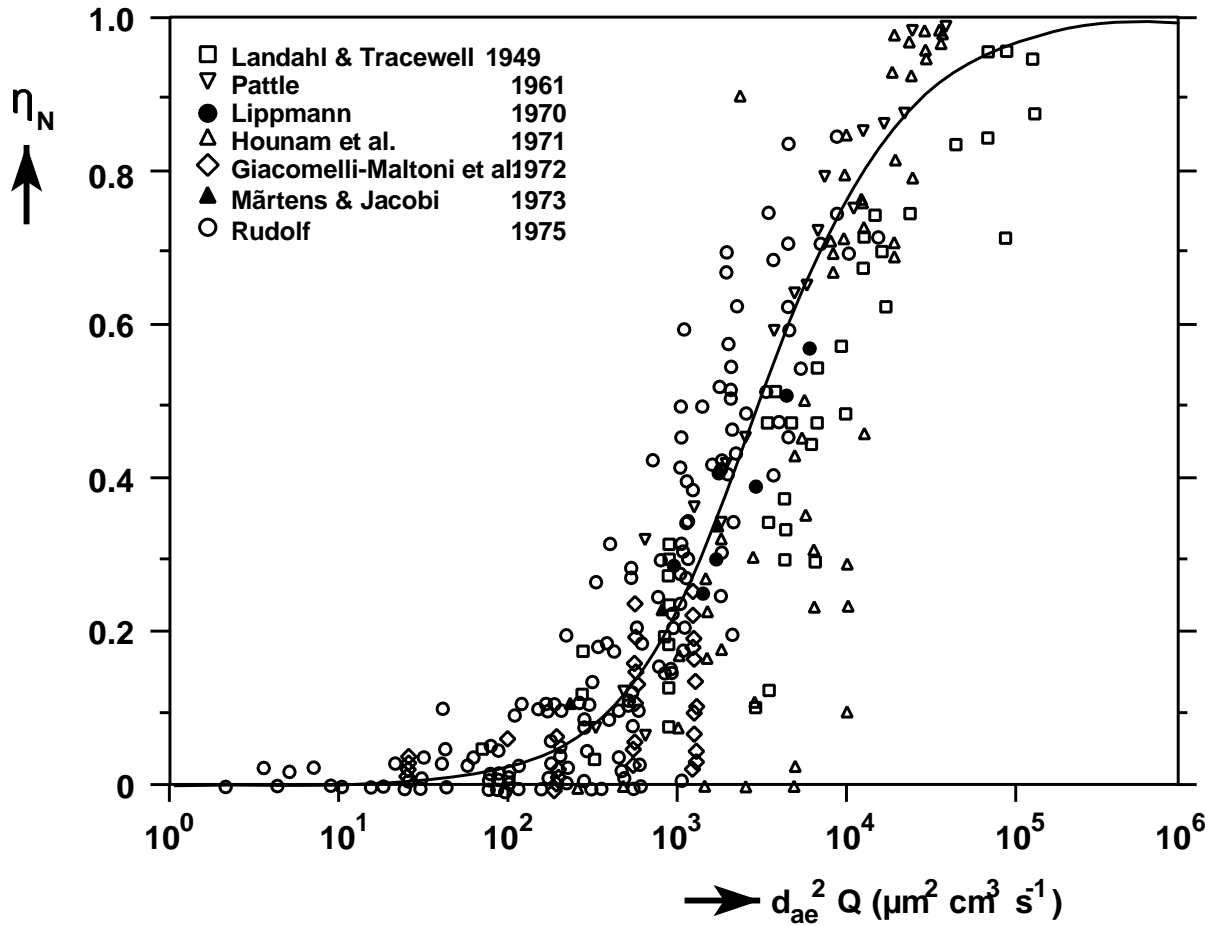


**Figure 10-22. Inspiratory deposition of the human nose as a function of particle aerodynamic diameter and flow rate ( $d_{ae}^2 Q$ ). The curve represents Equation 10-22.**

Source: Stahlhofen et al. (1988).

inclusion of  $V_T$  in Equation 10-23 is caused by the fact that the size of the ET region during mouth breathing increases with increasing flow rate and with increasing tidal volume.

For ultrafine particles ( $d < 0.1 \mu\text{m}$ ), deposition in the ET region is controlled by the mechanism of diffusion which depends only on the particle geometric diameter,  $d$ . At this time, ET deposition for this particle size range has not been studied extensively in humans. George and Breslin (1969) measured nasal deposition of radon progeny in three subjects but the diffusion coefficient of the progeny was uncertain. Schiller et al. (1986, 1988) later obtained inspiratory nasal deposition from total deposition measurements using a nose in -

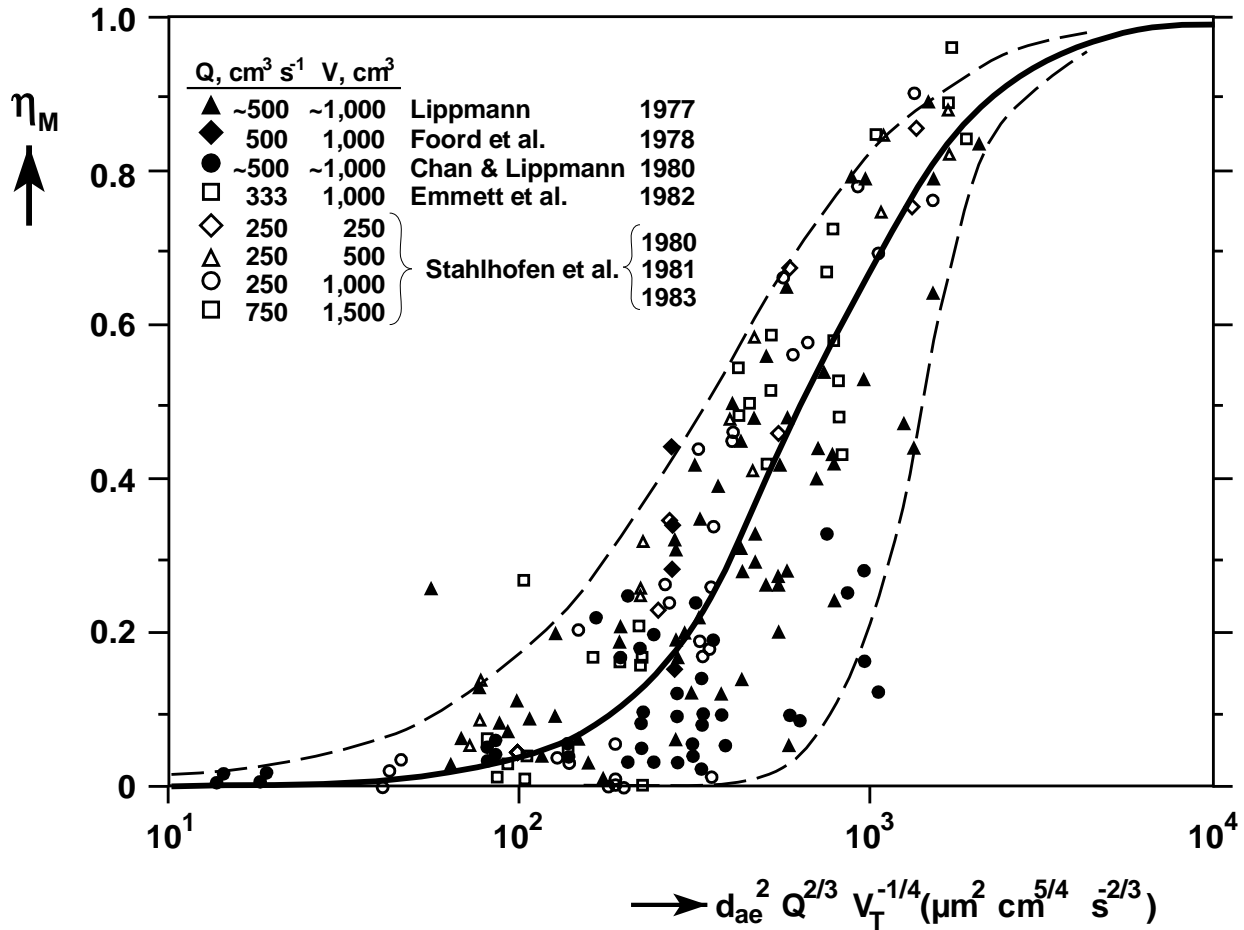


**Figure 10-23. Inspiratory extrathoracic deposition data in humans during mouth breathing as a function of particle aerodynamic diameter, flow rate, and tidal volume ( $d_{ae}^2 Q^{2/3} V_T^{-1/4}$ ). The curve represents Equation 10-23.**

Source: Stahlhofen et al. (1988).

mouth out and mouth in-nose out maneuver. However, their data cannot be considered reliable because mouth deposition is not negligible compared to nose deposition.

The only data available to date for ET deposition of ultrafine particles are from cast measurements (Cheng et al., 1988, 1990, 1993; Yamada et al., 1988; Gradon and Yu, 1989; Swift et al., 1992). Figure 10-24 shows these data on inspiratory nasal deposition from several laboratories reported by Swift et al. (1992) as a function of the diffusion parameter,  $D^{1/2} Q^{-1/8}$ , where  $D$  is the particle diffusion coefficient in cm<sup>2</sup>/sec and  $Q$  is the flow rate in L/min. Swift et al. (1992) also proposed an equation to fit the data in the form

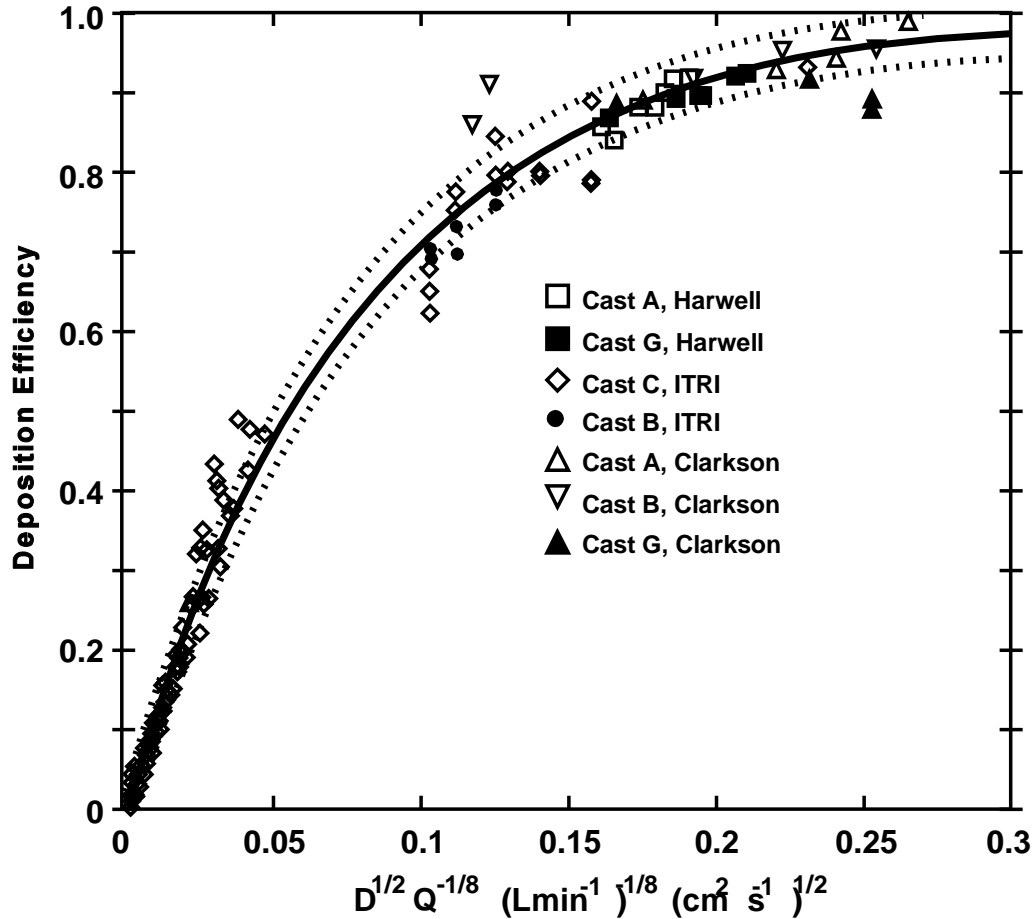


**Figure 10-24.** Inspiratory deposition efficiency data and fitted curve for human nasal casts plotted versus  $Q^{-1/8} D^{1/2} (\text{Lmin}^{-1})^{-1/8} (\text{cm}^2 \text{s}^{-1})^{1/2}$ . The solid curve represents Equation 10-24 and the dotted lines are 95% confidence limits on the mean.

Source: Swift et al. (1992).

$$\eta_N = 1 - \exp[-12.65 D^{1/2} Q^{-1/8}], \quad (10-24)$$

which was adopted by ICRP66 in the 1994 model. Expiratory nasal deposition for particles between  $0.005 \mu\text{m}$  to  $0.2 \mu\text{m}$  was found to have the same trend as Figure 10-24 but was approximately 10% higher than the inspiratory nasal deposition (Yamada et al., 1988). Cheng et al. (1993) derived the following empirical equations to fit the data for expiratory nasal deposition

$$\eta_N = 1 - \exp[-15.0D^{1/2}Q^{-1/8}]. \quad (10-25)$$

Diffusional deposition in human oral casts was found to be smaller than that in nasal casts (Cheng et al., 1990). Based upon these data, Cheng et al. (1993) derived the following equation for oral deposition

$$\eta_M = 1 - \exp(-10.3D^{1/2}Q^{-1/8}), \quad (10-26)$$

on inspiration, and

$$\eta_M = 1 - \exp(-8.51D^{1/2}Q^{-1/8}), \quad (10-27)$$

for deposition on expiration. Contrary to nasal deposition, deposition in the mouth is slightly higher for inspiration than for expiration. Figure 10-25 shows the inspiratory oral deposition data and Equation 10-26.

ICRP66 (1994) took a more conservative view of the experimental data on deposition of small particles in the oral passageway. Oropharyngeal deposition for mouth breathing was assumed to be only half the value for nose breathing so that

$$\eta_m = 1 - \exp(-6.33 D^{1/2} Q^{-1/8}). \quad (10-28)$$

### 10.5.1.3 Tracheobronchial Deposition

Particles escaping from deposition in the ET region enter the lung, but their regional deposition in the lung cannot be precisely measured. All the available regional deposition data have been obtained from experiments with radioactive labeled poorly soluble particles above 0.1  $\mu\text{m}$  in diameter. The amount of activity retained in the lung as a function of time normally exhibits a fast and slow decay component that have been identified as mucociliary and macrophage clearance. Since the tracheobronchial airways are ciliated, the rapidly

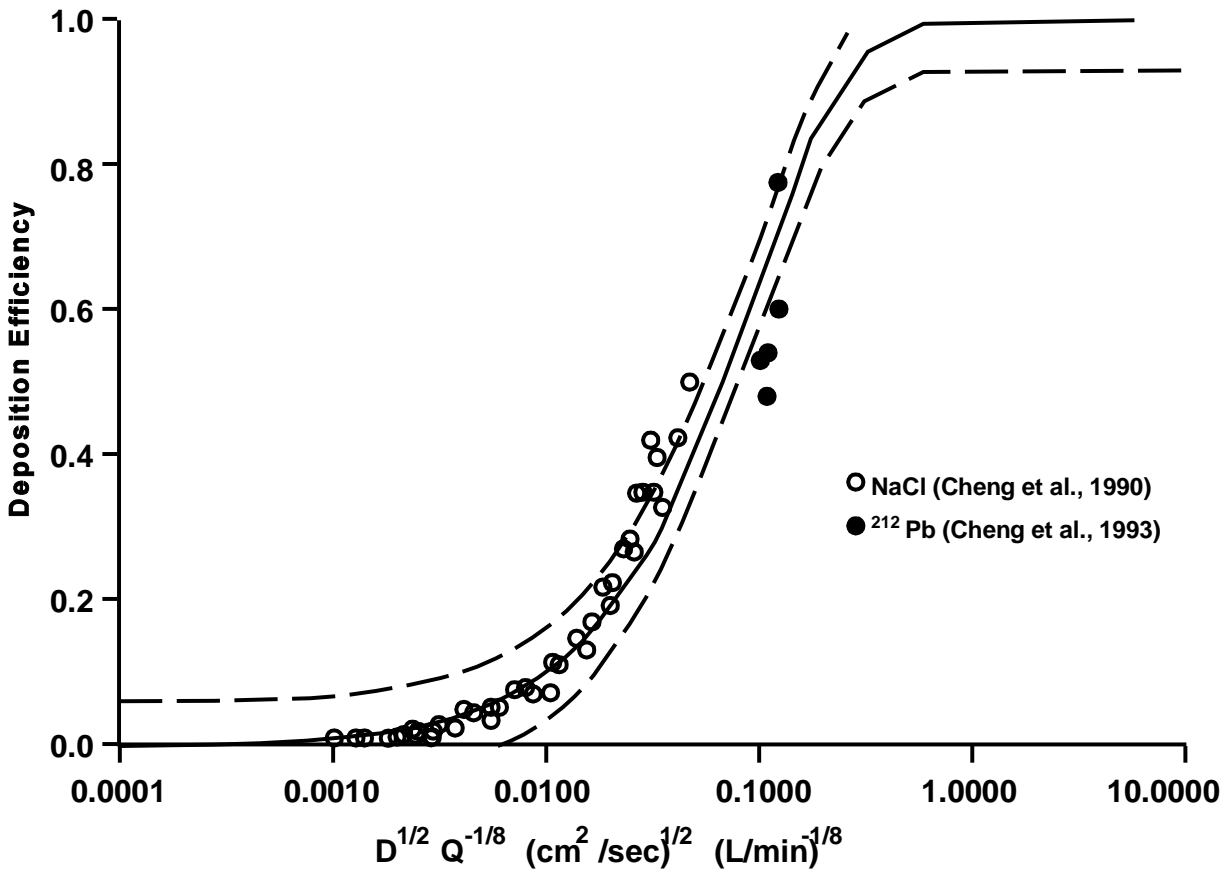


**Figure 10-25. Inspiratory deposition efficiency data in human oral casts plotted versus flow rate and particle diffusion coefficient [ $Q^{-1/8}D^{1/2}$  ( $Lmin^{-1})^{-1/8} (cm^2s^{-1})^{1/2}$ ]. The solid curve represents Equation 10-26 and the dotted lines are the 95% confidence limits.**

Source: Cheng et al. (1993).

cleared fraction of initial activity can be considered as a measure of the amount of material deposited in the TB region, whereas the slowly cleared fraction corresponds to the material deposited in the A region. However, there is experimental evidence that a significant fraction of material deposited in the TB region is retained much longer than 24 h (Stahlhofen et al., 1986a,b; Scheuch and Stahlhofen, 1988; Smaldone et al., 1988). This may be caused by the fact that the TB airway surface is lined with ciliated epithelium, but not all of the ciliated epithelium is covered with mucus all the time (Stahlhofen et al., 1989). Other mechanisms for prolonged TB clearance include phagocytosis by airway macrophages and

deposition of particles further down into the A region due to mixing of flow during inspiration. Thus, TB and A deposition measured based upon the clearance of radioactive labeled particles have been suggested as the "fast-cleared" and "slow-cleared" thoracic deposition (Stahlhofen et al., 1989).

Figure 10-26 shows the data from various investigators (Lippmann, 1977; Foord et al., 1978; Chan and Lippmann, 1980; Emmett et al., 1982; and Stahlhofen et al., 1980, 1981, 1983) on TB deposition or fast-cleared thoracic deposition for mouth breathing as a function of  $d_{ae}$  reported by Stahlhofen et al. (1989). Again, the data are quite scattered due to differences in experimental technique and intersubject and intrasubject variabilities that have been cited previously. Another cause for the scatter is from the difference in the flow rate employed by various studies. For  $d_{ae} > 0.5 \mu\text{m}$ , deposition in the TB region is caused by both impaction and sedimentation. Whereas the impaction deposition is governed by the parameter  $d_{ae}^2 Q$ , sedimentation deposition is controlled by the parameter  $d_{ae}^2/Q$ . It is therefore not possible to have a single relationship between deposition and  $d_{ae}$  for different flow rates.

Data in Figure 10-26 show that TB deposition does not increase monotonically with  $d_{ae}$ . A higher  $d_{ae}$  leads to a greater ET deposition and consequently a lower TB deposition. For the range of flow rates employed in various studies, the maximum TB deposition occurs at about  $4 \mu\text{m}$   $d_{ae}$ . It is also seen that the data by Stahlhofen et al. (1980, 1981, 1983) in Figure 10-26 are considerably lower than those from other investigators. Chan and Lippmann (1980) cited two possible reasons for this difference. One was that Stahlhofen and coworkers used constant respiratory flow rates in their studies as opposed to the variable flow rates used by others. The second reason was that different methods of separating the initial thoracic burden into TB and A regions were used. Stahlhofen et al. (1980) extrapolated the thoracic retention values during the week after the end of fast clearance back to the time of inhalation; they considered A deposition to be the intercept at that time, with the remainder of the thoracic burden considered as TB deposition. This approach yields results similar to, but not identical with, those obtained by treating TB deposition as equivalent to the particles cleared within 24 h.

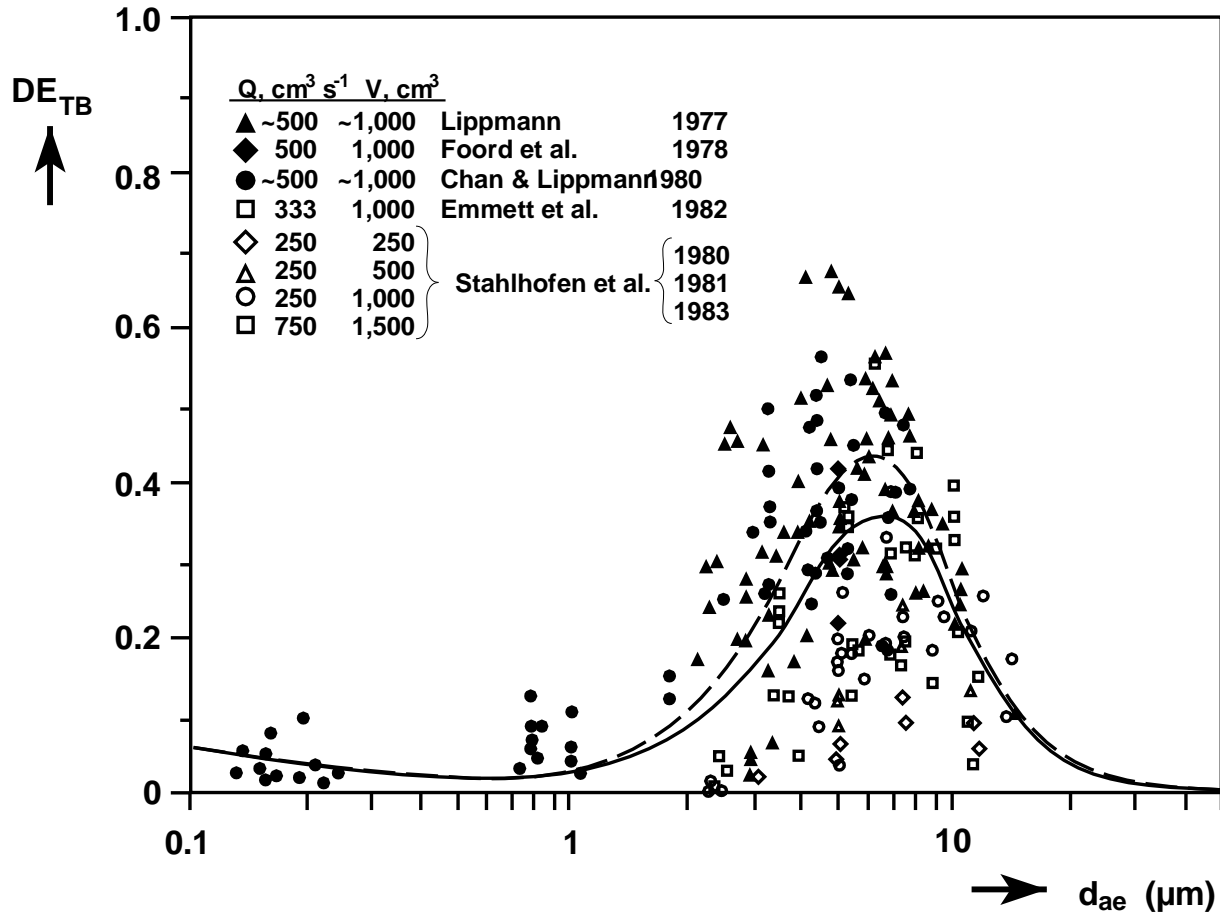
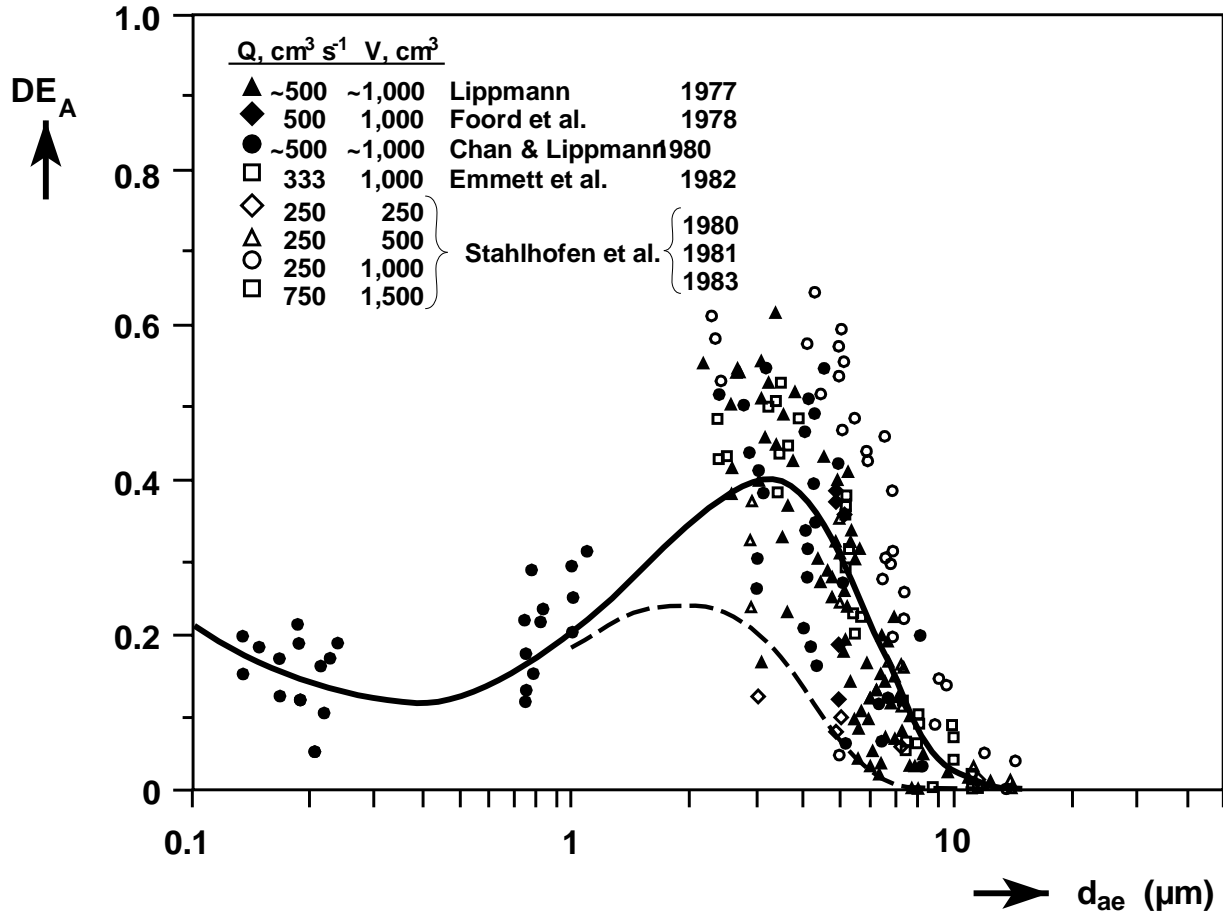


Figure 10-26. Tracheobronchial deposition data in humans at mouth breathing as a function of particle aerodynamic diameter ( $d_{ae}$ ). The solid curve represents the approximate mean of all the experimental data; the broken curve represents the mean excluding the data of Stahlhofen et al.

Source: Stahlhofen et al. (1988).

#### 10.5.1.4 Alveolar Deposition

The A deposition data as a function of  $d_{ae}$  for mouth breathing are shown in Figure 10-27. These data are from the same studies that reported TB deposition in Figure 10-25 but there is a better agreement between different studies than with the TB data. Alveolar deposition is favored by slow and deep breathing. The data of Stahlhofen et al. (1980, 1981, 1983) at 1000 cm<sup>3</sup> tidal volume and 250 cm<sup>3</sup>/sec flow rate thus are higher than other data. Figure 10-27 also shows (1) that A deposition reaches the maximum at about



**Figure 10-27.** Alveolar deposition data in humans as a function of particle aerodynamic diameter ( $d_{ae}$ ). The solid curve represents the mean of all the data; the broken curve is an estimate of deposition for nose breathing by Lippmann (1977).

Source: Stahlhofen et al. (1988).

3.5  $\mu\text{m}$   $d_{ae}$  and (2) that for  $d_{ae}$  between 0.2  $\mu\text{m}$  and 1.0  $\mu\text{m}$ , A deposition does not show significant change although a minimum deposition may occur near 0.5  $\mu\text{m}$ .

By switching from mouth breathing to nose breathing, alveolar deposition will decrease. Lippmann (1977) made an estimate by analysis of the difference in the ET deposition for nose and mouth breathing. The nose breathing (dashed line) result is also shown in Figure 10-26. For  $d_{ae}$  greater than 7  $\mu\text{m}$ , practically no particles deposit in the A region in this breathing mode.

During exercise, most subjects switch from nose breathing to breathing partly through the mouth (Niinimaa et al., 1981). The amount of inhaled material that deposits in the lungs is affected because the mouth and nose have different filtration efficiencies. Niinimaa et al. (1981) found that in thirty subjects, twenty switched to oro-nasal breathing (normal augmenters), typically at a ventilation rate of about 35 L/min, five continued to breathe through the nose, and the rest who were habitual mouth breathers breathed oro-nasally at all levels of exercise. These data were reviewed by Miller et al. (1988) and used to estimate thoracic deposition (TB and A deposition) at different ventilation rates. At higher ventilation rates, Miller et al. (1988) predicted little difference in thoracic deposition between normal augmenters and mouth breathers, but for ventilation rates less than 35 L/min they predicted substantially lower deposition in normal argumenters compared to mouth breathers. Based upon this finding, ICRP (1994) recommended a different breathing pattern for normal augmenters and mouth breathers that typifies the breathing habits of adult males as a function of ventilation rate. The split in airflow for the recommended breathing patterns by ICRP (1994) is shown in Figure 10-28. Table 10-10 provides the same information on the percentages of total ventilatory airflow passing through the nose versus mouth at reference levels of physical exertion for a normal augmenter and a mouth breather adult male. These are the same levels of exercise and values for fraction of nasal ventilatory airflow used to construct the activity patterns in Section 10.7. In the absence of specific data, it must be assumed that a similar breathing pattern applies to young healthy subjects at equivalent levels of exercise. Alveolar deposition at different ventilation rates can be estimated from Figure 10-28 or Table 10-10. For example, a mouth breather doing light exercise ( $\dot{V}_E = 1.5 \text{ m}^3/\text{h}$ ) has about 40% ventilatory air-flow passing through the nasal route. At a particle size of  $2 \mu\text{m } d_{ae}$ , Figure 10-28 gives, respectively, 0.24 and 0.36 A deposition for mouth and nose breathing. Thus, the resultant A deposition at this ventilation rate is  $0.4 \times 0.36 + 0.6 \times 0.24 = 0.288$ .

#### **10.5.1.5 Nonuniform Distribution of Deposition and Local Deposition Hot Spots**

The deposition data in different regions of the respiratory tract do not provide information on deposition nonuniformity in each region and local deposition intensity at a specific site. Such information may be of great importance from a toxicology perspective.

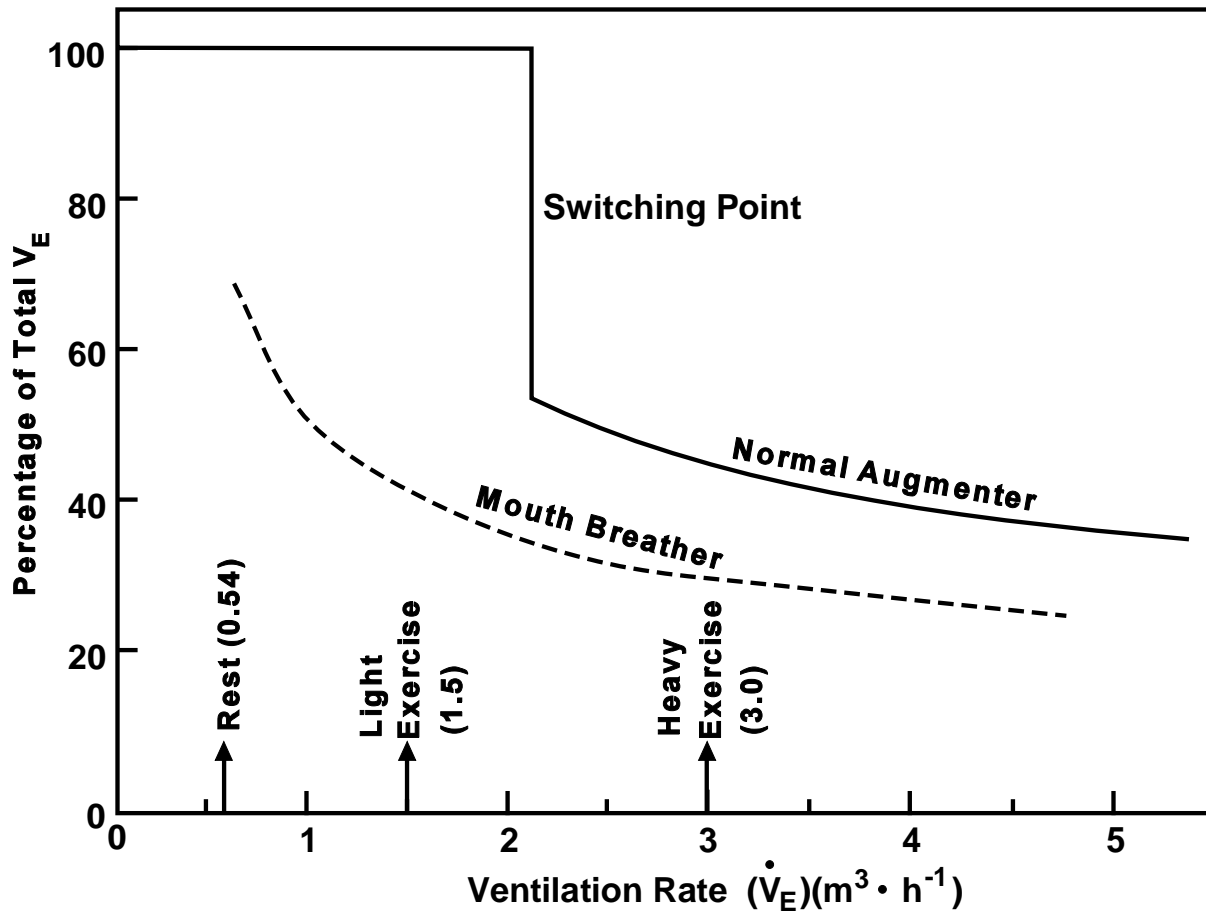


Figure 10-28. Percentage of total ventilatory airflow passing through the nasal route in human "normal augmenter" (solid curve) and in habitual "mouth breather" (broken curve).

Source: International Commission on Radiological Protection (ICRP66, 1994).

**TABLE 10-10. FRACTION OF VENTILATORY AIRFLOW PASSING THROUGH THE NOSE IN HUMAN "NORMAL AUGMENTER" AND "MOUTH BREATHER"<sup>a</sup>**

Level of Exertion	$F_n$	
	Nasal Augmenter	Mouth Breather
Sleep	1.0	0.7
Rest	1.0	0.7
Light exercise	1.0	0.4
Heavy exercise	0.5	0.3

<sup>a</sup>(ICRP66, 1994) as derived from Miller et al. (1988).

Because airway structure and its associated air flow patterns are exceedingly complex (Chang and Menon, 1993), and ventilation distribution of air in different parts of the lung is uneven (Milic-Emili et al., 1966), it is expected that particle deposition patterns in ET, TB, and A regions are highly nonuniform. Fry and Black (1973) measured regional deposition in the human nose using radiolabelled particles and found that most of deposition occurred in the anterior region of the nose. Schlesinger and Lippmann (1978) found nonuniform deposition in the trachea to be caused by the airflow disturbance of the larynx. In a single airway bifurcation model, measurements show that deposition occurs principally around the carinal ridge (e.g., Bell and Friedlander, 1973; Lee and Wang, 1977); Martonen and Lowe, 1983; Kim and Iglesias, 1989 a,b). A similar result was observed in the alveolar duct bifurcations in rats and mice (Brody and Roe, 1983). Figure 10-29 shows the data on local deposition pattern obtained by Kim and Iglesias (1989) and Kim et al. (1989) in a bifurcating tube for both inspiration and expiration. The peak deposition occurs in the daughter tube during inspiration and the parent tube during expiration, but always near the carinal ridge. In addition, airways are not smooth tubes. More recently, Martonen et al. (1994 a,b,c) have called attention to the existence of cartilaginous rings on the wall of airways in the tracheobronchial region. Using a numerical analysis, they showed that such surface structure can lead to a considerable alteration of the flow pattern and enhancement of deposition.

Deposition measurements in small laboratory rodents (Raabe et al., 1977) also showed differences in lobar distribution with up to 60 percent higher deposition than the average in the right apical lobe (corresponding to the human upper lobe). The difference was greater for large particles than for small particles. Raabe et al. (1977) further showed that these differences in relative lobar deposition were related to geometric mean number of airway bifurcations between trachea and terminal bronchioles in each lobe for rats and hamsters. Since similar morphologic differences occur in the human lungs, nonuniform lobar distribution should also occur.

#### **10.5.1.6 Approaches to Deposition Modeling**

Mathematical models of lung deposition have been developed in recent years to help interpret experimental data and to make predictions of deposition for cases where data are not available. A review of various mathematical models was given by Morrow and Yu

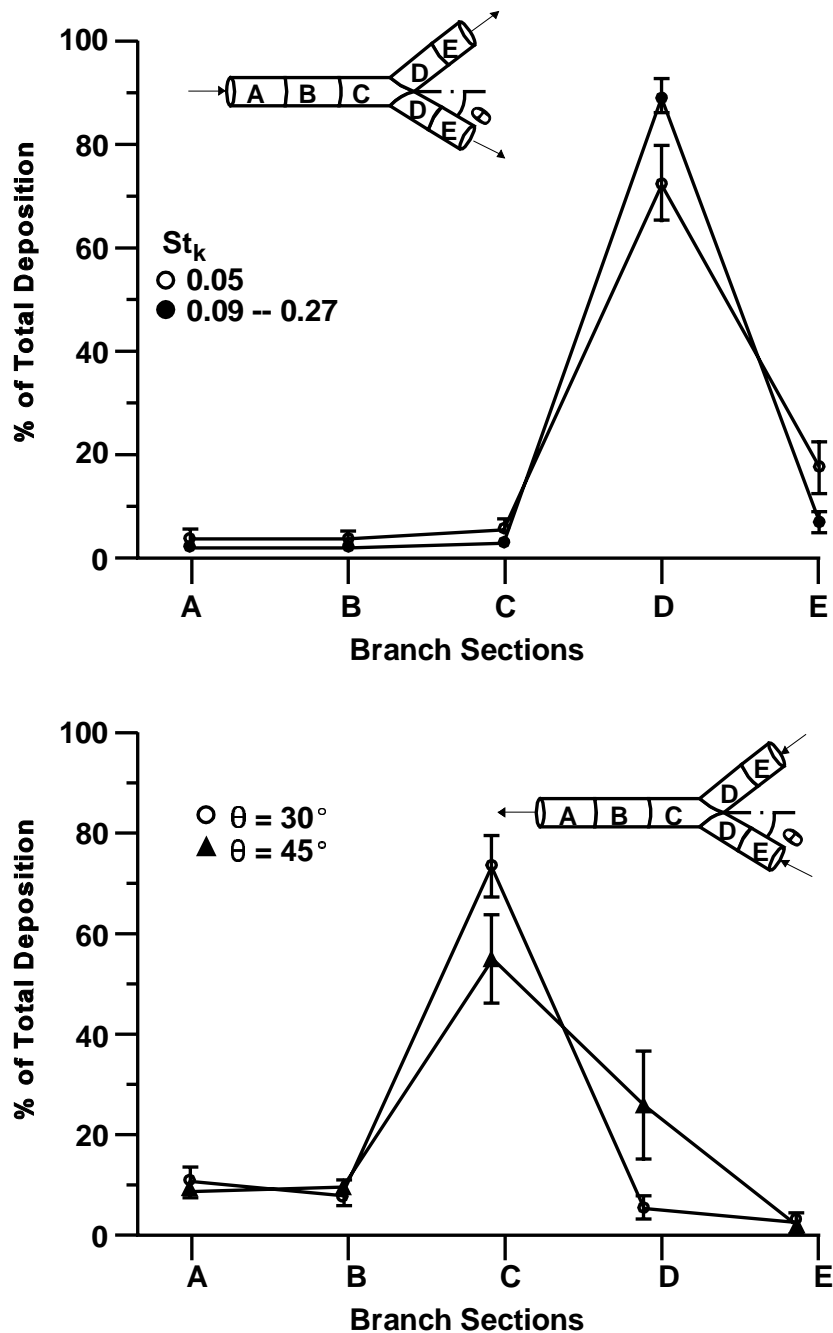


**Figure 10-29.** Local deposition pattern in a bifurcating tube for inhalation (top panel) and exhalation (bottom panel). Deposition in each section is expressed as a percent of total deposition for the entire model. Symbols and error bars in the top panel represent means and standard deviations of the  $\theta = 30^\circ$  and  $45^\circ$ . Symbols and error bars in the bottom panel represent means and standard deviations of the entire data obtained in the Stokes number range from 0.05 to 0.28.

Source: Kim and Iglesias (1989); Kim et al. (1989).

(1993). There are three major elements involved in mathematical modeling. First, a model of airways simulating the real structure must be specified. Secondly, deposition efficiency in each airway due to various mechanisms must be derived. Finally, a computational procedure must be developed to account for the transport and deposition of the particles in the airways.

Three different approaches have been used in the mathematical modeling. The first approach is a compartmental model first formulated by Findeisen (1935). Starting with the trachea, Findeisen divided the airways into nine compartments based upon the anatomical structure. Particles which did not deposit in one compartment remained airborne and transported to the next compartment for deposition. Findeisen's lung model and analysis were later modified by Landahl (1950a, 1963) and Beeckmans (1965). Detailed calculations of regional deposition with additional consideration of nasal deposition based upon the Findeisen-Landahl-Beeckmans theory were later published in a report by the Task Group on Lung Dynamics (TGLD) in 1966.

Because of advancement in measuring techniques, refined airway models have become available (as discussed in Section 10.2). Several new models based upon the compartmental analysis have been proposed (e.g., Gerrity et al., 1979; Yeh and Schum, 1980; Martonen and Graham, 1987). The expressions used for deposition efficiency of each compartment differed somewhat in these models. In the absence of any careful comparison with the experimental data, it is difficult to assess the applicability of these models to deposition prediction. However, one difficulty often encountered in the compartmental model is the derivation of deposition efficiency in each airway for combined mechanisms of impaction, sedimentation and diffusion. A commonly used assumption is that each deposition mechanism is independent, thus the joint efficiency can be written in the form

$$\eta = 1 - (1 - \eta_I)(1 - \eta_S)(1 - \eta_D), \quad (10-29)$$

where  $\eta_I$ ,  $\eta_S$ , and  $\eta_D$  are, respectively, deposition efficiency in an airway or compartment by the individual mechanisms of impaction, sedimentation and diffusion, and  $\eta$  is the joint efficiency. Yu et al. (1977) have shown, in a detailed mathematical analysis of a combined sedimentation and diffusion problem, that the above equation is an inaccurate expression for deposition when  $\eta_S$  and  $\eta_D$  are not small and have about the same magnitude. Another

difficulty in the compartmental model is that the air-mixing effect (i.e., mixing of tidal air and lung air) on deposition cannot be easily accounted for. Such an effect is important for transient exposure. However, the compartmental model is easy to formulate and to understand conceptually.

The second approach to deposition modeling was put forward by Yu and coworkers (Taulbee and Yu, 1975; Yu, 1978; Yu and Diu, 1983) and later by Egan and Nixon (1985, 1989). In this approach, the many generations of airways are viewed as a chamber shaped like a trumpet. The cross-sectional area of the chamber varies with airway depth measured from the beginning of the trachea, according to anatomical data. The concentration of inhaled particles in the chamber as a function of airway depth and time during breathing is described by a convective diffusion equation with a loss-term accounting for airway deposition. This equation can be solved either exactly (without longitudinal diffusion) or numerically with appropriate initial and boundary conditions. Deposition at different sites in the airways is then calculated once the concentration is known.

The deposition model formulated in this manner has some advantages over the compartmental model. The use of differential airway length in the model allows the joint deposition efficiency per unit airway length to be the superposition of efficiencies by each individual mechanism. Variation of airway dimensions during breathing is accounted for in the model. The model is time-dependent and can thus be applied to any breathing pattern and transient exposure condition. Air-mixing and uneven airway path lengths can be accounted for with the use of an equivalent longitudinal diffusion term in the convective-diffusion equation. Finally, in the case of no longitudinal diffusion, the exact solution of the convective-diffusion is obtainable, thus reducing the time required for calculating deposition.

The airway geometry of the human lung is not identical within a population. In a given lung, the dimension of the airways in a specified generation is also not uniform and the bifurcation is not symmetric (Weibel, 1963). The above two modeling approaches have been extended to account for the randomness of airway geometry (Yu et al., 1979; Yu and Diu, 1982a,b; Koblinger and Hofmann, 1990; Hofmann and Koblinger, 1990). Yu and Diu (1982b) compared their modeling results with total and regional deposition data of Stahlhofen et al. (1981) and Heyder et al. (1982) for controlled breathing and suggested that differences

in lung morphology were probably the principal cause for intersubject variability in deposition.

Another approach to deposition modeling is an empirical one proposed by Rudolf et al. (1983, 1984, 1986, 1990) similar to that developed for ET deposition. This model considers the lung as a series of two filters representing the TB and A regions of the lung. The model requires no assumptions about airway geometry, airflow pattern and distribution, or particle deposition efficiency in each airway. However, the construction of the model relies heavily on experimental data of regional deposition for a wide range of particle sizes (monodisperse) and breathing conditions. These data are not always available. An additional difficulty in empirical modeling is the development of deposition equations in each region for combined deposition mechanisms. As discussed earlier, impaction, sedimentation and diffusion deposition depend, respectively, on the parameters  $d_{ae}^2 Q$ ,  $D_{ae}^2/Q$  and  $D/Q$ , where  $D$  is a function of particle geometric diameter. It is a very difficult task to come up with an equation for deposition in terms of these parameters which can match all experimental data. Furthermore, because only a few compartments are used in the empirical model, more detailed deposition information such as deposition at a specific airway generation cannot be predicted. However, as mentioned, with an empirical model the geometry and relative importance of mechanisms and airflow splits are all "correct" in the subjects tested and are reflected in the measured deposition. This may be an advantage over theoretical models that must rely on extremely limited information on geometry. As described in Appendix 10A, the ICRP based their 1994 model of respiratory tract deposition on a theoretical calculation of the type introduced by Taulbee and Yu (1975), which was found to be consistent with the experimental data taken as a whole. However, for mathematical simplicity in applying the results of these complex calculations, which included the effects of airway dimension scaling for subject gender and age, the ICRP developed a set of algebraic expressions to represent regional lung deposition in terms of the controlling parameters, i.e., particle diameter, density, shape factor, breathing mode (nose or mouth), tidal volume, respiratory frequency, functional residual capacity, gender, and subject height.

## 10.5.2 Laboratory Animals

Since much information concerning inhalation toxicology is collected from laboratory animals, the comparative regional deposition in these laboratory animals must be considered to help interpret, from a dosimetric viewpoint, the possible implications of animal toxicological results for humans. In evaluating deposition studies in terms of interspecies extrapolation, it is not adequate to express the amount of deposition merely as a percentage of the total inhaled. For some particle sizes, regional deposition in humans and laboratory animals may be quite similar and appears to be species independent (McMahon et al., 1977; Brain and Mensah, 1983). However, different species exposed to identical particles at the same exposure concentration will not receive the same particle mass per unit exposure time because of their differences in tidal volume and breathing rate. In addition, because of differences in the lung weight and airway surface area, the amount of deposition normalized to these quantities is also very different between species.

It is difficult to systematically compare interspecies deposition patterns obtained from various reported studies, because of variations in experimental protocols, measurement techniques, definitions of specific respiratory tract regions, and so on. For example, tests with humans are generally conducted under protocols that standardize the breathing pattern, whereas those using laboratory animals involve a wider variation in respiratory exposure conditions (for example, spontaneous breathing versus ventilated breathing as well as various degrees of sedation). Much of the variability in the reported data for individual species may be due to the lack of normalization for specific respiratory parameters during exposure. In addition, the various studies have used different exposure techniques, such as nasal mask, oral mask, oral tube, or tracheal intubation. Regional deposition may be affected by the exposure route and delivery technique employed.

Figure 10-30 shows the regional deposition data versus particle diameter in commonly used laboratory animals obtained by various investigators and compiled by Schlesinger (1988). Although there is much variability in the data, it is possible to make some generalizations concerning comparative deposition patterns. The relationship between total respiratory tract deposition and particle size is approximately the same in humans and most of these animals; deposition increases on both sides of a minimum, which occurs for particles of 0.2 to 0.9  $\mu\text{m}$ . Interspecies differences in regional deposition occur due to anatomical and

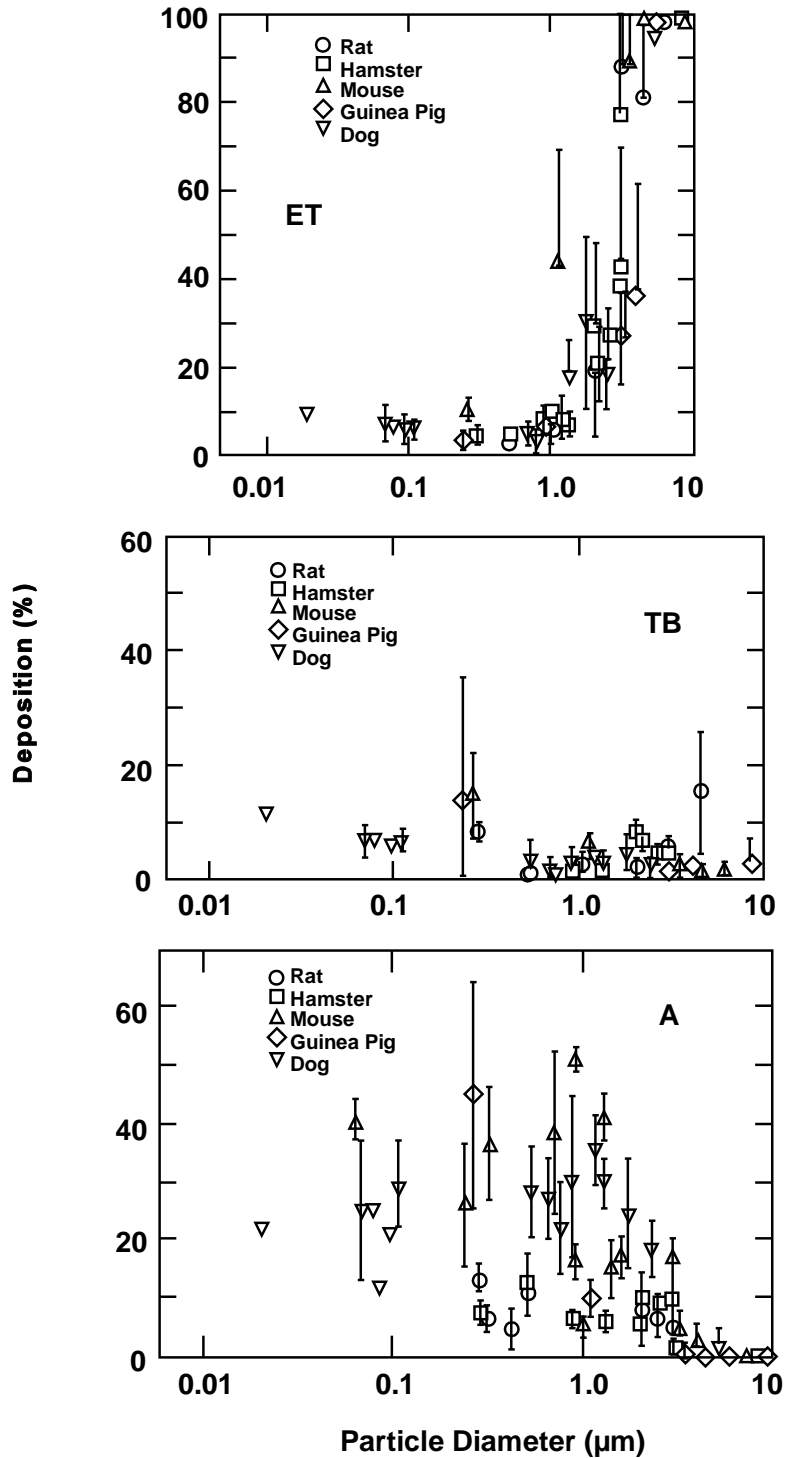


**Figure 10-30.** Regional deposition fraction in laboratory animals as a function of particle size. Particle diameters are aerodynamic (MMAD) for those  $> 0.5 \mu\text{m}$  and geometric (or diffusion equivalent) for those  $< 0.5 \mu\text{m}$ .

Source: Schlesinger (1988).

physiological factors. In most laboratory animal species, deposition in the ET region is near 100 percent for  $d_{ae}$  greater than 5  $\mu\text{m}$  (Raabe et al., 1988), indicating greater efficiency than that seen in humans. In the TB region, there is a relatively constant, but lower, deposition fraction for  $d_{ae}$  greater than 1  $\mu\text{m}$  in all species compared to humans. Finally, in the A region, deposition fraction peaks at a lower particle size ( $d_{ae}$  about 1  $\mu\text{m}$ ) in laboratory animals, than in humans.

Mathematical deposition models for rats, hamsters, and guinea pigs have been developed by several investigators (e.g., Schum and Yeh, 1980; Xu and Yu, 1987; Martonen et al., 1992) in a similar manner as the human models without including diffusion deposition in the ET region. Although the modeling results are generally in agreement with experimental data, there is a considerable uncertainty in the respiratory and anatomical parameters of the laboratory animals used in the modeling studies. In addition, the airway branching patterns in the animals are commonly monopodial as compared to the dichotomous branching in the human lung. The deposition efficiency of an airway (the amount of deposition in an airway divided by the amount entered) developed in the human model may not be applicable to laboratory animal species. Despite some of these difficulties, modeling studies in laboratory animals remain a useful step in extrapolating exposure-dose-response relationships from laboratory animals to the human (Yu et al., 1991).

Asgharian et al. (1995) developed an empirical model of particle deposition in the A region based on the published data reviewed by Schlesinger (1985a). Although restricted to the A region, the approach could be applied to other regions. A deposition function ( $F_A$ ) was described using a polynomial regression of the form

$$F_A = \sum_{i=0}^N a_i(\log_{10}d)^i \text{ for } d \leq d_{\text{cut-off}}, \text{ and} \quad (10-30)$$

$$F_A(d)=0 \text{ for } d \geq d_{\text{cut-off}}. \quad (10-31)$$

where  $N = 4$  is the degree of the polynomial,  $d$  is the particle diameter in micrometers, and  $d_{\text{cut-off}}$  is the diameter at which the deposition efficiency becomes zero. Since Equation 10-30 is a 4<sup>th</sup>-degree polynomial, it will give a non-zero value for  $d_{\text{cut-off}}$ . For this

reason, Equation 10-31 was added to be consistent with the deposition data and  $d_{\text{cut-off}}$  was determined by setting Equation 10-30 to zero. Newton's method was employed to find  $d_{\text{cut-off}}$  for different cases. Particle deposition was then integrated with particle distributions differing in median particle diameter and  $\sigma_g$  to calculate deposition mass fraction for specific polydisperse size distributions.

Ménache et al. (1996) developed an empirical model to estimate fractional regional deposition efficiency. This model represents a revised version of previously published models used for dosimetric interspecies extrapolation (Jarabek et al., 1989, 1990; Miller et al., 1988) that have been useful to develop inhalation reference concentration (RfC) estimates for dose-response assessment of air toxics (U.S. Environmental Protection Agency, 1994). For example, rather than linear interpolation between the published (Raabe et al., 1988) means for deposition measured at discrete particle diameters, as previously done for the rat deposition modeling, equations have now been fit to the individual animal data for each of the discrete, monodisperse particle exposures (U.S. Environmental Protection Agency, 1994; Ménache et al., 1996).

A description of the complete study including details of the exposure may be found elsewhere (Raabe et al., 1988). Briefly, the animals were exposed to radiolabelled ytterbium ( $^{169}\text{Yb}$ ) fused aluminosilicate spheres in a nose-only exposure apparatus. Twenty unanesthetized rodents or eight rabbits were exposed to particles of aerodynamic diameters ( $d_{ae}$ ) approximately 1, 3, 5, or 10  $\mu\text{m}$ . Half the animals were sacrificed immediately post exposure; the remaining half were held 20 h post exposure. One-half of the animals at each time point were female. The animals were dissected into 15 tissue compartments, and radioactivity was counted in each compartment. The compartments included the head, larynx, GI tract, trachea, and the five lung lobes. This information was used directly in the calculation of the deposition fractions. Radioactivity was also measured in other tissues including heart, liver, kidneys, and carcass; and additionally in the urine and feces of a group of animals held 20 h. Data for the animals sacrificed immediately post exposure were used to ensure that there was no contamination of other tissue, whereas the data from the animals held 20 h were used in the calculation of a fraction used to partition bronchial deposition between the TB and A regions. Radioactivity was measured in the pelt, paws, tail, and headskin as a control on the exposure.

Although there are some other studies of particle deposition in laboratory animals (see review by Schlesinger, 1985a), no other data have the level of detail or the experimental design (i.e., freely breathing, unanesthetized, nose-only exposure to monodisperse particle size distributions) required to provide deposition equations representative of the animal exposures used in many inhalation toxicology studies. However, many inhalation toxicology studies are not nose-only exposures. While nose-only exposures are necessary to determine fractional particle deposition, adjustments can be made to estimate deposition fractions under whole-body exposure conditions. Similarly, deposition of polydisperse size distributions can be estimated by integrating the size distribution and monodisperse fractional deposition.

The advantages of using the data of Raabe et al. (1988) to develop the deposition efficiency equations include:

- the detailed measurements were made in all tissues in the animal, providing mass balance information and indicating that there was no contamination of nonrespiratory tract tissue with radioactivity immediately post exposure,
- the use of unanesthetized, freely breathing animals, and
- the use of monodisperse or near monodisperse particle size distributions in the exposures

Regional fractional deposition,  $F_r$ , was calculated as activity counted in a region normalized by total inhaled activity (Table 10-11). The proportionality factor,  $f_L$ , in Equations 10-33 and 10-34 was used to partition thoracic deposition between the TB and A regions. It was calculated using the 0 and 20-h data and is described in detail by Raabe and co-workers (1977).

These regional deposition fractions,  $F_r$ , however, are affected not only by the minute volume ( $V_E$ ), MMAD and  $\sigma_g$ , but also by deposition in regions through which the particles have already passed. Deposition efficiency,  $\eta_r$ , on the other hand, is affected only by MMAD,  $\sigma_g$  and  $V_E$ . The relationships between deposition fraction and efficiency are calculated as provided below and are described in more detail elsewhere (Ménache et al., 1995). In the aerodynamic domain, that is for particles with diameters  $>0.5 \mu\text{m}$ , efficiencies increase monotonically and are bounded below by 0 and above by 1. The

**TABLE 10-11. REGIONAL FRACTIONAL DEPOSITION**

	$F_r = \frac{\text{Activity Counted in a Region}}{\text{Total Inhaled Activity}}$	
Extrathoracic (ET): $F_{ET}$	$= \frac{[\text{head} + \text{GI tract} + \text{larynx}]_{0\ h}}{\text{Total Inhaled Activity}}$	(10-32)
Tracheobronchial (TB): $F_{TB}$	$= \frac{\text{trachea}_{0\ h} + f_L \times \sum_{i=1}^5 \text{lobe}_{i,0\ h}}{\text{Total Inhaled Activity}}$	(10-33)
Alveolar (A): $F_A$	$= \frac{(1 - f_L) \times \sum_{i=1}^5 \text{lobe}_{i,0\ h}}{\text{Total Inhaled Activity}}$	(10-34)

Source: U.S. Environmental Protection Agency (1994).

logistic function has mathematical properties that are consistent with the shape of the efficiency function (Miller et al., 1988)

$$E(\eta_r) = \frac{1}{1 + e^{\alpha + \beta \log_{10} x}}, \quad (10-35)$$

where  $E(\eta_r)$  is the expected value of deposition efficiency ( $\eta_r$ ) for region  $r$ , and  $x$  is expressed as an impaction parameter,  $d_{ae}^2 Q$ , for extrathoracic deposition efficiency and as aerodynamic particle size,  $d_{ae}$ , for TB and A deposition efficiencies. The flow rate,  $Q$  (mL/s), in the impaction parameter may be approximated by  $(2V_E/60)$ . The parameters  $\alpha$  and  $\beta$  are estimated using nonlinear regression techniques.

To fit this model, efficiencies must be derived from the deposition fractions that were calculated as described in Table 10-11. Efficiency may be defined as activity counted in a region divided by activity entering that region. Then, considering the region as a sequence of filters in steady state, efficiencies may be calculated as follows

$$\eta_{ET} = F_{ET} \quad (10-36)$$

$$\eta_{\text{TB}} = \frac{\text{trachea}_{0\text{ h}} + f_{\text{L}} \times \sum_{i=1}^5 \text{lobe}_{i,0\text{ h}}}{(1 - \eta_{\text{ET}})} \quad (10-37)$$

$$\eta_{\text{A}} = \frac{(1 - f_{\text{L}}) \times \sum_{i=1}^5 \text{lobe}_{i,0\text{ h}}}{(1 - \eta_{\text{ET}}) (1 - \eta_{\text{TB}})}. \quad (10-38)$$

Using these calculated regional efficiencies in the individual animals, the logistic function was fit for the ET, TB, and A regions for the five animal species and humans. Figure 10-31 shows the deposition efficiency in the rat ET region versus the impaction parameter,  $d_{\text{ac}}^2 Q$ . The logistic curve was fit to the experimental data assuming negligible deposition on exhalation. The open circles represent the data for animals having extreme studentized residuals ( $>1.96$ ) compared to the data for other animals (closed circles) in the ET region. Deposition efficiency curves were fit for the TB and A regions also. In all three regions, the curve fits provided good descriptions of the data with asymptotic  $R^2$  of 0.98 or greater (Ménache et al., 1996). The root MSE, an estimate of the average error in the regression model in the data units, ranged between 0.08 and 0.10. These differences are well within the limits of biological variability seen in this study and other studies (Schlesinger, 1988). The parameter estimates from these fits are listed in Table 10-12.

The fitted equations are then used to generate predicted efficiencies ( $\hat{\eta}$ ) as a function of impaction in the ET region and of  $d_{\text{ac}}$  in the TB and A regions. Finally, the predicted efficiencies are multiplied together and adjusted for inhalability,  $I$ , as shown in Equations 10-39 through 10-41 to produce predicted deposition fractions ( $\hat{F}_{\text{T}}$ ) for monodisperse and near monodisperse ( $\sigma_{\text{g}} < 1.3$ ) particles

$$\hat{F}_{\text{ET}} = I \times \hat{\eta}_{\text{ET}} \quad (10-39)$$

$$\hat{F}_{\text{TB}} = I \times (1 - \hat{\eta}_{\text{ET}}) \times \hat{\eta}_{\text{TB}} \quad (10-40)$$

$$\hat{F}_{\text{A}} = I \times (1 - \hat{\eta}_{\text{ET}}) \times (1 - \hat{\eta}_{\text{TB}}) \times \hat{\eta}_{\text{A}}. \quad (10-41)$$

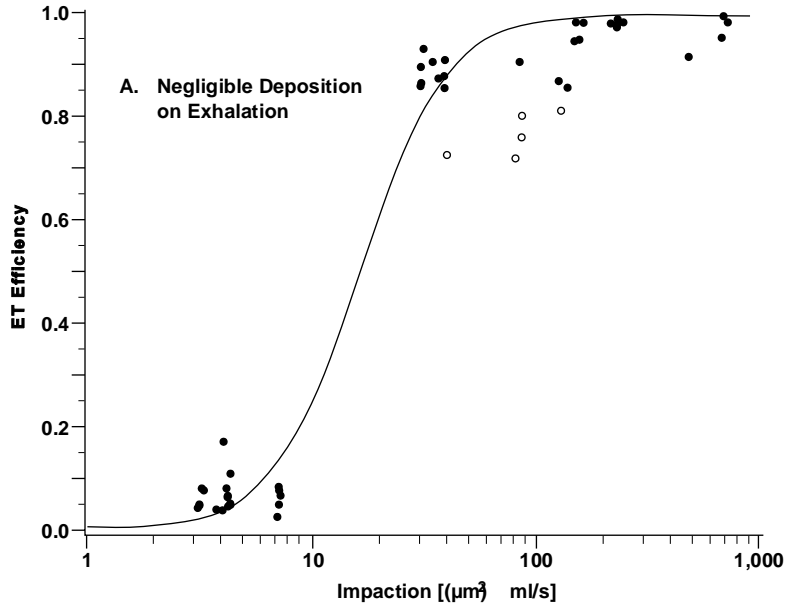


**Figure 10-31. Regional deposition efficiency in the rat extrathoracic (ET) region versus an impaction parameter ( $d_{ac}^2 Q$ ) as predicted by model of Ménache et al. (1996).**

Source: Ménache et al. (1996).

Inhalability,  $I$ , is an adjustment for the particles in an ambient exposure concentration that are not inhaled at all. For humans, an equation has been fit applying the logistic function (Ménache et al., 1995) to the experimental data of Breysse and Swift (1990)

$$I = 1 - \frac{1}{1 + e^{10.32 - 7.17 \log_{10} d_{ac}}} \quad (10-42)$$

The logistic function was also fit to the data of Raabe et al. (1988) for laboratory animals (Ménache et al., 1995)

$$I = 1 - \frac{1}{1 + e^{2.57 - 2.81 \log_{10} d_{ac}}} \quad (10-43)$$

Figure 10-32 illustrates the relationship between the predicted efficiencies and predicted depositions using this model for the rats. The particles were assumed to be monodisperse.

**TABLE 10-12. DEPOSITION EFFICIENCY EQUATION ESTIMATED PARAMETERS  
AND 95% ASYMPTOTIC CONFIDENCE INTERVALS**

Species	ET (Nasal)		TB		A	
	$\alpha$	$\beta$	$\alpha$	$\beta$	$\alpha$	$\beta$
Human	7.129 <sup>a</sup>	-1.957 <sup>a</sup>	3.298 <sup>a</sup>	-4.588 <sup>a</sup>	0.523 <sup>a</sup>	-1.389 <sup>a</sup>
Rat	6.348 (5.14, 7.56)	-5.269 (-6.19, -4.35)	2.822 (2.54, 3.11)	-4.576 (-5.06, -4.10)	2.241 (1.72, 2.77)	-10.463 (-12.74, -8.19)

<sup>a</sup>Source: Miller et al. (1988).

A default body weight (BW) for the rats of 0.38 kg was used to calculate a default  $\dot{V}_E$  using allometric scaling (U.S. Environmental Protection Agency, 1994). Regional deposition efficiencies and fractions were calculated for particles with  $d_{ae}$  ranging from 1.0 to 10  $\mu\text{m}$ . These calculated points were connected to produce the smooth curves shown in Figure 10-30. The three panels on the left of Figure 10-32 are plots of the predicted regional deposition efficiencies; the three panels on the right show the predicted regional deposition fractions derived from the estimated efficiencies and adjusted for inhalability. The vertical axis for the predicted deposition efficiency panels range from 0 to 1. Although the deposition fraction is also bounded by 0 and 1, the vertical axes in the figure are less than 1 in the TB and A regions. The top two panels of Figure 10-32 are the predicted deposition efficiency and fraction, respectively, for the ET region. These two curves are plotted as a function of the impaction parameter described for Equation 10-35. The middle two and lower two panels show the predicted deposition efficiencies and fractions for the TB and A regions, respectively. These four curves are plotted as a function of  $d_{ae}$ .

When a particle is from a monodisperse size distribution, the  $d_{ae}$  and the MMAD are the same. If, however, the particle is from a polydisperse size distribution, the particle cannot be described by a single  $d_{ae}$ ; the average value of the distribution, the MMAD, must be used. In the aerodynamic particle size range, the deposition efficiency curves all increase monotonically as a function of the independent variable (i.e., either the impaction parameter or  $d_{ae}$ ) and have both lower and upper asymptotes. The curves describing the deposition fractions, however, have different shapes that are dependent on the respiratory tract region. Deposition fractions in all three regions are nonmonotonic—initially increasing as a function of particle size but decreasing as particle sizes become larger. This is because particles that have been deposited in proximal regions are no longer available for deposition in distal regions. As an extreme example, if all particles are deposited in the ET region, no particles are available for deposition in either the TB or A regions. In the ET region, the nonmonotonic shape for fractional deposition is due to the fact that not all particles in an ambient concentration are inhalable.

As discussed in Section 10.2, particles in an experimental or ambient exposure are rarely all a single size but rather have some distribution in size around an average value.

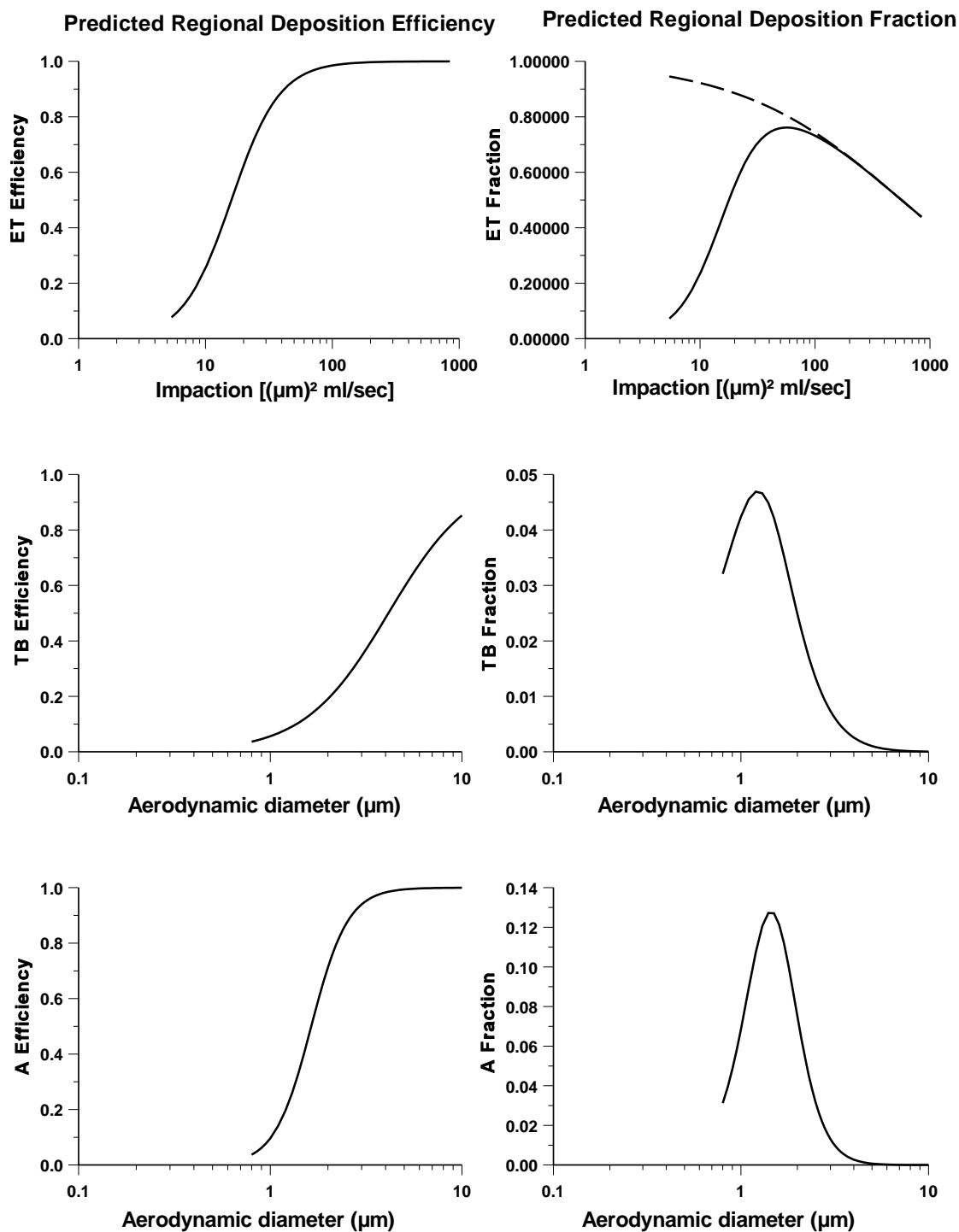


**Figure 10-32. Comparison of regional deposition efficiencies and fractions for the rat. A default body weight of 0.38 kg (U.S. Environmental Protection Agency, 1994) was used in these calculations. The fractional deposition (solid line) and inhalability (dashed line) are shown in the upper right panel.**

As this distribution becomes greater, the particle is said to be polydisperse. The empirical model of Ménache et al. (1996) was developed from exposures using essentially monodisperse particles (which are treated as though they are exactly monodisperse). It is therefore possible to multiply the particle size distribution function (which is customarily considered to be the lognormal distribution) by the predicted depositions (calculated as described in Equations 10-39 through 10-41) and integrate over the entire particle size range. Mathematically, this calculation is performed as described by Equation 10-44

$$[\hat{F}_r]_p = \int_0^{\infty} [\hat{F}_r]_m \times \frac{I}{d_{ae}(\log \sigma_g)\sqrt{2\pi}} \times \exp\left[-1/2 \frac{(\log d_{ae} - \log MMAD)^2}{(\log \sigma_g)^2}\right] dd_{ae}, \quad (10-44)$$

where log refers to the natural logarithm,  $[\hat{F}_r]_p$  is the predicted polydisperse fractional deposition for a given MMAD and  $\sigma_g$ , and  $[\hat{F}_r]_m$  is the predicted monodisperse fractional deposition for particles of size  $d_{ae}$ . The limits of integration are defined from 0 to  $\infty$  but actually include only four standard deviations (99.95% of the complete distribution). For each particle size in the integration,  $[\hat{F}_r]_m$  is calculated and then multiplied by the probability of observing a particle of that size in a particle size distribution with that MMAD and  $\sigma_g$ . Rudolf and colleagues (1988) have also investigated the effect of polydisperse particle size distributions on predicted regional uptake of aerosols in humans and present a more detailed discussion of these and related issues.

As discussed by Schlesinger (1985a), there are many sources of variability that could explain differences in predicted deposition using the model of Ménache et al. (1996) and the observed deposition data in the studies reported by Schlesinger (1985a). However, results from the model of Asgharian et al. (1995), based on the data reported in Schlesinger (1985a), are similar to estimates derived using the model of Ménache et al. (1996).

Data from inhalation studies, particularly chronic inhalation exposures, are often difficult to interpret in terms of respiratory tract deposition efficiency, because the amounts of material retained in the respiratory tract and other body organs are often determined by complex relationships between initial lung deposition, lung retention, subsequent organ uptake and retention, and body uptake by ingestion of material contaminating the body surface. As an example, review of the literature indicates that data from most inhalation

deposition studies are not appropriate for direct comparison or model validation with the estimates from the Ménache et al. (1996) model because the data are normalized to the deposition in or on the animal rather than to what was inhaled (Newton and Pfladderer, 1986; Dahlbäck et al., 1989), used anesthetized animals (McMahon et al., 1977; Johnson and Ziemer, 1971; Raabe et al., 1977), or used cannulated animals (Shiotsuka et al., 1987). Berteau and Biermann (1977) exposed female Sprague Dawley rats to an aerosol with a mass median diameter (MMD) of  $2.1 \mu\text{m}$  and a  $\sigma_g$  of 2.0 for 20 minutes. These authors calculated total deposition in 8 animals to be  $28 \pm 9.3\%$ . The model of Ménache et al. (1996) would predict approximately 60% deposition, assuming the MMD = MMAD. Berteau and Biermann (1977) noted substantially lower deposition in rats than in mice for this same study and proposed a decrease in  $\dot{V}_E$  as a possible reason. Some adjustment of  $\dot{V}_E$  would bring the model prediction into closer agreement with the data. Differences in exposure such as whole-body and group housing versus nose-only could also contribute to some of the variability. Although there is substantial disagreement between the model prediction and the experimental measurement for this polydisperse aerosol, it seems likely that the experimental data are unusually low.

Dahlbäck and Eirefelt (1994) exposed male Sprague Dawley rats to monodisperse fluorescent polystyrene latex microspheres ranging in size from 0.63 to  $5.7 \mu\text{m}$  count median diameter. Deposition was reported as the sum of nose, esophagus, stomach, and lung normalized to the amount deposited in the sum of these four compartments. Ménache et al. (1996) compared their model predictions with the experimental data for all particles  $> 1 \mu\text{m}$ . Because the experimental data were expressed as regional deposition normalized to total respiratory tract deposition, the model predictions were also normalized to total predicted respiratory tract deposition. To distinguish this presentation from presentation of deposition fractions elsewhere in this chapter, upper respiratory tract (URT) deposition is defined as the sum of the nose, esophagus, and stomach deposition divided by those three compartments plus the lung for the data of Dahlbäck and Eirefelt (1994); and as deposition in the ET region divided by deposition in the sum of the ET, TB, and A regions for the predictions using the Ménache et al. (1996). Lower respiratory tract (LRT) deposition may then be defined as

$$\text{LRT deposition} = 1 - \text{URT deposition.} \quad (10-45)$$

The experimental and model-predicted deposition fractions are shown in Figure 10-33 for the data of Dahlbäck and Eirefelt (1994), as well as for the data of Raabe et al. (1988) that were used to develop the model. The solid line is the line of identity and represents the situation in which the predicted and observed deposition match exactly. As can be seen in Figure 10-33, there is considerable scatter in the data, particularly in the range associated generally with particles of about 2 to 3  $\mu\text{m}$  MMAD. Under the conditions for which the model would predict 50 to 60 percent deposition, the observed deposition for both the URT and LRT ranges from 10 to 80 percent. As noted earlier (Figure 10-31) deposition in rats increases very rapidly from low to high values in this range. Similarly, in humans, regional deposition associated with particles of 2 to 3  $\mu\text{m}$  ranges from 10 to 20 percent to 60 to 80 percent (Figure 10-22, 10-26, and 10-27).

## 10.6 CLEARANCE DATA AND MODELS

As discussed in previous sections, the biologic effects of inhaled particles are a function of their disposition. This, in turn, depends on their patterns of both deposition (i.e., the sites within which they initially come into contact with airway epithelial surfaces and the amount removed from the inhaled air at these sites) and clearance (i.e., the rates and routes by which deposited materials are removed from the respiratory tract). Removal of deposited materials involves the competing processes of macrophage - mediated clearance and dissolution - absorption. Deposition and clearance mechanisms were discussed in Sections 10.5 and 10.6, respectively.

Respiratory-tract clearance begins immediately upon deposition of inhaled particles. Given sufficient time, the deposited particles may be completely removed by these clearance processes. However, single inhalation exposures may be the exception rather than the rule. It is generally accepted that repeated or chronic exposures are common for environmental aerosols. As a result of such exposures, accumulations of the particles may occur. Chronic exposures produce respiratory tract burdens of inhaled particles that continue to increase with time until the rate of deposition is balanced by the rate of clearance. This is defined as the "equilibrium respiratory tract burden". The accumulation patterns are unique to each

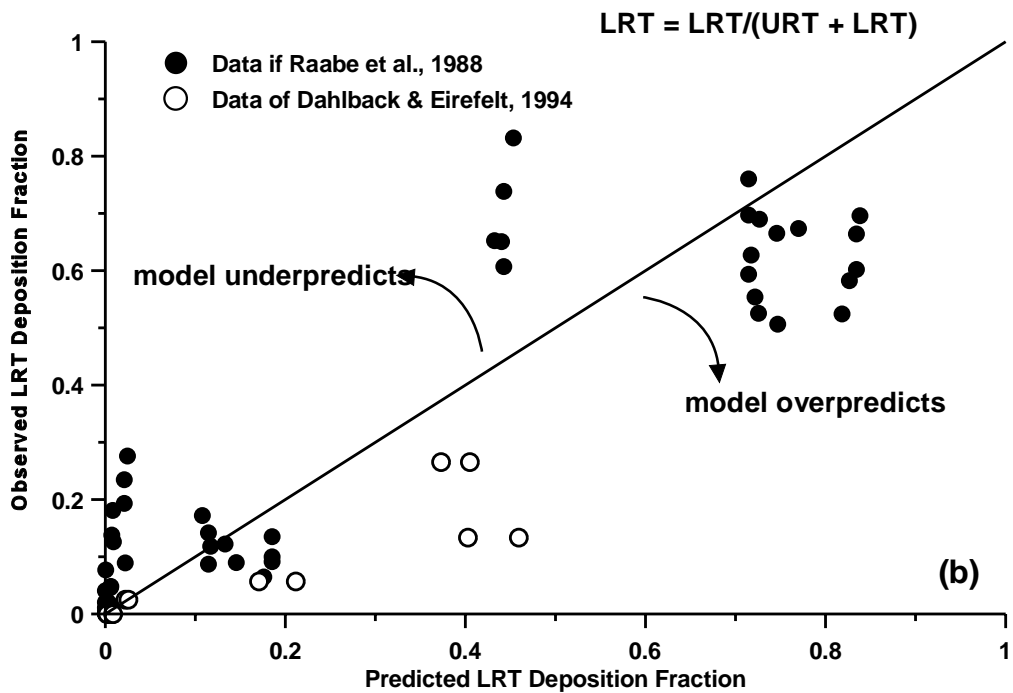
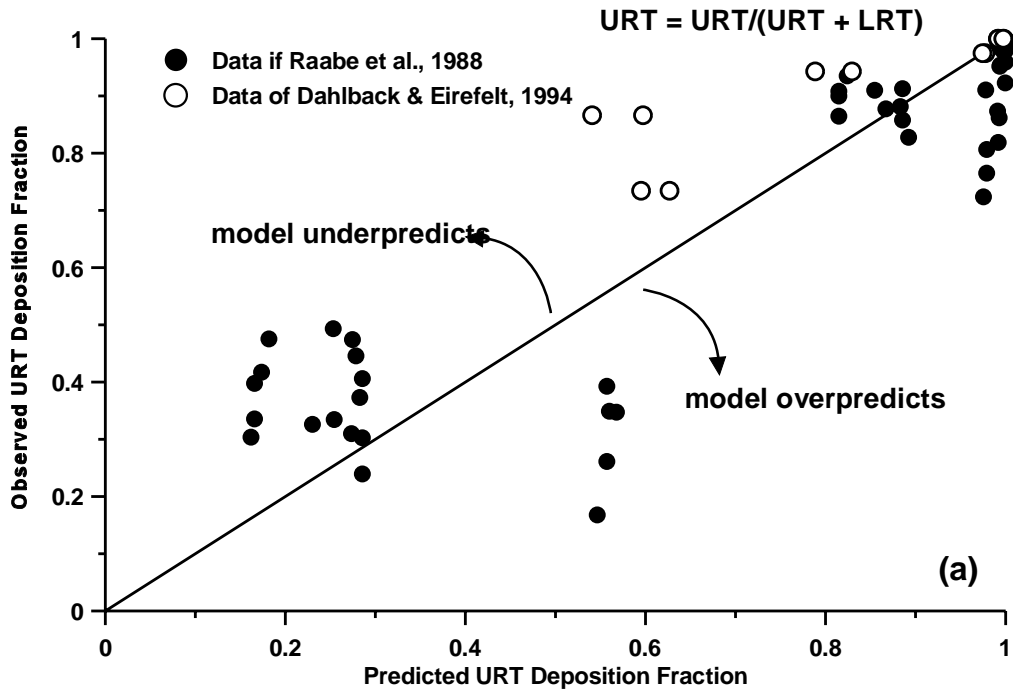


**Figure 10-33.** Experimental deposition fraction data and predicted estimates using model of Ménache et al. (1996). The solid line is the line of identity and represents the situation in which the predicted and observed deposition match exactly.  
Source: Ménache et al. (1996).

laboratory animal species, and possibly unique to the inhaled material, especially if the inhaled material alters deposition and/or clearance patterns.

It is important to evaluate these accumulation patterns, especially when assessing ambient chronic exposures, because they dictate what the equilibrium respiratory tract burdens of inhaled particles will be for a specified exposure atmosphere. Equivalent concentrations can be defined as "species-dependent concentrations of airborne particles which, when chronically inhaled, produce equal lung deposits of inhaled particles per gram of lung during a specified exposure period". This section presents available data and approaches to evaluating exposure atmospheres that produce similar respiratory tract burdens in laboratory animals and humans.

### **10.6.1 Humans**

Models for deposition, clearance, and dosimetry of the respiratory tract of humans have been available for the past four decades and continue to evolve. The International Commission on Radiological Protection (ICRP) has recommended three different mathematical models during this time period (ICRP 1959, 1979, 1994). The models changed substantially in structure, expanding from two compartments in the 1959 model (ICRP, 1959) to five compartments in the 1994 model (ICRP, 1994). These models have been an important aspect of radiation protection programs for inhaled radioactive materials. However, they make it possible to calculate the mass deposition and retention by different parts of the respiratory tract and provide, if needed, mathematical descriptions of the translocation of portions of the deposited material to other organs and tissues beyond the respiratory tract. The structure and complexity of the ICRP models increased with each version. These increases in complexity reflect both the expanded knowledge of the behavior and dosimetry of inhaled materials in the respiratory tract that has become available and an increased need for models that can be applied to a broader range of uses.

The 1959 model (ICRP, 1959) had a very simple structure in which the respiratory tract was divided into an upper respiratory tract (URT), and a lower respiratory tract (LRT). No information was given on the anatomical division between the URT and the LRT. In the 1959 model, 50% of inhaled particles deposited in the URT, 25% deposited in the LRT, and the remaining 25% was exhaled. No information on the effects of the sites or magnitude of

particle deposition was given, and relationships between particle size, deposition, and clearance were not incorporated into the 1959 model. The URT was considered an air passage from which all deposited particles cleared quickly by mucociliary activity and swallowed. Particles deposited in the LRT were classified as soluble or insoluble. For soluble particles, chemical constituents of all 25% of the inhaled particles that reach the LRT were assumed to be rapidly absorbed into the systemic circulation. For poorly soluble particles, 12.5% were assumed to clear by mucociliary activity and be swallowed during the first 24 h following deposition. The remaining 12.5% was assumed to be retained with a biological half-time of 120 d. No clearance of particles to the regional lymph nodes was included in the 1959 model.

The 1979 model (ICRP, 1979) was based on the Task Group Lung Model (TGLM) report (Morrow et al., 1966) and was divided into three compartments (nasopharyngeal, NP; tracheobronchial, TB; and pulmonary, PU). The NP region included anatomical structures from the tip of the nose to the larynx. The TB region extended from the trachea to the end of the terminal bronchioles. The PU region (equivalent to the A regional as described in Table 10-1) was the remaining, non-ciliated pulmonary parenchyma. Deposition probabilities were given for the NP, TB, and PU regions for activity median aerodynamic diameters (AMAD) of inhaled particles that covered about two orders of magnitude (0.2 - 10  $\mu\text{m}$ ). This incorporation of particle size considerations and the AMAD concept were major improvements in the health protection aspects of modeling related to inhaled radioactive particles. The 1979 ICRP model also incorporated consideration for clearance rates using three classes (D, W, Y). Class D particles cleared rapidly ( $T_{1/2} = 0.5$  d), class W particles cleared at an intermediate rate ( $T_{1/2} = 50$  d), and class Y particles cleared slowly ( $T_{1/2} = 500$  d). It was also recognized that the competing processes of dissolution-absorption and physical clearance operated on the deposited particles, but inadequate information was available to differentiate between the two mechanisms. This model also included a clearance pathway to the tracheobronchial lymph nodes. The long-term clearance of particles by either physical transport processes or by dissolution-absorption processes are described by the same clearance half-time.

A substantial increase in knowledge about the effects of particle size on the deposition of inhaled particles occurred since the publication of the TGLM report (Morrow et al.,

1966). This new information is reflected in the latest ICRP66 model (ICRP66, 1994). This new ICRP66 model considers the respiratory tract as four anatomical regions. The extrathoracic (ET) region is divided into two sub-regions: the anterior nasal airways, which clear only by extrinsic processes such as nose blowing, defined as  $ET_1$ , and the posterior nasal passages, pharynx, mouth and larynx defined as  $ET_2$ , which clears to the gastrointestinal tract via a combination of mucociliary action and fluid flow. The airways within the lungs are comprised of the bronchial (BB) and bronchiolar (bb) regions, which combined are equivalent to the Tracheobronchial (TB) region described in Table 10-3. The division of the TB region into two parts (bronchi and bronchiolar) by the ICRP enables mass deposition in the small airways to be evaluated separately, and possible related to such effects as small airways constriction. The gas-exchange tissues are defined as the alveolar-interstitial (AI) region, which is exactly comparable to the pulmonary region or A region (see Tables 10-1 and 10-3). There are two lymph node regions;  $LN_{ET}$  drains the extrathoracic region and  $LN_{TH}$  drains the BB, bb, and AI regions.

Deposition in the four anatomical regions (ET, BB, bb, and AI) is given as a function of particle size covering five orders of magnitude, and two different types of particle size parameters are used. The activity median thermodynamic diameter (AMTD) is used to describe the deposition of particles ranging in size from 0.0005 to 1.0 micrometer; the AMAD is used to describe deposition for the size range of 0.1 to 100 micrometer. The model applies to hygroscopic particles by estimating particle growth in each region during inhalation. Reference values of regional deposition are provided, and guidance is given for extrapolating to specific individuals and populations under different levels of activity. Deposition is expressed as a fraction of the number or activity of particles of a given size that is present in a volume of ambient air before inspiration, and activity is assumed to be log-normally distributed as a function of particle size for a typical particle density of  $3 \text{ g/cm}^3$  and dynamic shape factor of 1.5, although particle density and shape factor are included as variables in the deposition calculations. As discussed in Section 10.5, the 1994 ICRP66 model also includes consideration of particle inhalability, which is a measure of the degree to which particles can enter the respiratory tract and be available for deposition.

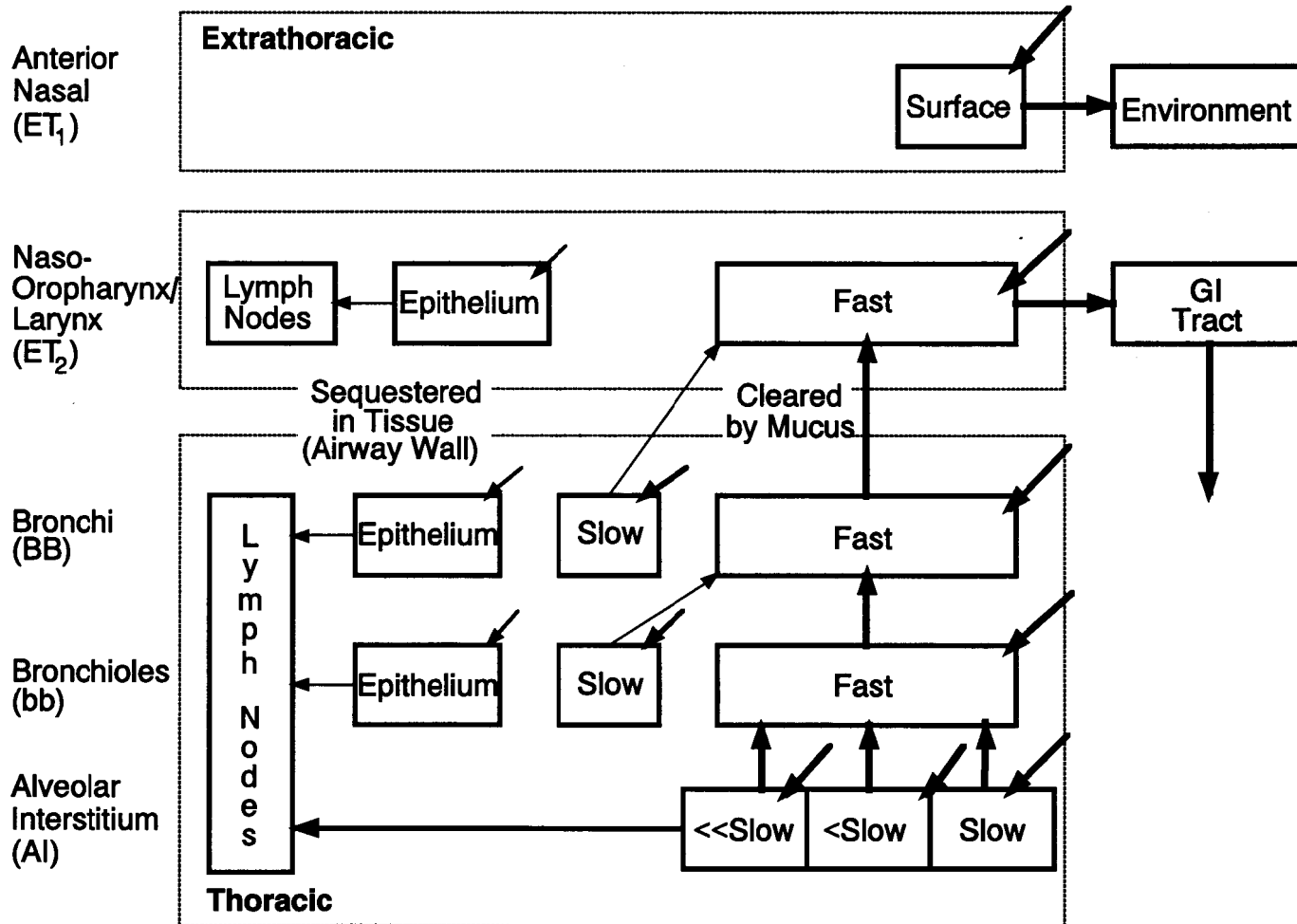
After deposition occurs in a given region, two different clearance processes act competitively on the deposited particles, except in the  $ET_1$  region where the only clearance

process is extrinsic. These processes are particle transport, which includes mucociliary clearance from the respiratory tract and physical clearance of particles to the regional lymph nodes, and absorption, which includes movement of material to blood including both dissolution-absorption and transport of ultra fine particles. Rates of particle clearance which were derived from studies with human subjects are assumed to be the same for all types of particles. Particle clearance from the BB and bb regions includes two slow phases: (1) to account for observations of slow mucociliary clearance in humans and (2) to account for observations of long term retention of small fractions of deposited material in the tracheobronchial tissues of both laboratory animals and humans. The structure for the ICRP66 1994 model is shown in Figure 10-34. A summary of the development of the ICRP66 1994 model is provided in Appendix 10A. This includes comparison of model predictions against the available deposition data discussed in Section 10.5.

A considerable amount of information has accumulated relevant to the biokinetics of inhaled radioactive materials. The radiation associated with these materials allows relative ease of analysis to determine temporal patterns for retention, distribution, and excretion of inhaled radioactive particles and their constituents. Non-radioactive particles are difficult to study because the particles and their chemical constituents are generally difficult to detect in biological systems, tissues, and excreta. Some studies have shown that the physicochemical forms and sites of deposition of chemical toxicants influence clearance rates. Also, adsorption of chemicals onto particles can influence deposition patterns and alter rates of dissolution-absorption of the particles and their constituents. For example, vapors that would not normally reach the A region will do so if they are adsorbed onto particles. Also, adsorption onto particles might slow the rates at which chemicals can be absorbed into lung tissue or the circulatory system. Amounts of inhaled material may markedly influence clearance as a consequence of particle overload. The cytotoxicity and shapes of particles (i.e., fibers) also influence clearance. Additionally, metabolic products of the inhaled materials may cause pathology and disease states that may result in nonpredictable retention and clearance patterns.

Absorption into blood is material specific, acts in all regions except ET<sub>1</sub>, and is assumed to occur at the same rates for all regions. Absorption into blood is a two stage process. The first step (dissolution) involves dissociation of the particles into a form that can

## The ICRP 1994 Human Respiratory Tract Model



10-125

**Figure 10-34. Schematic of the International Commission on Radiological Protection (ICRP66, 1994) model. Respiratory tract compartments in which inhaled particles may be deposited are illustrated. An explanation of clearance pathways, clearance rates, and subfractions of activity committed to different pathways is provided in the text.**

Source: International Commission on Radiological Protection (ICRP66, 1994).

be absorbed into blood; the second step involves absorption of the subunits of the particles. Because these processes act independently on the regionally deposited particles, each can be specified separately and allowed to compete against the other processes involved in the model. This approach makes it possible to use time-dependent functions to describe processes such as dissolution-absorption. However, for ease of calculation it is assumed that time dependent dissolution can be approximated by dividing the material into two fractions with different dissolution rates: material in an initial state dissolves at a constant rate, simultaneously changing to a transformed state in which it dissolves at another rate. Uptake into blood is treated as instantaneous for the material immediately absorbed after dissolution. Another fraction of dissolved material may be absorbed more slowly as a result of binding with tissue components. The model can use observed rates of absorption for compounds for which there are reliable human or laboratory animal data. The absorption of other compounds are specified as fast, moderate or slow. In the absence of specific information, compounds are classified as fast, moderate or slow according to their former classification as D, W or Y, respectively, under the previous ICRP model. Greater attention to the transfer of particles to regional lymph nodes is given in this model than in the 1979 model by incorporating these clearance processes at each level in the respiratory tract, not just in the A or pulmonary region as in the 1979 model. Additionally, while the new ICRP66 model (ICRP66, 1994) was developed primarily for use with airborne radioactive particles and gases, its use for describing the dosimetry of inhaled mass of non-radioactive substances is also appropriate.

An alternative new respiratory tract dosimetry model that developed concurrently with the new ICRP model is being proposed by the National Council on Radiation Protection (NCRP). This model was described in outline by Phalen et al. (1991) and at the time of writing, a full report of the model is undergoing final approval by the NCRP. As with the 1994 ICRP66 model (ICRP66, 1994), the proposed NCRP model addresses (1) inhalability of particles, (2) new sub-regions of the respiratory tract, (3) dissolution-absorption as an important aspect of the model, and (4) body size (and age). The proposed NCRP model defines the respiratory tract in terms of a naso-oro-pharyngo-laryngeal (NOPL) region, a tracheobronchial (TB) region, a pulmonary (P) region, and the lung-associated lymph nodes (LN). As with the 1994 ICRP66 model, inhalability of aerosol particles is considered, and

deposition in the various regions of the respiratory tract is modeled using methods that relate to mechanisms of inertial impaction, sedimentation, and diffusion. The rates of dissolution-absorption of particles and their constituents are derived from clearance data from humans and laboratory animals. The effect of body growth on particle deposition is also considered in the model, but particle clearance rates are assumed to be independent of age. The NCRP model does not consider the fate of inhaled materials after they leave the respiratory tract. Although the proposed NCRP model describes respiratory tract deposition, clearance, and dosimetry for radioactive substances inhaled by humans, the model can also be used for evaluating inhalation exposures to all types of particles.

Both the NCRP and ICRP had the benefit of contributions from respected investigators in respiratory tract toxicology and biomedical aerosol research. Similar mathematical assessments were arrived at by both commissions, although detailed calculations for specific radionuclides can be different. Comparison of regional deposition fraction predictions between the two models are shown in Figures 10-35 through 10-37. As noted above, the various compartments of the two models are equivalent. That is, the ET region as described in Table 10-3 is equivalent to the  $ET_1$  plus  $ET_2$  compartments of the ICRP66 1944 model and the NOPL compartment of the proposed NCRP model. The TB region of Table 10-3 is equivalent to the BB plus bb compartments of the ICRP66 1994 model and to the TB compartment of the proposed NCRP model. The A region of Table 10-3 is equivalent to the AI compartment of the ICRP66 1994 model and to the P compartment of the proposed NCRP model. These differences in nomenclature are retained in these figures to aid distinguishing the predictions from each. Figures 10-35 and 10-36 show predictions for an adult male during mild exercise and at rest. Figure 10-37 shows predictions for a 5-year old child. These comparisons show that the behavior of the models are quite comparable, that is, the predicted deposition fraction for a given particle size is similar if the models use the same ventilation parameters as input. In fact, in order to insure a uniform course of action that provides a coherent and consistent international approach, the NCRP recommends adoption of the ICRP66 1994 model for calculating exposures for radiation workers and the public (e.g., for computing annual reference levels of intake and derived reference air concentrations).

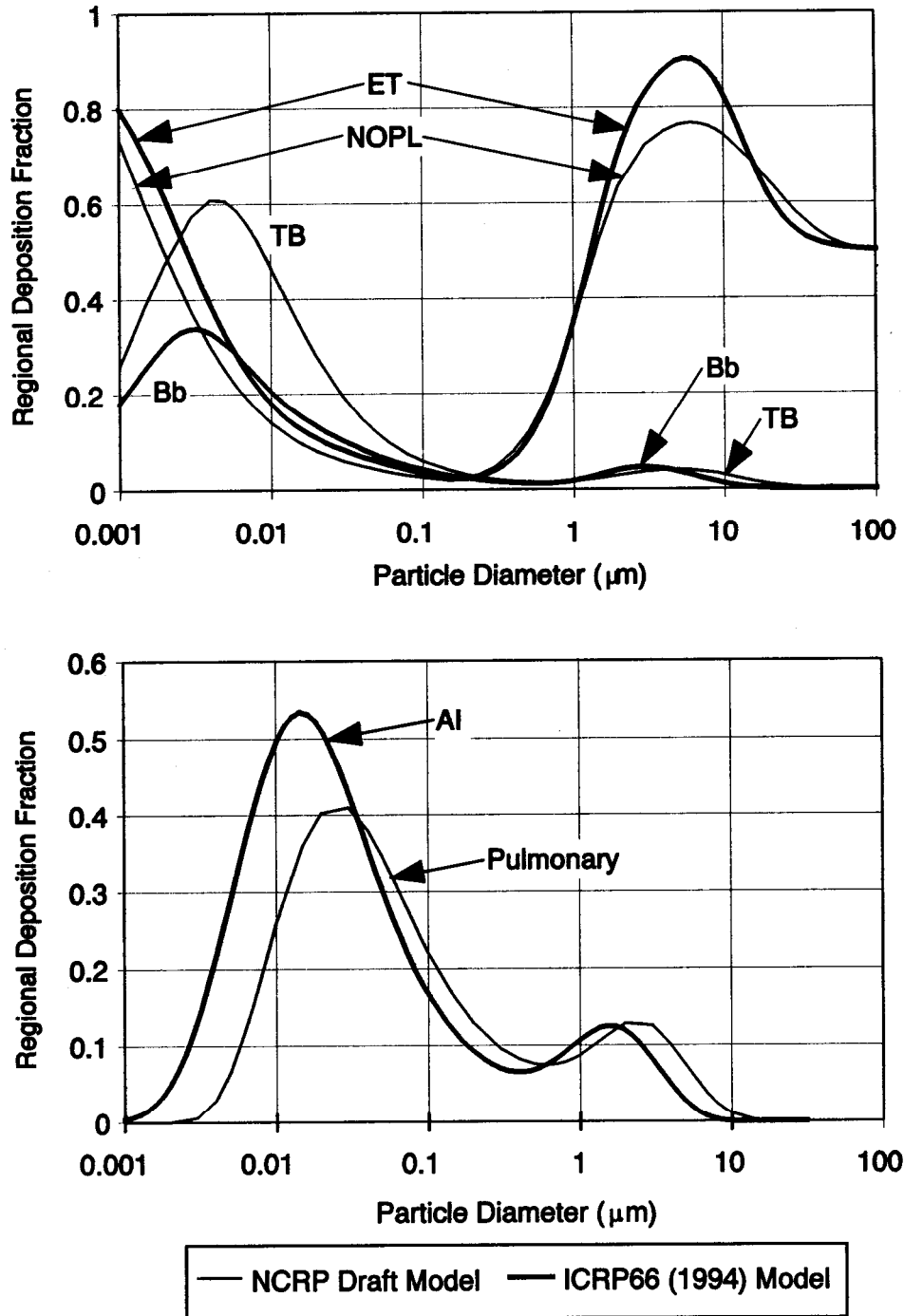
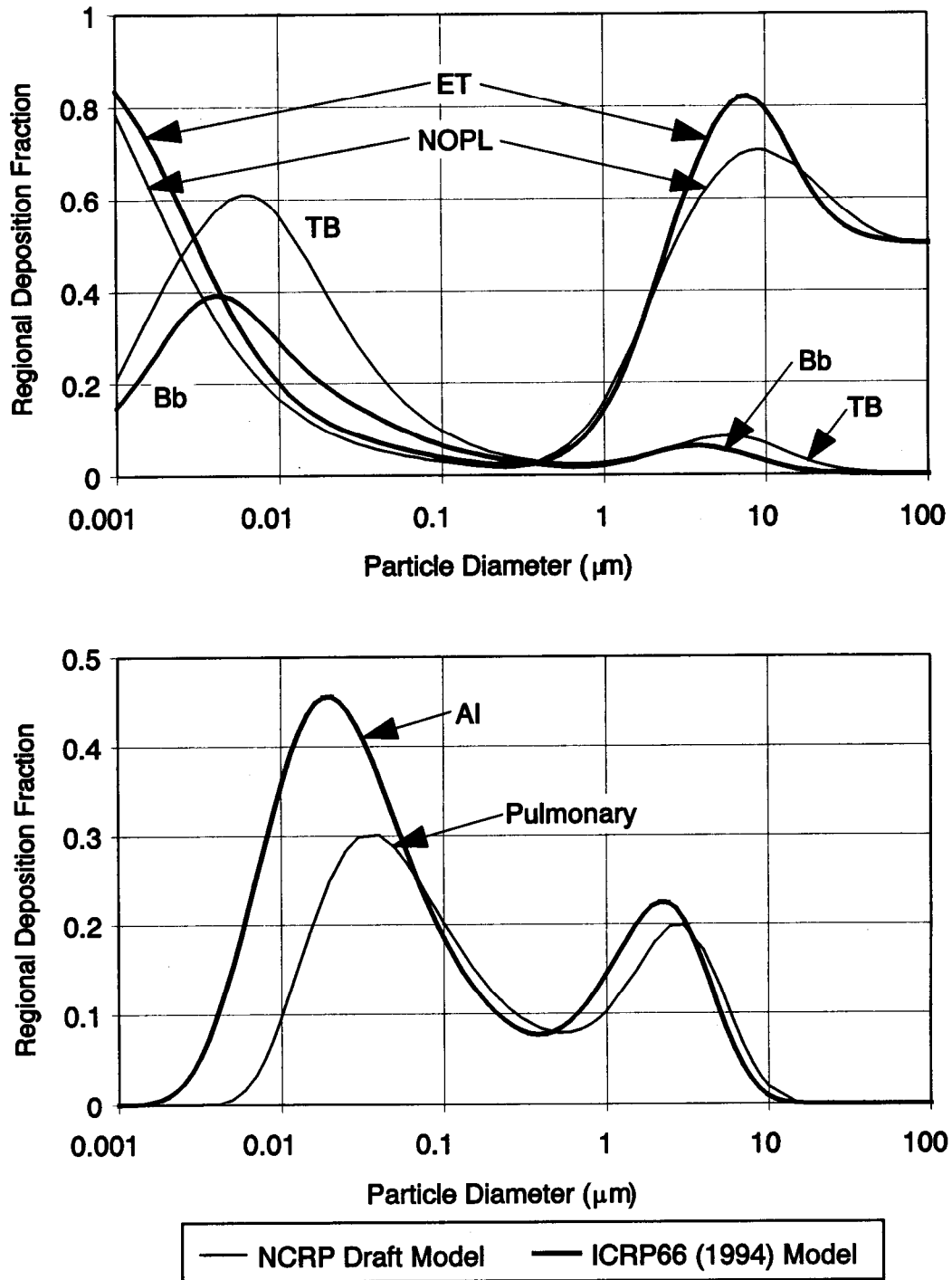
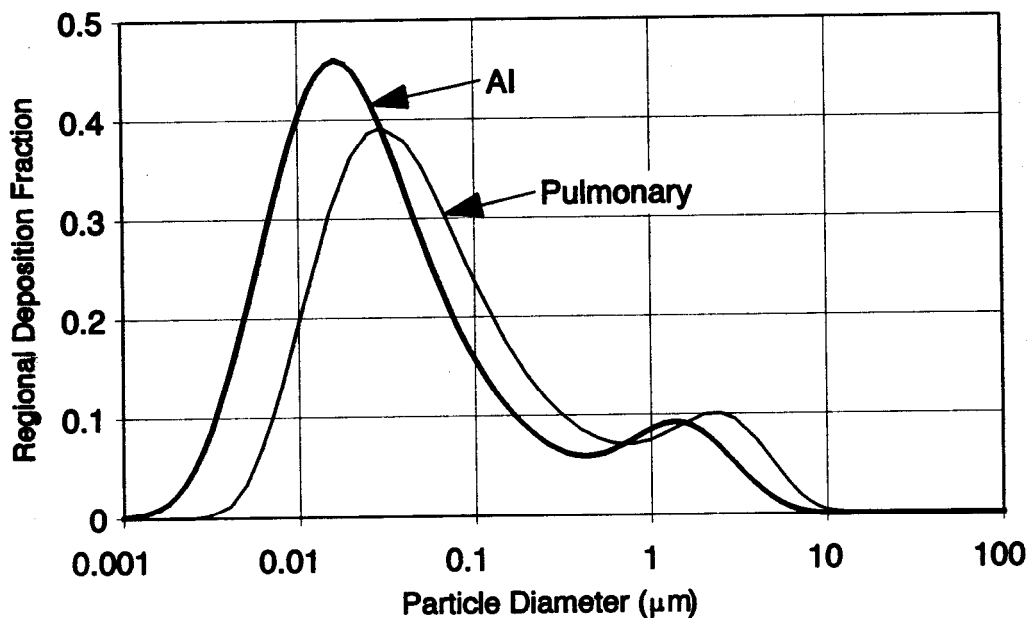
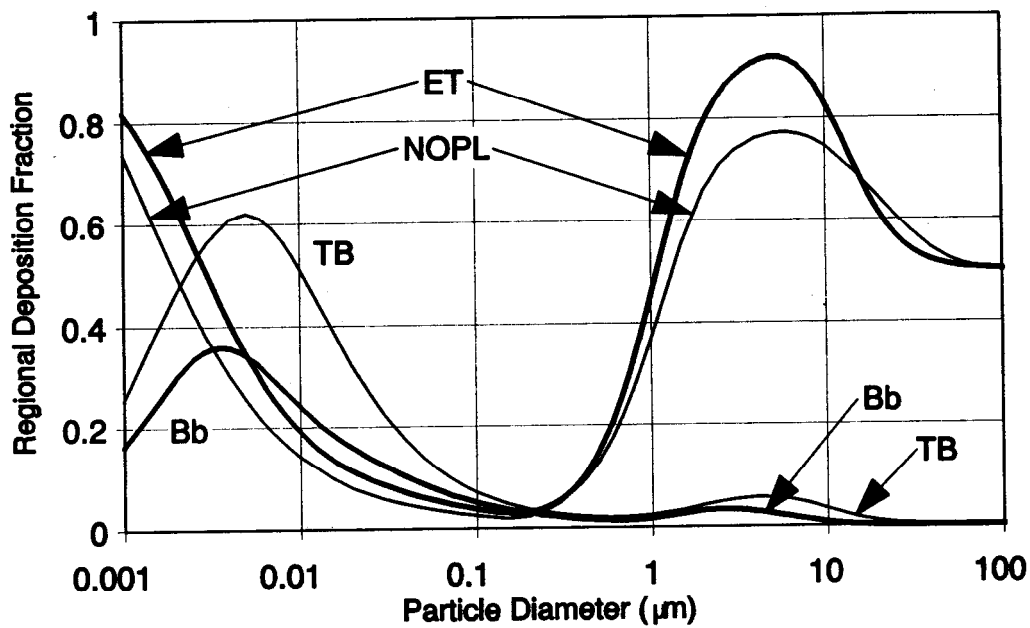


Figure 10-35.

Comparison of regional deposition fractions predicted by the proposed National Council on Radiation Protection (NCRP) model with those of the International Commission on Radiological Protection (ICRP) Publication 66 (1994) model. Predictions are for unit density, spherical particles inhaled through the nose by an adult male with a tidal volume of 1250 mL, respiratory frequency of 20 min<sup>-1</sup>, and functional residual capacity (FRC) of 3300 mL. See text for an explanation of abbreviations for respiratory tract compartments.



**Figure 10-36.** Comparison of regional deposition fractions predicted by the proposed National Council on Radiation Protection (NCRP) model with those of the International Commission on Radiological Protection (ICRP) Publication 66 (1994) model. Predictions are for unit density, spherical particles inhaled through the nose by an adult male with a tidal volume of 750 mL, respiratory frequency of 12 min<sup>-1</sup>, and functional residual capacity (FRC) of 3300 mL. See text for an explanation of abbreviations for respiratory tract compartments.



— NCRP Draft Model — ICRP66 (1994) Model

**Figure 10-37.** Comparison of regional deposition fractions predicted by the proposed National Council on Radiation Protection (NCRP) model with those of the International Commission on Radiological Protection (ICRP) Publication 66 (1994) model. Predictions are for unit density, spherical particles inhaled through the nose by a 5-year-old child with a tidal volume of 244 mL, respiratory frequency of  $39 \text{ min}^{-1}$ , and functional residual capacity (FRC) of 767 mL. See text for an explanation of abbreviations for respiratory tract compartments.

## 10.6.2 Laboratory Animals

Several laboratory animal models have been developed to help interpret results from specific studies that involved chronic inhalation exposures to non-radioactive particles (Wolff et al., 1987; Strom et al., 1988; Stöber et al., 1994). These models were adapted to data from studies involving high level chronic inhalation exposures in which massive lung burdens of low toxicity, poorly soluble particles were accumulated and the models have not been adapted to chronic exposures to low concentrations of aerosols in which particle overload does not occur.

Snipes et al. (1983) adapted a materials balance simulation model to evaluate repeated or chronic inhalation exposures. The simulation model language for a single inhalation exposure was described by Pritsker (1974) and uses a Fortran-based numerical integration of differential equations. The integration method is a fourth order, variable step-size Runge-Kutta-England routine for integrating systems of first order ordinary differential equations with initial values. The model was used to describe the retention and clearance of poorly soluble aerosol inhaled by mice, rats, and dogs (Snipes et al., 1983) and guinea pigs (Snipes et al., 1984). A distinct advantage of this kind of model is the requirement that dissolution-absorption rates for particles retained in the respiratory tract are approximated as part of the modeling process. The model output includes an estimate of the pulmonary burden of dust for each day of interest following an inhalation exposure.

Compartments and pathways of the model used in this chapter were kept as simple as necessary and were limited to those associated with the alveolar region of the respiratory tract. Figure 10-38 depicts the model, where

$D(t)$  = alveolar deposit of aerosol particles at time  $t$  ( $\mu\text{g/g}$  lung);

$MP(t)$  = mechanical transfer rate (fraction/day) for particles from the alveolar region to the mucociliary escalator for clearance to the gastrointestinal tract;

$ML(t)$  = mechanical transfer rate (fraction/day) for particles from the alveolar region to the thoracic lymph nodes;

$S(t)$  = dissolution-absorption rate (fraction/day) for particles in the alveolar region or thoracic lymph nodes.

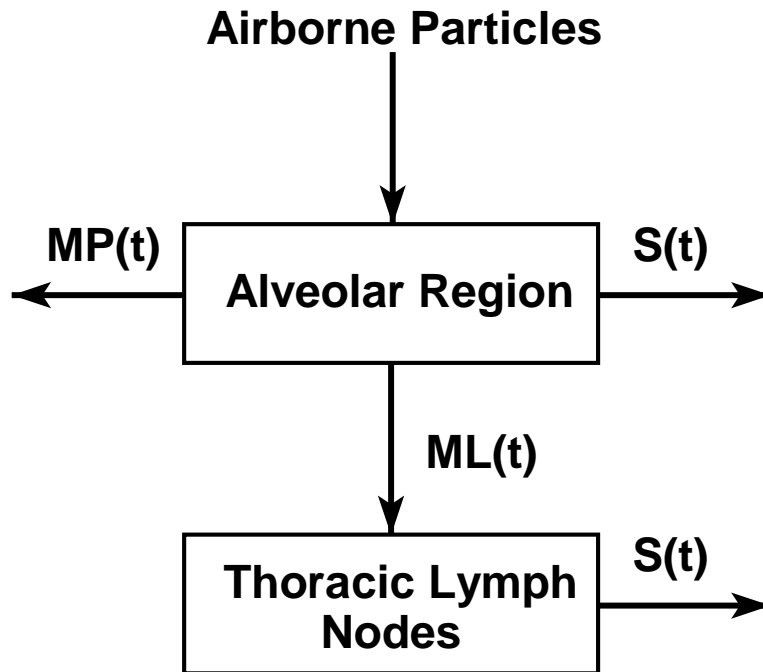


**Figure 10-38.** Compartments of the simulation model used to predict alveolar burdens of particles acutely inhaled by mice, hamsters, rats, guinea pigs, monkeys, and dogs. Definitions for parameters are provided in the text.

The retention of particles in the alveolar region as a function of time after a single inhalation exposure is described by

$$dD(t)/dt = -D(t) \cdot [MP(t) + ML(t) + S(t)], \quad (10-46)$$

with appropriate initial conditions for a single inhalation exposure. The solution of differential equations in the GASP IV simulation language is based upon numerical analysis techniques which adapt to produce solutions to a prespecified accuracy on either an absolute or relative scale. To maintain the specified accuracy the algorithm adjusts the size of the time step, making the step smaller or larger depending upon the estimated error. If the algorithm detects that the error is growing too large, it goes back to an earlier time and proceeds with smaller steps.

The simulation models for acute exposures were adapted to chronic exposures for the selected species using the assumption that each individual exposure during a chronic exposure

is the same with regard to deposition and clearance kinetics. Chronic exposures were simulated by defining the exposure duration in days and summing the amounts of dust retained in the lung from each daily inhalation exposure throughout the defined chronic exposure period. The model for chronic inhalation exposures therefore simply integrated the results of the individual exposures to predict the burdens of dust in the alveolar region during the course of the chronic exposures.

This model adequately accounted for the observed lung burdens of diesel exhaust particles (DEP) achieved in rats over the course of a 2-year chronic inhalation exposure to 0.35 mg DEP/m<sup>3</sup> (Snipes, 1989). The specific lung burdens of DEP achieved in the rats during the 2-year study were about 0.4 mg DEP/g lung, which is less than the amount that is generally predicted to cause particle overload. This model, and alternatives that are easily adapted to inhalation exposure scenarios, appears to be useful for predicting alveolar clearance patterns for a variety of inhaled materials as long as exposure concentrations are reasonably low and particle overload has not occurred.

### **10.6.3 Species Similarities and Differences**

Rates for particle translocation from the A region to thoracic lymph nodes (TLNs) appear to vary considerably among species. Rats and mice have particle translocation rates from the A region to TLNs that are quite different from those of guinea pigs, dogs, and possibly humans (Snipes et al., 1983; 1984). Translocation from the A region to TLNs begins soon after an acute inhalation exposure. However, after a few days following the acute exposure, the transport of particles from the A region to TLNs appears to be negligible in mice and rats (Snipes et al., 1983), but continues at a constant rate in guinea pigs and dogs (Snipes et al., 1983; 1984). No experimental information is available about the rates of translocation of particles from the A region to TLNs in humans. However, data for amounts of particles accumulated in the lungs of humans exposed repeatedly to dusty environments (Stöber et al., 1967; Carlberg et al., 1971; McInroy et al., 1976; Cottier et al., 1987) suggest that poorly soluble particles accumulate in TLNs of humans at rates that may be comparable to those observed for guinea pigs, dogs, and monkeys. However, based on human autopsy data for particles found in thoracic lymph nodes and lung tissue, the ICRP (1994) determined a transport rate for particle from lung to lymph nodes that would result in

a lymph node/lung particle concentration ratio of 20 at 10,000 days after inhalation. The transport rate was  $2 \times 10^{-5}$ /day, i.e., lower than the rate for dogs and monkey by approximately a factor of ten.

Physical movement of particles from the A region to the TLNs affords the opportunity to transport particles out of the lung, but the result is to sequester, or trap the particles in what is generally perceived to be a dead-end compartment. Because the TLNs represent traps for particles cleared from the lung, particles can accumulate to high concentrations in the TLNs. Thomas (1968, 1972) discussed the implications of particle translocation from the A region to TLNs when the particles contain specific radionuclides, but he presented information that is relevant to all types of particles. Translocation of particles from the A region to the TLNs results in concentrations of particles in the lymph nodes that can be more than 2 orders of magnitude higher than concentrations in the lung. The implications of this consequence of inhalation exposures have not been fully evaluated but may have important implications for immunological responses in humans exposed to specific kinds of aerosols.

Many measurements of alveolar retention and clearance have been conducted on humans and a variety of laboratory animal species. In some cases, at least two laboratory animal species were exposed to the same aerosolized material, so direct comparisons among species are possible. Few human inhalation exposure studies have been performed using the same materials as used for the laboratory animal studies. Therefore, only a limited number of direct comparisons are possible between laboratory animals and humans.

Table 10-13 contains a summary of selected results for alveolar retention of inhaled materials after single inhalation exposures to small masses of poorly soluble particles. Studies of less than about 3 mo duration were not included. The variability in these results was caused by several factors. In many cases, the reported results did not allow division of the alveolar burden between short- and long-term clearance. Also, for most studies, dissolution-absorption of the exposure materials were not known or were not reported. The broad range of particle sizes would have influenced deposition patterns, and dissolution-absorption rates, but probably not physical clearance of particles from the A region. The alveolar burden as a function of time in days after acute inhalation is given by

**TABLE 10-13. COMPARATIVE ALVEOLAR RETENTION PARAMETERS FOR POORLY SOLUBLE PARTICLES INHALED BY LABORATORY ANIMALS AND HUMANS**

Species	Aerosol Matrix	Particle Size <sup>a</sup>		Alveolar Burden <sup>b</sup>				Study Duration (days)	References
		µm	Measure	P	T <sub>1</sub> (d)	P <sub>2</sub>	T <sub>2</sub> (d)		
Mouse	FAP <sup>c</sup>	0.7	AMAD	<sup>d</sup> 0.93	34	0.07	146	850	Snipes et al. (1983)
	FAP	1.5	AMAD	0.93	35	0.07	171	850	Snipes et al. (1983)
	FAP	2.8	AMAD	0.93	36	0.07	201	850	Snipes et al. (1983)
	Ru oxide	0.38	CMD	0.88	28	<sup>e</sup> 0.12	230	490	Bair (1961)
	Pu oxide	0.2	CMD	0.86	20	0.14	460	525	Bair (1961)
Hamster	FAP	1.2	CMD	0.73	50	0.27	220	463	Bailey et al. (1985a)
Rat	Diesel soot	0.12	MMAD	0.37	6	0.63	80	330	Lee et al. (1983)
	FAP	1.25	CMD	0.62	20	0.38	180	492	Bailey et al. (1985b)
	FAP	0.7	AMAD	0.91	34	0.09	173	850	Snipes et al. (1983)
	FAP	1.5	AMAD	0.91	35	0.09	210	850	Snipes et al. (1983)
	FAP	2.8	AMAD	0.91	36	0.09	258	850	Snipes et al. (1983)
	FAP	1.2	AMAD	0.83	33	0.17	310	365	Finch et al. (1994)
	FAP	1.4	AMAD	0.76	26	0.24	210	180	Finch et al. (1995)
	Asbestos fibers	1.2-2.3	AMAD			1.00	46-76	101-171	Morgan et al. (1977)
	Latex	3.0	CMD	0.39	18	0.61	63	190	Snipes et al. (1988)
	Pu oxide	<1.0	CMD	0.20	20	0.80	180	350	Langham (1956)
	Pu oxide	2.5	AMAD	0.75	30	0.25	250	800	Sanders et al. (1976)
	UO <sub>2</sub>	2.7-3.2	AMAD			1.00	247	720	Morris et al. (1990)
	U <sub>3</sub> O <sub>8</sub>	≈1-2	CMD	0.67	20	0.33	500	768	Galibin and Parfenov (1971)
Co <sub>3</sub> O <sub>4</sub>	2.69	MMAD	0.70	19	0.30	125	180	Kreyling et al. (1993)	
Guinea pig	FAP	2.0	AMAD	0.22	29	0.78	385	1100	Snipes et al. (1984)
	Diesel soot	0.12	MMAD			1.00	>2,000	432	Lee et al. (1983)
	Latex	3.0	CMD			1.00	83	190	Snipes et al. (1988)

**TABLE 10-13 (cont'd). COMPARATIVE ALVEOLAR RETENTION PARAMETERS FOR POORLY SOLUBLE PARTICLES INHALED BY LABORATORY ANIMALS AND HUMANS**

Species	Aerosol Matrix	Particle Size		Alveolar Burden				Study Duration (days)	References
		µm	Measure	P	T <sub>1</sub> (d)	P <sub>2</sub>	T <sub>2</sub> (d)		
Dog, (cont'd)	Coal dust	2.4	MMAD			1.00	1,000	160	Gibb et al. (1975)
	Coal dust	1.9	MMAD			1.00	≈700	301-392	Morrow and Yuile (1982)
	Ce oxide	0.09-1.4	MMD			1.00 <sup>g</sup>	>570	140	Stuart et al. (1964)
	FAP	2.1-2.3	AMAD	0.09	13	0.91	440	181	Boecker and McClellan, (1968)
	FAP	0.7	AMAD	0.15	20	0.85	257	850	Snipes et al. (1983)
	FAP	1.5	AMAD	0.15	21	0.85	341	850	Snipes et al. (1983)
	FAP	2.8	AMAD	0.15	21	0.85	485	850	Snipes et al. (1983)
	FAP	2.01	AMAD	0.05		0.95	910	1,000	Kreyling et al. (1988)
	Nb oxide	1.6 -2.5	AMAD			1.00	>300	128	Cuddihy (1978)
	Pu oxide	1-5	CMD			1.00	1,500	280	Bair (1961)
	Pu oxide	4.3	MMD			1.00	300	300	Bair et al. (1962)
	Pu oxide	1.1-4.9	MMAD		≈1		400	468	Morrow et al. (1967)
	Pu oxide	0.1-0.65	CMD	0.10	200	0.90	1,000	≈4,000	Park et al. (1972)
	Pu oxide	0.72	AMAD	0.10	3.9	0.90	680	730	Guilmette et al. (1984)
	Pu oxide	1.4	AMAD	0.32	87	0.68	1,400	730	Guilmette et al. (1984)
	Pu oxide	2.8	AMAD	0.22	32	0.78	1,800	730	Guilmette et al. (1984)
	Pu oxide	4.3	MMD	0.50	20	0.50	1,600	270	Bair and McClanahan (1961)
	Tantalum	4.0	AMAD	0.40	1.9	0.60	860	155	Bianco et al. (1974)
U <sub>3</sub> O <sub>8</sub>	0.3	CMD	0.47	4.5	0.53	120	127	Fish (1961)	
Zr oxide	2.0	AMAD			1.0	340	128	Waligora (1971)	
Monkey	Pu oxide	2.06	CMAD			1.0	500-900	200	Nolibe et al. (1977)
	Pu oxide	1.6	AMAD			1.0	770-1,100	990	LaBauve et al. (1980)
Human	FAP	1	CMD	0.14	40	0.86	350	372-533	Bailey et al. (1985a)
	FAP	4	CMD	0.27	50	0.73	670	372-533	Bailey et al. (1985a)

**TABLE 10-13 (cont'd). COMPARATIVE ALVEOLAR RETENTION PARAMETERS FOR POORLY SOLUBLE PARTICLES INHALED BY LABORATORY ANIMALS AND HUMANS**

Species	Aerosol Matrix	Particle Size		Alveolar Burden				<sup>b</sup> Study Duration (days)	References
		µm	Measure	P	T <sub>1</sub> (d)	P <sub>2</sub>	T <sub>2</sub> (d)		
Human, (cont'd)	Latex	3.6	CMD	0.27	30	0.73	296	≈480	Bohning et al. (1982)
	Latex	5	CMD	0.42	0.5	0.58	150-300	160	Booker et al. (1967)
	Pu oxide	0.3	MMD			1.00	240	300	Johnson et al. (1972)
	Graphite and PuO <sub>2</sub>	6	AMAD			1.00	240-290	566	Ramsden et al. (1970)
	Pu oxide	<4-5	CMD			1.00	1,000	427	Newton (1968)
	Th oxide	<4-5	CMD			1.00	300-400	427	Newton (1968)
	Teflon	4.1	CMD	0.30	4.5-45	0.70	200-2,500	300	Philipson et al. (1985)
	Zr oxide	2.0	AMAD			1.00	224	261	Waligora (1971)

<sup>a</sup>Some aerosols were monodisperse, but most were polydisperse, with geometric standard deviations in the range of 1.5 to 4.

<sup>b</sup>Alveolar burden =  $P_1 \cdot e^{-(\ln 2)t/T_1} + P_2 \cdot e^{-(\ln 2)t/T_2}$ , where P<sub>1</sub> and P<sub>2</sub> are fractions constrained to total 1.00, T<sub>1</sub> and T<sub>2</sub> equal retention half-times in (d), and

t equals days after exposure. Retention half-times are approximations and are the net result of dissolution-absorption and physical clearance

processes. In some examples, the original data were subjected to a computer curve-fit procedure to derive the values for P<sub>1</sub> and T<sub>1</sub> presented in this table.

<sup>c</sup>FAP = fused aluminosilicate particles.

<sup>d</sup>AMAD = activity median aerodynamic diameter.

<sup>e</sup>CMD = count median diameter.

<sup>f</sup>MMAD = mass median aerodynamic diameter.

<sup>g</sup>MMD = mass median diameter.

$$P_1 \cdot e^{-(\ln 2)t/T_1} + P_2 \cdot e^{-(\ln 2)t/T_2}, \quad (10-47)$$

where  $P_1$  and  $P_2$  are fractions constrained to total 1.0,  $T_1$  and  $T_2$  equal retention half-times in days, and  $t$  equals days after acute exposure.

The information shown in Table 10-13 was used to approximate biological clearance rates for particles inhaled by the species listed in Table 10-14. In addition, approximations are included for the fractions of alveolar burdens initially deposited in the A region that were subjected to short- or long-term clearance. These trends clearly will not apply to all types of inhaled particles. For example, in some cases, deposition and clearance may be influenced by the physicochemical and/or biological characteristics of the inhaled material. Further, the generalizations that led to Table 10-14 allow comparisons for the consequences of chronic inhalation exposures among these animal species and humans that might not otherwise be possible.

**TABLE 10-14. AVERAGE ALVEOLAR RETENTION PARAMETERS FOR POORLY SOLUBLE PARTICLES INHALED BY SELECTED LABORATORY ANIMAL SPECIES AND HUMANS**

Species	Alveolar Retention Parameters <sup>a</sup>			
	$P_1$	$T_1$	$P_2$	$T_2$
Mouse	0.9	30	0.1	240
Rat, Syrian hamster	0.9	25	0.1	210
Guinea pig	0.2	29	0.8	570
Monkey, dog, human	0.3	30	0.7	700

<sup>a</sup>Alveolar burden (fraction of initial deposition) =

$$P_1 \exp^{-(\ln 2)t/T_1} + P_2 \exp^{-(\ln 2)t/T_2},$$

where:

- $P_1$  and  $P_2$  = fractions of alveolar burden in fast and slow-clearing components;
- $T_1$  and  $T_2$  = retention half-times (days) for  $P_1$  and  $P_2$ ; and
- $t$  = time in days after an acute inhalation exposure.

The mathematical expressions for fitting curves to data are dependent on the study duration. The values for percent initial alveolar burden (% IAB) versus time in the following table were obtained by simulating alveolar retention of poorly soluble particles in the rat using the physical clearance rates from Table 10-14. Two-component exponential curves were next fit for % IAB versus time using the model results for days 1 to 150, 1 to 300, and 1 to 730. As indicated in Table 10-15, the curve fitting parameters for the data for days 1 to 150 agree well with results typically seen in relatively short-term alveolar clearance studies with rats.

**TABLE 10-15. PHYSICAL CLEARANCE RATES**

<b>Days</b>	<b>% IAB</b>	<b>P<sub>1</sub></b>	<b>T<sub>1</sub></b>	<b>P<sub>2</sub></b>	<b>T<sub>2</sub></b>
<b>1</b>	<b>96.96</b>				
<b>7</b>	<b>81.21</b>				
<b>14</b>	<b>66.89</b>				
<b>28</b>	<b>47.00</b>				
<b>35</b>	<b>40.03</b>				
<b>42</b>	<b>34.43</b>				
<b>49</b>	<b>29.87</b>				
<b>56</b>	<b>26.14</b>				
<b>63</b>	<b>23.06</b>				
<b>70</b>	<b>20.49</b>				
<b>100</b>	<b>13.26</b>				
<b>150</b>	<b>7.80</b>	<b>71.6</b>	<b>18.4</b>	<b>29.4</b>	<b>78.3</b>
<b>200</b>	<b>5.39</b>				
<b>250</b>	<b>4.10</b>				
<b>300</b>	<b>3.30</b>	<b>84.4</b>	<b>22.0</b>	<b>15.6</b>	<b>131</b>
<b>400</b>	<b>2.36</b>				
<b>500</b>	<b>1.78</b>				
<b>600</b>	<b>1.37</b>				
<b>730</b>	<b>0.99</b>	<b>91.0</b>	<b>25.6</b>	<b>9.0</b>	<b>221</b>

Physical clearance patterns for alveolar burdens of particles are similar for guinea pigs, monkeys, dogs, and humans. For these species, about 20 to 30% of the initial burden of particles clears with a half-time on the order of 1 mo, the balance clears with a half-time of several hundred days. Mice, Syrian hamsters, and rats clear about 90% of the deposited

particles with a half-time of about 1 month and 10% with a half-time greater than 100 days. The relative division of the alveolar burden between short-term and long-term clearance represents a significant difference between most rodents and larger mammals and has considerable impact on long-term patterns for retention of material acutely inhaled, as well as for accumulation patterns for materials inhaled in repeated exposures.

#### **10.6.4 Models To Estimate Retained Dose**

Models have routinely been used to express retained dose in terms of temporal patterns for alveolar retention of acutely inhaled materials. Available information for a variety of mammalian species and humans can be used to predict deposition patterns in the respiratory tract for inhalable aerosols with reasonable degrees of accuracy. Additionally, as indicated above, alveolar clearance data for mammalian species commonly used in inhalation studies are available from numerous experiments that involved small amounts of inhaled radioactive particles. The amounts of particles inhaled in those studies were small and can be presumed to result in clearance patterns characteristic of the species unless radiation damage was a confounding factor, which was probably not the case except where acute effects were an experimental objective.

A very important factor in using models to predict retention patterns in laboratory animals or humans is the dissolution-absorption rate of the inhaled material. Factors that affect the dissolution of materials or the leaching of their constituents in physiological fluids, and the subsequent absorption of these constituents, are not fully understood. Solubility is known to be influenced by the surface-to-volume ratio and other surface properties of particles (Mercer, 1967; Morrow, 1973). The rates at which dissolution and absorption processes occur are influenced by factors that include chemical composition of the material. Temperature history of materials is an important consideration for some metal oxides. For example, in controlled laboratory environments, the solubility of oxides usually decreases when the oxides are produced at high temperatures, which generally results in compact particles having small surface-to-volume ratios. It is sometimes possible to accurately predict dissolution-absorption characteristics of materials based on physical/chemical considerations. However, predictions for *in vivo* dissolution-absorption rates for most materials, especially if they contain multivalent cations or anions, should be confirmed experimentally.

Phagocytic cells, primarily macrophages, clearly play a role in dissolution-absorption of particles retained in the respiratory tract (Kreyling, 1992). Some particles dissolve within the phagosomes due to the acidic milieu in those organelles (Lundborg et al., 1984, 1985), but the dissolved material may remain associated with the phagosomes or other organelles in the macrophage rather than diffuse out of the macrophage to be absorbed and transported elsewhere (Cuddihy, 1984). Examples of delayed absorption of presumably soluble inorganic materials are beryllium (Reeves and Vorwald, 1967) and americium (Mewhinney and Griffith, 1983). This same phenomenon has been reported for organic materials. For example, covalent binding of benzo(a)pyrene or metabolites to cellular macromolecules resulted in an increased alveolar retention time for that compound after inhalation exposures of rats (Medinsky and Kampcik, 1985). Certain chemical dyes are also retained in the lung (Medinsky et al., 1986), where they may dissolve and become associated with lipids or react with other constituents of lung tissue. Understanding these phenomena and recognizing species similarities and differences are important for evaluating alveolar retention and clearance processes and interpreting results of inhalation studies.

In one study related to the issue of species differences in dissolution-absorption, Oberdörster et al. (1987) evaluated clearance of  $^{109}\text{Cd}$  from the lungs of rats and monkeys after inhalation of  $^{109}\text{Cd}$ -labeled aerosols of  $\text{CdCl}_2$  and  $\text{CdO}$ . The inhaled Cd was cleared 10 times faster from lungs of the rats than from the lungs of monkeys. Cadmium in the lungs of mammalian species is probably bound to metallothionein, and these differences in rates of Cd clearance appear to be the result of species differences in metallothionein metabolism. Bailey et al. (1989) conducted a study that included an interspecies comparison of the translocation of  $^{57}\text{Co}$  from the A region to blood after inhalation of  $^{57}\text{Co}_3\text{O}_4$ . The results of this multi-species study suggest that mammalian species demonstrate considerable variability with regard to rates of dissolution of particles retained in lung tissue, degree of binding of solubilized materials with constituents of lung tissue, and rates of absorption into the circulatory system.

Dissolution-absorption of materials in the respiratory tract is clearly dependent on the chemical and physical attributes of the material. While it is possible to predict rates of dissolution-absorption, it is prudent to experimentally determine this important clearance parameter to understand the importance of this clearance process for the lung, TLNs,

and other body organs that might receive particles or fibers, or their constituents which enter the circulatory system from the lung.

#### **10.6.4.1 Extrathoracic and Conducting Airways**

Insufficient data are available to adequately model long-term retention of particles deposited in the conducting airways of any mammalian species. It is probable that some particles that deposit in the airways of the head and TB region during an inhalation exposure are retained for long times and may represent significant dosimetry concerns. Additionally, some of the particles that are cleared from the A region via the mucociliary transport pathway may become trapped in the TB epithelium during their transit through the airways. Additional research must be done to provide the information needed to properly evaluate retention of particles in conducting airways.

Based on the results of longitudinal studies of dogs who inhaled promethium oxide particles, Stuart (1966) concluded that some particles were retained for relatively long times in the heads. A study by Snipes et al. (1983) included mice, rats, and dogs exposed by inhalation to monodisperse or polydisperse <sup>134</sup>Cs-labeled fused aluminosilicate particles. In all three species, 0.001 to 1% of the initial internally deposited burden of particles was retained in the head airways and was removed only by dissolution-absorption. Tissue autoradiography revealed that retained particles were in close proximity to the basement membrane of nasal airway epithelium. In another study by Snipes et al. (1988), 3-, 9-, and 15- $\mu$ m latex microspheres were inhaled by rats and guinea pigs. About 1 and 0.1% of all three sizes of microspheres were retained in the head airways of the rats and guinea pigs, respectively. For rats, the 9- and 15- $\mu$ m microspheres cleared with half-times of 23 days; for guinea pigs, microspheres of this size cleared with half-times of about 9 days. The 3- $\mu$ m microspheres were cleared from the head airways of the rats and guinea pigs with biological half-times of 173 and 346 days, respectively. The smaller particles are apparently more likely to penetrate the epithelium and reach long-term retention sites.

Whaley et al. (1986) studied retention and clearance of radiolabeled, 3- $\mu$ m polystyrene latex particles instilled onto the epithelium of the maxillary and ethmoid turbinates of Beagle dogs. Retention of the particles at both sites after 30 days was about 0.1% of the amount

initially deposited. Autoradiographs of turbinate tissue indicated that the particles were retained in the epithelial submucosa of both regions.

It is also generally concluded that most inhaled particles that deposit in the TB region clear within hours or days. However, results from a number of studies in recent years challenge this supposition. These studies have demonstrated that small portions of the particles that deposit in, or are cleared through, the TB region are retained with half-times on the order of weeks or months. Patrick and Stirling (1977) noted that about 1% of barium sulfate particles instilled intratracheally into rats remained in the bronchial tissue for at least 30 days. In a followup study, Stirling and Patrick (1980) used autoradiography to demonstrate the temporal retention patterns for some of the retained  $^{133}\text{BaSO}_4$  particles in TB airways. The particles were retained within macrophages in the tracheal wall for at least 7 days after intratracheal instillation of  $^{133}\text{BaSO}_4$ . By two h after instillation, some of the particles were buried in the tracheal wall. After 24 h, when most of the initial deposition of particles had cleared, 74% of  $^{133}\text{BaSO}_4$  particles located by autoradiography were in macrophages proximate to the basement membrane. After 7 days, practically all of the remaining particles were incorporated into the walls of the airways. The authors did not determine the mechanisms by which the particles were moved into the airway epithelium. It is possible that the particles were phagocytized by macrophages and transported into the airway epithelium. Another possibility is direct uptake by epithelial cells of the airways. It is also probable that intratracheal instillation procedures perturb airway epithelium and influence the results of these kinds of studies.

Gore and Thorne (1977) exposed rats by inhalation to polydisperse aerosols of  $\text{UO}_2$ . At 2, 4, 7, and 35 days after inhalation of the  $\text{UO}_2$ , autoradiography was used to determine the locations of particles retained in the TB and A regions. The authors did not report seeing particles of  $\text{UO}_2$  retained in the airways, but did note two phases of clearance. The first phase was associated with a clearance half-time of 1.4 days, the second phase with a clearance half-time of about 16 days. The faster clearance was presumably associated with particles deposited on the conducting airways during the inhalation exposure; the longer-term clearance was associated with clearance of  $\text{UO}_2$  particles from the A region. In a separate study, Gore and Patrick (1978) evaluated the distribution of  $\text{UO}_2$  particles in the trachea and bronchi of rats for up to 14 days after inhalation of aerosols similar to those used by Gore

and Thorne (1977). Retention of  $\text{UO}_2$  at airway bifurcations was noted, as was retention of particles in the trachea.

In another study, Gore and Patrick (1982) also compared the retention sites of inhaled  $\text{UO}_2$  particles and intratracheally instilled barium sulphate particles. Both types of particles were found in macrophages at sites near the basement membrane of the airways of the TB region. The macrophages appeared to have engulfed the particles in the airways, then passed through the airway epithelium and remained in the vicinity of the basement membrane. About 4% of the  $\text{UO}_2$  in lungs of rats was associated with intrapulmonary airways (Gore, 1983; Patrick, 1983). Watson and Brain (1979) observed similar results with aerosols of gold colloid and iron oxide. Both types of particles were found in bronchial epithelium, but more of the iron oxide was observed, suggesting a possible particle size effect, or a relationship between the process of material uptake and chemical composition of the material. Both types of particles were found in bronchial epithelial cells, but neither gold nor iron oxide particles were seen in interstitial macrophages.

In another inhalation study, Briant and Sanders (1987) exposed rats to 0.7  $\mu\text{m}$  AMAD chain-aggregate aerosols of U-Pu. These authors observed retained particles of U-Pu in the larynx, trachea, carina, and bronchial airways throughout the course of their 84-day study. The amounts retained varied, but were at any time approximately 1% of the concurrent alveolar burden. The alveolar burden of U-Pu cleared with a biological half-time of 100 days, and the relative amounts of U-Pu in the airways suggested comparable particle clearance rates from the airways. Particles of U-Pu retained in the airways were located in epithelial cells.

Stahlhofen et al. (1981, 1986) conducted inhalation studies with humans to directly assess deposition and retention of poorly soluble particles that deposit in the TB region by inhalation. Human subjects inhaled small volumes of aerosols using procedures that theoretically allowed deposition to occur at specific depths in the TB region, but not in the A region. Results of those studies suggested that as much as 50% of the particles that deposited in the TB region clear slowly, presumably because they become incorporated into the airway epithelium. Smaldone et al. (1988) reported the results from gamma camera imaging analyses of aerosol retention in normal and diseased human subjects, and also suggested that particles deposited on central airways of the human lung do not completely

clear within 24 h. There have also been a few reports indicating that poorly soluble particles associated with cigarette smoke are retained in the epithelium of the tracheobronchial tree of humans (Little et al., 1965; Radford and Martell, 1977; Cohen et al., 1988). The cumulative results of these studies strongly suggest that a portion of particles that deposit on the conducting airways can be retained for long periods of time, or indefinitely.

Long-term retention and clearance patterns for radioactive particles that deposit in the head airways and TB region must be thoroughly evaluated because of the implications of this information for respiratory tract dosimetry and risk assessment (James et al., 1991; Johnson and Milencoff, 1989; Roy, 1989; ICRP, 1994). Similar concerns exist for non-radioactive particles that might be cytotoxic or elicit inflammatory, allergic, or immune responses at or near retention sites in conducting airways.

#### **10.6.4.2 Alveolar Region**

Model projections are possible for the A region using the cumulative information in the scientific literature relevant to deposition, retention, and clearance of inhaled particles. Table 10-16 summarizes reasonable approximations for physical alveolar clearance parameters for six laboratory animal species. Alveolar clearance curves produced using the parameters in Table 10-16 agree with curves produced using the parameters in Table 10-14. An advantage to using the parameters in Table 10-16 is that they separate physical clearance from the A region into its two components, physical clearance via the mucociliary clearance pathway to the GI tract and clearance to TLNs. To model the biokinetics of a specific type of particle in the A regions of these laboratory animal species, the physical clearance parameters in Table 10-16 were used in conjunction with a dissolution-absorption parameter to derive rates for effective clearance from the A region. As explained below, biokinetic modeling for particles deposited in the A region of humans was done using the new ICRP66 respiratory tract model (ICRP66, 1994). To model the alveolar biokinetics of a specific type of particle, the physical clearance parameters in Table 10-16 are used in conjunction with a dissolution-absorption parameter to derive rates for effective clearance from the A region.

**TABLE 10-16. PHYSICAL CLEARANCE RATES<sup>a</sup> FOR MODELING  
ALVEOLAR CLEARANCE OF PARTICLES INHALED BY  
SELECTED MAMMALIAN SPECIES**

Species	Clearance via Mucociliary Transport Pathway	Clearance to Thoracic Lymph Nodes
Mouse <sup>b</sup>	$0.023 \exp^{-0.008t} + 0.0013$	$0.0007 \exp^{-0.5t}$
Rat <sup>b</sup> , Syrian hamster <sup>c</sup>	$0.028 \exp^{-0.01t} + 0.0018$	$0.0007 \exp^{-0.5t}$
Guinea pig <sup>b</sup>	$0.007 \exp^{-0.03t} + 0.0004$	0.00004
Monkey <sup>d</sup> , dog <sup>b</sup>	$0.008 \exp^{-0.022t} + 0.0001$	0.0002

<sup>a</sup>Fraction of existing alveolar burden physically cleared per day.

<sup>b</sup>Adapted from Snipes (1989)

<sup>c</sup>Clearance rates assumed to be the same as for rats.

<sup>d</sup>Clearance rates assumed to be the same as for dogs.

## **10.7 APPLICATION OF DOSIMETRY MODELS TO DOSE-RESPONSE ASSESSMENT**

For the purposes of this document an attempt was made to ascertain whether dosimetry modeling can provide insight into the apparent discrepancies between the epidemiologic and laboratory animal data, to identify plausible dose metrics of relevance to the available health endpoints, and to identify modifying factors that may enhance susceptibility to inhaled particles. In order to accomplish these objectives, this section presents an application of dosimetry modeling to data typically available from the epidemiologic and laboratory animal studies. Choice of a dosimetry model for humans and laboratory animals, respectively, is discussed and these models are used to simulate deposition and retained doses of various exposures. Different dose metrics and their relevance to observed health endpoints are also discussed.

Application of the chosen dosimetry models to calculate these estimates are intended to illustrate the potential influence dosimetry may have on estimation of dose to provide a linkage between the exposure and the available epidemiologic and toxicologic data. At present, respiratory tract dosimetry must rely on many simplifications and empiricisms, but even a somewhat rudimentary effort will assist in linking dose to effects and in species extrapolations. As more information on mechanistic determinants of dose, target tissues, and target dose and tissue interaction relationships become available, the more complex and

realistic the dosimetry construct will become. It is foreseen that choice of dose metrics will go beyond dependence on average mass or number concentration in the future as physiologically-based models become available. The human and laboratory animal models chosen for the simulations represent semi-empirical and empirical approaches to characterizing the available deposition and retention data. Default values for key parameters such as ventilation rate and body weight have been used in these simulation exercises. Disagreement with the limited published deposition and retention data is considered to be within the known variability among these parameters as well as biological detectability of the current state of measurement. As with any data-driven process, when additional data become available, the model structures can be reviewed and revised as appropriate. Additional experimental measurements would provide more information to strengthen the predictions and provide better description of intersubject and interspecies variability.

### **10.7.1 General Considerations for Extrapolation Modeling**

Major factors that affect the disposition (deposition, uptake, distribution, metabolism, and elimination) of inhaled particles include the physicochemical properties of the particles (e.g., particle diameter, distribution, hygroscopicity) and anatomic (e.g., upper respiratory tract architecture, regional surface areas, airway diameters, airway lengths, branching patterns) and physiologic (e.g., ventilation rates, clearance mechanisms) parameters of individual mammalian species. The relative contribution of each of these factors is a dynamic relationship. Further, the relative contribution of these determinants is also influenced by exposure conditions such as concentration and duration. A comprehensive description of the exposure-dose-response continuum is desired for accurate extrapolation. Therefore, a dosimetry model should incorporate all of the various deterministic factors into a computational structure. Clearly, many advances in the understanding and quantification of the mechanistic determinants of particle disposition, toxicant-target interactions, and tissue responses (including species sensitivity) are required before an overall model of pathogenesis can be developed for a specific aerosol. Such data exist to varying degrees, however, and may be incorporated into less comprehensive models that nevertheless are useful in describing delivered doses or in some cases, target tissue interactions.

### **10.7.1.1 Model Structure and Parameterization**

Data on the mechanistic determinants of particle disposition, toxicant-target interactions, and tissue responses to incorporate into a model vary in degree of availability for chemicals and animal species. An ideal theoretical mathematical model to describe particle deposition would require detailed information on all of the influential parameters (e.g., respiratory rates, exact airflow patterns, complete measurement of the branching structure of the respiratory tract, alveolar region mechanics) across different humans or across various laboratory species of interest. An empirical model (i.e., a system of equations fit to experimental data) is an alternative approach. A third approach, the hybrid approach adopted in ICRP66, is to fit a system of empirical equations to the results of theoretical modeling. Depending on the relative importance of these various mechanistic determinants, models with less detail may be used to adequately describe differences in respiratory dosimetry for the purposes of extrapolation.

An understanding of the bases for model structures also allows development of a framework for the evaluation of whether one available model structure may be considered optimal relative to another. A model structure might be considered more appropriate than another for extrapolation when default assumptions or parameters are replaced by more detailed, biologically-motivated descriptions or actual data, respectively. For example, a model could be preferred if it incorporates more chemical or species-specific information or if it accounts for more mechanistic determinants. Empirical models may differ in the quality or appropriateness of the data used to fit the descriptive equations. These considerations are summarized in Table 10-17.

The sensitivity of the model to differences in structure may be gauged by their relative importance in describing the response function for a given chemical. For example, a model that incorporates many parameters may not be any better at describing ("fitting") limited response data than a simpler model.

### **10.7.1.2 Intraspecies Variability**

There are essentially three areas of concern in assessing the quality of epidemiologic or toxicity data. These involve the design and methodological approaches for (1) exposure

**TABLE 10-17. HIERARCHY OF MODEL STRUCTURES FOR  
DOSIMETRY AND EXTRAPOLATION**

---

---

**Optimal model structure**

**Structure describes all significant mechanistic determinants of particle disposition, toxicant-target interaction, and tissue response**

**Uses chemical-specific and species-specific parameters**

**Dose metric described at level of detail commensurate with the epidemiologic or toxicity data**

**Default model structure**

**Limited or default description of mechanistic determinants of particle disposition, toxicant-target interaction, and tissue response**

**Uses categorical or default values for chemical and species parameters**

**Dose metric at generic level of detail**

---

---

Source: Adapted from U.S. Environmental Protection Agency (1994); Jarabek (1995).

measures, (2) effect measures, and (3) the control of covariables and confounding variables. Although these topics are discussed in detail in other chapters, it is also important to consider these concerns when evaluating potential dosimetry models for extrapolation of epidemiologic or toxicity data. For example, although the epidemiologic investigations attempt to relate an exposure to a given health effect, the way the exposure is characterized may influence the choice of an appropriate dosimetry model. Characterization of a particular health effect in a human population may include pre-existing pathologic conditions (e.g., lung disease) that may alter inhalation dosimetry and have implications for model choice. The broad genetic variation of the human population in processes related to chemical disposition and tissue response (e.g., age, gender, disease status) may cause individual differences in sensitivity to inhaled aerosols. Sensitivity analyses could be used to determine ranges of dosimetry model outputs for specific ranges of input for various parameters (e.g., range in ventilation rate due to gender).

### **10.7.1.3 Extrapolation of Laboratory Animal Data to Humans**

Toxicological data in laboratory animals typically can aid the interpretation of human clinical and epidemiological data because they provide concentration- and duration-response information on a fuller array of effects and exposures than can be evaluated in humans.

However, historically, use of laboratory animal toxicological data has been limited because of difficulties in quantitative extrapolation to humans. The various species used in inhalation toxicology studies do not receive identical doses in comparable respiratory tract regions (ET, TB, A) when exposed to the same aerosol (same composition,  $\mu\text{g}/\text{m}^3$ , MMAD,  $\sigma_g$ ). Such interspecies differences are important because the adverse toxic effect is likely more related to the quantitative pattern of deposition within the respiratory tract than to the exposure; this pattern determines not only the initial respiratory tract tissue dose but also the specific pathways by which the inhaled particles are cleared and redistributed.

Both qualitative and quantitative extrapolation of laboratory animal data to humans are of interest. Qualitative extrapolation refers to the "class" of the effects. For example, if the function of rabbit alveolar macrophages is depressed by sulfuric acid, will it also be depressed in humans, albeit at an unknown exposure? This type of extrapolation is limited to known homologous effects. For example, given the similarities in human and laboratory animal alveolar macrophages, and likely toxicity mechanisms, the qualitative extrapolation is reasonable. However, in some cases, the homology is not understood adequately. For example, what is the laboratory animal model homology to the mortality effects observed in the epidemiological studies? Would PM exposures of aged animals or animal models of respiratory or cardiac disease states more closely mimic the mortality observed among the elderly or those with pre-existing cardiopulmonary disease? Several hypotheses exist, but at present there is inadequate evidence for consensus.

Once a qualitative extrapolation has been justified, a quantitative extrapolation can be initiated. In order for the laboratory animal data to be useful to the risk assessment of PM, interspecies extrapolation should account for differences in particle dosimetry and species sensitivity. Dosimetry, here, is used broadly to represent the effective dose to target site which may be some complex combination of regional delivered or retained particle burdens. Given the identical exposure, these particle burdens may be different in different species. Even if there is a comprehensive understanding of dose, there still needs to be an understanding of species differences in sensitivity to that dose. For example, perhaps one species has more efficient repair or chemical defense mechanisms than another, making that one species less sensitive to a given dose.

## 10.7.2 Dosimetry Model Selection

Available deposition models for humans and laboratory animals were presented in Section 10.5.1 and 10.5.2, respectively. Clearance models, required to calculate retained doses, were discussed in Section 10.6. This section focuses on modeling efforts intended to present informative and comparative data relevant to lung burdens that result in humans and laboratory animals as a consequence of acute and chronic inhalation exposures. The information and predictions are intended to illustrate examples of approaches to lung dosimetry, metrics of deposited and retained particle burdens, and species similarities and differences that influence exposure and dose metrics.

### 10.7.2.1 Human Model

The theoretically-based, semi-empirical lung deposition model of the International Commission on Radiological Protection (ICRP66, 1994) was chosen and used to model the dosimetry of inhaled particles in humans (Sections 10.7.4 and 10.7.5 below). A distinct advantage of this model is that it incorporates both deposition and clearance mechanisms so that both deposited and retained particles burdens can be calculated. LUDEP® software version 1.1 was used to run the ICRP66 1994 model simulations (National Radiological Protection Board, 1994).

Although the highly-detailed theoretical models described in Section 10.5 might allow prediction to more localized regions of the respiratory tract, information about the dimensions of the numerous gross and microscopic structures of the respiratory tract are extremely limited. Human experimental data are still available only for gross regional deposition, for the adult Caucasian male, and for a limited range of particle size ( $d_{ae}$  from about 1  $\mu\text{m}$  to 10  $\mu\text{m}$ ), making validation of the most detailed theoretical models impossible at the present time. For these reasons, the analysis of respiratory tract deposition by gross anatomical region adopted by the ICRP was viewed as advantageous. The parametric analysis of regional lung desposition, developed by Rudolf et al. (1986, 1990) and described in Section 10.5, was used to represent the results of complex theoretical modeling by relatively simple algebraic approximations. A theoretical model of gas transport and particle deposition (Egan et al., 1989) was applied to apportion particle deposition among the lower respiratory tract regions (BB, bb, AI — see Section 10.6), and to quantify the effects of lung

size and breathing rate. The structure of the respiratory tract is represented explicitly by a morphometric anatomical model as described in Table 10-3 and Figure 10-4. The 1994 ICRP model reasonably describes the experimental data relating total thoracic deposition to particle size and breathing behavior. The model also succeeds in simulating the variation of regional deposition with particle size and breathing pattern that was inferred by Stahlhofen et al. (1980,1983) from their measurements of thoracic deposition and retention. In common with earlier theoretical models of Yeh and Schum (1980) and Yu and Diu (1982b), the 1994 ICRP model predicts less thoracic deposition for particles in the range of  $d_{ae}$  from 1  $\mu\text{m}$  to 5  $\mu\text{m}$  than the median values reported by Lippmann (1977) and Chan and Lippmann (1980). These data are crucial since they represent the largest group of experimental subjects studied to date. However, as described in Appendix 10A, according to the analysis in ICRP66 (1994), there is direct experimental evidence (Gebhart et al., 1988) that particulate material used in the New York University (NYU) studies exhibits a degree of hygroscopic growth in the respiratory tract. When allowance is made in the deposition calculation for these supplementary data, the key set of experimental measurements from NYU is also found to support the 1994 ICRP66 deposition model. The problem of time-dependent functions to describe clearance from the various regions in the respiratory tract was overcome by using a combination of compartments with constant rates of clearance. Clearance from each region by three routes (absorption into blood, transport to GI tract, and transport to lymphatics) is accomplished by pathways with assigned rate constants.

Mathematical models such as the ICRP66 model do not provide site-specific dosimetry at the level of individual lung lobes, but the objective of this exercise is to provide useful insights about dose metrics such as average concentrations and average numbers of particles per unit area of respiratory regions. The ICRP model provides average concentration or average number values on a regional basis, i.e., mass or number deposited or retained in the ET, TB, or A regions. An important aspect of modeling and dosimetry is to relate the modeling effort to the level or accuracy of measurements. Neither the available deposition and clearance data nor the response data such as the mortality effects provide a level of detail that support more physiologically-based parameters and compartments.

The available deposition data were from radioactive tracer studies, in which accurate measurements were obtained at very low particulate mass burdens. As such, the particle

mass deposited in the respiratory tract was negligible, and did not introduce the possibility of experimental artifact due to particle overload phenomena. Biphasic or multiphasic clearance processes do not necessarily imply specific physiologic associations. The ICRP model makes use of convenient mathematical approaches to vary the rates of specific processes involved in clearance. The time dependence of clearance processes (both physical and dissolution-absorption) may well be determined by a decrease in the availability of the particles, e.g., because of (1) burial of the particles in the interstitial tissue, (2) sequestering in macrophages in areas that have low probability of physical clearance, or (3) altered dissolution-absorption rates related to physical or chemical changes in the particle with time.

Both the NCRP and ICRP had the benefit of contributions from respected investigators in respiratory tract toxicology and biomedical aerosol research. Similar mathematical assessments were arrived at by both commissions, although detailed calculations for specific radionuclides can be different. Comparisons between the models presented earlier and in Appendix 10A show that the behavior of the models are quite comparable, that is, the predicted deposition fraction for a given particle size is similar if the models use the same ventilation parameters as input. In fact, in order to ensure a uniform course of action that provides a coherent and consistent international approach, the NCRP recommends adoption of the ICRP 1994 model for modeling the effects of exposure for radiation workers and the public (e.g., for computing reference levels of annual intake and derived reference air concentrations corresponding to recommended dose limits).

Some of the human parameter values used in the ICRP66 model (ICRP66, 1994) and the LUDEP® software are provided in Appendix 10B. Surface area values were derived by the ICRP based on the morphometry provided previously in Table 10-3. LUDEP® allows simulations of either normal augmenter or mouth breather adult male humans. The proportion of nasal airflow for these two types of breathing at different levels of activity previously provided in Figure 10-27 and Table 10-11 in Section 10.5. The levels of activity to apportion nasal airflow are the same as those used to construct the three different activity patterns (general population; worker, light work; and worker, heavy work) shown in Table 10B-1.

### 10.7.2.2 Laboratory Animal Model

The particle dosimetry model of Ménache et al. (1996) described in Section 10.5.2 was chosen to calculate deposited dose estimates for rats as an illustration of dosimetric adjustment for laboratory animal species. Attributes of the model that were viewed as especially advantageous for this exercise included the detailed measurements made in all tissues that served as the source of deposition data (Raabe et al., 1988); that the deposition data were available for unanesthetized, freely breathing animals; and that inhalability was accounted for and used to adjust the logistic function to describe deposition efficiency. This model represents a revised version of previous models (Miller et al., 1988; Jarabek et al., 1989, 1990) that have been useful to develop inhalation reference concentration (RfC) estimates for dose-response assessment of air toxics (U.S. EPA, 1994). The same approach will be used to calculate deposited doses as discussed below in greater detail (Section 10.7.4). The range for application of the Ménache et al. (1996) model to interspecies extrapolation was restricted to 1 to 4  $\mu\text{m}$  MMAD because this is the range that had the most deposition data for model development and it is also the range most likely of use for evaluating the available inhalation toxicology investigations.

For calculation of retained doses, the simulation model based on Pritsker (1974) and described in Section 10.6 was used. This clearance model was applied to output of the Ménache et al. (1996) deposition model in order to calculate retained dose as discussed below in Section 10.7.5.

The broad spectrum of mammals used in inhalation toxicology research have body weights ranging upwards from a few grams to tens of kg; these mammals also exhibit a broad range of respiratory parameters. Table 10B-2 in Appendix 10B lists body weights, lung weights, respiratory minute ventilation and respiratory tract region surface areas for six laboratory animal species. Lung weights and ventilation parameters are important variables for inhalation toxicology because these parameters dictate the amounts of inhaled materials potentially deposited in the lung, as well as the specific alveolar burdens (mass of particles/g lung) that will result from inhalation exposures. The inverse relationship between body size and metabolic rate is demonstrated by the values for respiratory minute ventilation and body weight or lung tissue volume. For example, liters of air inhaled per minute per gram of lung is about 20 times higher for resting mice than for resting humans, which is an important

factor to consider relative to potential amounts of aerosol deposited in the respiratory tract per unit time during inhalation exposures.

### **10.7.3 Choice of Dose Metrics**

As discussed in the preceding sections, inhaled dose, especially to different regions or locations within the respiratory tract, is not necessarily related linearly to the exposure concentration. For this reason, an internal dose to characterize the dose-response relationship of PM is desired. In general, the objective is to provide a metric that is mechanistically-motivated by the observed response. Unfortunately, at this point in time, the crucial definition and determination of the relevant dose has not been accomplished for PM. Mechanistic determinants of the observed health effects have not been adequately elucidated. The health effects data discussed later (Chapter 11, 12, and 13) include effects that could be characterized as either "acute" (e.g., effects associated with mortality) or "chronic" (e.g., morbidity or laboratory animal pathology after two-year bioassays). Dose may be accurately described by particle deposition alone if the particles exert their primary action on the surface contacted (Dahl et al., 1991), i.e., deposited dose may be an appropriate metric for acute effects. For longer-term effects, the initially deposited dose may not be as decisive a metric since particles clear at varying rates from different lung compartments. To characterize these effects, a retained dose that accounts for differences between deposition and clearance is more appropriate.

Conventionally and conveniently, doses usually are expressed in terms of particle mass (gravimetric dose). However, when different types of particles are compared, doses may be more appropriately expressed as particle volume, particle surface area, or numbers of particles, depending on the effect in question (Oberdörster et al., 1994). For example, the retardation of alveolar macrophage-mediated clearance due to particle overload appears to be better correlated with phagocytized particle volume rather than mass (Morrow, 1988). As shown in Figures 10-2 and 10-3, the smaller size fractions of aerosols are associated with greater amounts of particles when characterized by surface area or by number rather than by mass. That is, concentrations in this size fraction are very small by mass but extremely high by number. The need to consider this is accentuated when the high rate of deposition of small particles in the lower respiratory tract (TB and A regions), the putative target for the

mortality and morbidity effects of PM exposures, is also taken into account. Anderson et al. (1990) have shown that the deposition of ultrafine particles in patients with COPD is greater than in healthy subjects.

Miller et al. (1995) recently investigated considerations for both intraspecies and interspecies dosimetry. Using a multipath dosimetric model, simulations for different particle sizes (0.1, 1, and 5  $\mu\text{m}$ ) were performed and different dose metrics calculated for the rat and both normal and compromised human lung status. A summary table of this exercise is provided as Table 10-18. These simulations support the conclusion that particle number per various anatomical normalizing factors indicate a need to examine the role of fine particles in eliciting acute morbidity and mortality, particularly in patients with compromised lung status (Miller et al., 1995).

For the present document, average deposited particle mass burden in each region of the respiratory tract has been selected as the dose metric for "acute" effects in both humans and laboratory animals. Average retained particle mass burden in each region for humans and in the lower respiratory tract for laboratory animals has been selected as the dose metric for "chronic" effects. These choices were dictated by the selection of the dosimetry models and the availability of anatomical and morphometric information.

Because mass may not be the appropriate metric, especially to characterize effects of the fine fraction, average particle number burdens and the number of particles deposited per day were calculated in addition for humans. An attempt to address the variability due to differences in the population was made by calculating deposited particle mass burdens in each region for eight different demographic groups that included a range of ages and one selected for cardiopulmonary symptoms.

### **10.7.3.1 Interspecies Extrapolation**

In order to gain insight on species similarities and differences that may account for the apparent discrepancies between epidemiologic and laboratory animal data, interspecies adjustments to the observed exposure levels must be made for the dose metrics selected for "acute" and "chronic" effects. This section discusses an approach to calculate human equivalent concentration (HEC) estimates based on the observed laboratory animal toxicological data.

**TABLE 10-18. SPECIES COMPARISONS BY MILLER ET AL. (1995) OF VARIOUS DOSE METRICS AS A FUNCTION OF PARTICLE SIZE FOR 24-HOUR EXPOSURES TO 150  $\mu\text{g}/\text{m}^3$**

Particle Size	Dose Metric	Rat	Human Lung Status		Ratio: Human/Rat	
			<sup>a</sup> Normal	Compromised	Normal	Compromised
0.1 $\mu\text{m}$	Mass/unit area	$3.74\text{-}3.76 \times 10$	$5.0 \times 10^{-4}$	NC <sup>d</sup>	0.13	NC
	No. deposited	$1.2 \times 10^{10}$	$5.9 \times 10^{11}$	$4.3 \times 10^{11}$	49	37
	No./unit surface area	$7.1 \times 10^6$	$9.5 \times 10^5$	$2.8 \times 10^6$	0.1	0.4
	No./ventilatory unit	$4.9 \times 10^6$	$1.8 \times 10^7$	$5.3 \times 10^7$	4	11
	No./alveolus <sup>c</sup>	303-598	1,190-1,930	3,570-5,790	2-5	6-15
	No./macrophage <sup>c</sup>	262-399	100-61	298-482	0.3-0.6	0.8-1.8
1 $\mu\text{m}$	Mass/unit area	$1.1\text{-}1.2 \times 10$	$2.8 \times 10^{-4}$	NC <sup>d</sup>	<sup>-3</sup> 0.23-0.25	NC
	No. deposited	$3.5 \times 10$	$3.5 \times 10^6$	$2.4 \times 10^8$	92	69
	No./unit surface area	2,130	532	1,590	0.3	0.8
	No./ventilatory unit	1,470	9,910	29,700	7	20
	No./alveolus <sup>c</sup>	0.12-0.18	0.7-1.1	2.0-3.3	4-9	11-28
	No./macrophage <sup>c</sup>	0.08-0.12	0.06-0.09	0.2-0.3	0.5-1.2	1.4 -3.5
5 $\mu\text{m}$	Mass/unit area	$2.8\text{-}4.4 \times 10$	$9.1 \times 10^4$	NC <sup>d</sup>	<sup>-4</sup> 2.09-3.23	NC
	No. deposited	$7.1 \times 10$	$8.5 \times 10^6$	$6.4 \times 10^6$	1,195	897
	No./unit surface area	4	14	42	3.2	9.7
	No./ventilatory unit	3	260	780	88	263
	No./alveolus <sup>c</sup>	0.0002	0.02-0.03	0.05-0.09	49-120	145-359

10-157

d

d

d

A HEC would be calculated by

$$\text{HEC } (\mu\text{g}/\text{m}^3) = \text{NOAEL}_{[\text{ADJ}]} (\mu\text{g}/\text{m}^3) \times \text{DAF}_r, \quad (10-48)$$

where the  $\text{NOAEL}_{[\text{ADJ}]}$  is the no-observed-adverse-effect level (or other effect level) of the laboratory animal study (this level, if from an intermittent exposure regimen, is often adjusted for the number of hours per day and days per week ( $\#/24 \times \#/7$ ) in order to model a continuous exposure) and  $\text{DAF}_r$  is a dosimetric adjustment factor for a specific respiratory tract region,  $r$  (ET, TB, A). The  $\text{DAF}_r$  is either the regional deposited dose ratio ( $\text{RDDR}_r$ ) for "acute" effects of deposited particles or the regional gas dose ratio ( $\text{RGDR}_r$ ) for "chronic" effects of retained particles. The  $\text{DAF}_r$  is a multiplicative factor that represents the laboratory animal to human ratio of a specific inhaled particle burden. The HEC is expected to be associated with the same delivered particle burden to the observed target tissue as in the laboratory animal species. A  $\text{DAF}_r$  above the value of 1.0 indicates that the human receives a relatively smaller deposited or retained particle burden than the particular laboratory animal species. Values of the  $\text{DAF}_r$  below 1.0 indicate that the human receives a relatively larger deposited or retained particle burden than the laboratory animal species, and application of the  $\text{DAF}_r$  would adjust the resultant HEC lower than the laboratory animal exposure level.

For deposited particle burdens, regional deposited dose ( $\text{RDD}_r$ ) can be calculated as

$$\text{RDD}_r = 10^{-3} \times C_i \times \dot{V}_E \times F_r, \quad (10-49)$$

where:

- $\text{RDD}_r$  = dose deposited in region  $r$  ( $\mu\text{g}/\text{min}$ ),
- $C_i$  = concentration ( $\mu\text{g}/\text{m}^3$ ),
- $\dot{V}_E$  = minute ventilation (L/min), and
- $F_r$  = fractional deposition in region  $r$ .

If the RDD in laboratory animals is expressed relative to humans, the resultant regional deposited dose ratio ( $\text{RDDR}_r$ ) can be used as the  $\text{DAF}_r$  in Equation 10-48 to adjust an inhalation particulate exposure in a laboratory species to a predicted HEC that would be

expected to be associated with the same particle burden delivered to the r<sup>th</sup> region of the respiratory tract. The RDDR<sub>r</sub> can be calculated as a series of ratios

$$\text{RDDR}_r = \frac{(10^{-3} \times C_i)_A}{(10^{-3} \times C_i)_H} \times \frac{(\text{Normalizing Factor})_H}{(\text{Normalizing Factor})_A} \times \frac{(\dot{V}_E)_A}{(\dot{V}_E)_H} \times \frac{(F_r)_A}{(F_r)_H} \quad (10-50)$$

where the normalizing factor can be selected based on consideration of the mechanism of action. Because poorly soluble particles deposit along the surface of the respiratory tract, the surface area of an affected respiratory tract region (e.g., TB or A region) could be used as the normalizing factor. For the purposes of calculating the RDDR<sub>r</sub>, the exposure concentration for the laboratory animal (A) and human (H) are assumed to be the same because it is assumed that the observed effect in the laboratory animal is relevant to human health risk. The RDDR<sub>r</sub> is used as a factor to adjust for interspecies differences in delivered dose under the same exposure scenario. The first term in Equation 10-50, therefore, equals one and will not be discussed further. The last term, the ratio of deposition fractions in a given respiratory region, (F<sub>r</sub>), is calculated using the respective human and laboratory animal dosimetry models.

Because the ICRP66 model utilizes an activity pattern, Equation 10-50 must be modified to account for the fraction of time spent at each different ventilation rate, corresponding to each different activity levels, as

$$\text{RDDR}_{t_{[\text{ACT}]}} = \frac{a}{t_{[1]} \times \dot{V}_{E_{H[1]}} \times F_{r_{H[1]}} + t_{[2]} \times \dot{V}_{E_{H[2]}} \times F_{r_{H[2]}} + \dots + t_{[n]} \times \dot{V}_{E_{H[n]}}} \quad (10-51)$$

where t<sub>[i]</sub> is the fractional time spent breathing minute volume [i],

$$t_{[1]} + t_{[2]} + \dots + t_{[n]} = 1, \quad \text{and} \quad (10-52)$$

$$a = \frac{(\text{Normalizing Factor})_H}{(\text{Normalizing Factor})_A} \times \dot{V}_{E_A} \times F_{r_A}, \quad (10-53)$$

where  $\dot{V}_{E_A}$  is a daily average ventilation rate (L/min  $\times$  1440 min/day). It should be noted that the human denominator is the fractional deposition value output from the ICRP model simulations using the LUDEP® software using an activity pattern.

Although clearance is dependent on the site of initial deposition, calculation of retained dose is probably more appropriate for assessing chronic health effects. Different normalizing factors such as retained mass per region, retained mass per surface area, or retained mass per other available morphometric information may be worthwhile to explore. The regional retained dose ratio (RRDR<sub>r</sub>) for interspecies dosimetric adjustment is calculated as a series of five ratios

$$\text{RRDR}_r = \frac{(10^{-3} \times \text{Ci})_A}{(10^{-3} \times \text{Ci})_H} \times \frac{(\text{Normalizing Factor})_H}{(\text{Normalizing Factor})_A} \times \frac{(\dot{V}_E)_A}{(\dot{V}_E)_H} \times \frac{(F_r)_A}{(F_r)_H} \times \frac{(AI_t)_A}{(AI_t)_H} \quad (10-54)$$

where:

RRDR<sub>r</sub> = relative  $\mu\text{g}$  of particles retained in region (r),

Ci = exposure atmosphere concentration ( $\mu\text{g}/\text{m}^3$ ),

Normalizing Factor = lung weight (g),

$\dot{V}_E$  = minute ventilation (L/min),

$F_r$  = fractional aerosol deposition in region r, and

(AI<sub>t</sub>) = relative accumulated alveolar interstitial burden of particles as a function of time from the start of a chronic exposure.

Again, since the ICRP66 model allows simulation of an activity pattern, Equation 10-54 must be adjusted to account for the fraction of time spent at each different ventilation rate corresponding to different activity levels so that

$$\text{RRDR}_{r[\text{ACT}]} = \frac{a}{t_{[1]} \times \dot{V}_{E_{H[1]}} \times F_{r_{H[1]}} \times (AI_t)_{H[1]} \times t_{[2]} \times \dot{V}_{E_{H[2]}} \times F_{r_{H[2]}} \times (AI_t)_{H[2]} + \dots + t_{[n]} \times \dot{V}_{E_{H[n]}} \times (AI_t)_{H[n]}} \quad (10-55)$$

where  $t_{[i]}$  is the fractional time spent breathing at minute ventilation  $[i]$ ,

$$t_{[1]} + t_{[2]} + \dots + t_{[n]} = 1, \text{ and} \quad (10-56)$$

$$a = \frac{(\text{NormalizingFactor}_r)_H}{(\text{NormalizingFactor}_r)_A} \times (\dot{V}D_E)_A \times (Fr)_A \times (AI_v)_A, \quad (10-57)$$

and  $(\dot{V}D_{E_A})$  is a daily average ventilation rate (L/min  $\times$  1440 min/day).

The relative accumulated alveolar interstitial burden of particles as a function of time from the start of a chronic exposure must be calculated for specific exposure scenarios to account for species differences in clearance, as well as the dissolution-absorption characteristics of the inhaled particles. This ratio is not a constant and must be calculated for the chronic exposure time of interest. Physical clearance functions and dissolution-absorption rates for particles deposited in the A region are used to integrate daily deposition and clearance over the chronic exposure time period of interest. The equations for laboratory animals are derived using the information in Table 10-16. Physical clearance parameters for humans are in the ICRP model (ICRP66, 1994) and the calculation of A burden for humans can be made using LUDEP®.

Calculating these ratios (either deposited or retained) depends on particle diameter (MMAD) and distribution ( $\sigma_g$ ) but not on aerosol concentration, i.e., it assumes no altered deposition or clearance due to exposure concentration or chemical-specific toxicity.

The calculation of the  $DAF_r$  currently uses point estimates for all the terms used to construct the ratios, that is, a default  $\dot{V}_E$  for each species, a default regional surface area or lung weight for the normalizing factor, and an estimate of fractional deposition or retained particle burden. These single values are assumed to be representative of the average value of that term for a member of the laboratory animal species or human population. As discussed in the previous sections of this chapter, there are many sources of intraspecies variability that contribute to the range of responses observed to a given external exposure to an inhaled toxicant. Host factors may affect both the delivered dose of the toxicant to the target tissue as well as the sensitivity of that tissue to interaction with the toxicant. The procedures described in this interspecies extrapolation section could provide some limited capability to

examine the effects of population variability on the  $DAF_r$  by changing the default  $\dot{V}_E$  and surface areas or lung weights in an iterative fashion. However, because of correlations between  $\dot{V}_E$ , surface area, and lung weight, such changes should be made with caution. Confidence intervals were provided on the parameters for the deposition efficiency equations. Iterative computational procedures could be used to generate envelopes of regional fractional deposition that could be used with distributions of  $\dot{V}_E$ , surface areas, and lung weights to provide ranges of  $DAF_r$  estimates. Actual implementation of this procedure is not straightforward due to the complex nature of the correlation structures. Future versions of the deposition and clearance models used to calculate the laboratory animal species values could estimate distributions that reflect the range of available data for key parameters.

## 10.7.4 Choice of Exposure Metrics

### 10.7.4.1 Human Exposure Data

Ambient exposure data provided elsewhere in Chapter 3 of this document were selected to represent typical human exposures. Three different aerosols were selected as presented in Appendix 10C. As discussed in Chapter 3, it is not known at this time whether the intermodal mode for the trimodal aerosols is real or whether it is an artifact of sampling procedures.

The first is the trimodal aerosol shown in Figure 10C-1. Table 10C-1 shows the upper size cut (in  $\mu\text{m}$ ) for various particle size intervals based on the distribution of particle count, surface area, mass, or aerodynamic diameter ( $d_{ae}$ ). Recall from Section 10.2 that the 50% size cut for each of these diameters would be the respective median diameter of the distribution, i.e., the 50% size-cut diameter of the  $d_{ae}$  is the MMAD. Table 10C-2a,b,c shows the particle number, surface, area, and mass distribution, respectively, for the aerosol from Figure 10C-1. The distribution of particle mass in Table 10C-2c was used as input to the human dosimetry (ICRP66, 1994) model to estimate total particle mass deposition.

The two trimodal aerosols depicted in Figure 10C-2, panel (a) and (b) for Philadelphia and Phoenix respectively, were also chosen and treated similarly. Table 10C-3 shows the upper size cut (in  $\mu\text{m}$ ) for various particle size intervals from the Philadelphia aerosol (Panel a), based on the distribution of particle count, surface area, mass, or aerodynamic diameter ( $d_{ae}$ ). Table 10C-4a,b,c shows the particle number, surface area, and mass

distribution, respectively, from Figure 10C-2(a). The distribution of particle mass in Table 10C-4c was used as input to the human dosimetry model (ICRP, 1994) to estimate total particle mass deposition. Tables 10C-5 and 10-C6a,b,c are analogous to Tables 10-C3 and 10C-4a,b,c but show the data for Phoenix (Figure 10C-2b).

#### **10.7.4.2 Laboratory Animal Data**

As noted previously, the range of application for the Ménache et al. (1996) model was limited to that typically used in laboratory animal studies that are the basis of the toxicity data in Chapter 11. For calculation of deposited doses, fractional deposition was estimated for a range of particle diameters ( $d_{ae}$ ) and two distributions ( $\sigma_g$ ), one representing a relatively monodisperse ( $\sigma_g = 1.3$ ) and the other a polydisperse ( $\sigma_g = 2.4$ ) aerosol. Deposited doses for two different particle diameters and distributions were then used in clearance models to calculate retained doses (see Section 10.7.5).

### **10.7.5 Deposited Dose Estimations**

The respective models discussed in Section 10.7.1 were used to estimate deposition in each of the respiratory tract regions. Note that the ICRP66 human model divides the ET region into compartments,  $ET_1$  and  $ET_2$ . The ICRP66 model also divides the TB region into two compartments, the bronchi (BB) and bronchiole (bb). The alveolar interstitial (AI) compartment is equivalent to the A region. When compared to the laboratory animal data, deposition fractions for  $ET_1$  and  $ET_2$  were summed to calculate ET deposition. Likewise, the BB and bb deposition fractions were summed to calculate the TB fraction.

#### **10.7.5.1 Human Estimates**

Tables 10-19 through 10-24 present the regional deposition fractions (% deposition) and regional deposited particle mass ( $\mu\text{g}$ ) for each of the three ambient human exposure aerosols depicted in Figures 10C-1, 10C-2a (Philadelphia), and 10C-2b (Phoenix). Data are shown for normal augmenters (Tables 10-19, 10-21, and 10-23) versus mouth breathers (Tables 10-20, 10-22, and 10-24) for three different activity patterns.

**TABLE 10-19. DAILY MASS DEPOSITION OF PARTICLES FROM AEROSOL DEFINED IN FIGURE 10C-1 IN THE RESPIRATORY TRACT OF  
“NORMAL AUGMENTER” ADULT MALE HUMANS EXPOSED TO  
A PARTICLE MASS CONCENTRATION OF 50 µg/m<sup>3</sup>**

Activity Pattern	Region of Respiratory Tract	Contribution to Total Deposited Particle Mass from Each Aerosol Mode <sup>a</sup>					
		Nuclei Mode		Accumulation Mode		Coarse Mode	
		Percent Deposited <sup>b</sup>	Mass of Particles (µg)	Percent Deposition	Mass of Particles (µg)	Percent Deposition	Mass of Particles (µg)
General population <sup>c</sup>	ET <sub>1</sub>	1.0	10	0.7	7	16.3	162
	ET <sub>2</sub>	1.1	11	0.7	7	19.0	189
	BB	0.4	4	0.2	2	0.9	9
	bb	2.4	24	1.1	11	0.7	7
	AI	7.0	69	4.2	42	2.5	25
	<b>Total</b>	<b>11.7</b>	<b>117</b>	<b>6.8</b>	<b>68</b>	<b>39.4</b>	<b>392</b>
Workers, light work <sup>d</sup>	ET <sub>1</sub>	0.9	10	0.7	8	15.4	176
	ET <sub>2</sub>	1.1	12	0.7	8	19.2	220
	BB	0.3	4	0.2	2	1.5	18
	bb	2.2	26	1.0	11	0.8	9
	AI	7.2	82	4.1	47	2.4	28
	<b>Total</b>	<b>11.7</b>	<b>134</b>	<b>6.6</b>	<b>76</b>	<b>39.4</b>	<b>451</b>
Workers, heavy work <sup>e</sup>	ET <sub>1</sub>	0.8	11	0.7	9	8.8	117
	ET <sub>2</sub>	1.0	14	0.7	9	20.0	267
	BB	0.3	4	0.2	2	6.0	80
	bb	2.1	29	0.9	12	1.2	16
	AI	7.4	98	4.0	54	2.7	36
	<b>Total</b>	<b>11.7</b>	<b>156</b>	<b>6.5</b>	<b>87</b>	<b>38.6</b>	<b>517</b>

<sup>a</sup>Nuclei mode MMAD = 0.0169 µm,  $\sigma_g = 1.6$ , density = 1.4 g/cm<sup>3</sup>, 15.6% of the aerosol mass; accumulation mode MMAD = 0.180 µm,  $\sigma_g = 1.8$ , density = 1.2 g/cm<sup>3</sup>, 38.7% of the aerosol mass; coarse mode MMAD = 5.95 µm,  $\sigma_g = 1.87$ , density = 2.2 g/cm<sup>3</sup>, 45.7% of the aerosol mass (see Tables 10C-1 and 10C-2c).

<sup>b</sup>Expressed as a percentage of the total mass of particles in the volume of ambient air inhaled.

<sup>c</sup>Average for 24 h, as derived from ICRP-66 (1994): for 33.3% sleep, 33.3% sitting, and 33.3% light exercise (see Table 10B-1).

<sup>d</sup>Average for 24 h, as derived from ICRP-66 (1994): for 33.3% sleep, 27.1% sitting, and 35.4% light exercise, 4.2% heavy exercise (see Table 10B-1).

<sup>e</sup>Average for 24 h, as derived from ICRP-66 (1994): for 33.3% sleep, 16.7% sitting, and 41.7% light exercise, 8.3% heavy exercise. (see Table 10B-1).

**TABLE 10-20. DAILY MASS DEPOSITION OF PARTICLES FROM AEROSOL DEFINED IN FIGURE 10C-1 IN THE RESPIRATORY TRACT OF “MOUTH BREATHER” ADULT MALE HUMANS EXPOSED TO A PARTICLE MASS CONCENTRATION OF 50 µg/m<sup>3</sup>**

Activity Pattern	Region of Respiratory Tract	Contribution to Total Deposited Particle Mass from Each Aerosol Mode <sup>a</sup>					
		Nuclei Mode		Accumulation Mode		Coarse Mode	
		Percent Deposited <sup>b</sup>	Mass of Particles (µg)	Percent Deposition	Mass of Particles (µg)	Percent Deposition	Mass of Particles (µg)
General population <sup>c</sup>	ET <sub>1</sub>	0.5	5	0.3	3	7.3	72
	ET <sub>2</sub>	1.1	11	0.5	5	16.2	162
	BB	0.4	4	0.2	2	4.2	42
	bb	2.4	24	1.1	11	2.1	21
	AI	7.2	71	4.2	42	6.2	62
	Total	11.6	116	6.3	63	36.0	358
Workers, light work <sup>d</sup>	ET <sub>1</sub>	0.5	6	0.3	3	6.8	78
	ET <sub>2</sub>	1.1	12	0.5	6	16.8	192
	BB	0.4	4	0.2	2	4.8	55
	bb	2.3	26	1.0	11	2.1	24
	AI	7.4	84	4.1	47	5.8	66
	Total	11.6	133	6.1	70	36.3	415
Workers, heavy work <sup>e</sup>	ET <sub>1</sub>	0.5	6	0.3	4	6.4	86
	ET <sub>2</sub>	1.0	14	0.5	7	17.2	230
	BB	0.3	4	0.2	2	5.4	72
	bb	2.2	29	0.9	12	2.0	27
	AI	7.5	101	4.1	54	5.4	73
	Total	11.6	155	5.9	79	36.5	488

<sup>a</sup>Nuclei mode MMAD = 0.0169 µm,  $\sigma_g = 1.6$ , density = 1.4 g/cm<sup>3</sup>, 15.6% of the aerosol mass; accumulation mode MMAD = 0.180 µm,  $\sigma_g = 1.8$ , density = 1.2 g/cm<sup>3</sup>, 38.7% of the aerosol mass; coarse mode MMAD = 5.95 µm,  $\sigma_g = 1.87$ , density = 2.2 g/cm<sup>3</sup>, 45.7% of the aerosol mass (see Tables 10C-1 and 10C-2c).

<sup>b</sup>Expressed as a percentage of the total mass of particles in the volume of ambient air inhaled.

<sup>c</sup>Average for 24 h, as derived from ICRP-66 (1994): for 33.3% sleep, 33.3% sitting, and 33.3% light exercise. (See Table 10B-1).

<sup>d</sup>Average for 24 h, as derived from ICRP-66 (1994): for 33.3% sleep, 27.1% sitting, and 35.4% light exercise, 4.2% heavy exercise. (See Table 10B-1).

<sup>e</sup>Average for 24 h, as derived from ICRP-66 (1994): for 33.3% sleep, 16.7% sitting, and 41.7% light exercise, 8.3% heavy exercise. (See Table 10B-1).

**TABLE 10-21. DAILY MASS DEPOSITION OF PARTICLES FROM PHILADELPHIA AEROSOL DEFINED IN FIGURE 10C-2(a) IN THE RESPIRATORY TRACT OF “NORMAL AUGMENTER” ADULT MALE HUMANS EXPOSED TO A PARTICLE MASS CONCENTRATION OF 50 µg/m<sup>3</sup>**

Activity Pattern	Region of Respiratory Tract	Contribution to Total Deposited Particle Mass from Each Aerosol Mode <sup>a</sup>					
		Accumulation Mode		Intermodal Mode		Coarse Mode	
		Percent Deposited <sup>b</sup>	Mass of Particles (µg)	Percent Deposition	Mass of Particles (µg)	Percent Deposition	Mass of Particles (µg)
General population <sup>c</sup>	ET <sub>1</sub>	2.0	19	1.9	19	13.0	130
	ET <sub>2</sub>	1.9	19	2.6	26	13.4	134
	BB	0.2	2	0.2	2	0.2	2
	bb	0.7	7	0.2	2	0.1	1
	AI	3.7	37	1.1	11	0.1	1
	Total	8.5	84	6.0	60	26.8	267
Workers, light work <sup>d</sup>	ET <sub>1</sub>	1.9	22	1.8	21	12.2	139
	ET <sub>2</sub>	1.9	22	2.6	30	14.2	162
	BB	0.2	2	0.2	3	0.3	3
	bb	0.6	7	0.2	2	0.1	1
	AI	3.6	42	1.1	13	0.1	1
	Total	8.3	95	5.9	68	26.8	307
Workers, heavy work <sup>e</sup>	ET <sub>1</sub>	1.9	26	1.8	24	11.6	156
	ET <sub>2</sub>	2.0	26	2.6	35	14.7	197
	BB	0.2	3	0.3	4	0.3	5
	bb	0.6	8	0.2	2	0.1	1
	AI	3.6	48	1.1	14	0.1	1
	Total	8.3	111	6.0	80	26.8	359

<sup>a</sup>Accumulation mode MMAD = 0.436 µm,  $\sigma_g = 1.51$ , density = 1.3 g/cm<sup>3</sup>, 48.2% of the aerosol mass; intermodal mode MMAD = 2.20 µm,  $\sigma_g = 1.16$ , density = 1.3 g/cm<sup>3</sup>, 7.4% of the aerosol mass; coarse mode MMAD = 28.8 µm,  $\sigma_g = 2.16$ , density = 1.3 g/cm<sup>3</sup>, 44.4% of the aerosol mass (see Tables 10C-3 and 10C-4c).

<sup>b</sup>Expressed as a percentage of the total mass of particles in the volume of ambient air inhaled.

<sup>c</sup>Average for 24 h, as derived from ICRP-66 (1994): for 33.3% sleep, 33.3% sitting, and 33.3% light exercise. (See Table 10B-1).

<sup>d</sup>Average for 24 h, as derived from ICRP-66 (1994): for 33.3% sleep, 27.1% sitting, and 35.4% light exercise, 4.2% heavy exercise. (See Table 10B-1).

<sup>e</sup>Average for 24 h, as derived from ICRP-66 (1994): for 33.3% sleep, 16.7% sitting, and 41.7% light exercise, 8.3% heavy exercise. (See Table 10B-1)

**TABLE 10-22. DAILY MASS DEPOSITION OF PARTICLES FROM PHILADELPHIA AEROSOL DEFINED IN FIGURE 10C-2(a) IN THE RESPIRATORY TRACT OF “MOUTH BREATHER” ADULT MALE HUMAN EXPOSED TO A PARTICLE MASS CONCENTRATION OF 50 µg/m<sup>3</sup>**

Activity Pattern	Region of Respiratory Tract	Contribution to Total Deposited Particle Mass from Each Aerosol Mode <sup>a</sup>					
		Accumulation Mode		Intermodal Mode		Coarse Mode	
		Percent Deposited <sup>b</sup>	Mass of Particles (µg)	Percent Deposition	Mass of Particles (µg)	Percent Deposition	Mass of Particles (µg)
General population <sup>c</sup>	ET <sub>1</sub>	0.5	5	0.7	7	6.6	66
	ET <sub>2</sub>	0.6	6	1.0	10	18.3	182
	BB	0.2	2	0.3	3	1.1	11
	bb	0.7	7	0.3	3	0.2	2
	AI	3.9	39	1.9	19	0.4	4
	Total	5.9	59	4.2	42	26.6	265
Workers, light work <sup>d</sup>	ET <sub>1</sub>	0.5	6	0.6	7	6.1	70
	ET <sub>2</sub>	0.6	7	1.1	12	18.8	215
	BB	0.2	2	0.4	5	1.1	13
	bb	0.7	8	0.3	3	0.2	3
	AI	3.8	43	1.8	21	0.3	4
	Total	5.8	66	4.2	48	26.7	305
Workers, heavy work <sup>e</sup>	ET <sub>1</sub>	0.5	7	0.6	8	5.7	76
	ET <sub>2</sub>	0.6	8	1.1	15	19.3	259
	BB	0.2	3	0.5	6	1.2	16
	bb	0.6	8	0.3	4	0.2	3
	AI	3.7	50	1.8	24	0.3	4
	Total	5.7	76	4.3	57	26.7	357

<sup>a</sup>Accumulation mode MMAD = 0.436 µm,  $\sigma_g = 1.51$ , density = 1.3 g/cm<sup>3</sup>, 48.2% of the aerosol mass; intermodal mode MMAD = 2.20 µm,  $\sigma_g = 1.16$ , density = 1.3 g/cm<sup>3</sup>, 7.4% of the aerosol mass; coarse mode MMAD = 28.8 µm,  $\sigma_g = 2.16$ , density = 1.3 g/cm<sup>3</sup>, 44.4% of the aerosol mass (see Tables 10C-3 and 10C-4c).

<sup>b</sup>Expressed as a percentage of the total mass of particles in the volume of ambient air inhaled.

<sup>c</sup>Average for 24 h, as derived from ICRP-66 (1994): for 33.3% sleep, 33.3% sitting, and 33.3% light exercise. (See Table 10B-1).

<sup>d</sup>Average for 24 h, as derived from ICRP-66 (1994): for 33.3% sleep, 27.1% sitting, and 35.4% light exercise, 4.2% heavy exercise. (See Table 10B-1).

<sup>e</sup>Average for 24 h, as derived from ICRP-66 (1994): for 33.3% sleep, 16.7% sitting, and 41.7% light exercise, 8.3% heavy exercise. (See Table

**TABLE 10-23. DAILY MASS DEPOSITION OF PARTICLES FROM PHOENIX AEROSOL DEFINED IN FIGURE 10C-2(b) IN THE RESPIRATORY TRACT OF “NORMAL AUGMENTER” ADULT MALE HUMAN EXPOSED TO A PARTICLE MASS CONCENTRATION OF 50 µg/m<sup>3</sup>**

Activity Pattern	Region of Respiratory Tract	Contribution to Total Deposited Particle Mass from Each Aerosol Mode <sup>a</sup>					
		Accumulation Mode		Intermodal Mode		Coarse Mode	
		Percent Deposited <sup>b</sup>	Mass of Particles (µg)	Percent Deposition	Mass of Particles (µg)	Percent Deposition	Mass of Particles (µg)
General population <sup>c</sup>	ET <sub>1</sub>	0.4	4	2.9	29	20.3	202
	ET <sub>2</sub>	0.4	4	3.8	38	21.9	218
	BB	0.1	1	0.2	2	0.6	6
	bb	0.7	7	0.3	3	0.4	4
	AI	2.7	26	1.7	17	1.2	12
	Total	4.2	42	8.9	89	44.4	441
Workers, light work <sup>d</sup>	ET <sub>1</sub>	0.4	4	2.8	32	19.1	218
	ET <sub>2</sub>	0.4	4	3.8	43	22.8	260
	BB	0.1	1	0.3	4	1.0	11
	bb	0.6	7	0.3	3	0.4	4
	AI	2.6	30	1.7	19	1.2	13
	Total	4.1	47	8.9	101	44.3	507
Workers, heavy work <sup>e</sup>	ET <sub>1</sub>	0.4	5	2.8	37	18.3	244
	ET <sub>2</sub>	0.4	5	3.8	51	23.4	313
	BB	0.1	1	0.4	6	1.3	17
	bb	0.6	8	0.3	4	0.4	5
	AI	2.6	34	1.6	22	1.1	14
	Total	4.0	53	8.9	119	44.4	594

<sup>a</sup>Accumulation mode MMAD = 0.188 µm,  $\sigma_g = 1.54$ , density = 1.7 g/cm<sup>3</sup>, 22.4% of the aerosol mass; intermodal mode MMAD = 1.70 µm,  $\sigma_g = 1.9$ , density = 1.7 g/cm<sup>3</sup>, 13.8% of the aerosol mass; coarse mode MMAD = 16.4 µm,  $\sigma_g = 2.79$ , density = 1.7 g/cm<sup>3</sup>, 63.9% of the aerosol mass (see Tables 10C-5 and 10C-6c).

<sup>b</sup>Expressed as a percentage of the total mass of particles in the ambient air inhaled.

<sup>c</sup>Average for 24 h, as derived from ICRP-66 (1994): for 33.3% sleep, 33.3% sitting, and 33.3% light exercise. (See Table 10B-1).

<sup>d</sup>Average for 24 h, as derived from ICRP-66 (1994): for 33.3% sleep, 27.1% sitting, and 35.4% light exercise, 4.2% heavy exercise. (See Table 10B-1).

<sup>e</sup>Average for 24 h, as derived from ICRP-66 (1994): for 33.3% sleep, 16.7% sitting, and 41.7% light exercise, 8.3% heavy exercise. (See Table 10B-1).

**TABLE 10-24. DAILY MASS DEPOSITION OF PARTICLES FROM PHOENIX AEROSOL DEFINED IN FIGURE 10C-2(b) IN THE RESPIRATORY TRACT OF “MOUTH BREATHER” ADULT MALE HUMANS EXPOSED TO A PARTICLE MASS CONCENTRATION OF 50 µg/m<sup>3</sup>**

Activity Pattern	Region of Respiratory Tract	Contribution to Total Deposited Particle Mass from Each Aerosol Mode <sup>a</sup>					
		Accumulation Mode		Intermodal Mode		Coarse Mode	
		Percent Deposited <sup>b</sup>	Mass of Particles (µg)	Percent Deposition	Mass of Particles (µg)	Percent Deposition	Mass of Particles (µg)
General population <sup>c</sup>	ET <sub>1</sub>	0.2	2	1.0	10	9.8	98
	ET <sub>2</sub>	0.3	3	1.7	17	25.5	254
	BB	0.1	1	0.5	5	3.1	31
	bb	0.7	7	0.5	5	1.2	12
	AI	2.7	27	2.7	27	3.0	30
	Total	4.0	40	6.4	63	42.7	425
Workers, light work <sup>d</sup>	ET <sub>1</sub>	0.2	2	1.0	11	9.2	105
	ET <sub>2</sub>	0.3	4	1.7	20	26.3	301
	BB	0.1	1	0.6	7	3.4	39
	bb	0.6	7	0.5	5	1.1	13
	AI	2.6	30	2.6	30	2.8	31
	Total	3.9	44	6.4	73	42.8	490
Workers, heavy work <sup>e</sup>	ET <sub>1</sub>	0.2	2	1.0	13	8.5	114
	ET <sub>2</sub>	0.3	4	1.8	24	27.0	362
	BB	0.1	1	0.8	10	3.7	50
	bb	0.6	8	0.4	6	1.1	14
	AI	2.6	35	2.5	34	2.6	34
	Total	3.8	50	6.5	86	42.9	574

<sup>a</sup>Accumulation mode MMAD = 0.188 µm,  $\sigma_g = 1.54$ , density = 1.7 g/cm<sup>3</sup>, 22.4% of the aerosol mass; intermodal mode MMAD = 1.70 µm,  $\sigma_g = 1.9$ , density = 1.7 g/cm<sup>3</sup>, 13.8% of the aerosol mass; coarse mode MMAD = 16.4 µm,  $\sigma_g = 2.79$ , density = 1.7 g/cm<sup>3</sup>, 63.9% of the aerosol mass (see Tables 10C-5 and 10C-6c).

<sup>b</sup>Expressed as a percentage of the total mass of particles in the volume of ambient air inhaled.

<sup>c</sup>Average for 24 h, as derived from ICRP-66 (1994): for 33.3% sleep, 33.3% sitting, and 33.3% light exercise. (See Table 10B-1).

<sup>d</sup>Average for 24 h, as derived from ICRP-66 (1994): for 33.3% sleep, 27.1% sitting, and 35.4% light exercise, 4.2% heavy exercise. (See Table 10B-1).

<sup>e</sup>Average for 24 h, as derived from ICRP-66 (1994): for 33.3% sleep, 16.7% sitting, and 41.7% light exercise, 8.3% heavy exercise. (See Table 10B-1).

Recall from Section 10.4 that deposition of a particular aerosol (MMAD and  $\sigma_g$ ) in the respiratory tract is a function of inhalability and deposition efficiency. This is illustrated schematically in Figure 10-39. The inhalability function (Figure 10-39b) for a specific respiratory tract region (or for the total respiratory tract as depicted in the figure) is integrated with the deposition efficiency function (Figure 10-39c). These are integrated with an aerosol characterized by its particle diameter and mass distribution data (Figure 10-39a) to estimate the mass deposition fraction (Figure 10-39d) in that region.

As expected from experimental studies, these simulations predict different deposition fractions for mouth breathing versus nasal breathing. This is most noticeable for deposition of the intermodal and coarse modes of the Philadelphia and Phoenix aerosols (depicted in Figures 10C-2a and 10C-2b), which showed significant increases in BB and AI deposition fractions. The MMAD for the intermodal and coarse modes were 2.20 and 28.8, respectively, for the Philadelphia aerosol; and 1.70 and 16.4, respectively, for the Phoenix aerosol. Deposition in these regions of the accumulation mode was less effected by mouth breathing as would be anticipated for these smaller MMADs.

Activity pattern influenced the deposition fractions greatly. ET deposition of all three modes increased with the ventilation rates associated with work activity patterns. A noticeable increase in both BB and A deposition occurred with percent changes of increased deposition ranging up to 60%. Differences were also apparent in the nuclei and accumulation modes. For the aerosol depicted in Figure 10C-1, the nuclei mode (MMAD = 0.0169  $\mu\text{m}$ ), deposition fractions decreased in the bb and AI regions with the heavy work activity pattern compared to that for the general population. For the Philadelphia aerosol, deposition of the accumulation mode (MMAD = 0.436  $\mu\text{m}$ ) stayed the same in the BB region but decreased slightly in the bb and A regions with the heavy work activity pattern. For the Phoenix aerosol, deposition of the accumulation mode (MMAD = 0.188) increased in the bb and A compartments with the heavy work activity pattern. Figures 10-40 and 10-41 show the daily mass deposition ( $\mu\text{g}/\text{d}$ ) predicted for normal augmenters versus mouth breathers and these different minute volume activity patterns for the Philadelphia and Phoenix aerosols, respectively.

Differences among the aerosols were also apparent and reflected the differences in the MMAD values and percent mass of each mode. Table 10-25 presents summary data for each

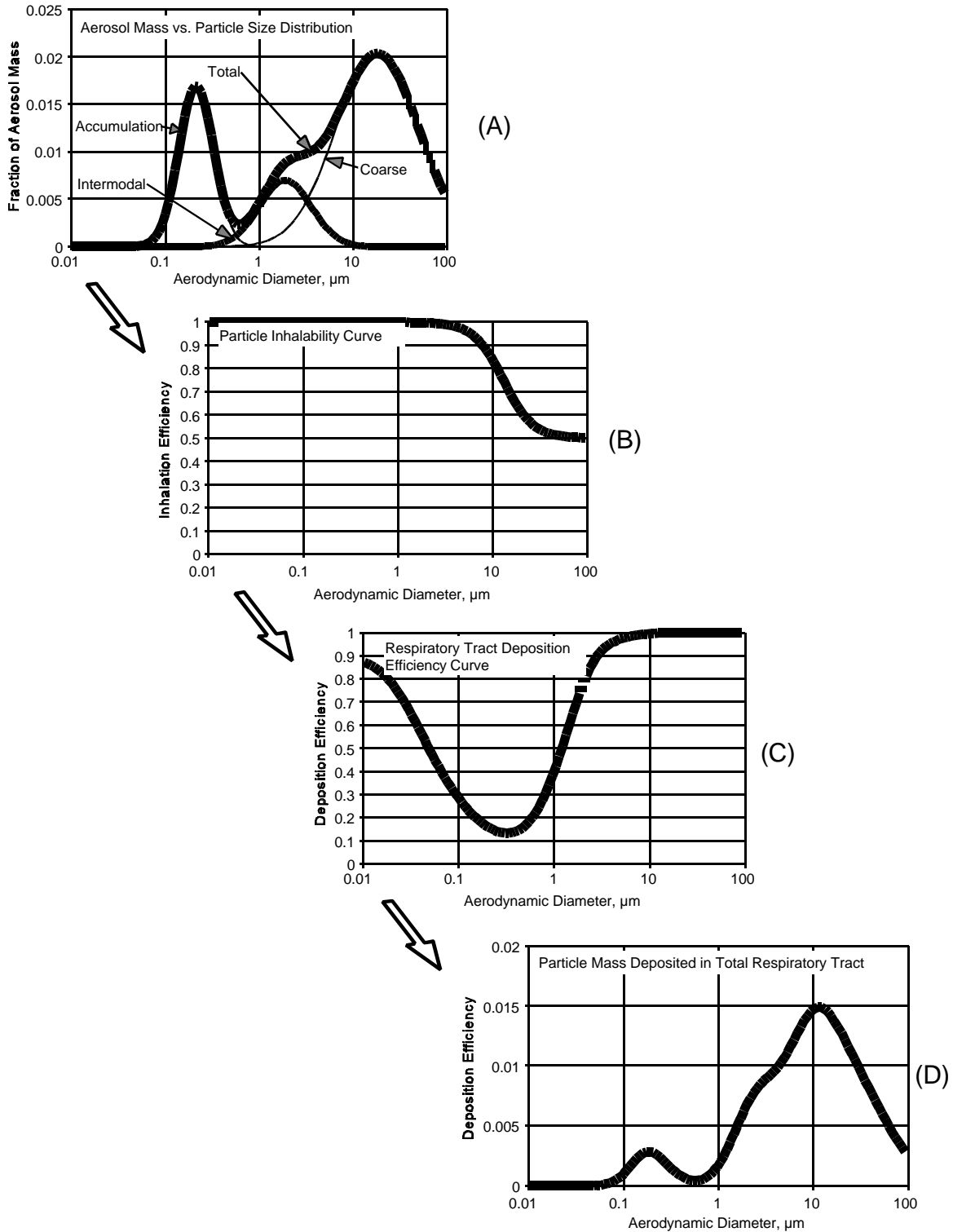


**Figure 10-39. Schematic showing integration of inhalability (b) with deposition efficiency (c) functions. These functions are integrated with particle diameter and distribution data (a) to estimate deposition fractions of particle mass in each region of the respiratory tract (d). The particle mass fraction deposited in the total respiratory tract is illustrated.**

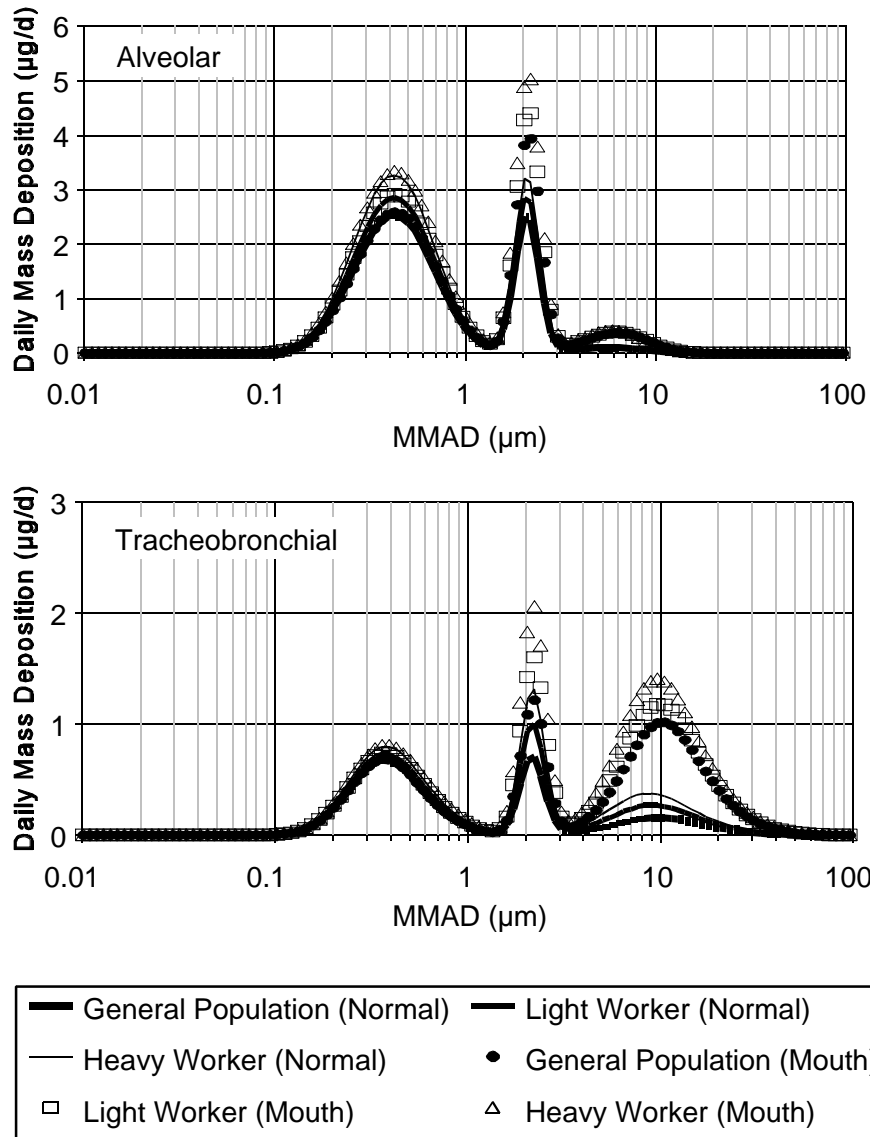


**Figure 10-40. Daily mass deposition ( $\mu\text{g}/\text{day}$ ) in tracheobronchial and alveolar regions for normal augmenter versus mouth breather adult males using International Commission on Radiological Protection Publication 66 (ICRP66) (1994) minute volume activity patterns (general population; worker-light activity; worker-heavy activity). The 1994 ICRP66 model simulated an exposure at  $50 \mu\text{g}/\text{m}^3$  to the Philadelphia aerosol described in Appendix 10C.**

of the three chosen ambient aerosols. To better understand the deposition differences for each mode, however, the previous Tables 10-19 through 10-24 should also be consulted.

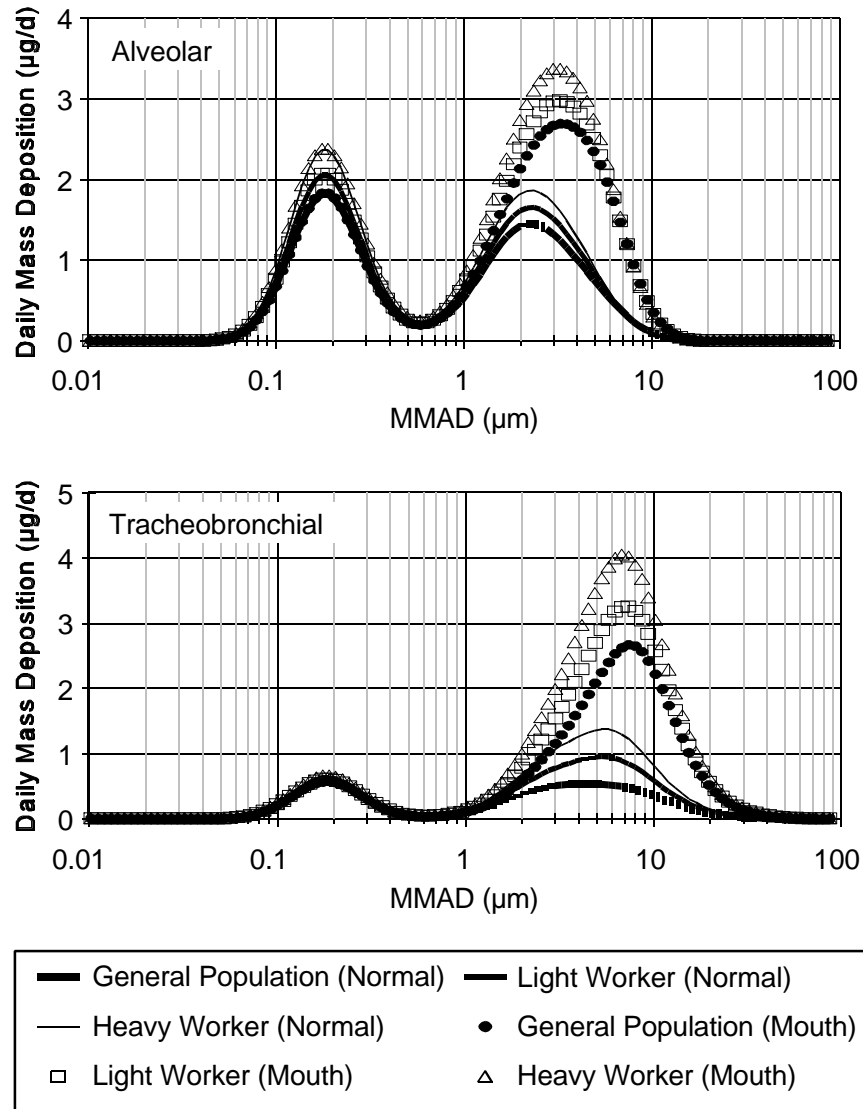


**Figure 10-41. Daily mass deposition ( $\mu\text{g}/\text{day}$ ) in tracheobronchial and alveolar regions for normal augmenter versus mouth breather adult males using International Commission on Radiological Protection Publication 66 (ICRP66) (1994) minute volume activity patterns (general population; worker-light activity; worker-heavy activity). The 1994 ICRP66 model simulated an exposure at  $50 \mu\text{g}/\text{m}^3$  to the Phoenix aerosol described in Appendix 10C.**

### *Intraspecies Variability*

The different deposition predictions for normal augmenter versus mouth breathing humans illustrates the variability that differences in ventilation rate introduces to deposition estimates. As discussed in Section 10.4.1.6., age, gender, and disease status can influence

**TABLE 10-25. DAILY MASS DEPOSITION OF AEROSOL PARTICLES IN  
THE RESPIRATORY TRACTS OF "NORMAL AUGMENTER" AND "MOUTH BREATHER"  
ADULT MALE HUMANS EXPOSED TO 50  $\mu\text{g}$  PARTICLES/ $\text{m}^3$**

Aerosol Figure		10C-1		10C-2(a) (Philadelphia)		10C-2(b) (Phoenix)	
Activity Pattern	Region of Respiratory Tract	Normal Augmenter	Mouth Breather	Normal Augmenter	Mouth Breather	Normal Augmenter	Mouth Breather
Mass of Particle ( $\mu\text{g}$ )							
General population <sup>a</sup>	ET <sub>1</sub>	179	80	168	78	235	110
	ET <sub>2</sub>	207	178	179	198	260	274
	BB	15	48	6	16	9	37
	bb	42	56	10	12	14	24
	AI	136	175	49	62	55	84
	Total	577	537	411	366	572	528
Workers, light work <sup>b</sup>	ET <sub>1</sub>	194	87	182	83	254	118
	ET <sub>2</sub>	240	210	214	234	307	325
	BB	24	61	8	20	16	47
	bb	46	61	10	14	14	25
	AI	157	197	56	68	62	91
	Total	661	618	470	419	655	607
Workers, heavy work <sup>c</sup>	ET <sub>1</sub>	137	96	206	91	286	129
	ET <sub>2</sub>	290	251	258	282	369	390
	BB	86	78	12	25	24	61
	bb	57	68	11	15	17	28
	AI	188	228	63	78	70	103
	Total	760	722	550	490	766	710

<sup>a</sup>Average for 24 h, as derived from ICRP-66 (1994): for 33.3% sleep, 33.3% sitting, and 33.3% light exercise. (See Table 10B-1).

<sup>b</sup>Average for 24 h, as derived from ICRP-66 (1974): for 33.3% sleep, 27.1% sitting, 35.4% light exercise, 4.2% heavy exercise. (See Table 10B-1).

<sup>c</sup>Average for 24 h, as derived from ICRP-66 (1994): for 33.3% sleep, 16.7% sitting, 41.7% light exercise, 8.3% heavy exercise. (See Table 10B-1).

deposition in the respiratory tract. Because the simulations in the preceding section were performed with parameters for adult males using an activity pattern for the general population, an effort to develop activity patterns for different demographic groups was undertaken.

Previous efforts on establishing and revising the NAAQS for ozone and carbon monoxide have attempted to simulate the movement of people through zones of varying air quality so as to approximate the actual exposure patterns of people living within a defined area (Johnson et al., 1989; 1990; 1995a,b). The approach has been implemented through an evolving methodology referred to as the NAAQS exposure model (NEM). The NEM includes data on ventilation rates for various cohort populations.

These cohort data were analyzed to create daily ventilation breathing pattern data for eight demographic groups as follows:

1. Adult Male (18 to 44 years)
2. Adult Female (18 to 44 years)
3. Elderly Male (over 65 years)
4. Elderly Female (over 65 years)
5. Children (0 to 5 years)
6. Children (6 to 13 years)
7. Children (14 to 18 years)
8. Compromised

The compromised demographic group was limited to adults  $\geq 19$  years of age. The objective of identifying this cohort was to construct an activity pattern for subjects with symptoms consistent with cardiopulmonary disease. Those who met this age criterion were included if they answered "yes - it limits my activity" to one of the following questions from a study of the activity patterns affecting exposure to air pollution (Johnson, 1989):

1. Has a doctor ever determined that you have asthma?
2. Has a doctor ever determined that you have a heart condition?
3. Has a doctor ever determined that you have angina?
4. Have you had a stroke?
5. Have you ever had a heart attack?

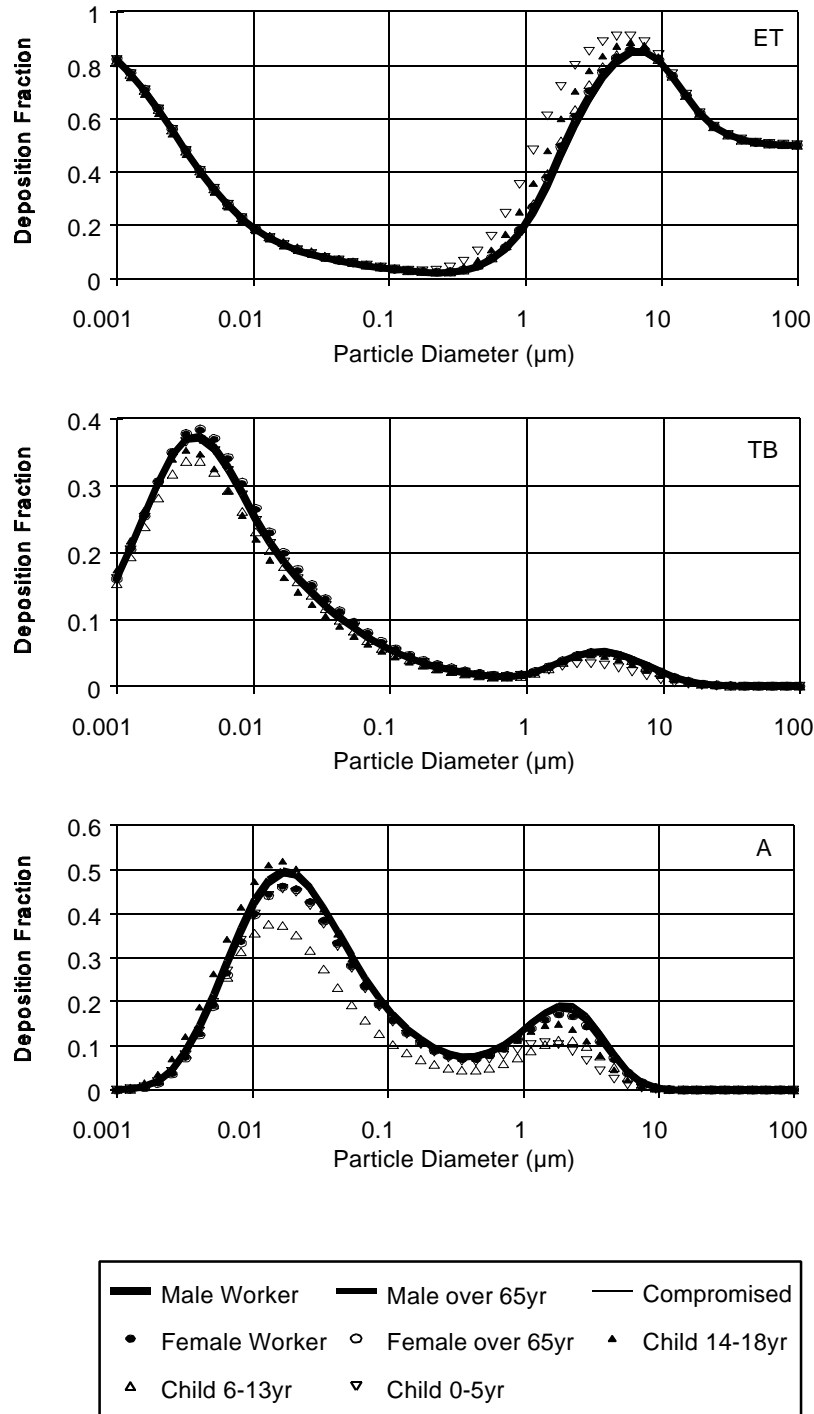
6. Has a doctor ever determined that you have hypertension (high blood pressure)?
7. Has a doctor ever determined that you have chronic bronchitis?
8. Do you have any other diagnosed respiratory or heart ailment which limits your activity?

Respondents were also included if they answered "yes - it does not limit my activity" to question numbers 1, 2, 3, 4, 5, or 7.

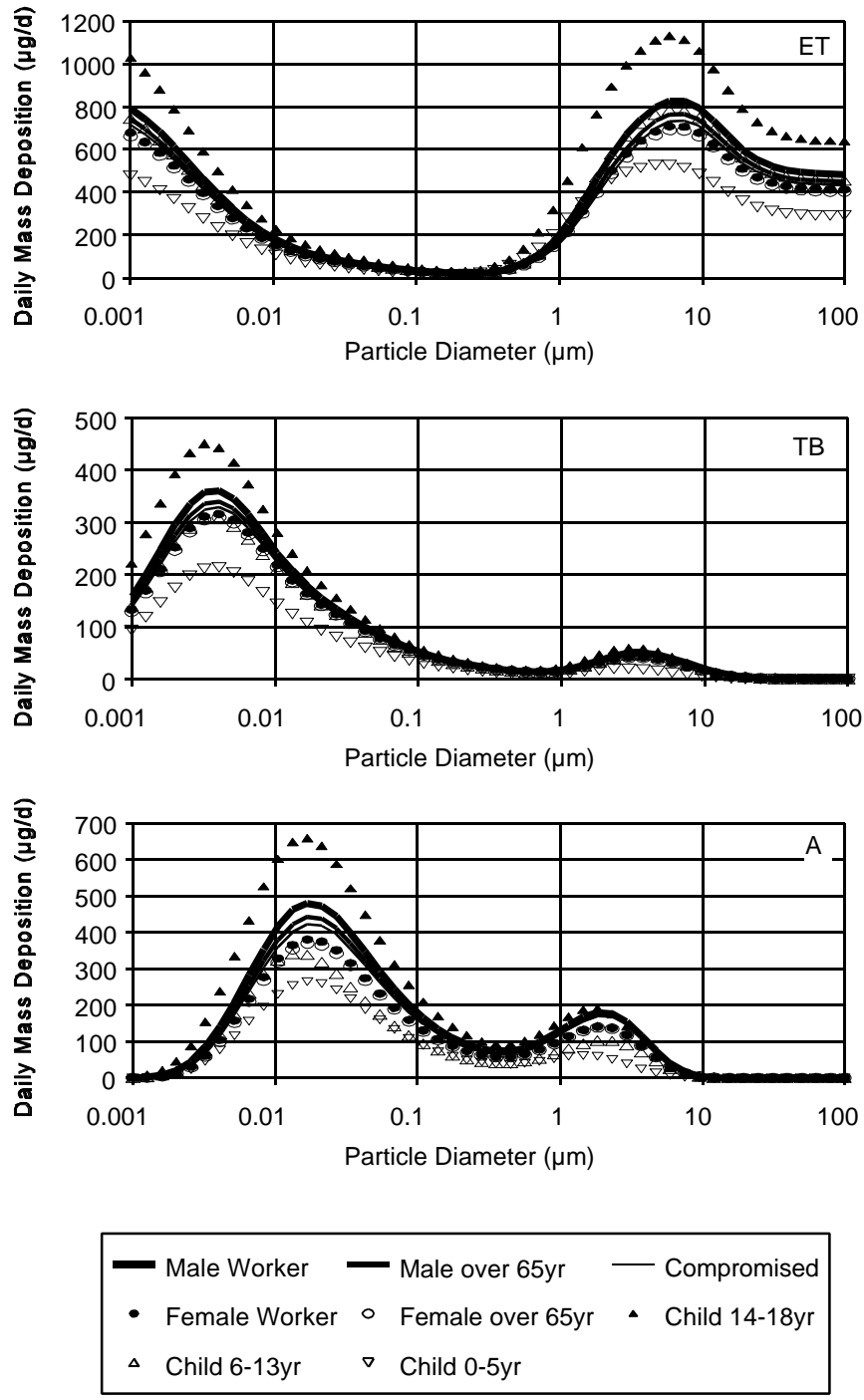
Figures 10B-1 through 10B-3 in Appendix 10B show the daily minute volume patterns for each of these demographic groups. The average minute volume for each of 4 time periods: (1) 24:00 to 06:00; (2) 06:00 to 12:00; (3) 12:00 to 21:00; and (4) 21:00 to 24:00 was used as input to the 1994 ICRP model in order to create a total 24-h daily breathing pattern for each demographic group.

Figure 10-42 shows the fractional deposition in each of the three respiratory tract regions for these demographic groups. Figure 10-43 shows the daily deposition rate ( $\mu\text{g}/\text{day}$ ) of an exposure to  $50 \mu\text{g}/\text{m}^3$ . Some variation between the cohorts exists in the mass deposition fraction for particles in the aerodynamic size range of the ET region; the cohorts of children, especially the 0 to 5 year age group, show an increased deposition. In the A region, the cohort of children 14 to 18 years showed an enhanced deposition rate ( $\mu\text{g}/\text{d}$ ) for submicron-sized particles in all three regions of the respiratory tract, whereas the cohort of children 0 to 5 years showed a decreased deposition rate relative to male and female adults. For larger particles (micron-sized and above), the 14 to 18 year cohort showed no enhanced deposition rate in the tracheo bronchial or alveolar regions compared to adults, and younger children cohorts showed a progressive decrease with decreasing age. When evaluated on the basis of daily mass deposition rate ( $\mu\text{g}/\text{d}$ ), the cohort of children ages 14 to 18 years showed an increase in deposition for all three regions of the respiratory tract (Figure 10-43) compared to other cohorts, whereas the cohort of children 0 to 5 years showed a decrease. This is due primarily to differences in respiratory frequency.

Although constructed for differences in age, gender, and health status, the cohorts as constructed represent differences for these factors only characterized in terms of differences in hourly minute volume patterns. Other effects on dosimetry such as altered respiratory tract architecture leading to altered flow pattern or differences in susceptibility of the target



**Figure 10-42. Deposition fraction in each respiratory tract region as predicted by the International Commission on Radiological Protection Publication 66 (ICRP66) (1994) model. Simulations used daily minute volume activity patterns for different demographic groups as provided in Appendix 10B.**



**Figure 10-43.** Daily mass particle deposition rates ( $\mu\text{g/d}$ ) for 24-hour exposure at  $50 \mu\text{g/m}^3$  in each respiratory tract region as predicted by the International Commission on Radiological Protection Publication 66 (ICRP66) (1994) model. Simulations used daily minute volume activity patterns for different demographic groups as provided in Appendix 10B.

tissue are not addressed in these simulations. As discussed earlier, Anderson et al. (1990) have shown enhanced deposition in patients with COPD compared to healthy subjects. Miller et al. (1995) used a more detailed theoretical multipath model and estimated enhanced deposition in a compromised lung status model defined by decreased ventilation to respiratory tract region adjustment. The simulations performed herein were limited to average mass particle burdens per region of the respiratory tract. Nevertheless, these simulations do suggest differences for these cohorts. For example, the cohort for children 14 to 18 years showed an enhanced deposition rate (ug/d) in all three respiratory tract regions whereas children 0 to 5 years showed a decrease.

### ***Relevance to $PM_{10}$ Versus $PM_{2.5}$ Sampling***

The dosimetry of particles of different sizes in the human respiratory tract formed one of the primary bases for selecting the  $PM_{10}$  size fraction in the 1987 review. Particles in this size range pose the greatest risk to human health because they penetrate to the putative target regions in the lower respiratory tract associated with mortality and morbidity, i.e., the TB and A regions.

Ambient aerosols have been established as bimodal distributions of particles. Fine and coarse particles generally have different sources, formation mechanisms, physical properties, chemical composition and properties, atmospheric lifetimes, and outdoor to indoor infiltration ratios. The fine fraction has been suggested to provide a better exposure surrogate for the epidemiological data (See Chapters 12 and 13). In addition, some of the properties of fine particles may play a role in possible mechanisms of toxicity. For example, the fine mode accounts for most of the particle number and much of the surface area. Also, several chemical classes of concern such as acids and sulfates are found predominantly in the fine fraction. If particle number and not mass alone is an important determinant of response, then a refined characterization of this mode may enhance the ability to discern effects in the exposed populations.

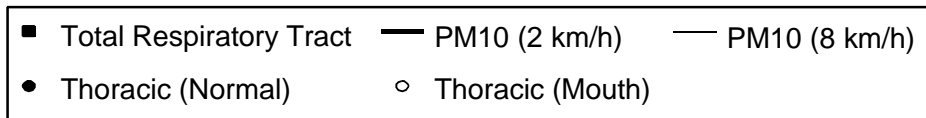
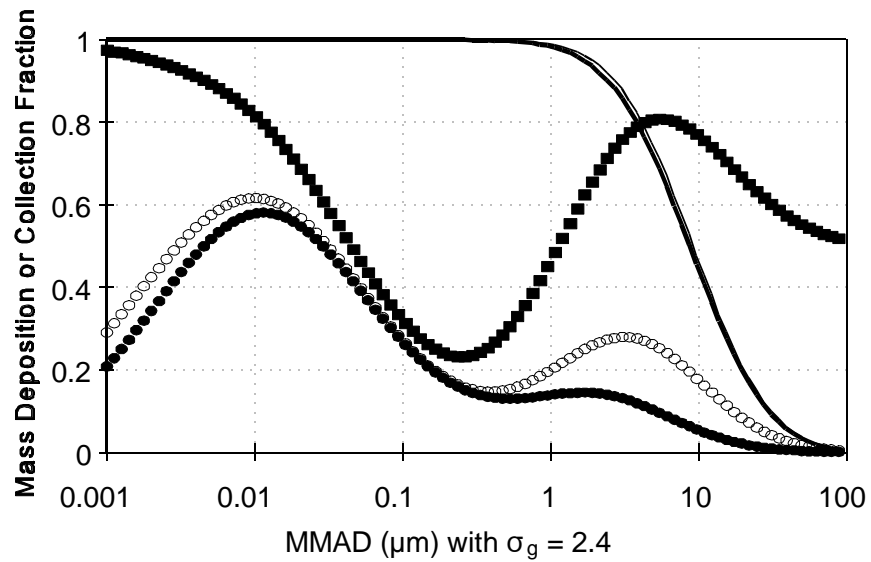
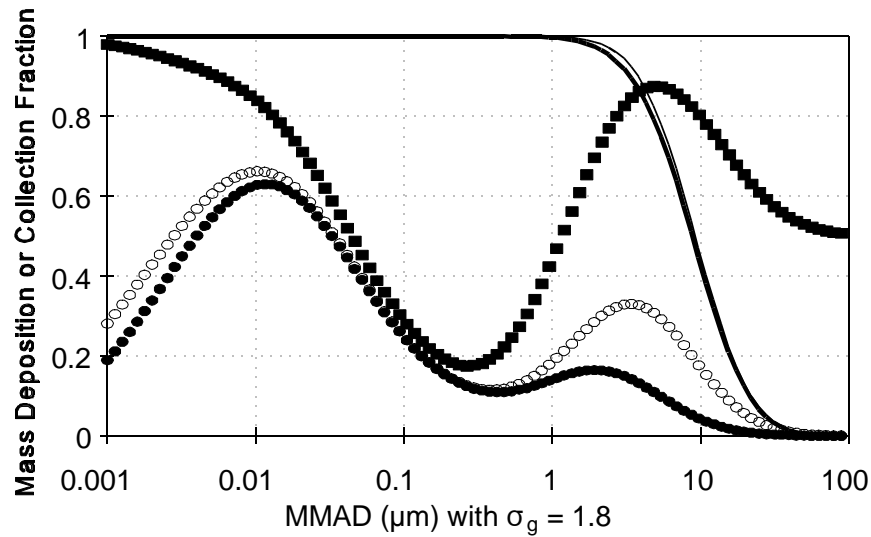
Simulations were performed using the 1994 ICRP66 dosimetry model to illustrate the relationship between deposition efficiency of the respiratory tract, mass burden of particles in the thoracic portion of the respiratory tract, and the mass distribution of aerosols collected by a  $PM_{10}$  or  $PM_{2.5}$  sampler.

Figure 10-44 shows the predicted regional deposition fraction in the respiratory tract, relative to unit mass concentration in ambient air, as a function of the aerosol size (represented by the mass median aerodynamic diameter, MMAD, in  $\mu\text{m}$ ). The top graph is for aerosols with a

geometric standard deviation ( $\sigma_g$ ) of 1.8 and the other with a  $\sigma_g$  of 2.4. Deposition fraction based on model simulations are shown for the thoracic region (i.e., tracheobronchial plus alveolar deposition, TB + A), as well as for the total respiratory tract deposition fraction. The difference between total respiratory tract and total thoracic fractions represents the extrathoracic or upper airway deposition fraction. In addition these figures show curves representing the fraction collected by a  $PM_{10}$  sampler. This illustrates that the  $PM_{10}$  sample accounts for almost all of the thoracic deposition, but does not account for many of the larger particles which would be deposited in the ET region. Two curves for the  $PM_{10}$  collection fraction are shown illustrating different wind speed characteristics (i.e., for 2 km/h or 8 km/h). It is seen that wind speed is not a major factor. These curves represent the deposition fractions for healthy people who breathe oronasally during exercise (normal augmenters) and healthy people who breathe predominantly through their mouth (mouth breather). As before, it is clear that mouth breathers have a greater deposition of particles  $>1 \mu\text{m}$  than do oronasal breathers.

Figures 10-45 and 10-46 expand on the information presented in 10-44 by illustrating deposition fraction in each of the two thoracic regions, the alveolar and the TB region, again for normal augmenters and for mouth breathers. In addition, the collection fraction for a  $PM_{2.5}$  sampler is illustrated. Whereas  $PM_{10}$  accounts for all particles in the thoracic size deposition mode, the  $PM_{2.5}$  sample does not include some larger particles that would be deposited in the TB and A regions of mouth breathers, under the simulated conditions (general population activity pattern 8 h sleep, 8 h sitting, 8 h light activity [see Appendix 10B, Table 10B-1(b)]. Mouth breathers do not represent a large percentage of the population, but are cited here to illustrate the effect of breathing habit. Figure 10-46 provides the same information as Figure 10-45 but expands the scale for micron-sized particles by excluding particles smaller than  $0.1 \mu\text{m}$ .

These simulations (Figures 10-44 through 10-46) represent single mode aerosols of various MMAD and two different  $\sigma_g$ . However, the real world ambient aerosols are



**Figure 10-44. Respiratory tract deposition fractions and PM<sub>10</sub> sampler collection versus mass median aerodynamic diameter (MMAD) with two different geometric standard deviations ( $\sigma_g = 1.8$  or  $\sigma_g = 2.4$ ). Thoracic deposition fraction predicted for normal augments versus mouth breather adult male using a general population (ICRP66) minute volume activity pattern and the 1994 ICRP66 model. Total respiratory tract deposition fraction also shown for normal augments. PM<sub>10</sub> sampler collection shown at two different wind speeds (8 km/h or 2 km/h).**

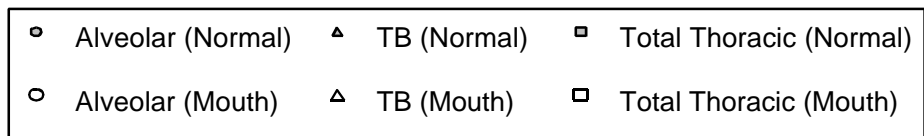
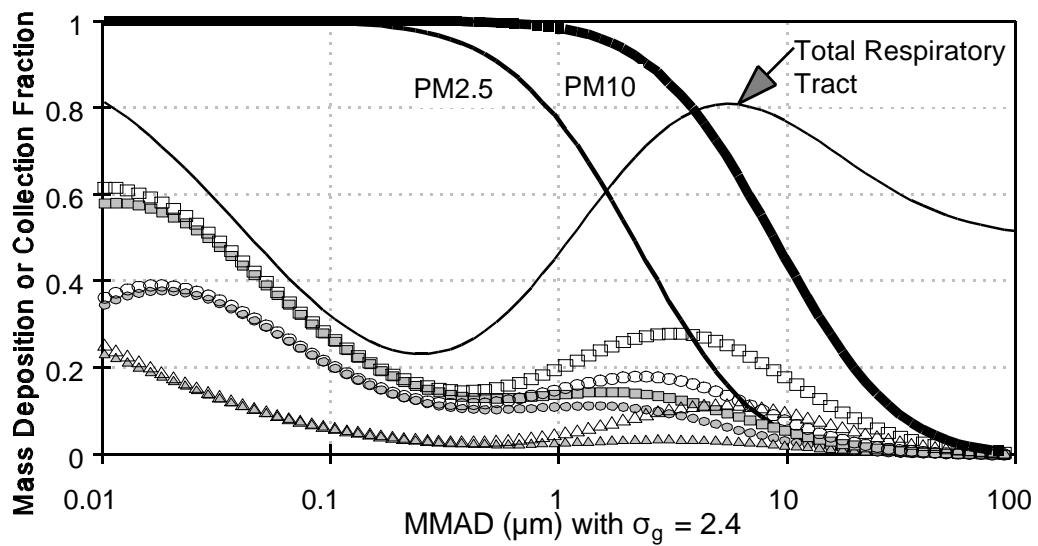
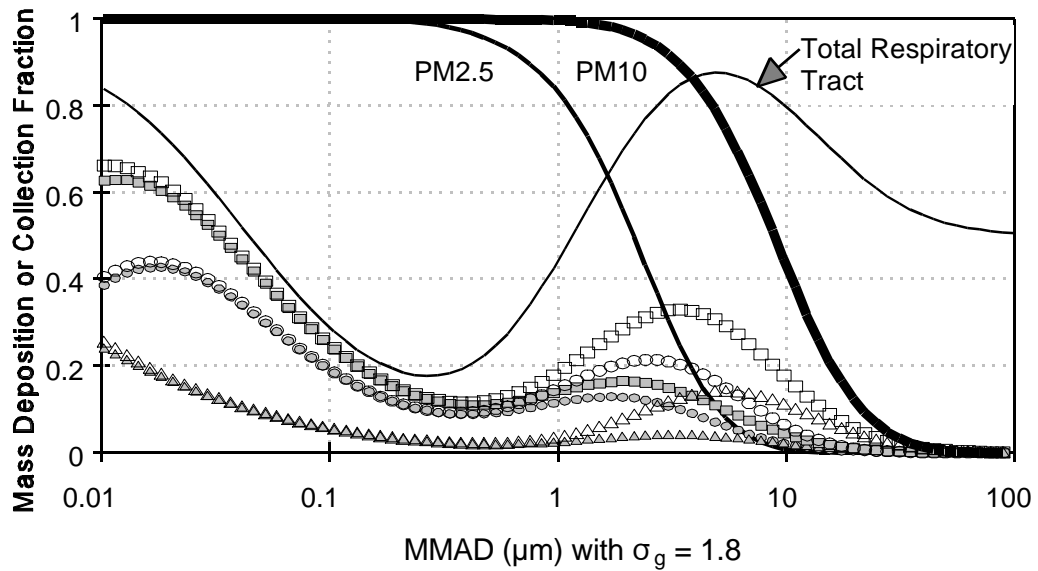


**Figure 10-45. Respiratory tract deposition fractions and  $\text{PM}_{10}$  or  $\text{PM}_{2.5}$  sampler collection versus mass median aerodynamic diameter (MMAD) with two different geometric standard deviations ( $\sigma_g = 1.8$  or  $\sigma_g = 2.4$ ). Alveolar, tracheobronchial, or total thoracic deposition fractions predicted for normal augmenter versus mouth breather adult male using a general population (ICRP66) minute volume activity pattern and the 1994 ICRP66 model.**

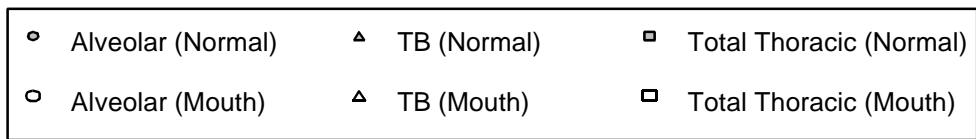
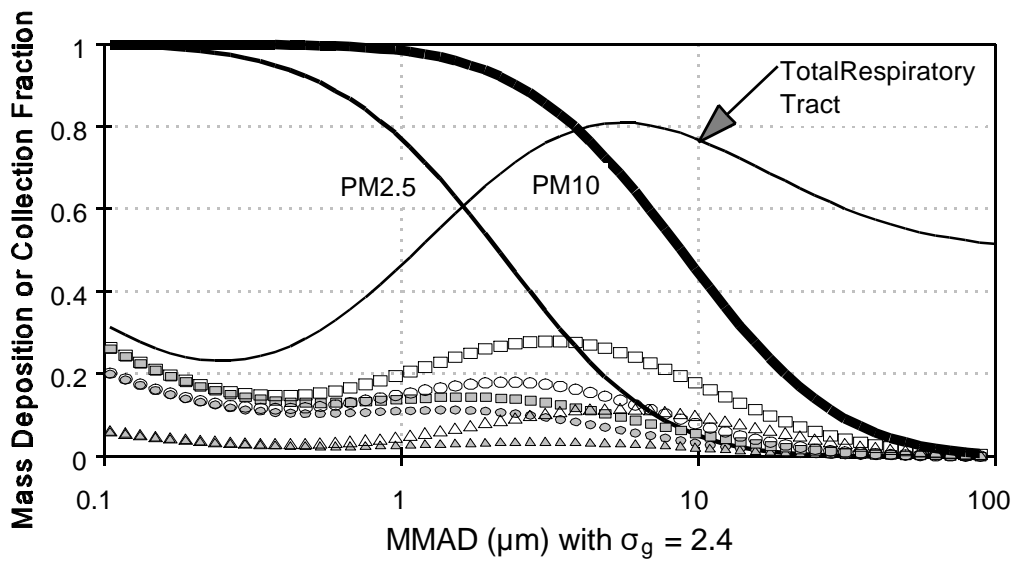
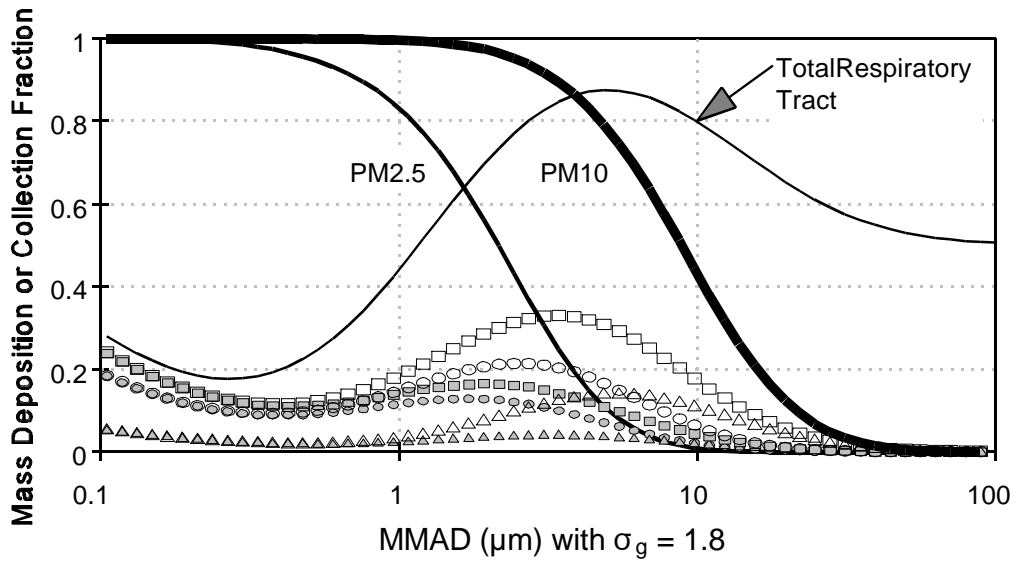


**Figure 10-46. Respiratory tract deposition fractions and  $\text{PM}_{10}$  or  $\text{PM}_{2.5}$  sampler collection fractions versus mass median aerodynamic diameter (MMAD) with two different geometric standard deviations ( $\sigma_g = 1.8$  or  $\sigma_g = 2.4$ ). Alveolar, tracheobronchial, or total thoracic deposition fractions predicted for normal augments versus mouth breather adult male using a general population (ICRP66) minute volume activity pattern and the 1994 ICRP66 model.**

multi-modal, having a broad distribution of particle sizes and composition. Figure 10-47 illustrates graphically the process of taking the mass distribution for an ambient aerosol and the deposition efficiency curve for a “typical” (general population adult male) human and deriving the distribution of particle mass deposited in the lung. This is shown in the sequence of graphs in Figure 10-47. The mass distribution of the ambient aerosol (Figure 10-47a) is combined with the deposition efficiency curve (Figure 10-47b; similar to Figure 10-39) to obtain the thoracic mass deposition for the ambient aerosol (Figure 10-47c). The corresponding process for collection with a PM<sub>10</sub> sampler is also shown. Figure 10-47a (ambient mass distribution) is combined with the sampler efficiency curve (Figure 10-47d), resulting in Figure 10-47e, which shows the collected mass distribution for the ambient aerosol. If Figure 10-47c is superimposed on Figure 10-47e, figures such as 10-48 and 10-49 will be generated.

Figures 10-48 and 10-49 illustrate the fractional mass deposition seen with representative ambient aerosols for the cities of Phoenix and Philadelphia. These trimodal aerosols were described in Chapter 3, and their parameters are provided in Appendix 10C. From these graphs it is shown that the PM<sub>2.5</sub> sampler distribution accounts for the particle mass in the fine (<1.0 μm) mode and the transition mode (MMAD ~2.5 μm) but does not account for the smaller mass of coarse mode particles that would be deposited in the thorax (mainly affecting tracheobronchial deposition in mouth breathers). Failure of the PM<sub>2.5</sub> sampler to account for coarse mode particle thoracic deposition is more evident for the Phoenix aerosol than for the Philadelphia aerosol.

Because mass deposition is not the only dose metric that is of interest, a similar modeling exercise was conducted for particle number, using the Philadelphia and Phoenix aerosols. Simulations were again performed with parameters for adult males and a general population activity pattern. Figure 10-50 shows the predicted fraction of total number of particles inhaled that is deposited in each region of the respiratory tract (ET, TB, A) for the Philadelphia aerosol. Figure 10-51 shows the number of particles deposited each day in each respiratory tract region for the Philadelphia aerosol assuming an exposure to a total particulate mass concentration of 50 μg/m<sup>3</sup>. These figures show that a large fraction of the number of deposited particles is contributed, as anticipated, by the fine fraction mode, and that this can represent a very large number of particles deposited per day (on the order of

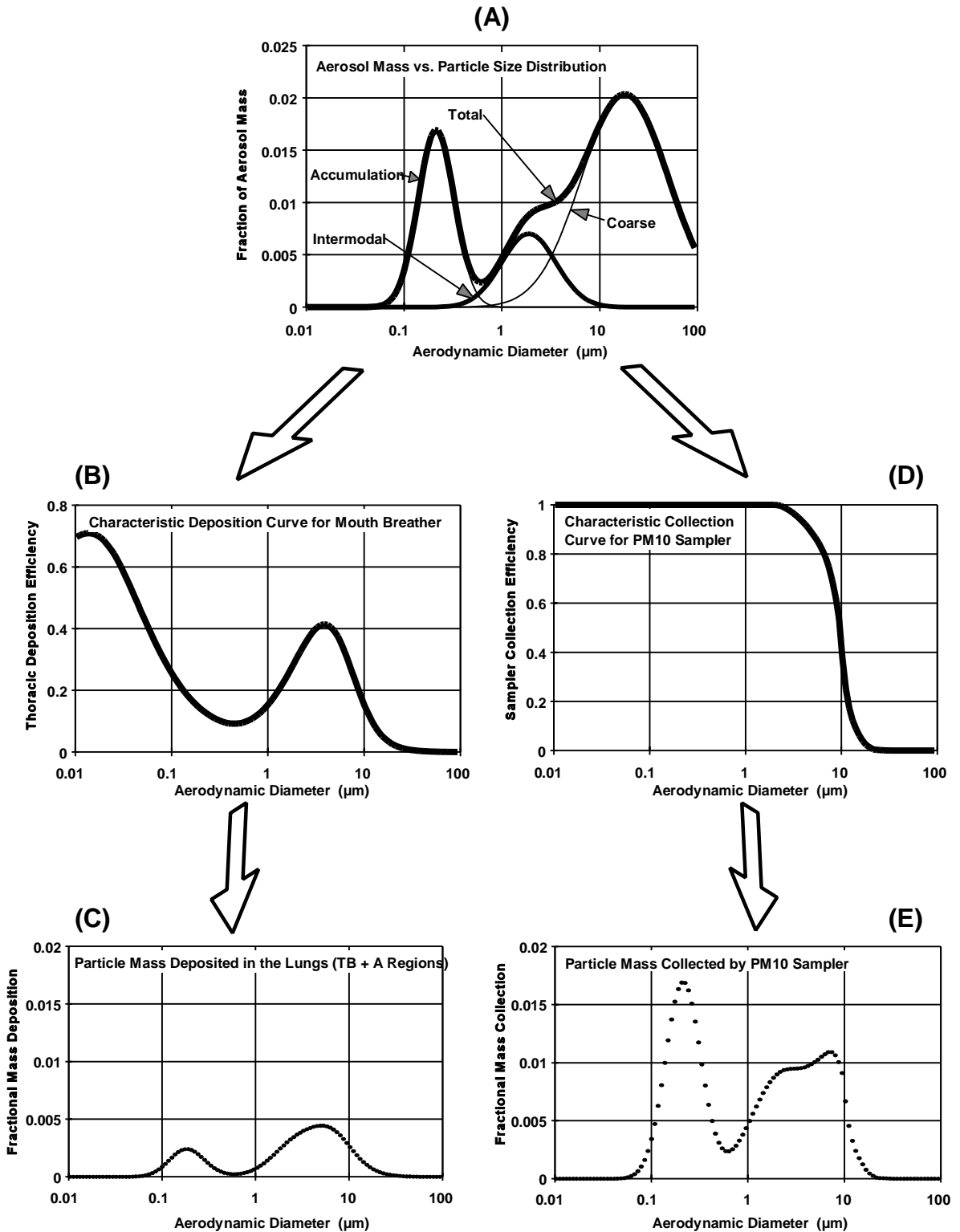
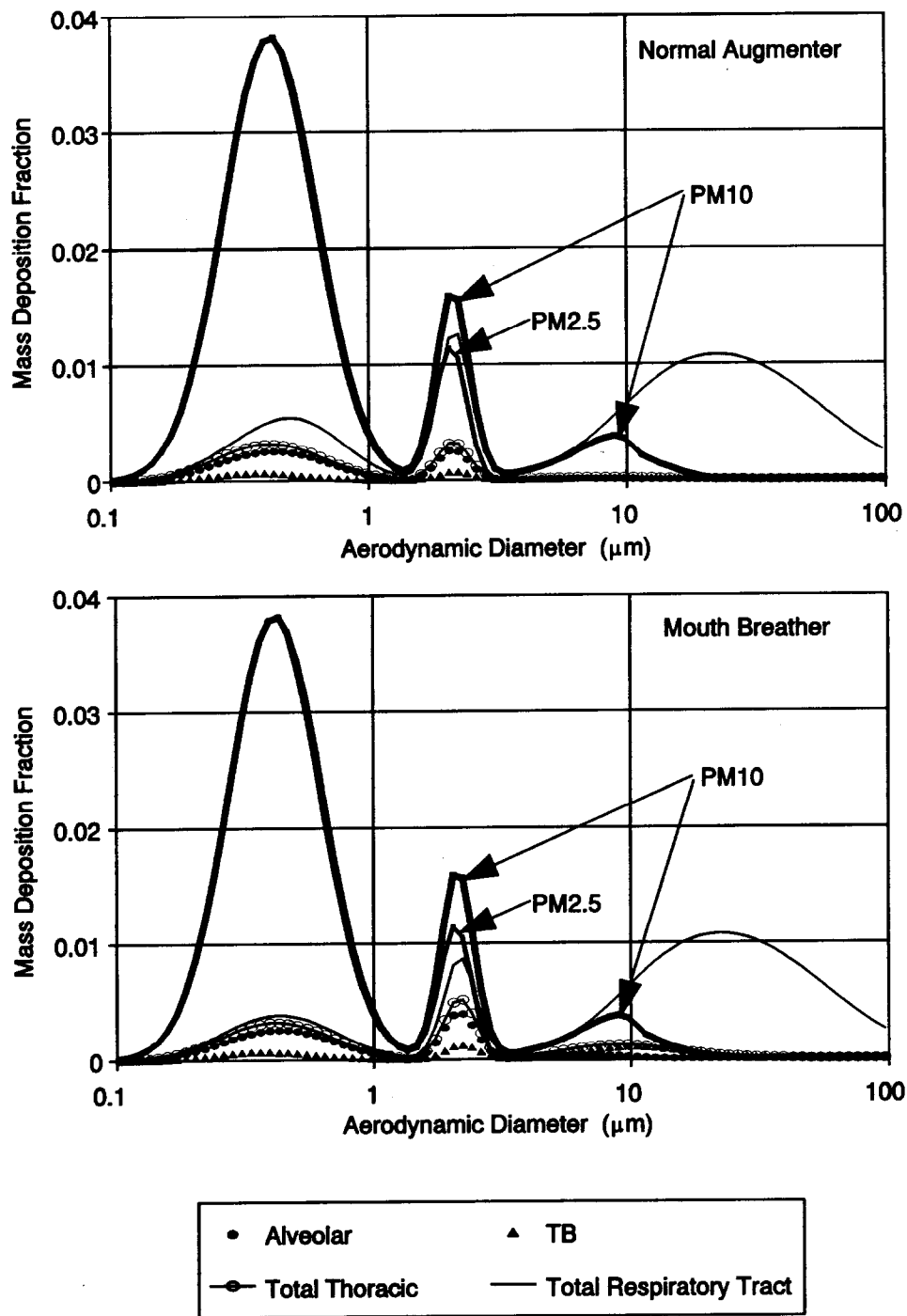
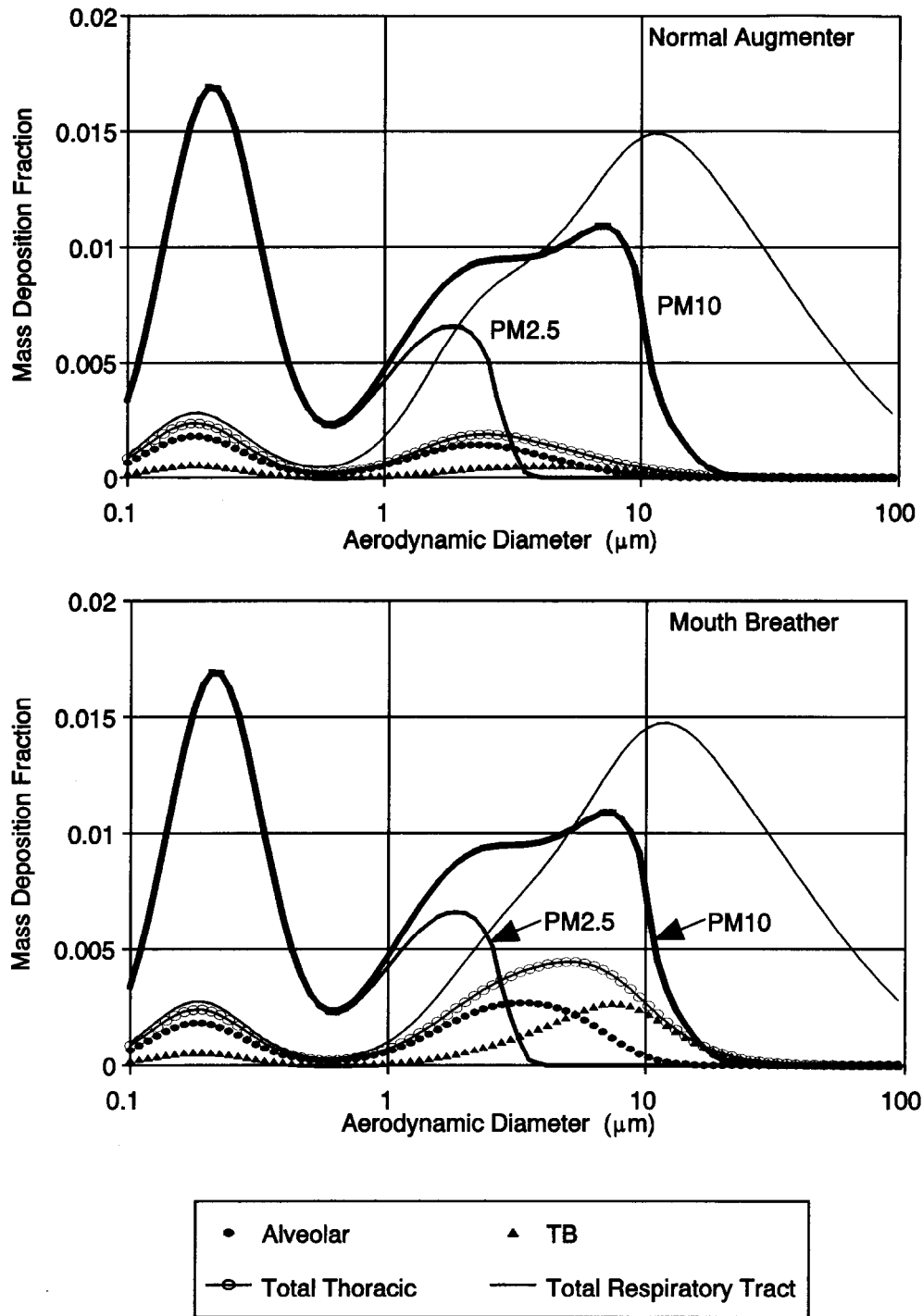


Figure 10-47. Schematic illustration of how ambient aerosol distribution data were integrated with respiratory tract deposition efficiency (using 1994 ICRP66 model) or sampler efficiency to calculate deposition in respiratory tract regions or mass collected by sampler.



**Figure 10-48.** Mass deposition fraction in normal augmenter versus mouth breather adult male with a general population minute volume activity pattern predicted by the International Commission on Radiological Protection Publication 66 (1994) model and the mass collected by PM<sub>10</sub> or PM<sub>2.5</sub> samplers for Philadelphia aerosol (described in Appendix 10C).



**Figure 10-49.** Mass deposition fraction in normal augmenter versus mouth breather adult male with a general population minute volume activity pattern predicted by the International Commission on Radiological Protection Publication 66 (1994) model and the mass collected by  $\text{PM}_{10}$  or  $\text{PM}_{2.5}$  samplers for Phoenix aerosol (described in Appendix 10C).

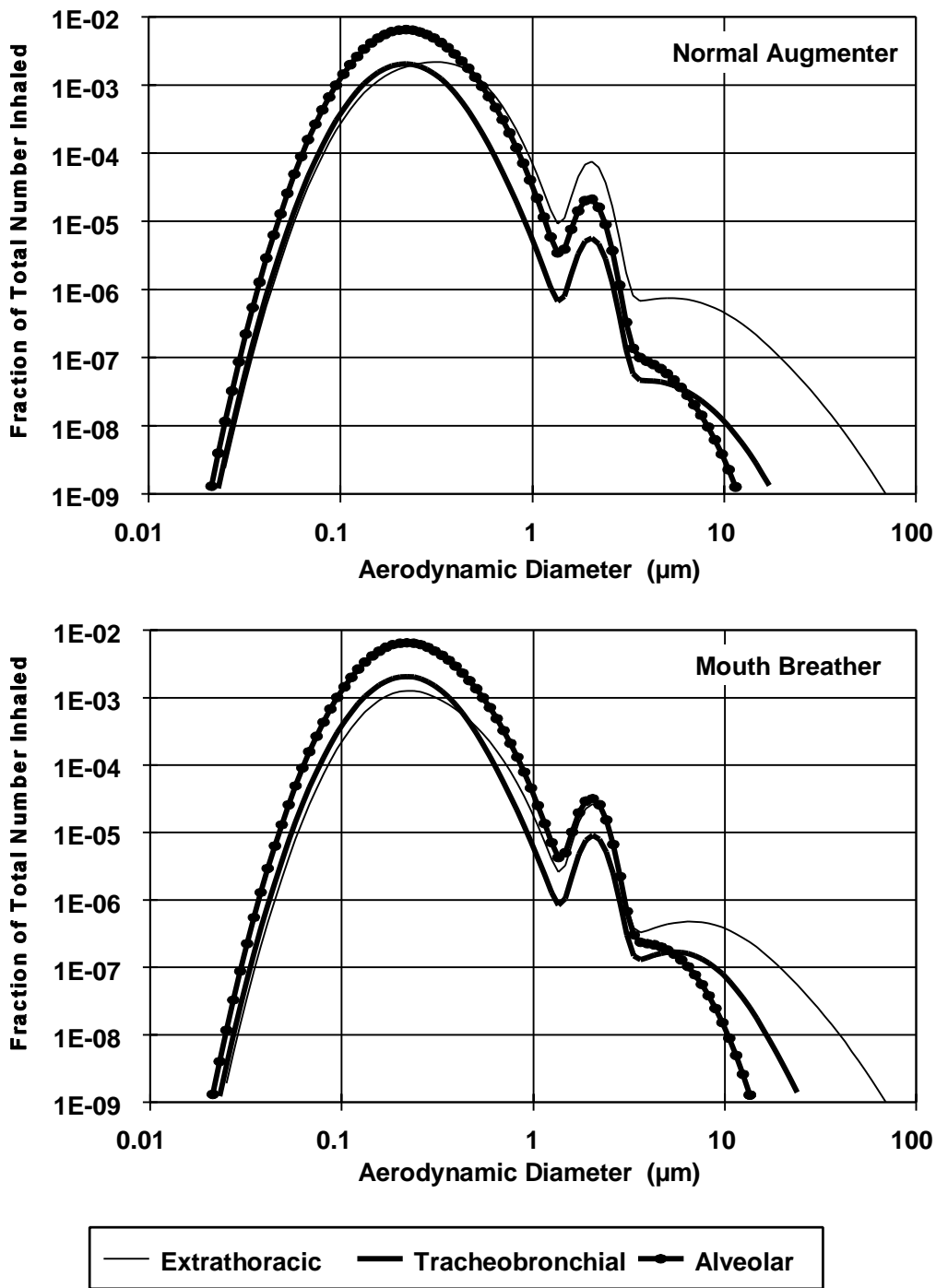


**Figure 10-50.** Fractional number deposition in each respiratory tract region for normal augmenter versus mouth breather adult male with a general population activity pattern as predicted by the International Commission on Radiological Protection Publication 66 (1994) model for an exposure to the Philadelphia aerosol (described in Appendix 10C).

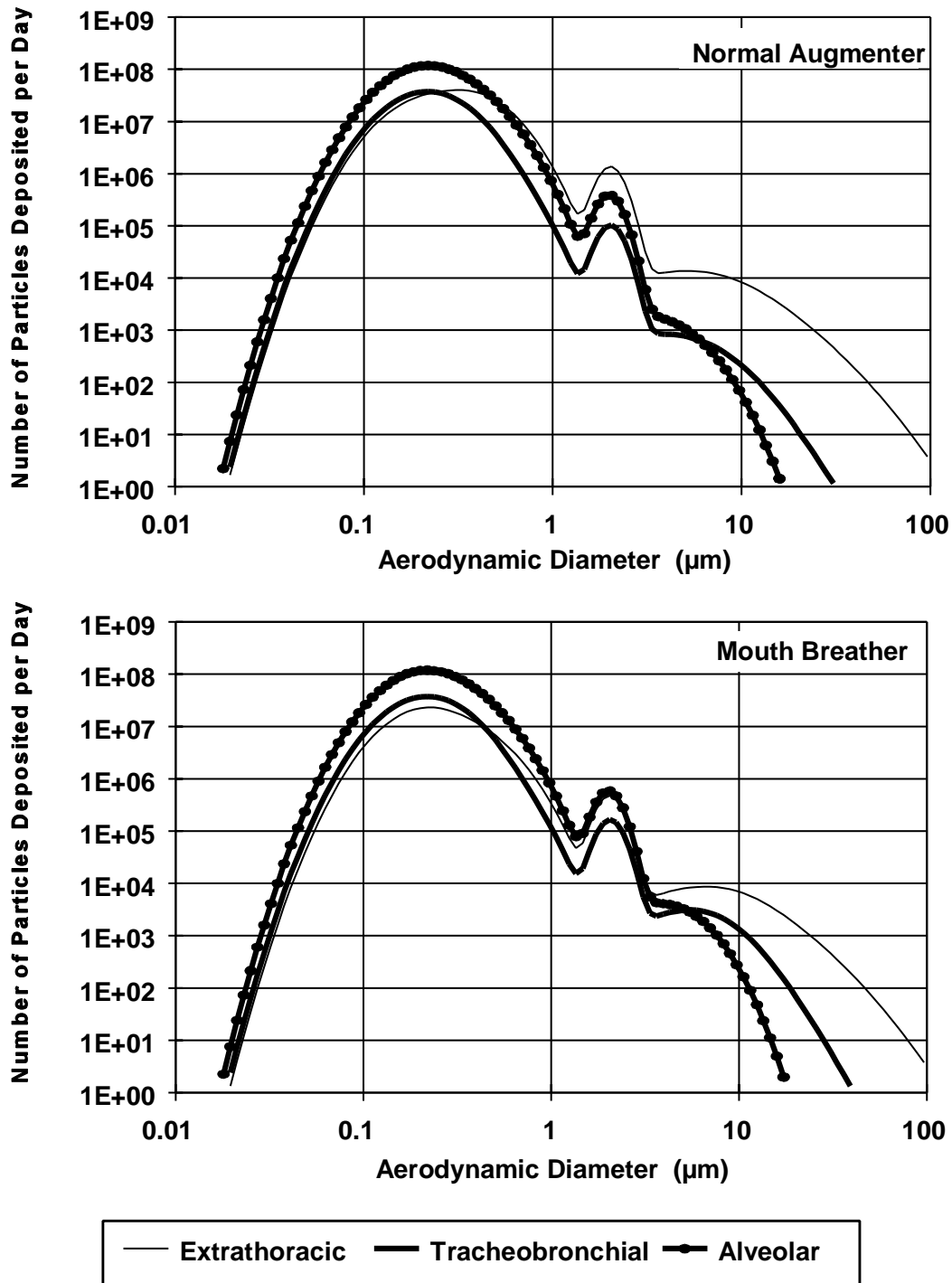


Figure 10-51. Number of particles deposited per day in each respiratory tract region for normal augmenter versus mouth breather adult male with a general population activity pattern as predicted by the International Commission on Radiological Protection Publication 66 (1994) model for an exposure to the Philadelphia aerosol (described in Appendix 10C) at a concentration of  $50 \mu\text{g}/\text{m}^3$ .

100,000,000) in the alveolar region. Figure 10-52 shows the predicted fraction of total number of particles inhaled that is deposited in each respiratory tract region for the Phoenix aerosol, and Figure 10-53 shows the number of particles deposited each day in each respiratory tract region for this aerosol assuming an exposure to a total particulate mass concentration of  $50 \mu\text{g}/\text{m}^3$ . The more disperse intermodal fraction of the Phoenix aerosol (see Figure 10C-2 in Appendix 10C) contributes more particles to the fine mode size-range than that of the Philadelphia aerosol.

### ***Hygroscopic Aerosols***

The ICRP66 (1994) deposition model as so far described relates to the distribution of activity or mass of aerosol particles with respect to their size on entering the respiratory tract. However, in the case of a hygroscopic material, it is necessary to take account of the increase in particle size that occurs when such materials are exposed to the near-saturated air in the respiratory tract. The ICRP66 model can be applied for hygroscopic materials by replacing the values of particle aerodynamic diameter,  $d_{ae}$ , and diffusion coefficient,  $D$ , in ambient air with the values  $d_{ae}(j)$  and  $D_j$  attained in each region,  $j$ , of the respiratory tract.

Annexe D of ICRP66 describes how the growth of a hygroscopic particle can be approximated in general terms as a function of its residence time in saturated air at body temperature. For a residence time,  $t_j^r$ , in region,  $j$ , measured from inspiration of the particle (*i.e.*, entry to the nose or mouth), the particle aerodynamic diameter and diffusion coefficient attained by hygroscopic growth are approximately related to  $d_{ae}(0)$  and  $D(0)$ , the respective values in ambient air (*i.e.*, the external environment), and the values at equilibrium,  $d_{ae}(\infty)$  and  $D(\infty)$  are

$$d_{ae}(t_j^r) = d_{ae}(\infty) - [d_{ae}(\infty) - d_{ae}(0)] \left[ \exp \left( \frac{-\{10 t_j^r\}^{0.55}}{d_{ae}(0)} \right) \right]^{0.6}, \text{ and} \quad (10-58)$$

$$D(t_j^r) = D(0) - \left[ \frac{d_{ae}(t_j^r) - d_{ae}(0)}{d_{ae}(\infty) - d_{ae}(0)} \right] [D(0) - D(\infty)]. \quad (10-59)$$

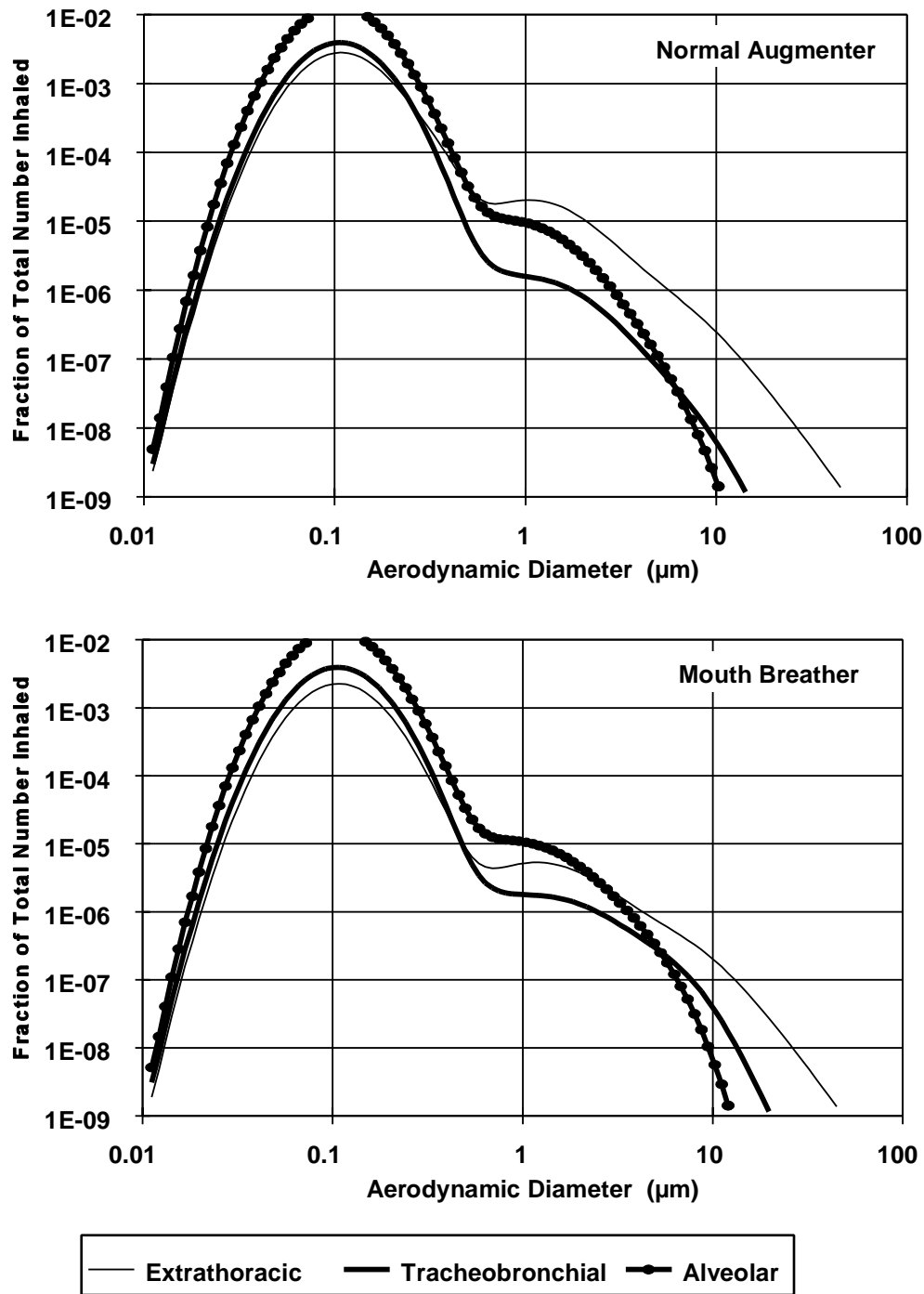


**Figure 10-52. Fractional number deposition in normal augmenter versus mouth breather adult male with a general population activity pattern predicted by the International Commission on Radiological Protection Publication 66 (1994) model for an exposure to the Phoenix aerosol (described in Appendix 10C).**

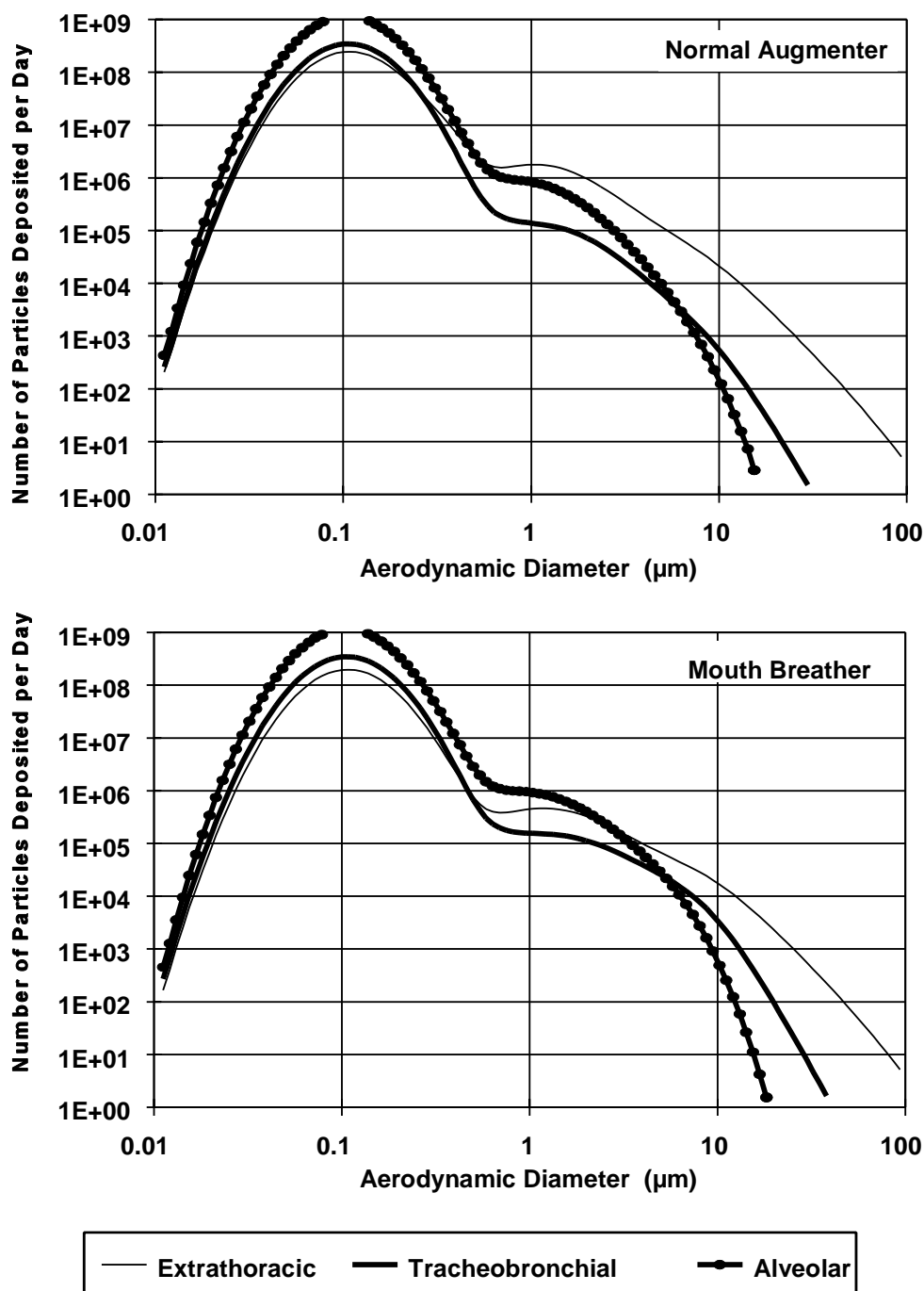


**Figure 10-53.** Number of particles deposited per day in each respiratory tract region for normal augmenter versus mouth breather adult male with a general population activity pattern predicted by the International Commission on Radiological Protection Publication 66 (1994) model for an exposure to the Phoenix aerosol (described in Appendix 10C) at a concentration of  $50 \mu\text{g}/\text{m}^3$ .

To solve the model for a specific material, it is necessary to specify the degree of particle size growth at equilibrium. This generally lies in the range of two- to fourfold growth, depending on the amount of hygroscopic material associated with the particle. However, ICRP66 suggests that it is likely to be adequate to assume by default a threefold growth factor at equilibrium, for substitution in these equations. Note that the initial aerodynamic diameter,  $d_{ac}(0)$ , is increased by particle growth, whereas the initial diffusion coefficient,  $D(0)$ , is decreased.

The effect of hygroscopic particle growth is generally to decrease total lung deposition for submicron-sized particles, and to increase it for larger particles. As discussed in some detail in Annexe D of ICRP66, the particle size in ambient air corresponding to minimum lung deposition is reduced from about 0.4  $\mu\text{m}$  for non-hygroscopic particles to about 0.1  $\mu\text{m}$  for hygroscopic particles (Tu and Knutson, 1984; Blanchard and Willeke, 1984).

### ***Intrahuman Variability in Regional Deposition***

The experimental data on regional deposition of particles in the human respiratory tract indicate substantial intersubject variability, even if the particles are inhaled under identical exposure conditions. In ICRP66, the upper and lower 95% confidence bounds of the data are represented by a variable coefficient,  $a$ , which is incorporated into each algebraic expression for deposition efficiency (see ICRP66, Chapter 5, Tables 12 and 13, pp. 45 and 46). In each case, the coefficient is taken to be log-normally distributed, (i.e.,  $a_{\text{upper}} = a_{\text{median}} \times \sigma_g^2$ , and  $a_{\text{lower}} = a_{\text{median}} \div \sigma_g^2$ ) where  $\sigma_g$  is the fitted geometric standard deviation. Other confidence bounds on the predicted regional deposition efficiency are given by substituting an appropriate value of the coefficient,  $a$ , that is sampled from the defined log-normal distribution.

Representing the median (or expectation) value of the coefficient,  $a$ , for each region,  $j$ , by  $a_j$ , then it is convenient to use a dimensionless scaling constant,  $c_j$ , as a multiplier or divisor of the median value. In Table 14 of ICRP66 (Chapter 5, p. 49), the ICRP gives values of this scaling constant that are estimated to describe the spread in the experimental data for regional respiratory tract deposition. The scaling factors defining the upper and lower 95% confidence bounds of regional deposition range from  $\times$  or  $\div$  by 1.4 in the expression for “thermodynamic” deposition efficiency of the extrathoracic (ET) region, to  $\times$  or  $\div$  by 3.3 for the “aerodynamic” deposition efficiency of the ET region. To evaluate the uncertainty distribution of the predicted deposition

fractions in all five regions of the respiratory tract (i.e., ET<sub>1</sub>, ET<sub>2</sub>, BB, bb, and AI) it is necessary to select the respective values of  $c_j$  at random from their assumed log-normal distributions.

#### 10.7.5.2 Laboratory Animal Estimates

Tables 10-26 through 10-31 provide the deposition fractions of various particle sizes (MMAD) for either a relatively monodisperse ( $\sigma_g = 1.3$ ) versus a more polydisperse ( $\sigma_g = 2.4$ ) distribution in humans or rats. Deposition fractions of these aerosols for an adult male human normal augments and mouth breather with a general population activity pattern were calculated using the ICRP66 model (ICRP66, 1994). The deposition fraction for each respiratory tract region is presented: ET in Tables 10-26 and 10-27; TB in Tables 10-28 and 10-29; and A in Tables 10-30 and 10-31. These regional deposition fractions are shown plotted in Figure 10-54. The left side in each panel represents the deposition fractions for the relatively monodisperse aerosol ( $\sigma_g = 1.3$ ) and the right side in each panel represents the more polydisperse aerosol ( $\sigma_g = 2.4$ ). Note that the y-axis scale changes from one panel to the other and from panel to panel. As discussed in Section 10.5, polydispersity in the aerodynamic particle size range tends to smear the regional deposition across the range of particles. The interspecies differences in fractional deposition are readily apparent from these figures.

In the TB region, Figure 10-54 illustrates that at the smaller particle diameters (MMAD < 2  $\mu\text{m}$  for  $\sigma_g = 1.3$ ) the rats have higher deposition fractions than normal augments (nasal breathing) humans. At larger particle diameters (MMAD > 2.5  $\mu\text{m}$  for  $\sigma_g = 1.3$ ), rats have very little deposition in the TB or A regions due to the low inhalability of these particles. This may help explain why inhalation exposures of rodents to high concentrations of larger particles have exhibited little effect in some bioassays.

The information in Tables 10-26 through 10-31 and depicted in the panels of Figure 10-54 can be used to calculate the deposition fraction term in Equations 10-50 and 10-54. The average ventilation rates and parameters such as surface area which could be used for normalizing factors for laboratory animals are found in Appendix 10B, Table 10B-2.

**TABLE 10-26. EXTRATHORACIC DEPOSITION FRACTIONS OF INHALED MONODISPERSE AEROSOLS ( $\sigma_g=1.3$ ) IN RATS AND HUMAN "NORMAL AUGMENTER" AND "MOUTH BREATHER"**

MMAD	Normal Augmenter	Mouth Breather	Rat
1	0.273	0.074	0.18
1.5	0.443	0.141	0.55
2	0.566	0.209	0.74
2.5	0.651	0.270	0.77
3	0.711	0.326	0.76
3.5	0.754	0.375	0.73
4	0.785	0.420	0.70

**TABLE 10-27. EXTRATHORACIC DEPOSITION FRACTIONS OF INHALED POLYDISPERSE AEROSOLS ( $\sigma_g=2.4$ ) IN RATS AND HUMAN "NORMAL AUGMENTER" AND "MOUTH BREATHER"**

MMAD	Normal Augmenter	Mouth Breather	Rat
1	0.326	0.126	0.30
1.5	0.442	0.193	0.42
2	0.524	0.250	0.49
2.5	0.582	0.299	0.53
3	0.624	0.340	0.55
3.5	0.655	0.374	0.56
4	0.678	0.404	0.56

**TABLE 10-28. TRACHEOBRONCHIAL DEPOSITION FRACTIONS OF INHALED MONODISPERSE AEROSOLS ( $\sigma_g=1.3$ ) IN RATS AND HUMAN "NORMAL AUGMENTER" AND "MOUTH BREATHER"**

MMAD	Normal Augmenter	Mouth Breather	Rat
1	0.022	0.026	0.10
1.5	0.033	0.048	0.06
2	0.042	0.074	0.03
2.5	0.048	0.101	0.01
3	0.050	0.125	0.005
3.5	0.050	0.144	0.002
4	0.049	0.159	0.001

**TABLE 10-29. TRACHEOBRONCHIAL DEPOSITION FRACTIONS OF INHALED  
POLYDISPERSE AEROSOLS ( $\sigma_g=2.4$ ) IN RATS AND HUMAN  
"NORMAL AUGMENTER" AND "MOUTH BREATHER"**

MMAD	Normal Augmenter	Mouth Breather	Rat
1	0.028	0.049	0.06
1.5	0.032	0.068	0.05
2	0.035	0.084	0.04
2.5	0.036	0.096	0.031
3	0.036	0.104	0.025
3.5	0.036	0.110	0.021
4	0.035	0.114	0.017

**TABLE 10-30. ALVEOLAR DEPOSITION FRACTIONS OF INHALED  
MONODISPERSE AEROSOLS ( $\sigma_g=1.3$ ) IN RATS AND HUMAN  
"NORMAL AUGMENTER" AND "MOUTH BREATHER"**

MMAD	Normal Augmenter	Mouth Breather	Rat
1	0.119	0.140	0.06
1.5	0.146	0.120	0.10
2	0.150	0.237	0.06
2.5	0.142	0.256	0.02
3	0.126	0.258	0.011
3.5	0.109	0.248	0.005
4	0.092	0.230	0.002

**TABLE 10-31. ALVEOLAR DEPOSITION FRACTIONS OF INHALED  
POLYDISPERSE AEROSOLS ( $\sigma_g=2.4$ ) IN RATS AND HUMAN  
"NORMAL AUGMENTER" AND "MOUTH BREATHER"**

MMAD	Normal Augmenter	Mouth Breather	Rat
1	0.111	0.151	0.04
1.5	0.112	0.171	0.04
2	0.109	0.180	0.035
2.5	0.103	0.179	0.031
3	0.096	0.175	0.027
3.5	0.089	0.169	0.023
4	0.082	0.161	0.020

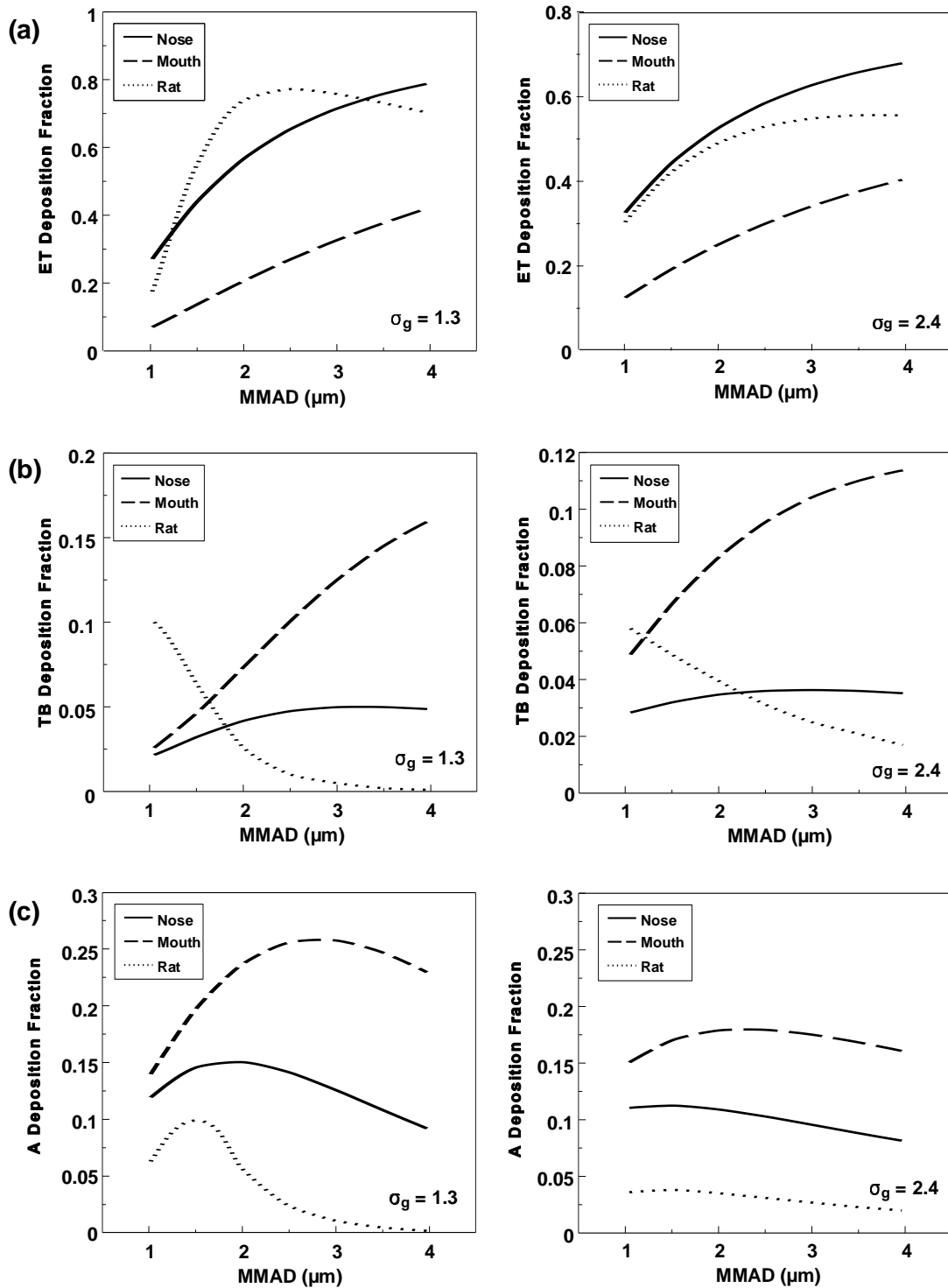


**Figure 10-54.** Predicted extrathoracic deposition fractions versus mass median aerodynamic diameter (MMAD) of inhaled monodisperse ( $\sigma_g = 1.3$ ) aerosols shown in left-side panels or polydisperse ( $\sigma_g = 2.4$ ) aerosols shown in right-side panels for humans (nose versus mouth breathing) and rats (obligatory nose breathers), for (a) the extrathoracic region, (b) tracheobronchial region, and (c) alveolar region.

Respiratory tract region surface areas for humans are found in Table 10B-1. The human male adult general population activity pattern in Table 10B-1 corresponds to a daily ventilation volume of 19.9 m<sup>3</sup>/day. This is the average ventilation rate that was used to run the LUDEP<sup>®</sup> simulations and would be used in the denominator of Equations 10-51 or 10-55. The normal augments or mouth breather deposition fractions found in Tables 10-26 through 10-31 represents the sum of the Fr<sub>H</sub> factors in the denominator of the expression found in Equations 10-51 and 10-55. Likewise, the deposition fractions for the rat represent the Fr<sub>A</sub> factor in Equations 10-53 and 10-57.

Because particles initially deposit along the surface of the respiratory tract, regional surface area is chosen as the normalizing factor for calculation of the regional deposited dose ratio (RDDR), as described in Equation 10-50, in order to characterize "acute" effects. Assuming an exposure to an aerosol with a MMAD of 1.0 μm and σ<sub>g</sub> = 1.3, Equation 10-51 can be used to calculate RDDR<sub>A[ACT]</sub> estimates using the deposition fractions provided in Tables 10-26 through 10-31 and surface area and ventilation rate parameters provided in Tables 10B-1 and 10B-2 in Appendix 10B. A RDDR<sub>A[ACT]</sub> value of 1.54 is calculated for rats using the alveolar surface area as a normalizing factor. The RDDR<sub>A[ACT]</sub> value for each species would be applied to an experimental exposure concentration from a laboratory toxicology study using rats to calculate a human equivalent concentration.

Interspecies extrapolation to HEC values allows for comparison among species. For example, if a rat exhibited an effect in the alveolar region when exposed to an aerosol with a MMAD = 1.0 μm and σ<sub>g</sub> = 1.3 at an exposure concentration of 100 μg/m<sup>3</sup>, the resultant HEC value calculated for the rat would be 154 μg/m<sup>3</sup>. This HEC would result in a similar alveolar deposited dose and thereby a similar effect in humans, assuming species sensitivity to a given dose is equal. Although laboratory species may be exposed to the same aerosol at the same concentration, each would have a different fractional deposition, which when normalized to regional surface area, could result in different HEC estimates. Thus, taking into account species differences in dosimetry is necessary before comparing effective concentrations when interpreting toxicity data.

For tracheobronchial effects, the RDDR<sub>TB[ACT]</sub> would be used to adjust exposure concentrations for interspecies differences in dosimetry. For an aerosol with an MMAD = 1.0 μm and σ<sub>g</sub> = 1.3, the RDDR<sub>TB[ACT]</sub> value is 9.95 for rats. For an aerosol with an MMAD = 2.5

and  $\sigma_g = 2.4$ , the  $RDDR_{TB[ACT]}$  value is 1.89. The decrease in the value is due to the decreased inhalability of the larger particle diameter and the effect of polydispersity. Similarly, the  $RDDR_{A[ACT]}$  value for an aerosol with an MMAD = 2.5  $\mu\text{m}$  and  $\sigma_g = 2.4$  is 0.88 for rats, whereas it was 1.54 for the more monodisperse aerosol.

### **10.7.6 Retained Dose Estimates**

An important issue in inhalation toxicology is the relationship between repeated or chronic inhalation exposures and the resulting alveolar burdens of exposure material achieved in the human lung versus the lungs of laboratory animal species. It is generally assumed that the magnitude of the alveolar burden of particles produced during an inhalation exposure is an important determinant of biological responses to the inhaled particles. Therefore, understanding the basis for differences among species in alveolar burdens that will result from well-defined inhalation exposures will provide investigators with a better understanding of alveolar burdens that would result from exposures of various mammalian species to the same aerosol.

Alternatively, the exposure conditions could be tailored for each species to produce desired alveolar burdens of particles.

Predictable deposition, retention, and clearance patterns are possible for acute inhalation exposures of laboratory animal species and humans. Repeated exposures also occur for humans and are used routinely in laboratory animals to study the inhalation toxicology of a broad spectrum of potentially hazardous particulates. The predicted biokinetics of particles acutely inhaled can be readily extrapolated to repeated exposures. However, the predictions become increasingly questionable as exposure conditions deviate from those used for acute inhalation exposures. The following predictions for repeated inhalation exposures are therefore intended to be relative, rather than absolute, and were made using the assumption that physical clearance parameters for the A region are the same for acute and repeated inhalation exposures.

#### **10.7.6.1 Human Estimates**

The LUDEP® software version 1.1 for the 1994 ICRP66 model was also used to simulate chronic exposures of adult male "normal augmenters" to the trimodal aerosols described in Appendix 10C for Philadelphia (Figure 10C-2a, and Tables 10C-3 and 10C-4) and Phoenix (Figure 10C-2b, and Tables 10C-5 and 10C-6). The simulations were of a continuous 24 h/d and

7 d/week exposure at an air concentration of  $50 \mu\text{g}/\text{m}^3$ . For both aerosols, the particles in the accumulation, intermediate, and coarse modes were assumed to have dissolution/absorption half times of 10, 100, and 1000 days, respectively.

Predicted particle mass ( $\mu\text{g}$ ) lung burdens as a function of exposure days are presented in Figure 10-55a for the Philadelphia trimodal aerosol and in Figure 10-55b for the Phoenix trimodal aerosol. The assumed dissolution/absorption rates and default values for clearance parameters in the ICRP66 1994 model yielded predicted particle mass lung burdens from the accumulation, intermediate, and coarse modes that reached equilibrium between deposition and clearance after about 100, 700, and 7,000 days, respectively. Table 10-32 presents the predicted ratios of particle mass in the lungs for each of the three modes and for the total amount of particles. Individuals breathing the Phoenix aerosol would have about 0.7 the amount of the accumulation mode particles in their lungs as would individuals breathing the Philadelphia aerosol, and about 1.5 times as much of the intermediate and 11 times as much of the coarse modes. Overall, individuals exposed for long periods to the Phoenix aerosol would have almost 4 times as much total mass of particles in their lungs as would individuals exposed to the Philadelphia aerosol. Interestingly, the biggest difference is in the predicted amounts of particles from the coarse mode.

Another way to present these model simulation results is to express them in terms of specific lung burden ( $\mu\text{g dust} / \text{g lung}$ ) versus time. This is presented in Figure 10-56a for the Philadelphia aerosol and in Figure 10-56b for the Phoenix aerosol. Note that the time of exposure was converted to age in years. Assuming that humans of all ages and gender deposit and clear about the same amounts of particles from these aerosols per day per gram of lung, this presentation of data approximates the specific lung burdens of particle mass as a function of age for young and old alike. For both aerosols, equilibrium amounts of dust are achieved after about 16-18 years. Assuming that clearance rates are not altered with age or these levels of particle burden, this suggests that an individual who has lived in these environments for longer than about 18 years has accumulated a specific lung burden of these particles and that the burdens will remain relatively constant as long as exposure conditions and health status are not appreciably changed. Note again that the data in Table 10-33 predict different relative amounts of accumulated particles from the three modes.

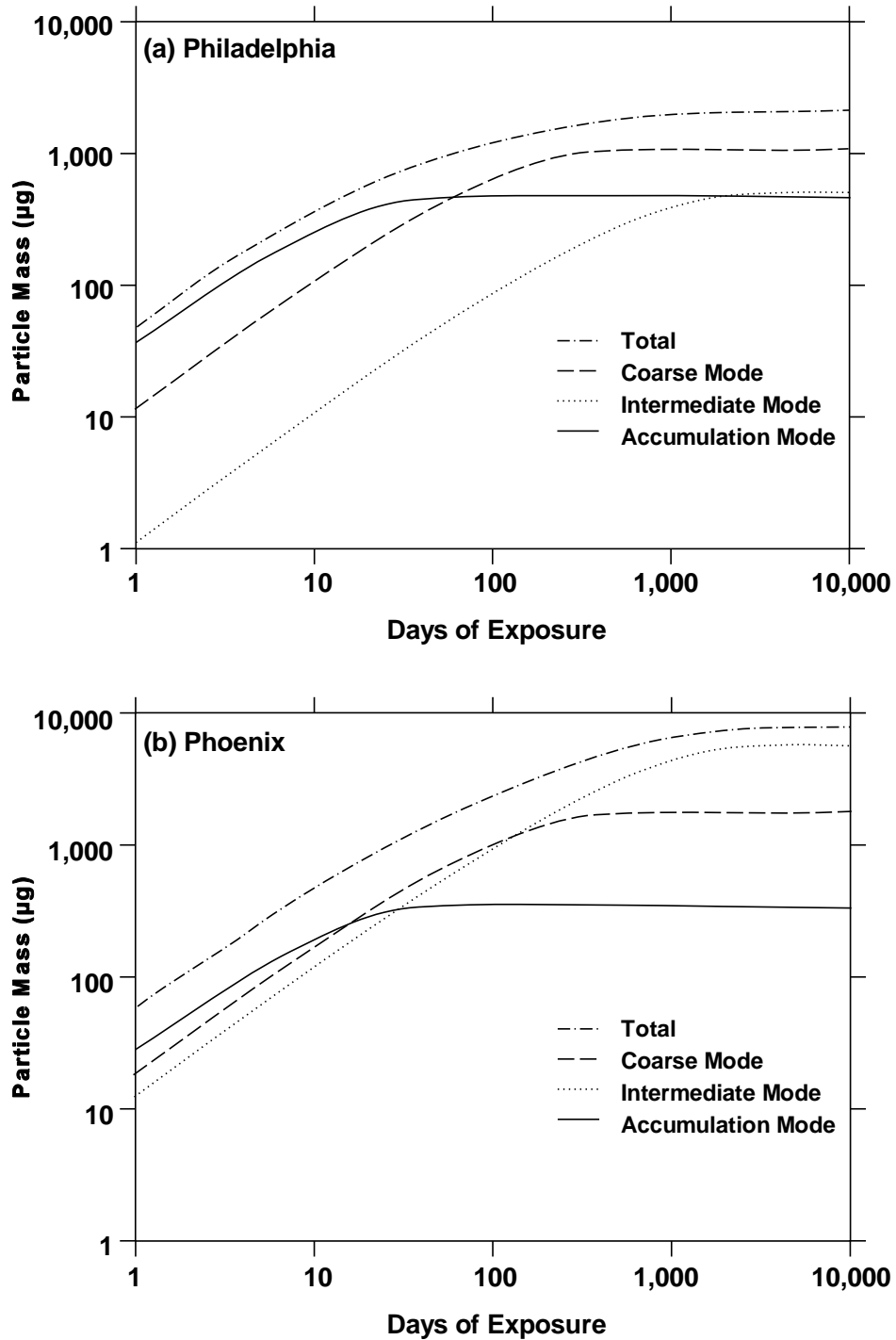


**Figure 10-55.** Particle mass ( $\mu\text{g}$ ) retained in the lung versus time (days of exposure) predicted by the International Commission on Radiological Protection Publication 66 (1994) model, assuming dissolution-absorption half-times of 10, 100, and 1,000 days for the accumulation, intermodal, and coarse modes, respectively, of continuous exposures to Philadelphia and Phoenix aerosols (described in Appendix 10C) at  $50 \mu\text{g}/\text{m}^3$ . Predictions shown for a normal augmenter adult male with a general population activity level.

**TABLE 10-32. PREDICTED RELATIVE PARTICLE MASS ( $\mu\text{g}$ ) IN LUNGS OF ADULT MALE "NORMAL AUGMENTER" EXPOSED CHRONICALLY TO PHOENIX TRIMODAL AEROSOL VERSUS PHILADELPHIA TRIMODAL AEROSOL**

Day	Particle Mass ( $\mu\text{g}$ ) Versus Mode: Ratio of Phoenix to Philadelphia Aerosols			
	Accum.	Intermed.	Coarse	Total
1	0.71	1.52	10.8	1.14
2	0.71	1.52	10.8	1.14
4	0.71	1.52	10.8	1.16
6	0.71	1.52	10.8	1.18
8	0.71	1.52	10.8	1.20
10	0.71	1.52	10.8	1.23
12	0.72	1.52	10.8	1.25
14	0.72	1.52	10.8	1.27
16	0.72	1.52	10.8	1.29
18	0.72	1.52	10.8	1.31
20	0.72	1.52	10.8	1.32
25	0.72	1.52	10.8	1.37
30	0.72	1.52	10.8	1.42
40	0.72	1.52	10.8	1.50
60	0.72	1.52	10.8	1.64
80	0.72	1.52	10.8	1.75
100	0.72	1.52	10.8	1.84
150	0.72	1.52	10.8	2.01
200	0.72	1.52	10.8	2.15
250	0.72	1.52	10.8	2.26
300	0.72	1.52	10.8	2.36
400	0.72	1.52	10.8	2.55
500	0.72	1.53	10.8	2.70
600	0.72	1.53	10.8	2.83
700	0.72	1.53	10.8	2.94
800	0.72	1.53	10.8	3.04
900	0.72	1.53	10.8	3.12
1000	0.72	1.53	10.8	3.19
1200	0.72	1.53	10.8	3.28
1500	0.72	1.53	10.8	3.41
2000	0.72	1.53	10.8	3.51
2500	0.72	1.53	10.8	3.57
3000	0.72	1.53	10.8	3.60
3500	0.72	1.53	10.8	3.62
4000	0.72	1.53	10.8	3.63
4500	0.72	1.53	10.8	3.64
5000	0.72	1.53	10.8	3.64
5500	0.72	1.53	10.8	3.64
6000	0.72	1.53	10.8	3.64
7000	0.72	1.53	10.8	3.65
8000	0.72	1.53	10.8	3.65
9000	0.72	1.53	10.8	3.65
10,000	0.72	1.53	10.8	3.65

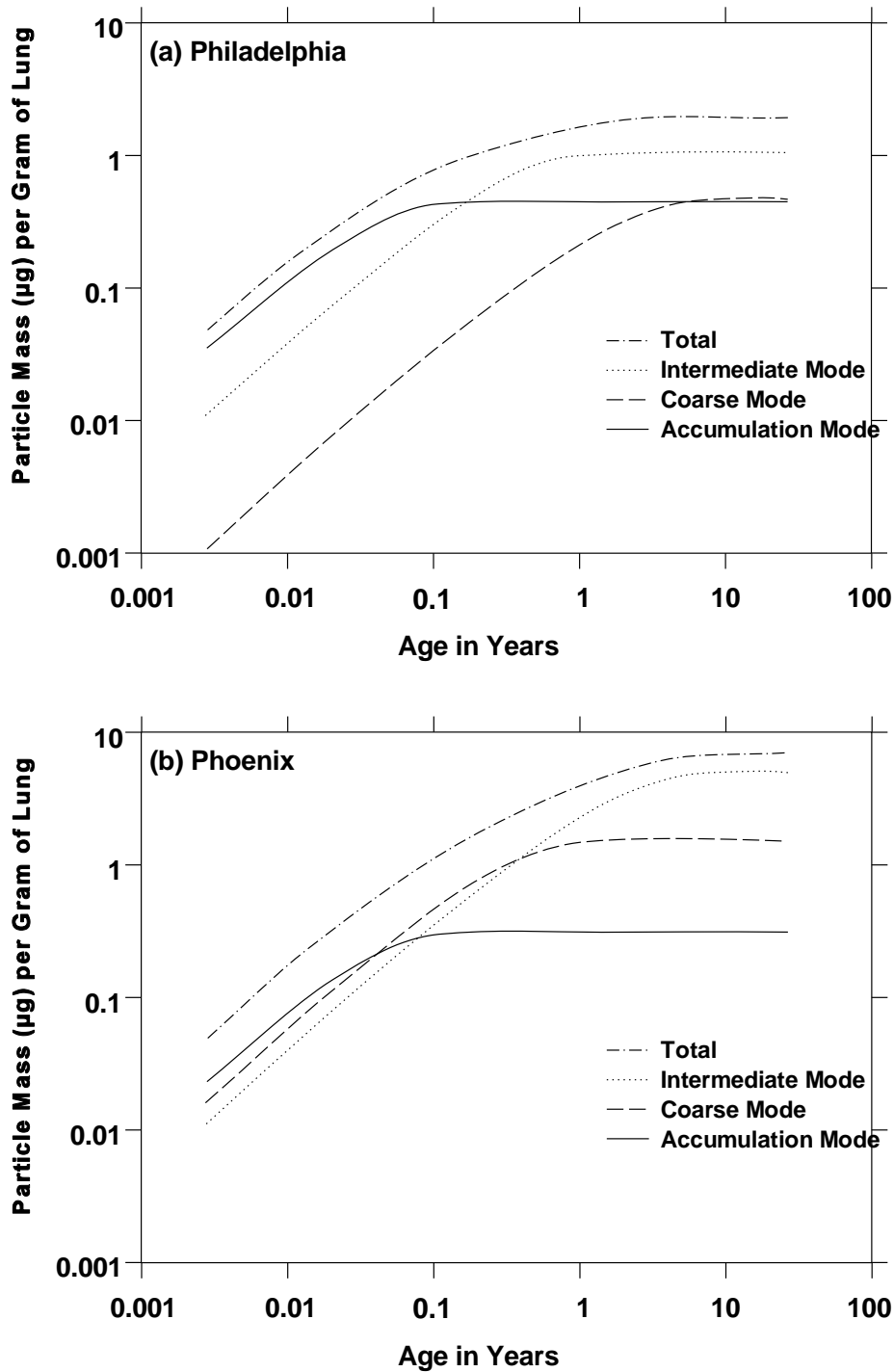


**Figure 10-56. Specific lung burden ( $\mu\text{g}$  particles/g lung) versus time (age in years) predicted by the International Commission on Radiological Protection Publication 66 (1994) model, assuming dissolution-absorption half-times of 10, 100, and 1,000 days for the accumulation, intermodal, and coarse modes, respectively, of continuous exposures to Philadelphia and Phoenix aerosols (described in Appendix 10C) at  $50 \mu\text{g}/\text{m}^3$ . Predictions shown for a normal augmenter adult male with a general population activity level.**

### 10.7.6.2 Laboratory Animal Estimates

Deposition data for two different aerosols, one with an MMAD of 1.0 and  $\sigma_g$  of 1.3, the other with an MMAD of 2.55 and a  $\sigma_g = 2.4$  were chosen to calculate total alveolar retention (Table 10-33). The aerosol with an MMAD of 1.0  $\mu\text{m}$  and  $\sigma_g$  of 1.3 was chosen as the smallest particle diameter for which the laboratory animal dosimetry model calculates fractional deposition and to represent a relatively monodisperse distribution. The aerosol with an MMAD of 2.55  $\mu\text{m}$  and a  $\sigma_g$  of 2.4 was chosen to approximate a hypothetical  $\text{PM}_{10}$  aerosol in which the  $\text{PM}_{2.5}$  to  $\text{PM}_{10}$  sample size cut ratio is 0.6 Dockery and Pope (1994).

**TABLE 10-33. FRACTION OF INHALED PARTICLES DEPOSITED IN THE ALVEOLAR REGION OF THE RESPIRATORY TRACT FOR RATS AND ADULT MALE HUMANS**

Aerosol Parameters	Fraction of Aerosol Deposited in Alveolar Region	
	Rat <sup>a</sup>	Human <sup>b</sup>
1.0 $\mu\text{m}$ MMAD, $\sigma_g = 1.3$	0.063	0.119
2.55 $\mu\text{m}$ MMAD, $\sigma_g = 2.4$	0.031	0.102

<sup>a</sup>From Tables 10-30 and 10-31.

<sup>b</sup>From (ICRP 66, 1994) average for general population activity pattern (8 h sleeping, 8 h sitting, and 8 h light activity) for adult male "normal augmentor" (See Table 10-18).

Table 10-34 provides fractional deposition data in the alveolar region for three different aerosols as predicted for the various demographic groups. Table 10-35 provides the particle deposition rates ( $\mu\text{g}/\text{d}$ ) in the alveolar regional for a 24-h exposure to an airborne mass concentration of 50  $\mu\text{g}/\text{m}^3$ . Although model simulations of retained particle burdens were not performed for these various cohorts, differences in retained particle burdens can be expected because the clearance modeling output is proportional to the deposition fractions used as input. Note the greater deposition efficiency for the larger diameter aerosols in elderly males and in those with respiratory disease.

Table 10-36 summarizes the common and specific parameters used for predicting alveolar burdens for exposures of humans and rats of the two different aerosols at a concentration of 50  $\mu\text{g}$  particles/ $\text{m}^3$ . Exposures were assumed to take place 24 h/day at the

**TABLE 10-34. FRACTION OF INHALED PARTICLES DEPOSITED IN THE ALVEOLAR REGION OF THE RESPIRATORY TRACT FOR DIFFERENT DEMOGRAPHIC GROUPS**

Aerosol Parameters	Fraction of Aerosol Deposited in Alveolar Region <sup>a</sup>						
	Male Worker (18-44) <sup>b</sup>	Female Worker (18-44) or Elderly Female (over 65) <sup>c</sup>	Elderly Male over 65 <sup>d</sup>	Male Respiratory Compromised <sup>e</sup>	Child (14-18) <sup>f</sup>	Child (6-13) <sup>g</sup>	Child (0-5) <sup>h</sup>
0.5 $\mu\text{m}$ MMAD, $\sigma_g = 1.3$	0.085	0.079	0.085	0.086	0.079	0.067	0.069
1.0 $\mu\text{m}$ MMAD, $\sigma_g = 1.3$	0.135	0.125	0.138	0.139	0.120	0.098	0.094
2.55 $\mu\text{m}$ MMAD, $\sigma_g = 2.4$	0.118	0.108	0.123	0.126	0.091	0.073	0.062

<sup>a</sup>Calculated using ICRP Publication 66 lung deposition model with EPA's hourly lung ventilation rates for each demographic group.

<sup>b</sup>Total daily volume of air breathed by a male worker is 19.4 m<sup>3</sup>.

<sup>c</sup>Total daily volume of air breathed by a female worker is 16.5 m<sup>3</sup>, and 16.1 m<sup>3</sup> for a female over age 65.

<sup>d</sup>Total daily volume of air breathed by a male over 65 years old is 18.1 m<sup>3</sup>.

<sup>e</sup>Total daily volume of air breathed by an adult male with compromised respiratory system is 17.4 m<sup>3</sup>.

<sup>f</sup>Total daily volume of air breathed by a child of age 14-18 years is 25.5 m<sup>3</sup>.

<sup>g</sup>Total daily volume of air breathed by a child of age 6-13 years is 18.2 m<sup>3</sup>.

<sup>h</sup>Total daily volume of air breathed by a child of age 0-5 years is 11.6 m<sup>3</sup>.

10-205

**TABLE 10-35. PARTICLE DEPOSITION RATES ( $\mu\text{g}/\text{d}$ ) IN THE ALVEOLAR REGION (FOR 24-H EXPOSURE TO AN AIRBORNE MASS CONCENTRATION OF 50  $\mu\text{g}/\text{m}^3$ )**

Aerosol Parameters	Daily Mass Deposition in Alveolar Region						
	Male Worker (18-44)	Female Worker (18-44)	Male over 65	Male Respiratory Compromised	Child (14-18)	Child (6-13)	Child (0-5)
0.5 $\mu\text{m}$ MMAD, $\sigma_g = 1.3$	82.5	65.2	76.9	74.8	100.7	61.0	40.0
1.0 $\mu\text{m}$ MMAD, $\sigma_g = 1.3$	131.3	102.8	124.7	121.2	153.0	88.7	54.6
2.55 $\mu\text{m}$ MMAD, $\sigma_g = 2.4$	114.5	89.1	111.3	109.6	116.0	66.4	36.0

**TABLE 10-36. SUMMARY OF COMMON AND SPECIFIC INHALATION EXPOSURE PARAMETERS USED FOR PREDICTING ALVEOLAR BURDENS OF PARTICLES INHALED BY RATS AND HUMANS**

A. Common Parameters:

Exposure atmosphere	50 $\mu\text{g}/\text{m}^3$
Particle MMAD, $\sigma_g$	1.0 $\mu\text{m}$ , 1.3; or 2.55 $\mu\text{m}$ , 2.4
Particle dissolution-absorption half-time	10, 100, or 1,000 days
Chronic inhalation exposure pattern	24 h/day; 7 days/week
Duration of continuous exposure	2 years

B. Specific Parameters: Particle deposition rates in the alveolar region; data calculated using information in Tables 10-33 and Appendix 10B, Tables 10B-1 and 10B-2

Species	Daily Deposition of 1.0 $\mu\text{m}$ MMAD, $\sigma_g = 1.3$		Daily Deposition of 2.55 $\mu\text{m}$ MMAD, $\sigma_g = 2.4$	
	$\mu\text{g}$	$\mu\text{g}/\text{g lung}$	$\mu\text{g}$	$\mu\text{g}/\text{g lung}$
	Rat	1.14	0.26	0.56
Human <sup>a</sup>	118	0.11	101	0.092

<sup>a</sup>Based on human deposition parameters from ICRP66 (ICRP, 1994) for an average general population activity pattern (8 h sleeping, 8 h sitting, and 8 h light activity) for adult male "normal augments" (See Table 10B-1 in Appendix 10B).

average minute respiratory ventilation and deposition fractions presented in Tables 10B-1, 10B-2, and 10-34. Daily alveolar deposition was expressed in units of  $\mu\text{g}$  particles/g lung to normalize deposition rates between the two species. Particle dissolution-absorption rates were varied; half-times of 10, 100, and 1000 days were used to simulate particles that are relatively soluble, moderately soluble, and poorly soluble. The A clearance parameters in Table 10-16 derived from the results of acute inhalation exposures of laboratory animals, were used to predict the consequences of repeated exposures of these animals. For human modeling of acute or repeated inhalation exposures, the clearance parameters as recommended by the ICRP (ICRP66, 1994) were used in the human model LUDEP<sup>®</sup> version 1.1 software.

Table 10-37 shows the calculated alveolar particle burdens of the 1.0  $\mu\text{m}$  MMAD ( $\sigma_g = 1.3$ ) aerosol in rats and an adult human normal augments for a general population activity pattern, assuming a particle dissolution-absorption half-time of 10, 100, and 1,000 days, respectively. Table 10-38 shows the analogous calculated alveolar particle

**TABLE 10-37. ALVEOLAR PARTICLE BURDENS ( $\mu\text{g}$ ) OF EXPOSURE TO  
 $50 \mu\text{g}/\text{m}^3$  OF  $1.0 \mu\text{m}$  MASS MEDIAN AERODYNAMIC DIAMETER (MMAD) AEROSOL,  
 ASSUMING PARTICLE DISSOLUTION-ABSORPTION HALF-TIME OF 10, 100, OR 1,000 DAYS**

Exposure Days	10 Days		100 Days		1000 Days	
	Rat	Human	Rat	Human	Rat	Human
1	1.04	114	1.11	117	1.11	117
7	5.52	642	6.96	790	7.13	808
14	8.31	1020	12.4	1510	13.0	1580
21	9.74	1250	16.8	2170	17.8	2310
28	10.5	1380	20.2	2780	21.9	3020
35	10.9	1460	23.1	3340	25.3	3700
50	11.2	1540	27.5	4400	31.2	5090
75	11.3	1570	32.1	5840	37.9	7210
91	11.3	1580	33.9	6600	40.9	8460
100	11.3	1580	34.7	6980	42.4	9160
150	11.3	1580	37.4	8610	48.1	12700
200	11.3	1580	38.6	9690	51.8	15900
300	11.3	1580	39.7	10900	56.6	21600
400	11.3	1580	40.1	11500	59.8	26400
500	11.3	1580	40.2	11700	62.1	30500
600	11.3	1580	40.3	11800	63.9	34100
700	11.3	1580	40.3	11900	65.3	37100
730	11.3	1580	40.3	11900	65.7	38000

10-207

**TABLE 10-38. ALVEOLAR PARTICLE BURDENS ( $\mu\text{g}$ ) OF EXPOSURE TO  
 $50 \mu\text{g}/\text{m}^3$  OF  $2.55 \mu\text{m}$  MASS MEDIAN AERODYNAMIC DIAMETER (MMAD) AEROSOL,  
 ASSUMING PARTICLE DISSOLUTION-ABSORPTION HALF-TIME OF 10, 100, OR 1,000 DAYS**

Exposure Days	10 Days		100 Days		1000 Days	
	Rat	Human	Rat	Human	Rat	Human
1	0.51	96.0	0.54	99.1	0.54	99.3
7	2.70	542	3.40	666	3.49	681
14	4.06	861	6.07	1280	6.34	1330
21	4.76	1050	8.19	1830	8.71	1950
28	5.12	1160	9.89	2340	10.7	2540
35	5.31	1230	11.3	2820	12.4	3120
50	5.47	1300	13.5	3710	15.2	4290
75	5.53	1320	15.7	4930	18.5	6080
91	5.53	1330	16.6	5570	20.0	7140
100	5.53	1330	17.0	5890	20.7	7730
150	5.53	1330	18.3	7260	23.5	10700
200	5.53	1330	18.9	8170	25.3	13400
300	5.53	1330	19.4	9200	27.7	18200
400	5.53	1330	19.6	9660	29.2	22200
500	5.53	1330	19.6	9890	30.4	25800
600	5.53	1330	19.7	9980	31.2	28700
700	5.53	1330	19.7	10000	31.9	31300
730	5.53	1330	19.7	10000	32.1	32000

10-208

burdens for the 2.55  $\mu\text{m}$  MMAD ( $\sigma_g = 2.4$ ) aerosol. Note the different patterns for accumulations of A burdens of particles for these species. These simulations suggest that significant A burdens of particles can be reached with exposures to relatively low aerosol concentrations of 50  $\mu\text{g}/\text{m}^3$ . Particle burdens increase with time until an equilibrium burden is achieved. This burden is achieved more rapidly for less soluble particles. The maximal equilibrium particle burden is much higher for poorly soluble particles and also slightly higher for the smaller diameter (1  $\mu\text{m}$ ) particles.

The exposure concentration is representative of environmental ambient aerosols that have been recorded for numerous American and European cities. An important point to make is that the composition of the ambient aerosols vary from one place to another and constituents of the aerosols undoubtedly cover a broad range of solubilization and absorption characteristics. Therefore, the composition of the retained particles would be expected to change with time and the accumulated A burdens would consist of the more persistent types of particles or constituents of particles present in ambient aerosols. The more soluble, and perhaps more toxic, constituents of the aerosols will be rapidly absorbed into the circulatory system, metabolized, excreted, or redeposited in body organs.

Data in Tables 10-37 and 10-38 were used together with the data in Table 10B-2 to calculate the  $\mu\text{g}$  of particles per gram of lung tissue for each aerosol at each of the assumed particle dissolution-absorption half-life times. Panels a, b, and c in Figure 10-57 show the alveolar particle burdens normalized to lung tissue weight ( $\mu\text{g}$  particles per g lung tissue) for the 1.0  $\mu\text{m}$  MMAD ( $\sigma_g = 1.3$ ) aerosol assuming particle dissolution-absorption half-times of 10, 100, and 1,000 days, respectively. Panels a, b, and c in Figure 10-58 show the alveolar particle burdens normalized to lung tissue weight ( $\mu\text{g}$  particles per g lung tissue) for the 2.55  $\mu\text{m}$  MMAD ( $\sigma_g = 2.4$ ) aerosol assuming particle dissolution-absorption half-times of 10, 100, and 1,000 days, respectively. The rat alveolar burden is predicted to be greater than that of humans if a dissolution-absorption half-time of 10 days is assumed but remains at lower alveolar particle burdens than the humans if 100 or 1,000 days is assumed for the dissolution-absorption half-time.

Figure 10-58 shows the rat and human alveolar particle burdens for the larger diameter and more polydisperse aerosol (2.55  $\mu\text{m}$  MMAD,  $\sigma_g = 2.4$ ). At short dissolution-absorption half-times, the rat and human are predicted to have very similar alveolar particle burdens,

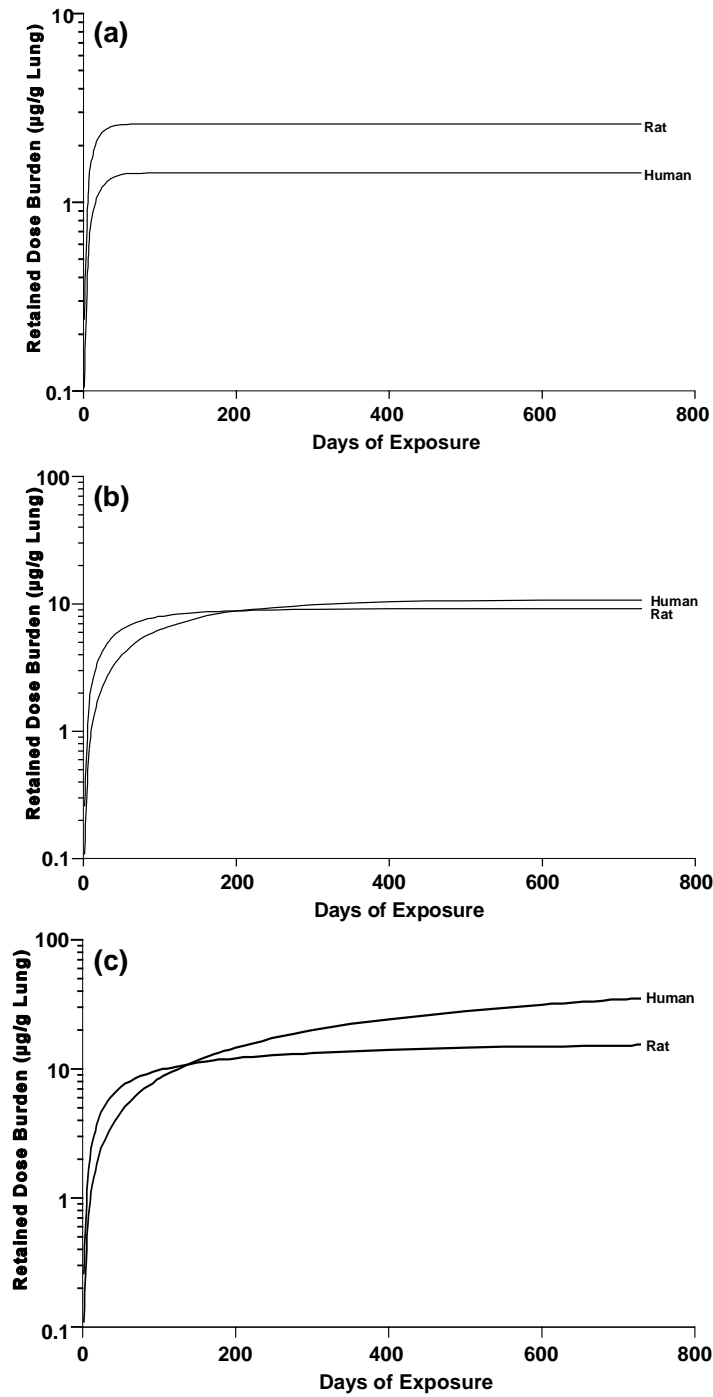


**Figure 10-57.** Predicted retained alveolar dose ( $\mu\text{g/g}$  lung) in a normal augmenter human or in a rat for exposure at  $50 \mu\text{g}/\text{m}^3$  to  $1.0 \mu\text{m}$  mass median aerodynamic diameter (MMAD) monodisperse ( $\sigma_g = 1.3$ ) aerosol, assuming a dissolution-absorption half-time of (a) 10 days, (b) 100 days, or (c) 1,000 days.

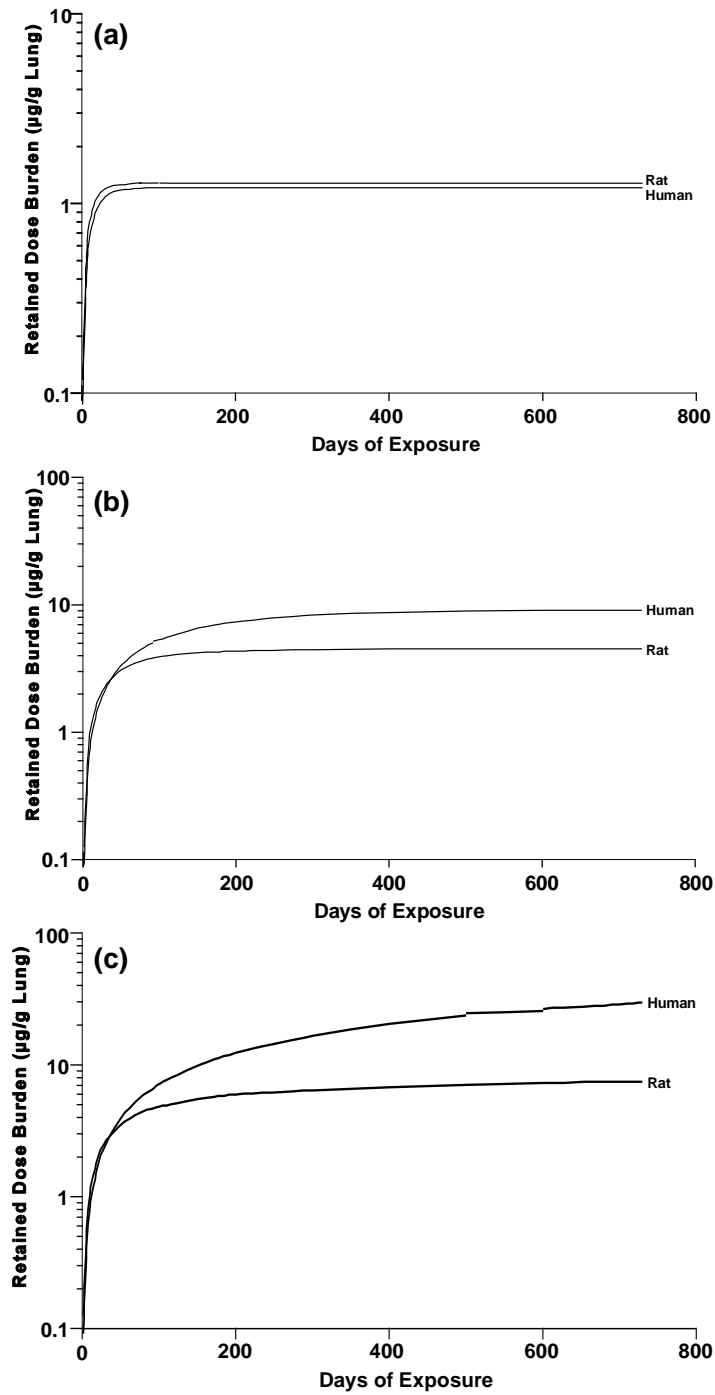


**Figure 10-58. Predicted retained alveolar dose ( $\mu\text{g/g}$  lung) in a normal augmenter human or in a rat for exposure at  $50 \mu\text{g}/\text{m}^3$  to  $2.55 \mu\text{m}$  mass median aerodynamic diameter (MMAD) polydisperse aerosol ( $\sigma_g = 2.4$ ), assuming a dissolution-absorption half-time (a) of 10 days, (b) 100 days, or (c) 1,000 days.**

with the rat having a slightly greater burden at an assumed dissolution-absorption half-time of 10-days. At an assumed dissolution-absorption half-time of 100 days, rat alveolar particle burden less than that of humans. By 1000 days, the rat burden is considerably lower.

Panels (a) through (c) in Figure 10-59 show the rat to human alveolar retained dose ratios ( $\mu\text{g}/\text{d lung}$ ) for both aerosols and assuming particle dissolution-absorption half-times of 10, 100, and 1,000 days, respectively. Because retention involves clearance processes that can translocate particle mass, the particle mass burden was normalized to lung tissue weight ( $\mu\text{g particles per g lung tissue}$ ). These ratios could be calculated using Equation 10-54 and could be used for interspecies extrapolation of "chronic" effects. Tables 10-38 and 10-39 provide the  $(AI_r)$  term. Tables 10-27 through 10-32 provide the  $(F_{rA})$  term. Normalizing factor data and ventilation rates for laboratory humans and laboratory animals are provided in Tables 10B-1 and 10B-2, respectively. These figures present the  $RRDR_{A[ACT]}$  values that would be applied to a given concentration to calculate an HEC for the rat for these simulated continuous exposures. It is apparent that a substantial range of exposure concentrations would be required to produce the same specific A burdens in these mammalian species, and the exposure concentrations depend on the exposure protocol, or study duration. These results demonstrate the importance of understanding respiratory, deposition, and physical clearance parameters of humans and laboratory animals, as well as the dissolution-absorption characteristics of the inhaled particles. This combination of factors results in significant species differences in A accumulation patterns of inhaled particles during the course of repeated or chronic exposures which must be considered in experiments designed to achieve equivalent alveolar burdens, or in evaluating the results of inhalation exposures of different mammalian species to the same aerosolized test materials.

These retained dose ratios are different than those predicted for deposited dose, reflecting both a difference in normalizing factor as well as differences in clearance rates and the dissolution-absorption characteristics of the inhaled particles.

### **10.7.7 Summary**

Major factors that affect the disposition (deposition, uptake, distribution, metabolism, and elimination) of inhaled particles in the respiratory tract include physicochemical characteristics of the inhaled aerosol (e.g., particle size, distribution, solubility,

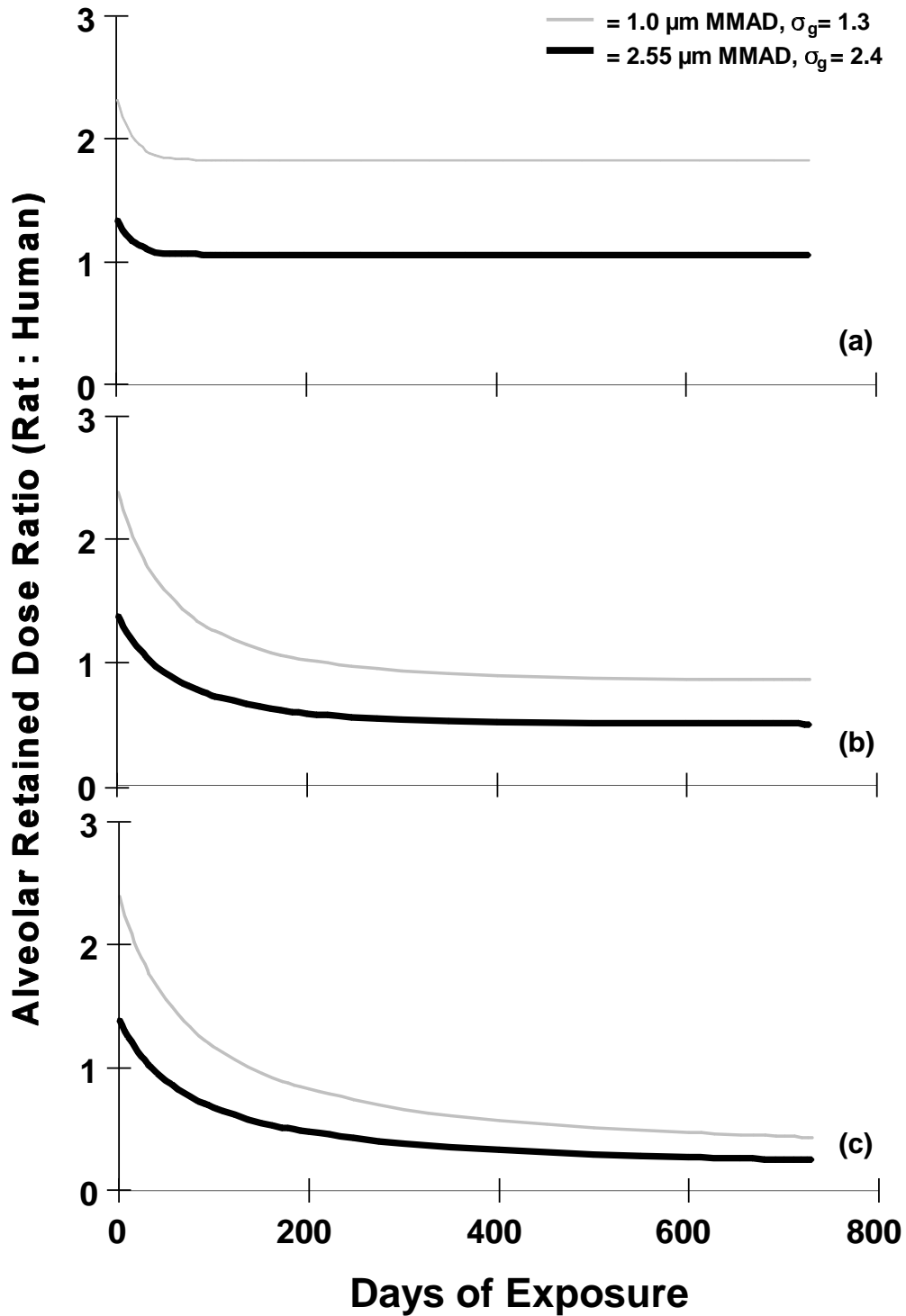


Figure 10-59. Predicted alveolar region retained dose ratios in rats versus humans for chronically inhaled exposure at  $50 \mu\text{g}/\text{m}^3$  to  $1.0 \mu\text{m}$  mass median aerodynamic diameter (MMAD) monodisperse ( $\sigma_g = 1.3$ ) and  $2.55 \mu\text{m}$  MMAD polydisperse ( $\sigma_g = 2.4$ ) aerosols, assuming a dissolution- absorption half-time of (a) 10 days, (b) 100 days, or (c) 1,000 days.

hygroscopicity) and anatomic (e.g., architecture and size of upper and lower airways, airway diameters, airway lengths, branching patterns) and physiological (e.g., ventilation rates, clearance mechanisms) parameters of individual mammalian species.

Differences in susceptibility can be due to either differences in dosimetry (i.e., differences in deposited and retained particle mass or number) or tissue sensitivity. The simulations performed herein were limited to an exploration of differences in dosimetry. At present, respiratory tract dosimetry must rely on many simplifications and empiricisms, but even a somewhat rudimentary effort assists in linking exposure to potential effects, provides insight on intrahuman variability, and aids interspecies extrapolations.

The objective of this exercise was to provide useful insights about dose metrics such as average mass concentrations and average numbers of particles per unit area of respiratory regions. Construction of more detailed theoretical or PBPK model structures to explore site-specific dosimetry at the level of individual lung lobes awaits the availability of data with which to estimate parameters.

Dose may be accurately described by particle deposition alone if the particles exert their primary action on the surface contacted (Dahl et al., 1991), i.e., deposited dose may be an appropriate metric for acute effects. For longer-term effects, the initially deposited dose may not be as decisive a metric since particles clear at varying rates from different lung regions. To characterize these effects, a retained dose that includes the effects of both deposition and clearance is more appropriate. For the present document, average deposited particle mass burden in each region of the respiratory tract was selected as the dose metric for "acute" effects in both humans and laboratory animals. Average retained particle mass burden in each region for humans and in the lower respiratory tract for laboratory animals was selected as the dose metric for "chronic" effects. These choices were dictated by the availability of the dosimetry models and the input of anatomical and morphometric information.

Ventilatory activity pattern and breathing mode (nose or mouth) were confirmed as major factors affecting inhaled particle deposition. Variations in mass deposition fraction were shown for adult males with a general population activity pattern versus adult male workers with light or heavy activity patterns. Eight demographic groups were constructed that differed in ventilation pattern by age, gender, and cardiopulmonary health status. In the alveolar (A) region, the cohort of children 14 to 18 years showed slightly higher deposition of particles less than approximately

0.1  $\mu\text{m}$  when compared to the other cohorts, whereas the cohort of children 0 to 5 years showed a decrease. When evaluated on the basis of daily mass deposition ( $\mu\text{g}/\text{d}$ ), the cohort of children ages 14 to 18 years showed an increase in deposition for all three regions of the respiratory tract compared to other cohorts, whereas the cohort of children 0 to 5 years showed a decrease. This is due primarily to differences in minute volume relative to lung size.

Other differences in dosimetry such as altered respiratory tract architecture with altered flow pattern or differences in susceptibility of the target tissue are not addressed in these simulations. As discussed earlier, Anderson et al. (1990) have shown enhanced deposition of ultrafine particles in patients with COPD compared to healthy subjects. Miller et al. (1995) used a more detailed theoretical multipath model and estimated enhanced deposition in a model of compromised lung status defined by decreased ventilation to some parts of the respiratory tract. The simulations performed herein were limited to average particle mass burdens in each region of the respiratory tract. Nevertheless, these simulations do suggest differences for these cohorts. For example, the cohort of children 14 to 18 years showed an enhanced deposition rate ( $\mu\text{g}/\text{d}$ ) for submicron-sized particles in all three respiratory tract regions whereas children 0 to 5 years showed a decrease deposition rate relative to male and female adults. For larger particles (micron-sized and above), the 14 to 18-year cohort showed no enhanced deposition rate in the tracheobronchial or alveolar regions compared to adults, and younger children cohorts showed a progressive decrease with decreasing age.

A number of simulations were performed in order to illustrate the relationship between deposition efficiency of the respiratory tract, mass burden of particles in the thoracic portion of the respiratory tract, and the mass distribution of aerosols collected by a  $\text{PM}_{10}$  or  $\text{PM}_{2.5}$  sampler. Simulations were performed for single mode aerosols of different particle diameters. It is clear that mouth (habitually oronasal) breathers have a greater deposition of particles  $>1 \mu\text{m}$  than do normal augmenter (habitually nasal) breathers. Whereas  $\text{PM}_{10}$  accounts for all particles in the thoracic size deposition mode, the  $\text{PM}_{2.5}$  sample does not include some larger particles that would be deposited in the TB and A regions of mouth breathers, under the simulated conditions (general population activity pattern 8 h sleep, 8 h sitting, 8 h light activity). Habitual oronasal (mouth) breathers do not represent a large percentage of the population, but are cited here to illustrate the difference effect of breathing habit.

Because the real world situation is more complex and ambient aerosols are multi-modal having a broad distribution of particle size and composition, similar simulations were performed using ambient aerosols, as characterized for either Philadelphia or Phoenix. These simulations of ambient aerosols showed that the  $PM_{2.5}$  sampler distribution accounts for the particle mass in the fine ( $<1.0 \mu\text{m}$ ) mode and the transition mode (MMAD  $\sim 2.5 \mu\text{m}$ ) but does not account for the smaller mass of coarse mode particles that would be deposited in the thorax (mainly affecting tracheobronchial deposition in mouth breathers). Failure of  $PM_{2.5}$  to account for coarse mode particle thoracic deposition is more severe for the Phoenix aerosol than for the Philadelphia aerosol.

Doses are conventionally expressed in terms of particle mass (gravimetric dose). However, when different types of particles are compared, doses may be more appropriately expressed as particle volume, particle surface area, or numbers of particles, depending on the effect in question (Oberdörster et al., 1994). For example, the retardation of alveolar macrophage-mediated clearance due to particle overload appears to be better correlated with phagocytized particle volume rather than mass (Morrow, 1988). The smaller size fractions of aerosols are associated with the bulk of surface area and particle number. That is, concentrations in this size fraction are very small by mass but extremely high by number. The need to consider alternative dose metrics such as number is accentuated when the high rate of deposition of small particles in the lower respiratory tract (TB and A regions), the putative target for the mortality and morbidity effects of PM exposures, is also taken into account. Simulations of particle number deposition fraction for ambient aerosols characterized for Philadelphia and Phoenix confirm that the fine mode contributes the highest deposition fraction in each region of the respiratory tract. Particle numbers deposited per day were shown to be on the order of 100,000,000 and 1,000,000,000 for the fine mode of Philadelphia and Phoenix, respectively, for hypothetical exposure to a total aerosol mass concentration of  $50 \mu\text{g}/\text{m}^3$ .

Inhalability is a major factor influencing interspecies variability. At the larger particle diameters (MMAD  $> 2.5 \mu\text{m}$  for  $g = 1.3$ ), the laboratory animal species have very little lower respiratory tract deposition due to the low inhalability of these particles. This may help explain why inhalation exposures of laboratory animals to high concentrations of larger diameter particles have exhibited little effect in some bioassays.

Simulations of retained particle burdens confirmed solubility as a major factor influencing clearance. Assumptions with respect to dissolution-half-times (10, 100, or 1,000 days) were shown to dramatically influence the predicted particle mass burdens. Data on in vivo solubility are needed to enhance modeling of clearance in all species. Retained particle burden accumulates more rapidly and reaches a higher equilibrium burden when the particles are poorly soluble.

## REFERENCES

- Adamson, I. Y. R.; Bowden, D. H. (1978) Adaptive responses of the pulmonary macrophagic system to carbon: II. morphologic studies. *Lab. Invest.* 38: 430-438.
- Adamson, I. Y. R.; Bowden, D. H. (1981) Dose response of the pulmonary macrophagic system to various particulates and its relationship to transepithelial passage of free particles. *Exp. Lung Res.* 2: 165-175.
- Albert, R. E.; Petrow, H. G.; Salam, A. S.; Spiegelman, J. R. (1964) Fabrication of monodisperse lucite and iron oxide particles with a spinning disk generator. *Health Phys.* 10: 933-940.
- Albert, R. E.; Lippmann, M.; Spiegelman, J.; Strehlow, C.; Briscoe, W.; Wolfson, P.; Nelson, N. (1967) The clearance of radioactive particles from the human lung. In: Davies, C. N., ed. *Inhaled particles and vapours II: proceedings of an international symposium; September-October 1965; Cambridge, United Kingdom.* Oxford, United Kingdom: Pergamon Press; pp. 361-378.
- Albert, R. E.; Lippmann, M.; Peterson, H. T., Jr. (1971) The effects of cigarette smoking on the kinetics of bronchial clearance in humans and donkeys. In: Walton, W. H., ed. *Inhaled particles III: proceedings of an international symposium, v. I; September 1970; London, United Kingdom.* Old Woking, Surrey, United Kingdom: Unwin Brothers Ltd.; pp. 165-182.
- Albert, R. E.; Lippmann, M.; Peterson, H. T., Jr.; Berger, J.; Sanborn, K.; Bohning, D. (1973) Bronchial deposition and clearance of aerosols. *Arch. Intern. Med.* 131: 115-127.
- Albert, R. E.; Berger, J.; Sanborn, K.; Lippmann, M. (1974) Effects of cigarette smoke components on bronchial clearance in the donkey. *Arch. Environ. Health* 29: 96-101.
- Altose, M. D. (1980) Pulmonary mechanics. In: Fishman, A. P., ed. *Pulmonary diseases and disorders.* New York, NY: McGraw-Hill Book Company; pp. 359-372.
- American Conference of Governmental Industrial Hygienists. (1968) Threshold limit values of airborne contaminants for 1968. Cincinnati, OH: American Conference of Governmental Industrial Hygienists.
- American Conference of Governmental Industrial Hygienists. (1985) Particle size-selective sampling in the workplace: report of the ACGIH technical committee on air sampling procedures. Cincinnati, OH: American Conference of Governmental Industrial Hygienists.
- Andersen, M. E.; Krishnan, K.; Conolly, R. B.; McClellan, R. O. (1992) Mechanistic toxicology research and biologically-based modeling: partners for improving quantitative risk assessments. *CIIT Activities* 12(1): 1-7.
- Anderson, E.; Browne, N.; Duletsky, S.; Ramig, J.; Warn, T. (1985) Development of statistical distributions or ranges of standard factors used in exposure assessments. Washington, DC: U.S. Environmental Protection Agency, Office of Research and Development; EPA report no. EPA-600/8-85-010. Available from: NTIS, Springfield, VA; PB85-242667.
- Anderson, P. J.; Wilson, J. D.; Hiller, F. C. (1990) Respiratory tract deposition of ultrafine particles in subjects with obstructive or restrictive lung disease. *Chest* 97: 1115-1120.
- Anonymous. (1986) Aerosols: formation and reactivity, proceedings of the second international aerosol conference; September; Berlin, Federal Republic of Germany. Oxford, United Kingdom: Pergamon Press.
- Anselm, A.; Heibel, T.; Gebhart, J.; Ferron, G. (1990) "In vivo"—studies of growth factors of sodium chloride particles in the human respiratory tract. *J. Aerosol Sci.* 21(suppl. 1): S427-S430.

- Arms, A. D.; Travis, C. C. (1988) Reference physiological parameters in pharmacokinetic modeling. Washington, DC: U.S. Environmental Protection Agency, Office of Health and Environmental Assessment; EPA report no. EPA/600/6-88/004. Available from: NTIS, Springfield, VA; PB88-196019.
- Asgharian, B.; Yu, C. P. (1988) Deposition of inhaled fibrous particles in the human lung. *J. Aerosol Med.* 1: 37-50.
- Asgharian, B.; Yu, C. P. (1989) Deposition of fibers in the rat lung. *J. Aerosol Sci.* 20: 355-366.
- Asgharian, B.; Wood, R.; Schlessinger, R. B. (1995) Empirical modeling of particle deposition in the alveolar region of the lungs: a basis for interspecies extrapolation. *Fundam. Appl. Toxicol.* 27: 232-238.
- Bailey, M. R.; Roy, M. (1994) Clearance of particles from the respiratory tract: annexe E. In: Human respiratory tract model for radiological protection: a report of a task group of the International Commission on Radiological Protection. Oxford, United Kingdom: Elsevier Science Ltd.; pp. 301-413. (ICRP publication 66; Annals of the ICRP: v. 24, nos. 1-3).
- Bailey, M. R.; Fry, F. A.; James, A. C. (1982) The long-term clearance kinetics of insoluble particles from the human lung. *Ann. Occup. Hyg.* 26: 273-290.
- Bailey, M. R.; Hodgson, A.; Smith, H. (1985a) Respiratory tract retention of relatively insoluble particles in rodents. *J. Aerosol Sci.* 16: 279-293.
- Bailey, M. R.; Fry, F. A.; James, A. C. (1985b) Long-term retention of particles in the human respiratory tract. *J. Aerosol Sci.* 16: 295-305.
- Bailey, M. R.; Kreyling, W. G.; Andre, S.; Batchelor, A.; Collier, C. G.; Drosselmeyer, E.; Ferron, G. A.; Foster, P.; Haider, B.; Hodgson, A.; Masse, R.; Metivier, H.; Morgan, A.; Müller, H.-L.; Patrick, G.; Pearman, I.; Pickering, S.; Ramsden, D.; Stirling, C.; Talbot, R. J. (1989) An interspecies comparison of the lung clearance of inhaled monodisperse cobalt oxide particles—part 1: objectives and summary of results. *J. Aerosol Sci.* 20: 169-188.
- Bair, W. J. (1961) Deposition, retention, translocation and excretion of radioactive particles. In: Davies, C. N., ed. Inhaled particles and vapours: proceedings of an international symposium; March-April 1960; Oxford, United Kingdom; New York, NY: Pergamon Press; pp. 192-208.
- Bair, W. J.; McClanahan, B. J. (1961) Plutonium inhalation studies: II. excretion and translocation of inhaled Pu<sup>239</sup>O<sub>2</sub> dust. *Arch. Environ. Health* 2: 48-55.
- Bair, W. J.; Willard, D. H.; Herring, J. P.; George, L. A., II. (1962) Retention, translocation and excretion of inhaled Pu<sup>239</sup>O<sub>2</sub>. *Health Phys.* 8: 639-649.
- Becquemin, M. H.; Roy, M.; Bouchikhi, A.; Teillac, A. (1987) Deposition of inhaled particles in healthy children. In: Hoffman, W., ed. Deposition and clearance of aerosols in the human respiratory tract. Vienna, Austria: Facultas; pp. 22-27.
- Becquemin, M. H.; Yu, C. P.; Roy, M.; Bouchikhi, A.; Teillac, A. (1991) Total deposition of inhaled particles related to age: comparison with age-dependent model calculations. *Radiat. Prot. Dosim.* 38: 23-28.
- Beeckmans, J. M. (1965) The deposition of aerosols in the respiratory tract: a mathematical analysis and comparison with experimental data. *Can. J. Physiol. Pharmacol.* 43: 157-175.
- Bell, K. A. (1978) Local particle deposition in respiratory airway models. In: Shaw, D. T., ed. Recent developments in aerosol science. New York, NY: John Wiley and Sons; pp. 97-134.

- Bell, K. A.; Friedlander, S. K. (1973) Aerosol deposition in models of a human lung bifurcation. *Staub Reinhalt. Luft* 33: 178-182.
- Bennett, W. D. (1988) Human variation in spontaneous breathing deposition fraction: a review. *J. Aerosol Med.* 1: 67-80.
- Bennett, W. D.; Smaldone, G. C. (1987) Human variation in the peripheral air-space deposition of inhaled particles. *J. Appl. Physiol.* 62: 1603-1610.
- Berteau, P. B.; Biermann, A. H. (1977) Respiratory deposition and early distribution of inhaled vegetable oil aerosols in mice and rats. *Toxicol. Appl. Pharmacol.* 39: 177-183.
- Bianco, A.; Gibb, F. R.; Kilpper, R. W.; Landman, S.; Morrow, P. E. (1974) Studies of tantalum dust in the lungs. *Radiology (Eaton, PA)* 112: 549-556.
- Bice, D. E.; Harmsen, A. G.; Muggenburg, B. A. (1990) Role of lung phagocytes in the clearance of particles by the mucociliary apparatus. *Inhalation Toxicol.* 2: 151-160.
- Birnbaum, L.; Bischoff, K.; Blancato, J.; Clewell, H.; Dedrick, R.; Delp, M.; Rhomberg, L.; Schaeffer, V. (1994) Physiological parameter values for PBPK models. Washington, DC: International Life Sciences Institute Risk Science Institute.
- Boat, T. F.; Cheng, P.-W.; Leigh, M. W. (1994) Biochemistry of mucus. In: Takishima, T.; Shimura, S., eds. *Airway secretion*. New York, NY: Marcel Dekker, Inc.; pp. 217-282. (*Lung biology in health and disease* v. 72).
- Boecker, B. B.; McClellan, R. O. (1968) The effects of solubility on the bioassay for inhaled radionuclides. In: Kornberg, H. A.; Norwood, W. D., eds. *Diagnosis and treatment of deposited radionuclides: proceedings of a symposium*; May 1967; Richland, WA. New York, NY: Excerpta Medica Foundation; pp. 236-242.
- Bohning, D. E.; Atkins, H. L.; Cohn, S. H. (1982) Long-term particle clearance in man: normal and impaired. In: Walton, W. H., ed. *Inhaled particles V: proceedings of an international symposium*; September 1980; Cardiff, Wales. *Ann. Occup. Hyg.* 26: 259-271.
- Booker, D. V.; Chamberlain, A. C.; Rundo, J.; Muir, D. C. F.; Thomson, M. L. (1967) Elimination of 5  $\mu$ m particles from the human lung. *Nature (London)* 215: 30-33.
- Bowden, D. H.; Adamson, I. Y. R. (1984) Pathways of cellular efflux and particulate clearance after carbon instillation to the lung. *J. Pathol.* 143: 117-125.
- Bowes, S. M., III; Swift, D. L. (1989) Deposition of inhaled particles in the oral airway during oronasal breathing. *Aerosol Sci. Technol.* 11: 157-167.
- Boyden, E. A. (1972) The structure of the pulmonary acinus in a child of six years and eight months. *Am. J. Anat.* 132: 275-300.
- Brain, J. D. (1971) The effects of increased particles on the number of alveolar macrophages. In: Walton, W. H., ed. *Inhaled particles III: proceedings of an international symposium*, v. I; September 1970; London, United Kingdom. Old Woking, Surrey, United Kingdom: Unwin Brothers, Ltd.; pp. 209-223.
- Brain, J. D.; Blanchard, J. D. (1993) Mechanisms of particle deposition and clearance. In: Morén, F.; Dolovich, M. B.; Newhouse, M. T.; Newman, S. P., eds. *Aerosols in medicine: principles, diagnosis and therapy*. 2nd rev. ed. Amsterdam, The Netherlands: Elsevier; pp. 117-156.
- Brain, J. D.; Mensah, G. A. (1983) Comparative toxicology of the respiratory tract. *Am. Rev. Respir. Dis.* 128: S87-S90.

- Breuer, H. (1971) Problems of gravimetric dust sampling. In: Walton, W. H., ed. *Inhaled particles III*. London, United Kingdom: Unwin Bros.; pp. 1031-1042.
- Breyse, P. N.; Swift, D. L. (1990) Inhalability of large particles into the human nasal passage: in vivo studies in still air. *Aerosol Sci. Technol.* 13: 459-464.
- Briant, J. K.; Sanders, C. L. (1987) Inhalation deposition and retention patterns of a U-Pu chain aggregate aerosol. *Health Phys.* 53: 365-375.
- Brody, A. R.; Davis, G. S. (1982) Alveolar macrophage toxicology. In: Witschi, H.; Nettesheim, P., eds. *Mechanisms in respiratory toxicology: volume II*. Boca Raton, FL: CRC Press, Inc.; pp. 3-28.
- Brody, A. R.; Hill, L. H.; Adkins, B., Jr.; O'Connor, R. W. (1981) Chrysotile asbestos inhalation in rats: deposition pattern and reaction of alveolar epithelium and pulmonary macrophages. *Am. Rev. Respir. Dis.* 123: 670-679.
- Brown, J. H.; Cook, K. M.; Ney, F. G.; Hatch, T. (1950) Influence of particle size upon the retention of particulate matter in the human lung. *Am. J. Public Health* 40: 450-458, 480.
- Brundelet, P. J. (1965) Experimental study of the dust-clearance mechanism of the lung: I. histological study in rats of the intra-pulmonary bronchial route of elimination. *Acta Pathol. Microbiol. Scand. Suppl.* 175: 1-141.
- Camner, P.; Mossberg, B.; Philipson, K.; Strandberg, K. (1979) Elimination of test particles from the human tracheobronchial tract by voluntary coughing. *Scand. J. Respir. Dis.* 60: 56-62.
- Camner, P.; Curstedt, T.; Jarstrand, C.; Johannsson, A.; Robertson, B.; Wiernik, A. (1985) Rabbit lung after inhalation of manganese chloride: a comparison with the effects of chlorides of nickel, cadmium, cobalt, and copper. *Environ. Res.* 38: 301-309.
- Carlberg, J. R.; Crable, J. V.; Limtiaca, L. P.; Norris, H. B.; Holtz, J. L.; Mauer, P.; Wolowicz, F. R. (1971) Total dust, coal, free silica, and trace metal concentrations in bituminous coal miners' lungs. *Am. Ind. Hyg. Assoc. J.* 32: 432-440.
- Casarett, L. J. (1975) Toxicology of the respiratory system. In: Casarett, L. J.; Doull, J., eds. *Toxicology: the basic science of poisons*. New York, NY: MacMillan Publishing Co., Inc.; pp. 201-224.
- Chan, T. L.; Lippmann, M. (1980) Experimental measurements and empirical modelling of the regional deposition of inhaled particles in humans. *Am. Ind. Hyg. Assoc. J.* 41: 399-409.
- Chan, T. L.; Lippmann, M.; Cohen, V. R.; Schlesinger, R. B. (1978) Effect of electrostatic charges on particle deposition in a hollow cast of the human larynx-tracheobronchial tree. *J. Aerosol Sci.* 9: 463-468.
- Chang, H. K.; Menon, A. S. (1993) Airflow dynamics in the human airways. In: Morén, F.; Dolovich, M. B.; Newhouse, M. T.; Newman, S. P., eds. *Aerosols in medicine: principles, diagnosis and therapy*. 2nd rev. ed. Amsterdam, The Netherlands: Elsevier; pp. 85-116.
- Chen, L. C.; Wu, C. Y.; Qu, Q. S.; Schlesinger, R. B. (1995) Number concentration and mass concentration as determinants of biological response to inhaled irritant particles. In: Phalen, R. F.; Bates, D. V., eds. *Proceedings of the colloquium on particulate air pollution and human mortality and morbidity, part II; January 1994; Irvine, CA*. *Inhalation Toxicol.* 7: 577-588.
- Cheng, Y.-S.; Yamada, Y.; Yeh, H.-C.; Swift, D. L. (1988) Diffusional deposition of ultrafine aerosols in a human nasal cast. *J. Aerosol. Sci.* 19: 741-751.

- Cheng, Y.-S.; Yamada, Y.; Yeh, H.-C.; Swift, D. L. (1990) Deposition of ultrafine aerosols in a human oral cast. *Aerosol Sci. Technol.* 12: 1075-1081.
- Cheng, Y.-S.; Su, Y.-F.; Yeh, H.-C.; Swift, D. L. (1993) Deposition of thoron progeny in human head airways. *Aerosol Sci. Technol.* 18: 359-375.
- Cocks, A. T.; Fernando, R. P. (1982) The growth of sulphate aerosols in the human airways. *J. Aerosol Sci.* 13: 9-19.
- Cocks, A. T.; McElroy, W. J. (1984) Modeling studies of the concurrent growth and neutralization of sulfuric acid aerosols under conditions in the human airways. *Environ. Res.* 35: 79-96.
- Coenen, W. (1971) Berechnung von Umrechnungsfaktoren für verschiedene Feinstaubmessverfahren [Estimation of conversion factors for different fine dust measurement methods]. In: Walton, W. H., ed. *Inhaled particles III*. London, United Kingdom: Unwin Brothers; pp. 1045-1050.
- Cohen, D.; Arai, S. F.; Brain, J. D. (1979) Smoking impairs long-term dust clearance from the lung. *Science* (Washington, DC) 204: 514-517.
- Cohen, B. S.; Harley, N. H.; Schlesinger, R. B.; Lippmann, M. (1988) Nonuniform particle deposition on tracheobronchial airways: implications for lung dosimetry. *Ann. Occup. Hyg.* 32(suppl. 1): 1045-1053.
- Collett, P. W.; Roussos, C.; Macklem, P. T. (1988) Respiratory mechanics. In: Murray, J. F.; Nadel, J. A., eds. *Textbook of respiratory medicine*. Philadelphia, PA: W.B. Saunders Company; pp. 85-128.
- Connolly, T. P.; Noujaim, A. A.; Man, S. F. P. (1978) Simultaneous canine tracheal transport of different particles. *Am. Rev. Respir. Dis.* 118: 965-968.
- Conolly, R. B. (1990) Biologically-based models for toxic effects: tools for hypothesis testing and improving health risk assessments. *CIIT Activities* 10: 1-8.
- Corry, D.; Kulkarni, P.; Lipscomb, M. F. (1984) The migration of bronchoalveolar macrophages into hilar lymph nodes. *Am. J. Pathol.* 115: 321-328.
- Cotes, J. E. (1979) *Lung function: assessment and application in medicine*. 4th ed. Oxford, United Kingdom: Blackwell Scientific Publications.
- Cottier, H.; Meister, F.; Zimmermann, A.; Kraft, R.; Burkhardt, A.; Gehr, P.; Poretti, G. (1987) Accumulation of anthracotic particles along lymphatics of the human lung: relevance to "hot spot" formation after inhalation of poorly soluble radionuclides. *Radiat. Environ. Biophys.* 26: 275-282.
- Crapo, J. D.; Barry, B. E.; Gehr, P.; Bachofen, M.; Weibel, E. R. (1982) Cell characteristics of the normal human lung. *Am. Rev. Respir. Dis.* 125: 740-745.
- Crapo, J. D.; Young, S. L.; Fram, E. K.; Pinkerton, K. E.; Barry, B. E.; Crapo, R. O. (1983) Morphometric characteristics of cells in the alveolar region of mammalian lungs. *Am. Rev. Respir. Dis.* 128: S42-S46.
- Crawford, D. J. (1982) Identifying critical human subpopulations by age groups: radioactivity and the lung. *Phys. Med. Biol.* 27: 539-552.
- Creasia, D. A.; Nettesheim, P.; Hammons, A. S. (1973) Impairment of deep lung clearance by influenza virus infection. *Arch. Environ. Health* 26: 197-201.
- Cuddihy, R. G. (1978) Deposition and retention of inhaled niobium in beagle dogs. *Health Phys.* 34: 167-176.

- Cuddihy, R. G. (1984) Mathematical models for predicting clearance of inhaled radioactive materials. In: Smith, H.; Gerber, G., eds. Lung modeling for inhalation of radioactive materials. Luxembourg: Commission of the European Communities; pp. 167-176; report no. EUR9384EN.
- Cuddihy, R. G.; Yeh, H. C. (1988) Respiratory tract clearance of particles and substances dissociated from particles. In: Mohr, U.; Dungworth, D.; Kimmerle, G.; Lewkowski, J.; McClellan, R.; Stöber, W., eds. Inhalation toxicology: the design and interpretation of inhalation studies and their use in risk assessment. New York, NY: Springer-Verlag; pp. 169-193.
- Cuddihy, R. G.; Hall, R. P.; Hobbs, C. H.; Boecker, B. B.; Muggenburg, B. A. (1972) Tissue blood volumes and weights in adult Beagle dogs. In: McClellan, R. O.; Rupperecht, F. C., eds. Annual report of the fission product inhalation program, Lovelace Foundation for Medical Education and Research, Albuquerque, New Mexico, October 1, 1971 through September 30, 1972. Washington, DC: U.S. Atomic Energy Commission, Division of Biomedical and Environmental Research; contract no. AT(29-2)-1013. Available from: NTIS, Springfield, VA; LF-45.
- Cuddihy, R. G.; McClellan, R. O.; Griffith, W. C. (1979) Variability in target organ deposition among individuals exposed to toxic substances. *Toxicol. Appl. Pharmacol.* 49: 179-187.
- Cuddihy, R. G.; Fisher, G. L.; Moss, O. R.; Phalen, R. F.; Schlesinger, R. B.; Swift, D. L.; Yeh, H. C. (1988) New approaches to respiratory tract dosimetry modeling for inhaled radionuclides. *Ann. Occup. Hyg.* 32(suppl. 1): 833-841.
- Dahl, A. R.; Griffith, W. C. (1983) Deposition of sulfuric acid mist in the respiratory tracts of guinea pigs and rats. *J. Toxicol. Environ. Health* 12: 371-383.
- Dahl, A. R.; Snipes, M. B.; Muggenburg, B. A.; Young, T. C. (1983) Deposition of sulfuric acid mists in the respiratory tract of beagle dogs. *J. Toxicol. Environ. Health* 11: 141-149.
- Dahl, A. R.; Schlesinger, R. B.; Heck, H. D' A.; Medinsky, M. A.; Lucier, G. W. (1991) Comparative dosimetry of inhaled materials: differences among animal species and extrapolation to man. *Fundam. Appl. Toxicol.* 16: 1-13.
- Dahlbäck, M.; Eirefelt, S. (1994) Total deposition of fluorescent monodisperse particles in rats. *Ann. Occup. Hyg.* 38: suppl. 1; pp. 127-134.
- Dahlbäck, M.; Eirefelt, S.; Karlberg, I.-B.; Nerbrink, O. (1989) Total deposition of Evans blue in aerosol exposed rats and guinea pigs. *J. Aerosol Sci.* 20: 1325-1327.
- Damon, E. G.; Mokler, B. V.; Jones, R. K. (1983) Influence of elastase-induced emphysema and the inhalation of an irritant aerosol on deposition and retention of an inhaled insoluble aerosol in Fischer-344 rats. *Toxicol. Appl. Pharmacol.* 67: 322-330.
- Davies, C. N. (1952) Dust sampling and lung disease. *Br. J. Ind. Med.* 9: 120-126.
- Davies, C. N., ed. (1961) Discussion [of particle deposition in the human respiratory system]. In: Inhaled particles and vapours: proceedings of an international symposium; March-April 1960; Oxford, United Kingdom. New York, NY: Pergamon Press; pp. 88-91.
- Davies, C. N. (1972) An algebraical model for the deposition of aerosols in the human respiratory tract during steady breathing. *J. Aerosol Sci.* 3: 297-306.
- Dennis, W. L. (1961) Discussion. In: Davies, C. N., ed. Inhaled particles and vapours: proceedings of an international symposium; March-April 1960; Oxford, United Kingdom. New York, NY: Pergamon Press; pp. 82-91.

- Diu, C. K.; Yu, C. P. (1983) Respiratory tract deposition of polydisperse aerosols in humans. *Am. Ind. Hyg. Assoc. J.* 44: 62-65.
- Dockery, D. W.; Pope, C. A., III. (1994) Acute respiratory effects of particulate air pollution. *Annu. Rev. Public Health* 15: 107-132.
- Dolovich, M. B.; Sanchis, J.; Rossman, C.; Newhouse, M. T. (1976) Aerosol penetrance: a sensitive index of peripheral airways obstruction. *J. Appl. Physiol.* 40: 468-471.
- Edwards, A. W. T.; Velasquez, T.; Farhi, L. E. (1963) Determination of alveolar capillary temperature. *J. Appl. Physiol.* 18: 107-113.
- Egan, M. J.; Nixon, W. (1985) A model of aerosol deposition in the lung for use in inhalation dose assessments. *Radiat. Prot. Dosim.* 11: 5-17.
- Egan, M. J.; Nixon, W. (1989) On the relationship between experimental data for total deposition and model calculations—part II: application to fine particle deposition in the respiratory tract. *J. Aerosol Sci.* 20: 149-156.
- Egan, M. J.; Nixon, W.; Robinson, N. I.; James, A. C.; Phalen, R. F. (1989) Inhaled aerosol transport and deposition calculations for the ICRP Task Group. *J. Aerosol Sci.* 20: 1301-1304.
- Emmett, P. C.; Aitken, R. J. (1982) Measurements of the total and regional deposition of inhaled particles in the human respiratory tract. *J. Aerosol Sci.* 13: 549-560.
- Emmett, P. C.; Aitken, R. J.; Hannan, W. J. (1982) Measurements of the total and regional deposition of inhaled particles in the human respiratory tract. *J. Aerosol Sci.* 13: 549-560.
- Esposito, A. L.; Pennington, J. E. (1983) Effects of aging on antibacterial mechanisms in experimental pneumonia. *Am. Rev. Respir. Dis.* 128: 662-667.
- Evans, J. C.; Evans, R. J.; Holmes, A.; Hounam, R. F.; Jones, D. M.; Morgan, A.; Walsh, M. (1973) Studies on the deposition of inhaled fibrous material in the respiratory tract of the rat and its subsequent clearance using radioactive tracer techniques: 1. UICC crocidolite asbestos. *Environ. Res.* 6: 180-201.
- Felicetti, S. A.; Wolff, R. K.; Muggenburg, B. A. (1981) Comparison of tracheal mucous transport in rats, guinea pigs, rabbits, and dogs. *J. Appl. Physiol.: Respir. Environ. Exercise Physiol.* 51: 1612-1617.

- Ferin, J. (1977) Effect of particle content of lung on clearance pathways. In: Sanders, C. L.; Schneider, R. P.; Dagle, G. E.; Ragan, H. A., eds. Pulmonary macrophages and epithelial cells: proceedings of the sixteenth annual Hanford biology symposium; September 1976; Richland, WA. Oak Ridge, TN: Energy Research and Development Administration; pp. 414-423. Available from: NTIS, Springfield, VA; CONF-760927. (ERDA symposium series 43).
- Ferin, J.; Feldstein, M. L. (1978) Pulmonary clearance and hilar lymph node content in rats after particle exposure. *Environ. Res.* 16: 342-352.
- Ferin, J.; Leach, L. J. (1977) The effects of selected air pollutants on clearance of titanic oxide particles from the lungs of rats. In: Walton, W. H.; McGovern, B., eds. Inhaled particles IV: proceedings of an international symposium, part 1; September 1975; Edinburgh, United Kingdom. Oxford, United Kingdom: Pergamon Press, Ltd.; pp. 333-341.
- Ferin, J.; Oberdörster, G.; Penney, D. P. (1992) Pulmonary retention of ultrafine and fine particles in rats. *Am. J. Respir. Cell Mol. Biol.* 6: 535-542.
- Ferron, G. A.; Haider, B.; Kreyling, W. G. (1983) Aerosol particle growth in the human airways using a calculated humidity profile. *J. Aerosol Sci.* 14: 196-199.
- Ferron, G. A.; Haider, B.; Kreyling, W. G. (1985) A method for the approximation of the relative humidity in the upper human airways. *Bull. Math. Biol.* 47: 565-589.
- Ferron, G. A.; Kreyling, W. G.; Haider, B. (1988) Inhalation of salt aerosol particles—II. growth and deposition in the human respiratory tract. *J. Aerosol Sci.* 19: 611-631.
- Ferron, G. A.; Karg, E.; Rudolf, G. (1992) Deposition of polydisperse hygroscopic aerosol particles in the human respiratory tract: estimation of errors in the calculation methods. *J. Aerosol Sci.* 23(suppl. 1) S465-S468.
- Ferron, G. A.; Karg, E.; Peter, J. E. (1993) Estimation of deposition of polydisperse hygroscopic aerosols in the human respiratory tract. *J. Aerosol Sci.* 24: 655-670.
- Finch, G. L.; Haley, P. J.; Hoover, M. D.; Snipes, M. B.; Cuddihy, R. G. (1994) Responses of rat lungs to low lung burdens of inhaled beryllium metal. *Inhalation Toxicol.* 6: 205-224.
- Finch, G. L.; Nikula, K. J.; Chen, B. T.; Barr, E. B.; Chang, I.-Y.; Hobbs, C. H. (1995) Effect of chronic cigarette smoke exposure on lung clearance of tracer particles inhaled by rats. *Fundam. Appl. Toxicol.* 24: 76-85.
- Findeisen, W. (1935) Über das Absetzen kleiner, in der Luft suspendierter Teilchen in der menschlichen Lunge bei der Atmung [The deposition of small airborne particles in the human lung during respiration]. *Pfluegers Arch. Gesamte Physiol. Menschen Tiere* 236: 367-379.
- Fine, J. M.; Gordon, T.; Thompson, J. E.; Sheppard, D. (1987) The role of titratable acidity in acid aerosol-induced bronchoconstriction. *Am. Rev. Respir. Dis.* 135: 826-830.
- Fish, B. R. (1961) Inhalation of uranium aerosols by mouse, rat, dog and man. In: Davies, C. N., ed. Inhaled particles and vapours: proceedings of an international symposium organized by the British Occupational Hygiene Society; March-April 1960; Oxford, United Kingdom. New York, NY: Pergamon Press; pp. 151-166.
- Foord, N.; Black, A.; Walsh, M. (1978) Regional deposition of 2.5-7.5  $\mu\text{m}$  diameter inhaled particles in healthy male non-smokers. *J. Aerosol Sci.* 9: 343-357.
- Forrest, J. B. (1993) Lower airway: structure and function. In: Morén, F.; Dolovich, M. B.; Newhouse, M. T.; Newman, S. P., eds. *Aerosols in medicine: principles, diagnosis and therapy*. 2nd rev. ed. Amsterdam, The Netherlands: Elsevier; pp. 27-60.

- Foster, W. M.; Langenback, E.; Bergofsky, E. H. (1980) Measurement of tracheal and bronchial mucus velocities in man: relation to lung clearance. *J. Appl. Physiol.: Respir. Environ. Exercise Physiol.* 48: 965-971.
- Fry, F. A.; Black, A. (1973) Regional deposition and clearance of particles in the human nose. *J. Aerosol Sci.* 4: 113-124.
- Fukuta, N.; Walter, L. A. (1970) Kinetics of hydrometeor growth from a vapor-spherical model. *J. Atmos. Sci.* 27: 1160-1172.
- Fung, Y. C. (1990) *Biomechanics: motion, flow, stress, and growth.* New York, NY: Springer-Verlag; pp. 230-231.
- Galibin, G. P.; Parfenov, Yu. D. (1971) Inhalation study on metabolism of insoluble uranium compounds. In: Walton, W. H., ed. *Inhaled particles III: proceedings of an international symposium, v. I; September 1970; London, United Kingdom.* Old Woking, Surrey, United Kingdom: Unwin Brothers Ltd; pp. 201-208.
- Gardner, D. E. (1984) Alterations in macrophage functions by environmental chemicals. *Environ. Health Perspect.* 55: 343-358.
- Gardner, I. D.; Lim, S. T. K.; Lawton, J. W. M. (1981) Monocyte function in ageing humans. *Mech. Ageing Dev.* 16: 233-239.
- Gatto, L. A. (1981) pH of mucus in rat trachea. *J. Appl. Physiol.: Respir. Environ. Exercise Physiol.* 50: 1224-1226.
- Gebhart, J.; Heigwer, G.; Heyder, J.; Roth, C.; Stahlhofen, W. (1988) The use of light scattering photometry in aerosol medicine. *J. Aerosol Med.* 1: 89-112.
- Gebhart, J.; Schiller-Scotland, C. F.; Egan, M. J.; Nixon, W. (1989) On the relationship between experimental data for total deposition and model calculations—part I: effect of instrumental dead space. *J. Aerosol Sci.* 20: 141-147.
- Gehr, P. (1984) Lung morphometry. In: Smith, H.; Gerber, G., eds. *Lung modeling for inhalation of radioactive materials.* Luxembourg: Commission of the European Communities; pp. 1-11; report no. EUR9384EN.
- Gehr, P. (1994) Anatomy and morphology of the respiratory tract: annexe A. In: *Human respiratory tract model for radiological protection: a report of the International Commission on Radiological Protection.* Oxford, United Kingdom: Elsevier Science, Ltd.; pp. 121-166. (ICRP publication 66; *Annals of the ICRP*: v. 24, nos. 1-3).
- Gehr, P.; Schürch, S.; Berthiaume, Y.; Im Hof, V.; Geiser, M. (1990) Particle retention in airways by surfactant. *J. Aerosol Med.* 3: 27-43.
- George, A.; Breslin, A. J. (1969) Deposition of radon daughters in humans exposed to uranium mine atmospheres. *Health Phys.* 17: 115-124.
- Gerrard, C. S.; Gerrity, T. R.; Yeates, D. B. (1986) The relationships of aerosol deposition, lung size, and the rate of mucociliary clearance. *Arch. Environ. Health* 41: 11-15.
- Gerrity, T. R.; Lee, P. S.; Hass, F. J.; Marinelli, A.; Werner, P.; Lourenço, R. V. (1979) Calculated deposition of inhaled particles in the airway generations of normal subjects. *J. Appl. Physiol.: Respir. Environ. Exercise Physiol.* 47: 867-873.
- Giacomelli-Maltoni, G.; Melandri, C.; Prodi, V.; Tarroni, G. (1972) Deposition efficiency of monodisperse particles in human respiratory tract. *Am. Ind. Hyg. Assoc. J.* 33: 603-610.
- Gibb, F. R.; Beiter, H. B.; Morrow, P. E. (1975) Studies of coal dust retention in the lungs utilizing neutron-activated coal. report no. UR-3490-679. Available from: NTIS, Springfield, VA.

- Godard, P.; Chaintreuil, J.; Damon, M.; Coupe, M.; Flandre, O.; de Paulet, A. C.; Michel, F. B. (1982) Functional assessment of alveolar macrophages: comparison of cells from asthmatics and normal subjects. *J. Allergy Clin. Immunol.* 70: 88-93.
- Goodman, R. M.; Yergin, B. M.; Landa, J. F.; Golinvaux, M. H.; Sackner, M. A. (1978) Relationship of smoking history and pulmonary function tests to tracheal mucous velocity in nonsmokers, young smokers, ex-smokers, and patients with chronic bronchitis. *Am. Rev. Respir. Dis.* 117: 205-214.
- Gore, D. J. (1983) The spatial and temporal distribution of inhaled  $UO_2$  particles in the respiratory tract of the rat: II. the relative concentration of  $UO_2$  between the intrapulmonary airways and the pulmonary tissue. *Radiat. Res.* 93: 276-287.
- Gore, D. J.; Patrick, G. (1978) The distribution and clearance of inhaled  $UO_2$  particles on the first bifurcation and trachea of rats. *Phys. Med. Biol.* 23: 730-737.
- Gore, D. J.; Patrick, G. A. (1982) A quantitative study of the penetration of insoluble particles into the tissue of the conducting airways. In: Walton, W. H., ed. *Inhaled particles V: proceedings of an international symposium; September 1980; Cardiff, Wales.* *Ann. Occup. Hyg.* 26: 149-161.
- Gore, D. J.; Thorne, M. C. (1977) The distribution and clearance of inhaled uranium dioxide particles in the respiratory tract of the rat. In: Walton, W. H., McGovern, B., eds. *Inhaled particles IV: proceedings of an international symposium, part 1; September 1975; Edinburgh, United Kingdom.* Oxford, United Kingdom: Pergamon Press, Ltd.; pp. 275-283.
- Gradon, L.; Yu, C. P. (1989) Diffusional particle deposition in the human nose and mouth. *Aerosol Sci. Technol.* 11: 213-220.
- Green, G. M. (1973) Alveolobronchiolar transport mechanisms. *Arch. Intern. Med.* 131: 109-114.
- Green, H. L.; Lane, W. R. (1957) *Particulate clouds: dusts, smokes and mists.* Princeton, NJ: D. Van Nostrand Company, Inc. (Bunbury, H. M., ed. *General and industrial chemistry series.*)
- Greenspan, B. J.; Morrow, P. E.; Ferin, J. (1988) Effects of aerosol exposures to cadmium chloride on the clearance of titanium dioxide from the lungs of rats. *Exp. Lung Res.* 14: 491-499.
- Griffith, W. C.; Cuddihy, R. G.; Boecker, B. B.; Guilmette, R. A.; Medinsky, M. A.; Mewhinney, J. A. (1983) Comparison of solubility of aerosols in lungs of laboratory animals. *Health Phys.* 45: 233.
- Gross, E. A.; Morgan, K. T. (1992) Architecture of nasal passages and larynx. In: Parent, R. A., ed. *Comparative biology of the normal lung: v. I, treatise on pulmonary toxicology.* Boca Raton, FL: CRC Press, Inc.; pp. 7-25.
- Guilmette, R. A.; Diel, J. H.; Muggenburg, B. A.; Mewhinney, J. A.; Boecker, B. B.; McClellan, R. O. (1984) Biokinetics of inhaled  $^{239}PuO_2$  in the beagle dog: effect of aerosol particle size. *Int. J. Radiat. Biol.* 45: 563-581.
- Guilmette, R. A.; Wicks, J. D.; Wolff, R. K. (1989) Morphometry of human nasal airways *in vivo* using magnetic resonance imaging. *J. Aerosol. Med.* 2: 365-377.
- Guyton, A. C. (1947) Measurement of the respiratory volumes of laboratory animals. *Am. J. Physiol.* 150: 70-77.
- Haefeli-Bleuer, B.; Weibel, E. R. (1988) Morphometry of the human pulmonary acinus. *Anat. Rec.* 220: 401-414.
- Hägerstrand, I.; Seifert, B. (1973) Asbestos bodies and pleural plaques in human lungs at necropsy. *Acta Pathol. Microbiol. Scand. Sect. A* 81: 457-460.

- Hahn, F. F.; Hobbs, C. H. (1979) The effect of enzyme-induced pulmonary emphysema in Syrian hamsters on the deposition and long-term retention of inhaled particles. *Arch. Environ. Health* 34: 203-211.
- Hallworth, C. W. (1993) Particle size analysis of therapeutic aerosols. In: Moren, F.; Dolovich, M. B.; Newhouse, M. T.; Newman, S. P., eds. *Aerosols in medicine: principles, diagnosis and therapy*. New York, NY: Elsevier Science Publishers; pp. 351-.
- Hammad, Y. Y. (1984) Deposition and elimination of MMMF. In: Guthe, T., ed. *Biological effects of man-made mineral fibres: proceedings of a WHO/IARC conference in association with JEMRB and TIMA, v. 2; April 1982; Copenhagen, Denmark*. Copenhagen, Denmark: World Health Organization, Regional Office for Europe; pp. 126-142.
- Hammad, Y.; Simmons, W.; Abdel-Kader, H.; Reynolds, C.; Weill, H. (1988) Effect of chemical composition on pulmonary clearance of man-made mineral fibres. *Ann. Occup. Hyg.* 32(suppl. 1): 769-779.
- Hansen, J. E.; Ampaya, E. P. (1975) Human air space shapes, sizes, areas, and volumes. *J. Appl. Physiol.* 38: 990-995.
- Hansen, J. E.; Ampaya, E. P.; Bryant, G. H.; Navin, J. J. (1975) Branching pattern of airways and air spaces of a single human terminal bronchiole. *J. Appl. Physiol.* 38: 983-989.
- Harkema, J. R. (1991) Comparative aspects of nasal airway anatomy: relevance to inhalation toxicology. *Toxicol. Pathol.* 19: 321-336.
- Harmsen, A. G.; Muggenburg, B. A.; Snipes, M. B.; Bice, D. E. (1985) The role of macrophages in particle translocation from lungs to lymph nodes. *Science (Washington, DC)* 230: 1277-1280.
- Hatch, T.; Choate, S. P. (1929) Statistical description of the size properties of non-uniform particulate substances. *J. Franklin Inst.* 207: 369-387.
- Hatch, T. F.; Gross, P. (1964) *Pulmonary deposition and retention of inhaled aerosols*. New York, NY: Academic Press, Inc.
- Henshaw, D. L.; Fewes, A. P. (1984) The microdistribution of alpha emitting particles in the human lung. In: Smith, H.; Gerber, G., eds. *Lung modeling for inhalation of radioactive materials*. Luxembourg: Commission of the European Communities; pp. 199-208; report no. EUR9384EN.
- Heppleston, A. G. (1953) The pathological anatomy of simple pneumokoniosis in coal workers. *J. Pathol. Bacteriol.* 66: 235-246.
- Heyder, J.; Rudolf, G. (1977) Deposition of aerosol particles in the human nose. In: Walton, W. H.; McGovern, B., eds. *Inhaled particles IV: proceedings of an international symposium, part 1; September 1975; Edinburgh, United Kingdom*. Oxford, United Kingdom: Pergamon Press, Ltd.; pp. 107-126.
- Heyder, J.; Rudolf, G. (1984) Mathematical models of particle deposition in the human respiratory tract. In: Smith, H.; Gerber, G., eds. *Lung modeling for inhalation of radioactive materials*. Luxembourg: Commission of the European Communities; pp. 17-38; report no. EUR9384EN.
- Heyder, J.; Scheuch, G. (1983) Diffusional transport of nonspherical aerosol particles. *Aerosol Sci. Technol.* 2: 41-44.
- Heyder, J.; Gebhart, J.; Stahlhofen, W.; Stuck, B. (1982) Biological variability of particle deposition in the human respiratory tract during controlled and spontaneous mouth-breathing. In: Walton, W. H., ed. *Inhaled particles V: proceedings of an international symposium; September 1980; Cardiff, Wales*. *Ann. Occup. Hyg.* 26: 137-147.

- Heyder, J.; Gebhart, J.; Scheuch, G. (1985) Interaction of diffusional and gravitational particle transport in aerosols. *Aerosol Sci. Technol.* 4: 315-326.
- Heyder, J.; Gebhart, J.; Rudolf, G.; Schiller, C. F.; Stahlhofen, W. (1986) Deposition of particles in the human respiratory tract in the size range 0.005-15  $\mu\text{m}$ . *J. Aerosol Sci.* 17: 811-825.
- Heyder, J.; Gebhart, J.; Scheuch, G. (1988) Influence of human lung morphology on particle deposition. *J. Aerosol Med.* 1: 81-88.
- Hilding, A. C. (1963) Phagocytosis, mucous flow, and ciliary action. *Arch. Environ. Health* 6: 67-79.
- Hiller, F. C. (1991) Health implications of hygroscopic particle growth in the human respiratory tract. *J. Aerosol Med.* 4: 1-23.
- Hofmann, W. (1982) Dose calculations for the respiratory tract from inhaled natural radioactive nuclides as a function of age - II. basal cell dose distributions and associated lung cancer risk. *Health Phys.* 43: 31-44.
- Hofmann, W.; Koblinger, L. (1990) Monte Carlo modeling of aerosol deposition in human lungs. Part II: Deposition fractions and their sensitivity to parameter variations. *J. Aerosol Sci.* 21: 675-688.
- Hofmann, W.; Martonen, T. B.; Graham, R. C. (1989) Predicted deposition of nonhygroscopic aerosols in the human lung as a function of subject age. *J. Aerosol Med.* 2: 49-68.
- Holma, B. (1985) Influence of buffer capacity and pH-dependent rheological properties of respiratory mucus on health effects due to acidic pollution. *Sci. Total Environ.* 41: 101-123.
- Holma, B.; Lindegren, M.; Andersen, J. M. (1977) pH effects on ciliomotility and morphology of respiratory mucosa. *Arch. Environ. Health* 32: 216-226.
- Holt, P. F. (1981) Transport of inhaled dust to extrapulmonary sites. *J. Pathol.* 133: 123-129.
- Horsfield, K.; Cumming, G. (1968) Morphology of the bronchial tree in man. *J. Appl. Physiol.* 24: 373-383.
- Hounam, R. F.; Black, A.; Walsh, M. (1969) Deposition of aerosol particles in the nasopharyngeal region of the human respiratory tract. *Nature (London)* 221: 1254-1255.
- Hounam, R. F.; Black, A.; Walsh, M. (1971) The deposition of aerosol particles in the nasopharyngeal region of the human respiratory tract. *J. Aerosol Sci.* 2: 47-61.
- Hühnerbein, J.; Otto, J.; Thal, W. (1984) Untersuchungsergebnisse der mukoziliären Clearance bei lungengesunden Kindern [Results of research on mucociliary clearance in the healthy lungs of children]. *Pediatr. Grenzgeb.* 23: 437-443.
- International Commission on Radiological Protection. (1960) Report of Committee II on permissible dose for internal radiation (1959). *Health Phys.* 3.
- International Commission on Radiological Protection. (1975) Report of the task group on reference man. ICRP publication 23.
- International Commission on Radiological Protection. (1979) Limits for intakes of radionuclides by workers. Oxford, United Kingdom: International Commission on Radiological Protection; ICRP publication 30, part 1.
- International Commission on Radiological Protection. (1994) Human respiratory tract model for radiological protection: a report of a task group of the International Commission on Radiological Protection. Oxford, United Kingdom: Elsevier Science Ltd. (ICRP publication 66; *Annals of the ICRP*: v. 24, nos. 1-3).

- International Commission on Radiological Protection. (1995) Age-dependent doses to members of the public from intake of radionuclides: part 4, inhalation dose coefficients (includes ingestion dose coefficients from ICRP publications 56, 67, and 69): a report of a task group of committee 2 adopted in September 1995 [draft]. Oxford, United Kingdom: International Commission on Radiological Protection; pp. 24-25; ICRP publication 74; July.
- Israel, G. (1986) Aerosols: formation and reactivity: proceedings of the second international aerosol conference; September; Berlin, Federal Republic of Germany. New York, NY: Pergamon Press.
- Itoh, H.; Ishii, Y.; Maeda, H.; Todo, G.; Torizuka, K.; Smaldone, G. C. (1981) Clinical observations of aerosol deposition in patients with airways obstruction. *Chest* 80(suppl.): 837-840.
- James, A. C. (1988) Lung dosimetry. In: Nazaroff, W. W.; Nero, A. V., Jr., eds. Radon and its decay products in indoor air. New York, NY: John Wiley & Sons; pp. 259-309.
- James, A. C.; Stahlhofen, W.; Rudolf, G.; Egan, M. J.; Nixon, W.; Gehr, P.; Briant, J. K. (1991) The respiratory tract deposition model proposed by the ICRP Task Group. *Radiat. Prot. Dosim.* 38: 159-165.
- James, A. C.; Stahlhofen, W.; Rudolf, G.; Köbrich, R.; Briant, J. K.; Egan, M. J.; Nixon, W.; Birchall, A. (1994) Deposition of inhaled particles: annexe D. In: Human respiratory tract model for radiological protection: a report of a task group of the International Commission on Radiological Protection. Oxford, United Kingdom: Elsevier Science Ltd.; pp. 231-299. (ICRP publication 66; *Annals of the ICRP*: v. 24, nos. 1-3).
- Jammet, H.; Drutel, P.; Parrot, R.; Roy, M. (1978) Étude de l'épuration pulmonaire chez l'homme après administration d'aérosols de particules radioactives [Study of pulmonary function in man after administration of radioactive particulate aerosols]. *Radioprotection* 13: 143-166.
- Jarabek, A. M. (1995) The application of dosimetry models to identify key processes and parameters for default dose-response assessment approaches. *Toxicol. Lett.* 79: 171-184.
- Jarabek, A. M.; Ménache, M. G.; Overton, J. H., Jr.; Dourson, M. L.; Miller, F. J. (1989) Inhalation reference dose (RfD): an application of interspecies dosimetry modeling for risk assessment of insoluble particles. In: Proceedings of the 26th Hanford life sciences symposium, "modeling for scaling to man;" October 1987; Richland, WA. *Health Phys.* 57(suppl. 1): 177-183.
- Jarabek, A. M.; Ménache, M. G.; Overton, J. H., Jr.; Dourson, M. L.; Miller, F. J. (1990) The U.S. Environmental Protection Agency's inhalation RfD methodology: risk assessment for air toxics. *Toxicol. Ind. Health* 6: 279-301.
- John, W.; Wall, S. M.; Ondo, J. L.; Wong, H. C. (1986) Acidic aerosol concentrations and size distributions in California. In: Aerosols: formation and reactivity, proceedings of the second international aerosol conference; September; Berlin, Federal Republic of Germany. Oxford, United Kingdom: Pergamon Press; pp. 25-28.
- John, W.; Wall, S. M.; Ondo, J. L.; Winklmayr, W. (1990) Modes in the size distributions of atmospheric inorganic aerosol. *Atmos. Environ. Part A* 24: 2349-2359.
- John, J.; Wollmer, P.; Dahlbäck, M.; Luts, A.; Jonson, B. (1994) Tidal volume and alveolar clearance of insoluble particles. *J. Appl. Physiol.* 76: 584-588.
- Johnson, T. (1989) Human activity patterns in Cincinnati, Ohio [final report]. Palo Alto, CA: Electric Power Research Institute; project no. RP940-06; report no. EN-6204.
- Johnson, N. F. (1992) The utility of animal inhalation studies to assess the risk of mineral fiber-induced pulmonary cancer. In: D'Amato, R.; Slaga, T. J.; Farland, W. H.; Henry, C., eds. Relevance of animal studies to the

- evaluation of human cancer risk: proceedings of a symposium; December 1990; Austin, TX. New York, NY: Wiley-Liss; pp. 19-36. (Progress in clinical and biological research: v. 374).
- Johnson, T. R. (1994) One-minute ozone exposure sequences for selected New York cohorts [letter to Dr. John H. Overton, U.S. EPA]. Durham, NC: International Technology Corporation; November 22.
- Johnson, J. R.; Milencoff, S. (1989) A comparison of excretion and retention between the current ICRP lung model and a proposed new model. *Health Phys.* 57(suppl. 1): 263-270.
- Johnson, R. F., Jr.; Zeimer, P. L. (1971) The deposition and retention of inhaled <sup>152-154</sup>europium oxide in the rat. *Health Phys.* 20: 187-193.
- Johnson, L. J.; Dean, P. N.; Ide, H. M. (1972) *In vivo* determination of the late-phase lung clearance of <sup>239</sup>Pu following accidental exposure. *Health Phys.* 22: 410-412.
- Johnson, N. F.; Griffiths, D. M.; Hill, R. J. (1984) Size distribution following long-term inhalation of MMMF. In: Guthe, T., ed. *Biological effects of man-made mineral fibres: proceedings of a WHO/IARC conference in association with JEMRB and TIMA, v. 2; April 1982; Copenhagen, Denmark.* Copenhagen, Denmark: World Health Organization, Regional Office for Europe; pp. 102-125.
- Johnson, T.; Capel, J.; Wijnberg, L. (1990) The incorporation of serial correlation into a version of NEM applicable to carbon monoxide. Research Triangle Park, NC: U.S. Environmental Protection Agency, Atmospheric Research and Exposure Assessment Laboratory; contract no. 68-02-4406.
- Johnson, T.; Capel, J.; McCoy, M.; Mozier, J. W. (1995a) Estimation of ozone exposures experienced by outdoor workers in nine urban areas using a probabilistic version of NEM. Research Triangle Park, NC: U.S. Environmental Protection Agency, Office of Air Quality Planning and Standards; contract no. 63-D-30094.
- Johnson, T.; Capel, J.; Mozier, J. W.; McCoy, M. (1995b) Estimation of ozone exposures experienced by outdoor children in nine urban areas using a probabilistic version of NEM. Research Triangle Park, NC: U.S. Environmental Protection Agency, Office of Air Quality Planning and Standards; contract no. 63-D-30094.
- Jones, A. D.; Vincent, J. H.; Johnston, A. M.; McMillan, C. H. (1988) Effects of electrostatic charge on the pulmonary deposition of mineral dust aerosols inhaled by rats. *J. Aerosol Sci.* 19: 565-575.
- Kilburn, K. H. (1968) A hypothesis for pulmonary clearance and its implications. *Am. Rev. Respir. Dis.* 98: 449-463.
- Kim, C. S.; Iglesias, A. J. (1989) Deposition of inhaled particles in bifurcating airway models: I. inspiratory deposition. *J. Aerosol Med.* 2: 1-14.
- Kim, C. S.; Trujillo, D.; Sackner, M. A. (1985) Size aspects of metered-dose inhaler aerosols. *Am. Rev. Respir. Dis.* 132: 137-142.
- Kim, C. S.; Lewars, G. A.; Sackner, M. A. (1988) Measurement of total lung aerosol deposition as an index of lung abnormality. *J. Appl. Physiol.* 64: 1527-1536.
- Kim, C. S.; Iglesias, A. J.; Garcia, L. (1989) Deposition of inhaled particles in bifurcating airway models: II. expiratory deposition. *J. Aerosol Med.* 2: 15-27.
- Kliment, V. (1973) Similarity and dimensional analysis, evaluation of aerosol deposition in the lungs of laboratory animals and man. *Folia Morphol. (Prague)* 21: 59-64.
- Knight, G.; Lichti, K. (1970) Comparison of cyclone and horizontal elutriator size selectors. *Am. Ind. Hyg. Assoc. J.* 31: 437-441.

- Koblinger, L.; Hofmann, W. (1990) Monte Carlo modeling of aerosol deposition in human lungs. Part I: simulation of particle transport in a stochastic lung structure. *J. Aerosol Sci.* 21: 661-674.
- Kreyling, W. G. (1992) Intracellular particle dissolution in alveolar macrophages. *Environ. Health Perspect.* 97: 121-126.
- Kreyling, W. G.; Schumann, G.; Ortmaier, A.; Ferron, G. A.; Karg, E. (1988) Particle transport from the lower respiratory tract. *J. Aerosol Med.* 1: 351-370.
- Kreyling, W. G.; Cox, C.; Ferron, G. A.; Oberdörster, G. (1993) Lung clearance in Long-Evans rats after inhalation of porous, monodisperse cobalt oxide particles. *Exp. Lung Res.* 19: 445-467.
- Kwart, H.; Moseley, W. W., Jr.; Katz, M. (1963) The chemical characterization of human tracheobronchial secretion: a possible clue to the origin of fibrocystic mucus. *Ann. N. Y. Acad. Sci.* 106: 709-721.
- LaBauve, R. J.; Brooks, A. L.; Mauderly, J. L.; Hahn, F. F.; Redman, H. C.; Macken, C.; Slauson, D. O.; Mewhinney, J. A.; McClellan, R. O. (1980) Cytogenetic and other biological effects of  $^{239}\text{PuO}_2$  inhaled by the rhesus monkey. *Radiat. Res.* 82: 310-335.
- LaBelle, C. W.; Brieger, H. (1961) Patterns and mechanisms in the elimination of dust from the lung. In: Davies, C. N., ed. *Inhaled particles and vapours: proceedings of an international symposium; March-April 1960; Oxford, United Kingdom.* New York, NY: Pergamon Press; pp. 356-368.
- Landahl, H. D. (1950a) On the removal of air-borne droplets by the human respiratory tract: I. the lung. *Bull. Math. Biophys.* 12: 43-56.
- Landahl, H. D. (1950b) On the removal of air-borne droplets by the human respiratory tract: II. the nasal passages. *Bull. Math. Biophys.* 12: 161-169.
- Landahl, H. D. (1963) Particle removal by the respiratory system: note on the removal of airborne particulates by the human respiratory tract with particular reference to the role of diffusion. *Bull. Math. Biophys.* 25: 29-39.
- Landahl, H. D.; Tracewell, T. (1949) Penetration of air-borne particles through the human nose II. *J. Ind. Hyg. Toxicol.* 31: 55-59.
- Langham, W. H. (1956) Determination of internally deposited radioactive isotopes from excretion analyses. *Am. Ind. Hyg. Assoc. Q.* 17: 305-318.
- Larson, T. V. (1989) The influence of chemical and physical forms of ambient air acids on airway doses. In: *Symposium on the health effects of acid aerosols; October 1987; Research Triangle Park, NC.* *Environ. Health Perspect.* 79: 7-13.
- Larson, T. V.; Covert, D. S.; Frank, R.; Charlson, R. J. (1977) Ammonia in the human airways: neutralization of inspired acid sulfate aerosols. *Science (Washington, DC)* 197: 161-163.
- Larson, T. V.; Frank, R.; Covert, D. S.; Holub, D.; Morgan, M. S. (1982) Measurements of respiratory ammonia and the chemical neutralization of inhaled sulfuric acid aerosol in anesthetized dogs. *Am. Rev. Respir. Dis.* 125: 502-506.
- Larson, T. V.; Hanley, Q. S.; Koenig, J. Q.; Bernstein, O. (1993) Calculation of acid aerosol dose. In: Mohr, U., ed. *Advances in controlled clinical inhalation studies.* Berlin, Federal Republic of Germany: Springer-Verlag; pp. 109-121.

- Lauweryns, J. M.; Baert, J. H. (1974) The role of the pulmonary lymphatics in the defenses of the distal lung: morphological and experimental studies of the transport mechanisms of intratracheally instilled particles. *Ann. N. Y. Acad. Sci.* 221: 244-275.
- Le Bouffant, L.; Henin, J. P.; Martin, J. C.; Normand, C.; Tichoux, G.; Trolard, F. (1984) Distribution of inhaled MMMF in the rat lung - long-term effects. In: Guthe, T., ed. *Biological effects of man-made mineral fibres: proceedings of a WHO/IARC conference in association with JEMRB and TIMA*, v. 2; April 1982; Copenhagen, Denmark. Copenhagen, Denmark: World Health Organization, Regional Office for Europe; pp. 143-168.
- Le Bouffant, L.; Daniel, H.; Henin, J. P.; Martin, J. C.; Normand, C.; Tichoux, G.; Trolard, F. (1987) Experimental study on long-term effects of inhaled MMMF on the lungs of rats. *Ann. Occup. Hyg.* 31: 765-790.
- Leak, L. V. (1980) Lymphatic removal of fluids and particles in the mammalian lung. *Environ. Health Perspect.* 35: 55-76.
- Lee, W. C.; Wang, C. S. (1977) Particle deposition in systems of repeatedly bifurcating tubes. In: Walton, W. H., ed. *Inhaled particles IV*. Oxford, United Kingdom: Pergamon Press; pp. 49-59.
- Lee, P. S.; Gerrity, T. R.; Hass, F. J.; Lourenço, R. V. (1979) A model for tracheobronchial clearance of inhaled particles in man and a comparison with data. *IEEE Trans Biomed. Eng.* BME-26: 624-630.
- Lee, P. S.; Chan, T. L.; Hering, W. E. (1983) Long-term clearance of inhaled diesel exhaust particles in rodents. *J. Toxicol. Environ. Health* 12: 801-813.
- Lee, K. P.; Trochimowicz, H. J.; Reinhardt, C. F. (1985) Transmigration of titanium dioxide (TiO<sub>2</sub>) particles in rats after inhalation exposure. *Exp. Mol. Pathol.* 42: 331-343.
- Lehnert, B. E. (1990) Alveolar macrophages in a particle "overload" condition. *J. Aerosol Med.* 3(suppl. 1): S9-S30.
- Lehnert, B. E. (1992) Pulmonary and thoracic macrophage subpopulations and clearance of particles from the lung. *Environ. Health Perspect.* 97: 17-46.
- Lehnert, B. E.; Morrow, P. E. (1985) Association of <sup>59</sup>iron oxide with alveolar macrophages during alveolar clearance. *Exp. Lung Res.* 9: 1-16.
- Lehnert, B. E.; Valdez, Y. E.; Holland, L. M. (1985) Pulmonary macrophages: alveolar and interstitial populations. *Exp. Lung Res.* 9: 177-190.
- Lehnert, B. E.; Valdez, Y. E.; Bomalaski, S. H. (1988) Analyses of particles in the lung free cell, tracheobronchial lymph nodal, and pleural space compartments following their deposition in the lung as related to lung clearance mechanisms. *Ann. Occup. Hyg.* 32: 125-140.
- Leikauf, G.; Yeates, D. B.; Wales, K. A.; Spektor, D.; Albert, R. E.; Lippmann, M. (1981) Effects of sulfuric acid aerosol on respiratory mechanics and mucociliary particle clearance in healthy nonsmoking adults. *Am. Ind. Hyg. Assoc. J.* 42: 273-282.
- Leikauf, G. D.; Spektor, D. M.; Albert, R. E.; Lippmann, M. (1984) Dose-dependent effects of submicrometer sulfuric acid aerosol on particle clearance from ciliated human lung airways. *Am. Ind. Hyg. Assoc. J.* 45: 285-292.
- Lippmann, M. (1970) Deposition and clearance of inhaled particles in the human nose. *Ann. Otol. Rhinol. Laryngol.* 79: 519-528.

- Lippmann, M. (1977) Regional deposition of particles in the human respiratory tract. In: Lee, D. H. K.; Falk, H. L.; Murphy, S. D.; Geiger, S. R., eds. Handbook of physiology, section 9: reactions to physical agents. Bethesda, MD: American Physiological Society; pp. 213-232.
- Lippmann, M. (1978) Respirable dust sampling. In: Air sampling instruments for evaluation of atmospheric contaminants. 5th ed. Cincinnati, OH: American Conference of Governmental Industrial Hygienists; pp. g-1 - g-23.
- Lippmann, M.; Albert, R. E. (1967) A compact electric-motor driven spinning disc aerosol generator. Am. Ind. Hyg. Assoc. J. 28: 501-506.
- Lippmann, M.; Albert, R. E. (1969) The effect of particle size on the regional deposition of inhaled aerosols in the human respiratory tract. Am. Ind. Hyg. Assoc. J. 30: 257-263.
- Lippmann, M.; Schlesinger, R. B. (1984) Interspecies comparisons of particle deposition and mucociliary clearance in tracheobronchial airways. J. Toxicol. Environ. Health 13: 441-469.
- Lippmann, M.; Albert, R. E.; Yeates, D. B.; Berger, J. M.; Foster, W. M.; Bohning, D. E. (1977) Factors affecting tracheobronchial mucociliary transport. In: Walton, W. H.; McGovern, B., eds. Inhaled particles IV: proceedings of an international symposium, part 1; September 1975; Edinburgh, United Kingdom. Oxford, United Kingdom: Pergamon Press, Ltd.; pp. 305-319.
- Little, J. B.; Radford, E. P., Jr.; McCombs, H. L.; Hunt, V. R. (1965) Distribution of polonium<sup>210</sup> in pulmonary tissues of cigarette smokers. N. Engl. J. Med. 273: 1343-1351.
- Lourenço, R. V.; Cotromanca, E. (1982) Clinical aerosols. I. Characterization of aerosols and their diagnostic uses. Arch. Intern. Med. 142: 2163-2172.
- Lourenço, R. V.; Stanley, E. D.; Gatmaitan, B.; Jackson, G. G. (1971) Abnormal deposition and clearance of inhaled particles during upper respiratory viral infections. J. Clin. Invest. 50: 62a.
- Lundborg, M.; Lind, B.; Camner, P. (1984) Ability of rabbit alveolar macrophages to dissolve metals. Exp. Lung Res. 7: 11-22.
- Lundborg, M.; Eklund, A.; Lind, B.; Camner, P. (1985) Dissolution of metals by human and rabbit alveolar macrophages. Br. J. Ind. Med. 42: 642-645.
- Lundgren, D. A.; Hausknecht, B. J. (1982) Ambient aerosol size distribution determination using a mobile wide range aerosol classifier. Research Triangle Park, NC: U.S. Environmental Protection Agency, Environmental Monitoring Systems Laboratory; EPA contract no. CR-808606-01-1.
- Lynch, J. R. (1970) Evaluation of size-selective presamplers: I. theoretical cyclone and elutriator relationships. Am. Ind. Hyg. Assoc. J. 31: 548-551.
- Maguire, B. A.; Barker, D. (1969) A gravimetric dust sampling instrument (SIMPEDS): preliminary underground trials. Ann. Occup. Hyg. 12: 197-201.
- Majima, Y.; Sakakura, Y.; Matsubara, T.; Murai, S.; Miyoshi, Y. (1983) Mucociliary clearance in chronic sinusitis: related human nasal clearance and in vitro bullfrog palate clearance. Biorheology 20: 251-262.
- Man, S. F. P.; Lee, T. K.; Gibney, R. T. N.; Logus, J. W.; Noujaim, A. A. (1980) Canine tracheal mucus transport of particulate pollutants: comparison of radiolabeled corn pollen, ragweed pollen, asbestos, silica, and talc to Dowex® anion exchange particles. Arch. Environ. Health 35: 283-286.

- Marafante, E.; Lundborg, M.; Vahter, M.; Camner, P. (1987) Dissolution of two arsenic compounds by rabbit alveolar macrophages *in vitro*. *Fundam. Appl. Toxicol.* 8: 382-388.
- Martens, A.; Jacobi, W. (1973) Die In-Vivo Bestimmung der Aerosolteilchen-deposition im Atemtrakt bei Mund-Bzw. Nasenatmung [In vivo determination of aerosol particle deposition in the total respiratory tract]. In: *Aerosole in Physik, Medizin und Technik*. Bad Soden, West Germany: Gesellschaft für Aerosolforschung; pp. 117-121.
- Martonen, T. B.; Lowe, J. (1983) Assessment of aerosol deposition patterns in human respiratory tract casts. In: Marple, V. A.; Liu, B. Y. H., eds. *Aerosols in the mining and industrial work environments: papers presented at the international symposium: volume 1, fundamentals and status; November 1981; Minneapolis, MN*. Ann Arbor, MI: Ann Arbor Science; pp. 151-164.
- Martonen, T. B.; Graham, R. C. (1987) Hygroscopic growth: its effect on aerosol therapy and inhalation toxicology. Research Triangle Park, NC: U.S. Environmental Protection Agency, Health Effects Research Laboratory; report no. EPA/600/D-87/172. Available from: NTIS, Springfield, VA; PB87-194734.
- Martonen, T. B.; Zhang, Z. (1993) Deposition of sulfate acid aerosols in the developing human lung. *Inhalation Toxicol.* 5: 165-187.
- Martonen, T. B.; Zhang, Z.; Yang, Y. (1992) Extrapolation modeling of aerosol deposition in human and laboratory rat lungs. *Inhalation Toxicol.* 4: 303-324.
- Martonen, T. B.; Zhang, Z.; Lessmann, R. C. (1993) Fluid dynamics of the human larynx and upper tracheobronchial airways. *Aerosol Sci. Technol.* 19: 133-156.
- Martonen, T. B.; Yang, Y.; Xue, Z. Q. (1994a) Influences of cartilaginous rings on tracheobronchial fluid dynamics. *Inhalation Toxicol.* 6: 185-203.
- Martonen, T. B.; Yang, Y.; Xue, Z. Q. (1994b) Effects of carinal ridge shapes on lung airstreams. *Aerosol Sci. Technol.* 21: 119-136.
- Martonen, T. B.; Yang, Y.; Xue, Z. Q.; Zhang, Z. (1994c) Motion of air within the human tracheobronchial tree. Part. *Sci. Technol.* 12: 175-188.
- Masse, R.; Ducouso, R.; Nolibe, D.; Lafuma, J.; Chretien, J. (1974) Passage transbronchique des particules metalliques [Transbronchial passage of metallic particulates]. *Rev. Fr. Mal. Respir.* 1: 123-129.
- Matthys, H.; Vastag, E.; Köhler, D.; Daikeler, G.; Fischer, J. (1983) Mucociliary clearance in patients with chronic bronchitis and bronchial carcinoma. *Respiration* 44: 329-337.
- Matulionis, D. H. (1984) Chronic cigarette smoke inhalation and aging in mice: 1. morphologic and functional lung abnormalities. *Exp. Lung Res.* 7: 237-256.
- Mauderly, J. L. (1994) Contribution of inhalation bioassays to the assessment of human health risks from solid airborne particles. In: Mohr, U.; Dungworth, D. L.; Mauderly, J. L.; Oberdörster, G., eds. *Toxic and carcinogenic effects of solid particles in the respiratory tract: [proceedings of the 4th international inhalation symposium]; March 1993; Hannover, Germany*. Washington, DC: International Life Sciences Institute Press; pp. 355-365.
- Mauderly, J. L.; Bice, D. E.; Cheng, Y. S.; Gillett, N. A.; Griffith, W. C.; Henderson, R. F.; Pickrell, J. A.; Wolff, R. K. (1990) Influence of preexisting pulmonary emphysema on susceptibility of rats to diesel exhaust. *Am. Rev. Respir. Dis.* 141: 1333-1341.
- McInroy, J. F.; Stewart, M. W.; Moss, W. D. (1976) Studies of plutonium in human tracheobronchial lymph nodes. In: Ballou, J. E., ed. *Radiation and the lymphatic system: proceedings of the fourteenth annual Hanfor Biology*

Symposium; September-October 1974; Richland, WA. Oak Ridge, TN: Energy Research and Development Administration; pp. 54-58. (ERDA symposium series: 37).

McMahon, T. A.; Brain, J. D.; Lemott, S. (1977) Species differences in aerosol deposition. In: Walton, W. H.; McGovern, B., eds. Inhaled particles IV: proceedings of an international symposium, part 1; September 1975; Edinburgh, United Kingdom. Oxford, United Kingdom: Pergamon Press, Ltd.; pp. 23-33.

Medinsky, M. A.; Kampcik, S. J. (1985) Pulmonary retention of [<sup>14</sup>C]benzo[*a*]pyrene in rats as influenced by the amount instilled. *Toxicology* 35: 327-336.

Medinsky, M. A.; Cheng, Y. S.; Kampcik, S. J.; Henderson, R. F.; Dutcher, J. S. (1986) Disposition and metabolism of <sup>14</sup>C-solvent yellow and solvent green aerosols after inhalation. *Fundam. Appl. Toxicol.* 7: 170-178.

- Melandri, C.; Prodi, V.; Tarroni, G.; Formignani, M.; De Zaiacomo, T.; Bompane, G. F.; Maestri, G.; Maltoni, G. G. (1977) On the deposition of unipolarly charged particles in the human respiratory tract. In: Walton, W. H.; McGovern, B., eds. Inhaled particles IV: proceedings of an international symposium, part 1; September 1975; Edinburgh, United Kingdom. Oxford, United Kingdom: Pergamon Press, Ltd.; pp. 193-201.
- Melandri, C.; Tarroni, G.; Prodi, V.; De Zaiacomo, T.; Formignani, M.; Lombardi, C. C. (1983) Deposition of charged particles in the human airways. *J. Aerosol Sci.* 14: 657-669.
- Ménache, M. G.; Miller, F. J.; Raabe, O. G. (1995) Particle inhalability curves for humans and small laboratory animals. *Ann. Occup. Hyg.* 39: 317-328.
- Ménache, M. G.; Raabe, O. G.; Miller, F. J. (1996) An empirical dosimetry model of aerodynamic particle deposition in the rat respiratory tract. *Inhalation Toxicol.*: accepted.
- Mercer, T. T. (1967) On the role of particle size in the dissolution of lung burdens. *Health Phys.* 13: 1211-1221.
- Mercer, T. T. (1973a) Aerosol technology in hazard evaluation. New York, NY: Academic Press; pp. 285-290. (McCormick, W. E., ed. Monograph series on industrial hygiene).
- Mercer, T. T. (1973b) Aerosol technology in hazard evaluation. New York, NY: Academic Press; pp. 22-33. (McCormick, W. E., ed. Monograph series on industrial hygiene).
- Mercer, T. T. (1973c) Aerosol technology in hazard evaluation. New York, NY: Academic Press; pp. 28-29. (McCormick, W. E., ed. Monograph series on industrial hygiene).
- Mercer, T. T. (1975) The deposition model of the task group on lung dynamics: a comparison with recent experimental data. *Health Phys.* 29: 673-680.
- Mercer, R. R.; Crapo, J. D. (1987) Three-dimensional reconstruction of the rat acinus. *J. Appl. Physiol.* 63: 785-794.
- Mercer, R. R.; Crapo, J. D. (1992) Architecture of the acinus. In: Parent, R. A., ed. Comparative biology of the normal lung: volume I, treatise on pulmonary toxicology. Boca Raton, FL: CRC Press; pp. 109-119.
- Mercer, R. R.; Laco, J. M.; Crapo, J. D. (1987) Three-dimensional reconstruction of alveoli in the rat lung for determination of pressure-volume relationships. *J. Appl. Physiol.* 62: 1480-1487.
- Mewhinney, J. A.; Griffith, W. C. (1983) A tissue distribution model for assessment of human inhalation exposures to <sup>241</sup>AmO<sub>2</sub>. *Health Phys.* 44(suppl.1): 537-544.
- Milic-Emili, J.; Henderson, J. A. M.; Dolovich, M. B.; Trop, D.; Kaneko, K. (1966) Regional distribution of inspired gas in the lung. *J. Appl. Physiol.* 21: 749-759.
- Miller, F. J.; Martonen, T. B.; Ménache, M. G.; Graham, R. C.; Spektor, D. M.; Lippmann, M. (1988) Influence of breathing mode and activity level on the regional deposition of inhaled particles and implications for regulatory standards. In: Dodgson, J.; McCallum, R. I.; Bailey, M. R.; Fisher, D. R., eds. Inhaled particles VI: proceedings of an international symposium and workshop on lung dosimetry; September 1985; Cambridge, United Kingdom. *Ann. Occup. Hyg.* 32(suppl. 1): 3-10.
- Miller, F. J.; Angilvel, S.; Ménache, M. G.; Asgharian, B.; Gerrity, T. R. (1995) Dosimetric issues relating to particulate toxicity. In: Phalen, R. F.; Bates, D. V., eds. Proceedings of the colloquium on particulate air pollution and human mortality and morbidity, part II; January 1994; Irvine, CA. *Inhalation Toxicol.* 7: 615-632.
- Morgan, A.; Evans, J. C.; Evans, R. J.; Hounam, R. F.; Holmes, A.; Doyle, S. G. (1975) Studies on the deposition of inhaled fibrous material in the respiratory tract of the rat and its subsequent clearance using radioactive tracer techniques. II. Deposition of the UICC standard reference samples of asbestos. *Environ. Res.* 10: 196-207.

- Morgan, A.; Evans, J. C.; Holmes, A. (1977) Deposition and clearance of inhaled fibrous minerals in the rat. Studies using radioactive tracer techniques. In: Walton, W. H.; McGovern, B., eds. Inhaled particles IV: proceedings of an international symposium, part 1; September 1975; Edinburgh, United Kingdom. Oxford, United Kingdom: Pergamon Press, Ltd.; pp. 259-272.
- Morgan, A.; Evan, J. C.; Holmes, A. (1978) Deposition and clearance of inhaled fibrous materials in the rat: studies using radioactive tracer techniques. In: Walton, W. H.; McGovern, B., eds. Inhaled particles IV: proceedings of an international symposium, part 1; September 1975; Edinburgh, United Kingdom. Oxford, United Kingdom: Pergamon Press, Ltd.; pp. 259-272.
- Morgan, A.; Black, A.; Evans, N.; Holmes, A.; Pritchard, J. N. (1980) Deposition of sized glass fibres in the respiratory tract of the rat. *Ann. Occup. Hyg.* 23: 353-366.
- Morgan, A.; Holmes, A.; Davison, W. (1982) Clearance of sized glass fibres from the rat lung and their solubility in vivo. *Ann. Occup. Hyg.* 25: 317-331.
- Morgan, K. T.; Patterson, D. L.; Gross, E. A. (1986) Responses of the nasal mucociliary apparatus to airborne irritants. In: Barrow, C. S., ed. *Toxicology of the nasal passages: based on the seventh CIIT conference on toxicology; February 1984; Raleigh, NC. Washington, DC: Hemisphere Publishing Corporation; pp. 123-133. (Chemical Industry Institute of Toxicology series).*
- Morrow, P. E. (1972) Lymphatic drainage of the lung in dust clearance. *Ann. N. Y. Acad. Sci.* 22: 46-65.
- Morrow, P. E. (1973) Alveolar clearance of aerosols. *Arch. Intern. Med.* 131: 101-108.
- Morrow, P. E. (1977) Clearance kinetics of inhaled particles. In: Brain, J. D.; Proctor, D. F.; Reid, L. M., eds. *Respiratory defense mechanisms (in two parts), part II. New York, NY: Marcel Dekker, Inc.; pp. 491-543. (Lenfant, C., ed. Lung biology in health and disease: v. 5).*
- Morrow, P. E. (1986) Factors determining hygroscopic aerosol deposition in airways. *Physiol. Rev.* 66: 330-376.
- Morrow, P. E. (1988) Possible mechanisms to explain dust overloading of the lungs. *Fundam. Appl. Toxicol.* 10: 369-384.
- Morrow, P. E. (1994) Mechanisms and significance of "particle overload." In: Mohr, U.; Dungworth, D. L.; Mauderly, J. L.; Oberdörster, G., eds. *Toxic and carcinogenic effects of solid particles in the respiratory tract: [proceedings of the 4th international inhalation symposium]; March 1993; Hannover, Germany. Washington, DC: International Life Sciences Institute Press; pp. 17-25.*
- Morrow, P. E.; Yu, C. P. (1993) Models of aerosol behavior in airways and alveoli. In: Morén, F.; Dolovich, M. B.; Newhouse, M. T.; Newman, S. P., eds. *Aerosols in medicine: principles, diagnosis and therapy. 2nd rev. ed. Amsterdam, The Netherlands: Elsevier; pp. 157-193.*
- Morrow, P. E.; Yuile, C. L. (1982) The disposition of coal dusts in the lungs and tracheobronchial lymph nodes of dogs. *Fundam. Appl. Toxicol.* 2: 300-305.

- Morrow, P. E.; Gibb, F. R.; Gazioglu, K. (1967a) The clearance of dust from the lower respiratory tract of man. An experimental study. In: Davies, C. N., ed. Inhaled particles and vapours II: proceedings of an international symposium; September-October 1965; Cambridge, United Kingdom. Oxford, United Kingdom: Pergamon Press; pp. 351-359.
- Morrow, P. E.; Gibb, F. R.; Gazioglu, K. M. (1967b) A study of particulate clearance from the human lungs. *Am. Rev. Respir. Dis.* 96: 1209-1221.
- Mueller, H.-L.; Robinson, B.; Muggenburg, B. A.; Gillett, N. A.; Guilmette, R. A. (1990) Particle distribution in lung and lymph node tissues of rats and dogs and the migration of particle-containing alveolar cells in vitro. *J. Toxicol. Environ. Health* 30: 141-165.
- Muhle, H.; Bellmann, B.; Heinrich, U. (1988) Overloading of lung clearance during chronic exposure of experimental animals to particles. *Ann. Occup. Hyg.* 32(suppl. 1): 141-147.
- Muhle, H.; Creutzenberg, O.; Bellmann, B.; Heinrich, U.; Mermelstein, R. (1990) Dust overloading of lungs: investigations of various materials, species differences, and irreversibility of effects. *J. Aerosol Med.* 3(suppl. 1): S111-S128.
- Murray, M. J.; Driscoll, K. E. (1992) Immunology of the respiratory system. In: Parent, R. A., ed. *Comparative biology of the normal lung: v. I*. Boca Raton, FL: CRC Press, Inc.; pp. 725-746.
- Myojo, T. (1987) Deposition of fibrous aerosol in model bifurcating tubes. *J. Aerosol Sci.* 18: 337-347.
- Myojo, T. (1990) The effect of length and diameter on the deposition of fibrous aerosol in a model lung bifurcation. *J. Aerosol Sci.* 21: 651-659.
- National Research Council. (1979) *Airborne particles*. Baltimore, MD: University Park Press.
- Naumann, B. D.; Schlesinger, R. B. (1986) Assessment of early alveolar particle clearance and macrophage function following an acute inhalation of sulfuric acid mist. *Exp. Lung Res.* 11: 13-33.
- Newton, D. (1968) A case of accidental inhalation of protactinium-231 and actinium-227. *Health Phys.* 15: 11-17.
- Newton, P. E.; Pfledderer, C. (1986) Measurement of the deposition and clearance of inhaled radiolabeled particles from rat lungs. *J. Appl. Toxicol.* 6: 113-119.
- Newton, D.; Fry, F. A.; Taylor, B. T.; Eagle, M. C.; Sharma, R. C. (1978) Interlaboratory comparison of techniques for measuring lung burdens of low-energy photon-emitters. *Health Phys.* 35: 751-771.
- Niinimaa, V.; Cole, P.; Mintz, S.; Shephard, R. J. (1981) Oronasal distribution of respiratory airflow. *Respir. Physiol.* 43: 69-75.
- Nixon, W.; Egan, M. J. (1987) Modelling study of regional deposition of inhaled aerosols with special reference to effects of ventilation asymmetry. *J. Aerosol Sci.* 18: 563-579.
- Nolibé, D.; Metivier, H.; Masse, R.; LaFuma, J. (1977) Therapeutic effect of pulmonary lavage *in vivo* after inhalation of insoluble radioactive particles. In: Walton, W. H.; McGovern, B., eds. *Inhaled particles IV: proceedings of an international symposium, part 2*; September 1975; Edinburgh, United Kingdom. Oxford, United Kingdom: Pergamon Press, Ltd.; pp. 597-613.
- Oberdörster, G. (1988) Lung clearance of inhaled insoluble and soluble particles. *J. Aerosol Med.* 1: 289-330.
- Oberdörster, G. (1993) Lung dosimetry: pulmonary clearance of inhaled particles. *Aerosol Sci. Technol.* 18: 279-289.

- Oberdörster, G.; Cox, C.; Baggs, R. (1987) Long term lung clearance and cellular retention of cadmium in rats and monkeys. *J. Aerosol Sci.* 18: 745-748.
- Oberdörster, G.; Morrow, P. E.; Spurny, K. (1988) Size dependent lymphatic short term clearance of amosite fibres in the lung. *Ann. Occup. Hyg.* 32(suppl. 1): 149-156.
- Oberdörster, G.; Ferin, J.; Gelein, R.; Soderholm, S. C.; Finkelstein, J. (1992a) Role of the alveolar macrophage in lung injury: studies with ultrafine particles. *Environ. Health Perspect.* 97: 193-199.
- Oberdörster, G.; Ferin, J.; Morrow, P. E. (1992b) Volumetric loading of alveolar macrophages (AM): a possible basis for diminished AM-mediated particle clearance. *Exp. Lung Res.* 18: 87-104.
- Oberdörster, G.; Ferin, J.; Lehnert, B. E. (1994) Correlation between particle size, *in vivo* particle persistence, and lung injury. *Environ. Health Perspect.* 102(suppl. 5): 173-179.
- Oghiso, Y.; Matsuoka, O. (1979) Distribution of colloidal carbon in lymph nodes of mice injected by different routes. *Jpn. J. Exp. Med.* 49: 223-234.
- Orenstein, A. J., ed. (1960) Proceedings of the pneumoconiosis conference; February 1959; Johannesburg, South Africa. London, United Kingdom: J. & A. Churchill, Ltd.
- Owen, P. R. (1969) Turbulent flow and particle deposition in the trachea. In: Wolstenholme, G. E. W.; Knight, J., eds. *Circulatory and respiratory mass transport*. Boston, MA: Little, Brown and Company; pp. 236-255.
- Pack, A.; Hooper, M. B.; Nixon, W.; Taylor, J. C. (1977) A computational model of pulmonary gas transport incorporating effective diffusion. *Respir. Physiol.* 29: 101-123.
- Parent, R. A., ed. (1992) *Comparative biology of the normal lung; volume I, treatise on pulmonary toxicology*. Boca Raton, FL: CRC Press.
- Park, J. F.; Bair, W. J.; Busch, R. H. (1972) Progress in beagle dog studies with transuranium elements at Battelle-Northwest. *Health Phys.* 22: 803-810.
- Parker, H.; Horsfield, K.; Cumming, G. (1971) Morphology of distal airways in the human lung. *J. Appl. Physiol.* 31: 386-391.
- Parra, S. C.; Burnette, R.; Price, H. P.; Takaro, T. (1986) Zonal distribution of alveolar macrophages, Type II pneumonocytes, and alveolar septal connective tissue gaps in adult human lungs. *Am. Rev. Respir. Dis.* 133: 908-912.
- Passali, D.; Bianchini Ciampoli, M. (1985) Normal values of mucociliary transport time in young subjects. *Int. J. Pediatr. Otorhinolaryngol.* 9: 151-156.
- Patra, A. L. (1986) Comparative anatomy of mammalian respiratory tracts: the nasopharyngeal region and the tracheobronchial region. *J. Toxicol. Environ. Health* 17: 163-174.
- Patrick, G. (1983) The retention of various types and sizes of particle in the large airways of the rat: implications for assessing the risk of lung cancer. In: Fisher, D. R., ed. *Current concepts in lung dosimetry*. Oak Ridge, TN: U.S. Department of Energy; pp. 66-72.
- Patrick, G. (1989) Requirements for local dosimetry and risk estimation in inhomogeneously irradiated lung. In: Baverstock, K. F.; Stather, J. W., eds. *Low dose radiation: biological bases of risk assessment*. London, United Kingdom: Taylor and Francis; pp. 269-277.

- Patrick, G.; Stirling, C. (1977) The retention of particles in large airways of the respiratory tract. *Proc. R. Soc. London B* 198: 455-462.
- Pattle, R. E. (1961) The retention of gases and particles in the human nose. In: Davies, C. N., ed. *Inhaled particles and vapours: proceedings of an international symposium; March-April 1960; Oxford, United Kingdom*. New York, NY: Pergamon Press; pp. 302-311.
- Pavia, D. (1984) Lung mucociliary clearance. In: Clarke, S. W.; Pavia, D., eds. *Aerosols and the lung: clinical and experimental aspects*. London, United Kingdom: Butterworths; pp. 127-155.
- Pavia, D.; Bateman, J. R. M.; Sheahan, N. F.; Agnew, J. E.; Clarke, S. W. (1985) Tracheobronchial mucociliary clearance in asthma: impairment during remission. *Thorax* 40: 171-175.
- Phalen, R. F. (1984) Aerosols and gases. In: *Inhalation studies: foundations and techniques*. Boca Raton, FL: CRC Press, Inc.; pp. 1-30.
- Phalen, R. F.; Oldham, M. J. (1983) Tracheobronchial airway structure as revealed by casting techniques. *Am. Rev. Respir. Dis.* 128: S1-S4.
- Phalen, R. F.; Oldham, M. J.; Beaucage, C. B.; Crocker, T. T.; Mortensen, J. D. (1985) Postnatal enlargement of human tracheobronchial airways and implications for particle deposition. *Anat. Rec.* 212: 368-380.
- Phalen, R. F.; Stuart, B. O.; Liroy, P. J. (1988) Rationale for and implications of particle size-selective sampling. In: *Advances in air sampling: [papers from the ACGIH symposium]; February 1987; Pacific Grove, CA*. Chelsea, MI: Lewis Publishers, Inc.; p. 6. (Industrial hygiene science series).
- Phalen, R. F.; Cuddihy, R. G.; Fisher, G. L.; Moss, O. R.; Schlesinger, R. B.; Swift, D. L.; Yeh, H.-C. (1991) Main features of the proposed NCRP respiratory tract model. *Radiat. Prot. Dosim.* 38: 179-184.
- Phalen, R. F.; Mannix, R. C.; Kleinman, M. T. (1994) Effects of oxidants, acids and other agents on particle clearance in the rat. In: Dodgson, J.; McCallum, R. I., eds. *Inhaled particles VII: proceedings of an international symposium; September 1991; Edinburgh, United Kingdom*. *Ann. Occup. Hyg.* 38(suppl. 1): 927-931.
- Philipson, K.; Falk, R.; Camner, P. (1985) Long-term lung clearance in humans studied with Teflon particles labeled with chromium-51. *Exp. Lung Res.* 9: 31-42.
- Pritchard, J. N. (1989) Dust overloading causes impairment of pulmonary clearance: evidence from rats and humans. *Exp. Pathol.* 37: 39-42.
- Pritchard, J. N.; Jefferies, S. J.; Black, A. (1986) Sex differences in the regional deposition of inhaled particles in the 2.5—7.5  $\mu\text{m}$  size range. *J. Aerosol Sci.* 17: 385-389.
- Pritsker, A. A. B. (1974) *The GASP IV simulation language*. New York, NY: John Wiley & Sons.
- Proctor, D. F. (1977) The upper airways: I. nasal physiology and defense of the lungs. *Am. Rev. Respir. Dis.* 115: 97-129.
- Proctor, D. F. (1980) The upper respiratory tract. In: Fishman, A. P., ed. *Pulmonary diseases and disorders*. New York, NY: McGraw-Hill Book Company; pp. 209-223.
- Puchelle, E.; Zahm, J.-M.; Bertrand, A. (1979) Influence of age on mucociliary transport. *Scand. J. Respir. Dis.* 60: 307-313.
- Puchelle, E.; Zahm, J. M.; Girard, F.; Bertrand, A.; Polu, J. M.; Aug, F.; Sadoul, P. (1980) Mucociliary transport *in vivo* and *in vitro*: relations to sputum properties in chronic bronchitis. *Eur. J. Respir. Dis.* 61: 254-264.

- Pump, K. K. (1964) The morphology of the finer branches of the bronchial tree of the human lung. *Dis. Chest* 46: 379-398.
- Raabe, O. G. (1971) Particle size analysis utilizing grouped data and the log-normal distribution. *J. Aerosol Sci.* 2: 289-303.
- Raabe, O. G. (1979) Deposition and clearance of inhaled aerosols. Washington, DC: U.S. Department of Energy, Laboratory for Energy-Related Health Research; report no. UCD-472-503. Available from: NTIS, Springfield, VA; UCD-472-503.
- Raabe, O. G. (1982) Deposition and clearance of inhaled aerosols. In: Witschi, H., ed. *Mechanisms in respiratory toxicology*. Boca Raton, FL: CRC Press; pp. 27-76.
- Raabe, O. G. (1984a) Size-selective sampling criteria for thoracic and respirable mass fractions. *Ann. Am. Conf. Gov. Ind. Hyg.* 11: 53-65.
- Raabe, O. G. (1984b) Deposition and clearance of inhaled particles. In: Gee, J. B. L.; Morgan, W. K. C.; Brooks, S. M., eds. *Occupational lung disease*. New York, NY: Raven Press; pp. 1-37.
- Raabe, O. G.; Yeh, H. C.; Schum, G. M.; Phalen, R. F. (1976) *Tracheobronchial geometry: human, dog, rat, hamster*. Albuquerque, NM: Lovelace Foundation; report no. LF-53.
- Raabe, O. G.; Yeh, H.-C.; Newton, G. J.; Phalen, R. F.; Velasquez, D. J. (1977) Deposition of inhaled monodisperse aerosols in small rodents. In: Walton, W. H.; McGovern, B., eds. *Inhaled particles IV: proceedings of an international symposium, part 1; September 1975; Edinburgh, United Kingdom*. Oxford, United Kingdom: Pergamon Press, Ltd.; pp. 3-21.
- Raabe, O. G.; Al-Bayati, M. A.; Teague, S. V.; Rasolt, A. (1988) Regional deposition of inhaled monodisperse, coarse, and fine aerosol particles in small laboratory animals. In: Dodgson, J.; McCallum, R. I.; Bailey, M. R.; Fischer, D. R., eds. *Inhaled particles VI: proceedings of an international symposium and workshop on lung dosimetry; September 1985; Cambridge, United Kingdom*. *Ann. Occup. Hyg.* 32(suppl. 1): 53-63.
- Radford, E. P.; Martell, E. A. (1977) Polonium-210: lead-210 ratios as an index of residence time of insoluble particles from cigarette smoke in bronchial epithelium. In: Walton, W. H.; McGovern, B., eds. *Inhaled particles IV: proceedings of an international symposium, part 2; September 1975; Edinburgh, United Kingdom*. Oxford, United Kingdom: Pergamon Press, Ltd.; pp. 567-581.
- Ramsden, D.; Bains, M. E. D.; Fraser, D. C. (1970) In-vivo and bioassay results from two contrasting cases of plutonium-239 inhalation. *Health Phys.* 19: 9-17.
- Reeves, A. L.; Vorwald, A. J. (1967) Beryllium carcinogenesis: II. pulmonary deposition and clearance of inhaled beryllium sulfate in the rat. *Cancer Res.* 27: 446-451.
- Robertson, B. (1980) Basic morphology of the pulmonary defence system. *Eur. J. Respir. Dis.* 61(suppl. 107): 21-40.
- Rodriguez, M.; Bur, S.; Weibel, E. R. (1987) Pulmonary acinus: geometry and morphometry of the peripheral airway system in rat and rabbit. *Am. J. Anat.* 180: 143-155.
- Rossmann, C. M.; Lee, R. M. K. W.; Forrest, J. B.; Newhouse, M. T. (1984) Nasal ciliary ultrastructure and function in patients with primary ciliary dyskinesia compared with that in normal subjects and in subjects with various respiratory diseases. *Am. Rev. Respir. Dis.* 129: 161-167.
- Roy, M. (1989) Lung clearance modeling on the basis of physiological and biological parameters. *Health Phys.* 57(suppl. 1): 255-262.

- Rudolf, G. (1975) Deposition von aerosolteilchen in der nase [Deposition of aerosol particles in the nose] [diploma thesis]. Frankfurt, Federal Republic of Germany: University Frankfurt/Main.
- Rudolf, G. (1984) A mathematical model for the deposition of aerosol particles in the human respiratory tract. *J. Aerosol Sci.* 15: 195-199.
- Rudolf, G.; Gebhart, J.; Heyder, J.; Scheuch, G.; Stahlhofen, W. (1983) Modelling the deposition of aerosol particles in the human respiratory tract. *J. Aerosol Sci.* 14: 188-192.
- Rudolf, G.; Gebhart, J.; Heyder, J.; Schiller, Ch. F.; Stahlhofen, W. (1986) An empirical formula describing aerosol deposition in man for any particle size. *J. Aerosol Sci.* 17: 350-355.
- Rudolf, G.; Gebhart, J.; Heyder, J.; Scheuch, G.; Stahlhofen, W. (1988) Mass deposition from inspired polydisperse aerosols. *Ann. Occup. Hyg.* 32: 919-938.
- Rudolf, G.; Köbrich, R.; Stahlhofen, W. (1990) Modelling and algebraic formulation of regional aerosol deposition in man. *J. Aerosol Sci.* 21(suppl. 1): S403-S406.
- Ruppel, G. (1979) Manual of pulmonary function testing. 2nd ed. St. Louis, MO: The C. V. Mosby Company.
- Rutland, J.; Cole, P. J. (1981) Nasal mucociliary clearance and ciliary beat frequency in cystic fibrosis compared with sinusitis and bronchiectasis. *Thorax* 36: 654-658.
- Sanders, C. L.; Dagle, G. E.; Cannon, W. C.; Craig, D. K.; Powers, G. J.; Meier, D. M. (1976) Inhalation carcinogenesis of high-fired  $^{239}\text{PuO}_2$  in rats. *Radiat. Res.* 68: 349-360.
- Scheuch, G.; Stahlhofen, W. (1988) Particle deposition of inhaled aerosol boluses in the upper human airways. *J. Aerosol Med.* 1: 29-36.
- Scheuch, G.; Gebhart, J.; Roth, C. (1990) Uptake of electrical charges in the human respiratory tract during exposure to air loaded with negative ions. *J. Aerosol Sci.* 21(suppl. 1): 439-442.
- Schiller, C. F.; Gebhart, J.; Heyder, J.; Rudolf, G.; Stahlhofen, W. (1986) Factors influencing total deposition of ultrafine aerosol particles in the human respiratory tract. *J. Aerosol Sci.* 17: 328-332.
- Schiller, C. F.; Gebhart, J.; Heyder, J.; Rudolf, G.; Stahlhofen, W. (1988) Deposition of monodisperse insoluble aerosol particles in the 0.095 to 0.2  $\mu\text{m}$  size range within the human respiratory tract. *Ann. Occup. Hyg.* 32(suppl.): 41-49.
- Schiller-Scotland, C. F.; Hlawa, R.; Gebhart, J.; Wönne, R.; Heyder, J. (1992) Total deposition of aerosol particles in the respiratory tract of children during spontaneous and controlled mouth breathing. *J. Aerosol Sci.* 23(suppl. 1): S457-S460.
- Schlesinger, R. B. (1985a) Comparative deposition of inhaled aerosols in experimental animals and humans: a review. *J. Toxicol. Environ. Health* 15: 197-214.
- Schlesinger, R. B. (1985b) Clearance from the respiratory tract. *Fundam. Appl. Toxicol.* 5: 435-450.
- Schlesinger, R. B. (1985c) Effects of inhaled acids on respiratory tract defense mechanisms. *Environ. Health Perspect.* 63: 25-38.
- Schlesinger, R. B. (1988) Biological disposition of airborne particles: basic principles and application to vehicular emissions. In: Watson, A. Y.; Bates, R. R.; Kennedy, D., eds. *Air pollution, the automobile, and public health*. Washington, DC: National Academy Press; pp. 239-298.

- Schlesinger, R. B. (1989) Deposition and clearance of inhaled particles. In: McClellan, R. O.; Henderson, R. F., eds. Concepts in inhalation toxicology. New York, NY: Hemisphere Publishing Corp.; pp. 163-192.
- Schlesinger, R. B. (1990) The interaction of inhaled toxicants with respiratory tract clearance mechanisms. *Crit. Rev. Toxicol.* 20: 257-286.
- Schlesinger, R. B. (1995) Deposition and clearance of inhaled particles. In: McClellan, R. O.; Henderson, R. F., eds. Concepts in inhalation toxicology. 2nd ed. Washington, DC: Taylor & Francis; pp. 191-224.
- Schlesinger, R. B.; Chen, L. C. (1994) Comparative biological potency of acidic sulfate aerosols: implications for the interpretation of laboratory and field studies. *Environ. Res.* 65: 69-85.
- Schlesinger, R. B.; Lippmann, M. (1978) Selective particle deposition and bronchogenic carcinoma. *Environ. Res.* 15: 424-431.
- Schlesinger, R. B.; Driscoll, K. E.; Naumann, B. D.; Vollmuth, T. A. (1988) Particle clearance from the lungs: assessment of effects due to inhaled irritants. *Ann. Occup. Hyg.* 32(suppl. 1): 113-123.
- Schreider, J. P. (1983) Nasal airway anatomy and inhalation deposition in experimental animals and people. In: Reznik, G.; Stinson, S. F., eds. Nasal tumors in animals and man: v. III, experimental nasal carcinogenesis. Boca Raton, FL: CRC Press; pp. 1-26.
- Schreider, J. P.; Raabe, O. G. (1981) Anatomy of the nasal-pharyngeal airway of experimental animals. *Anat. Rec.* 200: 195-205.
- Schulte, P. A. (1989) A conceptual framework for the validation and use of biologic markers. *Environ. Res.* 48: 129-144.
- Schum, M.; Yeh, H.-C. (1980) Theoretical evaluation of aerosol deposition in anatomical models of mammalian lung airways. *Bull. Math. Biol.* 42: 1-15.
- Schürch, S.; Gehr, P.; Im Hof, V.; Geiser, M.; Green, F. (1990) Surfactant displaces particles toward the epithelium in airways and alveoli. *Respir. Physiol.* 80: 17-32.
- Scott, W. R.; Taulbee, D. B.; Yu, C. P. (1978) Theoretical study of nasal deposition. *Bull. Math. Biol.* 40: 581-604.
- Sebastien, P.; Fondimare, A.; Bignon, J.; Monchaux, G.; Desbordes, J.; Bonnard, G. (1977) Topographic distribution of asbestos fibers in human lung in relation to occupational and non-occupational exposure. In: Walton, W. H.; McGovern, B., eds. Inhaled particles IV: proceedings of an international symposium, part 2; September 1975; Edinburgh, United Kingdom. Oxford, United Kingdom: Pergamon Press, Ltd.; pp. 435-446.
- Shiotsuka, R. N.; Costa, D. L.; Osheroff, M. R.; Drew, R. T. (1987) Method of measuring deposition of unlabeled monodisperse microspheres in rat lungs. *J. Toxicol. Environ. Health* 21: 1-13.
- Slauson, D. O.; Lay, J. C.; Castleman, W. L.; Neilsen, N. R. (1987) Alveolar macrophage phagocytic kinetics following pulmonary parainfluenza-3 virus infection. *J. Leukocyte Biol.* 41: 412-420.
- Slauson, D. O.; Lay, J. C.; Castleman, W. L.; Neilsen, N. R. (1989) Influence of acute pulmonary interstitial inflammation on kinetics of phagocytosis by alveolar macrophages. *Inflammation (NY)* 13: 429-441.
- Smaldone, G. C.; Perry, R. J.; Bennett, W. D.; Messina, M. S.; Zwang, J.; Ilowite, J. (1988) Interpretation of "24 hour lung retention" in studies of mucociliary clearance. *J. Aerosol Med.* 1: 11-20.
- Snipes, M. B. (1989) Long-term retention and clearance of particles inhaled by mammalian species. *CRC Crit. Rev. Toxicol.* 20: 175-211.

- Snipes, M. B. (1994) Biokinetics of inhaled radionuclides. In: Raabe, O. G., ed. Internal radiation dosimetry, Health Physics Society summer school 1994. Madison, WI: Medical Physics Publishing; pp. 181-196.
- Snipes, M. B.; Clem, M. F. (1981) Retention of microspheres in the rat lung after intratracheal instillation. *Environ. Res.* 24: 33-41.
- Snipes, M. B.; Boecker, B. B.; McClellan, R. O. (1983) Retention of monodisperse or polydisperse aluminosilicate particles inhaled by dogs, rats, and mice. *Toxicol. Appl. Pharmacol.* 69: 345-362.
- Snipes, M. B.; Böcker, B. B.; McClellan, R. O. (1984) Respiratory tract clearance of inhaled particles in laboratory animals. In: Smith, H.; Gerber, G., eds. Lung modeling for inhalation of radioactive materials. Luxembourg: Commission of the European Communities; pp. 63-71; report no. EUR9384EN.
- Snipes, M. B.; Olson, T. R.; Yeh, H. C. (1988) Deposition and retention patterns for 3-, 9-, and 15- $\mu$ m latex microspheres inhaled by rats and guinea pigs. *Exp. Lung Res.* 14: 37-50.
- Snyder, W. S.; Cook, M. J.; Nasset, E. S.; Karhausen, L. R.; Howells, G. P.; Tipton, I. H. (1975) Report of the task group on reference man. New York, NY: Pergamon Press. (International Commission on Radiological Protection no. 23).
- Soderholm, S. C. (1989) Proposed international conventions for particle size-selective sampling. *Ann. Occup. Hyg.* 33: 301-320.
- Sorokin, S. P.; Brain, J. D. (1975) Pathways of clearance in mouse lungs exposed to iron oxide aerosols. *Anat. Rec.* 181: 581-625.
- Stahl, W. R. (1967) Scaling of respiratory variables in mammals. *J. Appl. Physiol.* 22: 453-460.
- Stahlhofen, W.; Gebhart, J.; Heyder, J. Stuck, B. (1979) Herstellung von monodispersen Fe<sub>2</sub>O<sub>3</sub>-testaerosolen mit Hilfe der Zentrifugalzerstäubung. *Staub Reinhalt. Luft* 39: 73-77.
- Stahlhofen, W.; Gebhart, J.; Heyder, J. (1980) Experimental determination of the regional deposition of aerosol particles in the human respiratory tract. *Am. Ind. Hyg. Assoc. J.* 41: 385-398a.
- Stahlhofen, W.; Gebhart, J.; Heyder, J. (1981a) Biological variability of regional deposition of aerosol particles in the human respiratory tract. *Am. Ind. Hyg. Assoc. J.* 42: 348-352.
- Stahlhofen, W.; Gebhart, J.; Heyder, J.; Philipson, K.; Camner, P. (1981b) Intercomparison of regional deposition of aerosol particles in the human respiratory tract and their long-term elimination. *Exp. Lung Res.* 2: 131- 139.
- Stahlhofen, W.; Gebhart, J.; Heyder, J.; Scheuch, G. (1983) New regional deposition data of the human respiratory tract. *J. Aerosol Sci.* 14: 186-188.
- Stahlhofen, W.; Gebhart, J.; Rudolf, G.; Scheuch, G. (1986a) Measurement of lung clearance with pulses of radioactively-labelled aerosols. *J. Aerosol Sci.* 17: 333-336.
- Stahlhofen, W.; Gebhart, J.; Rudolf, G.; Scheuch, G.; Philipson, K. (1986b) Clearance from the human airways of particles of different sizes deposited from inhaled aerosol boli. In: *Aerosols: formation and reactivity, proceedings of the second international aerosol conference; September; Berlin, Federal Republic of Germany.* Oxford, United Kingdom: Pergamon Press; pp. 192-196.
- Stahlhofen, W.; Gebhart, J.; Rudolf, G.; Scheuch, G. (1987) Retention of radioactively labelled Fe<sub>2</sub>O<sub>3</sub> particles in human lungs. In: Hofmann, W., ed. *Deposition and clearance of aerosols in the human respiratory tract.* Vienna, Austria: Facultas Universitätsverlag mbH; pp. 123-128.

- Stahlhofen, W.; Rudolf, G.; James, A. C. (1989) Intercomparison of experimental regional aerosol deposition data. *J. Aerosol Med.* 2: 285-308.
- Stahlhofen, W.; Koebrich, R.; Rudolf, G.; Scheuch, G. (1990) Short-term and long-term clearance of particles from the upper human respiratory tract as function of particle size. *J. Aerosol Sci.* 21(suppl. 1): S407-S410.
- Stanley, P. J.; Wilson, R.; Greenstone, M. A.; Mackay, I. S.; Cole, P. J. (1985) Abnormal nasal mucociliary clearance in patients with rhinitis and its relationship to concomitant chest disease. *Br. J. Dis. Chest* 79: 77-82.
- Stirling, C.; Patrick, G. (1980) The localisation of particles retained in the trachea of the rat. *J. Pathol.* 131: 309-320.
- Stöber, W.; Einbrodt, H. J.; Klosterkötter, W. (1967) Quantitative studies of dust retention in animal and human lungs after chronic inhalation. In: Davies, C. N., ed. *Inhaled particles and vapours II: proceedings of an international symposium; September-October 1965; Cambridge, United Kingdom.* Oxford, United Kingdom: Pergamon Press; pp. 409-418.
- Stöber, W.; Morrow, P. E.; Koch, W.; Morawietz, G. (1994) Alveolar clearance and retention of inhaled insoluble particles in rats simulated by a model inferring macrophage particle load distributions. *J. Aerosol Sci.* 25: 975-1002.
- Stone, K. C.; Mercer, R. R.; Gehr, P.; Stockstill, B.; Crapo, J. D. (1992) Allometric relationships of cell numbers and size in the mammalian lung. *Am. J. Respir. Cell. Mol. Biol.* 6: 235-243.
- Strom, K. A.; Chan, T. L.; Johnson, J. T. (1988) Pulmonary retention of inhaled submicron particles in rats: diesel exhaust exposures and lung retention model. In: Dodgson, J.; McCallum, R. I.; Bailey, M. R.; Fischer, D. R., eds. *Inhaled particles VI: proceedings of an international symposium and workshop on lung dosimetry; September 1985; Cambridge, United Kingdom.* Ann. Occup. Hyg. 32(suppl. 1): 645-658.
- Stuart, B. O. (1966) Promethium oxide inhalation studies. In: Pacific Northwest Laboratory annual report for 1965 in the biological sciences. Richland, WA: Battelle-Northwest; report no. BNWL-280m.
- Stuart, B. O. (1973) Deposition of inhaled aerosols. *Arch. Intern. Med.* 131: 60-73.
- Stuart, B. O.; Casey, H. W.; Bair, W. J. (1964) Acute and chronic effects of inhaled  $^{144}\text{CeO}_2$  in dogs. *Health Phys.* 10: 1203-1209.
- Sussman, R. G.; Cohen, B. S.; Lippmann, M. (1991a) Asbestos fiber deposition in a human tracheobronchial cast. I. Experimental. *Inhalation Toxicol.* 3: 145-160.
- Sussman, R. G.; Cohen, B. S.; Lippmann, M. (1991b) Asbestos fiber deposition in a human tracheobronchial cast. II. Empirical model. *Inhalation Toxicol.* 3: 161-179.
- Svartengren, M.; Widtskiöld-Olsson, K.; Philipson, K.; Camner, P. (1981) Retention of particles on the first bifurcation and the trachea of rabbits. *Clin. Respir. Physiol.* 17: 87-91.
- Svartengren, M.; Philipson, K.; Linnman, L.; Camner, P. (1986) Regional deposition of particles in human lung after induced bronchoconstriction. *Exp. Lung Res.* 10: 223-233.
- Svartengren, M.; Philipson, K.; Camner, P. (1989) Individual differences in regional deposition of  $6\text{-}\mu\text{m}$  particles in humans with induced bronchoconstriction. *Exp. Lung Res.* 15: 139-149.
- Svartengren, M.; Anderson, M.; Bylin, G.; Philipson, K.; Camner, P. (1990) Regional deposition of  $3.6\text{-}\mu\text{m}$  particles in subjects with mild to moderately severe asthma. *J. Aerosol Med.* 3: 197-207.

- Svartengren, M.; Anderson, M.; Bylin, G.; Philipson, K.; Camner, P. (1991) Mouth and throat deposition of 3.6  $\mu\text{m}$  radiolabelled particles in asthmatics. *J. Aerosol Med.* 4: 313-321.
- Swift, D. L. (1976) Design of the human respiratory tract to facilitate removal of particulates and gases. *AIChE Symp. Ser.* 72(156): 137-144.
- Swift, D. L. (1989) Age-related scaling for aerosol and vapor deposition in the upper airways of humans. In: Mahaffey, J. A., ed. 26th Hanford life sciences symposium, modeling for scaling to man: biology, dosimetry, and response. *Health Phys.* 57(suppl. 1): 293-297.
- Swift, D. L. (1993) Aerosol measurement in the health care field. In: Willeke, K.; Baron, P. A., eds. *Aerosol measurement: principles, techniques, and applications*. New York, NY: Van Nostrand Reinhold.
- Swift, D. L.; Proctor, D. F. (1988) A dosimetric model for particles in the respiratory tract above the trachea. *Ann. Occup. Hyg.* 32(suppl. 1): 1035-1044.
- Swift, D. L.; Montassier, N.; Hopke, P. K.; Karpen-Hayes, K.; Cheng, Y.-S.; Su, Y. F.; Yeh, H. C.; Strong, J. C. (1992) Inspiratory deposition of ultrafine particles in human nasal replicate cast. *J. Aerosol Sci.* 23: 65-72.
- Tabata, Y.; Ikada, Y. (1988) Effect of the size and surface charge of polymer microspheres on their phagocytosis by macrophage. *Biomaterials* 9: 356-362.
- Takahashi, S.; Asaho, S.; Kubota, Y.; Sato, H.; Matsuoka, O. (1987) Distribution of  $^{198}\text{Au}$  and  $^{133}\text{Ba}$  in thoracic and cervical lymph nodes of the rat following the intratracheal instillation of  $^{198}\text{Au}$ -colloid and  $^{133}\text{BaSO}_4$ . *J. Radiat. Res.* 28: 227-231.
- Takahashi, S.; Kubota, Y.; Hatsuno, H. (1992) Effect of size on the movement of latex particles in the respiratory tract following local administration. *Inhalation Toxicol.* 4: 113-123.
- Tang, I. N.; Munkelwitz, H. R. (1977) Aerosol growth studies—III. ammonium bisulfate aerosols in a moist atmosphere. *J. Aerosol Sci.* 8: 321-330.
- Tang, I. N.; Munkelwitz, H. R.; Davis, J. G. (1977) Aerosol growth studies - II. preparation and growth measurements of monodisperse salt aerosols. *J. Aerosol Sci.* 8: 149-159.
- Tarroni, G.; Melandri, C.; Prodi, V.; De Zaiacomo, T.; Formignani, M.; Bassi, P. (1980) An indication on the biological variability of aerosol total deposition in humans. *Am. Ind. Hyg. Assoc. J.* 41: 826-831.
- Task Group on Lung Dynamics. (1966) Deposition and retention models for internal dosimetry of the human respiratory tract. *Health Phys.* 12: 173-207.
- Taulbee, D. B.; Yu, C. P. (1975) A theory of aerosol deposition in the human respiratory tract. *J. Appl. Physiol.* 38: 77-85.
- Thomas, R. G. (1968) Transport of relatively insoluble materials from lung to lymph nodes. *Health Phys.* 14: 111-117.
- Thomas, R. G. (1972) Tracheobronchial lymph node involvement following inhalation of alpha emitters. In: Stover, B. J.; Jee, W. S. S., eds. *Radiobiology of plutonium*. Salt Lake City, UT: The J. W. Press; pp. 231-241.
- Thomson, M. L.; Short, M. D. (1969) Mucociliary function in health, chronic obstructive airway disease, and asbestosis. *J. Appl. Physiol.* 26: 535-539.
- Tryka, A. F.; Sweeney, T. D.; Brain, J. D.; Godleski, J. J. (1985) Short-term regional clearance of an inhaled submicrometric aerosol in pulmonary fibrosis. *Am. Rev. Respir. Dis.* 132: 606-611.

- Tu, K. W.; Knutson, E. O. (1984) Total deposition of ultrafine hydrophobic and hygroscopic aerosols in the human respiratory system. *Aerosol Sci. Technol.* 3: 453-465.
- U.S. Environmental Protection Agency. (1982) Air quality criteria for particulate matter and sulfur oxides. Research Triangle Park, NC: Office of Health and Environmental Assessment, Environmental Criteria and Assessment Office; EPA report no. EPA-600/8-82-029aF-cF. 3v. Available from: NTIS, Springfield, VA; PB84-156777.
- U.S. Environmental Protection Agency. (1988) Recommendations for and documentation of biological values for use in risk assessment. Cincinnati, OH: Office of Health and Environmental Assessment, Environmental Criteria and Assessment Office; EPA report no. EPA-600/6-87-008. Available from: NTIS, Springfield, VA; PB88-179874.
- U.S. Environmental Protection Agency. (1989) An acid aerosols issue paper: health effects and aerometrics. Research Triangle Park, NC: Office of Health and Environmental Assessment, Environmental Criteria and Assessment Office; EPA report no. EPA-600/8-88-005F. Available from: NTIS, Springfield, VA; PB91-125864.
- U.S. Environmental Protection Agency. (1994) Methods for derivation of inhalation reference concentrations and application of inhalation dosimetry [draft final]. Research Triangle Park, NC: Office of Health and Environmental Assessment, Environmental Criteria and Assessment Office; report no. EPA/600/8-88/066F.
- Utell, M. J.; Mariglio, J. A.; Morrow, P. E.; Gibb, F. R.; Speers, D. M. (1989) Effects of inhaled acid aerosols on respiratory function: the role of endogenous ammonia. *J. Aerosol Med.* 2: 141-147.

- Valberg, P. A. (1985) Determination of retained lung dose. In: Witschi, H. P.; Brain, J. D., eds. Toxicology of inhaled materials: general principles of inhalation toxicology. Berlin, Federal Republic of Germany: Springer-Verlag; pp. 57-91. (Born, G. V. R.; Farah, A.; Herken, H.; Welch, A. D., eds. Handbook of experimental pharmacology: v. 75).
- Valberg, P. A.; Blanchard, J. D. (1992) Pulmonary macrophage physiology: origin, motility, endocytosis. In: Parent, R. A., ed. Comparative biology of the normal lung: v. I. Boca Raton, FL: CRC Press; pp. 681-724.
- Valberg, P. A.; Wolff, R. K.; Mauderly, J. L. (1985) Redistribution of retained particles: effect of hyperpnea. *Am. Rev. Respir. Dis.* 131: 273-280.
- Vastag, E.; Matthys, H.; Zsomboki, G.; Köhler, D.; Daikeler, G. (1986) Mucociliary clearance in smokers. *Eur. J. Respir. Dis.* 68: 107-113.
- Vincent, J. H. (1990) The fate of inhaled aerosols: a review of observed trends and some generalizations. *Ann. Occup. Hyg.* 34: 623-637.
- Vollmuth, T. A.; Schlesinger, R. B. (1984) Measurement of respiratory tract ammonia in the rabbit and implications to sulfuric acid inhalation studies. *Fundam. Appl. Toxicol.* 4: 455-464.
- Waite, D. A.; Ramsden, D. (1971) The inhalation of insoluble iron oxide particles in the sub-micron range. Part I: Chromium 51 labelled aerosols. London, United Kingdom: Atomic Energy Authority; report no. AEEW-R740.
- Wales, K. A.; Petrow, H.; Yeates, D. B. (1980) Production of <sup>99m</sup>Tc-labeled iron oxide aerosols for human lung deposition and clearance studies. *Int. J. Appl. Radiat. Isot.* 31: 689-694.
- Waligora, S. J., Jr. (1971) Pulmonary retention of zirconium oxide (<sup>95</sup>Nb) in man and beagle dogs. *Health Phys.* 20: 89-91.
- Wanner, A. (1977) Clinical aspects of mucociliary transport. *Am. Rev. Respir. Dis.* 116: 73-125.
- Wanner, A. (1980) Pulmonary defense mechanisms: mucociliary clearance. In: Simmons, D. H., ed. *Current pulmonology*: v. 2. Boston, MA: Houghton Mifflin Professional Publishers; pp. 325-355.
- Warheit, D. B.; Hartsky, M. A. (1988) Assessments of pulmonary macrophage clearance responses to inhaled particulates. *Scanning Microsc.* 2: 1069-1078.
- Warheit, D. B.; Hartsky, M. A. (1990) Species comparisons of proximal alveolar deposition patterns of inhaled particulates. *Exp. Lung Res.* 16: 83-99.
- Warheit, D. B.; Hartsky, M. A. (1994) Influences of gender, species, and strain differences in pulmonary toxicological assessments of inhaled particles and/or fibers. In: Mohr, U.; Dungworth, D. L.; Mauderly, J. L.; Oberdörster, G., eds. Toxic and carcinogenic effects of solid particles in the respiratory tract: [proceedings of the 4th international inhalation symposium]; March 1993; Hannover, Germany. Washington, DC: International Life Sciences Institute Press; pp. 254-265.
- Warheit, D. B.; Overby, L. H.; George, G.; Brody, A. R. (1988) Pulmonary macrophages are attracted to inhaled particles through complement activation. *Exp. Lung Res.* 14: 51-66.
- Warner, A. E.; Brain, J. D. (1990) The cell biology and pathogenic role of pulmonary intravascular macrophages. *Am. J. Physiol.* 258: L1-L12.
- Warr, G. A.; Martin, R. R. (1978) Histochemical staining and in vitro spreading of human pulmonary alveolar macrophages: variability with cigarette smoking status. *J. Reticuloendothel. Soc.* 23: 53-62.

- Warwick, R.; Williams, P. L., eds. (1973) *Gray's anatomy*. 35th British ed. Philadelphia, PA: W. B. Saunders Company.
- Watson, A. Y.; Brain, J. D. (1979) Uptake of iron oxide aerosols by mouse airway epithelium. *Lab. Invest.* 40: 450-459.
- Watson, A. Y.; Brain, J. D. (1980) The effect of SO<sub>2</sub> on the uptake of particles by mouse bronchial epithelium. *Exp. Lung Res.* 1: 67-87.
- Weibel, E. R. (1963) *Morphometry of the human lung*. New York, NY: Academic Press Inc.
- Weibel, E. R. (1980) *Stereological methods: practical methods for biological morphometry*. New York, NY: Academic Press.
- Whaley, S. L.; Wolff, R. K.; Muggenburg, B. A.; Snipes, M. B. (1986) Mucociliary clearance and particle retention in the maxillary and ethmoid turbinate regions of beagle dogs. *J. Toxicol. Environ. Health* 19: 569-580.
- Whaley, S. L.; Wolff, R. K.; Muggenburg, B. A. (1987) Clearance of nasal mucus in nonanesthetized and anesthetized dogs. *Am. J. Vet. Res.* 48: 204-206.
- Whitby, K. T. (1975) Modeling of atmospheric aerosol particle size distributions: a progress report on EPA research grant no. R800971, "sampling and analysis of atmospheric aerosols." Minneapolis, MN: University of Minnesota, Mechanical Engineering Department; p. III-21; particle technology laboratory publication no. 253.
- Whitby, K. T. (1978) The physical characteristics of sulfur aerosols. *Atmos. Environ.* 12: 135-159.
- Wilson, W. E.; Spiller, L. L.; Ellestad, T. G.; Lamothe, P. J.; Dzubay, T. G.; Stevens, R. K.; Macias, E. S.; Fletcher, R. A.; Husar, J. D.; Husar, R. B.; Whitby, K. T.; Kittelson, D. B.; Cantrell, B. K. (1977) General Motors sulfate dispersion experiment: summary of EPA measurements. *J. Air Pollut. Control Assoc.* 27: 46-51.
- Wolff, R. K. (1986) Effects of airborne pollutants on mucociliary clearance. *Environ. Health Perspect.* 66: 223-237.
- Wolff, R. K. (1992) Mucociliary function. In: Parent, R. A., ed. *Comparative biology of the normal lung: v. I*. Boca Raton, FL: CRC Press; pp. 659-680.
- Wolff, R. K.; Dolovich, M. B.; Obminski, G.; Newhouse, M. T. (1977) Effects of exercise and eucapnic hyperventilation on bronchial clearance in man. *J. Appl. Physiol.: Respir. Environ. Exercise Physiol.* 43: 46-50.
- Wolff, R. K.; Henderson, R. F.; Snipes, M. B.; Griffith, W. C.; Mauderly, J. L.; Cuddihy, R. G.; McClellan, R. O. (1987) Alterations in particle accumulation and clearance in lungs of rats chronically exposed to diesel exhaust. *Fundam. Appl. Toxicol.* 9: 154-166.
- Xu, G. B.; Yu, C. P. (1985) Theoretical lung deposition of hygroscopic NaCl aerosols. *Aerosol Sci. Technol.* 4: 455-461.
- Xu, G. B.; Yu, C. P. (1986) Effects of age on deposition of inhaled aerosols in the human lung. *Aerosol Sci. Technol.* 5: 349-357.
- Xu, G. B.; Yu, C. P. (1987) Deposition of diesel exhaust particles in mammalian lungs: a comparison between rodents and man. *Aerosol Sci. Technol.* 7: 117-123.
- Yamada, Y.; Cheng, Y. S.; Yeh, H. C.; Swift, D. L. (1988) Inspiratory and expiratory deposition of ultrafine particles in a human nasal cast. *Inhalation Toxicol.* 1: 1-11.
- Yeates, D. B.; Aspin, M. (1978) A mathematical description of the airways of the human lungs. *Respir. Physiol.* 32: 91-104.

- Yeates, D. B.; Aspin, N.; Levison, H.; Jones, M. T.; Bryan, A. C. (1975) Mucociliary tracheal transport rates in man. *J. Appl. Physiol.* 19: 487-495.
- Yeates, D. B.; Gerrity, T. R.; Garrard, C. S. (1981a) Particle deposition and clearance in the bronchial tree. *Ann. Biomed. Eng.* 9: 577-592.
- Yeates, D. B.; Pitt, B. R.; Spektor, D. M.; Karron, G. A.; Albert, R. E. (1981b) Coordination of mucociliary transport in human trachea and intrapulmonary airways. *J. Appl. Physiol.: Respir. Environ. Exercise Physiol.* 51: 1057-1064.
- Yeh, H.-C.; Schum, G. M. (1980) Models of human lung airways and their application to inhaled particle deposition. *Bull. Math. Biol.* 42: 461-480.
- Yeh, H. C.; Schum, G. M.; Duggan, M. T. (1979) Anatomic models of the tracheobronchial and pulmonary regions of the rat. *Anat. Rec.* 195: 483-492.
- Yeh, H. C.; Zhuang, Y.; Chang, I. Y. (1993) Mathematical model of particle deposition from inhaled polydisperse aerosols. In: Nikula, K. J.; Belinsky, S. A.; Bradley, P. L., eds. *Inhalation Toxicology Research Institute annual report 1992—1993*. Albuquerque, NM: U. S. Department of Energy, Lovelace Biomedical and Environmental Research Institute; pp. 127-129; report no. ITRI-140. Available from: NTIS, Springfield, VA; AD-A277 924/7/XAB.
- Yu, C. P. (1978) Exact analysis of aerosol deposition during steady breathing. *Powder Technol.* 21: 55-62.
- Yu, C. P. (1985) Theories of electrostatic lung deposition of inhaled aerosols. *Ann. Occup. Hyg.* 29: 219-227.
- Yu, C. P.; Asgharian, B. (1993) Mathematical models of fiber deposition in the lung. In: Warheit, D. B., ed. *Fiber toxicology*. San Diego, CA: Academic Press, Inc.; pp. 73-98.
- Yu, C. P.; Diu, C. K. (1982a) A comparative study of aerosol deposition in different lung models. *Am. Ind. Hyg. Assoc. J.* 43: 54-65.
- Yu, C. P.; Diu, C. K. (1982b) A probabilistic model for intersubject deposition variability of inhaled particles. *Aerosol Sci. Technol.* 1: 355-362.
- Yu, C. P.; Diu, C. K. (1983) Total and regional deposition of inhaled aerosols in humans. *J. Aerosol Sci.* 5: 599-609.
- Yu, C. P.; Xu, G. B. (1987) Predicted deposition of diesel particles in young humans. *J. Aerosol Sci.* 18: 419-429.
- Yu, C. P.; Liu, C. S.; Taulbee, D. B. (1977) Simultaneous diffusion and sedimentation of aerosols in a horizontal cylinder. *J. Aerosol Sci.* 8: 309-316.
- Yu, C. P.; Nicolaidis, P.; Soong, T. T. (1979) Effect of random airway sizes on aerosol deposition. *Am. Ind. Hyg. Assoc. J.* 40: 999-1005.
- Yu, C. P.; Diu, C. K.; Soong, T. T. (1981) Statistical analysis of aerosol deposition in nose and mouth. *Am. Ind. Hyg. Assoc. J.* 42: 726-733.
- Yu, C. P.; Chen, Y. K.; Morrow, P. E. (1989) An analysis of alveolar macrophage mobility kinetics at dust overloading of the lungs. *Fundam. Appl. Toxicol.* 13: 452-459.
- Yu, C. P.; Yoon, K. J.; Chen, Y. K. (1991) Retention modeling of diesel exhaust particles in rats and humans. *J. Aerosol Med.* 4: 79-115.

- Yu, C. P.; Zhang, L.; Becquemin, M. H.; Roy, M.; Bouchikhi, A. (1992) Algebraic modeling of total and regional deposition of inhaled particles in the human lung of various ages. *J. Aerosol Sci.* 23: 73-79.
- Zeltner, T. B.; Sweeney, T. D.; Skornik, W. A.; Feldman, H. A.; Brain, J. D. (1991) Retention and clearance of 0.9- $\mu\text{m}$  particles inhaled by hamsters during rest or exercise. *J. Appl. Physiol.* 70: 1137-1145.
- Zhang, L.; Yu, C. P. (1993) Empirical equations for nasal deposition of inhaled particles in small laboratory animals and humans. *Aerosol Sci. Technol.* 19: 51-56.
- Zwicker, G. M.; Filipy, R. E.; Park, J. F.; Loscutoff, S. M.; Ragan, H. A.; Stevens, D. L. (1978) Clinical and pathological effects of cigarette smoke exposure in beagle dogs. *Arch. Pathol. Lab. Med.* 102: 623-628.

## **APPENDIX 10A**

# **PREDICTION OF REGIONAL DEPOSITION IN THE HUMAN RESPIRATORY TRACT USING THE INTERNATIONAL COMMISSION ON RADIOLOGICAL PROTECTION PUBLICATION 66 MODEL**

## 10A.1 INTRODUCTION

This Appendix gives an overview of how the regional deposition values that are calculated using the ICRP's newly recommended model of the human respiratory tract (ICRP66, 1994) compare with the available body of experimental data. A more complete description and discussion of these data is given in Annexe D (James et al., 1994) of the ICRP66 report. That Annexe also discusses both the theoretical model (Egan et al., 1989) of gas and aerosol particle transport in the human respiratory tract, which underlies ICRP66's analysis of the experimental data, and ICRP66's methodology in developing the recommended algebraic expressions to predict regional deposition for various subjects.

The deposition of particles in the respiratory tract, and the underlying physical mechanisms that determine regional deposition, have been intensively studied. However, in the main, experimental data are available only for the adult Caucasian male, and for a limited range of particle size (from about 1- $\mu\text{m}$  to 10- $\mu\text{m}$  aerodynamic diameter), whereas the application of this human respiratory tract model is required to be much broader. Because of the need to extrapolate the available data to aerosol particles and vapors from atomic dimensions up to very coarse wind-borne particles, and also to subjects of different body size and level of physical exertion, the ICRP66 report applied both theoretical and/or empirical modeling methods, as appropriate, to develop the recommended predictive deposition model.

Since the publication of ICRP's previous deposition model (TGLD, 1966; ICRP, 1979), substantial progress has been made in theoretical modeling of aerosol transport and deposition within the lungs (Taulbee and Yu, 1975; Pack et al., 1977; Yu, 1978; Nixon and Egan, 1987). The development of this theoretical modeling approach was reviewed by Heyder and Rudolf (1984). As a working hypothesis, the ICRP66 report utilized the particular formulation described by Egan and Nixon (1985), and later improved by Egan et al. (1989), as the basis for modeling regional aerosol deposition in the lungs of different subjects as a function of their respiratory characteristics.

In parallel with this more fundamental approach to modeling in purely physical terms, substantial developments have occurred in the analysis of measured particle deposition in the respiratory tract in terms of empirically defined parameters (TGLD, 1966; Davies, 1972; Rudolf et al., 1986, 1990). As a working hypothesis, the ICRP66 report utilized the parametric analysis of regional lung deposition developed by Rudolf et al. (1990) to represent the results of complex

theoretical modeling by relatively simple algebraic approximations. The algebraic formulae so developed and described in the Annexe to ICRP66 constitute ICRP's recommended respiratory tract deposition model.

In ICRP66, and in this annex, the term "deposition" denotes the mean probability of an inspired particle being deposited. The fraction of the number of inhaled particles deposited in the whole respiratory tract is referred to as "total" deposition. The fraction of the number of inhaled particles deposited in a single region of the respiratory tract is referred to as "regional" deposition. The total deposition is therefore the sum of the regional deposition values. The term "deposition efficiency" denotes the fraction of the number of particles that enter a single region of the respiratory tract that is deposited in that region.

## **10A.2 EXTRATHORACIC DEPOSITION**

The processes that govern deposition of particles in the extrathoracic region of the respiratory tract, i.e., the nose, naso-oropharyngeal passages, and larynx, depend strongly on particle size (as they do within the thoracic airways). In broad terms, particles with an aerodynamic diameter larger than about 0.5  $\mu\text{m}$  are deposited primarily by the so-called "aerodynamic" transport processes of inertial motion, referred to as "impaction," and gravitational settling, referred to as "sedimentation." For very large particles and fibers, interception with surfaces in the extrathoracic airways also contributes to their deposition. Particles with an equivalent physical diameter less than a few tenths of a micrometer are deposited primarily by the "thermodynamic" transport process of Brownian "diffusion."

### **10A.2.1 Nasal Deposition**

The aerodynamic filtration efficiency of the nose is much better documented than that of any other part of the respiratory tract. A large number of studies have been reported for aerosols with aerodynamic particle diameters above 0.2  $\mu\text{m}$ . These studies have been reviewed by Mercer (1975), Lippmann (1977), Yu et al. (1981), Schlesinger (1985a), and Stahlhofen et al. (1989). As discussed in Annexe D of ICRP66, different experimental techniques and evaluation procedures were used in the various studies, and the published data are not all directly comparable. The artificial technique of measuring nasal deposition when aerosol particles were drawn in continuously through the nose and exhausted through a filter at the mouth gave

generally lower values than other techniques which utilized normal breathing. Accordingly, ICRP66 fitted the recommended empirical model of nasal deposition efficiency to the experimental data obtained with normal breathing.

Figure 10A-1 shows the experimental data on the aerodynamic deposition efficiency of the nose during normal inspiration, plotted as a function of the inertial impaction parameter,  $d_{ae}^2 V$ , where  $d_{ae}$  is the aerodynamic particle diameter (in  $\mu\text{m}$ ), and  $V$  is the volumetric flow rate (in  $\text{cm}^3 \text{s}^{-1}$ ). Each of the studies by Lippmann (1970), Giacomelli-Maltoni et al. (1972), and Rudolf (1975) exhibit a large degree of variability in nasal deposition measured in different subjects.

ICRP66 adopted the empirical analysis reported by Rudolf et al. (1986) and Stahlhofen et al. (1989) to represent the trend of the mean of these data for aerodynamic deposition efficiency of the nose on inhalation in terms of the impaction parameter,  $d_{ae}^2 V$ . The recommended function is shown in Figure 10A-1(a), together with the estimated 95% confidence bounds based on the variability of the data. The fitted function accounts for the observed slow increase in deposition efficiency for low values of  $d_{ae}^2 V$ , and also predicts an asymptotic approach to unity for high values of this impaction parameter. As shown in the figure, for intermediate values of  $d_{ae}^2 V$ , the predicted deposition efficiency is similar to that given by Pattle's (1961) log-linear approximation, which was adopted by the Task Group on Lung Dynamics (TGLD, 1966).

Nasal deposition for submicron-sized particles has not been studied intensively in human subjects. Accordingly, to define the "thermodynamic" deposition efficiency of the nose, ICRP66 relied on the experimental measurements made in hollow, anatomical casts of the nasal airways (Swift et al., 1992). (See ICRP66 Annexe D for discussion of these data, and their empirical representation).

### **10A.2.2 Oropharyngeal Deposition**

Most experimental studies of oropharyngeal deposition have been performed with mouth breathing through a tube, since this is a convenient method for aerosol administration. The oral deposition was measured by repeated mouth-washings directly after inhalation. The remainder of the extrathoracic deposition, i.e., that in the oropharynx and larynx, was measured by external gamma counting. Emmett and Aitken (1982) showed that, for particles

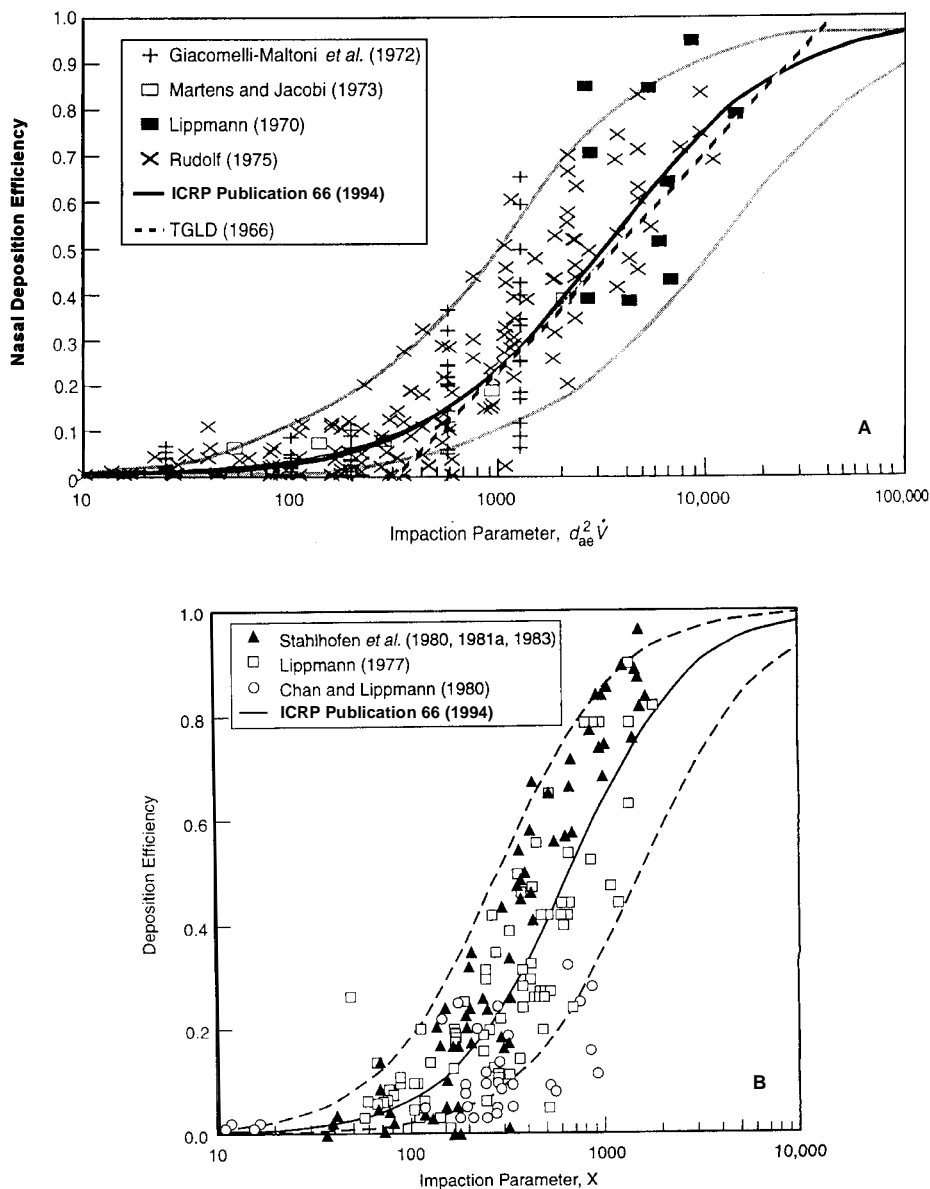


**Figure 10A-1.** Nasal deposition efficiency measured in adult Caucasian males during normal breathing (A) and data on extrathoracic deposition when particles are inhaled and exhaled through a mouthpiece (B). The solid curves show the empirical model used in ICRP Publication 66 (1994). The outer curves on either side represent the estimated 95% confidence bounds in predicted extrathoracic deposition based on the variability of the data. The heavy dashed line in (A) shows the expression for nasal deposition efficiency used in the ICRP Publication 30 (1979) lung model (TGLD, 1966). The impactation parameter,  $x$ , is described in the text as  $d_{ae}^2 \dot{V}^{0.6} V_T^{-0.2}$  ( $\mu\text{m}^2 \text{cm}^{1.2} \text{s}^{0.6}$ ).

Source: ICRP Publication 66 (1994).

less than about 10- $\mu$ m aerodynamic diameter, the bulk of the extrathoracic deposition during mouth breathing occurs in the larynx.

Figure 10A-1(b) compares the experimental data on extrathoracic deposition during mouth breathing through tube mouthpieces obtained by Lippmann (1977), Chan and Lippmann (1980), and Stahlhofen et al. (1980, 1981a, 1983). Again, the measured variability in extrathoracic deposition is high. The curves shown in the figure represent the empirical model adopted in ICRP66 to describe the underlying trend of deposition efficiency as a function of an impaction parameter, (see also Figure 10-22 of Chapter 10), together with the upper and lower 95% confidence bounds of this estimate.

### **10A.2.3 Scaling for Body Size**

Extrathoracic deposition has not been studied systematically in children, nor has the degree to which the intersubject variability measured in adult subjects is related to variation in anatomical dimensions. In the absence of data, ICRP66 utilized the dimensional scaling procedure proposed by Swift (1989) to predict the effect of a subject's body size on nasal and oropharyngeal deposition of particles in the aerodynamic size-range, and by Cheng et al. (1988) to predict body-size effects on thermodynamic deposition efficiency, in relation to values modeled for a reference adult male.

## **10A.3 REGIONAL LUNG DEPOSITION**

Although the experimental data obtained for the adult human male are sufficient to model empirically and accurately the deposition efficiency of the lungs as a whole, as a function of breathing behavior and particle size (Rudolf et al., 1983, 1986), they are not complete enough nor mutually consistent enough to define precisely the regional deposition in a reference adult male, nor the effects of different airway size in other subjects. ICRP66 therefore used the theoretical model developed by Egan and Nixon (1985), and Nixon and Egan (1987), as updated by Egan et al. (1989), to predict the effects of breathing behavior and airway size on the deposition of particles in discrete anatomical regions of the lungs, i.e., in the bronchial (BB), bronchiolar (bb), and alveolar-interstitial (AI) airways, of various subjects. These theoretical predictions formed the basis for the simplified algebraic model of regional deposition in the

lungs of various subjects that is recommended in ICRP66, and is applied in Chapter 10. The model evaluates the combined effects of convective and diffusive gas transport, and aerosol loss processes, within the airways of the lungs, on the basis of the mathematical formalisms introduced by Taulbee and Yu (1975) and Pack et al. (1977).

### **10A.3.1 Comparison with Data from GSF Frankfurt Laboratory**

Stahlhofen et al. (1980, 1981a,b, 1983) measured the fractional deposition of insoluble monodisperse aerosols of iron oxide particles labeled with  $^{198}\text{Au}$ , in a total of nine different subjects under closely controlled breathing conditions. In these tests, the subjects inhaled and exhaled particles of various sizes through a mouthpiece, at a constant flow rate of either  $250\text{ cm}^3\text{ s}^{-1}$  or  $750\text{ cm}^3\text{ s}^{-1}$ . Four different tidal volumes were studied:  $250\text{ cm}^3$ ,  $500\text{ cm}^3$ ,  $1000\text{ cm}^3$  at the flow rate of  $250\text{ cm}^3\text{ s}^{-1}$ , and  $1500\text{ cm}^3$  at the flow rate of  $750\text{ cm}^3\text{ s}^{-1}$ . The fraction of inhaled gamma activity deposited initially in the thorax was measured using a calibrated and well-characterized array of collimated NaI(Tl)-detectors. The retention of the deposited iron oxide particles in the lungs (obtained by correcting the thorax measurements for the activity of particles cleared to the stomach) was followed in each subject for several days. In general, two distinct phases of particle retention were observed: an initial rapid phase, succeeded by continued slow clearance with a fitted half-time of several tens of days. The exponential clearance curve fitted to the "slow-cleared" fraction was extrapolated back to the time of exposure to define the complementary "fast-cleared" fraction of the initial lung deposit. The "slow-" and "fast-cleared" fractions of the thoracic deposit are conventionally assumed to represent particles deposited in the A region and tracheobronchiolar airways (BB and bb regions), respectively.

To simulate these experimental data, ICRP66 utilized the theoretical deposition model of Egan et al. (1989) to calculate the expected fractional deposition summed for all airways in the A region and the combined BB and bb regions. Figures 10A-2 and 10A-3 compare the theoretical predictions of tracheobronchiolar and alveolar-interstitial deposition, respectively, with the "fast-" and "slow-cleared" fractions of thoracic deposition measured at the GSF Frankfurt Laboratory.

It is seen from these figures that both measured fractions of the thoracic deposition exhibit substantial variability under otherwise identical experimental conditions (as does the

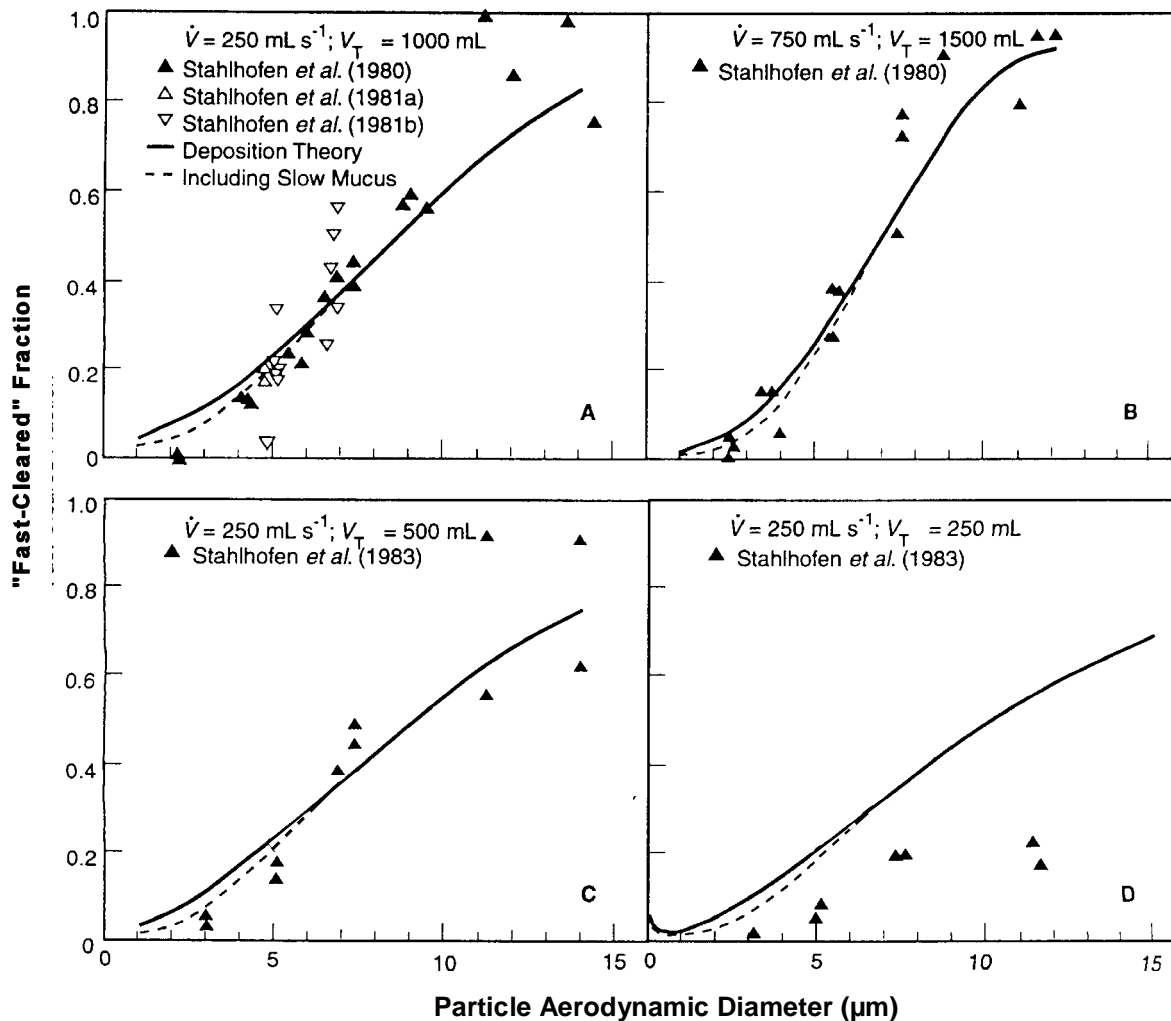


**Figure 10A-2.** Comparisons of the "fast-cleared" fraction of lung deposition measured at the GSF Frankfurt Laboratory with the tracheobronchiolar deposition predicted by the theoretical model (shown by the solid curves) of Egan et al. (1989). The dashed curves show the effect on the predicted "fast-cleared" fraction of allowing for slow clearance of a fraction of the number of particles deposited in the tracheobronchiolar airways. This "slow-cleared" fraction is assumed to tend to zero for large particles.

Source: ICRP Publication 66 (1994).

total thoracic deposition). It is also seen that, overall, the calculated deposition curves provide an accurate prediction of the trends in measured values with particle aerodynamic diameter.

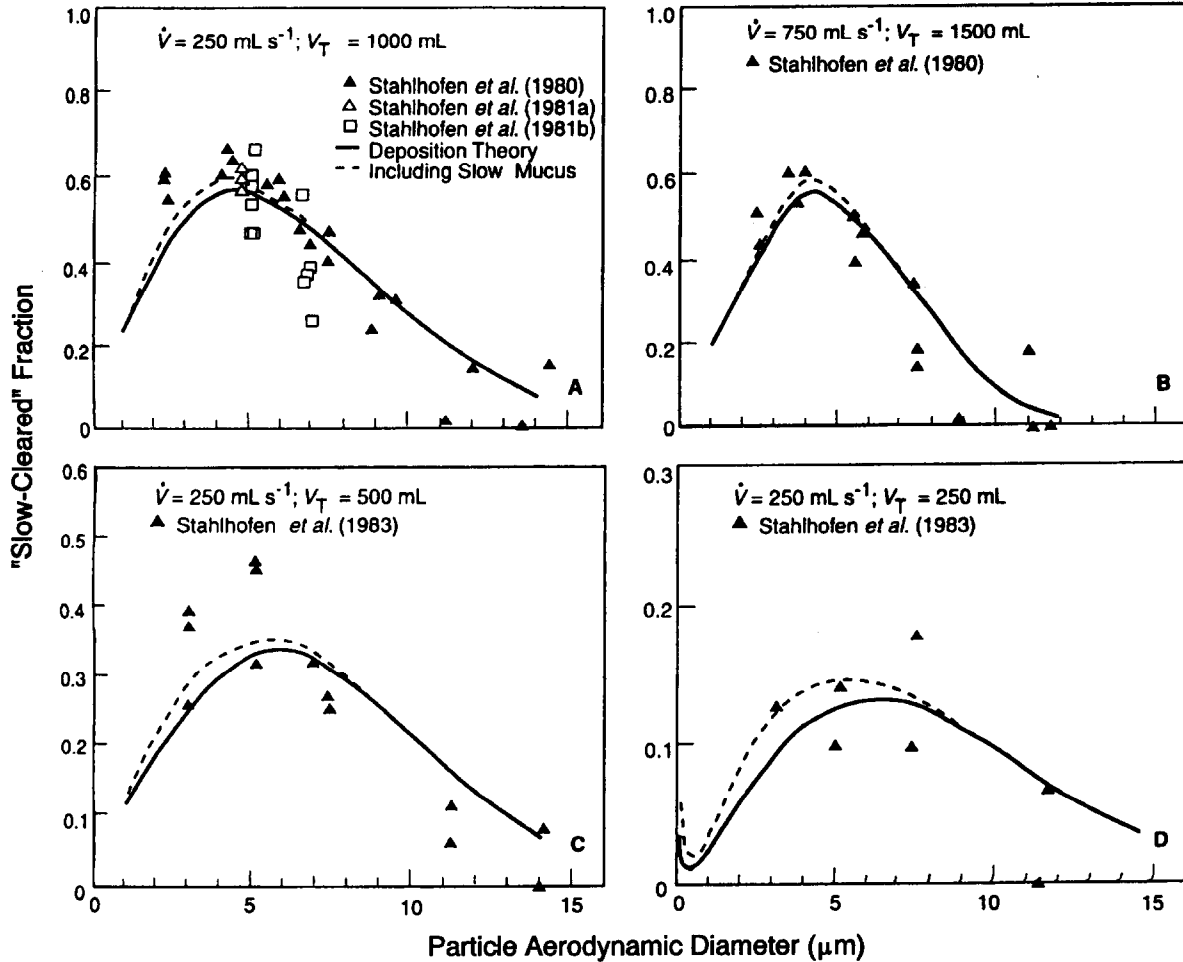


**Figure 10A-3.** Comparisons of the "slow-cleared" fraction of lung deposition measured at the GSF Frankfurt Laboratory with the alveolar deposition predicted by the theoretical model (shown by the solid curves) of Egan *et al.* (1989). The dashed curves show the effect on the predicted "slow-cleared" fraction of allowing for additional slow clearance of a fraction of the number of particles deposited in the tracheobronchiolar airways.

Source: ICRP Publication 66 (1994).

In Figure 10A-2, except for the experiments carried out at a flow rate of  $250 \text{ cm}^3 \text{ s}^{-1}$  and a low tidal volume of  $250 \text{ cm}^3$  (Figure 10A-2(d)), it is seen that the predicted curves match the measured "fast-cleared" fractions. The closest match is obtained for the experiments carried out at a flow rate of  $750 \text{ cm}^3 \text{ s}^{-1}$  and tidal volume of  $1500 \text{ cm}^3$

approximates the breathing rate of ICRP66's "reference worker." The apparently poor match to the data at low flow rate and low tidal volume arises principally from the two measurements for 12- $\mu$ m-aerodynamic-diameter particles. Bronchial deposition efficiency for these particles should clearly be substantially higher than for the next smallest particles (of 7.5- $\mu$ m aerodynamic diameter). The fact that the measured efficiency is lower suggests an experimental artifact in correcting for extrathoracic particle losses.

On the whole, the predicted deposition fractions are seen to match the data with increased accuracy as the particle aerodynamic diameter is increased. For several of the smallest particle sizes studied, there is a general tendency for the predicted tracheobronchial deposition to be higher than the measured "fast-cleared" fraction. However, for these particles (with aerodynamic diameter less than about 5  $\mu$ m), the fit of the predicted curves to the measured values is significantly improved by allowing for the incomplete "rapid" clearance of particles deposited in the human tracheobronchial tree that has been observed directly in other experimental studies. Those studies were discussed in detail in Annexe E (Bailey and Roy, 1994) of ICRP66. Based on that discussion, ICRP66 concluded that, for particles with a physical diameter of 2.5  $\mu$ m or less, only 50% of the number deposited in the tracheobronchial airways is cleared rapidly. The remaining 50% is cleared at a rate that is indistinguishable experimentally from particles deposited in the alveolar-interstitial airways. For larger particles, the fraction of the tracheobronchial deposition that is cleared slowly is found to decrease steeply with particle size. The dashed curves shown in Figure 10A-2 make allowance for slow clearance of a part of the tracheobronchial deposition. It is seen that, by making this allowance, the fit of the predicted "fast-cleared" fraction to the measured values is improved.

Figure 10A-3 compares the experimental data and theoretical predictions of the complementary "slow-cleared" fraction of lung deposition. For particles with aerodynamic diameter 5  $\mu$ m or greater, the fit between predicted and measured values is generally good. Allowance for part of the predicted tracheobronchiolar deposition being cleared slowly is again seen to improve the predictions for smaller particles.

### 10A.3.2 Comparison with Data for Polystyrene Particles

The GSF Laboratory used a so-called "academic" breathing pattern, in which the subject inhaled and exhaled at a closely controlled rate. Other investigators exposed their subjects under so-called "spontaneous" breathing conditions, where the subject maintains a more natural variation in flow rate through the breathing cycle, but is trained to achieve a relatively constant tidal volume and respiratory frequency. In this manner, Foord et al. (1978) measured the fractional deposition of  $^{99m}\text{Tc}$ -labelled polystyrene particles in the mouth and lungs of 15 different subjects. The lung deposition was divided into a "tracheobronchiolar" fraction, which was assumed to consist of the activity cleared from the lungs within 24 h of inhalation, and the remaining "pulmonary" fraction. These authors used three different sizes of particles, i.e., 2.5- $\mu\text{m}$ , 5- $\mu\text{m}$ , and 7.5- $\mu\text{m}$  diameter, and studied regional deposition for several different breathing patterns. Figure 10A-4 shows their results for 6 subjects (with an average tidal volume of 1 L, and a mean respiratory frequency of  $10 \text{ min}^{-1}$ ), together with the deposition of  $^{99m}\text{Tc}$ -labelled polystyrene particles in the lungs of 12 different subjects measured by Emmett and Aitken (1982), using the same breathing pattern.

The figure shows that, after correcting for the extrathoracic deposition measured for each test, the recommended lung deposition model accurately matches the trend of tracheobronchiolar "deposition" with particle size measured by Foord et al (1978). (See panel labeled "TB"). The calculated curve here includes ICRP66's recommended allowance for an assumed fraction of 50% the TB deposition of the 2.5- $\mu\text{m}$  particles not being cleared from the TB region within the 24-h measurement period. The tracheobronchiolar deposition reported by Emmett and Aitken (1982), i.e., the activity deposited in the lungs that is cleared within 24 h, is generally higher than that found by Foord et al. (1978), with relatively little variability between the three subjects studied at each particle size.

The panel labeled "A" in Figure 10A-4 shows the measured values of activity deposited in the lungs that was retained longer than 24 h. In this case, the data of Foord et al. are generally higher than the modeled values, while Emmett and Aitken's values are lower by a similar factor. Both sets of data show a similar trend of "slow-cleared" lung deposition with particle size to that modeled, but with higher or lower absolute values, respectively, for the same breathing pattern.

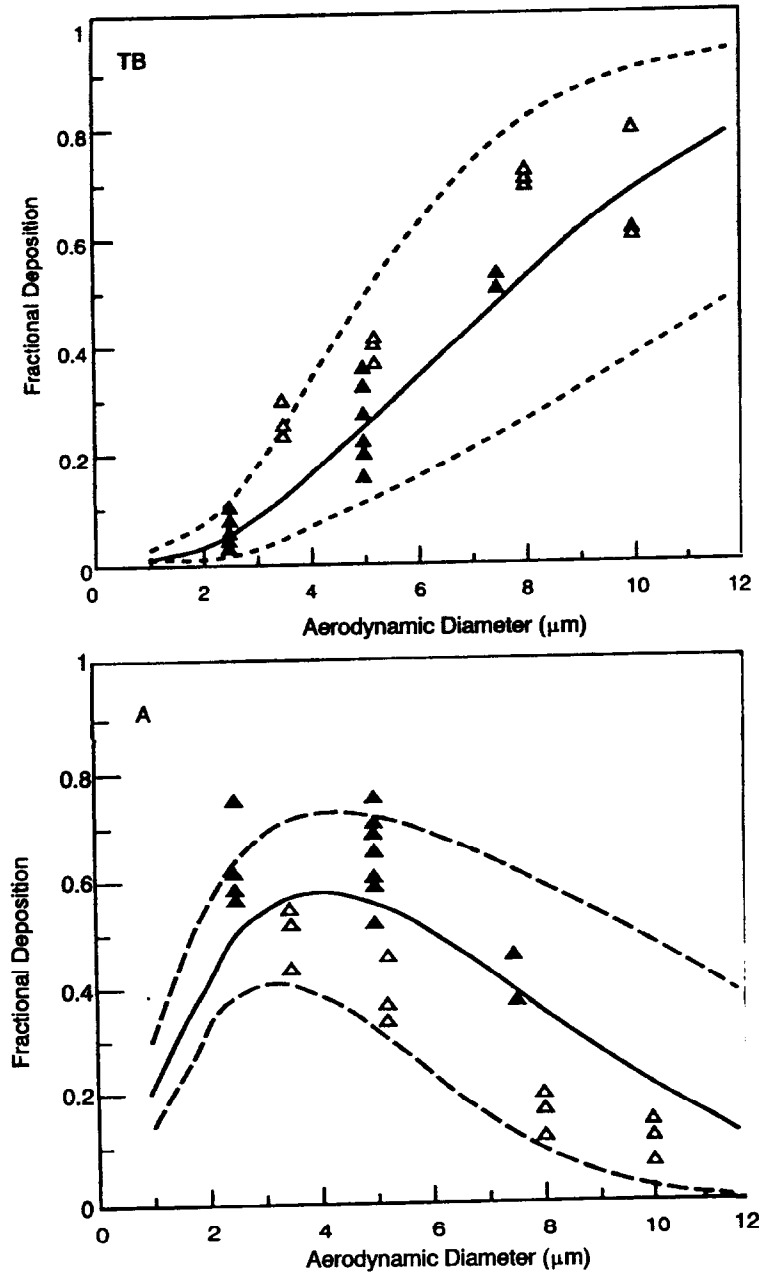


**Figure 10A-4. Comparison of fractional deposition measured by Foord et al. (1978) (solid triangles) and Emmett and Aitken (1982) (open triangles) in different subjects with values given by the International Commission on Radiological Protection (ICRP) Publication 66 (1994) lung model (solid curves). The fractional deposition shown has been adjusted to correspond to zero extrathoracic deposition in the tracheobronchial (TB) and alveolar (A) regions. The dashed curves represent the upper and lower 95% confidence bounds of regional deposition predicted for an individual subject by the ICRP lung model.**

Source: ICRP Publication 66 (1994).

When the experimental data on thoracic deposition in "fast-" and "slow-cleared" fractions are pooled, as is done in Figure 10A-4, the deposition model recommended in ICRP66 represents the data as a whole. It is also seen from Figure 10A-4 that ICRP66's estimated 95% confidence bounds on regional lung deposition predicted for individual subjects include all but 3 of the data points.

### **10A.3.3 Comparison with Data for Submicron-Sized Particles**

For particles in the submicron, thermodynamic size range (with equivalent diameter between about 5 nm and 0.2  $\mu\text{m}$ ), extrathoracic deposition during mouth breathing (in the oral cavity and larynx) is small compared to that in the lungs. Schiller et al. (1986) measured the total respiratory tract deposition for several subjects exposed via a mouthpiece to monodisperse, uncharged spherical particles of silver over a range of particle diameter extending from 5 nm to about 0.2  $\mu\text{m}$ . These experimental results were corrected by Gebhart et al. (1989) for the effects of instrumental dead space, which tended to reduce the measured deposition fraction for nanometer-sized particles. Egan and Nixon (1989) compared the resulting mean values of total thoracic deposition with the values predicted by the theoretical model developed by Egan et al. (1989). These authors showed that the theoretically modeled fractional deposition in the lungs matches the measured values. Figure 10A-5 shows that the calculated values also represent the data obtained earlier for hydrophobic submicron-sized spheres of aluminosilicate by Tu and Knutson (1984).

### **10A.3.4 Influence of "Controlled" Versus "Spontaneous" Breathing**

The data from the GSF Frankfurt Laboratory shown above apply to controlled breathing at a constant inspiratory and expiratory flow rate, whereas, during normal spontaneous breathing, the flow rate varies throughout each breath in an approximately sinusoidal manner. However, Heyder et al. (1982) showed in a study of 20 different subjects that the mean total deposition for spontaneous breathing is virtually identical to that for controlled breathing at the same average flow rate. Heyder et al.'s data are given in Figure 10A-6, together with the values predicted for a reference male subject by the ICRP66 lung model. It is seen that, for both controlled and spontaneous mouth breathing, there is a large amount of variation

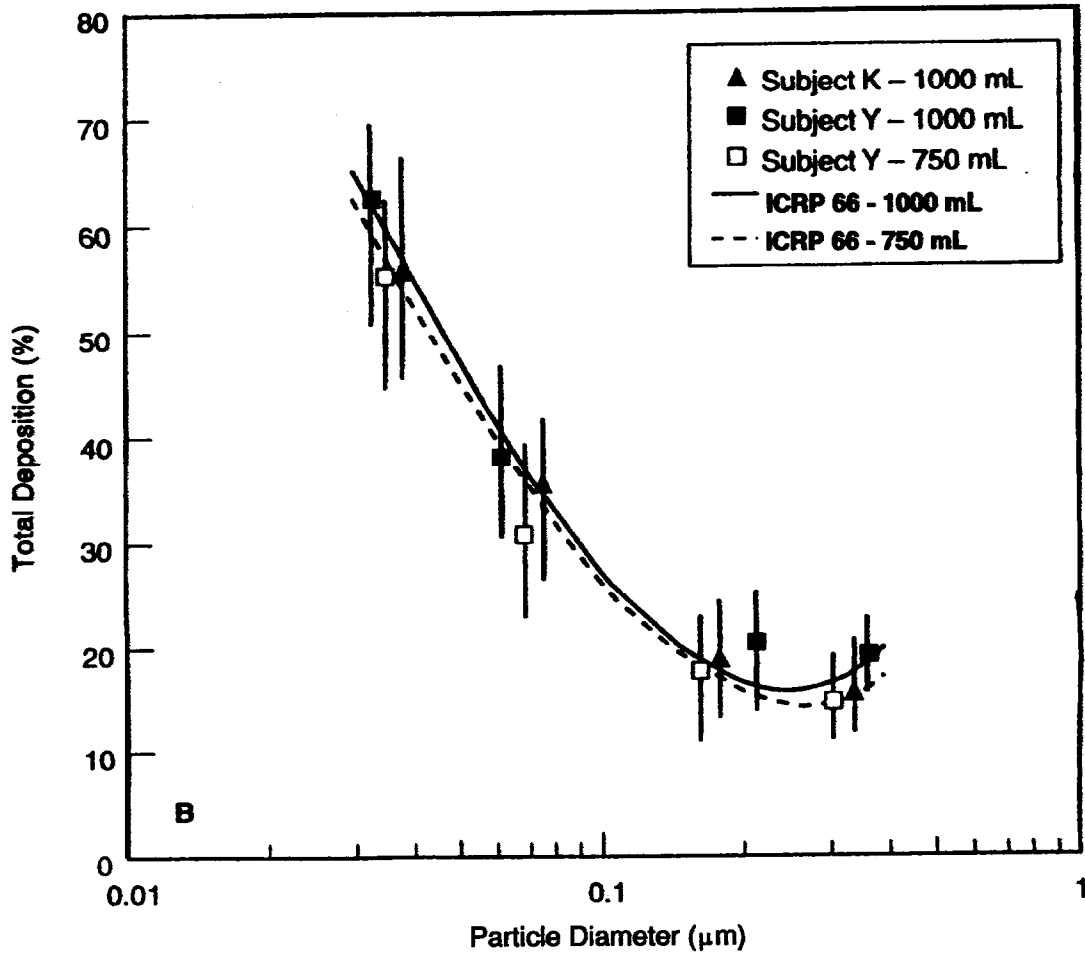


**Figure 10A-5. Comparison of total respiratory tract deposition of submicron-sized alumino-silicate particles measured by Tu and Knutson (1984) in two subjects (at tidal volumes of 1000 mL or 750 mL), with the values calculated as a function of particle diameter by Egan et al. (1989). The ICRP Publication 66 (1994) lung model reproduces these calculated values.**

Source: ICRP Publication 66 (1994).

between different subjects, although in any one subject under controlled breathing conditions, total deposition measurements are highly repeatable (Heyder et al., 1982).

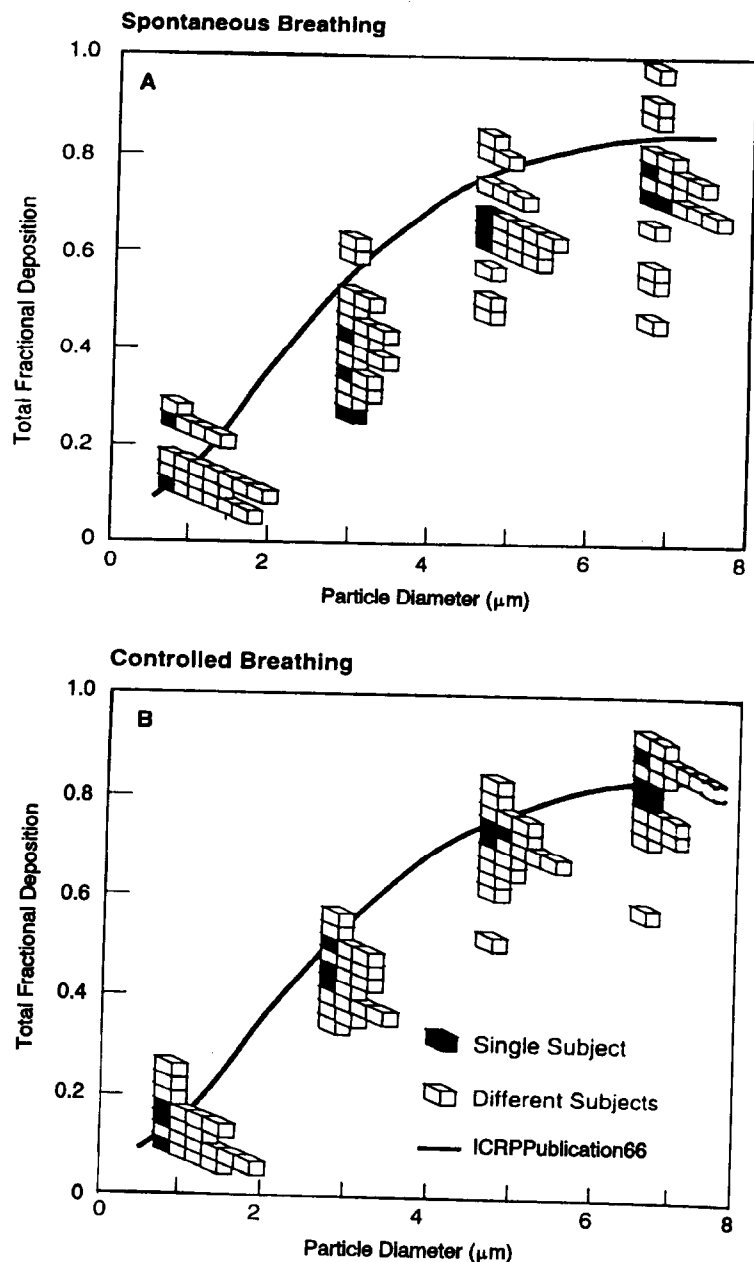


**Figure 10A-6.** Comparison of the distributions of total respiratory tract deposition measured in 20 different subjects (A) breathing spontaneously at rest or (B) breathing at a controlled rate at rest. In case (A), the individual mean flow rate varied from 220 to 740 mL/s, with a collective mean value of 380 mL/s. In case (B), the mean flow rate was held constant at 400 mL/s for each subject. Each box shown in the figure represents one experimental measurement. Shaded boxes represent repeat measurements on a single subject (see inset key in bottom figure). The curves show values predicted by the ICRP Publication 66 (1994) model.

Source: ICRP Publication 66 (1994).

### 10A.3.5 Comparison with Data for Iron Oxide Particles from New York University

Lippmann (1977) and Chan and Lippmann (1980) reported measurements of lung deposition and 24-h retention in a large number of different subjects at New York University (NYU). These studies involved iron oxide particles tagged in aqueous suspension with  $^{99m}\text{Tc}$  (Wales et al., 1980). Each subject was allowed to breathe normally, and the average tidal volume and breathing frequency were monitored. Typical values of these respiratory parameters were  $500 \text{ cm}^3 \text{ s}^{-1}$  and  $15 \text{ min}^{-1}$ , respectively.

Figure 10A-7 shows the values of "fast-" and "slow-cleared" lung deposition obtained in these studies at NYU (adjusted from the measured value to zero extrathoracic deposition). In common with the earlier theoretical lung deposition models described by Yeh and Schum (1980) and Yu and Diu (1982b), and with the NCRP's currently proposed lung model, ICRP66's deposition model predicts substantially less bronchial ("fast-cleared") deposition for particles of aerodynamic diameter larger than  $1 \mu\text{m}$  than is indicated by the bulk of the NYU data. Likewise, the predicted alveolar ("slow-cleared") deposition for particles of about  $1\text{-}\mu\text{m}$  aerodynamic diameter is also low compared to the NYU data.

These data from NYU provide an excellent measure of intersubject variability in the deposition efficiencies of the tracheobronchiolar and alveolar-interstitial regions of the lungs. However, according to ICRP66's review of the literature, the interpretation of the NYU results is complicated by the possibility that the labeled iron oxide particles used may have grown hygroscopically in the humid air of the respiratory tract. Monodisperse iron oxide particles are produced by atomization of an aqueous suspension of colloidal iron oxide with a spinning top generator (Albert et al., 1964; Lippmann and Albert, 1967; Stahlhofen et al., 1979). The colloidal suspension is prepared by converting iron chloride in aqueous solution by hydrolysis to iron oxide. In order to remove all traces of the dissolvable chloride, the aqueous iron oxide colloid must be dialyzed extremely thoroughly.

Gebhart et al. (1988) used light-scattering photometry to examine the effect of the degree to which a suspension of colloidal iron oxide is dialyzed on the hygroscopicity of the resulting monodisperse particles, by comparing the physical properties of these particles on inhalation and exhalation. These authors found that even when the particles are produced from extremely well dialyzed iron oxide there is a distinct change in light-scattering

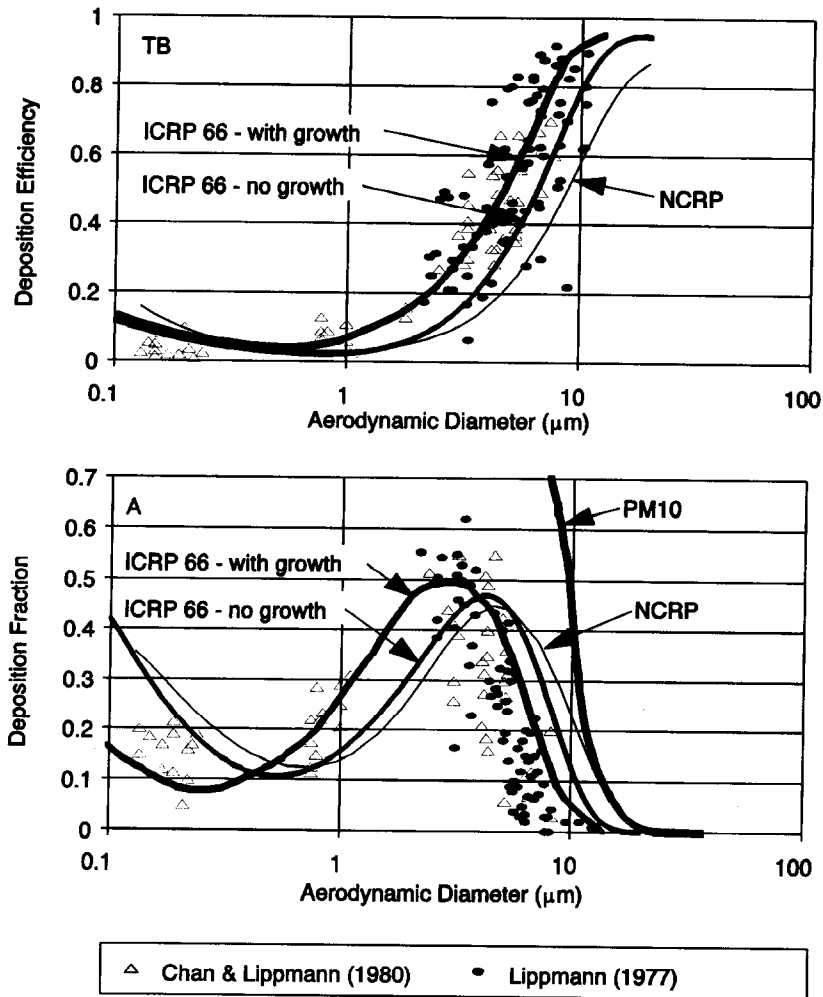


**Figure 10A-7. Experimental data on deposition efficiency of the tracheobronchial (TB) region and fractional deposition in the alveolar (A) region for the large group of subjects studied at New York University (NYU). These subjects inhaled monodisperse particles of iron oxide through a mouthpiece at a tidal volume of approximately 1000 mL and respiratory frequency of 15/min. The measured values are normalized to zero extrathoracic deposition. The curves show the corresponding values predicted by the NCRP (proposed) and ICRP Publication 66 (1994) models. Two curves are shown for the ICRP 66 model: (1) "no growth" represents the values calculated on the assumption that the size of the iron oxide particles was stable in the respiratory tract, and (2) "with growth" represents the partial hygroscopic growth of similar particles indicated by the experimental study of Gebhart et al. (1988). The lower figure (marked as "A") also shows the characteristic particle collection efficiency curve for a PM<sub>10</sub> sampler.**

Source: Adapted from ICRP Publication 66 (1994).

properties between the inhaled and exhaled particles. Since the total respiratory tract deposition of these particles was indistinguishable from that of oil droplets of the same aerodynamic size in ambient air, Gebhart et al. (1988) concluded that their measured shift in optical properties was caused by the presence of a thin film of condensed water on the surface of the exhaled particles.

Using this same technique on a sample of the dialyzed iron oxide suspension prepared at NYU by their published method (Wales et al., 1980), Gebhart et al. (1988) found a much greater shift in light-scattering properties of the final monodisperse particles between inhalation and exhalation. This observed shift in light-scattering properties was accompanied by increased total respiratory tract deposition compared with that of oil droplets of the same aerodynamic size in ambient air. The deposition measured under identical exposure conditions was found to increase from 44% for the hydrophobic oil droplets to 68% for the iron oxide particles. The same change in measured respiratory tract deposition would be obtained by inhaling oil droplets of 3.8- $\mu\text{m}$  aerodynamic diameter in place of the 2.4- $\mu\text{m}$ -aerodynamic-diameter iron oxide particles.

The ICRP66 report includes a recommended method for extending the algebraic deposition model to evaluate regional lung deposition for aerosols that are subject to hygroscopic particle growth. Figure 10A-7 shows the effect on the modeled fast- and slow-cleared lung deposition including in the calculation the rate of hygroscopic growth of the NYU iron oxide particles that was derived from the results of the Gebhart et al. (1988) study. It is seen that this correction of the modeled lung deposition improves substantially the overall fit of the predicted values to the measurements.

## **APPENDIX 10B**

### **SELECTED MODEL PARAMETERS**

**TABLE 10B-1(a). BODY WEIGHT AND RESPIRATORY TRACT REGION SURFACE AREAS**

Body Weight (kg)	Lung Weight (g)	Respiratory Tract Surface Areas		
		ET (cm <sup>2</sup> )	TB (cm <sup>2</sup> )	A (m <sup>2</sup> )
73.0	1,100	470	2,690	54.0

**TABLE 10B-1(b). HUMAN ACTIVITY PATTERNS AND ASSOCIATED RESPIRATORY MINUTE VENTILATION**

Activity Pattern	Sleeping (.45 m <sup>3</sup> /h)		Sitting (.54 m <sup>3</sup> /h)		Activity Light (1.5 m <sup>3</sup> /h)		Activity Heavy (3.0 m <sup>3</sup> /h)		Total/Day	
	Hours	Total m <sup>3</sup>	Hours	Total m <sup>3</sup>	Hours	Total m <sup>3</sup>	Hours	Total m <sup>3</sup>	Hours	Total m <sup>3</sup>
Adult male, general population	8	3.6	8	4.32	8	12	0	0	24	19.9
Adult male, light work	8	3.6	6.5	3.5	8.5	12.75	1	3	24	22.85
Adult male, heavy work	8	3.6	4	2.16	10	15	2	6	24	26.76

10B-2

<sup>a</sup>International Commission on Radiological Protection (ICRP66, 1994).

**TABLE 10B-2. BODY WEIGHTS, LUNG WEIGHTS, RESPIRATORY MINUTE VENTILATION, AND RESPIRATORY TRACT REGION SURFACE AREA FOR SELECTED LABORATORY ANIMAL SPECIES**

Species	Body Weight (kg)	Lung Weight <sup>b</sup> (g)	Minute Ventilation <sup>b</sup> (L/min)	Minute Ventilation per g lung (l/min · g lung)	Respiratory Region Surface Area		
					ET (cm <sup>2</sup> )	TB (cm <sup>2</sup> )	A (m <sup>2</sup> )
Mouse (B6C3F1)	0.037 <sup>a</sup>	0.43 <sup>b</sup>	0.044 <sup>a</sup>	0.063	3 <sup>a</sup>	3.5 <sup>a</sup>	0.05 <sup>a</sup>
Syrian hamster	0.134 <sup>a</sup>	1.54 <sup>b</sup>	0.057 <sup>a</sup>	0.049	14 <sup>a</sup>	20.0 <sup>a</sup>	0.30 <sup>a</sup>
Rat (F344)	0.380 <sup>a</sup>	4.34 <sup>b</sup>	0.253 <sup>a</sup>	0.040	15 <sup>a</sup>	22.5 <sup>a</sup>	0.34 <sup>a</sup>
Guinea pig	0.890 <sup>a</sup>	10.1 <sup>b</sup>	0.286 <sup>a</sup>	0.034	30 <sup>a</sup>	200 <sup>a</sup>	0.90 <sup>a</sup>
Monkey	2.5 <sup>c</sup>	28.0 <sup>b</sup>	0.789 <sup>b</sup>	0.028	NA <sup>e</sup>	NA <sup>e</sup>	4.3 <sup>f</sup>
Dog	10.0 <sup>d</sup>	110.0 <sup>d</sup>	2.39 <sup>b</sup>	0.022	NA <sup>e</sup>	NA <sup>e</sup>	42.5 <sup>f</sup>

<sup>a</sup>U.S. Environmental Protection Agency (1994, 1988a). Default values for male laboratory animals in chronic bioassays.

<sup>b</sup>Stahl, 1967: lung weight in g = 11.3 · (kg BW)<sup>0.99</sup>; minute ventilation = 379 · (kg BW)<sup>0.8</sup>.

<sup>c</sup>Phalen (1984).

<sup>d</sup>Cuddihy et al. (1972).

<sup>e</sup>Not available.

<sup>f</sup>Scaled from results of dogs and baboons in Crapo et al. (1983).

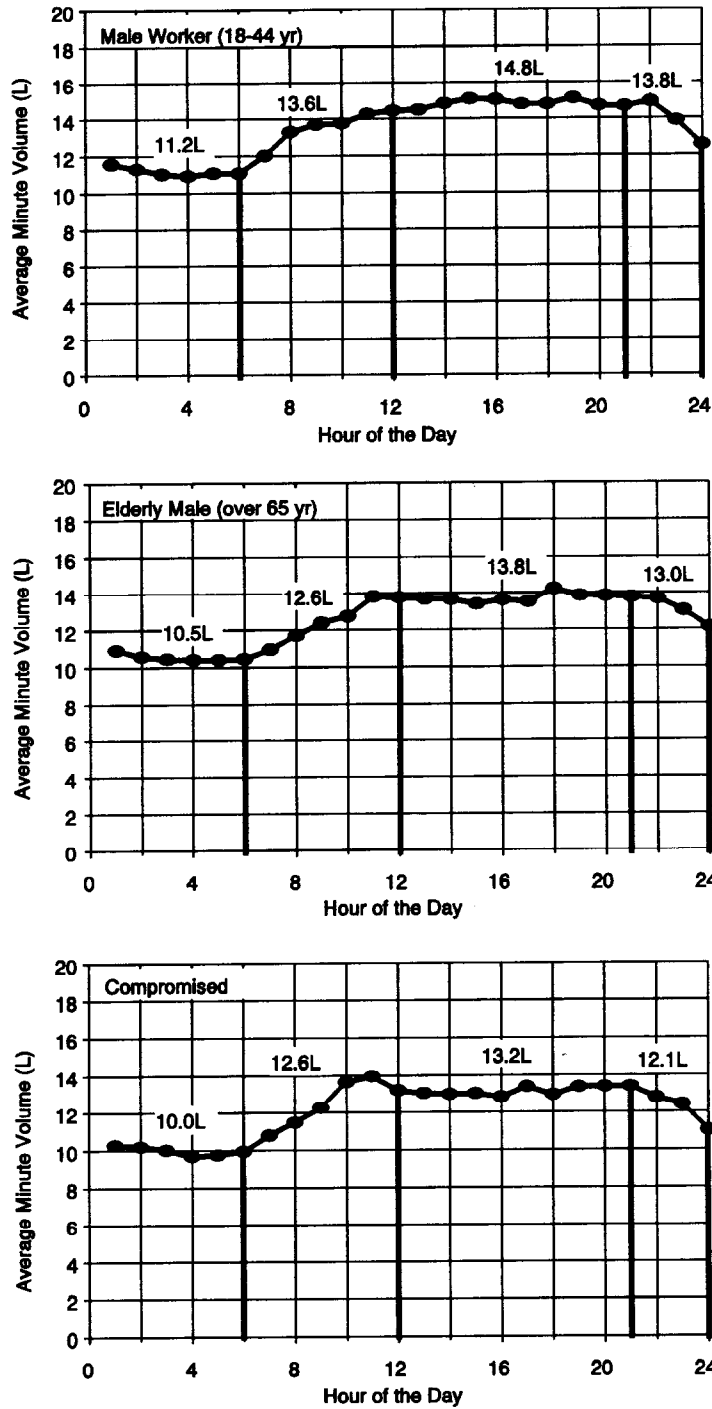


**Figure 10B-1. Daily minute volume pattern for male demographic groups. The average rates for each of four time intervals are shown. Total volume ( $m^3$ ) breathed in 24 hours for male worker (18-44 yr) is 19.4; for elderly male (over 65 yr) is 18.1; and for compromised subjects is 17.4.**

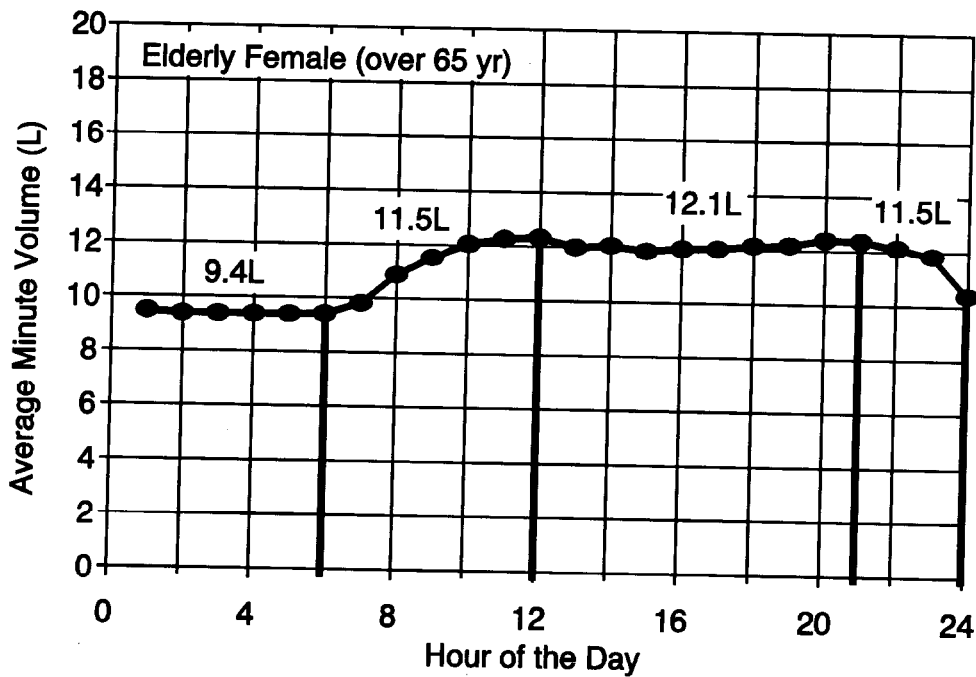
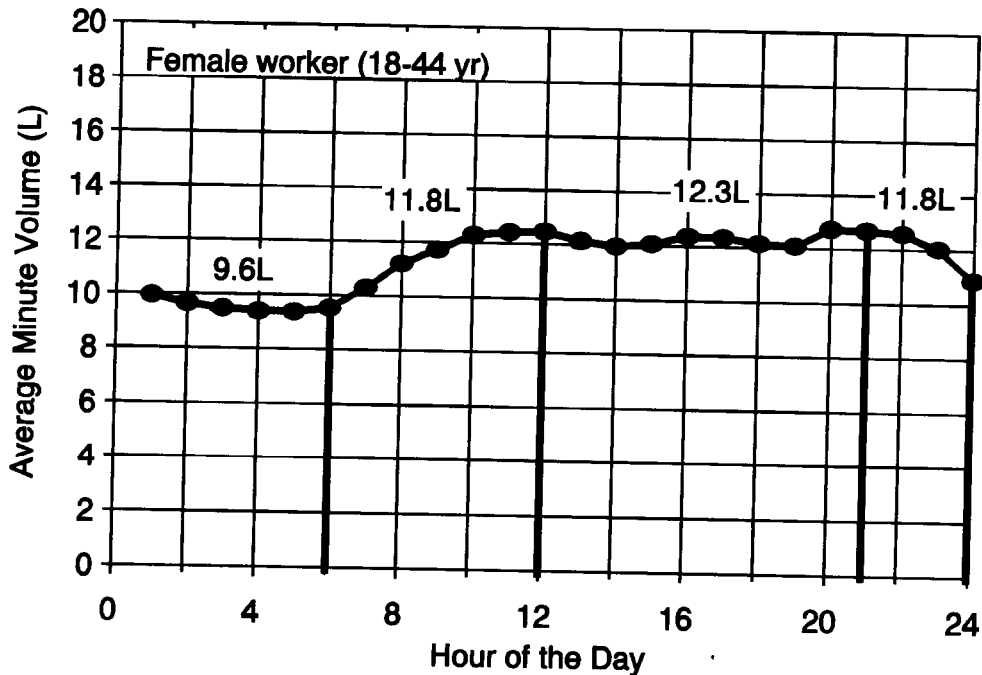


**Figure 10B-2. Daily minute volume pattern for female demographic groups. The average rates for each of four time intervals are shown. Total volume (m<sup>3</sup>) breathed in 24 hours for female worker (18-44 yr) is 16.5 and for elderly female (over 65 yr) is 16.1.**

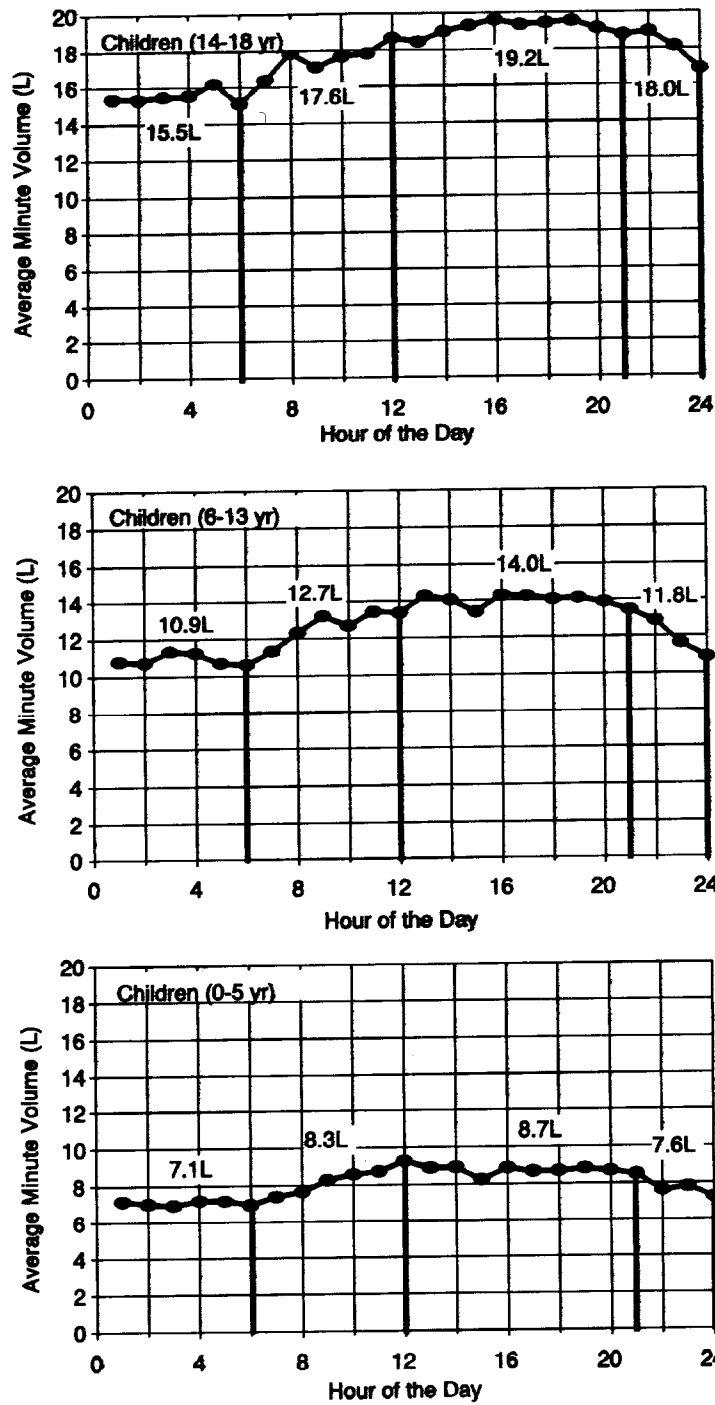


**Figure 10B-3. Daily minute volume pattern for demographic groups for children. The average rates for each of four time intervals are shown. Total volume ( $m^3$ ) breathed in 24 hours for children (0-5 yr) is 11.6; children (6-13 yr) is 18.2; and for children (14-18 yr) is 25.5.**

**APPENDIX 10C**

**SELECTED AMBIENT AEROSOL  
PARTICLE DISTRIBUTIONS**

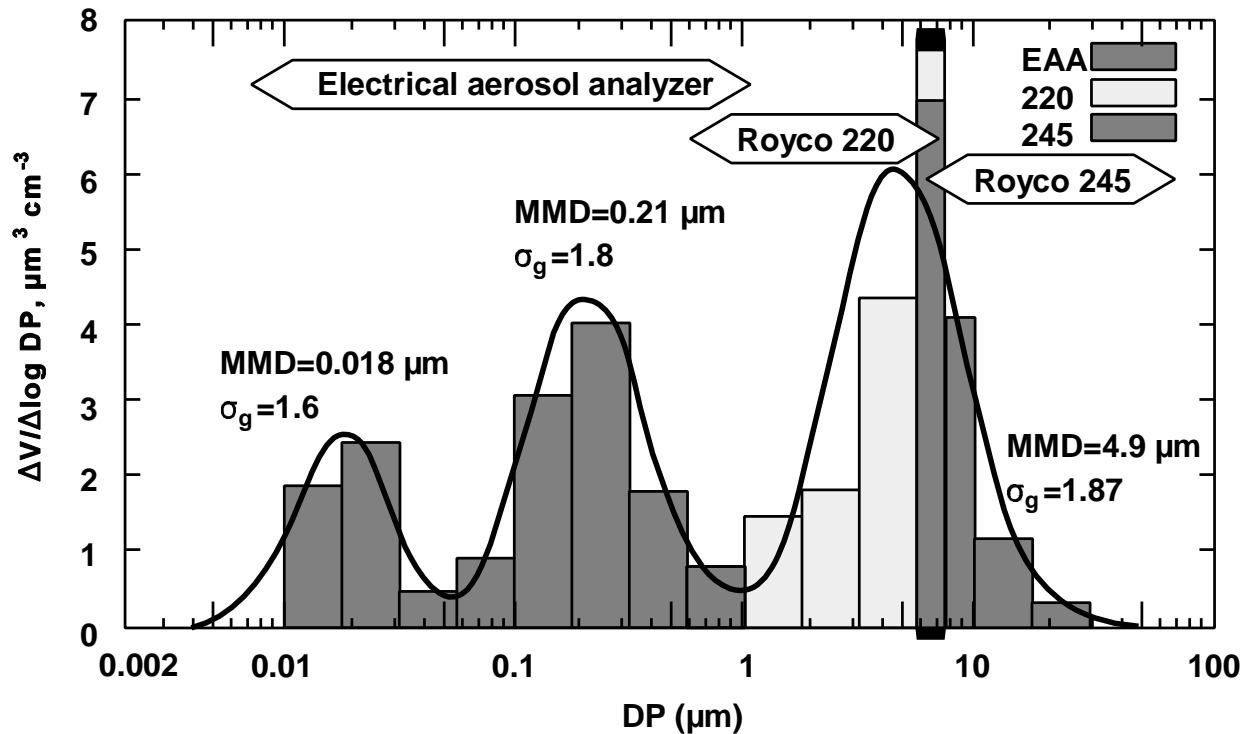


**Figure 10C-1.** An example of histogram display and fitting to log-normal functions for particle-counting size distribution data. Instruments used and the range covered by each are shown. Counts are combined into reasonably-sized bins and displayed. Lognormal functions, fitted to the data, are shown with geometric mass median diameter (MMD) of each mode and the width ( $\sigma_g$ ) of each mode. Data taken from a study of fine sulfate and other particles generated by catalyst equipped cars as part of a cooperative study by EPA and General Motors Corporation. Note the clear separation of the nuclei mode (MMD = 0.018  $\mu\text{m}$ ), the accumulation mode (MMD = 0.21  $\mu\text{m}$ ) and coarse mode (MMD = 4.9  $\mu\text{m}$ ). Fine particles, as defined by Whitby (1978), include the nuclei and accumulation mode.

Source: Wilson et al. (1977).

**TABLE 10C-1 DISTRIBUTION OF PARTICLE COUNT, SURFACE AREA OR MASS IN THE TRIMODAL POLYDISPERSE AEROSOL DEFINED IN FIGURE 10C-1**

**(The tabulated numbers represent the upper size cut [in  $\mu\text{m}$ ] for each particle size interval based on the distribution of particle count vs. physical diameter [ $d_p\{c\}$ ], distribution of surface area vs. physical diameter [ $d_p\{s\}$ ], distribution of mass vs. physical diameter [ $d_p\{m\}$ ], or distribution of mass vs. Aerodynamic diameter [ $d_{ac}\{m\}$ ].<sup>a</sup>)**

Aerosol Mode	Particle Parameter	Percent of Total Count, Surface Area or Mass Associated with Particles Smaller than Size Cut												
		1	5	10	20	30	40	50	60	70	80	90	95	99
Accumulation <sup>b</sup>	count; $d_p\{c\}$	0.0053	0.0073	0.0087	0.011	0.012	0.014	0.016	0.018	0.020	0.024	0.029	0.034	0.047
	surface; $d_p\{s\}$	0.0058	0.0080	0.0094	0.012	0.013	0.015	0.017	0.019	0.022	0.026	0.032	0.037	0.051
	mass; $d_p\{m\}$	0.0060	0.0083	0.010	0.012	0.014	0.016	0.018	0.020	0.023	0.027	0.033	0.039	0.054
	mass; $d_{ac}\{m\}$	0.0056	0.078	0.093	0.011	0.013	0.015	0.017	0.019	0.022	0.025	0.031	0.037	0.051
Intermodal <sup>c</sup>	count; $d_p\{c\}$	0.044	0.066	0.081	0.105	0.127	0.149	0.173	0.201	0.235	0.283	0.367	0.454	0.676
	surface; $d_p\{s\}$	0.050	0.075	0.093	0.120	0.145	0.170	0.197	0.228	0.268	0.323	0.418	0.517	0.768
	mass; $d_p\{m\}$	0.053	0.080	0.099	0.128	0.154	0.181	0.210	0.244	0.286	0.345	0.447	0.551	0.820
	mass; $d_{ac}\{m\}$	0.044	0.066	0.083	0.108	0.131	0.155	0.180	0.211	0.248	0.301	0.437	0.485	0.725
Coarse <sup>d</sup>	count; $d_p\{c\}$	0.915	1.40	1.76	2.32	2.83	3.35	3.93	4.60	5.45	6.66	8.76	11.0	16.8
	surface; $d_p\{s\}$	1.06	1.63	2.04	2.69	3.28	3.88	4.55	5.34	6.32	7.71	10.2	12.7	19.5
	mass; $d_p\{m\}$	1.14	1.75	2.20	2.89	3.53	4.18	4.90	5.75	6.81	8.30	10.9	13.7	20.9
	mass; $d_{ac}\{m\}$	1.40	2.14	2.68	3.52	4.29	5.08	5.95	6.98	8.27	10.1	13.2	16.6	25.3

<sup>a</sup>Values for  $d_{ac}$  were calculated iteratively from  $d_p$  using Equations D.13 and D.14 of ICRP Publication 66, Annexe D (James *et al.*, 1994).

<sup>b</sup>Mass median aerodynamic diameter (MMAD) = 0.018  $\mu\text{m}$ ; geometric standard deviation ( $\sigma_g$ ) = 1.6; density ( $\rho$ ) = 1.4  $\text{g}/\text{cm}^3$ .

<sup>c</sup>MMAD = 0.21  $\mu\text{m}$ ;  $\sigma_g$  = 1.8;  $\rho$  = 1.2  $\text{g}/\text{cm}^3$ .

<sup>d</sup>MMAD = 4.9  $\mu\text{m}$ ;  $\sigma_g$  = 1.87;  $\rho$  = 2.2  $\text{g}/\text{cm}^3$ .

**TABLE 10C-2a. DISTRIBUTION OF PARTICLE NUMBER IN THE TRIMODAL POLYDISPERSE AEROSOL DEFINED IN FIGURE 10C-1**  
**(Each individual mode of the trimodal aerosol is separated into the size fractions containing the 1, 5, 10, 20, 30, 40, 50, 60, 70, 80, 90, 95, and 99% number fractiles.**  
**The “nuclei mode” contains about 99.6% of the total number of particles;**  
**the “accumulation mode” about 0.39%; and the “coarse mode” about 0.01%.)**

Mode	Number Fractile (%)	Percent of Trimodal Aerosol	Upper Limit of Particle Size Interval (µm)
Nuclei <sup>a</sup>	1	1.0	0.0027
	5	4.0	0.0038
	10	5.0	0.0045
	20	10	0.0055
	30	10	0.0064
	40	10	0.0073
	50	10	0.0082
	60	10	0.0092
	70	10	0.0105
	80	10	0.0122
	90	10	0.0149
	95	5.0	0.0177
99	4.0	0.0244	
Accumulation <sup>b</sup>	1	0.004	0.0156
	5	0.0159	0.0233
	10	0.0198	0.0289
	20	0.0397	0.0374
	30	0.0397	0.0450
	40	0.0397	0.0528
	50	0.0397	0.0613
	60	0.0397	0.0711
	70	0.0397	0.0834
	80	0.0397	0.101
	90	0.0397	0.130
	95	0.0198	0.161
99	0.0159	0.241	

**TABLE 10C-2a (cont'd). DISTRIBUTION OF PARTICLE NUMBER IN THE TRIMODAL POLYDISPERSE AEROSOL DEFINED IN FIGURE 10C-1**  
**(Each individual mode of the trimodal aerosol is separated into the size fractions containing the 1, 5, 10, 20, 30, 40, 50, 60, 70, 80, 90, 95, and 99% number fractiles.**  
**The “nuclei mode” contains about 99.6% of the total number of particles; the “accumulation mode” about 0.39%; and the “coarse mode” about 0.01%.)**

Mode	Number Fractile (%)	Percent of Trimodal Aerosol	Upper Limit of Particle Size Interval ( $\mu\text{m}$ )
Coarse <sup>c</sup>	1	$2.7 \times 10^{-7}$	0.283
	5	$1.1 \times 10^{-6}$	0.432
	10	$1.3 \times 10^{-6}$	0.543
	20	$2.7 \times 10^{-6}$	0.716
	30	$2.7 \times 10^{-6}$	0.873
	40	$2.7 \times 10^{-6}$	1.03
	50	$2.7 \times 10^{-6}$	1.21
	60	$2.7 \times 10^{-6}$	1.42
	70	$2.7 \times 10^{-6}$	1.68
	80	$2.7 \times 10^{-6}$	2.05
	90	$2.7 \times 10^{-6}$	2.71
	95	$1.3 \times 10^{-6}$	3.40
	99	$1.1 \times 10^{-6}$	5.21

<sup>a</sup>Mass median diameter (MMD) = 0.018  $\mu\text{m}$ ; geometric standard deviation ( $\sigma_g$ ) = 1.6; density ( $\rho$ ) = 1.4  $\text{g}/\text{cm}^3$ .

<sup>b</sup>MMD = 0.21  $\mu\text{m}$ ;  $\sigma_g$  = 1.8; density ( $\rho$ ) = 1.2  $\text{g}/\text{cm}^3$ .

<sup>c</sup>MMD = 4.9  $\mu\text{m}$ ;  $\sigma_g$  = 1.87; density ( $\rho$ ) = 2.2  $\text{g}/\text{cm}^3$ .

**TABLE 10C-2b. DISTRIBUTION OF PARTICLE SURFACE AREA IN THE TRIMODAL POLYDISPERSE AEROSOL DEFINED IN FIGURE 10C-1**  
**(Each individual mode of the trimodal aerosol is separated into the size fractions containing the 1, 5, 10, 20, 30, 40, 50, 60, 70, 80, 90, 95, and 99% surface area fractiles. The “nuclei mode” contains about 77.4% of the total particle surface area; the “accumulation mode” about 21.9%; and the “coarse mode” about 0.64%.)**

Mode	Surface Area Fractile (%)	Percent of Trimodal Aerosol	Upper Limit of Particle Size Interval (µm)
Nuclei <sup>a</sup>	1	0.78	0.0043
	5	3.1	0.0059
	10	3.9	0.0070
	20	7.8	0.0086
	30	7.8	0.0100
	40	7.8	0.0113
	50	7.8	0.0127
	60	7.8	0.0144
	70	7.8	0.0163
	80	7.8	0.0189
	90	7.8	0.0233
	95	3.9	0.0277
	99	3.1	0.0381
Accumulation <sup>b</sup>	1	0.22	0.0312
	5	0.89	0.0465
	10	1.1	0.0575
	20	2.2	0.0746
	30	2.2	0.0899
	40	2.2	0.105
	50	2.2	0.122
	60	2.2	0.142
	70	2.2	0.167
	80	2.2	0.201
	90	2.2	0.260
	95	1.1	0.322
	99	0.89	0.481

**TABLE 10C-2b (cont'd). DISTRIBUTION OF PARTICLE SURFACE AREA IN THE TRIMODAL POLYDISPERSE AEROSOL DEFINED IN FIGURE 10C-1**  
**(Each individual mode of the trimodal aerosol is separated into the size fractions containing the 1, 5, 10, 20, 30, 40, 50, 60, 70, 80, 90, 95, and 99% surface area fractiles. The “nuclei mode” contains about 77.4% of the total particle surface area; the “accumulation mode” about 21.9%; and the “coarse mode” about 0.64%.)**

Mode	Number Fractile (%)	Percent of Trimodal Aerosol	Upper Limit of Particle Size Interval ( $\mu\text{m}$ )
Coarse <sup>c</sup>	1	0.006	0.618
	5	0.026	0.947
	10	0.032	1.19
	20	0.064	1.57
	30	0.064	1.91
	40	0.064	2.27
	50	0.064	2.65
	60	0.064	3.11
	70	0.064	3.69
	80	0.064	4.50
	90	0.064	5.92
	95	0.032	7.44
	99	0.026	11.4

<sup>a</sup>Mass median diameter (MMD) = 0.018  $\mu\text{m}$ ; geometric standard deviation ( $\sigma_g$ ) = 1.6; density ( $\rho$ ) = 1.4  $\text{g}/\text{cm}^3$ .

<sup>b</sup>MMD = 0.21  $\mu\text{m}$ ;  $\sigma_g$  = 1.8; density ( $\rho$ ) = 1.2  $\text{g}/\text{cm}^3$ .

<sup>c</sup>MMD = 4.9  $\mu\text{m}$ ;  $\sigma_g$  = 1.87; density ( $\rho$ ) = 2.2  $\text{g}/\text{cm}^3$ .

**TABLE 10C-2c. DISTRIBUTION OF PARTICLE MASS IN THE TRIMODAL POLYDISPERSE AEROSOL DEFINED IN FIGURE 10C-1**  
**(Each individual mode of the trimodal aerosol is separated into the size fractions containing the 1, 5, 10, 20, 30, 40, 50, 60, 70, 80, 90, 95, and 99% mass fractiles. The “nuclei mode” contains 15.6% of the total particle mass; the “accumulation mode” 38.7%; and the “coarse mode” about 45.7%.)**

Mode	Mass Fractile (%)	Percent of Trimodal Aerosol	Upper Limit of Particle Size Interval (µm)
Nuclei <sup>a</sup>	1	0.16	0.0053
	5	0.63	0.0073
	10	0.79	0.0087
	20	1.58	0.0107
	30	1.58	0.0124
	40	1.58	0.0141
	50	1.58	0.0159
	60	1.58	0.0179
	70	1.58	0.0203
	80	1.58	0.0236
	90	1.58	0.0290
	95	0.79	0.0345
99	0.63	0.0474	
Accumulation <sup>b</sup>	1	0.39	0.0312
	5	1.56	0.0465
	10	1.95	0.0575
	20	3.91	0.0746
	30	3.91	0.0899
	40	3.91	0.105
	50	3.91	0.122
	60	3.91	0.142
	70	3.91	0.167
	80	3.91	0.201
	90	3.91	0.260
	95	1.95	0.322
99	1.56	0.481	

**TABLE 10C-2c (cont'd). DISTRIBUTION OF PARTICLE MASS IN THE TRIMODAL POLYDISPERSE AEROSOL DEFINED IN FIGURE 10C-1**  
**(Each individual mode of the trimodal aerosol is separated into the size fractions containing the 1, 5, 10, 20, 30, 40, 50, 60, 70, 80, 90, 95, and 99% mass fractiles. The “nuclei mode” contains 15.6% of the total particle mass; the “accumulation mode” about 38.7%; and the “coarse mode” about 45.7%.)**

Mode	Number Fractile (%)	Percent of Trimodal Aerosol	Upper Limit of Particle Size Interval (µm)
Coarse <sup>c</sup>	1	0.46	0.915
	5	1.85	1.40
	10	2.31	1.76
	20	4.62	2.32
	30	4.62	2.83
	40	4.62	3.35
	50	4.62	3.93
	60	4.62	4.60
	70	4.62	5.45
	80	4.62	6.66
	90	4.62	8.76
	95	2.31	11.0
	99	1.85	16.9

<sup>a</sup>Mass median diameter (MMD) = 0.018 µm; geometric standard deviation ( $\sigma_g$ ) = 1.6; density ( $\rho$ ) = 1.4 g/cm<sup>3</sup>.

<sup>b</sup>MMD = 0.21 µm;  $\sigma_g$  = 1.8; density ( $\rho$ ) = 1.2 g/cm<sup>3</sup>.

<sup>c</sup>MMD = 4.9 µm;  $\sigma_g$  = 1.87; density ( $\rho$ ) = 2.2 g/cm<sup>3</sup>.

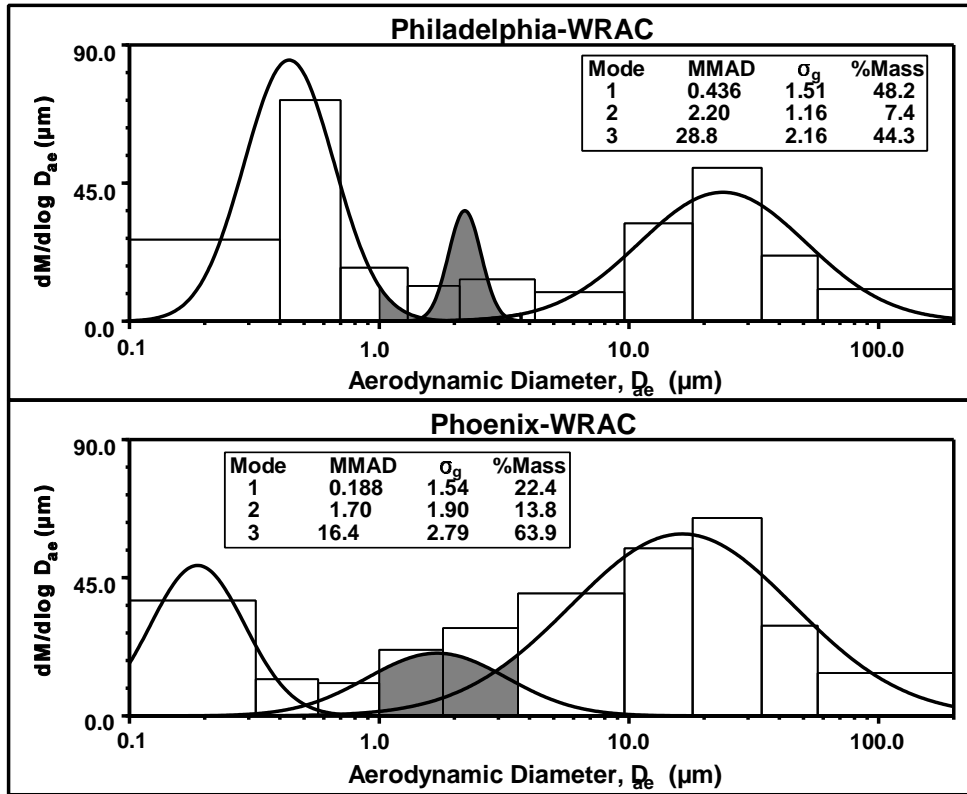


**Figure 10C-2. Impactor size distribution measurement generated by Lundgren et al. with the Wide Range Aerosol Classifier: (a) Philadelphia and (b) Phoenix. Note the much larger, small size tail to the coarse mode in the dryer environment of Phoenix.**

Source: Lundgren and Hausknecht (1982).

**TABLE 10C-3. DISTRIBUTION OF PARTICLE COUNT, SURFACE AREA OR MASS IN THE TRIMODAL POLYDISPERSE AEROSOL FOR PHILADELPHIA DEFINED IN FIGURE 10C-2(a)**  
 (The tabulated numbers represent the upper size cut [in  $\mu\text{m}$ ] for each particle size interval based on the distribution of particle count vs. aerodynamic diameter [ $d_{ae}\{c\}$ ], distribution of surface area vs. aerodynamic diameter [ $d_{ae}\{s\}$ ], distribution of mass vs. aerodynamic diameter [ $d_{ae}\{m\}$ ], or distribution of mass vs. equivalent physical diameter [ $d_p\{m\}$ ]<sup>a</sup>.)

Aerosol Mode	Particle Parameter	Percent of Total Count, Surface Area or Mass Associated with Particles Smaller than Size Cut												
		1	5	10	20	30	40	50	60	70	80	90	95	99
Accumulation <sup>b</sup>	count; $d_{ae}\{c\}$	0.152	0.201	0.233	0.280	0.319	0.357	0.396	0.440	0.492	0.561	0.673	0.781	1.03
	surface; $d_{ae}\{s\}$	0.162	0.214	0.249	0.298	0.340	0.381	0.422	0.469	0.525	0.597	0.717	0.831	1.10
	mass; $d_{ae}\{m\}$	0.167	0.221	0.257	0.308	0.351	0.393	0.436	0.484	0.541	0.618	0.741	0.860	1.13
	mass; $d_p\{m\}$	0.185	0.243	0.282	0.336	0.383	0.428	0.474	0.526	0.587	0.670	0.802	0.930	1.22
Intermodal <sup>c</sup>	count; $d_{ae}\{c\}$	1.53	1.70	1.79	1.92	2.01	2.09	2.17	2.26	2.35	2.47	2.63	2.78	3.06
	surface; $d_{ae}\{s\}$	1.54	1.72	1.80	1.93	2.03	2.11	2.19	2.28	2.37	2.49	2.66	2.80	3.09
	mass; $d_{ae}\{m\}$	1.55	1.73	1.81	1.94	2.04	2.12	2.20	2.29	2.38	2.50	2.67	2.81	3.11
	mass; $d_p\{m\}$	1.67	1.86	1.95	2.09	2.20	2.28	2.37	2.47	2.56	2.69	2.87	3.02	3.34
Coarse <sup>d</sup>	count; $d_{ae}\{c\}$	3.43	5.80	7.67	10.8	13.8	16.9	20.6	25.0	30.8	39.4	55.3	73.1	122.5
	surface; $d_{ae}\{s\}$	4.29	7.25	9.60	13.5	17.2	21.2	25.7	31.3	38.6	49.2	69.0	91.4	153.5
	mass; $d_{ae}\{m\}$	4.80	8.12	10.7	15.1	19.2	23.7	28.8	35.0	43.2	55.1	77.3	102.1	171.5
	Mass; $d_p\{m\}$	5.16	8.73	11.5	16.2	20.6	25.5	30.9	37.6	46.4	59.2	83.0	109.7	184.2

<sup>a</sup>Values for  $d_p$  were calculated iteratively from  $d_{ae}$  using Equations D.13 and D.14 of ICRP Publication 66, Annexe D (James *et al.*, 1994).

<sup>b</sup>Mass median aerodynamic diameter (MMAD) = 0.436  $\mu\text{m}$ ; geometric standard deviation ( $\sigma_g$ ) = 1.51; density ( $\rho$ ) = 1.3  $\text{g}/\text{cm}^3$ .

<sup>c</sup>MMAD = 2.20  $\mu\text{m}$ ;  $\sigma_g$  = 1.16;  $\rho$  = 1.3  $\text{g}/\text{cm}^3$ .

<sup>d</sup>MMAD = 28.8  $\mu\text{m}$ ;  $\sigma_g$  = 2.16;  $\rho$  = 1.3  $\text{g}/\text{cm}^3$ .

**TABLE 10C-4a. DISTRIBUTION OF PARTICLE NUMBER IN THE TRIMODAL POLYDISPERSE PHILADELPHIA AEROSOL DEFINED IN FIGURE 10C-2a (Each individual mode of the trimodal aerosol is separated into the size fractions containing the 1, 5, 10, 20, 30, 40, 50, 60, 70, 80, 90, 95, and 99% number fractiles. The “accumulation mode” contains about 99.95% of the total number of particles; the “intermodal mode” about 0.05%; and the “coarse mode” about 0.004%.)**

Mode	Number Fractile (%)	Percent of Trimodal Aerosol	Upper Limit of Particle Size Interval (µm)
Accumulation <sup>a</sup>	1	1.0	0.0912
	5	4.0	0.121
	10	5.0	0.140
	20	10	0.168
	30	10	0.192
	40	10	0.215
	50	10	0.238
	60	10	0.264
	70	10	0.296
	80	10	0.337
	90	10	0.404
	95	5.0	0.469
	99	4.0	0.623
Intermodal <sup>b</sup>	1	$4.8 \times 10^{-4}$	1.43
	5	$1.9 \times 10^{-3}$	1.60
	10	$2.4 \times 10^{-3}$	1.68
	20	$4.8 \times 10^{-3}$	1.79
	30	$4.8 \times 10^{-3}$	1.88
	40	$4.8 \times 10^{-3}$	1.96
	50	$4.8 \times 10^{-3}$	2.03
	60	$4.8 \times 10^{-3}$	2.12
	70	$4.8 \times 10^{-3}$	2.20
	80	$4.8 \times 10^{-3}$	2.31
	90	$4.8 \times 10^{-3}$	2.47
	95	$2.4 \times 10^{-3}$	2.59
	99	$1.9 \times 10^{-3}$	2.89

**TABLE 10C-4a (cont'd). DISTRIBUTION OF PARTICLE NUMBER IN THE TRIMODAL POLYDISPERSE PHILADELPHIA AEROSOL DEFINED IN FIGURE 10C-2a (Each individual mode of the trimodal aerosol is separated into the size fractions containing the 1, 5, 10, 20, 30, 40, 50, 60, 70, 80, 90, 95, and 99% number fractiles. The “accumulation mode” contains about 99.95% of the total number of particles; the “intermodal mode” about 0.05%; and the “coarse mode” about 0.004%.)**

Mode	Number Fractile (%)	Percent of Trimodal Aerosol	Upper Limit of Particle Size Interval ( $\mu\text{m}$ )
Coarse <sup>c</sup>	1	$4.4 \times 10^{-5}$	0.579
	5	$1.8 \times 10^{-4}$	0.979
	10	$2.2 \times 10^{-4}$	1.30
	20	$4.4 \times 10^{-4}$	1.82
	30	$4.4 \times 10^{-4}$	2.32
	40	$4.4 \times 10^{-4}$	2.86
	50	$4.4 \times 10^{-4}$	3.48
	60	$4.4 \times 10^{-4}$	4.22
	70	$4.4 \times 10^{-4}$	5.21
	80	$4.4 \times 10^{-4}$	6.65
	90	$4.4 \times 10^{-4}$	9.34
	95	$2.2 \times 10^{-4}$	12.3
	99	$1.8 \times 10^{-4}$	20.9

<sup>a</sup>Mass median aerodynamic diameter (MMAD) = 0.436  $\mu\text{m}$ ; geometric standard deviation ( $\sigma_g$ ) = 1.51; density ( $\rho$ ) = 1.3  $\text{g}/\text{cm}^3$ .

<sup>b</sup>MMAD = 2.20  $\mu\text{m}$ ;  $\sigma_g$  = 1.16; density ( $\rho$ ) = 1.3  $\text{g}/\text{cm}^3$ .

<sup>c</sup>MMAD = 28.8  $\mu\text{m}$ ;  $\sigma_g$  = 2.16; density ( $\rho$ ) = 1.3  $\text{g}/\text{cm}^3$ .

**TABLE 10C-4b. DISTRIBUTION OF PARTICLE SURFACE AREA IN THE TRIMODAL POLYDISPERSE PHILADELPHIA AEROSOL DEFINED IN FIGURE 10C-2a (Each individual mode of the trimodal aerosol is separated into the size fractions containing the 1, 5, 10, 20, 30, 40, 50, 60, 70, 80, 90, 95, and 99% surface area fractiles. The “accumulation mode” contains about 95.4% of the total particle surface area; the “intermodal mode” about 2.5%; and the “coarse mode” about 2.1%.)**

Mode	Surface Area Fractile (%)	Percent of Trimodal Aerosol	Upper Limit of Particle Size Interval ( $\mu\text{m}$ )
Accumulation <sup>a</sup>	1	0.96	0.128
	5	3.9	0.170
	10	4.8	0.197
	20	9.6	0.236
	30	9.6	0.269
	40	9.6	0.301
	50	9.6	0.334
	60	9.6	0.371
	70	9.6	0.415
	80	9.6	0.473
	90	9.6	0.568
	95	4.8	0.659
	99	3.9	0.875
Intermodal <sup>b</sup>	1	0.025	1.50
	5	0.10	1.66
	10	0.13	1.75
	20	0.25	1.88
	30	0.25	1.96
	40	0.25	2.05
	50	0.25	2.13
	60	0.25	2.21
	70	0.25	2.30
	80	0.25	2.41
	90	0.25	2.57
	95	0.13	2.73
	99	0.10	3.02

**TABLE 10C-4b (cont'd). DISTRIBUTION OF PARTICLE SURFACE AREA IN THE TRIMODAL POLYDISPERSE PHILADELPHIA AEROSOL DEFINED IN FIGURE 10C-2a (Each individual mode of the trimodal aerosol is separated into the size fractions containing the 1, 5, 10, 20, 30, 40, 50, 60, 70, 80, 90, 95, and 99% surface area fractiles. The “accumulation mode” contains about 95.4% of the total particle surface area; the “intermodal mode” about 2.5%; and the “coarse mode” about 2.1%.)**

Mode	Surface Area Fractile (%)	Percent of Trimodal Aerosol	Upper Limit of Particle Size Interval ( $\mu\text{m}$ )
Coarse <sup>c</sup>	1	0.02	1.90
	5	0.08	3.20
	10	0.11	4.24
	20	0.21	5.95
	30	0.21	7.60
	40	0.21	9.37
	50	0.21	11.4
	60	0.21	13.8
	70	0.21	17.0
	80	0.21	21.8
	90	0.21	30.5
	95	0.11	40.4
	99	0.08	68.1

<sup>a</sup>Mass median aerodynamic diameter (MMAD) = 0.436  $\mu\text{m}$ ; geometric standard deviation ( $\sigma_g$ ) = 1.51; density ( $\rho$ ) = 1.3  $\text{g}/\text{cm}^3$ .

<sup>b</sup>MMAD = 2.20  $\mu\text{m}$ ;  $\sigma_g$  = 1.16; density ( $\rho$ ) = 1.3  $\text{g}/\text{cm}^3$ .

<sup>c</sup>MMAD = 28.8  $\mu\text{m}$ ;  $\sigma_g$  = 2.16; density ( $\rho$ ) = 1.3  $\text{g}/\text{cm}^3$ .

**TABLE 10C-4c. DISTRIBUTION OF PARTICLE MASS IN THE TRIMODAL POLYDISPERSE PHILADELPHIA AEROSOL DEFINED IN FIGURE 10C-2a (Each individual mode of the trimodal aerosol is separated into the size fractions containing the 1, 5, 10, 20, 30, 40, 50, 60, 70, 80, 90, 95, and 99% mass fractiles. The “accumulation mode” contains 48.2% of the total particle mass; the “intermodal mode” 7.4%; and the “coarse mode” 44.3%.)**

Mode	Mass Fractile (%)	Percent of Trimodal Aerosol	Upper Limit of Particle Size Interval (µm)
Accumulation <sup>a</sup>	1	0.49	0.152
	5	2.0	0.201
	10	2.4	0.233
	20	4.9	0.280
	30	4.9	0.319
	40	4.9	0.357
	50	4.9	0.396
	60	4.9	0.440
	70	4.9	0.492
	80	4.9	0.561
	90	4.9	0.673
	95	2.4	0.782
	99	2.0	1.04
Intermodal <sup>b</sup>	1	0.07	1.53
	5	0.30	1.70
	10	0.37	1.79
	20	0.75	1.92
	30	0.75	2.01
	40	0.75	2.09
	50	0.75	2.17
	60	0.75	2.26
	70	0.75	2.35
	80	0.75	2.47
	90	0.75	2.63
	95	0.37	2.78
	99	0.30	3.06

**TABLE 10C-4c (cont'd). DISTRIBUTION OF PARTICLE MASS IN THE TRIMODAL POLYDISPERSE PHILADELPHIA AEROSOL DEFINED IN FIGURE 10C-2a (Each individual mode of the trimodal aerosol is separated into the size fractions containing the 1, 5, 10, 20, 30, 40, 50, 60, 70, 80, 90, 95, and 99% mass fractiles. The “accumulation mode” contains 48.2% of the total particle mass; the “intermodal mode” 7.4%; and the “coarse mode” 44.3%.)**

Mode	Mass Fractile (%)	Percent of Trimodal Aerosol	Upper Limit of Particle Size Interval (μm)
Coarse <sup>c</sup>	1	0.45	3.43
	5	1.8	5.80
	10	2.2	7.67
	20	4.5	10.8
	30	4.5	13.7
	40	4.5	16.9
	50	4.5	20.6
	60	4.5	25.0
	70	4.5	30.8
	80	4.5	39.2
	90	4.5	55.0
	95	2.2	72.4
	99	1.8	118.7

<sup>a</sup>Mass median aerodynamic diameter (MMAD) = 0.436 μm; geometric standard deviation ( $\sigma_g$ ) = 1.51; density ( $\rho$ ) = 1.3 g/cm<sup>3</sup>.

<sup>b</sup>MMAD = 2.20 μm;  $\sigma_g$  = 1.16; density ( $\rho$ ) = 1.3 g/cm<sup>3</sup>.

<sup>c</sup>MMAD = 28.8 μm;  $\sigma_g$  = 2.16; density ( $\rho$ ) = 1.3 g/cm<sup>3</sup>.

**TABLE 10C-5. DISTRIBUTION OF PARTICLE COUNT, SURFACE AREA OR MASS IN THE TRIMODAL POLYDISPERSE AEROSOL FOR PHOENIX DEFINED IN FIGURE 10C-2(b) (The tabulated numbers represent the upper size cut [in  $\mu\text{m}$ ] for each particle size interval based on the distribution of particle count vs. aerodynamic diameter [ $d_{ac}\{c\}$ ], distribution of surface area vs. aerodynamic diameter [ $d_{ac}\{s\}$ ], distribution of mass vs. aerodynamic diameter [ $d_{ac}\{m\}$ ], or distribution of mass vs. equivalent physical diameter [ $d_p\{m\}$ ]<sup>a</sup>.)**

Aerosol Mode	Particle Parameter	Percent of Total Count, Surface Area or Mass Associated with Particles Smaller than Size Cut												
		1	5	10	20	30	40	50	60	70	80	90	95	99
Accumulation <sup>b</sup>	count; $d_{ac}\{c\}$	0.062	0.083	0.097	0.118	0.135	0.152	0.169	0.189	0.212	0.243	0.295	0.345	0.461
	surface; $d_{ac}\{s\}$	0.066	0.089	0.104	0.126	0.145	0.163	0.182	0.203	0.228	0.261	0.316	0.369	0.495
	mass; $d_{ac}\{m\}$	0.069	0.092	0.108	0.131	0.150	0.169	0.188	0.210	0.236	0.271	0.327	0.383	0.511
	mass; $d_p\{m\}$	0.062	0.083	0.098	0.119	0.137	0.155	0.172	0.193	0.217	0.250	0.303	0.355	0.475
Intermodal <sup>c</sup>	count; $d_{ac}\{c\}$	0.302	0.469	0.592	0.785	0.962	1.14	1.35	1.58	1.89	2.31	3.06	3.87	5.96
	surface; $d_{ac}\{s\}$	0.353	0.548	0.691	0.916	1.12	1.34	1.57	1.85	2.20	2.70	3.58	4.52	6.95
	mass; $d_{ac}\{m\}$	0.381	0.592	0.747	0.991	1.21	1.45	1.70	2.00	2.38	2.91	3.87	4.89	7.52
	mass; $d_p\{m\}$	0.353	0.552	0.697	0.926	1.13	1.36	1.59	1.87	2.23	2.73	3.63	4.59	7.06
Coarse <sup>d</sup>	count; $d_{ac}\{c\}$	0.831	1.67	2.43	3.81	5.28	6.97	9.04	11.7	15.5	21.4	33.7	48.8	97.4
	surface; $d_{ac}\{s\}$	1.24	2.49	3.61	5.67	7.85	10.4	13.4	17.4	23.0	31.9	50.0	72.6	144.8
	mass; $d_{ac}\{m\}$	1.51	3.03	4.40	6.92	9.58	12.7	16.4	21.3	28.1	38.9	61.1	88.4	176.9
	mass; $d_p\{m\}$	1.41	2.34	4.13	6.50	8.99	11.9	15.4	20.0	26.4	36.5	57.4	83.0	166.2

<sup>a</sup>Values for  $d_p$  were calculated iteratively from  $d_{ac}$  using Equations D.13 and D.14 of ICRP Publication 66, Annexe D (James *et al.*, 1994).

<sup>b</sup>Mass median aerodynamic diameter (MMAD) = 0.188  $\mu\text{m}$ ; geometric standard deviation ( $\sigma_g$ ) = 1.54; density ( $\rho$ ) = 1.7  $\text{g}/\text{cm}^3$ .

<sup>c</sup>MMAD = 1.70  $\mu\text{m}$ ;  $\sigma_g$  = 1.90;  $\rho$  = 1.7  $\text{g}/\text{cm}^3$ .

<sup>d</sup>MMAD = 16.4  $\mu\text{m}$ ;  $\sigma_g$  = 2.79;  $\rho$  = 1.7  $\text{g}/\text{cm}^3$ .

**TABLE 10C-6a. DISTRIBUTION OF PARTICLE NUMBER IN THE TRIMODAL POLYDISPERSE PHOENIX AEROSOL DEFINED IN FIGURE 10C-2b**  
**(Each individual mode of the trimodal aerosol is separated into the size fractions containing the 1, 5, 10, 20, 30, 40, 50, 60, 70, 80, 90, 95, and 99% number fractiles. The “accumulation mode” contains about 99.6% of the total number of particles; the “intermodal mode” about 0.3%; and the “coarse mode” about 0.1%.)**

Mode	Number Fractile (%)	Percent of Trimodal Aerosol	Upper Limit of Particle Size Interval (µm)
Accumulation <sup>a</sup>	1	1.0	0.0353
	5	4.0	0.0475
	10	5.0	0.0556
	20	10	0.0672
	30	10	0.0771
	40	10	0.0867
	50	10	0.0967
	60	10	0.108
	70	10	0.122
	80	10	0.139
	90	10	0.169
	95	5.0	0.197
	99	4.0	0.264
Intermodal <sup>b</sup>	1	0.0034	0.0878
	5	0.014	0.136
	10	0.017	0.172
	20	0.034	0.228
	30	0.034	0.280
	40	0.034	0.333
	50	0.034	0.391
	60	0.034	0.461
	70	0.034	0.548
	80	0.034	0.673
	90	0.034	0.891
	95	0.017	1.13
	99	0.014	1.74

**TABLE 10C-6a (cont'd). DISTRIBUTION OF PARTICLE NUMBER IN THE TRIMODAL POLYDISPERSE PHOENIX AEROSOL DEFINED IN FIGURE 10C-2b**  
**(Each individual mode of the trimodal aerosol is separated into the size fractions containing the 1, 5, 10, 20, 30, 40, 50, 60, 70, 80, 90, 95, and 99% number fractiles. The “accumulation mode” contains about 99.6% of the total number of particles; the “intermodal mode” about 0.3%; and the “coarse mode” about 0.1%.)**

Mode	Number Fractile (%)	Percent of Trimodal Aerosol	Upper Limit of Particle Size Interval ( $\mu\text{m}$ )
Coarse <sup>c</sup>	1	$9.3 \times 10^{-4}$	0.0353
	5	$3.7 \times 10^{-3}$	0.0711
	10	$4.6 \times 10^{-3}$	0.103
	20	$9.3 \times 10^{-3}$	0.162
	30	$9.3 \times 10^{-3}$	0.224
	40	$9.3 \times 10^{-3}$	0.296
	50	$9.3 \times 10^{-3}$	0.385
	60	$9.3 \times 10^{-3}$	0.499
	70	$9.3 \times 10^{-3}$	0.658
	80	$9.3 \times 10^{-3}$	0.912
	90	$9.3 \times 10^{-3}$	1.43
	95	$4.6 \times 10^{-3}$	2.08
99	$3.7 \times 10^{-3}$	4.18	

<sup>a</sup>Mass median aerodynamic diameter (MMAD) = 0.188  $\mu\text{m}$ ; geometric standard deviation ( $\sigma_g$ ) = 1.54; density ( $\rho$ ) = 1.7  $\text{g}/\text{cm}^3$ .

<sup>b</sup>MMAD = 1.70  $\mu\text{m}$ ;  $\sigma_g$  = 1.90; density ( $\rho$ ) = 1.7  $\text{g}/\text{cm}^3$ .

<sup>c</sup>MMAD = 16.4  $\mu\text{m}$ ;  $\sigma_g$  = 2.79; density ( $\rho$ ) = 1.7  $\text{g}/\text{cm}^3$ .

**TABLE 10C-6b. DISTRIBUTION OF PARTICLE SURFACE AREA IN THE TRIMODAL POLYDISPERSE PHOENIX AEROSOL DEFINED IN FIGURE 10C-2b**  
**(Each individual mode of the trimodal aerosol is separated into the size fractions containing the 1, 5, 10, 20, 30, 40, 50, 60, 70, 80, 90, 95, and 99% surface area fractiles. The “accumulation mode” contains about 85.5% of the total particle surface area; the “intermodal mode” about 7.4%; and the “coarse mode” about 7.0%.)**

Mode	Surface Area Fractile (%)	Percent of Trimodal Aerosol	Upper Limit of Particle Size Interval (µm)
Accumulation <sup>a</sup>	1	0.86	0.0514
	5	3.5	0.0689
	10	4.3	0.0807
	20	8.6	0.0977
	30	8.6	0.112
	40	8.6	0.126
	50	8.6	0.141
	60	8.6	0.157
	70	8.6	0.176
	80	8.6	0.202
	90	8.6	0.244
	95	4.3	0.285
	99	3.5	0.385
Intermodal <sup>b</sup>	1	0.075	0.202
	5	0.30	0.311
	10	0.37	0.392
	20	0.75	0.520
	30	0.75	0.637
	40	0.75	0.758
	50	0.75	0.892
	60	0.75	1.05
	70	0.75	1.25
	80	0.75	1.53
	90	0.75	2.03
	95	0.37	2.57
	99	0.30	3.97

**TABLE 10C-6b (cont'd). DISTRIBUTION OF PARTICLE SURFACE AREA IN THE TRIMODAL POLYDISPERSE PHOENIX AEROSOL DEFINED IN FIGURE 10C-2b**  
**(Each individual mode of the trimodal aerosol is separated into the size fractions containing the 1, 5, 10, 20, 30, 40, 50, 60, 70, 80, 90, 95, and 99% surface area fractiles.**  
**The “accumulation mode” contains about 85.5% of the total particle surface area; the “intermodal mode” about 7.4%; and the “coarse mode” about 7.0%.)**

Mode	Surface Area Fractile (%)	Percent of Trimodal Aerosol	Upper Limit of Particle Size Interval (μm)
Coarse <sup>c</sup>	1	0.07	0.290
	5	0.29	0.583
	10	0.36	0.847
	20	0.71	1.33
	30	0.71	1.84
	40	0.71	2.43
	50	0.71	3.16
	60	0.71	4.09
	70	0.71	5.40
	80	0.71	7.48
	90	0.71	11.8
	95	0.36	17.1
	99	0.29	34.4

<sup>a</sup>Mass median aerodynamic diameter (MMAD) = 0.188 μm; geometric standard deviation ( $\sigma_g$ ) = 1.54; density ( $\rho$ ) = 1.7 g/cm<sup>3</sup>.

<sup>b</sup>MMAD = 1.70 μm;  $\sigma_g$  = 1.90; density ( $\rho$ ) = 1.7 g/cm<sup>3</sup>.

<sup>c</sup>MMAD = 16.4 μm;  $\sigma_g$  = 2.79; density ( $\rho$ ) = 1.7 g/cm<sup>3</sup>.

**TABLE 10C-6c. DISTRIBUTION OF PARTICLE MASS IN THE TRIMODAL POLYDISPERSE PHOENIX AEROSOL DEFINED IN FIGURE 10C-2b**  
**(Each individual mode of the trimodal aerosol is separated into the size fractions containing the 1, 5, 10, 20, 30, 40, 50, 60, 70, 80, 90, 95, and 99% mass fractiles. The “accumulation mode” contains 22.4% of the total particle mass; the “intermodal mode” 13.8%; and the “coarse mode” 63.9%.)**

Mode	Mass Fractile (%)	Percent of Trimodal Aerosol	Upper Limit of Particle Size Interval (µm)
Accumulation <sup>a</sup>	1	0.23	0.0618
	5	0.91	0.0832
	10	1.1	0.0973
	20	2.3	0.118
	30	2.3	0.135
	40	2.3	0.152
	50	2.3	0.169
	60	2.3	0.189
	70	2.3	0.213
	80	2.3	0.243
	90	2.3	0.295
	95	1.1	0.345
	99	0.91	0.462
Intermodal <sup>b</sup>	1	0.14	0.302
	5	0.56	0.469
	10	0.70	0.592
	20	1.4	0.785
	30	1.4	0.962
	40	1.4	1.14
	50	1.4	1.35
	60	1.4	1.58
	70	1.4	1.89
	80	1.4	2.31
	90	1.4	3.06
	95	0.70	3.87
	99	0.56	6.00

**TABLE 10C-6c (cont'd). DISTRIBUTION OF PARTICLE MASS IN THE TRIMODAL POLYDISPERSE PHOENIX AEROSOL DEFINED IN FIGURE 10C-2b**  
**(Each individual mode of the trimodal aerosol is separated into the size fractions containing the 1, 5, 10, 20, 30, 40, 50, 60, 70, 80, 90, 95, and 99% mass fractiles. The “accumulation mode” contains 22.4% of the total particle mass; the “intermodal mode” 13.8%; and the “coarse mode” 63.9%.)**

Mode	Mass Fractile (%)	Percent of Trimodal Aerosol	Upper Limit of Particle Size Interval ( $\mu\text{m}$ )
Coarse <sup>c</sup>	1	0.65	0.831
	5	2.6	1.67
	10	3.2	2.43
	20	6.5	3.81
	30	6.5	5.27
	40	6.5	6.96
	50	6.5	9.03
	60	6.5	11.7
	70	6.5	15.5
	80	6.5	21.4
	90	6.5	33.5
	95	3.2	48.4
	99	2.6	94.1

<sup>a</sup>Mass median aerodynamic diameter (MMAD) = 0.188  $\mu\text{m}$ ; geometric standard deviation ( $\sigma_g$ ) = 1.54; density ( $\rho$ ) = 1.7  $\text{g}/\text{cm}^3$ .

<sup>b</sup>MMAD = 1.70  $\mu\text{m}$ ;  $\sigma_g$  = 1.90; density ( $\rho$ ) = 1.7  $\text{g}/\text{cm}^3$ .

<sup>c</sup>MMAD = 16.4  $\mu\text{m}$ ;  $\sigma_g$  = 2.79; density ( $\rho$ ) = 1.7  $\text{g}/\text{cm}^3$ .

# 11. TOXICOLOGICAL STUDIES OF PARTICULATE MATTER

## 11.1 INTRODUCTION

This chapter assesses results of exposure to particulate matter (PM) in controlled human clinical studies, selected occupational studies, and animal toxicology studies. It focuses mainly on those studies published since the 1982 Air Quality Criteria Document for Particulate Matter and Sulfur Oxides (U.S. Environmental Protection Agency, 1982), emphasizing coverage of selected constituents of ambient air PM that may contribute to those types of health effects found by epidemiological studies discussed in Chapter 12 of this document. The data discussed in Chapter 12 indicate that increased levels of PM in the ambient atmosphere are associated with increased mortality risk, especially among the elderly (aged 65+ years) and individuals with preexisting cardiopulmonary diseases, such as chronic obstructive pulmonary disease (COPD), pneumonia, and chronic heart disease. The epidemiology studies also provide evidence for associations of ambient PM exposures with increased risk of respiratory and cardiovascular morbidity effects (e.g., increased hospital admissions or emergency room visits for asthma or other respiratory problems, increased incidence of respiratory symptoms, or alterations in pulmonary function).

Chronic obstructive pulmonary disease is defined as a disease state characterized by the presence of airflow obstruction due to chronic bronchitis or emphysema; the airflow obstruction is generally progressive, may be accompanied by airway hyperreactivity, and may be partially reversible (American Thoracic Society, 1995). The biological responses occurring in the respiratory tract following controlled PM inhalation encompass a continuum of changes, including changes in pulmonary function, respiratory symptoms (i.e., wheeze, coughing, etc.), inflammation, and tumor formation. The responses observed are dependent on the physicochemical characteristics of the particulate matter, the total exposure and the health status of the host. However, many of the responses are usually seen only at distinctly higher level exposures characteristic of occupational and laboratory animal studies but not at typically much lower ambient particle concentrations.

Particulate matter is a broad term that encompasses thousands of chemical species, many of which have not been investigated in controlled laboratory animal or human studies. However, a full discussion of all the types of particles that have been studied is well beyond the scope of this chapter. Thus, criteria were used to select topics for presentation. High priority was placed on studies that: (1) may elucidate health effects of major common constituents of ambient PM (e.g., sulfates, carbon, silica) and/or (2) contribute to enhanced understanding of the epidemiological studies (e.g., real-world particles, "surrogate" particles; or particles with low inherent toxicity that may cause effects due to their generic nature as a particle, such as their ultrafine size). Based on these criteria, full summaries of acid aerosols, ultrafine particles, real-world particles, and "surrogate" particles are provided.

Diesel exhaust particles generally fit the criteria; but, because they are described in great detail elsewhere (U.S. Environmental Protection Agency, 1994; Health Effects Institute, 1995), they are only summarized briefly here. Diesel particles also differ from other particles in this classification because they are regulated pursuant to mobile source sections of the Clean Air Act (g/mi emission standards), although there is still a relationship of these regulations to the PM<sub>10</sub> standard. Medium priority was placed on particles with high inherent toxicity that are of concern primarily because of point source emissions and more local exposures (as contrasted to ubiquitous pollutants). Metals having air concentrations greater than 0.5  $\mu\text{g}/\text{m}^3$  were placed in this class. The health effects of particles in this prioritization class are summarized far more briefly here. It must be emphasized that this prioritization is not related to a judgement or decision about potency or health risk. For example, it should not be inferred that on an individual exposure basis, a "high priority" particle is of more inherent health concern than a "medium priority" particle. The split is primarily related to regulatory issues. The Clean Air Act requires a criteria document for criteria pollutants. Except for lead, individual metals are not criteria pollutants. Rather, they are regulated as hazardous air pollutants under the Clean Air Act. Thus, their inclusion here is only intended to be generally instructive because they can be part of the complex mixture of PM in the ambient air.

As noted above, lead is a criteria air pollutant that, like particulate matter, is also regulated under Sections 108 and 109 of the Clean Air Act. Earlier extensive evaluations in Air Quality Criteria for Lead (U.S. Environmental Protection Agency, 1977) led to setting of

the current National Ambient Air Quality Standard (primary as well as secondary) for lead at  $1.5 \mu\text{g}/\text{m}^3$  on a quarterly average basis (Federal Register, 1978 [51594]). Subsequent to promulgation of that standard, the U.S. Environmental Protection Agency issued a revised Air Quality Criteria for Lead (1986a) and a Supplement (U.S. Environmental Protection Agency, 1990). These and other such assessments found blood lead levels of  $10 \mu\text{g}/\text{dl}$  in young children and women of child bearing age (due to risk to the fetus in utero) to be associated with unacceptable risk of slowed prenatal and postnatal growth and neuropsychological development. Air levels below  $0.50$  to  $0.75 \mu\text{g}/\text{m}^3$  lead have been proposed as adequate to protect against such risk (World Health Organization, 1987). Typical ambient air levels of lead in U.S. urban areas almost invariably now fall below  $0.10$  to  $0.25 \mu\text{g}/\text{m}^3$ . The reader is referred to the above-noted air quality criteria documents/supplement and Federal Register notices concerning the lead National Ambient Air Quality Standard for detailed information on particulate lead health effects.

In some widespread geographic areas of the United States, silica can be among major ambient PM constituents and is discussed briefly here. The reader is referred to more extensive evaluation of silica elsewhere (U.S. Environmental Protection Agency, 1996). Asbestos fibers are also well established as a fibrogenic pollutant and they are known to cause mesothelial tumors following chronic exposures in laboratory animals. However, asbestos is not discussed as a separate entity in the present document, but reviews on asbestos effects can be found elsewhere (U.S. Environmental Protection Agency, 1986b; Mossman and Gee, 1989; Rom, et al., 1991; Health Effects Institute, 1991).

The effects of exposure to combinations of particles or particles and gases are important to understand because people are not exposed to single ambient air pollutants. The responses to pollutant mixtures may be different from those of the individual chemical constituents. Effects can be additive, antagonistic, or synergistic. Controlled exposure studies of humans or animals rarely involve more than two pollutants simultaneously or sequentially. Significant exceptions to this are the bodies of work on diesel and gasoline engine emissions, where the exposure has been to the specific mixture. In studies involving more complex mixtures (e.g., ambient air) it is difficult, if not impossible, to assess the relative contributions of individual specific components.

The different nature of the data bases also influences the structure of the chapter. For example, community epidemiology studies that sought associations between health effects and some type of ambient PM metric are described in Chapter 12 to permit full portrayal and integrated evaluation of the results. For the metals and diesel particles, discussed to reach a different goal, epidemiological studies are included here in Chapter 11 to facilitate a full hazard identification, and as appropriate, exposure-response information. Besides the summary of the effects portion of the literature, this chapter also attempts to identify and characterize key factors that may have significant influences on the health effects of PM.

Most of the investigations reported herein were conducted with laboratory animals, raising the question of their quantitative extrapolation to humans. Of the dosimetric and species sensitivity aspects of extrapolation, most is known about the former, which is presented in Chapter 10. Both Chapters 10 and 11 must be jointly considered for interpretation. For example, was one aerosol more toxic than another because it had a greater deposition in a sensitive lung target site or because it had higher potency?

Similarly, most particles considered in the laboratory animal toxicology and occupational studies are mainly in the fine and coarse mode size range. However, the enormous numbers and huge surface area of the ultrafine particles demonstrate the importance of considering the size of the particle. Ultrafine particles with a diameter of 20 nm when inhaled at the same mass concentration have an approximately 6 orders of magnitude higher number concentration than a 2.5  $\mu\text{m}$  diameter particle; particle surface area is also greatly increased (Table 11-1).

**TABLE 11-1. NUMBERS AND SURFACE AREAS OF MONODISPERSE PARTICLES OF UNIT DENSITY OF DIFFERENT SIZES AT A MASS CONCENTRATION OF 10  $\mu\text{g}/\text{m}^3$**

Particle Diameter $\mu\text{m}$	Particle Number per $\text{cm}^3$ Air	Particle Surface Area $\mu\text{m}^2$ per $\text{cm}^3$ Air
0.02	2,400,000	3,016
0.1	19,100	600
0.5	153	120
1.0	19	60
2.5	1.2	24

Source: Oberdörster et al. (1995a).

Most of the laboratory animal and occupational epidemiological studies summarized here used high particulate mass concentrations, relative to ambient, even when laboratory animal-to-human dosimetric differences are considered. This raises a question about the relevance of, for example, a rat study at  $5,000 \mu\text{g}/\text{m}^3$  in terms of direct extrapolation to humans in ambient exposure scenarios.

In spite of these difficulties, the array of laboratory animal studies does illustrate certain toxicological principles for particles. To identify but a few here, the data base clearly shows that the site of respiratory tract deposition (and hence particle size) influences the health outcome and that toxicity is dependent on the chemical species (e.g., cadmium is different from sulfuric acid, and cadmium chloride is different from cadmium oxide).

## 11.2 ACID AEROSOLS

The ubiquitous presence of acidic aerosols in the ambient air and concern about their potential health effects led to considerable research over the past 15 years on the response of humans and laboratory animals to exposure to acid aerosols. In Section 11.2.1, responses of both healthy and sensitive humans to acid aerosols and acidic aerosol mixtures with other pollutants are reviewed. Human studies primarily consider brief exposures, whereas the laboratory animal toxicology studies discussed in Section 11.2.2 also consider the effects of chronic exposure to acid aerosols and acidic aerosol mixtures.

Section 11.2 focuses mainly on sulfate-related species (e.g., sulfuric acid [ $\text{H}_2\text{SO}_4$ ]). Information on certain other aerosol species (e.g., nitrates) was reviewed in the previous PM/SO<sub>x</sub> CD (U.S. Environmental Protection Agency, 1982), the EPA Acid Aerosols Issue Paper (U.S. Environmental Protection Agency, 1989), and the Oxides of Nitrogen Criteria Document (U.S. Environmental Protection Agency, 1993). Those earlier assessments yielded only very limited information indicative of health effects being associated with exposures to aerosol species such as sodium nitrate ( $\text{NaNO}_3$ ) or ammonium nitrate ( $\text{NH}_4\text{NO}_3$ ) at levels very much in excess of ambient (i.e., at three orders of magnitude [about 1000 times] above nitrate concentrations typically found in ambient air). Ambient levels of airborne nitrate salts are typically less than  $5 \mu\text{g}/\text{m}^3$  and rarely exceed  $50 \mu\text{g}/\text{m}^3$  (Sackner et al., 1979). Given that little, if any, important new information on nitrate-related health

effects has appeared in the past few years since the above noted assessments were completed, they are not treated further here, except as components of some particle mixtures discussed later in the chapter.

## **11.2.1 Controlled Human Exposure Studies**

### **11.2.1.1 Introduction**

Human clinical exposure studies utilize controlled laboratory conditions to test responses to atmospheric pollutants. Advantages include the opportunity to study the species of interest (i.e., humans), and the ability to carefully control the atmosphere with regard to pollutant concentration, aerosol characteristics, temperature, and relative humidity. Concentrations can be varied while other conditions are held constant to determine exposure-response relationships. Mixtures of pollutants or sequential exposures to different pollutants can be used to elucidate interactions.

Methods of inhalation used in clinical studies include mouthpiece, face mask, head-dome, and environmental chamber. Breathing through a mouthpiece alters breathing patterns, and bypasses the normal filtering and humidifying role of the nasal passages, thereby increasing delivery of particles to the lower airways. Environmental chamber and head-dome exposures allow the assessment of shifts between nasal and oral-nasal breathing that normally occur with exercise.

Several factors limit the utility of human clinical studies. To meet legal and ethical requirements, exposures must be without significant harm. Studies are typically limited to short-term exposures, since long-term exposures are impractical, and may be more likely to cause harm. Sample sizes are small, and therefore may not be representative of populations at risk. Finally, individuals likely to be at greatest risk (i.e., the very young and very old, those with severe obstructive lung disease, or combined heart and lung disease) have not been studied. The data from human clinical studies should therefore be used together with information from laboratory animal exposure studies, epidemiologic studies, and *in vitro* exposure studies, in the process of health assessment.

The endpoints most commonly measured in human clinical studies are symptoms and pulmonary function tests. The latter are well standardized, and their use in these studies has been reviewed (Utell et al., 1993). Effects in clinical studies can be directly compared to

acute changes in field studies, as has been done extensively in studies of ozone health effects (U.S. Environmental Protection Agency, 1995).

Airway responsiveness is another endpoint commonly measured in human clinical studies. This test measures changes in lung function in response to pharmacologic bronchoconstricting agents, typically methacholine, carbachol, or histamine (see also Section 11.2.1.4). A dose-response curve is obtained for the agent, and airway responsiveness is expressed as the dose of the bronchoconstricting agent resulting in a specific change in lung function: e.g., the  $PD_{20}$  is the provocative dose resulting in a 20% fall in forced expiratory volume in 1 sec ( $FEV_1$ ). Individuals with asthma almost always have hyperresponsive airways, with a  $PD_{20}$  well below the normal range. Increase in airway reactivity in response to pollutant exposure could reflect airway inflammation or edema. However, smaller airway caliber as a consequence of the exposure will also increase measured responsiveness because of factors related to airways geometry. It is therefore important to measure responsiveness at a time when spirometric function has returned to baseline. Likewise, performing airway challenge testing prior to pollutant exposure may alter subsequent lung function responses to the pollutant by changing the baseline airways caliber. Differences among laboratories in the protocols and provocative agents used for airway challenge make comparison of experimental results problematic.

Endpoints in human clinical studies have extended beyond measures of air flow and lung volume. Mucociliary clearance is measured using inhaled radio-labelled aerosols. As reviewed in the Acid Aerosols Issue Paper (U.S. Environmental Protection Agency, 1989), exposure to acid aerosols alters mucociliary clearance in humans as well as in several laboratory animal species. Within the past decade, fiberoptic bronchoscopy has been used to examine the lower respiratory tract in healthy volunteers exposed to pollutants. Cells that populate the alveolar space, including alveolar macrophages (AM), lymphocytes, and polymorphonuclear leukocytes (PMN), can be recovered by bronchoalveolar lavage (BAL); bronchial epithelial cells can be sampled using bronchial brushing and endobronchial biopsies. Nasal lavage can be used to quantitate inflammation in the nose.

Features of experimental design of particular importance with regard to human clinical studies are method of exposure, exercise, and selection of control exposures. Exposure by mouthpiece reduces humidification of inhaled air that normally occurs in the nasal passages;

inhalation of dry cold air into the airways may cause bronchoconstriction in asthmatic subjects. Exercise plays an important role in enhancing pollutant effects by causing a change from nasal to oral-nasal breathing, hence decreasing upper airways deposition, and by increasing pollutant dose through increased minute ventilation ( $\dot{V}_E$ ).

Selection of control exposures is of particular importance. Typically, each subject serves as his/her own control to eliminate intersubject variability. The control atmosphere depends on the study objectives and may consist of clean air, or, when acidic aerosols are being tested, a pH neutral aerosol, such as sodium chloride (NaCl), to distinguish non-specific effects of the aerosol from pollutant or hydrogen ion ( $H^+$ ) effects. It is important that control exposures be performed under similar conditions of temperature, relative humidity,  $\dot{V}_E$ , and time of day; that control and pollutant exposure be separated by sufficient time to avoid carry-over effects; and that the order of the exposures be randomized among the study group. Double blind procedures (by which neither the investigators collecting data nor the subjects know the contents of exposure atmospheres) should be used to the extent possible.

Human exposure studies of the effects of acid aerosols were reviewed in the *Acid Aerosols Issue Paper* (U.S. Environmental Protection Agency, 1989). That review reached the following conclusions:

- (1) In healthy subjects, no effects on spirometry have been observed after exposure to concentrations of  $H_2SO_4$  less than  $500 \mu g/m^3$ , and no consistent effects have been observed at levels up to  $1,000 \mu g/m^3$  with exposure durations up to 4 h. Studies of a variety of other sulfate and nitrate aerosols have similarly demonstrated an absence of spirometric effects on healthy subjects.
- (2) Combinations of sulfates with ozone or  $SO_2$  have not demonstrated synergistic or interactive effects.
- (3) Asthmatic subjects experience modest bronchoconstriction after exposure to  $\approx 400$  to  $1000 \mu g/m^3$   $H_2SO_4$ , and small decrements in spirometry have been observed in adolescent asthmatics at concentrations as low as  $68 \mu g/m^3$  for 30 min.
- (4) Some studies suggest that delayed effects may occur in healthy and asthmatic subjects following exposure to  $H_2SO_4$ .
- (5) Effects of sulfate aerosols are related to their acidity, and neutralization by oral ammonia tends to mitigate these effects.

- (6) Exposure to H<sub>2</sub>SO<sub>4</sub> at concentrations as low as 100 μg/m<sup>3</sup> for 60 min alters mucociliary clearance.
- (7) Airway reactivity increases in healthy and asthmatic subjects following exposure to 1,000 μg/m<sup>3</sup> H<sub>2</sub>SO<sub>4</sub> for 16 min.
- (8) Differences in estimated respiratory intake explain only a portion of the differences in responses among studies.

In the five years since the publication of the *Acid Aerosol Issue Paper*, several of these summary statements have been further confirmed. For example, recent studies confirm the absence of spirometric effects following acute exposure to H<sub>2</sub>SO<sub>4</sub> and other acid aerosols in healthy subjects, at or below 1,000 μg/m<sup>3</sup>. The observation of effects on adolescent asthmatics at levels as low as 68 μg/m<sup>3</sup> has not been confirmed, and studies utilizing longer exposures have raised further questions about the relationship between dosimetry and health effects. However, additional evidence supports the conclusion that lung function effects in asthmatic subjects are related to hydrogen ion exposure, which is in part determined by the degree of neutralization by oral ammonia. Two recent studies examining sequential exposure to H<sub>2</sub>SO<sub>4</sub> and ozone (Linn et al., 1994; Frampton et al., 1995) suggest that acid aerosols may potentiate the response to ozone in some asthmatic subjects. Finally, clinical studies of acid aerosols have been expanded to include endpoints associated with fiberoptic bronchoscopy and BAL.

Table 11-2 summarizes, in alphabetical order by author, controlled human exposure studies of particle exposure published since 1988. The majority of the human clinical studies have focused on the pulmonary function effects of exposure to acid aerosols. These studies are therefore summarized separately below, first reviewing studies of effects on healthy subjects, followed by subjects with asthma. Subsequent sections deal with effects other than lung function, and with studies of particulate pollutants other than acid aerosols.

#### **11.2.1.2 Pulmonary Function Effects of Sulfuric Acid in Healthy Subjects**

Since 1988, ten studies have examined the effects of H<sub>2</sub>SO<sub>4</sub> exposure on pulmonary function in healthy subjects. Exposure levels ranged from 100 μg/m<sup>3</sup> to 2,000 μg/m<sup>3</sup>, with exposure durations ranging from 16 min to 6.5 h on two successive days. All of these studies confirmed the findings from previous studies of an absence of spirometric effects on

**TABLE 11-2. CONTROLLED HUMAN EXPOSURES TO ACID AEROSOLS AND OTHER PARTICLES**

Ref.	Subjects	Exposures <sup>1</sup>	MMAD <sup>2</sup> ( $\mu\text{m}$ )	GSD <sup>3</sup> ( $\mu\text{m}$ )	Duration	Exercise	Temp (°C)	RH <sup>4</sup> (%)	Symptoms	Lung Function	Other Effects	Comments
Anderson et al. (1992)	15 healthy 15 asthmatic 18 to 45 years	(1): air (2): H <sub>2</sub> SO <sub>4</sub> $\approx$ 100 $\mu\text{g}/\text{m}^3$ (3): carbon black $\approx$ 200 $\mu\text{g}/\text{m}^3$ (4): acid-coated carbon with $\approx$ 100 $\mu\text{g}/\text{m}^3$ H <sub>2</sub> SO <sub>4</sub>	1.0	2	1 h	$\dot{V}_E \approx$ 50 L/min	22	50	Healthy subjects more symptomatic in air.	Largest decrements in FVC with air exposure.	No change in airway responsiveness	Smoking status of subjects not stated.
Aris et al. (1990)	19 asthmatic 20 to 40 years	Mouthpiece study: HMSA <sup>5</sup> 0 to 1000 $\mu\text{M}$ + H <sub>2</sub> SO <sub>4</sub> 6.1 50 $\mu\text{M}$ vs H <sub>2</sub> SO <sub>4</sub> 50 $\mu\text{M}$ Chamber study: HMSA 1 Mm + H <sub>2</sub> SO <sub>4</sub> 5 Mm vs H <sub>2</sub> SO <sub>4</sub> 5 Mm	$\approx$ 7		3 min. 1 h	100 W on cycle	$\approx$ 25	100	HMSA did not increase symptoms in comparison with H <sub>2</sub> SO <sub>4</sub> alone.	No effects on SRaw <sup>6</sup>		
Aris et al. (1991a)	10 healthy nonsmokers 21 to 31 years ozone sensitive	HNO <sub>3</sub> 500 $\mu\text{g}/\text{m}^3$ or H <sub>2</sub> O, or air followed by ozone 0.2 ppm	$\approx$ 6		2 h 3 h	50 min of each h 40 L/min	22	100	No effects of fog exposure	No direct effects of fog exposures. Greatest decrements when ozone preceded by air.	No change in airway responsiveness	Fog may have reduced ozone effects on lung function.
Aris et al. (1991b)	18 asthmatics 23 to 37 years	Mouthpiece study: H <sub>2</sub> SO <sub>4</sub> vs NaCl, $\approx$ 3000 $\mu\text{g}/\text{m}^3$ with varying particle size, osmolarity, relative humidity  Chamber study: H <sub>2</sub> SO <sub>4</sub> vs NaCl, 960 to 1400 $\mu\text{g}/\text{m}^3$ with varying water content	0.4 vs $\approx$ 6  6		16 min 1 h	With and without exercise. 100 W on cycle	$\approx$ 24	<10 vs 100	No effects	Increases in Sraw with low RH conditions; no pollutant-related effects		Postulated that effects seen in other studies due to secretions or effects on larynx

**TABLE 11-2 (cont'd). CONTROLLED HUMAN EXPOSURES TO ACID AEROSOLS AND OTHER PARTICLES**

Ref.	Subjects	Exposures <sup>1</sup>	MMAD <sup>2</sup> ( $\mu\text{m}$ )	GSD <sup>3</sup> ( $\mu\text{m}$ )	Duration	Exercise	Temp (°C)	RH <sup>4</sup> (%)	Symptoms	Lung Function	Other Effects	Comments
Avol et al. (1988a)	21 healthy 21 asthmatic 18 to 45 years	Air H <sub>2</sub> SO <sub>4</sub> : Healthy: 363, 1128, 1578 $\mu\text{g}/\text{m}^3$ Asthmatic: 396, 999, 1,460 $\mu\text{g}/\text{m}^3$	0.85 to 0.91	2.4 to 2.5	1 h	10 min $\times$ 3 47 to 49 L/min	21	50	Healthy: Slight increase in cough with highest concentrations.  Asthma: dose-related increase in lower resp. symptoms.	Healthy: No effects on lung function or airway reactivity.  Asthma: $\downarrow$ FEV <sub>1</sub> 0.26 L with H <sub>2</sub> SO <sub>4</sub> 1,460 $\mu\text{g}/\text{m}^3$		
Avol et al. (1988b)	22 healthy 22 asthmatic 18 to 45 years	H <sub>2</sub> O H <sub>2</sub> SO <sub>4</sub> : Healthy: 647, 1,100, 2,193 $\mu\text{g}/\text{m}^3$ Asthmatic: 516, 1,085, 2,034 $\mu\text{g}/\text{m}^3$	9.7 to 10.7		1 h	10 min $\times$ 3 41 to 46 L/min	9	100	Dose-related increase in lower resp. symp. in both groups.	Healthy: No effects on lung function.  Asthma: $\downarrow$ peak flow 16% at 2,034 $\mu\text{g}/\text{m}^3$ H <sub>2</sub> SO <sub>4</sub> .	No effects on airway responsiveness	Half the subjects received acidic gargle; no difference in effects.
Avol et al. (1990)	32 asthmatics 8 to 16 years	Air H <sub>2</sub> SO <sub>4</sub> 46, 127, and 134 $\mu\text{g}/\text{m}^3$	0.5	1.9	40 min	30 min rest, 10 min exercise 20L/min/m <sup>2</sup>	21	48	No pollutant effect	No pollutant effect. One subject increased Sraw 14.2% with acid exposure.		Did not reproduce findings of Koenig et al., 1983.
Balmes et al. (1988)	12 asthmatics responsive to hyposmolar saline aerosol 25 to 41 years	Mouthpiece, 5,900 to 87,100 $\mu\text{m}^3$ : NaCl 30 mOsm H <sub>2</sub> SO <sub>4</sub> 30 mOsm HNO <sub>3</sub> 30 mOsm H <sub>2</sub> SO <sub>4</sub> +HNO <sub>3</sub> 30 mOsm H <sub>2</sub> SO <sub>4</sub> 300 mOsm	$\approx$ 5 to 6	1.5		At rest	$\approx$ 23			Concentration of acid aerosol required to increase Sraw by 100% lower than for NaCl. No difference between acid species.		Exposures did not mimic environmental conditions. No mitigation by oral ammonia.
Culp et al. (1995)	16 healthy 20 to 39 yrs	NaCl 1000 $\mu\text{g}/\text{m}^3$ H <sub>2</sub> SO <sub>4</sub> 1,000 $\mu\text{g}/\text{m}^3$	0.9	1.9	2 h	10 min $\times$ 4 $\approx$ 40 L/min	22	40			Mucins from bronchoscopy: no effects on mucin recovery or changes in glycoproteins	

**TABLE 11-2 (cont'd). CONTROLLED HUMAN EXPOSURES TO ACID AEROSOLS AND OTHER PARTICLES**

Ref.	Subjects	Exposures <sup>1</sup>	MMAD <sup>2</sup> ( $\mu\text{m}$ )	GSD <sup>3</sup> ( $\mu\text{m}$ )	Duration	Exercise	Temp (°C)	RH <sup>4</sup> (%)	Symptoms	Lung Function	Other Effects	Comments
Fine et al. (1987b)	8 asthmatics 22 to 29 yrs	Mouthpiece: Buffered and unbuffered HCl and H <sub>2</sub> SO <sub>4</sub> at varying pH	5.3 to 6.2	1.6 to 1.8	3 min.	At rest			Cough with inhalation of unbuffered pH 2 aerosols	≈50% increase in airway resistance with buffered acid aerosols at pH 2. Little response to unbuffered acids.		Titrateable acidity important determinant of response to acid aerosols.
Fine et al. (1987a)	10 asthmatics 22 to 34 yrs	Mouthpiece: Na <sub>2</sub> SO <sub>3</sub> 0 to 10 mg/ml, pH 9, 6.6, 4; buffered acetic acid pH 4; SO <sub>2</sub> 0.25 to 8 ppm	5.6 to 6.1	1.6 to 1.7	1 min.	At rest				For Na <sub>2</sub> SO <sub>3</sub> , bronchoconstriction greater at lower pH; no response to acetic acid.		Suggests effects related to release of SO <sub>2</sub> or bisulfite, but not sulfite.
Frampton et al. (1992)	12 healthy 20 to 39 yrs	NaCl 1,000 $\mu\text{g}/\text{m}^3$ H <sub>2</sub> SO <sub>4</sub> 1,000 $\mu\text{g}/\text{m}^3$	0.9	1.9	2 h	10 min × 4 ≈40 L/min	22	40	4/12 subjects: throat irritation with acid exposure.	No pollutant effects	BAL findings: No effects on cell recovery, lymphocyte subsets, AM function, fluid proteins.	
Frampton et al. (1995)	30 healthy 30 asthmatics 20 to 42 yrs	NaCl or H <sub>2</sub> SO <sub>4</sub> 100 $\mu\text{g}/\text{m}^3$ followed by ozone 0.08, 0.12, or 0.18 ppm	0.45 0.64	4.05 2.50	3 h  3 h	10 min × 6. Healthy: 33 to 40 L/min; asthmatics: 31 to 36 L/min	21	40	No pollutant effects	Healthy subjects: no significant effects.  Asthmatics: ozone dose-response following H <sub>2</sub> SO <sub>4</sub> pre-exposure, but not NaCl		
Hanley et al. (1992)	22 asthmatics 12 to 19 yrs	Mouthpiece: (1): Air; H <sub>2</sub> SO <sub>4</sub> 70, 130 $\mu\text{g}/\text{m}^3$ (2): Air; H <sub>2</sub> SO <sub>4</sub> 70 $\mu\text{g}/\text{m}^3$ with and without lemonade	0.72	1.5	40 min. 45 min.	10 min 30 min ≈30 L/min	22	65	No effects	Significant decreases in FEV <sub>1</sub> (≈37 ml/ $\mu\text{mol}$ H <sup>+</sup> ) and FVC at 2 to 3 min but not 20 min after exposure.	Significant correlation between baseline airways responsiveness and $\Delta\text{FEV}_{1}/\text{H}^+$ (R <sup>2</sup> =0.3).	Large variability in oral NH <sub>3</sub> levels.

**TABLE 11-2 (cont'd). CONTROLLED HUMAN EXPOSURES TO ACID AEROSOLS AND OTHER PARTICLES**

Ref.	Subjects	Exposures <sup>1</sup>	MMAD <sup>2</sup> ( $\mu\text{m}$ )	GSD <sup>3</sup> ( $\mu\text{m}$ )	Duration	Exercise	Temp (°C)	RH <sup>4</sup> (%)	Symptoms	Lung Function	Other Effects	Comments
Koenig et al. (1989)	9 asthmatics with exercise-induced bronchospasm 12 to 18 yrs	Mouthpiece: Air; $\text{H}_2\text{SO}_4$ 68 $\mu\text{g}/\text{m}^3$ ; $\text{SO}_2$ 0.1 ppm; $\text{H}_2\text{SO}_4+\text{SO}_2$ ; $\text{HNO}_3$ 0.05 ppm	0.6	1.5	40 min	10 min	25	65	No effects	$\downarrow$ FEV <sub>1</sub> 6% after $\text{H}_2\text{SO}_4$ compared with 2% after air.		
Koenig et al. (1992)	14 asthmatics with exercise-induced bronchospasm 13 to 18 yrs	Mouthpiece: Air; $\text{H}_2\text{SO}_4$ 35 or 70 $\mu\text{g}/\text{m}^3$	0.6	1.5	45 or 90 min	$\approx$ 23 L/min	22	65		$\downarrow$ FEV <sub>1</sub> 6% after $\text{H}_2\text{SO}_4$ 35 $\mu\text{g}/\text{m}^3$ for 45 min, 3% after 70 $\mu\text{g}/\text{m}^3$ (NS). Smaller changes after 90 min exposures.		Responses unrelated to $\text{C}\times\text{T}\times\dot{V}_E$
Koenig et al. (1993)	8 healthy 9 asthmatic 60 to 76 yrs	Mouthpiece: Air; $(\text{NH}_4)_2\text{SO}_4 \approx 70 \mu\text{g}/\text{m}^3$ ; $\text{H}_2\text{SO}_4 \approx 74$ to 82 $\mu\text{g}/\text{m}^3$ with and without lemonade	0.6	1.5	40 min	10 min 17.5 L/min for asthmatics, 19.7 for healthy	22	65		No significant effects. Correlation between increase in resistance and oral ammonia levels in asthmatics ( $R^2 = 0.575$ ).		
Koenig et al. (1994)	28 asthmatics 12 to 19 yrs	Mouthpiece: Air; ozone 0.12 ppm+ $\text{NO}_2$ 0.3 ppm; 0.6 ozone 0.12 ppm+ $\text{NO}_2$ 0.3 ppm+ $\text{H}_2\text{SO}_4$ 68 $\mu\text{g}/\text{m}^3$ ; ozone 0.12 ppm+ $\text{NO}_2$ 0.3 ppm+ $\text{HNO}_3$ 0.05 ppm		1.5	90 min $\times$ 2 days	$\dot{V}_E$ 3 $\times$ resting	22	65	No pollutant effects	No pollutant effects	No effects on airway responsiveness	6 subjects with moderate or severe asthma did not complete protocol
Laube et al. (1993)	7 healthy 20 to 31 yrs	Head dome: $\text{NaCl} \approx 500 \mu\text{g}/\text{m}^3$ $\text{H}_2\text{SO}_4 \approx 500 \mu\text{g}/\text{m}^3$	10.3 10.9		1 h	20 min	22 to 25	99	No pollutant effects	No pollutant effects	Tracheal clearance increased (4/4 subjects). Outer zone clearance increased (6/7 subjects). No effects on airway responsiveness	

**TABLE 11-2 (cont'd). CONTROLLED HUMAN EXPOSURES TO ACID AEROSOLS AND OTHER PARTICLES**

Ref.	Subjects	Exposures <sup>1</sup>	MMAD <sup>2</sup> ( $\mu\text{m}$ )	GSD <sup>3</sup> ( $\mu\text{m}$ )	Duration	Exercise	Temp (°C)	RH <sup>4</sup> (%)	Symptoms	Lung Function	Other Effects	Comments
Linn et al. (1989)	22 healthy 19 asthmatic 18 to 48 yrs	H <sub>2</sub> O H <sub>2</sub> SO <sub>4</sub> $\approx$ 2,000 $\mu\text{g}/\text{m}^3$	20 10 1		1 h	40 to 45 L/min	$\approx$ 10	74 to 100	Increased total score with larger acid particles.	No pollutant effects	No effects on airway reactivity	4 asthmatic subjects unable to complete exposures because of symptoms.
Linn et al. (1994)	15 healthy 30 asthmatic 18 to 50 yrs	Air; ozone 0.12 ppm; H <sub>2</sub> SO <sub>4</sub> 100 $\mu\text{g}/\text{m}^3$ ; ozone+H <sub>2</sub> SO <sub>4</sub>	$\approx$ 0.5	$\sim$ 2	6.5 h/d $\times$ 2d	50 min $\times$ 6 29 L/min	21	50	Symptoms unrelated to atmosphere	$\downarrow$ FEV <sub>1</sub> & FVC in ozone, similar for healthy & asthmatic subjects. Greater fall in FEV <sub>1</sub> for acid+ozone than ozone alone, marginally significant interaction.	Increased airway responsiveness with ozone, marginal further increase with ozone+acid	Average subject lost 100 ml FEV <sub>1</sub> with ozone, 189 ml with ozone+acid  Original findings replicated in 13 subjects
Morrow et al. (1994)	17 asthmatic 20 to 57 yrs 17 COPD 52 to 70 yrs	NaCl $\approx$ 100 $\mu\text{g}/\text{m}^3$ H <sub>2</sub> SO <sub>4</sub> $\approx$ 90 $\mu\text{g}/\text{m}^3$			2 h	Asthmatics: 10 min $\times$ 4 COPD: 7 min $\times$ 1	21	30	No pollutant effects.	Asthmatics: $\downarrow$ FEV <sub>1</sub> slightly greater after acid than after NaCl. COPD: No effects.		
Utell et al. (1989)	15 asthmatic 19 to 50 yrs	Mouthpiece: NaCl 350 $\mu\text{g}/\text{m}^3$ ; H <sub>2</sub> SO <sub>4</sub> 350 $\mu\text{g}/\text{m}^3$ , high NH <sub>3</sub> ; H <sub>2</sub> SO <sub>4</sub> , low NH <sub>3</sub>	0.80	1.7	30 min	10 min V <sub>E</sub> 3 $\times$ resting		20 to 25		Greater fall in FEV <sub>1</sub> with low NH <sub>3</sub> (19%) than with high NH <sub>3</sub> (8%).		

<sup>1</sup>Exposures in environmental chamber unless otherwise stated.

<sup>2</sup>Mass median aerodynamic diameter. In some studies expressed as volume median diameter; see text.

<sup>3</sup>Geometric standard deviation.

<sup>4</sup>Relative humidity.

<sup>5</sup>Hydroxymethanesulfonic acid.

<sup>6</sup>Specific airways resistance.

BAL=Bronchoalveolar lavage.

AM=Alveolar macrophage.

healthy subjects. Exposures at the highest concentrations (i.e. 1,000  $\mu\text{g}/\text{m}^3$  or greater) were associated with mild increases in respiratory symptoms (cough, substernal discomfort, throat irritation), especially those exposures with particle sizes in the 10 to 20  $\mu\text{m}$  range.

Two studies reported by Avol and colleagues (Avol et al., 1988a,b) examined effects of 1-h  $\text{H}_2\text{SO}_4$  aerosol exposures in an environmental chamber. In the first study (Avol et al., 1988b), 22 healthy nonsmoking subjects between the ages of 18 and 45 years, some reporting allergies, were exposed for 1 h to large particle aerosols (volume median diameter (VMD) 9.7 to 10.3  $\mu\text{m}$ , GSD not stated) consisting of  $\text{H}_2\text{O}$  (control) or  $\text{H}_2\text{SO}_4$  at 647, 1,100, and 2,193  $\mu\text{g}/\text{m}^3$ . Three 10-min periods of moderate exercise (46 L/min) were included. All subjects were exposed to each atmosphere, separated by one week. Half the subjects received an acidic gargle to reduce oral ammonia levels prior to exposure; no difference in effects was observed with or without the gargle, so data were combined in the analysis. Healthy subjects experienced a slight concentration-related increase in lower respiratory symptoms (cough, sputum, dyspnea, wheeze, chest tightness, substernal irritation), but no effect was found on spirometry or on airway reactivity to methacholine measured 1 h after exposure.

A second study (Avol et al., 1988a) essentially duplicated this protocol for  $\text{H}_2\text{SO}_4$  aerosols with a smaller particle size (MMAD = 0.85 to 0.91  $\mu\text{m}$ , geometric standard deviation [GSD = 2.4 to 2.5]). Twenty-one healthy subjects, 12 with allergies by skin testing, were exposed on separate occasions to air and  $\text{H}_2\text{SO}_4$  aerosol at each of three concentrations: 363, 1128, 1578  $\mu\text{g}/\text{m}^3$ . A slight increase in cough was found at the two highest concentrations of  $\text{H}_2\text{SO}_4$ , but no effects were found on spirometry, specific airway resistance (Sraw), or airway reactivity to methacholine.

Linn et al. (1989) examined the effects of droplet size on 22 healthy subjects exposed to nominally 2,000  $\mu\text{g}/\text{m}^3$   $\text{H}_2\text{SO}_4$  for 1 h, with three, 10-min exercise periods. Distilled  $\text{H}_2\text{O}$  was used for control aerosols. Aerosol VMDs were 1, 10, and 20  $\mu\text{m}$ . Actual exposure concentrations were 1,496, 2,170, and 2,503  $\mu\text{g}/\text{m}^3$ . Results were similar to the previous fog studies by this group, with no significant effects on lung function or airway reactivity to methacholine. Total symptom scores were increased with exposure to 10  $\mu\text{m}$  and 20  $\mu\text{m}$   $\text{H}_2\text{SO}_4$  particles, but not to 1  $\mu\text{m}$ .

Frampton et al. (1992) exposed 12 healthy nonsmokers to aerosols of NaCl (control) or H<sub>2</sub>SO<sub>4</sub> (MMAD = 0.9 μm, GSD = 1.9) at 1,175 μg/m<sup>3</sup> for 2 h in an environmental chamber. Four 10-min exercise periods at  $\dot{V}_E$  of ≈40 L/min were included. Subjects brushed their teeth and rinsed with mouthwash prior to and once during each exposure to reduce oral ammonia levels. Mild throat irritation was described by 4 of 12 subjects after acid exposure and 3 of 12 subjects after NaCl exposure. No effects on lung function were found.

Five other recent studies (Anderson et al., 1992; Koenig et al., 1993; Laube et al., 1993; Linn et al., 1994; Frampton et al., 1995) have included healthy subjects in exposures to H<sub>2</sub>SO<sub>4</sub> aerosols at levels below 1000 μg/m<sup>3</sup>; none have shown meaningful effects on lung function. Anderson et al., (1992) studied the responses of 15 healthy subjects exposed for 1 h in a chamber to air, 100 μg/m<sup>3</sup> H<sub>2</sub>SO<sub>4</sub>, 200 μg/m<sup>3</sup> carbon black, and carbon black coated with H<sub>2</sub>SO<sub>4</sub>, (MMAD ≈ 1 μm). Lemonade or citrus juice gargles were used to reduce oral ammonia levels. Exposures containing acid were without effects on symptoms, lung function, or airway reactivity. Healthy subjects were actually more symptomatic and demonstrated greater increases in Sraw after air than after pollutant exposure, contrary to expectation. In a study designed to examine effects of acid fog on pulmonary clearance, Laube et al., (1993) exposed seven healthy volunteers to NaCl or H<sub>2</sub>SO<sub>4</sub> at 470 μg/m<sup>3</sup>, MMAD ≈ 11 μm, for 1 h with 20 min of exercise. Acid exposure did not alter symptoms or lung function. Two chamber studies designed to examine the effects of combined or sequential exposure to acid aerosols and ozone found no direct effects of exposure to ≈100 μg/m<sup>3</sup> H<sub>2</sub>SO<sub>4</sub> on lung function of healthy subjects, using exposure durations of 3 h (Frampton et al., 1995) or 6.5 h for two successive days (Linn et al., 1994). Both studies included exercise and acidic mouthwash to minimize oral ammonia. Also of particular interest, Koenig et al, (1993) studied eight elderly subjects age 60 to 76 years exposed to air, H<sub>2</sub>SO<sub>4</sub>, or ammonium sulfate at approximately 82 μg/m<sup>3</sup> H<sub>2</sub>SO<sub>4</sub> for 40 min, delivered by mouthpiece. No effects were found on spirometry or total respiratory resistance.

Thus, for young healthy adults, brief exposures to H<sub>2</sub>SO<sub>4</sub> at mass concentrations more than an order of magnitude above ambient levels do not alter lung function. Some subjects report increased lower respiratory symptoms, including cough, at 1000 μg/m<sup>3</sup> and higher

levels, particularly with larger particle sizes ( $> 5 \mu\text{m}$ ). One small study suggests that the elderly do not demonstrate decrements in lung function at low  $\text{H}_2\text{SO}_4$  exposure levels of (approximately  $82 \mu\text{g}/\text{m}^3$ ). There are no data on the responses to particle exposure for healthy adolescents or children.

### 11.2.1.3 Pulmonary Function Effects of Sulfuric Acid in Asthmatic Subjects

Individuals with asthma often experience bronchoconstriction in response to a variety of stimuli, including exercise, cold dry air, or exposure to strong odors, smoke, and dusts. Considerable individual variability exists in the nature of stimuli that provoke a response, and in the degree of responsiveness. Thus, for clinical studies involving asthmatic subjects, subject selection and sample size deserve particular consideration. Differences among subjects may explain, in part, the widely differing results between laboratories studying effects of acid aerosols. For example, in some studies described below, asthmatic subjects were specifically selected to have exercise-induced bronchoconstriction (Koenig et al., 1989, 1992, 1994; Hanley et al., 1992), or responsiveness to hypo-osmolar aerosols (Balmes et al., 1988). The interval for withholding medications prior to exposure differed among various laboratories and different studies. In addition, the severity of asthma differed among studies; severity is often difficult to compare because published information describing clinical severity and baseline lung function is often incomplete. Table 11-3 lists the characteristics of asthmatic subjects exposed to acid aerosols and other particles.

Several studies have suggested that asthmatics are more sensitive than healthy subjects to effects of acid aerosols on lung function. Utell et al., (1982) found significant decrements in specific airway conductance (SGaw) in asthmatic subjects exposed by mouthpiece for 16 min to 450 and 1,000  $\mu\text{g}/\text{m}^3$   $\text{H}_2\text{SO}_4$  (MMAD 0.5 to 1.0  $\mu\text{m}$ ). Moreover, exposure to neutralization products of  $\text{H}_2\text{SO}_4$  produced smaller decrements in function, roughly in proportion to their acidity ( $\text{H}_2\text{SO}_4 > \text{NH}_4\text{HSO}_4 > \text{NaHSO}_4$ ).

The role of  $\text{H}^+$  in the responsiveness of asthmatics to acid aerosols was explored by Fine et al. (1987b), who found that titratable acidity and chemical composition, rather than pH alone, are key determinants of response in asthmatics. Eight asthmatic subjects were challenged by mouthpiece for 3 min at rest, with buffered or unbuffered hydrochloric acid (HCl) or  $\text{H}_2\text{SO}_4$  at varying pH levels, and changes in SRaw were measured. Solutions were

**TABLE 11-3. ASTHMA SEVERITY IN STUDIES OF ACID AEROSOLS AND OTHER PARTICLES**

Ref.	Subject # (F/M)	Age Range (mean)	Exposures <sup>1</sup>	Allergies	Medications	FEV <sub>1</sub> (% pred.)	FEV <sub>1</sub> /FVC (%)	Airway Responsiveness	Exercise/ $\dot{V}_E$
Anderson et al. (1992)	15 (6/9)	19 to 45 years (29)	(1): Air (2): H <sub>2</sub> SO <sub>4</sub> $\approx$ 100 $\mu$ g/m <sup>3</sup> (3): carbon black $\approx$ 200 $\mu$ g/m <sup>3</sup> (4): acid-coated carbon	Not stated	Not stated	Not stated	69 $\pm$ 14 (SD)	Methacholine: PD <sub>20</sub> $\leq$ 56 "breath-units"	Intermittent at $\approx$ 50 L/min
Aris et al. (1990)	19 (8/11)	20 to 40 years	Mouthpiece study: HMSA 0 to 1,000 mM + H <sub>2</sub> SO <sub>4</sub> 50 mM vs H <sub>2</sub> SO <sub>4</sub> 50 mM Chamber study: HMSA 1 mM + H <sub>2</sub> SO <sub>4</sub> 5 mM vs H <sub>2</sub> SO <sub>4</sub> 5 mM	Not stated	All but one on albuterol. 3 on inhaled steroids. No meds 24 h before study.	82 $\pm$ 20 (SD)	Not stated	Methacholine: All responded to <2 mg/ml	Intermittent, 100 W on cycle ergometer
Aris et al. (1991b)	18	23 to 37 years	Mouthpiece study: H <sub>2</sub> SO <sub>4</sub> vs NaCl to test changes in particle size, osmolarity (30 to 300 mOsm), relative humidity Chamber study: H <sub>2</sub> SO <sub>4</sub> vs NaCl with varying water content	Not stated	Most subjects on albuterol. Several on inhaled steroids. No meds 24 h before study.	79 $\pm$ 23 (SD)	Not stated	Methacholine: All responded to <1 mg/ml	Mouthpiece study: with and without exercise.  Chamber study: intermittent exercise at 100 W on cycle ergometer.
Avol et al. (1988a)	21 (9/12)	18 to 45 years (30)	Air H <sub>2</sub> SO <sub>4</sub> 396, 999, 1,460 $\mu$ g/m <sup>3</sup>	Positive skin tests in 20	11 on no regular meds; 10 on regular meds. 3 unable to hold meds prior to exposure.	Not stated	73 $\pm$ 14 (SD)	Hyperresponsive by methacholine challenge, not further specified	10 min $\times$ 3 47 to 49 L/min
Avol et al. (1988b)	22 (9/13)	18 to 45 years (26)	H <sub>2</sub> O H <sub>2</sub> SO <sub>4</sub> 516, 1,085, 2,034 $\mu$ g/m <sup>3</sup>	Positive skin tests in 18	"Majority had mild extrinsic disease". 9 on regular meds.	Not stated	45 to 98	Methacholine: PD <sub>20</sub> $\leq$ 295 "dose units"	10 min $\times$ 3 41 to 46 L/min

**TABLE 11-3 (cont'd). ASTHMA SEVERITY IN STUDIES OF ACID AEROSOLS AND OTHER PARTICLES**

Ref.	Subject # (F/M)	Age Range (mean)	Exposures <sup>1</sup>	Allergies	Medications	FEV <sub>1</sub> (% pred.)	FEV <sub>1</sub> / FVC (%)	Airway Responsiveness	Exercise/ $\dot{V}_E$
Avol et al. (1990)	32 (12/20)	8 to 16 years	Air H <sub>2</sub> SO <sub>4</sub> 46, 127, and 134 $\mu\text{g}/\text{m}^3$	All had history of allergy	18 on regular meds, 2 on no meds, rest intermittent. None on steroids.	Less than 70 in 25 subjects	Not stated	Hyperresponsive by exercise, cold air, or methacholine.	30 min rest, 10 min exercise 20L/min/m <sup>2</sup>
Balmes et al. (1988)	12 (6/6)	25 to 41 years	Mouthpiece, doubling outputs, 5,900 to 87,100 $\mu\text{g}/\text{m}^3$ : NaCl 30 mOsm H <sub>2</sub> SO <sub>4</sub> 30 mOsm HNO <sub>3</sub> 30 mOsm H <sub>2</sub> SO <sub>4</sub> +HNO <sub>3</sub> 30 mOsm H <sub>2</sub> SO <sub>4</sub> 300 mOsm	Not stated	All on inhaled meds, 3 on inhaled steroids. No meds 24 h before study.	94±15 (SD)	61 to 89	Responsive to hypoosmolar saline aerosol, methacholine <2 mg/ml.	At rest
Fine et al. (1987b)	8 (6/2)	22 to 29 years	Mouthpiece: Buffered and unbuffered HCl and H <sub>2</sub> SO <sub>4</sub> at varying pH	Not stated	6 on inhaled meds and/or theophylline, no steroids. No meds 12 h before study.	41 to 108	74±11 (SD)	Methacholine: All responded to <3 mg/ml.	At rest
Fine et al. (1987a)	10 (5/5)	22 to 34 years (26.7)	Mouthpiece: Na <sub>2</sub> SO <sub>3</sub> 0 to 10,000 $\mu\text{g}/\text{ml}$ , pH 9, 6.6, 4; buffered acetic acid pH 4; SO <sub>2</sub> 0.25 to 8 ppm	Not stated	7 on inhaled meds, no steroids. No meds 12 h before study.	Not stated	Not stated	9 subjects had bronchoconstrict- ion and greater response to aerosol with lower pH. Response to NaSO <sub>3</sub> aerosols may be due to release of SO <sub>2</sub> gas in bisulfite ions.	At rest
Frampton et al. (1995)	30 (20/10)	20 to 42 years	NaCl or H <sub>2</sub> SO <sub>4</sub> 100 $\mu\text{g}/\text{m}^3$ followed by ozone 0.08, 0.12, or 0.18 ppm	All had positive skin tests. † IgE in 10.	All on intermittent or daily bronchodilators. None on steroids. Meds held 24 h before study.	81±4 (SE)	75±2 (SE)	Positive carbamol challenge if normal spirometry	10 min × 6 for each exposure

**TABLE 11-3 (cont'd). ASTHMA SEVERITY IN STUDIES OF ACID AEROSOLS AND OTHER PARTICLES**

Ref.	Subject # (F/M)	Age Range (mean)	Exposures <sup>1</sup>	Allergies	Medications	FEV <sub>1</sub> (% pred.)	FEV <sub>1</sub> / FVC(%)	Airway Responsiveness	Exercise/ $\dot{V}_E$
Hanley et al. (1992)	22 (7/15)	12 to 19 years	Mouthpiece: (1): Air or H <sub>2</sub> SO <sub>4</sub> 70, 130 $\mu\text{g}/\text{m}^3$ (2): Air or H <sub>2</sub> SO <sub>4</sub> 70 $\mu\text{g}/\text{m}^3$ , with and without lemonade	"All had allergic asthma". ↑ IgE in 8.	All but 2 on meds, no steroids. No meds 4 h before study.	Not stated	Not stated	Methacholine: PD <sub>20</sub> 0.25 to 25 mg/ml; not available for 3 subjects. 18 were responsive to exercise by treadmill test	(1): 10 min (2): 30 min ≈30 L./min
Koenig et al. (1989)	9 (3/6)	12 to 18 years	Mouthpiece: Air H <sub>2</sub> SO <sub>4</sub> 68 $\mu\text{g}/\text{m}^3$ SO <sub>2</sub> 0.1 ppm H <sub>2</sub> SO <sub>4</sub> +SO <sub>2</sub> HNO <sub>3</sub> 0.05 ppm	5 "allergic asthma"	Not stated	Not stated	Not stated	Methacholine: All responded to <20 mg/ml. All had ↓FEV <sub>1</sub> >15% with treadmill test	"Moderate", on treadmill for 10 min
Koenig et al. (1992)	14 (5/9)	13 to 18 years	Mouthpiece: Air H <sub>2</sub> SO <sub>4</sub> 35 or 70 $\mu\text{g}/\text{m}^3$	"Allergic asthma"	Not stated	Not stated	Not stated	Methacholine: PD <sub>20</sub> 0.25 to 25 mg/ml; not available for 1 subject; 8 had pos. treadmill tests, 4 history of exercise responsiveness, 2 did not meet stated criteria for exercise responsiveness.	Intermittent ≈23 L/min
Koenig et al. (1993)	9 (7/2)	60 to 76 years	Mouthpiece: (1): Air (2): (NH <sub>4</sub> ) <sub>2</sub> SO <sub>4</sub> ≈70 $\mu\text{g}/\text{m}^3$ (3&4): H <sub>2</sub> SO <sub>4</sub> ≈74 $\mu\text{g}/\text{m}^3$ with and without lemonade	Not stated	All on "bronchodilator and/or anti- inflammatory treatment". Steroids not specified.	75	Not stated	Methacholine: PD <sub>20</sub> ≤ 10 mg/ml	10 min 17.5 L/min

**TABLE 11-3 (cont'd). ASTHMA SEVERITY IN STUDIES OF ACID AEROSOLS AND OTHER PARTICLES**

Ref.	Subject # (F/M)	Age Range (mean)	Exposures <sup>1</sup>	Allergies	Medications	FEV <sub>1</sub> (% pred.)	FEV <sub>1</sub> / FVC (%)	Airway Responsiveness	Exercise/ $\dot{V}_E$
Koenig et al. (1994)	28 (9/19)	12 to 19 years	Mouthpiece: (1): Air (2): ozone 0.12 ppm +NO <sub>2</sub> 0.3 ppm (3): ozone 0.12 ppm+NO <sub>2</sub> 0.3 ppm+H <sub>2</sub> SO <sub>4</sub> 68 μg/m <sup>3</sup> (4): ozone 0.12 ppm +NO <sub>2</sub> 0.3 ppm +HNO <sub>3</sub> 0.05 ppm	"Personal history of allergic asthma"	3 on no meds, rest on regular meds. 4 on inhaled steroids.	87	Not stated	Methacholine: PD <sub>20</sub> <25 mg/ml. All but 1 responsive to exercise by treadmill test.	Intermittent $\dot{V}_E$ 3 × resting
Linn et al. (1989)	19 (13/6)	18 to 48 years (29)	H <sub>2</sub> O H <sub>2</sub> SO <sub>4</sub> ≈ 2,000 μg/m <sup>3</sup>	"Some" subjects had history of allergy	All on bronchodilators at least weekly. No regular steroid use. No meds 12 h before study.	Not stated	70±11 (SD)	Hyperresponsive- ness based on methacholine PD <sub>20</sub> <38 "breath units", exercise responsiveness, or bronchodilator response.	Intermittent 40 to 45 L/min
Linn et al. (1994)	30 (17/13)	18 to 50 years (30)	(1): Air (2): ozone 0.12 ppm (3): H <sub>2</sub> SO <sub>4</sub> 100 μg/m <sup>3</sup> (4): ozone+H <sub>2</sub> SO <sub>4</sub>	Some subjects had positive skin tests.	Wide range of medication usage. Some on inhaled steroids. No meds 4 h before study.	Not stated	72	Responsive to methacholine or exercise, or bronchodilator response	50 min × 6 29 L/min
Morrow et al. (1994)	17	20 to 57 years (35)	NaCl ≈ 100 μg/m <sup>3</sup> H <sub>2</sub> SO <sub>4</sub> ≈ 90 μg/m <sup>3</sup>	Positive skin tests	Requirement for bronchodilators	Not stated	65±8 (SD)	Positive carbachol challenge if normal spirometry	10 min × 4

**TABLE 11-3 (cont'd). ASTHMA SEVERITY IN STUDIES OF ACID AEROSOLS AND OTHER PARTICLES**

Ref.	Subject # (F/M)	Age Range (mean)	Exposures <sup>1</sup>	Allergies	Medications	FEV <sub>1</sub> (% pred.)	FEV <sub>1</sub> /FVC (%)	Airway Responsiveness	Exercise/ $\dot{V}_E$
Utell et al. (1989)	15	19 to 50 years	Mouthpiece: (1): NaCl 350 $\mu\text{g}/\text{m}^3$ (2): H <sub>2</sub> SO <sub>4</sub> 350 $\mu\text{g}/\text{m}^3$ high NH <sub>3</sub> (3): H <sub>2</sub> SO <sub>4</sub> low NH <sub>3</sub>	Not stated	All on intermittent or daily bronchodilators. None on steroids. Meds held 24 h before study.	88±4 (SE)	70±3 (SE)	Positive carbachol challenge if normal spirometry	10 min $\dot{V}_E$ 3 × resting
Yang and Yang (1994)	25 (15/10)	23 to 48 years	Mouthpiece: Bagged polluted air, TSP = 202 $\mu\text{g}/\text{m}^3$	All $\uparrow$ IgE	No steroids. Holding of medications not stated.	Not stated	Not stated	Hyperresponsive to methacholine	Rest

<sup>1</sup>Exposures in environmental chamber unless otherwise stated.

buffered with glycine, which, by itself, was found to have no direct effect on lung function. Aerosol MMAD ranged from 5.3 to 6.2  $\mu\text{m}$  (GSD 1.6 to 1.8), simulating acid fogs. There was no group response to unbuffered acid, even at pH 2. However, SRaw increased in seven of eight subjects after inhalation of  $\text{H}_2\text{SO}_4$  and glycine at pH 2, suggesting that titratable acidity or available  $\text{H}^+$ , rather than pH, plays a role in mediating acid fog-induced bronchoconstriction. Nevertheless, the response occurred at  $\text{H}_2\text{SO}_4$  concentrations estimated in excess of 10,000  $\mu\text{g}/\text{m}^3$ , more than an order of magnitude higher than the concentration producing a response in the study of Utell et al. (1982).

Fine et al. (1987a) further examined the role of pH in sulfite-induced bronchoconstriction in asthmatics. Ten subjects with asthma were challenged with increasing concentrations of sodium sulfite ( $\text{Na}_2\text{SO}_3$ ) at three different pH levels. Challenge with buffered acetic acid aerosols at pH 4 was used to control for the airway effects of acid aerosols. Subjects also inhaled increasing concentrations of  $\text{SO}_2$  gas during eucapneic hyperpnea. Exposures consisted of 1 min of tidal breathing on a mouthpiece at rest. Particle MMAD ranged from 5.6 to 6.1  $\mu\text{m}$ . Nine of ten subjects experienced bronchoconstriction with  $\text{Na}_2\text{SO}_3$ , with greater responses to aerosols made from solutions with lower pH. No response was seen following acetic acid. The authors concluded that bronchoconstriction in response to  $\text{Na}_2\text{SO}_3$  aerosols may be caused by the release of  $\text{SO}_2$  gas or by bisulfite ions, but not by sulfite ions and not merely by alterations of airway pH. These studies of Fine et al., as pointed out by the authors, addressed potential mechanisms for bronchoconstriction in response to acidic sulfates, but did not attempt to mimic the effects of environmental exposures.

Hypo-osmolar aerosols can induce bronchoconstriction in some asthmatics. To test the effects of varying osmolarity of acidic aerosols, Balmes et al. (1988) administered aerosols of  $\text{NaCl}$ ,  $\text{H}_2\text{SO}_4$ ,  $\text{HNO}_3$ , or  $\text{H}_2\text{SO}_4 + \text{HNO}_3$  to 12 asthmatic subjects via mouthpiece. All solutions were prepared at an osmolarity of 30 mOsm, and delivered at doubling concentrations until SRaw increased by 100%. An additional series of challenges with  $\text{H}_2\text{SO}_4$  at 300 mOsm was performed. The 12 subjects were selected from a group of 17 asthmatics on the basis of responsiveness to challenge with hypo-osmolar saline aerosol. Aerosol particle size was similar to coastal fogs, with MMAD ranging from 5.3 to 6.1. Delivered nebulizer output during exposure was quite high, ranging from 5,900 to

approximately  $87,000 \mu\text{g}/\text{m}^3$ . All hypo-osmolar aerosols caused bronchoconstriction. Lower concentrations of hypo-osmolar acidic aerosols were required to induce bronchoconstriction than with NaCl, and there was no difference between acidic species. No bronchoconstriction occurred with isosmolar  $\text{H}_2\text{SO}_4$ , even at maximum nebulizer output (estimated  $\text{H}_2\text{SO}_4$  concentration greater than  $40,000 \mu\text{g}/\text{m}^3$ ). The authors concluded that acidity can potentiate bronchoconstriction caused by hypo-osmolar aerosols. As in the studies of Fine et al. (1987a,b), these exposures did not mimic environmental conditions.

Koenig and colleagues have studied the responses of adolescents with allergic asthma to  $\text{H}_2\text{SO}_4$  aerosols with particle sizes in the respirable range, and concentrations only slightly above peak, worst-case ambient levels. In one study (Koenig et al., 1983), ten adolescents were exposed to  $110 \mu\text{g}/\text{m}^3 \text{H}_2\text{SO}_4$  (MMAD =  $0.6 \mu\text{m}$ ) by mouthpiece for a total of 40 min, 30 min at rest followed by 10 min of exercise. The FEV<sub>1</sub> decreased 8% after exposure to  $\text{H}_2\text{SO}_4$ , and 3% after a similar exposure to NaCl, a statistically significant difference. In another study (Koenig et al., 1989), nine allergic adolescents were exposed to  $68 \mu\text{g}/\text{m}^3 \text{H}_2\text{SO}_4$  (MMAD =  $0.6 \mu\text{m}$ ) for 30 min at rest followed by 10 min of exercise ( $\dot{V}_E = 32 \text{ L}/\text{min}$ ). Although only five subjects were described as having "allergic asthma", all subjects had exercise-induced bronchoconstriction; thus all subjects were asthmatic by generally accepted criteria (Sheffer, 1991). Effects were compared with similar exposures to air, 0.1 ppm  $\text{SO}_2$ ,  $68 \mu\text{g}/\text{m}^3 \text{H}_2\text{SO}_4 + 0.1 \text{ ppm } \text{SO}_2$ , and 0.05 ppm  $\text{HNO}_3$ . The FEV<sub>1</sub> decreased 6% after exposure to  $\text{H}_2\text{SO}_4$  alone, and 4% after exposure to  $\text{H}_2\text{SO}_4 + \text{SO}_2$ , compared to a 2% decrease after air. Increases in total respiratory resistance were not significant. These results were presented as preliminary findings, in that a total of 15 subjects were to be studied; formal statistical comparison of  $\text{H}_2\text{SO}_4$  versus air was not presented. Findings from the full group of 15 subjects have not been published. These studies suggest that allergic asthmatics with exercise-induced bronchoconstriction may be more sensitive to effects of  $\text{H}_2\text{SO}_4$  than adult asthmatics, and that small changes in lung function may be observed at exposure levels below  $100 \mu\text{g}/\text{m}^3$ .

Two studies reported by Avol et al. (1988a,b) examined effects of  $\text{H}_2\text{SO}_4$  aerosols and fogs on asthmatic subjects. The results for healthy subjects in these studies were described in Section 11.2.1.2. In the first study, 21 adult asthmatics, 20 of whom had positive skin tests to common allergens, were exposed to air or 396, 999, and  $1,460 \mu\text{g}/\text{m}^3 \text{H}_2\text{SO}_4$

(MMAD 0.85 to 0.91  $\mu\text{m}$ ) for one hour with intermittent exercise. The asthmatic subjects experienced concentration-related increases in lower respiratory symptoms (most notably, cough), with some persistence of symptoms at 24 h. The FEV<sub>1</sub> decreased by a mean of 0.26 L after exposure to 999  $\mu\text{g}/\text{m}^3$ , and 0.28 L after exposure to 1,460  $\mu\text{g}/\text{m}^3$ . Results using analysis of variance (ANOVA) were significant for concentration effects on change in FEV<sub>1</sub> and FVC. However, decrements at 396  $\mu\text{g}/\text{m}^3$  were identical to those seen with air exposure. The SRaw approximately doubled following exposure to both air and 396  $\mu\text{g}/\text{m}^3$  H<sub>2</sub>SO<sub>4</sub>, and approximately tripled following exposure to 999 and 1,460  $\mu\text{g}/\text{m}^3$ . Although absolute change in SRaw related to concentration was not significant, percent change in SRaw was not analyzed as was done for FEV<sub>1</sub> and FVC; ANOVA of percent change for each of these measures may have proved more sensitive. These findings are similar to those of Utell, et al. (1983b), who found significant effects on SGaw following exposure to 450 and 1,000  $\mu\text{g}/\text{m}^3$ , and significant effects on FEV<sub>1</sub> at 1,000  $\mu\text{g}/\text{m}^3$  (MMAD = 0.8  $\mu\text{m}$ ). However, exposures in the Utell study were performed at rest for a considerably shorter duration (16 minutes).

The second study (Avol et al., 1988b) utilized an identical protocol to examine effects of a large particle aerosol (MMAD = 10  $\mu\text{m}$ ). Twenty-two asthmatic subjects were exposed to fogs containing 516, 1,085 and 2,034  $\mu\text{g}/\text{m}^3$  H<sub>2</sub>SO<sub>4</sub>, compared with H<sub>2</sub>O. Although concentration-related increases in respiratory symptoms were similar to those in the study of submicron aerosols, no significant effects were found on FEV<sub>1</sub>, FVC, or SRaw, even at the highest concentration of greater than 2,000  $\mu\text{g}/\text{m}^3$ . The findings from these two studies suggest that aerosols of submicron particle size may alter lung function to a greater degree than large particle aerosols in asthmatic subjects. Deep breaths of air containing acid aerosol would often provoke cough. However, the concentrations required to produce an effect (> 5000  $\mu\text{g}/\text{m}^3$ ) differ strikingly from the studies of adolescent asthmatics of Koenig and colleagues (1983, 1989).

Linn et al. (1989) utilized a similar exposure protocol to specifically examine effects of particle size. Nineteen asthmatic adults were exposed for 1 h to a pure water aerosol or approximately 2,000  $\mu\text{g}/\text{m}^3$  H<sub>2</sub>SO<sub>4</sub> at 3 different droplet sizes: 1, 10, and 20  $\mu\text{m}$ . Subjects exercised for 3 10-min periods at  $\dot{V}_E$  of 40 to 45 L/min. Grapefruit juice gargles were used to minimize oral ammonia. As in previous studies by this group, symptoms increased in acid

atmospheres with larger particles. Four of the 19 asthmatic subjects were unable to complete one or more exposures because of respiratory symptoms. All but one of the aborted exposures was in an acid aerosol-containing atmosphere: three subjects did not complete the 1  $\mu\text{m}$  acid exposure, one the 10  $\mu\text{m}$  exposure, and three the 20  $\mu\text{m}$  exposure. The authors reported significant decrements in lung function in these subjects, requiring administration of a bronchodilator. As stated by the authors, "the patterns of these appreciable clinical responses by asthmatics suggests a causal relationship to acid exposure, without obvious dependence on droplet size". These more dramatic responses to acid aerosols are not reflected in the mean responses, and suggest the existence of a few particularly susceptible individuals. Mean responses of FEV<sub>1</sub> to acid aerosol exposure were about -21%, with responses to exercise in clean air of about -12%. Some subjects experienced decreases in FEV<sub>1</sub> in excess of 50%, as a result of combined exercise and acid aerosol exposure. Analysis of variance found significant effects of acid  $\times$  time on SRaw and FEV<sub>1</sub>. There was no apparent effect of droplet size.

Utell et al. (1989) examined the influence of oral ammonia levels on responses to H<sub>2</sub>SO<sub>4</sub>. Fifteen subjects with mild asthma inhaled H<sub>2</sub>SO<sub>4</sub> aerosols (350  $\mu\text{g}/\text{m}^3$ , MMAD = 0.8  $\mu\text{m}$ ) via mouthpiece for 20 min at rest followed by 10 min of exercise. Sodium chloride aerosol served as control. Low oral ammonia levels were achieved using a lemon juice gargle and toothbrushing prior to exposure, and high levels were achieved by eliminating oral hygiene and food intake for 12 h prior to exposure. These procedures achieved a five-fold difference in oral ammonia levels. The FEV<sub>1</sub> decreased 19% with low ammonia versus 8% with high ammonia (p<0.001). The FEV<sub>1</sub> also decreased 8% with NaCl aerosol. These findings extended the authors' previous findings (Utell et al., 1983b) of decrements in SGaw following exposure to 450  $\mu\text{g}/\text{m}^3$  H<sub>2</sub>SO<sub>4</sub>, and demonstrated the importance of oral ammonia in mitigating the clinical effects of submicron H<sub>2</sub>SO<sub>4</sub> aerosols.

The findings of Koenig et al. (1989) in adolescent asthmatics prompted an attempt by Avol and colleagues (1990) to replicate the study using a larger group of subjects. Thirty-two subjects with mild asthma, aged 8 to 16 years, were exposed to 46 and 127  $\mu\text{g}/\text{m}^3$  H<sub>2</sub>SO<sub>4</sub> (MMAD  $\approx$  0.5  $\mu\text{m}$ ) for 30 min at rest followed by 10 min of exercise at 20 L/min/m<sup>2</sup> body surface area. Subjects gargled citrus juice prior to exposure to reduce oral ammonia. Bronchoconstriction occurred after exercise in all atmospheres, with no statistically

significant difference between clean air and acid exposures at any concentration. Because these exposures were undertaken in an environmental chamber with unencumbered oral/nasal breathing, in contrast to mouthpiece exposure in the Koenig et al. studies (1983, 1989), a subsequent study was performed to examine the effects of oral breathing only. Twenty-one of these subjects were therefore exposed to  $134 \mu\text{g}/\text{m}^3 \text{H}_2\text{SO}_4$  while breathing chamber air through an open mouthpiece. Again, no acid effect was found. One subject who was "unusually susceptible to exercise-induced bronchospasm" also showed the largest decrements in lung function with both exposures to the highest acid concentrations. It is possible that the subjects in the Koenig et al. (1989) study, all of whom demonstrated exercise-induced bronchoconstriction during a specific exercise challenge test, represented a more responsive subgroup of adolescent asthmatics. Only 15 of the 32 subjects in the Avol et al. (1990) study were known to have exercise-induced bronchoconstriction. Indeed, subsequent data (Hanley et al., 1992) suggest exercise responsiveness is predictive of  $\text{H}_2\text{SO}_4$  responsiveness (see below).

Aris et al. (1990) examined the effects of hydroxymethanesulfonic acid (HMSA), which has been identified as a component of west coast acidic fogs. They postulated that HMSA might cause bronchoconstriction in asthmatics because, at the pH of airway lining fluid, it dissociates into  $\text{CH}_2\text{O}$  and  $\text{SO}_2$ . In the first part of the study, nine asthmatics were serially challenged by mouthpiece with 0, 30, 100, 300 and 1,000  $\mu\text{M}$  HMSA in 50  $\mu\text{M}$   $\text{H}_2\text{SO}_4$  (MMAD = 6.1  $\mu\text{m}$ ). The SRaw was measured after each challenge. These findings were compared on a separate day to a similar series of exposures to 50  $\mu\text{M}$   $\text{H}_2\text{SO}_4$  alone. No effect was found for HMSA on symptoms or airways resistance. An environmental chamber exposure study was then performed in which 10 asthmatic subjects were exposed to 1 mM HMSA + 5 mM  $\text{H}_2\text{SO}_4$  for 1 h with intermittent exercise. The control was exposure to 5 mM  $\text{H}_2\text{SO}_4$  alone. Three subjects underwent additional exposures to NaCl aerosol. Particle MMAD was approximately 7  $\mu\text{m}$ . Both acid exposures slightly increased respiratory symptoms, but no significant effects on SRaw were found.

In a subsequent series of studies, Aris et al. (1991b) examined the effects of varying particle size, osmolarity, and relative humidity on airways resistance in response to  $\text{H}_2\text{SO}_4$  aerosol. To study effects of particle size and osmolarity, 11 asthmatics inhaled five different aerosols for 16 min by mouthpiece at rest: (1)  $\text{H}_2\text{SO}_4$  at 300 mOsm (VMD approximately 6  $\mu\text{m}$ ); (2)  $\text{H}_2\text{SO}_4$  30 mOsm (VMD approximately

6  $\mu\text{m}$ ); (3) sodium chloride 30 mOsm (VMD approximately 6  $\mu\text{m}$ ); (4)  $\text{H}_2\text{SO}_4$  (VMD approximately 0.4  $\mu\text{m}$ ); and (5)  $\text{H}_2\text{SO}_4$ , (VMD approximately 0.4  $\mu\text{m}$ ). Sulfuric acid concentrations were high, at approximately 3000  $\mu\text{g}/\text{m}^3$ . Airway resistance actually decreased slightly with all aerosol exposures and there were no significant effects on respiratory symptoms.

In a second mouthpiece study, nine subjects were exposed at rest (part 1) to  $\text{H}_2\text{SO}_4$  at approximately 3000  $\mu\text{g}/\text{m}^3$ , with large (VMD  $\approx$  6  $\mu\text{m}$ ) versus small (0.3  $\mu\text{m}$ ) particle size and low (< 10%) versus high (100%) relative humidity. Sodium chloride aerosols under similar conditions served as control. Because these exposures caused no decrements in SRaw, six subjects underwent exposures to small particle, low humidity  $\text{H}_2\text{SO}_4$  versus sodium chloride while exercising at 40 L/min (part 2). Although SRaw increased significantly with exercise, there was no difference between  $\text{H}_2\text{SO}_4$  and sodium chloride exposures. These results are shown in Figure 11-1. A significant increase in throat irritation was observed with the low humidity, small particle  $\text{H}_2\text{SO}_4$  inhalation in part 1 of this study (n=9) but was not replicated in part 2 (n=6).

Finally, an environmental chamber exposure study was undertaken to examine effects of  $\text{H}_2\text{SO}_4$  fogs (VMD approximately 6  $\mu\text{m}$ ) with varying water content on airways resistance. Ten subjects were exposed for 1 h with intermittent exercise to  $\text{H}_2\text{SO}_4$  and NaCl at low (0.5  $\mu\text{g}/\text{m}^3$ ) and high (1.8  $\mu\text{g}/\text{m}^3$ ) liquid water content. The mean sulfate concentrations were 960  $\mu\text{g}/\text{m}^3$  for low water content fogs and 1,400  $\mu\text{g}/\text{m}^3$  for high liquid water content fog. Surprisingly, SRaw decreased slightly with most exposures, with no significant difference among the 4 atmospheres. The authors speculated that the decrements in pulmonary function following exposure to acid aerosols in previous studies may have been due to increases in airway secretions or effects on the larynx rather than bronchoconstriction.

Responsiveness of adolescent asthmatic subjects to  $\text{H}_2\text{SO}_4$  aerosols was further explored by Hanley et al. (1992). Fourteen allergic asthmatics aged 12 to 19 years inhaled air or  $\text{H}_2\text{SO}_4$  at targeted concentrations of 70 and 130  $\mu\text{g}/\text{m}^3$ , for 30 min at rest and 10 min with exercise. In a second protocol, nine subjects were exposed to targeted concentrations of 70  $\mu\text{g}/\text{m}^3$   $\text{H}_2\text{SO}_4$ , with and without drinking lemonade to reduce oral ammonia. Actual exposure concentrations ranged from 51 to 176  $\mu\text{g}/\text{m}^3$   $\text{H}_2\text{SO}_4$ . Exposures lasted 45 min, including two 15-min exercise periods. Aerosol MMAD was 0.72  $\mu\text{m}$ . For the purposes of

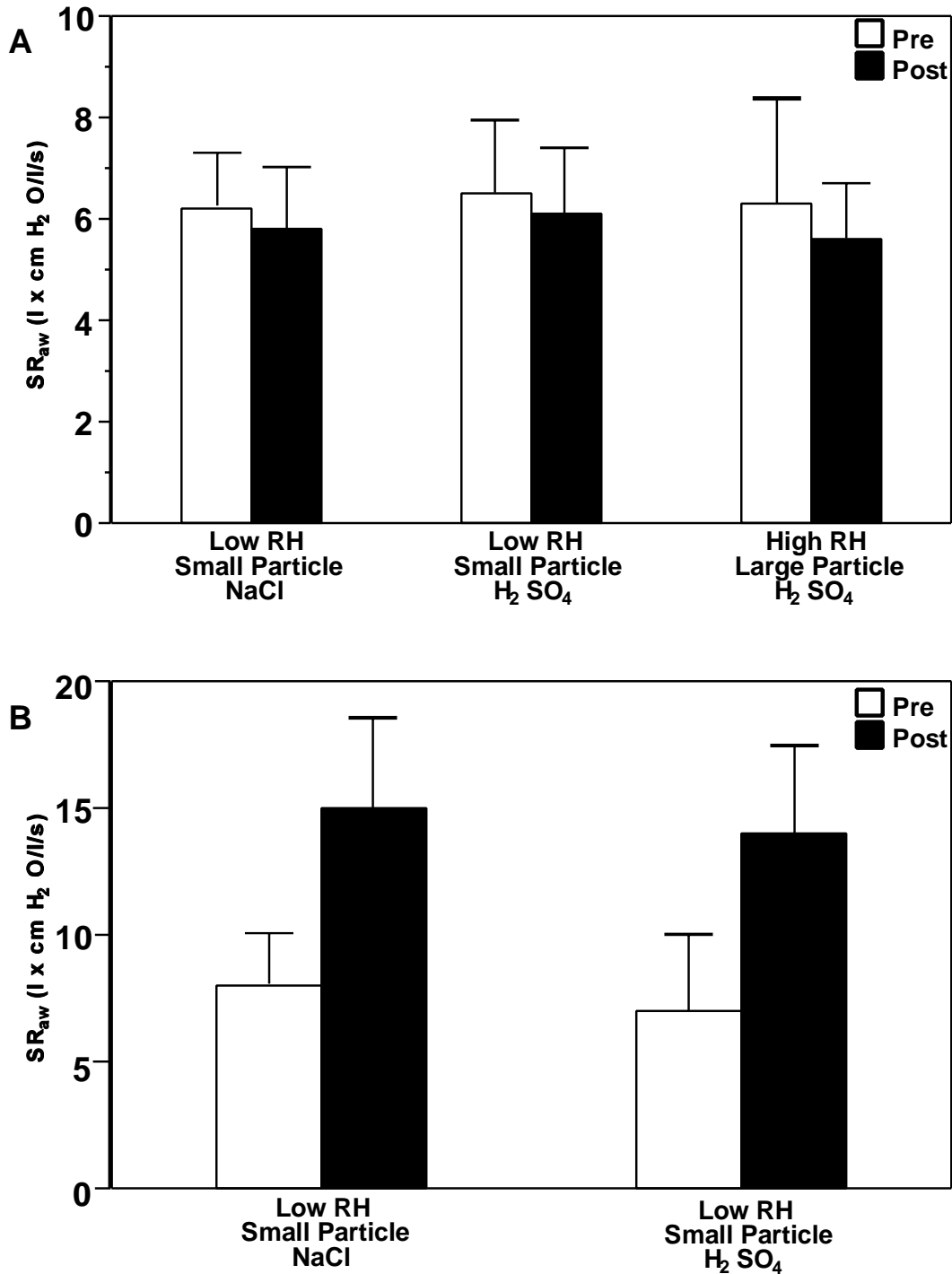


**Figure 11-1.** Mean plus or minus standard error of the mean specific airway resistance ( $SR_{aw}$ ) before and after a 16-min exposure for (A) nine subjects who inhaled low relative-humidity (RH) sodium chloride (NaCl), low-RH sulfuric acid ( $H_2SO_4$ ), and high-RH  $H_2SO_4$  aerosols at rest, and (B) six subjects who inhaled low-RH NaCl and low-RH  $H_2SO_4$  aerosols during exercise.

Source: Aris et al. (1991b).

this document, mean changes in FEV<sub>1</sub> were calculated from individual subject data provided in the published report. In the first protocol, FEV<sub>1</sub> fell 0.05 ± 0.08 L after air and 0.15 ± 0.14 L after nominal 70 μg/m<sup>3</sup> H<sub>2</sub>SO<sub>4</sub>. In the second protocol, FEV<sub>1</sub> fell 0.00 ± 0.23 L without lemonade gargle and 0.13 ± 0.09 L with lemonade gargle. Results from the 22 subjects exposed in the two protocols were combined for the published analyses, and changes in pulmonary function were regressed against H<sup>+</sup> concentration for each subject. Decrements in FEV<sub>1</sub> and FVC were statistically significant at 2 to 3 min after exposure, but not at 20 min after exposure. Changes in Vmax<sub>50</sub> and total respiratory resistance were not significantly different. The findings corresponded to a fall in FEV<sub>1</sub> of approximately 37 ml/μM H<sup>+</sup>. A significant correlation was found between exercise-induced bronchoconstriction, determined prior to exposure using a treadmill test, and the slope of Δ FEV<sub>1</sub>/H<sup>+</sup>. A similar observation linking baseline airways reactivity to H<sub>2</sub>SO<sub>4</sub> responsiveness had been made previously by Utell et al. (1983b).

Koenig et al. (1992) examined the effects of more prolonged mouthpiece exposures to H<sub>2</sub>SO<sub>4</sub> (MMAD = 0.6 μm). Fourteen allergic asthmatic subjects aged 13 to 18, with exercise-induced bronchoconstriction, were exposed to air or 35 and 70 μg/m<sup>3</sup> H<sub>2</sub>SO<sub>4</sub>, for 45 min and 90 min, on separate occasions. Oral ammonia was reduced by drinking lemonade. The exposures included alternate 15-min periods of exercise at three times resting  $\dot{V}_E$ . The largest decrements in FEV<sub>1</sub> (6%) actually occurred with the shorter exposure to the lower concentration of H<sub>2</sub>SO<sub>4</sub> (35 μg/m<sup>3</sup>). Changes following exposure to 70 μg/m<sup>3</sup> and following 90 min exposures were not significant. The authors concluded that duration of exposure did not play a role in the response to H<sub>2</sub>SO<sub>4</sub> aerosols. However, the absence of a concentration response in the studies suggests that the statistical findings may be due to chance. Therefore, the study does not appear to demonstrate a convincing effect of H<sub>2</sub>SO<sub>4</sub> at these exposure levels.

Anderson et al. (1992) included 15 asthmatic adults in a study comparing the effects of exposure for 1 h to air, 100 μg/m<sup>3</sup> H<sub>2</sub>SO<sub>4</sub>, 200 μg/m<sup>3</sup> carbon black particles, and acid-coated carbon black (MMAD ≈ 1.0 μm). Decrements in FEV<sub>1</sub> were observed for all exposures, averaging about 9%. Analysis of variance for FVC showed a significant interaction of acid, carbon, and time factors (p = 0.02), but the largest decrements actually occurred with air exposure.

In the only study of elderly asthmatics, Koenig et al. (1993) exposed nine subjects, 60 to 76 years of age, by mouthpiece to air,  $(\text{NH}_4)_2\text{SO}_4$ , or  $70 \mu\text{g}/\text{m}^3 \text{H}_2\text{SO}_4$  (MMAD =  $0.6 \mu\text{m}$ ), with and without lemonade gargle. Exposures were 30 min at rest followed by 10 min of mild exercise ( $\dot{V}_E = 17.5 \text{ L}/\text{min}$ ). Greater increases in total respiratory resistance occurred following  $\text{H}_2\text{SO}_4$  without lemonade than following the other atmospheres, but the difference between atmospheres was not significant.

In a study comparing effects of  $\text{H}_2\text{SO}_4$  exposure in subjects with asthma and COPD, Morrow et al. (1994) exposed 17 allergic asthmatic subjects in an environmental chamber to  $90 \mu\text{g}/\text{m}^3 \text{H}_2\text{SO}_4$  or NaCl (MMAD <  $1 \mu\text{m}$ ) for 2 h with intermittent exercise. Pulmonary function was measured after each of four 10 min exercise periods, and again 24 h after exposure, before and after exercise. Decrements in  $\text{FEV}_1$  were consistently greater in  $\text{H}_2\text{SO}_4$  than NaCl, although the difference was statistically significant only following the second exercise period.  $\text{FEV}_1$  decreased  $\approx 18\%$  after  $\text{H}_2\text{SO}_4$  compared with  $\approx 14\%$  after NaCl ( $p = 0.02$ ). Reductions in SGaw were significantly different only following the fourth exercise period ( $p = 0.009$ ). No changes were found in symptoms or arterial oxygen saturation, and there were no significant changes in lung function 24 h after exposure.

Finally, two recent studies have examined combined exposures to  $\text{H}_2\text{SO}_4$  and ozone, one using a combined pollutant atmosphere for 6 h per day over 2 days, (Linn et al., 1994) and the other using sequential 3 h exposures to  $\text{H}_2\text{SO}_4$  followed 1 day later by ozone (Frampton et al., 1995). These reports will be discussed in detail in section 11.2.1.7. However, neither study found any significant changes in lung function in asthmatics exposed to  $100 \mu\text{g}/\text{m}^3 \text{H}_2\text{SO}_4$  alone.

In summary, asthmatic subjects appear to be more sensitive than healthy subjects to the effects of acid aerosols on lung function, but the effective concentrations differ widely among laboratories. Although the reasons for these differences remain largely unclear, subject selection and differences in neutralization of acid by  $\text{NH}_3$  may be important factors. Adolescent asthmatics may be more sensitive than adults, and may experience small decrements in lung function in response to acid aerosols at exposure levels only slightly above peak ambient levels. Even in studies reporting an overall absence of effects on lung function, some individual asthmatic subjects appear to demonstrate clinically important effects. Submicron aerosols appear to have greater effects on spirometry and airway

resistance than particles in the  $10\mu\text{-}20\ \mu\text{m}$  range. However, respiratory symptoms (cough, irritation, etc.) are observed with both large and small aerosols.

#### **11.2.1.4 Effects of Acid Aerosols on Airway Responsiveness**

Human airways may undergo bronchoconstriction in response to a variety of stimuli. Airway responsiveness can be quantitated by measuring changes in expiratory flow or airways resistance in response to inhalation challenge. Typically, the challenging agent is a non-specific pharmacologic bronchoconstrictor such as methacholine or histamine. Other agents include carbamylcholine (carbachol), cold dry air, sulfur dioxide, hypo-osmolar aerosols, or exercise. In allergic subjects, airway challenge with specific allergens can be performed, although the responses are variable, and late phase reactions can result in bronchoconstriction beginning 4 to 8 h after challenge and lasting 24 h or more. Although many individuals with airway hyperresponsiveness do not have asthma, virtually all asthmatics have airway hyperresponsiveness, possibly reflecting underlying airway inflammation. Changes in clinical status are often accompanied by changes in airway responsiveness. Thus alterations in airway responsiveness may be clinically significant, even in the absence of direct effects on lung function (Godfrey, 1993; Weiss et al., 1993). Molfino et al. (1992) have provided a brief review of air pollution effects on allergic bronchial responsiveness.

As noted in section 11.2.1.3, two studies (Utell et al., 1983b; Hanley et al., 1992) have suggested that the degree of baseline airway responsiveness may predict responsiveness to acid aerosol exposure in asthmatic subjects. This section will deal only with studies examining changes in airway responsiveness with exposure to particles.

Despite the absence of effects on lung function in healthy subjects, Utell et al. (1983a) observed, in healthy nonsmokers, an increase in airway responsiveness to carbachol following exposure to  $450\ \mu\text{g}/\text{m}^3\ \text{H}_2\text{SO}_4$  (MMAD = 0.8). The increase occurred 24 h, but not immediately, after exposure. In addition, some subjects reported throat irritation between 12 and 24 h after exposure to  $\text{H}_2\text{SO}_4$ . These findings suggested the possibility of delayed effects. These investigators also observed increases in airway responsiveness among asthmatic subjects following exposure to 450 and  $1000\ \mu\text{g}/\text{m}^3$ , but not  $100\ \mu\text{g}/\text{m}^3\ \text{H}_2\text{SO}_4$ . These findings have been reviewed (Utell et al., 1991).

Avol et al. (1988a,b) included airway responsiveness as an outcome measure in their studies of healthy and asthmatic subjects exposed to varying concentrations of H<sub>2</sub>SO<sub>4</sub>. No effects on responsiveness were reported, with either acidic fogs or submicron aerosols, at H<sub>2</sub>SO<sub>4</sub> concentrations as high as 2000 μg/m<sup>3</sup>. However, airway challenge was performed using only two concentrations of methacholine. This limited challenge may have been insufficiently sensitive to detect small changes in airway responsiveness.

Using a similar 2-dose methacholine challenge protocol, Linn et al. (1989) found no change in airway responsiveness of healthy subjects following exposure to 2000 μg/m<sup>3</sup> H<sub>2</sub>SO<sub>4</sub> for 1 h, at particle sizes ranging from 1 to 20 μm. Anderson et al. (1992), in their study of responses to 100 μg/m<sup>3</sup> H<sub>2</sub>SO<sub>4</sub>, 200 μg/m<sup>3</sup> carbon black, and acid coated carbon, found no effects on airway responsiveness in healthy or asthmatic subjects. In this study, a conventional methacholine challenge was used, administering doubling increases in methacholine concentration until FEV<sub>1</sub> decreased more than 20%.

In a study primarily designed to examine effects of acid fog exposure on mucociliary clearance, Laube et al. (1993) examined changes in airway responsiveness to methacholine in 7 asthmatic subjects exposed to 500 μg/m<sup>3</sup> H<sub>2</sub>SO<sub>4</sub> or NaCl (MMAD ≈ 10 μm) for 1 h with 20 min of exercise. Responsiveness was measured at screening and 30 min after each exposure. No difference was observed between H<sub>2</sub>SO<sub>4</sub> and NaCl exposures.

A recent study (Linn et al., 1994) has suggested that exposure to ozone with H<sub>2</sub>SO<sub>4</sub> may enhance the increase in airway responsiveness seen with ozone exposure alone. Fifteen healthy and 30 asthmatic subjects were exposed to air, 0.12 ppm ozone, 100 μg/m<sup>3</sup> H<sub>2</sub>SO<sub>4</sub> (MMAD ≈ 0.5), and ozone + H<sub>2</sub>SO<sub>4</sub> for 6.5 h on 2 successive days, with intermittent exercise. Airway responsiveness was measured after each exposure day using a conventional methacholine incremental challenge, and compared with baseline measured on a separate day. An ANOVA using data from all subjects found an increase in airway responsiveness in association with ozone exposure (p=0.003), but showed no significant change following exposure to air or H<sub>2</sub>SO<sub>4</sub> alone. Multiple comparisons did not reveal significant differences in airway responsiveness between ozone and ozone + H<sub>2</sub>SO<sub>4</sub> in healthy or asthmatic subjects. However, asthmatic subjects showed the greatest increase in airway responsiveness following the first day of ozone + H<sub>2</sub>SO<sub>4</sub>, and ANOVA revealed a significant interaction of clinical status, ozone, acid, and day (p=0.03). Decreases in FEV<sub>1</sub> following methacholine

challenge for healthy subjects were 8% after air, 6% after H<sub>2</sub>SO<sub>4</sub>, 9% after ozone, and 13% after ozone + H<sub>2</sub>SO<sub>4</sub>. Changes were smaller following the second exposure day, suggesting attenuation of responsiveness with repeated exposure, as seen in previous studies of ozone alone (U.S. Environmental Protection Agency, 1995). These studies suggest that exposure to low concentrations of H<sub>2</sub>SO<sub>4</sub> may enhance ozone-induced increases in airway responsiveness in both healthy and asthmatic subjects.

Koenig et al. (1994) sought to determine whether exposure to H<sub>2</sub>SO<sub>4</sub> or HNO<sub>3</sub> enhanced changes in lung function or airway responsiveness seen with exposure to ozone + nitrogen dioxide (NO<sub>2</sub>). Adolescent asthmatic subjects were exposed to air, 0.12 ppm ozone + 0.3 ppm NO<sub>2</sub>, ozone + NO<sub>2</sub> + 73 μg/m<sup>3</sup> H<sub>2</sub>SO<sub>4</sub> (MMAD = 0.6), and ozone + NO<sub>2</sub> + 0.05 ppm HNO<sub>3</sub>. Exposures were by mouthpiece for 90 min, with intermittent exercise, on two consecutive days. Airway responsiveness was measured by methacholine challenge at screening and on the day following the second pollutant exposure. No effects on airway responsiveness were found for any atmosphere. However, challenge following pollutant exposure utilized only doses of methacholine well below the level causing significant reductions in FEV<sub>1</sub> for these subjects at baseline, making it unlikely that small or transient changes in responsiveness would be detected. Six subjects did not complete the protocol because of illness, symptoms, and other factors which may or may not have been related to pollutant exposure; these data were not included in the analysis.

In summary, the data suggest that there is little, if any, effect of low concentration acid aerosol exposure (regardless of particle size) on airway responsiveness in healthy or asthmatic subjects. Observations of possible delayed increases in responsiveness in healthy subjects exposed to 450 μg/m<sup>3</sup> H<sub>2</sub>SO<sub>4</sub> (Utell et al., 1983a), and H<sub>2</sub>SO<sub>4</sub> enhancement of ozone effects on airway responsiveness in healthy and asthmatic subjects (Linn et al., 1994) require confirmation in additional studies, utilizing standard challenge protocols.

#### **11.2.1.5 Effects of Acid Aerosols on Lung Clearance Mechanisms**

Brief (1- to 2-h) exposures to H<sub>2</sub>SO<sub>4</sub> aerosols have shown consistent effects on mucociliary clearance in three species: donkeys, rabbits, and humans. The direction and magnitude of the effect are dependent on the concentration and duration of the acid aerosol

exposure, the size of the acid particle, and the size of the tracer particle. Clearance studies in animals are discussed in Section 11.2.2.5.

Initial studies in healthy nonsmokers by Leikauf et al. (1981) found that exposure to  $110 \mu\text{g}/\text{m}^3 \text{H}_2\text{SO}_4$  (MMAD  $\approx 0.5 \mu\text{m}$ ) for 1 h at rest accelerated bronchial mucociliary clearance of  $7.5 \mu\text{m}$  tracer particles, while a similar exposure to  $980 \mu\text{g}/\text{m}^3 \text{H}_2\text{SO}_4$  slowed clearance. A second study (Leikauf et al., 1984) utilizing a smaller tracer particle ( $4.2 \mu\text{m}$ ) to assess more peripheral airways, found slowing of clearance with both  $108$  and  $983 \mu\text{g}/\text{m}^3 \text{H}_2\text{SO}_4$ , in comparison with distilled water aerosol. Spektor et al. (1989) extended these studies, exposing ten healthy subjects to  $\text{H}_2\text{SO}_4$  (MMAD =  $0.5 \mu\text{m}$ ) or distilled water aerosols for up to 2 h. Two different  $4.2 \mu\text{m}$  tracer aerosols were used, one administered before and the other after exposure. Following a 2 h exposure to  $100 \mu\text{g}/\text{m}^3 \text{H}_2\text{SO}_4$ , clearance halftime tripled compared with control, with reduced clearance rates still evident 3 h after exposure. These findings suggested that brief, resting exposures to  $\text{H}_2\text{SO}_4$  at  $\approx 100 \mu\text{g}/\text{m}^3$  accelerate clearance in large bronchi but slow clearance in more peripheral airways in a dose-dependent fashion.

Data from studies in asthmatics are less clear. Spektor et al. (1985) exposed ten asthmatic subjects to 0, 110, 319, and  $911 \mu\text{g}/\text{m}^3 \text{H}_2\text{SO}_4$  (MMAD =  $0.5 \mu\text{m}$ ) for 1 h. The effects were difficult to interpret because of inhomogeneous distribution of the tracer aerosol in the more severe asthmatics. However, clearance was decreased following the highest concentration of acid exposure in the six subjects with the mildest asthma (not dependent on regular medications). These responses were similar to those of healthy subjects reported above.

Laube et al. (1993) recently examined the effects of acid fog on mucociliary clearance in asthmatics. Seven nonsmoking subjects with mild asthma (baseline FEV<sub>1</sub> 90 to 118% predicted) were exposed in a head dome to  $500 \mu\text{g}/\text{m}^3 \text{H}_2\text{SO}_4$  or NaCl (MMAD  $\approx 10 \mu\text{m}$ ) for 1 h with 20 min of exercise. Mucociliary clearance was measured using inhalation of a technetium-99M sulfur colloid aerosol after exposure to the test aerosol. Tracheal clearance was measured in four subjects, and was increased in all four after  $\text{H}_2\text{SO}_4$  exposure (no statistical analysis was performed because of the small number of subjects). Outer zone lung clearance was increased in six of seven subjects after  $\text{H}_2\text{SO}_4$  exposure ( $p < 0.05$ ). The

dose of H<sup>+</sup> inhaled orally correlated significantly with the change in outer zone lung clearance ( $r = 0.79$ ,  $p = 0.05$ ).

#### **11.2.1.6 Effects of Acid Aerosols Studied by Bronchoscopy and Airway Lavage**

Fiberoptic bronchoscopy with BAL has proved a useful technique for sampling the lower airways of humans in clinical studies of oxidant air pollutants. The type and number of cells recovered in BAL fluid reflect changes in alveolar and distal airway cell populations, providing a relatively sensitive measure of inflammation. Increases in serum proteins recovered in BAL fluid can be a result of increased epithelial permeability, a consequence of injury and/or inflammation. Alveolar macrophages obtained by BAL can be assessed *in vitro* for functional changes important in inflammation and host defense. In addition, proximal airway cells and secretions can be recovered using airway washes or proximal airway lavage (Eschenbacher and Gravelyn, 1987).

Only one study has utilized bronchoscopy to evaluate the effects of exposure to acid aerosols. Frampton et al. (1992) exposed 12 healthy nonsmokers to aerosols of NaCl (control) or H<sub>2</sub>SO<sub>4</sub> (MMAD = 0.9, GSD = 1.9) at 1000  $\mu\text{g}/\text{m}^3$  for 2 h. Four 10-min exercise periods at  $\approx 40$  L/min were included. Subjects brushed their teeth and rinsed with mouthwash prior to and once during each exposure to reduce oral ammonia levels. Fiberoptic bronchoscopy with BAL was performed 18 h after exposure. No evidence for airway inflammation was found. Markers for changes in host defense, including lymphocyte subset distribution, antibody-dependent cellular cytotoxicity of alveolar macrophages, and alveolar macrophage inactivation of influenza virus, were not significantly different between H<sub>2</sub>SO<sub>4</sub> and NaCl exposures.

In an effort to define possible effects of H<sub>2</sub>SO<sub>4</sub> exposure on airway mucus, Culp et al. (1995) determined the composition of mucins recovered during bronchoscopy of subjects studied by Frampton et al. (1992), as well as from some subjects not exposed. Secretions were lipid extracted from airway wash samples and analyzed with regard to glycoprotein content, protein staining profiles, and amino acid and carbohydrate composition. Mucin composition was similar when non-exposed subjects were compared with NaCl-exposed subjects, indicating that aerosol exposure *per se* did not alter mucus composition. No differences were found between H<sub>2</sub>SO<sub>4</sub> and NaCl exposure with regard to absolute yields

of high-density material, proportion of glycoproteins, presence of glycoprotein degradation products, carbohydrate composition, or protein composition.

In these studies, bronchoscopy was performed 18 h after exposure in order to detect delayed effects. Transient effects of exposure to acid aerosols on alveolar macrophage function or mucous composition have therefore not been excluded.

#### **11.2.1.7 Human Exposure Studies of Acid Aerosol Mixtures**

In human subjects, previous studies have suggested that exposure to  $\text{H}_2\text{SO}_4$  does not potentiate responses to other pollutants. A number of more recent studies have also failed to find interactions in effects of pollutant mixtures that include  $\text{H}_2\text{SO}_4$ . Anderson et al. (1992) found no effects on lung function following exposure to  $200 \mu\text{g}/\text{m}^3$  carbon black alone, or carbon particles coated with  $\text{H}_2\text{SO}_4$ . Aris et al. (1990) found no effects on airways resistance of exposure to mixtures of hydroxymethanesulfonic acid and  $\text{H}_2\text{SO}_4$ . Balmes et al. (1988) found no differences between the effects of  $\text{H}_2\text{SO}_4$  and  $\text{HNO}_3$  exposure in asthmatics, and no interaction with exposure to both aerosols by mouthpiece. Koenig et al. (1989) found that exposure of adolescent asthmatic subjects to  $68 \mu\text{g}/\text{m}^3$   $\text{H}_2\text{SO}_4$  with 0.1 ppm  $\text{SO}_2$  did not increase the responses seen with  $\text{H}_2\text{SO}_4$  alone.

In one recent study funded by the Health Effects Institute, 28 adolescent asthmatic subjects were exposed to air, 0.12 ppm ozone + 0.3 ppm  $\text{NO}_2$ , ozone +  $\text{NO}_2$  +  $68 \mu\text{g}/\text{m}^3$   $\text{H}_2\text{SO}_4$ , and ozone +  $\text{NO}_2$  + 0.05 ppm  $\text{HNO}_3$  (Koenig et al., 1994). Exposures were by mouthpiece for 90 min, with intermittent exercise, on two consecutive days. No significant effects on lung function were seen for any of the atmospheres. However, six subjects did not complete the study protocol for a variety of reasons; these subjects were characterized by the authors as having moderate to severe asthma, based on results of methacholine challenge. Although the reasons for withdrawal of these subjects were not clearly related to exposures, all discontinued participation following exposure to pollutants rather than to clean air. As noted in the published comments of the Health Effects Institute Health Review Committee accompanying the Koenig et al. report, "...the conclusions of the study may have been based on a group of subjects more tolerant to oxidants, acid aerosols, or both, than those constituting the original study group" (Koenig et al., 1994, page 103).

Two recent studies suggest that exposure to  $100 \mu\text{g}/\text{m}^3 \text{H}_2\text{SO}_4$  may enhance airway effects of exposure to ozone. Linn et al. (1994) exposed 15 healthy and 30 asthmatic subjects to air, 0.12 ppm ozone,  $100 \mu\text{g}/\text{m}^3 \text{H}_2\text{SO}_4$  (MMAD  $\approx 0.5 \mu\text{m}$ ), and ozone +  $\text{H}_2\text{SO}_4$  for 6.5 h on two consecutive days. Each subject received all 4 pairs of exposures, each separated by one week. Subjects were exposed in small groups in an environmental chamber, with six, 50-min exercise periods each day. Acidic gargles were used to reduce oral ammonia. Lung function and methacholine responsiveness were measured at the end of each exposure day. Reductions in FEV<sub>1</sub> and FVC, and increases in airway responsiveness, were observed in association with ozone exposure in both healthy and asthmatic subjects. Some subjects in both the asthmatic and nonasthmatic group demonstrated greater declines in lung function after the first day of acid + ozone than after ozone alone (Figure 11-2), although the group mean differences were only marginally significant by ANOVA. From these data, a "hypothetical average subject", under the specific conditions of the study, would be expected to lose 100 ml FEV<sub>1</sub> during ozone exposure relative to clean air exposure, and would lose 189 ml FEV<sub>1</sub> during ozone +  $\text{H}_2\text{SO}_4$  exposure. When the responsive subjects were re-studied months later, increased responsiveness to acid + ozone compared with ozone was again demonstrated, although individual responses to O<sub>3</sub> +  $\text{H}_2\text{SO}_4$  in the original and repeat studies were not significantly correlated.

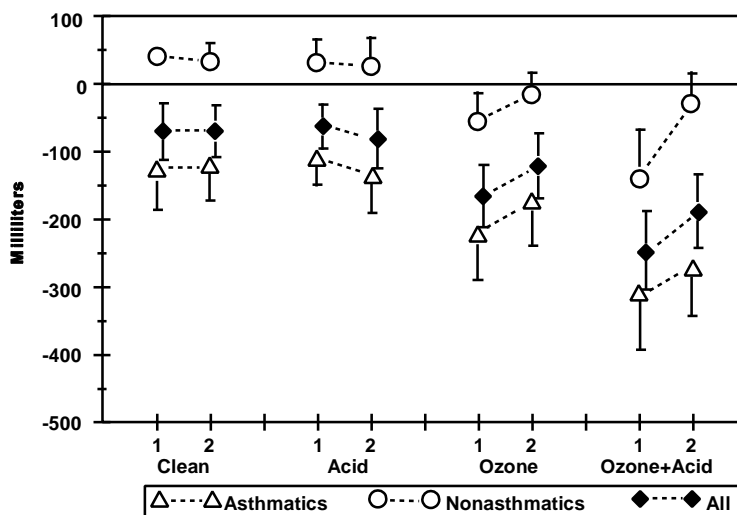


**Figure 11-2. Decrements in forced expiratory volume in 1 s (plus or minus standard error) following 6.5-h exposures on 2 successive days.**

Source: Linn et al. (1994).

Frampton et al. (1995) exposed 30 healthy and 30 asthmatic subjects to  $100 \mu\text{g}/\text{m}^3$   $\text{H}_2\text{SO}_4$  or NaCl for 3 h followed the next day by 0.08, 0.12, or 0.18 ppm ozone for 3 h. All exposures included intermittent exercise. Each subject received two of the three ozone exposure levels. Exposure to  $\text{H}_2\text{SO}_4$  or NaCl did not alter lung functions. As shown in Table 11-4, changes in spirometry following exposure to ozone were small, consistent with the relatively low concentrations, short exposure duration, and moderate exercise levels ( $\dot{V}_E$  30.6 to 36.2 L/min for a total of 60 min). Figure 11-3 shows the percentage changes in FVC 4 h after ozone exposure; these changes were similar to those found immediately after exposure. With  $\text{H}_2\text{SO}_4$  pre-exposure, FVC decreased following ozone in a concentration-response fashion. The ANOVA revealed significant main effects of ozone exposure as well as a significant interaction between aerosol and ozone exposure for effects on  $\text{FEV}_1$  and FVC among the asthmatic subjects, but not the healthy subjects. Four-way ANOVA revealed an interaction between ozone and aerosol for the entire group ( $p=0.0022$ ) and a difference between healthy subjects and subjects with asthma ( $p=0.0048$ ). Surprisingly, the largest decrements in FVC with the NaCl preexposure were found with 0.08 ppm ozone, whereas no effect was seen at 0.18. With 0.18 ppm ozone preceded by  $\text{H}_2\text{SO}_4$ , the responses were similar to those seen at 0.08 with NaCl. The authors concluded that, for asthmatic subjects,  $\text{H}_2\text{SO}_4$  alters the response to ozone in comparison with NaCl pre-exposure. Interpretation of these findings would be facilitated by a similar study including air as a further control pre-exposure atmosphere. However, considered together, these two studies (Frampton et al., 1995 and Linn et al., 1994) suggest that  $\text{H}_2\text{SO}_4$  aerosol exposure may enhance airway responsiveness to ozone.

#### **11.2.1.8 Summary and Conclusions**

Controlled human studies offer the opportunity to study the responses of human subjects under carefully controlled conditions, but are limited to short-term exposures to pollutant atmospheres without severe health risks. Outcome measures are limited by safety issues, but have been extended beyond measures of lung function and symptoms to include mucociliary clearance, BAL, and airway biopsies.

Human clinical studies of particle exposure remain almost completely limited to the study of acid aerosols, primarily of  $\text{H}_2\text{SO}_4$ , with the majority of these focussing on

**TABLE 11-4. PULMONARY FUNCTION RESPONSES AFTER AEROSOL AND OZONE EXPOSURES IN SUBJECTS WITH ASTHMA<sup>a</sup>**

Time of Measurement	FVC (L)		FEV <sub>1</sub> (L)		sGaw (cm H <sub>2</sub> O/L/sec)	
	NaCl	H <sub>2</sub> SO <sub>4</sub>	NaCl	H <sub>2</sub> SO <sub>4</sub>	NaCl	H <sub>2</sub> SO <sub>4</sub>
<b>0.08 ppm Ozone</b>						
Baseline	3.80 ± 0.17	3.73 ± 0.17	2.85 ± 0.11	2.79 ± 0.10	0.204 ± 0.021	0.209 ± 0.020
After exercise	3.64 ± 0.17	3.59 ± 0.18	2.84 ± 0.12	2.72 ± 0.12	-	-
Immediately after exposure	3.51 ± 0.18	3.64 ± 0.17	2.73 ± 0.12	2.79 ± 0.11	0.176 ± 0.024	0.177 ± 0.022
2 Hours after exposure	3.67 ± 0.17	3.70 ± 0.16	2.91 ± 0.12	2.89 ± 0.11	-	-
4 Hours after exposure	3.67 ± 0.15	3.74 ± 0.18	2.92 ± 0.10	2.92 ± 0.13	-	-
<b>0.12 ppm Ozone</b>						
Baseline	3.97 ± 0.22	3.95 ± 0.22	2.98 ± 0.17	3.05 ± 0.17	0.220 ± 0.015	0.236 ± 0.020
After exercise	3.72 ± 0.20	3.76 ± 0.19	2.94 ± 0.17	3.01 ± 0.16	-	-
Immediately after exposure	3.72 ± 0.21	3.76 ± 0.20	2.90 ± 0.19	2.97 ± 0.18	0.186 ± 0.019	0.209 ± 0.025
2 Hours after exposure	3.91 ± 0.22	3.85 ± 0.21	3.10 ± 0.18	3.08 ± 0.17	-	-
4 Hours after exposure	3.87 ± 0.22	3.87 ± 0.21	3.07 ± 0.18	3.04 ± 0.18	-	-
<b>0.18 ppm Ozone</b>						
Baseline	3.89 ± 0.23	3.99 ± 0.22	2.92 ± 0.16	3.04 ± 0.17	0.183 ± 0.016	0.207 ± 0.016
After exercise	3.76 ± 0.23	3.71 ± 0.22	2.90 ± 0.19	2.99 ± 0.16	-	-
Immediately after exposure	3.76 ± 0.23	3.74 ± 0.24	2.90 ± 0.19	2.96 ± 0.18	0.170 ± 0.016	0.179 ± 0.018
2 Hours after exposure	3.81 ± 0.25	3.87 ± 0.23	3.03 ± 0.19	3.03 ± 0.17	-	-
4 Hours after exposure	3.90 ± 0.24	3.84 ± 0.25	3.06 ± 0.17	2.99 ± 0.18	-	-

<sup>a</sup> Values are expressed as means ± SEM.

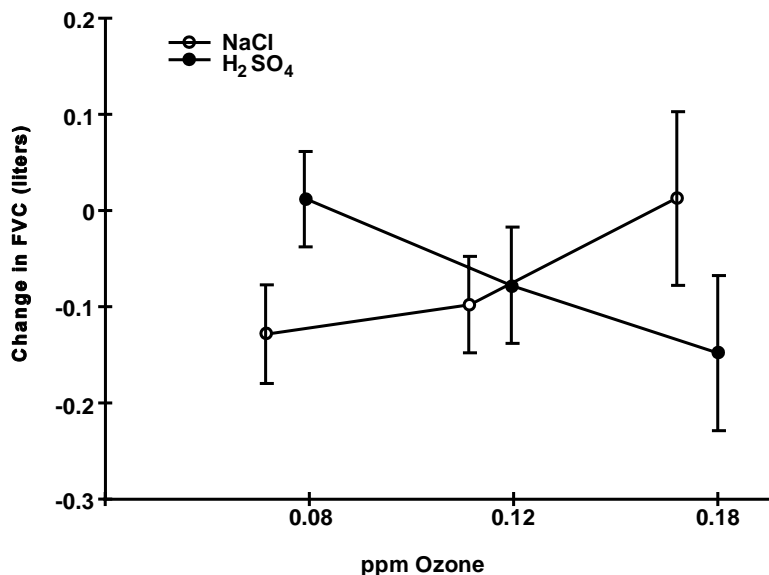


**Figure 11-3. Asthmatic subjects. The absolute change in FVC (means  $\pm$  SE) 4-h after exposure to each of the three ozone concentrations for the NaCl and H<sub>2</sub>SO<sub>4</sub> aerosol preexposure conditions.**

Source: Frampton et al. (1995).

symptoms and pulmonary function. Only two studies (Frampton et al., 1992; Culp et al., 1995) have utilized BAL to examine effects of particle exposure in humans. No studies have examined effects of particle or acid aerosol exposure on airway inflammation in asthmatic subjects. There are no studies examining the effects of particle exposure on antigen challenge in allergic or asthmatic subjects.

Ten studies since 1988 have confirmed previous findings that healthy subjects do not experience decrements in lung function following single exposures to H<sub>2</sub>SO<sub>4</sub> of various particle sizes at levels up to 2,000  $\mu\text{g}/\text{m}^3$  for 1 h, even with exercise and use of acidic gargles to minimize neutralization by oral ammonia. Mild lower respiratory symptoms occur at exposure concentrations in the  $\text{mg}/\text{m}^3$  range, particularly with larger particle sizes. Acid aerosols alter mucociliary clearance in healthy subjects at levels as low as 100  $\mu\text{g}/\text{m}^3$ , with effects dependent on exposure concentration, acid aerosol particle size, and the region of the lung being studied.

Asthmatic subjects appear to be more sensitive than healthy subjects to the effects of acid aerosols on lung function, but the effective concentration differs widely among studies.

Adolescent asthmatics may be more sensitive than adults and may experience small decrements in lung function in response to H<sub>2</sub>SO<sub>4</sub> at exposure levels only slightly above peak ambient levels. Although the reasons for the inconsistency among studies remain largely unclear, subject selection and acid neutralization by NH<sub>3</sub> may be important factors. Even in studies reporting an overall absence of effects on lung function, occasional asthmatic subjects appear to demonstrate clinically important effects. Two studies from different laboratories have suggested that responsiveness to acid aerosols may correlate with degree of baseline airway hyperresponsiveness. There is a need to identify determinants of responsiveness to H<sub>2</sub>SO<sub>4</sub> exposure in asthmatic subjects. In very limited studies, elderly and individuals with chronic obstructive pulmonary disease do not appear to be particularly susceptible to the effects of submicron acid aerosols on lung function.

Two recent studies have examined the effects of exposure to both H<sub>2</sub>SO<sub>4</sub> aerosols and ozone on lung function in healthy and asthmatic subjects. Both studies found evidence that 100 μg/m<sup>3</sup> H<sub>2</sub>SO<sub>4</sub> may potentiate the response to ozone, in contrast with previous studies.

Human studies of particles other than acid aerosols provide insufficient data to draw conclusions regarding health effects. However, available data suggest that inhalation of inert particles in the respirable range, including three studies of carbon particles, have little or no effect on symptoms or lung function in healthy subjects at levels above peak ambient concentrations.

## **11.2.2 Laboratory Animal Studies**

### **11.2.2.1 Introduction**

This section reviews the effects of acidic aerosols on laboratory animals. Almost all of the available data have been derived from studies using acidic sulfates, namely ammonium bisulfate (NH<sub>4</sub>HSO<sub>4</sub>) and sulfuric acid (H<sub>2</sub>SO<sub>4</sub>).

### **11.2.2.2 Mortality**

The previous CD (U.S. Environmental Protection Agency, 1982) examined animal studies of the acute lethality of acid aerosols (mainly H<sub>2</sub>SO<sub>4</sub>), and there are few new data to add here. As for other toxicologic endpoints, large interspecies differences occurred, with the guinea pig being the most sensitive, compared to the mouse, rat and rabbit. But high

concentrations of  $\text{H}_2\text{SO}_4$ , generally in excess of  $10,000 \mu\text{g}/\text{m}^3$ , were required for lethality, even in a species as sensitive as the guinea pig. Also, within a particular species of experimental animal, the  $\text{H}_2\text{SO}_4$  concentration required for lethality was dependent upon particle size, with smaller particles being less effective than larger ones. As noted in the previous CD, the cause of death due to acute, high-level  $\text{H}_2\text{SO}_4$  exposure was laryngeal or bronchial spasm. Since these are irritant responses, differences in the deposition pattern of smaller and larger acid droplets may account for the aforementioned particle size dependence of lethal concentration; larger particles deposit to a greater extent in the larynx and upper bronchial tree, where the bulk of irritant receptors are located. As acid particle size is reduced, deeper pulmonary damage occurs prior to death. Lesions commonly seen are focal atelectasis, hemorrhage, congestion, pulmonary and perivascular edema, and desquamation of bronchiolar epithelium; hyperinflation is also often evident.

Few data allow assessment of lethality for acid sulfate aerosols other than  $\text{H}_2\text{SO}_4$ . Pattle et al. (1956) noted that if sufficient ammonium carbonate was added into the chamber where guinea pigs were exposed to  $\text{H}_2\text{SO}_4$  so as to provide excess  $\text{NH}_3$ , protection was afforded to acid levels which would have produced 50% mortality in the absence of  $\text{NH}_3$ . This implies that  $\text{H}_2\text{SO}_4$  is more acutely toxic than its neutralization products [i.e.,  $\text{NH}_4\text{HSO}_4$  and/or  $(\text{NH}_4)_2\text{SO}_4$ ]. Pepelko et al. (1980a) found no mortality among rats exposed for 8 h/day for 3 days to  $(\text{NH}_4)_2\text{SO}_4$  at 1,000,000 to 1,200,000  $\mu\text{g}/\text{m}^3$  (2 to 3  $\mu\text{m}$ , MMAD); but 40 and 17% mortality occurred in guinea pigs exposed once for 8 h to 800,000 to 900,000, or 600,000 to 700,000  $\mu\text{g}/\text{m}^3$ , respectively, of similarly sized-particles. Death was ascribed to airway constriction, rather than to extensive lung damage. As with  $\text{H}_2\text{SO}_4$ , guinea pigs were more sensitive than other species.

In summary, very high concentrations of acid sulfates are required to cause mortality in otherwise healthy animals, with variations in effective concentrations depending on acid particle size and the animal species tested.

### **11.2.2.3 Pulmonary Mechanical Function**

Many studies examining the toxicology of inhaled acid aerosols at sublethal levels used changes in pulmonary function as indices of response. A survey of the database since

publication of the previous CD (U.S. Environmental Protection Agency, 1982) is presented in Table 11-5.

One of the major exposure parameters which affects response is particle size. Studies by Amdur (1974) and Amdur et al. (1978a,b), summarized in the previous CD, showed that the irritant potency of  $\text{H}_2\text{SO}_4$ ,  $(\text{NH}_4)_2\text{SO}_4$ , or  $\text{NH}_4\text{HSO}_4$ , as measured by pulmonary resistance in guinea pigs, increased with decreasing particle size (i.e., the degree of response per unit mass of sulfate [ $\text{SO}_4^-$ ] at any specific exposure concentration increased as particle size decreased, at least within the size range of 1 to  $0.1 \mu\text{m}$ ). If this is compared to the relationship between particle size and mortality, it is evident that the relative toxicity of different particle sizes also depends upon the exposure concentration. At high concentrations above the threshold for lethality, large particles were more effective in eliciting response, while at lower (sublethal) levels, smaller particles were more effective.

Pulmonary functional responses to  $\text{H}_2\text{SO}_4$  described previously suggested a major site of action to be the conducting airways, as evidenced by exposure-induced alterations in airflow resistance. However, some earlier data also suggested that high exposure levels may affect more distal lung regions, as evidenced by changes in pulmonary diffusing capacity ( $\text{DL}_{\text{co}}$ ) noted in dogs exposed to  $889 \mu\text{g}/\text{m}^3$  ( $\text{MMAD} = 0.5 \mu\text{m}$ ) (Lewis et al., 1973). Deep lung effects of  $\text{H}_2\text{SO}_4$  are also evident from studies of morphologic and lung defense endpoints, discussed in subsequent sections.

Studies reported in the previous CD (U.S. Environmental Protection Agency, 1982) indicated that the particle size of the acid aerosol affected the temporal pattern of any pulmonary function response. For example, the response to  $100 \mu\text{g}/\text{m}^3 \text{H}_2\text{SO}_4$  at  $1 \mu\text{m}$  was slight and rapidly reversible, while that with  $0.3 \mu\text{m}$  droplets was greater and more persistent. At any particular size, however, the degree of change in resistance and compliance in guinea pigs was observed to be concentration related.

Although the earlier studies by Amdur and colleagues appeared to provide a reasonable picture of the relative effects of acid particle size and exposure concentration on the bronchoconstrictive response of guinea pigs at sublethal exposure levels, there is some conflict between these results and reports by others discussed in the previous CD (U.S. Environmental Protection Agency, 1982). Whereas the Amdur work supported a concentration dependence for respiratory mechanics alterations (i.e., animals in each

**TABLE 11-5. EFFECTS OF ACIDIC SULFATE PARTICLES ON PULMONARY MECHANICAL FUNCTION**

Particle	Species, Gender, Strain, Age, or Body Weight		Exposure Technique (RH)	Mass Concentration ( $\mu\text{g}/\text{m}^3$ )	Particle Characteristics		Observed Effect	Reference
					Size ( $\mu\text{m}$ ); $\sigma_g$	Exposure Duration		
H <sub>2</sub> SO <sub>4</sub>	Rat		Whole body	2,370	0.5 (MMD)	14 weeks	NC: V <sub>T</sub> , f, R <sub>L</sub> , Cd, pH, PaCO <sub>2</sub>	Lewkowski et al. (1979)
H <sub>2</sub> SO <sub>4</sub>	Rat		Whole body	6,350	0.44 (MMD)	6 weeks	↓ PaCO <sub>2</sub>	Lewkowski et al. (1979)
H <sub>2</sub> SO <sub>4</sub>	Rat		Whole body	6,590	0.31 (MMD)	13 weeks	↑ pH	Lewkowski et al. (1979)
H <sub>2</sub> SO <sub>4</sub>	Guinea pig, M Hartley		Whole body	1,000, 3,200	0.54 (MMD); 1.32	24 h/d, 3-30 d	Hypo- to hyperresponsive airways	Kobayashi and Shinozaki (1993)
H <sub>2</sub> SO <sub>4</sub>	Rabbit, M NZW		Nose-only (50%)	250	0.3 (MMAD); 1.6	1 h/day, 5 days/week, up to 12 mo	NC: R <sub>L</sub> Hyperresponsive by 4 mo	Gearhart and Schlesinger (1986)
H <sub>2</sub> SO <sub>4</sub>	Guinea pig, M Hartley, 260-325 g		Nose-only (50%)	300	0.08 (MMD); 1.3	1 h	NC: VC, IC, VA, TLC; ↓ DLco, (3 h post exp)	Chen et al. (1991)
H <sub>2</sub> SO <sub>4</sub>	Guinea pig, M Hartley, 290-410 g		Head-only (50%)	200	0.06 (MMD); 1.4	1 h	NC: R <sub>L</sub>	Chen et al. (1992b)
(NH <sub>4</sub> ) <sub>2</sub> SO <sub>4</sub>	Guinea pig, M Hartley, 10 wk		Whole body (50-60%)	1,000	0.4 (MMAD); 2.2	6 h/day, 5 days/week, 1 or 4 weeks	NC: RV; ↑ FRC, VC, TLC, DLco, Cd, ΔN <sub>2</sub>	Loscutt et al. (1985)
(NH <sub>4</sub> ) <sub>2</sub> SO <sub>4</sub>	Rat, M SD, 14 wk		Whole body (50-60%)	1,000	0.4 (MMAD); 2.3	6 h/day, 5 days/week, 1 or 4 weeks	↑ RV, ↑ FRC, ΔN <sub>2</sub>	Loscutt et al. (1985)

Key to abbreviations:

NC: No significant change

↑: Significant increase

↓: Significant decrease

Cd: Dynamic compliance

DLco: Diffusing capacity, CO

f: Respiratory frequency

FRC: Functional residual capacity

IC: Inspiratory capacity

ΔN<sub>2</sub>: Change in distribution of ventilation as measured by nitrogen washout technique

PaCO<sub>2</sub>: Partial pressure of CO<sub>2</sub> in arterial blood

pH: Arterial pH

R<sub>L</sub>: Pulmonary resistance

RV: Residual volume

TLC: Total lung capacity

V<sub>T</sub>: Tidal volume

VA: Alveolar volume

VC: Vital capacity

exposure group responded uniformly and the degree of response was related to the exposure concentration), others found that individual guinea pigs exposed to H<sub>2</sub>SO<sub>4</sub> at similar sizes showed an "all-or-none" constrictive response (i.e., in atmospheres above a threshold concentration), some animals manifested major changes in pulmonary mechanics ("responders"), while others were not affected at all ("nonresponders") (Silbaugh et al., 1981b). As the exposure concentration was increased further, the percentage of the group which was affected (i.e., the ratio of responders to nonresponders) increased, producing an apparent concentration response relationship. However, the magnitude of the change in pulmonary function was similar for all responders, regardless of exposure concentration. Sensitivity to this all-or-none response may be related to an animal's baseline airway caliber prior to H<sub>2</sub>SO<sub>4</sub> exposure, because responders had higher pre-exposure values for resistance and lower values for compliance, compared to nonresponders. In any case, the threshold concentration for the all-or-none response was fairly high (>10,000 μg/m<sup>3</sup> H<sub>2</sub>SO<sub>4</sub>). Reasons for the discrepancy with the studies of Amdur and colleagues are not known; they may involve differences in guinea pig strains, ages, or exposure conditions, or differences in techniques used to measure functional parameters. In any case, the dyspneic response of the guinea pig responders is similar to asthma episodes in humans, in both its rapidity of onset and in the associated characteristic obstructive pulmonary function changes.

A more recent approach used to evaluate the acute pulmonary functional response to H<sub>2</sub>SO<sub>4</sub> involves co-inhalation of CO<sub>2</sub> (Wong and Alarie, 1982; Matijak-Schaper et al., 1983; Schaper et al., 1984). This procedure assesses the response to irritants by measuring a decrease in tidal volume (V<sub>T</sub>) (based upon changes in inspiratory volume and pressure) which is routinely increased above normal by adding 10% CO<sub>2</sub> to the exposure atmosphere. Although the exact mechanism underlying a reduction in response to CO<sub>2</sub> is not clear, the assumption is that the change in ventilatory response after irritant exposure is due to direct stimulation of irritant receptors. A concentration-dependent decrease in CO<sub>2</sub>-enhanced ventilation has been found in guinea pigs following 1-h exposures to H<sub>2</sub>SO<sub>4</sub> (≈ 1 μm, MMD) at levels ≥ 40,100 μg/m<sup>3</sup> (Wong and Alarie, 1982). Subsequently, Schaper et al. (1984) exposed guinea pigs for 0.5 h to H<sub>2</sub>SO<sub>4</sub> at 1,800 to 54,900 μg/m<sup>3</sup> (0.6 μm, AED). At concentrations >10,000 μg/m<sup>3</sup>, the level of response (i.e., the maximum decrease in ventilatory response to CO<sub>2</sub>) increased as a function of exposure concentration.

At concentrations below 10,000  $\mu\text{g}/\text{m}^3$ , there was no clear relationship between exposure concentration and response; any effects were transient, occurring only at the onset of acid exposure.

The results of the studies with  $\text{CO}_2$  differ from those of both Silbaugh et al. (1981b) and Amdur and colleagues, in that there was neither an "all or none" response as seen by the former, nor was there a concentration-response relationship observed at  $\text{H}_2\text{SO}_4$  concentrations  $<10,000 \mu\text{g}/\text{m}^3$ , as reported by the latter. In addition, Amdur and colleagues observed sustained changes in lung function, rather than a fading response, at low concentrations. The reasons for these differences are unknown, but may partly reflect inherent sensitivity differences in the measurement techniques used as noted above.

The specific mechanisms underlying acid sulfate-induced pulmonary functional changes are not known, but may be due to irritant receptor stimulation resulting from direct contact by deposited acid particles or from humoral mediators released as a result of exposure. In terms of the latter, a possible candidate in mediation of the bronchoconstrictive response, at least in guinea pigs, is histamine (Charles and Menzel, 1975). On the other hand, evidence for a direct response to  $\text{H}_2\text{SO}_4$  in altering pulmonary function was found using the  $\text{CO}_2$  co-inhalation procedure. Schaper and Alarie (1985) noted that the responses to histamine and  $\text{H}_2\text{SO}_4$  differed in both their magnitude and temporal relationship, suggesting direct action of the inhaled acid, or a role of other humoral factors.

Whatever the underlying mechanism, the results of pulmonary function studies indicate that  $\text{H}_2\text{SO}_4$  is a bronchoactive agent that can alter lung mechanics of exposed animals primarily by constriction of smooth muscle; however, the threshold concentration for this response is quite variable, depending upon the animal species and measurement procedure used. In general, exposure to  $\text{H}_2\text{SO}_4$  at levels  $<1,000 \mu\text{g}/\text{m}^3$  does not produce physiologically significant changes in standard tests of pulmonary mechanics, except in the guinea pig. Although in this species such effects may be markers of exposure, any health significance in normal individuals is not clear. On the other hand, all subgroups of an exposed population may not be equally sensitive.

### *Airway Responsiveness*

Some lung diseases (e.g., asthma) involve a change in airway "responsiveness", which is an alteration in the degree of reactivity to exogenous (or endogenous) bronchoactive agents, resulting in increased airway resistance at levels of these agents which would not affect airways of normal individuals. Such altered airways are called hyperresponsive. The use of pharmacologic agents capable of inducing smooth muscle contraction, a technique known as bronchoprovocation challenge testing, can assess the state of airway responsiveness after exposure to a nonspecific stimulus such as an inhaled irritant. Human asthmatics and, to some extent, chronic bronchitis, typically have hyperresponsive airways, but the exact role of this in the pathogenesis of airway disease is uncertain. Hyperresponsiveness may be a predisposing factor in clinical disease, or it may be a reflection of other changes in the airways which precede it. In any case, current evidence supports the hypothesis that an increase in airway responsiveness is a factor in the pathogenesis of obstructive airway disease (O'Connor et al., 1989).

The ability of H<sub>2</sub>SO<sub>4</sub> aerosols to alter airway responsiveness has been assessed in a number of studies. Silbaugh et al. (1981a) exposed guinea pigs for 1 h to 4,000 to 40,000 μg/m<sup>3</sup> H<sub>2</sub>SO<sub>4</sub> (1.01 μm, MMAD) and examined the subsequent response to inhaled histamine. Some of the animals showed an increase in pulmonary resistance and a decrease in compliance at H<sub>2</sub>SO<sub>4</sub> concentrations ≥ 19,000 μg/m<sup>3</sup> without provocation challenge; only the animals showing this constrictive response during acid exposure also had major increases in histamine sensitivity. This suggested that airway constriction may have been a prerequisite for the development of hyperresponsiveness. On the other hand, Chen et al. (1992b) found bronchial hyperresponsiveness, but no change in baseline resistance, in guinea pigs exposed for 1 h to 200 μg/m<sup>3</sup> H<sub>2</sub>SO<sub>4</sub> (0.06 μm, MMD). Perhaps the smaller size of this aerosol was responsible for producing effects at a lower concentration.

Kobayashi and Shinozaki (1993) exposed guinea pigs to fairly high H<sub>2</sub>SO<sub>4</sub> levels, namely 1,000 and 3,200 μg/m<sup>3</sup> (0.54 μm), 24 h/day for 3, 7, 14 or 30 days, and examined airway response to inhaled histamine. Unlike the study of Silbaugh et al. (1981a) and similar to that of Chen et al. (1992b), acid exposure did not change the baseline resistance measured prior to bronchoprovocation challenge. Exposure to 3,200 μg/m<sup>3</sup> of acid resulted in airway hyporesponsiveness at 3 days, hyperresponsiveness at 14 days and a return to normal levels of responsiveness by 30 days of exposure. Thus, acid exposure resulted in a transient alteration in airway function. The authors speculated that the hyporesponsiveness, and eventual return to

normal, was due to changes in mucous secretion in the airways, which would affect the ability of the inhaled histamine challenge aerosol to contact airway receptors.

Airway responsiveness following chronic exposure to H<sub>2</sub>SO<sub>4</sub> was examined by Gearhart and Schlesinger (1986), who exposed rabbits to 250 μg/m<sup>3</sup> H<sub>2</sub>SO<sub>4</sub> (0.3 μm, MMD) for 1 h/day, 5 days/week, and assessed responsiveness after 4, 8 and 12 mo of exposure, using acetylcholine administered intravenously rather than inhaled. Hyperresponsiveness was evident at 4 mo, and a further increase was found by 8 mo; the response at 12 mo was similar to that at 8 mo, indicating a stabilization of effect. There was no change in baseline resistance. Thus, repeated exposures to H<sub>2</sub>SO<sub>4</sub> produced hyperresponsive airways in previously normal animals.

The mechanism which underlies H<sub>2</sub>SO<sub>4</sub>-induced airway hyperresponsiveness is not clear. However, some recent studies have suggested possibilities. One may involve an increased sensitivity to mediators involved in airway smooth muscle control. For example, guinea pigs exposed to H<sub>2</sub>SO<sub>4</sub> showed a small degree of enhanced response to histamine, but a much more pronounced sensitivity to substance P, a neuropeptide having effects on bronchial muscle tone (Stengel et al., 1993). El-Fawal and Schlesinger (1994) exposed rabbits for 3 h to 50 to 500 μg/m<sup>3</sup> H<sub>2</sub>SO<sub>4</sub> (0.3 μm), following which bronchial airways were examined in vitro for responsiveness to acetylcholine and histamine. Exposures at ≥75 μg/m<sup>3</sup> produced increased responsiveness to both constrictor agents. Detailed examination of the response in tracheal segments suggested that the acid effect may result from interference with airway contractile/dilatory homeostatic processes, in that there was a potentiation of the response of airway constrictor receptors and a diminution of the response of dilatory receptors.

#### **11.2.2.4 Pulmonary Morphology and Biochemistry**

Morphologic alterations associated with exposure to acid aerosols are summarized in Table 11-6.

**TABLE 11-6. EFFECTS OF ACIDIC SULFATE PARTICLES ON RESPIRATORY TRACT MORPHOLOGY**

Particle	Species, Gender, Strain, Age, or Body Weight	Exposure Technique (RH)	Mass Concentration ( $\mu\text{g}/\text{m}^3$ )	Particle Characteristics	Exposure Duration	Observed Effect	Reference
				Size ( $\mu\text{m}$ ); $\sigma_g$			
H <sub>2</sub> SO <sub>4</sub>	Guinea pig	Whole body (70-90%)	32,600	1 (MMAD); 1.49	4 h	Focal atelectasis; epithelial desquamation in terminal bronchioles	Brownstein (1980)
H <sub>2</sub> SO <sub>4</sub>	Guinea pig, M/F Hartley, 2-3 mo	Whole body (80%)	1,200, 9,000, 27,000	0.8-1 (MMAD); 1.5-1.6	6 h	At 27,000 $\mu\text{g}/\text{m}^3$ : interstitial edema only in "responders"; no change in "nonresponders" or at 1,000 and 10,000 $\mu\text{g}/\text{m}^3$ . Concentration-dependent increase in height of tracheal mucus layer at all concentrations.	Wolff et al. (1986)
H <sub>2</sub> SO <sub>4</sub>	Rabbit, M mixed, 2.5-2.7 kg	Oral tube or nose- only (80%)	250-500	0.3 (MMAD); 1.6	1 h/day, 5 days/week, 4 weeks	Increased epithelial thickness in small airways; increase in secretory cells in mid to small airways	Schlesinger et al. (1983)
H <sub>2</sub> SO <sub>4</sub>	Rabbit, M mixed, 2.5-2.7 kg	Nose-only (80%)	250	0.3 (MMAD); 1.6	1 h/day, 5 days/week up to 52 weeks	Increase in secretory cell no. density throughout bronchial tree increase in number of small airways	Gearhart and Schlesinger (1988)
H <sub>2</sub> SO <sub>4</sub>	Rabbit, M NZ White, 3-3.5 kg	Nose-only (60%)	125	0.3 (MMD); 1.6	2 h/day, 5 days/week up to 12 mo	No bronchial inflammation; increase in secretory cell number density in small airways at 12 mo	Schlesinger et al. (1992b)
H <sub>2</sub> SO <sub>4</sub>	Rat	Whole body (40-60%)	2,000	0.3 (MMD); $\approx 2$	8 h/day, 82 days	Some hypertrophy of epithelial cells, mainly at alveolar duct level; no effect on turnover rate of terminal bronchiolar epithelial or Type II cells	Juhos et al. (1978)
H <sub>2</sub> SO <sub>4</sub>	Rat	Whole body (50%)	700-1,200	0.03-0.04 (CMD); 1.8-2.1	Continuous, up to 180 days	No effect	Moore and Schwartz (1981)
H <sub>2</sub> SO <sub>4</sub>	Rat	Whole body ( $\leq 60\%$ )	45,000 68,000 172,000	0.52 (CMD) 0.4 (MMAD) 0.45 (CMD)	11 days 6 days 7 days	No effect in nasal passages, trachea, bronchi, alveolar region	Schwartz et al. (1977)
H <sub>2</sub> SO <sub>4</sub>	Rhesus monkey	Whole body ( $\leq 60\%$ )	150,000 361,000 502,000	0.3-0.5 (CMD) 0.43 (MMAD); 1.6 0.48 (MMAD); 1.5	3 days 7 days 7 days	No effect	Schwartz et al. (1977)
H <sub>2</sub> SO <sub>4</sub>	Guinea Pig	Whole body ( $\leq 60\%$ )	30,000 38,000 71,000	0.31 (MMAD); 1.6 0.31 (MMAD); 1.6 0.52 (CMD)	7 days 7 days 4 days	At 71,000 $\mu\text{g}/\text{m}^3$ : focal edema, necrosis of alveolar septa, inflammatory cell infiltration; necrosis of bronchiolar epithelium; focal epithelial necrosis in larger bronchi; ciliary denudation. At 38,000 $\mu\text{g}/\text{m}^3$ : minimal effects; some change in density and length of cilia	Schwartz et al. (1977)

**TABLE 11-6 (cont'd). EFFECTS OF ACIDIC SULFATE PARTICLES ON RESPIRATORY TRACT MORPHOLOGY**

Particle	Species, Gender, Strain, Age, or Body Weight	Exposure Technique (RH)	Mass Concentration ( $\mu\text{g}/\text{m}^3$ )	Particle Characteristics	Exposure Duration	Observed Effect	Reference
				Size ( $\mu\text{m}$ ); $\sigma_g$			
H <sub>2</sub> SO <sub>4</sub>	Mouse	Whole body (<60%)	140,000	0.32 (MMAD); 1.4	14 days	Lesions in larynx and upper trachea; epithelial ulceration, edema, inflammatory infiltration	Schwartz et al. (1977)
			170,000	0.62 (MMAD); 1.7	10 days		
H <sub>2</sub> SO <sub>4</sub>	Rat	Whole body	1,000-100,000	0.6-1.1 (MMAD); 1.7-1.8	6 h	At 100,000 $\mu\text{g}/\text{m}^3$ : some cilia loss; ulceration of larynx. <100,000 $\mu\text{g}/\text{m}^3$ : no effect	Henderson et al. (1980a)
H <sub>2</sub> SO <sub>4</sub>	Rat, M/F, F344/Crl 12-16 weeks	Whole body (80%)	1,100, 11,000, 96,000	0.8-1 (MMAD); 1.6-1.8	6 h	Laceration of larynx and cilia loss in bronchi at 96,000 $\mu\text{g}/\text{m}^3$ ; no deep lung lesions; some thickening of mucus lining in trachea at 11,000 and 96,000 $\mu\text{g}/\text{m}^3$	Wolff et al. (1986)
H <sub>2</sub> SO <sub>4</sub>	Rat, M Fischer, 250-300 g	Whole body (55%)	10,000	0.89 (MMD)	5 days	No effect	Cavender et al. (1977b)
			30,000	0.83 (MMD)	5 days		
			100,000	0.72 (MMD)	5 days		
H <sub>2</sub> SO <sub>4</sub>	Guinea pig	Whole body (55%)	10,000	0.89 (MMD)	5 days	No effect } Mortality }	Cavender et al. (1977b)
			30,000	0.83 (MMD)	5 days		
			100,000	0.72 (MMD)	5 days		
(NH <sub>4</sub> ) <sub>2</sub> SO <sub>4</sub>	Guinea pig, M, Hartley adult	Whole body	1,030	0.42 (MMD); 2.25	6 h/day, 5 days/week, 20 days	Interstitial thickening; hypertrophy and hyperplasia of Type II cells and secretory cells in bronchioli	Busch et al. (1984)
(NH <sub>4</sub> ) <sub>2</sub> SO <sub>4</sub>	Rat, M, SD/Crl, 70-75 g	Whole body	5000	0.8-1 (MMD); 1.8-2.0	7 days	No effect (proximal acinar region)	Last et al. (1983)
(NH <sub>4</sub> ) <sub>2</sub> SO <sub>4</sub>	Hamster, M, Syrian, 10 weeks	Whole body	187	0.3 (MMD); 2.02	6 h/day, 5 days/week, 15 weeks	Emphysematic lesions; no hyperplasia of bronchial glands or metaplasia of goblet cells	Godleski et al. (1984)
(NH <sub>4</sub> ) <sub>2</sub> SO <sub>4</sub>	Rat, M, adult	Whole body	300,000	1-2 (MMAD)	8 h/day, 1-14 days	No effect	Pepelko et al. (1980a)
(NH <sub>4</sub> ) <sub>2</sub> SO <sub>4</sub>	Rat, M, SD adult	Whole body	1,030	0.42 (MMAD); 2.25	6 h/day, 5 days/week, 20 days	Interstitial thickening	Busch et al. (1984)
(NH <sub>4</sub> ) <sub>2</sub> SO <sub>4</sub>	Rat	Nose-only	70	0.2 (MMAD)	4 h/day, 4 days/week, 8 weeks	Increased alveolar septal thickness; decreased average alveolar diameter	Kleinman et al. (1995)

Single or multiple exposures to H<sub>2</sub>SO<sub>4</sub> at fairly high levels (>1,000 μg/m<sup>3</sup>) produce a number of characteristic morphologic responses (e.g., alveolitis, bronchial and/or bronchiolar epithelial desquamation, and edema). As with other endpoints, the sensitivity to H<sub>2</sub>SO<sub>4</sub> is dependent upon the animal species. Comparative sensitivities of the rat, mouse, rhesus monkey and guinea pig were examined by Schwartz et al. (1977), using concentrations of H<sub>2</sub>SO<sub>4</sub> ≥30,000 μg/m<sup>3</sup> at comparable particle sizes (0.3 to 0.6 μm) and assessing airways from the larynx to the deep lung. Both the rat and monkey were quite resistant, while the guinea pig and mouse were the more sensitive species. The nature of the lesions in the latter pair were similar, but differed in location; this was, perhaps, a reflection of differences in the deposition pattern of the acid droplets. Mice would tend to have greater deposition in the upper respiratory airways than would the guinea pig (Schlesinger, 1985), which could account for the laryngeal and upper tracheal location of the lesions seen in the mice. The relative sensitivity of the guinea pig and relative resistance of the rat to acid sulfates is supported by results from other morphological studies (Busch et al., 1984; Cavender et al., 1977b; Wolff et al., 1986).

Repeated or chronic exposures to H<sub>2</sub>SO<sub>4</sub> at concentrations ≤1,000 μg/m<sup>3</sup> produce a response characterized by hypertrophy and hyperplasia of epithelial secretory cells. In morphometric studies of rabbits exposed to 125 to 500 μg/m<sup>3</sup> H<sub>2</sub>SO<sub>4</sub> (0.3 μm) for 1 to 2 h/day, 5 d/week (Schlesinger et al., 1983; Gearhart and Schlesinger, 1988; Schlesinger et al., 1992b), increases in the relative number density of secretory cells (as determined by histochemical staining) have been found to extend to the bronchiolar level, where these cells are normally rare or absent. Depending upon the study, the changes began within 4 weeks of exposure and persisted for up to 3 mo following the end of exposure. The mechanism underlying increases in secretory cell numbers at low H<sub>2</sub>SO<sub>4</sub> exposure levels is also unknown; it may involve an increase in secretory activity of existing cells, or a transition from another cell type.

An increase in the relative number of smaller airways (<0.25 mm) in rabbits was found by 4 mo of exposure to 250 μg/m<sup>3</sup> (0.3 μm) for 1 h/day, 5 days/week (Gearhart and Schlesinger, 1988). Changes in airway size distribution due to irritant exposure, specifically cigarette smoke, has been reported in humans (Petty et al., 1983; Cosio et al., 1977), and this seems to be an early change relevant to clinical small airways disease.

The specific pathogenesis of acid-induced lesions is not known. As with pulmonary mechanics, both a direct effect of deposited acid droplets on the epithelium and/or indirect effects, perhaps mediated by humoral factors, may be involved. For example, similar lesions have been produced in guinea pig lungs by exposure to either histamine or  $\text{H}_2\text{SO}_4$  (Cavender et al., 1977a). In addition, some lesions may be secondary to reflex bronchoconstriction, to which guinea pigs are very vulnerable, rather than primary effects separable from constriction. Thus, damage at the small bronchi and bronchiolar level may be due not only to direct acid droplet-induced injury, but to indirect, reflex-mediated injury as well (Brownstein, 1980).

Morphologic and cellular damage to the respiratory tract following exposure to acid aerosols may be determined by methods other than direct microscopic observation. Analysis of bronchoalveolar lavage fluid can also provide valuable information, and this procedure has seen increasing use since publication of the previous CD. Levels of cytoplasmic enzymes, such as lactate dehydrogenase (LDH) and glucose-6-phosphate dehydrogenase (G-6PD), are markers of cytotoxicity; increases in lavageable protein suggest increased permeability of the alveolar epithelial barrier; levels of membrane enzymes, such as alkaline phosphatase, are markers of disrupted membranes; the presence of fibrin degradation products (FDP) provides evidence of general damage; and sialic acid, a component of mucoglycoprotein, indicates mucus-secretory activity. (It should, however, be noted that lavage analysis may not be able to provide identification of the site of injury nor indicate effects in the interstitial tissue.)

Henderson et al. (1980b) exposed rats for 6 h to  $\text{H}_2\text{SO}_4$  ( $0.6 \mu\text{m}$ , MMAD) at 1,500, 9,500, and  $98,200 \mu\text{g}/\text{m}^3$ , and found FDP in blood serum after exposure at all concentrations. No FDP was found in lavage fluid, but since the washing procedure did not include the upper respiratory tract (i.e., anterior to and including the larynx), FDP in the serum was concluded to be an indicator of upper airway injury. A concentration-dependent increase in sialic acid content of the lavage fluid was also observed, indicating increased secretory activity within the tracheobronchial tree.

Chen et al. (1992a) exposed guinea pigs to fine ( $0.3 \mu\text{m}$ ) and ultrafine ( $0.04 \mu\text{m}$ ) aerosols of  $\text{H}_2\text{SO}_4$  at  $300 \mu\text{g}/\text{m}^3$  for 3 h/day for 1 or 4 days. Animals were sacrificed 24 h after each of these exposures. Following the single exposure to either size, lavage fluid showed increases in LDH and total protein, and the change in LDH was evident at 24 h with

the fine, but not the ultrafine, particles. These responses did not occur following the 4 day exposure.

Wolff et al. (1986) exposed both rats and guinea pigs for 6 h to H<sub>2</sub>SO<sub>4</sub> (0.8 to 1 μm, MMAD), at concentrations of 1,100 to 96,000 μg/m<sup>3</sup> for rats and 1,200 to 27,000 μg/m<sup>3</sup> for guinea pigs. No changes in lavageable LDH, protein, or sialic acid were found in the rat. However, some of the guinea pigs exhibited bronchoconstriction after exposure to 27,000 μg/m<sup>3</sup>, and only these animals showed increased levels of lavageable protein, sialic acid and LDH. In other studies, no changes in lavageable protein were found in the lungs of rats exposed for 3 days to 1,000 μg/m<sup>3</sup> (0.4 to 0.5 μm, MMAD) H<sub>2</sub>SO<sub>4</sub> (Warren and Last, 1987), nor for 2 days to 5,000 μg/m<sup>3</sup> (0.5 μm, MMAD) (NH<sub>4</sub>)<sub>2</sub>SO<sub>4</sub> (Warren et al., 1986).

An important group of biological mediators of the inflammatory response, as well as of smooth muscle tone, are the eicosanoids, (e.g., prostaglandins and leukotrienes). Modulation of these mediators could be involved in damage to the respiratory tract due to inhaled particles. Preziosi and Ciabattini (1987) exposed isolated, perfused guinea pig lungs for 10 min to aerosols of H<sub>2</sub>SO<sub>4</sub> (no concentration or particle sizes were given). An increase in thromboxane B<sub>2</sub> but no change in leukotriene B<sub>4</sub> in the perfusate was found. Schlesinger et al. (1990b) exposed rabbits to 250 to 1,000 μg/m<sup>3</sup> H<sub>2</sub>SO<sub>4</sub> (0.3 μm) for 1 h/day for 5 days. Lungs were lavaged and the fluid assayed for eicosanoids. A concentration-dependent decrease in levels of prostaglandins E<sub>2</sub> and F<sub>2α</sub> and thromboxane B<sub>2</sub> were noted, while there was no change in leukotriene B<sub>4</sub>. The effects, which were determined to be due to the hydrogen ion rather than the sulfate ion, indicate that acid sulfates can upset the normally delicate balance of eicosanoid synthesis/metabolism which is necessary to maintain pulmonary homeostasis. Since some of the prostaglandins are involved in regulation of muscle tone, this imbalance may be involved in the development of airway hyperresponsiveness found with exposure to acid sulfates.

Other biochemical markers of pulmonary damage have been used to assess the toxicity of acid sulfate particles. The proline content of the lungs may provide an index of collagen metabolism. No change in soluble proline content was found in rat lungs after exposure for 7 days to 4,840 μg/m<sup>3</sup> (0.5 μm, MMAD) (NH<sub>4</sub>)<sub>2</sub>SO<sub>4</sub>, nor due to a 7 day exposure to 1,000 μg/m<sup>3</sup> (0.5 μm) H<sub>2</sub>SO<sub>4</sub> (Last et al., 1986). A series of studies assessed collagen synthesis in rat lung minces after in vivo exposure; this is a possible indicator of the potential

for pollutants to produce fibrosis. Exposure for 7 days to H<sub>2</sub>SO<sub>4</sub> at 40, 100, 500, and 1,000 μg/m<sup>3</sup> (0.4 to 0.5 μm, MMAD) resulted in an increase in collagen synthesis rate only at 100 μg/m<sup>3</sup>; higher levels had no effect (Warren and Last, 1987). No effect on collagen synthesis by rat lung minces was found due to 7-day exposures to (NH<sub>4</sub>)<sub>2</sub>SO<sub>4</sub> at 5,000 μg/m<sup>3</sup> (0.8 to 1 μm, MMAD) (Last et al., 1983).

Other parameters of pulmonary damage are changes in lung DNA, RNA, or total protein content. No significant changes in any of these parameters were found in rats after exposure to 1,000 μg/m<sup>3</sup> H<sub>2</sub>SO<sub>4</sub> (<1 μm) for 3 days (Last and Cross, 1978), nor in protein content in rats exposed for up to 9 days to a similar concentration of H<sub>2</sub>SO<sub>4</sub> (Warren and Last, 1987).

#### 11.2.2.5 Pulmonary Defenses

Responses to air pollutants often depend upon their interaction with an array of non-specific and specific respiratory tract defenses. The former consists of nonselective mechanisms protecting against a wide variety of inhaled materials; the latter requires antigenic stimulation of the immune system for activation. Although these systems may function independently, they are linked, and response to an immunologic insult may enhance the subsequent response to nonspecific materials. The overall efficiency of lung defenses determines the local residence times for inhaled deposited material, which has a major influence upon the degree of pulmonary response; furthermore, either depression or over-activity of these systems may be involved in the pathogenesis of lung diseases.

Studies of altered lung defenses resulting from inhaled acid aerosols have concentrated on conducting and respiratory region clearance function and nonspecific activity of macrophages; there are only a few studies of effects upon immunologic competence.

**Clearance Function:** Clearance, a major nonspecific defense mechanism, is the physical removal of material that deposits on airway surfaces. As discussed in Chapter 10, the mechanisms involved are regionally distinct. In the tracheobronchial region, clearance occurs via the mucociliary system, whereby a mucus "blanket" overlying the ciliated epithelium is moved by the coordinated beating of the cilia towards the oropharynx. In the alveolar region of the lungs, clearance occurs via a number of mechanisms and pathways, but the major one for both microbes and nonviable particles is the alveolar macrophage (AM).

These cells exist freely within the fluid lining of the alveolar epithelium, where they move by ameboid motion. The phagocytic ingestion of deposited particles helps prevent particle penetration through the alveolar epithelium and subsequent translocation to other sites. These cells contain proteolytic enzymes, which digest a wide variety of organic materials, and they also kill bacteria through oxidative mechanisms. In addition, AMs are involved in the induction and expression of immune reactions. Thus, the AM provides a link between the lung's non-specific and specific defense systems. These cells also are in the effector chain for lung damage (e.g., by release of proinflammatory cytokines).

***Mucociliary Transport:*** The assessment of acid effects upon mucociliary clearance often involved examination only of mucus transport rates in the trachea, since this is a readily accessible airway and tracheal mucociliary clearance measurements are more straightforward to perform than are those aimed at assessing clearance from the entire tracheobronchial tree. Table 11-7 outlines studies of acid sulfate effects upon tracheal mucociliary clearance.

Although many of the studies involved fairly high concentrations of acid aerosols, most demonstrated a lack of effect. The most likely explanation for this is that the sizes of the aerosols were such that significant tracheal deposition did not occur. This is supported by the results of Wolff et al. (1981), who found tracheal transport rates in dogs to be depressed only when using  $0.9 \mu\text{m}$   $\text{H}_2\text{SO}_4$ ; no effect was seen with a  $0.3 \mu\text{m}$  aerosol at an equivalent mass concentration. In addition, the use of tracheal clearance rate as a sole toxicologic endpoint may be misleading, inasmuch as a number of studies have demonstrated alterations in bronchial clearance patterns in the absence of changes in tracheal mucous transport.

Studies assessing the effects of acid aerosols upon bronchial mucociliary clearance are also outlined in Table 11-7. Responses following acute exposure to  $\text{H}_2\text{SO}_4$  indicate that the nature of clearance change (i.e., a slowing or speeding) is concentration (C) and exposure-duration (t) dependent; stimulation of clearance generally occurs after low Ct exposures, and retardation generally occurs at higher Ct levels. However, the actual Ct needed to alter clearance rate may depend upon the anatomic location within the bronchial tree from which clearance is being measured, in relation to the region which is most affected by the deposited acid. Studies in humans indicated that low  $\text{H}_2\text{SO}_4$  concentrations (i.e.,  $\approx 100$  to  $500 \mu\text{g}/\text{m}^3$ ) may accelerate clearance, compared to unexposed subjects, from the large proximal airways

**TABLE 11-7. EFFECTS OF ACIDIC SULFATE PARTICLES ON RESPIRATORY TRACT CLEARANCE**

Particle	Species, Gender, Strain, Age, or Body Weight	Exposure Technique (RH)	Mass Concentration ( $\mu\text{g}/\text{m}^3$ )	Particle Characteristics		Exposure Duration	Observed Effect	Reference
				Size ( $\mu\text{m}$ ); $\sigma_g$				
Tracheal								
H <sub>2</sub> SO <sub>4</sub>	Dog, M/F Beagle, 3 years	Nose-only (80%)	1,000	0.3 (MMAD); 1.2		1 h	NC	Wolff et al. (1981)
			5,000	0.3 (MMAD); 1.2		1 h	NC	
			1,000	0.9 (MMAD); 1.3		1 h	↓	
			500	0.9 (MMAD); 1.3		1 h	↓	
H <sub>2</sub> SO <sub>4</sub>	Donkey, M/F adult	Nasopharyngeal catheter (45%)	200-1,400	0.4 (MMAD); 1.5		1 h	NC	Schlesinger et al. (1978)
H <sub>2</sub> SO <sub>4</sub>	Rat	Whole body (82%)	1,000-100,000	0.6-0.8 (MMAD); 1.5-2.6		6 h	↑	Wolff et al. (1980)
H <sub>2</sub> SO <sub>4</sub>	Rat	Nose-only (80%)	10,000-100,000	0.4-0.6 (MMAD); 1.3-1.4		0.5 h	↑	
H <sub>2</sub> SO <sub>4</sub>	Rat, M/F F344/Crl 12-16 weeks	Whole body (80%)	1,100, 11,000, 96,000	0.9-1 (MMAD); 1.6-1.8		6 h	↑ at 96,000 $\mu\text{g}/\text{m}^3$	Wolff et al. (1986)
H <sub>2</sub> SO <sub>4</sub>	Guinea pig, M/F Hartley 2-3 mo	Whole body (80%)	1,400, 9,000, 27,000	0.8-0.9 (MMAD); 1.5-1.6		6 h	↓ at 1,400 $\mu\text{g}/\text{m}^3$	
NH <sub>4</sub> HSO <sub>4</sub>	Sheep	Head-only (20-30%)	1,000	0.1 (CMD); 2.1		4 h	NC	Sackner et al. (1981)
(NH <sub>4</sub> ) <sub>2</sub> SO <sub>4</sub>	Donkey	Nasopharyngeal catheter (45%)	300-3,000	0.4 (MMAD); 1.5		1 h	NC	Schlesinger et al. (1978)
(NH <sub>4</sub> ) <sub>2</sub> SO <sub>4</sub>	Sheep	Head-only (20-30%)	1,100	0.1 (CMD); 2.1		4 h	NC	Sackner et al. (1981)
Bronchial								
H <sub>2</sub> SO <sub>4</sub>	Rabbit, M NZW/mixed, 2.5-3 kg	Oral tube (75%)	100-2,200	0.3 (MMAD); 1.6		1 h	↑, ↓ (depending on concentration and duration)	Chen and Schlesinger (1983); Schlesinger et al. (1984)
H <sub>2</sub> SO <sub>4</sub>	Rabbit, M mixed 2.5-2.7 kg	Oral tube or nose-only (80%)	250-500	0.3 (MMAD); 1.6		1 h/days, 5 days/week, 4 weeks	↑; persistent	Schlesinger et al. (1983)
H <sub>2</sub> SO <sub>4</sub>	Rabbit, M NZW 2.5-3 kg	Nose-only (80%)	250	0.3 (MMAD); 1.6		1 h/day, 5 days/week, 12 mo	↓ by 1 week; progressive slowing after 19 weeks; persistent	Gearhart and Schlesinger (1988)
H <sub>2</sub> SO <sub>4</sub>	Rabbit, M NZW 2.5-3 kg	Nose-only (60%)	125	0.3 (MMD); 1.6		2 h/day, 5 days/week up to 12 mo	↑ followed by ↓ PE; persistent	Schlesinger et al. (1992b)

**TABLE 11-7 (cont'd). EFFECTS OF ACIDIC SULFATE PARTICLES ON RESPIRATORY TRACT CLEARANCE**

Particle	Species, Gender, Strain, Age, or Body Weight	Exposure Technique (RH)	Mass Concentration ( $\mu\text{g}/\text{m}^3$ )	Particle Characteristics		Exposure Duration	Observed Effect	Reference
				Size ( $\mu\text{m}$ ); $\sigma_g$				
Bronchial								
H <sub>2</sub> SO <sub>4</sub>	Rabbit, M mixed 6 mo	oral tube nose-only	250; 250; 500	0.3 (MMAD); 1.6		1 h/day, 5 days/week, 4 weeks	↑ only some days at 250/oral and 500/nasal; persistent ↑ up to 14 days PE for all.	Schlesinger et al. (1983)
H <sub>2</sub> SO <sub>4</sub>	Donkey	Nasopharyngeal catheter (45%)	200-1,400	0.4 (MMAD); 1.5		1 h	↓ in some animals at all concentrations; progressive slowing in some animals with continued exposures.	Schlesinger et al. (1978)
H <sub>2</sub> SO <sub>4</sub>	Rat, M SD 200 g	Nose-only (39%; 85%)	3,600	1.0 (MMAD); 1.9-2.3		4 h	NC	Phalen et al. (1980)
NH <sub>4</sub> HSO <sub>4</sub>	Rabbit, M mixed 2.5-2.7 kg	Oral tube (78%)	600-1,700	0.4 (MMAD); 1.6		1 h	↓ at 1,700 $\mu\text{g}/\text{m}^3$	Schlesinger (1984)
(NH <sub>4</sub> ) <sub>2</sub> SO <sub>4</sub>	Rabbit, M mixed 2.5-2.7 kg	Oral tube (78%)	2,000	0.4 (MMAD); 1.6		1 h	NC	Schlesinger (1984)
(NH <sub>4</sub> ) <sub>2</sub> SO <sub>4</sub>	Rat, M SD 200 g	Nose-only (39%; 85%)	3,600	0.4 (MMAD); 1.9-2.3		4 h	NC	Phalen et al. (1980)
Alveolar								
H <sub>2</sub> SO <sub>4</sub>	Rat, M SD 200 g	Whole body (30-80%)	3,600	1.0		4 h	NC	Phalen et al. (1980)
H <sub>2</sub> SO <sub>4</sub>	Rabbit, M NZW 2.5-3 kg	Oral tube	1,000	0.3 (MMAD); 1.5		1 h	↑	Naumann and Schlesinger (1986)
H <sub>2</sub> SO <sub>4</sub>	Rabbit, M NZW 2.5-3 kg	Nose-only (80%)	250	0.3 (MMAD); 1.6		1 h/day, 5 days/week, 1, 57, 240 day	↑	Schlesinger and Gearhart (1986)

**TABLE 11-7 (cont'd). EFFECTS OF ACIDIC SULFATE PARTICLES ON RESPIRATORY TRACT CLEARANCE**

Particle	Species, Gender, Strain, Age, or Body Weight	Exposure Technique (RH)	Mass Concentration ( $\mu\text{g}/\text{m}^3$ )	Particle Characteristics		Exposure Duration	Observed Effect	Reference
				Size ( $\mu\text{m}$ ); $\sigma_g$				
Alveolar (cont'd)								
H <sub>2</sub> SO <sub>4</sub>	Rabbit, M NZW 3-3.5 kg	Nose-only (80%)	500	0.3 (MMAD); 1.6		2 h/day, 14 days	↓	Schlesinger and Gearhart (1987)

Key to abbreviations:  
 NC: No significant change  
 ↑: Significant increase  
 ↓: Significant decrease  
 PE: Post exposure

where little acid deposits, while slowing clearance from the distal ciliated airways where there is greater acid deposition. At higher concentrations, mucociliary clearance from both the proximal and distal bronchial tree becomes depressed (Leikauf et al., 1984).

Comparison of responses to  $\text{H}_2\text{SO}_4$  show interspecies differences in the sensitivity of mucociliary clearance to acid aerosols. As an example, the acceleration of tracheal transport found by Wolff et al. (1986) in the rat with  $\approx 100,000 \mu\text{g}/\text{m}^3 \text{H}_2\text{SO}_4$  seems anomalous since, in other species, levels  $\geq 1,000 \mu\text{g}/\text{m}^3$  depress mucociliary function. The reasons for this apparent discrepancy are not known. The rat is less susceptible to the lethal effects of  $\text{H}_2\text{SO}_4$ , and it does not have strong bronchoconstrictive reflex responses following  $\text{H}_2\text{SO}_4$  exposures. These characteristics suggest that the mucociliary system of the rat may also differ in sensitivity from the other species studied, a view supported by the lack of effect of  $\text{H}_2\text{SO}_4$  on bronchial clearance found by Phalen et al. (1980) following exposure at  $3,600 \mu\text{g}/\text{m}^3$  for 4 h and by the similarity in bronchial clearance response in donkeys and rabbits to single 1-h exposures of  $\text{H}_2\text{SO}_4$  (Table 11-7). Although the lack of response of tracheal transport in the guinea pig at  $\text{H}_2\text{SO}_4$  levels  $>1,000 \mu\text{g}/\text{m}^3$  is also surprising, its response at  $1,000 \mu\text{g}/\text{m}^3$  is also different from that of the rat and more in line with other species (Wolff, 1986).

The relative potency of acid sulfate aerosols, in terms of altering mucociliary clearance, is related to their acidity ( $\text{H}^+$  content). Schlesinger (1984) exposed rabbits for 1 h to submicrometer aerosols of  $\text{NH}_4\text{HSO}_4$ ,  $(\text{NH}_4)_2\text{SO}_4$ , and  $\text{Na}_2\text{SO}_4$ . Exposure to  $\text{NH}_4\text{HSO}_4$  at concentrations of  $\approx 600$  to  $1,700 \mu\text{g}/\text{m}^3$  significantly depressed clearance rate only at the highest exposure level. No significant effects were observed with the other sulfur oxides at levels up to  $\approx 2,000 \mu\text{g}/\text{m}^3$ . When these results are compared to those from a study using  $\text{H}_2\text{SO}_4$  (Schlesinger et al., 1984), the ranking of potency was  $\text{H}_2\text{SO}_4 > \text{NH}_4\text{HSO}_4 > (\text{NH}_4)_2\text{SO}_4, \text{Na}_2\text{SO}_4$ ; this strongly suggests a relation between the hydrogen ion concentration and the extent of alteration in bronchial mucociliary clearance.

The mechanism by which deposited acid aerosol alters clearance is not certain. The effective functioning of mucociliary transport depends upon optimal beating of cilia and the presence of mucus having appropriate physicochemical properties, and both ciliary beating as well as mucus viscosity may be affected by acid deposition. At alkaline pH, mucus is more fluid than at acid pH, so a small increase in viscosity due to deposited acid could "stiffen"

the mucus blanket, perhaps promoting the clearance mechanism and, thus, increasing its efficiency (Holma et al., 1977). Such a scenario may occur at low H<sub>2</sub>SO<sub>4</sub> exposure concentrations, where ciliary activity would not be directly affected by the acid, and is consistent with clearance acceleration observed at these concentrations with acute exposure. However, the exact relation between mucus viscosity and transport rate is not certain.

High concentrations of H<sub>2</sub>SO<sub>4</sub> may affect ciliary beating, as discussed in the previous CD (U.S. Environmental Protection Agency, 1982; Schiff et al., 1979; Grose et al., 1980). An additional mechanism by which deposited acid may affect mucociliary clearance is via altering the rate and/or amount of mucus secreted. A small increase in mucus production could facilitate clearance, while more excessive production could result in a thickened mucus layer which would be ineffectively coupled to ciliary beat. Finally, the airways actively transport ions, and the interaction between transepithelial ion transport and consequent fluid movement is important in maintaining the mucus lining. A change in ion transport due to deposited acid particles may alter the depth and/or composition of the sol layer (Nathanson and Nadel, 1984), perhaps affecting clearance rate. In any case, the pathological significance of transient alterations in bronchial clearance rates in healthy individuals is not certain, but such changes are an indication of a lung defense response. On the other hand, persistent impairment of clearance may lead to the inception or progression of acute or chronic respiratory disease and, as such, may be a plausible link between inhaled acid aerosols and respiratory disease.

Short-term exposures to acid aerosols may lead to persistent clearance changes, as indicated previously (Schlesinger et al., 1978). The effects of long-term exposures were investigated by Schlesinger et al. (1983), who exposed rabbits to 250 or 500 μg/m<sup>3</sup> H<sub>2</sub>SO<sub>4</sub> (0.3 μm, MMAD) for 1 h/day, 5 days/week for 4 weeks, during which time bronchial mucociliary clearance was monitored. Clearance was accelerated on individual days during the course of the acid exposures, especially at 500 μg/m<sup>3</sup>. In addition, clearance was significantly faster, compared to preexposure levels, during a 2 week follow-up period after acid exposures had ceased.

Another long-term exposure at relatively low H<sub>2</sub>SO<sub>4</sub> levels was conducted by Gearhart and Schlesinger (1988). Rabbits were exposed to 250 μg/m<sup>3</sup> H<sub>2</sub>SO<sub>4</sub> for 1 h/day, 5 days/week for up to 52 weeks, and some animals were also provided a 3 mo follow-up

period in clean air. Clearance was slower during the first month of exposure and this slowing was maintained throughout the rest of the exposure period. After cessation of exposure, clearance became extremely slow and did not return to normal by the end of the follow-up period. Differences in the nature of clearance change between this study and that of Schlesinger et al. (1983) may be due to differences in exposure protocol daily (duration) and/or concentration. In both studies, however, and as discussed earlier, histologic analyses indicated the development of increased numbers of epithelial secretory cells, especially in small airways, the likely consequence of which would be an increase in mucus production. In addition, the slowing of clearance seen by Gearhart and Schlesinger (1988) was also associated with a shift in the histochemistry of mucus towards a greater content of acidic glycoproteins; this would tend to make mucus more viscous.

The longest duration study at the lowest concentration of H<sub>2</sub>SO<sub>4</sub> yet reported is that of Schlesinger et al. (1992b), in which rabbits were exposed to 125 μg/m<sup>3</sup> H<sub>2</sub>SO<sub>4</sub> for 2 h/day, 5 days/week for up to 52 weeks. The variability of measured bronchial clearance time was increased with acid exposure, and acceleration of clearance was noted at various times during the one-year exposure period. However, following a 6-mo observation period after exposures had ceased, a trend towards slowing of clearance was noted (compared to both control and rates during acid exposure). In addition, and consistent with previous studies, an increase in the number density of epithelial secretory cells was observed in small airways (<0.5 mm) following 12 mo of acid exposure. This histological change had resolved by the end of the 6-mo post-exposure period.

***Alveolar Region Clearance and Alveolar Macrophage Function:*** Only a few studies have examined the ability of acid aerosols to alter clearance of particles from the alveolar region of the lungs (Table 11-7). Rats exposed to 3,600 μg/m<sup>3</sup> H<sub>2</sub>SO<sub>4</sub> (1 μm) for 4 h showed no change in clearance (Phalen et al., 1980). On the other hand, acceleration of clearance was seen in rabbits exposed for 1 h to 1,000 μg/m<sup>3</sup> H<sub>2</sub>SO<sub>4</sub> (0.3 μm, MMAD) (Naumann and Schlesinger, 1986).

Two studies involving repeated exposures to acid aerosols have been reported. In one, rabbits were exposed to 250 μg/m<sup>3</sup> (0.3 μm, MMAD) H<sub>2</sub>SO<sub>4</sub> for 1 h/day, 5 days/week, and inert tracer particles were administered on days 1, 57 and 240 following the start of the acid exposures (Schlesinger and Gearhart, 1986). Clearance (measured for 14 days after each

tracer exposure) was accelerated during the first test, and this acceleration was maintained throughout the acid exposure period. In the other study (Schlesinger and Gearhart, 1987), rabbits were exposed 2 h/day for 14 days to  $500 \mu\text{g}/\text{m}^3 \text{H}_2\text{SO}_4$  ( $0.3 \mu\text{m}$ , MMAD); retardation of early alveolar region clearance of tracer particles administered on the first day of exposure was noted. The results of these two studies suggest a graded response, whereby a low exposure concentration accelerates early alveolar region clearance and a high level retards it, such as was seen with mucociliary transport following acute  $\text{H}_2\text{SO}_4$  exposure.

The mechanisms responsible for the altered alveolar region clearance patterns seen in the above studies are not known. Observed clearance is the net consequence of a number of differential underlying responses, which can include change in mucociliary transport rates and altered functioning of AMs.

A number of studies have examined the functional response of AMs following acidic sulfate aerosol exposures. To adequately perform their role in clearance, AMs must be competent in a number of functions, including phagocytosis, mobility and attachment to a surface. Alterations in any one, or combination, of these individual functions may affect clearance function. Naumann and Schlesinger (1986) noted a reduction in surface adherence and an enhancement of phagocytosis in AMs obtained by lavage from rabbits following a 1-h exposure to  $1,000 \mu\text{g}/\text{m}^3 \text{H}_2\text{SO}_4$  ( $0.3 \mu\text{m}$ ). The acid exposure produced no change in the viability or numbers of recoverable AMs.

In a study with repeated  $\text{H}_2\text{SO}_4$  exposures, AMs were lavaged from rabbits exposed to  $500 \mu\text{g}/\text{m}^3 \text{H}_2\text{SO}_4$  ( $0.3 \mu\text{m}$ ) for 2 h/day for up to 13 consecutive days (Schlesinger, 1987). Macrophage counts increased after 2 of the daily exposures, but returned to control levels thereafter. Neutrophil counts remained at control levels throughout the study, suggesting no acute inflammatory response. Random mobility of AMs decreased after 6 and 13 of the daily exposures. The number of phagocytically active AMs and the level of such activity increased after 2 exposures, but phagocytosis became depressed by the end of the exposure series. Although such studies demonstrate that  $\text{H}_2\text{SO}_4$  can alter AM function, they have not as yet been able to provide a complete understanding of the cellular mechanisms which may underly the changes in pulmonary region clearance observed with exposure to acid aerosols.

The relative potency of acidic sulfate aerosols in terms of altering AM numbers or function has been examined. Aranyi et al. (1983) found no change in total or differential

counts of free cells lavaged from mice exposed to  $1,000 \mu\text{g}/\text{m}^3$   $(\text{NH}_4)_2\text{SO}_4$  for 3 h/day for 20 days; this suggests a lack of inflammatory response to this sulfate aerosol. Additional studies seem to suggest that the response to acid sulfates of AM is a function of the  $\text{H}^+$ . Schlesinger et al. (1990a) examined phagocytic activity of AMs recovered from rabbits exposed for 1 h/day for 5 days to either 250 to  $2,000 \mu\text{g}/\text{m}^3$   $\text{H}_2\text{SO}_4$  ( $0.3 \mu\text{m}$ ) or 500 to  $4,000 \mu\text{g}/\text{m}^3$   $\text{NH}_4\text{HSO}_4$  ( $0.3 \mu\text{m}$ ); the levels were chosen such that the  $\text{H}^+$  concentration in the exposure atmospheres were equivalent for both sulfate species. Phagocytic activity of AMs was reduced following exposure to  $\geq 1,000 \mu\text{g}/\text{m}^3$   $\text{H}_2\text{SO}_4$  or to  $4,000 \mu\text{g}/\text{m}^3$   $\text{NH}_4\text{HSO}_4$ ; exposure to  $2,000 \mu\text{g}/\text{m}^3$   $\text{NH}_4\text{HSO}_4$  resulted in increased phagocytic activity. While these exposure concentrations were quite high, the interesting observation was that for a given level of sulfate, the response to  $\text{H}_2\text{SO}_4$  was greater than that to  $\text{NH}_4\text{HSO}_4$ . However, even when the data were assessed in terms of  $\text{H}^+$  concentration in the exposure atmosphere, it was noted that exposure to the same concentrations of  $\text{H}^+$  did not result in identical responses for the two different acid sulfate species;  $\text{H}^+$  appeared to be more effective as the  $\text{H}_2\text{SO}_4$  species. On the other hand, when AMs were incubated in acidic environments in vitro, the phagocytic activity response was identical, regardless of the sulfate species used, as long as the pH was the same. These results suggested an enhanced potency of  $\text{H}_2\text{SO}_4$  during inhalation exposures. Experimental evidence provided by Schlesinger and Chen (1994) indicated that this difference noted in vivo was likely a reflection of different degrees of neutralization by respiratory tract ammonia of the two species of inhaled acid aerosols. It was shown that, for a given concentration of ammonia and within a given residence time within the respiratory tract, more total  $\text{H}^+$  remained available from inhaled sulfuric acid than from inhaled ammonium bisulfate when the exposure atmospheres had the same total  $\text{H}^+$  concentration. Thus, the greater observed potency of inhaled sulfuric acid compared to ammonium bisulfate for exposure atmospheres containing the same total  $\text{H}^+$  concentration is likely due to a greater degree of neutralization of the latter, and a resultant greater loss of  $\text{H}^+$  prior to particle deposition onto airway surfaces. Thus, the respiratory "fate" of inhaled acid sulfate particles should be considered in assessing the relationship between exposure atmosphere and biological response, since a lower  $\text{H}^+$  concentration will likely deposit onto lung tissue than is inhaled at the mouth or nose.

Interspecies differences in the effects of acid sulfates on AM function were examined by Schlesinger et al. (1992a). Based upon in vitro exposures of AM to acidic media, a ranking of response in order of decreasing sensitivity to acidic challenge and subsequent effect on phagocytic activity was found to be: guinea pig>rat>rabbit>human.

As noted with other endpoints, the effect of H<sub>2</sub>SO<sub>4</sub> upon AM function may be dependent upon particle size. Chen et al. (1992a) observed that 300 μg/m<sup>3</sup> H<sub>2</sub>SO<sub>4</sub> enhanced the phagocytic activity of AMs recovered from guinea pigs after 4 days (3 h/day) of exposure to fine particles (0.3 μm), while an identical exposure to ultrafine particles (0.04 μm) depressed phagocytic function.

The effects of acid sulfates upon the intracellular pH of AMs has been examined, because this may be one of the determinants of the rate of many cellular functions (Nucitelli and Deamer, 1982). Internal pH of AMs recovered from guinea pigs exposed to 300 μg/m<sup>3</sup> H<sub>2</sub>SO<sub>4</sub> was depressed after a single 3-h exposure to both 0.3 and 0.04 μm particles, but the depression persisted for 24 h following exposure to the smaller size (Chen et al., 1992a). A depression in pH was also noted 24 h following 4 days of exposure to the ultrafine, but not the fine, aerosol. Thus, acid exposure produced a change in intracellular pH of the AMs and the effect was particle size dependent.

It is possible that this and other differences in response between fine and ultrafine particles reflect, to some extent, differences in the number of particles in aerosols of these two size modes, in that at a given mass concentration of acid sulfate, there are a greater number of ultrafine than fine particles. To examine this possibility, Chen et al. (1995) noted that changes in intracellular pH of macrophages obtained following inhalation exposure to H<sub>2</sub>SO<sub>4</sub> aerosols were dependent both upon the number of particles as well as upon the total mass concentration of H<sup>+</sup> in the exposure atmosphere, with a threshold existing for both exposure parameters. The role of size in modulating toxicity due to PM is discussed further in Section 11.4. It should, however, be noted that aside from number, differences in deposition and neutralization may also affect differential responses to fine and ultrafine particles.

A possible mechanism underlying the acid-induced alterations in intracellular pH was examined by Qu et al. (1993), who exposed guinea pigs to 969 μg/m<sup>3</sup> H<sub>2</sub>SO<sub>4</sub> (0.3 μm MMD, σ<sub>g</sub> 1.73) for 3 h or to 974 μg/m<sup>3</sup> for 3 h/day for 5 days. Macrophages were

obtained following the end of each exposure protocol and examined for the ability of internal pH to recover from an added intracellular acid load. Both H<sub>2</sub>SO<sub>4</sub> exposures resulted in a depression of internal pH recovery compared to air control. Subsequent analysis indicated that this alteration in internal pH regulation was attributable to effects on the Na<sup>+</sup>/H<sup>+</sup> exchanger located in the cell membrane.

Macrophages are the source of numerous biologically active chemicals, and the effects of acid sulfate upon some of these have been investigated. Zelikoff and Schlesinger (1992) exposed rabbits to 50 - 500 μg/m<sup>3</sup> H<sub>2</sub>SO<sub>4</sub> (0.3 μm) for 2 h. AM recovered by lavage following exposure were assessed for effects on tumor necrosis factor (TNF) release/activity and production of superoxide radical, both of which are biological mediators involved in host defense. Exposure to H<sub>2</sub>SO<sub>4</sub> at ≥ 75 μg/m<sup>3</sup> produced a reduction in TNF cytotoxic activity, as well as a reduction in stimulated production of superoxide radical. Subsequently, Zelikoff et al. (1994) exposed rabbits for 2 h/day for 4 days to sulfuric acid at 500, 750 or 1,000 μg/m<sup>3</sup>. AM recovered from animals exposed at the highest acid level showed a reduction in TNF and interleukin (IL)-1α production/activity, both immediately and 24 h following the last exposure. On the other hand, increased release of TNF from macrophages obtained from guinea pigs was observed immediately following a single 3 h exposure, and 24 h following a 3 h/day 4 day exposure, to 300 μg/m<sup>3</sup> H<sub>2</sub>SO<sub>4</sub> (0.3 μm or 0.04 μm) (Chen et al., 1992a); in addition, production of hydrogen peroxide by these cells was enhanced immediately after the 4 day exposure. These differences in TNF may reflect interspecies differences in response to acid exposure and/or differences in experimental conditions.

### ***Resistance to Infectious Disease***

The development of an infectious disease requires both the presence of the appropriate pathogen, as well as host vulnerability. There are numerous anti-microbial host defenses with different specific functions for different microbes (e.g., there are some differences in defenses against viruses and bacteria). The AM represents the main defense against gram positive bacteria depositing in the alveolar region of the lungs. The ability of acid aerosols to modify resistance to bacterial infection could result from a decreased ability to clear microbes, and a resultant increase in their residence time, due to alterations in AM function. To test this possibility, a rodent infectivity model has been frequently used. In this

technique, mice are challenged with a bacterial aerosol after exposure to the pollutant of interest; mortality rate and/or survival time are then examined within a particular postexposure time period. Any decrease in the latter or increase in the former indicates impaired defense against respiratory infection. A number of studies which have used the infectivity model (primarily with *Streptococcus sp.*) to assess effects of acid aerosols were discussed in the previous CD (U.S. Environmental Protection Agency, 1982). It was evident that acute exposures to H<sub>2</sub>SO<sub>4</sub> aerosols at concentrations up to 5,000 μg/m<sup>3</sup> were not very effective in enhancing susceptibility to this bacterially-mediated respiratory disease in the murine model. More recent studies with mice, shown in Table 11-8, continue to support this conclusion.

However, a study using another animal suggests that H<sub>2</sub>SO<sub>4</sub> may indeed alter antimicrobial defense. Zelikoff et al. (1994) exposed rabbits for 2 h/day for 4 days to 500, 750, or 1,000 μg/m<sup>3</sup> H<sub>2</sub>SO<sub>4</sub>. Intracellular killing of a bacterium, *Staphylococcus aureus*, by AMs recovered by lavage 24 h following the last exposure at the two highest acid concentrations was reduced; bacterial uptake was also reduced at the same time point, but only at the highest acid level. Thus, repeated H<sub>2</sub>SO<sub>4</sub> exposures may reduce host resistance to bacteria in the rabbit, in contrast to no effect on this endpoint in the mouse.

### ***Specific Immune Response***

Most of the database involving effects of acid aerosols on lung defense is concerned with non-specific mechanisms. Little is known about the effects of these pollutants on humoral (antibody) or cell-mediated immunity. Since numerous potential antigens are present in inhaled air, the possibility exists that acid sulfates may enhance immunologic reaction and, thus, produce a more severe response, and one with greater pulmonary pathogenic potential. Pinto et al. (1979) found that mice which inhaled H<sub>2</sub>SO<sub>4</sub> for 0.5 h daily and were then exposed weekly to a particulate antigen (sheep red blood cells) exhibited higher serum and bronchial lavage antibody titers than did animals exposed to the antigen alone; unfortunately, neither the exposure mass concentration nor particle size of the H<sub>2</sub>SO<sub>4</sub> was described. The combination of acid with antigen also produced morphologic damage, characterized by mononuclear cell infiltration around the bronchi and blood vessels, while

**TABLE 11-8. EFFECTS OF ACID SULFATES ON BACTERIAL INFECTIVITY IN VIVO**

Particle	Species, Gender, Strain, Age, or Body Weight	Exposure Technique (RH)	Mass Concentration ( $\mu\text{g}/\text{m}^3$ )	Particle Characteristics		Exposure Duration	Observed Effect	References
				Size ( $\mu\text{m}$ ); $\sigma_g$				
H <sub>2</sub> SO <sub>4</sub>	Mouse, F CD-1 30 days	Head-only (31%)	543	0.08 (VMD); 2.3		2 h	NC	Grose et al. (1982)
H <sub>2</sub> SO <sub>4</sub>	Mouse, F CD-1 30 days	Head-only (31%)	365	0.06 (VMD); 2.3		2 h/day, 5 days	NC	Grose et al. (1982)
(NH <sub>4</sub> ) <sub>2</sub> SO <sub>4</sub>	Mouse, F CD-1 30 days	Whole body	1,000	Submicrometer		3 h/day, 20 days	NC	Aranyi et al. (1983)

NC: No change

exposure to acid or antigen alone did not. Thus, the apparent adjuvant effect of H<sub>2</sub>SO<sub>4</sub> may be a factor promoting lung inflammation.

Osebold et al. (1980) exposed mice to 1,000 μg/m<sup>3</sup> H<sub>2</sub>SO<sub>4</sub> (0.04 μm, CMD) to determine whether this enhanced the sensitization to an inhaled antigen (ovalbumin). The exposure regimen involved intermittent 4 day exposures, up to 16 total days of exposure; no increase in sensitization compared to controls was found. Kitabatake et al. (1979) exposed guinea pigs to 1,910 μg/m<sup>3</sup> H<sub>2</sub>SO<sub>4</sub> (<1 μm, MMAD) for 0.5 h twice per week for 4 weeks, followed by up to 10 additional paired treatments with the H<sub>2</sub>SO<sub>4</sub> for 0.5 h each; the animals were then exposed to aerosolized albumin for another 0.5 h. The breathing pattern of the animals was monitored for evidence of dyspnea. Enhanced sensitization was found after ≈4 of the albumin exposures. A subsequent challenge with acetylcholine suggested hyperresponsive airways.

Fujimaki et al. (1992) exposed guinea pigs to 300, 1,000, and 3,200 μg/m<sup>3</sup> H<sub>2</sub>SO<sub>4</sub> for 2 or 4 weeks, following which lung mast cell suspensions were examined for antigen-induced histamine release. Exposure for 2 weeks at the two highest concentrations resulted in enhanced histamine release, but this response dissipated by 4 weeks of exposure. Thus, H<sub>2</sub>SO<sub>4</sub>, at high concentrations, may affect the functional properties of mast cells; these cells are involved in allergic responses, including bronchoconstriction.

### 11.2.3

#### **Mixtures Containing Acidic Sulfate Particles**

Most of the toxicological data concerning effects of PM are derived from exposures using single compounds. Although such information is essential, it is also important to study responses which result from inhalation of typical combinations of materials, because population exposures are generally to mixtures. Toxicological interaction provides a basis whereby ambient pollutants may show synergism (effect greater than the sum of the parts) or antagonism (effect less than the sum of the parts). Thus, the lack of any toxic effect following exposure to an individual pollutant should always be interpreted with caution, because mixtures may act differently than expected from the same pollutants acting separately. Most toxicologic studies of pollutant mixtures involved exposures to mixtures containing only two materials. These are summarized first below for mixtures containing

acidic aerosols (see Table 11-9); complex acid aerosol mixture studies (i.e., those using more than 2 compounds) are then discussed.

The extent of any toxicological interaction involving acidic sulfate aerosols has been shown to depend on the endpoint being examined, as well as on the co-inhalant. Most studies of interactions using acidic sulfates employed ozone ( $O_3$ ) as the co-pollutant. Depending upon the exposure regimen, endpoint, and animal species, either additivity, synergism, or antagonism has been observed. These studies are summarized in the  $O_3$  criteria document (U.S. Environmental Protection Agency, 1995). Interaction studies of  $H_2SO_4$  and nitrogen dioxide ( $NO_2$ ) are discussed in the nitrogen oxides criteria document pollutant (U.S. Environmental Protection Agency, 1993). The nature of interactions was dependent on the protocol; no unifying principles emerged. It is important to recognize that the nature of particle-pollutant interactions are specific for a given endpoint and set of exposure conditions and no attempt should be made to generalize from those specific observations discussed in the  $O_3$  and  $NO_x$  criteria documents.

Kitabatake et al. (1979) exposed guinea pigs to  $H_2SO_4$  aerosol (average  $1910 \mu g/m^3$ ) or  $SO_2 + H_2SO_4$  aerosol (average 145 ppm and  $1890 \mu g/m^3$ ) for 30 min, twice a week for 4 weeks prior to albumin exposure. After the preexposures, the guinea pigs were treated 10 times with paired exposures to the sulfur oxides for 30 min followed by treatment with the antigen (albumin) aerosol for another 30 min. The results indicate that exposures to high concentrations of sulfur oxides ( $SO_2 + H_2SO_4$  aerosol or  $H_2SO_4$  aerosol alone) may increase hyperreactivity to albumin in guinea pigs.

In a study designed to determine if effects of exposure to  $H_2SO_4$  aerosol were exacerbated in the presence of other particulate matter, Henderson et al. (1980a) exposed rats to  $H_2SO_4$  aerosol (MMAD =  $.8 \mu m$ ,  $\sigma_g = 1.7$ ) in the presence or absence of 70,000  $\mu g/m^3$  fly ash (MMAD =  $6.0 \mu m$ ,  $\sigma_g = 2.0$ ). Lung damage in the rats was determined by BAL one day after exposure to the fly ash and 1,000, 10,000, or 100,000  $\mu g/m^3$   $H_2SO_4$  for 6 h. BAL from animals exposed to high levels of sulfuric acid alone, to the ash alone, or to both showed an increase in sialic acid and in acid phosphatase activity. Lactate dehydrogenase and glutathione reductase activities were elevated in the combined exposures. The presence of a separate particulate aerosol did not greatly modify the response of the rat lung to  $H_2SO_4$ .

**TABLE 11-9. TOXICOLOGIC EFFECTS OF MIXTURES CONTAINING ACIDIC AEROSOLS**

Co-Pollutant			Acid Particle			Exposure Conditions	Species, Gender Strain, Age and Body Weight	Endpoints	Response to Mixture	Interaction	Reference
Chemical	$\mu\text{g}/\text{m}^3$	ppm	Chemical	$\mu\text{g}/\text{m}^3$ ( $\mu\text{m}$ )	Exposure Regime						
ZnO	(0.05 $\mu\text{m}$ , MMAD, $\sigma_g = 1.86$ )		H <sub>2</sub> SO <sub>4</sub>	25 or 84	3 h	Nose-only	GP, M Hartley 250-300 g	BAL eicosanoids PE		Concentration dependent ↑ in PGF2 $\alpha$ compared to ZnO alone	Chen et al. (1989)
ZnO	(0.05 CMD, $\sigma_g = 2$ )		H <sub>2</sub> SO <sub>4</sub> (coated on particles)	24 or 84		Nose-only	Guinea pig, M, Hartley 260-325 g	Pulmonary function	Animals exposed to acid had greater decrease in lung volume and DL <sub>co</sub>	Acid layered on particle enhanced response to subsequent O <sub>3</sub> or acid exposure	Chen et al. (1991)
O <sub>3</sub>	0.15		H <sub>2</sub> SO <sub>4</sub> pure	300 (0.08)							
ZnO	up to 2,760 $\mu\text{g}/\text{m}^3$ (0.05 $\mu\text{m}$ MMAD, $\sigma_g = 2.0$ )		H <sub>2</sub> SO <sub>4</sub> (coated on particle)	20-30 $\mu\text{g}/\text{m}^3$ (0.05 $\mu\text{m}$ MMAD, $\sigma = 2.0$ )	1 h	Head-only	Guinea pig	Airway responsiveness to acetylcholine		Acid-coated particles caused hyperresponsiveness	Chen et al. (1992b)
			H <sub>2</sub> SO <sub>4</sub>	202 $\mu\text{g}/\text{m}^3$ (0.06 $\mu\text{m}$ MMAD, $\sigma = 1.36$ )						Similar changes at 10 × concentration of coated particles	
SO <sub>2</sub>		145	H <sub>2</sub> SO <sub>4</sub>	1,890 (<1 $\mu\text{m}$ , MMAD)	0.5 h, twice weekly for 4 weeks; then 0.5 h twice weekly with antigen or constrictor challenge	Head-only	Guinea pig	Sensitization to inhaled antigen (albumin); responsiveness to acetylcholine		Enhanced response compared to H <sub>2</sub> SO <sub>4</sub> alone	Kitabatake et al. (1979)
Fly ash	70,000 (6 $\mu\text{m}$ , MMAD)		H <sub>2</sub> SO <sub>4</sub>	1,000, 10,000, 100,000 (0.8 $\mu\text{m}$ , MMAD, $\sigma_g = 1.7-1.8$ )	6 h	Chamber	Rat	Lavage indices (LDH, acid phosphatase, glutathione reductase)		Minimal interaction: response largely due to H <sub>2</sub> SO <sub>4</sub> ; increase in LDH and glutathione reductase only in combined exposure	Henderson et al. (1980a)

**TABLE 11-9 (cont'd). TOXICOLOGIC EFFECTS OF MIXTURES CONTAINING ACIDIC AEROSOLS**

Co-Pollutant		Acid Particle		Exposure Regime	Exposure Conditions	Species, Gender Strain, Age and Body Weight	Endpoints	Response to Mixture	Interaction	Reference
Chemical	$\mu\text{g}/\text{m}^3$ ppm	Chemical	$\mu\text{g}/\text{m}^3$ ( $\mu\text{m}$ )							
HNO <sub>3</sub> (vapor) Diesel exhaust	380 460 (0.15)	H <sub>2</sub> SO <sub>4</sub>	180 (no size stated)	5 h/day, 5 days		Rat, M, Sprague-Dawley	Macrophage phagocytosis; receptor activity	Macrophage phagocytosis, F <sub>c</sub> receptor activity decreased	Not determined	Prasad et al. (1988)
HNO <sub>3</sub> (vapor) Diesel exhaust	380 550 (0.15 $\mu\text{m}$ MMAD)	H <sub>2</sub> SO <sub>4</sub>	180 (no size stated)	5 h/day, 5 days	Nose-only	Rat, M, Sprague-Dawley, 6 wk	Macrophage phagocytosis; morphology; tracheobronchial and mucociliary clearance	No change in cell turnover in nose, trachea, alveolar epithelium; no deep lung lesions; ↓ phagocytosis; no clearance effects	Not determinable	Prasad et al. (1990)
ZnO	up to 2500 $\mu\text{g}/\text{m}^3$ (0.05 $\mu\text{m}$ emd, $\sigma_g = 2$ )	H <sub>2</sub> SO <sub>4</sub> (coated on ZnO particles)	20-30 $\mu\text{g}$	3 h/day for 5 days		Guinea pig	Pulmonary function	Reductions in total lung vol. vital capacity, DL <sub>50</sub> severity inc. with increasing exposure duration, inc. protein, PMNs in BAL		Amdur and Chen (1989)

A few studies have examined the effects of exposure to multicomponent (complex) atmospheres containing acidic sulfate particles. Studies of mixtures containing O<sub>3</sub> or NO<sub>2</sub> are summarized elsewhere (U.S. Environmental Protection Agency, 1993, 1995).

A series of studies discussed in the previous PM/SO<sub>x</sub> CD (U.S. Environmental Protection Agency, 1982) involved exposure of dogs to simulated auto exhaust atmospheres (e.g., Hyde et al., 1978) for 16 h/day for 68 mo followed by a 32- to 36-mo period in clean air. The mixture consisted of 90 μg/m<sup>3</sup> H<sub>2</sub>SO<sub>4</sub> + 1,100 μg/m<sup>3</sup> SO<sub>2</sub>, with and without irradiated auto exhaust (which results in production of oxidants) and nonirradiated auto exhaust. The results were dependent on the time of examination, exposure, and the endpoint. The primary finding was that groups exposed to SO<sub>2</sub> and H<sub>2</sub>SO<sub>4</sub> showed emphysema like changes, observed 32- to 36-mo postexposure. The authors considered the specific changes to be analogous to an incipient stage of human centrilobular emphysema. SO<sub>2</sub> alone would be unlikely to produce such a deep lung response. Also, from the pulmonary function results, it did not appear that auto exhaust exacerbated the effects of the SO<sub>2</sub>-H<sub>2</sub>SO<sub>4</sub> mixture.

Prasad et al. (1988) exposed rats for 5 h/day for 5 days to an atmosphere consisting of 460 μg/m<sup>3</sup> diluted diesel exhaust (0.15 μm), 380 μg/m<sup>3</sup> HNO<sub>3</sub> vapor, and 180 μg/m<sup>2</sup> H<sub>2</sub>SO<sub>4</sub> (present as a surface coat on the diesel particles). Reduced activity of macrophage surface (Fc) receptors and phagocytosis were noted, but interaction could not be determined since the individual components were not tested separately. In another related study, Prasad et al. (1990) examined particle clearance, lung histology and macrophage phagocytic activity following nose-only exposures of rats (Sprague-Dawley, M, 6 weeks) for 5 h/day for 5 days to atmospheres consisting of 380 μg/m<sup>3</sup> HNO<sub>3</sub> vapor, 550 μg/m<sup>3</sup> diluted diesel exhaust, and 180 μg/m<sup>3</sup> H<sub>2</sub>SO<sub>4</sub> coated on the diesel particles (0.15 μm). There was no change in tracheobronchial or pulmonary clearance of tracer particles with this mixture, compared to air controls. While no deep lung lesions nor any change in turnover rate of epithelial cells from the nose, trachea or alveolar region were noted, there was a decrease in the percentage of total macrophages assessed which had internalized diesel particles following exposure to the mixture, compared to cells recovered from animals exposed to the diesel particles alone. Furthermore, phagocytosis was depressed up to 3 days following exposure to the mixture.

The enhanced effect of the particles with the surface acid coat is consistent with studies, described below, with other acid-coated particles.

Amdur and Chen (1989) exposed guinea pigs to simulated primary emissions from coal combustion processes, produced by mixing ZnO, SO<sub>2</sub>, and water in a high temperature combustion furnace. The animals were exposed 3 h/day for 5 days to ultrafine (0.05 μm CMD, σ<sub>g</sub>=2) aerosols of zinc oxide (ZnO) at up to 2,500 μg/m<sup>3</sup> having a surface coating of H<sub>2</sub>SO<sub>4</sub> resulting from this process (ZnO had no effect in this study). Levels of SO<sub>2</sub> in the effluent ranged from 0.2 to 1 ppm. Acid sulfate concentrations as low as 20 to 30 μg/m<sup>3</sup> as equivalent H<sub>2</sub>SO<sub>4</sub> delivered in this manner resulted in significant reductions in total lung volume, vital capacity, and DL<sub>co</sub>. The effects appeared to be cumulative, in that the severity was increased with increasing exposure duration. These exposures also resulted in an increase in the protein content of pulmonary lavage fluid and an increase in PMNs. The investigators noted that much higher exposure levels of pure H<sub>2</sub>SO<sub>4</sub> aerosol were needed to produce comparable results, suggesting that the physical state of the associated acid in the pollutant mixture was an important determinant of response. But one confounder in these studies was that the number concentration was greater for the coated particles than for the pure acid particles and, as mentioned earlier, both number and mass concentrations of the exposure atmosphere likely play roles in the biological responses.

Other studies have examined responses to acid-coated particles. Chen et al. (1989) exposed (nose-only) guinea pigs (male, Hartley, 250 to 300g) for 3 h to ultrafine ZnO (0.05 μm, σ<sub>g</sub>=1.86) onto which was coated 25 or 84 μg/m<sup>3</sup> H<sub>2</sub>SO<sub>4</sub>. Selected eicosanoids were examined in lavage fluid obtained at 0, 72, and 96 h post-exposure. Immediately following exposure, animals exposed to the higher acid concentration showed increased levels of prostaglandin F<sub>2α</sub> compared to those found in animals exposed to ZnO alone. Levels of prostaglandins E<sub>1</sub> and 6-keto-PGF<sub>1α</sub>, thromboxane B<sub>2</sub> and leukotriene B<sub>4</sub> were similar to those found in animals exposed to the metal alone. During the post-exposure period, changes in prostaglandin E<sub>1</sub>, leukotriene B<sub>4</sub> and thromboxane B<sub>2</sub> were noted. But the authors suggested that there was no causal relationship between these changes and alterations in pulmonary function noted earlier (Amdur et al., 1986).

Chen et al. (1992b) exposed guinea pigs to acid-coated ZnO for 1 h, and examined airway responsiveness to acetylcholine administered 1.5 h after exposure. In this study, the

equivalent concentrations of  $\text{H}_2\text{SO}_4$  were 20 and 30  $\mu\text{g}/\text{m}^3$  coated on the 0.05  $\mu\text{m}$  ZnO particles. Animals were also exposed to pure  $\text{H}_2\text{SO}_4$  droplets at 202  $\mu\text{g}/\text{m}^3$  and having a similar size as the coated particles (0.06  $\mu\text{m}$ ,  $\sigma_g=1.36$ ). Hyperresponsiveness was found in animals exposed to the acid-coated particles, but not in those exposed to furnace gases (particle-free control) or to the ZnO alone. A similar quantitative change was noted in those animals exposed to the pure droplet at about 10 times the concentration of the coated particles (Amdur and Chen, 1989).

Amdur and Chen (1989) exposed guinea pigs for 3 h or for 3 h/day for 5 days to a similar atmosphere as above and examined pulmonary function. Levels of 30  $\mu\text{g}/\text{m}^3$   $\text{H}_2\text{SO}_4$  produced a significant depression in diffusing capacity (DLco). Repeated exposures at the equivalent of 21  $\mu\text{g}/\text{m}^3$   $\text{H}_2\text{SO}_4$  resulted in reduced DLco after the 4th exposure day; at the higher (30  $\mu\text{g}/\text{m}^3$ ) level of coated acid, DLco decreased gradually from the first exposure day.

The interaction of acid coated particles with ozone was examined by Chen et al. (1991). Guinea pigs (male, Hartley, 260 to 325 g) were exposed (nose-only) to sulfuric acid coated ZnO particles (0.050  $\mu\text{m}$  CMD,  $\sigma_g=2$ ) at 24 or 84  $\mu\text{g}/\text{m}^3$   $\text{H}_2\text{SO}_4$  or pure acid (0.08  $\mu\text{m}$ ) at 300  $\mu\text{g}/\text{m}^3$  for 2 h, followed by 2 h rest period and 1 h additional exposure (whole body) to air or 0.15 ppm  $\text{O}_3$ . Other animals were exposed to acid coated ZnO having an equivalent acid concentration (24  $\mu\text{g}/\text{m}^3$ ) for 3 h/day for 5 days. This was followed by exposure for 1 h to 0.15 ppm  $\text{O}_3$  on day 9, or to two additional 3 h exposures to 24  $\mu\text{g}/\text{m}^3$   $\text{H}_2\text{SO}_4$  layered-ZnO on days 8 and 9. In the single exposure series, animals exposed only to the higher coated acid concentration followed by ozone showed greater than additive changes in vital capacity and DLco, while those exposed first to the pure acid droplet did not show any change greater than that due to ozone alone. Animals exposed repeatedly and then to the two added acid exposures showed greater reductions in lung volumes and DLco than did those that did not receive the additional acid exposures. Finally, animals exposed to ozone after acid showed reduced lung volumes and DLco not observed in animals exposed to either ozone alone or acid alone. In terms of acid alone, neither single exposure to the coated acid affected the endpoints, while exposure to the pure acid decreased DLco. The investigators concluded that single or multiple exposures to the acid-coated ZnO resulted in an enhanced response to subsequent exposures to acid or ozone and that the manner in which the acid was

delivered (i.e., as a pure droplet or as a surface coating) affected whether or not any interaction occurred. However, it is likely that the number concentration of particles was greater in the zinc oxide aerosol than in the pure acid aerosol, and the interaction may reflect this greater particle number. It should also be noted that ZnO itself may have produced some biological response, or contributed to any interaction with the acid, in some of the studies reported for some endpoints.

Wong et al. (1994) exposed rats (M; F-344, nose-only) for 4 h/day, 4 days/week for 8 weeks to a complex mixture consisting of 350  $\mu\text{g}/\text{m}^3$  California road dust (5  $\mu\text{m}$  MMAD) + 65  $\mu\text{g}/\text{m}^3$   $(\text{NH}_4)_2\text{SO}_4$  (0.3  $\mu\text{m}$ ) + 365  $\mu\text{g}/\text{m}^3$   $\text{NH}_4\text{NO}_3$  (0.6  $\mu\text{m}$ ) +  $\text{O}_3$  (0.2 ppm), as well as to  $\text{O}_3$  alone. Animals were sacrificed at 4 or 17 days after the last exposure to assess stress inducible heat shock protein as an indicator of early pulmonary injury. An increase in heat shock protein was observed with the mixture at both time points, but the effect of  $\text{O}_3$  was greater than that due to the mixture.

Mannix et al. (1982) examined the effects of a 4 h exposure of rats to a  $\text{SO}_2$ -sulfate mix, consisting of  $\text{SO}_2$  (13,000  $\mu\text{g}/\text{m}^3$ ) plus 1,500  $\mu\text{g}/\text{m}^3$  (0.5  $\mu\text{m}$ , MMAD) of an aerosol containing  $(\text{NH}_4)_2\text{SO}_4$  and  $\text{Fe}_2(\text{SO}_4)_3$ . No change in particle clearance from the tracheobronchial tree or pulmonary region was found.

## 11.3 METALS

### 11.3.1 Introduction

The metals discussed in this section are generally present in the ambient atmosphere of U.S. urban areas in concentrations greater than 0.5  $\mu\text{g}/\text{m}^3$  (see Chapter 3, Table 3-10) and include arsenic, cadmium, copper, iron, lead, vanadium, and zinc. While other metals are present in the ambient air, they are found at concentrations less than 0.5  $\mu\text{g}/\text{m}^3$  and are not reviewed here. There are no reported toxicological studies of acute effects of inhaled metals at or below this concentration.

The information presented has primarily been obtained from occupational and laboratory animal studies. Both of these data sources have limitations that affect their usefulness to ambient particulate matter discussion. In the occupational studies, the exposures are not well-characterized and may be confounded by exposure to other materials

such as PAH, toxic gases, and other respirable particulate. Moreover, the concentrations of metals experienced in occupational settings as well as the exposure concentrations and the doses administered in the laboratory animal studies are generally hundreds to several thousand times greater than the concentrations found in the ambient air (about 1-14  $\mu\text{g}/\text{m}^3$ ).

These sections are intended as general summaries of each metal since the majority, with the exception of lead, do not have current documentation or health risk standards. However, review articles and criteria documents from other agencies are cited as sources of additional information. While there are many studies available using higher concentrations and other routes of administration than inhalation, a select summary only of the effects of inhaling metals on humans and animals is presented in Table 11-10 where an attempt was made, where possible, to focus on those studies that reported effects at the lowest exposures. Each section briefly discusses data on acute and chronic effects from inhaling metals in humans and laboratory animals. Endpoints (developmental effects and other non-respiratory endpoints) not immediately related to the epidemiological findings presented in Chapter 12 are not included in this discussion but are presented in the references cited. End points seen with routes of exposure other than inhalation are not discussed.

### **11.3.2 Arsenic**

***Human Data:*** The toxicity data on inhalation exposures to arsenic are limited in number and quality. Long-term occupational exposure to arsenic leads to a range of health effects such as lung cancer, skin changes and peripheral nerve damage in workers. Most of the available human inhalation data on arsenic are based on occupational exposures to arsenic trioxide.

In humans, acute symptoms are seen after airborne exposure to high levels of arsenic trioxide in an occupational setting. Symptoms include severe irritation of the nasal mucosa, larynx, and bronchi (Holmqvist, 1951; Pinto and McGill, 1953). It is not clear if these effects were chemically related to arsenic or a result of irritation due to the dusts inhaled. Irritation of mucous membranes of the nose and throat leading to hoarseness, laryngitis, bronchitis, or rhinitis and sometimes perforation of the nasal septa have been reported in workers exposed to arsenic dusts (Pinto and McGill, 1953), but effect levels cannot be set due to insufficient exposure data. Increased peripheral vasospastic disorders and Raynaud's

**TABLE 11-10. RESPIRATORY SYSTEM EFFECTS OF INHALED METALS ON HUMANS AND LABORATORY ANIMALS**

Metal (Ambient Concentrations) <sup>a</sup>	Subjects	Effects <sup>b</sup>	References
Arsenic (0.002-2.32 $\mu\text{g}/\text{m}^3$ )	In humans	Resp. tract irritation, laryngitis, bronchitis, rhinitis. Effects absent at 100-1,000 $\mu\text{g}/\text{m}^3$ .	Agency for Toxic Substances and Disease Registry (1993)
	In animals	Decreased bactericidal activity, inc mortality in streptococcal assay at 500-940 $\mu\text{g}/\text{m}^3$ .	Aranyi et al. (1985)
Cadmium (0.0002-7.0 $\mu\text{g}/\text{m}^3$ )	In humans	Acute exposure: resp. tract irritation, bronchiolitis, alveolitis, impaired lung function, and emphysema; mild and reversible symptoms with exposure to 200-500 $\mu\text{g}/\text{m}^3$ . Chronic exposure: kidneys and resp. tract affected; effects include proteinuria and emphysema, with exposure to 20 $\mu\text{g}/\text{m}^3$ for 27 years.	Agency for Toxic Substances and Disease Registry (1989)
		In animals	Mild inflammation; AM and epithelial hyperplasia in rat at 500 $\mu\text{g}/\text{m}^3$ for 3 h; lesions repaired at 7-15 days postexposure. Effects similar to humans. Dose-dependent fibrotic lesions in lungs of rats exposed to 300-1,000 $\mu\text{g}/\text{m}^3$ for 12 weeks.
		Hyperplasia of terminal bronchioles, cell flattening, inflammation and proliferation of fibroblasts in rat at $\geq 300$ $\mu\text{g}/\text{m}^3$ , 6 h/day, 5 days/week, 62 days.	Kutzman et al. (1986)
		BAL fluid changes at 1,600 $\mu\text{g}/\text{m}^3$ , 3 h/day, 5 days/week, 1-6 weeks indicative of lung damage. Aggregates of PMNs in interstitium, thickening of alveolar septa. Effects peaked at 2 weeks, then dec.	Hart (1986)
		Inc number and size of AM in rat at 100 $\mu\text{g}/\text{m}^3$ , 22 h/day, 7 days/week, 30 days, returning to normal 2 mo postexposure.	Glaser et al. (1986a)
		In rabbit at 400 $\mu\text{g}/\text{m}^3$ , 6 h/day, 5 days/week, 4-6 weeks, inc lung weight, interstitial infiltration of PMNs and lymphocytes, intraalveolar accumulation of large, vacuolated macrophages, inc phospholipid content.	Johansson et al. (1984)
		In mouse at 30-90 $\mu\text{g}/\text{m}^3$ , 8 or, 19 h/day, 5 days/week, 42-69 weeks inc incidence of alveolar lipoproteinosis, interstitial fibrosis, bronchoalveolar hyperplasia.	Heinrich et al. (1989a)

**TABLE 11-10 (cont'd). RESPIRATORY SYSTEM EFFECTS OF INHALED METALS ON HUMANS AND LABORATORY ANIMALS**

Metal (Ambient Concentrations) <sup>a</sup>	Subjects	Effects <sup>b</sup>	References
Copper (0.003-5.14 $\mu\text{g}/\text{m}^3$ )	In humans	Subjective symptoms and clinical tests (CBC, LDH determination, urinalysis) after outbreak of metal fume fever: fever, dyspnea, chills, headache, nausea, myalgia, cough, shortness of breath, sweet metallic taste, vomiting, 1-10 h occup exposure. Complaints of discomfort similar to onset of common cold; chills or warmth; stuffiness of the head, 75-120 $\mu\text{g}/\text{m}^3$ , few weeks occup exposure.	Agency for Toxic Substances and Disease Registry (1990)
	In animals	Mild respiratory tract effects in hamster: Decreased cilia beating frequency and abnormal epithelium at 3,300 $\mu\text{g}/\text{m}^3$ , 3 h/day.	Agency for Toxic Substances and Disease Registry (1990)
		In mouse exposed for 3 h/day, 5 days/week, 1-2 weeks slight alveolar thickening and irregularities after 5 exposures at 120 $\mu\text{g}/\text{m}^3$ , extensive thickening with many walls fused into irregular masses and dec mean survival time after 10 exposures at 130 $\mu\text{g}/\text{m}^3$ . Dec bactericidal activity in both exposure groups.	Agency for Toxic Substances and Disease Registry (1990)
Iron (0.13-13.80 $\mu\text{g}/\text{m}^3$ )	In humans	Subjective symptoms, chest X ray: siderosis in 3 males. Note: concurrent exposure to several other chemicals; $\geq 10,000 \mu\text{g}/\text{m}^3$ , 2 mo-12 years (occup).	Sentz and Rakow (1969)
		34% prevalence of siderosis; complaints of chronic coughing and breathlessness, 3,500-269,000 $\mu\text{g}/\text{m}^3$ , 10 year (avg).	Teculescu and Albu (1973)
	In animals	Respiratory tract cell injury (not specified) in hamsters, alveolar fibrosis, 14,000 $\mu\text{g}/\text{m}^3$ , 1 mo.	Creasia and Nettesheim (1974)
		Impaired respiration in rats, blood nasal discharge at 6,800 and 22,000 $\mu\text{g}/\text{m}^3$ , 6 h/day 5 days/week, 4 weeks.	BASF Corporation (1991)

**TABLE 11-10 (cont'd). RESPIRATORY SYSTEM EFFECTS OF INHALED METALS  
ON HUMANS AND LABORATORY ANIMALS**

Metal (Ambient Concentrations) <sup>a</sup>	Subjects	Effects <sup>b</sup>	References
Vanadium (0.0004-1.46 $\mu\text{g}/\text{m}^3$ )	In humans	Bronchial irritation (cough, mucous formation) postexposure at 60 $\mu\text{g}/\text{m}^3$ . Cough at 100, 600 $\mu\text{g}/\text{m}^3$ 8 h lasted about 1 week.	Zenz and Berg (1967)
		Productive cough, runny nose, sore throat, wheezing, 100-300 $\mu\text{g}/\text{m}^3$ , 2 years (occup).	Lewis (1959)
	In humans	Rhinitis, nasal discharge, irritated throat, bronchopneumonia, "asthmatic" bronchitis, est $\leq 6,500$ , 1-2 years (occup)	Sjöberg (1950)
	In animals	Alveolar proteinosis in rat at 17,000 $\mu\text{g}/\text{m}^3$ , 6 h/day, 5 days/week, 2 weeks; dose-related inc lung weight, inc accumulation of macrophages, collagen deposition, lung lipid content, and Type II pneumocytes.	Lee and Gillies (1986)
		Reduced lung function in monkey at 2,500 $\mu\text{g}/\text{m}^3$ , 6 h, inc pulmonary resistance; inc leukocytes in bronchoalveolar lavage.	Knecht et al. (1985)
		In rat, nasal discharge (sometimes containing blood), difficulty breathing, dec BW; hemorrhages in lung, heart, liver, kidney, brain. bronchitis, focal interstitial pneumonia in lungs. Effects mainly in lungs at low concentration. Mild signs of toxicity at 2,800 $\mu\text{g}/\text{m}^3$ .	Roshchin (1967a)
	In rats	Capillary congestion, perivascular edema, hemorrhages in lungs. Also focal edema and bronchitis in some cases, lymphocyte infiltration of interstitial spaces, constriction of small bronchi, 1,700-2,800 $\mu\text{g}/\text{m}^3$ , 2 h/every other day, 3 mo.	Roshchin (1967a)

**TABLE 11-10 (cont'd). RESPIRATORY SYSTEM EFFECTS OF INHALED METALS  
ON HUMANS AND LABORATORY ANIMALS**

Metal (Ambient Concentrations) <sup>a</sup>	Subjects	Effects <sup>b</sup>	References
Zinc (0.015-8.328 $\mu\text{g}/\text{m}^3$ )	In humans	Symptoms metal fume fever: Nausea, chills, shortness of breath and chest pains at 320,000-580,000 $\mu\text{g}/\text{m}^3$ , 1-3 h.	Agency for Toxic Substances and Disease Registry (1994)
		Fever, chills, chest tightness, muscle/joint pain, sore throat, headache at 4-8 h postexposure; inc airway resistance of 16%, 4,900 $\mu\text{g}/\text{m}^3$ , 2 h/day, 1 day (face mask).	Gordon et al. (1992)
		Significant correlation between change in peak expiratory flow rate and dust concentration, 6-8 h workshift.	Marquart et al. (1989)
		BAL fluid changes; inc number of leukocytes, T cells, T suppressor cells, and NK cells; inc PMN leukocytes, with 77,000-153,000 $\mu\text{g}/\text{m}^3$ , 15-30 min (occup).	Blanc et al. (1991)
		Miminal substernal irritation and throat irritation during exposure, 3.6 $\mu\text{g}/\text{m}^3$ , 2 h.	Linn et al. (1981)
	In animals	BAL fluid: Inc protein, LDH, and $\beta$ -glucuronidase, inflammation at 2,200 $\mu\text{g}/\text{m}^3$ , 3 h/day 1 day in rat.	Gordon et al. (1992)
		BAL fluid: Inc protein, LDH, and $\beta$ -glucuronidase (suggesting altered macrophage function), inflammation at 2,200 $\mu\text{g}/\text{m}^3$ , 3 h/day 1 day in guinea pig.	
		Impaired lung function (dec compliance and lung volume, inc pulmonary resistance, dec CO diffusing capacity at 3,700 $\mu\text{g}/\text{m}^3$ , 3 h/day 6 day in guinea pig.	Lam et al. (1985)
		Inc lung weight; inflammation, and increased interstitial thickening, fibroblasts, and interstitial infiltrates at 4,300 $\mu\text{g}/\text{m}^3$ .	
		Dec pulmonary compliance, followed by inc during 2-h postexposure, at 730 $\mu\text{g}/\text{m}^3$ , 1 h in guinea pig.	Amdur et al. (1982)

<sup>a</sup>Ambient air concentration range associated with metal particulate matter in the United States atmosphere (see Chapter 1, Table 1-4).

<sup>b</sup>Abbreviations: dec = decreased; inc = increased; occup = occupational; PAH = polycyclic aromatic hydrocarbons; ALK = alkaline phosphatase; BAL = bronchoalveolar lavage; AM = pulmonary alveolar macrophage; PMN = polymorphonuclear leukocyte; res = respiratory.

phenomenon were found in Swedish arsenic workers exposed to airborne arsenic dusts (Lagerkvist et al., 1986).

*Laboratory Animal Data:* Limited acute data were available on the inhalation toxicity of arsenic in animals. Aranyi et al. (1985) exposed mice to an aerosol of arsenic trioxide for 3 h at levels of 0, 270, 500, or 940  $\mu\text{g arsenic}/\text{m}^3$ . Additional groups were exposed for 3 h/day for 5 or 20 days. At the end of exposure, mice were challenged with an aerosol exposure of viable streptococci, and death of exposed and controls was recorded over 14 days. Separate groups were challenged with aerosols of  $^{35}\text{S}$ -labeled *Klebsiella pneumoniae* to evaluate macrophage function (bacterial killing) in a 3-h period. In the streptococcal assay, a concentration-related increase in mortality occurred. Bactericidal activity was markedly decreased after a single exposure to 940  $\mu\text{g arsenic}/\text{m}^3$ , but no consistent or significant effects were seen at lower exposure levels after one or several exposures.

In a chronic inhalation study, male Wistar rats (20 to 40/group) were continuously exposed to 0, 60, or 200  $\mu\text{g arsenic}/\text{m}^3$  as arsenic trioxide for 18 mo (Glaser et al., 1986b). No effects on body weight, hematology, clinical chemistry, or macroscopic and microscopic examination outcomes were observed.

### **11.3.3 Cadmium**

Recent reviews and health criteria documents have detailed the toxicological and carcinogenic effects of cadmium by different routes of administration including inhalation (Oberdörster, 1989a,b; Waalkes and Oberdörster, 1990; International Agency for Research on Cancer, 1993). Acute and chronic health effects observed after cadmium exposure were mostly related to occupational settings and occurred after exposures to concentrations far exceeding those occurring environmentally. Average airborne cadmium concentrations in rural areas range from 0.0002 to 0.006  $\mu\text{g}/\text{m}^3$ , and in urban areas concentrations from 0.002 to 0.025  $\mu\text{g}/\text{m}^3$  have been found which can increase in industrial areas by a factor of 3 to 5. Health effects at these low airborne concentrations of cadmium have not been reported; the following summary indicates that health effects observed in humans and animals are correlated with higher occupational exposure concentrations ranging up to the  $\text{mg}/\text{m}^3$  levels. Thus, exposure to much lower ambient environmental airborne concentrations of cadmium

are unlikely to contribute to acute health effects. It should also be considered that exposure to cadmium occurring in cigarette smoke by far exceeds background ambient air concentrations. When evaluating health effects of inhaled cadmium compounds it should be considered that *in vivo* solubility of the different cadmium compounds is different from their water solubility. For example, CdO and CdS are both insoluble in water, yet CdO is rapidly soluble in the lung, possibly in the acidic milieu of alveolar macrophages after phagocytosis, whereas CdS is highly insoluble in the lung, behaving more like a low toxicity particle (Oberdörster, 1989b).

### 11.3.3.1 Health Effects

**Human Data:** Table 11-10 summarizes data from studies of occupationally-exposed workers which show that the main target organs for cadmium toxicity are the kidney and the respiratory tract. This table is restricted to those studies where exposures to airborne cadmium concentrations were less than  $100 \mu\text{g}/\text{m}^3$  since it is felt that effects observed from exposures to higher airborne cadmium concentrations are irrelevant for low concentrations of environmental cadmium and particulate matter. With respect to renal damage, these low environmental concentrations will not lead to significant accumulation of cadmium in the kidney to reach the critical concentration of  $200 \mu\text{g}/\text{g}$  which will result in symptoms of kidney damage, e.g., proteinuria. Earlier studies found evidence of proteinuria after occupational exposures to  $50 \mu\text{g}/\text{m}^3$  for up to 12 years (Kjellstrom et al., 1977). More recent analyses found the threshold of cadmium exposure for proteinuria at close to  $1,000 \mu\text{g}/\text{m}^3 \times \text{year}$  (Elinder et al., 1985a,b; Mason et al., 1988). Obviously, these exposure concentrations are far above those encountered environmentally and will not be considered further in the context of this document.

Acute respiratory effects of inhaled cadmium have been reported as pneumonitis and edema if exposure concentrations exceed  $1,000 \mu\text{g}/\text{m}^3$  for periods of 1 h or more. Chronic cadmium exposures resulting in emphysema and dyspnea have also been reported when exposure concentrations are very high, exceeding for extended periods of time several hundred  $\mu\text{g}/\text{m}^3$ . Chronic exposure concentrations below  $100 \mu\text{g}/\text{m}^3$  at occupational settings have been associated with induction of lung tumors (International Agency for Research on Cancer, 1993). Recent analyses of English and Swedish cohorts as well as an American

cohort found a statistically significant excess risk of lung cancer in the highest exposure groups (Elinder et al., 1985c; Sorahan, 1987; Thun et al., 1985). Based on these studies, IARC determined that cadmium is a human carcinogen. However, environmentally encountered airborne cadmium concentrations are too low to induce lung cancer, unless it is postulated that a combination of cadmium plus other air contaminants results in a synergistic carcinogenic effect. Excess of prostate cancer due to occupational inhalation of cadmium observed in earlier epidemiological studies have not been confirmed in later studies (IARC, 1993).

*Laboratory Animal Data:* Health effects of inhaled cadmium compounds are summarized in Table 11-10. Like with the human studies, only those studies are listed where exposure concentrations below  $100 \mu\text{g}/\text{m}^3$  were used. These studies in laboratory animals confirm that inhalation exposure to cadmium compounds can result in respiratory tract injury. Very high exposure concentrations ( $\text{mg}/\text{m}^3$ ) are needed to cause acute effects such as lung edema and alveolar epithelial cell necrosis, whereas lower exposure concentrations at  $\sim 50 - 100 \mu\text{g}/\text{m}^3$  can induce chronic inflammatory responses including bronchoalveolar hyperplasia, proliferation of connective tissue leading to interstitial fibrosis (Takenaka et al., 1983). The most striking effect at low exposure concentrations in rats is that different cadmium compounds were shown to cause lung cancer (Takenaka et al., 1983; Glaser et al., 1990). These studies reported primary lung tumors (bronchoalveolar adenoma, adenocarcinoma, squamous cell tumors) following exposure to  $\text{CdCl}_2$ ,  $\text{CdSO}_4$ ,  $\text{CdS}$  and  $\text{CdO}$  inhaled as dust or fume. Exposure concentrations were as low as  $10 \mu\text{g}/\text{m}^3$ , adding to the evidence from human occupational exposure studies that inhaled Cd-compounds can induce lung tumors. In contrast to rats, mice and hamsters exposed to the different cadmium compounds at similar concentrations did not induce lung tumors (Heinrich et al., 1989a). The reason for the significant species differences may be the different inducibility of metallothionein (MT) as well as different baseline levels of MT in the lungs of mice and rats which was demonstrated by Oberdörster et al. (1994a). These authors found that a four-week inhalation exposure to  $\text{CdCl}_2$  aerosols at an exposure concentration of  $100 \mu\text{g}/\text{m}^3$  caused greater and more persistent inflammation and cell proliferation in the lungs of mice than in rats. At the same time MT was induced to a greater degree in mice, possibly protecting the lungs of this species from the cytotoxic effects of inhaled cadmium.

In summary, these studies demonstrate that measured low environmental cadmium concentrations alone are not likely to be causally associated with acute effects on mortality and morbidity observed in epidemiological studies; nor are they likely to cause long-term chronic effects. Cadmium exposure at relatively high exposure concentrations has been shown to lead to a decreased immune response in mice (Graham et al., 1978; Krzystyniak et al., 1987) which could suggest that people with a compromised immune system may also be affected more than healthy people by exposure to cadmium. However, environmental low level cadmium concentrations have not been shown to induce these effects.

### 11.3.4 Copper

**Human Data:** The data on human exposure to copper by inhalation are limited. The major target organ appears to be the respiratory system, but the data are limited to occupational studies. Data are primarily based on subjective symptoms without indications of pulmonary function changes as a result of occupational exposure to copper. The observed symptoms may also be due to exposure to copper by both oral and inhalation routes since exposures were confounded. The lack of control workers is also a limitation in evaluating the human data available for copper exposure by inhalation. A combination of respiratory symptoms has been reported following acute inhalation exposure to copper in humans. Armstrong et al. (1983) reported the following symptoms (in order of number of workers affected): fever, dyspnea, chills, headache, nausea, myalgia, cough, shortness of breath, a sweet metallic taste and vomiting in factory workers accidentally exposed to copper dust or fumes for 1 to 10 h as a result of cutting pipes known to contain copper. These symptoms are consistent with metal fume fever, an acute disease induced by inhalation of metal oxides that temporarily impairs pulmonary function but does not progress to chronic lung disease (Stokinger, 1981a). Airborne copper concentration during the exposure period was not reported. It was reported that 5 of 12 workers hospitalized following the acute exposure had urine copper levels greater than 50  $\mu\text{g/L}$ . Since the major route of excretion of copper is biliary, the elevated urine copper levels reported suggest that the exposure concentration was relatively high. Copper levels were not determined for control workers in this study which limits the interpretation of the urinary copper values as an indicator of copper inhalation exposure. Armstrong et al. (1983) also reported evidence of minimal elevation of serum

lactate dehydrogenase (in 3 of 14 workers evaluated) and leukocytosis (in 21 of 24 workers evaluated). Nonspecific complaints of discomfort and chills were reported among several workers within a few weeks of beginning operation of a copper plate polishing operation. Exposure levels of 75 to 120  $\mu\text{g}/\text{m}^3$  were measured (Gleason, 1968).

In an epidemiological study by Suciú et al. (1981), factory workers exposed to copper dust received annual physical and clinical examinations during a 4 year exposure period. The reported air copper levels were not reported for the first year, were 464,000  $\mu\text{g Cu}/\text{m}^3$  in the second year; 132,000  $\mu\text{g Cu}/\text{m}^3$  in the third year; and 111,000  $\mu\text{g Cu}/\text{m}^3$  in the fourth year. Although inhalation was considered to be the major route of exposure for these workers, it was likely that a portion of the airborne copper was trapped in the upper respiratory tract and swallowed. This assumption was made based on the gastrointestinal effects that were observed in these workers in addition to the respiratory effects. Respiratory effects reported included symptoms of coughing, sneezing, yellowish-green expectoration, dyspnea, and thoracic pain. Radiography revealed linear pulmonary fibrosis and in some cases nodulation. Limitations of this study include the absence of a control group, poor description of study design and the lack of statistical analysis of data.

Respiratory effects were also noted in a report by Askergrén and Mellgren (1975). Nose and throat examinations were performed in sheet-metal workers exposed to copper dust. Six of 11 workers had nasal mucosa characterized by increased vascularity and superficial epistatic vessels. This was accompanied by symptoms of runny nose and mucosal irritation in the mouth and eyes. However, the levels of airborne copper were not measured.

**Laboratory Animal Data:** As with human exposure, the respiratory system appears to be the primary site of injury following inhalation exposure to copper. Drummond et al. (1986) reported a decrease in tracheal cilia beating frequency following a single exposure to 3,300  $\mu\text{g Cu}/\text{m}^3$  (as a copper sulfate aerosol) in hamsters, but not in mice exposed to the same level. Alveolar thickening was observed in mice exposed repeatedly and the severity of the effect increased with the duration of exposure. Histological examination of the trachea revealed abnormal epithelium in mice at 5 exposures at 120  $\mu\text{g Cu}/\text{m}^3$ , extensive thickening and decreased mean survival time after 10 exposures at 130  $\mu\text{g Cu}/\text{m}^3$ .

Immunological effects were observed in mice (Drummond et al., 1986) and in rabbits (Johansson et al., 1983) exposed to copper sulfate aerosols. Mice exposed to either a single

concentration of 560  $\mu\text{g Cu/m}^3$  or 10 exposures to 130  $\mu\text{g Cu/m}^3$ , and simultaneously challenged with an aerosol of *Streptococcus zooepidemicus* had decreased survival time (Drummond et al., 1986). Decreased bactericidal activity was also observed in mice after exposure to an aerosol of *Klebsiella pneumonia* after single or repeated exposures to copper sulfate aerosols (Drummond et al., 1986), suggesting that copper can inhibit the function of alveolar macrophages. After inhalation exposure, Johansson et al. (1983) also observed a slight increase in the amount of lamellated cytoplasmic inclusions in alveolar macrophages. Exposures of rabbits to copper chloride aerosols for 4 to 6 weeks resulted in a minor increase in volume density of alveolar Type 2 cells and minor levels of lymphocytic or eosinophilic inflammatory infiltrates (Johansson et al., 1984).

### 11.3.5 Iron

**Human Data:** Most of the available human inhalation data on iron are based on occupational exposures to iron oxide, with effects limited to respiratory symptoms and dysfunction. There are no acute human inhalation data on the effects of iron exposure. Health effects information via inhalation route is limited to iron pentacarbonyl. No information was located on the soluble iron salts including ferric chloride, ferric nitrate, and ferric sulfate.

Occupational exposure occurs from mining of iron ores, consisting mainly of oxide forms. During the mining and during smelting and welding process, workers are often exposed to dust containing iron oxides and silica, as well as other metals and substances. It is known that exposure to iron oxides results in roentgenological changes in the lung due to deposition of inhaled iron particles (Doig and McLaughlin, 1936; Musk et al., 1988; Plamenac et al., 1974), designated variously as siderosis, iron pneumoconiosis, hematite pneumoconiosis, iron pigmentation of the lung, and arc welder lung (Elinder, 1986). Siderosis is prevalent in 5 to 15% of iron workers exposed for more than 5 years (Buckell et al., 1946; Schuler et al., 1962; Sentz and Rakow, 1969). Exposure levels were reported to exceed 10,000  $\mu\text{g iron/m}^3$  by Sentz and Rakow (1969); but no exposure data were presented for the other studies. A Romanian study (Teculescu and Albu, 1973) reported a 34% prevalence of siderosis in workers exposed to ferric oxide dust (3,500 to 269,000  $\mu\text{g/m}^3$ ); but radiological evidence of lung fibrosis was not observed. Complaints of

chronic coughing were reported by 80% of the workers. Morgan (1978) found a male subject exposed chronically to ferric oxide (magnetite;  $\text{Fe}_3\text{O}_4$ ) had symptoms of coughing and sputum for 8-9 years and exhibited an abnormal chest x-ray, but pulmonary function tests revealed no abnormalities. Stokinger (1984) reviewed the literature on occupational exposure to iron oxide fumes, and concluded that most investigators considered the roentgenological pulmonary changes, secondary to inhalation of iron dust (i.e., siderosis), as benign and did not suspect them to progress to fibrosis. Although several case reports have described iron oxide workers, with coughing and shortness of breath, exhibiting diffuse fibrosis in their chest x-rays (Charr, 1956; Friede and Rachow, 1961; Stanescu et al., 1967), concurrent exposure to other chemicals may have contributed to this finding (Chan-Yeung et al., 1982; Sitas et al., 1989).

Several studies report high incidence of lung cancer mortality among workers exposed to iron oxide in mines and smelters; but, in all cases, there was simultaneous exposure to other potentially carcinogenic substances (Boyd et al., 1970; Faulds, 1957). Improvements in dust control and ventilation of mines after 1967 have also resulted in reduction of lung cancer mortality in iron ore mine workers (Kinlen and Willows, 1988).

Iron oxide particles have been used both as a tracer and as a carrier particle for radioactive tracers (e.g., Te) in human (Leikauf et al., 1984; Gerrard et al., 1986; Ilowite et al., 1989; Bennett et al., 1992; Bennett and Zeman, 1994; Bennett et al., 1993) and laboratory animal studies (Okuhata et al., 1994, Brain et al., 1994; Warheit and Hartsky, 1993; Dorries and Valberg, 1992; Warheit et al., 1991a,c; Bellmann et al., 1991; Lehnert and Morrow, 1985; Brain et al., 1984; Valberg, 1984; Skornik and Brain, 1983) to measure different aspects of pulmonary deposition and clearance. In general, the exposures were brief and the concentrations of iron used in these studies were extremely high compared to those found in the ambient atmosphere. There were no reported acute effects of exposure to these iron oxide particles.

**Laboratory Animal Data:** Two acute inhalation studies reported clinical signs relating to respiratory distress in rats exposed to iron pentacarbonyl for 4 h or 1 mo (BASF Corporation, 1991; Bio/Dynamics Incorporated, 1988). However, histopathology was not performed on the lungs. Acute exposure of rats to  $500,000 \mu\text{g iron}/\text{m}^3$  as iron oxide for greater than 30 min also resulted in coughing, respiratory difficulties, and nasal irritation

(Hewitt and Hicks, 1972 as cited in Elinder, 1986) and histopathology of the lungs revealed iron oxide particles in macrophage cells. Ten intratracheal installations of ferric oxide in hamsters produced loss of ciliated cells, and hyperplasia and proliferation of non-ciliated epithelial cells in the lungs (Port et al., 1973). Intratracheal instillation of iron oxides in female rats produced tumors in 70% of the animals but did not reduce the life-span (Pott et al., 1994). At a longer duration of 1 mo, hamsters inhaling 14,000  $\mu\text{g iron}/\text{m}^3$  as ferric oxide dust (MMAD of 0.11  $\mu\text{m}$ ) revealed respiratory tract cell injury and alveolar fibrosis (Creasia and Nettesheim, 1974).

See also the discussion below on transition metals (Section 11.3.8) regarding ferric iron ( $\text{Fe}^{3+}$ ) complexed on the surface of silicates. There it is noted, for example that newly emerging studies by Ghio et al. (1992) and others suggest that  $\text{Fe}^{3+}$  complexed on the surface of silicate particles may be responsible for inflammatory responses associated with silicate inhalation.

### 11.3.6 Vanadium

**Human Data:** Acute and chronic inhalation studies in humans are generally limited to occupational case studies and epidemiology studies in workers engaged in the industrial production and use of vanadium. Based on these studies, the respiratory tract is the primary target of vanadium inhalation. Most of the reported exposures are to vanadium pentoxide dusts.

Acute and chronic respiratory effects were most commonly seen following exposure to vanadium pentoxide dusts. Mild respiratory distress (cough, wheezing, chest pain, runny nose, or sore throat) was observed in workers exposed to vanadium pentoxide dusts or vanadium in fuel oil smoke for as few as 5 h (Levy et al., 1984; Musk and Tees, 1982; Thomas and Stiebris, 1956; Zenz et al., 1962) or as long as 6 years (Lewis, 1959; Orris et al., 1983; Sjöberg, 1956; Vintinner et al., 1955; Wyers, 1946). Most clinical signs reflect the irritative effects of vanadium on the respiratory tract; only at concentrations  $>1,000 \mu\text{g vanadium}/\text{m}^3$  were more serious effects on the lower respiratory tract observed (bronchitis, pneumonitis). Rhinitis, pharyngitis, bronchitis, chronic productive cough, wheezing, shortness of breath, and fatigue were reported by workers following chronic inhalation of vanadium pentoxide dusts (Sjöberg, 1956; Vintinner et al., 1955; Wyers, 1946).

Two volunteers exposed to  $60 \mu\text{g vanadium}/\text{m}^3$  as vanadium pentoxide reported a delay of 7 to 24 h in the onset of mucus formation and coughing (Zenz and Berg, 1967).

Vanadium induced asthma in vanadium pentoxide refinery workers without previous history of asthma, with symptoms continuing for 8 weeks following cessation of exposure (Musk and Tees, 1982). Increased neutrophils in the nasal mucosa were reported in chronically exposed workers (Kiviluoto, 1980; Kiviluoto et al., 1979, 1981c).

Chronic occupational exposure to vanadium dusts was also associated with some electrocardiographic changes (Sjöberg, 1950). Vanadium dusts had no effect on hematology following acute exposure (Zenz and Berg, 1967) or chronic exposure (Kiviluoto et al., 1981a; Sjöberg, 1950; Vintinner et al., 1955). Blood pressure and gross neurologic signs were not affected following chronic exposure to vanadium pentoxide dusts at levels up to  $58,800 \mu\text{g vanadium}/\text{m}^3$  (Vintinner et al., 1955), although other authors reported anemia or leukopenia (Roshchin, 1964; Watanabe et al., 1966). Based on serum biochemistry and urinalysis, there was no indication of kidney or liver toxicity in workers chronically exposed to 200 to  $58,800 \mu\text{g vanadium}/\text{m}^3$  as vanadium dusts (Kiviluoto et al., 1981a,b; Sjöberg, 1950; Vintinner et al., 1955). Vanadium green discoloration of the tongue resulting from direct deposition of vanadium is often reported (Orris et al., 1983; Lewis, 1959; Musk and Tees, 1982).

**Laboratory Animal Data:** Acute and chronic laboratory animal studies support the respiratory tract as the main target of inhaled vanadium compounds. The animal data indicate that vanadium toxicity increases with increasing compound valency, and that vanadium is toxic both as a cation and as an anion (Venugopal and Luckey, 1978).

The mechanism of vanadium's effect on the respiratory system is similar to that of other metals. *In vitro* tests show that vanadium damages alveolar macrophages (Castranova et al., 1984; Sheridan et al., 1978; Waters et al., 1974; Wei and Misra, 1982) by affecting the integrity of the alveolar membrane, thus impairing the cells' phagocytotic ability, viability, and resistance to bacterial infection. Cytotoxicity, tested on rabbit alveolar macrophages *in vitro*, was directly related to solubility in the order  $\text{V}_2\text{O}_5 > \text{V}_2\text{O}_3 > \text{VO}_2$ . Dissolved vanadium pentoxide ( $6 \mu\text{g}/\text{ml}$ ) also reduces phagocytosis (Waters, 1977).

Respiratory effects in laboratory animals following acute inhalation of vanadium compounds include increased pulmonary resistance and significantly increased

polymorphonuclear leukocytes in bronchioalveolar lavage fluid. These effects were observed in monkeys 24 h following a 6-h inhalation exposure to 2,800  $\mu\text{g vanadium}/\text{m}^3$  as vanadium pentoxide (Knecht et al., 1985). In addition, increased lung weight and alveolar proteinosis were observed in rats after inhaling bismuth orthovanadate 6 h daily for two weeks (Lee and Gillies, 1986). Rabbits exposed to high concentrations of vanadium pentoxide dust for 1 to 3 days exhibited dyspnea and mucosal discharge from the nose and eyes (Sjöberg, 1950). In a follow-up experiment, rabbits had difficulty breathing following a daily 1-h exposure for 8 mo (Sjöberg, 1950).

The effects of acute exposure to 5,600 to 39,200  $\mu\text{g vanadium}/\text{m}^3$  as vanadium pentoxide fume or 44,800 to 392,000  $\mu\text{g vanadium}/\text{m}^3$  as vanadium pentoxide dust were investigated by Roshchin (1967a); the exposure duration was not described in the available literature. For vanadium pentoxide fume, "mild toxicity" occurred at 5,600  $\mu\text{g vanadium}/\text{m}^3$ , and deaths were observed at the high level. The vanadium pentoxide dust was described as one-fifth as toxic as the fume. Effects at the lower levels were mostly observed in the lungs. These included irritation of respiratory mucosa, perivascular and focal edema, bronchitis, and interstitial pneumonia. In a subchronic experiment, rats were exposed to vanadium pentoxide fume (1,700 to 2,800  $\mu\text{g vanadium}/\text{m}^3$ ) or vanadium pentoxide dust (5,600 to 17,000  $\mu\text{g vanadium}/\text{m}^3$ ) for 2 h every other day for 3 to 4 mo (Roshchin, 1967a). Histopathological effects were limited to the lungs and were similar to those observed following acute exposure. The study author concluded that vanadium inhalation resulted in irritation of the respiratory mucosa, hemorrhagic inflammation, a spastic effect on smooth muscle of the bronchi, and vascular changes in internal organs (at higher levels). Similar effects were observed with the trivalent vanadium compounds vanadium trioxide and vanadium trichloride, although vanadium trichloride caused more severe histological changes in internal organs (Roshchin, 1967b); further details were not available.

Rats exposed to vanadium pentoxide condensation aerosol (15  $\mu\text{g vanadium}/\text{m}^3$ ) continuously for 70 days developed marked lung congestion, focal lung hemorrhages, and extensive bronchitis (Pazynich, 1966).

### **11.3.7 Zinc**

Inhalation of zinc compounds, most notably zinc oxide fumes, can result in significant pulmonary irritation and inflammation referred to as metal fume fever. However, zinc is an essential element with low intrinsic toxicity, and exposure concentrations have to be in the  $\text{mg}/\text{m}^3$  range to induce these symptoms which are accompanied by increased inflammatory cell and protein levels in pulmonary lavage both in experimental animals and humans (Gordon et al., 1992). A number of studies in experimental animals and also in humans occupationally-exposed to zinc fumes have been reported, and almost all of these were related to high exposure concentrations which are irrelevant for low environmental exposure levels. A recent review of the toxicity of inhaled metal compounds including zinc in the respiratory tract (Gordon, 1995) describes a number of studies from which it can be concluded that inhaled zinc compounds including zinc oxide are rapidly solubilized in the lung and do not appear to accumulate in the respiratory tract. Elevated levels of zinc can be found in blood and urine of exposed workers as well as in exposed animals. Occupational exposures at concentrations below  $50 \mu\text{g}/\text{m}^3$  have not resulted in the occurrence of metal fume fever (Marquart et al., 1989; Linn et al., 1981). Higher exposure concentrations inhaled repeatedly result in the development of tolerance after initial symptoms of zinc fume fever subside (Gordon et al., 1992). Effects observed after acute high level exposures include dyspnea, cough, pleuritic chest pain, bilateral diffuse infiltrations, pneumothorax and acute pneumonitis from respiratory tract irritations. However, exposure concentrations have to be extremely high for the more severe symptoms to occur which has no relevance for ambient low level particulate pollutants.

### **11.3.8 Transition Metals**

An area of current investigation is the potential for the particle-associated transition metals to induce oxidant injury. The transition metals are characterized by being electronically stable in more than one oxidation state and, as a result, have the ability to catalyze the oxidative deterioration of biological macromolecules. Considering that the transition metals can catalyze the oxidative deterioration of biological macromolecules it is plausible that inhalation of PM containing these metals could cause oxidative injury to the

respiratory tract. However, the data available thus far is derived from studies using in vitro systems and intratracheal administration and can not be used for risk estimation.

Iron, the best studied of the transition metals, has the ability to catalyze the formation of reactive oxygen species (ROS) and initiate lipid peroxidation (Aust, 1989; Minotti and Aust, 1987; Imlay et al., 1988; Halliwell and Gutteridge, 1986). Guilianelli et al. (1993) studied the importance of iron to the toxicity of iron-containing particles in cultured tracheal epithelial cells. Nemalite, the most cytotoxic of the three minerals tested, contained the most surface  $\text{Fe}^{2+}$ . Moreover, pretreatment with the iron chelating compound desferrioxamine, reduced the toxic effects of nemalite.

Garrett et al. (1981a) exposed rabbit alveolar macrophages in vitro to fly ash with and without surface coatings of various metal oxides. Cellular viability and cellular adenosine triphosphate content were reduced only with the metal-coated ash particles. Berg and co-workers (1993) measured the release of ROS from bovine alveolar macrophages stimulated with heavy metal-containing dusts  $<4 \mu\text{m}$  in diameter. Dusts, derived from waste incineration, sewage sludge incineration, an electric power station, and from two factories, incubated with alveolar macrophages caused a concentration-dependent increase in ROS release. The ratio of superoxide anion ( $\text{O}_2\cdot^-$ ) and hydrogen peroxide ( $\text{H}_2\text{O}_2$ ) secreted varied, depending on the dust, but the release of  $\text{H}_2\text{O}_2$  correlated best, in descending order, with the content of iron, manganese, chromium, vanadium, and arsenic in the dusts. The positioning of iron first in this array is consistent with other studies examining the biological effects of iron coating the surface of particles.

Certain particles, including silica, crocidolite, kaolinite, and talc, complex considerable concentrations of ferric iron ( $\text{Fe}^{3+}$ ) onto their surfaces. The potential biological importance of iron complexation was assessed by Ghio and co-workers (1992) who examined the effects of surface  $\text{Fe}^{3+}$  on several indices of oxidative injury. Three varieties of silicate dusts were studied: (1) iron-loaded, (2) unmodified, and (3) desferrioxamine-treated. The ability of silicates to catalyze oxidant generation in an ascorbate/ $\text{H}_2\text{O}_2$  system in vitro, to trigger respiratory burst activity and leukotriene  $\text{B}_4$  release by alveolar macrophages, and induce lung inflammation in the rat following intra-tracheal instillation all increased in proportion to the amount of  $\text{Fe}^{3+}$  complexed onto their surfaces. Ghio and Hatch (1993) noted that an extracellular accumulation of surfactant following instillation of silica into the lungs of rats

was associated with the concentration of  $\text{Fe}^{3+}$  complexed to the surface of the particles, and that surfactant-enriched material was a target for oxidants, the production of which was catalyzed by  $\text{Fe}^{3+}$ . Moreover, iron, drawn from body stores, has been shown to complex to the surface of intratracheally instilled silica particles and increase concentrations of iron in bronchoalveolar lavage fluid, lung tissue and plasma, and decrease antioxidant molecules in lung tissue, including ascorbate, urate, and glutathione (Ghio et al., 1994).

Surface complexed iron has been implicated in pulmonary injury due to a variety of environmental particles (Costa et al., 1994a,b; Tepper et al., 1994). Three particle types (Mt. St. Helen's volcanic ash, ambient particles of Dusseldorf, Germany, and residual oil fly ash), which represented a range of inflammatory potential, were intratracheally instilled into rats. Both the degree of acute inflammation (as measured by assessing PMNs, eosinophils, LDH and protein in lavage) and nonspecific bronchial responsiveness correlated with the iron (specifically  $\text{Fe}^{+3}$ ) loading of the particles. An interesting observation was that surface iron was correlated with particle acidity, yet when instillation of  $\text{H}_2\text{SO}_4$  at comparable pH was performed, the lavage analysis indicated much less inflammation with the pure acid compared to the high surface iron particles. In fact, neutralization of the fly ash instillate (which could occur if similar particles were inhaled, due to endogeneous respiratory tract ammonia) actually enhanced particle toxicity, while the pulmonary response diminished when iron was removed from the fly ash by acid washing. These preliminary results generally support the notion that oxidant generation by iron present on the surface of particles may increase lung injury; but, clearly, other factors are likely to contribute to this response.

Tepper et al. (1994) reported that the concentration of iron ( $\text{Fe}^{3+}$ ) complexed on the surface of a particle was associated with the ability of the particle to support electron transfer and to generate oxidants in vitro and to increase lung inflammation and airway hyperresponsiveness in vivo. Particles with or without iron complexed on the surface were instilled into the lungs of rats and evaluated for their potential to produce inflammation and airway hyperactivity. The effects of a high-iron particle (coal fly ash) before and after surface iron was removed by acid washing and the effects of an inert particle (titanium), with or without iron added to the particle surface, were evaluated. The effects of pretreating the rats with drugs to reduce iron-associated ROS formation also were studied. Although coal ash caused considerable inflammation and hyperactivity, acid washing to remove surface iron

reduced the deleterious effects of the particle. However, compared to titanium alone, instillation of a titanium particle coated with iron did not increase lung injury. Pretreatment with allopurinol partially blocked lung inflammation, but desferrioxamine and an anti-neutrophil antibody were less effective. The authors concluded that the results generally support the hypothesis that ROS generation by iron on the surface of particles may exacerbate lung injury.

The inflammatory potential of 10 different metal-containing dusts of either natural or anthropogenic origin was evaluated following intratracheal instillation in rats (Pritchard et al., 1995). Measurements included (1) oxidized products of deoxyribose catalyzed by particulates, (2) induction of a neutrophilic alveolitis after particulate instillation, (3) increments in airway reactivity after particulate instillation, and (4) mortality after exposures to both dust and a microbial agent. Except for titanium, in vitro generation of oxidized products of deoxyribose increased with ionizable concentrations of all metals associated with the particles. After intratracheal instillation of the dusts in rats, the neutrophil influx and lavage protein both increased with ionizable concentrations of the same metals. Changes in airway reactivity following instillation of the dusts also appeared to be associated with the ionizable concentrations of these metals. Similarly, mortality after instillation of particles in mice followed by exposure to aerosolized *Streptococcus zooepidemicus* reflected metal concentrations. The authors concluded that in vitro measures of oxidant production and in vivo indices of lung injury increased with increasing concentrations of the metals instilled intratracheally.

Thus, it is clear that ROS produced through chemical reactions involving iron can initiate lipid peroxidation, cell injury, and ultimately cell death. It may be possible that other transition metals, by virtue of their ability to redox between valence states, also can generate ROS in the presence of precursor oxidants and reducing agents. However, it has not been established in inhalation studies that these reactions can occur in vivo.

### **11.3.9 Summary**

Data from occupational studies and laboratory animal studies indicate that acute exposures to high levels or chronic exposures to low levels (albeit high compared to ambient levels) of metal particulate can have an effect on the respiratory tract. However, it is

doubtful that the metals at concentrations present in the ambient atmosphere (1 to 14  $\mu\text{g}/\text{m}^3$ ) could have a significant acute effect in healthy individuals.

Acute and chronic inhalation exposures to arsenic, cadmium, copper, iron, and vanadium are associated with respiratory effects, and, in the case of cadmium, renal effects. However, in general, the levels used in the laboratory animal studies or experienced in occupational settings are considerably higher (at least 10-fold and as much as  $10^3$ - or  $10^4$ -fold) than those found in the ambient environment, and the results of these studies provide little insight into the morbidity and mortality studies discussed in Chapter 12. This is not unexpected because of the patterns of exposure and the total exposures, as well as differences in the populations exposed. Some of the effects noted in the human occupational studies such as respiratory tract irritation, bronchitis, impaired pulmonary function, cough, wheezing, are also observed in the epidemiological studies discussed in Chapter 12 and may indicate a general effect of PM. However, these effects are evident at exposures much greater than experienced in the ambient atmosphere. Nevertheless, the toxicological studies of the metals do not appear to provide insight into the effects observed in the epidemiological studies discussed in Chapter 12. While studies examining the potential for the transition metals to cause lung injury have been conducted in vitro and in animals by intratracheal instillation are interesting, these results thus far are of limited value.

## **11.4 ULTRAFINE PARTICLES**

This section on ultrafine particles is designed to provide an overview of current concepts concerning the potential pulmonary toxicity of this class of particulates. The occurrence of ultrafine particles in the ambient environment as well as their sources are reviewed in Chapters 3 and 6. Studies assessing the comparative toxicity of particles of different sizes using intratracheal instillation are reviewed in Section 11.9.1. Particles used in toxicological studies are mainly in the fine and coarse mode size range. This section addresses the hypothesis that ultrafine particles can cause acute lung injury and focuses on experimental studies in which ultrafine particles generated as fumes were used. The ultrafine (nucleation mode) particle phase has a median diameter of  $\approx 20$  nm (see Figure 3-13). Ultrafine particles with a diameter of 20 nm have an approximately 6 order of magnitude

higher number concentration than a 2.5  $\mu\text{m}$  diameter particle when inhaled at the same mass concentration; particle surface area is also highly increased (Table 11-1).

At present, no toxicological studies with relevant ambient ultrafine particles have been performed. Although ultrafine particles have been used in animal inhalation studies, the studies did not focus on two potentially important aspects of ultrafine particles which are addressed in this chapter; their presence in the exposure atmosphere as single particles rather than aggregates and their low solubility. Single ultrafine particles occur regularly in the urban atmosphere at high number concentrations ( $5 \times 10^4 - 3 \times 10^5$  particles/cm<sup>3</sup>) but very low mass concentrations (Brand et al., 1991; 1992; Castellani, 1993). These single ultrafine particles are not very stable and eventually aggregate with larger particles but they are always freshly-generated by a number of natural anthropogenic sources (e.g., gas to particle conversion; combustion processes; incinerator emissions). Because results of studies with relevant ambient ultrafine particles at relevant low mass concentrations (10 to 50  $\mu\text{g}/\text{m}^3$ ) are not available in the literature, effects of single ultrafine particles generated as polymer fumes are discussed in this section. Obviously, polymer fume particles do not occur in the ambient atmosphere and they serve only as a surrogate to indicate the toxic potential that some inhaled ultrafine particles may have. The hypothesis that other ultrafine particles have this toxic potential as well needs still to be tested but cannot be refuted at this time since studies with ultrafine copper oxide particles described in this section also indicate their potential to cause acute effects. Human exposure to very fine acid aerosols ( $\approx 100$  nm; 1,500  $\mu\text{g}/\text{m}^3$ ) have also been conducted (Horvath et al., 1987). No pulmonary function or symptom responses were observed suggesting that the soluble nature of these particles or their tendency to either grow or aggregate may be responsible for the fact that they did not induce responses similar to other (less soluble) ultrafine particles.

Inhalation studies in rats with aggregated ultrafine particles have shown that these particles still required high concentrations (in the mg/m<sup>3</sup> range) and repeated exposures to produce effects in laboratory animals, although they were more active than larger-sized particles of the same composition. These particles included ultrafine TiO<sub>2</sub> aggregates (Ferin et al., 1992; Oberdörster et al., 1992; Heinrich, 1994), aggregated carbon black particles (Heinrich, et al., 1995; Mauderly et al., 1994a; Nikula et al., 1995), and diesel soot (White and Garg, 1981; Rudell et al., 1990). Effects observed after subchronic or chronic exposure

of rats included chronic pulmonary inflammation, pulmonary fibrosis, and induction of lung tumors. No acute effects were observed, even at the highest exposure concentrations. Although the studies with TiO<sub>2</sub> and carbon black involved particles of ultrafine size (~20 nm), they were inhaled as aggregates which are considerably larger than single 20 nm ultrafine particles. Thus, these results may not fully reflect the toxicity of single 20 nm particles.

From these studies with aggregate ultrafine particles, it appeared that particle surface area is an important parameter for expressing exposure-response and dose-response relationships of inhaled highly insoluble particles. The significantly increased pulmonary inflammatory response of aggregated ultrafine particles is presumably because of their highly increased surface area. If the dose for particles of different sizes is expressed relative to their surface area, then responses elicited by ultrafines would be comparable with those for larger-sized particles (Oberdörster et al., 1992, 1994b). The finding that ultrafine particles can penetrate into the interstitium more easily than larger-sized particles (Takenaka et al., 1986; Ferin et al., 1992) is also very important. Transport across the epithelium appears to be facilitated if ultrafine aggregates deaggregate upon deposition and are present as single particles.

As stated above, acute pulmonary effects were not observed after inhalation of aggregates of ultrafine particles. In contrast, specific types of inhaled single ultrafine particles described below can induce severe acute lung injury at low inhaled mass concentrations relative to aggregated ultrafine particles (Oberdörster, 1995). Such model ultrafine particles can be generated by heating of polytetrafluoroethylene (Teflon<sup>®</sup>; PTFE); the resulting condensation aerosol consists of single ultrafine particles. More than 25 years ago it was recognized that the toxicity of pyrolysis products of PTFE is associated with the particulate phase rather than with gas phase constituents (Waritz and Kwon, 1968). It was demonstrated more recently that these particles are of ultrafine size (Lee and Seidel, 1991a,b; Seidel et al., 1991). These particles form upon heating of Teflon<sup>®</sup> to a critical temperature of ~420 to 450 °C and have diameters from <10 - 60 nm (median diameter of ~26 nm) (Oberdörster et al., 1995a). The toxicity of PTFE fumes has been recognized dating back to the 1950's, when exposures of rabbits, guinea pigs, rats, mice, cats, and dogs resulted in acute mortality (Treon et al., 1955). Further studies in experimental animals by several

investigators (Scheel et al., 1968; Coleman et al., 1968; Griffith et al., 1973; Lee et al., 1976; Alarie and Anderson, 1981) confirmed that these fumes are highly toxic to birds and mammals. Extensive pulmonary epithelial and interstitial damage and alveolar flooding occurred after only short-durations of exposure. Accidental exposures of humans to fumes generated from polymers also demonstrated the high toxicity of these fumes for humans (Nuttall et al., 1964; Goldstein et al., 1987; Dahlgvist et al., 1992). Associated effects include pulmonary edema, nausea and headaches, together characterized by the term "polymer fume fever" in analogy to the well-known symptoms of metal fume fever (Rose, 1992).

The toxicity of polymer fumes was initially thought to be associated with toxic gas phase products, such as hydrogen fluoride (HF), carbonyl fluoride, and perfluoroisobutylene (PFIB). However, detailed studies by Waritz and Kwon (1968) as well as more recent studies have shown that the high toxicity is associated with the particulate phase. For example, HF studies showed that concentrations as high as 1300 ppm are needed to cause effects in the upper respiratory tract of exposed rats; effects did not occur in the lung periphery where the fume particles have been shown to be most effective (Stavert et al., 1991). Concentrations of HF in fumes generated at the critical temperature are only  $\approx 10$  ppm, and therefore, cannot be responsible for the observed toxicity of the fumes (Oberdörster et al., 1995a). The more toxic gas phase compounds, carbonyl fluoride and PFIB are generated only at temperatures approaching  $500^{\circ}\text{C}$  when heating PTFE (Coleman et al., 1968; Waritz and Kwon, 1968). Furthermore, rat inhalation studies with PFIB alone showed that lung pathology was detected only when a high concentration of  $90,000 \mu\text{g}/\text{m}^3$  was exceeded (Lehnert et al., 1993). Further proof that the particles of polymer fumes represent the toxic entity is provided by studies in which the particulate phase was removed by filters and subsequently the gas phase compounds did not show toxicity in exposed rats (Waritz and Kwon, 1968; Warheit et al., 1990; Lee and Seidel, 1991a).

It has also been suggested that highly toxic radicals on the surface of the polymer fume particles may cause the acute effects. However, studies by Seidel et al. (1991) with fumes from different polymers showed similar toxicities to the lung regardless as to whether significant amounts of radicals could be detected on those particles or not. Although this still does not exclude that some reactive toxic compounds may be attached to the particle surface,

all of these studies provide strong evidence that the ultrafine particles are the cause of the PTFE fume-associated, acute lung injury. It has also been shown that aging of the fumes leading to particle aggregation diminishes their toxicity, indicating that the presence of ultrafine particles as singlets is highly important for the toxicity of these particles (Lee and Seidel, 1991b; Warheit et al., 1990).

To exclude the possibility that oxygen-derived radicals from the generation process may be responsible for the observed pulmonary toxicity, PTFE particles were generated in a nitrogen atmosphere (Waritz and Kwon, 1968) or in an argon gas atmosphere (Oberdörster et al., 1995b). Results showed that the inhaled PTFE fumes generated in this way showed the same high pulmonary toxicity in rats that was observed with PTFE fumes generated in air. The toxicity consisted of severe hemorrhagic, pulmonary edema and influx of PMNs into the alveolar space within 4 h after a 15-min exposure of healthy rats to an ultrafine particle mass concentration of about 40 to 50  $\mu\text{g}/\text{m}^3$ ; this was accompanied by high mortality (Oberdörster et al., 1995a; Johnston et al., 1995). It was also determined by these investigators that a number concentration of  $1 \times 10^5$  PTFE particles/ $\text{cm}^3$  is equivalent to a mass concentration of  $\approx 10 \mu\text{g}/\text{m}^3$ . Pulmonary lavage data showed that up to 80% of lavageable cells consisted of PMNs. Acute mortality was also observed in up to 50% of rats exposed to these concentrations of  $5 \times 10^5$  particles/ $\text{cm}^3$ . Epithelial as well as endothelial cell damage occurred, resulting in both interstitial and alveolar edema. The authors concluded that freshly-generated ultrafine PTFE particles inhaled as singlets at low mass concentrations can cause severe acute lung injury and that ultrafine particles, in general, penetrate readily through epithelial-endothelial barriers.

Additional results from studies with ultrafine PTFE particles directed at evaluating mechanistic events in the lung by using in situ hybridization techniques on lung tissue showed that the highly inflammatory reaction was characterized by significant increases in message for the pro-inflammatory cytokine  $\text{TNF}\alpha$  and the low molecular weight protein metallothionein (Johnston et al., 1995). Furthermore, increases in abundance for messages encoding  $\text{IL-1}\alpha$ ,  $\text{IL-1}\beta$ ,  $\text{IL-6}$ ,  $\text{TNF}\alpha$  and the antioxidants MnSOD and metallothionein were found in RNA extracted from lung tissues. In addition to the increase in message of these pro-inflammatory cytokines and antioxidants, abundance for message of inducible NOS was also increased, whereas message for VEGF (vascular endothelial growth factor) was

decreased in the acute phase (Johnston et al., 1995). The authors suggested that the acute lung damage affecting epithelial and endothelial barrier functions may be due to the activities of reactive oxygen species originating from activated inflammatory cells and reactive nitrogen species produced via inducible NOS.

In another effort to evaluate acute effects and disposition of inhaled ultrafine particles Stearns et al. (1994) exposed hamsters for 60 minutes to ultrafine CuO, Cu<sub>2</sub>O and Cu(OH)<sub>2</sub> particles (11 nm diameter,  $\sigma_g = 1.8$ ; approximately  $10^9$  particles/cm<sup>3</sup>). A marked 4-fold increase in pulmonary resistance was found which persisted for 24 hours. Immediately after exposure, using electron spectroscopic imaging, copper oxide particles were found not only on and within airway mucus and extracellular alveolar lining layers but also in airway and alveolar epithelial cells, in the pulmonary interstitium and in alveolar macrophages. These particles were even found in the alveolar capillaries and in pulmonary lymphatics. In addition, animals at 24 hours post-exposure showed evidence of a pulmonary inflammatory response, including the appearance of neutrophils and eosinophils.

Roth et al. (1994) demonstrated in human subjects that clearance of ultrafine particles is delayed. These workers exposed three male subjects to ultrafine particles (18 nm CMD; 27 nm MMD) of <sup>111</sup>In-labeled indium oxide for two or three breathing cycles and measured radioactivity present in the head, chest, and stomach immediately after inhalation and for 4 to 8 days at ensuing intervals. The clearance curves showed a fast clearance for particles deposited in the thorax with a mean value of 7% and a slow clearance fraction with a mean value of 93%. The half-life of the slow phase appeared to be on the order of 40 days, indicating greater persistence of the ultrafine particles rather than the larger particles (>2  $\mu$ m) in the lung.

Hatch et al. (1994) evaluated to what extent ultrafine particles (<100 nm) are present in ambient air by determining their presence in alveolar macrophages of healthy people. Alveolar macrophages isolated from lung lavage samples of 7 workers of an oil-fired power plant, 4 welders of the power plant and 3 university employees (no known occupational or environmental exposures) were studied by electron energy loss spectroscopy and electron spectroscopic imaging. Regardless of the occupation, ultrafine particles were observed in phagolysosomes of macrophages of all volunteers, there was no correlation of ultrafine particle quantity with occupation. Spectral analysis of the ultrafine particles revealed a

variety of metals including cadmium, vanadium, titanium and iron. This study demonstrates the presence of large numbers of ultrafine particles in alveolar macrophages of healthy people even in the absence of specific occupational exposure. Whether all of these particles have been inhaled as ultrafines or whether some of them dissolved in the macrophages from larger particles to the ultrafine size is not known. However, since ultrafine particles occur in the ambient air (Chapter 6) their presence in large numbers in alveolar macrophages of people demonstrates that they are effectively deposited in the deep lung, although some of them may have been inhaled as particles adsorbed to larger particles as suggested by the authors. The high deposition efficiency of inhaled single ultrafine particles in the alveolar region (Chapter 10) contributes to the plausibility of the suggestion by Hatch et al. (1994) that many of these particles were inhaled as ultrafines.

In summary, certain freshly-generated ultrafine particles, when inhaled as singlets at very low mass concentrations ( $<50 \mu\text{g}/\text{m}^3$ ), can be highly toxic to the lung. After inhalation and deposition in the lung, ultrafine particles of low solubility can rapidly penetrate epithelial cell barriers and penetrate to interstitial and endothelial sites (Stearns et al., 1994). Obviously, ultrafine particles studied in experimental animals so far (PTFE-fume, copper oxides) are not constituents of the ambient atmosphere and it is not clear how well these particles might serve as surrogates for ambient ultrafines.

Mechanisms responsible for a potential high toxicity could include: (1) high pulmonary deposition efficiencies of inhaled single ultrafine particles; (2) the large numbers per unit mass of these particles; (3) their increased surface area available for reaction; (4) their rapid penetration of epithelial layers and access of pulmonary interstitial sites; and (5) the presence of radicals and perhaps acids on the particle surface depending on the process of generation of the particles. Results of studies with model ultrafine particles indicate that particle number or total particle surface area could be more important than mass concentration (see Table 11-1).

## **11.5 DIESEL EXHAUST EMISSIONS**

Diesel engines emit both gas phase pollutants (hydrocarbons, oxides of nitrogen, and carbon monoxide) and carbonaceous PM into the ambient atmosphere. The concentration of diesel particulate in the ambient atmosphere although low is ubiquitous. The concentration of

diesel particulate in the ambient atmosphere has been estimated to be about 1-6  $\mu\text{g}/\text{m}^3$  in Los Angeles (Health Effects Institute, 1995). A description of the diesel engine, its combustion system, pollutant formation mechanisms and emission factors as well as the cancer and noncancer health effects of diesel exhaust emissions have been recently reviewed elsewhere in the Health Assessment Document for Diesel Emissions (U.S. Environmental Protection Agency, 1994) and in Diesel Exhaust: A Critical Analysis of Emissions, Exposure and Health Effects (Health Effects Institute, 1995). The endpoints discussed in this section are those associated with diesel particulate and directly related to the epidemiological results discussed in Chapter 12. Other components of diesel exhaust, such as sulfur dioxide ( $\text{SO}_2$ ), nitrogen dioxide ( $\text{NO}_2$ ), formaldehyde, acrolein, and sulfuric acid may contribute to some of these potential health effects. Endpoints not directly related to the epidemiological findings are not included in the discussion but are presented elsewhere (International Agency for Research on Cancer, 1989; Claxton, 1983; Lewtas, 1982; Ishinishi et al., 1986; Pepelko and Peirano, 1983; Pepelko et al., 1980b,c; U.S. Environmental Protection Agency, 1994; Health Effects Institute, 1995).

Within the text, exposures are expressed in terms of the mass concentration of diesel particles. Other major measured components in the studies are presented in the tables which have additional details about the studies, including references. The Health Assessment Document for Diesel Emissions (U.S. Environmental Protection Agency, 1994) that is in preparation and the Diesel Exhaust Document (Health Effects Institute, 1995) should be consulted for a complete evaluation of the health effects associated with diesel emissions.

### **11.5.1 Effects of Diesel Exhaust on Humans**

It is difficult to study the health effects of diesel exhaust in the general population because diesel emissions are diluted in the ambient air; hence, exposure is very low. Thus, populations occupationally exposed to diesel exhaust are studied to determine the potential health effects in humans. The occupations involving potential high exposure to diesel exhaust are miners, truck drivers, transportation works, railroad workers, and heavy-equipment operators. All the occupational studies considered in this section have a common problem—an inability to measure accurately the actual exposure to diesel exhaust.

The effects of short term exposure to diesel exhaust have been investigated primarily in occupationally-exposed workers (Table 11-11). Symptoms of acute exposure to high levels of diesel exhaust include mucous membrane, eye, and respiratory tract irritation (including chest tightness and wheezing) and neuropsychological effects of headache, lightheadedness, nausea, heartburn, vomiting, weakness, and numbness and tingling in the extremities. Diesel exhaust odor can cause nausea, headache, and loss of appetite.

There have been a few experimental exposures of humans to diesel exhaust, but all were single exposures. No significant changes in respiratory function were found in subjects exposed for 1 (Battigelli 1965) or 3.7 (Ulfvarsson et al., 1987) hours to diesel exhaust at approximately 1,000  $\mu\text{g soot}/\text{m}^3$  or less.

Rudell et al. (1990, 1994) exposed eight healthy subjects in an exposure chamber to diluted exhaust from a diesel engine for one hour, with intermittent exercise. Dilution of the diesel exhaust was controlled to provide a median  $\text{NO}_2$  level of approximately 1.6 ppm. Median particle number was  $4.3 \times 10^6/\text{cm}^3$ , and median levels of NO and CO were 3.7 and 27 ppm, respectively (particle size and mass concentration were not provided). There were no effects on spirometry or on closing volume using nitrogen washout. Five of eight subjects experienced unpleasant smell, eye irritation, and nasal irritation during exposure. Bronchoalveolar lavage was performed 18 hours after exposure and was compared with a control BAL performed 3 weeks prior to exposure. There was no control air exposure. Small but statistically significant reductions were seen in BAL mast cells, AM phagocytosis of opsonized yeast particles, and lymphocyte CD4/CD8 ratios. A small increase in recovery of PMNs was also observed. These findings suggest that diesel exhaust may induce mild airway inflammation in the absence of spirometric changes.

In underground miners, bus garage workers, dock workers, and locomotive repairmen exposed to diesel exhaust, minimal and not statistically significant changes were reported in respiratory symptoms and pulmonary function over the course of a workshift. In diesel bus garage workers, there was an increased reporting of burning and watering of the eyes, cough, labored breathing, chest tightness, and wheezing, but no reductions in pulmonary function associated with exposure to diesel exhaust. In stevedores pulmonary function was adversely affected over a workshift exposure to diesel exhaust but normalized after a few days without exposure.

**TABLE 11-11. HUMAN STUDIES OF DIESEL EXHAUST EXPOSURE**

<b>Study</b>	<b>Description</b>	<b>Findings</b>
Kahn et al. (1988)	13 Cases of acute exposure, Utah and Colorado coal miners.	Acute reversible sensory irritation, headache; nervous system effects, bronchoconstriction were reported at unknown exposures.
El Batawi and Noweir (1966)	161 Workers, two diesel bus garages.	Eye irritation (42%), headache (37%), dizziness (30%), throat irritation (19%), and cough and phlegm (11%) were reported in this order of incidence by workers exposed in the service and repair of diesel powered buses.
Battigelli (1965)	Six subjects, eye exposure chamber, three dilutions.	Time to onset was inversely related and severity of eye irritation was associated with the level of exposure to diesel exhaust.
Katz et al. (1960)	14 Persons monitoring diesel exhaust in a train tunnel.	Three occasions of minor eye and throat irritation; no correlation established with concentrations of diesel exhaust components.
Hare and Springer (1971) Hare et al. (1974)	Volunteer panelists who evaluated general public's response to odor of diesel exhaust.	Slight odor intensity, 90% perceived, 60% objected; slight to moderate odor intensity, 95% perceived, 75% objected; almost 75% objected; almost 95% objected.
Linnell and Scott (1962)	Odor panel under highly controlled conditions determined odor threshold for diesel exhaust.	In six panelists, the volume of air required to dilute raw diesel exhaust to an odor threshold ranged from a factor of 140 to 475.
Battigelli (1965)	13 Volunteers exposed to three dilutions of diesel exhaust for 15 min to 1 h.	No significant effects on pulmonary resistance were observed as measured by plethysmography.
Reger (1979)	Five or more VC maneuvers by each of 60 coal miners exposed to diesel exhaust at the beginning and end of a work shift.	FEV <sub>1</sub> , FVC, and PEF <sub>R</sub> were similar between diesel and non-diesel-exposed miners. Smokers had an increased number of decrements over shift than nonsmokers.
Ames et al. (1982)	Pulmonary function of 60 diesel-exposed compared with 90 non-diesel-exposed coal miners over work shift.	Significant work shift decrements occurred in miners in both groups who smoked; no significant differences in ventilatory function changes between miners exposed to diesel exhaust and those not exposed.
Jorgensen and Svensson (1970)	240 Iron ore miners matched for diesel exposure, smoking and age were given bronchitis questionnaires and spirometry pre- and postwork shift.	Among underground (surrogate for diesel exposure) miners, smokers and older age groups, frequency of bronchitis was higher. Pulmonary function was similar between groups and subgroups except for differences accountable to age.

**TABLE 11-11 (cont'd). HUMAN STUDIES OF DIESEL EXHAUST EXPOSURE**

Study	Description	Findings
Gamble et al. (1979)	200 Salt miners performed before and after workshift spirometry. Personal environmental NO <sub>2</sub> and inhalable particle samples were collected.	Smokers had greater but not significant reductions in spirometry than ex- or nonsmokers. NO <sub>2</sub> , but not particulate, levels significantly decreased FEV <sub>1</sub> , FEF <sub>25</sub> , FEF <sub>50</sub> , and FEF <sub>75</sub> over the workshift.
Gamble et al. (1987a)	232 Workers in four diesel bus garages were administered acute respiratory questionnaires and before and after workshift spirometry. Compared to lead, acid battery workers previously found to be unaffected by their exposures.	Prevalence of burning eyes, headache, difficult or labored breathing, nausea, and wheeze were higher in diesel bus workers than in comparison population.
Ulfvarson et al. (1987)	Workshift changes in pulmonary function were evaluated in crews of roll-on/ roll-off ships and car ferries and bus garage staff. Pulmonary function was evaluated in six volunteers exposed to diluted diesel exhaust, 2.1 ppm NO <sub>2</sub> , and 600 µg/m <sup>3</sup> particulate matter.	Pulmonary function was affected during a workshift exposure to diesel exhaust, but it normalized after a few days with no exposure. Decrements were greater with increasing intervals between exposures. No effect on pulmonary function was observed in the experimental exposure study.
Battigelli et al. (1964)	210 Locomotive repairmen exposed to diesel exhaust for an average of 9.6 years in railroad engine houses were compared with 154 railroad yard workers of comparable job status but no exposure to diesel exhaust.	No significant differences in VC, FEV <sub>1</sub> , peak flow, nitrogen washout, or diffusion capacity nor in the prevalence of dyspnea, cough, or sputum were found between the diesel exhaust-exposed and nonexposed groups.
Gamble et al. (1987b)	283 Male diesel bus garage workers from four garages in two cities were examined for impaired pulmonary function (FVC, FEV <sub>1</sub> , and flow rates). Study population with a mean tenure of 9 ± 10 years S.D. was compared to a nonexposed "blue collar" population.	Analyses within the study populations population showed no association of respiratory symptoms with tenure. Reduced FEV <sub>1</sub> and FEF <sub>50</sub> (but not FEF <sub>75</sub> ) were associated with increasing tenure. The study population had a higher incidence of cough, phlegm, and wheezing unrelated to tenure. Pulmonary function was not affected in the total cohort of diesel-exposed of diesel-exposed but was reduced with 10 or more years of tenure.

**TABLE 11-11 (cont'd). HUMAN STUDIES OF DIESEL EXHAUST EXPOSURE**

<b>Study</b>	<b>Description</b>	<b>Findings</b>
Purdham et al. (1987)	Respiratory symptoms and pulmonary function were evaluated in 17 stevedores exposed to both diesel and gasoline exhausts in car ferry operations; control group was 11 on-site office workers.	No differences between the two groups for respiratory symptoms. Stevedores had lower baseline lung function consistent with an obstructive ventilatory defect compared with controls and those of Sydney, Nova Scotia, residents. Caution in interpretation is warranted due to small sample size. No significant changes in lung function over workshift nor difference between two groups.
Reger et al. (1982)	Differences in respiratory symptoms and pulmonary function were assessed in 823 coal miners from six diesel equipped mines compared to 823 matched coal miners not exposed to diesel exhaust.	Underground miners in diesel-use mines reported more symptoms of cough and phlegm and had lower pulmonary function. Similar trends were noted for surface workers at diesel-use mines. Pattern was consistent with small airway disease but factors other than exposure to diesel exhaust thought to be responsible.
Ames et al. (1984)	Changes in respiratory symptoms and function were measured during a 5-year period in 280 diesel-exposed and 838 nonexposed U.S. underground coal miners.	No decrements in pulmonary function or increased prevalence of respiratory symptoms were found attributable to diesel exhaust. In fact, 5-year incidences of cough, phlegm, and dyspnea were greater in miners without exposure to diesel exhaust than in miners exposed to diesel exhaust.
Attfield (1978)	Respiratory symptoms and function were assessed in 2,659 miners from 21 underground metal mines (1,709 miners) and nonmetal mines (950 miners). Years of diesel usage in the mines were surrogate for exposure to diesel exhaust.	Questionnaire found an association between an increased prevalence of cough and aldehyde exposure; this finding was not substantiated by spirometry data. No adverse symptoms or pulmonary function decrements were related to exposure to NO <sub>2</sub> , CO, CO <sub>2</sub> , dust, or quartz.
Attfield et al. (1982)	Respiratory symptoms and function were assessed in 630 potash miners from six potash mines using a questionnaire, chest radiographs and spirometry. A thorough assessment of the environment of each mine was made concurrently.	No obvious association indicative of diesel exposure was found between health indices, dust exposure, and pollutants. A higher prevalence of cough and phlegm, but no differences in FVC and FEV <sub>1</sub> , were found in these diesel-exposed potash workers when compared to predicted values from a logistic model based on blue-collar staff working in nondusty jobs.

**TABLE 11-11 (cont'd). HUMAN STUDIES OF DIESEL EXHAUST EXPOSURE**

Study	Description	Findings
Gamble et al. (1983)	Respiratory morbidity was assessed in 259 miners in 5 salt mines by respiratory symptoms, radiographic findings and spirometry. Two mines used diesels extensively, 2 had limited use, one used no diesels in 1956, 1957, 1963, or 1963 through 1967. Several working populations were compared to the salt mine cohort.	After adjustment for age and smoking, salt miners showed no symptoms, increased prevalence of cough, phlegm, dyspnea or air obstruction (FEV <sub>1</sub> /FVC) compared to aboveground coal miners, potash workers or blue collar workers. FEV <sub>1</sub> , FVC, FEF <sub>50</sub> , and FEF <sub>75</sub> were uniformly lower for salt miners in comparison to all the comparison populations. No changes in pulmonary function were associated with years of exposure or cumulative exposure to inhalable particles or NO <sub>2</sub> .
Gamble and Jones (1983)	Same as above. Salt miners were grouped into low, intermediate and high exposure categories based on tenure in jobs with diesel exposure.	A statistically significant dose-related association of phlegm and diesel exposure was noted. Changes in pulmonary function showed no association with diesel tenure. Age- and smoking-adjusted rates of cough, phlegm, and dyspnea were 145, 169, and 93% of an external comparison population. Predicted pulmonary function indices showed small but significant reductions; there was no dose-response relationship.
Edling and Axelson (1984)	Pilot study of 129 bus company employees classified into three diesel exhaust exposure categories clerks (0), bus drivers (1), and bus garage workers.	The most heavily exposed group (bus garage workers) had a fourfold increase in risk of dying from cardiovascular disease, even after correction for smoking and allowing for 10 years of exposure and 15 years or more of induction latency time.
Edling et al. (1987)	Cohort of 694 male bus garage employees followed from 1951 through 1983 were evaluated for mortality from cardiovascular disease. Subcohorts categorized by levels of exposure were clerks (0), bus drivers (1), and bus garage employees (2).	No increased mortality from cardiovascular disease was found among the members of these five bus companies when compared with the general population or grouped as sub-cohorts with different levels of exposure.
Rudell et al. (1989, 1990, 1994)	Eight healthy non-smoking subjects exposed for 60 min in chamber to diesel exhaust (3.7 ppm NO, 1.5 ppm NO <sub>2</sub> , 27 ppm CO, 0.5 mg/m <sup>3</sup> formaldehyde, particles 4.3 × 10 <sup>6</sup> /cm <sup>3</sup> ). Exercise, 10 of each 20 min (75 W).	Odor, eye and nasal irritation in 5/8 subjects. BAL findings small decrease in mast cells, lymphocyte subsets and macrophage phagocytosis, small increase in PMNs.

The chronic effects of exposure to diesel exhaust have been evaluated in humans in epidemiologic studies of occupationally exposed workers. Most of the epidemiologic data indicate the absence of an excess of chronic respiratory disease associated with exposure to diesel exhaust. In a few of these studies, a higher prevalence of respiratory symptoms, primarily cough, phlegm, or dyspnea was observed in the exposed workers. Reductions in several pulmonary function parameters including FVC and FEV<sub>1</sub>, and to a lesser extent forced expiratory flow at 50 and 75% of vital capacity (FEF<sub>50</sub> and FEF<sub>75</sub>), have also been reported. Two studies (Reger et al., 1982; Purdham et al., 1987), each with methodological problems, detected statistically significant decrements in pulmonary function when compared with matched controls. These two studies coupled with other reported nonsignificant trends in respiratory flow-volume measurements suggest that diesel exhaust exposure may impair pulmonary function among occupational populations. A preliminary study of the association of cardiovascular mortality and exposure to diesel exhaust found a risk ratio of 4.0. A more comprehensive study by the same investigators, however, found no significant difference between the observed and expected number of deaths due to cardiovascular disease.

The results of the epidemiologic studies addressing noncarcinogenic health effects resulting from exposure to diesel exhaust must be interpreted cautiously because of a myriad of methodological problems, including incomplete information on the extent of exposure to diesel exhaust, the presence of confounding variables (smoking, occupational exposures to other toxic substances), and the short duration and low intensity of exposure. These limitations restrict definitive conclusions about diesel exhaust being the cause of any noncarcinogenic health effects, observed or reported.

### **11.5.2 Effects of Diesel Exhaust on Laboratory Animals**

In short-term and chronic exposure studies, toxic effects have been related to high concentrations of diesel particulate matter. Data from short-term exposures indicate minimal effects on pulmonary function, even though histological and cytological changes were observed in the lungs (Table 11-12). Exposures for several months or longer to levels markedly above environmental ambient concentrations resulted in accumulation of particles in the lungs, increases in lung weight, increases in AMs and leukocytes, macrophage aggregation, hyperplasia of alveolar epithelium, and thickening of the alveolar septa. Similar

**TABLE 11-12. SHORT-TERM EFFECTS OF DIESEL EXHAUST ON LABORATORY ANIMALS**

Species/Sex	Exposure Period	Particles ( $\mu\text{g}/\text{m}^3$ )	C $\times$ T ( $\mu\text{g}\cdot\text{h}/\text{m}^3$ )	CO (ppm)	NO <sub>2</sub> (ppm)	SO <sub>2</sub> (ppm)	Effects	References
Rat, F-344, M; Mouse, A/J; Hamster, Syrian	20 h/day 7 days/week 10-13 weeks	1,500 0.19 $\mu\text{m}$ , MMD	2,100,000 to 2,730,000	6.9	0.49	—	Increase in lung wt; increase in thickness of alveolar walls; no species difference	Kaplan et al. (1982)
Rat, F-344, M, F; Mouse, CD-1, M, F	7 h/day 5 days/week 19 weeks	210 1,000 4,400	140,000 665,000 2,926,000	—	—	—	No effects on lung function; increase in PMNs and proteases and AM aggregation in both species	Mauderly et al. (1981)
Cat, Inbred, M	20 h/day 7 days/week 4 weeks	6,400	3,584,000	14.6	2.1	2.1	Few effects on lung function; focal pneumonitis or alveolitis	Pepelko et al. (1980d)
Rat, Sprague-Dawley, M	20 h/day 7 days/week 4 weeks	6,400 6,800 <sup>a</sup>	3,584,000 3,808,000	16.9 16.1 <sup>a</sup>	2.49 2.76 <sup>a</sup>	2.10 1.86 <sup>a</sup>	Decreased body wt; arterial blood pH reduced; both vital and total lung capacities increased	Pepelko (1982a)
Guinea Pig, Hartley, M, F	20 h/day 7 days/week 4 weeks	6,800 <sup>a</sup>	3,808,000	16.7	2.9	( $<0.01$ ppm O <sub>3</sub> ) <sup>a</sup>	Exposure started when animals were 4 days old; increase in pulmonary flow; bradycardia	Wiester et al. (1980)
Rat, F-344, M	20 h/day 5.5 days/week 4 weeks	6,000 6.8 $\mu\text{m}$ , MMD	2,640,000	—	—	—	Macrophage aggregation; increase in PMNs; Type 2 cell proliferation; thickened alveolar walls	White and Garg (1981)
Guinea Pig, Hartley M, F	20 h/day 7 days/week 8 weeks	6,300	7,056,000	17.4	2.3	( $<0.01$ ppm O <sub>3</sub> ) <sup>a</sup>	Increase in relative lung wt; AM aggregation; hypertrophy of goblet cells; focal hyperplasia of alveolar epithelium	Weister et al. (1980)

<sup>a</sup>Irradiated exhaust.

PMN = Polymorphonuclear leukocyte.

AM = Alveolar macrophage.

Source: quoted from U.S. Environmental Protection Agency (1994).

histological changes, as well as reductions in growth rates and alterations in indices of pulmonary function, have been observed in chronic exposure studies. Chronic studies have been carried out using rats, mice, guinea pigs, hamsters, cats, and monkeys. Reduced resistance to respiratory tract infections has been reported in mice exposed to diesel exhaust.

Reduced growth rates have been observed most often in studies with exposures of at least 2,000  $\mu\text{g}/\text{m}^3$  diesel particulate matter which lasted for 16 h or more per day (Table 11-13). No effects on growth or survival were noted at levels of 6,000 to 8,000  $\mu\text{g}/\text{m}^3$  of PM when the daily exposures were only 6 to 8 h/day.

Changes in pulmonary function have been noted in a number of different species chronically exposed to diesel exhaust (Table 11-14). The lowest exposure levels that resulted in impaired pulmonary function varied among the species tested but were in excess of 1,000  $\mu\text{g}/\text{m}^3$ .

Histological changes occurring in the respiratory tract tissue of animal exposed chronically to high concentrations of diesel exhaust include alveolar histiocytosis, macrophage aggregation, tissue inflammation, increases in polymorphonuclear leukocytes, hyperplasia of bronchiolar and alveolar Type 2 cells, thickened alveolar septa, edema, fibrosis, and emphysema (Table 11-15). Biochemical changes in the lung associated with these histopathological findings included increases in lung DNA, total protein, and activities of alkaline and acid phosphatase, and glucose-6-phosphate dehydrogenase; increased synthesis of collagen; and release of inflammatory mediators such as leukotriene LTB and prostaglandin  $\text{PGF}_{2\alpha}$ . Some studies have also suggested that there may be a threshold of exposure to diesel exhaust below which pathologic changes do not occur. These no-effect levels were reported to be 2,000  $\mu\text{g}/\text{m}^3$  for cynomolgus monkeys, 110 to 350  $\mu\text{g}/\text{m}^3$  for rats, and 250  $\mu\text{g}/\text{m}^3$  PM for guinea pigs exposed for 7 to 20 h/day, 5 to 5.5 days/week for 104 to 130 weeks.

The pathological effects of diesel exhaust particulate matter appear to be strongly dependent on the relative rates of pulmonary deposition and clearance (Table 11-16). At particle concentrations of about 1,000  $\mu\text{g}/\text{m}^3$  or above, pulmonary clearance becomes reduced, with concomitant focal aggregations of particle-laden AMs. The principal mechanism of reduced particle clearance appears to be the result of impaired AM function. This impairment seems to be nonspecific and applies to insoluble particles deposited in the

**TABLE 11-13. EFFECTS OF CHRONIC EXPOSURES TO DIESEL EXHAUST  
ON SURVIVAL AND GROWTH OF LABORATORY ANIMALS**

Species/Sex	Exposure Period	Particles ( $\mu\text{g}/\text{m}^3$ )	C × T ( $\mu\text{g}\cdot\text{h}/\text{m}^3$ )	CO (ppm)	NO <sub>2</sub> (ppm)	SO <sub>2</sub> (ppm)	Effects	References
Rat, F-344, M, F; Monkey, cynomolgus, M	7 h/day 5 days/week 104 weeks	2,000 0.23–0.36 $\mu\text{m}$ , MMD	7,280,000	11.5	1.5	0.8	No effects on growth or survival	Lewis et al. (1989)
Rat, F344, M; Guinea Pig, Hartley, M	20 h/day 5 days/week 106 weeks	250 750 1,500 0.19 $\mu\text{m}$ , MMD	2,650,000 7,950,000 15,900,000	2.7 <sup>a</sup> 4.4 <sup>a</sup> 7.1 <sup>a</sup>	0.1 <sup>b</sup> 0.27 <sup>b</sup> 0.5 <sup>b</sup>	— — —	Reduced body weight in rats at 1,500 $\mu\text{g}/\text{m}^3$	Schreck et al. (1981)
Hamster, Chinese, M	8 h/day 7 days/week 26 weeks	6,000 12,000	8,736,000 17,472,000	— —	— —	— —	No effect on growth	Vinegar et al. (1981a,b)
Rat, Wistar, M	6 h/day 5 days/week 87 weeks	8,300 0.71 $\mu\text{m}$ , MMD	21,663,000	50.0	4.0–6.0	—	No effect on growth or mortality rates	Karagianes et al. (1981)
Rat, F-344, M, F; Mouse CD-1	7 h/day 5 days/week 130 weeks	350 3,500 7,000 0.25 $\mu\text{m}$ , MMD	1,592,000 15,925,000 31,850,000	2.9 16.5 29.7	0.05 0.34 0.68	— — —	No effect on growth or mortality rates	Mauderly et al. (1984, 1987b)
Rat, Wistar, F; Mouse, MMRI, F	19 h/day 5 days/week 104 weeks	4,240 0.35 $\mu\text{m}$ , MMD	41,891,000	12.5	1.5	1.1	Reduced body wts; increased mortality in mice	Heinrich et al. (1986a)
Rat, F-344 M, F	16h/day 5 days/week 104 weeks	700 2,200 6,600	5,824,000 18,304,000 54,912,000	— — 32.0	— — —	— — —	Growth reduced at 2,200 and 6,600 $\mu\text{g}/\text{m}^3$	Brightwell et al. (1986)
Rat <sup>c</sup> F-344/Jcl.	16 h/day 6 days/week 130 weeks	110 <sup>d</sup> 410 <sup>d</sup> 1,080 <sup>d</sup> 2,310 <sup>d</sup> 3,720 <sup>e</sup> 0.2–0.3 $\mu\text{m}$ , MMD	1,373,000 5,117,000 13,478,000 28,829,000 46,426,000	1.23 2.12 3.96 7.10 12.9	0.08 0.26 0.70 1.41 3.00	0.38 1.06 2.42 4.70 4.57	Concentration-dependent decrease in body weight; earlier deaths in females exposed to 3,720 $\mu\text{g}/\text{m}^3$ , stabilized by 15 mo	Research Committee for HERP Studies (1988)

<sup>a</sup>Estimated from graphically depicted mass concentration data.

<sup>b</sup>Estimated from graphically presented mass concentration data for NO<sub>2</sub> (assuming 90% NO and 10% NO<sub>2</sub>).

<sup>c</sup>Data for tests with light-duty engine; similar results with heavy-duty engine.

<sup>d</sup>Light-duty engine.

<sup>e</sup>Heavy-duty engine.

Source: Quoted from U.S. Environmental Protection Agency (1994).

**TABLE 11-14. EFFECTS OF DIESEL EXHAUST ON  
PULMONARY FUNCTION OF LABORATORY ANIMALS**

Species/Sex	Exposure Period	Particles ( $\mu\text{g}/\text{m}^3$ )	C × T ( $\mu\text{g}\cdot\text{h}/\text{m}^3$ )	CO (ppm)	NO <sub>2</sub> (ppm)	SO <sub>2</sub> (ppm)	Effects	References
Rat, F-344 M, F	7 h/day 5 days/week 104 weeks	2,000 0.23–0.36 $\mu\text{m}$ MMD	7,280,000	11.5	1.5	0.8	No effect on pulmonary function	Lewis et al. (1989)
Monkey, M Cynomolgus	7 h/day 5 days/week 104 weeks	2,000 0.23–0.36 $\mu\text{m}$ , MMD	7,280,000	11.5	1.5	0.8	Decreased expiratory flow; no effect on vital or diffusing capabilities	Lewis et al. (1989)
Rat, F-344, M	20 h/day 5.5 days/week 87 weeks	1,500 0.19 $\mu\text{m}$ , MMD	14,355,000	7.0	0.5	—	Increased functional residual capacity, expiratory volume and flow	Gross (1981)
Rat, Wistar, F	7–8 h/day 5 days/week 104 weeks	3,900 0.1 $\mu\text{m}$ , MMD	14,196,000– 16,224,000	18.5	1.2	3.1	No effect on minute volume, compliance or resistance	Heinrich et al. (1982)
Hamster, Chinese, M	8 h/day 7 days/week 26 weeks	6,000 12,000	8,736,000 17,472,000	— —	— —	— —	Decrease in vital capacity, residual volume, and diffusing capacity; increase in static deflation lung volume	Vinegar et al. (1980, 1981a,b)
Rat, F-344, M, F	7 h/day 5 days/week 130 weeks	350 3,500 7,000 0.23–0.26 $\mu\text{m}$ , MMD	1,593,000 15,925,000 31,850,000	2.9 16.5 29.7	0.05 0.34 0.68	— — —	Diffusing capacity, lung compliance reduced at 3,500 and 7,000 $\mu\text{g}/\text{m}^3$	Mauderly et al. (1988) McClellan et al. (1986)
Hamster, Syrian M, F	19 h/day 5 days/week 120 weeks	4,240 0.35 $\mu\text{m}$ , MMD	48,336,000	12.5	1.5	1.1	Significant increase in airway resistance	Heinrich et al. (1986a)
Rat, F-344; Hamster Syrian	16 h/day 5 days/week 104 weeks	700 2,200 6,600	5,824,000 18,304,000 54,912,000	— — —	— — —	— — —	Large number of pulmonary function changes consistent with obstructive and restrictive airway diseases at 6,600 $\mu\text{g}/\text{m}^3$ (no specific data provided)	Brightwell et al. (1986)
Rat, Wistar, F	19 h/day 5 days/week 140 weeks	4,240 0.35 $\mu\text{m}$ , MMD	56,392,000	12.5	1.5	1.1	Decrease in dynamic lung compliance; increase in airway resistance	Heinrich et al. (1986a)
Cat, inbred, M	8 h/day 7 days/week 124 weeks	6,000 <sup>a</sup> 12,000 <sup>b</sup>	41,664,000 83,328,000	20.2 33.3	2.7 4.4	2.1 5.0	Decrease in vital capacity, total lung capacity, and diffusing capacity after 2 years; no effect on expiratory flow	Pepelko et al. (1980e, 1981) Moorman et al. (1985)

<sup>a</sup>1 to 61 weeks exposure.

<sup>b</sup>62 to 124 weeks of exposure.

Source: Quoted from U.S. Environmental Protection Agency (1994).

**TABLE 11-15. HISTOPATHOLOGICAL EFFECTS OF DIESEL EXHAUST  
IN THE LUNGS OF LABORATORY ANIMALS**

Species/Sex	Exposure Period	Particles ( $\mu\text{g}/\text{m}^3$ )	C $\times$ T ( $\mu\text{g}\cdot\text{h}/\text{m}^3$ )	CO (ppm)	NO <sub>2</sub> (ppm)	SO <sub>2</sub> (ppm)	Effects	References
Rat, F-344, M Mouse A/J, M; Hamster, Syrian, M	20 h/day 7 days/week 12-13 weeks	1,500 0.19 $\mu\text{m}$ , MMD	2,520,000- 2,730,000	—	—	—	Inflammatory changes; increase in lung weight; increase in thickness of alveolar walls	Kaplan et al. (1982)
Monkey, Cynomolgus, M	7 h/day 5 days/week 104 weeks	2,000 0.23–0.36 $\mu\text{m}$ , MMD	7,280,000	11.5	1.5	0.8	AM aggregation; no fibrosis, inflammation or emphysema	Lewis et al. (1989)
Rat, F-344, M, F	7 h/day 5 days/week 104 weeks	2,000 0.23–0.36 $\mu\text{m}$ , MMD	3,640,000	11.5	1.5	0.8	Multifocal histiocytosis; inflammatory changes; Type II cell proliferation; fibrosis	Bhatnagar et al. (1980) Pepelko (1982a)
Rat, Sprague- Dawley, M; Mouse, A/HEJ, M	8 h/day 7 days/week 39 weeks	6,000	13,104,000	—	—	—	Increase in lung protein content and collagen synthesis but a decrease in overall lung protein synthesis in both species; prolyl-hydroxylase activity increased in rats in utero	Bhatnagar et al. (1980) Pepelko (1982a)
Hamster, chinese, M	8 h/day 5 days/week 26 weeks	6,000 12,000	6,240,000 12,480,000	—	—	—	Inflammatory changes; AM accumulation; thickened alveolar lining; Type II cell hyperplasia; edema; increase in collagen	Pepelko (1982b)
Hamster, Syrian, M, F	7-8 h/day 5 days/week 120 weeks	3,900 0.1 $\mu\text{m}$ , MMD	16,380,000- 18,720,000	18.5	1.2	3.1	Inflammatory changes, 60% adenomatous cell proliferation	Heinrich et al. (1982)
Rat, Wistar, M	6 h/day 5 days/week 87 weeks	8,300 0.71 $\mu\text{m}$ , MMD	21,663,000	50.0	4.0-6.0	—	Inflammatory changes; AM aggregation; alveolar cell hypertrophy; interstitial fibrosis, emphysema (diagnostic methodology not described)	Karagianes et al. (1981)
Rat, F-344, F	8 h/day 7 days/week 104 weeks	4,900	28,538,000	7.0	1.8	13.1	Type II cell proliferation; inflammatory changes; bronchial hyperplasia; fibrosis	Iwai et al. (1986)
Rat, F-344, M, F; Mouse CD-1, M, F	7 h/day 5 days/week 130 weeks	350 3,500 7,000 0.23 $\mu\text{m}$ , MMD	1,592,000 15,925,000 31,850,000	2.9 16.5 29.7	0.05 0.34 0.68	— — —	Alveolar and bronchiolar epithelial metaplasia in rats at 3,500 and 7,000 $\mu\text{g}/\text{m}^3$ ; fibrosis at 7,000 $\mu\text{g}/\text{m}^3$ in rats and mice; inflammatory changes	Mauderly et al. (1987a,b) Henderson et al. (1988)

**TABLE 11-15 (cont'd). HISTOPATHOLOGICAL EFFECTS OF DIESEL EXHAUST  
IN THE LUNGS OF LABORATORY ANIMALS**

Species/Sex	Exposure Period	Particles ( $\mu\text{g}/\text{m}^3$ )	C × T ( $\mu\text{g}\cdot\text{h}/\text{m}^3$ )	CO (ppm)	NO <sub>2</sub> (ppm)	SO <sub>2</sub> (ppm)	Effects	References
Rat, M, F, F-344/Jcl.	16 h/day	110 <sup>a</sup>	1,373,000	1.23	0.08	0.38	Inflammatory changes; Type II cell hyperplasia and lung tumors seen at >400 $\mu\text{g}/\text{m}^3$ ; shortening and loss of cilia in trachea and bronchi	Research Committee for HERP Studies (1988)
	6 days/week	410 <sup>a</sup>	5,117,000	2.12	0.26	1.06		
	130 weeks	1,080 <sup>a</sup>	13,478,000	3.96	0.70	2.42		
		2,310 <sup>a</sup>	28,829,000	7.10	1.41	4.70		
		3,720 <sup>b</sup>	46,336,000	12.9	3.00	4.57		
Hamster, Syrian, M, F	19 h/day 5 days/week 120 weeks	4,240	48,336,000	12.5	1.5	1.1	Inflammatory changes; thickened alveolar septa; bronchioalveolar hyperplasia; emphysema (diagnostic methodology not described)	Heinrich et al. (1986a)
Mouse, NMRI, F	19 h/day 5 days/week 120 weeks	4,240	48,336,000	12.5	1.5	1.1	Inflammatory changes; bronchioalveolar hyperplasia; alveolar lipoproteinosis; fibrosis	Heinrich et al. (1986a)
Rat, Wistar, F	19 h/day 5 days/week 140 weeks	4,240	56,392,000	12.5	1.5	1.1	Thickened alveolar septa; AM aggregation; inflammatory changes; hyperplasia; lung tumors	Heinrich et al. (1986a)
Guinea Pig, Hartley, M	20 h/day	250	2,860,000	—	—	—	Minimal response at 250 and ultrastructural changes at 750 $\mu\text{g}/\text{m}^3$ ; thickened alveolar membranes; cell proliferation; fibrosis at 6,000 $\mu\text{g}/\text{m}^3$ ; increase in PMN at 750 $\mu\text{g}/\text{m}^3$ and 1,500 $\mu\text{g}/\text{m}^3$	Barnhart et al. (1981, 1982) Vostal et al. (1981)
	5.5 days/week	750	8,580,000	—	—	—		
	104 weeks	1,500	17,160,000	—	—	—		
		6,000	68,640,000	—	—	—		
Cat, inbred, M	8 h/day	6,000 <sup>c</sup>	41,664,000	20.2	2.7	2.1	Inflammatory changes; AM aggregation; bronchiolar epithelial metaplasia; Type II cell hyperplasia; peribronchiolar fibrosis	Plopper et al. (1983) Hyde et al. (1985)
	7 days/week	12,000 <sup>d</sup>	83,328,000	33.2	4.4	5.0		
	124 weeks							
Rat, Wistar, F	18 h/day	840	7,400,000	2.6	0.3	0.3	No effect on mortality. Reduced body wt., bronchioalveolar hyperplasia, and Inc. lung wt. at 2,500 and 7,000 $\mu\text{g}/\text{m}^3$	Heinrich et al. (1995)
	5 days/week	2,500	21,800,000	8.3	1.2	1.1		
	up to 24 mo	7,000	61,700,000	21.2	3.8	3.4		
							Alveolar clearance rates reduced in all groups at 3 mo. BAL showed clear exposure-related effects in all except lowest diesel exposure group	

**TABLE 11-15 (cont'd). HISTOPATHOLOGICAL EFFECTS OF DIESEL EXHAUST  
IN THE LUNGS OF LABORATORY ANIMALS**

Species/Sex	Exposure Period	Particles ( $\mu\text{g}/\text{m}^3$ )	C × T ( $\mu\text{g}\cdot\text{h}/\text{m}^3$ )	CO (ppm)	NO <sub>2</sub> (ppm)	SO <sub>2</sub> (ppm)	Effects	References
Rats, M, F F-344/N	16 h/day 5 day/week up to 24 mo	2,500 6,500	— —	10.3 26.9	0.73 3.78	— —	Higher mortality in males. Reduced body weight in males and females at 6,500 $\mu\text{g}/\text{m}^3$ . Inc lung weight in males and females at 2,500 and 6,500 $\mu\text{g}/\text{m}^3$ . Dose related increases in AM hyperplasia, alveolar epithelial hyperplasia, chronic active inflammation, septal fibrosis, alveolar proteinosis bronchioalveolar metaplasia, focal fibrosis with alveolar epithelial hyperplasia, squamous metaplasia, and squamous cysts	Nikula et al. (1995)
Mice NMRI/C5L F	18 h/day 5 days/week up to 24 mo	4,500	39,000,000	14.2	2.3	2.8	Reduced body weight, inc. lung weight.	Heinrich et al. (1995)

<sup>a</sup>Light-duty engine.

<sup>b</sup>Heavy-duty engine.

<sup>c</sup>1 to 61 weeks exposure.

<sup>d</sup>62 to 124 weeks of exposure.

AM = Alveolar macrophage.

PMN = Polymorphonuclear leukocyte.

Source: U.S. Environmental Protection Agency (1994).

**TABLE 11-16. EFFECTS OF EXPOSURE TO DIESEL EXHAUST ON THE PULMONARY DEFENSE MECHANISMS OF LABORATORY ANIMALS**

Species	Exposure Period	Particles ( $\mu\text{g}/\text{m}^3$ )	C $\times$ T ( $\mu\text{g}\cdot\text{h}/\text{m}^3$ )	CO (ppm)	NO <sub>2</sub> (ppm)	SO <sub>2</sub> (ppm)	Effects	Reference
<b>ALVEOLAR MACROPHAGE STATUS</b>								
Guinea Pig, Hartley	20 h/day 5.5 days/week 8 weeks	250 1,500 0.19 $\mu\text{m}$ , MMD	220,000 1,320,000	2.9 7.5	— —	— —	No significant changes in absolute numbers of AMs	Chen et al. (1980)
Rat, F-344, M	7 h/day 5 days/week 104 weeks	2,000 0.23–0.36 $\mu\text{m}$ MMD	7,280,000	11.5	1.5	0.81	Little effect on viability, cell number, oxygen consumption, membrane integrity, lysosomal enzyme activity, or protein content of AMs; decreased cell volume and ruffling of cell membrane and depressed luminescence of AM	Castranova et al. (1985)
Rat, F-344, M	20 h/day 5.5 days/week 26, 48, or 52 weeks	250 <sup>a</sup> 750 <sup>a</sup> 1,500 <sup>b</sup> 0.19 $\mu\text{m}$ , MMD	715,000- 8,580,000	2.9 4.8 7.5	— — —	— — —	AM cell counts proportional to concentration of DP at 750 and 1,500 $\mu\text{g}/\text{m}^3$ ; AM increased in lungs in response to rate of DP mass entering lung rather than total DP burden in lung; increased PMNs were proportional to inhaled concentrations and/or duration of exposure; PMNs affiliated with clusters of aggregated AM rather than DP	Strom (1984) Vostal et al. (1982)
Rat F-344/Crl, M, F Mouse, CD, M,F	7 h/day 5 days/week 104 weeks (rat), 78 weeks (mouse)	350 3,500 7,000 0.25 $\mu\text{m}$ , MMD	1,274,000 <sup>c</sup> 12,740,000 <sup>c</sup> 25,480,000 <sup>c</sup>	2.9 16.5 29.7	0.05 0.34 0.68	— — —	Significant increases of AM in rats and mice exposed to 7,000 $\mu\text{g}/\text{m}^3$ DP for 24 and 18 mo, respectively, but not at concentrations of 3,500 or 350 $\mu\text{g}/\text{m}^3$ DP for the same exposure durations; PMNs increased in a dose-dependent fashion in both rats and mice exposed to 3,500 or 7,000 $\mu\text{g}/\text{m}^3$ DP and were greater in mice than rats	Henderson et al. (1988)
<b>CLEARANCE</b>								
Rat	7 h/day 5 day/week 12 weeks	200 1,000 4,500 0.25 $\mu\text{m}$ , MMD	84,000 420,000 1,890,000	— — —	— — —	— — —	Evidence of apparent speeding of tracheal clearance at the 4,500 $\mu\text{g}/\text{m}^3$ level after 1 week of <sup>99m</sup> Tc macroaggregated-albumin and reduced clearance of tracer aerosol in each of the three exposure levels at 12 weeks; indication of a lower percentage of ciliated cells at the 1,000 and 4,500 $\mu\text{g}/\text{m}^3$ levels	Wolff and Gray (1980)
Rat, F-344 M, F	7 h/day 5 days/week 18 weeks <0.5 $\mu\text{m}$ , MMD	150 940 4,100	94,500 592,000 2,583,000	— — —	— — —	— — —	Lung burdens of DP were concentration-related; clearance half-time of DP almost double in 4,100 $\mu\text{g}/\text{m}^3$ group compared to 150 $\mu\text{g}/\text{m}^3$ group	Griffis et al. (1983)

**TABLE 11-16 (cont'd). EFFECTS OF EXPOSURE TO DIESEL EXHAUST ON THE PULMONARY DEFENSE MECHANISMS OF LABORATORY ANIMALS**

Species	Exposure Period	Particles ( $\mu\text{g}/\text{m}^3$ )	C $\times$ T ( $\mu\text{g}\cdot\text{h}/\text{m}^3$ )	CO (ppm)	NO <sub>2</sub> (ppm)	SO <sub>2</sub> (ppm)	Effects	Reference
Rat, F-344, M	7 h/day 5 days/week 26-104 weeks	2,000 0.23-0.36 $\mu\text{m}$ MMD	1,820,000- 7,280,000	11.5	1.5	0.8	No difference in clearance of <sup>59</sup> Fe <sub>3</sub> O <sub>4</sub> particles 1 day after tracer aerosol administration; 120 days after exposure tracer aerosol clearance was enhanced; Lung burden of DP increased significantly between 12 to 24 months of exposure	Lewis et al. (1989)
Rat, Sprague-Dawley	4-6 h/day 7 days/week 0.1 to 14.3 weeks	900 8,000 17,000	2,500- 10,210,000	— — —	5.0 2.7 8.0	0.2 0.6 1.0	Impairment of tracheal mucociliary clearance in a concentration-response manner	Battigelli et al. (1966)
Rat, F-344, M, F	7 h/day 5 days/week 130 weeks	350 3,500 7,000 0.25 $\mu\text{m}$ , MMD	1,593,000 15,925,000 31,850,000	2.9 16.5 29.7	0.1 0.3 0.7	— — —	No changes in tracheal mucociliary clearance after 6, 12, 18, 24, or 30 mo of exposure; increases in lung clearance half-times as early as 6 mo at 7,000 $\mu\text{g}/\text{m}^3$ level and 18 mo at 3,500 $\mu\text{g}/\text{m}^3$ level; no changes seen at 350 $\mu\text{g}/\text{m}^3$ level; after 24 mo of diesel exposure, long-term clearance half-times were increased in the 3,500 and 7,000 $\mu\text{g}/\text{m}^3$ groups	Wolff et al. (1987)
<b>MICROBIAL-INDUCED MORTALITY</b>								
Mice, CD-1, F	—	—	—	—	—	—	No change in mortality in mice exposed intratracheally to 100 $\mu\text{g}$ of DP prior to exposure to aerosolized <i>Streptococcus</i> sp.	Hatch et al. (1985)
Mice CD-1, F	7 h/day 5 days/week 4, 12, or 26 weeks	2,000 0.23-0.36 $\mu\text{m}$ MMD	280,000- 1,820,000	11.5	1.5	0.8	Mortality similar at each exposure duration when challenged with Ao/PR/8/34 influenza virus; in mice exposed for 3 and 6 mo, but not 1 mo, there were increases in the percentages of mice having lung consolidation, higher virus growth, depressed interferon levels and a four-fold reduction in hemagglutinin antibody levels	Hahon et al. (1985)

**TABLE 11-16 (cont'd). EFFECTS OF EXPOSURE TO DIESEL EXHAUST ON THE PULMONARY DEFENSE MECHANISMS OF LABORATORY ANIMALS**

Species	Exposure Period	Particles ( $\mu\text{g}/\text{m}^3$ )	C x T ( $\mu\text{g}\cdot\text{h}/\text{m}^3$ )	CO (ppm)	NO <sub>2</sub> (ppm)	SO <sub>2</sub> (ppm)	Effects	Reference
Mice, CR/CD-1, F	8 h/day 7 days/week 2 h up to 46 weeks	5,300 to 7,900	11,000- 20,350,000	19 to 22	1.8 to 3.6	0.9 to 2.8	Enhanced susceptibility to lethal effects of <i>S. pyogenes</i> infections at all exposure durations (2 and 6 h; 8, 15, 16, 307, and 321 days); inconclusive results with <i>S. typhimurium</i> because of high mortality rates in controls; no enhanced mortality when challenged with A/PR8-3 influenza virus	Campbell et al. (1980, 1981)

<sup>a</sup>Chronic exposure lasted 52 weeks.

<sup>b</sup>Chronic exposure lasted 48 weeks.

<sup>c</sup>Calculated for 104-week exposure.

DP = Diesel exhaust particles.

AM = Alveolar macrophage.

PMN = Polymorphonuclear leukocyte.

Source: Quoted from U.S. Environmental Protection Agency (1994).

alveolar region. Other data suggest that the inability of particle-laden AMs to translocate to the mucociliary escalator is correlated to the average composite particle volume per AM in the lung. Data from rats indicate that when this particle volume exceeds a critical level, impairment appears to be initiated. Such data for other laboratory species and humans, unfortunately, are very limited.

There is a considerable body of evidence that the major noncancerous health hazards posed by exposure to diesel exhaust are to the lung. These data also show that the exposures that cause pulmonary injury are lower than those inducing detectable increases in lung tumors. These same data further indicate that the inflammatory and proliferative changes in the lung play a key role in the etiology of pulmonary tumors in exposed rats. A range of no adverse effect levels has been estimated as 200-400  $\mu\text{g}/\text{m}^3$  (Health Effects Institute, 1995).

### **11.5.3 Species Differences**

The responses to inhaled diesel exhaust as well as other particulate differs markedly among rodents. Data on the response to diesel exhaust for a number of species has been reviewed by Mauderly (1994a). The data indicate that as with cancer, the non-cancer pulmonary effects of diesel exhaust differ greatly in rats, mice and Syrian hamsters. Thus far, all animals show epithelial proliferation with chronic high level exposure to diesel exhaust but the changes in the respiratory bronchioles of cats differ from the changes in the alveolar ducts of rodents. Rats appear to have a greater epithelial proliferative response to dusts than do mice. Guinea pigs differ from other species in that the inflammatory response to dust is eosinophil-based rather than neutrophil-based. Thus, it is unclear which of the animals used in inhalation studies is the best model for predicting the responses of humans to dust exposure. Pepelko and Perrano (1983) exposed 8 male cats to diluted DE ( $6000 \mu\text{g}/\text{m}^3$ ) for 5 days/week for 61 weeks, then to  $12,000 \mu\text{g}/\text{m}^3$  for another 27 mo. At the end of the exposure, a restrictive respiratory function impairment with nonuniform gas distribution was observed (Moorman et al., 1985). The accompanying histopathology included peribronchiolar fibrosis and epithelial metaplasia in terminal and respiratory bronchioles (Plopper et al., 1983). The epithelial changes lessened but the fibrosis worsened during 6 mo after the exposure ended.

The rat is the species for which most information about the noncancer effects of diesel exhaust (Table 11-15) as well as other inhaled dusts has been obtained. The responses of rats chronically exposed to carbon black or diesel particulate without the organic fraction, are essentially identical to their responses to diesel exhaust (Mauderly, 1994b; Heinrich et al., 1995). Heinrich et al. (1995) also demonstrated that the noncancer responses of rats to titanium dioxide were also similar qualitatively and quantitatively. Muhle et al. (1991) reported that the responses to chronically inhaled copying toner, a plastic dust pigmented with carbon black, titanium dioxide and silica were also similar qualitatively to titanium dioxide and diesel exhaust. Similar responses resulting from chronic exposure of rats to a range of other dusts including oil shale dusts (Mauderly et al., 1994b), talc (National Toxicology Program, 1993), and coal dust (Martin et al., 1977) have been described.

Few studies have examined the effects of exposure to diesel exhaust mixed with other dusts. The response of rats chronically exposed to diesel exhaust soot and mineral dust was studied by Mauderly et al. (1994b). Male and female F344 rats were exposed 7 hours/day 5 days/week for 30 mo to diesel exhaust, raw or retorted oil shale dust, or additive combinations of diesel exhaust and shale dust. The diesel exhaust soot accumulated more rapidly in the lungs than did the shale dust, due to differences in particle size, but the lung burdens of the two types of dust were additive. The long-term effects on lung weight and density, and BALF constituents, were greater than additive, the effects on respiratory function were approximately additive, and the effects on particle clearance were less than additive. The noncancer health effects of the combined exposures were more closely correlated with the total lung dust burden than with the combined dust exposure concentrations.

Lewis et al. (1989) studied the effects of diesel exhaust and mineral dust in rats and cynomolgus monkeys exposed to either diesel exhaust or coal dust at 2,000  $\mu\text{g}$  respirable particles/ $\text{m}^3$ , or to a combination of 1,000  $\mu\text{g}/\text{m}^3$  of each material. Lung burdens of the dusts were approximately additive in rats but were not measured in the monkeys. Local histopathological responses were similar and approximately additive for the two dusts in both species.

#### **11.5.4 Effects of Mixtures Containing Diesel Exhaust**

Mauderly (1993) reviewed the results of studies in which laboratory animals were exposed to complex mixtures. In a study of diesel and coal dust, rats were exposed for 24 mo to atmospheres containing diesel exhaust at  $2000 \mu\text{g}/\text{m}^3$  coal dust at the same concentration, and a combination of diesel exhaust and coal dust at  $1000 \mu\text{g}/\text{m}^3$  each. Among the health end points evaluated, the effects of diesel exhaust and coal dust were similar with coal dust being slightly less toxic. No synergistic interactions between the exposure materials were noted. In another study of diesel and shale oil dust, Mauderly et al. (1994b) exposed rats by inhalation for 7 h/day 5 days/week for up to 30 mo to raw or retorted oil shale dusts at  $5,000 \mu\text{g}/\text{m}^3$ , to diesel exhaust at  $3,500 \mu\text{g}/\text{m}^3$  or to additive combinations at total particulate concentrations of  $8,500 \mu\text{g}/\text{m}^3$ . The three agents all accumulated progressively in the lungs and caused similar pneumoconiotic responses. The magnitude of effects was more closely correlated to particle lung burdens than to exposure concentrations. The effects of diesel exhaust and shale dusts generally were less than additive for delay of particle clearance; additive for respiratory function impairment; and greater than additive for lung collagen, airway fluid indicators of inflammation, and lung tumors.

Mauderly (1989) discussed the susceptibility of the aging lung to inhaled pollutants. Although the data is extremely limited in that only two particulate pollutants are discussed, it appears that the aging lung might be more sensitive to particulate pollution. Rats were exposed repeatedly for 6 mo to diluted, whole diesel exhaust at a concentration of  $3,500 \mu\text{g}/\text{m}^3$ . The results indicated that rats exposed between 6 and 12 mo were more sensitive than rats born in the chambers and exposed up to 6 mo of age. The results indicated that mice exposed as adults were more susceptible than mice exposed at the onset of breeding age but while lung maturation was still underway.

#### **11.5.5 Particle Effect in Diesel Exhaust Studies**

Diesel PM is composed of an insoluble carbon core with a surface coating of relatively soluble organic constituents. Studies of diesel particle composition have shown that the insoluble carbon core makes up about 80% of the particle mass and that the organic phase

can be resolved into a more slowly dissolving component and a more quickly dissolving component.

The relative contribution of the carbon core of the diesel particles versus organics adsorbed to the surface of the particles to cancer induction and the uncertainty involved has been reviewed (Health Effects Institute, 1995). The primary evidence for the importance of the adsorbed organics is the presence of known carcinogens among these chemicals. These include polycyclic aromatics as well as nitroaromatics. Organic extracts of particles have also been shown to induce tumors in a variety of injection, intratracheal instillation and skin painting studies, and Grimmer et al. (1987) has, in fact, shown that the great majority of the carcinogenic potential following intratracheal instillation resided in the fraction containing four- to seven-ring PAHs.

Evidence for the importance of the carbon core is provided by studies of Kawabata et al. (1986), that showed induction of lung tumors following intratracheal instillation of CB that contained no more than traces of organics and studies of Heinrich et al. (1995) that indicated that exposure via inhalation to CB (Printex 90) particles induced lung tumors at concentrations similar to those effective in diesel studies. Other particles of low solubility such as titanium dioxide (Lee et al., 1986) have also been shown to induce lung tumors, although at much higher concentrations than necessary for carbon particles or diesel exhaust. Pyrolyzed pitch, on the other hand, essentially lacking a carbon core but having PAH concentrations at least three orders of magnitude greater than diesel exhaust, was no more effective in tumor induction than was diesel exhaust (Heinrich et al., 1986b). These studies suggest that the insoluble carbon core of the particle is at least as important as the organic components and possibly more so for lung tumor induction at high particle concentrations ( $>2,000 \mu\text{g}/\text{m}^3$ ).

Diesel soot and carbon black appear to elicit similar responses in animal inhalation studies (Mauderly et al., 1994a; Heinrich et al., 1995; Nikula et al., 1995). Macrophage accumulation, epithelial histopathology, and reduced clearance have been observed in rodents exposed to high concentrations of chemically inert particles (Morrow, 1992), furthering the possibility that the toxicity of diesel particles results from the carbon core rather than the associated organics. However, the organic component of diesel particles consists of a large number of polycyclic aromatic hydrocarbons and heterocyclic compounds and their

derivatives. A large number of specific compounds have been identified. These components of diesel particles may also be responsible for the pulmonary toxicity of diesel particles. It is not possible to separate the carbon core from the adsorbed organics in order to compare the toxicity. As an approach to this question, a study has been performed in which rats were exposed to either diesel exhaust or to carbon black, an inert analog of the carbon core of diesel particles. Rats were exposed for 16 h/day, 5 days/week, for up to 24 mo to either 2,500 or 6,500  $\mu\text{g}/\text{m}^3$  of either particle (Nikula et al., 1995). Although the study is primarily concerned with the role of particle associated organics in the carcinogenicity of diesel exhaust, non-neoplastic effects are also mentioned. Both diesel exhaust and carbon black exposure resulted in macrophage hyperplasia, epithelial hyperplasia, bronchiolar-alveolar metaplasia, and focal fibrosis. In general, the number and intensity of the lesions seems to correspond to the exposure time and concentration and that the morphological characteristics of the lesions were similar in the animals exposed to diesel and to carbon black. The results suggest that the chronic noncancer effects of diesel exhaust exposure are caused by the persistence of the insoluble carbon core of the particles, rather than by the extractable organic layer. These studies have been reviewed (Health Effects Institute, 1995) and the consensus is that particulate matter is primarily responsible for the rat lung response to diesel exhaust.

### **11.5.6 Gasoline Engine Emissions**

Mauderly (1994c) reviewed the toxicological and epidemiological evidence for health risks from inhaled gasoline engine emissions. Although the data bank is more extensive for diesel exhaust, animal studies have shown that heavy, chronic exposure to gasoline engine exhaust can cause lung pathology and associated physiological effects.

In female beagle dogs exposed to gasoline engine exhaust for over 5 years (16 h/day, 7 days/week) there was little effect on respiratory function during the exposure. However, subsequent tests revealed increases in lung volumes, dead space ventilation, and dynamic lung compliance, and a decrease in alveolar-capillary gas exchange efficiency (Hyde et al., 1978). There were also slight but distinct histopathological changes in the tracheobronchial and alveolar regions.

The effects of gasoline engine exhaust on the lungs of rodents were evaluated in a series of studies in rats and Syrian golden hamsters exposed for up to 24 mo to two dilutions of gasoline engine exhaust with particle concentrations of approximately 50 or 100  $\mu\text{g}/\text{m}^3$  (Bellman et al., 1983; Muhle et al., 1984; Heinrich et al., 1986a). While gasoline engine exhaust did not cause any substantial histopathology or alterations of lavage fluid in either species, gasoline engine exhaust in the higher concentration increased lung weight, retarded particle clearance, reduced lung compliance, and increased acetylcholine sensitivity in rats. No significant changes in function were found at either concentration in the hamster, or at the lower concentration in the rat. In rats and hamsters exposed to gasoline engine exhaust and diesel engine exhaust (16 h/day, 5 days/week, for 24 mo), there were no significant changes in respiratory function (Brightwell et al., 1989).

While the laboratory animal toxicological data base is limited there is some indication that long term exposure to gasoline engine exhaust can produce effects on the respiratory tract. It is unclear to what extent the other constituents of gasoline engine exhaust may have contributed to the effects.

### **11.5.7 Summary**

In summary, diesel particulate is a widespread pollutant that is present in low concentrations in the ambient atmosphere (1 to 6  $\mu\text{g}/\text{m}^3$  in Los Angeles). Data from occupational studies and laboratory animal studies indicate that acute exposures to high levels or chronic exposures to low levels (albeit high compared to ambient levels) of diesel particulate can have an effect on the respiratory tract. However, it is doubtful that the diesel particulate at concentrations present in the ambient atmosphere could have a significant effect.

Acute and chronic inhalation exposures to diesel particulate are associated with respiratory effects. However, in general, the levels used in the laboratory animal studies or experienced in occupational settings are considerably higher than those experienced in the ambient environment and the results of these studies provide little insight into the morbidity and mortality studies discussed in Chapter 12. This is not unexpected because of the patterns of exposure and the total exposures, as well as differences in the populations exposed. Some of the effects noted in the occupational studies such as respiratory tract irritation, bronchitis,

impaired pulmonary function, cough, wheezing, are also observed in the epidemiological studies discussed in Chapter 12. Although these responses were specific to diesel exhaust, the effects appear to be due to the particles, per se. However, these effects are evident at exposures much higher than those experienced in the ambient atmosphere. Accordingly, the toxicological studies of specific diesel particulate do not appear to provide insight into the effects observed in the epidemiological studies discussed in Chapter 12 which relate to PM in general.

## **11.6 SILICA**

This section on silica particle toxicity is designed to give an overview of current concepts regarding the pulmonary toxicity of these environmental pollutants as they relate to different species, different polymorphs (crystalline vs. amorphous), and biological mechanisms of action. No attempt has been made to review all of the relevant animal toxicity data, which is voluminous. Silica is well established as a fibrogenic pollutant which causes lung tumors following chronic exposures in rats. A review of the literature on the effects of silica can be found elsewhere (U.S. Environmental Protection Agency, 1996).

The pulmonary response to inhaled silica has long been considered to be a major occupational hazard, causing disability and deaths among workers in a variety of industries. Some of the processes and work environments which are frequently associated with silica exposure include mining, sandblasting of abrasive materials, quarrying and tunneling, stonecutting, glass and pottery manufacturing, metal casting, boiler scaling, and vitreous enameling (Ziskind et al., 1976).

### **11.6.1 Physical and Chemical Properties of Silica**

Silica is one of the most common substances to which workers are exposed. Silica particle emissions in the environment can arise from natural, industrial, and farming activities. There are only limited data on ambient air concentrations of either crystalline or amorphous silica particles, due in part, to the limits in accurately quantifying crystalline silica and to the inability, under existing measurement methods, of separating the identity of crystalline silica from other particulate matter. Davis et al., (1984) used radiographic

diffraction to determine the inhalable composition and concentration of quartz in ambient aerosols collected on dichotomous filters at 25 U.S. metropolitan areas. They reported the average weight percentage of quartz in the coarse and fine particle mass to be 4.9 (+ 2.3) and 0.4 (+ 0.7), respectively. Combining the weight percentage data for the coarse fraction and 7 year average annual arithmetic mean PM<sub>10</sub> information available for 17 of the 25 areas, annual average and high U.S. ambient quartz levels of 3 and 8  $\mu\text{g}/\text{m}^3$ , respectively, have been estimated (U.S. Environmental Protection Agency, 1996). The actual fraction of quartz in PM<sub>10</sub> samples may be slightly lower than that which was estimated by Davis et al. (1984) in the coarse fraction of dichotomous filters. However, these estimated U.S. levels are considered to be reasonable upper bound estimates (U.S. Environmental Protection Agency, 1996). There are at least four polymorphs or forms of crystalline silica dust. These include quartz, cristobalite, tridymite and tripoli. Although identical chemically, they differ in their crystal parameters. The basic structural units of the silica minerals are silicon tetrahedra, arranged in such a manner so that each oxygen atom is common to two tetrahedra. However, there are considerable differences in the arrangement of the silicon tetrahedra among the various crystalline forms of silica (Coyle, 1982). Naturally occurring rocks that contain amorphous forms of silica include diatomite or diatomaceous earth, a hydrate form such as opal, and an unhydrated form, flint (Stokinger, 1981b). Silica is also a component of many naturally occurring silicate minerals in which various cations and anions are substituted into a crystalline silica matrix. Examples of such silicates are kaolin, talc, vermiculite, micas, bentonite, feldspar, asbestos, and Fuller's earth (Silicosis and Silicate Disease Committee, 1988). Commonly encountered synthetic amorphous silica, according to their method of preparation, are SiO<sub>2</sub> gel (silica G), precipitated SiO<sub>2</sub> (silica P), and fumed SiO<sub>2</sub> (silica F). The most outstanding characteristics of synthetic amorphous silica compounds are their particle size and high specific surface area, which determine their numerous applications (Stokinger, 1981b).

### **11.6.2 Health Effects of Silica**

The causal relationship between inhalation of dust containing crystalline silica and pulmonary inflammation and the consequent development of silica-induced pulmonary fibrosis (i.e., silicosis) is well established (Spencer, 1977; Morgan et al., 1980; Bowden,

1987). During the acute phase of exposure, a pulmonary inflammatory response develops and may progress to alveolar proteinosis and a granulomatous-type pattern of disease in rats and other rodent species. A pattern of nodular fibrosis occurs in chronically exposed animals and humans (Ziskind, 1976; Spencer, 1977; Morgan et al., 1980; Bowden, 1987). Although there is experimental evidence that quartz can also cause lung cancer, a clear correlation between pulmonary fibrosis and neoplasia has been suggested but has not been definitively established. Acute high occupational exposures can elicit a rapid onset of lung inflammation, leading to serious, if not fatal, lung dysfunction.

The pulmonary pathological effects of inhaled crystalline silica are well established, however, there is a paucity of information on the effects of inhaled amorphous forms of silica on the respiratory tract. The limited toxicological information available suggests that the respiratory tract effects following exposures to amorphous silicates may be reversible in the absence of continuing exposures (Groth et al., 1981; Schepers, 1981; Goscicki et al., 1978; Pratt, 1983). Thus, current evidence suggests that synthetic amorphous silica is not as severe a hazard as the various polymorphs of crystalline silica.

Parameters which have been commonly used to assess the respiratory effects of silica exposure in experimental animals include lung weight, development of pulmonary fibrosis, or biomarkers for fibrosis, such as collagen content, cytotoxicity, pulmonary inflammation, biochemical indices of homogenized lung samples or bronchoalveolar lavage samples, and immunologic responses. Few studies have provided exposure dose-response data from which definitive effect levels could be derived, thus necessitating comparisons among studies in which experimental conditions may vary considerably. A review of the published laboratory animal toxicology studies is available (U.S. Environmental Protection Agency, 1996).

### **11.6.3 Differences Between Chemical Forms of Silica**

A few studies have been carried out to compare the effects of inhaled crystalline and amorphous silica particulates (see Table 11-17). Pratt (1983) exposed guinea pigs for 21 to 24 mo to atmospheric suspensions of either cristobalite crystalline silica, amorphous diatomaceous earth, or to amorphous volcanic glass. The index of lung pathogenicity was substantially higher for the cristobalite-exposed animals compared to the other two polymorphs of amorphous silica particles (Pratt, 1983). Hemenway et al. (1986) exposed

**TABLE 11-17. COMPARATIVE INHALATION TOXICITY STUDIES WITH DIFFERENT SILICA POLYMORPHS**

Particle	Species, Gender	Mass Concentration	Exposure Duration	Observed Effect	References
Cristobalite	Guinea pig (GP)	151,000 $\mu\text{g}/\text{m}^3$	7-8 h/d 5.5 d/wk	Total amount of silica accum. varied inversely with the pulmonary tissue damage. Cristobalite produced the greatest pulmonary effects.	Pratt et al. (1983)
Diatomaceous earth (amorphous)	Same	100,000 $\mu\text{g}/\text{m}^3$	21-24 mo		
Volcanic glass (amorphous)	Same	>151,000 $\mu\text{g}/\text{m}^3$			
Cristobalite	Male Fischer 344 rats	58,000 & 73,000 $\mu\text{g}/\text{m}^3$	6 h/d 8 days	Cristobalite produced the most dramatic inflammation and fibrotic response. Amorph. silica-transient inflamm. AQ initial mild response but progressive.	Hemenway et al. (1986)
Alpha-quartz	Same	36,000 & 81,000 $\mu\text{g}/\text{m}^3$			
Amorphous silica (Zeofree 80)	Same	30,000 $\mu\text{g}/\text{m}^3$			
Fumed silica	Male SD rats Male Hartley GP Male cynomolgus monkeys	15,000 $\mu\text{g}/\text{m}^3$	5.5-6 h/d 5 d/wk up to 18 mo		
Precip. silica	Same	Same	Same	Monkeys developed greater response to fumed silica than rats or guinea pig. Fumed silica produced greater fibrotic and pulmonary function effects compared to gel or ppt. silica	Groth et al. (1981)
Gel silica	Same	Same	Same		
Cristobalite	Male SD rats	10,000 or 100,000 $\mu\text{g}/\text{m}^3$	6 h/d for 3 days	Exposures to cristobalite or AQ produced persistent and progressive pulmonary inflammation and $\uparrow$ biomarkers of cytotoxicity. Ludox and amorphous silica elicited transient pulmonary inflammatory responses.	Warheit et al. (1995)
Alpha-quartz (Min-U-Sil)	Same	10,000, 50,000 or 100,000 $\mu\text{g}/\text{m}^3$	6 h/d for 3 days		
Amorphous silica (Zeofree 80)	Same	10,000 or 100,000 $\mu\text{g}/\text{m}^3$	6 h/d for 3 days		
Ludox (Colloidal silica)	Same	10,000, 50,000 or 150,000 $\mu\text{g}/\text{m}^3$	6 h/d for 2 or 4 wk		

rats for 8 days to aerosols of one of three silicon dioxide species,  $\alpha$ -cristobalite,  $\alpha$ -quartz, and amorphous silica particulates. The greatest measure of lung injury was produced with cristobalite, which caused substantial inflammation and fibrosis. Exposures to  $\alpha$ -quartz produced mild but progressive effects, while amorphous silica produced transient inflammation. Warheit and coworkers carried out a number of short-term inhalation studies using cristobalite, ( $\alpha$ -quartz Min-U-Sil), Ludox colloidal silica, a form of precipitated amorphous silica, and amorphous silica. Rats were exposed to silica aerosols for periods ranging from 3 days to 4 weeks and evaluated by bronchoalveolar lavage and cellular proliferation indices at several postexposure time periods. Brief exposures to 2 different forms of crystalline silica particles at  $100 \mu\text{g}/\text{m}^3$  produced persistent pulmonary inflammation characterized by neutrophil recruitment and elevated biomarkers of cytotoxicity in BAL fluids. Progressive histopathologic lesions previously were observed within 1 mo after a 3-day exposure (Warheit et al., 1991a). In contrast, a 3-day exposure to amorphous silica, produced transient lung inflammation, and 2 or 4-week exposures to Ludox elicited pulmonary inflammation at 50,000 or 150,000  $\mu\text{g}/\text{m}^3$  but not at 10,000  $\mu\text{g}/\text{m}^3$ ; most elevated biochemical effects were reversible. These results demonstrated that the crystalline forms of silica dust were substantially more potent in producing pulmonary toxicity compared to the amorphous or colloidal forms of silica (Warheit et al., 1991a, 1991b, 1995). In addition, the pulmonary effects of inhaled ( $\alpha$ -quartz particles in rats were much more potent than in the study reported by Hemenway and coworkers (1986).

#### **11.6.4 Species Differences**

The fibrogenic effects of crystalline silica exposure may vary depending on the species used in experimental studies. Rats appear to be more sensitive to the development of silica-induced lung injury and lung tumors in comparison to other rodent species such as mice and hamsters (Saffioti, 1992; Saffioti et al., 1993; Uber and McReynolds, 1982). Warheit et al., (1994) reported that inhalation exposure to silica in complement-normal and complement-deficient mice produced an acute pulmonary inflammatory response which was mild and transient, compared to the pulmonary effects observed in rats wherein silica produced a sustained and progressive pulmonary inflammatory response. In support of these results, mice intratracheally injected with silica particles had a milder fibrogenic response

when compared with rats (Hatch et al., 1984). It seems clear, however, that the silica-induced response in mice depends upon the strain, as there appear to be low and high responding strains of mice to silica (Callis et al., 1985; Hubbard, 1989).

Differences are not only apparent across and within rodent species, but also between rodents and humans. Unlike the nodules observed in human radiographs, silicosis is manifested in rat radiographs as a diffuse "haziness", described as a ground-glass appearance with some peripheral striation (Kutzman, 1984). In a chronic study by Muhle et al. (1989), the principal non-neoplastic finding in the silica-exposed rats, extensive subpleural and peribronchiolar fibrosis, was described as being unlike the nodular fibrosis observed in human silicosis. Such interspecies differences and the fact that most of the available laboratory studies only examined one dose level may limit the utility of laboratory animal data for extrapolation of the silicosis risk observed in higher exposure conditions of human occupational studies.

For additional information on the pathogenic development of silica-related lung disease in humans and experimental animals, the reader is referred to a variety of informative reviews (Ziskind et al., 1976; Spencer, 1977; Reiser and Last, 1986; Bowden, 1987; Crouch, 1990; Goldstein and Fine, 1986; Warheit and Gavett, 1993).

## **11.7 BIOAEROSOLS**

### **11.7.1 Types of Health Effects Associated with Bioaerosols**

Exposure to biological aerosols can produce three general classes of health effects: infections, hypersensitivity disease, and toxicoses. It is possible that these afflictions may make people more susceptible to air pollutant effects.

#### **11.7.1.1 Infections**

Infections result when a living (micro)organism invades another organism, multiplies using some component of the host as a nutrient source, and either directly (via digestion) or indirectly (via release of toxins) causes disease. The number of individual living particles required to cause disease depends on the virulence (ability to invade the host) of the organism, and on the status of the host's immune system (Pennington, 1989). The organisms

that most commonly cause infectious disease are viruses (e.g., influenza, measles, common colds) and bacteria (e.g., Legionnaires' disease, tuberculosis). A few fungi can also cause infections in healthy people (e.g., *Histoplasma capsulatum*) or those with damaged immunity (e.g., *Aspergillus fumigatus*) (Rippon, 1988).

Particle size is an important consideration for disease. Some agents can only cause infection in the upper respiratory tract, and are best transmitted via large droplets (many common colds). Others must reach the lower airway to cause infection, and large droplets that impact in the upper airway are not usually part of the disease process (e.g., *Mycobacterium tuberculosis*) (Burge, 1989). Infectious aerosols must remain alive and be able to invade and replicate in the host in order to cause disease. Over time, infectious aerosols decay physically (becoming less concentrated) and biologically (each remaining cell becoming less able to cause disease). Airborne infectious diseases are generally caused by relatively resistant organisms that are highly virulent (Cox, 1987).

#### **11.7.1.2 Hypersensitivity Diseases**

Hypersensitivity diseases are caused by exposure to allergens (a specific type of antigen) and result from specific responses of the immune system (Pope et al., 1993). They are always caused by two step processes. Initial exposures induce sensitization (i.e., cause the production of circulating or fixed immune cells that recognize the agent), and subsequent exposures precipitate symptoms (the agent reacts with the specific immune cell and releases mediators such as histamine that result in overt symptoms). Thus the first exposure to a sensitizing agent does not cause symptoms. The kinds of hypersensitivity diseases that are caused by bioaerosols include asthma, allergic rhinitis and (rarely) allergic dermatitis (the "immediate" or IgE-mediated diseases), and hypersensitivity pneumonitis (also called allergic alveolitis) which is mediated primarily by the cellular immune system. Approximately 30% of the US population is affected by IgE-mediated allergies. The incidence of hypersensitivity pneumonitis remains unknown. Farmer's lung disease (a form of the disease) probably occurs in less than 3% of the farm population.

Very little good data have been accumulated on the actual doses of an allergen (the agent that stimulates the response) required for either sensitization or symptom development. For the IgE-mediated diseases, relatively low level long-term exposure is considered to be

important for sensitization and higher levels are needed to precipitate symptoms. For hypersensitivity pneumonitis, intense short term exposures may result in sensitization, while very low levels may induce symptoms.

Any allergen could probably cause either type of disease depending on the conditions of exposure. Pollen and fungal allergens are well-known agents that precipitate hay fever and asthma symptoms, while proteins released from dust mite fecal particles are apparently highly effective sensitizers. Historically, the agents most commonly associated with hypersensitivity pneumonitis are the thermophilic actinomycetes. In addition, fungal spores, bird droppings, bacterial enzymes, and other agents have been reported to cause the disease.

Allergen-bearing particles that induce IgE-mediated disease range in size from  $<0.1 \mu\text{m}$  (cat secretions) to  $60 \mu\text{m}$  (some grass pollen). Apparently allergen-bearing particles must be  $<5 \mu\text{m}$  in order to cause hypersensitivity pneumonitis. In both diseases, there may be synergistic effects between allergens and irritants (i.e., endotoxin, chemical air pollutants) with respect to sensitization. Note that allergens are always water soluble, and must diffuse out of the allergen-bearing particle before inducing their effect. It is likely, then, that the larger the particle, the more slowly the allergen exposure, and hence the response, will occur.

### **11.7.1.3 Toxicoses**

Microbial toxins are (essentially) chemicals that are produced by living organisms. The microbial toxicoses are basically similar to the comparable diseases caused by non-biological toxins. Microbial toxins are known that are mutagenic, teratogenic, tumorigenic, and cytotoxic. In addition, some (like endotoxin) have adjuvant activity (i.e., they stimulate the immune system).

Exposure/response relationships for biological toxins are poorly known with the possible exception of endotoxin. Endotoxin clearly affects pulmonary function and at high levels may cause serious disease (Burge, 1995). Organic dust toxic syndrome has been associated with massive exposure to endotoxins (along with mycotoxins and other components of grain dust). The incidence of the disease (the percent of the farm worker population with at least one attack) ranges from 1% in Sweden to up to 44% in the United States (Do Pico, 1992). Grain dust also causes a less acute disease with prolonged

exposures at relatively low exposure levels. Whether a component of the grain itself or of contaminating bacteria or fungi is actually the toxic agent remains unknown.

Mycotoxin-related lung disease remains poorly documented. There is some evidence that exposure to *Aspergillus flavus* aerosols containing aflatoxin B1 is a risk for lung and esophageal cancer in peanut handlers (Sorenson et al., 1984) and in farmers handling moldy corn (Baxter et al., 1981). Exposure to trichothecene toxins contained in *Stachybotrys atra* has been blamed for central nervous system symptoms, skin rashes, and pulmonary hemorrhages in specific cases, although in all cases, exposure was inferred rather than measured (Croft et al., 1986).

Particle sizes required for disease related to biological toxin exposure depend on the nature of the disease. Pulmonary effects of endotoxin probably require pulmonary deposition, while systemic effects could be precipitated by larger particles impacting in the upper airway. The fungal spores that have been blamed for mycotoxin-induced airway disease range from about 3 to 5  $\mu\text{m}$  in diameter. The location of the mycotoxins in fungal spores is unknown. The toxins may not be present on the surface of particles, and, in some cases, must be released from the particle to be effective. Endotoxin is a part of the outer cell wall.

### **11.7.2 Ambient Bioaerosols**

Ambient bioaerosols include fungal spores, pollen, bacteria, viruses, endotoxins, and animal and plant debris. Bacteria, viruses and endotoxins are mainly found attached to aerosol particles, while entities in the other categories are found as separate particles. Data for characterizing ambient concentrations and size distributions of bioaerosols are sparse. Matthias-Maser and Jaenicke (1994) found that bioaerosols constituted about 30% of the total number of particles in samples collected on a clean day in Mainz, Germany. The proportion of particles that were bioaerosols was higher in the fine size mode (as much as a third) and slightly lower in the coarse size mode. In Brisbane, Australia, Glikson et al. (1995) found that fungal spores dominate the bioaerosol count in the coarse fraction of  $\text{PM}_{10}$  and that the overall contribution of bioaerosols to total  $\text{PM}_{10}$  particulate mass was on the order of 5 to 10%. However, the cytoplasmic content of spores and pollen was often found to be adhered to particles emitted by motor vehicles and particles of crustal origin.

Fungal spores range in size from 1.5  $\mu\text{m}$  to  $>100 \mu\text{m}$ , although most are 2 to 4  $\mu\text{m}$  MMAD. They form the largest and most consistently present component of biological aerosols in ambient air. Levels vary seasonally, usually being lowest when snow is on the ground. Fungal spores often reach levels of 1000 to 10,000 spores/ $\text{m}^3$  during the summer months (Lacey and Dutkiewicz, 1994; Madelin, 1994) and may be as high as 100,000/ $\text{m}^3$  near some anthropogenic sources (agriculture activities, compost, etc.).

Asthma mortality has been associated with ambient levels of fungal spores, unadjusted OR of 2.16 (95% CI = 1.31 to 3.56) per increment of 1000 spores/ $\text{m}^3$ ; controlling for time and pollen counts reduced the RR to 1.2 (95% CI = 1.07 to 1.34) (Targonski et al., 1995). Asthma mortality in Scotland shows a seasonal peak that follows the peak in ambient pollen levels (MacKay et al., 1992). Exposure to fungal spores has also been identified as a possible precipitating factor in respiratory arrest in asthmatics (O'Hollaren et al., 1991). Such exposure can lead to allergic alveolitis (hypersensitivity pneumonitis) or pulmonary mycoses such as coccidioidomycosis or histoplasmosis (Lacey and Dutkiewicz, 1994).

Bioaerosols can contribute to increased mortality and morbidity. Most commonly, bioaerosols appear to exacerbate allergic rhinitis and asthma. Induction of hypersensitivity generally requires exposure to concentrations that are substantially higher than in ambient air, although subsequent antigenic responses require much lower concentrations. Association of fungal and pollen spores with exacerbations of asthma or allergic rhinitis is well established (Ayres, 1986) and fungal spore levels may be associated with asthma mortality (Targonski et al., 1995). The incidence of many other diseases (e.g., coccidioidomycosis) induced by fungal spores is relatively low, although there is no doubt about the causal organisms (Lacey and Dutkiewicz, 1994). The potential for fungal induced diseases is much higher in immunocompromised patients and those with unusually high exposures, such as military personnel.

In addition to fungal spores and pollen, other bioaerosol material can exacerbate asthma and can also induce responses in nonasthmatics. For example, in grain workers who experience symptoms, spirometry decrements, and airway hyperresponsiveness in response to breathing grain dust, the severity of responses is associated with levels of endotoxin in the bioaerosol rather than the total dust concentration (Schwartz et al., 1995). A classic series of studies (Antó and Sunyer, 1990) proved that airborne dust from soybean husks was

responsible for asthma epidemics and increased emergency room visits in Barcelona, Spain. These studies indicate that airborne fragments of biological substances can produce severe health effects.

Bacterial aerosol counts may range as high as 30,000 bacteria/m<sup>3</sup> downwind of sewage treatment facilities, composting areas, waterfalls from polluted rivers, or certain agricultural activities. Typical levels in urban areas range from several hundred to several thousand bacteria/m<sup>3</sup> (Lighthart and Stetzenbach, 1994). Human pathogenic activity of such bacteria is not well understood or characterized. Infective potential of aerosolized bacteria depends on size (smaller are more effective), virulence, host immune status, and host species sensitivity (Salem and Gardner, 1994). Aerosolized bacteria can cause bacterial infections of the lung including tuberculosis and legionnaire's disease. The *Legionella pneumophila* bacterium is one of the few infectious agents known to reside outside an infected host and is commonly found in water, including lakes and streams. Levels of bioaerosols (fungi and bacteria) are generally higher in urban than in rural areas (Lighthart and Stetzenbach, 1994).

Exposures to bioaerosols of the above types, while clearly capable of producing serious health effects (especially at high concentrations often encountered in indoor environments) appear unlikely to account for observed ambient (outdoor) PM effects on human mortality and morbidity demonstrated by epidemiology studies reviewed in Chapter 12. This conclusion is based on (1) bioaerosols generally represent only a very small percentage (< 5 to 10%) of measured urban ambient PM mass; (2) they typically have even lower concentrations in ambient air during winter months, when notable ambient PM effects have been demonstrated; and they tend to be in the coarse fraction size range.

## **11.8 TOXICOLOGY OF OTHER PARTICULATE MATTER**

### **11.8.1 Introduction**

This section reviews the toxicology of other PM within the framework described in the introduction to the chapter. The particle classes chosen for inclusion here are those which may actually occur in ambient air or may be surrogates for these. For example, some of the particles discussed are considered to be models of "nuisance" or "inert" dusts (i.e., those having low intrinsic toxicity) and, as such, are likely to be representative of similar ambient

PM. In many instances, there are only a few studies examining the response on specific biological endpoints following inhalation exposure. In these cases, and where available, intratracheal instillation studies have been used to compare the toxicity of different particle types. While instillation may produce more severe pulmonary damage than would inhalation (largely due to differences in delivered doses and dose rates), the relative toxicities of different particles seem to be similar when given by either method (Driscoll et al., 1991). Thus, intratracheal instillation studies can be used for comparative potency purposes, but it is not possible to quantitatively extrapolate the resulting exposure-response data to inhalation exposure-responses. In a number of cases, particles with low intrinsic toxicity have been used in instillation studies to delineate nonspecific particle effects from effects of known toxicants. Some of these studies are discussed herein, as they offer the only database for such materials.

### **11.8.2 Mortality**

Examples of studies in which effects on mortality were reported using particles  $>1 \mu\text{m}$  in diameter are presented in Table 11-18; all of these studies involved repeated or chronic exposures to high concentrations of various PM, some of which are considered to be of low toxicity. While incomplete, the studies are of a variety of materials and indicate that essentially no treatment-related mortality was induced in any of the studies.

Recent interest has been focused on the inherent toxicity of a smaller size class of particles, namely the ultrafine particles which are discussed in Section 11.4. While the mass concentration of ultrafine particles in ambient air may be low, their number concentration may be quite high, as discussed previously.

### **11.8.3 Pulmonary Mechanical Function**

Assessments of pulmonary mechanical function have generally been carried out with particles having some inherent toxicity, as well as other studies examining effects of other particles with low intrinsic toxicity (see Table 11-19). Wright et al. (1988) instilled rats (Sprague-Dawley; F; 200g) with 10,000  $\mu\text{g}$  iron oxide ( $0.1 \mu\text{m}$  GMD,  $\sigma_g = 1.7$ ) or silica (quartz) ( $1.3 \mu\text{m}$ ,  $\sigma_g = 2.5$ ). At 1 mo after exposure, they noted no changes in various indices of pulmonary mechanics (total lung capacity [TLC];

**TABLE 11-18. EFFECTS OF PARTICULATE MATTER ( $\geq 1 \mu\text{m}$ ) ON MORTALITY**

Particle	Species, Gender, Strain, Age, or Body Weight	Exposure Technique	Mass Concentration ( $\mu\text{g}/\text{m}^3$ )	Particle Characteristics		Exposure Duration	Observed Effect <sup>a</sup>	Reference
				Size ( $\mu\text{m}$ ); $\sigma_g$				
TiO <sub>2</sub>	Rat, M/F, F-344, 8 weeks	Whole body	5,000	1.1 (MMAD); 1.5		6 h/day, 5 days/week, 2 years	None	Muhle et al. (1991)
Toner	Rat, M/F, F-344, 8 weeks	Whole body	16,000	4 (MMAD)		6 h/days, 5 days/week, 2 years	None	Muhle et al. (1991)
Coal dust	Rat, M, Wistar, 18 weeks	Whole body	6,600, 14,900	2.1 (MMAD); 2.7		6 h/day, 5 days/week, 20 mo	None	Karagianes et al. (1981)
Petroleum coke (micronized)	Rat, M, SD	Whole body	10,000, 30,000	3.1 (AED); 1.9		6 h/day, 5 days/week, 2 years	None	Klonne et al. (1987)
Petroleum coke (micronized)	Monkey, adult, cynomologous	Whole body	10,000, 30,000	3.1 (AED); 1.9		6 h/day, 5 days/week, 2 years	None	Klonne et al. (1987)
Volcanic ash	Rat, M/F, F-344, 3 mo	Whole body	5,000, 50,000	Respirable (unspecified size)		6 h/day, 5 days/week, 2 years	None	Wehner et al. (1983)
TiO <sub>2</sub>	Rat, M/F, CD	Whole body	10,000, 50,000, 250,000	1.5-1.7 (MMD)		6 h/day, 5 days/week, 2 years	None	Lee et al. (1985)
Fly ash (coal)	Rat, M, Wistar, 3 mo	Whole body	270,000	47% $\leq 3.75 \mu\text{m}$		6 h/day, 15 days	None	Chauhan et al. (1987)
California road dust	Rat, F-344	Nose-only	300, 900	4 (MMAD); 2.2		4 h/day, 4 days/week, 8 weeks	None	Kleinman et al. (1995)
Talc	Rat, M/F, F-344	Whole body	6,000, 18,000	2.7-3.2 (MMAD); 1.9		6 h/day, 5 days/week, 2 years	None	National Toxicology Program (1993)

<sup>a</sup>Effect indicates "treatment related" mortality.

**TABLE 11-19. EFFECTS OF INHALED PM ON PULMONARY MECHANICAL FUNCTION**

Particle	Species, Gender, Strain, Age, or Body Weight	Exposure Technique	Mass Concentration ( $\mu\text{g}/\text{m}^3$ )	Particle Characteristics		Exposure Duration	Observed Effect <sup>a</sup>	Reference
				Size ( $\mu\text{m}$ ); $\sigma_g$				
Volcanic ash	Rat, Sprague-Dawley, 40 days	Whole body	9,400	0.65 (MMAD); 1.78		2 h/days, 5 days	No changes (f, $V_T$ , $V_{\text{insp}}$ , $V_{\text{exp}}$ )	Raub et al. (1985)
Fly ash (coal) (Illinois # 6)	Guinea pig, Hartley, 250-320 g	Nose-only	5,800	0.21 (MMAD); 4.14		1 or 2 h	2 h: $\downarrow$ TLC, VC, $DL_{\text{co}}$ up to 96 h PE 1 h: no effect	Chen et al. (1990)
Fly ash (coal) (Montana lignite)	Guinea pig, Hartley, 250-320 g	Nose-only	5,800	0.21 (MMAD); 4.14		1 or 2 h	2 h: $\downarrow$ TLC, VC; no change in $DL_{\text{co}}$	Chen et al. (1990)
Volcanic ash	Rat, M/F, F-344, 3 mo	Whole body	5,000, 50,000	Respirable		6 h/day, 5 days/week, 24 mo	$\uparrow$ f for 50,000 $\mu\text{g}/\text{m}^3$ by 8 mo; no change for 5,000 $\mu\text{g}/\text{m}^3$	Wehner et al. (1983)
Volcanic ash	Guinea pig, Hartley, 300-425 g	Head	9,400	0.65 (MMAD); 1.78		2 h	No change in $R_{\text{aw}}$ , $C_{\text{dyn}}$ , f, $V_T$ , $\dot{V}_E$	Wiester et al. (1985)
Coal dust	Rat, Wistar, 200-300 g, conventional and germ free	Whole body	10,000	Geometric mean $<5 \mu\text{m}$		8 h/day, 120 days	$\downarrow$ FEV <sub>1</sub> , $\dot{V}_{\text{max}}$ (10%) (Germfree); only $\downarrow \dot{V}_{\text{max}}$ (10%) conv.	Moorman et al. (1977)
TiO <sub>2</sub>	Rat, F, F-344, 8 weeks	Whole body	5,000	—		6 h/day, 5 days/week, 24 mo	No changes (C, $V_T$ , IC, VC, RV, TLC, $DL_{\text{co}}$ , N <sub>2</sub> washout)	Heinrich et al. (1989b)

Key to abbreviations:

f: breathing frequency  
 $V_T$ : tidal volume  
 $V_{\text{insp}}$ : inspiratory flow  
 $V_{\text{exp}}$ : expiratory flow  
TLC: total lung capacity  
VC: vital capacity  
 $DL_{\text{co}}$ : carbon monoxide diffusing capacity  
PE: post exposure  
IC: inspiratory capacity

RV: residual volume  
 $R_{\text{aw}}$ : airway resistance  
 $C_{\text{dyn}}$ : dynamic compliance  
 $\dot{V}_I$  = max inspiratory flow  
 $\dot{V}_E$  = expiratory minute volume  
FEV<sub>1,0</sub> = forced expiratory volume (1 sec)  
 $\dot{V}_{\text{max}}$  (10%) = maximal flow at 10% FVC  
FVC = forced vital capacity

functional residual capacity [FRC]; nitrogen [ $N_2$ ] washout; FEV<sub>1</sub>; or peak expiratory flow [PEF]) in animals exposed to iron oxide, but silica exposure resulted in changes in the  $N_2$  washout curve and decreased compliance. Bégin et al. (1985) instilled into sheep (Male; 25 to 45 kg BW) 100,000  $\mu\text{g}$  latex beads (0.1  $\mu\text{m}$ ) or asbestos fibers. The latex produced no change in pulmonary function (TLC, residual volume [RV]; vital capacity [VC]; expiratory reserve volume [ERV]; pulmonary compliance [ $C_{\text{pulm}}$ ]; pulmonary resistance [ $R_{\text{pulm}}$ ]; FRC), while the asbestos produced a reduction in compliance, abnormalities in the  $N_2$  washout curve, and changes in forced expiratory flow measurements.

There are a few studies of pulmonary function responses following inhalation exposures to PM. Chen et al. (1990) evaluated pulmonary function of guinea pigs exposed to coal fly ash (5.8  $\mu\text{g}/\text{m}^3$ , MMAD = 0.21  $\mu\text{m}$ ) produced during combustion of Illinois no. 6 coal (high sulfur) or Montana lignite (low sulfur). Total lung capacity (TLC), vital capacity (VC), and diffusing capacity for carbon monoxide ( $DL_{\text{CO}}$ ) were all significantly reduced below control values at 2h and 8h postexposure in guinea pigs exposed to Illinois no. 6 ash. The  $DL_{\text{CO}}$  was still 10% below control values 96h postexposure. Guinea pigs exposed to the Montana lignite fly ash at comparable concentration and particle size did not show alterations in diffusing capacity. The authors suggested that the different effects could be due to sulfuric acid produced during combustion of the two coals but neutralized by the high alkali content of the Montana lignite.

Wehner et al. (1983) exposed rats (F-344; M/F, 3mo) to 5,000 or 50,000  $\mu\text{g}/\text{m}^3$  volcanic ash (Mt. St. Helens) for 6 h/day, 5 days/week for up to 24 mo (Table 11-19). By 12 mo of exposure, no changes in lung volume were noted. By 8 mo of exposure, there was an increase in respiratory frequency in animals exposed at the higher concentration, but no change at the lower concentration.

Heinrich et al. (1989b) exposed rats for 6 h/day, 5 days/week up to 24 mo to titanium dioxide ( $\text{TiO}_2$ ) at 5,000  $\mu\text{g}/\text{m}^3$  and silica at 1,000  $\mu\text{g}/\text{m}^3$ . Exposure to silica produced a reduction in quasistatic lung compliance, tidal volume, ( $V_T$ ), inspiratory capacity (IC), VC, RV, and TLC. Diffusion capacity for carbon monoxide ( $DL_{\text{CO}}$ ) was also reduced, and the  $N_2$  washout curve was altered; these changes indicate a functionally restrictive lung, a finding often noted in humans occupationally exposed to silicates. None of these variables were altered by exposure to  $\text{TiO}_2$ .

Acidic sulfates have been associated with alterations in bronchial responsiveness, but there are few studies with other particles which examined this response. Fedan et al. (1985) exposed rats (F344, whole body) for 7 h/day, 5 days/week for 2 years to coal dust (size described as respirable, but not specifically stated) at  $2,000 \mu\text{g}/\text{m}^3$ , and examined the pharmacological response of isolated tracheal preparations to various agonists. The coal dust exposure increased the maximal contractile response of the tracheal smooth muscle to acetylcholine (a bronchoconstrictor), compared to air exposed control tissue, but did not alter the slope of the acetylcholine concentration-response curve nor sensitivity (i.e., EC50). No change in response to isoproterenol (a bronchodilator) was noted. Wiester et al. (1985) exposed guinea pigs for 2 h to  $9,400 \mu\text{g}/\text{m}^3$  of Mt. St. Helens volcanic ash ( $0.65 \mu\text{m}$ ). No changes in pulmonary mechanics measured during exposure (airway resistance, dynamic compliance, breathing frequency, maximum inspiratory flow or expiratory minute volume) were noted. However, following exposure, airway hyporesponsiveness to histamine challenge was observed.

It should be noted that, as with acidic sulfates, changes in pulmonary function may not be the most sensitive marker of response to other PM. For example, inflammatory changes in sheep following the instillation of latex particles ( $100,000 \mu\text{g}$  in 100 ml fluid) were not associated with any changes in lung volumes, resistance, or compliance (Bégin et al., 1985).

#### **11.8.4 Pulmonary Morphology and Biochemistry**

A considerable amount of the information concerning morphologic alterations from inhaled particles has been obtained in studies of diesel exhaust, and this is discussed in this chapter and reviewed elsewhere (U.S. Environmental Protection Agency, 1994; Health Effects Institute, 1995). In addition, and as previously mentioned with acidic sulfate particles, markers in lung BAL have been used to assess damage following PM exposure.

The ability of ambient particles to affect lung morphology was strongly suggested by Böhm et al. (1989). They exposed rats (Wistar, F, 2.5 mo) for 6 mo to the ambient air of two cities in Brazil, namely São Paulo and Cubatao. Although characterization of air pollution levels was vague, pollution in the former appeared to be dominated by automobile exhaust gases, while that in the latter by industrially derived particulate matter. Rats exposed in Cubatao showed various responses, such as mucus hypersecretion and epithelial

hyperplasia, in both the upper and lower bronchial tree, while those exposed in São Paulo showed effects generally limited to the upper bronchial tree. Particle concentrations ( $PM_{10}$ ) were as high as  $164 \mu\text{g}/\text{m}^3$  in Cubatao. Thus, high PM levels were suggested to be responsible for the observed effects, although the contribution of other components of the pollutant mix could not be discounted.

Some intratracheal instillation studies have compared morphological effects resulting from exposure to different particles. Wright et al. (1988) instilled  $10,000 \mu\text{g}$  iron oxide ( $\text{Fe}_2\text{O}_3$ ;  $0.1 \mu\text{m}$  GMD,  $\sigma_g = 1.7$ ) or  $10,000 \mu\text{g}$  quartz ( $1.3 \mu\text{m}$  GMD,  $\sigma_g = 2.5$ ) into rats, and examined the lungs 30 days following each exposure. The iron oxide did not produce any histological or morphometric changes, while the quartz exposure resulted in aggregations of PMNs and AMs around small airways, alveolar proteinosis, increased alveolar distances, airspace enlargement, and increased thickness of respiratory bronchiolar walls.

Another example of an instillation study which may be used to compare effects from different types of particles is that of Sanders et al. (1982), who instilled rats (F-344, female, young adult) with  $40,000 \mu\text{g}$  of either soil (sandy loam,  $1.6 \mu\text{m}$  CMD), volcanic ash (Mt. St. Helens,  $0.5$  to  $1.5 \mu\text{m}$  CMD), or crystalline quartz ( $1.5 \mu\text{m}$  CMD). Mononuclear cell infiltration was noted with both the soil and ash particles in regions of high particle aggregation. There was also some Type 2 epithelial cell hyperplasia 7 to 37 days following ash or soil instillation. However, the ash produced a fibrotic response to a greater extent than did the soil, with indications from the former of a simple pneumoconiosis and moderate lipoproteinosis. Some foci of particle-laden macrophages were noted in the mediastinal lymph nodes of soil exposed animals, but the ash-exposed animals showed reactive lymphoid hyperplasia. Quartz resulted in production of granulomas, deposition of collagen, widespread lipoproteinosis, and fibrosis in regional lymph nodes.

The comparative fibrogenic potential of a number of particle types was examined by Schreider et al. (1985). Male Sprague-Dawley rats were exposed by intratracheal instillation to  $5,000$ ,  $15,000$ , or  $45,000 \mu\text{g}$  of Montmorillonite clay ( $0.84 \mu\text{m}$  CMD), quartz ( $1.1 \mu\text{m}$ ), Mt. St. Helens volcanic ash ( $1.2 \mu\text{m}$ ), stack-collected coal fly ash ( $1.5 \mu\text{m}$ ) or hopper-collected fly ash ( $1.9 \mu\text{m}$ ), or to  $5,000$  or  $15,000 \mu\text{g}$  of a coal-oil ash mixture ( $3.9 \mu\text{m}$ ). Lung histology was assessed at 90 days post instillation. Neutrophils were noted in alveoli only with quartz (all concentrations), stack ash (at high concentration), and

volcanic ash (low and mid concentrations). Some fibrosis was produced by all of the particles, although there were qualitative and quantitative differences among the different exposure groups. The order of fibrosis potential, from greatest to least, was as follows: quartz > clay > volcanic ash > hopper coal ash > stack coal ash > oil-coal ash mixture.

Bégin et al. (1985) instilled 100,000  $\mu\text{g}$  of 0.1  $\mu\text{m}$  latex beads or asbestos fibers into the lungs of sheep (25 to 45 kg) and examined lavage fluid at 1 to 60 days post instillation. The latex produced only transient alveolitis and transient increases in the number of AMs and PMNs in lavage beginning at day 1, whereas the asbestos-exposed animals had a persistent inflammatory response and more severe damage. Callis et al. (1985) instilled silica or latex particles (0.9  $\mu\text{m}$ ) into the lungs of mice. While the latter produced some increase in protein and cell number in lavage, the response to the former was much greater. Finally, Lindenschmidt et al. (1990) instilled rats with either of two inert dusts, ( $\text{Al}_2\text{O}_3$ ; 5.3  $\mu\text{m}$ ) and  $\text{TiO}_2$  (2.2  $\mu\text{m}$ ) at 1,000 or 5,000  $\mu\text{g}/100\text{g}$  body weight and examined the lungs up to 63 days post instillation. Both particle types produced similar increases in N-acetylglucosamine and total recovered cells in lavage, while a minimal Type 2 cell hyperplasia noted with  $\text{Al}_2\text{O}_3$  was even less severe with  $\text{TiO}_2$ . However, when results were compared with those for instilled silica, any responses seen with the inert particles decreased towards control level during the 2-mo study period, while changes with silica progressed. This highlights the difference between the inert and fibrogenic materials. Thus, the instillation studies suggest that there may be some nonspecific particle effect, but clearly the chemical characteristics of the particle affects the ultimate biological response. In any case, levels of particles with low intrinsic toxicity are not associated with major nonspecific effects.

The effects of inhaled PM on pulmonary morphology are outlined in Table 11-20. Most of the studies used fly ash and volcanic ash;  $\text{TiO}_2$  has also been used to assess effects of a "nuisance" (low intrinsic toxicity) type of particle. However, with the exception of the study of road dust by Kleinman et al. (1995), exposure concentrations ranged from very high to extremely high and likely caused overload with long-term exposures. Responses, when they did occur, were quite similar for the various particles, characterized by focal aggregates of particle-laden macrophages with evidence of an inflammatory response; the intensity of both effects was related to exposure duration and concentration. On the other

**TABLE 11-20. EFFECTS OF PARTICULATE MATTER ON RESPIRATORY TRACT MORPHOLOGY**

Particle	Species, Gender, Strain, Age or Body Weight	Exposure Technique	Mass Concentration ( $\mu\text{g}/\text{m}^3$ )	Particle Characteristics		Exposure Duration	Observed Effect	Reference
				Size ( $\mu\text{m}$ ); $\sigma_g$				
Coal dust (micronized bituminous)	Rat, M, Wistar, 18 weeks	Whole body	6,600, 14,900	2.1 (MMAD); 2.7		6 h/day, 5 days/week, 20 mo	Accumulation of aggregates of particles in AMs immed. after exposure; alveolar histiocytosis, interstitial fibrosis and emphysema, indication of simple pneumoconiosis; no lesions in upper respiratory tract.	Karagianes et al. (1981)
Petroleum coke (micronized raw)	Rat, M/F, S-D; Monkey, cynomologous (mature)	Whole body	10,000, 30,000	3.1 (AED); 1.9		6 h/day, 5 days/week, 2 years	Rat: chronic pulmonary inflammation at 3, 6, 12, and 18 mo observation times at both conc; focal fibrosis; sclerosis; squamous alveolar metaplasia. Monkey: accumulation of particle-laden AMs; no inflammation	Klonne et al. (1987)
Fly ash (coal)	Rat, M/F, F-344, 10-13 mo	Whole body	36,000	3.6 (MMAD); 2		7 h/day for 3 days on week 1, 5 days/week next 3 weeks, 2 days in week 5	No exposure-related histopathology in large or small airways; but increased cell division; slight increase in number of hypertrophic Type 2 cells by 2 weeks; small areas of thickened alveolar walls and some perivenous inflammatory cell infiltration; by 4 weeks, aggregation of AMs with particles and greater alveolar wall thickening and inflammation; some resolution by 42 weeks in pathology.	Shami et al. (1984)
Volcanic ash (Mt. St. Helens)	Rat, M/F, F-344, 3 mo	Whole body	5,000, 50,000	Respirable (no size given)		6 h/day, 5 days/week, up to 24 mo	At 5,000 $\mu\text{g}/\text{m}^3$ : small aggregations of particle-laden AMs at 4 mo and some thickening of alveolar septa. Aggregates of dust deposits at 8 mo, and some peribronchiolar lymphoid hyperplasia which increased by 12 mo. Enlargement of mediastinal nodes by 12 mo. At 50,000 $\mu\text{g}/\text{m}^3$ : more severe lesions; low to moderate AM accumulation by 4 mo which increased by 8 mo and stabilized by 12 mo. Prominent peribronchial and mediastinal node reaction by 4 mo, which increased by 8 mo and stabilized by 12 mo; alveolar proteinosis by 8 mo.	Wehner et al. (1983)
TiO <sub>2</sub>	Rat, F, F-344, 8 weeks	Whole body	5,000			6 h/day, 5 days/week, up to 24 mo	No fibrosis; no bronchiolar hyperplasia; no accumulation of AMs in lung tissue.	Heinrich et al. (1989b)

**TABLE 11-20 (cont'd). EFFECTS OF PARTICULATE MATTER ON RESPIRATORY TRACT MORPHOLOGY**

Particle	Species, Gender, Strain, Age or Body Weight	Exposure Technique	Mass Concentration ( $\mu\text{g}/\text{m}^3$ )	Particle Characteristics	Exposure Duration	Observed Effect	Reference
				Size ( $\mu\text{m}$ ); $\sigma_g$			
Fly ash (coal)	Mice, M, C57BL/6, 12 weeks	Nose-only	200,000	1.6-1.7 (MMAD); 1.4-1.5	100 min	Increased no. of AMs; no other lesions evident by light microscopy.	Fisher and Wilson (1980)
TiO <sub>2</sub>	Guinea pig, F, Dunkin-Hartley, 300-350 g	Whole body	23,000	95% < 1.98 (MMAD)	20 h/day, 14 days	At 1 day PE: dust laden cells in bronchial lymph nodes and BALT; some thickening of alveolar septa in areas of high dust conc.; some degenerative changes in AMs; no PMNs. At 6 d PE: increased number of dust laden AMs.	Baskerville et al. (1988)
Volcanic ash	Rat, Sprague-Dawley, 40 days	Whole body	9,400	0.65 (MMAD); 1.78	2 h/day, 5 days	Slight peribronchial and perivascular mononuclear cell infiltration.	Raub et al. (1985)
California road dust	Rat, F-344	Nose-only	900	4 (MMAD); 2.2	4 h/day, 4 days/week, 8 weeks	↑ Alveolar septal wall thickness; ↓ Alveolar diameter	Kleinman et al. (1995)
TiO <sub>2</sub>	Rat, M/F, CD	Whole body	10,000, 50,000, 250,000	1.5-1.7 (MMAD)	6 h/day, 5 days/week, 2 years	At 10,000 $\mu\text{g}/\text{m}^3$ : slight alveolar epithelial hyperplasia. At 50,000 $\mu\text{g}/\text{m}^3$ : marked alveolar epithelial hyperplasia; bronchioarization of alveoli adjacent to terminal bronchioles; alveolar proteinosis. At 250,000 $\mu\text{g}/\text{m}^3$ : increased alveolar hyperplasia and bronchioarization; deposition of collagen fibers.	Lee et al. (1985)
Fly ash (fluidized bed coal combustion)	Rat, M/F, F-344, 12-16 weeks	Whole body	142,000	3 (MMAD); 2.6	6 h	No pathology, except accumulation of particles.	Hackett (1983)
Fly ash (coal)	Hamster, golden, 8 weeks	Whole body	2,000, 1,000, 2,000, 20,000	2.3-2.4 (MMAD); 1.5	20 h/day, 7 days/week, 6 mo	Accumulation of particle-laden AMs in proximal alveoli in concentration/duration dependent fashion; ↑ PMNs at 20,000 $\mu\text{g}/\text{m}^3$ in peripheral alveoli.	Negishi (1994)
Fly ash (fluidized bed coal combustion)	Rat, M/F, F-344, 12 weeks	Whole body	36,000	3.6 (MMAD); 2.0	7 h/day, 5 days/week, 4 weeks	Slight enlargement of lung associated lymph nodes due to increased no. of lymphoid cells (persistent up to 48 weeks PE); small cluster of particle laden AMs in alveoli.	Bice et al. (1987)
Fly ash (pulverized coal combustion)	Rat, M/F, F-344, 12 weeks	Whole body	37,000	2.7 (MMAD); 2.1	7 h/day, 5 days/week, 4 weeks	Moderate enlargement of lung associated lymph nodes due to hyperplasia and cell accumulation (persistent up to 48 weeks PE); small granulomas in lungs.	Bice et al. (1987)

**TABLE 11-20 (cont'd). EFFECTS OF PARTICULATE MATTER ON PULMONARY MORPHOLOGY**

Particle	Species, Gender, Strain, Age or Body Weight	Exposure Technique	Mass Concentration ( $\mu\text{g}/\text{m}^3$ )	Particle Characteristics		Exposure Duration	Observed Effect	Reference
				Size ( $\mu\text{m}$ ); $\sigma_g$				
Carbon black	Rat, M, F-344, 14-15 weeks	Whole body	10,000	2.0/0.12 (MMAD) (bimodal distr. with 70% in smaller mode) 2.5/2.3		7 h/day, 5 days/week, 12 weeks	Mild hyperplasia of Type 2 cells; particle laden AMs in distal terminal bronchioles and proximal alveolar ducts.	Wolff et al. (1990)
Carbon black	Rat, F, Wistar 6 weeks		6,000	n/s		18 h/day, 5 days/week, 10 mo	Moderate to severe hyperplasia in bronchioalveolar region; some inflammation; alveolar lipoproteinosis	Nolte et al. (1994)
Fly ash (coal)	Rat, M, Wistar, 160-175 g	Whole body	270,000	47% <3.75 $\mu\text{m}$		6 h/day, 15 days	Mild infiltration of mononuclear cells and mild pneumonitis 45 days PE; numerous particle-laden AMs outside alveoli up to 105 days PE; $\uparrow$ lung weight by 30 days PE.	Chauhan et al. (1987)
Shale dust (raw or spent)	Monkey, cynomolgus, M/F, 2-4.5 kg  Rat, M/F, F344, 90-95 g	Whole body	10,000, 30,000	3.9-4.5; (1.8-2.2)		6 h/day, 5 days/week, 2 years	Concentration-related accumulation of AMs; subacute bronchiolitis and alveolitis  Concentration-related proliferative bronchiolitis and alveolitis, chronic inflammation with spent shale; no lymph node inflammation; accumulation of AMs	MacFarland et al. (1982)
Coal dust	Monkey cynomolgus, M Rat, M/F, F-344 Mice, M/F CD-1	Whole body	2,000	8.6 $\mu\text{m}$ (MMAD)		7-h/day, 5 days/week, up to 2 years	Type II cell hyperplasia and pulmonary lipodosis in rats; increased phagocytosis. Mild obstructive airway disease in monkeys.	Lewis et al. (1989)

Key to abbreviations:

NS: Not specified

PE: Post-exposure

AM: Alveolar macrophage

PMNs: Polymorphonuclear leukocytes

hand, the Kleinman et al. (1995) study at relatively low particle concentrations showed a more diffuse pattern of morphological change and no inflammatory loci.

There is some evidence for interspecies differences in response to comparable exposure atmospheres (Klone et al., 1987). In the study of Shami et al. (1984), increased proliferation of large and small airway epithelial cells occurred in the absence of overt histopathology following exposure to fly ash. The authors suggested that this may indicate some potential for the interaction of fly ash with carcinogens.

Clark et al. (1990) exposed dogs (mongrel, 15 to 20 kg) for 5 min to wood smoke (from fir plywood sawdust and kerosene; no specified particle size or exposure concentration) via an endotracheal tube. The lungs were examined for increased extravascular water around the pulmonary arteries, which was found to occur with smoke exposure but not in air sham controls. This response was suggested to be due to increased microvascular permeability without any increase in capillary pressure. A decrease in lung compliance was also noted with smoke exposure.

Table 11-21 outlines studies in which lavage fluid was analyzed following inhalation exposure to PM. As with morphology, most exposure concentrations were very high, but effects, when they occurred, indicated inflammation.

As mentioned earlier, eicosanoids are potent mediators of various biological functions, and alterations in arachidonic acid metabolism, which may be involved in lung pathology, can be assessed in lavage fluid. Exposure to coal dust ( $25,000 \mu\text{g}/\text{m}^3$ ) produced decreases in prostaglandin  $E_2$ , and increases in thromboxane  $A_2$  and leukotriene  $B_4$ , perhaps suggesting smooth muscle constriction, vasoconstriction and increased chemotactic activity of macrophages (Kuhn et al., 1990).

Table 11-22 outlines studies examining lung biochemistry following particle inhalation, mostly to fly ash. In some cases, effects on the xenobiotic metabolizing system of the lungs were examined. For example, van Bree et al. (1990) exposed rats to coal fly ash (10,000, 30,000, 100,000  $\mu\text{g}/\text{m}^3$ ) and examined cytosolic antioxidant enzymes and the microsomal P-450 linked mixed function oxidase system involved in lung metabolic defense against reactive oxygen species and xenobiotic compounds. They noted both exposure-related increases and decreases in different components of this system, which they ascribed to differential effects of organic and trace metal components of the ash. Srivastava et al. (1985)

**TABLE 11-21. EFFECTS OF PARTICULATE MATTER ON MARKERS IN LAVAGE FLUID**

Particle	Species, Gender, Strain, Age or Body Weight	Exposure Technique	Mass Concentration ( $\mu\text{g}/\text{m}^3$ )	Particle Characteristics		Exposure Duration	Observed Effect	Reference
				Size ( $\mu\text{m}$ ); $\sigma_g$				
Carbon black	Mouse, F, Swiss, 20-23 days	Nose-only	10,000	2.45 (MMAD); 2.54		4 h/day, 4 days	No change in total cell no. or differential counts; no change in albumin levels.	Jakab (1992, 1993)
Volcanic ash	Mouse, F, CD-1, 4-8 weeks	Whole body	9,400	0.65 (MMAD); 1.8		2 h	Increase in PMNs.	Grose et al. (1985)
TiO <sub>2</sub>	Rat, M, F-344 180-200 g	Whole body	50,000	1 (MMAD); 2.6		6 h/day, 5 days	No change in: AMs, PMNs, lymphocytes; LDH; protein; to 63 days PE.	Driscoll et al. (1991)
TiO <sub>2</sub>	Rat, HAN	Whole body	50,000			8 h/day, 5 days/week (up to 15 weeks)	Slight increase in PMNs at 15 weeks.	Brown et al. (1992)
Coal dust	Rat, HAN	Whole body	10,000, 50,000			8 h/day, 5 days/week (up to 15 weeks)	Increased PMNs (persistent).	Brown et al. (1992)
California road dust	Rat, F-344	Nose-only	300, 900	4 (MMAD); 2.2		4 h/day, 4 days/week, 8 weeks	↑ Albumin at 900 $\mu\text{g}/\text{m}^3$ ; no change in total cells or differential counts	Kleinman et al. (1995)
TiO <sub>2</sub>	Rat, M/F, F-344, 8 weeks	Whole body	5,000	1.1 (MMAD); 1.6		6 h/day, 5 days/week, 24 mo	No change in total cell no. in lavage but ↑ AMs and ↓ PMNs some time points; no change in LDH, protein, β-glucuronidase in lavage.	Muhle et al. (1991)
Fe <sub>2</sub> O <sub>3</sub>	Rat, M, Long-Evans, 225-250 g	Nose-only	18,000-24,000	1.45-1.7 (MMAD); 2.9-3		2 h	No change total cell no. or differential counts.	Lehnert and Morrow (1985)
Carbon black	Rat, M, F-344, 14-15 weeks	Whole body	10,000	2.0/0.12 (MMAD) (bimodal distr. with 70% in smaller mode); 2.5/2.3		7 h/day, 5 days/week, 12 weeks	↑ PMNs in lavage; ↑ acid proteinase in lavage.	Wolff et al. (1990)
Carbonyl iron	Rat, M Crl:CDBR, 8 weeks	Nose-only	100,000	3.6 (MMAD); 1.7		6 h; 6 h/day, 3 days	No change in total cell no, protein, or LDH.	Warheit et al. (1991a)
Carbon black	Mouse, F, Swiss 20-23 g	Nose-only	10,000	2.4 (MMD); 2.75		4 h	No change in total cell no. or differential count at 20 h PE.	Jakab and Hemenway (1993)
TiO <sub>2</sub>	Guinea pig, M/F, 400 g	Whole body	24,000	85% < 2 $\mu\text{m}$		8 h/day, 5 days/week, 3 weeks	No change in LDH, AP, AG, Cathepsin D at 4-24 h PE.	Kuhn et al. (1990)
Coal dust	Rat, F, F-344, 180 g	Whole body	25,000	4-5		16 h/day, 7 days/week, 2 weeks	↑ TxA <sub>2</sub> , LTB <sub>4</sub> , protein; ↓ PGE <sub>2</sub> at 1 day PE; TxA <sub>2</sub> , and LTB <sub>4</sub> change persistent for 2 weeks.	Sjöstrand and Rylander (1984)

**TABLE 11-21 (cont'd). EFFECTS OF PARTICULATE MATTER ON MARKERS IN LAVAGE FLUID**

Particle	Species, Gender, Strain, Age or Body Weight	Exposure Technique	Mass Concentration ( $\mu\text{g}/\text{m}^3$ )	Particle Characteristics	Exposure Duration	Observed Effect	Reference
				Size ( $\mu\text{m}$ ); $\sigma_g$			
TiO <sub>2</sub>	Guinea pig, M/F, 400 g	Whole body	24,000	Most between 0.5-2 (GMD)	8 h/day, 5 days/week, 3 week	No change PMNs; ↑ no. AMs, eosinophils by 16 weeks PE.	Fogelmark et al. (1983)

Key to abbreviations:

- LDH: lactate dehydrogenase
- AP: acid phosphatase
- AG: N-acetyl-β-d-glucosaminidase
- TxA<sub>2</sub>: thromboxane A<sub>2</sub>
- LTB<sub>4</sub>: Leukotrine B<sub>4</sub>
- PGE<sub>2</sub>: Prostaglandin E<sub>2</sub>
- AM: alveolar macrophage
- PE: post-exposure
- PMN: polymorphonuclear leukocyte
- ↑: increase
- ↓: decrease

**TABLE 11-22. EFFECTS OF PARTICULATE MATTER ON LUNG BIOCHEMISTRY**

Particle	Species, Gender, Strain, Age or Body Weight	Exposure Technique	Mass Concentration ( $\mu\text{g}/\text{m}^3$ )	Particle Characteristics	Exposure Duration	Observed Effect	Reference
				Size ( $\mu\text{m}$ ); $\sigma_g$			
Fly ash (coal)	Rat, M, Wistar, 5 weeks	Whole body	10,000, 30,000, 100,000	80-95% mass was $\leq 42 \mu\text{m}$ (AED)	6 h/day, 5 days/week, 4 weeks	↑ Cytosolic GSHP <sub>x</sub> , protein at 30,000 100,000; ↓ G6PDH at 100,000; ↓ lung microsomal protein, ↓ microsomal BROD at 30,000/100,000; no change microsomal P-450 content; induction of EROD activity at all conc. (all in lung tissue).	van Bree et al. (1990)
Carbon black	Rat, M, F-344, 200-250 g	Whole body	6,000	0.22 (MMAD)	20 h/day, 1-14 days	No change in synthesis of lung total DNA; no change in DNA synthesis of Type 2 cells.	Wright (1986)
Fly ash (fluidized bed coal)	Rat, M/F, F-344	Whole body	142,000	3 (MMAD); 2.6	6 h	↑ Labeling of Type 2 cells; ↑ incorporation of thymidine in AM DNA, persisting 4 days PE; ↑ labeling airway epithelial cells, persistent up to 4 days PE.	Hackett (1983)
Carbonyl iron	Rat, M, Crl:CD BR, 8 weeks	Nose-only	100,000	3.6 (MMAD); 2.6	6 h/day, 3 days	No effect on labeling index of lung parenchymal or airway cells.	Warheit et al. (1991a)
Fly ash (fluidized bed coal combustion)	Rat, M/F, F-344, 10-13 weeks	Whole body	36,000	3.6 (MMAD); 2	7 h/day, 3 days week 1; 5 days/week week 2-4; 2 days week 5	↑ Labeling index of large airway basal cells and bronchiolar Clara cells at 2 weeks, resolved by 2 weeks PE; ↑ labeling index of Type 2 cells by 4 weeks, resolved by 2 weeks PE.	Shami et al. (1984)
Fly ash (coal)	Rat, M, Wistar, 160-175 g	Whole body	270,000	47% < 3.75 $\mu\text{m}$	6 h/day, 15 days	↑ P-450 content; ↑ activity of aryl hydrocarbon hydroxylase, glutathione S-transferase, $\delta$ -amino levulinic acid synthetase; inhibition of hemoxygenase.	Chauhan et al. (1989)
Fly ash (coal)	Rat, M, Wistar, 160-170 g	Whole body	270,000	47% < 3.75 $\mu\text{m}$	6 h/day, 15 days	↑ Total lung phospholipids; ↑ phosphatidylcholine up to 45 days PE.	Chauhan and Misra (1991)

Key to abbreviations:

GSHP<sub>x</sub> = glutathione peroxidase

G6PDH = glucose 6 phosphate dehydrogenase

BROD = benzoxyresorufin O-dearylyase

EROD = NADPH-mediated ethoxyresorufin O-deethylase

↑: increase

↓: decrease

PE = post exposure

AM = alveolar macrophage

also found that the effects of fly ash were likely due to chemicals adsorbed onto, or that were part of, the fly ash particle, rather than to some nonspecific particle effect. This was because the activity of the lung mixed function oxidase system was induced in rats by instillation of coal fly ash ( $<0.5 \mu\text{m}$ ), but not by instillation of glass beads.

There is some evidence that fly ash exposure can initiate cell division and DNA synthesis in the lungs (Hackett, 1983; Shami et al., 1984), but exposure levels were very high ( $>30,000 \mu\text{g}/\text{m}^3$ ).

## **11.8.5 Pulmonary Defenses**

### **11.8.5.1 Clearance Function**

#### ***Mucociliary Transport***

Grose et al. (1985) exposed (whole-body) rats (Sprague-Dawley CD, M, 60 to 70 days) to volcanic ash from Mt. St. Helens ( $0.65 \mu\text{m}$ ,  $\sigma_g=1.8$ ) at  $9,400 \mu\text{g}/\text{m}^3$  for 2 h. At 24 h post exposure, a depression in ciliary beat frequency in excised tracheas was noted. Whether this would contribute to any change in mucociliary transport function in the intact animal is unknown.

#### ***Pulmonary Region Clearance and Alveolar Macrophage Function***

A number of studies have examined particle retention following exposure to high concentrations of inhaled particles, some of which have low intrinsic toxicity. Such exposures resulted in a phenomenon known as overload, in which the effectiveness of lung clearance mechanisms is significantly reduced. This response, which is nonspecific to a wide range of particles, is discussed in detail in Chapter 10.

While there are no studies of effects of exposure to nonacidic sulfate particles on alveolar region clearance, there have been several studies examining AM function following inhalation exposures (Table 11-23) or with in vitro exposure. High exposure concentrations of various particles can depress the phagocytic activity of AMs following inhalation.

To examine the effects of different fly ashes, Garrett et al. (1981b) incubated rabbit AMs with  $\leq 1,000 \mu\text{g}$  of either conventional coal combustion fly ash or fluidized bed combustion fly ash at  $>3$  and  $<3 \mu\text{m}$ , for 20 h. While all exposures caused reductions in cell viability and cell ATP levels, conventional coal fly ash  $<3 \mu\text{m}$  produced the greatest

**TABLE 11-23. EFFECTS OF PARTICULATE MATTER ON ALVEOLAR MACROPHAGE FUNCTION**

Particle	Species, Gender, Strain, Age, or Body Weight	Exposure Technique	Mass Concentration ( $\mu\text{g}/\text{m}^3$ )	Particle Characteristics		Exposure Duration	Observed Effect <sup>a</sup>	Reference
				Size ( $\mu\text{m}$ ); $\sigma_g$				
Carbon black	Mouse, F, Swiss, 20-23 g	Nose-only	10,000	2.45 (MMAD); 2.54		4 h/day, 4 days	No change in F <sub>c</sub> -mediated AM phagocytic activity up to 40 days PE.	Jakab (1992, 1993); Jakab and Hemenway (1993)
Volcanic ash	Mouse, F, CD-1, 4-8 weeks	Whole body	9,400	0.65 (MMAD); 1.8		2 h	No change in viability of recovered cells; no effect on AM phagocytosis at 0 or 24 h PE.	Grose et al. (1985)
TiO <sub>2</sub>	Rat, M, F-344 180-200 g	Whole body	50,000	1 (MMAD); 2.6		6 h/day, 5 days	No change in spontaneous/stimulated release of IL-1 by AMs up to 63 days PE.	Driscoll et al. (1991)
Fly ash (coal)	Mouse, F, BALB/C; C57BL; 6-8 weeks	Whole body	535 (fine particle fraction < 2.1 $\mu\text{m}$ )	32% < 2.1 $\mu\text{m}$ (by wt)		148 days	↓ AM phagocytic activity by 21 days of exposure.	Zarkower et al. (1982)
TiO <sub>2</sub>	Rat, HAN	Whole body	50,000	"respirable fraction"		8 h/day, 5 days/week	No change in chemotactic activity of AM.	Brown et al. (1992)
Coal dust	Rat, HAN	Whole body	10,000, 50,000	"respirable fraction"		8 h/day, 5 days/week	Decreased AM chemotactic activity.	Brown et al. (1992)
California road dust	Rat, F-344	Nose-only	300, 900	4 (MMAD)		4 h/day, 4 days/week, 8 weeks	↓ Production of superoxide at high concentration; no change in F <sub>c</sub> receptor mediated phagocytic activity.	Kleinman et al. (1995)
Iron oxide (Fe <sub>2</sub> O <sub>3</sub> )	Rat, M, Long-Evans, 225-250 g	Nose-only	18,000-24,000	1.45-1.7 (MMAD); 2.9-3		2 h	No change in AM adherence; ↑ phagocytic activity of AM (F <sub>c</sub> -mediated) up to 20 days PE.	Lehnert and Morrow (1985)
Carbonyl iron	Rat, M, Crl:CDBR, 8 weeks	Nose-only	100,000	3.6 (MMAD); 1.7		6 h; 6 h/day, 3 days	No change in AM chemotactic activity; cell viability; slight ↑ AM phagocytic activity for single exp.	Warheit et al. (1991a)
Carbon black	Mouse, F, Swiss, 20-23 g	Nose only	10,000	2.4 (MMD); 2.75		4 h	No change in F <sub>c</sub> -receptor mediated AM phagocytic activity.	Jakab and Hemenway (1993)
TiO <sub>2</sub>	Guinea pig, M/F 400g	Whole body	24,000	Most between 0.5-2 (GMD)		8 h/d, 5 days/week, 3 weeks	No change in AM phagocytic activity.	Fogelmark et al. (1983)

effect. These results suggest toxicity somewhat dependent on size, as observed previously with other endpoints.

There is little available data on complex mixtures of other PM. Fick et al. (1984) exposed rabbits (NZW, 1.5 to 2 kg) for 0.2 to 2 h to the pyrolysis products derived from Douglas fir wood (exposure concentrations and particle size were not stated). They noted an increase in the total number of cells recovered by lavage immediately postexposure, and the magnitude of this increase was related to the exposure duration. The ratio of AMs, PMNs and lymphocytes was constant at all exposure durations except for the longest, in which case lymphocyte numbers increased. A depression in the uptake and intracellular killing of *Pseudomonas aeruginosa* was found in AMs obtained from the smoke-exposed animals compared to cells from air controls. Furthermore, cells from the smoke-exposed animals were smaller, and had reduced surface adherence.

To examine for a nonspecific particle effect on phagocytosis, Finch et al. (1987) exposed bovine AMs in vitro to TiO<sub>2</sub> (1.57 μm MMD, σ<sub>g</sub>=2.3) or to glass beads (2.1 μm, σ<sub>g</sub>=1.8), the former at 2.3 or 5 μg/ml, and the latter at 5 or 8.4 μg/ml. Neither exposure altered phagocytic activity, but TiO<sub>2</sub> did produce some decrease in cell viability.

Macrophages may contact particles via chemotactic-directed movement. Constituents of lung fluid having high chemotactic activity are components of complement, and particles which activate complement tend to show greater chemoattractant activity for macrophage accumulation at sites of particle deposition (Warheit et al., 1988). For example, in an in vitro study, iron-coated asbestos and carbonyl iron particles activated chemotactic activity in rat serum and concentrated rat lavage proteins, while volcanic ash did not. When the rats were exposed by inhalation to 10,000 to 20,000 μg/m<sup>3</sup> of these particles, only the volcanic ash failed to produce an increased number of macrophages on the first alveolar duct bifurcations, the primary deposition site for these particles and fibers. Complement proteins on alveolar surfaces are likely to be derived primarily from normal transudation of serum components from the pulmonary vasculature (Warheit et al., 1986). The generation of chemotactic factors at particle deposition sites may facilitate clearance for some particle types, but not for others, such as silica (Warheit et al., 1988, 1991a).

In a somewhat related study, Hill et al. (1982) examined the interaction with complement of coal combustion fly ash particles (2 to 3 μm MMAD) from different sites,

using serum from dogs. In addition to releasing peptides that are chemotactic for macrophages and other inflammatory cells, fly ash also induced release of lysosomal enzymes and increased vascular permeability, all processes involved in inflammation. While the authors noted that some fly ash samples activated complement, while others did not, they were not able to determine which component on or in the ash was responsible for this action. A possibility was suggested to be some metals, such as Mn, which are potent activators of the complement cascade (Lew et al., 1975).

Thorén (1992) examined the metabolic activity of AMs by measuring heat exchange rates after exposing cell monolayers to TiO<sub>2</sub> or manganese dioxide (MnO<sub>2</sub>) at 0.6 – 4 × 10<sup>6</sup> particles/ml. The former affected metabolism only at the highest concentration used, while the latter caused changes at lower concentrations as well.

The response of AMs to PM is influenced by both physical and chemical characteristics of the particles with which they come into contact. Shanbhag et al. (1994) exposed a macrophage cell line (P388D1) to particles of two different composition (TiO<sub>2</sub> or latex) at comparable sizes, 0.15 and 0.45 μm for the former, and 0.11 and 0.49 for the latter. They also used pure titanium at 1.76 μm for comparison to latex at 1.61 μm. Titanium dioxide decreased cellular proliferation, depending upon both size and concentration. Similar sizes and concentrations of latex produced lesser responses. In addition, cells incubated with latex released factors, into the medium, which produced fibroblast proliferation to a greater extent than did cells incubated with TiO<sub>2</sub> of a similar size and concentration.

#### **11.8.5.2 Resistance to Infectious Disease**

Susceptibility of mice to challenge with several infectious agents has been used to assess effects of various inhaled particles on microbial defense of the lungs (Table 11-24). The study of Jakab (1993) is of particular interest because the infectious agents used were selected based upon differences in the antimicrobial defense mechanism most effective in eliminating each organism. Thus, *Staphylococcus aureus* defense depends primarily upon the integrity of AMs, while that for *Proteus mirabilis* involves both AMs and PMNs. *Listeria monocytogenes* defenses involve specific acquired immunity, namely the integrity of the lymphokine-mediated components of the cell-mediated immune response (e.g., AMs and lymphocytes). A number of host defenses play a role in defense against influenza, including

**TABLE 11-24. EFFECTS OF PARTICULATE MATTER ON MICROBIAL INFECTIVITY**

Particle	Species, Gender, Strain, Age, or Body Weight	Exposure Technique	Mass Concentration ( $\mu\text{g}/\text{m}^3$ )	Particle Characteristics	Exposure Duration	Observed Effect	Reference
				Size ( $\mu\text{m}$ ); $\sigma_g$			
Carbon black	Mouse, F, Swiss, 20-23 g	Nose-only	4,700-6,100	2.45 (MMAD); 2.54	4 h/day, 4 days	No effect on susceptibility to infection from <i>S. aureus</i> administered 1 day PE; no effect on intrapulmonary killing of bacteria by AM.	Jakab (1992)
Carbon black	Mouse, F, Swiss, 20-23 g	Nose-only	10,000	2.4 (MMAD); 2.75	4 h/day, 4 days	No change in no. of <i>S. aureus</i> or <i>P. mirabilis</i> recovered in lung after bacterial challenge or on intrapulmonary killing of bacteria administered 1 d PE; no effect on proliferation of <i>L. monocytogenes</i> ; no effect on proliferation or elimination of influenza A virus; no change in albumin level in lavage 4 h after bacterial challenge; no change in PMN in lavage 4 h after challenge.	Jakab (1993)
TiO <sub>2</sub>	Guinea pig, F, Dunkin-Hartley 300-350 g	Whole body	23,000	95% < 1.98 $\mu\text{m}$ (MMAD)	20 h/day, 14 days	No change in susceptibility to <i>Legionella pneumophila</i> administered 1-6 days PE but AM with heavy particle burden did not ingest bacteria.	Baskerville et al. (1988)
Coal dust	Mouse, F, Swiss CD-1, 20-24 g	Whole body	2,000	80% < 10 $\mu\text{m}$ ; 50% < 5 $\mu\text{m}$	7 h/day, 5 days/week, 6 mo	No change in susceptibility to influenza virus administered after 1, 3 and 6 mo exposure; decrease in interferon level in lung at 3 mo; no change in inflammatory response to virus.	Hahon et al. (1985)
Volcanic ash	Mouse, F, CD-1, 4-8 weeks	Whole body	9,400	0.65 (MMAD); 1.8	2 h	No change in susceptibility to bacteria ( <i>Streptococcus</i> ) or virus administered 0 or 24 h PE; no change in lymphocyte response to mitogens.	Grose et al. (1985)
TiO <sub>2</sub>	Mouse, Harlan-Olac, 8 weeks	Whole body	2,000, 20,000	95% < 1.98 $\mu\text{m}$ (UDS)	20 h/day, 2 or 4 weeks	↓ Clearance of <i>P. haemolytica</i> administered after exposure in proportion to exposure duration at 20,000 $\mu\text{g}/\text{m}^3$ only.	Gilmour et al. (1989a)
TiO <sub>2</sub>	Mouse, Harlan-Olac, 8 weeks	Whole body	20,000	95% < 1.98 $\mu\text{m}$ (UDS)	20 h/day, 10 days	↓ Clearance of <i>P. haemolytica</i> , persistent up to 10 days PE.	Gilmour et al. (1989a)

**TABLE 11-24 (cont'd). EFFECTS OF PARTICULATE MATTER ON MICROBIAL INFECTIVITY**

Particle	Species, Gender, Strain, Age, or Body Weight	Exposure Technique	Mass Concentration ( $\mu\text{g}/\text{m}^3$ )	Particle Characteristics	Exposure Duration	Observed Effect	Reference
				Size ( $\mu\text{m}$ ); $\sigma_g$			
TiO <sub>2</sub>	Mouse, Harlan-Olac, 8 weeks	Whole body	20,000	95% <1.98 $\mu\text{m}$ (UDS)	20 h/day, 7 days	↓ Response to bacterial antigens of mediastinal lymph node lymphocytes from mice inoculated with <i>P. haemolytica</i> after exposure.	Gilmour et al. (1989b)

Key to abbreviations:

↓: decrease

PE: post-exposure

specific cytotoxic lymphocytes. However, repeated exposure to 10,000  $\mu\text{g}/\text{m}^3$  carbon black did not alter any of these antimicrobial defense systems.

Particles of low intrinsic toxicity may impair mechanisms involved in the clearance of bacteria, perhaps increasing their persistence and resulting in increased infectivity. To examine this possibility, a study was aimed at determining whether animals (guinea pigs) in which phagocytic activity was impaired by exposure to a high concentration (23,000  $\mu\text{g}/\text{m}^3$ ) of an "inert" dust ( $\text{TiO}_2$ ) were more susceptible to bacterial infection, in this case due to *Legionella pneumophila* (Baskerville et al., 1988). While those AMs having heavy burdens of  $\text{TiO}_2$  particles did not phagocytize the bacteria, there was no increase in infectivity in particle-exposed compared to air-exposed control animals; this was suggested to be due to the recruitment of monocytes into the lungs of the  $\text{TiO}_2$ -exposed animals, and these cells were able to phagocytize the bacteria.

The studies presented in Table 11-24 indicate that particles inhaled even at high concentrations did not reduce resistance to microbial infections. However, some changes were noted in an instillation study. Hatch et al. (1985) examined various particles administered by intratracheal instillation for their ability to alter infectivity in mice subsequently exposed to a bacterium (*Streptococcus sp.*). The specific particle types and their sizes (VMD) were as follows: conventional coal combustion fly ash from various sources (0.5  $\mu\text{m}$ ); various samples of fluidized bed combustion coal fly ash (0.4 to 1.3  $\mu\text{m}$ ); various samples of oil combustion fly ash (0.8-1.3 $\mu\text{m}$ ); volcanic ash (1.4 and 2.3 $\mu\text{m}$ ); latex (0.5 and 5  $\mu\text{m}$ ); and urban air particles (0.4  $\mu\text{m}$ ) from Dusseldorf, Germany, Washington, DC, and St. Louis, MO. The instillation dose was 100  $\mu\text{g}$  particles/mouse. An increase in infectivity was found with all oil fly ash samples, some of the combustion and fluidized bed coal fly ash samples, ambient air particles from Dusseldorf and Washington, latex, and also from carbon and ferric oxide particles of unstated size. Exposure to volcanic ash, St. Louis ambient particles, and other coal fly ash samples did not have an effect. It was postulated that the activity of the fly ash reflected either the speculated presence of metals or the ability of the ash to alter the pH of airway fluid. In a corollary to the above study, rabbit AMs were incubated for 20 h with the various particles and cell viability assessed. Viability was reduced by all oil fly ash samples, coal fly ash, ambient particles from all three sites,

volcanic ash and latex. These results did not totally correlate with the response following in vivo exposures.

To examine effects of particles on nonimmunological antiviral defense, Hahon et al. (1983) exposed monolayers of mammalian cells (rhesus monkey kidney cell line) to coal combustion fly ash ( $2.5 \mu\text{m}$ ) at 500 to 5,000  $\mu\text{g}/10 \text{ ml}$  medium and assessed effects on interferon. Induction of interferon due to infection with influenza and parainfluenza virus was reduced when the cells were pretreated with the fly ash. This was suggested to be due to either the matrix itself, or to some surface component which was not extractable with either polar or nonpolar solvents.

One study examined the effect of two larger particles on infectivity. Grose et al. (1985) instilled (42  $\mu\text{g}/\text{animal}$ ) mice (CD-1, F, 4 to 8 weeks) with two sizes of volcanic ash from Mt. St. Helens, namely coarse mode (12.1  $\mu\text{m}$  MMAD,  $\sigma\text{g}=2.3$ ) and fine mode (2.2  $\mu\text{m}$  MMAD,  $\sigma\text{g}=1.9$ ), followed by challenge with bacteria (*Streptococcus sp.*) immediately or 24 h postexposure. No particle size related difference was noted in susceptibility to bacterial infection, with both sizes producing a similar increase in infection following bacterial challenge at 24 h, but not immediately, after pollutant exposure. However, inhalation exposure to 9,400  $\mu\text{g}/\text{m}^3$  volcanic ash (0.65  $\mu\text{m}$ ) for 2 h produced no change in infectivity (Table 11-24).

### 11.8.5.3 Immunologic Defense

The few studies on effects of inhaled particles on respiratory tract immune function are shown in Table 11-25. Particles may affect some aspects of immune defense and not others. For example, fly ash did not produce any change in the cellular immune response, namely delayed hypersensitivity, but did depress the ability of macrophages to enhance T-cell mitogenesis (Zarkower et al., 1982).

### 11.8.6 Systemic Effects

A few studies have examined systemic effects of inhaled particles. One assessed the ability of particles to affect systemic immune responses (Eskew et al., 1982). Mice (F, BALB/C) were continuously exposed for various times to coal combustion fly ash (32% by wt  $<2.1 \mu\text{m}$ ), and the antigenic response of spleen cells to protein derivatives after

**TABLE 11-25. EFFECTS OF PARTICULATE MATTER ON RESPIRATORY TRACT IMMUNE FUNCTION**

Particle	Species, Gender, Strain, Age, or Body Weight	Exposure Technique	Mass Concentration ( $\mu\text{g}/\text{m}^3$ )	Particle Characteristics		Exposure Duration	Observed Effect	Reference
				Size ( $\mu\text{m}$ ); $\sigma_g$				
Fly ash (fluidized bed coal combustion)	Rat, M/F, F-344, 12 weeks	Whole body	36,000	3.6 (MMAD); 2.0		7 h/day, 5 days/week, 4 weeks	No effect on humoral immune function.	Bice et al. (1987)
Fly ash (pulverized coal combustion)	Rat, M/F, F-344, 12 weeks	Whole body	37,000	2.7 (MMAD); 2.1		7 h/day, 5 days/week, 4 weeks	↓ Antibody response at 48 weeks PE.	Bice et al. (1987)
Fly ash (coal)	Mouse, F BALB/C; C57BL 6-8 weeks	Whole body	760 (fine particle fraction, <2.1 $\mu\text{m}$ )	32% < 2.1 $\mu\text{m}$ (by wt)		28 days (continuous)	↓ Ability of AMs to stimulate PHA-induced T-lymphocyte mitogenesis.	Zarkower et al. (1982)
			2,200 (fine particle fraction, <2.1 $\mu\text{m}$ )			160 days (continuous)	No change in ability of animals sensitized with BCG during exposure to respond to purified protein derivative challenge (delayed hypersensitivity cellular immune response).	

Key to abbreviations:

AM: macrophage

PE: post-exposure

IL = interleukin

↑: increase

↓: decrease

sensitization with BCG (delayed hypersensitivity reaction) was examined, as was the mitogenic response of spleen cells to concanavalin A or lipopolysaccharide (LPS). Exposure for 1 to 8 weeks to  $1,150 \mu\text{g}/\text{m}^3$  reduced the mitogenic response of spleen cells after 3 weeks of exposure, but not after 5 or 8 weeks and only for concanavalin A. Exposure for 5 mo to  $2,220 \mu\text{g}/\text{m}^3$  increased thymidine incorporation into spleen cells from BCG-sensitized mice. Finally, exposure for 5 weeks to  $871 \mu\text{g}/\text{m}^3$  reduced the number of antibody plaque forming cells in the spleen and the hemagglutinin titer. These results suggest that fly ash has little effect on the cellular immune response, but depresses the humoral response. The implications of the increase in thymidine incorporation into the spleen of BCG-sensitized mice was not clear, but may indicate an increase in resistance to infection.

In another study of systemic immunity, Mentnech et al. (1984) exposed rats (F344, M, whole body) to  $2,000 \mu\text{g}/\text{m}^3$  coal dust (40%  $<7\mu\text{m}$ ) for 7 h/day, 5 days/week for 12 or 24 mo. The number of antibody-producing cells in the spleen 4 days after immunization with sheep red blood cells was used as a test of effects on humoral immunity, while the proliferative response of splenic T-lymphocytes to the mitogens concanavalin A and phytohemagglutinin was used to assess cellular immunity. No changes were found.

## **11.8.7 Toxicological Interactions of Other Particulate Matter Mixtures**

### **11.8.7.1 Laboratory Animal Toxicology Studies of Particulate Matter Mixtures**

Toxicological interactions with PM may be antagonistic, additive, or synergistic (Mauderly, 1993). The presence and nature of any interaction seems to depend upon the concentration of pollutants in the mixture, the exposure duration, and the endpoint being examined, and it is not possible to predict a priori from the presence of certain pollutants whether there will be any interaction.

Mechanisms responsible for the various forms of interaction are generally not known. The greatest hazard in terms of potential health effects from pollutant interaction is the possibility of synergism, especially if effects occur at all with mixtures which do not occur at all when the individual constituents are inhaled. Various broad mechanisms may underly synergism. One is physical, the result of adsorption or absorption of one material on a particle and subsequent transport to more sensitive sites, or sites where this material would not normally deposit in toxic amounts. This may explain the interaction found in studies of

mixtures of carbon black and formaldehyde, or carbon black and acrolein (Jakab, 1992, 1993), especially since formaldehyde has been shown to be absorbed onto particles (Rothenberg et al., 1989).

Somewhat related to this hypothesis is the possibility of reactions on particle surfaces, forming some secondary products which may be more toxicologically active than the primary material and which is then carried to some sensitive site. This may explain the results of the Jakab and Hemenway (1993) study, wherein mice were exposed to carbon black either prior to or after exposure to O<sub>3</sub>, and then to both materials simultaneously. Simultaneous exposure produced evidence of interaction, while exposure to carbon black either before or after O<sub>3</sub> did not produce responses which were different from that due to exposure to O<sub>3</sub> alone. The authors' suggested that this was due to a reaction of O<sub>3</sub> on the surface of the carbon black particles in the presence of adsorbed water, producing surface bound, highly toxicologically active reactive oxygen species. Production of these species would not occur when the exposures were sequential.

Another mechanism may involve a pollutant-induced change in the local microenvironment of the lung, enhancing the effects of the co-inhalant. Thus, the observed synergism in rats between O<sub>3</sub> and acidic sulfates was suggested to be due to a shift in the local microenvironmental pH of the lung following deposition of acid, enhancing the effects of O<sub>3</sub> by producing a change in the reactivity or residence time of reactants, such as radicals, involved in O<sub>3</sub>-induced tissue injury (Last et al., 1984). This hypothesis was examined in a series of studies (Last et al., 1983, 1984, 1986; Last and Cross, 1978; Warren and Last, 1987; Warren et al., 1986) in which rats were exposed to various sulfur oxide aerosols [H<sub>2</sub>SO<sub>4</sub>, (NH<sub>4</sub>)<sub>2</sub>SO<sub>4</sub>, Na<sub>2</sub>SO<sub>4</sub>] with and without oxidant gases (O<sub>3</sub> or NO<sub>2</sub>), and various biochemical endpoints examined. Acidic sulfate aerosols alone did not produce any response at concentrations that caused a response in conjunction with O<sub>3</sub> or NO<sub>2</sub>. Further evidence that the synergism was due to H<sup>+</sup> was the finding that neither Na<sub>2</sub>SO<sub>4</sub> nor NaCl was synergistic with O<sub>3</sub> (Last et al., 1986). But if this was the only explanation for acid/O<sub>3</sub> interaction, then the effects of ozone should be consistently enhanced by the presence of acid in an exposure atmosphere regardless of endpoint examined. However, in the study of Schlesinger et al. (1992b), in which rabbits were exposed for 3 h to combinations of 0.1, 0.3, and 0.6 ppm O<sub>3</sub> with 50, 75, and 125 μg/m<sup>3</sup> H<sub>2</sub>SO<sub>4</sub> (0.3 μm), antagonism was noted

when evaluating stimulated production of superoxide anion by AMs harvested by lavage immediately after exposure to 0.1 or 0.3 ppm ozone in combination with 75 or 125  $\mu\text{g}/\text{m}^3$   $\text{H}_2\text{SO}_4$ , and also for AM phagocytic activity at all of the ozone/acid combinations; there was no change in cell viability compared to air control.

The database for binary mixtures containing PM other than acid sulfates is quite sparse. But as with acidic sulfates, interaction depends upon pollutant combinations, exposure regimen and biological endpoints (see Table 11-26). Some interaction was noted following exposure of mice to mixtures of 9,400  $\mu\text{g}/\text{m}^3$  volcanic ash and 2.5 ppm  $\text{SO}_2$  (Grose et al., 1985), in that synergism was suggested in terms of immune cell activity and numbers but no interaction was found with overall bacterial infectivity. On the other hand, exposure of mice to various concentrations of carbon black and formaldehyde (HCHO) produced no evidence of interaction in terms of bacterial infectivity but possible synergism in terms of macrophage phagocytic activity (Jakab, 1992).

The infectivity study of Jakab (1993), in which mice were exposed to acrolein and carbon black (Table 11-26), is of interest because, as mentioned earlier, the microbial agents were selected on the basis of the defense mechanisms they elicited. The results indicated that while particle or acrolein exposure alone did not alter infectivity from any of the microbes, exposure to the mixture did, and also suggested differential effects on different aspects of antimicrobial defense. For example, the increase in intracellular killing of *P. mirabilis* was ascribed to the increase in PMN levels after bacterial challenge. The reduced effectiveness for *L. monocytogenes* and influenza virus were somewhat more persistent, which led the authors to suggest that the particle/gas mixture had a greater impact upon acquired immune defenses than on innate defense mediated by AMs and PMNs, this being the major defense against *S. aureus* and *P. mirabilis*.

Another complex mixture examined was a combination of gaseous sulfur (IV), particulate sulfur (IV) and particulate sulfur (VI). A series of studies involved exposures (whole body) of Beagle dogs (M, 34 mo old) for 22.5 h/day, 7 days/week for up to 290 days to such an atmosphere, in which respirable sulfur IV ( $0.6 \mu\text{m}$  MMAD,  $\sigma_g=2$ ) was maintained at a concentration of 300  $\mu\text{g}/\text{m}^3$  (Heyder et al., 1992; Maier et al., 1992; Kreyling et al., 1992; Schulz et al., 1992; Takenaka et al., 1992). Various biological endpoints were examined, and responses included reductions in nonspecific defense

**TABLE 11-26. TOXICOLOGIC INTERACTIONS TO MIXTURES CONTAINING NON-ACID AEROSOL PARTICLES**

Co-pollutant			Particle		Exposure Regime	Exposure Conditions	Species, Gender		Endpoints	Response to Mixture	Interaction	Reference
Chemical	$\mu\text{g}/\text{m}^3$	ppm	Chemical	$\mu\text{g}/\text{m}^3$ ( $\mu\text{m}$ )			Strain, Age or Body Weight					
SO <sub>2</sub>	2,500	—	Volcanic ash	9,400 (0.65 $\mu\text{m}$ , MMAD, $\sigma\text{g}=1.8$ )	2 h	Whole body	Mouse, F, CD-1, 4-8 weeks	Infectivity to Group C <i>Streptococcus</i> or virus given 0 or 24 h after exposure	No change in susceptibility to infection	None	Grose et al. (1985)	
SO <sub>2</sub>	2,500	—	Volcanic ash	9,400 (0.65 $\mu\text{m}$ , MMAD, $\sigma\text{g}=1.8$ )	2 h	Whole body	Rat, M, Sprague-Dawley, 60-70 days	Lavaged cell nos. at 0 or 24 h PE	↑ PMN; ↑ lymphocytes; ↓ AM (no change in total cell no.)	Possible at 0 h: effect greater than either pollutant alone; similar to SO <sub>2</sub> alone at 24 h	Grose et al. (1985)	
SO <sub>2</sub>	2,500	—	Volcanic ash	9,400 (0.65 $\mu\text{m}$ , MMAD, $\sigma\text{g}=1.8$ )	2 h	Whole body	Rat, M, Sprague-Dawley, 60-70 days	AM phagocytosis at 0 or 24 h PE	↓ phagocytic activity	Possible at 0 hr: effect greater than either pollutant alone; at 24 h: similar to SO <sub>2</sub> alone	Grose et al. (1985)	
SO <sub>2</sub>	2,500	—	Volcanic ash	9,400 (0.65 $\mu\text{m}$ , MMAD, $\sigma\text{g}=1.8$ )	2 h/day, 5 days	Whole body	Rat, M, Sprague-Dawley, 60-70 days	Splenic lymphocyte response to mitogen (phytohemagglutinin)	Decrease	Possible synergism: no effect with either pollutant alone	Grose et al. (1985)	
HCHO	1,000;	2.4-3	C black	1,000; 2,400-6,800 (2.45 $\mu\text{m}$ , MMAD, $\sigma\text{g}=2.54$ )	4 h	Nose-only	Mouse, F, Swiss, 20-23 g	Infectivity of <i>S. aureus</i> administered prior to pollutant; differential counts in lavage	None	None	Jakab (1992)	
HCHO	—	4.1-5	C black	4,800-13,200	4 h	Nose-only	Mouse, F, Swiss, 20-23 g	Infectivity of <i>S. aureus</i> administered prior to pollutant; differential counts in lavage	None	None	Jakab (1992)	
SO <sub>2</sub>	2,500	—	Volcanic ash	9,400 (0.65 $\mu\text{m}$ , MMAD, $\sigma\text{g}=1.8$ )	2 h	Whole body	Rat, M, Sprague-Dawley, 60-70 days	Tracheal ciliary beat frequency at 0, 24, 72 h PE	Decrease	None: same as ash alone	Grose et al. (1985)	
HCHO	—	2.4-3	C black	2,400-6,800 (2.45 $\mu\text{m}$ , MMAD, $\sigma\text{g}=2.54$ )	4 h	Nose-only	Mouse, F, Swiss, 20-23 g	Infectivity of <i>S. aureus</i> administered prior to pollutant; differential counts in lavage	None	None	Jakab (1992)	

**TABLE 11-26 (cont'd). TOXICOLOGIC INTERACTIONS TO MIXTURES  
CONTAINING NON-ACID AEROSOL PARTICLES**

Co-pollutant			Particle		Exposure Regime	Exposure Conditions	Species, Gender Strain, Age or Body Weight	Endpoints	Response to Mixture	Interaction	Reference
Chemical	$\mu\text{g}/\text{m}^3$	ppm	Chemical	$\mu\text{g}/\text{m}^3$ ( $\mu\text{m}$ )							
HCHO	—	1	C black	1,000; and 2,400-6,800 (2.45 $\mu\text{m}$ MMAD, $\sigma\text{g} = 2.54$ )	4 h	Nose-only	Mouse, F, Swiss, 20-23 g	Infectivity of <i>S. aureus</i> administered prior to pollutant; differential counts in lavage	None	None	Jakab (1992)
HCHO	—	4.1-5	C black	4,800-13,200 (2.45 $\mu\text{m}$ , MMAD, $\sigma\text{g}=2.54$ )	4 h	Nose-only	Mouse, F, Swiss, 20-23 g	Infectivity of <i>S. aureus</i> administered prior to pollutant; differential counts in lavage	None	None	Jakab (1992)
HCHO	—	1.8-2.8 ; 5	C black	4,700-6,100; 10,000	4 h/day, 4 days	Nose-only	Mouse, F, Swiss, 20-23 g	Infectivity of <i>S. aureus</i> administered 1 day after last pollutant exposure; differential counts in lavage	None	None	Jakab (1992)
HCHO	—	5	C black	10,000	4 h/day, 4 days	Nose-only	Mouse, F, Swiss, 20-23 g	F <sub>c</sub> -receptor mediated M $\phi$ phagocytosis up to 40 days PE	↓ Phagocytic activity from day 25 PE, return to normal by day 40 PE	Possible synergism: no 3-day effect of C black or HCHO alone	Jakab (1992)
Acrolein	—	2.5	C black	10,000 (2.4 $\mu\text{m}$ , MMAD, $\sigma=2.75$ )	4 h/day, 4 days	Nose-only	Mouse, F, Swiss, 20-23 g	Infectivity to <i>S. aureus</i> , <i>P. mirabilis</i> , <i>L. monocytogenes</i> ; influenza A virus administered 1 day PE	↓ Elimination of virus; ↓ killing of <i>L. monocytogenes</i> ;  ↓ killing of <i>S. aureus</i> ; ↓ killing of <i>P. mirabilis</i>  ↑ PMN count 4 h after <i>P. mirabilis</i> challenge;  No change total cell no. by lavage after <i>S. aureus</i>	Possible synergism: no effect of either alone  Possible: no effect of C black  Possible: greater than either alone  None	Jakab (1993)

**TABLE 11-26 (cont'd). TOXICOLOGIC INTERACTIONS TO MIXTURES  
CONTAINING NON-ACID AEROSOL PARTICLES**

Co-pollutant			Particle		Exposure Regime	Exposure Conditions	Species, Gender Strain, Age or Body Weight	Endpoints	Response to Mixture	Interaction	Reference
Chemical	$\mu\text{g}/\text{m}^3$	ppm	Chemical	$\mu\text{g}/\text{m}^3$ ( $\mu\text{m}$ )							
SO <sub>2</sub>	2,700	—	Volcanic ash	9,400 (0.65, MMAD, $\sigma=1.78$ )	2 h/day, 5 days	Whole body	Rat, Sprague-Dawley (40 days)	Pulmonary mechanics	Reduced tidal volume and peak expiratory flow; no effect on breathing frequency	None: effect due to SO <sub>2</sub>	Raub et al. (1985)

capabilities of AMs such as phagocytosis and production of reactive oxygen species; increases in protein and  $\beta$ -N-acetylglucosaminidase in lavage fluid; increased rate of clearance of test particles from lungs to blood (suggesting a change in the permeability of the epithelium); minor changes in pulmonary function; and some histopathological effects, such as hyperplasia of respiratory epithelium of the posterior nasal passages and a slight (but not statistically significant) decrease in the volume density of alveolar septa. The exact role played by specific components of this mixture could not be determined because responses to individual components were not examined.

#### **11.8.7.2 Human Studies of Particulate Matter Mixtures Other Than Acid Aerosols**

Few studies have examined the effects of particles other than acid aerosols, despite the fact that ambient particulate matter consists of a mixture of soluble and insoluble material of varying chemical composition. Human safety considerations limit experimental exposures to particles considered to be essentially inert and non-carcinogenic. As reviewed in the 1982 Criteria Document (U.S. Environmental Protection Agency, 1982), Andersen et al. (1979) examined effects on healthy subjects of exposure to Xerox toner at concentrations ranging from 2,000 to 25,000  $\mu\text{g}/\text{m}^3$ . These concentrations are not relevant to outdoor environmental exposures. Nevertheless, the studies were remarkable for the virtual absence of symptomatic or lung functional responses.

Utell et al. (1980) exposed healthy young subjects with acute influenza to a  $\text{NaNO}_3$  aerosol (0.5  $\mu\text{m}$ ) or  $\text{NaCl}$  (control), and observed significant reductions in specific airway conductance in response to the  $\text{NaNO}_3$  aerosol, but not to  $\text{NaCl}$  aerosol, for up to 1 week following the acute illness. These studies suggested that individuals with acute viral illness may experience bronchoconstriction from particulate nitrate pollutants that do not have effects on healthy subjects. However, the concentration of particles in these experiments was  $\approx 7,000 \mu\text{g}/\text{m}^3$ , more than 100 times greater than peak ambient concentrations.

Three more recent studies have attempted to examine effects of exposure to carbon black particles, either alone or in combination with other pollutants (see Table 11-27). First, Kulle et al. (1986) exposed 20 healthy nonsmokers (10 males and 10 females) to air, 0.99 ppm  $\text{SO}_2$ , 517  $\mu\text{g}/\text{m}^3$  activated carbon aerosol (MMAD = 1.5  $\mu\text{m}$ , GSD = 1.5), and  $\text{SO}_2$  + activated carbon for four hours in an environmental chamber. Two 15-minute

**TABLE 11-27. CONTROLLED HUMAN EXPOSURE STUDIES OF PARTICULATE MATTER MIXTURES OTHER THAN ACID AEROSOLS**

Ref.	Subjects	Exposures <sup>1</sup>	MMAD <sup>2</sup> ( $\mu\text{m}$ )	GSD <sup>3</sup> ( $\mu\text{m}$ )	Duration	Exercise	Temp (°C)	RH (%)	Symptoms	Lung Function	Other Effects	Comments
Green et al. (1989)	24 healthy 18 to 35 yrs	Air; activated carbon 510 $\mu\text{g}/\text{m}^3$ ; HCHO 3.01 ppm; carbon 510 $\mu\text{g}/\text{m}^3$ + HCHO 3.01 ppm	1.4	1.8	2 h	15 of each 30 min., 57 L/min	22	65	Increased cough with carbon + HCHO	No direct effects of carbon. Additive effects of carbon + HCHO on FVC, FEV <sub>3</sub> , peak flow; decrements less than 5%.		
Kulle et al. (1986)	20 healthy 20 to 35 yrs	Air; activated carbon 517 $\mu\text{g}/\text{m}^3$ ; SO <sub>2</sub> 0.99 ppm; carbon 517 $\mu\text{g}/\text{m}^3$ + SO <sub>2</sub> 0.99 ppm.	1.5	1.5	4 h	15 min × 2, 35 L/min	22	60	No symptoms related to carbon exposure	No direct or additive effects of carbon exposure		
Yang and Yang (1994)	30 healthy 25 asthmatic 23 to 48 yrs	Mouthpiece: Bagged polluted air, TSP = 202 $\mu\text{g}/\text{m}^3$			30 min	At rest				Healthy subjects: no change Asthmatics: ↓FEV <sub>1</sub> ≈7%	Increased airway responsiveness in asthmatics reported; no allowance for change in airway caliber	No control exposure

exercise periods ( $\dot{V}_E = 35$  L/min) were included in the exposure. The exposure days were separated by one week and were bracketed by control air exposures on the day prior to and the day following the experimental exposure. Measurements included respiratory symptoms, spirometry, lung volumes, and airway responsiveness to methacholine. The carbon aerosol exposure resulted in no significant effects on symptoms or lung function, and exposure to carbon + SO<sub>2</sub> did not enhance the very small effects on lung function seen with SO<sub>2</sub> alone. Results of methacholine challenge testing were not provided.

Second, a separate report from the same laboratory (Green et al., 1989) examined potential interactions between formaldehyde (HCHO) and carbon exposure. Twenty-four healthy nonsmokers without airway hyperresponsiveness were exposed for two hours to air, 3 ppm HCHO, 510  $\mu\text{g}/\text{m}^3$  activated carbon aerosol (MMAD = 1.4  $\mu\text{m}$ , GSD = 1.8) and HCHO + carbon. Exposures incorporated exercise ( $\dot{V}_E = 57$  L/min) for 15 of each 30 minutes. The exposures were separated by one week. Measurements included symptoms, spirometry, lung volumes, and serial measurements of peak flow. There were no significant effects on symptoms or decrements in lung function with exposure to carbon alone. The combination of carbon and HCHO increased cough at 20 and 80 minutes of exposure when compared to either pollutant alone. There were also small (less than 5%) but statistically significant decrements in FVC, FEV<sub>3</sub>, and peak flow with carbon + HCHO, compared with either pollutant alone. The authors speculated that the enhancement of cough with carbon + HCHO resulted from increased delivery of HCHO adsorbed to carbon.

Finally, the studies by Anderson et al. (1992), summarized previously, were designed to test the hypothesis that inert particles in ambient air may become coated with acid, thereby delivering increased concentrations of acid sulfates to "sensitive" areas of the respiratory tract. Carbon black particles (MMAD  $\approx 1$   $\mu\text{m}$ , GSD  $\approx 2$   $\mu\text{m}$ ) were coated with H<sub>2</sub>SO<sub>4</sub> using fuming H<sub>2</sub>SO<sub>4</sub>. Electron microscopy findings suggested successful coating of the particles. Fifteen healthy and 15 asthmatic subjects were exposed for 1 h to acid-coated carbon, with a total suspended particulate concentration of 358  $\mu\text{g}/\text{m}^3$  for asthmatic subjects and 505  $\mu\text{g}/\text{m}^3$  for healthy subjects. On separate occasions, subjects were also exposed to carbon black alone ( $\approx 200$   $\mu\text{g}/\text{m}^3$ , estimated as the difference between total suspended particulate and non-carbon particulate concentrations), H<sub>2</sub>SO<sub>4</sub> alone ( $\approx 100$   $\mu\text{g}/\text{m}^3$ ), and air.

No adverse effects of particle exposure on lung function or airway responsiveness were observed for either study group.

Clinical studies of single particulate pollutants or simple mixtures may not be representative of effects that occur in response to complex ambient mixtures. In an attempt to examine effects of an ambient air pollution atmosphere under controlled laboratory conditions, Yang and Yang (1994) exposed 25 asthmatic and 30 healthy subjects to polluted air collected in a motor vehicle tunnel in Taiwan. This compressed air sample contained 202  $\mu\text{g}/\text{m}^3$  particles as well as 0.488 ppm  $\text{NO}_2$ , 0.112 ppm  $\text{SO}_2$ , and 3.4 ppm carbon monoxide (CO). The chemical and size characteristics of the particles were not provided. Mouthpiece exposure to polluted air was performed at rest for 30 min, and lung function and methacholine responsiveness were assessed after exposure. Small but significant decrements in  $\text{FEV}_1$  and FVC were observed in asthmatic, but not healthy subjects when compared with baseline measurements. However, no control exposure to air was performed, which seriously limits interpretation of these results. The small decrements in lung function could have resulted from exposure conditions other than the pollutants, such as humidity or temperature of the inhaled air, which were not specified.

Thus, few studies have examined effects of particles other than acid aerosols on lung function, although available data suggest inert particles in the respirable range have little or no acute effects at levels well above ambient concentrations. Other than the studies of Rudell et al. on diesel exhaust discussed in Section 11.5.1, no studies have examined effects on mucociliary clearance, epithelial inflammation, or host defense functions of the distal respiratory tract in humans.

## **11.9 PHYSICOCHEMICAL AND HOST FACTORS INFLUENCING PARTICULATE MATTER TOXICITY**

### **11.9.1 Physicochemical Factors Affecting Particulate Matter Toxicity**

The physicochemical factors modulating biological responses to PM are not always clear. However, the available toxicological database does allow for some speculation as to factors which may influence biological responses to diverse types of PM. For example, the toxic potency of inorganic particles may be related to certain physicochemical characteristics.

While the bulk chemical makeup of a particle would clearly influence its toxicity, responses may also be driven by chemical species adsorbed onto the particle surface, even for those particles considered to have low intrinsic toxicity. Furthermore, certain physical properties of particles, such as size or surface area, and of aerosols, such as number concentration, may be factors in determining responses to PM. This section provides an overview of current hypotheses concerning particle characteristics which may relate to toxicity.

**Particle Acidity:** It should be clear from discussions in Section 11.2 that the deposition of acidic particles in the respiratory tract can result in various biological effects. The bulk of the toxicologic database on acidic PM involves sulfate particles, primarily  $\text{H}_2\text{SO}_4$  and the available evidence indicates that the observed responses to these are likely due to the  $\text{H}^+$ , rather than to the  $\text{SO}_4^-$ . Thus, effects observed for this pollutant likely apply to any acidic particle having a similar deposition pattern in the respiratory tract, although the specific chemical composition of different acids may be a factor mediating the quantitative response (Fine et al., 1987a). In terms of  $\text{H}^+$ , the irritant potency of an acid aerosol may be related more to the total available  $\text{H}^+$  concentration (i.e., titratable acidity in lung fluids following deposition) rather than to the free  $\text{H}^+$  concentration as measured by pH (Fine et al., 1987b). In any case, the response to acidic particles appears to be due to a direct irritant action and/or the subsequent release of humoral mediators.

Acidic particles exert their action throughout the respiratory tract, with the response and location of effect dependent upon particle size and mass concentration. They have been shown to alter bronchial responsiveness, mucociliary transport, clearance from the pulmonary region, regulation of internal cellular pH, production of cytokines and reactive oxygen species, pulmonary mechanical function, and airway morphology.

Particles do not have to be pure acid droplets to elicit health effects. The acid may be associated with another particle type. For example, in the study of Chen et al. (1990), guinea pigs were exposed to two different fly ashes, one derived from a low sulfur coal and one from a high sulfur coal (Table 11-19). Levels of acidic sulfates associated with the fly ash were found to be proportional to the coal sulfur content, and greater effects on pulmonary functional endpoints were noted for the high sulfur fly ash than for the low sulfur fly ash.

**Particle Surface Coatings:** The presence of surface coatings may make certain particles more toxic than expected based solely upon particle core composition. This was noted in studies of acid-coated metal oxides (Section 11.2.3) and is discussed in greater detail in Section 11.3.8. Certain surface metals may be especially important in this regard, and because trace metal species vary geographically, this may account to some extent for particles in different areas having different toxic potentials.

**Particle Size:** Studies which have examined PM-induced mortality seem to suggest some inherent potential toxicity of inhaled ultrafine particles (Section 11.4), and other endpoints appear to show this as well. This is especially important when considering particles which may have low inherent toxicity at one size, yet greater potency at another. However, the mechanism which underlies a size-related difference in toxicity is not known at this time.

To compare toxic potency of particles of different sizes, intratracheal instillation has often been used. This technique allows the delivery of equivalent doses of different materials and avoids differences in deposition which would occur if particles of different sizes were inhaled. While this approach may highlight inherent similarities and differences in responses to particles of various sizes, in reality, there would be greater deposition of singlet ultrafine particles (in the size range used in the toxicology studies described) in the lungs, especially within the alveolar region, than for the larger fine or coarse mode particles.

The release of proinflammatory mediators may be involved in lung disease, and their levels may be increased with exposure to ultrafine particles. For example, Driscoll and Maurer (1991) compared effects of instilled fine ( $0.3\ \mu\text{m}$ ) or ultrafine ( $0.02\ \mu\text{m}$ )  $\text{TiO}_2$ , in rat (F344) lungs. Concentrations were  $10,000\ \mu\text{g}$  particles/kg BW. Lavage was performed up to 28 days post-exposure, and pathology was assessed at this 28-day time point. While both size modes produced an increase in the number of AMs and PMNs in lavage, the increase was greater and more persistent with the ultrafine particles. The release of another monokine, tumor necrosis factor (TNF), by AMs was stimulated with both sizes, but again the response was greater and more persistent for the ultrafines. A similar response was noted for fibronectin produced by AMs. Finally, fine particle exposure resulted in a minimally increased prominence of

particle-laden macrophages associated with alveolar ducts, while ultrafine particle exposures produced somewhat of a greater prominence of macrophages, some necrosis of macrophages and slight interstitial inflammation associated with the alveolar duct region. In addition, increased collagen occurred only with ultrafine particle exposure.

Oberdörster et al. (1992) instilled rats with 500  $\mu\text{g}$   $\text{TiO}_2$  in either fine (0.25  $\mu\text{m}$ ) or ultrafine (0.02  $\mu\text{m}$ ) sizes, and performed lavage 24 h later. Various indicators of acute inflammation were altered with the ultrafine particles; this included an increase in the number of total cells recovered, a decrease in percentage of AMs and increase in percentage of PMNs, and an increase in protein. On the other hand, instillation of the fine particles did not cause statistically significant effects. Thus, the ultrafine particles had greater pulmonary inflammatory potency than did the larger size particles of this material. The investigators attributed enhanced toxicity to greater interaction of the ultrafine particles, with their large surface area, with alveolar and interstitial macrophages, resulting in enhanced release of inflammatory mediators. They suggested that ultrafine particles of materials of low in vivo solubility appear to enter the interstitium more readily than do larger size particles of the same material, which accounted for the increased contact with macrophages in this compartment of the lung. In support of these results, Driscoll and Maurer (1991) noted that the pulmonary retention of ultrafine  $\text{TiO}_2$  particles instilled into rat lungs was greater than for the same mass of fine mode  $\text{TiO}_2$  particles.

Not all ultrafine particles will enter the interstitium to the same extent, and this may influence toxicity. For example, both  $\text{TiO}_2$  (~20 nm) and carbon black (~20 nm) elicit an inflammatory response, yet much less of the latter appears to enter the interstitium after exposure (Oberdörster et al., 1992). Since different particles may induce chemotactic factors to different extents, it is possible that less chemotoxicity with  $\text{TiO}_2$  results in less contact with and phagocytosis by macrophages, a longer residence time at the area of initial deposition, and a resultant greater translocation into the interstitium. Similarly, Brown et al. (1992; Table 11-23) noted following inhalation exposure of rats to  $\text{TiO}_2$  or coal mine dust that the former did not affect macrophage chemotaxis, while the latter reduced it; the coal dust also produced a greater inflammatory response than did the  $\text{TiO}_2$ . This is consistent with less interaction of coal dust with AMs and greater movement into the interstitium.

The above studies appear to support the concept of some inherent toxicity of ultrafine particles compared to larger ones. Both particle size and the resultant surface area of a unit

mass of particles likely influences toxic potential. Surface area is important because, as noted above, adsorption of certain chemical species on particles may enhance their toxicity, and this could be an even greater factor for ultrafine particles with their larger surface area per unit mass.

Other studies have compared effects following exposures to larger than ultrafine particle sizes, and the results ranged from none detectable to some particle size-related differences. Raub et al. (1985) instilled into rats coarse mode (12.2  $\mu\text{m}$ ) and fine mode (2.2  $\mu\text{m}$ ) volcanic ash at two dose levels, 50,000 or 300  $\mu\text{g}$  particles/animal. The coarse mode produced a change in end expiratory volume, but no changes in other pulmonary function endpoints (i.e., frequency,  $V_T$ , peak inspiratory and expiratory flows, VC, RV, TLC). When lungs were examined 6 mo after instillation, animals exposed to the low dose of either size fraction showed no changes in lung weight or hydroxyproline content compared to control, while those exposed to the high concentration of coarse mode ash showed increased lung weight. In terms of histopathology, both size modes produced some focal alveolitis. Thus, there were essentially no differences in responses between the two size modes, especially at the low exposure dose. In a similar study, Grose et al. (1985) instilled mice with 42  $\mu\text{g}$ /animal of volcanic ash in the same two size fractions as above, coarse and fine, 24 h prior to challenge with bacteria (*Streptococcus sp.*). A small, but similar, increase in susceptibility to infection was noted with both particle sizes.

Shanbhag et al. (1994) exposed a mouse macrophage cell line (P388D1) to particles of two different composition ( $\text{TiO}_2$  or latex) at comparable sizes, 0.15 and 0.45  $\mu\text{m}$  for the former, and 0.11 and 0.49 for the latter. They also used pure titanium at 1.76  $\mu\text{m}$  for comparison to latex at 1.61  $\mu\text{m}$ . In order to examine effects of particle surface area, the cells were exposed to a constant surface area of particles, expressed in terms of  $\text{mm}^2$  per unit number of cells. This was obtained based upon particle size and density and, therefore, the weight percentage was greater for larger particles than for smaller ones for the same surface area. Furthermore, because of particle density differences, the weight percentage for similarly sized particles of different materials to obtain the same surface area also differed. The authors noted that at a constant total particle surface area to cell ratio, the 0.15 and 0.45  $\mu\text{m}$  particles were likely to be less inflammatory than were the 1.76  $\mu\text{m}$  particles, in that the smaller particles produced lower elicited levels of interleukin-1 and less cell

proliferation. These results indicate that the larger particles had greater toxicity than the smaller ones in this experimental system. Thus, the exact relationship between particle size and toxicity is not resolved. It may differ for different size modes and may also depend on the specific experimental system used.

**Particle Number Concentration:** The number concentration of particles within an aerosol will increase as the size of the constituent particles decrease. Thus, for a given mass concentration of a material, there would be greater particle numbers in an ultrafine aerosol than in a fine aerosol. As previously discussed (Section 11.2.3), studies have shown various biological responses, such as reductions in lung volumes and diffusion capacity, alterations in biochemical markers, and changes in lung tissue morphology, in guinea pigs following exposure to ultrafine ZnO having a surface layer of H<sub>2</sub>SO<sub>4</sub>. These responses were much greater than were found following exposure to H<sub>2</sub>SO<sub>4</sub> aerosols in pure droplet form yet having a similar mass concentration.

A possible contribution to this differential response is that the number concentration of particles in the exposure atmospheres were different, resulting in different numbers of particles deposited at target sites. At an equal total sulfate mass concentration, H<sub>2</sub>SO<sub>4</sub> existed on many more particles when layered on the ZnO carrier particles than when dissolved into aqueous droplets (i.e., pure acid aerosol); this was because the particle size distribution of the former aerosol was smaller than that of the latter. Therefore, it is possible that the greater the number of particles containing H<sub>2</sub>SO<sub>4</sub>, the greater will be the number of cells affected after these particles deposit in the lungs, and the more severe will be the overall biological response. While differences in particle size distributions between the coated and pure acid particles may have influenced the results to some extent, a recent study (Chen et al., 1995) confirmed that the number of particles in the exposure atmosphere, not just total mass concentration, is an important factor in biological responses following acidic sulfate particle inhalation when aerosols having the same size distribution were compared.

### **11.9.2 Host Factors Affecting Particulate Matter Toxicity**

Not only do the differences in particle chemistry and morphology influence responses to inhalation of particulate matter, but also various factors related to host susceptibility. One obvious example is the differences associated with species susceptibility as well as differences

in dosimetry related to animal mass and lung structure and geometry. Host health status, specifically the presence of pulmonary inflammation or bacterial or viral infection or nutritional status also may markedly alter responses to PM. The presence of chronic pulmonary disease is also a factor in both animals and humans. Age of the animal, especially very young or very old, can influence susceptibility.

**Host Health Status:** Epidemiological studies suggest there may be subsegments of the population that are especially susceptible to effects from inhaled particles (see Chapter 12). One particular group may be those having lungs compromised by respiratory disease. However, most toxicology studies have used healthy adult animals, and there are very few data to allow examination of the effects of different disease states upon the biological response to PM. A number of studies have examined the effects of lung disease on deposition and/or clearance of inhaled aerosols, and these are discussed in Chapter 10. Alterations in deposition sites and clearance rates/pathways due to concurrent disease may impact upon dose delivered from inhaled particles, and thus influence ultimate toxicity.

Some work has been performed with sulfate and nitrate aerosols using models of compromised hosts. Rats and guinea pigs with elastase-induced emphysema were examined to assess whether repeated exposures (6 h/day, 5 days/week, 20 days) to  $(\text{NH}_4)_2\text{SO}_4$  (1,000  $\mu\text{g}/\text{m}^3$ , 0.4  $\mu\text{m}$  MMAD) or  $\text{NH}_4\text{NO}_3$  (1,000  $\mu\text{g}/\text{m}^3$ , 0.6  $\mu\text{m}$  MMAD) would alter pulmonary function compared to saline-treated controls (Loscutoff et al., 1985). Similarly, dogs having lungs impaired by exposure to  $\text{NO}_2$  were treated with  $\text{H}_2\text{SO}_4$  (889  $\mu\text{g}/\text{m}^3$ , 0.5  $\mu\text{m}$ , 21 h/day, 620 days) (Lewis et al., 1973). Results of both of these studies indicated that the specific induced disease state did not enhance the effect of acidic sulfate aerosols in altering pulmonary function; in some cases, there were actually fewer functional changes in the diseased lungs than in the unimpaired animals. It is possible, however, that other types of disease states could result in enhanced response to inhaled acidic aerosols; as mentioned, asthma is a likely one, but there are no data to evaluate whether effects are enhanced in animal models of human asthma.

Few studies have examined effects of other particles in health compromised host models. Mauderly et al. (1990) exposed young rats having elastase-induced emphysema to whole diesel exhaust (3,500  $\mu\text{g}$  soot/ $\text{m}^3$ ) for 24 mo (7 h/day, 5 days/week). Various endpoints were examined after exposure, including pulmonary function (e.g., respiratory

pattern, lung compliance, DLco), biochemical components of BAL (e.g., enzymes, protein, collagen), and histopathology and morphometry. There was no evidence that the diseased lungs were more susceptible to the diesel exhaust than were normal lungs. In fact, in some cases, there seemed to be a reduced effect of the diesel exhaust in the emphysematous lungs. But this could be due to a reduced lung burden in the diseased lungs, resulting from differences in deposition and/or clearance compared to normal lungs.

Rats having elastase-induced emphysema were exposed to 9,400  $\mu\text{g}/\text{m}^3$  (0.65  $\mu\text{m}$ ) Mt. St. Helens volcanic ash for 2 h/day for 5 days (Raub et al., 1985; Table 11-19), with and without 2,700  $\mu\text{g}/\text{m}^3$   $\text{SO}_2$ . Effects on pulmonary mechanics were similar to those noted in normal animals exposed to the same atmospheres.

Raabe et al. (1994) exposed rats with elastase-induced emphysema to two particle atmospheres, a California-type aerosol and a London-type aerosol. The former consisted of 1.1 to 1.5  $\mu\text{m}$  (MMAD;  $\sigma_g = 1.7$  to 2.4) particles of graphitic carbon, natural clay,  $\text{NH}_4\text{HSO}_4$ ,  $(\text{NH}_4)_2\text{SO}_4$ ,  $\text{NH}_4\text{NO}_3$ , and trace amounts of metals ( $\text{PbSO}_4$ ,  $\text{VOSO}_4$ ,  $\text{MnSO}_4$ , and  $\text{NiSO}_4$ ). The latter consisted of 0.8 to 0.9  $\mu\text{m}$  particles ( $\sigma_g = 1.7$  to 1.8) of  $\text{NH}_4\text{HSO}_4$ ,  $(\text{NH}_4)_2\text{SO}_4$ , coal fly ash, and lamp black carbon. The elastase treated rats showed increased lung DNA and RNA, a general marker for repair of cell damage. Exposure for 3 days (23 h/day) to the London aerosol produced a further increase not seen in exposed normal rats. A 30-day exposure to the California aerosol enhanced small airway lesions in the elastase-treated animals. These preliminary results suggest that the California aerosol and the London aerosol both caused significant responses in animals with elastase-induced emphysema, but clarification of these responses must await a more comprehensive treatment of these data.

Thus, the available toxicological database indicates only limited evidence of enhanced susceptibility to PM of "compromised" hosts. However, these studies were restricted to emphysema models and it is not known whether other simulated pulmonary diseases would enhance susceptibility to PM in laboratory animals.

**Species Differences:** The effects of asbestos-free talc at 6,000 or 18,000  $\mu\text{g}/\text{m}^3$  (2.7-3.2  $\mu\text{m}$ ) were studied in male and female F344 rats and B6C3F1 mice exposed 6 hours/day 5 days/week for 24 mo (National Toxicology Program, 1993). In rats and mice exposed to the higher concentration for 24 mo the specific talc lung burdens (mg/g lung)

were nearly identical. Rats had a greater increase than mice in lung weight as well as greater elevations of neutrophils, enzymes and protein in BALF. The histopathology of rats, including accumulations of talc-filled macrophages, inflammation, epithelial hyperplasia and squamous metaplasia, and focal fibrosis was identical to that described for other dusts. The histopathology differed in that the epithelial hyperplasia and metaplasia, and focal fibrosis observed in rats was absent in mice. These findings illustrate that differences between the responses of rats and mice persist across a wide range of different types of inhaled dusts.

There are a few reports comparing the responses of other species to chronic dust inhalation (Mauderly, 1994a). Alarie et al. (1973, 1975) studied the response of cynomolgus monkeys and guinea pigs chronically exposed to coal combustion fly ash in combination with  $\text{H}_2\text{SO}_4$ . In the study (Alarie et al., 1973), monkeys and guinea pigs were exposed 23+ hours/day 7 days/week for either 52 weeks (guinea pigs) or 78 weeks (monkeys) to approximately  $500 \mu\text{g ash}/\text{m}^3$  (MMAD  $\approx 2.6 \mu\text{m}$ ) in combination with 0.1 to 5.0 ppm sulfur dioxide. Although particles accumulated in the lungs in both species (including bronchial and alveolar deposition) and caused slight inflammation, type II cell proliferation was observed in guinea pigs but not monkeys. In the second study (Alarie et al., 1975), guinea pigs and monkeys were exposed 23+ hours/day 7 days/week for 18 mo to approximately  $500 \mu\text{g ash}/\text{m}^3$  (MMAD  $\approx 4\text{-}5 \mu\text{m}$ ) in combination with 100 or 1,000  $\mu\text{g sulfuric acid mist}/\text{m}^3$ . The effects attributed to fly ash were similar to those described in the first study. Comparison between guinea pigs and monkeys in this series of studies is complicated because the concentrations of co-pollutants and fly ash were not always equivalent and the deposition pattern of the  $2.6\text{-}5.3 \mu\text{m}$  fly ash particles is undoubtedly different in monkeys than in guinea pigs.

***Comparison of Human and Laboratory Animal Response:*** There are limited data allowing direct comparisons of responses of humans and laboratory animals to ambient particulate matter constituents. Chronic occupational exposures to high concentrations of mineral dusts cause pneumoconioses in human lungs, consisting primarily of fibrotic responses with many features similar to those observed in animals. Exposure to silica and dusts with high quartz content causes granulomatous lesions in both human and animal lungs. Merchant et al. (1986) provided a comprehensive review of the pulmonary responses to coal dust in coal workers. The focal collections of dust (macules) and the progressive focal

fibrosis have many (1989). features similar to the responses of rats (Martin et al., 1977; Lewis et al., 1989). Although little information is available on the effects of coal dust in other animals, Heppleston (1954) reported dust accumulations and responses in the lungs of rabbits and ponies that were similar to the responses seen in humans. Emphysema, a common feature of pneumoconiosis even in nonsmoking coal workers (Green et al., 1992) is not a prevalent finding in other species and is usually found only in association with large scars in rats (Mauderly et al., 1988). Other features including the epithelial hyperplasia of rodents and squamous metaplasia of rats are not seen in coal workers' pneumoconiosis.

There are obviously similarities and differences between animals and humans and among animals in their responses to chronic dust inhalation. It is not yet clear which, if any, animal species is a good model for predicting noncancer pulmonary responses of humans to chronic dust exposure. The most common bioassay species, rats and mice, clearly differ in their responses, but it is not clear which best represents humans.

**Age of Animals:** There is limited information on the effects of inhaled particles as a function of changes occurring with age in laboratory animals Mauderly (1989). Mauderly et al. (1987c) exposed rats for 6 mo to diluted, whole diesel exhaust containing  $3500 \mu\text{g}/\text{m}^3$  (MMAD  $\approx 0.25 \mu\text{m}$ ) soot particles. Effects in rats conceived and born in the exposure chambers and exposed up to 6 mo of age were compared to those of rats exposed between 6 and 12 mo of age. Soot accumulated in similar amounts in the lungs of both the young and adult groups, but soot-laden macrophages formed more intraalveolar aggregates in the adults. Tissue responses adjacent to the aggregated macrophages were greater in the adults than in the young rats. Lung weight and the cellularity of pulmonary lymph nodes increased and particle clearance was delayed in the older group, but not in the younger group. Exposure throughout the period of lung development did not cause differences between the lung morphology or respiratory function of exposed and sham-exposed young rats after they reached adulthood (6 mo of age). These results indicate that rats with developing lungs may be less susceptible than adults to the effects of diesel exhaust.

Mauderly (1989) indicates that there is insufficient information on the influence of age on the effects of inhaled particles. It is therefore inappropriate to draw conclusions regarding age-related susceptibility at the present time.

## **11.10 POTENTIAL PATHOPHYSIOLOGICAL MECHANISMS FOR THE EFFECT CONCENTRATIONS OF PARTICULATE POLLUTION**

### **11.10.1 Physiological Mechanisms**

The pathophysiologic mechanisms by which low level ambient particle concentrations may increase morbidity and mortality are not clear. Potential mechanisms might be posited through examining hypotheses considering the pathological mechanisms by which inhaled particles might alter normal physiological, immunological, and biochemical processes in the lung.

In the healthy person, air is drawn into the respiratory tract through a branching airway network. Although the large airways of the tracheobronchial region continuously branch into narrower airways the increase in total cross sectional area makes resistance to airflow low. The inspired air ultimately enters the alveolar or gas exchange region of the lung where the area available for the diffusion of gases is large and the distances for diffusion across the respiratory membrane are minimal.

In the healthy person, the pulmonary circulation is a low resistance system requiring only about 1/5 of the pressure required to pump blood through the high resistance systemic circuit. Any changes in the pulmonary vasculature that increase the resistance to blood flow through the lungs will impose an additional work load on the right ventricle which, if severe enough in a compromised individual, could result in right heart failure.

In considering the potential mechanisms by which increases in ambient PM might affect morbidity and mortality, it is important to consider the physiological characteristics of the population most affected. In general, the population most susceptible to elevations in ambient PM is older (see chapter 12) and may have preexisting respiratory disease. As the healthy older population (Folkow and Svanborg, 1993; Dice, 1993; Lakatta, 1993) ages, cardiorespiratory function, including lung volumes, FEV<sub>1</sub>, and cardiac output reserve (Kenney, 1989) decline. Many of the decrements in physiological function associated with the aging process also may be associated with pathological changes caused by disease or other environmental stressors impacting a person over their lifespan.

There is little information on the extent to which an elderly population might be more susceptible to the effects of particulate pollution in the ambient environment (Cooper et al., 1991). The elderly might be expected to be more susceptible to particulate pollution because

of numerous changes in the body's protective mechanisms. While young and healthy animals might be more adaptable, older animals and those with chronic illness have a more limited ability to adapt to environmental stressors.

### **11.10.2 Physiological-Particle Interaction**

Particles inhaled into the respiratory tract deposit at a variety of sites depending on their size, shape, and the pulmonary ventilation characteristics of the organism. Once deposited, the particles may be cleared by from the lung, sequestered in the lymphatics, metabolized or otherwise transformed by mechanisms described in Chapter 10.

If the particle mass inhaled into the lung is so excessive that the normal pulmonary clearance mechanisms are overwhelmed, or if repeated insult from toxic particles has somehow reduced the ability of normal mechanisms to clear particles, then particles, their degradation products, and metabolic products associated with the clearance process may accumulate and present an additional stress to the organism. This stress may affect the entire organism and not just the respiratory tract. While a young healthy organism may tolerate or adapt to the consequences of an excessive particle load, an older organism or one with chronic respiratory disease or one rendered more susceptible by other stressors (dietary, crowding, thermal, etc.) may become sicker or may die. Thus, it is possible that death of an organism may be the result of an accumulation of lifetime stressors (or, the response to these stressors) that is exacerbated by the addition of an incremental particle load on the system.

Cardiorespiratory system function may be compromised and become less efficient in older people or as a result of disease. Inhaled particles could, conceivably, further compromise the functional status in such individuals. Because a small increase in environmental particle concentrations would not be lethal to most subjects, the terminal event(s) must presumably result from a triggering or exacerbating of a lethal failing of a critical function, such as ventilation, gas exchange, pulmonary circulation, lung fluid balance, or cardiovascular function in subjects already approaching the limits of tolerance due to preexisting conditions.

### 11.10.3 Pathophysiologic Mechanisms

It is conceivable that inhaled particles, their reaction products, or the physiological response to deposited particles may further impair ventilation in the chronically ill individual. Inhaled particles may induce further bronchoconstriction and increase resistance to air flow by activating airways smooth muscle, as in asthmatics. Inhaled particles may also influence various airway secretions that could add to and thicken the mucous blanket leading to mucus plugging or decreased mucociliary clearance. Increases in airways resistance would increase the work of breathing and, in turn, the increased effort would require a greater proportion of the inhaled oxygen for the respiratory muscles and increase the potential risk of respiratory failure.

Inhaled particles or their pathophysiological reaction products could also act at the alveolar capillary membrane. At this site, inhaled particles could decrease the diffusing capacity of the lungs by increasing diffusion distances across the respiratory membrane (by increasing the thickness of the respiratory membrane) and causing abnormal ventilation-perfusion ratios in parts of the lung by altering ventilation distribution.

Inhaled particles, especially ultrafine particles could also act at the level of the pulmonary vasculature. Inhaled particles or the pathophysiological reaction to inhaled particles could elicit changes in pulmonary vascular resistance that could further alter ventilation perfusion abnormalities in people with respiratory disease. Particles could also cause alteration of the distribution of ventilation by causing changes in airway resistance. Diseases such as emphysema destroy alveolar walls as well as the pulmonary capillaries they contain. This causes a progressive increases in pulmonary vascular resistance and elevates pulmonary blood pressure. The generalized systemic hypoxia could result in further pulmonary hypertension and interstitial edema that would impose an increased workload on the heart.

Potential mechanisms which might be evoked to explain the phenomenon of particle related mortality have been considered by Utell and Frampton (1995). Mechanisms which could conceivably account for the particle-related mortality include: (1) "premature" death, that is the hastening of death for individuals already near death (i.e., hastening of an already certain death by hours or days); (2) increased susceptibility to infectious disease; and (3) exacerbation of chronic underlying cardiac or pulmonary disease.

Particulate pollution could contribute to daily mortality rates by affecting those at greatest risk of dying; those individuals for whom death is already imminent. Elevated concentrations of particulate matter, which might be only a minor irritant to healthy people, could be the "last straw" that tips over the precariously balanced physiology of a dying patient. In developing this possibility, Utell and Frampton (1995) have compared the effect associated with particulate matter with that associated with temperature deviations. Time-series analyses have shown relationships between temperature changes, regardless of the direction change, and increasing mortality of a magnitude similar to that described for air pollution (Kunst et al., 1993). While there are a few deaths that can be attributed to hyperthermia and hypothermia, the excess mortality due to moderate temperature deviations is associated primarily with the chronically and terminally ill. It is this excess mortality that is likely caused by further stress on overburdened compensatory mechanisms.

However, if particulate air pollution simply represents a physiological stress similar to thermal stress, and the excess mortality is occurring among individuals who would have died within days or weeks, one would expect to see a "harvesting effect". That is, following the increase in mortality associated with an increase in particulate pollution mortality should fall below baseline, because some of those at risk will have already died. Although Kunst et al. (1993) have reported such an effect with temperature-related mortality, it has not been evident in epidemiology studies of ambient particulate exposure. It is possible however, that epidemiologic studies may not be sensitive enough to detect a harvesting effect because the overall changes in mortality are small. However, even in the 1952 London Fog episode, there was no decline in mortality following the peak in excess deaths; instead, increased mortality appeared to remain somewhat elevated in the days after pollution levels had returned to baseline (Logan, 1953).

Other studies suggest that the effect of particles on mortality cannot be explained solely by death-bed effects. In longitudinal studies, Dockery et al. (1993) and Pope et al. (1995) found a strong association between particulate air pollution and mortality in U.S. cities after adjusting for cigarette smoking and other risk factors. Moreover, mortality and respiratory illness in the Utah Valley have been linked with particulate exposure associated with a steel mill. These findings indicate an effect on annual mortality rates that cannot be explained by hastening death for individuals already near death.

Particle exposure could increase susceptibility to infection with bacteria or respiratory viruses, leading to an increased incidence of, and death from, pneumonia in susceptible members of the population. Potential mechanisms could include effects on mucociliary clearance, alveolar macrophage function, adherence of microorganisms to epithelia, and other specific or nonspecific effects on the immune response. However, pneumonia rarely results in death within 24 h of onset; serious infections of the lower respiratory tract generally take days or weeks to evolve. This would potentially contribute to morbidity effects from PM that are lagged by several days or weeks (Chapter 12). If pollutant exposure increased susceptibility to infectious disease, it should be possible to detect differences in the incidence of such diseases in communities with low vs. high particulate concentrations. It might be expected that emergency room visits and hospitalizations for pneumonia caused by the relevant agent should be measurably higher on days with elevated ambient particle concentrations. Examples of this are evident in data from several cities (see Chapter 12). Laboratory animal studies indicate that PM exposure can impair host defenses. Exposure to acidic aerosols has been linked with alterations in mucociliary clearance and macrophage function. However, bacterial infectivity studies with exposure to non-acidic aerosols and other particulate species have not been shown experimentally to cause increased infection.

What chronic disease processes are most likely to be affected by inhaled particulate matter? To explain the daily mortality statistics, there must be common conditions that contribute significantly to overall mortality from respiratory causes. The most likely candidates are the chronic airways diseases, particularly chronic obstructive pulmonary disease (COPD). COPD is the fourth leading cause of death in the US, and is the most common cause of non-malignant respiratory deaths, accounting for more than 84,000 deaths in 1989 (U.S. Bureau of the Census, 1992). This group of diseases encompasses both emphysema and chronic bronchitis, however, information on death certificates does not allow differentiation between these diagnoses. The pathophysiology includes chronic inflammation of the distal airways as well as destruction of the lung parenchyma. There is loss of supportive elastic tissue, so that the airways collapse more easily during expiration, obstructing flow. Processes that enhance airway inflammation or edema, increase smooth muscle contraction in the conducting airways, or slow mucociliary clearance could adversely affect gas exchange and host defense. Moreover, the uneven ventilation-perfusion matching

characteristics of this disease, with dependence on fewer functioning airways and alveoli for gas exchange, means inhaled particles may be directed to the few functioning lung units in higher concentration than in normal lungs (Bates, 1992)

Asthma is a common chronic respiratory disease that may be exacerbated by air pollution. Mortality from asthma (about 3% of all respiratory deaths) has been rising in the last 15 years (Gergen and Weiss, 1992), and air pollution has been implicated as a potential causative factor. Atmospheric particle levels have been linked with increased hospital admissions for asthma, worsening of symptoms, decrements in lung function, and increased medication use. The incidence of asthma is higher among children and young adults. Although asthma deaths are rare below the age of 35, asthma is the leading cause of non-infectious respiratory mortality below the age of 55. Nevertheless, approximately 70% of all asthma-related deaths occur after age 55 (National Center for Health Statistics, 1993). Death due to asthma may contribute to overall PM-related mortality but it is doubtful that asthma is a leading cause.

Particulate pollutants have been associated with increases in cardiovascular mortality both in the major air pollution episodes and in the more recent time-series analysis. Bates (1992) has postulated three ways in which pollutants could affect cardiovascular mortality statistics. These include: acute airways disease misdiagnosed as pulmonary edema; increased lung permeability, leading to pulmonary edema in people with underlying heart disease and increased left atrial pressure; and, acute bronchiolitis or pneumonia induced by air pollutants precipitating congestive heart failure in those with pre-existing heart disease. Moreover, the pathophysiology of many lung diseases is closely intertwined with cardiac function. Many individuals with COPD also have cardiovascular disease caused by: smoking; aging; or pulmonary hypertension accompanying COPD. Terminal events in patients with end-stage COPD are often cardiac, and may therefore be misclassified as cardiovascular deaths. Hypoxemia associated with abnormal gas exchange can precipitate cardiac arrhythmias and sudden death.

In comparison to healthy people, individuals with respiratory disease have greater deposition of inhaled aerosols in the fine ( $PM_{2.5}$ ) mode. The deposition of particles in the lungs of a COPD patient may be as much as three-fold greater than in a healthy adult. Thus, the potential for greater target tissue dose in susceptible patients is present. The lungs of

individuals with chronic lung diseases, such as asthma, bronchitis, emphysema, etc. are often in a chronic state of inflammation. In addition to the fact that particles can induce an inflammatory response in the respiratory region, the influence of particles on generation of proinflammatory cytokines may be enhanced by the prior existence of inflammation. Phagocytosis by alveolar macrophages is down-regulated both by inflammation and the increased levels of ingested particles. Therefore, people with lung disease not only have greater particle deposition, but the conditions that exist in their lungs prior to exposure are conducive to amplification of the effects of particles and depression of their clearance.

## **11.11 SUMMARY AND CONCLUSIONS**

### **11.11.1 Acid Aerosols**

The results of human studies indicate that healthy subjects do not experience decrements in lung function following single exposures to  $\text{H}_2\text{SO}_4$  at levels up to  $2,000 \mu\text{g}/\text{m}^3$  for 1 h, even with exercise and use of acidic gargles to minimize neutralization by oral ammonia. Mild lower respiratory symptoms (cough, irritation, dyspnea) occur at exposure concentrations in the  $\text{mg}/\text{m}^3$  range. Acid aerosols alter mucociliary clearance in healthy subjects, with effects dependent on exposure concentration and the region of the lung being studied.

Asthmatic subjects appear to be more sensitive than healthy subjects to the effects of acid aerosols on lung function, but the effective concentration differs widely among studies. Adolescent asthmatics may be more sensitive than adults, and may experience small decrements in lung function in response to  $\text{H}_2\text{SO}_4$  at exposure levels only slightly above peak ambient levels. Although the reasons for the inconsistency among studies remain largely unclear, subject selection and acid neutralization by  $\text{NH}_3$  may be important factors. Even in studies reporting an overall absence of effects on lung function, occasional asthmatic subjects appear to demonstrate clinically important effects. Two studies from different laboratories have suggested that responsiveness to acid aerosols may correlate with degree of baseline airway hyperresponsiveness. There is a need to identify determinants of responsiveness to  $\text{H}_2\text{SO}_4$  exposure in asthmatic subjects. In very limited studies, elderly and individuals with

chronic obstructive pulmonary disease do not appear to be particularly susceptible to the effects of acid aerosols on lung function.

Two recent studies have examined the effects of exposure to both H<sub>2</sub>SO<sub>4</sub> and ozone on lung function in healthy and asthmatic subjects. In contrast with previous studies, both studies found evidence that 100 μg/m<sup>3</sup> H<sub>2</sub>SO<sub>4</sub> may potentiate the response to ozone.

Human studies of particles other than acid aerosols provide insufficient data to draw conclusions regarding health effects. However, available data suggest that inhalation of inert particles in the respirable range, including three studies of carbon particles, have little or no effect on symptoms or lung function in healthy subjects at levels above peak ambient concentrations.

The bulk of the laboratory animal toxicologic data base on PM involves sulfur oxide particles, primarily H<sub>2</sub>SO<sub>4</sub>, and the available evidence indicates that the observed responses to these are likely due to H<sup>+</sup> rather than to SO<sub>4</sub><sup>=</sup>.

Acidic sulfates exert their action throughout the respiratory tract, with the response and location of effect dependent upon particle size and mass and number concentration. At very high concentrations that are not environmentally realistic, mortality will occur following acute exposure, due primarily to laryngospasm or bronchoconstriction; larger particles are more effective in this regard than are smaller ones. Extensive pulmonary damage, including edema, hemorrhage, epithelial desquamation, and atelectasis can also cause mortality, but even in the most sensitive animal species, concentrations causing mortality are quite high, at least a thousand-fold greater than current ambient levels.

Both acute and chronic exposure to H<sub>2</sub>SO<sub>4</sub> at levels well below lethal ones will produce functional changes in the respiratory tract. The pathological significance of some of these are greater than for others. Acute exposure will alter pulmonary function, largely due to bronchoconstrictive action. However, attempts to produce changes in airway resistance in healthy animals at levels below 1,000 μg/m<sup>3</sup> have been largely unsuccessful, except when the guinea pig has been used. The lowest effective level of H<sub>2</sub>SO<sub>4</sub> producing a small transient change in airway resistance in the guinea pig is 100 μg/m<sup>3</sup> (1-h exposure). In general, the smaller size droplets (submicron) were more effective in altering pulmonary function, especially at low concentrations. Very low concentrations (< 100 μg/m<sup>3</sup>) of acid-coated ultrafine particles are associated with lung function and diffusion decrements, as well as

airway hyperresponsiveness. Yet even in the guinea pig, there are inconsistencies in the type of response exhibited towards acid aerosols. Chronic exposure to  $\text{H}_2\text{SO}_4$  is also associated with alterations in pulmonary function (e.g., changes in the distribution of ventilation and in respiratory rate in monkeys). But, in these cases, the effective concentrations are  $\geq 500 \mu\text{g}/\text{m}^3$ . Hyperresponsive airways have been induced with repeated exposures to  $250 \mu\text{g}/\text{m}^3 \text{H}_2\text{SO}_4$  in rabbits, and have been suggested to occur following single exposures at  $75 \mu\text{g}/\text{m}^3$ .

Severe morphologic alterations in the respiratory tract will occur at high ( $\gg 1,000 \mu\text{g}/\text{m}^3$ ) acid levels. At low ( $> 100 \mu\text{g}/\text{m}^3$ ) levels and with chronic exposure, the main response seems to be hypertrophy and/or hyperplasia of mucus secretory cells in the epithelium; these alterations may extend to the small bronchi and bronchioles, where secretory cells are normally rare or absent.

The lungs have an array of defense mechanisms to detoxify and physically remove inhaled material, and available evidence indicates that certain of these defenses may be altered by exposure to  $\text{H}_2\text{SO}_4$  levels  $< 1,000 \mu\text{g}/\text{m}^3$ . Defenses such as resistance to bacterial infection may be altered even by acute exposure to concentrations of  $\text{H}_2\text{SO}_4$  around  $1,000 \mu\text{g}/\text{m}^3$ . However, the bronchial mucociliary clearance system is very sensitive to inhaled acids; fairly low levels of  $\text{H}_2\text{SO}_4$  produce alterations in mucociliary transport rates in healthy animals. The lowest level shown to have such an effect,  $100 \mu\text{g}/\text{m}^3$  with repeated exposures, is well below that which results in other physiological changes in most experimental animals. Furthermore, exposures to somewhat higher levels that also alter clearance have been associated with various morphometric changes in the bronchial tree indicative of mucus hypersecretion.

Limited data also suggest that exposure to acid aerosols may affect the functioning of AMs. The lowest level examined in this regard to date is  $500 \mu\text{g}/\text{m}^3 \text{H}_2\text{SO}_4$ . Alveolar region particle clearance is affected by repeated  $\text{H}_2\text{SO}_4$  exposures to as low as  $125 \mu\text{g}/\text{m}^3$  (Schlesinger et al., 1992a).

The assessment of the toxicology of acid aerosols requires some examination of potential interactions with other air pollutants. Such interactions may be antagonistic, additive, or synergistic. Evidence for interactive effects may depend upon the sequence of exposure as well as on the endpoint examined. Low levels of  $\text{H}_2\text{SO}_4$  ( $100 \mu\text{g}/\text{m}^3$ ) have been

shown to react synergistically with O<sub>3</sub> in simultaneous exposures using biochemical endpoints (Warren and Last, 1987). In this case, the H<sub>2</sub>SO<sub>4</sub> enhanced the damage due to the O<sub>3</sub>. The most realistic exposures are to multicomponent atmospheres, but the results of these are often difficult to assess due to chemical interactions of components and a resultant lack of precise control over the composition of the exposure environment.

### 11.11.2 Metals

Data from occupational studies and laboratory animal studies indicate that acute exposures to high levels or chronic exposures to low levels (albeit high compared to ambient levels) of metal particulate can have an effect on the respiratory tract. However, it is doubtful that the metals at concentrations present in the ambient atmosphere (1 to 14 μg/m<sup>3</sup>) could have a significant acute effect in healthy individuals.

The toxicity data on inhalation exposures to arsenic are limited in humans and laboratory animals. Acute data are largely lacking for this route of exposure. In humans, inhalation exposure data, primarily limited to long-term occupational exposure of smelter workers, indicate that chronic exposure leads to lung cancer. In laboratory animals, intratracheal administration of arsenic compounds in the lungs have not indicated tumor development in rats and mice, but insufficient exposure duration may have been used in these studies. However, respiratory tract tumors occurred in hamsters exposed to intratracheal doses of arsenic when a charcoal carbon carrier dust was used to increase arsenic retention in the lungs.

Chronic inhalation exposure to arsenic has also been shown to cause both skin changes (such as hyperpigmentation and hyperkeratosis) and peripheral nerve damage in workers; however, the available inhalation studies in laboratory animals have not evaluated these endpoints. The laboratory animal inhalation data are limited and thus do not allow a thorough comparison of the toxicological and carcinogenic potential of arsenic with the human data. Species differences in dosimetry, absorption, clearance, and elimination of arsenic (i.e., strong affinity to rat hemoglobin) exist between rats and other animal species, including humans, which complicate comparisons of quantitative toxicity.

The kidney is clearly the primary target of chronic inhalation exposure to cadmium in the human; toxicity is dependent on cumulative exposure. Tubular proteinuria occurs after kidney levels of cadmium accumulate to a certain level, estimated at 200 µg/g kidney weight.

The respiratory system is also a target of inhaled cadmium in humans and animals. Intense irritation occurs following high-level exposure in humans and more mild effects on pulmonary function (dyspnea, decreased forced vital capacity) occur following chronic low-level exposure. These effects and their mechanism have been investigated to a greater degree in laboratory animals, although spirometry has not been conducted in animals. The observed effects (increased lung weight, inhibition of macrophages and edema) are consistent with the irritation observed in human studies. In humans, symptoms reverse with cessation or lessening of exposure; laboratory animal studies have reported no progression or slight reversal with continued exposure.

Rat studies show that several forms of cadmium (cadmium chloride, cadmium oxide dust or fume, cadmium sulfide, or cadmium sulfate) can cause lung cancer. There is some evidence that lung cancer has been observed in humans following high occupational exposure, although confounding exposures were present. Because animal cancer studies only examined the lung, they did not address the suggestive evidence of cadmium-related prostate cancer found in several occupational studies.

Although both human and laboratory animal data are limited, both data bases support the respiratory system as a major target of inhaled copper and copper compounds, including copper sulfate and copper chloride. In humans, the data are limited primarily to subjective reporting of respiratory symptoms following acute and chronic inhalation exposures to copper fumes or dust supported with radiographic evidence of pulmonary involvement. The human data do not include pulmonary function tests or histopathology of the respiratory tract. In laboratory animal studies, supporting evidence exists for the involvement of the respiratory system after copper inhalation exposure. Respiratory tract abnormalities in mice repeatedly exposed to copper sulfate aerosols, and decreased tracheal cilia beating frequency in singly exposed hamsters have been reported. Respiratory effects, although minor, have also been observed in rabbits; these included a slight increase in amount of lamellated cytoplasmic inclusions in alveolar macrophages, and a slight increase in volume density of alveolar Type 2 cells. Although respiratory effects were observed in both human and

laboratory animal studies, direct comparisons are not possible since different parameters were examined in the different species for which limited data exist. Immunological effects have been investigated in only one animal study. In the one study addressing the issue, immunotoxic effects observed included: decreased survival time after simultaneous *S. zooepidemicus* aerosol challenge, and decreased bactericidal activity after simultaneous *K. pneumonia* aerosol exposure.

There is limited information on iron toxicity, with human data primarily from chronic occupational exposures. Both human and laboratory animal data, mostly qualitative information, do demonstrate that the respiratory system is the primary target organ for iron oxides following inhalation exposure. However, the differences in toxicity (if any) for different particle sizes or valence states of iron have not been well studied. In humans, respiratory effects (coughing, siderosis) have been reported in workers chronically exposed to iron dust. In laboratory animals, hyperplasia and alveolar fibrosis have been reported after inhalation or intratracheal administration of iron oxide. The lack of information on the histopathological changes in the lungs of exposed workers precludes direct comparison with animal data. Brief exposure to relatively high concentrations of large iron oxide particles in humans have not been associated with adverse responses. The available human and laboratory animal studies are limited and do not provide conclusive evidence regarding the respiratory carcinogenicity of iron oxide.

Human and laboratory animal data confirm the respiratory tract as the primary target of inhaled vanadium compounds. Laboratory animal data suggest that vanadium compounds damage alveolar macrophages, and that toxicity is related to compound solubility and valence. Because of the difficulty in obtaining clinical signs of respiratory distress in laboratory animals, most reported animal data consisted of histological findings (increased leukocytes and lung weights, perivascular edema, alveolar proteinosis, and capillary congestion). Human occupational case studies and epidemiological studies generally emphasize clinical symptoms of respiratory distress, including wheezing, chest pain, bronchitis, rhinitis, productive cough, and fatigue including the possibility of vanadium induced asthma. No human data were found describing histopathology following oral or inhalation exposure.

No major differences in the pharmacokinetics of zinc in humans and laboratory animals were evident. Both human and laboratory animal data demonstrate that the respiratory system is the primary target organ for zinc following inhalation exposure; the toxic compounds most studied are zinc chloride and zinc oxide. In humans, the development of metal fume fever, characterized by respiratory symptoms and pulmonary dysfunction, was observed in workers and experimental subjects during acute exposures to zinc oxide. An immunological component is believed to be responsible for these respiratory responses. Quantitative data on chronic exposures in humans are not available. Inflammation with altered macrophage function, morphological changes in the lungs, and impaired pulmonary function (decreased compliance, total lung capacity, decreased diffusing capacity) were observed in guinea pigs. Rats also showed altered macrophage function in the lungs. At subchronic durations, histopathological changes in the lungs (increased macrophages) were observed in rats, mice, and guinea pigs exposed to zinc chloride. It is clear that zinc can produce inflammatory response in both human and animal species. Alveogenic carcinomas have been observed in mice exposed to zinc chloride for 20 weeks; however, human studies have shown no evidence of increased tumor incidences at exposure levels found in occupational settings. Zinc compounds are soluble in lung fluids and do not appear to accumulate in the respiratory tract.

Studies examining the potential for the transition metals to cause lung injury by the generation of ROS have been conducted in vitro and in animals by intratracheal instillation. While these studies are interesting, the results thus far are of limited value.

### **11.11.3 Ultrafine Particles**

There are only limited data available from human studies or laboratory animal studies on ultrafine aerosols. They are present in the ambient environment as singlet particles but represent an extremely small portion of the mass. However, ultrafine particles are present in high numbers and have a high collective surface area. There are in vitro studies that show ultrafine particles have the capacity to cause injury to cells of the respiratory tract. High levels of ultrafine particles, as metal or polymer "fume", are associated with toxic respiratory responses in humans and other mammals. Such exposures are associated with cough, dyspnea, pulmonary edema, and acute inflammation. Presence of ultrafine particles,

especially the metals Cd, V, Ti, Fe, in human alveolar macrophages indicates widespread exposure to ultrafines as single particles in ambient air. At concentrations less than  $50 \mu\text{g}/\text{m}^3$ , freshly generated insoluble ultrafine particles can be severely toxic to the lung. There are also studies on a number of ultrafine particles (diesel, carbon black, acidic aerosols) where the particles are not present in the exposure atmosphere as singlet particles. Insufficient information is available at the present time to determine whether ambient ultrafine particles may play a role in PM-induced mortality.

#### **11.11.4 Diesel Emissions**

Acute toxic effects caused by exposure to diesel exhaust are mainly attributable to the gaseous components (i.e., mortality from carbon monoxide intoxication and lung injury from respiratory irritants). When the exhaust is diluted to limit the concentrations of these gases, acute effects are not seen.

The focus of the long-term (> 1 year) animal inhalation studies of diesel engine emissions studies has been on the respiratory tract effects in the alveolar region. Effects in the upper respiratory tract and in other organs were not found consistently in chronic animal exposures. Several of these studies are derived from research programs on the toxicology of diesel emissions that consisted of large-scale chronic exposures, which are represented by multiple published accounts of results from various aspects of the overall research program. The respiratory system response has been well characterized in terms of histopathology, biochemistry, cytology, pulmonary function, and respiratory tract clearance. The pathogenic sequence following the inhalation of diesel exhaust as determined histopathologically and biochemically begins with the phagocytosis of diesel particles by AMs. These activated macrophages release chemotactic factors that attract neutrophils and additional AMs. As the lung burden of diesel particles increases, there is an aggregation of particle-laden AMs in alveoli adjacent to terminal bronchioles, increases in the number of Type 2 cells lining particle-laden alveoli, and the presence of particles within alveolar and peribronchial interstitial tissues and associated lymph nodes. The PMNs and macrophages release mediators of inflammation and oxygen radicals and particle-laden macrophages are functionally altered resulting in decreased viability and impaired phagocytosis and clearance of particles. There is a substantial body of evidence for an impairment of particulate

clearance from the bronchioalveolar region of rats following exposure to diesel exhaust. The latter series of events may result in the presence of pulmonary inflammatory, fibrotic, or emphysematous lesions. The noncancer toxicity of diesel emissions is considered to be due to the particle rather than the gas phase, since the long-term effects seen with whole diesel are not found or are found to a much lesser extent in animals exposed to similar dilutions of diesel exhaust filtered to remove most of the particles. Chronic studies in rodents have demonstrated pulmonary effects at 200 to 700  $\mu\text{g}/\text{m}^3$  (expressed as equivalent continuous exposure to adjust for protocol differences). A range of no adverse effect levels has been estimated as from 200 to 400  $\mu\text{g}/\text{m}^3$ .

Several epidemiologic studies have evaluated the effects of chronic exposure to diesel exhaust on occupationally exposed workers. None of these studies are useful for a quantitative evaluation of noncancer toxicity because of inadequate exposure characterization, either because exposures were not well defined or because the possible confounding effects of concurrent exposures could not be evaluated.

#### **11.11.5 Silica**

Emissions of silica into the environment can arise from natural, industrial, and farming activities. There are only limited data on ambient air concentrations of amorphous or crystalline silica, principally because existing measurement methods are not well suited for distinguishing silica from other particulate matter. Using available data on the quartz fraction of coarse dust (Davis et al., 1984) and average annual arithmetic mean  $\text{PM}_{10}$  measurements for 17 U.S. metropolitan areas, annual average and high U.S. ambient quartz levels of 3 and 8  $\mu\text{g}/\text{m}^3$ , respectively, have been estimated (U.S. Environmental Protection Agency, 1996). Davis et al. (1984) found that most of the quartz was in the fraction between 2.5 to 15  $\mu\text{m}$  MMAD.

Silica can occur in two chemical forms, amorphous and crystalline. Crystalline forms include quartz, which is the most prevalent; cristobalite, tridymite, and a few other rare forms. Freshly fractured crystalline silica is more toxicologically reactive than aged forms of crystalline silica. Amorphous silica is less well studied but is considered less potent than crystalline silica. Occupational studies show that chronic exposure to crystalline silica causes inflammation of the lung which can progress to fibrosis and silicosis, a human fibrotic

disease, which can lead to early mortality. Some occupational studies also show a concurrent incidence of lung cancer. The role, if any, of silica-induced lung inflammation, fibrosis, and silicosis in the development of lung cancer is postulated but not adequately demonstrated. Crystalline silica interaction with DNA has been shown under in vitro conditions. Chronic exposure studies in rats also show a similar pattern of lung inflammation, fibrosis, and lung cancer. The International Agency for Research on Cancer (1987) classified crystalline silica as a "possible" human carcinogen owing to a sufficient level of evidence in animal studies, but with inadequate evidence in human studies. The health statistics of the U.S. do not reveal a general population increase in the incidence of these silica-related disease, although there is an increase within segments of the occupational work force.

These effective occupational exposures are greater and the particle sizes smaller than those likely to be experienced by the general public, including susceptible populations. Information gaps still exist for the exposure-response relationship for levels of exposure within the general population.

#### **11.11.6 Bioaerosols**

Ambient bioaerosols include fungal spores, pollen, bacteria, viruses, endotoxins, and plant and animal debris. Such biological aerosols can produce three general classes of health effects: infections, hypersensitivity reactions, and toxicoses. Bioaerosols present in the ambient environment have the potential to cause disease in humans under certain conditions. However, it is improbable that bioaerosols, at the concentrations present in the ambient environment, could account for the observed effects of particulate matter on human mortality and morbidity reported in PM epidemiological studies. Moreover, bioaerosols generally represent a rather small fraction of the measured urban ambient PM mass and are typically present even at lower concentrations during the winter months when notable ambient PM effects have been demonstrated. Bioaerosols also tend to be in the coarse fraction of PM.

#### **11.11.7 "Other Particulate Matter"**

Toxicologic studies of other particulate matter species besides acid aerosols, metals, ultrafine particles, diesel emissions, silica, and bioaerosols were discussed in this chapter.

These studies included exposure to fly ash, volcanic ash, coal dust, carbon black, TiO<sub>2</sub>, and miscellaneous other particles, either alone or in mixtures.

A number of studies of the effects of "Other PM" examined effects of up to 50,000  $\mu\text{g}/\text{m}^3$  of respirable particles with inherently low toxicity on mortality and found no effects. Some mild pulmonary function effects of 5,000 to 10,000  $\mu\text{g}/\text{m}^3$  of similar particles were observed in rats and guinea pigs. Lung morphology studies revealed focal inflammatory responses, some epithelial hyperplasia, and fibrotic responses to exposure generally  $>5,000 \mu\text{g}/\text{m}^3$ . Changes in macrophage clearance after exposure to  $>10,000 \mu\text{g}/\text{m}^3$  were equivocal (no infectivity effects). In studies of mixtures of particles and other pollutants, effects were variable depending on the toxicity of the associated pollutant. In humans, associated particles may increase responses to formaldehyde but not to acid aerosol. None of the "other" particles mentioned above are present in ambient air in more than trace quantities. The relevance of any of these studies to ambient particulate standard setting is extremely limited.

## REFERENCES

- Agency for Toxic Substances and Disease Registry. (1989) Toxicological profile for cadmium. Atlanta, GA: U.S. Department of Health and Human Services, Public Health Service; report no. ATSDR/TP-88/08.
- Agency for Toxic Substances and Disease Registry. (1990) Toxicological profile for copper. Atlanta, GA: U.S. Department of Health & Human Services, Public Health Service; report no. TP-90-08.
- Agency for Toxic Substances and Disease Registry. (1993) Toxicological profile for arsenic. Atlanta, GA: U.S. Department of Health and Human Services, Public Health Service; report no. TP-92/02.
- Agency for Toxic Substances and Disease Registry. (1994) Toxicological profile for zinc. Atlanta, GA: U.S. Department of Health and Human Services, Public Health Service; report no. ASTDR/TP-93/15.
- Alarie, Y.; Anderson, R. C. (1981) Toxicologic classification of thermal decomposition products of synthetic and natural polymers. *Toxicol. Appl. Pharmacol.* 57: 181-188.
- Alarie, Y.; Kantz, R. J., II; Ulrich, C. E.; Krumm, A. A.; Busey, W. M. (1973) Long-term continuous exposure to sulfur dioxide and fly ash mixtures in cynomolgus monkeys and guinea pigs. *Arch. Environ. Health* 27: 251-253.
- Alarie, Y. C.; Krumm, A. A.; Busey, W. M.; Ulrich, C. E.; Kantz, R. J., II. (1975) Long-term exposure to sulfur dioxide, sulfuric acid mist, fly ash, and their mixtures: results of studies in monkeys and guinea pigs. *Arch. Environ. Health* 30: 254-262.
- Amdur, M. O. (1974) 1974 Cummings memorial lecture: the long road from Donora. *Am. Ind. Hyg. Assoc. J.* 35: 589-597.
- Amdur, M. O.; Chen, L. C. (1989) Furnace-generated acid aerosols: speciation and pulmonary effects. In: *Symposium on the health effects of acid aerosols; October 1987; Research Triangle Park, NC.* *Environ. Health Perspect.* 79: 147-150.
- Amdur, M. O.; Dubriel, M.; Creasia, D. A. (1978a) Respiratory response of guinea pigs to low levels of sulfuric acid. *Environ. Res.* 15: 418-423.
- Amdur, M. O.; Bayles, J.; Ugro, V.; Underhill, D. W. (1978b) Comparative irritant potency of sulfate salts. *Environ. Res.* 16: 1-8.
- Amdur, M. O.; McCarthy, J. F.; Gill, M. W. (1982) Respiratory response of guinea pigs to zinc oxide fume. *Am. Ind. Hyg. Assoc. J.* 43: 887-889.
- Amdur, M. O.; Sarofim, A. F.; Neville, M.; Quann, R. J.; McCarthy, J. F.; Elliott, J. F.; Lam, H. F.; Rogers, A. E.; Conner, M. W. (1986) Coal combustion aerosols and SO<sub>2</sub>: an interdisciplinary analysis. *Environ. Sci. Technol.* 20: 138-145.
- American Thoracic Society. (1995) Standards for the diagnosis and care of patients with chronic obstructive pulmonary disease: definitions, epidemiology, pathophysiology, diagnosis, and staging. *Am. J. Respir. Crit. Care Med.* 152(suppl.): S78-S83.
- Ames, R. G.; Attfield, M. D.; Hankinson, J. L.; Hearl, F. J.; Reger, R. B. (1982) Acute respiratory effects of exposure to diesel emissions in coal miners. *Am. Rev. Respir. Dis.* 125: 39-42.
- Ames, R. G.; Reger, R. B.; Hall, D. S. (1984) Chronic respiratory effects of exposure to diesel emissions in coal mines. *Arch. Environ. Health* 39: 389-394.

- Andersen, I. B.; Lundqvist, G. R.; Proctor, D. F.; Swift, D. L. (1979) Human response to controlled levels of inert dust. *Am. Rev. Respir. Dis.* 119: 619-627.
- Anderson, K. R.; Avol, E. L.; Edwards, S. A.; Shamoo, D. A.; Peng, R.-C.; Linn, W. S.; Hackney, J. D. (1992) Controlled exposures of volunteers to respirable carbon and sulfuric acid aerosols. *J. Air Waste Manage. Assoc.* 42: 770-776.
- Antó, J. M.; Sunyer, J. (1990) Epidemiologic studies of asthma epidemics in Barcelona. *Chest* 90(suppl.): 185S-190S.
- Aranyi, C.; Vana, S. C.; Thomas, P. T.; Bradof, J. N.; Fenters, J. D.; Graham, J. A.; Miller, F. J. (1983) Effects of subchronic exposure to a mixture of O<sub>3</sub>, SO<sub>2</sub>, and (NH<sub>4</sub>)<sub>2</sub>SO<sub>4</sub> on host defenses of mice. *J. Toxicol. Environ. Health* 12: 55-71.
- Aranyi, C.; Bradof, J. N.; O'Shea, W. J.; Graham, J. A.; Miller, F. J. (1985) Effects of arsenic trioxide inhalation exposure on pulmonary antibacterial defenses in mice. *J. Toxicol. Environ. Health* 15: 163-172.
- Aris, R.; Christian, D.; Sheppard, D.; Balmes, J. R. (1990) Acid fog-induced bronchoconstriction: the role of hydroxymethanesulfonic acid. *Am. Rev. Respir. Dis.* 141: 546-551.
- Aris, R.; Christian, D.; Sheppard, D.; Balmes, J. R. (1991a) The effects of sequential exposure to acidic fog and ozone on pulmonary function in exercising subjects. *Am. Rev. Respir. Dis.* 143: 85-91.
- Aris, R.; Christian, D.; Sheppard, D.; Balmes, J. R. (1991b) Lack of bronchoconstrictor response to sulfuric acid aerosols and fogs. *Am. Rev. Respir. Dis.* 143: 744-750.
- Armstrong, C. W.; Moore, L. W., Jr.; Hackler, R. L.; Miller, G. B., Jr.; Stroube, R. B. (1983) An outbreak of metal fume fever: diagnostic use of urinary copper and zinc determinations. *J. Occup. Med.* 25: 886-888.
- Askergren, A.; Mellgren, M. (1975) Changes in the nasal mucosa after exposure to copper salt dust: a preliminary report. *Scand. J. Work Environ. Health* 1: 45-49.
- Attfield, M. D. (1978) The effect of exposure to silica and diesel exhaust in underground metal and nonmetal miners. In: Kelley, W. D., ed. *Industrial hygiene for mining and tunneling: proceedings of an American Conference of Governmental Industrial Hygienists topical symposium*; November 1978; Denver, CO. pp. 129-135.
- Attfield, M. D.; Trabant, G. D.; Wheeler, R. W. (1982) Exposure to diesel fumes and dust at six potash mines. *Ann. Occup. Hyg.* 26: 817-831.
- Aust, S. D. (1989) Metal ions, oxygen radicals and tissue damage. In: Somogyi, J. C.; Müller, H. R., eds. *Nutritional impact of food processing: 25th symposium of the Group of European Nutritionists*; September 1987; Reykjavik, Iceland. New York, NY: S. Karger; pp. 266-277. (Somogyi, J. C., ed. *Bibliotheca nutritio et dieta*: no. 43).
- Avol, E. L.; Linn, W. S.; Whynot, J. D.; Anderson, K. R.; Shamoo, D. A.; Valencia, L. M.; Little, D. E.; Hackney, J. D. (1988a) Respiratory dose-response study of normal and asthmatic volunteers exposed to sulfuric acid aerosol in the sub-micrometer size range. *Toxicol. Ind. Health* 4: 173-184.
- Avol, E. L.; Linn, W. S.; Wightman, L. H.; Whynot, J. D.; Anderson, K. R.; Hackney, J. D. (1988b) Short-term respiratory effects of sulfuric acid in fog: a laboratory study of healthy and asthmatic volunteers. *JAPCA* 38: 258-263.
- Avol, E. L.; Linn, W. S.; Shamoo, D. A.; Anderson, K. R.; Peng, R.-C.; Hackney, J. D. (1990) Respiratory responses of young asthmatic volunteers in controlled exposures to sulfuric acid aerosol. *Am. Rev. Respir. Dis.* 142: 343-348.

- Ayres, J. G. (1986) Trends in asthma and hay fever in general practice in the United Kingdom 1976-83. *Thorax* 41: 111-116.
- BASF Corporation. (1991) Notice in accordance with Section 8(e) - preliminary results of acute inhalation study of iron pentacarbonyl [letter to Office of Toxic Substances]. Wyandotte, MI: BASF Corporation; February 14. Available for inspection at: U.S. Environmental Protection Agency, Central Docket Section, Washington, DC; document no. 8EHQ-0291-1177.
- Balmes, J. R.; Fine, J. M.; Christian, D.; Gordon, T.; Sheppard, D. (1988) Acidity potentiates bronchoconstriction induced by hypoosmolar aerosols. *Am. Rev. Respir. Dis.* 138: 35-39.
- Barnhart, M. I.; Chen, S.-t.; Salley, S. O.; Puro, H. (1981) Ultrastructure and morphometry of the alveolar lung of guinea pigs chronically exposed to diesel engine exhaust: six month's experience. *J. Appl. Toxicol.* 1: 88-103.
- Barnhart, M. I.; Salley, S. O.; Chen, S.-t.; Puro, H. (1982) Morphometric ultrastructural analysis of alveolar lungs of guinea pigs chronically exposed by inhalation to diesel exhaust (DE). In: Lewtas, J., ed. *Toxicological effects of emissions from diesel engines: proceedings of the Environmental Protection Agency diesel emissions symposium; October, 1981; Raleigh, NC.* New York, NY: Elsevier Biomedical; pp. 183-200. (Developments in toxicology and environmental science: v. 10).
- Baskerville, A.; Fitzgeorge, R. B.; Gilmour, M. I.; Dowsett, A. B.; Williams, A.; Featherstone, A. S. R. (1988) Effects of inhaled titanium dioxide dust on the lung and on the course of experimental Legionnaires' disease. *Br. J. Exp. Pathol.* 69: 781-792.
- Bates, D. V. (1992) Health indices of the adverse effects of air pollution: the question of coherence. *Environ. Res.* 59: 336-349.
- Battigelli, M. C. (1965) Effects of diesel exhaust. *Arch. Environ. Health* 10: 165-167.
- Battigelli, M. C.; Mannella, R. J.; Hatch, T. F. (1964) Environmental and clinical investigation of workmen exposed to diesel exhaust in railroad engine houses. *Ind. Med. Surg.* 33: 121-124.
- Battigelli, M. C.; Hengstenberg, F.; Mannella, R. J.; Thomas, A. P. (1966) Mucociliary activity. *Arch. Environ. Health* 12: 460-466.
- Baxter, C. S.; Wey, H. E.; Burg, W. R. (1981) A prospective analysis of the potential risk associated with inhalation of aflatoxin-contaminated grain dusts. *Food Cosmet. Toxicol.* 19: 765-769.
- Bégin, R.; Massé, S.; Rola-Pleszczynski, M.; Drapeau, G.; Dalle, D. (1985) Selective exposure and analysis of the sheep tracheal lobe as a model for toxicological studies of respirable particles. *Environ. Res.* 36: 389-404.
- Bellmann, B.; Muhle, H.; Heinrich, U. (1983) Lung clearance after long time exposure of rats to airborne pollutants. *J. Aerosol Sci.* 14: 194-196.
- Bellmann, B.; Muhle, H.; Creutzenberg, O.; Dasenbrock, C.; Kilpper, R.; MacKenzie, J. C.; Morrow, P.; Mermelstein, R. (1991) Lung clearance and retention of toner, utilizing a tracer technique, during chronic inhalation exposure in rats. *Fundam. Appl. Toxicol.* 17: 300-313.
- Bennett, W. D.; Zeman, K. L. (1994) Effect of enhanced supramaximal flows on cough clearance. *J. Appl. Physiol.* 77: 1577-1583.
- Bennett, W. D.; Chapman, W. F.; Gerrity, T. R. (1992) Ineffectiveness of cough for enhancing mucus clearance in asymptomatic smokers. *Chest* 102: 412-416.

- Bennett, W. D.; Chapman, W. F.; Mascarella, J. M. (1993) The acute effect of ipratropium bromide bronchodilator therapy on cough clearance in COPD. *Chest* 103: 488-495.
- Berg, I.; Schlüter, T.; Gercken, G. (1993) Increase of bovine alveolar macrophage superoxide anion and hydrogen peroxide release by dusts of different origin. *J. Toxicol. Environ. Health* 39: 341-354.
- Bhatnagar, R. S.; Hussain, M. Z.; Sorensen, K. R.; Von Dohlen, F. M.; Danner, R. M.; McMillan, L.; Lee, S. D. (1980) Biochemical alterations in lung connective tissue in rats and mice exposed to diesel emissions. In: Pepelko, W. E.; Danner, R. M.; Clarke, N. A., eds. *Health effects of diesel engine emissions: proceedings of an international symposium, v. 1; December 1979; Cincinnati, OH. Cincinnati, OH: U.S. Environmental Protection Agency, Health Effects Research Laboratory; pp. 557-570; EPA report no. EPA-600/9-80-057a. Available from: NTIS, Springfield, VA; PB81-173809.*
- Bice, D. E.; Hahn, F. F.; Benson, J.; Carpenter, R. L.; Hobbs, C. H. (1987) Comparative lung immunotoxicity of inhaled quartz and coal combustion fly ash. *Environ. Res.* 43: 374-379.
- Bio/dynamics Incorporated. (1988) An acute inhalation toxicity study of iron pentacarbonyl in the rat [with cover letter dated February 27, 1992]. East Millstone, NJ: Bio/dynamics Inc.; project no. 87-8024.
- Blanc, P.; Wong, H.; Bernstein, M. S.; Boushey, H. A. (1991) An experimental human model of metal fume fever. *Ann. Intern. Med.* 114: 930-936.
- Böhm, G. M.; Saldiva, P. H. N.; Pasqualucci, C. A. G.; Massad, E.; Martins, M. D. A.; Zin, W. A.; Cardoso, W. V.; Criado, P. M. P.; Komatsuzaki, M.; Sakae, R. S.; Negri, E. M.; Lemos, M.; Capelozzi, V. D. M.; Crestana, C.; da Silva, R. (1989) Biological effects of air pollution in São Paulo and Cubatão. *Environ. Res.* 49: 208-216.
- Bowden, D. H. (1987) Macrophages, dust, and pulmonary diseases. *Exp. Lung Res.* 12: 89-107.
- Boyd, J. T.; Doll, R.; Faulds, J. S.; Leiper, J. (1970) Cancer of the lung in iron ore (haematite) miners. *Br. J. Ind. Med.* 27: 97-105.
- Brain, J. D.; Bloom, S. B.; Valberg, P. A.; Gehr, P. (1984) Correlation between the behavior of magnetic iron oxide particles in the lungs of rabbits and phagocytosis. *Exp. Lung Res.* 6: 115-131.
- Brain, J. D.; Godleski, J.; Kreyling, W. (1994) *In vivo* evaluation of chemical biopersistence of nonfibrous inorganic particles. *Environ. Health Perspect.* 102(suppl. 5): 119-125.
- Brand, P.; Gebhart, J.; Below, M.; Georgi, B.; Heyder, J. (1991) Characterization of environmental aerosols on Heligoland Island. *Atmos. Environ. Part A* 25: 581-585.
- Brand, P.; Ruob, K.; Gebhart, J. (1992) Performance of a mobile aerosol spectrometer for an *in situ* characterization of environmental aerosols in Frankfurt city. *Atmos. Environ. Part A* 26: 2451-2457.
- Brightwell, J.; Fouillet, X.; Cassano-Zoppi, A.-L.; Gatz, R.; Duchosal, F. (1986) Neoplastic and functional changes in rodents after chronic inhalation of engine exhaust emissions. In: Ishinishi, N.; Koizumi, A.; McClellan, R. O.; Stöber, W., eds. *Carcinogenic and mutagenic effects of diesel engine exhaust: proceedings of the international satellite symposium on toxicological effects of emissions from diesel engines; July; Tsukuba Science City, Japan. Amsterdam, Holland: Elsevier Science Publishers B. V.; pp. 471-485. (Developments in toxicology and environmental science: v. 13).*

- Brightwell, J.; Fouillet, X.; Cassano-Zoppi, A.-L.; Bernstein, D.; Crawley, F.; Duchosal, R.; Gatz, R.; Perczel, S.; Pfeifer, H. (1989) Tumors of the respiratory tract in rats and hamsters following chronic inhalation of engine exhaust emissions. *J. Appl. Toxicol.* 9: 23-31.
- Brown, G. M.; Brown, D. M.; Donaldson, K. (1992) Persistent inflammation and impaired chemotaxis of alveolar macrophages on cessation of dust exposure. *Environ. Health Perspect.* 97: 91-94.
- Brownstein, D. G. (1980) Reflex-mediated desquamation of bronchiolar epithelium in guinea pigs exposed acutely to sulfuric acid aerosol. *Am. J. Pathol.* 98: 577-590.
- Buckell, M.; Garrad, J.; Jupe, M. H.; McLaughlin, A. I. G.; Perry, K. M. A. (1946) The incidence of siderosis in iron turners and grinders. *Br. J. Ind. Med.* 3: 78-82.
- Buckley, B. J.; Bassett, D. J. P. (1987) Pulmonary cadmium oxide toxicity in the rat. *J. Toxicol. Environ. Health* 21: 233-250.
- Burge, H. A. (1989) Indoor air and infectious disease. In: Cone, J. E.; Hodgson, M. J., eds. *Problem buildings: building-associated illness and the sick building syndrome.* *Occup. Med.: State of the Art Rev.* 4: 713-721.
- Busch, R. H.; Buschbom, R. L.; Cannon, W. C.; Lauhala, K. E.; Miller, F. J.; Graham, J. A.; Smith, L. G. (1984) Effects of ammonium sulfate aerosol exposure on lung structure of normal and elastase-impaired rats and guinea pigs. *Environ. Res.* 33: 454-472.
- Callis, A. H.; Sohnle, P. G.; Mandel, G. S.; Wiessner, J.; Mandel, N. S. (1985) Kinetics of inflammatory and fibrotic pulmonary changes in a murine model of silicosis. *J. Lab. Clin. Med.* 105: 547-553.
- Campbell, K. I.; George, E. L.; Washington, I. S., Jr. (1980) Enhanced susceptibility to infection in mice after exposure to dilute exhaust from light duty diesel engines. In: Pepelko, W. E.; Danner, R. M.; Clarke, N. A., eds. *Health effects of diesel engine emissions: proceedings of an international symposium, v. 2; December 1979; Cincinnati, OH.* Cincinnati, OH: U.S. Environmental Protection Agency, Health Effects Research Laboratory; pp. 772-785; EPA report no. EPA-600/9-80-057b. Available from: NTIS, Springfield, VA; PB81-173817.
- Campbell, K. I.; George, E. L.; Washington, I. S., Jr. (1981) Enhanced susceptibility to infection in mice after exposure to dilute exhaust from light duty diesel engines. *Environ. Int.* 5: 377-382.
- Castellani, C. M. (1993) Characterization of the atmospheric aerosol in an urban area and the vicinity of a main highway. In: ENEA Environment Department meetings and seminars; Bologna and Rome, Italy. *INTO* 7(93): 35-55.
- Castranova, V.; Bowman, L.; Wright, J. R.; Colby, H.; Miles, P. R. (1984) Toxicity of metallic ions in the lung: effects on alveolar macrophages and alveolar type II cells. *J. Toxicol. Environ. Health* 13: 845-856.
- Castranova, V.; Bowman, L.; Reasor, M. J.; Lewis, T.; Tucker, J.; Miles, P. R. (1985) The response of rat alveolar macrophages to chronic inhalation of coal dust and/or diesel exhaust. *Environ. Res.* 36: 405-419.
- Cavender, F. L.; Steinhagen, W. H.; McLaurin, D. A., III; Cockrell, B. Y. (1977a) Species difference in sulfuric acid mist inhalation. *Am. Rev. Respir. Dis.* 115(suppl.): 204.
- Cavender, F. L.; Steinhagen, W. H.; Ulrich, C. E.; Busey, W. M.; Cockrell, B. Y.; Haseman, J. K.; Hogan, M. D.; Drew, R. T. (1977b) Effects in rats and guinea pigs of short-term exposures to sulfuric acid mist, ozone, and their combination. *J. Toxicol. Environ. Health* 3: 521-533.

- Chan-Yeung, M.; Johnson, A.; MacLean, L.; Cheng, F.; Enarson, D. (1982) Respiratory abnormalities among workers in a iron and steel foundry in B.C. In: 77th annual meeting of the American Thoracic Society; May; Los Angeles, CA. *Am. Rev. Respir. Dis.* 125(4): 161.
- Charles, J. M.; Menzel, D. B. (1975) Ammonium and sulfate ion release of histamine from lung fragments. *Arch. Environ. Health* 30: 314-316.
- Charr, R. (1956) Pulmonary changes in welders: a report of three cases. *Ann. Intern. Med.* 44: 806-812.
- Chauhan, S. S.; Misra, U. K. (1991) Elevation of rat pulmonary, hepatic and lung surfactant lipids by fly ash inhalation. *Biochem. Pharmacol.* 41: 191-198.
- Chauhan, S. S.; Chaudhary, V. K.; Narayan, S.; Misra, U. K. (1987) Cytotoxicity of inhaled coal fly ash in rats. *Environ. Res.* 43: 1-12.
- Chauhan, S. S.; Singh, S. K.; Misra, U. K. (1989) Induction of pulmonary and hepatic cytochrome *P*-450 species by coal fly ash inhalation in rats. *Toxicology* 56: 95-105.
- Chen, L. C.; Schlesinger, R. B. (1983) Response of the bronchial mucociliary clearance system in rabbits to inhaled sulfite and sulfuric acid aerosols. *Toxicol. Appl. Pharmacol.* 71: 123-131.
- Chen, S.; Weller, M. A.; Barnhart, M. I. (1980) Effects of diesel engine exhaust on pulmonary alveolar macrophages. *Scanning Electron Microsc.* 3: 327-338.
- Chen, L. C.; Miller, P. D.; Amdur, M. O. (1989) Effects of sulfur oxides on eicosanoids. *J. Toxicol. Environ. Health* 28: 99-109.
- Chen, L. C.; Lam, H. F.; Kim, E. J.; Guty, J.; Amdur, M. O. (1990) Pulmonary effects of ultrafine coal fly ash inhaled by guinea pigs. *J. Toxicol. Environ. Health* 29: 169-184.
- Chen, L. C.; Miller, P. D.; Lam, H. F.; Guty, J.; Amdur, M. O. (1991) Sulfuric acid-layered ultrafine particles potentiate ozone-induced airway injury. *J. Toxicol. Environ. Health* 34: 337-352.
- Chen, L. C.; Fine, J. M.; Qu, Q.-S.; Amdur, M. O.; Gordon, T. (1992a) Effects of fine and ultrafine sulfuric acid aerosols in guinea pigs: alterations in alveolar macrophage function and intracellular pH. *Toxicol. Appl. Pharmacol.* 113: 109-117.
- Chen, L. C.; Miller, P. D.; Amdur, M. O.; Gordon, T. (1992b) Airway hyperresponsiveness in guinea pigs exposed to acid-coated ultrafine particles. *J. Toxicol. Environ. Health* 35: 165-174.
- Chen, L. C.; Wu, C. Y.; Qu, Q. S.; Schlesinger, R. B. (1995) Number concentration and mass concentration as determinants of biological response to inhaled irritant particles. In: Phalen, R. F.; Bates, D. V., eds. *Proceedings of the colloquium on particulate air pollution and human mortality and morbidity, part II*; January 1994; Irvine, CA. *Inhalation Toxicol.* 7: 577-588.
- Clark, W. R.; Nieman, G.; Hakim, T. S. (1990) Distribution of extravascular lung water after acute smoke inhalation. *J. Appl. Physiol.* 68: 2394-2402.
- Claxton, L. D. (1983) Characterization of automotive emissions by bacterial mutagenesis bioassay: a review. *Environ. Mutagen.* 5: 609-631.
- Coleman, W. E.; Scheel, L. D.; Kupel, R. E.; Larkin, R. L. (1968) The identification of toxic compounds in the pyrolysis products of polytetrafluoroethylene (PTFE). *Am. Ind. Hyg. Assoc. J.* 29: 33-40.
- Cooper, R. L.; Goldman, J. M.; Harbin, T. J., eds. (1991) *Aging and environmental toxicology: biological and behavioral perspectives*. Baltimore, MD: The Johns Hopkins University Press. (Annau, Z., ed. *Series in environmental toxicology*).

- Cosio, M. D.; Ghezzi, H.; Hogg, J. C.; Corbin, R.; Loveland, M.; Dosman, J.; Macklem, P. T. (1977) The relations between structural changes in small airways and pulmonary-function tests. *N. Engl. J. Med.* 298: 1277-1281.
- Costa, D. L.; Tepper, J. S.; Lehmann, J. R.; Winsett, D. W.; Dreher, K.; Ghio, A. J. (1994a) Surface complexed iron ( $\text{Fe}^{+3}$ ) on particles: its role in the induction of lung inflammation and hyperreactivity. Presented at: Colloquium on particulate air pollution and human mortality and morbidity: program and abstracts; January; Irvine, CA. Irvine, CA: University of California Irvine, Air Pollution Health Effects Laboratory; p. S3.4; report no. 94-02.
- Costa, D. L.; Lehmann, J. R.; Frazier, L. T.; Doerfler, D.; Ghio, A. (1994b) Pulmonary hypertension: a possible risk factor in particulate toxicity. *Am. Rev. Respir. Dis.* 149 (4, pt. 2): A840.
- Cox, C. S. (1987) *The aerobiological pathway of microorganisms*. New York, NY: John Wiley & Sons.
- Coyle, T. D. (1982) Silica. In: Grayson, M.; Eckroth, D., eds. *Kirk-Othmer encyclopedia of chemical technology*: v. 20, refractories to silk. 3rd ed. New York, NY: John Wiley & Sons; pp. 748-766.
- Creasia, D. A.; Nettesheim, P. (1974) Respiratory cocarcinogenesis studies with ferric oxide: a test case of current experimental models. In: Karbe, E.; Park, J. F., eds. *Experimental lung cancer: carcinogenesis and bioassays: international symposium held at the Battelle Seattle Research Center*; June; Seattle, WA. New York, NY: Springer-Verlag; pp. 234-245.
- Croft, W. A.; Jarvis, B. B.; Yatawara, C. S. (1986) Airborne outbreak of trichothecene toxicosis. *Atmos. Environ.* 20: 549-552.
- Crouch, E. (1990) Pathobiology of pulmonary fibrosis. *Am. J. Physiol.* 259: L159-L184.
- Culp, D. J.; Latchney, L. R.; Frampton, M. W.; Jahnke, M. R.; Morrow, P. E.; Utell, M. J. (1995) Composition of human airway mucins and effects after inhalation of acid aerosol. *Am. J. Physiol.* 269: L358-L370.
- Dahlqvist, M.; Alexandersson, R.; Andersson, B.; Andersson, K.; Kolmodin-Hedman, B.; Malker, H. (1992) Exposure to ski-wax smoke and health effects in ski waxers. *Appl. Occup. Environ. Hyg.* 7: 689-693.
- Davis, B. L.; Johnson, L. R.; Stevens, R. K.; Courtney, W. J.; Safriet, D. W. (1984) The quartz content and elemental composition of aerosols from selected sites of the EPA inhalable particulate network. *Atmos. Environ.* 18: 771-782.
- Dice, J. F. (1993) Cellular and molecular mechanisms of aging. *Physiol. Rev.* 73: 149-159.
- Do Pico, G. A. (1992) Hazardous exposure and lung disease among farm workers. *Clin. Chest Med.* 13: 311-328.
- Dockery, D. W.; Pope, C. A., III; Xu, X.; Spengler, J. D.; Ware, J. H.; Fay, M. E.; Ferris, B. G., Jr.; Speizer, F. E. (1993) An association between air pollution and mortality in six U.S. cities. *N. Engl. J. Med.* 329: 1753-1759.
- Doig, A. T.; McLaughlin, A. I. G. (1936) X ray appearances of the lungs of electric arc welders. *Lancet*: 771-774.
- Dorries, A. M.; Valberg, P. A. (1992) Heterogeneity of phagocytosis for inhaled versus instilled material. *Am. Rev. Respir. Dis.* 146: 831-837.
- Driscoll, K. E.; Maurer, J. K. (1991) Cytokine and growth factor release by alveolar macrophages: potential biomarkers of pulmonary toxicity. *Toxicol. Pathol.* 19: 398-405.

- Driscoll, K. E.; Lindenschmidt, R. C.; Maurer, J. K.; Perkins, L.; Perkins, M.; Higgins, J. (1991) Pulmonary response to inhaled silica or titanium dioxide. *Toxicol. Appl. Pharmacol.* 111: 201-210.
- Drummond, J. G.; Aranyi, C.; Schiff, L. J.; Fenters, J. D.; Graham, J. A. (1986) Comparative study of various methods used for determining health effects of inhaled sulfates. *Environ. Res.* 41: 514-528.
- Edling, C.; Axelson, O. (1984) Risk factors of coronary heart disease among personnel in a bus company. *Int. Arch. Occup. Environ. Health* 54: 181-183.
- Edling, C.; Anjou, C.-G.; Axelson, O.; Kling, H. (1987) Mortality among personnel exposed to diesel exhaust. *Int. Arch. Occup. Environ. Health* 59: 559-565.
- El Batawi, M. A.; Noweir, M. H. (1966) Health problems resulting from prolonged exposure to air pollution in diesel bus garages. *Ind. Health* 4: 1-10.
- El-Fawal, H. A. N.; Schlesinger, R. B. (1994) Nonspecific airway hyperresponsiveness induced by inhalation exposure to sulfuric acid aerosol: an *in vitro* assessment. *Toxicol. Appl. Pharmacol.* 125: 70-76.
- Elinder, C.-G. (1986) Iron. In: Friberg, L.; Nordberg, G. F.; Vouk, V., eds. *Handbook on the toxicology of metals: v. II, specific metals*. 2nd ed. Amsterdam, The Netherlands: Elsevier; pp. 276-297.
- Elinder, C. G.; Edling, C.; Lindberg, E.; Kagedal, B.; Vesterberg, O. (1985a) Assessment of renal function in workers previously exposed to cadmium. *Br. J. Ind. Med.* 42: 754-760.
- Elinder, C.-G.; Edling, C.; Lindberg, E.; Kagedal, B.; Vesterberg, O. (1985b)  $\beta_2$ -microglobulinuria among workers previously exposed to cadmium: follow-up and dose-response analyses. *Am. J. Ind. Med.* 8: 553-564.
- Elinder, C.-G.; Kjellström, T.; Hogstedt, C.; Andersson, K.; Spång, G. (1985c) Cancer mortality of cadmium workers. *Br. J. Ind. Med.* 42: 651-655.
- Eschenbacher, W. L.; Gravelyn, T. R. (1987) A technique for isolated airway segment lavage. *Chest* 92: 105-109.
- Eskew, M. L.; Zarkower, A.; Scheuchenzuber, W. J.; Graham, J. A. (1982) Effects of fly ash inhalation on murine immune function: effects on systemic response. *Environ. Res.* 28: 375-385.
- Faulds, J. S. (1957) Haematite pneumonconiosis in Cumberland miners. *J. Clin. Pathol.* 10: 187-199.
- Fedan, J. S.; Frazier, D. G.; Moorman, W. J.; Attfield, M. D.; Franczak, M. S.; Kosten, C. J.; Cahill, J. F.; Lewis, T. R.; Green, F. H. Y. (1985) Effects of a two-year inhalation exposure of rats to coal dust and/or diesel exhaust on tension responses of isolated airway smooth muscle. *Am. Rev. Respir. Dis.* 131: 651-655.
- Federal Register. (1978) National ambient air quality standard for lead: final rules and proposed rulemaking. *F. R.* (October 5) 43: 46246-46263.
- Ferin, J.; Oberdörster, G.; Penney, D. P. (1992) Pulmonary retention of ultrafine and fine particles in rats. *Am. J. Respir. Cell Mol. Biol.* 6: 535-542.
- Fick, R. B., Jr.; Paul, E. S.; Merrill, W. W.; Reynolds, H. Y.; Loke, J. S. O. (1984) Alterations in the antibacterial properties of rabbit pulmonary macrophages exposed to wood smoke. *Am. Rev. Respir. Dis.* 129: 76-81.

- Finch, G. L.; McNeill, K. L.; Hayes, T. L.; Fisher, G. L. (1987) *In vitro* interactions between pulmonary macrophages and respirable particles. *Environ. Res.* 44: 241-253.
- Fine, J. M.; Gordon, T.; Sheppard, D. (1987a) The roles of pH and ionic species in sulfur dioxide- and sulfite-induced bronchoconstriction. *Am. Rev. Respir. Dis.* 136: 1122-1126.
- Fine, J. M.; Gordon, T.; Thompson, J. E.; Sheppard, D. (1987b) The role of titratable acidity in acid aerosol-induced bronchoconstriction. *Am. Rev. Respir. Dis.* 135: 826-830.
- Fisher, G. L.; Wilson, F. D. (1980) The effects of coal fly ash and silica inhalation of macrophage function and progenitors. *J. Reticuloendothel. Soc.* 27: 513-524.
- Fogelmark, B. Sjöstrand, M.; Bergström, R.; Rylander, R. (1983) Pulmonary macrophage phagocytosis and enzyme production after *in vivo* exposure to silica dust. *Toxicol. Appl. Pharmacol.* 68: 152-159.
- Folkow, B.; Svanborg, A. (1993) Physiology of cardiovascular aging. *Physiol. Rev.* 73: 725-764.
- Frampton, M. W.; Voter, K. Z.; Morrow, P. E.; Roberts, N. J., Jr.; Culp, D. J.; Cox, C.; Utell, M. J. (1992) Sulfuric acid aerosol exposure in humans assessed by bronchoalveolar lavage. *Am. Rev. Respir. Dis.* 146: 626-632.
- Frampton, M. W.; Morrow, P. E.; Cox, C.; Levy, P. C.; Condemi, J. J.; Speers, D.; Gibb, F. R.; Utell, M. J. (1995) Sulfuric acid aerosol followed by ozone exposure in healthy and asthmatic subjects. *Environ. Res.* 69: 1-14.
- Friede, E.; Rachow, D. O. (1961) Symptomatic pulmonary disease in arc welders. *Ann. Intern. Med.* 54: 121-127.
- Fujimaki, H.; Katayama, N.; Wakamori, K. (1992) Enhanced histamine release from lung mast cells of guinea pigs exposed to sulfuric acid aerosols. *Environ. Res.* 58: 117-123.
- Gamble, J. F.; Jones, W. G. (1983) Respiratory effects of diesel exhaust in salt miners. *Am. Rev. Respir. Dis.* 128: 389-394.
- Gamble, J.; Jones, W.; Hudak, J.; Merchant, J. (1979) Acute changes in pulmonary function in salt miners. Presented at: Industrial hygiene for mining and tunneling: proceedings of a topical symposium; November 1978; Denver, CO. Cincinnati, OH: American Conference of Governmental Industrial Hygienists; pp. 119-128.
- Gamble, J.; Jones, W.; Hudak, J. (1983) An epidemiological study of salt miners in diesel and nondiesel mines. *Am. J. Ind. Med.* 4: 435-458.
- Gamble, J.; Jones, W.; Minshall, S. (1987a) Epidemiological-environmental study of diesel bus garage workers: acute effects of NO<sub>2</sub> and respirable particulate on the respiratory system. *Environ. Res.* 42: 201-214.
- Gamble, J.; Jones, W.; Minshall, S. (1987b) Epidemiological-environmental study of diesel bus garage workers: chronic effects of diesel exhaust on the respiratory system. *Environ. Res.* 44: 6-17.
- Garrett, N. E.; Campbell, J. A.; Stack, H. F.; Waters, M. D.; Lewtas, J. (1981a) The utilization of the rabbit alveolar macrophage and Chinese hamster ovary cell for evaluation for the toxicity of particulate materials: I. model compounds and metal-coated fly ash. *Environ. Res.* 24: 345-365.
- Garrett, N. E.; Campbell, J. A.; Stack, H. F.; Waters, M. D.; Lewtas, J. (1981b) The utilization of the rabbit alveolar macrophage and Chinese hamster ovary cell for evaluation of the toxicity of particulate materials: II. particles from coal-related processes. *Environ. Res.* 24: 366-376.

- Gearhart, J. M.; Schlesinger, R. B. (1986) Sulfuric acid-induced airway hyperresponsiveness. *Fundam. Appl. Toxicol.* 7: 681-689.
- Gearhart, J. M.; Schlesinger, R. B. (1988) Response of the tracheobronchial mucociliary clearance system to repeated irritant exposure: effect of sulfuric acid mist on function and structure. *Exp. Lung Res.* 14: 587-605.
- Gergen, P. J.; Weiss, K. B. (1992) The increasing problem of asthma in the United States. *Am. Rev. Respir. Dis.* 146: 823-824.
- Gerrard, C. S.; Gerrity, T. R.; Yeates, D. B. (1986) The relationships of aerosol deposition, lung size, and the rate of mucociliary clearance. *Arch. Environ. Health* 41: 11-15.
- Ghio, A. J.; Hatch, G. E. (1993) Lavage phospholipid concentration after silica instillation in the rat is associated with complexed  $[Fe^{3+}]$  on the dust surface. *Am. J. Respir. Cell Mol. Biol.* 8: 403-407.
- Ghio, A. J.; Kennedy, T. P.; Whorton, A. R.; Crumbliss, A. L.; Hatch, G. E.; Hoidal, J. R. (1992) Role of surface complexed iron in oxidant generation and lung inflammation induced by silicates. *Am. J. Physiol.* 263: L511-L518.
- Ghio, A. J.; Jaskot, R. H.; Hatch, G. E. (1994) Lung injury after silica instillation is associated with an accumulation of iron in rats. *Am. J. Physiol.* 267: L686-L692.
- Gilmour, M. I.; Taylor, F. G. R.; Baskerville, A.; Wathes, C. M. (1989a) The effect of titanium dioxide inhalation on the pulmonary clearance of *Pasteurella haemolytica* in the mouse. *Environ. Res.* 50: 157-172.
- Gilmour, M. I.; Taylor, F. G. R.; Wathes, C. M. (1989b) Pulmonary clearance of *Pasteurella haemolytica* and immune responses in mice following exposure to titanium dioxide. *Environ. Res.* 50: 184-194.
- Glaser, U.; Klöppel, H.; Hochrainer, D. (1986a) Bioavailability indicators of inhaled cadmium compounds. *Ecotoxicol. Environ. Saf.* 11: 261-271.
- Glaser, U.; Hochrainer, D.; Oldiges, H.; Takenaka, S. (1986b) Long-term inhalation studies with NIO and  $As_2O_3$  aerosols in Wistar rats. In: Proceedings of the international conference on health hazards and biological effects of welding fumes and gases; February 1985; Copenhagen, Denmark. *Int. Congr. Ser. Excerpta Med.* 676: 325-328.
- Glaser, U.; Hochrainer, D.; Otto, F. J.; Oldiges, H. (1990) Carcinogenicity and toxicity of four cadmium compounds inhaled by rats. *Toxicol. Environ. Chem.* 27: 153-162.
- Gleason, R. P. (1968) Exposure to copper dust. *Am. Ind. Hyg. Assoc. J.* 29: 461-462.
- Glikson, M.; Rutherford, S.; Simpson, R. W.; Mitchell, C. A.; Yago, A. (1995) Microscopic and submicron components of atmospheric particulate matter during high asthma periods in Brisbane, Queensland, Australia. *Atmos. Environ.* 29: 549-562.
- Godfrey, S. (1993) Airway inflammation, bronchial reactivity and asthma. *Agents Actions Suppl.* 40: 109-143.
- Godleski, J. J.; Melnicoff, M. J.; Sadri, S.; Garbeil, P. (1984) Effects of inhaled ammonium sulfate on benzo[a]pyrene carcinogenesis. *J. Toxicol. Environ. Health* 14: 225-238.
- Goldstein, R. H.; Fine, A. (1986) Fibrotic reactions in the lung: the activation of the lung fibroblast. *Exp. Lung Res.* 11: 245-261.

- Goldstein, M.; Weiss, H.; Wade, K.; Penek, J.; Andrews, L.; Brandt-Rauf, P. (1987) An outbreak of fume fever in an electronics instrument testing laboratory. *J. Occup. Med.* 29: 746-749.
- Gordon, T. (1995) Respiratory system. In: Goyer, R. A.; Klaasen, C. D.; Waalkes, M. P., eds. *Metal toxicity*. San Diego, CA: Academic Press; pp. 237-263.
- Gordon, T.; Chen, L. C.; Fine, J. M.; Schlesinger, R. B.; Su, W. Y.; Kimmel, T. A.; Amdur, M. O. (1992) Pulmonary effects of inhaled zinc oxide in human subjects, guinea pigs, rats, and rabbits. *Am. Ind. Hyg. Assoc. J.* 53: 503-509.
- Gościcki, J.; Woźniak, H.; Szendzikowski, S.; Więcek, E.; Lao, I.; Bielichowska, G.; Kołakowski, J. (1978) [Experimental silicosis. II. Fibrogenic effect of natural amorphous silica.] *Med. Pr.* 29: 281-291.
- Graham, J. A.; Miller, F. J.; Daniels, M. J.; Payne, E. A.; Gardner, D. E. (1978) Influence of cadmium, nickel, and chromium on primary immunity in mice. *Environ. Res.* 16: 77-87.
- Green, D. J.; Bascom, R.; Healey, E. M.; Hebel, J. R.; Sauder, L. R.; Kulle, T. J. (1989) Acute pulmonary response in healthy, nonsmoking adults to inhalation of formaldehyde and carbon. *J. Toxicol. Environ. Health* 28: 261-275.
- Green, F. H. Y.; Vallyathan, V.; Schleiff, P.; Attfield, M. (1992) Emphysema in coal workers' pneumoconiosis: contribution by coal and cigarette smoking. *Am. Rev. Respir. Dis.* 145(suppl.): A321.
- Griffis, L. C.; Wolff, R. K.; Henderson, R. F.; Griffith, W. C.; Mokler, B. V.; McClellan, R. O. (1983) Clearance of diesel soot particles from rat lung after a subchronic diesel exhaust exposure. *Fundam. Appl. Toxicol.* 3: 99-103.
- Griffith, F. D.; Stephens, S. S.; Tayfun, F. O. (1973) Exposure of Japanese quail and parakeets to the pyrolysis products of fry pans coated with Teflon™ and common cooking oils. *Am. Ind. Hyg. Assoc. J.* 34: 176-178.
- Grimmer, G.; Brune, H.; Deutsch-Wenzel, R.; Dettbarn, G.; Jacob, J.; Naujack, K.-W.; Mohr, U.; Ernst, H. (1987) Contribution of polycyclic aromatic hydrocarbons and nitro-derivatives to the carcinogenic impact of diesel engine exhaust condensate evaluated by implantation into the lungs of rats. *Cancer Lett. (Shannon, Irel.)* 37: 173-180.
- Grose, E. C.; Gardner, D. E.; Miller, F. J. (1980) Response of ciliated epithelium to ozone and sulfuric acid. *Environ. Res.* 22: 377-385.
- Grose, E. C.; Richards, J. H.; Illing, J. W.; Miller, F. J.; Davies, D. W.; Graham, J. A.; Gardner, D. E. (1982) Pulmonary host defense responses to inhalation of sulfuric acid and ozone. *J. Toxicol. Environ. Health* 10: 351-362.
- Grose, E. C.; Grady, M. A.; Illing, J. W.; Daniels, M. J.; Selgrade, M. K.; Hatch, G. E. (1985) Inhalation studies of Mt. St. Helens volcanic ash in animals: III. host defense mechanisms. *Environ. Res.* 37: 84-92.
- Gross, K. B. (1981) Pulmonary function testing of animals chronically exposed to diluted diesel exhaust. *J. Appl. Toxicol.* 1: 116-123.
- Groth, D. H.; Moorman, W. J.; Lynch, D. W.; Stettler, L. E.; Wagner, W. D.; Hornung, R. W. (1981) Chronic effects of inhaled amorphous silicas in animals. In: Dunnom, D. D., ed. *Health effects of synthetic silica particulates: a symposium sponsored by ASTM Committee E-34 on Occupational Health and Safety and the Industrial Health Foundation; November 1979; Benalmadena-Costa (Torremolinos), Spain*. Philadelphia, PA: American Society for Testing and Materials; pp. 118-143; ASTM special technical publication 732.

- Guilianelli, C.; Baeza-Squiban, A.; Boisvieux-Ulrich, E.; Houcine, O.; Zalma, R.; Guennou, C.; Pezerat, H.; Marano, F. (1993) Effect of mineral particles containing iron on primary cultures of rabbit tracheal epithelial cells: possible implication of oxidative stress. *Environ. Health Perspect.* 101: 436-442.
- Hackett, N. A. (1983) Cell proliferation in lung following acute fly ash exposure. *Toxicology* 27: 273-286.
- Hahon, N.; Booth, J. A.; Sepulveda, M.-J. (1983) Effects of lignite fly ash particulates and soluble components on the interferon system. *Environ. Res.* 32: 329-343.
- Hahon, N.; Booth, J. A.; Green, F.; Lewis, T. R. (1985) Influenza virus infection in mice after exposure to coal dust and diesel engine emissions. *Environ. Res.* 37: 44-60.
- Halliwell, B.; Gutteridge, J. M. C. (1986) Iron and free radical reactions: two aspects of antioxidant protection. *Trends Biochem. Sci.* 11: 372-375.
- Hanley, Q. S.; Koenig, J. Q.; Larson, T. V.; Anderson, T. L.; Van Belle, G.; Rebolledo, V.; Covert, D. S.; Pierson, W. E. (1992) Response of young asthmatic patients to inhaled sulfuric acid. *Am. Rev. Respir. Dis.* 145: 326-331.
- Hare, C. T.; Springer, K. J. (1971) Public response to diesel engine exhaust odors [final report]. San Antonio, TX: Southwest Research Institute; report no. AR-804. Available from: NTIS, Springfield, VA; PB-204012.
- Hare, C. T.; Springer, K. J.; Somers, J. H.; Huls, T. A. (1974) Public opinion of diesel odor. Warrendale, PA: Society of Automotive Engineers; SAE technical paper no. 740214.
- Hart, B. A. (1986) Cellular and biochemical response of the rat lung to repeated inhalation of cadmium. *Toxicol. Appl. Pharmacol.* 82: 281-291.
- Hatch, G. E.; Raub, J. A.; Graham, J. A. (1984) Functional and biochemical indicators of pneumoconiosis in mice: comparison with rats. *J. Toxicol. Environ. Health* 13: 487-497.
- Hatch, G. E.; Boykin, E.; Graham, J. A.; Lewtas, J.; Pott, F.; Loud, K.; Mumford, J. L. (1985) Inhalable particles and pulmonary host defense: *in vivo* and *in vitro* effects of ambient air and combustion particles. *Environ. Res.* 36: 67-80.
- Hatch, V.; Hauser, R.; Hayes, G. B.; Stearns, R.; Christiani, D.; Godleski, J. J. (1994) Detection of ultrafine particles in the lung macrophages of healthy people. In: Bailey, G. W.; Garratt-Reed, A. J., eds. Proceedings fifty-second annual meeting, Microscopy Society of America, twenty-ninth annual meeting, Microbeam Analysis Society; August; New Orleans, LA. San Francisco, CA: San Francisco Press, Inc.; pp. 1004-1005.
- Health Effects Institute-Asbestos Research. (1991) Asbestos in public and commercial buildings: a literature review and synthesis of current knowledge. Cambridge, MA: Health Effects Institute-Asbestos Research.
- Health Effects Institute. (1995) Diesel exhaust: a critical analysis of emissions, exposure, and health effects: a special report of the Institute's Diesel Working Group. Cambridge, MA: Health Effects Institute.
- Heinrich, U. (1994) Carcinogenic effects of solid particles. In: Mohr, U.; Dungworth, D. L.; Mauderly, J. L.; Oberdörster, G., eds. Toxic and carcinogenic effects of solid particles in the respiratory tract: [proceedings of the 4th international inhalation symposium]; March 1993; Hannover, Germany. Washington, DC: International Life Sciences Institute Press; pp. 57-73.

- Heinrich, U.; Peters, L.; Funcke, W.; Pott, F.; Mohr, U.; Stöber, W. (1982) Investigation of toxic and carcinogenic effects of diesel exhaust in long-term inhalation exposure of rodents. In: Lewtas, J., ed. Toxicological effects of emissions from diesel engines: proceedings of the Environmental Protection Agency diesel emissions symposium; October 1981; Raleigh, NC. New York, NY: Elsevier Biomedical; pp. 225-242. (Developments in toxicology and environmental science: v. 10).
- Heinrich, U.; Pott, F.; Rittinghausen, S. (1986a) Comparison of chronic inhalation effects in rodents after long-term exposure to either coal oven flue gas mixed with pyrolyzed pitch or diesel engine exhaust. In: Ishinishi, N.; Koizumi, A.; McClellan, R. O.; Stöber, W., eds. Carcinogenic and mutagenic effects of diesel engine exhaust: proceedings of the international satellite symposium on toxicological effects of emissions from diesel engines; July; Tsukuba Science City, Japan. Amsterdam, Holland: Elsevier Science Publishers B. V.; pp. 441-457. (Developments in toxicology and environmental science: v. 13).
- Heinrich, U.; Muhle, H.; Takenaka, S.; Ernst, H.; Fuhst, R.; Mohr, U.; Pott, F.; Stöber, W. (1986b) Chronic effects on the respiratory tract of hamsters, mice, and rats after long-term inhalation of high concentrations of filtered and unfiltered diesel engine emissions. *J. Appl. Toxicol.* 6: 383-395.
- Heinrich, U.; Peters, L.; Ernst, H.; Rittinghausen, S.; Dasenbrock, C.; König, H. (1989a) Investigation on the carcinogenic effects of various cadmium compounds after inhalation exposure in hamsters and mice. *Exp. Pathol.* 37: 253-258.
- Heinrich, U.; Muhle, H.; Hoymann, H. G.; Mermelstein, R. (1989b) Pulmonary function changes in rats after chronic and subchronic inhalation exposure to various particulate matter. *Exp. Pathol.* 37: 248-252.
- Heinrich, U.; Fuhst, R.; Rittinghausen, S.; Creutzenberg, O.; Bellmann, B.; Koch, W.; Levsen, K. (1995) Chronic inhalation exposure of Wistar rats and two different strains of mice to diesel engine exhaust, carbon black, and titanium dioxide. *Inhalation Toxicol.* 7: 533-556.
- Hemenway, D. R.; Absher, M.; Landesman, M.; Trombley, L.; Emerson, R. J. (1986) Differential lung response following silicon dioxide polymorph aerosol exposure. In: Goldsmith, D. F.; Winn, D. M.; Shy, C. M., eds. Silica, silicosis, and cancer: controversy in occupational medicine. New York, NY: Praeger Publishers; pp. 105-116.
- Henderson, R. F.; Gray, R. H.; Hahn, F. F. (1980a) Acute inhalation toxicity of sulfuric acid mist in the presence and absence of respirable particles. In: Diel, J. H.; Bice, D. E.; Martinez, B. S., eds. Inhalation Toxicology Research Institute annual report 1979—1980. Albuquerque, NM: U. S. Department of Energy, Lovelace Biomedical and Environmental Research Institute; pp. 466-469; report no. LMF-84. Available from: NTIS, Springfield, VA; LMF-84.
- Henderson, R. F.; Rebar, A. H.; DeNicola, D. B.; Henderson, T. R. (1980b) The use of pulmonary lavage fluid in screening for early indicators of lung injury. In: Sanders, C. L.; Cross, F. T.; Dagle, G. E.; Mahaffey, J. A., eds. Pulmonary toxicology of respirable particles: proceedings of the nineteenth annual Hanford life sciences symposium; October 1979; Richland, WA. Washington, DC: U.S. Department of Energy, Technical Information Center; pp. 378-391; report no. CONF-791002. (DOE symposium series 53). Available from: NTIS, Springfield, VA; CONF-791002.
- Henderson, R. F.; Pickrell, J. A.; Jones, R. K.; Sun, J. D.; Benson, J. M.; Mauderly, J. L.; McClellan, R. O. (1988) Response of rodents to inhaled diluted diesel exhaust: biochemical and cytological changes in bronchoalveolar lavage fluid and in lung tissue. *Fundam. Appl. Toxicol.* 11: 546-567.
- Heppleston, A. G. (1954) Changes in the lungs of rabbits and ponies inhaling coal dust underground. *J. Pathol. Bacteriol.* 67: 349-359.

- Hewitt, P. J.; Hicks, R. (1972) Neutron activation analysis of blood and body tissue from rats exposed to welding fume. In: Krippner, M., ed. Nuclear activation techniques in the life sciences 1972: proceedings of a symposium; April; Bled, Yugoslavia. Vienna, Austria: International Atomic Energy Agency; pp. 219-232.
- Heyder, J.; Beck-Speier, I.; Ferron, G. A.; Heilmann, P.; Karg, E.; Kreyling, W. G.; Lenz, A. G.; Maier, K.; Schulz, H.; Takenaka, S.; Tuch, T. (1992) Early response of the canine respiratory tract following long-term exposure to a sulfur(IV) aerosol at low concentration. I. Rationale, design, methodology, and summary. *Inhalation Toxicol.* 4: 159-174.
- Hill, J. O.; Rothenberg, S. J.; Kanapilly, G. M.; Hanson, R. L.; Scott, B. R. (1982) Activation of immune complement by fly ash particles from coal combustion. *Environ. Res.* 28: 113-122.
- Holma, B.; Lindegren, M.; Andersen, J. M. (1977) pH effects on ciliomotility and morphology of respiratory mucosa. *Arch. Environ. Health* 32: 216-226.
- Holmqvist, I. (1951) Occupational arsenical dermatitis: a study among employees at a copper ore smelting work including investigations of skin reactions to contact with arsenic compounds. *Acta Derm. Venereol.* 31(suppl. 26): 1-214.
- Horvath, S. M.; Folinsbee, L. J.; Bedi, J. F. (1987) Combined effect of ozone and sulfuric acid on pulmonary function in man. *Am. Ind. Hyg. Assoc. J.* 48: 94-98.
- Hubbard, A. K. (1989) Role for T lymphocytes in silica-induced pulmonary inflammation. *Lab. Invest.* 61: 46-52.
- Hyde, D.; Orthoefer, J.; Dungworth, D.; Tyler, W.; Carter, R.; Lum, H. (1978) Morphometric and morphologic evaluation of pulmonary lesions in beagle dogs chronically exposed to high ambient levels of air pollutants. *Lab. Invest.* 38: 455-469.
- Hyde, D. M.; Plopper, C. G.; Weir, A. J.; Murnane, R. D.; Warren, D. L.; Last, J. A.; Pepelko, W. E. (1985) Peribronchiolar fibrosis in lungs of cats chronically exposed to diesel exhaust. *Lab. Invest.* 52: 195-206.
- Ilowite, J. S.; Smaldone, G. C.; Perry, R. J.; Bennett, W. D.; Foster, W. M. (1989) Relationship between tracheobronchial particle clearance rates and sites of initial deposition in man. *Arch. Environ. Health* 44: 267-273.
- Imlay, J. A.; Chin, S. M.; Linn, S. (1988) Toxic DNA damage by hydrogen peroxide through the Fenton reaction in vivo and in vitro. *Science (Washington, DC)* 240: 640-642.
- International Agency for Research on Cancer. (1987) Silica and some silicates. Lyon, France: World Health Organization. (IARC monographs on the evaluation of carcinogenic risks to humans: v. 42).
- International Agency for Research on Cancer. (1989) Diesel and gasoline engine exhausts and some nitroarenes. Lyon, France: World Health Organization. (IARC monographs on the evaluation of carcinogenic risks to humans: v. 46).
- International Agency for Research on Cancer. (1993) IARC monographs on the evaluation of carcinogenic risks to humans: v. 58, beryllium, cadmium, mercury, and exposures in the glass manufacturing industry. Lyon, France: World Health Organization.
- Ishinishi, N.; Kuwabara, N.; Nagase, S.; Suzuki, T.; Ishiwata, S.; Kohno, T. (1986) Long-term inhalation studies on effects of exhaust from heavy and light duty diesel engines on F344 rats. In: Ishinishi, N.; Koizumi, A.; McClellan, R. O.; Stöber, W., eds. Carcinogenic and mutagenic effects of diesel engine exhaust: proceedings of the international satellite symposium on toxicological effects of emissions from diesel engines; July; Tsukuba Science City, Japan.

- Amsterdam, Holland: Elsevier Science Publishers B. V.; pp. 329-348. (Developments in toxicology and environmental science: v. 13).
- Iwai, K.; Udagawa, T.; Yamagishi, M.; Yamada, H. (1986) Long-term inhalation studies of diesel exhaust on F344 SPF rats. Incidence of lung cancer and lymphoma. In: Ishinishi, N.; Koizumi, A.; McClellan, R. O.; Stöber, W., eds. Carcinogenic and mutagenic effects of diesel engine exhaust: proceedings of the international satellite symposium on toxicological effects of emissions from diesel engines; July; Tsukuba Science City, Japan. Amsterdam, Holland: Elsevier Science Publishers B. V.; pp. 349-360. (Developments in toxicology and environmental science: v. 13).
- Jakab, G. J. (1992) Relationship between carbon black particulate-bound formaldehyde, pulmonary antibacterial defenses, and alveolar macrophage phagocytosis. *Inhalation Toxicol.* 4: 325-342.
- Jakab, G. J. (1993) The toxicologic interactions resulting from inhalation of carbon black and acrolein on pulmonary antibacterial and antiviral defenses. *Toxicol. Appl. Pharmacol.* 121: 167-175.
- Jakab, G. J.; Hemenway, D. R. (1993) Inhalation coexposure to carbon black and acrolein suppresses alveolar macrophage phagocytosis and TNF- $\alpha$  release and modulates peritoneal macrophage phagocytosis. *Inhalation Toxicol.* 5: 275-289.
- Johansson, A.; Camner, P.; Jarstrand, C.; Wiernik, A. (1983) Rabbit alveolar macrophages after inhalation of soluble cadmium, cobalt, and copper: a comparison with the effects of soluble nickel. *Environ. Res.* 31: 340-354.
- Johansson, A.; Curstedt, T.; Robertson, B.; Camner, P. (1984) Lung morphology and phospholipids after experimental inhalation of soluble cadmium, copper, and cobalt. *Environ. Res.* 34: 295-309.
- Johnston, C. J.; Finkelstein, J. N.; Gelein, R.; Baggs, R.; Oberdörster, G. (1995) Characterization of the early pulmonary inflammatory response associated with ultrafine PTFE particle exposure. *Toxicol. Appl. Pharmacol.*: submitted
- Jørgensen, H.; Svensson, A. (1970) Studies on pulmonary function and respiratory tract symptoms of workers in an iron ore mine where diesel trucks are used underground. *J. Occup. Med.* 12: 348-354.
- Juhos, L. T.; Evans, M. J.; Mussenden-Harvey, R.; Furiosi, N. J.; Lapple, C. E.; Freeman, G. (1978) Limited exposure of rats to H<sub>2</sub>SO<sub>4</sub> with and without O<sub>3</sub>. *J. Environ. Sci. Health Part C* 13: 33-47.
- Kahn, G.; Orris, P.; Weeks, J. (1988) Acute overexposure to diesel exhaust: report of 13 cases. *Am. J. Ind. Med.* 13: 405-406.
- Kaplan, H. L.; MacKenzie, W. F.; Springer, K. J.; Schreck, R. M.; Vostal, J. J. (1982) A subchronic study of the effects of exposure of three species of rodents to diesel exhaust. In: Lewtas, J., ed. Toxicological effects of emissions from diesel engines: proceedings of the Environmental Protection Agency diesel emission symposium; October, 1981; Raleigh, NC. New York, NY: Elsevier Biomedical; pp. 161-182. (Developments in toxicology and environmental science: v. 10).
- Karagianes, M. T.; Palmer, R. F.; Busch, R. H. (1981) Effects of inhaled diesel emissions and coal dust in rats. *Am. Ind. Hyg. Assoc. J.* 42: 382-391.
- Katz, M.; Rennie, R. P.; Jegier, Z. (1960) Air pollution and associated health hazards from diesel locomotive traffic in a railroad tunnel. *Occup. Health Rev.* 11: 2-15.

- Kawabata, Y.; Iwai, K.; Udagawa, T.; Tukagoshi, K.; Higuchi, K. (1986) Effects of diesel soot on unscheduled DNA synthesis of tracheal epithelium and lung tumor formation. In: Ishinishi, N.; Koizumi, A.; McClellan, R. O.; Stöber, W., eds. Carcinogenic and mutagenic effects of diesel engine exhaust: proceedings of the international satellite symposium on toxicological effects of emissions from diesel engines; July; Tsukuba Science City, Japan. Amsterdam, The Netherlands: Elsevier Science Publishers B. V.; pp. 213-222. (Developments in toxicological and environmental science: v. 13).
- Kenney, R. A., ed. (1989) Physiology of aging: a synopsis. Chicago, IL: Year Book Medical Publishers, Inc.
- Kinlen, L. J.; Willows, A. N. (1988) Decline in the lung cancer hazard: a prospective study of the mortality of iron ore miners in Cumbria. *Br. J. Ind. Med.* 45: 219-224.
- Kitabatake, M.; Imai, M.; Kasama, K.; Kobayashi, I.; Tomita, Y.; Yoshida, K. (1979) Effects of air pollutants on the experimental induction of asthma attacks in guinea pigs: sulfuric acid mist and mixture of the mist and sulfur dioxide. *Mie Med. J.* 29: 29-36.
- Kiviluoto, M. (1980) Observations on the lungs of vanadium workers. *Br. J. Ind. Med.* 37: 363-366.
- Kiviluoto, M.; Räsänen, O.; Rinne, A.; Rissanen, M. (1979) Effects of vanadium on the upper respiratory tract of workers in a vanadium factory: a macroscopic and microscopic study. *Scand. J. Work Environ. Health* 5: 50-58.
- Kiviluoto, M.; Pakarinen, A.; Pyy, L. (1981a) Clinical laboratory results of vanadium-exposed workers. *Arch. Environ. Health* 36: 109-113.
- Kiviluoto, M.; Pyy, L.; Pakarinen, A. (1981b) Serum and urinary vanadium of workers processing vanadium pentoxide. *Int. Arch. Occup. Environ. Health* 48: 251-256.
- Kiviluoto, M.; Räsänen, O.; Rinne, A.; Rissanen, M. (1981c) Intracellular immunoglobulins in plasma cells of nasal biopsies taken from vanadium-exposed workers: a retrospective case control study by the peroxidase-antiperoxidase (PAP) method. *Anat. Anz.* 149: 446-450.
- Kjellstrom, T.; Evrin, P.-E.; Rahnster, B. (1977) Dose-response analysis of cadmium-induced tubular proteinuria: a study of urinary  $\beta_2$ -microglobulin excretion among workers in a battery factory. *Environ. Res.* 13: 303-317.
- Kleinman, M. T.; Bhalla, D. K.; Mautz, W. J.; Phalen, R. F. (1995) Cellular and immunologic injury with PM-10 inhalation. In: Phalen, R. F.; Bates, D. V., eds. Proceedings of the colloquium on particulate air pollution and human mortality and morbidity, part II; January 1994; Irvine, CA. *Inhalation Toxicol.* 7: 589-602.
- Klonne, D. R.; Burns, J. M.; Halder, C. A.; Holdsworth, C. E.; Ulrich, C. E. (1987) Two-year inhalation toxicity study of petroleum coke in rats and monkeys. *Am. J. Ind. Med.* 11: 375-389.
- Knecht, E. A.; Moorman, W. J.; Clark, J. C.; Lynch, D. W.; Lewis, T. R. (1985) Pulmonary effects of acute vanadium pentoxide inhalation in monkeys. *Am. Rev. Respir. Dis.* 132: 1181-1185.
- Kobayashi, T.; Shinozaki, Y. (1993) Effects of exposure to sulfuric acid-aerosol on airway responsiveness in guinea pigs: concentration and time dependency. *J. Toxicol. Environ. Health* 39: 261-272.
- Koenig, J. Q.; Pierson, W. E.; Horike, M. (1983) The effects of inhaled sulfuric acid on pulmonary function in adolescent asthmatics. *Am. Rev. Respir. Dis.* 128: 221-225.
- Koenig, J. Q.; Covert, D. S.; Pierson, W. E. (1989) Effects of inhalation of acidic compounds on pulmonary function in allergic adolescent subjects. In: Symposium on the health effects of

- acid aerosols; October 1987; Research Triangle Park, NC. *Environ. Health Perspect.* 79: 173-178.
- Koenig, J. Q.; Covert, D. S.; Larson, T. V.; Pierson, W. E. (1992) The effect of duration of exposure on sulfuric acid-induced pulmonary function changes in asthmatic adolescent subjects: a dose-response study. *Toxicol. Ind. Health* 8: 285-296.
- Koenig, J. Q.; Dumler, K.; Rebolledo, V.; Williams, P. V.; Pierson, W. E. (1993) Respiratory effects of inhaled sulfuric acid on senior asthmatics and nonasthmatics. *Arch. Environ. Health* 48: 171-175.
- Koenig, J. Q.; Covert, D. S.; Pierson, W. E.; Hanley, Q. S.; Rebolledo, V.; Dumler, K.; McKinney, S. E. (1994) Oxidant and acid aerosol exposure in healthy subjects and subjects with asthma. Part I: effects of oxidants, combined with sulfuric or nitric acid, on the pulmonary function of adolescents with asthma. Cambridge, MA: Health Effects Institute; pp. 1-36; research report no. 70.
- Kreyling, W. G.; Ferron, G. A.; Fürst, G.; Heilmann, P.; Neuner, M.; Ruprecht, L.; Schumann, G.; Takenaka, S.; Heyder, J. (1992) Early response of the canine respiratory tract following long-term exposure to a sulfur(IV) aerosol at low concentration. III. Macrophage-mediated long-term particle clearance. *Inhalation Toxicol.* 4: 197-233.
- Krzystyniak, K.; Fournier, M.; Trottier, B.; Nadeau, D.; Chevalier, G. (1987) Immunosuppression in mice after inhalation of cadmium aerosol. *Toxicol. Lett.* 38: 1-12.
- Kuhn, D. C.; Stanley, C. F.; El-Ayouby, N.; Demers, L. M. (1990) Effect of in vivo coal dust exposure on arachidonic acid metabolism in the rat alveolar macrophage. *J. Toxicol. Environ. Health* 29: 157-168.
- Kulle, T. J.; Sauder, L. R.; Hebel, J. R.; Miller, W. R.; Green, D. J.; Shanty, F. (1986) Pulmonary effects of sulfur dioxide and respirable carbon aerosol. *Environ. Res.* 41: 239-250.
- Kunst, A. E.; Looman, C. W. N.; Mackenbach, J. P. (1993) Outdoor air temperature and mortality in the Netherlands: a time-series analysis. *Am. J. Epidemiol.* 137: 331-341.
- Kutzman, R. S. (1984) A study of Fischer-344 rats exposed to silica dust at concentrations of 0, 2, 10 or 20 mg/m<sup>3</sup>, then maintained for six months prior to assessment. Upton, NY: Brookhaven National Laboratory; report no. BNL-35735.
- Kutzman, R. S.; Drew, R. T.; Shiotsuka, R. N.; Cockrell, B. Y. (1986) Pulmonary changes resulting from subchronic exposure to cadmium chloride aerosol. *J. Toxicol. Environ. Health* 17: 175-189.
- Lacey, J.; Dutkiewicz, J. (1994) Bioaerosols and occupational lung disease. *J. Aerosol. Sci.* 25: 1371-1404.
- Lagerkvist, B.; Linderholm, H.; Nordberg, G. F. (1986) Vasospastic tendency and Raynaud's phenomenon in smelter workers exposed to arsenic. *Environ. Res.* 39: 465-474.
- Lakatta, E. G. (1993) Cardiovascular regulatory mechanisms in advanced age. *Physiol. Rev.* 73: 413-467.
- Lam, H. F.; Conner, M. W.; Rogers, A. E.; Fitzgerald, S.; Amdur, M. O. (1985) Functional and morphologic changes in the lungs of guinea pigs exposed to freshly generated ultrafine zinc oxide. *Toxicol. Appl. Pharmacol.* 78: 29-38.
- Last, J. A.; Cross, C. E. (1978) A new model for health effects of air pollutants: evidence for synergistic effects of mixtures of ozone and sulfuric acid aerosols on rat lungs. *J. Lab. Clin. Med.* 91: 328-339.

- Last, J. A.; Gerriets, J. E.; Hyde, D. M. (1983) Synergistic effects on rat lungs of mixtures of oxidant air pollutants (ozone or nitrogen dioxide) and respirable aerosols. *Am. Rev. Respir. Dis.* 128: 539-544.
- Last, J. A.; Hyde, D. M.; Chang, D. P. Y. (1984) A mechanism of synergistic lung damage by ozone and a respirable aerosol. *Exp. Lung Res.* 7: 223-235.
- Last, J. A.; Hyde, D. M.; Guth, D. J.; Warren, D. L. (1986) Synergistic interaction of ozone and respirable aerosols on rat lungs. I. Importance of aerosol acidity. *Toxicology* 39: 247-257.
- Laube, B. L.; Bowes, S. M., III; Links, J. M.; Thomas, K. K.; Frank, R. (1993) Acute exposure to acid fog: effects on mucociliary clearance. *Am. Rev. Respir. Dis.* 147: 1105-1111.
- Lee, K. P.; Gillies, P. J. (1986) Pulmonary response and intrapulmonary lipids in rats exposed to bismuth orthovanadate dust by inhalation. *Environ. Res.* 40: 115-135.
- Lee, K. P.; Seidel, W. C. (1991a) Pulmonary response of rats exposed to polytetrafluoroethylene and tetrafluoroethylene hexafluoropropylene copolymer fume and isolated particles. *Inhalation Toxicol.* 3: 237-264.
- Lee, K. P.; Seidel, W. C. (1991b) Pulmonary response to perfluoropolymer fume and particles generated under various exposure conditions. *Fundam. Appl. Toxicol.* 17: 254-269.
- Lee, K. P.; Zapp, J. A., Jr.; Sarver, J. W. (1976) Ultrastructural alterations of rat lung exposed to pyrolysis products of polytetrafluoroethylene (PTFE, Teflon). *Lab. Invest.* 35: 152-160.
- Lee, K. P.; Trochimowicz, H. J.; Reinhardt, C. F. (1985) Pulmonary response of rats exposed to titanium dioxide (TiO<sub>2</sub>) by inhalation for two years. *Toxicol. Appl. Pharmacol.* 79: 179-192.
- Lee, K. P.; Henry, N. W., III; Trochimowicz, H. J.; Reinhardt, C. F. (1986) Pulmonary response to impaired lung clearance in rats following excessive TiO<sub>2</sub> dust deposition. *Environ. Res.* 41: 144-167.
- Lehnert, B. E.; Morrow, P. E (1985) Characteristics of alveolar macrophages following the deposition of a low burden of iron oxide in the lung. *J. Toxicol. Environ. Health* 16: 855-868.
- Lehnert, B. E.; Archuleta, D.; Behr, M. J.; Stavert, D. M. (1993) Lung injury after acute inhalation of perfluoroisobutylene: exposure concentration-response relationships. *Inhalation Toxicol.* 5: 1-32.
- Leikauf, G.; Yeates, D. B.; Wales, K. A.; Spektor, D.; Albert, R. E.; Lippmann, M. (1981) Effects of sulfuric acid aerosol on respiratory mechanics and mucociliary particle clearance in healthy nonsmoking adults. *Am. Ind. Hyg. Assoc. J.* 42: 273-282.
- Leikauf, G. D.; Spektor, D. M.; Albert, R. E.; Lippmann, M. (1984) Dose-dependent effects of submicrometer sulfuric acid aerosol on particle clearance from ciliated human lung airways. *Am. Ind. Hyg. Assoc. J.* 45: 285-292.
- Levy, B. S.; Hoffman, L.; Gottsegen, S. (1984) Boilermakers' bronchitis: respiratory tract irritation associated with vanadium pentoxide exposure during oil-to-coal conversion of a power plant. *J. Occup. Med.* 26: 567-570.
- Lew, F. T.; Yukiyaama, Y.; Waks, H. S.; Osler, A. G. (1975) Activation of the alternative (properdin) pathway by divalent cations. *J. Immunol.* 155: 884-888.
- Lewis, C. E. (1959) The biological effects of vanadium: II. the signs and symptoms of occupational vanadium exposure. *AMA Arch. Ind. Health* 19: 497-503.

- Lewis, T. R.; Moorman, W. J.; Ludmann, W. F.; Campbell, K. I. (1973) Toxicity of long-term exposure to oxides of sulfur. *Arch. Environ. Health* 26: 16-21.
- Lewis, T. R.; Green, F. H. Y.; Moorman, W. J.; Burg, J. R.; Lynch, D. W. (1989) A chronic inhalation toxicity study of diesel engine emissions and coal dust, alone and combined. *J. Am. Coll. Toxicol.* 8: 345-375.
- Lewkowski, J. P.; Malanchuk, M.; Hastings, L.; Vinegar, A.; Cooper, G. P. (1979) Effects of chronic exposure of rats to automobile exhaust, H<sub>2</sub>SO<sub>4</sub>, SO<sub>2</sub>, Al<sub>2</sub>(SO<sub>4</sub>)<sub>3</sub> and CO. In: Lee, S. D.; Mudd, J. B., eds. *Assessing toxic effects of environmental pollutants*. Ann Arbor, MI: Ann Arbor Science Publishers Inc.; pp. 187-217.
- Lewtas, J. (1982) Mutagenic activity of diesel emissions. In: Lewtas, J., ed. *Toxicological effects of emissions from diesel engines: proceedings of the Environmental Protection Agency 1981 diesel emissions symposium; October 1981; Raleigh, NC*. New York, NY: Elsevier Biomedical; pp. 243-264. (*Developments in toxicology and environmental science: v. 10*).
- Lighthart, B.; Stetzenbach, L. D. (1994) Distribution of microbial bioaerosol. In: Lighthart, B.; Mohr, A. J., eds. *Atmospheric microbial aerosols: theory and applications*. New York, NY: Chapman & Hall; pp. 68-98.
- Lindenschmidt, R. C.; Driscoll, K. E.; Perkins, M. A.; Higgins, J. M.; Maurer, J. K.; Belfiore, K. A. (1990) The comparison of a fibrogenic and two nonfibrogenic dusts by bronchoalveolar lavage. *Toxicol. Appl. Pharmacol.* 102: 268-281.
- Linn, W. S.; Kleinman, M. T.; Bailey, R. M.; Medway, D. A.; Spier, C. E.; Whynot, J. D.; Anderson, K. R.; Hackney, J. D. (1981) Human respiratory responses to an aerosol containing zinc ammonium sulfate. *Environ. Res.* 25: 404-414.
- Linn, W. S.; Avol, E. L.; Anderson, K. R.; Shamoo, D. A.; Peng, R.-C.; Hackney, J. D. (1989) Effect of droplet size on respiratory responses to inhaled sulfuric acid in normal and asthmatic volunteers. *Am. Rev. Respir. Dis.* 140: 161-166.
- Linn, W. S.; Shamoo, D. A.; Anderson, K. R.; Peng, R.-C.; Avol, E. L.; Hackney, J. D. (1994) Effects of prolonged, repeated exposure to ozone, sulfuric acid, and their combination in healthy and asthmatic volunteers. *Am. J. Respir. Crit. Care Med.* 150: 431-440.
- Linnell, R. H.; Scott, W. E. (1962) Diesel exhaust composition and odor studies. *J. Air Pollut. Control Assoc.* 12: 510-515, 545.
- Logan, W. P. D. (1953) Mortality in the London fog incident, 1952. *Lancet* (Feb. 14): 336-339.
- Loscutoff, S. M.; Cannon, W. C.; Buschbom, R. L.; Busch, R. H.; Killand, B. W. (1985) Pulmonary function in elastase-treated guinea pigs and rats exposed to ammonium sulfate or ammonium nitrate aerosols. *Environ. Res.* 36: 170-180.
- MacFarland, H. N.; Coate, W. B.; Disbennett, D. B.; Ackerman, L. J. (1982) Long-term inhalation studies with raw and processed shale dusts. In: Walton, W. H., ed. *Inhaled particles V: proceedings of an international symposium organized by the British Occupational Society; September 1980; Cardiff, Wales*. *Ann. Occup. Hyg.* 26: 213-225.
- Mackay, T. W.; Wathen, C. G.; Sudlow, M. F.; Elton, R. A.; Caulton, E. (1992) Factors affecting asthma mortality in Scotland. *Scott. Med. J.* 37: 5-7.
- Madelin, T. M. (1994) Fungal aerosols: a review. *J. Aerosol Sci.* 25: 1405-1412.
- Maier, K.; Beck-Speier, I.; Dayal, N.; Heilmann, P.; Hinze, H.; Lenz, A.-G.; Leuschel, L.; Matejkova, E.; Miaskowski, U.; Heyder, J.; Ruprecht, L. (1992) Early response of the canine respiratory

tract following long-term exposure to a sulfur(IV) aerosol at low concentration. II. Biochemistry and cell biology of lung lavage fluid. *Inhalation Toxicol.* 4: 175-195.

- Mannix, R. C.; Phalen, R. F.; Kenoyer, J. L.; Crocker, T. T. (1982) Effect of sulfur dioxide-sulfate exposure on rat respiratory tract clearance. *Am. Ind. Hyg. Assoc. J.* 43: 679-685.
- Marquart, H.; Smid, T.; Heederik, D.; Visschers, M. (1989) Lung function of welders of zinc-coated mild steel: cross-sectional analysis and changes over five consecutive work shifts. *Am. J. Ind. Med.* 16: 289-296.
- Martin, J. C.; Daniel, H.; Le Bouffant, L. (1977) Short- and long-term experimental study of the toxicity of coal mine dust and some of its constituents. In: Walton, W. H., ed. *Inhaled particles IV, part 1: proceedings of an international symposium; September 1975; Edinburgh, United Kingdom.* Oxford, United Kingdom: Pergamon Press; pp. 361-371.
- Mason, H. J.; Davison, A. G.; Wright, A. L.; Guthrie, C. J. G.; Fayers, P. M.; Venables, K. M.; Smith, N. J.; Chettle, D. R.; Franklin, D. M.; Scott, M. C.; Holden, H.; Gompertz, D.; Newman-Taylor, A. J. (1988) Relations between liver cadmium, cumulative exposure, and renal function in cadmium alloy workers. *Br. J. Ind. Med.* 45: 793-802.
- Matijak-Schaper, M.; Wong, K.-L.; Alarie, Y. (1983) A method to rapidly evaluate the acute pulmonary effects of aerosols in unanesthetized guinea pigs. *Toxicol. Appl. Pharmacol.* 69: 451-460.
- Matthias-Maser, S.; Jaenicke, R. (1994) Examination of atmospheric bioaerosol particles with radii > 0.2  $\mu\text{m}$ . *J. Aerosol Sci.* 25: 1605-1613.
- Mauderly, J. L. (1989) Susceptibility of young and aging lungs to inhaled pollutants. In: Utell, M. J.; Frank, R., eds. *Susceptibility to inhaled pollutants: [papers presented at the conference]; October 1987; Williamsburg, VA. Philadelphia, PA: American Society for Testing and Materials; pp. 148-161. (ASTM special technical publication no. STP 1024).*
- Mauderly, J. L. (1993) Toxicological approaches to complex mixtures. *Environ. Health Perspect.* 101(suppl. 4): 155-165.
- Mauderly, J. L. (1994a) Noncancer pulmonary effects of chronic inhalation exposure of animals to solid particles. In: Mohr, U.; Dungworth, D. L.; Mauderly, J. L.; Oberdörster, G., eds. *Toxic and carcinogenic effects of solid particles in the respiratory tract: [proceedings of the 4th international inhalation symposium]; March 1993; Hannover, Germany. Washington, DC: International Life Sciences Institute Press; pp. 43-55.*
- Mauderly, J. L. (1994b) Contribution of inhalation bioassays to the assessment of human health risks from solid airborne particles. In: Mohr, U.; Dungworth, D. L.; Mauderly, J. L.; Oberdörster, G., eds. *Toxic and carcinogenic effects of solid particles in the respiratory tract: [proceedings of the 4th international inhalation symposium]; March 1993; Hannover, Germany. Washington, DC: International Life Sciences Institute Press; pp. 355-365.*
- Mauderly, J. L. (1994c) Toxicological and epidemiological evidence for health risks from inhaled engine emissions. In: *Symposium of risk assessment of urban air: emissions, exposure, risk identification, and risk quantitation; May-June 1992; Stockholm, Sweden. Environ. Health Perspect.* 102(suppl. 4): 165-171.
- Mauderly, J. L.; Benson, J. M.; Bice, D. E.; Henderson, R. F.; Jones, R. K.; McClellan, R. O.; Mokler, B. V.; Pickrell, J. A.; Redman, H. C.; Wolff, R. K. (1981) Observations on rodents exposed for 19 weeks to diluted diesel exhaust. In: *Inhalation Toxicology Research Institute annual report 1980-1981. Albuquerque, NM: Lovelace Biomedical and Environmental Research Institute; pp. 305-311; report no. LMF-91.*
- Mauderly, J. L.; Benson, J. M.; Bice, D. E.; Carpenter, R. L.; Evans, M. J.; Henderson, R. F.; Jones, R. K.; McClellan, R. O.; Pickrell, J. A.; Shami, S. G.; Wolff, R. K. (1984) Life-span study of

rodents inhaling diesel exhaust: effect on body weight and survival. Albuquerque, NM: Lovelace Biomedical and Environmental Research Institute; report no. LMF-113; pp. 287-291.

- Mauderly, J. L.; Bice, D. E.; Carpenter, R. L.; Hanson, R. L.; Henderson, R. F.; Jones, R. K.; McClellan, R. O.; Wolff, R. K. (1987a) Effects of 4-week inhalation exposure of rats to oil shale dust and diesel exhaust. In: Gray, R. H.; Chess, E. K.; Mellinger, P. J.; Riley, R. G.; Springer, D. L., eds. Health & environmental research on complex organic mixtures: twenty-fourth Hanford life sciences symposium; October 1985; Richland, WA. Richland, WA: Pacific Northwest Laboratory; pp. 421-432. (DOE symposium series 62). Available from: NTIS, Springfield, VA; CONF-851027.
- Mauderly, J. L.; Jones, R. K.; Griffith, W. C.; Henderson, R. F.; McClellan, R. O. (1987b) Diesel exhaust is a pulmonary carcinogen in rats exposed chronically by inhalation. *Fundam. Appl. Toxicol.* 9: 208-221.
- Mauderly, J. L.; Bice, D. E.; Carpenter, R. L.; Gillett, N. A.; Henderson, R. F.; Pickrell, J. A.; Wolff, R. K. (1987c) Effects of inhaled nitrogen dioxide and diesel exhaust on developing lung. Cambridge, MA: Health Effects Institute; research report no. 8.
- Mauderly, J. L.; Gillett, N. A.; Henderson, R. F.; Jones, R. K.; McClellan, R. O. (1988) Relationships of lung structural and functional changes to accumulation of diesel exhaust particles. In: Dodgson, J.; McCallum, R. I.; Bailey, M. R.; Fisher, D. R., eds. Inhaled particles VI: proceedings of an international symposium and workshop on lung dosimetry; September 1985; Cambridge, United Kingdom. *Ann. Occup. Hyg.* 32(suppl. 1): 659-669.
- Mauderly, J. L.; Bice, D. E.; Cheng, Y. S.; Gillett, N. A.; Griffith, W. C.; Henderson, R. F.; Pickrell, J. A.; Wolff, R. K. (1990) Influence of preexisting pulmonary emphysema on susceptibility of rats to diesel exhaust. *Am. Rev. Respir. Dis.* 141: 1333-1341.
- Mauderly, J. L.; Snipes, M. B.; Barr, E. B.; Belinsky, S. A.; Bond, J. A.; Brooks, A. L.; Chang, I.-Y.; Cheng, Y. S.; Gillett, N. A.; Griffith, W. C.; Henderson, R. F.; Mitchell, C. E.; Nikula, K. J.; Thomassen, D. G. (1994a) Pulmonary toxicity of inhaled diesel exhaust and carbon black in chronically exposed rats. Part I: neoplastic and nonneoplastic lung lesions. Cambridge, MA: Health Effects Institute; research report no. 68.
- Mauderly, J. L.; Barr, E. B.; Eidson, A. F.; Harkema, J. R.; Henderson, R. F.; Pickrell, J. A.; Wolff, R. K. (1994b) Pneumoconiosis in rats exposed chronically to oil shale dust and diesel exhaust, alone and in combination. In: Dodgson, J.; McCallum, R. I., eds. Inhaled particles VII: proceedings of an international symposium; September 1991; Edinburgh, United Kingdom. *Ann. Occup. Hyg.* 38(suppl 1): 403-409.
- McClellan, R. O.; Bice, D. E.; Cuddihy, R. G.; Gillett, N. A.; Henderson, R. F.; Jones, R. K.; Mauderly, J. L.; Pickrell, J. A.; Shami, S. G.; Wolff, R. K. (1986) Health effects of diesel exhaust. In: Lee, S. D.; Schneider, T.; Grant, L. D.; Verkerk, P. J., eds. Aerosols: research, risk assessment and control strategies: proceedings of the second U.S.-Dutch international symposium; May 1985; Williamsburg, VA. Chelsea, MI: Lewis Publishers, Inc.; pp. 597-615.
- Mentnech, M. S.; Lewis, D. M.; Olenchock, S. A.; Mull, J. C.; Koller, W. A.; Lewis, T. R. (1984) Effects of coal dust and diesel exhaust on immune competence in rats. *J. Toxicol. Environ. Health* 13: 31-41.
- Merchant, J. A.; Taylor, G.; Hodous, T. K. (1986) Coal workers' pneumoconiosis and exposure to other carbonaceous dusts. In: Merchant, J. A., ed. Occupational respiratory diseases. Washington, DC: U.S. Department of Health and Human Services, National Institute for Occupational Safety and Health; pp. 329-384; DHHS(NIOSH) publication no. 86-102.
- Minotti, G.; Aust, S. D. (1987) The role of iron in the initiation of lipid peroxidation. *Chem. Phys. Lipids* 44: 191-208.

- Molfino, N. A.; Slutsky, A. S.; Zamel, N. (1992) The effects of air pollution on allergic bronchial responsiveness. *Clin. Exp. Allergy* 22: 667-672.
- Moore, P. F.; Schwartz, L. W. (1981) Morphological effects of prolonged exposure to ozone and sulfuric acid aerosol on the rat lung. *Exp. Mol. Pathol.* 35: 108-123.
- Moorman, W. J.; Hornung, R. W.; Wagner, W. D. (1977) Ventilatory functions in germfree and conventional rats exposed to coal dusts. *Proc. Soc. Exp. Biol. Med.* 155: 424-428.
- Moorman, W. J.; Clark, J. C.; Pepelko, W. E.; Mattox, J. (1985) Pulmonary function responses in cats following long-term exposure to diesel exhaust. *J. Appl. Toxicol.* 5: 301-305.
- Morgan, W. K. C. (1978) Magnetite pneumoconiosis. *J. Occup. Med.* 20: 762-763.
- Morgan, A.; Moores, S. R.; Homes, A.; Evans, J. C.; Evans, N. H.; Black, A. (1980) The effect of quartz, administered by intratracheal instillation, on the rat lung. I. The cellular response. *Environ. Res.* 22: 1-12.
- Morrow, P. E. (1992) Dust overloading of the lungs: update and appraisal. *Toxicol. Appl. Pharmacol.* 113: 1-12.
- Morrow, P. E.; Utell, M. J.; Bauer, M. A.; Speers, D. M.; Gibb, F. R. (1994) Effects of near ambient levels of sulphuric acid aerosol on lung function in exercising subjects with asthma and chronic obstructive pulmonary disease. In: Dodgson, J.; McCallum, R. I., eds. *Inhaled particles VII: proceedings of an international symposium; September 1991; Edinburgh, United Kingdom.* *Ann. Occup. Hyg.* 38(suppl. 1): 933-938.
- Mossman, B. T.; Gee, J. B. L. (1989) Asbestos-related diseases. *N. Engl. J. Med.* 320: 1721-1730.
- Muhle, H.; Bellmann, B.; Heinrich, U. (1984) Effect of combustion products of fossil fuels on lung metabolism in inhalation experiments. In: Grosdanoff, P.; Baß, R.; Hackenberg, U.; Henschler, D.; Müller, D.; Klimisch, H.-J., eds. *Problems of inhalation toxicity studies.* München, Germany: MMV Medizin Verlag München; pp. 359-371. (bga-Schriften 5/1984).
- Muhle, H.; Takenaka, S.; Mohr, U.; Dasenbrock, C.; Mermelstein, R. (1989) Lung tumor induction upon long-term low-level inhalation of crystalline silica. *Am. J. Ind. Med.* 15: 343-346.
- Muhle, H.; Bellmann, B.; Creutzenberg, O.; Dasenbrock, C.; Ernst, H.; Kilpper, R.; MacKenzie, J. C.; Morrow, P.; Mohr, U.; Takenaka, S.; Mermelstein, R. (1991) Pulmonary response to toner upon chronic inhalation exposure in rats. *Fundam. Appl. Toxicol.* 17: 280-299.
- Musk, A. W.; Tees, J. G. (1982) Asthma caused by occupational exposure to vanadium compounds. *Med. J. Aust.* 1: 183-184.
- Musk, A. W.; de Klerk, N. H.; Cookson, W. O. C.; Morgan, W. K. C. (1988) Radiographic abnormalities and duration of employment in Western Australian iron-ore miners. *Med. J. Aust.* 148: 332-334.
- Nathanson, I.; Nadel, J. A. (1984) Movement of electrolytes and fluid across airways. *Lung* 162: 125-137.
- National Center for Health Statistics. (1993) Advance report of final mortality statistics, 1991. Hyattsville, MD: U.S. Department of Health and Human Services, Public Health Service, Centers for Disease Control and Prevention. (Monthly vital statistics report: v. 42, no. 2, suppl.).
- National Toxicology Program. (1993) NTP technical report on the toxicology and carcinogenesis studies of talc (CAS no. 14807-96-6) in F344/N rats and B6C3F<sub>1</sub> mice (inhalation studies).

- Naumann, B. D.; Schlesinger, R. B. (1986) Assessment of early alveolar particle clearance and macrophage function following an acute inhalation of sulfuric acid mist. *Exp. Lung Res.* 11: 13-33.
- Negishi, T. (1994) Accumulation of alveolar macrophages induced by inhalation exposure of coal fly ash in golden hamster lungs. *Exp. Anim.* 43: 61-78.
- Nikula, K. J.; Snipes, M. B.; Barr, E. B.; Griffith, W. C.; Henderson, R. F.; Mauderly, J. L. (1995) Comparative pulmonary toxicities and carcinogenicities of chronically inhaled diesel exhaust and carbon black in F344 rats. *Fundam. Appl. Toxicol.* 25: 80-94.
- Nolte, T.; Thiedemann, K.-U.; Dungworh, D. L.; Ernst, H.; Paulini, I.; Heinrich, U.; Dasenbrock, C.; Peters, L.; Ueberschär, S.; Mohr, U. (1994) Histological and ultrastructural alterations of the bronchoalveolar region in the rat lung after chronic exposure to a pyrolyzed pitch condensate or carbon black, alone and in combination. *Inhalation Toxicol.* 6: 459-483.
- Nuccitelli, R.; Deamer, D. W., eds. (1982) Intracellular pH: its measurement, regulation, and utilization in cellular functions: proceedings of a conference; July 1981; Santa Ynez Valley, CA. New York, NY: Alan R. Liss, Inc. (The Kroc Foundation series: v. 15).
- Nuttall, J. B.; Kelly, R. J.; Smith, B. S.; Whiteside, C. K., Jr. (1964) Inflight toxic reactions resulting from fluorocarbon resin pyrolysis. *Aerosp. Med.* 35: 676-683.
- Oberdörster, G. (1989a) Deposition and retention modeling of inhaled cadmium in rat and human lung: an example for extrapolation of effects and risk estimation. In: Crapo, J. D.; Miller, F. J.; Smolko, E. D.; Graham, J. A.; Hayes, A. W., eds. *Extrapolation of dosimetric relationships for inhaled particles and gases*. San Diego, CA: Academic Press, Inc.; pp. 345-370.
- Oberdörster, G. (1989b) Pulmonary toxicity and carcinogenicity of cadmium. *J. Am. Coll. Toxicol.* 8: 1251-1263.
- Oberdörster, G. (1995) Effects of ultrafine particles in the lung and potential relevance to environmental particles. In: *Proceedings of the Warsaw particle workshop; 1995; Warsaw, Poland*. Delft, The Netherlands: Delft University Press; accepted for publication.
- Oberdörster, G.; Ferin, J.; Gelein, R.; Soderholm, S. C.; Finkelstein, J. (1992) Role of the alveolar macrophage in lung injury: studies with ultrafine particles. *Environ. Health Perspect.* 97: 193-199.
- Oberdörster, G.; Cherian, M. G.; Baggs, R. B. (1994a) Correlation between cadmium-induced pulmonary carcinogenicity, metallothionein expression, and inflammatory processes: a species comparison. Presented at: Second international meeting on molecular mechanisms of metal toxicity and carcinogenicity; January 1993; Madonna di Campiglio, Italy. *Environ. Health Perspect.* 102(suppl. 3): 257-263.
- Oberdörster, G.; Ferin, J.; Lehnert, B. E. (1994b) Correlation between particle size, *in vivo* particle persistence, and lung injury. *Environ. Health Perspect.* 102(suppl. 5): 173-179.
- Oberdörster, G.; Gelein, R. M.; Ferin, J.; Weiss, B. (1995a) Association of particulate air pollution and acute mortality: involvement of ultrafine particles? In: Phalen, R. F.; Bates, D. V., eds. *Proceedings of the colloquium on particulate air pollution and human mortality and morbidity; January 1994; Irvine, CA*. *Inhalation Toxicol.* 7: 111-124.
- Oberdörster, G.; Ferin, J.; Gelein, R.; Mercer, P.; Corson, N.; Godleski, J. (1995b) Low-level ambient air particulate levels and acute mortality/morbidity: studies with ultrafine Teflon™ particles. *Am. J. Respir. Crit. Care Med.* 151(suppl.): A66.

- O'Connor, G. T.; Sparrow, D.; Weiss, S. T. (1989) The role of allergy and nonspecific airway hyperresponsiveness in the pathogenesis of chronic obstructive pulmonary disease. *Am. Rev. Respir. Dis.* 140: 225-252.
- O'Hollaren, M. T.; Yunginger, J. W.; Offord, K. P.; Somers, M. J.; O'Connell, E. J.; Ballard, D. J.; Sachs, M. I. (1991) Exposure to an aeroallergen as a possible precipitating factor in respiratory arrest in young patients with asthma. *N. Engl. J. Med.* 324: 359-363.
- Okuhata, Y.; Xia, T.; Urahashi, S. (1994) Inhalation MR lymphography: a new method for selective enhancement of the lung hilar and mediastinal lymph nodes. *Magn. Reson. Imaging* 12: 1135-1138.
- Orris, P.; Cone, J.; McQuilkin, S. (1983) Health hazard evaluation report HETA 80-096-1359, Eureka Company, Bloomington, Illinois. Cincinnati, OH: U.S. Department of Health and Human Services, National Institute for Occupational Safety and Health; report no. 80-096. Available from: NTIS, Springfield, VA; PB85-163574.
- Osebold, J. W.; Gershwin, L. J.; Zee, Y. C. (1980) Studies on the enhancement of allergic lung sensitization by inhalation of ozone and sulfuric acid aerosol. *J. Environ. Pathol. Toxicol.* 3: 221-234.
- Pattle, R. E.; Burgess, F.; Cullumbine, H. (1956) The effects of a cold environment and of ammonia on the toxicity of sulphuric acid mist to guinea-pigs. *J. Pathol. Bacteriol.* 72: 219-232.
- Pazynich, V. M. (1966) Maximum permissible concentration of vanadium pentoxide in the atmosphere. *Hyg. Sanit. (USSR)* 31(7-9): 6-12.
- Pennington, J. E., ed. (1989) *Respiratory infections: diagnosis and management*. 2nd ed. New York, NY: Raven Press.
- Pepelko, W. E. (1982a) Effects of 28 days exposure to diesel engine emissions in rats. *Environ. Res.* 27: 16-23.
- Pepelko, W. E. (1982b) EPA studies on the toxicological effects of inhaled diesel engine emissions. In: Lewtas, J., ed. *Toxicological effects of emissions from diesel engines: proceedings of the Environmental Protection Agency diesel emissions symposium; October 1981; Raleigh, NC*. New York, NY: Elsevier Biomedical; pp. 121-142. (Developments in toxicology and environmental science: v. 10).
- Pepelko, W. E.; Peirano, W. B. (1983) Health effects of exposure to diesel engine emissions: a summary of animal studies conducted by the U.S. Environmental Protection Agency's Health Effects Research Laboratories at Cincinnati, Ohio. *J. Am. Coll. Toxicol.* 2: 253-306.
- Pepelko, W. E.; Mattox, J. K.; Cohen, A. L. (1980a) Toxicology of ammonium sulfate in the lung. *Bull. Environ. Contam. Toxicol.* 24: 156-160.
- Pepelko, W. E.; Danner, R. M.; Clarke, N. A., eds. (1980b) *Health effects of diesel engine emissions: proceedings of an international symposium, v. 1; December 1979; Cincinnati, OH*. Cincinnati, OH: U.S. Environmental Protection Agency, Health Effects Research Laboratory; EPA report no. EPA-600/9-80-057a. Available from: NTIS, Springfield, VA; PB81-173809.
- Pepelko, W. E.; Danner, R. M.; Clarke, N. A., eds. (1980c) *Health effects of diesel engine emissions: proceedings of an international symposium, v. 2; December 1979; Cincinnati, OH*. Cincinnati, OH: U.S. Environmental Protection Agency, Health Effects Research Laboratory; EPA report no. EPA-600/9-80-057b. Available from: NTIS, Springfield, VA; PB81-173817.
- Pepelko, W. E.; Mattox, J. K.; Yang, Y. Y.; Moore, W., Jr. (1980d) Pulmonary function and pathology in cats exposed 28 days to diesel exhaust. *J. Environ. Pathol. Toxicol.* 4: 449-458.

- Pepelko, W. E.; Mattox, J.; Moorman, W. J.; Clark, J. C. (1980e) Pulmonary function evaluation of cats after one year of exposure to diesel exhaust. In: Pepelko, W. E.; Danner, R. M.; Clarke, N. A., eds. Health effects of diesel engine emissions: proceedings of an international symposium, v. 2; December 1979; Cincinnati, OH. Cincinnati, OH: U.S. Environmental Protection Agency, Health Effects Research Laboratory; pp. 757-765; EPA report no. EPA-600/9-80-057b. Available from: NTIS, Springfield, VA; PB81-173817.
- Pepelko, W. E.; Mattox, J.; Moorman, W. J.; Clark, J. C. (1981) Pulmonary function evaluation of cats after one year of exposure to diesel exhaust. *Environ. Int.* 5: 373-376.
- Petty, T. L.; Silvers, G. W.; Stanford, R. E. (1983) The morphology and morphometry of small airways disease (relevance to chronic obstructive pulmonary disease). *Trans. Clin. Climatol. Assoc.* 94: 130-140.
- Phalen, R. F.; Kenoyer, J. L.; Crocker, T. T.; McClure, T. R. (1980) Effects of sulfate aerosols in combination with ozone on elimination of tracer particles inhaled by rats. *J. Toxicol. Environ. Health* 6: 797-810.
- Pinto, S. S.; McGill, C. M. (1953) Arsenic trioxide exposure in industry. Presented at: the 38th annual meeting of the Industrial Medical Association; April; Los Angeles, CA. *Ind. Med. Surg.* 22: 281-287.
- Pinto, M.; Birnbaum, S. C.; Kadar, T.; Goldberg, G. M. (1979) Lung injury in mice induced by factors acting synergistically with inhaled particulate antigen. *Clin. Immunol. Immunopathol.* 13: 361-368.
- Plamenac, P.; Nikulin, A.; Pikula, B. (1974) Cytologic changes of the respiratory epithelium in iron foundry workers. *Acta Cytol.* 18: 34-40.
- Plopper, C. G.; Hyde, D. M.; Weir, A. J. (1983) Centriacinar alterations in lungs of cats chronically exposed to diesel exhaust. *Lab. Invest.* 49: 391-399.
- Pope, A. M.; Patterson, R.; Burge, H. (1993) Indoor allergens: assessing and controlling adverse health effects. Washington, DC: National Academy Press.
- Pope, C. A., III; Thun, M. J.; Namboodiri, M. M.; Dockery, D. W.; Evans, J. S.; Speizer, F. E.; Heath, C. W., Jr. (1995) Particulate air pollution as a predictor of mortality in a prospective study of U.S. adults. *Am. J. Respir. Crit. Care Med.* 151: 669-674.
- Port, C. D.; Henry, M. C.; Kaufman, D. G.; Harris, C. C.; Ketels, K. V. (1973) Acute changes in the surface morphology of hamster tracheobronchial epithelium following benzo(a)pyrene and ferric oxide administration. *Cancer Res.* 33: 2498-2501.
- Pott, F.; Dungworth, D. L.; Heinrich, U.; Muhle, H.; Kamino, K.; Germann, P.-G.; Roller, M.; Rippe, R. M.; Mohr, U. (1994) Lung tumours in rats after intratracheal instillation of dusts. In: Dodgson, J.; McCallum, R. I., eds. Inhaled particles VII: proceedings of an international symposium; September 1991; Edinburgh, United Kingdom. *Ann. Occup. Hyg.* 38(suppl. 1): 357-363.
- Prasad, S. B.; Rao, V. S.; Mannix, R. C.; Phalen, R. F. (1988) Effects of pollutant atmospheres on surface receptors of pulmonary macrophages. *J. Toxicol. Environ. Health* 24: 385-402.
- Prasad, S. B.; Rao, V. S.; McClure, T. R.; Mannix, R. C.; Phalen, R. F. (1990) Toxic effects of short-term exposures to acids and diesel exhaust. *J. Aerosol Med.* 3: 147-163.
- Pratt, P. C. (1983) Lung dust content and response in guinea pigs inhaling three forms of silica. *Arch. Environ. Health* 38: 197-204.
- Preziosi, P.; Ciabattini, G. (1987) Acid rain: effects on arachidonic acid metabolism in perfused and ventilated guinea-pig lung. *Toxicol. Lett.* 39: 101-108.

- Pritchard, R. J.; Ghio, A. J.; Lehmann, J. R.; Winsett, D. W.; Tepper, J. S.; Park, P.; Gilmour, I.; Dreher, K. L.; Costa, D. L. (1995) Oxidant generation and lung injury after particulate air pollutant exposure increase with the concentrations of associated metals. *Inhalation Toxicol.*: in press.
- Purdham, J. T.; Holness, D. L.; Pilger, C. W. (1987) Environmental and medical assessment of stevedores employed in ferry operations. *Appl. Ind. Hyg.* 2: 133-139.
- Qu, Q.-S.; Chen, L. C.; Gordon, T.; Amdur, M.; Fine, J. M. (1993) Alteration of pulmonary macrophage intracellular pH regulation by sulfuric acid aerosol exposures. *Toxicol. Appl. Pharmacol.* 121: 138-143.
- Raabe, O. G.; Wilson, D. W.; Al-Bayati, M. A.; Hornof, W. J.; Rosenblatt, L. S. (1994) Biological effects of inhaled pollutant aerosols. In: Dodgson, J.; McCallum, R. I., eds. *Inhaled particles VII: proceedings of an international symposium; September 1991; Edinburgh, United Kingdom.* *Ann. Occup. Hyg.* 38(suppl. 1): 323-330.
- Raub, J. A.; Hatch, G. E.; Mercer, R. R.; Grady, M.; Hu, P.-C. (1985) Inhalation studies of Mt. St. Helens volcanic ash in animals: II. lung function, biochemistry, and histology. *Environ. Res.* 37: 72-83.
- Reger, R. (1979) Ventilatory function changes over a work shift for coal miners exposed to diesel emissions. In: Bridbord, K.; French, J., eds. *Toxicological and carcinogenic health hazards in the workplace: proceedings of the first annual NIOSH scientific symposium; 1978; Cincinnati, OH. Park Forest South, IL: Pathotox Publishers, Inc.,; pp. 346-347.*
- Reger, R.; Hancock, J.; Hankinson, J.; Hearl, F.; Merchant, J. (1982) Coal miners exposed to diesel exhaust emissions. *Ann. Occup. Hyg.* 26: 799-815.
- Reiser, K. M.; Last, J. A. (1986) Early cellular events in pulmonary fibrosis. *Exp. Lung Res.* 10: 331-355.
- Research Committee for HERP Studies. (1988) *Diesel exhaust and health risks: results of the HERP studies.* Tsukuba, Ibaraki, Japan: Japan Automobile Research Institute, Inc.
- Rippon, J. W. (1988) *Medical mycology: the pathogenic fungi and the pathogenic actinomycetes.* 3rd ed. Philadelphia, PA: W. B. Saunders Company.
- Rom, W. M.; Travis, W. D.; Brody, A. R. (1991) Cellular and molecular basis of the asbestos-related diseases. *Am. Rev. Respir. Dis.* 143: 408-422.
- Rose, C. S. (1992) Inhalation fevers. In: *Occupational lung diseases.* pp. 373-380.
- Roshchin, I. V. (1964) Metallurgiya vanadiya v svete gigiyeny truda i voprosy profilaktiki professionalnykh zabolevaniy i intoksikatsiy. [Vanadium metallurgy in the light of industrial hygiene and questions concerned with the prevention of occupational diseases and intoxication]. *Gig. Tr. Prof. Zabol.* 8: 3-10.
- Roshchin, I. V. (1967a) Vanadium. In: Izrael'son, Z. I., ed. *Toxicology of the rare metals.* Jerusalem, Israel: Israel Program for Scientific Translations; pp. 52-60.
- Roshchin, I. V. (1967b) Toxicology of vanadium compounds used in modern industry. *Gig. Sanit.* 32(6): 26-32.
- Roth, C.; Scheuch, G.; Stahlhofen, W. (1994) Clearance measurements with radioactively labelled ultrafine particles. In: Dodgson, J.; McCallum, R. I., eds. *Inhaled particles VII: proceedings of an international symposium; September 1991; Edinburgh, United Kingdom.* *Ann. Occup. Hyg.* 38(suppl. 1): 101-106.

- Rothenberg, S. J.; Nagy, P. A.; Pickrell, J. A.; Hobbs, C. H. (1989) Surface area, adsorption, and desorption studies on indoor dust samples. *Am. Ind. Hyg. Assoc. J.* 50: 15-23.
- Rudell, B.; Marqvardsen, O.; Lindström, K.; Kolmodin-Hedman, B. (1989) A method for controlled exposure to diesel exhaust from a continuously idling diesel engine. *J. Aerosol Sci.* 20: 1281-1284.
- Rudell, B.; Sandström, T.; Stjernberg, N.; Kolmodin-Hedman, B. (1990) Controlled diesel exhaust exposure in an exposure chamber: pulmonary effects investigated with bronchoalveolar lavage. *J. Aerosol Sci.* 21(suppl. 1): S411-S414
- Rudell, B.; Sandström, T.; Hammarström, U.; Ledin, M.-L.; Hörstedt, P.; Stjernberg, N. (1994) Evaluation of an exposure setup for studying effects of diesel exhaust in humans. *Int. Arch. Occup. Environ. Health* 66: 77-83.
- Sackner, M. A.; Dougherty, R. D.; Chapman, G. A.; Zarzecki, S.; Zarzemski, L.; Schreck, R. (1979) Effects of sodium nitrate aerosol on cardiopulmonary function of dogs, sheep, and man. *Environ. Res.* 18: 421-436.
- Sackner, M. A.; Dougherty, R. L.; Chapman, G. A.; Ciplej, J.; Perez, D.; Kwoka, M.; Reinhart, M.; Brito, M.; Schreck, R. (1981) Effects of brief and intermediate exposures to sulfate submicron aerosols and sulfate injections on cardiopulmonary function of dogs and tracheal mucous velocity of sheep. *J. Toxicol. Environ. Health* 7: 951-972.
- Saffiotti, U. (1992) Lung cancer induction by crystalline silica. In: D'Amato, R.; Slaga, T. J.; Farland, W. H.; Henry, C., eds. *Relevance of animal studies to the evaluation of human cancer risk: proceedings of a symposium; December 1990; Austin, TX.* New York, NY: Wiley-Liss; pp. 51-69. (Progress in clinical and biological research: v. 374).
- Saffiotti, U.; Daniel, L. H.; Mao, Y.; Williams, A. O.; Kaighn, M. E.; Ahmed, N.; Knapton, A. D. (1993) Biological studies on the carcinogenic effects of quartz. In: Guthrie, G. D.; Mossman, B. T., eds. *Health effects of mineral dusts.* *Rev. Mineral.* 28: 523-544.
- Salem, H.; Gardner, D. E. (1994) Health aspects of bioaerosols. In: Lighthart, B.; Mohr, A. J., eds. *Atmospheric microbial aerosols: theory and applications.* New York, NY: Chapman & Hall; pp. 304-330.
- Sanders, C. L.; Conklin, A. W.; Gelman, R. A.; Adey, R. R.; Rhoads, K. (1982) Pulmonary toxicity of Mount St. Helens volcanic ash. *Environ. Res.* 27: 118-135.
- Schaper, M.; Alarie, Y. (1985) The effects of aerosols of carbamylcholine, serotonin and propranolol on the ventilatory response to CO<sub>2</sub> in guinea pigs and comparison with the effects of histamine and sulfuric acid. *Acta Pharmacol. Toxicol.* 56: 244-249.
- Schaper, M.; Kegerize, J.; Alarie, Y. (1984) Evaluation of concentration-response relationships for histamine and sulfuric acid aerosols in unanesthetized guinea pigs for their effects on ventilatory response to CO<sub>2</sub>. *Toxicol. Appl. Pharmacol.* 73: 533-542.
- Scheel, L. D.; McMillan, L.; Phipps, F. C. (1968) Biochemical changes associated with toxic exposures to polytetrafluoroethylene pyrolysis products. *Am. Ind. Hyg. Assoc. J.* 29: 49-53.
- Schepers, G. W. H. (1981) Biological action of precipitation-process submicron amorphous silica (HI-SIL 233). In: Dunnom, D. D., ed. *Health effects of synthetic silica particulates: a symposium sponsored by ASTM Committee E-34 on Occupational Health and Safety and the Industrial Health Foundation; November 1979; Benalmadena-Costa (Torremolinos), Spain.* Philadelphia, PA: American Society for Testing and Materials; pp. 144-173; ASTM special technical publication 732.

- Schiff, L. J.; Bryne, M. M.; Fenters, J. D.; Graham, J. A.; Gardner, D. E. (1979) Cytotoxic effects of sulfuric acid mist, carbon particulates, and their mixtures on hamster tracheal epithelium. *Environ. Res.* 19: 339-354.
- Schlesinger, R. B. (1984) Comparative irritant potency of inhaled sulfate aerosols—effects on bronchial mucociliary clearance. *Environ. Res.* 34: 268-279.
- Schlesinger, R. B. (1985) Comparative deposition of inhaled aerosols in experimental animals and humans: a review. *J. Toxicol. Environ. Health* 15: 197-214.
- Schlesinger, R. B. (1987) Functional assessment of rabbit alveolar macrophages following intermittent inhalation exposures to sulfuric acid mist. *Fundam. Appl. Toxicol.* 8: 328-334.
- Schlesinger, R. B.; Chen, L. C. (1994) Comparative biological potency of acidic sulfate aerosols: implications for the interpretation of laboratory and field studies. *Environ. Res.* 65: 69-85.
- Schlesinger, R. B.; Gearhart, J. M. (1986) Early alveolar clearance in rabbits intermittently exposed to sulfuric acid mist. *J. Toxicol. Environ. Health* 17: 213-220.
- Schlesinger, R. B.; Gearhart, J. M. (1987) Intermittent exposures to mixed atmospheres of nitrogen dioxide and sulfuric acid: effect on particle clearance from the respiratory region of rabbit lungs. *Toxicology* 44: 309-319.
- Schlesinger, R. B.; Lippmann, M.; Albert, R. E. (1978) Effects of short-term exposures to sulfuric acid and ammonium sulfate aerosols upon bronchial airway function in the donkey. *Am. Ind. Hyg. Assoc. J.* 39: 275-286.
- Schlesinger, R. B.; Naumann, B. D.; Chen, L. C. (1983) Physiological and histological alterations in the bronchial mucociliary clearance system of rabbits following intermittent oral or nasal inhalation of sulfuric acid mist. *J. Toxicol. Environ. Health* 12: 441-465.
- Schlesinger, R. B.; Chen, L.-C.; Driscoll, K. E. (1984) Exposure-response relationship of bronchial mucociliary clearance in rabbits following acute inhalations of sulfuric acid mist. *Toxicol. Lett.* 22: 249-254.
- Schlesinger, R. B.; Chen, L. C.; Finkelstein, I.; Zelikoff, J. T. (1990a) Comparative potency of inhaled acidic sulfates: speciation and the role of hydrogen ion. *Environ. Res.* 52: 210-224.
- Schlesinger, R. B.; Gunnison, A. F.; Zelikoff, J. T. (1990b) Modulation of pulmonary eicosanoid metabolism following exposure to sulfuric acid. *Fundam. Appl. Toxicol.* 15: 151-162.
- Schlesinger, R. B.; Fine, J. M.; Chen, L. C. (1992a) Interspecies differences in the phagocytic activity of pulmonary macrophages subjected to acidic challenge. *Fundam. Appl. Toxicol.* 19: 584-589.
- Schlesinger, R. B.; Gorczynski, J. E.; Dennison, J.; Richards, L.; Kinney, P. L.; Bosland, M. C. (1992b) Long-term intermittent exposure to sulfuric acid aerosol, ozone and their combination: alterations in tracheobronchial mucociliary clearance and epithelial secretory cells. *Exp. Lung Res.* 18: 505-534.
- Schreck, R. M.; Soderholm, S. C.; Chan, T. L.; Smiler, K. L.; D'Arcy, J. B. (1981) Experimental conditions in GMR chronic inhalation studies of diesel exhaust. *J. Appl. Toxicol.* 1: 67-76.
- Schreider, J. P.; Culbertson, M. R.; Raabe, O. G. (1985) Comparative pulmonary fibrogenic potential of selected particles. *Environ. Res.* 38: 256-274.
- Schuler, P.; Maturana, V.; Cruz, E.; Guijon, C.; Vasquez, A.; Valenzuela, A.; Silva, R. (1962) Arc welder's pulmonary siderosis. *J. Occup. Med.* 4: 353-358.

- Schulz, H.; Eder, G.; Heilmann, P.; Ruprecht, L.; Schumann, G.; Takenaka, S.; Heyder, J. (1992) Early response of the canine respiratory tract following long-term exposure to a sulfur(IV) aerosol at low concentration. IV. Respiratory lung function. *Inhalation Toxicol.* 4: 235-246.
- Schwartz, L. W.; Moore, P. F.; Chang, D. P.; Tarkington, B. K.; Dungworth, D. L.; Tyler, W. S. (1977) Short-term effects of sulfuric acid aerosols on the respiratory tract. A morphological study in guinea pigs, mice, rats and monkeys. In: Lee, S. D., ed. *Biochemical effects of environmental pollutants*. Ann Arbor, MI: Ann Arbor Science Publishers Inc.; pp. 257-271.
- Schwartz, D. A.; Thorne, P. S.; Yagla, S. J.; Burmeister, L. F.; Olenchock, S. A.; Watt, J. L.; Quinn, T. J. (1995) The role of endotoxin in grain dust-induced lung disease. *Am. J. Respir. Crit. Care Med.* 152: 603-608.
- Seidel, W. C.; Scherer, K. V., Jr.; Cline, D., Jr.; Olson, A. H.; Bonesteel, J. K.; Church, D. F.; Nugehalli, S.; Pryor, W. A. (1991) Chemical, physical, and toxicological characterization of fumes produced by heating tetrafluoroethene homopolymer and its copolymers with hexafluoropropene and perfluoro(propyl vinyl ether). *Chem. Res. Toxicol.* 4: 229-236.
- Sentz, F. C., Jr.; Rakow, A. B. (1969) Exposure to iron oxide fume at arcair and powder-burning operations. *Am. Ind. Hyg. Assoc. J.* 30: 143-146.
- Shami, S. G.; Silbaugh, S. A.; Hahn, F. F.; Griffith, W. C.; Hobbs, C. H. (1984) Cytokinetic and morphological changes in the lungs and lung-associated lymph nodes of rats after inhalation of fly ash. *Environ. Res.* 35: 373-393.
- Shanbhag, A. S.; Jacobs, J. J.; Black, J.; Galante, J. O.; Glant, T. T. (1994) Macrophage/particle interactions: effect of size, composition and surface area. *J. Biomed. Mater. Res.* 28: 81-90.
- Sheffer, A. L., chairman. (1991) Guidelines for the diagnosis and management of asthma: National Heart, Lung, and Blood Institute National Asthma Education Program expert panel report. *J. Allergy Clin. Immunol.* 88(3, part 2).
- Sheridan, C. J.; Pflieger, R. C.; McClellan, R. O. (1978) Cytotoxicity of vanadium pentoxide on pulmonary alveolar macrophages from dog, rabbit, and rat: effect of viability and effect on lipid metabolism. *Ann. Respir. Inhalation Toxicol.* : 294-298.
- Silbaugh, S. A.; Mauderly, J. L.; Macken, C. A. (1981a) Effects of sulfuric acid and nitrogen dioxide on airway responsiveness of the guinea pig. *J. Toxicol. Environ. Health* 8: 31-45.
- Silbaugh, S. A.; Wolff, R. K.; Johnson, W. K.; Mauderly, J. L.; Macken, C. A. (1981b) Effects of sulfuric acid aerosols on pulmonary function of guinea pigs. *J. Toxicol. Environ. Health* 7: 339-352.
- Silicosis and Silicate Disease Committee. (1988) Diseases associated with exposure to silica and nonfibrous silicate minerals. *Arch. Pathol. Lab. Med.* 112: 673-720.
- Sitas, F.; Douglas, A. J.; Webster, E. C. (1989) Respiratory disease mortality patterns among South African iron moulders. *Br. J. Ind. Med.* 46: 310-315.
- Sjöberg, S.-G. (1950) Vanadium pentoxide dust: a clinical and experimental investigation on its effect after inhalation. *Acta Med. Scand. Suppl.* 238: 1-188.
- Sjöberg, S.-G. (1956) Vanadium dust, chronic bronchitis and possible risk of emphysema: a follow-up investigation of workers at a vanadium factory. *Acta Med. Scand.* 154: 381-386.
- Sjöstrand, M.; Rylander, R. (1984) Enzymes in lung lavage fluid after inhalation exposure to silica dust. *Environ. Res.* 33: 307-311.

- Skornik, W. A.; Brain, J. D. (1983) Relative toxicity of inhaled metal sulfate salts for pulmonary macrophages. *Am. Rev. Respir. Dis.* 128: 297-303.
- Sorahan, T. (1987) Mortality from lung cancer among a cohort of nickel cadmium battery workers: 1946-84. *Br. J. Ind. Med.* 44: 803-809.
- Sorenson, W. G.; Jones, W.; Simpson, J.; Davidson, J. I. (1984) Aflatoxin in respirable airborne peanut dust. *J. Toxicol. Environ. Health* 14: 525-533.
- Spektor, D. M.; Leikauf, G. D.; Albert, R. E.; Lippmann, M. (1985) Effects of submicrometer sulfuric acid aerosols on mucociliary transport and respiratory mechanics in asymptomatic asthmatics. *Environ. Res.* 37: 174-191.
- Spektor, D. M.; Yen, B. M.; Lippmann, M. (1989) Effect of concentration and cumulative exposure of inhaled sulfuric acid on tracheobronchial particle clearance in healthy humans. In: Symposium on the health effects of acid aerosols; October 1987; Research Triangle Park, NC. *Environ. Health Perspect.* 79: 167-172.
- Spencer, H. (1977) Pathology of the lung (excluding pulmonary tuberculosis). 3rd ed. Oxford, United Kingdom: Pergamon Press. 2 v.
- Srivastava, P. K.; Tyagi, S. R.; Misra, U. K. (1985) Induction of pulmonary drug metabolizing enzymes by coal fly ash in rats. *Toxicology* 36: 171-181.
- Stănescu, D. C.; Pilat, L.; Gavrilesco, N.; Teculescu, D. B.; Cristescu, I. (1967) Aspects of pulmonary mechanics in arc welders' siderosis. *Br. J. Ind. Med.* 24: 143-147.
- Stavert, D. M.; Archuleta, D. C.; Behr, M. J.; Lehnert, B. E. (1991) Relative acute toxicities of hydrogen fluoride, hydrogen chloride, and hydrogen bromide in nose- and pseudo-mouth-breathing rats. *Fundam. Appl. Toxicol.* 16: 636-655.
- Stearns, R. C.; Murthy, G. G. K.; Skornik, W.; Hatch, V.; Katler, M.; Godleski, J. J. (1994) Detection of ultrafine copper oxide particles in the lungs of hamsters by electron spectroscopic imaging. In: Proceedings of international conference of electron microscopy, ICEM 13; July; Paris, France; pp. 763-764.
- Stengel, P. W.; Bendele, A. M.; Cockerham, S. L.; Silbaugh, S. A. (1993) Sulfuric acid induces airway hyperresponsiveness to substance P in the guinea pig. *Agents Actions* 39: C128-C131.
- Stokinger, H. E. (1981a) Copper, Cu. In: Clayton, G. D.; Clayton, F. E., eds. *Patty's industrial hygiene and toxicology: v. 2A, toxicology.* 3rd rev. ed. New York, NY: John Wiley & Sons; pp. 1620-1630.
- Stokinger, H. E. (1981b) The halogens and the nonmetals boron and silicon. In: Clayton, G. D.; Clayton, F. E., eds. *Patty's industrial hygiene and toxicology: v. 2B, toxicology.* 3rd rev. ed. New York, NY: John Wiley & Sons; pp. 2937-3043.
- Stokinger, H. E. (1984) A review of world literature finds iron oxides noncarcinogenic. *Am. Ind. Hyg. Assoc. J.* 45: 127-133.
- Strom, K. A. (1984) Response of pulmonary cellular defenses to the inhalation of high concentrations of diesel exhaust. *J. Toxicol. Environ. Health* 13: 919-944.
- Suciu, I.; Prodan, L.; Lazar, V.; Ilea, E.; Cocîrla, A.; Olinici, L.; Paduraru, A.; Zagreanu, O.; Lengyel, P.; Györfi, L.; Andru, D. (1981) Research on copper poisoning. *Med. Lav.* 72: 190-197.
- Takenaka, S.; Oldiges, H.; König, H.; Hochrainer, D.; Oberdörster, G. (1983) Carcinogenicity of cadmium chloride aerosols in W rats. *JNCI, J. Natl. Cancer Inst.* 70: 367-371.

- Takenaka, S.; Dornhöfer-Takenaka, H.; Muhle, H. (1986) Alveolar distribution of fly ash and of titanium dioxide after long-term inhalation by Wistar rats. *J. Aerosol Sci.* 17: 361-364.
- Takenaka, S.; Fürst, G.; Heilman, P.; Heini, A.; Heinzmann, U.; Kreyling, W. G.; Murray, A. B.; Schulz, H.; Heyder, J. (1992) Early response of the canine respiratory tract following long-term exposure to a sulfur(IV) aerosol at low concentration. V. Morphology and morphometry. *Inhalation Toxicol.* 4: 247-272.
- Targonski, P. V.; Persky, V. W.; Ramekrishnan, V. (1995) Effect of environmental molds on risk of death from asthma during the pollen season. *J. Allergy Clin. Immunol.* 95: 955-961.
- Teculescu, D.; Albu, A. (1973) Pulmonary function in workers inhaling iron oxide dust. *Int. Arch. Arbeitsmed.* 31: 163-170.
- Tepper, J. S.; Lehmann, J. R.; Winsett, D. W.; Costa, D. L.; Ghio, A. J. (1994) The role of surface-complexed iron in the development of acute lung inflammation and airway hyperresponsiveness. *Am. Rev. Respir. Dis.* 149(4, pt. 2): A839.
- Thomas, D. L. G.; Stiebris, K. (1956) Vanadium poisoning in industry. *Med. J. Aust.* 1: 607-609.
- Thorén, S. A. (1992) Calorimetry: a new quantitative in vitro method in cell toxicology. A dose/effect study of alveolar macrophages exposed to particles. *J. Toxicol. Environ. Health* 36: 307-318.
- Thun, M. J.; Schnorr, T. M.; Smith, A. B.; Halperin, W. E.; Lemen, R. A. (1985) Mortality among a cohort of U.S. cadmium production workers - an update. *JNCI J. Natl. Cancer Inst.* 74: 325-333.
- Treon, J. F.; Cappel, J. W.; Cleveland, F. P.; Larson, E. E.; Atchley, R. W.; Denham, R. T. (1955) The toxicity of the products formed by the thermal decomposition of certain organic substances. Presented at: 15th annual meeting of the American Industrial Hygiene Association; April 1954; Chicago, IL. *Am. Ind. Hyg. Assoc. Q.* 16: 187-195.
- U.S. Bureau of the Census. (1992) Statistical abstract of the United States 1992. 112th ed. Washington, DC: U.S. Department of Commerce.
- U.S. Environmental Protection Agency. (1977) Air quality criteria for lead. Research Triangle Park, NC: Health Effects Research Laboratory, Criteria and Special Studies Office; EPA report no. EPA-600/8-77-017. Available from: NTIS, Springfield, VA; PB-280411.
- U.S. Environmental Protection Agency. (1982) Air quality criteria for particulate matter and sulfur oxides. Research Triangle Park, NC: Office of Health and Environmental Assessment, Environmental Criteria and Assessment Office; EPA report no. EPA-600/8-82-029aF-cF. 3v. Available from: NTIS, Springfield, VA; PB84-156777.
- U.S. Environmental Protection Agency. (1986a) Air quality criteria for lead. Research Triangle Park, NC: Office of Health and Environmental Assessment, Environmental Criteria and Assessment Office; EPA report no. EPA-600/8-83/028aF-dF. 4v. Available from: NTIS, Springfield, VA; PB87-142378.
- U.S. Environmental Protection Agency. (1986b) Airborne asbestos: health assessment update. Research Triangle Park, NC: Environmental Criteria and Assessment Office; report no. EPA/600/8-84/003F. Available from: NTIS, Springfield, VA; PB86-242864.
- U.S. Environmental Protection Agency. (1989) An acid aerosols issue paper: health effects and aerometrics. Research Triangle Park, NC: Office of Health and Environmental Assessment, Environmental Criteria and Assessment Office; EPA report no. EPA-600/8-88-005F. Available from: NTIS, Springfield, VA; PB91-125864.

- U.S. Environmental Protection Agency. (1990) Air quality criteria for lead: supplement to the 1986 addendum. Research Triangle Park, NC: Office of Health and Environmental Assessment, Environmental Criteria and Assessment Office; report no. EPA/600/8-89/049F. Available from: NTIS, Springfield, VA; PB91-138420/XAB.
- U.S. Environmental Protection Agency. (1993) Air quality criteria for oxides of nitrogen. Research Triangle Park, NC: Office of Health and Environmental Assessment, Environmental Criteria and Assessment Office; EPA report no. EPA/600/8-91/049aF-cF. 3v. Available from: NTIS, Springfield, VA; PB95-124533, PB95-124525, PB95-124517.
- U.S. Environmental Protection Agency. (1994) Health assessment document for diesel emissions [external review draft]. Research Triangle Park, NC: Office of Health and Environmental Assessment, Environmental Criteria and Assessment Office; report nos. EPA/600/8-90/057Ba-Bb. 2v.
- U.S. Environmental Protection Agency. (1995) Air quality criteria for ozone and related photochemical oxidants [draft final]. Research Triangle Park, NC: National Center for Environmental Assessment-RTP Office; EPA report nos. EPA/600/AP-93/004aF-cF. 3v.
- U.S. Environmental Protection Agency. (1996) Ambient levels and noncancer health effects of inhaled crystalline and amorphous silica: health issue assessment [draft]. Research Triangle Park, NC: National Center for Environmental Assessment; EPA report no. EPA/600/R-95/115.
- Uber, C. L.; McReynolds, R. A. (1982) Immunotoxicology of silica. *Crit. Rev. Toxicol.* 10: 303-319.
- Ulfvarson, U.; Alexandersson, R.; Aringer, L.; Svensson, E.; Hedenstierna, G.; Hogstedt, C.; Holmberg, B.; Rosen, G.; Sorsa, M. (1987) Effects of exposure to vehicle exhaust on health. *Scand. J. Work Environ. Health* 13: 505-512.
- Utell, M. J.; Frampton, M. W. (1995) Particles and mortality: a clinical perspective. In: Phalen, R. F.; Bates, D. V., eds. Proceedings of the colloquium on particulate air pollution and human mortality and morbidity, part II; January 1994; Irvine, CA. *Inhalation Toxicol.* 7: 645-655.
- Utell, M. J.; Aquilina, A. T.; Hall, W. J.; Speers, D. M.; Douglas, R. G., Jr.; Gibb, F. R.; Morrow, P. E.; Hyde, R. W. (1980) Development of airway reactivity to nitrates in subjects with influenza. *Am. Rev. Respir. Dis.* 121: 233-241.
- Utell, M. J.; Morrow, P. E.; Hyde, R. W. (1982) Comparison of normal and asthmatic subjects' responses to sulphate pollutant aerosols. In: Walton, W. H., ed. Inhaled particles V: proceedings of an international symposium organized by the British Occupational Hygiene Society; September 1980; Cardiff, Wales. *Ann. Occup. Hyg.* 26: 691-697.
- Utell, M. J.; Morrow, P. E.; Hyde, R. W. (1983a) Latent development of airway hyperreactivity in human subjects after sulfuric acid aerosol exposure. *J. Aerosol Sci.* 14: 202-205.
- Utell, M. J.; Morrow, P. E.; Speers, D. M.; Darling, J.; Hyde, R. W. (1983b) Airway responses to sulfate and sulfuric acid aerosols in asthmatics: an exposure-response relationship. *Am. Rev. Respir. Dis.* 128: 444-450.
- Utell, M. J.; Mariglio, J. A.; Morrow, P. E.; Gibb, F. R.; Speers, D. M. (1989) Effects of inhaled acid aerosols on respiratory function: the role of endogenous ammonia. *J. Aerosol Med.* 2: 141-147.
- Utell, M. J.; Frampton, M. W.; Morrow, P. E. (1991) Air pollution and asthma: clinical studies with sulfuric acid aerosols. *Allergy Proc.* 12: 385-388.
- Utell, M. J.; Frampton, M. W.; Morrow, P. E. (1993) Quantitative clinical studies with defined exposure atmospheres. In: Gardner, D. E.; Crapo, J. D.; McClellan, R. O., eds. Toxicology of the lung. 2nd ed. New York, NY: Raven Press; pp. 283-309. (Hayes, A. W.; Thomas, J. A.; Gardner, D. E., eds. Target organ toxicology series).

- Valberg, P. A. (1984) Magnetometry of ingested particles in pulmonary macrophages. *Science* (Washington, DC) 224: 513-516.
- Van Bree, L.; Reuzel, P. G. J.; Verhoef, M. A.; Bos, J.; Rombout, P. J. A. (1990) Effects of acute inhalation of respirable coal fly ash on metabolic defense capability of the rat lung. *Inhalation Toxicol.* 2: 361-373.
- Venugopal, B.; Luckey, T. D. (1978) Vanadium (V). In: *Metal toxicity in mammals: 2. chemical toxicity of metals and metalloids*. New York, NY: Plenum Press; pp. 220-226.
- Vinegar, A.; Carson, A. I.; Pepelko, W. E. (1980) Pulmonary function changes in Chinese hamsters exposed six months to diesel exhaust. In: Pepelko, W. E.; Danner, R. M.; Clarke, N. A., eds. *Health effects of diesel engine emissions: proceedings of an international symposium, v. 2; December, 1979; Cincinnati, OH*. Cincinnati, OH: U.S. Environmental Protection Agency, Health Effects Research Laboratory; pp. 749-756; EPA report no. EPA-600/9-80-057b. Available from: NTIS, Springfield, VA; PB81-173817
- Vinegar, A.; Carson, A.; Pepelko, W. E.; Orthofer, J. O. (1981a) Effect of six months of exposure to two levels of diesel exhaust on pulmonary function of Chinese hamsters. *Fed. Proc.* 40: 593.
- Vinegar, A.; Carson, A.; Pepelko, W. E. (1981b) Pulmonary function changes in Chinese hamsters exposed six months to diesel exhaust. *Environ. Int.* 5: 369-371.
- Vintinner, F. J.; Vallenias, R.; Carlin, C. E.; Weiss, R.; Macher, C.; Ochoa, R. (1955) Study of the health of workers employed in mining and processing of vanadium ore. *AMA Arch. Ind. Health* 12: 635-642.
- Vostal, J. J.; Chan, T. L.; Garg, B. D.; Lee, P. S.; Strom, K. A. (1981) Lymphatic transport of inhaled diesel particles in the lungs of rats and guinea pigs exposed to diluted diesel exhaust. *Environ. Int.* 5: 339-347.
- Vostal, J. J.; White, H. J.; Strom, K. A.; Siak, J.-S.; Chen, K.-C.; Dziedzic, D. (1982) Response of the pulmonary defense system to diesel particulate exposure. In: Lewtas, J., ed. *Toxicological effects of emissions from diesel engines: proceedings of the Environmental Protection Agency diesel emissions symposium; October 1981; Raleigh, NC*. New York, NY: Elsevier Biomedical; pp. 201-221. (Developments in toxicology and environmental science: v. 10).
- Waalkes, M. P.; Oberdörster, G. (1990) Cadmium carcinogenesis. In: Foulkes, E. C., ed. *Biological effects of heavy metals: vol. II, metal carcinogenesis*. CRC Press; ch. 5, pp. 129-157.
- Warheit, D. B.; Gavett, S. H. (1993) Current concepts in the pathogenesis of particulate-induced lung injury. In: Warheit, D. B., ed. *Fiber toxicology*. San Diego, CA: Academic Press; pp. 305-322.
- Warheit, D. B.; Hartsky, M. A. (1993) Role of alveolar macrophage chemotaxis and phagocytosis in pulmonary clearance responses to inhaled particles: comparisons among rodent species. *Microsc. Res. Tech.* 26: 412-422.
- Warheit, D. B.; Hill, L. H.; George, G.; Brody, A. R. (1986) Time course of chemotactic factor generation and the corresponding macrophage response to asbestos inhalation. *Am. Rev. Respir. Dis.* 134: 128-133.
- Warheit, D. B.; Overby, L. H.; George, G.; Brody, A. R. (1988) Pulmonary macrophages are attracted to inhaled particles through complement activation. *Exp. Lung Res.* 14: 51-66.
- Warheit, D. B.; Seidel, W. C.; Carakostas, M. C.; Hartsky, M. A. (1990) Attenuation of perfluoropolymer fume pulmonary toxicity: effect of filters, combustion method, and aerosol age. *Exp. Mol. Pathol.* 52: 309-329.

- Warheit, D. B.; Carakostas, M. C.; Hartsky, M. A.; Hansen, J. F. (1991a) Development of a short-term inhalation bioassay to assess pulmonary toxicity of inhaled particles: comparisons of pulmonary responses to carbonyl iron and silica. *Toxicol. Appl. Pharmacol.* 107: 350-368.
- Warheit, D. B.; Carakostas, M. C.; Kelly, D. P.; Hartsky, M. A. (1991b) Four-week inhalation toxicity study with Ludox colloidal silica in rats: pulmonary cellular responses. *Fundam. Appl. Toxicol.* 16: 590-601.
- Warheit, D. B.; Carakostas, M. C.; Bamberger, J. R.; Hartsky, M. A. (1991c) Complement facilitates macrophage phagocytosis of inhaled iron particles but has little effect in mediating silica-induced lung inflammatory and clearance responses. *Environ. Res.* 56: 186-203.
- Warheit, D. B.; McHugh, T. A.; Stanickyj, L.; Kellar, K. A.; Hartsky, M. A. (1994) Species differences in acute pulmonary responses to inhaled particles. In: Dodgson, J.; McCallum, R. L., eds. *Inhaled particles VII: proceedings of an international symposium; September 1991; Edinburgh, United Kingdom.* *Ann. Occup. Hyg.* 38(suppl. 1): 389-397.
- Warheit, D. B.; McHugh, T. A.; Hartsky, M. A. (1995) Differential pulmonary responses in rats inhaling various forms of silica dust (i.e., crystalline, colloidal and amorphous). *Scand. J. Work Environ. Health*: in press.
- Waritz, R. S.; Kwon, B. K. (1968) The inhalation toxicity of pyrolysis products of polytetrafluoroethylene heated below 500 degrees centigrade. *Am. Ind. Hyg. Assoc. J.* 29: 19-26.
- Warren, D. L.; Last, J. A. (1987) Synergistic interaction of ozone and respirable aerosols on rat lungs: III. ozone and sulfuric acid aerosol. *Toxicol. Appl. Pharmacol.* 88: 203-216.
- Warren, D. L.; Guth, D. J.; Last, J. A. (1986) Synergistic interaction of ozone and respirable aerosols on rat lungs: II. synergy between ammonium sulfate aerosol and various concentrations of ozone. *Toxicol. Appl. Pharmacol.* 84: 470-479.
- Watanabe, H.; Murayama, H.; Yamaoka, S. (1966) Some clinical findings on vanadium workers. *Sangyo Igaku* 8: 23-27.
- Waters, M. D. (1977) Toxicology of vanadium. In: Goyer, R. A.; Melman, M. A., eds. *Toxicology of trace elements.* New York, NY: Halsted Press; pp. 147-189. (*Advances in modern toxicology*: v. 2).
- Waters, M. D.; Gardner, D. E.; Coffin, D. L. (1974) Cytotoxic effects of vanadium on rabbit alveolar macrophages *in vitro*. *Toxicol. Appl. Pharmacol.* 28: 253-263.
- Wehner, A. P.; Dagle, G. E.; Clark, M. L. (1983) Lung changes in rats inhaling volcanic ash for one year. *Am. Rev. Respir. Dis.* 128: 926-932.
- Wei, C.; Misra, H. P. (1982) Cytotoxicity of ammonium metavanadate to cultured bovine alveolar macrophages. *J. Toxicol. Environ. Health* 9: 995-1006.
- Weiss, S. T.; Sparrow, D.; O'Connor, G. T. (1993) The interrelationship among allergy, airways responsiveness, and asthma. *J. Asthma* 30: 329-349.
- White, H. J.; Garg, B. D. (1981) Early pulmonary response of the rat lung to inhalation of high concentration of diesel particles. *J. Appl. Toxicol.* 1: 104-110.
- Wiester, M. J.; Iltis, R.; Moore, W. (1980) Altered function and histology in guinea pigs after inhalation of diesel exhaust. *Environ. Res.* 22: 285-297.
- Wiester, M. J.; Setzer, C. J.; Barry, B. E.; Mercer, R. R.; Grady, M. A. (1985) Inhalation studies of Mt. St. Helens volcanic ash in animals: respiratory mechanics, airway reactivity and deposition. *Environ. Res.* 36: 230-240.

- Wolff, R. K. (1986) Effects of airborne pollutants on mucociliary clearance. *Environ. Health Perspect.* 66: 223-237.
- Wolff, R. K.; Gray, R. L. (1980) Tracheal clearance of particles. In: Diel, J. H.; Bice, D. E.; Martinez, B. S., eds. *Inhalation Toxicology Research Institute annual report: 1979-1980*. Albuquerque, NM: Lovelace Biomedical and Environmental Research Institute; p. 252; report no. LMF-84.
- Wolff, R. K.; Henderson, R. F.; Dahl, A. R.; Felicetti, S. A.; Gray, R. H. (1980) Effects of H<sub>2</sub>SO<sub>4</sub> on tracheal mucus clearance. In: Sanders, C. L.; Cross, F. T.; Dagle, G. E.; Mahaffey, J. A., eds. *Pulmonary toxicology of respirable particles: proceedings of the nineteenth annual Hanford life sciences symposium; October 1979; Richland, WA*. Washington, DC: U.S. Department of Energy, Technical Information Center; pp. 119-133; report no. CONF-791002. (DOE symposium series 53). Available from: NTIS, Springfield, VA; CONF-791002.
- Wolff, R. K.; Muggenburg, B. A.; Silbaugh, S. A. (1981) Effect of 0.3 and 0.9  $\mu$ m sulfuric acid aerosols on tracheal mucous clearance in beagle dogs. *Am. Rev. Respir. Dis.* 123: 291-294.
- Wolff, R. K.; Henderson, R. F.; Gray, R. H.; Carpenter, R. L.; Hahn, F. F. (1986) Effects of sulfuric acid mist inhalation on mucous clearance and on airway fluids of rats and guinea pigs. *J. Toxicol. Environ. Health* 17: 129-142.
- Wolff, R. K.; Henderson, R. F.; Snipes, M. B.; Griffith, W. C.; Mauderly, J. L.; Cuddihy, R. G.; McClellan, R. O. (1987) Alterations in particle accumulation and clearance in lungs of rats chronically exposed to diesel exhaust. *Fundam. Appl. Toxicol.* 9: 154-166.
- Wolff, R. K.; Bond, J. A.; Henderson, R. F.; Harkema, J. R.; Mauderly, J. L. (1990) Pulmonary inflammation and DNA adducts in rats inhaling diesel exhaust or carbon black. *Inhalation Toxicol.* 2: 241-254.
- Wong, K. L.; Alarie, Y. (1982) A method for repeated evaluation of pulmonary performance in unanesthetized, unrestrained guinea pigs and its application to detect effects of sulfuric acid mist inhalation. *Toxicol. Appl. Pharmacol.* 63: 72-90.
- Wong, C. G.; Bonakdar, M.; Kleinman, M. T.; Chow, J.; Bhalla, D. K. (1994) Elevation of stress-inducible heat shock protein 70 in the rat lung after exposure to ozone and particle-containing atmosphere. *Inhalation Toxicol.* 6: 501-514.
- World Health Organization. (1987) *Air quality guidelines for Europe*. Copenhagen, Denmark: Regional Office for Europe (WHO regional publications, European series no. 23).
- Wright, E. S. (1986) Effects of short-term exposure to diesel exhaust on lung cell proliferation and phospholipid metabolism. *Exp. Lung Res.* 10: 39-55.
- Wright, J. L.; Harrison, N.; Wiggs, B.; Churg, A. (1988) Quartz but not iron oxide causes air-flow obstruction, emphysema, and small airways lesions in the rat. *Am. Rev. Respir. Dis.* 138: 129-135.
- Wyers, H. (1946) Some toxic effects of vanadium pentoxide. *Br. J. Ind. Med.* 3: 177-182.
- Yang, S.-C.; Yang, S.-P. (1994) Respiratory function changes from inhalation of polluted air. *Arch. Environ. Health* 49: 182-187.
- Zarkower, A.; Eskew, M. L.; Scheuchenzuber, W. J.; Graham, J. A. (1982) Effects of fly ash inhalation on murine immune function: changes in macrophage-mediated activities. *Environ. Res.* 29: 83-89.

- Zelikoff, J. T.; Schlesinger, R. B. (1992) Modulation of pulmonary immune defense mechanisms by sulfuric acid: effects on macrophage-derived tumor necrosis factor and superoxide. *Toxicology* 76: 271-281.
- Zelikoff, J. T.; Sisco, M. P.; Yang, Z.; Cohen, M. D.; Schlesinger, R. B. (1994) Immunotoxicity of sulfuric acid aerosol: effects on pulmonary macrophage effector and functional activities critical for maintaining host resistance against infectious diseases. *Toxicology* 92: 269-286.
- Zenz, C.; Berg, B. A. (1967) Human responses to controlled vanadium pentoxide exposure. *Arch. Environ. Health* 14: 709-712.
- Zenz, C.; Bartlett, J. P.; Thiede, W. H. (1962) Acute vanadium pentoxide intoxication. *Arch. Environ. Health* 5: 542-546.
- Ziskind, M.; Jones, R. N.; Weill, H. (1976) Silicosis. *Am. Rev. Respir. Dis.* 113: 643-665.